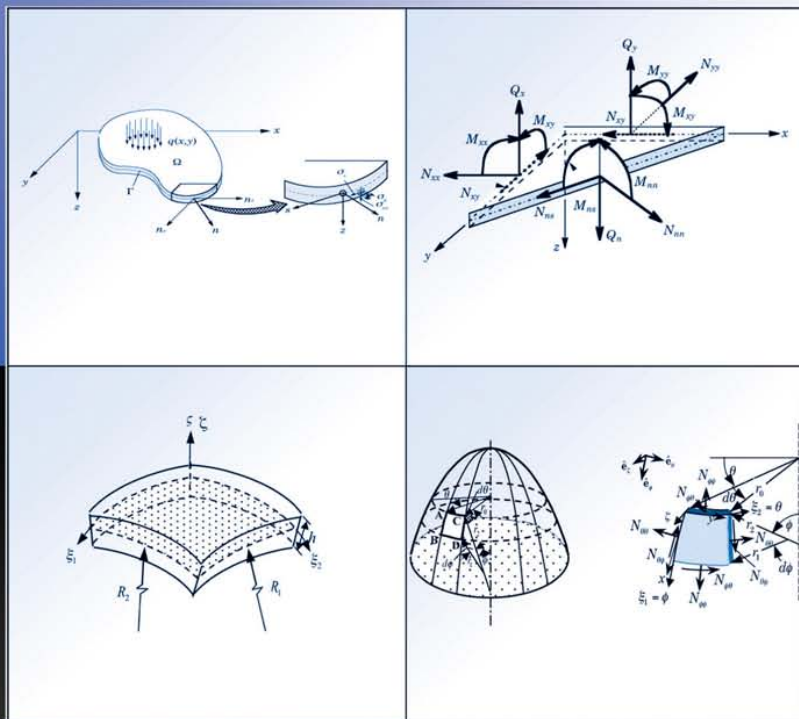


Theory and Analysis of Elastic Plates and Shells

Second Edition



J. N. Reddy

Theory and Analysis of Elastic Plates and Shells

Second Edition

Theory and Analysis of Elastic Plates and Shells

Second Edition

J. N. Reddy



CRC Press

Taylor & Francis Group

Boca Raton London New York

CRC Press is an imprint of the
Taylor & Francis Group, an informa business

CRC Press
Taylor & Francis Group
6000 Broken Sound Parkway NW, Suite 300
Boca Raton, FL 33487-2742

© 2007 by Taylor & Francis Group, LLC
CRC Press is an imprint of Taylor & Francis Group, an Informa business

No claim to original U.S. Government works
Printed in the United States of America on acid-free paper
10 9 8 7 6 5 4 3 2 1

International Standard Book Number-10: 0-8493-8415-X (Hardcover)
International Standard Book Number-13: 978-0-8493-8415-8 (Hardcover)

This book contains information obtained from authentic and highly regarded sources. Reprinted material is quoted with permission, and sources are indicated. A wide variety of references are listed. Reasonable efforts have been made to publish reliable data and information, but the author and the publisher cannot assume responsibility for the validity of all materials or for the consequences of their use.

No part of this book may be reprinted, reproduced, transmitted, or utilized in any form by any electronic, mechanical, or other means, now known or hereafter invented, including photocopying, microfilming, and recording, or in any information storage or retrieval system, without written permission from the publishers.

For permission to photocopy or use material electronically from this work, please access www.copyright.com (<http://www.copyright.com/>) or contact the Copyright Clearance Center, Inc. (CCC) 222 Rosewood Drive, Danvers, MA 01923, 978-750-8400. CCC is a not-for-profit organization that provides licenses and registration for a variety of users. For organizations that have been granted a photocopy license by the CCC, a separate system of payment has been arranged.

Trademark Notice: Product or corporate names may be trademarks or registered trademarks, and are used only for identification and explanation without intent to infringe.

Visit the Taylor & Francis Web site at
<http://www.taylorandfrancis.com>

and the CRC Press Web site at
<http://www.crcpress.com>

“Whence all creation had its origin,
he, whether he fashioned it or whether he did not,
 he, who surveys it all from highest heaven,
 he knows—or maybe even he does not know.”

Rig Veda

Contents

Preface to the Second Edition	xv
Preface	xvii
About the Author	xix
1 Vectors, Tensors, and Equations of Elasticity	1
1.1 Introduction	1
1.2 Vectors, Tensors, and Matrices	2
1.2.1 Preliminary Comments	2
1.2.2 Components of Vectors and Tensors	2
1.2.3 Summation Convention	3
1.2.4 The Del Operator	5
1.2.5 Matrices and Cramer's Rule	11
1.2.6 Transformations of Components	14
1.3 Equations of Elasticity	18
1.3.1 Introduction	18
1.3.2 Kinematics	18
1.3.3 Compatibility Equations	21
1.3.4 Stress Measures	23
1.3.5 Equations of Motion	25
1.3.6 Constitutive Equations	28
1.4 Transformation of Stresses, Strains, and Stiffnesses	32
1.4.1 Introduction	32
1.4.2 Transformation of Stress Components	32
1.4.3 Transformation of Strain Components	33
1.4.4 Transformation of Material Stiffnesses	34
1.5 Summary	35
Problems	35
2 Energy Principles and Variational Methods	39
2.1 Virtual Work	39
2.1.1 Introduction	39
2.1.2 Virtual Displacements and Forces	40
2.1.3 External and Internal Virtual Work	42
2.1.4 The Variational Operator	46
2.1.5 Functionals	47

2.1.6 Fundamental Lemma of Variational Calculus	48
2.1.7 Euler–Lagrange Equations	49
2.2 Energy Principles	51
2.2.1 Introduction	51
2.2.2 The Principle of Virtual Displacements	52
2.2.3 Hamilton’s Principle	55
2.2.4 The Principle of Minimum Total Potential Energy	58
2.3 Castigliano’s Theorems	61
2.3.1 Theorem I	61
2.3.2 Theorem II	66
2.4 Variational Methods	68
2.4.1 Introduction	68
2.4.2 The Ritz Method	69
2.4.3 The Galerkin Method	83
2.5 Summary	87
Problems	87
3 Classical Theory of Plates	95
3.1 Introduction	95
3.2 Assumptions of the Theory	96
3.3 Displacement Field and Strains	97
3.4 Equations of Motion	100
3.5 Boundary and Initial Conditions	105
3.6 Plate Stiffness Coefficients	110
3.7 Stiffness Coefficients of Orthotropic Plates	115
3.8 Equations of Motion in Terms of Displacements	118
3.9 Summary	121
Problems	121
4 Analysis of Plate Strips	125
4.1 Introduction	125
4.2 Governing Equations	126
4.3 Bending Analysis	126
4.3.1 General Solution	126
4.3.2 Simply Supported Plates	127
4.3.3 Clamped Plates	128
4.3.4 Plate Strips on Elastic Foundation	129
4.4 Buckling under Inplane Compressive Load	130
4.4.1 Introduction	130
4.4.2 Simply Supported Plate Strips	132
4.4.3 Clamped Plate Strips	133
4.4.4 Other Boundary Conditions	134

4.5 Free Vibration	135
4.5.1 General Formulation	135
4.5.2 Simply Supported Plate Strips	138
4.5.3 Clamped Plate Strips	139
4.6 Transient Analysis	140
4.6.1 Preliminary Comments.....	140
4.6.2 The Navier Solution	140
4.6.3 The Ritz Solution	142
4.6.4 Transient Response	143
4.6.5 Laplace Transform Method.....	144
4.7 Summary	146
Problems	146
5 Analysis of Circular Plates	149
5.1 Introduction	149
5.2 Governing Equations.....	149
5.2.1 Transformation of Equations from Rectangular Coordinates to Polar Coordinates	149
5.2.2 Derivation of Equations Using Hamilton's Principle	153
5.2.3 Plate Constitutive Equations.....	158
5.3 Axisymmetric Bending	160
5.3.1 Governing Equations.....	160
5.3.2 Analytical Solutions.....	162
5.3.3 The Ritz Formulation	166
5.3.4 Simply Supported Circular Plate under Distributed Load.....	167
5.3.5 Simply Supported Circular Plate under Central Point Load.....	171
5.3.6 Annular Plate with Simply Supported Outer Edge.....	174
5.3.7 Clamped Circular Plate under Distributed Load	178
5.3.8 Clamped Circular Plate under Central Point Load	179
5.3.9 Annular Plates with Clamped Outer Edges.....	181
5.3.10 Circular Plates on Elastic Foundation	185
5.3.11 Bending of Circular Plates under Thermal Loads	188
5.4 Asymmetrical Bending	189
5.4.1 General Solution	189
5.4.2 General Solution of Circular Plates under Linearly Varying Asymmetric Loading	190
5.4.3 Clamped Plate under Asymmetric Loading.....	192
5.4.4 Simply Supported Plate under Asymmetric Loading	193
5.4.5 Circular Plates under Noncentral Point Load	194
5.4.6 The Ritz Solutions	196

5.5 Free Vibration	200
5.5.1 Introduction	200
5.5.2 General Analytical Solution	201
5.5.3 Clamped Circular Plates	202
5.5.4 Simply Supported Circular Plates	204
5.5.5 The Ritz Solutions	204
5.6 Axisymmetric Buckling.....	207
5.6.1 Governing Equations.....	207
5.6.2 General Solution.....	208
5.6.3 Clamped Plates.....	209
5.6.4 Simply Supported Plates.....	209
5.6.5 Simply Supported Plates with Rotational Restraint.....	210
5.7 Summary	211
Problems	212
6 Bending of Simply Supported Rectangular Plates	215
6.1 Introduction	215
6.1.1 Governing Equations.....	215
6.1.2 Boundary Conditions	216
6.2 Navier Solutions	217
6.2.1 Solution Procedure.....	217
6.2.2 Calculation of Bending Moments, Shear Forces, and Stresses.....	221
6.2.3 Sinusoidally Loaded Plates	225
6.2.4 Plates with Distributed and Point Loads	228
6.2.5 Plates with Thermal Loads.....	233
6.3 Lévy's Solutions.....	236
6.3.1 Solution Procedure.....	236
6.3.2 Analytical Solution	237
6.3.3 Plates under Distributed Transverse Loads	242
6.3.4 Plates with Distributed Edge Moments	246
6.3.5 An Alternate Form of the Lévy Solution.....	249
6.3.6 The Ritz Solutions	254
6.4 Summary	258
Problems	259
7 Bending of Rectangular Plates with Various Boundary Conditions	263
7.1 Introduction	263
7.2 Lévy Solutions	263
7.2.1 Basic Equations.....	263
7.2.2 Plates with Edges $x = 0, a$ Clamped (CCSS).....	266
7.2.3 Plates with Edge $x = 0$ Clamped and Edge $x = a$ Simply Supported (CSSS)	273

7.2.4 Plates with Edge $x = 0$ Clamped and Edge $x = a$ Free (CFSS)	275
7.2.5 Plates with Edge $x = 0$ Simply Supported and Edge $x = a$ Free (SFSS)	277
7.2.6 Solution by the Method of Superposition	280
7.3 Approximate Solutions by the Ritz Method	283
7.3.1 Analysis of the Lévy Plates	283
7.3.2 Formulation for General Plates	287
7.3.3 Clamped Plates (CCCC)	291
7.4 Summary	293
Problems	293
8 General Buckling of Rectangular Plates	299
8.1 Buckling of Simply Supported Plates under Compressive Loads	299
8.1.1 Governing Equations	299
8.1.2 The Navier Solution	300
8.1.3 Biaxial Compression of a Plate	301
8.1.4 Biaxial Loading of a Plate	302
8.1.5 Uniaxial Compression of a Rectangular Plate	303
8.2 Buckling of Plates Simply Supported along Two Opposite Sides and Compressed in the Direction Perpendicular to Those Sides	309
8.2.1 The Lévy Solution	309
8.2.2 Buckling of SSSF Plates	310
8.2.3 Buckling of SSCF Plates	312
8.2.4 Buckling of SSCC Plates	315
8.3 Buckling of Rectangular Plates Using the Ritz Method	317
8.3.1 Analysis of the Lévy Plates	317
8.3.2 General Formulation	319
8.3.3 Buckling of a Simply Supported Plate under Combined Bending and Compression	321
8.3.4 Buckling of a Simply Supported Plate under Inplane Shear	324
8.3.5 Buckling of Clamped Plates under Inplane Shear	326
8.4 Summary	328
Problems	328
9 Dynamic Analysis of Rectangular Plates	331
9.1 Introduction	331
9.1.1 Governing Equations	331
9.1.2 Natural Vibration	331
9.1.3 Transient Analysis	332
9.2 Natural Vibration of Simply Supported Plates	332
9.3 Natural Vibration of Plates with Two Parallel Sides Simply Supported	334
9.3.1 The Lévy Solution	334

9.3.2 Analytical Solution	335
9.3.3 Vibration of SSSF Plates.....	336
9.3.4 Vibration of SSCF Plates	338
9.3.5 Vibration of SSCC Plates	340
9.3.6 Vibration of SSCS Plates.....	341
9.3.7 Vibration of SSFF Plates	342
9.3.8 The Ritz Solutions	345
9.4 Natural Vibration of Plates with General Boundary Conditions	346
9.4.1 The Ritz Solution.....	346
9.4.2 Simply Supported Plates (SSSS)	347
9.4.3 Clamped Plates (CCCC)	348
9.4.4 CCCS Plates.....	350
9.4.5 CSCS Plates	351
9.4.6 CFCF, CCFF, and CFFF Plates	351
9.5 Transient Analysis	354
9.5.1 Spatial Variation of the Solution	354
9.5.2 Time Integration.....	355
9.6 Summary	356
Problems	356
10 Shear Deformation Plate Theories.....	359
10.1 First-Order Shear Deformation Plate Theory	359
10.1.1 Preliminary Comments	359
10.1.2 Kinematics	359
10.1.3 Equations of Motion	361
10.1.4 Plate Constitutive Equations.....	365
10.1.5 Equations of Motion in Terms of Displacements	365
10.2 The Navier Solutions of FSDT	366
10.2.1 General Solution.....	366
10.2.2 Bending Analysis	368
10.2.3 Buckling Analysis.....	372
10.2.4 Natural Vibration.....	374
10.3 The Third-Order Plate Theory	376
10.3.1 General Comments	376
10.3.2 Displacement Field	376
10.3.3 Strains and Stresses.....	378
10.3.4 Equations of Motion	379
10.4 The Navier Solutions of TSDT	383
10.4.1 Preliminary Comments	383
10.4.2 General Solution.....	383
10.4.3 Bending Analysis	385
10.4.4 Buckling Analysis.....	387
10.4.5 Natural Vibration.....	389

10.5 Relationships between Solutions of Classical and Shear Deformation Theories	390
10.5.1 Introduction	390
10.5.2 Circular Plates	391
10.5.3 Polygonal Plates	394
10.6 Summary	399
Problems	399
11 Theory and Analysis of Shells	403
11.1 Introduction	403
11.1.1 Preliminary Comments	403
11.1.2 Classification of Shell Surfaces	405
11.2 Governing Equations	407
11.2.1 Geometric Properties of the Shell	407
11.2.2 General Strain–Displacement Relations	413
11.2.3 Stress Resultants	414
11.2.4 Displacement Field and Strains	415
11.2.5 Equations of Motion of a General Shell	419
11.2.6 Equations of Motion of Thin Shells	424
11.2.7 Constitutive Equations of a General Shell	425
11.2.8 Constitutive Equations of Thin Shells	428
11.3 Analytical Solutions of Thin Cylindrical Shells	430
11.3.1 Introduction	430
11.3.2 Membrane Theory	431
11.3.3 Flexural Theory for Axisymmetric Loads	436
11.4 Analytical Solutions of Shells with Double Curvature	441
11.4.1 Introduction and Geometry	441
11.4.2 Equations of Equilibrium	442
11.4.3 Membrane Stresses in Symmetrically Loaded Shells	444
11.4.4 Membrane Stresses in Unsymmetrically Loaded Shells	451
11.4.5 Bending Stresses in Spherical Shells	458
11.5 Vibration and Buckling of Circular Cylinders	464
11.5.1 Equations of Motion	464
11.5.2 Governing Equations in Terms of Displacements	465
11.5.3 The Lévy Solution	466
11.5.4 Boundary Conditions	471
11.5.5 Numerical Results	472
11.6 Summary	473
Problems	473
12 Finite Element Analysis of Plates	479
12.1 Introduction	479
12.2 Finite Element Models of CPT	480
12.2.1 Introduction	480

12.2.2 General Formulation	481
12.2.3 Plate-Bending Elements	483
12.2.4 Fully Discretized Finite Element Models	486
12.2.5 Numerical Results	488
12.3 Finite Element Models of FSDT	491
12.3.1 Virtual Work Statements	491
12.3.2 Lagrange Interpolation Functions	492
12.3.3 Finite Element Model	496
12.3.4 Numerical Results	498
12.4 Nonlinear Finite Element Models	504
12.4.1 Introduction	504
12.4.2 Classical Plate Theory	504
12.4.3 First-Order Shear Deformation Plate Theory	508
12.4.4 The Newton–Raphson Iterative Method	512
12.4.5 Tangent Stiffness Coefficients	513
12.4.6 Membrane Locking	519
12.4.7 Numerical Examples	520
12.5 Summary	524
Problems	526
References	531
Subject Index	543

Preface to the Second Edition

The objective of this second edition of *Theory and Analysis of Elastic Plates and Shells* remains the same – to present a complete and up-to-date treatment of classical as well as shear deformation plate and shell theories and their solutions by analytical and numerical methods. New material has been added in most chapters, along with some rearrangement of topics to improve the clarity of the overall presentation.

The first 10 chapters are the same as those in the first edition, with minor changes to the text. Section 2.3 on Castiglano's Theorems, Section 5.6 on axisymmetric buckling of circular plates, and Section 10.5 on relationships between the solutions of classical and shear deformation theories are new. Chapter 11 is entirely new and deals with theory and analysis of shells, while Chapter 12 is the same as the old Chapter 11, with the exception of a major new section on nonlinear finite element analysis of plates.

This edition of the book, like the first, is suitable as a textbook for a first course on theory and analysis of plates and shells in aerospace, civil, mechanical, and mechanics curricula. Due to the coverage of the linear and nonlinear finite element analysis, the book may be used as a reference for courses on finite element analysis. It can also be used as a reference by structural engineers and scientists working in industry and academia on plates and shell structures. An introductory course on mechanics of materials and elasticity should prove to be helpful, but not necessary, because a review of the basics is included in the first two chapters of the book.

A solutions manual is available from the publisher for those instructors who adopt the book as a textbook for a course.

J. N. Reddy
College Station, Texas

Preface

The objective of this book is to present a complete and up-to-date treatment of classical as well as shear deformation plate theories and their solutions by analytical and numerical methods. *Beams* and *plates* are common structural elements of most engineering structures, including aerospace, automotive, and civil engineering structures, and their study, both from theoretical and analysis points of view, is fundamental to the understanding of the behavior of such structures.

There exists a number of books on the theory of plates and most of them cover the classical Kirchhoff plate theory in detail and present the Navier solutions of the theory for rectangular plates. Much of the latest developments in shear deformation plate theories and their finite element models have not been compiled in a textbook form. The present book is aimed at filling this void in the literature.

The motivation that led to the writing of the present book has come from many years of the author's research in the development of shear deformation plate theories and their analysis by the finite element method, and also from the fact that there does not exist a book that contains a detailed coverage of shear deformation beam and plate theories, analytical solutions, and finite element models in one volume. The present book fulfills the need for a complete treatment of the classical and shear deformation theories of plates and their solution by analytical and numerical methods.

Some mathematical preliminaries, equations of elasticity, and virtual work principles and variational methods are reviewed in Chapters 1 and 2. A reader who has had a course in elasticity or energy and variational principles of mechanics may skip these chapters and go directly to Chapter 3, where a complete derivation of the equations of motion of the classical plate theory (CPT) is presented. Solutions for cylindrical bending, buckling, natural vibration, and transient response of plate strips are developed in Chapter 4. A detailed treatment of circular plates is undertaken in Chapter 5, and analytical and Rayleigh–Ritz solutions of axisymmetric and asymmetric bending are presented for various boundary conditions and loads. A brief discussion of natural vibrations of circular plates is also included here.

Chapter 6 is dedicated to the bending of rectangular plates with all edges simply supported, and the Navier and Rayleigh–Ritz solutions are presented. Bending of rectangular plates with general boundary conditions are treated in Chapter 7. The Lévy solutions are presented for rectangular plates with two parallel edges simply supported while the other two have arbitrary boundary conditions; the Rayleigh–Ritz solutions are presented for rectangular plates with arbitrary conditions. General buckling of rectangular plates under various boundary conditions is presented in Chapter 8. The Navier, Lévy, and Rayleigh–Ritz solutions are developed here. Chapter 9 is devoted to the dynamic analysis of rectangular plates, where solutions are developed for free vibration and transient response.

The first-order and third-order shear deformation plate theories are discussed in Chapter 10. Analytical solutions presented in these chapters are limited to rectangular plates with simply supported boundary conditions on all four edges (the Navier solution). Parametric effects of the material orthotropy and plate aspect ratio on bending deflections and stresses, buckling loads, and vibration frequencies are discussed. Finally, Chapter 11 deals with the linear finite element analysis of beams and plates. Finite element models based on both classical and first-order shear deformation plate theories are developed and numerical results are presented.

The book is suitable as a textbook for a first course on theory of plates in civil, aerospace, mechanical, and mechanics curricula. It can be used as a reference by engineers and scientists working in industry and academia. An introductory course on mechanics of materials and elasticity should prove to be helpful, but not necessary, because a review of the basics is included in the first two chapters of the book.

The author's research in the area of plates over the years has been supported through research grants from the Air Force Office of Scientific Research (AFOSR), the Army Research Office (ARO), and the Office of Naval Research (ONR). The support is gratefully acknowledged. The author also wishes to express his appreciation to Dr. Filis T. Kokkinos for his help with the illustrations in this book.

J. N. Reddy

College Station, Texas

About the Author

J. N. Reddy is Distinguished Professor and the Holder of Oscar S. Wyatt Endowed Chair in the Department of Mechanical Engineering at Texas A&M University, College Station, Texas.

Professor Reddy is internationally known for his contributions to theoretical and applied mechanics and computational mechanics. He is the author of over 350 journal papers and 14 books, including *Introduction to the Finite Element Method* (3rd ed.), McGraw-Hill, 2006; *An Introduction to Nonlinear Finite Element Analysis*, Oxford University Press, 2004; *Energy Principles and Variational Methods in Applied Mechanics* (2nd ed.), John Wiley & Sons, 2002; *Mechanics of Laminated Plates and Shells: Theory and Analysis*, (2nd ed.) CRC Press, 2004; *The Finite Element Method in Heat Transfer and Fluid Dynamics* (2nd ed.) (with D. K. Gartling), CRC Press, 2001; *An Introduction to the Mathematical Theory of Finite Elements* (with J. T. Oden), John Wiley & Sons, 1976; and *Variational Methods in Theoretical Mechanics* (with J. T. Oden), Springer-Verlag, 1976. For a complete list of publications, visit the websites <http://authors.isihighlycited.com/> and <http://www.tamu.edu/acml>.

Professor Reddy is the recipient of the *Walter L. Huber Civil Engineering Research Prize* of the American Society of Civil Engineers (ASCE), the *Worcester Reed Warner Medal* and the *Charles Russ Richards Memorial Award* of the American Society of Mechanical Engineers (ASME), the 1997 *Archie Higdon Distinguished Educator Award* from the American Society of Engineering Education (ASEE), the 1998 *Nathan M. Newmark Medal* from the American Society of Civil Engineers, the 2003 *Bush Excellence Award for Faculty in International Research* from Texas A&M University, the 2003 *Computational Solid Mechanics Award* from the U.S. Association of Computational Mechanics (USACM), and the 2000 *Excellence in the Field of Composites* and 2004 *Distinguished Research Award* from the American Society of Composites.

Professor Reddy is a Fellow of AIAA, ASCE, ASME, the American Academy of Mechanics (AAM), the American Society of Composites (ASC), the U.S. Association of Computational Mechanics (USACM), the International Association of Computational Mechanics (IACM), and the Aeronautical Society of India (ASI). Professor Reddy is the Editor-in-Chief of *Mechanics of Advanced Materials and Structures*, *International Journal of Computational Methods in Engineering Science and Mechanics*, and *International Journal of Structural Stability and Dynamics*, and he serves on the editorial boards of over two dozen other journals, including *International Journal of Non-Linear Mechanics*, *International Journal for Numerical Methods in Engineering*, *Computer Methods in Applied Mechanics and Engineering*, *Engineering Computations*, *Engineering Structures*, and *Applied Mechanics Reviews*.

Vectors, Tensors, and Equations of Elasticity

1.1 Introduction

The primary objective of this book is to study theories and analytical as well as numerical solutions of plate and shell structures, i.e., thin structural elements undergoing stretching and bending. The plate and shell theories are developed using certain assumed kinematics of deformation that facilitate writing the displacement field explicitly in terms of the thickness coordinate. Then the principle of virtual displacements and integration through the thickness are used to obtain the governing equations. The theories considered in this book are valid for *thin* and *moderately thick* plates and shells.

The governing equations of solid and structural mechanics can be derived by either vector mechanics or energy principles. In vector mechanics, better known as Newton's second law, the vector sum of forces and moments on a typical element of a structure is set to zero to obtain the equations of equilibrium or motion. In energy principles, such as the principle of virtual displacement or its derivative, the principle of minimum total potential energy, is used to obtain the governing equations. While both methods can give the same equations, the energy principles have the advantage of providing information on the form of the boundary conditions suitable for the problem. Energy principles also enable the development of refined theories of structural members that are difficult to formulate using vector mechanics. Finally, energy principles provide a natural means of determining numerical solutions of the governing equations. Hence, the energy approach is adopted in the present study to derive the governing equations of plates and shells.

In order to study theories of plates and shells, a good understanding of the basic equations of elasticity and the concepts of work done and energy stored is required. A study of these topics in turn requires familiarity with the notions of vectors, tensors, transformations of vector and tensor components, and matrices. Therefore, a brief review of vectors and tensors is presented first, followed by a review of the equations of elasticity. Readers familiar with these topics may skip the remaining portion of this chapter and go directly to Chapter 2, where the principles of virtual work and classical variational methods are discussed.

1.2 Vectors, Tensors, and Matrices

1.2.1 Preliminary Comments

All quantities appearing in analytical descriptions of physical laws can be classified into two categories: *scalars* and *nonscalars*. The scalars are given by a single real or complex number. Nonscalar quantities not only need a specified magnitude, but also additional information, such as direction and/or differentiability. Time, temperature, volume, and mass density are examples of scalars. Displacement, temperature gradient, force, moment, velocity, and acceleration are examples of nonscalars.

The term *vector* is used to imply a nonscalar that has magnitude and “direction” and obeys the parallelogram law of vector addition and rules of scalar multiplication. A vector in modern mathematical analysis is an abstraction of the elementary notion of a *physical vector*, and it is “an element from a linear vector space.” While the definition of a vector in abstract analysis does not require it to have a magnitude, in nearly all cases of practical interest it does, in which case the vector is said to belong to a “normed vector space.” In this book, we only need vectors from a special normed vector space – that is, physical vectors.

Not all nonscalar quantities are vectors. Some quantities require the specification of magnitude and two directions. For example, the specification of stress requires not only a force, but also an area upon which the force acts. Such quantities are called second-order tensors. Vector is a tensor of order one, while stress is a second-order tensor.

1.2.2 Components of Vectors and Tensors

In the analytical description of a physical phenomenon, a coordinate system in the chosen frame of reference is introduced and various physical quantities involved in the description are expressed in terms of measurements made in that system. The form of the equations thus depends upon the chosen coordinate system and may appear different in another type of coordinate system. The laws of nature, however, should be independent of the choice of a coordinate system, and we may seek to represent the law in a manner independent of a particular coordinate system. A way of doing this is provided by vector and tensor notation. When vector notation is used, a particular coordinate system need not be introduced. Consequently, use of vector notation in formulating natural laws leaves them *invariant* to coordinate transformations.

Often a specific coordinate system that facilitates the solution is chosen to express governing equations of a problem. Then the vector and tensor quantities appearing in the equations are expressed in terms of their components in that coordinate system. For example, a vector \mathbf{A} in a three-dimensional space may be expressed in terms of its components a_1 , a_2 , and a_3 and *basis vectors* \mathbf{e}_1 , \mathbf{e}_2 , and \mathbf{e}_3 as

$$\mathbf{A} = a_1 \mathbf{e}_1 + a_2 \mathbf{e}_2 + a_3 \mathbf{e}_3 \quad (1.2.1)$$

If the basis vectors of a coordinate system are constants, i.e., with fixed lengths and directions, the coordinate system is called a *Cartesian coordinate system*. The general Cartesian system is oblique. When the Cartesian system is orthogonal, it is

called *rectangular Cartesian*. When the basis vectors are of unit length and mutually orthogonal, they are called *orthonormal*. We denote an orthonormal Cartesian basis by

$$(\hat{\mathbf{e}}_1, \hat{\mathbf{e}}_2, \hat{\mathbf{e}}_3) \text{ or } (\hat{\mathbf{e}}_x, \hat{\mathbf{e}}_y, \hat{\mathbf{e}}_z) \quad (1.2.2)$$

The Cartesian coordinates are denoted by

$$(x_1, x_2, x_3) \text{ or } (x, y, z) \quad (1.2.3)$$

The familiar rectangular Cartesian coordinate system is shown in Figure 1.2.1. We shall always use a right-hand coordinate system.

A second-order tensor, also called a *dyad*, can be expressed in terms of its rectangular Cartesian system as

$$\begin{aligned} \Phi = & \varphi_{11}\hat{\mathbf{e}}_1\hat{\mathbf{e}}_1 + \varphi_{12}\hat{\mathbf{e}}_1\hat{\mathbf{e}}_2 + \varphi_{13}\hat{\mathbf{e}}_1\hat{\mathbf{e}}_3 \\ & + \varphi_{21}\hat{\mathbf{e}}_2\hat{\mathbf{e}}_1 + \varphi_{22}\hat{\mathbf{e}}_2\hat{\mathbf{e}}_2 + \varphi_{23}\hat{\mathbf{e}}_2\hat{\mathbf{e}}_3 \\ & + \varphi_{31}\hat{\mathbf{e}}_3\hat{\mathbf{e}}_1 + \varphi_{32}\hat{\mathbf{e}}_3\hat{\mathbf{e}}_2 + \varphi_{33}\hat{\mathbf{e}}_3\hat{\mathbf{e}}_3 \end{aligned} \quad (1.2.4)$$

Here we have selected a rectangular Cartesian basis to represent the second-order tensor Φ . The first- and second-order tensors (i.e., vectors and dyads) will be of greatest utility in the present study.

1.2.3 Summation Convention

It is convenient to abbreviate a summation of terms by understanding that a *once repeated* index means summation over all values of that index. For example, the component form of vector \mathbf{A}

$$\mathbf{A} = a^1\mathbf{e}_1 + a^2\mathbf{e}_2 + a^3\mathbf{e}_3 \quad (1.2.5)$$

where $(\mathbf{e}_1, \mathbf{e}_2, \mathbf{e}_3)$ are basis vectors (not necessarily unit), can be expressed in the form

$$\mathbf{A} = \sum_{j=1}^3 a^j \mathbf{e}_j = a^j \mathbf{e}_j \quad (1.2.6)$$

The repeated index is a *dummy index* in the sense that any other symbol that is not already used in that expression can be used:

$$\mathbf{A} = a^j \mathbf{e}_j = a^k \mathbf{e}_k = a^m \mathbf{e}_m \quad (1.2.7)$$

An index that is not repeated is called a *free index*, like j in $A_i B_i C_j$. The range of summation is always known in the context of the discussion. For example, in the present context, the range of j, k , and m is 1 to 3, because we are discussing vectors in a three-dimensional space.

A vector \mathbf{A} and a second-order tensor \mathbf{P} can be expressed in a short form using the summation convention

$$\mathbf{A} = A_i \hat{\mathbf{e}}_i, \quad \mathbf{P} = P_{ij} \hat{\mathbf{e}}_i \hat{\mathbf{e}}_j \quad (1.2.8)$$

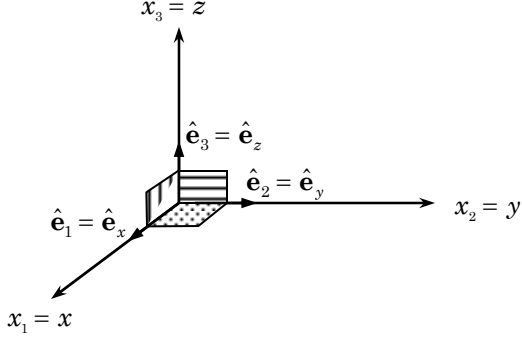


Figure 1.2.1 A rectangular Cartesian coordinate system, $(x_1, x_2, x_3) = (x, y, z)$; $(\hat{\mathbf{e}}_1, \hat{\mathbf{e}}_2, \hat{\mathbf{e}}_3) = (\hat{\mathbf{e}}_x, \hat{\mathbf{e}}_y, \hat{\mathbf{e}}_z)$ are the unit basis vectors.

and an n th-order tensor has the form

$$\Phi = \varphi_{ijkl\dots} \hat{\mathbf{e}}_i \hat{\mathbf{e}}_j \hat{\mathbf{e}}_k \hat{\mathbf{e}}_\ell \dots \quad (1.2.9)$$

A unit second-order tensor \mathbf{I} in a rectangular cartesian system is represented as

$$\mathbf{I} = \delta_{ij} \hat{\mathbf{e}}_i \hat{\mathbf{e}}_j \quad (1.2.10)$$

where δ_{ij} , called the *Kronecker delta*, is defined as

$$\delta_{ij} = \begin{cases} 0, & \text{if } i \neq j \\ 1, & \text{if } i = j \end{cases} \quad (1.2.11)$$

for any values of i and j . Note that $\delta_{ij} = \delta_{ji}$ and $\delta_{ij} \equiv \hat{\mathbf{e}}_i \cdot \hat{\mathbf{e}}_j$. In Eqs. (1.2.8)–(1.2.10) we have chosen a rectangular Cartesian basis to represent the tensors.

The *dot product* (or *scalar product*) and *cross product* (or *vector product*) of vectors can be defined in terms of their components with the help of Kronecker delta symbol and

$$\varepsilon_{ijk} = \begin{cases} 1, & \text{if } i, j, k \text{ are in cyclic order and } i \neq j \neq k \\ -1, & \text{if } i, j, k \text{ are not in cyclic order and } i \neq j \neq k \\ 0, & \text{if any of } i, j, k \text{ are repeated} \end{cases} \quad (1.2.12)$$

The symbol ε_{ijk} is called the *alternating symbol permutation symbol*, or *alternating tensor*, since it is a Cartesian component of a third-order tensor.

In an orthonormal basis, the scalar and vector products can be expressed in the index form using the Kronecker delta and the alternating symbol

$$\begin{aligned} \mathbf{A} \cdot \mathbf{B} &= (A_i \hat{\mathbf{e}}_i) \cdot (B_j \hat{\mathbf{e}}_j) = A_i B_j \delta_{ij} = A_i B_i \\ \mathbf{A} \times \mathbf{B} &= (A_i \hat{\mathbf{e}}_i) \times (B_j \hat{\mathbf{e}}_j) = A_i B_j \varepsilon_{ijk} \hat{\mathbf{e}}_k \end{aligned} \quad (1.2.13)$$

Note that

$$\hat{\mathbf{e}}_i \cdot (\hat{\mathbf{e}}_j \times \hat{\mathbf{e}}_k) = \varepsilon_{ijk} = \varepsilon_{kij} = \varepsilon_{jki}; \quad \varepsilon_{ijk} = -\varepsilon_{jik} = -\varepsilon_{ikj} \quad (1.2.14)$$

The parenthesis around $\hat{\mathbf{e}}_j \times \hat{\mathbf{e}}_k$ may be omitted since the expression makes no sense any other way. Thus, a cyclic permutation of the indices does not change the sign, while the interchange of any two indices will change the sign. Further, the Kronecker delta and the permutation symbol are related by the identity, known as the ε - δ *identity*

$$\varepsilon_{ijk}\varepsilon_{imn} = \delta_{jm}\delta_{kn} - \delta_{jn}\delta_{km} \quad (1.2.15)$$

Note that in the above expression i is a dummy index while j , k , m , and n are free indices.

The permutation symbol and the Kronecker delta prove to be very useful in proving vector identities and simplifying vector equations. The following example illustrates some of the uses of δ_{ij} and ε_{ijk} .

Example 1.2.1

We wish to simplify the vector operation $(\mathbf{A} \times \mathbf{B}) \cdot (\mathbf{C} \times \mathbf{D})$ in an alternate vector form and thereby establish a vector identity. We begin with

$$\begin{aligned} (\mathbf{A} \times \mathbf{B}) \cdot (\mathbf{C} \times \mathbf{D}) &= (A_i \hat{\mathbf{e}}_i) \times (B_j \hat{\mathbf{e}}_j) \cdot (C_m \hat{\mathbf{e}}_m) \times (D_n \hat{\mathbf{e}}_n) \\ &= (A_i B_j \varepsilon_{ijk} \hat{\mathbf{e}}_k) \cdot (C_m D_n \varepsilon_{mnp} \hat{\mathbf{e}}_p) \\ &= A_i B_j C_m D_n \varepsilon_{ijk} \varepsilon_{mnp} \delta_{kp} \\ &= A_i B_j C_m D_n \varepsilon_{ijk} \varepsilon_{mnk} \\ &= A_i B_j C_m D_n (\delta_{im} \delta_{jn} - \delta_{in} \delta_{jm}) \\ &= A_i B_j C_m D_n \delta_{im} \delta_{jn} - A_i B_j C_m D_n \delta_{in} \delta_{jm} \end{aligned}$$

where we have used the ε - δ identity. Since $C_m \delta_{im} = C_i$, $A_i \delta_{im} = A_m$, and $A_i C_i = \mathbf{A} \cdot \mathbf{C}$, and so on, we can write

$$\begin{aligned} (\mathbf{A} \times \mathbf{B}) \cdot (\mathbf{C} \times \mathbf{D}) &= A_i B_j C_i D_j - A_i B_j C_j D_i \\ &= A_i C_i B_j D_j - A_i B_j D_j C_i \\ &= (\mathbf{A} \cdot \mathbf{C})(\mathbf{B} \cdot \mathbf{D}) - (\mathbf{A} \cdot \mathbf{D})(\mathbf{B} \cdot \mathbf{C}) \end{aligned}$$

Although the above vector identity is established using an orthonormal basis, it holds in a general coordinate system.

1.2.4 The Del Operator

A position vector to an arbitrary point (x, y, z) or (x_1, x_2, x_3) in a body, measured from the origin, is given by (sometimes denoted by \mathbf{x})

$$\mathbf{r} = x \hat{\mathbf{e}}_x + y \hat{\mathbf{e}}_y + z \hat{\mathbf{e}}_z = x_1 \hat{\mathbf{e}}_1 + x_2 \hat{\mathbf{e}}_2 + x_3 \hat{\mathbf{e}}_3 \quad (1.2.16)$$

or, in summation notation, by

$$\mathbf{r} = x_j \hat{\mathbf{e}}_j \quad (= \mathbf{x}) \quad (1.2.17)$$

Consider a scalar field ϕ which is a function of the position vector, $\phi = \phi(\mathbf{r})$. The differential change is given by

$$d\phi = \frac{\partial \phi}{\partial x_i} dx_i \quad (1.2.18)$$

The differentials dx_i are components of $d\mathbf{r}$, that is,

$$d\mathbf{r} = dx_i \hat{\mathbf{e}}_i$$

We would now like to write $d\phi$ in such a way that we account for the *direction* as well as the magnitude of $d\mathbf{r}$. Since $dx_i = d\mathbf{r} \cdot \hat{\mathbf{e}}_i$, we can write

$$d\phi = d\mathbf{r} \cdot \left(\hat{\mathbf{e}}_i \frac{\partial \phi}{\partial x_i} \right)$$

Let us now denote the magnitude of $d\mathbf{r}$ by $ds \equiv |d\mathbf{r}|$. Then $\hat{\mathbf{e}} = d\mathbf{r}/ds$ is a unit vector in the direction of $d\mathbf{r}$, and we have

$$\left(\frac{d\phi}{ds} \right)_{\hat{\mathbf{e}}} = \hat{\mathbf{e}} \cdot \left(\hat{\mathbf{e}}_i \frac{\partial \phi}{\partial x_i} \right) \quad (1.2.19)$$

The derivative $(d\phi/ds)_{\hat{\mathbf{e}}}$ is called the *directional derivative of ϕ* . We see that it is the rate of change of ϕ with respect to distance and that it depends on the direction $\hat{\mathbf{e}}$ in which the distance is taken.

The vector that is scalar multiplied by $\hat{\mathbf{e}}$ can be obtained immediately whenever the scalar field is given. Because the magnitude of this vector is equal to the maximum value of the directional derivative, it is called the *gradient vector* and is denoted by $\text{grad } \phi$:

$$\text{grad } \phi \equiv \hat{\mathbf{e}}_i \frac{\partial \phi}{\partial x_i} \quad (1.2.20)$$

We interpret $\text{grad } \phi$ as some operator operating on ϕ , that is, $\text{grad } \phi = \nabla \phi$. This operator is denoted, in a general coordinate system (q^1, q^2, q^3) with basis $(\mathbf{e}^1, \mathbf{e}^2, \mathbf{e}^3)$, by

$$\nabla \equiv \mathbf{e}^1 \frac{\partial}{\partial q^1} + \mathbf{e}^2 \frac{\partial}{\partial q^2} + \mathbf{e}^3 \frac{\partial}{\partial q^3} = \mathbf{e}^i \frac{\partial}{\partial q^i} \quad (1.2.21)$$

and is called the del operator. In rectangular Cartesian system, we have

$$\nabla \equiv \hat{\mathbf{e}}_x \frac{\partial}{\partial x} + \hat{\mathbf{e}}_y \frac{\partial}{\partial y} + \hat{\mathbf{e}}_z \frac{\partial}{\partial z} \quad (1.2.22)$$

The del operator is a *vector differential* operator. However, it is important to note that the del operator has some of the properties of a vector, but it does not have them all because it is an operator. For example, $\nabla \cdot \mathbf{A}$ is a scalar, called the *divergence of \mathbf{A}* , whereas $\mathbf{A} \cdot \nabla$ is a scalar *differential operator*. Thus, the del operator does not commute in this sense. The operation $\nabla \times \mathbf{A}$ is called the *curl of \mathbf{A}* . The gradient of a vector is a second-order tensor. The scalar differential operator

$\nabla \cdot \nabla = \nabla^2$ is known as the *Laplacian* operator. The properties of the del operator are illustrated in Example 1.2.2.

Example 1.2.2

Here we illustrate the use of index notation and the del operator to rewrite the following vector expressions in alternative forms:

- (a) grad ($\mathbf{r} \cdot \mathbf{A}$)
- (b) div ($\mathbf{r} \times \mathbf{A}$)
- (c) curl ($\mathbf{r} \times \mathbf{A}$)

where $\mathbf{A} = \mathbf{A}(r)$ is a vector and \mathbf{r} is the position vector with magnitude r .

For simplicity, we use the rectangular Cartesian basis to establish the identities.

- (a) Expressing in components

$$\begin{aligned}\nabla(\mathbf{r} \cdot \mathbf{A}) &= \left(\hat{\mathbf{e}}_i \frac{\partial}{\partial x_i} \right) (x_j \hat{\mathbf{e}}_j \cdot A_k \hat{\mathbf{e}}_k) = \hat{\mathbf{e}}_i \frac{\partial}{\partial x_i} (x_j A_k \delta_{jk}) \\ &= \hat{\mathbf{e}}_i \frac{\partial}{\partial x_i} (x_j A_j) = \hat{\mathbf{e}}_i \left(\frac{\partial x_j}{\partial x_i} A_j + x_j \frac{\partial A_j}{\partial x_i} \right) \\ &= \hat{\mathbf{e}}_i (\delta_{ij} A_j + x_j A_{j,i}) = \hat{\mathbf{e}}_i A_i + \hat{\mathbf{e}}_i x_j A_{j,i}\end{aligned}$$

The first expression is clearly equal to \mathbf{A} . A close examination of the second expression on the right side of the equality indicates that the basis vector goes with the differential operator because both have the same subscript i . Also x_j and A_j have the same subscript, implying that there is a dot product operation between them. Hence, we can write

$$\hat{\mathbf{e}}_i \frac{\partial A_j}{\partial x_i} x_j = (\nabla \mathbf{A}) \cdot \mathbf{r}$$

Thus, we have

$$\nabla(\mathbf{r} \cdot \mathbf{A}) = \mathbf{A} + (\nabla \mathbf{A}) \cdot \mathbf{r}$$

Note that $\nabla \mathbf{A}$ is a second-order tensor $F_{ij} \hat{\mathbf{e}}_i \hat{\mathbf{e}}_j$ with components $F_{ij} = \partial A_j / \partial x_i$.

- (b) Writing in components form

$$\begin{aligned}\nabla \cdot (\mathbf{r} \times \mathbf{A}) &= \left(\hat{\mathbf{e}}_i \frac{\partial}{\partial x_i} \right) \cdot (x_j \hat{\mathbf{e}}_j \times A_k \hat{\mathbf{e}}_k) = \hat{\mathbf{e}}_i \cdot (\hat{\mathbf{e}}_j \times \hat{\mathbf{e}}_k) \frac{\partial}{\partial x_i} (x_j A_k) \\ &= \varepsilon_{ijk} \left(\frac{\partial x_j}{\partial x_i} A_k + x_j \frac{\partial A_k}{\partial x_i} \right) = \varepsilon_{ijk} (\delta_{ij} A_k + x_j A_{k,i}) \\ &= \varepsilon_{iik} A_k + \varepsilon_{ijk} x_j A_{k,i}\end{aligned}$$

Clearly the first term is zero on account of the repeated subscript in the permutation symbol. Now consider the second term

$$\varepsilon_{ijk} x_j A_{k,i} = -A_{k,i} \varepsilon_{ikj} x_j = -(\nabla \times \mathbf{A}) \cdot \mathbf{r}$$

Thus, we have

$$\nabla \cdot (\mathbf{r} \times \mathbf{A}) = -(\nabla \times \mathbf{A}) \cdot \mathbf{r}$$

(c) Writing in cartesian component form

$$\begin{aligned}
 \nabla \times (\mathbf{r} \times \mathbf{A}) &= \left(\hat{\mathbf{e}}_i \frac{\partial}{\partial x_i} \right) \times (x_j \hat{\mathbf{e}}_j \times A_k \hat{\mathbf{e}}_k) = \hat{\mathbf{e}}_i \times (\hat{\mathbf{e}}_j \times \hat{\mathbf{e}}_k) \frac{\partial}{\partial x_i} (x_j A_k) \\
 &= \varepsilon_{jkm} \hat{\mathbf{e}}_i \times \hat{\mathbf{e}}_m \left(\frac{\partial x_j}{\partial x_i} A_k + x_j \frac{\partial A_k}{\partial x_i} \right) \\
 &= \varepsilon_{jkm} \varepsilon_{imn} \hat{\mathbf{e}}_n (\delta_{ij} A_k + x_j A_{k,i}) \\
 &= (\delta_{jn} \delta_{ki} - \delta_{ji} \delta_{kn}) (\delta_{ij} A_k + x_j A_{k,i}) \hat{\mathbf{e}}_n \\
 &= (A_n - 3A_n + x_n A_{i,i} - x_i A_{n,i}) \hat{\mathbf{e}}_n \\
 &= -2\mathbf{A} + \mathbf{r}(\nabla \cdot \mathbf{A}) - (\mathbf{r} \cdot \nabla)\mathbf{A} \\
 &= \mathbf{r} \operatorname{div} \mathbf{A} - 2\mathbf{A} - \mathbf{r} \cdot \operatorname{grad} \mathbf{A}
 \end{aligned}$$

where we have used the identities $\delta_{jn} \delta_{ij} = \delta_{in}$, $\delta_{ij} \delta_{ij} = \delta_{ii}$ and $\delta_{ii} = 3$.

In an orthogonal curvilinear coordinate system, the del operator can be expressed in terms of its orthonormal basis. Two commonly used orthogonal curvilinear coordinate systems are *cylindrical coordinates* and *spherical coordinates*, which are shown in Figure 1.2.2. Here we summarize the relationships between the rectangular Cartesian and the two orthogonal curvilinear coordinate systems and the forms of the del and Laplacian operators.

Cylindrical Coordinates (r, θ, z)

The rectangular Cartesian coordinates (x, y, z) are related to the cylindrical coordinates (r, θ, z) by

$$x = r \cos \theta, \quad y = r \sin \theta, \quad z = z \quad (1.2.23)$$

and the inverse relations are

$$r = \sqrt{x^2 + y^2}, \quad \theta = \tan^{-1} \left(\frac{y}{x} \right), \quad z = z \quad (1.2.24)$$

The basis vectors are

$$\mathbf{e}_r = \hat{\mathbf{e}}_r, \quad \mathbf{e}_\theta = r \hat{\mathbf{e}}_\theta, \quad \mathbf{e}_z = \hat{\mathbf{e}}_z \quad (1.2.25)$$

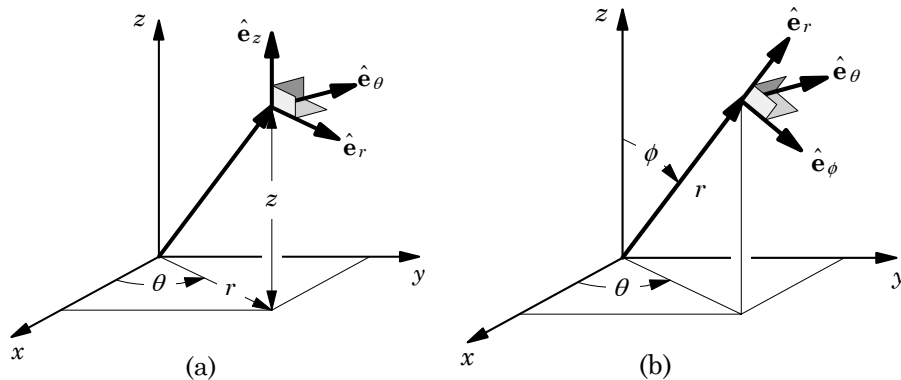


Figure 1.2.2 (a) Cylindrical coordinate system. (b) Spherical coordinate system.

In terms of the Cartesian basis, we have

$$\begin{aligned}\hat{\mathbf{e}}_r &= \cos \theta \hat{\mathbf{e}}_x + \sin \theta \hat{\mathbf{e}}_y \\ \hat{\mathbf{e}}_\theta &= -\sin \theta \hat{\mathbf{e}}_x + \cos \theta \hat{\mathbf{e}}_y \\ \hat{\mathbf{e}}_z &= \hat{\mathbf{e}}_z\end{aligned}\quad (1.2.26)$$

The Cartesian basis in terms of the cylindrical orthonormal basis is

$$\begin{aligned}\hat{\mathbf{e}}_x &= \cos \theta \hat{\mathbf{e}}_r - \sin \theta \hat{\mathbf{e}}_\theta \\ \hat{\mathbf{e}}_y &= \sin \theta \hat{\mathbf{e}}_r + \cos \theta \hat{\mathbf{e}}_\theta \\ \hat{\mathbf{e}}_z &= \hat{\mathbf{e}}_z\end{aligned}\quad (1.2.27)$$

The position vector is given by

$$\mathbf{r} = r\hat{\mathbf{e}}_r + z\hat{\mathbf{e}}_z \quad (1.2.28)$$

The nonzero derivatives of the basis vectors are

$$\begin{aligned}\frac{\partial \hat{\mathbf{e}}_r}{\partial \theta} &= -\sin \theta \hat{\mathbf{e}}_x + \cos \theta \hat{\mathbf{e}}_y = \hat{\mathbf{e}}_\theta \\ \frac{\partial \hat{\mathbf{e}}_\theta}{\partial \theta} &= -\cos \theta \hat{\mathbf{e}}_x - \sin \theta \hat{\mathbf{e}}_y = -\hat{\mathbf{e}}_r\end{aligned}\quad (1.2.29)$$

The del (∇) and Laplacian ($\nabla^2 = \nabla \cdot \nabla$) operators are given by

$$\nabla = \hat{\mathbf{e}}_r \frac{\partial}{\partial r} + \hat{\mathbf{e}}_\theta \frac{1}{r} \frac{\partial}{\partial \theta} + \hat{\mathbf{e}}_z \frac{\partial}{\partial z} \quad (1.2.30)$$

$$\nabla^2 = \frac{1}{r} \left[\frac{\partial}{\partial r} \left(r \frac{\partial}{\partial r} \right) + \frac{1}{r} \frac{\partial^2}{\partial \theta^2} + r \frac{\partial^2}{\partial z^2} \right] \quad (1.2.31)$$

Then the gradient, divergence, and curl of a vector \mathbf{u} in the cylindrical coordinate system can be obtained as (see Problems 1.10 and 1.11 at the end of the chapter)

$$\begin{aligned}\nabla \mathbf{u} &= \frac{\partial u_r}{\partial r} \hat{\mathbf{e}}_r \hat{\mathbf{e}}_r + \frac{1}{r} \left(u_r + \frac{\partial u_\theta}{\partial \theta} \right) \hat{\mathbf{e}}_\theta \hat{\mathbf{e}}_\theta + \frac{\partial u_z}{\partial z} \hat{\mathbf{e}}_z \hat{\mathbf{e}}_z + \frac{1}{r} \frac{\partial u_z}{\partial \theta} \hat{\mathbf{e}}_\theta \hat{\mathbf{e}}_z + \frac{\partial u_\theta}{\partial z} \hat{\mathbf{e}}_z \hat{\mathbf{e}}_\theta \\ &\quad + \frac{\partial u_r}{\partial z} \hat{\mathbf{e}}_z \hat{\mathbf{e}}_r + \frac{\partial u_z}{\partial r} \hat{\mathbf{e}}_r \hat{\mathbf{e}}_z + \frac{\partial u_\theta}{\partial r} \hat{\mathbf{e}}_r \hat{\mathbf{e}}_\theta + \frac{1}{r} \left(\frac{\partial u_r}{\partial \theta} - u_\theta \right) \hat{\mathbf{e}}_\theta \hat{\mathbf{e}}_r\end{aligned}\quad (1.2.32)$$

$$\nabla \cdot \mathbf{u} = \frac{1}{r} \frac{\partial(ru_r)}{\partial r} + \frac{1}{r} \frac{\partial u_\theta}{\partial \theta} + \frac{\partial u_z}{\partial z} \quad (1.2.33)$$

$$\nabla \times \mathbf{u} = \left(\frac{1}{r} \frac{\partial u_z}{\partial \theta} - \frac{\partial u_\theta}{\partial z} \right) \hat{\mathbf{e}}_r + \left(\frac{\partial u_r}{\partial z} - \frac{\partial u_z}{\partial r} \right) \hat{\mathbf{e}}_\theta + \frac{1}{r} \left(\frac{\partial(ru_\theta)}{\partial r} - \frac{\partial u_r}{\partial \theta} \right) \hat{\mathbf{e}}_z \quad (1.2.34)$$

Spherical Coordinates (r, ϕ, θ)

The rectangular Cartesian coordinates (x, y, z) are related to the spherical coordinates (r, ϕ, θ) by

$$\begin{aligned} x &= r \sin \phi \cos \theta \\ y &= r \sin \phi \sin \theta \\ z &= r \cos \phi \end{aligned} \quad (1.2.35)$$

and the inverse relations are

$$\begin{aligned} r &= \sqrt{x^2 + y^2 + z^2} \\ \phi &= \cos^{-1} \frac{z}{\sqrt{x^2 + y^2 + z^2}} \\ \theta &= \tan^{-1} \left(\frac{y}{x} \right) \end{aligned} \quad (1.2.36)$$

Note that r in the spherical coordinates is not the same as that in the cylindrical coordinate system.

The basis vectors are

$$\mathbf{e}_r = \hat{\mathbf{e}}_r, \quad \mathbf{e}_\phi = \hat{\mathbf{e}}_\phi, \quad \mathbf{e}_\theta = r \sin \theta \hat{\mathbf{e}}_\theta \quad (1.2.37)$$

It is clear that the basis vectors are not unit vectors in general. In terms of the Cartesian basis, we have

$$\begin{aligned} \hat{\mathbf{e}}_r &= \sin \phi \cos \theta \hat{\mathbf{e}}_x + \sin \phi \sin \theta \hat{\mathbf{e}}_y + \cos \phi \hat{\mathbf{e}}_z \\ \hat{\mathbf{e}}_\phi &= \cos \phi \cos \theta \hat{\mathbf{e}}_x + \cos \phi \sin \theta \hat{\mathbf{e}}_y - \sin \phi \hat{\mathbf{e}}_z \\ \hat{\mathbf{e}}_\theta &= -\sin \theta \hat{\mathbf{e}}_x + \cos \theta \hat{\mathbf{e}}_y \end{aligned} \quad (1.2.38)$$

On the other hand, the Cartesian basis in terms of the spherical orthonormal basis is

$$\begin{aligned} \hat{\mathbf{e}}_x &= \sin \phi \cos \theta \hat{\mathbf{e}}_r + \cos \phi \cos \theta \hat{\mathbf{e}}_\phi - \sin \theta \hat{\mathbf{e}}_\theta \\ \hat{\mathbf{e}}_y &= \sin \phi \sin \theta \hat{\mathbf{e}}_r + \cos \phi \sin \theta \hat{\mathbf{e}}_\phi + \cos \theta \hat{\mathbf{e}}_\theta \\ \hat{\mathbf{e}}_z &= \cos \phi \hat{\mathbf{e}}_r - \sin \phi \hat{\mathbf{e}}_\phi \end{aligned} \quad (1.2.39)$$

The position vector is given by

$$\mathbf{r} = r \hat{\mathbf{e}}_r \quad (1.2.40)$$

and the nonzero derivatives of the basis vectors are given by

$$\begin{aligned} \frac{\partial \hat{\mathbf{e}}_r}{\partial \phi} &= \hat{\mathbf{e}}_\phi, & \frac{\partial \hat{\mathbf{e}}_r}{\partial \theta} &= \sin \phi \hat{\mathbf{e}}_\phi, & \frac{\partial \hat{\mathbf{e}}_\phi}{\partial \phi} &= -\hat{\mathbf{e}}_r \\ \frac{\partial \hat{\mathbf{e}}_\phi}{\partial \theta} &= \cos \phi \hat{\mathbf{e}}_\theta, & \frac{\partial \hat{\mathbf{e}}_\theta}{\partial \theta} &= -\sin \phi \hat{\mathbf{e}}_r - \cos \phi \hat{\mathbf{e}}_\phi \end{aligned} \quad (1.2.41)$$

The del (∇) and Laplacian (∇^2) operators are given by

$$\nabla = \hat{\mathbf{e}}_r \frac{\partial}{\partial r} + \frac{\hat{\mathbf{e}}_\phi}{r} \frac{\partial}{\partial \phi} + \frac{1}{r \sin \phi} \hat{\mathbf{e}}_\theta \frac{\partial}{\partial \theta} \quad (1.2.42)$$

$$\nabla^2 = \frac{1}{r^2} \frac{\partial}{\partial r} \left(r^2 \frac{\partial}{\partial r} \right) + \frac{1}{r^2 \sin \phi} \frac{\partial}{\partial \phi} \left(\sin \phi \frac{\partial}{\partial \phi} \right) + \frac{1}{r^2 \sin^2 \phi} \frac{\partial^2}{\partial \theta^2} \quad (1.2.43)$$

The gradient, divergence, and curl of a vector \mathbf{u} in the spherical coordinate system can be obtained as (see Problem 1.15)

$$\begin{aligned} \nabla \mathbf{u} = & \frac{\partial u_r}{\partial r} \hat{\mathbf{e}}_r \hat{\mathbf{e}}_r + \frac{\partial u_\phi}{\partial r} \hat{\mathbf{e}}_r \hat{\mathbf{e}}_\phi + \frac{\partial u_\theta}{\partial r} \hat{\mathbf{e}}_r \hat{\mathbf{e}}_\theta \\ & + \frac{1}{r} \left(\frac{\partial u_r}{\partial \phi} - u_\phi \right) \hat{\mathbf{e}}_\phi \hat{\mathbf{e}}_r + \frac{1}{r} \left(\frac{\partial u_\phi}{\partial \phi} + u_r \right) \hat{\mathbf{e}}_\phi \hat{\mathbf{e}}_\phi + \frac{1}{r} \frac{\partial u_\theta}{\partial \phi} \hat{\mathbf{e}}_\phi \hat{\mathbf{e}}_\theta \\ & + \frac{1}{r \sin \phi} \left[\left(\frac{\partial u_r}{\partial \theta} - u_\theta \sin \phi \right) \hat{\mathbf{e}}_\theta \hat{\mathbf{e}}_r + \left(\frac{\partial u_\phi}{\partial \theta} - u_\theta \cos \phi \right) \hat{\mathbf{e}}_\theta \hat{\mathbf{e}}_\phi \right. \\ & \left. + \left(\frac{\partial u_\theta}{\partial \theta} + u_r \sin \phi + u_\phi \cos \phi \right) \hat{\mathbf{e}}_\theta \hat{\mathbf{e}}_\theta \right] \end{aligned} \quad (1.2.44)$$

$$\nabla \cdot \mathbf{u} = 2 \frac{u_r}{r} + \frac{\partial u_r}{\partial r} + \frac{1}{r \sin \phi} \frac{\partial (u_\phi \sin \phi)}{\partial \phi} + \frac{1}{R \sin \phi} \frac{\partial u_\theta}{\partial \theta} \quad (1.2.45)$$

$$\begin{aligned} \nabla \times \mathbf{u} = & \frac{1}{r \sin \phi} \left[\frac{\partial (u_\theta \sin \phi)}{\partial \phi} - \frac{\partial u_\phi}{\partial \theta} \right] \hat{\mathbf{e}}_r + \left[\frac{1}{r \sin \phi} \frac{\partial u_r}{\partial \theta} - \frac{1}{r} \frac{\partial (r u_\theta)}{\partial r} \right] \hat{\mathbf{e}}_\phi \\ & + \frac{1}{r} \left[\frac{\partial (r u_\phi)}{\partial r} - \frac{\partial u_r}{\partial \phi} \right] \hat{\mathbf{e}}_\theta \end{aligned} \quad (1.2.46)$$

1.2.5 Matrices and Cramer's Rule

A second-order tensor has nine components in any coordinate system. Equation (1.2.4) contains the Cartesian components of a tensor Φ . The form of the equation suggests writing down the scalars φ_{ij} (component in the i th row and j th column) in the rectangular array $[\Phi]$:

$$[\Phi] = \begin{bmatrix} \varphi_{11} & \varphi_{12} & \varphi_{13} \\ \varphi_{21} & \varphi_{22} & \varphi_{23} \\ \varphi_{31} & \varphi_{32} & \varphi_{33} \end{bmatrix}$$

The rectangular array of φ_{ij} 's is called a *matrix* when it satisfies certain properties. It is also common to use a boldface letter to denote a matrix (i.e., $[\Phi] = \Phi$).

Two matrices are equal if and only if they are identical, i.e., all elements of the two arrays are the same. If a matrix has m rows and n columns, we will say that it is m by n ($m \times n$), the number of rows always being listed first. The element in the i th row and j th column of a matrix $[C]$ is generally denoted by c_{ij} , and we

will sometimes write $[C] = [c_{ij}]$ to denote this. A square matrix is one that has the same number of rows as columns. The elements of a square matrix for which the row number and the column number are the same (i.e., $c_{11}, c_{22}, \dots, c_{nn}$) are called *diagonal elements*. The sum of the diagonal elements is called the *trace* of the matrix. The line of elements where the row number and the column number are the same is called the *diagonal*. A square matrix is said to be a *diagonal matrix* if all of the off-diagonal elements are zero (i.e., $c_{ij} = 0$ for $i \neq j$). An *identity matrix*, denoted by $[I]$, is a diagonal matrix whose elements are all 1's. The elements of the identity matrix can be written as $[I] = [\delta_{ij}]$.

We wish to associate with an $n \times n$ matrix $[C]$ a scalar that, in some sense, measures the “size” of $[C]$ and indicates whether $[C]$ is singular or nonsingular. The *determinant* of the matrix $[C] = [c_{ij}]$ is defined to be the scalar $\det[C] = |C|$ computed according to the rule (in this part of the chapter, the summation convention is not adopted)

$$\det[C] = |c_{ij}| = \sum_{i=1}^n (-1)^{i+1} c_{i1} |c_{i1}| \quad (1.2.47)$$

where $|c_{i1}|$ is the determinant of the $(n - 1) \times (n - 1)$ matrix that remains after deleting the i th row and the first column of $[C]$. For 1×1 matrices, the determinant is defined according to $|c_{11}| = c_{11}$. For convenience, we define the determinant of a *zeroth-order* matrix to be unity. In the above definition, special attention is given to the first column of the matrix $[C]$. We call it the expansion of $|C|$ according to the first column of $[C]$. One can expand $|C|$ according to any column or row:

$$|C| = \sum_{i=1}^n (-1)^{i+j} c_{ij} |c_{ij}| \quad (1.2.48)$$

where $|c_{ij}|$ is the determinant of the matrix obtained by deleting the i th row and j th column of matrix $[C]$.

For an $n \times n$ matrix $[C]$, the determinant of the $(n - 1) \times (n - 1)$ submatrix of $[C]$ obtained by deleting row i and column j of $[C]$ is called *minor* of c_{ij} and is denoted by $M_{ij}(C)$. The quantity $\text{cof}_{ij}(C) \equiv (-1)^{i+j} M_{ij}(C)$ is called the *cofactor* of c_{ij} . The determinant of $[C]$ can be cast in terms of the minor and cofactor of c_{ij} for any value of j :

$$\det[C] = \sum_{i=1}^n c_{ij} \text{cof}_{ij}(C) \quad (1.2.49)$$

The *adjunct* (also called *adjoint*) of a matrix $[C]$ is the transpose of the matrix obtained from $[C]$ by replacing each element by its cofactor. The adjunct of $[C]$ is denoted by $\text{Adj}(C)$.

Let $[C]$ be an $n \times n$ square matrix with elements c_{ij} . The cofactor of c_{ij} , denoted here by C_{ij} , is related to the minor M_{ij} of c_{ij} by

$$C_{ij} = (-1)^{i+j} M_{ij} \quad (1.2.50)$$

By definition, the determinant $|C|$ is given by

$$|C| = \sum_{k=1}^n c_{ik} C_{ik} = \sum_{k=1}^n c_{kj} C_{kj} \quad (1.2.51)$$

for any value of i and j ($i, j \leq n$). Then we have

$$\sum_{k=1}^n c_{rk} C_{ik} = |C| \delta_{ri}, \quad \sum_{k=1}^n c_{ks} C_{kj} = |C| \delta_{sj} \quad (1.2.52)$$

Using the above result, one can show that the solution to a set of n linear equations in n unknown quantities

$$\sum_{j=1}^n c_{ij} u_j = f_i, \quad i = 1, 2, \dots, n \quad (1.2.53)$$

in the case when the determinant of the matrix of coefficients is not zero ($|C| \neq 0$) is given by

$$u_j = \frac{1}{|C|} \sum_{i=1}^n C_{ij} b_i, \quad j = 1, 2, \dots, n \quad (1.2.54)$$

The result in Eq. (1.2.54) is known as *Cramer's rule*.

Example 1.2.3

Consider the system of equations

$$\begin{bmatrix} 6 & 3 & -1 \\ 1 & 4 & -3 \\ 2 & -2 & 5 \end{bmatrix} \begin{Bmatrix} u_1 \\ u_2 \\ u_3 \end{Bmatrix} = \begin{Bmatrix} f_1 \\ f_2 \\ f_3 \end{Bmatrix} = \begin{Bmatrix} 7 \\ -5 \\ 8 \end{Bmatrix}$$

Using Cramer's rule, we obtain

$$u_1 = \frac{1}{|C|} \begin{vmatrix} f_1 & 3 & -1 \\ f_2 & 4 & -3 \\ f_3 & -2 & 5 \end{vmatrix}, \quad u_2 = \frac{1}{|C|} \begin{vmatrix} 6 & f_1 & -1 \\ 1 & f_2 & -3 \\ 2 & f_3 & 5 \end{vmatrix}, \quad u_3 = \frac{1}{|C|} \begin{vmatrix} 6 & 3 & f_1 \\ 1 & 4 & f_2 \\ 2 & -2 & f_3 \end{vmatrix}$$

where $|C|$ is the determinant of the coefficient matrix

$$\begin{aligned} |C| &= \sum_{i=1}^3 (-1)^{i+1} c_{i1} |c_{i1}| \\ &= 6 \begin{vmatrix} 4 & -3 \\ -2 & 5 \end{vmatrix} - 3 \begin{vmatrix} 1 & -3 \\ 2 & 5 \end{vmatrix} + (-1) \begin{vmatrix} 1 & 4 \\ 2 & -2 \end{vmatrix} \\ &= 6(20 - 6) - 3(5 + 6) - (-2 - 8) = 61 \end{aligned}$$

Hence, the solution becomes

$$\begin{aligned} u_1 &= \frac{1}{61} (14f_1 - 13f_2 - 5f_3) = \frac{123}{61} \\ u_2 &= \frac{1}{61} (-11f_1 + 32f_2 + 17f_3) = -\frac{101}{61} \\ u_3 &= \frac{1}{61} (-10f_1 + 18f_2 + 21f_3) = \frac{8}{61} \end{aligned}$$

1.2.6 Transformations of Components

In structural analysis, one is required to refer all quantities used in the analytical description of a structure to a common coordinate system. Scalars, by definition, are independent of any coordinate system. While vectors and tensors are independent of a particular coordinate system, their components are not. The same vector, for example, can have different components in different coordinate systems. Any two sets of components of a vector and tensor can be related by writing one set of components in terms of the other. Such relationships are called transformations.

To establish the rules of the transformation of vector components, we consider barred $(\bar{x}_1, \bar{x}_2, \bar{x}_3)$ and unbarred (x_1, x_2, x_3) coordinate systems that are related by the equations

$$\begin{aligned} x_1 &= x_1(\bar{x}_1, \bar{x}_2, \bar{x}_3) \\ x_2 &= x_2(\bar{x}_1, \bar{x}_2, \bar{x}_3) \\ x_3 &= x_3(\bar{x}_1, \bar{x}_2, \bar{x}_3) \end{aligned} \quad (1.2.55)$$

The inverse relations are

$$\begin{aligned} \bar{x}_1 &= \bar{x}_1(x_1, x_2, x_3) \\ \bar{x}_2 &= \bar{x}_2(x_1, x_2, x_3) \\ \bar{x}_3 &= \bar{x}_3(x_1, x_2, x_3) \end{aligned} \quad (1.2.56)$$

The bases in the two systems are denoted $(\hat{\mathbf{e}}_1, \hat{\mathbf{e}}_2, \hat{\mathbf{e}}_3)$ and $(\hat{\hat{\mathbf{e}}}_1, \hat{\hat{\mathbf{e}}}_2, \hat{\hat{\mathbf{e}}}_3)$, as shown in Figure 1.2.3. The relations between the bases of the barred and unbarred coordinate systems can be written as $[\mathbf{A}] = [\mathbf{A} \cdot \hat{\mathbf{e}}_i] \hat{\mathbf{e}}_i$

$$\hat{\hat{\mathbf{e}}}_i = (\hat{\hat{\mathbf{e}}}_i \cdot \hat{\mathbf{e}}_k) \hat{\mathbf{e}}_k = a_{ik} \hat{\mathbf{e}}_k, \quad a_{ij} \equiv \hat{\hat{\mathbf{e}}}_i \cdot \hat{\mathbf{e}}_j = \hat{\mathbf{e}}_j \cdot \hat{\hat{\mathbf{e}}}_i \quad (1.2.57)$$

where the first subscript of a_{ij} comes from the base vector of the barred system. In matrix notation, we can write the relations in Eq. (1.2.57) as

$$\left\{ \begin{array}{c} \hat{\hat{\mathbf{e}}}_1 \\ \hat{\hat{\mathbf{e}}}_2 \\ \hat{\hat{\mathbf{e}}}_3 \end{array} \right\} = \begin{bmatrix} a_{11} & a_{12} & a_{13} \\ a_{21} & a_{22} & a_{23} \\ a_{31} & a_{32} & a_{33} \end{bmatrix} \left\{ \begin{array}{c} \hat{\mathbf{e}}_1 \\ \hat{\mathbf{e}}_2 \\ \hat{\mathbf{e}}_3 \end{array} \right\} \quad (1.2.58)$$

where $[A]$ denotes the 3×3 matrix array whose elements are the direction cosines, a_{ij} . We also have the inverse relation

$$\hat{\mathbf{e}}_j = (\hat{\mathbf{e}}_j \cdot \hat{\hat{\mathbf{e}}}_k) \hat{\hat{\mathbf{e}}}_k = a_{kj} \hat{\hat{\mathbf{e}}}_k \quad (1.2.59)$$

or, in matrix form

$$\left\{ \begin{array}{c} \hat{\mathbf{e}}_1 \\ \hat{\mathbf{e}}_2 \\ \hat{\mathbf{e}}_3 \end{array} \right\} = \begin{bmatrix} a_{11} & a_{21} & a_{31} \\ a_{12} & a_{22} & a_{32} \\ a_{13} & a_{23} & a_{33} \end{bmatrix} \left\{ \begin{array}{c} \hat{\hat{\mathbf{e}}}_1 \\ \hat{\hat{\mathbf{e}}}_2 \\ \hat{\hat{\mathbf{e}}}_3 \end{array} \right\} \quad (1.2.60)$$

From Eqs. (1.2.57) and (1.2.59), we note that

$$a_{ik} a_{jk} = a_{ki} a_{kj} = \delta_{ij} \quad (1.2.61)$$

or

$$[A][A]^T = [A]^T[A] = [I] \quad (1.2.62)$$

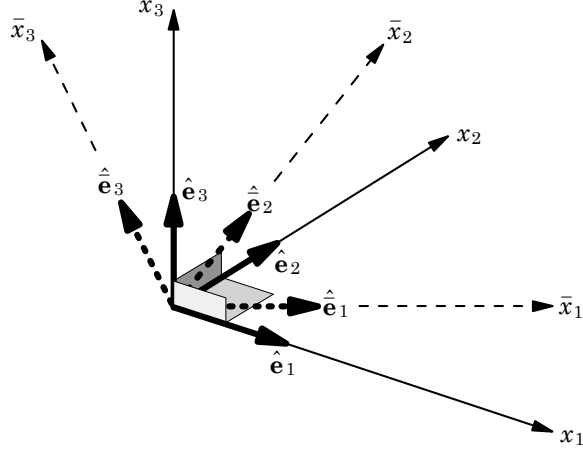


Figure 1.2.3 Unbarred and barred rectangular coordinate systems.

In other words, $[A]^T$ is equal to its inverse. Such transformations are called *orthogonal transformations* and $[A]$ is called an orthogonal matrix.

The transformations (1.2.57) and (1.2.59) between two orthogonal sets of bases also hold for their respective coordinates:

$$\bar{x}_i = a_{ik}x_k, \quad x_j = a_{kj}\bar{x}_k \quad (1.2.63)$$

Analogous to Eq. (1.2.63), the components of a vector \mathbf{u} in the barred and unbarred coordinate systems are related by the expressions

$$\bar{u}_i = a_{ij}u_j \quad (\{\bar{u}\} = [A]\{u\}), \quad u_i = a_{ji}\bar{u}_j \quad (\{u\} = [A]^T\{\bar{u}\}) \quad (1.2.64)$$

A second-order tensor can be expressed in two different coordinate systems using the corresponding bases. In a barred system, we have

$$\Phi = \bar{\varphi}_{mn}\hat{\mathbf{e}}_m\hat{\mathbf{e}}_n \quad (1.2.65)$$

and in an unbarred system, it is expressed as

$$\Phi = \varphi_{ij}\hat{\mathbf{e}}_i\hat{\mathbf{e}}_j \quad (1.2.66)$$

Using Eq. (1.2.59) for $\hat{\mathbf{e}}_i$ and $\hat{\mathbf{e}}_j$ in Eq. (1.2.66), we arrive at the equation

$$\Phi = \varphi_{ij}a_{mi}a_{nj}\hat{\mathbf{e}}_m\hat{\mathbf{e}}_n \quad (1.2.67)$$

Comparing Eq. (1.2.67) with Eq. (1.2.65), we arrive at the relations

$$\bar{\varphi}_{mn} = \varphi_{ij}a_{mi}a_{nj} \quad (1.2.68)$$

or, in matrix form, we have

$$[\bar{\varphi}] = [A][\varphi][A]^T \quad (1.2.69)$$

The inverse relation can be derived using the orthogonality property of $[A]$: $[A]^{-1} = [A]^T$. Premultiply both sides of Eq. (1.2.69) with $[A]^{-1} = [A]^T$ and postmultiply both sides of the resulting equation with $([A]^T)^{-1} = [A]$, and obtain the result

$$[\varphi] = [A]^T[\bar{\varphi}][A] \quad (1.2.70)$$

Equations (1.2.69) and (1.2.70) are useful in transforming second-order tensors (e.g., stresses and strains) from one coordinate system to another coordinate system, as we shall see shortly.

Example 1.2.4

Suppose that $(\bar{x}_1, \bar{x}_2, \bar{x}_3)$ is obtained from (x_1, x_2, x_3) by rotating the x_1x_2 -plane counter-clockwise by an angle θ about the x_3 -axis (see Figure 1.2.4). Then the two sets of coordinates are related by

$$\begin{Bmatrix} \bar{x}_1 \\ \bar{x}_2 \\ \bar{x}_3 \end{Bmatrix} = \begin{bmatrix} \cos \theta & \sin \theta & 0 \\ -\sin \theta & \cos \theta & 0 \\ 0 & 0 & 1 \end{bmatrix} \begin{Bmatrix} x_1 \\ x_2 \\ x_3 \end{Bmatrix} \quad (1.2.71)$$

and the inverse relation is given by

$$\begin{Bmatrix} x_1 \\ x_2 \\ x_3 \end{Bmatrix} = \begin{bmatrix} \cos \theta & -\sin \theta & 0 \\ \sin \theta & \cos \theta & 0 \\ 0 & 0 & 1 \end{bmatrix} \begin{Bmatrix} \bar{x}_1 \\ \bar{x}_2 \\ \bar{x}_3 \end{Bmatrix} \quad (1.2.72)$$

Clearly, we have $[A]^{-1} = [A]^T$. The components $\bar{\varphi}_{ij}$ and φ_{ij} of a second-order tensor Φ in the two coordinate systems, $(\bar{x}_1, \bar{x}_2, \bar{x}_3)$ and (x_1, x_2, x_3) , respectively, are related by Eqs. (1.2.69) and (1.2.70). Equation (1.2.69) in the present case gives

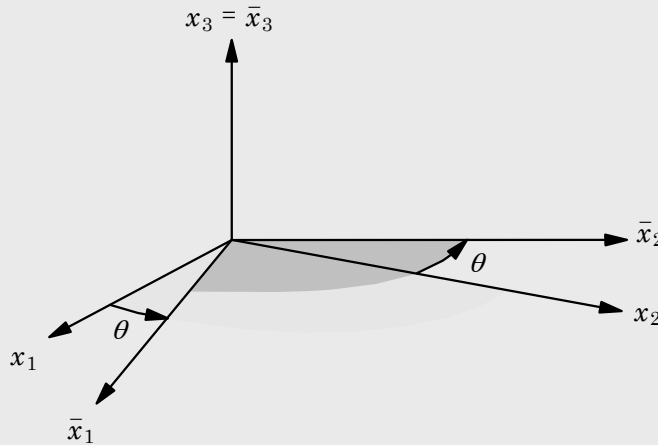


Figure 1.2.4 A special rotational transformation between unbarred and barred rectangular Cartesian coordinate systems.

$$\begin{aligned}
\bar{\varphi}_{11} &= \varphi_{11} \cos^2 \theta + \varphi_{22} \sin^2 \theta + (\varphi_{12} + \varphi_{21}) \cos \theta \sin \theta \\
\bar{\varphi}_{12} &= (\varphi_{22} - \varphi_{11}) \cos \theta \sin \theta + \varphi_{12} \cos^2 \theta - \varphi_{21} \sin^2 \theta \\
\bar{\varphi}_{21} &= (\varphi_{22} - \varphi_{11}) \cos \theta \sin \theta + \varphi_{21} \cos^2 \theta - \varphi_{12} \sin^2 \theta \\
\bar{\varphi}_{22} &= \varphi_{11} \sin^2 \theta + \varphi_{22} \cos^2 \theta - (\varphi_{12} + \varphi_{21}) \cos \theta \sin \theta \\
\bar{\varphi}_{13} &= \varphi_{13} \cos \theta + \varphi_{23} \sin \theta \\
\bar{\varphi}_{23} &= \varphi_{23} \cos \theta - \varphi_{13} \sin \theta \\
\bar{\varphi}_{31} &= \varphi_{31} \cos \theta + \varphi_{32} \sin \theta \\
\bar{\varphi}_{32} &= \varphi_{32} \cos \theta - \varphi_{31} \sin \theta \\
\bar{\varphi}_{33} &= \varphi_{33}
\end{aligned} \tag{1.2.73}$$

The inverse relations are provided by Eq. (1.2.70):

$$\begin{aligned}
\varphi_{11} &= \bar{\varphi}_{11} \cos^2 \theta + \bar{\varphi}_{22} \sin^2 \theta - (\bar{\varphi}_{12} + \bar{\varphi}_{21}) \cos \theta \sin \theta \\
\varphi_{12} &= (\bar{\varphi}_{11} - \bar{\varphi}_{22}) \cos \theta \sin \theta + \bar{\varphi}_{12} \cos^2 \theta - \bar{\varphi}_{21} \sin^2 \theta \\
\varphi_{21} &= (\bar{\varphi}_{11} - \bar{\varphi}_{22}) \cos \theta \sin \theta + \bar{\varphi}_{21} \cos^2 \theta - \bar{\varphi}_{12} \sin^2 \theta \\
\varphi_{22} &= \bar{\varphi}_{11} \sin^2 \theta + \bar{\varphi}_{22} \cos^2 \theta + (\bar{\varphi}_{12} + \bar{\varphi}_{21}) \cos \theta \sin \theta \\
\varphi_{13} &= \bar{\varphi}_{13} \cos \theta - \bar{\varphi}_{23} \sin \theta \\
\varphi_{23} &= \bar{\varphi}_{23} \cos \theta + \bar{\varphi}_{13} \sin \theta \\
\varphi_{31} &= \bar{\varphi}_{31} \cos \theta - \bar{\varphi}_{32} \sin \theta \\
\varphi_{32} &= \bar{\varphi}_{32} \cos \theta + \bar{\varphi}_{31} \sin \theta \\
\varphi_{33} &= \bar{\varphi}_{33}
\end{aligned} \tag{1.2.74}$$

The transformation law (1.2.68) is often taken to be the *definition* of a second-order tensor. In other words, Φ is a second-order tensor if and only if its components transform according to Eq. (1.2.68). In general, an n th-order tensor transforms according to the formula

$$\bar{\varphi}_{mnpq\dots} = \varphi_{ijkl\dots} a_{mi} a_{nj} a_{pk} a_{q\ell} \dots \tag{1.2.75}$$

The *trace* of a second-order tensor is defined to be the double-dot product of the tensor with the unit tensor \mathbf{I}

$$\text{tr } \Phi = \Phi : \mathbf{I} = \varphi_{ii} \tag{1.2.76}$$

The trace of a tensor is *invariant*, called the first principal invariant, and it is denoted by I_1 ; i.e., it is invariant under coordinate transformations ($\phi_{ii} = \bar{\phi}_{ii}$). The first, second, and third *principal invariants* of a second-order tensor are defined, in terms of the rectangular Cartesian components, as

$$I_1 = \varphi_{ii}, \quad I_2 = \frac{1}{2} (\varphi_{ii}\varphi_{jj} - \varphi_{ij}\varphi_{ji}), \quad I_3 = |\varphi| \tag{1.2.77}$$

1.3 Equations of an Elastic Body

1.3.1 Introduction

The objective of this section is to review the basic equations of an elastic body. The equations governing the motion and deformation of a solid body can be classified into four basic categories:

- (1) Kinematics (strain-displacement equations)
- (2) Kinetics (conservation of momenta)
- (3) Thermodynamics (first and second laws of thermodynamics)
- (4) Constitutive equations (stress-strain relations).

Kinematics is a study of the geometric changes or deformation in a body without the consideration of forces causing the deformation or the nature of the body. *Kinetics* is the study of the static or dynamic equilibrium of forces acting on a body. The thermodynamic principles are concerned with the conservation of energy and relations among heat, mechanical work, and thermodynamic properties of the body. The constitutive equations describe the constitutive behavior of the body and relate the dependent variables introduced in the kinetic description to those in the kinematic and thermodynamic descriptions. These equations are supplemented by appropriate boundary and initial conditions of the problem.

In the following sections, an overview of the kinematic, kinetic, and constitutive equations of an elastic body is presented. The thermodynamic principles are not reviewed, as we will account for thermal effects only through constitutive relations.

1.3.2 Kinematics

The term *deformation* of a body refers to relative displacements and changes in the geometry experienced by the body. In a rectangular Cartesian frame of reference (X_1, X_2, X_3) , every particle X in the body corresponds to a position $\mathbf{X} = (X_1, X_2, X_3)$. When the body is deformed, the particle X moves to a new position $\mathbf{x} = (x_1, x_2, x_3)$. If the displacement of every particle in the body is known, we can construct the deformed configuration κ from the reference (or undeformed) configuration κ_0 (Figure 1.3.1). In the Lagrangian description, the displacements are expressed in terms of the *material coordinates* \mathbf{X}

$$\mathbf{u}(\mathbf{X}, t) = \mathbf{x}(\mathbf{X}, t) - \mathbf{X} \quad (1.3.1)$$

The deformation of a body can be measured in terms of the strain tensor \mathbf{E} , which is defined such that it gives the change in the square of the length of the material vector $d\mathbf{X}$

$$\begin{aligned} 2d\mathbf{X} \cdot \mathbf{E} \cdot d\mathbf{X} &= d\mathbf{x} \cdot d\mathbf{x} - d\mathbf{X} \cdot d\mathbf{X} \\ &= d\mathbf{X} \cdot (\mathbf{I} + \nabla \mathbf{u}) \cdot [d\mathbf{X} \cdot (\mathbf{I} + \nabla \mathbf{u})] - d\mathbf{X} \cdot d\mathbf{X} \\ &= d\mathbf{X} \cdot [(\mathbf{I} + \nabla \mathbf{u}) \cdot (\mathbf{I} + \nabla \mathbf{u})^T - \mathbf{I}] \cdot d\mathbf{X} \end{aligned} \quad (1.3.2)$$

where ∇ denotes the gradient operator with respect to the material coordinates \mathbf{X} and \mathbf{E} is known as the *Green-Lagrange strain tensor* and it is defined by

$$\mathbf{E} = \frac{1}{2} [\nabla \mathbf{u} + (\nabla \mathbf{u})^T + \nabla \mathbf{u} \cdot (\nabla \mathbf{u})^T] \quad (1.3.3)$$

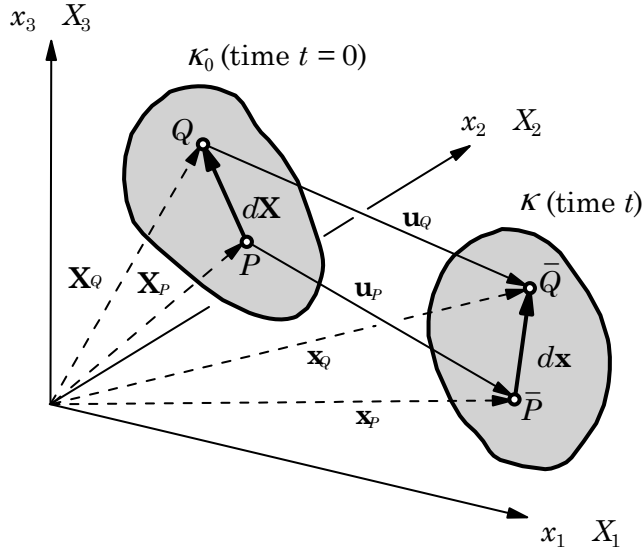


Figure 1.3.1 Undeformed and deformed configurations of a body.

Note that the Green–Lagrange strain tensor is symmetric, $\mathbf{E} = \mathbf{E}^T$. The strain components defined in Eq. (1.3.3) are called finite strain components because no assumption concerning the smallness (compared to unity) of the strains is made.

The rectangular Cartesian component form of \mathbf{E} is

$$E_{jk} = \frac{1}{2} \left(\frac{\partial u_j}{\partial X_k} + \frac{\partial u_k}{\partial X_j} + \frac{\partial u_m}{\partial X_j} \frac{\partial u_m}{\partial X_k} \right) \quad (1.3.4)$$

where summation on repeated subscripts is implied. In explicit form, we have

$$\begin{aligned} E_{11} &= \frac{\partial u_1}{\partial X_1} + \frac{1}{2} \left[\left(\frac{\partial u_1}{\partial X_1} \right)^2 + \left(\frac{\partial u_2}{\partial X_1} \right)^2 + \left(\frac{\partial u_3}{\partial X_1} \right)^2 \right] \\ E_{22} &= \frac{\partial u_2}{\partial X_2} + \frac{1}{2} \left[\left(\frac{\partial u_1}{\partial X_2} \right)^2 + \left(\frac{\partial u_2}{\partial X_2} \right)^2 + \left(\frac{\partial u_3}{\partial X_2} \right)^2 \right] \\ E_{33} &= \frac{\partial u_3}{\partial X_3} + \frac{1}{2} \left[\left(\frac{\partial u_1}{\partial X_3} \right)^2 + \left(\frac{\partial u_2}{\partial X_3} \right)^2 + \left(\frac{\partial u_3}{\partial X_3} \right)^2 \right] \\ E_{12} &= \frac{1}{2} \left(\frac{\partial u_1}{\partial X_2} + \frac{\partial u_2}{\partial X_1} + \frac{\partial u_1}{\partial X_1} \frac{\partial u_1}{\partial X_2} + \frac{\partial u_2}{\partial X_1} \frac{\partial u_2}{\partial X_2} + \frac{\partial u_3}{\partial X_1} \frac{\partial u_3}{\partial X_2} \right) \\ E_{13} &= \frac{1}{2} \left(\frac{\partial u_1}{\partial X_3} + \frac{\partial u_3}{\partial X_1} + \frac{\partial u_1}{\partial X_1} \frac{\partial u_1}{\partial X_3} + \frac{\partial u_2}{\partial X_1} \frac{\partial u_2}{\partial X_3} + \frac{\partial u_3}{\partial X_1} \frac{\partial u_3}{\partial X_3} \right) \\ E_{23} &= \frac{1}{2} \left(\frac{\partial u_2}{\partial X_3} + \frac{\partial u_3}{\partial X_2} + \frac{\partial u_1}{\partial X_2} \frac{\partial u_1}{\partial X_3} + \frac{\partial u_2}{\partial X_2} \frac{\partial u_2}{\partial X_3} + \frac{\partial u_3}{\partial X_2} \frac{\partial u_3}{\partial X_3} \right) \end{aligned} \quad (1.3.5)$$

The strain components in other coordinate systems can be derived from Eq. (1.3.3) by expressing the tensor \mathbf{E} and del operator ∇ in that coordinate system. See Eqs. (1.2.30) and (1.2.42) for the definition of ∇ in cylindrical and spherical coordinates systems, respectively. For example, the Green–Lagrange strain tensor components in the cylindrical coordinate system are given by

$$\begin{aligned} E_{rr} &= \frac{\partial u_r}{\partial r} + \frac{1}{2} \left[\left(\frac{\partial u_r}{\partial r} \right)^2 + \left(\frac{\partial u_\theta}{\partial r} \right)^2 + \left(\frac{\partial u_z}{\partial r} \right)^2 \right] \\ E_{\theta\theta} &= \frac{u_r}{r} + \frac{1}{r} \frac{\partial u_\theta}{\partial \theta} + \frac{1}{2} \left[\left(\frac{1}{r} \frac{\partial u_r}{\partial \theta} \right)^2 + \left(\frac{1}{r} \frac{\partial u_\theta}{\partial \theta} \right)^2 + \left(\frac{1}{r} \frac{\partial u_z}{\partial \theta} \right)^2 \right] \\ &\quad + \frac{1}{r^2} \left(2u_r \frac{\partial u_\theta}{\partial \theta} - 2u_\theta \frac{\partial u_r}{\partial \theta} + u_\theta^2 + u_r^2 \right) \\ E_{zz} &= \frac{\partial u_z}{\partial z} + \frac{1}{2} \left[\left(\frac{\partial u_r}{\partial z} \right)^2 + \left(\frac{\partial u_\theta}{\partial z} \right)^2 + \left(\frac{\partial u_z}{\partial z} \right)^2 \right] \\ E_{r\theta} &= \frac{1}{2} \left(\frac{1}{r} \frac{\partial u_r}{\partial \theta} + \frac{\partial u_\theta}{\partial r} - \frac{u_\theta}{r} \right) + \frac{1}{2r} \left(\frac{\partial u_r}{\partial r} \frac{\partial u_r}{\partial \theta} + \frac{\partial u_\theta}{\partial \theta} \frac{\partial u_\theta}{\partial r} \right. \\ &\quad \left. + \frac{\partial u_z}{\partial r} \frac{\partial u_z}{\partial \theta} + u_r \frac{\partial u_\theta}{\partial r} - u_\theta \frac{\partial u_r}{\partial r} \right) \\ E_{z\theta} &= \frac{1}{2} \left(\frac{\partial u_\theta}{\partial z} + \frac{1}{r} \frac{\partial u_z}{\partial \theta} \right) + \frac{1}{2r} \left(\frac{\partial u_r}{\partial \theta} \frac{\partial u_r}{\partial z} + \frac{\partial u_\theta}{\partial \theta} \frac{\partial u_\theta}{\partial z} + \frac{\partial u_z}{\partial \theta} \frac{\partial u_z}{\partial z} \right. \\ &\quad \left. - u_\theta \frac{\partial u_r}{\partial z} + u_r \frac{\partial u_\theta}{\partial z} \right) \\ E_{rz} &= \frac{1}{2} \left(\frac{\partial u_r}{\partial z} + \frac{\partial u_z}{\partial r} \right) + \frac{1}{2} \left(\frac{\partial u_r}{\partial r} \frac{\partial u_r}{\partial z} + \frac{\partial u_\theta}{\partial r} \frac{\partial u_\theta}{\partial z} + \frac{\partial u_z}{\partial r} \frac{\partial u_z}{\partial z} \right) \end{aligned} \tag{1.3.6}$$

If the displacement gradients are so small, $|u_{i,j}| \ll 1$, that their squares and products are negligible compared to $|u_{i,j}|$ and the difference between $\frac{\partial u_i}{\partial x_j}$ and $\frac{\partial u_i}{\partial X_j}$ vanishes, then the Green–Lagrange strain tensor reduces to the *infinitesimal strain tensor*:

$$\varepsilon = \frac{1}{2} \left[\nabla \mathbf{u} + (\nabla \mathbf{u})^T \right] \tag{1.3.7}$$

or in Cartesian component form

$$\varepsilon_{ij} = \frac{1}{2} \left(\frac{\partial u_i}{\partial x_j} + \frac{\partial u_j}{\partial x_i} \right) \equiv \frac{1}{2} (u_{i,j} + u_{j,i}) \tag{1.3.8}$$

Suppose that we use the notation $x_1 = x$, $x_2 = y$, and $x_3 = z$, and let $(u_1, u_2, u_3) = (u, v, w)$ denote the displacements along (x, y, z) . Then the infinitesimal strain components in Eq. (1.3.8) become

$$\varepsilon_{xx} = \frac{\partial u}{\partial x}, \quad \varepsilon_{yy} = \frac{\partial v}{\partial y}, \quad \varepsilon_{zz} = \frac{\partial w}{\partial z} \tag{1.3.9}$$

$$2\varepsilon_{xy} = \frac{\partial u}{\partial y} + \frac{\partial v}{\partial x}, \quad 2\varepsilon_{xz} = \frac{\partial u}{\partial z} + \frac{\partial w}{\partial x}, \quad 2\varepsilon_{yz} = \frac{\partial v}{\partial z} + \frac{\partial w}{\partial y} \tag{1.3.10}$$

Example 1.3.1

The displacement field of a beam under the Euler–Bernoulli kinematic hypothesis (i.e., a transverse normal line before deformation remains straight, inextensible, and normal after deformation) can be expressed as (with $X = x$, $Y = y$, and $Z = z$)

$$u(x, y, z) = u_0(x) - z \frac{dw_0}{dx}, \quad v = 0, \quad w(x, y, z) = w_0(x) \quad (1.3.11)$$

Then the only nonzero, nonlinear strains are given by

$$\begin{aligned} \varepsilon_{xx} &= \frac{du}{dx} + \frac{1}{2} \left[\left(\frac{du}{dx} \right)^2 + \left(\frac{dw}{dx} \right)^2 \right] \\ &= \frac{du_0}{dx} + \frac{1}{2} \left[\left(\frac{du_0}{dx} \right)^2 + \left(\frac{dw_0}{dx} \right)^2 \right] - z \left(\frac{d^2w_0}{dx^2} + \frac{du_0}{dx} \frac{d^2w_0}{dx^2} \right) + \frac{z^2}{2} \left(\frac{d^2w_0}{dx^2} \right)^2 \\ \varepsilon_{zz} &= \frac{dw}{dz} + \frac{1}{2} \left[\left(\frac{du}{dz} \right)^2 + \left(\frac{dw}{dz} \right)^2 \right] = \frac{1}{2} \left(\frac{dw_0}{dx} \right)^2 \\ 2\varepsilon_{xz} &= \frac{du}{dz} + \frac{dw}{dx} + \frac{du}{dx} \frac{du}{dz} + \frac{dw}{dx} \frac{dw}{dz} = -\frac{du_0}{dx} \frac{dw_0}{dx} + z \frac{d^2w_0}{dx^2} \frac{dw_0}{dx} \end{aligned} \quad (1.3.12)$$

If we assume that the following terms are negligible compared to du_0/dx ,

$$\left(\frac{du_0}{dx} \right)^2, \quad h \frac{du_0}{dx} \frac{d^2w_0}{dx^2}, \quad h^2 \left(\frac{d^2w_0}{dx^2} \right)^2, \quad \frac{du_0}{dx} \frac{dw_0}{dx}, \quad h \frac{dw_0}{dx} \frac{d^2w_0}{dx^2} \quad (1.3.13)$$

where h denotes the height of the beam, then the nonlinear strains in Eq. (1.3.12) can be simplified to

$$\varepsilon_{xx} = \frac{du_0}{dx} + \frac{1}{2} \left(\frac{dw_0}{dx} \right)^2 - z \frac{d^2w_0}{dx^2}, \quad \varepsilon_{zz} = \frac{1}{2} \left(\frac{dw_0}{dx} \right)^2, \quad 2\varepsilon_{xz} = 0 \quad (1.3.14)$$

1.3.3 Compatibility Equations

By definition, the components of the strain tensor can be computed from a differentiable displacement field using Eq. (1.3.3). However, if the *six* components of strain tensor are given and if we are required to find the *three* displacement components, the strains given should be such that a unique solution to the six differential equations relating the strains and displacements exists. For example, consider the relations

$$\frac{\partial u}{\partial x} = x^2 + 2y, \quad \frac{\partial u}{\partial y} = 3x + y^2$$

The two equations cannot be solved for u because they are inconsistent. The inconsistency can be verified by computing the second derivative $\partial^2 u / \partial x \partial y$ from the two relations. The first equation gives 2 and the second equation gives 3, which are unequal.

The existence of a unique solution to the six partial differential equations defined by the strain-displacement relations is guaranteed if the infinitesimal strain components satisfy certain integrability conditions, known in elasticity as the *compatibility conditions*. In Cartesian component form, these are

$$\varepsilon_{ikm}\varepsilon_{j\ell n}\varepsilon_{ij,k\ell} = 0 \quad (1.3.15)$$

or in vector form

$$\nabla \times (\nabla \times \varepsilon)^T = \mathbf{0} \quad (\text{zero dyad}) \quad (1.3.16)$$

Note that m and n are the free subscripts. In the three-dimensional case, Eq. (1.3.15) gives 81 relations among the strain components. However, due to the symmetry of $\varepsilon_{ij,k\ell}$ with respect to i and j and k and ℓ , there are only six independent relations. The sufficiency of the statements (1.3.15) and (1.3.16) can be verified.

Equation (1.3.15) can be written as

$$\frac{\partial^2 \varepsilon_{ij}}{\partial x_m \partial x_n} + \frac{\partial^2 \varepsilon_{mn}}{\partial x_i \partial x_j} - \frac{\partial^2 \varepsilon_{im}}{\partial x_j \partial x_n} - \frac{\partial^2 \varepsilon_{jn}}{\partial x_i \partial x_m} = 0 \quad (1.3.17)$$

for any $i, j, m, n = 1, 2, 3$. For the two-dimensional case, Eq. (1.3.17) reduces to the following single compatibility equation

$$\frac{\partial^2 \varepsilon_{11}}{\partial x_2^2} + \frac{\partial^2 \varepsilon_{22}}{\partial x_1^2} - 2 \frac{\partial^2 \varepsilon_{12}}{\partial x_1 \partial x_2} = 0 \quad (1.3.18)$$

It should be noted that the strain compatibility equations are satisfied automatically when the strains are computed from a displacement field. Thus, one needs to verify the compatibility conditions only when the strains are computed from stresses that are in equilibrium.

Example 1.3.2

(a) Consider the following two-dimensional strain field:

$$\varepsilon_{11} = c_1 x_1 (x_1^2 + x_2^2), \quad \varepsilon_{22} = \frac{1}{3} c_2 x_1^3, \quad \varepsilon_{12} = c_3 x_1^2 x_2$$

where c_1, c_2 , and c_3 are constants. We wish to check if the strain field is compatible. Using Eq. (1.3.18) we obtain

$$\frac{\partial^2 \varepsilon_{11}}{\partial x_2^2} + \frac{\partial^2 \varepsilon_{22}}{\partial x_1^2} - 2 \frac{\partial^2 \varepsilon_{12}}{\partial x_1 \partial x_2} = 2c_1 x_1 + 2c_2 x_1 - 4c_3 x_1$$

Thus, the strain field is, in general, not compatible unless $c_1 = c_2 = c_3$.

(b) Given the strain tensor $\mathbf{E} = E_{rr}\hat{\mathbf{e}}_r\hat{\mathbf{e}}_r + E_{\theta\theta}\hat{\mathbf{e}}_\theta\hat{\mathbf{e}}_\theta$ in an axisymmetric body (i.e., E_{rr} and $E_{\theta\theta}$ are functions of r and z only), we wish to determine the compatibility conditions on E_{rr} and $E_{\theta\theta}$.

Using the vector form of compatibility conditions, Eq. (1.3.16), we obtain (see Problem 1.11)

$$\mathbf{F} \equiv \nabla \times \mathbf{E} = \left(\frac{\partial E_{\theta\theta}}{\partial r} + \frac{E_{\theta\theta} - E_{rr}}{r} \right) \hat{\mathbf{e}}_z \hat{\mathbf{e}}_\theta + \frac{\partial E_{rr}}{\partial z} \hat{\mathbf{e}}_\theta \hat{\mathbf{e}}_r - \frac{\partial E_{\theta\theta}}{\partial z} \hat{\mathbf{e}}_r \hat{\mathbf{e}}_\theta$$

and

$$\begin{aligned} \nabla \times (\mathbf{F})^T &= \frac{\partial}{\partial r} \left(\frac{\partial E_{\theta\theta}}{\partial r} + \frac{E_{\theta\theta} - E_{rr}}{r} \right) (\hat{\mathbf{e}}_r \times \hat{\mathbf{e}}_\theta) \hat{\mathbf{e}}_z \\ &\quad - \frac{\partial^2 E_{\theta\theta}}{\partial r \partial z} (\hat{\mathbf{e}}_r \times \hat{\mathbf{e}}_\theta) \hat{\mathbf{e}}_r + \frac{1}{r} \left(\frac{\partial E_{\theta\theta}}{\partial r} + \frac{E_{\theta\theta} - E_{rr}}{r} \right) \left(\hat{\mathbf{e}}_\theta \times \frac{\partial \hat{\mathbf{e}}_\theta}{\partial \theta} \right) \hat{\mathbf{e}}_z \\ &\quad + \frac{1}{r} \frac{\partial E_{rr}}{\partial z} \left(\hat{\mathbf{e}}_\theta \times \frac{\partial \hat{\mathbf{e}}_r}{\partial \theta} \right) \hat{\mathbf{e}}_\theta + \frac{1}{r} \frac{\partial E_{rr}}{\partial z} (\hat{\mathbf{e}}_\theta \times \hat{\mathbf{e}}_r) \frac{\partial \hat{\mathbf{e}}_\theta}{\partial \theta} \\ &\quad - \frac{1}{r} \frac{\partial E_{\theta\theta}}{\partial z} \left(\hat{\mathbf{e}}_\theta \times \frac{\partial \hat{\mathbf{e}}_\theta}{\partial \theta} \right) \hat{\mathbf{e}}_r + \frac{\partial}{\partial z} \left(\frac{\partial E_{\theta\theta}}{\partial r} + \frac{E_{\theta\theta} - E_{rr}}{r} \right) (\hat{\mathbf{e}}_z \times \hat{\mathbf{e}}_\theta) \hat{\mathbf{e}}_z \\ &\quad + \frac{\partial^2 E_{rr}}{\partial z^2} (\hat{\mathbf{e}}_z \times \hat{\mathbf{e}}_r) \hat{\mathbf{e}}_\theta - \frac{\partial^2 E_{\theta\theta}}{\partial z^2} (\hat{\mathbf{e}}_z \times \hat{\mathbf{e}}_r) \hat{\mathbf{e}}_r = \mathbf{0} \end{aligned}$$

Noting that

$$\begin{aligned} \frac{\partial \hat{\mathbf{e}}_r}{\partial \theta} &= \hat{\mathbf{e}}_\theta, \quad \frac{\partial \hat{\mathbf{e}}_\theta}{\partial \theta} = -\hat{\mathbf{e}}_r \\ \hat{\mathbf{e}}_\theta \times \hat{\mathbf{e}}_r &= \hat{\mathbf{e}}_z, \quad \hat{\mathbf{e}}_\theta \times \hat{\mathbf{e}}_z = \hat{\mathbf{e}}_r, \quad \hat{\mathbf{e}}_z \times \hat{\mathbf{e}}_r = \hat{\mathbf{e}}_\theta \end{aligned} \tag{1.3.19}$$

and that a tensor is zero only when all its components are zero, we obtain

$$\begin{aligned} \hat{\mathbf{e}}_z \hat{\mathbf{e}}_z : \quad &\frac{\partial}{\partial r} \left(\frac{\partial E_{\theta\theta}}{\partial r} + \frac{E_{\theta\theta} - E_{rr}}{r} \right) + \frac{1}{r} \left(\frac{\partial E_{\theta\theta}}{\partial r} + \frac{E_{\theta\theta} - E_{rr}}{r} \right) = 0 \\ \hat{\mathbf{e}}_z \hat{\mathbf{e}}_r : \quad &-\frac{\partial^2 E_{\theta\theta}}{\partial r \partial z} + \frac{1}{r} \frac{\partial}{\partial z} (E_{rr} - E_{\theta\theta}) = 0 \\ \hat{\mathbf{e}}_r \hat{\mathbf{e}}_z : \quad &-\frac{\partial}{\partial z} \left(\frac{\partial E_{\theta\theta}}{\partial r} + \frac{E_{\theta\theta} - E_{rr}}{r} \right) = 0 \\ \hat{\mathbf{e}}_\theta \hat{\mathbf{e}}_\theta : \quad &\frac{\partial^2 E_{rr}}{\partial z^2} = 0, \quad \hat{\mathbf{e}}_\theta \hat{\mathbf{e}}_r : \quad -\frac{\partial^2 E_{\theta\theta}}{\partial z^2} = 0 \end{aligned}$$

1.3.4 Stress Measures

Stress at a point is a measure of force per unit area. The force per unit area acting on an elemental area ds of the deformed body is called the *stress vector* acting on the element. The concept also applies to the surface created by slicing the deformed body with a plane. The stress vector on the area element Δs is the vector $\Delta \mathbf{f}/\Delta s$, which has the same direction as $\Delta \mathbf{f}$, but with a magnitude equal to $|\Delta \mathbf{f}|/\Delta s$. The stress vector at a point P on Δs is defined by

$$\mathbf{T} \equiv \lim_{\Delta s \rightarrow 0} \frac{\Delta \mathbf{f}}{\Delta s} \tag{1.3.20}$$

Equation (1.3.20) implies that the stress vector at a point depends on the direction and magnitude of the force vector and the surface area on which it acts. The surface area in turn depends on the orientation of the plane used to slice the body. For example, if a constant cross-section member is sliced with a plane perpendicular to its axis, the resulting surface area A_0 is the same as the area of cross section of the member. However, if it is sliced at the same point with a plane oriented at an angle $0^\circ < \theta < 90^\circ$ to the vertical axis, the surface area A obtained will be different: $A = A_0 / \cos \theta$. Thus, the stress vector at a point depends on the force vector as well as the orientation of the surface on which it acts. For this reason, the stress vector acting on a plane with normal $\hat{\mathbf{n}}$ is denoted by $\mathbf{T}^{(\hat{\mathbf{n}})}$.

The state of stress at a point inside a body can be expressed in terms of stress vectors on three mutually perpendicular planes, say planes perpendicular to the rectangular coordinate axes. Let $\mathbf{T}^{(i)}$ denote the stress vector at a point P on a plane perpendicular to the x_i -axis [Figure 1.3.2(a)]. Each vector $\mathbf{T}^{(i)}$, ($i = 1, 2, 3$) can be resolved into components along the coordinate lines

$$\mathbf{T}^{(i)} = \sigma_{ij} \hat{\mathbf{e}}_j \quad (i = 1, 2, 3) \quad (1.3.21)$$

where the symbol σ_{ij} denotes the component of the stress vector $\mathbf{T}^{(i)}$ at the point P along the x_j -direction, and $\hat{\mathbf{e}}_j$ is the unit base vector along the x_j -direction. There are a total of nine stress components σ_{ij} , ($i, j = 1, 2, 3$) at the point P . It can be shown that the quantities σ_{ij} transform like the components of a second-order tensor called the stress tensor, σ . The stress components σ_{ij} are shown on three perpendicular planes in Figure 1.3.2(b). Note the cube that is used to indicate the stress components is a point cube, so that all nine components are acting at the point P .

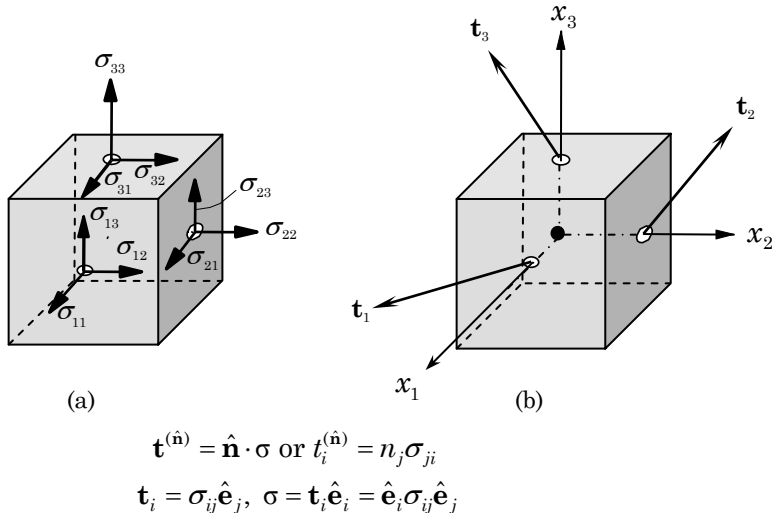


Figure 1.3.2 Stress vectors. (a) Components of stress tensor. (b) Stress vector on coordinate planes.

Using the linear momentum principle or Newton's second law of motion, it can be shown that the stress vector $\mathbf{T}^{(\hat{\mathbf{n}})}$ on a plane with unit normal $\hat{\mathbf{n}}$ is related to the stress tensor σ by the relation

$$\mathbf{T}^{(\hat{\mathbf{n}})} = \hat{\mathbf{n}} \cdot \sigma = \sigma^T \cdot \hat{\mathbf{n}} \quad \text{or} \quad \{T^{(\hat{\mathbf{n}})}\} = [\sigma]^T \{n\} \quad (1.3.22)$$

Equation (1.3.22) is known as the *Cauchy stress formula* and σ is called the *Cauchy stress tensor*.

In the above discussion, it is understood that stress at a point in a deformed body is measured as the force per unit area in the deformed body. The area element Δs in the deformed body corresponds to an area element ΔS in the reference configuration. The stress vector $\mathbf{T}^{(\hat{\mathbf{n}})}$ is *measured* with respect to the area element in the deformed body. Stress vectors can be *referred* to either the reference coordinate system (X_1, X_2, X_3) or the spatial coordinate system (x_1, x_2, x_3) . The stress that is measured and referred to the deformed configuration \mathcal{C} is called the *Cauchy stress* or *true stress*, σ . The components σ_{ij} can be interpreted as the j th component of the force per unit area in the current configuration \mathcal{C} acting on a surface segment whose outward normal at \mathbf{x} is in the i th direction.

A suitable strain measure to use with the Cauchy stress tensor σ would be the infinitesimal strain tensor ε of Eq. (1.3.7). Since we defined strain tensor \mathbf{E} as a function of the material point \mathbf{X} in a reference state, the stress must also be expressed as a function of the material point. The stress measure that is used in nonlinear analysis of solid bodies is the second Piola–Kirchhoff stress tensor, which is measured in the deformed body but referred to the material coordinates, X_i . The strain measure to use with the second Piola–Kirchhoff stress is the Green–Lagrange strain tensor. For small deformation problems, the difference between the two measures of stress disappears. In the present study, we consider only small strain problems and, therefore, will not distinguish between various measures of stress, although it should be understood that σ denotes the second Piola–Kirchhoff stress tensor in the rest of the study. The principle of conservation of moment of momentum, in the absence of any distributed moments, leads to the symmetry of the stress tensor, $\sigma = \sigma^T$ ($\sigma_{ij} = \sigma_{ji}$). Thus, there are only six independent components of the Cauchy and second Piola–Kirchhoff stress tensors.

1.3.5 Equations of Motion

Consider a given mass of a material body \mathcal{B} at any instant occupying a volume Ω bounded by a surface Γ . Suppose that the body is acted upon by external forces \mathbf{T} (per unit surface area) and \mathbf{f} (per unit mass). The principle of conservation of linear momentum states that the rate of change of the total linear momentum of a given continuous medium equals the vector sum of all the external forces acting on the body \mathcal{B} , which initially occupied a configuration \mathcal{C}^0 , provided Newton's Third Law of action and reaction governs the internal forces. The principle leads to the following result:

$$\nabla \cdot \sigma + \rho \mathbf{f} = \rho \frac{\partial^2 \mathbf{u}}{\partial t^2} \quad (1.3.23)$$

where ∇ is the gradient operator with respect to the coordinates $\mathbf{X} \approx \mathbf{x}$ and ρ is the material density in the undeformed body. In writing Eq. (1.3.23), all variables are

assumed to be functions of \mathbf{X} and time t . For the static case, Eq. (1.3.23) reduces to the equilibrium equations

$$\nabla \cdot \sigma + \rho \mathbf{f} = \mathbf{0} \quad (\sigma_{ji,j} + \rho f_i = 0) \quad (1.3.24)$$

The equations of motion or equilibrium are supplemented by the boundary conditions on the displacement vector and/or stress vector:

$$\mathbf{u} = \hat{\mathbf{u}}, \quad \sigma \cdot \hat{\mathbf{n}} = \hat{\mathbf{T}} \quad (1.3.25)$$

where $\hat{\mathbf{u}}$ and $\hat{\mathbf{T}}$ are specified displacement and stress vectors, respectively.

In rectangular Cartesian coordinates (x, y, z) , the equations of motion (1.3.23) can be expressed as

$$\begin{aligned} \frac{\partial \sigma_{xx}}{\partial x} + \frac{\partial \sigma_{xy}}{\partial y} + \frac{\partial \sigma_{xz}}{\partial z} + \rho f_x &= \rho \frac{\partial^2 u}{\partial t^2} \\ \frac{\partial \sigma_{xy}}{\partial x} + \frac{\partial \sigma_{yy}}{\partial y} + \frac{\partial \sigma_{yz}}{\partial z} + \rho f_y &= \rho \frac{\partial^2 v}{\partial t^2} \\ \frac{\partial \sigma_{xz}}{\partial x} + \frac{\partial \sigma_{yz}}{\partial y} + \frac{\partial \sigma_{zz}}{\partial z} + \rho f_z &= \rho \frac{\partial^2 w}{\partial t^2} \end{aligned} \quad (1.3.26)$$

For coordinate systems other than the rectangular Cartesian systems, the equations of motion can be derived from the vector form (1.3.23) by expressing σ , \mathbf{f} , \mathbf{u} , and ∇ in the chosen coordinate system. For example, the equations of motion (1.3.23) in the cylindrical coordinate system (r, θ, z) are given by (see Problem 1.18)

$$\begin{aligned} \frac{\partial \sigma_{rr}}{\partial r} + \frac{1}{r} \frac{\partial \sigma_{r\theta}}{\partial \theta} + \frac{\partial \sigma_{rz}}{\partial z} + \frac{1}{r} (\sigma_{rr} - \sigma_{\theta\theta}) + \rho f_r &= \rho \frac{\partial^2 u_r}{\partial t^2} \\ \frac{\partial \sigma_{r\theta}}{\partial r} + \frac{1}{r} \frac{\partial \sigma_{\theta\theta}}{\partial \theta} + \frac{\partial \sigma_{\theta z}}{\partial z} + \frac{2\sigma_{r\theta}}{r} + \rho f_\theta &= \rho \frac{\partial^2 u_\theta}{\partial t^2} \\ \frac{\partial \sigma_{rz}}{\partial r} + \frac{1}{r} \frac{\partial \sigma_{\theta z}}{\partial \theta} + \frac{\partial \sigma_{zz}}{\partial z} + \frac{\sigma_{rz}}{r} + \rho f_z &= \rho \frac{\partial^2 u_z}{\partial t^2} \end{aligned} \quad (1.3.27)$$

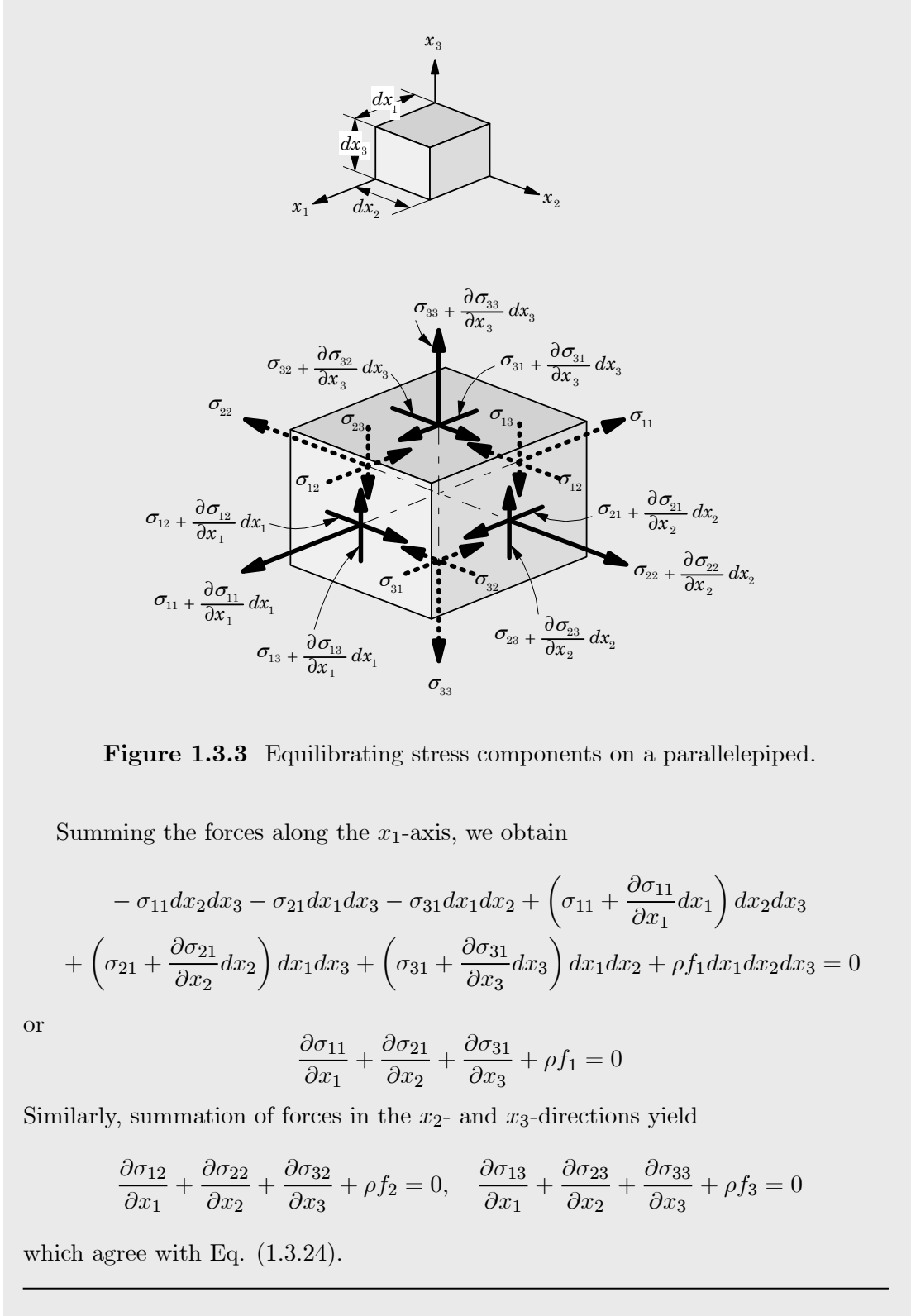
where u_r , u_θ , and u_z are, for example, the components of the displacement vector \mathbf{u} in the cylindrical coordinate system.

Example 1.3.3

Here we illustrate the derivation of the equations of equilibrium of an elastic body using Newton's laws. Consider the static equilibrium of an infinitesimal parallelepiped of dimensions dx_1 , dx_2 , and dx_3 and with its sides parallel to the coordinate planes, as shown in Figure 1.3.3. The stresses acting on typical planes are shown in the figure. Each stress component on a surface perpendicular to the negative x_k -axis is assumed to increase from its value σ_{ij} to

$$\sigma_{ij} + \frac{\partial \sigma_{ij}}{\partial x_k} dx_k$$

on the plane perpendicular to the positive x_k -axis. For example, the forces acting on the plane perpendicular to the negative x_1 -axis are $\sigma_{11}dx_2dx_3$, $\sigma_{12}dx_2dx_3$, and $\sigma_{13}dx_2dx_3$, all in the opposite directions to the positive coordinates.



1.3.6 Constitutive Equations

The kinematic relations and the mechanical and thermodynamic principles are applicable to any continuum irrespective of its physical constitution. Here we consider equations characterizing the individual material and its reaction to applied loads. These equations are called the *constitutive equations*. The formulation of the constitutive equations for a given material is guided by certain rules (i.e., constitutive axioms). We will not discuss them here, but will review the linear constitutive relations for solids undergoing small deformations.

A material body is said to be *homogeneous* if the material properties are the same throughout the body. In a *heterogeneous* body, the material properties are a function of position. An *anisotropic* body is one that has different values of a material property in different directions at a point, i.e., material properties are direction-dependent. An *isotropic* body is one for which every material property in all directions at a point is the same. An isotropic or anisotropic material can be nonhomogeneous or homogeneous.

A material body is said to be *ideally elastic* when, under isothermal conditions, the body recovers its original form completely upon removal of the forces causing deformation, and there is a one-to-one relationship between the state of stress and the state of strain. The constitutive equations described here do not include creep at constant stress and stress relaxation at constant strain. Thus, the material coefficients that specify the constitutive relationship between the stress and strain components are assumed to be constant during the deformation. This does not automatically imply that we neglect temperature effects on deformation. We account for the thermal expansion of the material, which can produce strains or stresses as large as those produced by the applied mechanical forces. A more detailed discussion of the thermoelastic constitutive relations will be presented in the chapter on mechanical behavior of a lamina. Here we review the basic constitutive equations of linear elasticity (i.e., generalized Hooke's law) for small displacements.

The generalized Hooke's law relates the six components of stress to the six components of strain as

$$\begin{Bmatrix} \sigma_1 \\ \sigma_2 \\ \sigma_3 \\ \sigma_4 \\ \sigma_5 \\ \sigma_6 \end{Bmatrix} = \begin{bmatrix} C_{11} & C_{12} & C_{13} & C_{14} & C_{15} & C_{16} \\ C_{21} & C_{22} & C_{23} & C_{24} & C_{25} & C_{26} \\ C_{31} & C_{32} & C_{33} & C_{34} & C_{35} & C_{36} \\ C_{41} & C_{42} & C_{43} & C_{44} & C_{45} & C_{46} \\ C_{51} & C_{52} & C_{53} & C_{54} & C_{55} & C_{56} \\ C_{61} & C_{62} & C_{63} & C_{64} & C_{65} & C_{66} \end{bmatrix} \begin{Bmatrix} \varepsilon_1 \\ \varepsilon_2 \\ \varepsilon_3 \\ \varepsilon_4 \\ \varepsilon_5 \\ \varepsilon_6 \end{Bmatrix} \quad (1.3.28)$$

where C_{ij} are the elastic coefficients and

$$\begin{aligned} \sigma_1 &= \sigma_{11}, \sigma_2 = \sigma_{22}, \sigma_3 = \sigma_{33}, \sigma_4 = \sigma_{23}, \sigma_5 = \sigma_{13}, \sigma_6 = \sigma_{12} \\ \varepsilon_1 &= \varepsilon_{11}, \varepsilon_2 = \varepsilon_{22}, \varepsilon_3 = \varepsilon_{33}, \varepsilon_4 = 2\varepsilon_{23}, \varepsilon_5 = 2\varepsilon_{13}, \varepsilon_6 = 2\varepsilon_{12} \end{aligned} \quad (1.3.29)$$

The single subscript notation (1.3.29) used for stresses and strains is called the *contracted notation* or the Voigt–Kelvin notation. The two-subscript components C_{ij} are obtained from C_{ijkl} by the following change of subscripts:

$$11 \rightarrow 1 \quad 22 \rightarrow 2 \quad 33 \rightarrow 3 \quad 23 \rightarrow 4 \quad 13 \rightarrow 5 \quad 12 \rightarrow 6$$

The resulting C_{ij} are also symmetric ($C_{ij} = C_{ji}$) by virtue of the assumption that there exists a potential function $U_0 = U_0(\varepsilon_{ij})$, called the *strain energy density function*, whose derivative with respect to a strain component determines the corresponding stress component

$$\sigma_{ij} = \frac{\partial U_0}{\partial \varepsilon_{ij}} \quad (1.3.30)$$

Such materials are termed *hyperelastic* materials. For hyperelastic materials, there are only 21 independent coefficients of the matrix $[C]$.

When three mutually orthogonal planes of material symmetry exist, the number of elastic coefficients is reduced to 9, and such materials are called *orthotropic*. The stress-strain relations for an orthotropic material take the form

$$\begin{Bmatrix} \sigma_1 \\ \sigma_2 \\ \sigma_3 \\ \sigma_4 \\ \sigma_5 \\ \sigma_6 \end{Bmatrix} = \begin{bmatrix} C_{11} & C_{12} & C_{13} & 0 & 0 & 0 \\ C_{12} & C_{22} & C_{23} & 0 & 0 & 0 \\ C_{13} & C_{23} & C_{33} & 0 & 0 & 0 \\ 0 & 0 & 0 & C_{44} & 0 & 0 \\ 0 & 0 & 0 & 0 & C_{55} & 0 \\ 0 & 0 & 0 & 0 & 0 & C_{66} \end{bmatrix} \begin{Bmatrix} \varepsilon_1 \\ \varepsilon_2 \\ \varepsilon_3 \\ \varepsilon_4 \\ \varepsilon_5 \\ \varepsilon_6 \end{Bmatrix} \quad (1.3.31)$$

The inverse relations, strain-stress relations, are given by

$$\begin{aligned} \begin{Bmatrix} \varepsilon_1 \\ \varepsilon_2 \\ \varepsilon_3 \\ \varepsilon_4 \\ \varepsilon_5 \\ \varepsilon_6 \end{Bmatrix} &= \begin{bmatrix} S_{11} & S_{12} & S_{13} & 0 & 0 & 0 \\ S_{12} & S_{22} & S_{23} & 0 & 0 & 0 \\ S_{13} & S_{23} & S_{33} & 0 & 0 & 0 \\ 0 & 0 & 0 & S_{44} & 0 & 0 \\ 0 & 0 & 0 & 0 & S_{55} & 0 \\ 0 & 0 & 0 & 0 & 0 & S_{66} \end{bmatrix} \begin{Bmatrix} \sigma_1 \\ \sigma_2 \\ \sigma_3 \\ \sigma_4 \\ \sigma_5 \\ \sigma_6 \end{Bmatrix} \\ &= \begin{bmatrix} \frac{1}{E_1} & -\frac{\nu_{21}}{E_2} & -\frac{\nu_{31}}{E_3} & 0 & 0 & 0 \\ -\frac{\nu_{12}}{E_1} & \frac{1}{E_2} & -\frac{\nu_{22}}{E_3} & 0 & 0 & 0 \\ -\frac{\nu_{13}}{E_1} & -\frac{\nu_{23}}{E_2} & \frac{1}{E_3} & 0 & 0 & 0 \\ 0 & 0 & 0 & \frac{1}{G_{23}} & 0 & 0 \\ 0 & 0 & 0 & 0 & \frac{1}{G_{13}} & 0 \\ 0 & 0 & 0 & 0 & 0 & \frac{1}{G_{12}} \end{bmatrix} \begin{Bmatrix} \sigma_1 \\ \sigma_2 \\ \sigma_3 \\ \sigma_4 \\ \sigma_5 \\ \sigma_6 \end{Bmatrix} \end{aligned} \quad (1.3.32)$$

where S_{ij} denote the compliance coefficients, $[S] = [C]^{-1}$; E_1, E_2, E_3 are Young's moduli in 1, 2, and 3 material directions, respectively; ν_{ij} is Poisson's ratio, defined as the ratio of transverse strain in the j th direction to the axial strain in the i th direction when stressed in the i -direction; and G_{23}, G_{13}, G_{12} = shear moduli in the 2-3, 1-3, and 1-2 planes, respectively. Since the compliance matrix $[S]$ is the inverse of the stiffness matrix $[C]$ and the inverse of a symmetric matrix is symmetric, it follows that the compliance matrix $[S]$ is also a symmetric matrix. This in turn implies, in view of Eq. (1.3.31), that the following reciprocal relations hold:

$$\frac{\nu_{21}}{E_2} = \frac{\nu_{12}}{E_1}; \quad \frac{\nu_{31}}{E_3} = \frac{\nu_{13}}{E_1}; \quad \frac{\nu_{32}}{E_3} = \frac{\nu_{23}}{E_2} \quad \text{or} \quad \frac{\nu_{ij}}{E_i} = \frac{\nu_{ji}}{E_j} \quad (\text{no sum on } i, j) \quad (1.3.33)$$

for $i, j = 1, 2, 3$. Thus, there are only nine independent material coefficients

$$E_1, E_2, E_3, G_{23}, G_{13}, G_{12}, \nu_{12}, \nu_{13}, \nu_{23}$$

for an orthotropic material.

When there exist no preferred directions in the material (i.e., the material has infinite number of planes of material symmetry), the number of independent elastic coefficients reduces to 2. Such materials are called *isotropic*. For isotropic materials, we have $E_1 = E_2 = E_3 = E$, $G_{12} = G_{13} = G_{23} \equiv G$, and $\nu_{12} = \nu_{23} = \nu_{13} \equiv \nu$. Of the three constants (E, ν, G), only two are independent and the third one is related to the other. For example, G can be determined from E and ν by the relation

$$G = \frac{E}{2(1 + \nu)} \quad (1.3.34)$$

A *plane stress state* is defined to be one in which all transverse stresses are negligible. The strain–stress relations of an orthotropic body in plane stress of state can be written as

$$\begin{Bmatrix} \varepsilon_1 \\ \varepsilon_2 \\ \varepsilon_6 \end{Bmatrix} = \begin{bmatrix} S_{11} & S_{12} & 0 \\ S_{12} & S_{22} & 0 \\ 0 & 0 & S_{66} \end{bmatrix} \begin{Bmatrix} \sigma_1 \\ \sigma_2 \\ \sigma_6 \end{Bmatrix} = \begin{bmatrix} \frac{1}{E_1} & -\frac{\nu_{21}}{E_2} & 0 \\ -\frac{\nu_{12}}{E_1} & \frac{1}{E_2} & 0 \\ 0 & 0 & \frac{1}{G_{12}} \end{bmatrix} \begin{Bmatrix} \sigma_1 \\ \sigma_2 \\ \sigma_6 \end{Bmatrix} \quad (1.3.35)$$

The strain–stress relations (1.3.35) are inverted to obtain the stress–strain relations

$$\begin{Bmatrix} \sigma_1 \\ \sigma_2 \\ \sigma_6 \end{Bmatrix} = \begin{bmatrix} Q_{11} & Q_{12} & 0 \\ Q_{12} & Q_{22} & 0 \\ 0 & 0 & Q_{66} \end{bmatrix} \begin{Bmatrix} \varepsilon_1 \\ \varepsilon_2 \\ \varepsilon_6 \end{Bmatrix} \quad (1.3.36)$$

where the Q_{ij} , called the *plane stress-reduced stiffnesses*, are given by

$$\begin{aligned} Q_{11} &= \frac{S_{22}}{S_{11}S_{22} - S_{12}^2} = \frac{E_1}{1 - \nu_{12}\nu_{21}} \\ Q_{12} &= \frac{S_{12}}{S_{11}S_{22} - S_{12}^2} = \frac{\nu_{12}E_2}{1 - \nu_{12}\nu_{21}} \\ Q_{22} &= \frac{S_{11}}{S_{11}S_{22} - S_{12}^2} = \frac{E_2}{1 - \nu_{12}\nu_{21}} \\ Q_{66} &= \frac{1}{S_{66}} = G_{12} \end{aligned} \quad (1.3.37)$$

Note that the reduced stiffnesses involve four independent material constants, E_1 , E_2 , ν_{12} , and G_{12} .

The transverse shear stresses are related to the transverse shear strains in an orthotropic material by the relations

$$\begin{Bmatrix} \sigma_4 \\ \sigma_5 \end{Bmatrix} = \begin{bmatrix} Q_{44} & 0 \\ 0 & Q_{55} \end{bmatrix} \begin{Bmatrix} \varepsilon_4 \\ \varepsilon_5 \end{Bmatrix} \quad (1.3.38)$$

where $Q_{44} = C_{44} = G_{23}$ and $Q_{55} = C_{55} = G_{13}$.

When temperature changes occur in the elastic body, we account for the thermal expansion of the material, even though the variation of elastic constants with temperature is neglected. When the strains, geometric changes, and temperature variations are sufficiently small, all governing equations are linear and superposition of mechanical and thermal effects is possible. The linear thermoelastic constitutive equations have the form

$$\sigma_j = C_{ji}[-\alpha_i(T - T_0) + \varepsilon_i] \quad (1.3.39)$$

$$\varepsilon_j = S_{ji}\sigma_i + \alpha_i(T - T_0) \quad (1.3.40)$$

where α_i ($i = 1, 2, 3$) are the linear coefficients of thermal expansion, T denotes temperature, and T_0 is the reference temperature of the undeformed body. In writing Eqs. (1.3.39) and (1.3.40), it is assumed that α_i and C_{ij} are independent of strain and temperature. For an isotropic material, we have $\alpha_1 = \alpha_2 = \alpha_3 \equiv \alpha$. The plane stress strain-stress relations for a thermoelastic case are given by

$$\begin{Bmatrix} \sigma_1 \\ \sigma_2 \\ \sigma_6 \end{Bmatrix} = \begin{bmatrix} Q_{11} & Q_{12} & 0 \\ Q_{12} & Q_{22} & 0 \\ 0 & 0 & Q_{66} \end{bmatrix} \begin{Bmatrix} \varepsilon_1 - \alpha_1 \Delta T \\ \varepsilon_2 - \alpha_2 \Delta T \\ \varepsilon_6 \end{Bmatrix} \quad (1.3.41)$$

where $\Delta T = T - T_0$ is the temperature change from the reference temperature T_0 and α_i ($i = 1, 2$) are the coefficients of thermal expansion of an orthotropic material in the x_i -coordinate direction. In addition, Eq. (1.3.38) holds for the thermoelastic case.

Tables 1.3.1 and 1.3.2 contain the values of typical engineering constants for some commonly used metals and polymeric materials. The engineering properties of polymeric materials depend on the processing conditions, which can be different for different manufacturers.

Table 1.3.1 Values of the engineering constants* for several materials.

Material	E_1	E_2	G_{12}	G_{13}	G_{23}	ν_{12}
Aluminum	10.6	10.6	3.38	3.38	3.38	0.33
Copper	18.0	18.0	6.39	6.39	6.39	0.33
Steel	30.0	30.0	11.24	11.24	11.24	0.29
Gr-Ep (AS)	20.0	1.3	1.03	1.03	0.90	0.30
Gr-Ep (T)	19.0	1.5	1.00	0.90	0.90	0.22
Gl-Ep (1)	7.8	2.6	1.30	1.30	0.50	0.25
Gl-Ep (2)	5.6	1.2	0.60	0.60	0.50	0.26
Br-Ep	30.0	3.0	1.00	1.00	0.60	0.30

*Moduli are in msi = million psi; 1 psi = 6.895 kN/m².

Gr-Ep (AS) = graphite-epoxy (AS/3501); Gr-Ep (T) = graphite-epoxy (T300/934); Gl-Ep = glass-epoxy; Br-Ep = boron-epoxy.

Table 1.3.2 Values of additional engineering constants* for the materials listed in Table 1.3.1.

Material	E_3	ν_{13}	ν_{23}	α_1	α_2
Aluminum	10.6	0.33	0.33	13.1	13.1
Copper	18.0	0.33	0.33	18.0	18.0
Steel	30.0	0.29	0.29	10.0	10.0
Gr-Ep (AS)	1.3	0.30	0.49	1.0	30.0
Gr-Ep (T)	1.5	0.22	0.49	-0.167	15.6
Gl-Ep (1)	2.6	0.25	0.34	3.5	11.4
Gl-Ep (2)	1.3	0.26	0.34	4.8	12.3
Br-Ep	3.0	0.25	0.25	2.5	8.0

* Units of E_3 are ksi, and the units of α_1 and α_2 are 10^{-6} in./in./°F.

1.4 Transformation of Stresses, Strains, and Stiffnesses

1.4.1 Introduction

In general, the coordinate system used in the solution of a problem does not coincide with the material coordinate system. Therefore, there is a need to establish transformation relations among stresses and strains in one coordinate system to the corresponding quantities in another coordinate system. These relations can be used to transform constitutive equations from the material coordinates to the coordinates used in the solution of a problem. Here we consider a special coordinate transformation. Let the principal material coordinates be denoted by (x_1, x_2, x_3) and the plate coordinates be (x, y, z) . Further, assume that the x_1x_2 -plane is parallel to the xy -plane, but rotated counterclockwise about the $z = x_3$ -axis by an angle θ (Figure 1.4.1). Conversely, (x, y, z) is obtained from (x_1, x_2, x_3) by rotating the x_1x_2 -plane clockwise by an angle θ . Then the coordinates of a material point in the two coordinate systems are related by Eq. (1.2.63). We wish to write the relationships between the components of stress and strain in the two coordinate systems.

1.4.2 Transformation of Stress Components

Let $\sigma_{11}, \sigma_{12}, \dots, \sigma_{33}$ denote the stress components in the material coordinates (x_1, x_2, x_3) and $\sigma_{xx}, \sigma_{xy}, \dots, \sigma_{zz}$ be the stress components referred to the plate coordinates (x, y, z) . In the notation of Section 1.2, (x_1, x_2, x_3) is the system with bars, (x, y, z) is the system without bars, and θ is the angle of rotation about the $x_3 = z$ axis in the counter-clockwise direction. Since stress is a second-order tensor, we have from Eqs. (1.2.73) and (1.2.74) the following relations among the two sets of components:

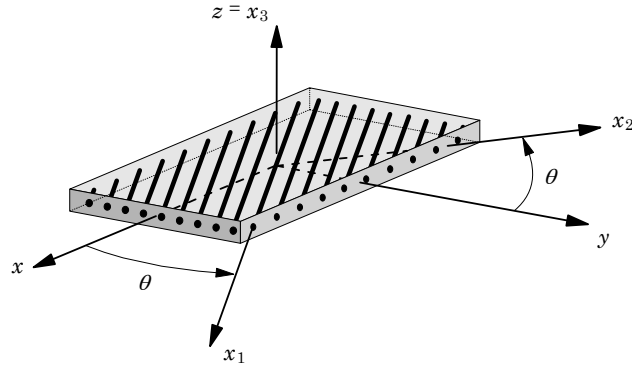


Figure 1.4.1 A plate with global and material coordinate systems.

$$\begin{aligned}
 \sigma_{11} &= \sigma_{xx} \cos^2 \theta + \sigma_{yy} \sin^2 \theta + 2\sigma_{xy} \cos \theta \sin \theta \\
 \sigma_{12} &= (\sigma_{yy} - \sigma_{xx}) \cos \theta \sin \theta + \sigma_{xy}(\cos^2 \theta - \sin^2 \theta) \\
 \sigma_{13} &= \sigma_{xz} \cos \theta + \sigma_{yz} \sin \theta \\
 \sigma_{22} &= \sigma_{xx} \sin^2 \theta + \sigma_{yy} \cos^2 \theta - 2\sigma_{xy} \cos \theta \sin \theta \\
 \sigma_{23} &= \sigma_{yz} \cos \theta - \sigma_{xz} \sin \theta \\
 \sigma_{33} &= \sigma_{zz}
 \end{aligned} \tag{1.4.1}$$

$$\begin{aligned}
 \sigma_{xx} &= \sigma_{11} \cos^2 \theta + \sigma_{22} \sin^2 \theta - 2\sigma_{12} \cos \theta \sin \theta \\
 \sigma_{xy} &= (\sigma_{11} - \sigma_{22}) \cos \theta \sin \theta + \sigma_{12}(\cos^2 \theta - \sin^2 \theta) \\
 \sigma_{xz} &= \sigma_{13} \cos \theta - \sigma_{23} \sin \theta \\
 \sigma_{yy} &= \sigma_{11} \sin^2 \theta + \sigma_{22} \cos^2 \theta + 2\sigma_{12} \cos \theta \sin \theta \\
 \sigma_{yz} &= \sigma_{23} \cos \theta + \sigma_{13} \sin \theta \\
 \sigma_{zz} &= \sigma_{33}
 \end{aligned} \tag{1.4.2}$$

1.4.3 Transformation of Strain Components

Since strains are also tensor quantities, transformation equations derived for stresses are also valid for *tensor* components of strains. We have (see Problem 1.20)

$$\begin{aligned}
 \varepsilon_{11} &= \varepsilon_{xx} \cos^2 \theta + \varepsilon_{yy} \sin^2 \theta + 2\varepsilon_{xy} \cos \theta \sin \theta \\
 \varepsilon_{12} &= (\varepsilon_{yy} - \varepsilon_{xx}) \cos \theta \sin \theta + \varepsilon_{xy}(\cos^2 \theta - \sin^2 \theta) \\
 \varepsilon_{13} &= \varepsilon_{xz} \cos \theta + \varepsilon_{yz} \sin \theta \\
 \varepsilon_{22} &= \varepsilon_{xx} \sin^2 \theta + \varepsilon_{yy} \cos^2 \theta - 2\varepsilon_{xy} \cos \theta \sin \theta \\
 \varepsilon_{23} &= \varepsilon_{yz} \cos \theta - \varepsilon_{xz} \sin \theta \\
 \varepsilon_{33} &= \varepsilon_{zz}
 \end{aligned} \tag{1.4.3}$$

$$\begin{aligned}
\varepsilon_{xx} &= \varepsilon_{11} \cos^2 \theta + \varepsilon_{22} \sin^2 \theta - 2\varepsilon_{12} \cos \theta \sin \theta \\
\varepsilon_{xy} &= (\varepsilon_{11} - \varepsilon_{22}) \cos \theta \sin \theta + \varepsilon_{12}(\cos^2 \theta - \sin^2 \theta) \\
\varepsilon_{xz} &= \varepsilon_{13} \cos \theta - \varepsilon_{23} \sin \theta \\
\varepsilon_{yy} &= \varepsilon_{11} \sin^2 \theta + \varepsilon_{22} \cos^2 \theta + 2\varepsilon_{12} \cos \theta \sin \theta \\
\varepsilon_{yz} &= \varepsilon_{23} \cos \theta + \varepsilon_{13} \sin \theta \\
\varepsilon_{zz} &= \varepsilon_{33}
\end{aligned} \tag{1.4.4}$$

1.4.4 Transformation of Material Stiffnesses

The material stiffnesses C_{ijkl} in their original form are the components of a fourth-order tensor. Hence, the tensor transformation law holds again. The fourth-order elasticity tensor components \bar{C}_{ijkl} in the problem coordinates can be related to the components C_{mnpq} in the material coordinates by the tensor transformation law

$$\bar{C}_{ijkl} = a_{im} a_{jn} a_{kp} a_{lq} C_{mnpq} \tag{1.4.5}$$

where a_{ij} are the direction cosines defined in (1.2.57). However, the above equation involves five matrix multiplications with four-subscript material coefficients. Alternatively, the same result can be obtained by using the stress-strain relations in the principal material coordinates and the stress and strain transformation equations in Eqs. (1.4.1)–(1.4.4).

For the plane stress case, the elastic stiffnesses Q_{ij} in the principal material system are related to \bar{Q}_{ij} in the reference coordinate system by the equations

$$\begin{aligned}
\bar{Q}_{11} &= Q_{11} \cos^4 \theta + 2(Q_{12} + 2Q_{66}) \sin^2 \theta \cos^2 \theta + Q_{22} \sin^4 \theta \\
\bar{Q}_{12} &= (Q_{11} + Q_{22} - 4Q_{66}) \sin^2 \theta \cos^2 \theta + Q_{12}(\sin^4 \theta + \cos^4 \theta) \\
\bar{Q}_{22} &= Q_{11} \sin^4 \theta + 2(Q_{12} + 2Q_{66}) \sin^2 \theta \cos^2 \theta + Q_{22} \cos^4 \theta \\
\bar{Q}_{16} &= (Q_{11} - Q_{12} - 2Q_{66}) \sin \theta \cos^3 \theta + (Q_{12} - Q_{22} + 2Q_{66}) \sin^3 \theta \cos \theta \\
\bar{Q}_{26} &= (Q_{11} - Q_{12} - 2Q_{66}) \sin^3 \theta \cos \theta + (Q_{12} - Q_{22} + 2Q_{66}) \sin \theta \cos^3 \theta \\
\bar{Q}_{66} &= (Q_{11} + Q_{22} - 2Q_{12} - 2Q_{66}) \sin^2 \theta \cos^2 \theta + Q_{66}(\sin^4 \theta + \cos^4 \theta) \\
\bar{Q}_{44} &= Q_{44} \cos^2 \theta + Q_{55} \sin^2 \theta \\
\bar{Q}_{45} &= (Q_{55} - Q_{44}) \cos \theta \sin \theta \\
\bar{Q}_{55} &= Q_{55} \cos^2 \theta + Q_{44} \sin^2 \theta
\end{aligned} \tag{1.4.6}$$

The thermal coefficients of expansion α_{ij} are the components of a second-order tensor and, therefore, they transform like the stress and strain components. For an orthotropic material, the only nonzero components of thermal expansion tensor referred to the principal materials coordinates are α_1 , α_2 , and α_3 . Hence, we can write the transformation relations among α_{ij} and $(\alpha_{xx}, \alpha_{yy}, \alpha_{xy})$ [see Eq. (1.4.4)]

$$\begin{aligned}
\alpha_{xx} &= \alpha_1 \cos^2 \theta + \alpha_2 \sin^2 \theta \\
\alpha_{yy} &= \alpha_1 \sin^2 \theta + \alpha_2 \cos^2 \theta \\
\alpha_{xy} &= 2(\alpha_1 - \alpha_2) \sin \theta \cos \theta \\
\alpha_{xz} &= 0, \quad \alpha_{yz} = 0, \quad \alpha_{zz} = \alpha_3
\end{aligned} \tag{1.4.7}$$

The stress-strain relations in the problem coordinates (x, y, z) for the thermoelastic case can now be expressed as

$$\begin{Bmatrix} \sigma_{xx} \\ \sigma_{yy} \\ \sigma_{yz} \\ \sigma_{xz} \\ \sigma_{xy} \end{Bmatrix} = \begin{bmatrix} \bar{Q}_{11} & \bar{Q}_{12} & 0 & 0 & \bar{Q}_{16} \\ \bar{Q}_{12} & \bar{Q}_{22} & 0 & 0 & \bar{Q}_{26} \\ 0 & 0 & \bar{Q}_{44} & \bar{Q}_{45} & 0 \\ 0 & 0 & \bar{Q}_{45} & \bar{Q}_{55} & 0 \\ \bar{Q}_{16} & \bar{Q}_{26} & 0 & 0 & \bar{Q}_{66} \end{bmatrix} \begin{Bmatrix} \varepsilon_{xx} - \alpha_{xx}\Delta T \\ \varepsilon_{yy} - \alpha_{yy}\Delta T \\ \varepsilon_{yz} \\ \varepsilon_{xz} \\ \varepsilon_{xy} - \alpha_{xy}\Delta T \end{Bmatrix} \quad (1.4.8)$$

1.5 Summary

In this chapter, a brief review of vectors, tensors, matrices, and equations of elasticity is presented. In particular, elements from vector and tensor calculus, summation convention, coordinate transformations, concepts of stress and strain, strain compatibility conditions, equations of motion and constitutive equations of linearized elasticity are presented. The concepts and equations presented in this chapter are useful in the forthcoming chapters of this book.

Problems

1.1 Prove the following properties of δ_{ij} and ε_{ijk} (assume $i, j = 1, 2, 3$ when they are dummy indices):

- (a) $F_{ij}\delta_{jk} = F_{ik}$
- (b) $\delta_{ij}\delta_{ij} = \delta_{ii} = 3$
- (c) $\varepsilon_{ijk}\varepsilon_{ijk} = 6$
- (d) $\varepsilon_{ijk}F_{ij} = 0$ whenever $F_{ij} = F_{ji}$ (symmetric)

1.2 Let \mathbf{r} denote a position vector. Show that:

- (a) $\text{grad } (r^n) = nr^{n-2}\mathbf{r}$
- (b) $\nabla^2(r^n) = n(n+1)r^{n-2}$
- (c) $\text{div } (\mathbf{r}) = 3$
- (d) $\text{curl } (\mathbf{r}f(r)) = \mathbf{0}$, where $f(r)$ is an arbitrary continuous function of r with continuous first derivatives

1.3 If $[B]$ is a symmetric $n \times n$ matrix and $[C]$ is any $n \times n$ matrix, show that $[C]^T[B][C]$ is symmetric.

1.4 Establish the ε - δ identity of Eq. (1.2.15).

1.5 Prove that the determinant of a 3×3 matrix $[C]$ can be expressed in the form

$$|C| = \varepsilon_{ijk} c_{1i} c_{2j} c_{3k} \quad (a)$$

and, thus, prove

$$|C| = \frac{1}{6} \varepsilon_{ijk} \varepsilon_{rst} c_{ir} c_{js} c_{kt} \quad (b)$$

where c_{ij} is the element occupying the i th row and the j th column of $[C]$.

1.6 Using Cramer's rule determine the solution to the following equations:

(a) (Ans: $x_1 = \frac{9}{4}$, $x_2 = \frac{7}{2}$, $x_3 = \frac{11}{4}$)

$$\begin{aligned} 2x_1 - x_2 &= 1 \\ -x_1 + 2x_2 - x_3 &= 2 \\ -x_2 + 2x_3 &= 2 \end{aligned}$$

(b) [Ans: $x_1 = \frac{3}{2}\alpha$, $x_2 = \frac{1}{2h}\alpha$, $x_3 = -\frac{2}{h}\alpha$, $\alpha = (f_0 h^4 / 24b)$]

$$\frac{2b}{h^3} \begin{bmatrix} 12 & 0 & 3h \\ 0 & 4h^2 & h^2 \\ 3h & h^2 & 2h^2 \end{bmatrix} \begin{Bmatrix} x_1 \\ x_2 \\ x_3 \end{Bmatrix} = \frac{f_0 h}{12} \begin{Bmatrix} 12 \\ 0 \\ h \end{Bmatrix}$$

where b , f_0 , and h are constants

1.7 Let $[C]$ be a 3×3 matrix, $[I]$ be a 3×3 identity matrix, and λ be a scalar. Show that

$$\det[C - \lambda I] = \lambda^3 - I_1 \lambda^2 + I_2 \lambda - I_3$$

where

$$I_1 = c_{ii}, \quad I_2 = \frac{1}{2}(c_{ii}c_{jj} - c_{ij}c_{ji}), \quad I_3 = |C|$$

1.8 If we identify a second-order tensor \mathbf{A} associated with the direction cosines $a_{ij} = \hat{\mathbf{e}}_i \cdot \hat{\mathbf{e}}_j$ [see Eq. (1.2.57)]

$$\mathbf{A} = a_{ij} \hat{\mathbf{e}}_i \hat{\mathbf{e}}_j$$

show that (a) $\mathbf{A} \cdot \mathbf{A} = \mathbf{A}$, (b) $\mathbf{A} \cdot \mathbf{A}^T = \mathbf{I}$, and (c) $\mathbf{A} : \mathbf{A} = 3$.

1.9 Use the definition $\nabla^2 = \nabla \cdot \nabla$ to show that the Laplacian operator in the cylindrical coordinate system is given by

$$\nabla^2 = \frac{1}{r} \left[\frac{\partial}{\partial r} \left(r \frac{\partial}{\partial r} \right) + \frac{1}{r} \frac{\partial^2}{\partial \theta^2} + r \frac{\partial^2}{\partial z^2} \right]$$

1.10 Show that the gradient of a vector \mathbf{u} in the cylindrical coordinate system is given by

$$\begin{aligned} \nabla \mathbf{u} &= \frac{\partial u_r}{\partial r} \hat{\mathbf{e}}_r \hat{\mathbf{e}}_r + \frac{1}{r} \left(u_r + \frac{\partial u_\theta}{\partial \theta} \right) \hat{\mathbf{e}}_\theta \hat{\mathbf{e}}_\theta + \frac{\partial u_z}{\partial z} \hat{\mathbf{e}}_z \hat{\mathbf{e}}_z \\ &\quad + \frac{1}{r} \frac{\partial u_z}{\partial \theta} \hat{\mathbf{e}}_\theta \hat{\mathbf{e}}_z + \frac{\partial u_\theta}{\partial z} \hat{\mathbf{e}}_z \hat{\mathbf{e}}_\theta + \frac{\partial u_r}{\partial z} \hat{\mathbf{e}}_z \hat{\mathbf{e}}_r + \frac{\partial u_z}{\partial r} \hat{\mathbf{e}}_r \hat{\mathbf{e}}_z \\ &\quad + \frac{\partial u_\theta}{\partial r} \hat{\mathbf{e}}_r \hat{\mathbf{e}}_\theta + \frac{1}{r} \left(\frac{\partial u_r}{\partial \theta} - u_\theta \right) \hat{\mathbf{e}}_\theta \hat{\mathbf{e}}_r \end{aligned}$$

- 1.11** Show that the curl of a vector \mathbf{u} in the cylindrical coordinate system is given by

$$\begin{aligned}\nabla \times \mathbf{u} &= \hat{\mathbf{e}}_r \left(\frac{1}{r} \frac{\partial u_z}{\partial \theta} - \frac{\partial u_\theta}{\partial z} \right) + \hat{\mathbf{e}}_\theta \left(\frac{\partial u_r}{\partial z} - \frac{\partial u_z}{\partial r} \right) \\ &\quad + \hat{\mathbf{e}}_z \left(\frac{\partial u_\theta}{\partial r} + \frac{u_\theta}{r} - \frac{1}{r} \frac{\partial u_r}{\partial \theta} \right)\end{aligned}$$

- 1.12** For an arbitrary second-order tensor \mathbf{S} , show that $\nabla \cdot \mathbf{S}$ in the cylindrical coordinate system is given by

$$\begin{aligned}\nabla \cdot \mathbf{S} &= \left[\frac{\partial S_{rr}}{\partial r} + \frac{1}{r} \frac{\partial S_{\theta r}}{\partial \theta} + \frac{\partial S_{zr}}{\partial z} + \frac{1}{r} (S_{rr} - S_{\theta \theta}) \right] \hat{\mathbf{e}}_r \\ &\quad + \left[\frac{\partial S_{r\theta}}{\partial r} + \frac{1}{r} \frac{\partial S_{\theta\theta}}{\partial \theta} + \frac{\partial S_{z\theta}}{\partial z} + \frac{1}{r} (S_{r\theta} + S_{\theta r}) \right] \hat{\mathbf{e}}_\theta \\ &\quad + \left[\frac{\partial S_{rz}}{\partial r} + \frac{1}{r} \frac{\partial S_{\theta z}}{\partial \theta} + \frac{\partial S_{zz}}{\partial z} + \frac{1}{r} S_{rz} \right] \hat{\mathbf{e}}_z\end{aligned}$$

- 1.13** For an arbitrary second-order tensor \mathbf{S} , show that $\nabla \times \mathbf{S}$ in the cylindrical coordinate system is given by

$$\begin{aligned}\nabla \times \mathbf{S} &= \hat{\mathbf{e}}_r \hat{\mathbf{e}}_r \left(\frac{1}{r} \frac{\partial S_{zr}}{\partial \theta} - \frac{\partial S_{\theta r}}{\partial z} - \frac{1}{r} S_{z\theta} \right) + \hat{\mathbf{e}}_\theta \hat{\mathbf{e}}_\theta \left(\frac{\partial S_{r\theta}}{\partial z} - \frac{\partial S_{z\theta}}{\partial r} \right) + \\ &\quad \hat{\mathbf{e}}_z \hat{\mathbf{e}}_z \left(\frac{1}{r} S_{\theta z} - \frac{1}{r} \frac{\partial S_{rz}}{\partial \theta} + \frac{\partial S_{\theta z}}{\partial r} \right) + \hat{\mathbf{e}}_r \hat{\mathbf{e}}_\theta \left(\frac{1}{r} \frac{\partial S_{z\theta}}{\partial \theta} - \frac{\partial S_{\theta\theta}}{\partial z} + \frac{1}{r} S_{zr} \right) + \\ &\quad \hat{\mathbf{e}}_\theta \hat{\mathbf{e}}_r \left(\frac{\partial S_{rr}}{\partial z} - \frac{\partial S_{zr}}{\partial r} \right) + \hat{\mathbf{e}}_r \hat{\mathbf{e}}_z \left(\frac{1}{r} \frac{\partial S_{zz}}{\partial \theta} - \frac{\partial S_{\theta z}}{\partial z} \right) + \\ &\quad \hat{\mathbf{e}}_z \hat{\mathbf{e}}_r \left(\frac{\partial S_{\theta r}}{\partial r} - \frac{1}{r} \frac{\partial S_{rr}}{\partial \theta} + \frac{1}{r} S_{r\theta} + \frac{1}{r} S_{\theta r} \right) + \hat{\mathbf{e}}_\theta \hat{\mathbf{e}}_z \left(\frac{\partial S_{rz}}{\partial z} - \frac{\partial S_{zz}}{\partial r} \right) + \\ &\quad \hat{\mathbf{e}}_z \hat{\mathbf{e}}_\theta \left(\frac{\partial S_{\theta\theta}}{\partial r} + \frac{1}{r} S_{\theta\theta} - \frac{1}{r} S_{rr} - \frac{1}{r} \frac{\partial S_{r\theta}}{\partial \theta} \right)\end{aligned}$$

- 1.14** Show that the curl of a tensor $\mathbf{E} = E_{rr}(r, z)\hat{\mathbf{e}}_r \hat{\mathbf{e}}_r + E_{\theta\theta}(r, z)\hat{\mathbf{e}}_\theta \hat{\mathbf{e}}_\theta$ in the cylindrical coordinate system is given by

$$\nabla \times \mathbf{E} = \left(\frac{\partial E_{\theta\theta}}{\partial r} + \frac{E_{\theta\theta} - E_{rr}}{r} \right) \hat{\mathbf{e}}_z \hat{\mathbf{e}}_\theta + \frac{\partial E_{rr}}{\partial z} \hat{\mathbf{e}}_\theta \hat{\mathbf{e}}_r - \frac{\partial E_{\theta\theta}}{\partial z} \hat{\mathbf{e}}_r \hat{\mathbf{e}}_\theta$$

- 1.15** Show that $\nabla \mathbf{u}$ in the spherical coordinate system is given by

$$\begin{aligned}\nabla \mathbf{u} &= \frac{\partial u_r}{\partial r} \hat{\mathbf{e}}_r \hat{\mathbf{e}}_r + \frac{\partial u_\phi}{\partial r} \hat{\mathbf{e}}_r \hat{\mathbf{e}}_\phi + \frac{\partial u_\theta}{\partial r} \hat{\mathbf{e}}_r \hat{\mathbf{e}}_\theta \\ &\quad + \frac{1}{r} \left(\frac{\partial u_r}{\partial \phi} - u_\phi \right) \hat{\mathbf{e}}_\phi \hat{\mathbf{e}}_r + \frac{1}{r} \left(\frac{\partial u_\phi}{\partial \phi} + u_r \right) \hat{\mathbf{e}}_\phi \hat{\mathbf{e}}_\phi + \frac{1}{r} \frac{\partial u_\theta}{\partial \phi} \hat{\mathbf{e}}_\phi \hat{\mathbf{e}}_\theta \\ &\quad + \frac{1}{r \sin \phi} \left[\left(\frac{\partial u_r}{\partial \theta} - u_\theta \sin \phi \right) \hat{\mathbf{e}}_\theta \hat{\mathbf{e}}_r + \left(\frac{\partial u_\phi}{\partial \theta} - u_\theta \cos \phi \right) \hat{\mathbf{e}}_\theta \hat{\mathbf{e}}_\phi \right. \\ &\quad \left. + \left(\frac{\partial u_\theta}{\partial \theta} + u_r \sin \phi + u_\phi \cos \phi \right) \hat{\mathbf{e}}_\theta \hat{\mathbf{e}}_\theta \right]\end{aligned}$$

1.16 Find the linear strains associated with the 2-D displacement field

$$\begin{aligned} u_1 &= -c_0 x_1 x_2 + c_1 x_2 + c_2 x_3 + c_4 \\ u_2 &= c_0 \left[\nu (x_2^2 - x_1^2) + x_1^2 \right] + c_4 x_3 + c_5 x_1 + c_6 \\ u_3 &= 0 \end{aligned}$$

where c_i and ν are constants.

1.17 Consider the displacement vector in polar axisymmetric system

$$\mathbf{u} = u_r \hat{\mathbf{e}}_r + u_z \hat{\mathbf{e}}_z$$

The strain tensor in the cylindrical coordinate system can be written in the dyadic form as

$$\begin{aligned} \varepsilon &= \varepsilon_{rr} \hat{\mathbf{e}}_{rr} + \varepsilon_{\theta\theta} \hat{\mathbf{e}}_\theta \hat{\mathbf{e}}_\theta + \varepsilon_{zz} \hat{\mathbf{e}}_z \hat{\mathbf{e}}_z + \varepsilon_{r\theta} (\hat{\mathbf{e}}_r \hat{\mathbf{e}}_\theta + \hat{\mathbf{e}}_\theta \hat{\mathbf{e}}_r) \\ &\quad + \varepsilon_{rz} (\hat{\mathbf{e}}_r \hat{\mathbf{e}}_z + \hat{\mathbf{e}}_z \hat{\mathbf{e}}_r) + \varepsilon_{\theta z} (\hat{\mathbf{e}}_\theta \hat{\mathbf{e}}_z + \hat{\mathbf{e}}_z \hat{\mathbf{e}}_\theta) \end{aligned}$$

Show that the only nonzero linear strains are given by

$$\varepsilon_{rr} = \frac{\partial u_r}{\partial r}, \quad \varepsilon_{\theta\theta} = \frac{u_r}{r}, \quad \varepsilon_{rz} = \frac{1}{2} \left(\frac{\partial u_r}{\partial z} + \frac{\partial u_z}{\partial r} \right), \quad \varepsilon_{zz} = \frac{\partial u_z}{\partial z}$$

1.18 Using the definitions of ∇ and \mathbf{u} in the cylindrical coordinate system, show that the linear strains (1.3.7) in the cylindrical coordinate system are given by

$$\begin{aligned} \varepsilon_{rr} &= \frac{\partial u_r}{\partial r}, \quad \varepsilon_{r\theta} = \frac{1}{2} \left(\frac{1}{r} \frac{\partial u_r}{\partial \theta} + \frac{\partial u_\theta}{\partial r} - \frac{u_\theta}{r} \right), \quad \varepsilon_{rz} = \frac{1}{2} \left(\frac{\partial u_r}{\partial z} + \frac{\partial u_z}{\partial r} \right) \\ \varepsilon_{\theta\theta} &= \frac{u_r}{r} + \frac{1}{r} \frac{\partial u_\theta}{\partial \theta}, \quad \varepsilon_{z\theta} = \frac{1}{2} \left(\frac{\partial u_\theta}{\partial z} + \frac{1}{r} \frac{\partial u_z}{\partial \theta} \right), \quad \varepsilon_{zz} = \frac{\partial u_z}{\partial z} \end{aligned}$$

1.19 Show that the equations of motion in the cylindrical coordinate system are given by

$$\begin{aligned} \frac{\partial \sigma_{rr}}{\partial r} + \frac{1}{r} \frac{\partial \sigma_{r\theta}}{\partial \theta} + \frac{\partial \sigma_{rz}}{\partial z} + \frac{1}{r} (\sigma_{rr} - \sigma_{\theta\theta}) + \rho f_r &= \rho \frac{\partial^2 u_r}{\partial t^2} \\ \frac{\partial \sigma_{r\theta}}{\partial r} + \frac{1}{r} \frac{\partial \sigma_{\theta\theta}}{\partial \theta} + \frac{\partial \sigma_{\theta z}}{\partial z} + \frac{2\sigma_{r\theta}}{r} + \rho f_\theta &= \rho \frac{\partial^2 u_\theta}{\partial t^2} \\ \frac{\partial \sigma_{rz}}{\partial r} + \frac{1}{r} \frac{\partial \sigma_{\theta z}}{\partial \theta} + \frac{\partial \sigma_{zz}}{\partial z} + \frac{\sigma_{rz}}{r} + \rho f_z &= \rho \frac{\partial^2 u_z}{\partial t^2} \end{aligned}$$

1.20 Derive the transformation relations (1.4.3) between the rectangular Cartesian components of strain ($\varepsilon_{xx}, \varepsilon_{yy}, \varepsilon_{xy}$) and the components of strain ($\varepsilon_{rr}, \varepsilon_{\theta\theta}, \varepsilon_{r\theta}$) in the cylindrical coordinate system.

Energy Principles and Variational Methods

2.1 Virtual Work

2.1.1 Introduction

The governing equations of a continuum can be derived using the laws of physics. For solid mechanics problems, the laws of physics may be expressed in several alternative forms. For example, the principle of conservation of linear momentum, which leads to the equations of motion, can be derived using either Newton's Second Law of motion or by using the *principle of virtual displacements*. The former is termed a vector approach and the latter an energy approach.

The use of Newton's laws to determine the governing equations of a structural problem requires the isolation of a typical volume element of the structure with all its applied and reactive forces (i.e., the free-body diagram of the element). Then the vector sum of all static and dynamic forces and moments acting on the element is set to zero to obtain the equations of motion. For simple mechanical systems for which the free-body diagram can be set up, the vector approach provides an easy and direct way of deriving the governing equations. However, for complicated systems the procedure becomes more cumbersome and intractable. In addition, the type of boundary conditions to be used in conjunction with the derived equations is not always clear.

In the energy approach, the total work done or energy stored in the body due to actual forces in moving through *virtual* displacements that are consistent with the geometric constraints of a body is set to zero to obtain the equations of motion. The energy approach yields not only the equations of motion, but also the force boundary conditions as well as the form of the variables involved in the specification of geometric boundary conditions. In addition, the energy expressions are useful in obtaining approximate solutions by direct variational methods, such as the Ritz and finite element methods.

In most of the present study, the principles of virtual work will be used to derive the equations of motion of plates and shells. We begin with the concepts of virtual displacements and virtual forces and work and energy. Mostly bar and beam problems are used to illustrate the concepts.

2.1.2 Virtual Displacements and Forces

From purely geometrical considerations, a given mechanical system can take many possible configurations consistent with the geometric constraints on the system. Of all the possible configurations, only one corresponds to the equilibrium configuration of the system under the prescribed forces. It is this configuration that satisfies Newton's second law (i.e., equations of equilibrium or motion of the system). The set of configurations that satisfy the geometric constraints, but not necessarily Newton's second law, is called the *set of admissible configurations*. These configurations are restricted to a neighborhood of the true configuration so that they are obtained from infinitesimal variations of the true configuration. During such variations, the geometric constraints of the system are not violated and all the forces are fixed at their actual values. When a mechanical system experiences such variations in its configuration, it is said to undergo *virtual displacements* from its actual configuration. These displacements need not have any relationship to the actual displacements that might occur due to a change in the applied loads. The displacements are called virtual because they are *imagined* to take place, while the actual loads are acting at their fixed values. *The virtual displacements at the boundary points at which the geometric boundary conditions are specified are zero.*

A boundary condition in which the specified value is zero is called a *homogeneous* boundary condition. For example, $u = \hat{u}$ is a nonhomogeneous boundary condition. If $\hat{u} = 0$, then the boundary condition $u = 0$ is said to be the *homogeneous form* of the boundary condition $u = \hat{u}$.

As an example, consider a bar fixed at one end and subjected to an axial load at the other end (Figure 2.1.1(a)). The bar can be imagined to have virtual displacements that are zero at the fixed end where the displacement is specified. One such virtual displacement is $v(x) = cx$, where c is a constant and the origin of the coordinate x is taken at the fixed end. In fact, polynomials of the form $v(x) = c_1x + c_2x^2 + \dots + c_nx^n$, with at least one of the constants c_k not zero, constitute a set of admissible variations. Note that any polynomial with a nonzero constant coefficient is *not* an admissible variation because it is not zero at $x = 0$. Similarly, for a cantilever beam (i.e., a beam fixed at $x = 0$ and free at $x = L$; Figure 2.1.2(b)) of length L and subjected to transverse distributed load, the set of virtual displacements consists of polynomials of the form $v(x) = c_1x^2 + c_2x^3 + \dots + c_nx^{n+1}$ with at least one of the c 's nonzero. Note that v and dv/dx are zero at $x = 0$, consistent with the geometric boundary conditions $w = 0$ and $dw/dx = 0$ at the fixed end of the beam.

Analogous to the concept of virtual displacements, one can think of virtual forces on a system. The virtual forces must be a set of forces that are in equilibrium among themselves. These forces can be internal and/or external and need not have any relation to the actual forces of the system. For example, a bar fixed at one end and subjected to an axial load at the other end can be imagined to have a variety of virtual forces. One such set is a force P applied at the right and left ends in opposite directions. Similarly, for a cantilever beam of length L , a virtual force system consists of applying a virtual point load δF acting upward at the free end and downward at the fixed end, and a virtual moment of $\delta M = \delta F \cdot L$ acting clockwise at the fixed end. The set of virtual forces $(\delta F, -\delta F, \delta M = \delta FL)$ is in self-equilibrium as can be verified by summing virtual forces and moments. The virtual

forces and moments are shown by dotted lines in Figures 2.1.1(b) and 2.1.2(b).

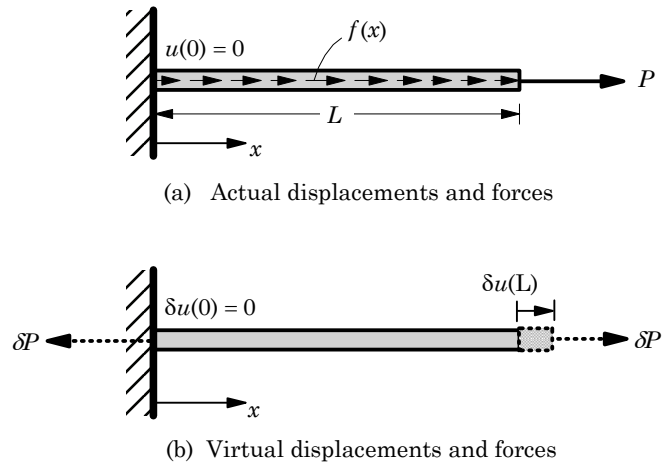


Figure 2.1.1 Virtual displacements and forces for a bar fixed at the left end (— actual forces; - - - virtual forces).

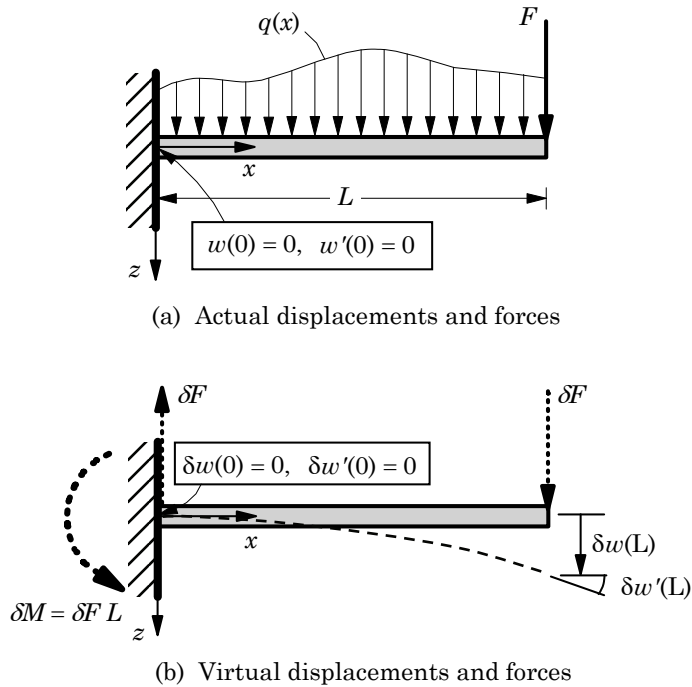


Figure 2.1.2 Virtual displacements and loads for a cantilever beam (— actual forces; - - - virtual forces).

2.1.3 External and Internal Virtual Work

Let us first recall the concept of work. When a force acts on a material point and moves through a displacement, the work done by the force is defined by the *projection* of the force in the direction of the displacement times the magnitude of the displacement. The work done by the actual forces through virtual displacements or the work done by virtual forces through actual displacements is called *virtual work*. The virtual work done by actual forces \mathbf{F} in a body Ω in moving through the virtual displacements $\delta\mathbf{u}$ is given by

$$\delta W = \int_{\Omega} \mathbf{F} \cdot \delta\mathbf{u} \, dv \quad (2.1.1)$$

where dv denotes the volume element in the material body Ω . The symbol δ is used to denote a virtual change in the variable it operates on.

Similar to the virtual displacements, we can imagine to apply forces on a body without disturbing its equilibrium. Then the virtual work done by virtual forces $\delta\mathbf{F}$ in moving through the actual displacement \mathbf{u} is

$$\delta W^* = \int_{\Omega} \delta\mathbf{F} \cdot \mathbf{u} \, dv \quad (2.1.2)$$

When a deformable body in equilibrium is subjected to virtual displacements, work is performed by externally applied forces and internally developed forces. The virtual work done by externally applied forces in moving through the respective virtual displacements is called *external virtual work* and it is denoted by δW_E . The virtual work done by internal forces in moving through the virtual displacements is called *internal virtual work*, and it is denoted by δW_I . In general, the internal energy W_I is composed of various types, mechanical, thermal, chemical, etc. In the present study, we consider only internal energy due to straining by mechanical forces, which is known as the strain energy, U . For rigid bodies, which experience no geometric changes and, therefore, no internal forces are developed, the internal work done $W_I = U$ is zero. In the following, we develop expressions for external and internal virtual works of a deformable body.

External Virtual Work

The external virtual work done due to virtual displacements $\delta\mathbf{u}$ in a solid body Ω subjected to body forces \mathbf{f} per unit volume and surface tractions \mathbf{T} per unit area of the boundary Γ_σ is given by

$$\delta W_E = - \left(\int_{\Omega} \mathbf{f} \cdot \delta\mathbf{u} \, dv + \int_{\Gamma_\sigma} \mathbf{T} \cdot \delta\mathbf{u} \, ds \right) \quad (2.1.3)$$

where ds denotes a surface element and Γ_σ denotes the portion of the boundary on which stresses are specified. The negative sign in Eq. (2.1.3) indicates that the work is performed on the body. It is understood that the displacements are specified on the remaining portion $\Gamma_u = \Gamma - \Gamma_\sigma$ of the boundary Γ . Therefore, the virtual displacements are zero on Γ_u , irrespective of whether \mathbf{u} is specified to be zero or not.

The external virtual work done due to virtual body forces $\delta\mathbf{f}$ and surface tractions $\delta\mathbf{t}$ on Γ_u of a solid body Ω in moving through the respective actual displacements \mathbf{u} is called the complementary virtual work δW_E^* , and it is given by

$$\delta W_E^* = - \left(\int_{\Omega} \delta\mathbf{f} \cdot \mathbf{u} \, dv + \int_{\Gamma_u} \delta\mathbf{t} \cdot \mathbf{u} \, ds \right) \quad (2.1.4)$$

Internal Virtual Work

The forces applied on a deformable body cause it to deform and the body experiences internal stresses. The relative movement of the material particles in the body can be measured in terms of strains. The forces associated with the internal stress field displace the material particles through displacements corresponding to the strain field in the body and, hence, work is done. Note that the work done on the body by external forces is responsible for the internal work.

The internal virtual work due to the virtual displacement $\delta\mathbf{u}$ can be computed as follows. Suppose that an infinitesimal material element of volume $dv = dx_1 dx_2 dx_3$ of the body experiences small virtual strains $\delta\varepsilon_{ij}$ due to the virtual displacements δu_i , where

$$\delta\varepsilon_{ij} = \frac{1}{2} \left(\frac{\partial \delta u_i}{\partial x_j} + \frac{\partial \delta u_j}{\partial x_i} \right) \quad (2.1.5)$$

The work done by the force due to actual stress σ_{11} , for example, in moving through the virtual displacement $\delta u_1 = \delta\varepsilon_{11} dx_1$ is (Figure 2.1.3)

$$(\sigma_{11} \, dx_2 dx_3)(\delta\varepsilon_{11} \, dx_1) = \sigma_{11} \delta\varepsilon_{11} \, dx_1 dx_2 dx_3$$

Similarly, the work done by the force due to stress σ_{12} in shearing the body is (Figure 2.1.4)

$$(\sigma_{12} \, dx_2 dx_3)(2\delta\varepsilon_{12} \, dx_1) = 2\sigma_{12} \delta\varepsilon_{12} \, dx_1 dx_2 dx_3$$

Thus, the total virtual work done (or virtual strain energy δU stored) by forces due to all the stresses in a volume element in moving through their respective displacements is

$$\begin{aligned} & (\sigma_{11} \delta\varepsilon_{11} + \sigma_{22} \delta\varepsilon_{22} + \sigma_{33} \delta\varepsilon_{33} + 2\sigma_{12} \delta\varepsilon_{12} + 2\sigma_{13} \delta\varepsilon_{13} + 2\sigma_{23} \delta\varepsilon_{23}) dx_1 dx_2 dx_3 \\ &= \sigma_{ij} \delta\varepsilon_{ij} \, dv \end{aligned} \quad (2.1.6)$$

The virtual strain energy per unit volume is called the virtual *strain energy density*, $\delta U_0 = \sigma_{ij} \delta\varepsilon_{ij}$. The total internal virtual work done δW_I is obtained by integrating the above expression over the entire volume of the body

$$\delta W_I = \delta U = \int_{\Omega} \sigma_{ij} \delta\varepsilon_{ij} \, dv = \int_{\Omega} \sigma : \delta\varepsilon \, dv \quad (2.1.7)$$

where “ $:$ ” denotes the double dot product. Equation (2.1.7) is valid for any material body irrespective of its constitutive behavior. The expression in Eq. (2.1.7) is also called the *virtual strain energy*. Although Eq. (2.1.7) was derived for infinitesimal strain case, it also holds for the finite strain case.

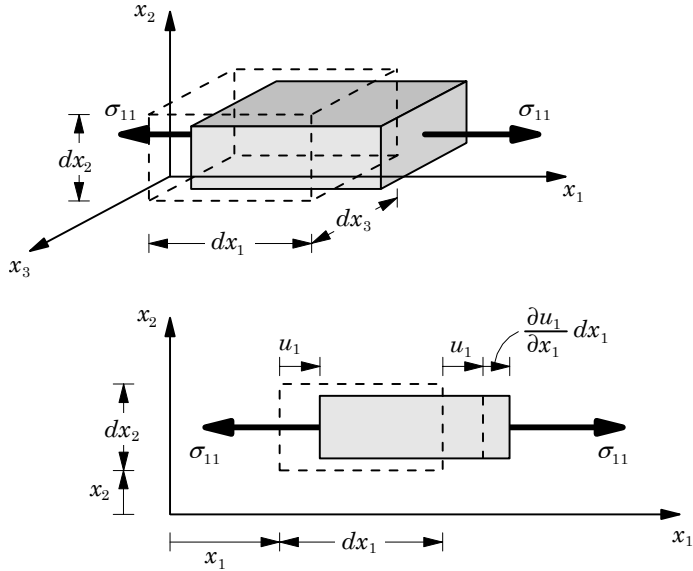


Figure 2.1.3 Virtual work done by normal stress σ_{11} .

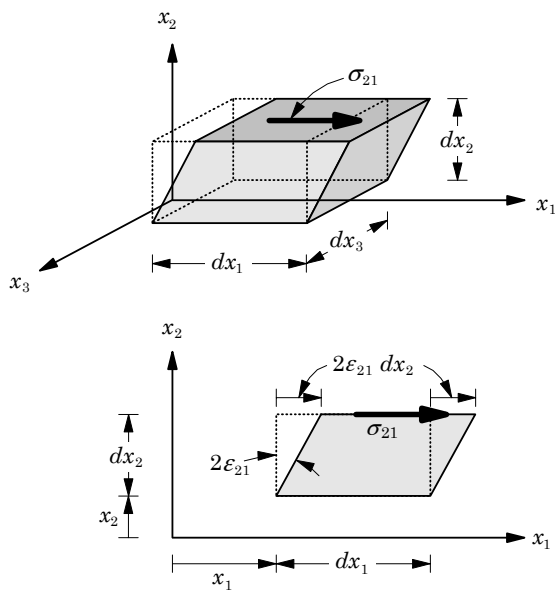


Figure 2.1.4 Virtual work done by shear stress σ_{21} .

The internal virtual work done by virtual stresses $\delta\sigma_{ij}$ in moving through the actual strains ε_{ij} is called the complementary internal virtual work δW_I^* , and it is given by

$$\delta W_I^* = \delta U^* = \int_{\Omega} \varepsilon_{ij} \delta\sigma_{ij} dv = \int_{\Omega} \varepsilon : \delta\sigma dv \quad (2.1.8)$$

The expression in Eq. (2.1.8) is also known as the *virtual complementary strain energy*. The virtual forces ($\delta\mathbf{f}, \delta\mathbf{T}$) and virtual stresses ($\delta\sigma$) should be such that the stress equilibrium equations

$$\frac{\partial \delta\sigma_{ij}}{\partial x_j} + \rho \delta f_i = 0 \quad \text{or} \quad \nabla \cdot \delta\sigma + \rho \delta\mathbf{f} = \mathbf{0} \quad (2.1.9)$$

and stress boundary conditions

$$\delta\sigma_{ij} n_j = \delta T_i \quad \text{or} \quad \delta\sigma \cdot \hat{\mathbf{n}} = \mathbf{T} = \mathbf{0} \quad (2.1.10)$$

are satisfied.

Next we consider an example of virtual work done by actual forces in moving through virtual displacements in a beam structure.

Example 2.1.1: Euler–Bernoulli Beam Theory

Consider the bending and stretching of an Euler–Bernoulli beam on a linear elastic foundation (modulus, k) and subjected to a transverse load $q(x)$ (Figure 2.1.5). We assume infinitesimal strains. Suppose that the displacements (u, v, w) along the coordinate directions $(X, Y, Z) = (x, y, z)$ are given by

$$u(x, y, z) = u_0(x) - z \frac{dw_0}{dx}, \quad v(x, y, z) = 0, \quad w(x, y, z) = w_0(x) \quad (2.1.11)$$

where u_0 and w_0 denote the axial and transverse displacements of a point on the x -axis of the beam. Then the only nonzero linear strain is

$$\varepsilon_{xx} = \frac{du_0}{dx} - z \frac{d^2 w_0}{dx^2} \quad (2.1.12)$$

Then the internal and external virtual works are given by

$$\begin{aligned} \delta W_E &= - \int_0^L q(x) \delta w_0(x) dx - \int_0^L F_s \delta w_0(x) dx \\ &= - \int_0^L q(x) \delta w_0(x) dx + \int_0^L k w_0(x) \delta w_0(x) dx \end{aligned} \quad (2.1.13)$$

$$\begin{aligned} \delta W_I &= \int_0^L \int_A \sigma_{xx} \delta \varepsilon_{xx} dA dx \\ &= \int_0^L \int_A \sigma_{xx} \left(\frac{d\delta u_0}{dx} - z \frac{d^2 \delta w_0}{dx^2} \right) dA dx \\ &= \int_0^L \left(N_{xx} \frac{d\delta u_0}{dx} - M_{xx} \frac{d^2 \delta w_0}{dx^2} \right) dx \end{aligned} \quad (2.1.14)$$

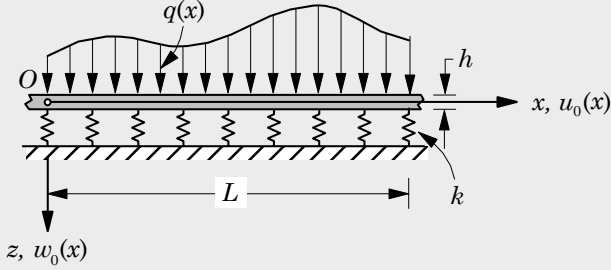


Figure 2.1.5 A beam on elastic foundation.

where k is the modulus of the elastic foundation, L the length, and A is the cross-sectional area of the beam, and N_{xx} and M_{xx} are axial force and bending moment (about the y -axis), respectively

$$N_{xx} = \int_A \sigma_{xx} dA, \quad M_{xx} = \int_A \sigma_{xx} z dA \quad (2.1.15)$$

The foundation reaction force F_s is replaced with $F_s = -kw_0(x)$ using the linear elastic constitutive equation for the foundation.

Note that the expression in (2.1.14) for internal virtual work is independent of the material of the beam, as we have not used any constitutive relation in arriving at the expression. For a given stress-strain relation, the stress resultants N_{xx} and M_{xx} in (2.1.15) can be expressed in terms of the displacements u_0 and w_0 .

2.1.4 The Variational Operator

The delta symbol “ δ ” used in conjunction with virtual displacements and forces can be interpreted as an operator, called the *variational operator*. It is used to denote a variation (or change) in a given quantity, i.e., δu denotes a variation in u . Thus, δ is an operator that produces virtual change or variation δu in a dependent variable u , in much the same way that dx denotes a change in x . In fact, the variational operator δ is a differential operator with respect to the dependent variables. Indeed, the laws of variation of sums, products, ratios, powers, and so forth are completely analogous to the corresponding laws of differentiation. For example, if $F_1 = F_1(u)$ and $F_2 = F_2(u)$, we have

- (1) $\delta(F_1 \pm F_2) = \delta F_1 \pm \delta F_2$
 - (2) $\delta(F_1 F_2) = \delta F_1 F_2 + F_1 \delta F_2$
 - (3) $\delta\left(\frac{F_1}{F_2}\right) = \frac{\delta F_1 F_2 - F_1 \delta F_2}{F_2^2}$
 - (4) $\delta(F_1)^n = n(F_1)^{n-1} \delta F_1$
- (2.1.16)

If $G = G(u, v, w)$ is a function of several dependent variables (and possibly their derivatives), the total variation is the sum of partial variations:

$$\delta G = \delta_u G + \delta_v G + \delta_w G \quad (2.1.17)$$

where, for example, δ_u denotes the partial variation with respect to u . The variational operator can be interchanged with differential and integral operators (commutativity):

$$(1) \quad \delta\left(\frac{du}{dx}\right) = \alpha \frac{dv}{dx} = \frac{d}{dx}(\alpha v) = \frac{d}{dx}(\delta u) \quad (2.1.18)$$

$$(2) \quad \delta\left(\int_{\Omega} u \, d\Omega\right) = \alpha \int_{\Omega} v \, d\Omega = \int_{\Omega} \alpha v \, d\Omega = \int_{\Omega} \delta u \, d\Omega \quad (2.1.19)$$

where Ω denotes a one-, two-, or three-dimensional domain and $d\Omega$ is an element of the domain.

The variational operator proves to be very useful in constructing virtual work statements and deriving governing equations from virtual work principles, as will be shown shortly. The delta operator can be viewed as a differential operator with respect to dependent variables.

Example 2.1.2

Given

$$(a) \quad F(x, u) = f(x) + x^2 u(x) - 2u \frac{du}{dx} + 2x \sin u$$

$$(b) \quad G(x, y, u, v, u) = 2xy + x^2 y + 2uv - y^2 \frac{\partial u}{\partial y} \partial v \partial x + x \left(\frac{\partial u}{\partial x} \right)^2 + xy \left(\frac{\partial v}{\partial x} \right)^2$$

we wish to determine the first and second variations of F and the first total variation of G .

(a) We have

$$\delta F = x^2 \delta u - 2\delta u \frac{du}{dx} - 2u \frac{d\delta u}{dx} + 2x \cos u \delta u$$

$$\delta^2 F = \delta(\delta F) = \left(x^2 - 2 \frac{du}{dx} + 2x \cos u \right) \delta^2 u - 4\delta u \frac{d\delta u}{dx} - 2u \frac{d^2 \delta u}{dx^2} - 2x \cos u (\delta u)^2$$

(b) The first total variation of G is

$$\delta G = 2\delta u v + 2u \delta v - y^2 \frac{\partial \delta u}{\partial y} \frac{\partial v}{\partial x} - y^2 \frac{\partial u}{\partial y} \frac{\partial \delta v}{\partial x} + 2x \frac{\partial u}{\partial x} \frac{\partial \delta u}{\partial x} + 2xy \frac{\partial v}{\partial x} \frac{\partial \delta v}{\partial x}$$

2.1.5 Functionals

A formal mathematical definition of a *functional* requires concepts from functional analysis. It is a real number (or scalar) obtained by operating on functions (dependent variables) from a given set of functions (or vector space). Thus, a functional is a real number $I(u)$ obtained by an operator $I(\cdot)$ that maps functions u of a vector space H into a real number $I(u)$ in the set of real numbers R :

$$I : H \rightarrow R \quad (2.1.20)$$

Note that $I(\cdot)$ is an operator and $I(u)$ is a functional.

A functional is said to be *linear* if

$$I(c_1u + c_2v) = c_1I(u) + c_2I(v) \quad (2.1.21)$$

for all constants c_1 and c_2 and dependent variables u and v . A *quadratic* functional is one that satisfies the relation

$$I(cu) = c^2I(u) \quad (2.1.22)$$

for all constants c and the dependent variable u .

The first variation of a functional of u (and its derivatives) can be calculated as follows. Let $I(u)$ denote the integral defined in the interval (a, b)

$$I(u) = \int_a^b F(x, u, u') dx \quad (2.1.23)$$

where F is a function, in general, of x , u , and $u' \equiv du/dx$. The first variation of the functional $I(u)$ is

$$\delta I(u) = \delta \int_a^b F(x, u, u') dx = \int_a^b \delta F dx = \int_a^b \left(\frac{\partial F}{\partial u} \delta u + \frac{\partial F}{\partial u'} \delta u' \right) dx \quad (2.1.24)$$

Thus, the variation of a functional can be readily calculated.

2.1.6 Fundamental Lemma of Variational Calculus

The *fundamental lemma of calculus of variations* is useful in obtaining differential equations from integral statements. The lemma can be stated as follows: *For any integrable function G , if the statement*

$$\int_a^b G \cdot \eta dx = 0 \quad (2.1.25)$$

holds for any arbitrary continuous function $\eta(x)$, for all x in (a, b) , then it follows that $G = 0$ in (a, b) .

A mathematical proof of the lemma can be found in most books on variational calculus. A simple proof of the lemma follows. Since η is arbitrary, it can be replaced by G . We have

$$\int_a^b G^2 dx = 0$$

Since an integral of a positive function is positive, the above statement implies that $G = 0$.

A more general statement of the fundamental lemma is as follows: If η is arbitrary in $a < x < b$ and $\eta(a)$ is arbitrary, then the statement

$$\int_a^b G \cdot \eta dx + B(a) \cdot \eta(a) = 0 \quad (2.1.26)$$

implies that $G = 0$ in $a < x < b$ and $B(a) = 0$ because $\eta(x)$ is independent of $\eta(a)$.

2.1.7 Euler–Lagrange Equations

Consider the problem of finding the extremum (i.e., minimum or maximum) of the functional

$$I(u) = \int_a^b F(x, u, u') dx, \quad u(a) = u_a, \quad u(b) = u_b \quad (2.1.27)$$

The necessary condition for the functional to have a minimum or maximum is (analogous to maxima or minima of functions) that its first variation be zero:

$$\delta I(u) = 0 \quad (2.1.28)$$

We have

$$0 = \int_a^b \left(\frac{\partial F}{\partial u} \delta u + \frac{\partial F}{\partial u'} \delta u' \right) dx$$

Note that $\delta u' = \delta(du/dx) = d(\delta u)/dx$. We cannot use the fundamental lemma in the above equation because it is not in the form of Eq. (2.1.25) or Eq. (2.1.26). To recast the above equation in the form of Eq. (2.1.25), we integrate the second term by parts and obtain

$$\begin{aligned} 0 &= \int_a^b \left(\frac{\partial F}{\partial u} \delta u + \frac{\partial F}{\partial u'} \delta u' \right) dx \\ &= \int_a^b \left(\frac{\partial F}{\partial u} \delta u + \frac{\partial F}{\partial u'} \frac{d\delta u}{dx} \right) dx \\ &= \int_a^b \left[\frac{\partial F}{\partial u} - \frac{d}{dx} \left(\frac{\partial F}{\partial u'} \right) \right] \delta u \, dx + \left[\frac{\partial F}{\partial u'} \delta u \right]_a^b \end{aligned} \quad (2.1.29)$$

Classification of variables and boundary conditions

Let us first examine the boundary expression:

$$\left[\frac{\partial F}{\partial u'} \right] \cdot \delta u$$

There are two parts to this expression: a varied quantity and its coefficient. The variable u that is subjected to variation is called the *primary variable*. The coefficient of the varied quantity, i.e., the expression next to δu in the boundary term, is called a *secondary variable*. The product of the primary variable (or its variation) with the secondary variable often represents the work done (or virtual work done). The specification of the primary variable at a boundary point is termed the *essential boundary condition*, and the specification of the secondary variable is called the *natural boundary condition*. In solid mechanics, these are known as the *geometric* and *force* boundary conditions, respectively. All admissible variations must satisfy the homogeneous form of the essential (or geometric) boundary conditions: $\delta u(a) = 0$ and $\delta u(b) = 0$. Elsewhere, $a < x < b$, δu is arbitrary.

Returning to Eq. (2.1.29), we note that the boundary terms drop out because of the conditions $\delta u(a) = 0$ and $\delta u(b) = 0$. We have

$$0 = \int_a^b \left[\frac{\partial F}{\partial u} - \frac{d}{dx} \left(\frac{\partial F}{\partial u'} \right) \right] \delta u \, dx$$

which must hold for any δu in (a, b) . In view of the fundamental lemma of calculus of variations ($\eta = \delta u$), it follows that [see Eq. (2.1.25)]

$$G \equiv \frac{\partial F}{\partial u} - \frac{d}{dx} \left(\frac{\partial F}{\partial u'} \right) = 0 \quad \text{in } a < x < b \quad (2.1.30)$$

Thus, the necessary condition for $I(u)$ to be an extremum at $u = u(x)$ is that $u(x)$ be the solution of Eq. (2.1.30), which is known as the *Euler–Lagrange equation* associated with the functional $I(u)$, i.e., $\delta I = 0$ is equivalent to Eq. (2.1.30).

If $u(a) = u_a$ and $\delta u(b)$ is arbitrary (i.e., $u(a)$ is specified but u is not specified at $x = b$), then $\delta u(a) = 0$ and we have from Eq. (2.1.29) the result

$$0 = \int_a^b \left[\frac{\partial F}{\partial u} - \frac{d}{dx} \left(\frac{\partial F}{\partial u'} \right) \right] \delta u \, dx + \left(\frac{\partial F}{\partial u'} \right)_{x=b} \delta u(b) \quad (2.1.31)$$

Since δu is arbitrary in (a, b) and $\delta u(b)$ is arbitrary, the above equation implies, in view of Eq. (2.1.26), that both the integral expression and the boundary term be zero separately:

$$\begin{aligned} \frac{\partial F}{\partial u} - \frac{d}{dx} \left(\frac{\partial F}{\partial u'} \right) &= 0, \quad a < x < b \\ \left(\frac{\partial F}{\partial u'} \right) &= 0 \quad \text{at } x = b \end{aligned} \quad (2.1.32)$$

Equations in (2.1.32) are called the *Euler–Lagrange equations*. Note that the boundary conditions that are a part of the Euler–Lagrange equations always belong to the class of natural boundary conditions.

Example 2.1.3

Consider the functional

$$I(u) = \int_{\Omega} \left[\frac{1}{2} (\nabla u \cdot \nabla u) - fu \right] dv - \int_{\Gamma_2} \hat{t} u \, ds \quad (a)$$

where u and f are functions of position, ds and dv denote the surface and volume elements of the domain Ω , and Γ_2 denotes a portion of the boundary Γ . We wish to determine the Euler–Lagrange equations associated with the functional when u is specified on the other portion of the boundary

$$u = \hat{u} \quad \text{on } \Gamma_1, \quad \Gamma_1 + \Gamma_2 = \Gamma$$

The first variation of $I(u)$ is given by

$$\begin{aligned} \delta I(u) &= \int_{\Omega} \left[\frac{1}{2} (\nabla \delta u \cdot \nabla u + \nabla u \cdot \nabla \delta u) - f \delta u \right] dv - \int_{\Gamma_2} \hat{t} \delta u \, ds \\ &= \int_{\Omega} (-\nabla \cdot \nabla u + f) \delta u \, dv + \oint_{\Gamma} \hat{\mathbf{n}} \cdot \nabla u \, \delta u \, ds - \int_{\Gamma_2} \hat{t} \delta u \, ds \end{aligned} \quad (b)$$

where the *divergence theorem* of vector calculus

$$\int_{\Omega} \nabla F \, dv = \oint_{\Gamma} \hat{\mathbf{n}} \cdot \nabla F \, ds \quad (2.1.33)$$

is used to relieve δu of the gradient operation:

$$\begin{aligned}\int_{\Omega} \nabla u \cdot \nabla \delta u \, dv &= \int_{\Omega} [\nabla \cdot (\nabla u \delta u) - (\nabla \cdot \nabla u) \delta u] \, dv \\ &= \oint_{\Gamma} (\hat{\mathbf{n}} \cdot \nabla u) \delta u \, ds - \int_{\Omega} (\nabla \cdot \nabla u) \delta u \, dv\end{aligned}$$

A circle on the boundary integral denotes integration over the closed boundary. Since the total boundary Γ is the direct sum of Γ_1 and Γ_2 and $\delta u = 0$ on Γ_1 , the integral on the total boundary of (b) is reduced to the boundary integral over Γ_2 and we obtain ($\nabla \cdot \nabla = \nabla^2$)

$$\delta I(u) = \int_{\Omega} (-\nabla^2 u + f) \delta u \, dv + \int_{\Gamma_2} \left(\frac{\partial u}{\partial n} - \hat{t} \right) \delta u \, ds \quad (c)$$

where

$$\frac{\partial u}{\partial n} = \hat{\mathbf{n}} \cdot \nabla u \quad (d)$$

is the *normal derivative* of u . Now, setting $\delta I = 0$ and using the fundamental lemma, we arrive at the Euler–Lagrange equations

$$\begin{aligned}-\nabla^2 u + f &= 0 \quad \text{in } \Omega \\ \frac{\partial u}{\partial n} - \hat{t} &= 0 \quad \text{on } \Gamma_2\end{aligned} \quad (e)$$

2.2 Energy Principles

2.2.1 Introduction

Recall that the virtual work due to virtual displacements is the work done by actual forces in moving the material particles of the body through virtual displacements that are consistent with the geometric constraints. All applied forces are kept constant during the virtual displacements. Consider a rigid body acted upon by a set of applied forces $\mathbf{F}_1, \mathbf{F}_2, \dots, \mathbf{F}_n$, and suppose that the points of application of these forces are subjected to the virtual displacements $\delta \mathbf{u}_1, \delta \mathbf{u}_2, \dots, \delta \mathbf{u}_n$, respectively. The virtual displacement $\delta \mathbf{u}_i$ has no relation to $\delta \mathbf{u}_j$, for $i \neq j$. The external virtual work done by the virtual displacements is

$$\delta W_E = -[\mathbf{F}_1 \cdot \delta \mathbf{u}_1 + \mathbf{F}_2 \cdot \delta \mathbf{u}_2 + \dots + \mathbf{F}_n \cdot \delta \mathbf{u}_n] = -\mathbf{F}_i \cdot \delta \mathbf{u}_i \quad (2.2.1)$$

where the sum on repeated indices (over the range of 1 to n) is implied. The internal virtual work done $\delta W_I = \delta U$ is zero because a rigid body does not undergo any strains (hence, virtual strains are zero). In addition, the virtual displacements $\delta \mathbf{u}_1, \delta \mathbf{u}_2, \dots, \delta \mathbf{u}_n$ should all be the same, say $\delta \mathbf{u}$, for a rigid body. Thus, we have

$$\delta W_E = -\mathbf{F}_i \cdot \delta \mathbf{u}_i = -\left(\sum_{i=1}^n \mathbf{F}_i \right) \cdot \delta \mathbf{u} \quad \text{and} \quad \delta W_I = 0 \quad (2.2.2)$$

But by Newton's second law, the vector sum of the forces acting on a body in static equilibrium is zero. This implies that the total virtual work, $\delta W_I + \delta W_E$, is equal to zero. Thus, for a body in equilibrium the total virtual work done due to virtual displacements is zero. This statement is known as *the principle of virtual displacements*. The principle also holds for continuous, deformable bodies for which δW_I is not zero.

2.2.2 The Principle of Virtual Displacements

Consider a continuous body \mathcal{B} in equilibrium under the action of body forces \mathbf{f} and surface tractions (i.e., boundary stresses) \mathbf{T} . Let the reference configuration be the initial configuration \mathcal{C}^0 whose volume is denoted as Ω . Suppose that over portion Γ_u of the total boundary Γ of the region Ω , the displacements are specified to be $\hat{\mathbf{u}}$, and on portion Γ_σ , the tractions are specified to be $\hat{\mathbf{T}}$. The boundary portions Γ_u and Γ_σ are disjoint (i.e., do not overlap), and their sum is the total boundary Γ . Let \mathbf{u} be the displacement vector corresponding to the equilibrium configuration of the body, and let σ and ε be the stress and strain tensors, respectively. The set of admissible configurations are defined by sufficiently differentiable functions that satisfy the geometric boundary conditions $\mathbf{u} = \hat{\mathbf{u}}$ on Γ_u .

If the body is in equilibrium, then of all admissible configurations, the actual one corresponding to the equilibrium configuration makes the total virtual work done zero. In order to determine the equations governing the equilibrium configuration \mathcal{C} , we let the body experience a virtual displacement $\delta\mathbf{u}$ from the true configuration \mathcal{C} . The virtual displacements are arbitrary, continuous functions except that they satisfy the homogeneous form of geometric boundary conditions, i.e., they must belong to the set of admissible variations.

The principle of virtual displacements can be stated as follows: *If a continuous body is in equilibrium, the virtual work of all actual forces in moving through a virtual displacement is zero:*

$$\delta W_I + \delta W_E \equiv \delta W = 0 \quad (2.2.3)$$

Just as we derived the Euler–Lagrange equations associated with the statement $\delta I = 0$, we can derive them for the statement in Eq. (2.2.3). However, first we must identify δW_I and δW_E for a given problem. The principle of virtual work is independent of any constitutive law and applies to both elastic (linear and nonlinear) and inelastic continua.

For a solid body, the expressions for external and internal virtual work done due to virtual displacements are given in Eqs. (2.1.3) and (2.1.7), respectively. Then the principle of virtual displacements for deformable body can be expressed as

$$\int_{\Omega} \sigma : \delta \varepsilon \, dv - \int_{\Omega} \rho \mathbf{f} \cdot \delta \mathbf{u} \, dv - \int_{\Gamma_\sigma} \mathbf{T} \cdot \delta \mathbf{u} \, ds = 0 \quad (2.2.4)$$

where Ω is the volume of the undeformed body, and dv and ds denote the volume and surface elements of Ω . Writing in terms of the Cartesian rectangular components, Eq. (2.2.4) takes the form (sum on repeated subscripts is implied)

$$\int_{\Omega} (\sigma_{ij} \delta \varepsilon_{ij} - \rho f_i \delta u_i) \, dv - \int_{\Gamma_\sigma} T_i \delta u_i \, ds = 0 \quad (2.2.5)$$

We will show that the Euler–Lagrange equations associated with the statement (2.2.4) or (2.2.5) of the principle of virtual displacements are nothing but the equilibrium equations of the 3-D elasticity [see Eq. (1.3.24)]. First we use the rectangular Cartesian component form to establish the result.

The virtual strains $\delta\varepsilon_{ij}$ are related to the virtual displacements δu_i by

$$\delta\varepsilon_{ij} = \frac{1}{2} (\delta u_{i,j} + \delta u_{j,i}), \quad u_{i,j} \equiv \frac{\partial u_i}{\partial x_j} \quad (2.2.6)$$

Substituting $\delta\varepsilon_{ij}$ from the above equation into Eq. (2.2.5) and using the divergence theorem to transfer differentiation from δu_i to its coefficient, one obtains ($\sigma_{ij} = \sigma_{ji}$)

$$\begin{aligned} 0 &= \int_{\Omega} \left[\frac{1}{2} \sigma_{ij} (\delta u_{i,j} + \delta u_{j,i}) - \rho f_i \delta u_i \right] dv - \int_{\Gamma_{\sigma}} T_i \delta u_i \, ds \\ &= \int_{\Omega} (\sigma_{ji} \delta u_{i,j} - \rho f_i \delta u_i) \, dv - \int_{\Gamma_{\sigma}} T_i \delta u_i \, ds \\ &= - \int_{\Omega} (\sigma_{ji,j} + \rho f_i) \delta u_i \, dv - \int_{\Gamma_{\sigma}} T_i \delta u_i \, ds + \oint_{\Gamma} \sigma_{ji} n_j \delta u_i \, ds \end{aligned} \quad (2.2.7)$$

Since $\delta u_i = 0$ on Γ_u and $\Gamma_{\sigma} = \Gamma - \Gamma_u$, we have

$$0 = - \int_{\Omega} (\sigma_{ji,j} + \rho f_i) \delta u_i \, dv + \int_{\Gamma_{\sigma}} (\sigma_{ji} n_j - T_i) \delta u_i \, ds \quad (2.2.8)$$

Because the virtual displacements are arbitrary in Ω_0 and on Γ_{σ} , Eq. (2.2.8) yields the following Euler–Lagrange equations

$$\sigma_{ji,j} + \rho f_i = 0 \quad \text{in } \Omega \quad (2.2.9)$$

$$\sigma_{ji} n_j - T_i = 0 \quad \text{on } \Gamma_{\sigma} \quad (2.2.10)$$

Equations (2.2.9) and (2.2.10) are the Euler–Lagrange equations associated with the principle of virtual displacements for a body undergoing small strains and displacements. The boundary conditions in Eq. (2.2.10) are the natural boundary conditions. The principle of virtual displacements is applicable to any continuous body with arbitrary constitutive behavior (i.e., elastic or inelastic).

Example 2.2.1

Consider the internal and external virtual works in Eqs. (2.1.13) and (2.1.14) of Example 2.1.1 associated with an Euler–Bernoulli beam on an elastic foundation (modulus k) and subjected to a transverse load $q(x)$ (see Figure 2.1.5). The principle of virtual work requires

$$\begin{aligned} 0 &= \int_0^L \left(N_{xx} \frac{d\delta u_0}{dx} - M_{xx} \frac{d^2 \delta w_0}{dx^2} \right) dx - \int_0^L (q - kw_0) \delta w_0 \, dx \\ &= \int_0^L \left[-\frac{dN_{xx}}{dx} \delta u_0 + \left(-\frac{d^2 M_{xx}}{dx^2} + kw_0 - q \right) \delta w_0 \right] dx \\ &\quad + \left[N_{xx} \delta u_0 + \frac{dM_{xx}}{dx} \delta w_0 - M_{xx} \frac{d\delta w_0}{dx} \right]_0^L \end{aligned} \quad (2.2.11)$$

where N_{xx} and M_{xx} are the stress resultants defined in Eq. (2.1.15). Hence, the Euler–Lagrange equations are

$$\delta u_0 : -\frac{dN_{xx}}{dx} = 0 \quad (2.2.12)$$

$$\delta w_0 : -\frac{d^2M_{xx}}{dx^2} + kw_0 - q = 0 \quad (2.2.13)$$

in $0 < x < L$ and the following boundary conditions at $x = 0, L$ are:

$$N_{xx} = 0, \quad \frac{dM_{xx}}{dx} = 0, \quad M_{xx} = 0 \quad (2.2.14)$$

For a linear elastic material, we have $\sigma_{xx} = E\varepsilon_{xx}$ and N_{xx} and M_{xx} can be expressed in terms of the displacements as

$$N_{xx} = EA \frac{du_0}{dx}, \quad M_{xx} = -EI \frac{d^2w_0}{dx^2} \quad (2.2.15)$$

where E is Young's modulus, A is the cross-sectional area, and I is the second moment of inertia of the beam.

Equations (2.2.12) and (2.2.13) can also be derived using the vector approach (i.e., application of Newton's second law). In vector approach, we isolate a typical element of the beam, located between x and $x+\Delta x$, with all its forces and moments, as shown in Figure 2.2.1. We have

$$\begin{aligned} \sum F_x &= 0 : -N_{xx}(x) + N_{xx}(x + \Delta x) = 0 \\ \sum F_z &= 0 : -V(x) + V(x + \Delta x) + q(x)\Delta x - F_k \cdot \Delta x = 0 \\ \sum M_y &= 0 : M_{xx}(x) + \Delta x \cdot V(x + \Delta x) - M_{xx}(x + \Delta x) \\ &\quad + (q(x) \cdot \Delta x)\alpha\Delta x = 0 \end{aligned}$$

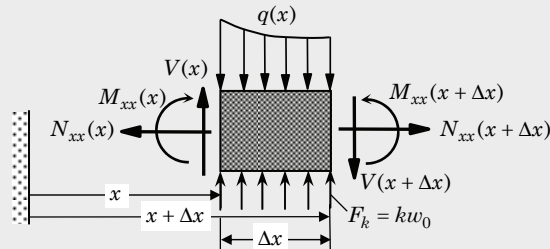
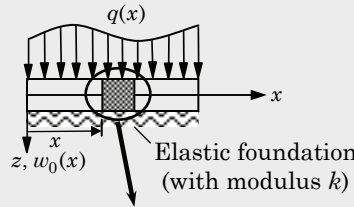


Figure 2.2.1 Free-body diagram of a beam element on elastic foundation.

where F_k is the force per unit length exerted by the foundation, $F_k(x) = kw_0(x)$, and α is a value between 0 and 1. Dividing each equation with Δx and taking the limit $\Delta x \rightarrow 0$ (to obtain the equations at an arbitrary point x), we obtain

$$\frac{dN_{xx}}{dx} = 0 \quad (2.2.16)$$

$$\frac{dV}{dx} + q - kw_0 = 0 \quad (2.2.17)$$

$$-\frac{dM_{xx}}{dx} + V = 0 \quad (2.2.18)$$

Substituting for V from Eq. (2.2.17) into Eq. (2.2.18) yields Eq. (2.2.13).

2.2.3 Hamilton's Principle

The principle of virtual displacements is limited to static equilibrium of solid bodies. Hamilton's principle is a generalization of the principle of virtual displacements to dynamics. The dynamics version of the principle of virtual displacements, i.e., Hamilton's principle, is based on the assumption that a dynamical system is characterized by two energy functions: a *kinetic energy* K and a *potential energy* W .

Newton's second law of motion expresses the global statement of the principle of conservation of linear momentum. However, Newton's second law of motion is not sufficient to determine the motion $\mathbf{u} = \mathbf{u}(\mathbf{x}, t)$. The kinematic conditions and constitutive equations derived in Chapter 1 are needed to completely determine the motion. The actual path $\mathbf{u} = \mathbf{u}(\mathbf{x}, t)$ followed by a material particle in position \mathbf{x} in the body is varied, consistent with kinematic (essential) boundary conditions, to $\mathbf{u} + \delta\mathbf{u}$, where $\delta\mathbf{u}$ is the admissible variation (or virtual displacement) of the path. We suppose that the varied path differs from the actual path except at initial and final times, t_1 and t_2 , respectively. Thus, an admissible variation $\delta\mathbf{u}$ satisfies the conditions

$$\begin{aligned} \delta\mathbf{u} &= 0 \text{ on } \Gamma_u \text{ for all } t \\ \delta\mathbf{u}(\mathbf{x}, t_1) &= \delta\mathbf{u}(\mathbf{x}, t_2) = 0 \text{ for all } \mathbf{x} \end{aligned} \quad (2.2.19)$$

where Γ_u denotes the portion of the surface of the body where the displacement vector \mathbf{u} is specified.

Hamilton's principle states that *of all possible paths that a material particle could travel from its position at time t_1 to its position at time t_2 , its actual path will be one for which the integral*

$$\int_{t_1}^{t_2} (K - W) dt \quad (2.2.20)$$

is an extremum. The difference between the kinetic and potential energies is called the *Lagrangian* function

$$L = K - W = K - W_I - W_E \quad (2.2.21)$$

Thus, Hamilton's principle can be expressed as

$$0 = \int_{t_1}^{t_2} (\delta K - \delta W_I - \delta W_E) dt \quad (2.2.22)$$

The kinetic energy of a continuous body is given by

$$K = \frac{1}{2} \int_{\Omega_0} \rho \frac{\partial \mathbf{u}}{\partial t} \cdot \frac{\partial \mathbf{u}}{\partial t} dv \quad (2.2.23)$$

where $\frac{\partial \mathbf{u}}{\partial t}$ denotes the velocity of the material particle.

The requirement that $\delta \mathbf{u}$ be zero at the final time when $\mathbf{u}(\mathbf{x}, t_2)$ is not known or specified is often a point of discussion and, for this reason, Hamilton's principle is sometimes referred to as a pseudo variational principle. The principle gives the equations of motion, but not the initial conditions. An application of Hamilton's principle is presented in the next example.

Example 2.2.2: The Timoshenko Beam Theory

The Euler–Bernoulli beam theory of Example 2.1.1 is based on the assumption that a straight line transverse to the axis of the beam before deformation remains (1) straight, (2) inextensible, and (3) normal to the mid-plane after deformation. In the Timoshenko beam theory, the first two assumptions are kept but the normality condition is relaxed by assuming that the rotation is independent of the slope ($w_{0,x}$) of the beam. Using these assumptions, the displacement field of the beam can be expressed as [cf. Eq. (2.1.11)]

$$u(x, z, t) = u_0(x, t) + z\phi(x, t), \quad v = 0, \quad w(x, z, t) = w_0(x, t) \quad (2.2.24)$$

where (u, v, w) are the displacements of a point along the (x, y, z) coordinates, (u_0, w_0) are the displacements of a point on the midplane of an undeformed beam, and ϕ is the rotation (about the y -axis) of a transverse normal line. We wish to derive the equations of motion of the Timoshenko beam theory using Hamilton's principle for the case of infinitesimal strains.

The only nonzero strains are

$$\begin{aligned} \varepsilon_{xx} &= \frac{\partial u}{\partial x} = \frac{\partial u_0}{\partial x} + z \frac{\partial \phi}{\partial x} \equiv \varepsilon_{xx}^0 + z\varepsilon_{xx}^1 \\ \gamma_{xz} &= \frac{\partial u}{\partial z} + \frac{\partial w}{\partial x} = \phi + \frac{\partial w_0}{\partial x} \equiv \gamma_{xz}^0 \end{aligned} \quad (2.2.25)$$

The virtual strains are

$$\delta\varepsilon_{xx}^0 = \frac{\partial \delta u_0}{\partial x}, \quad \delta\varepsilon_{xx}^1 = \frac{\partial \delta \phi}{\partial x}, \quad \delta\gamma_{xz}^0 = \delta\phi + \frac{\partial \delta w_0}{\partial x}$$

Next, we compute the virtual energies required in Eq. (2.2.22). We have

$$\begin{aligned} \delta W_I &= \int_v \sigma_{ij} \delta \varepsilon_{ij} dv = \int_0^L \int_A (\sigma_{xx} \delta \varepsilon_{xx} + \sigma_{xz} \delta \gamma_{xz}^0) dA dx \\ &= \int_0^L \int_A [\sigma_{xx} (\delta \varepsilon_{xx}^0 + z \delta \varepsilon_{xx}^1) + \sigma_{xz} \delta \gamma_{xz}^0] dA dx \\ &= \int_0^L (N_{xx} \delta \varepsilon_{xx}^0 + M_{xx} \delta \varepsilon_{xx}^1 + Q_x \delta \gamma_{xz}^0) dx \end{aligned}$$

$$\begin{aligned}\delta W_E &= - \int_0^L q \delta w_0 \, dx \\ \delta K &= \frac{1}{2} \delta \int_v \rho [(\dot{u})^2 + (\dot{w})^2] \, dv = \int_0^L \int_A \rho [(\dot{u}_0 + z\dot{\phi})^2 + (\dot{w}_0)^2] \, dA \, dx \\ &= \int_0^L [I_0 \dot{u}_0 \delta \dot{u}_0 + I_1 (\dot{u}_0 \delta \dot{\phi} + \dot{\phi} \delta \dot{u}_0) + I_2 \dot{\phi} \delta \dot{\phi} + I_0 \dot{w}_0 \delta \dot{w}_0] \, dx \quad (2.2.26)\end{aligned}$$

where ρ is the density, q is the distributed transverse load, and a superposed dot indicates differentiation with respect to time t , and

$$\begin{aligned}N_{xx} &= \int_A \sigma_{xx} \, dA, \quad M_{xx} = \int_A \sigma_{xx} z \, dA \\ Q_x &= K_s \int_A \sigma_{xz} \, dA, \quad I_i = \int_A \rho(z)^i \, dA \quad (2.2.27)\end{aligned}$$

The coefficient K_s is the *shear correction factor* introduced to account for the difference between the actual shear force and that predicted by the Timoshenko beam theory on account of constant state of shear stress through the beam height. For example, the shear stress distribution through the height of a homogeneous beam with rectangular cross section (width b and height h) can be computed from equilibrium as

$$\sigma_{xz}^E = \frac{3Q_x}{2bh} \left[1 - \left(\frac{2z}{h} \right)^2 \right], \quad -\frac{h}{2} \leq z \leq \frac{h}{2}$$

where Q_x is the transverse shear force. The transverse shear stress in the Timoshenko beam theory is a constant, $\sigma_{xz}^T = Q_x/bh$. The strain energies due to transverse shear stresses in the two theories are

$$\begin{aligned}U^E &= \frac{1}{2G} \int_A \left(\sigma_{xz}^E \right)^2 \, dA = \frac{6Q_x^2}{10Gbh} \\ U^T &= \frac{1}{2G} \int_A \left(\sigma_{xz}^T \right)^2 \, dA = \frac{Q_x^2}{2Gbh}\end{aligned}$$

The shear correction factor K_s is the ratio of U^T to U^E , which gives $K_s = 5/6$.

Substituting the expressions for δW_I , δW_E , and δK from Eq (2.2.26) into Eq. (2.2.22), we obtain

$$\begin{aligned}0 &= \int_0^T \int_0^L [I_0 \dot{u}_0 \delta \dot{u}_0 + I_1 (\dot{u}_0 \delta \dot{\phi} + \dot{\phi} \delta \dot{u}_0) + I_2 \dot{\phi} \delta \dot{\phi} + I_0 \dot{w}_0 \delta \dot{w}_0] \, dx \, dt \\ &\quad - \int_{t_1}^{t_2} \int_0^L \left[N_{xx} \frac{\partial \delta u_0}{\partial x} + M_{xx} \frac{\partial \delta \phi}{\partial x} + Q_x \left(\delta \phi + \frac{\partial \delta w_0}{\partial x} \right) - q \delta w_0 \right] \, dx \, dt \\ &= \int_0^T \int_0^L \left[\frac{\partial N_{xx}}{\partial x} - (I_0 \ddot{u}_0 + I_1 \ddot{\phi}) \right] \delta u_0 \, dx \, dt \\ &\quad + \int_0^T \int_0^L \left[\frac{\partial M_{xx}}{\partial x} - Q_x - (I_1 \ddot{u}_0 + I_2 \ddot{\phi}) \right] \delta \phi \, dx \, dt \\ &\quad + \int_0^T \int_0^L \left(\frac{\partial Q_x}{\partial x} + q - I_0 \ddot{w}_0 \right) \delta w_0 \, dx \, dt \\ &\quad - \left[N_{xx} \cdot \delta u_0 \right]_0^L - \left[M_{xx} \cdot \delta \phi \right]_0^L - \left[Q_x \cdot \delta w_0 \right]_0^L \quad (2.2.28)\end{aligned}$$

where it is assumed that ρ is independent of time. We note that

$$I_1 = \int_A \rho z \, dA = b \int_{-\frac{h}{2}}^{\frac{h}{2}} \rho z \, dz = 0 \quad (2.2.29)$$

whenever ρ is independent of z , where b is the width of the beam (when it is assumed to be of a rectangular cross section).

Integrating by parts (in space as well as time) to relieve δu_0 and δw_0 of any differentiations, collecting like terms together, noting that

$$\delta u_0(x, t_1) = \delta u_0(x, t_2) = \delta w_0(x, t_1) = \delta w_0(x, t_2) = 0$$

and using the fundamental lemma we arrive at the Euler–Lagrange equations:

$$\delta u_0 : \quad \frac{\partial N_{xx}}{\partial x} - I_0 \frac{\partial^2 u_0}{\partial t^2} = 0 \quad (2.2.30)$$

$$\delta \phi : \quad \frac{\partial M_{xx}}{\partial x} - Q_x - I_2 \frac{\partial^2 \phi}{\partial t^2} = 0 \quad (2.2.31)$$

$$\delta w_0 : \quad \frac{\partial Q_x}{\partial x} + q - I_0 \frac{\partial^2 w_0}{\partial t^2} = 0 \quad (2.2.32)$$

The force (natural) boundary conditions for the Timoshenko beam theory involve specifying the following secondary variables:

$$N_{xx}, \quad Q_x, \quad \text{and} \quad M_{xx} \quad \text{at } x = 0, L \quad (2.2.33)$$

The geometric boundary conditions involve specifying the following primary variables:

$$u_0, \quad w_0, \quad \text{and} \quad \phi \quad \text{at } x = 0, L \quad (2.2.34)$$

Thus, the pairing of the primary and secondary variables is as follows:

$$(u_0, N_{xx}), \quad (w_0, Q_x), \quad (\phi, M_{xx})$$

Only one member of each pair may be specified at a point in the beam.

2.2.4 The Principle of Minimum Total Potential Energy

A special case of the principle of virtual displacements that deals with linear as well as nonlinear elastic bodies is known as the *principle of minimum total potential energy*. For elastic bodies (in the absence of temperature variations), there exists a *strain energy density* function U_0 such that

$$\sigma_{ij} = \frac{\partial U_0}{\partial \varepsilon_{ij}} \quad (2.2.35)$$

Equation (2.2.35) represents the constitutive equation of an hyperelastic material. The strain energy density U_0 is a single-valued function of strains at a point, and is assumed to be positive definite. The statement of the principle of virtual

displacements, Eqs. (2.2.4) and (2.2.5), can be expressed in terms of the strain energy density U_0 :

$$\int_{\Omega} \frac{\partial U_0}{\partial \varepsilon_{ij}} \delta \varepsilon_{ij} dv - \left[\int_{\Omega} \rho f_i \delta u_i dv + \int_{\Gamma_\sigma} T_i \delta u_i ds \right] = 0 \quad (2.2.36)$$

The first integral is equal to

$$\int_{\Omega} \sigma_{ij} \delta \varepsilon_{ij} dv = \int_{\Omega} \delta U_0 dv = \delta U \quad (2.2.37)$$

where U is the strain energy

$$U = \int_{\Omega} U_0 dv = \int_{\Omega} \left(\int_0^{\varepsilon_{ij}} \sigma_{ij} d\varepsilon_{ij} \right) dv \quad (2.2.38)$$

For linear elastic material, the strain energy U can be expressed as

$$U = \frac{1}{2} \int_{\Omega} \sigma_{ij} \varepsilon_{ij} dv \quad (2.3.39)$$

The expression in the square brackets of (2.2.36) can be identified as $-\delta W_E$. We suppose that there exists a potential $V = W_E$ whose first variation is

$$\delta V = \delta W_E = - \left[\int_{\Omega} \rho f_i \delta u_i dv + \int_{\Gamma_\sigma} T_i \delta u_i ds \right] \quad (2.2.40)$$

Then the principle of virtual work takes the form

$$\delta U + \delta V = \delta(U + V) \equiv \delta \Pi = 0 \quad (2.2.41)$$

The sum $U + V = \Pi$ is called the *total potential energy* of the elastic body. The statement in Eq. (2.2.41) is known as the *principle of minimum total potential energy*. It states that *of all admissible displacements, those that satisfy the equilibrium equations make the total potential energy a minimum*, $\Pi(\mathbf{u}) \leq \Pi(\bar{\mathbf{u}})$, where \mathbf{u} is the true solution and $\bar{\mathbf{u}}$ is any admissible displacement field. The equality holds only if $\mathbf{u} = \bar{\mathbf{u}}$.

The difference between the principle of virtual displacements and the principle of minimum total potential energy is that, in the latter, a constitutive law is invoked. Thus, the principle of virtual displacements is more general and it applies to all material bodies independent of their constitutive behavior. The Euler–Lagrange equations resulting from the principle of virtual displacements are always in terms of the stresses or stress resultants, whereas those from the principle of minimum total potential energy are in terms of the strains or displacements.

The principle of minimum total potential energy for time-dependent problems is the same as Hamilton's principle, with the Lagrangian function of Eq. (2.2.21) being $L = K - \Pi$. We note that the principle becomes a stationary principle rather than a minimum principle due the addition of kinetic energy terms to the functional.

Example 2.2.3

Consider the Timoshenko beam theory of Example 2.2.2. For the static case, the principle of virtual displacements requires that

$$\delta W \equiv \delta W_I + \delta W_E$$

where δW_I and δW_E are given in Eq. (2.2.26). Thus, we have

$$0 = \int_0^L \left(N_{xx} \delta \varepsilon_{xx}^0 + M_{xx} \delta \varepsilon_{xx}^1 + Q_x \delta \gamma_{xz}^0 - q \delta w_0 \right) dx \quad (2.2.42)$$

Using the uniaxial constitutive relations

$$\sigma_{xx} = E \varepsilon_{xx} = E \left(\frac{\partial u_0}{\partial x} + z \frac{\partial \phi}{\partial x} \right), \quad \sigma_{xz} = G \gamma_{xz} = G \left(\phi + \frac{\partial w_0}{\partial x} \right) \quad (2.2.43)$$

the stress resultants N_{xx} , M_{xx} , and Q_x of Eq. (2.2.27) can be expressed in terms of the displacements (u_0, w_0, ϕ) as

$$N_{xx} = EA \frac{\partial u_0}{\partial x}, \quad M_{xx} = EI \frac{\partial \phi}{\partial x}, \quad Q_x = GAK_s \left(\phi + \frac{\partial w_0}{\partial x} \right) \quad (2.2.44)$$

where A denotes the area of cross section, I the moment of inertia, and K_s the shear correction coefficient of the beam.

Rewriting the statement in Eq. (2.2.42) in terms of the displacements, we obtain

$$0 = \int_0^L \left[EA \frac{\partial u_0}{\partial x} \frac{\partial \delta u_0}{\partial x} + EI \frac{\partial \phi}{\partial x} \frac{\partial \delta \phi}{\partial x} + GAK_s \left(\phi + \frac{\partial w_0}{\partial x} \right) \left(\delta \phi + \frac{\partial \delta w_0}{\partial x} \right) - q \delta w_0 \right] dx \quad (2.2.45)$$

The final step involves pulling the variational symbol out of the entire expression (2.2.45) by taking into consideration its operations on the dependent variables u_0 , w_0 and ϕ . We obtain

$$\begin{aligned} 0 &= \delta \int_0^L \left[\frac{EA}{2} \left(\frac{\partial u_0}{\partial x} \right)^2 + \frac{EI}{2} \left(\frac{\partial \phi}{\partial x} \right)^2 + \frac{GAK_s}{2} \left(\phi + \frac{\partial w_0}{\partial x} \right)^2 - qw_0 \right] dx \\ &= \delta \Pi(u_0, w_0, \phi) \end{aligned} \quad (2.2.46)$$

where Π is the total potential energy functional for the Timoshenko beam theory

$$\Pi = \int_0^L \left[\frac{EA}{2} \left(\frac{\partial u_0}{\partial x} \right)^2 + \frac{EI}{2} \left(\frac{\partial \phi}{\partial x} \right)^2 + \frac{GAK_s}{2} \left(\phi + \frac{\partial w_0}{\partial x} \right)^2 - qw_0 \right] dx \quad (2.2.47)$$

Thus, the principle of virtual displacements for the linear elastic case becomes the principle of minimum total potential energy, $\delta W = \delta \Pi = 0$.

2.3 Castigiano's Theorems

2.3.1 Theorem I

In Section 2.2, the principle of virtual displacements and its special case, the principle of minimum total potential energy, were used to derive governing equations of equilibrium or motion. The principle of virtual displacements for the static case can also be used to directly determine forces and displacements in structural members. Castigiano's Theorem I is a special case of the principle of virtual displacements to structures that allow representation of the displacement field as a linear combination of point displacements and known functions. A discussion of the method is presented below.

Suppose that the displacement field \mathbf{u} of the structure under consideration can be represented as a linear combination of n displacement parameters q_i and known functions of position $\phi_i(\mathbf{x})$

$$\mathbf{u} = \sum_{i=1}^n q_i \phi_i(\mathbf{x}) \quad (2.3.1)$$

Obviously, the representation in Eq. (2.3.1) is possible for only certain geometries. The displacement parameters q_1, q_2, \dots, q_n are called the *generalized displacements* of the structure. We further assume that the applied external resultant load vector \mathbf{F} on the structure can also be represented as a vector sum of point forces, called generalized forces, in the direction of the generalized displacements

$$\mathbf{F} = \sum_{i=1}^n F_i \hat{\mathbf{e}}_i \quad (2.3.2)$$

where $\hat{\mathbf{e}}_i$ is the unit vector along the generalized displacement q_i . Then the internal virtual work done by internal forces in moving through the virtual generalized displacements δq_i and external virtual work due to the applied point loads F_i in moving through the virtual generalized displacements δq_i are given by

$$\delta W_I = \int_v \sigma_{ij} \delta \varepsilon_{ij} dv = \delta U(q_1, q_2, \dots, q_n) \quad (2.3.3)$$

$$\delta W_E = -F_i \delta q_i \quad (2.3.4)$$

where summation on repeated subscripts is implied.

Now the principle of virtual displacements can be stated as

$$0 = \delta W = \delta W_I + \delta W_E = \left(\frac{\partial U}{\partial q_i} - F_i \right) \delta q_i \quad \text{or} \quad \frac{\partial U}{\partial q_i} = F_i \quad (2.3.5)$$

Equation (2.3.5) is known as Castigiano's Theorem I. Equation (2.3.5) can be used to determine generalized force F_i or displacement q_i in the structure.

Example 2.3.1

Consider the two-member truss shown in Figure 2.3.1(a). The members are made of linear elastic material and have the same geometric properties. We wish to

determine the horizontal displacement u_0 and vertical displacement v_0 of point O under horizontal point load Q and vertical point load P . We assume small strains and displacements.

For this problem, the strain energy U can be written in terms of the point displacements u_0 and v_0 directly (Figure 2.3.1(b)). The strains can be computed in terms of the displacements u_0 and v_0 from the deformed geometry of each member of the truss as follows:

$$\begin{aligned}\varepsilon^{(1)} &= \frac{1}{h} \left(\sqrt{(h+u_0)^2 + v_0^2} - h \right) = \sqrt{1 + 2\frac{u_0}{h}} - 1 \approx \frac{u_0}{h} \\ \varepsilon^{(2)} &= \frac{1}{\sqrt{2}h} \left(\sqrt{(h+u_0)^2 + (h-v_0)^2} - \sqrt{2}h \right) = \sqrt{1 + \frac{u_0 - v_0}{h}} - 1 \approx \frac{u_0 - v_0}{2h}\end{aligned}\quad (2.3.6)$$

where the squares of u_0 and v_0 were neglected due to the small strain assumption. The stresses are given by ($E^{(1)} = E^{(2)} = E$)

$$\sigma^{(1)} = E^{(1)}\varepsilon^{(1)} = E\frac{u_0}{h}, \quad \sigma^{(2)} = E^{(2)}\varepsilon^{(2)} = E\left(\frac{u_0 - v_0}{2h}\right) \quad (2.3.7)$$

The total strain energy of the structure is [see Eq. (2.2.35)]

$$\begin{aligned}U &= \frac{1}{2} \sum_{i=1}^2 \int_{A_i}^{L_i} \sigma^{(i)} \varepsilon^{(i)} dAdx = \frac{1}{2} \sum_{i=1}^2 A_i L_i E^{(i)} (\varepsilon^{(i)})^2 \\ &= \frac{EAh}{2} \left[\left(\frac{u_0}{h} \right)^2 + \sqrt{2} \left(\frac{u_0 - v_0}{2h} \right)^2 \right]\end{aligned}\quad (2.3.8)$$

Using Castigiano's Theorem I, we obtain

$$Q = \frac{\partial U}{\partial u_0} = EA \left[\frac{u_0}{h} + \sqrt{2} \left(\frac{u_0 - v_0}{4h} \right) \right] \quad (2.3.9)$$

$$P = \frac{\partial U}{\partial v_0} = -\sqrt{2}EA \left(\frac{u_0 - v_0}{4h} \right) \quad (2.3.10)$$

from which we obtain

$$u_0 = \frac{(Q+P)h}{AE}, \quad v_0 = \left[(1 + 2\sqrt{2})P + Q \right] \frac{h}{EA} \quad (2.3.11)$$

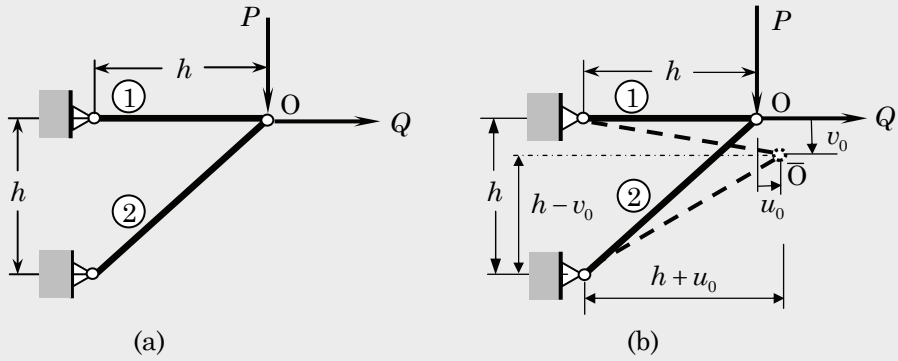


Figure 2.3.1 (a) Original truss. (b) Deformed truss (broken lines).

Example 2.3.2

We wish to determine the reactions and rotation at $x = 0$ of the beam shown in Figure 2.3.2. We assume small strains and displacements and use the Euler–Bernoulli beam theory (in which the energy due to transverse shear strain is neglected).

We assume that one can convert the distributed load $q(x)$ to statically equivalent point forces and moments, as will be shown shortly. Since these point forces and moments enter the expression for the work done by external forces V , we can take $q = 0$. Then the equilibrium equation is given by (2.2.13) with $k = 0$, $q = 0$, and M_{xx} [see Eq. (2.2.15)]

$$M_{xx} = \int_A z\sigma_{xx} dA = \int_A Ez\varepsilon_{xx} dA = -EI \frac{d^2w_0}{dx^2} \quad (2.3.12)$$

In terms of w_0 , Eq. (2.2.13) for the problem at hand reduces to

$$\frac{d^2}{dx^2} \left(EI \frac{d^2w_0}{dx^2} \right) = 0 \quad (2.3.13)$$

For constant EI , the general solution of this equation is

$$w_0(x) = c_1 + c_2x + c_3x^2 + c_4x^3 \quad (2.3.14)$$

where c_i ($i = 1, 2, 3, 4$) are constants of integration.

Next, we express the four constants c_i ($i = 1, 2, 3, 4$) in terms of the generalized displacements q_i . For pure bending of beams, the generalized displacements can be taken to be the transverse displacements q_1 and q_3 and rotations q_2 and q_4 at the two ends of a beam element, as shown in Figure 2.3.3(a). The associated generalized forces (which represent the reactions) are given by the transverse loads F_1 and F_3 and bending moments F_2 and F_4 , as shown in Figure 2.3.3(b).

The constants c_i now can be expressed in terms of the generalized displacements q_i as

$$\begin{aligned} q_1 &\equiv w_0(0) = c_1, \\ q_2 &\equiv \left(-\frac{dw_0}{dx} \right)_{x=0} = -c_2, \\ q_3 &\equiv w_0(L) = c_1 + c_2L + c_3L^2 + c_4L^3, \\ q_4 &\equiv \left(-\frac{dw_0}{dx} \right)_{x=L} = -c_2 - 2c_3L - 3c_4L^2 \end{aligned} \quad (2.3.15)$$

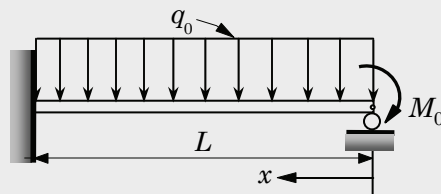


Figure 2.3.2 Indeterminate beam problem of Example 2.3.2.

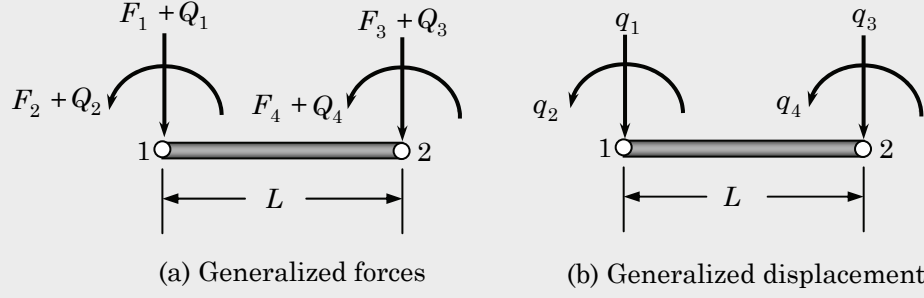


Figure 2.3.3 (a) Beam with end forces and moments (or generalized forces). (b) Generalized displacements.

These relations in Eq. (2.3.15) can be inverted to solve for q_i in terms of c_i . Then substituting the result into Eq. (2.3.14) yields

$$w_0(x) = \varphi_1(x)q_1 + \varphi_2(x)q_2 + \varphi_3(x)q_3 + \varphi_4(x)q_4 = \sum_{i=1}^4 \varphi_i(x) q_i \quad (2.3.16)$$

where

$$\begin{aligned} \varphi_1(x) &= 1 - 3\left(\frac{x}{L}\right)^2 + 2\left(\frac{x}{L}\right)^3, & \varphi_2(x) &= -x\left[1 - 2\left(\frac{x}{L}\right) + \left(\frac{x}{L}\right)^2\right] \\ \varphi_3(x) &= \left(\frac{x}{L}\right)^2\left(3 - 2\frac{x}{L}\right), & \varphi_4(x) &= x\frac{x}{L}\left(1 - \frac{x}{L}\right) \end{aligned} \quad (2.3.17)$$

Note the derivation of the expression in (2.3.16) is unique once we identify suitable generalized coordinates. Now the statically equivalent forces (Q_1, Q_3) and moments (Q_2, Q_4) due to the distributed load are computed using the formula

$$Q_i = \int_0^L q(x)\varphi_i(x) dx \quad (2.3.18)$$

We can write the strain energy U [see Eq. (2.2.39)] and potential energy V due to applied loads of an Euler–Bernoulli beam in terms of the generalized displacements q_i as

$$\begin{aligned} U &= \frac{1}{2} \int_0^L \int_A \sigma_{xx} \varepsilon_{xx} dA dx = \frac{1}{2} \int_0^L EI \left(\frac{d^2 w_0}{dx^2} \right)^2 dx \\ &= \frac{EI}{2} \int_0^L \left(\sum_{j=1}^4 \frac{d^2 \varphi_j}{dx^2} q_j \right)^2 dx \end{aligned} \quad (2.3.19)$$

$$\begin{aligned} V &= - \left[\int_0^L q(x)w_0(x) dx + \sum_{i=1}^4 F_i q_i \right] \\ &= - \left(\sum_{i=1}^4 q_i \int_0^L q(x)\varphi_i(x) dx + \sum_{i=1}^4 F_i q_i \right) = - \sum_{i=1}^4 (Q_i + F_i) q_i \end{aligned} \quad (2.3.20)$$

Castigliano's Theorem I (and the principle of minimum total potential energy, $(\partial U / \partial q_i) = -\partial V / \partial q_i$) gives

$$F_i + Q_i = \frac{\partial U}{\partial q_i} = \sum_{j=1}^4 \left(\int_0^L EI \frac{d^2 \varphi_j}{dx^2} \frac{d^2 \varphi_i}{dx^2} dx \right) q_j \equiv \sum_{j=1}^4 K_{ij} q_j \quad (2.3.21)$$

where

$$K_{ij} = \int_0^L EI \frac{d^2 \varphi_j}{dx^2} \frac{d^2 \varphi_i}{dx^2} dx, \quad i, j = 1, 2, \dots, 4 \quad (2.3.22)$$

Since $\varphi_i(x)$ are known from (2.3.17), K_{ij} can be evaluated exactly. Equations (2.3.21) can now be expressed as a set of matrix equations (recall that EI is assumed to be a constant)

$$\frac{2EI}{L^3} \begin{bmatrix} 6 & -3L & -6 & -3L \\ -3L & 2L^2 & 3L & L^2 \\ -6 & 3L & 6 & 3L \\ -3L & L^2 & 3L & 2L^2 \end{bmatrix} \begin{Bmatrix} q_1 \\ q_2 \\ q_3 \\ q_4 \end{Bmatrix} = \begin{Bmatrix} Q_1 \\ Q_2 \\ Q_3 \\ Q_4 \end{Bmatrix} + \begin{Bmatrix} F_1 \\ F_2 \\ F_3 \\ F_4 \end{Bmatrix} \quad (2.3.23)$$

Returning to the problem at hand, the known generalized displacements and generalized forces are

$$q_1 = q_2 = q_3 = 0, \quad F_4 = -M_0$$

In addition, the uniformly distributed load q_0 can be converted to statically equivalent load vector $\{Q\}$ by means of Eq. (2.3.20). We obtain

$$\{Q\}^T = \frac{q_0 L}{12} \{6 \ -L \ 6 \ L\} \quad (2.3.24)$$

Thus, of the four equations in (2.3.23), only the last equation contains only one unknown q_4 , the rotation (or slope) at $x = L$, and it can be easily solved for:

$$q_4 \equiv \left(-\frac{dw_0}{dx} \right)_{x=L} = \frac{L}{4EI} (Q_4 + F_4) = \frac{L}{4EI} \left(\frac{q_0 L^2}{12} - M_0 \right)$$

The reactions are now calculated from the first three equations of Eq. (2.3.23) as

$$\begin{aligned} F_1 &= -\frac{3}{L} \left(\frac{q_0 L^2}{12} - M_0 \right) - \frac{q_0 L}{2} = -\frac{3}{4} q_0 L + \frac{3}{L} M_0 \\ F_2 &= \frac{1}{2} \left(\frac{q_0 L^2}{12} - M_0 \right) + \frac{q_0 L^2}{12} = \frac{1}{8} q_0 L^2 - \frac{1}{2} M_0 \\ F_3 &= \frac{3}{2L} \left(\frac{q_0 L^2}{12} - M_0 \right) - \frac{q_0 L}{2} = -\frac{3}{8} q_0 L - \frac{3}{2L} M_0 \end{aligned}$$

This completes the example.

2.3.2 Theorem II

An equivalent procedure to that of Castigliano's Theorem I but based on the principle of minimum total complementary potential energy ($\delta\Pi^* = 0$ where $\Pi^* = U^* + V^*$) is known as Castigliano's Theorem II. The complementary strain energy and its variation are given by

$$U^* = \int_{\Omega} \left(\int_0^{\sigma_{ij}} \varepsilon_{ij} d\sigma_{ij} \right) dv, \quad \delta U^* = \int_{\Omega} \varepsilon_{ij} \delta \sigma_{ij} dv \quad (2.3.25)$$

where it is understood that the strains and stresses are known in terms of the generalized forces F_i . For linear elastic body, the complementary strain energy U^* is given by

$$U^* = \frac{1}{2} \int_{\Omega} \sigma_{ij} \varepsilon_{ij} dv \quad (2.3.26)$$

Although $U^* = U$ in value for a linear elastic body, U^* is expressed in terms of forces whereas U is expressed in terms of displacements. Then Castigliano's Theorem II requires that $(\partial U^*/\partial F_i = -\partial V^*/\partial F_i)$

$$\frac{\partial U^*}{\partial F_i} = q_i \quad (2.3.27)$$

Castigliano's Theorem II can be readily used for problems involving trusses and frames (i.e., bars and beams) to determine point forces and displacements. The problems considered in Examples 2.3.1 and 2.3.2 are used to illustrate the application of Castigliano's Theorem II.

Example 2.3.3

Consider the frame structure shown in Figure 2.3.4(a). We wish to determine the horizontal displacement u_0 and vertical displacement v_0 of point O due to the horizontal force Q and vertical force P .

Since the complementary strain energy U^* is written in terms of the forces, we must compute the member forces first. Using a section around joint O, the axial forces in each member are determined as (Figure 2.3.4(b))

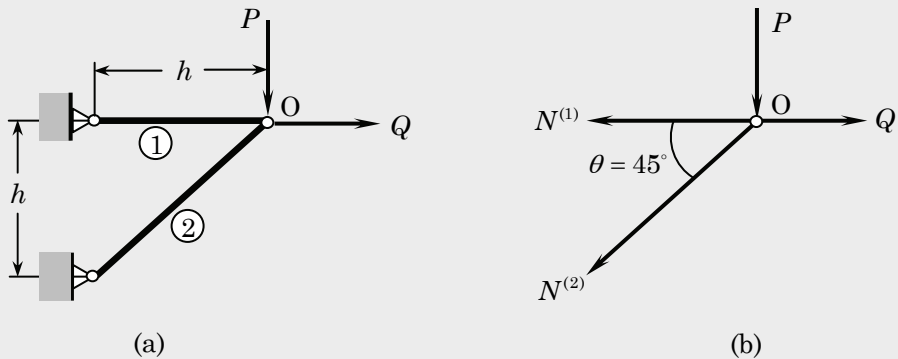


Figure 2.3.4 (a) Geometry and forces on the truss. (b) Member forces.

$$N^{(1)} + N^{(2)} \cos \theta = Q, \quad P + N^{(2)} \sin \theta = 0 \quad \rightarrow \quad N^{(1)} = P + Q, \quad N^{(2)} = -\sqrt{2}P$$

The complementary strain energy of the structure is given by

$$\begin{aligned} U^* &= \frac{1}{2} \sum_{i=1}^2 \int_{A_i} \int_0^{L_i} \sigma^{(i)} \varepsilon^{(i)} \, dA \, dx = \sum_{i=1}^2 \frac{A_i L_i}{2E_i} (\sigma^{(i)})^2 \\ &= \sum_{i=1}^2 \frac{L_i}{2E_i A_i} (N^{(i)})^2 = \frac{h}{2EA} [(P+Q)^2 + (-\sqrt{2}P)^2 \sqrt{2}] \end{aligned}$$

Using Castiglano's Theorem II, we obtain

$$u_0 = \frac{\partial U^*}{\partial Q} = \frac{(P+Q)h}{EA}, \quad v_0 = \frac{\partial U^*}{\partial P} = [(1+2\sqrt{2})P+Q] \frac{h}{EA}$$

which are the same as those obtained in Example 2.3.1.

Example 2.3.4

We wish to determine the reaction and rotation at $x = 0$ of the beam shown in Figure 2.3.5(a) using Castiglano's Theorem II.

The complementary strain energy due to bending of a beam is given by

$$\begin{aligned} U^* &= \frac{1}{2} \int_0^L \int_A \sigma_{xx} \varepsilon_{xx} \, dA \, dx = \frac{1}{2} \int_0^L \frac{1}{E} \int_A (\sigma_{xx})^2 \, dA \, dx \\ &= \frac{1}{2} \int_0^L \frac{1}{E} \int_A \left(-\frac{Mz}{I}\right)^2 \, dA \, dx = \frac{1}{2} \int_0^L \frac{M^2}{EI} \, dx \end{aligned} \quad (2.3.28)$$

where the result of Problem 2.1 is used to replace σ_{xx} in terms of the bending moment $M(x)$ ($N = 0$), which for the beam at hand is (Figure 2.3.5(b))

$$M(x) = \frac{1}{2}q_0x^2 + M_0 - F_0x, \quad 0 < x < L$$

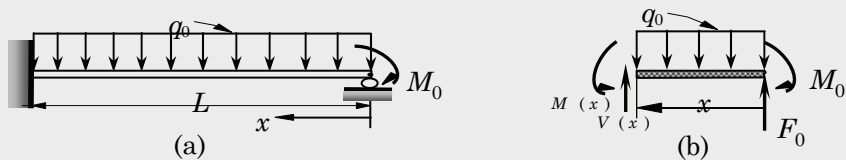


Figure 2.3.5 Indeterminate beam problem of Example 2.3.4.

Then U^* is given by

$$U^* = \frac{1}{2EI} \int_0^L \left(\frac{1}{2}q_0x^2 + M_0 - F_0x \right)^2 dx$$

Use of Castiglano's Theorem II gives

$$\begin{aligned}\theta_0 &= \frac{\partial U^*}{\partial M_0} = \frac{1}{EI} \int_0^L \left(\frac{1}{2}q_0x^2 + M_0 - F_0x \right) (1) dx = \frac{q_0L^3}{6EI} + \frac{M_0L}{EI} - \frac{F_0L^2}{2EI} \\ w_0 &= \frac{\partial U^*}{\partial F_0} = \frac{1}{EI} \int_0^L \left(\frac{1}{2}q_0x^2 + M_0 - F_0x \right) (-x) dx = \frac{q_0L^4}{8} + \frac{M_0L^2}{2} - \frac{F_0L^3}{3}\end{aligned}$$

where θ_0 is the rotation and w_0 is the deflection (which is zero) at point $x = 0$ (both in the direction of their respective force and moment). Thus, we have

$$F_0 = \frac{3}{8}q_0L + \frac{3}{2L}M_0, \quad \theta_0 = -\frac{1}{48}q_0L^3 + \frac{1}{4}M_0L$$

These results are the same as those obtained for $-q_4$ and $-F_4$ in Example 2.3.2. The sign difference is due to the convention adopted for the generalized displacements in Figure 2.3.3.

2.4 Variational Methods

2.4.1 Introduction

In Section 2.2, we have seen how the principles of virtual work and minimum total potential energy can be used to obtain governing differential equations and associated natural boundary conditions. Then in Section 2.3, Castiglano's theorems were used to determine exact values of deflections and forces at selective points. In this section, we study the use of the energy principles, $\delta W = 0$ or $\delta \Pi = 0$, in the solution of the underlying equations of these statements. The methods to be described here are known as the *classical* variational methods. In these methods, we seek an approximate solution to the problem in terms of *adjustable* parameters that are determined by substituting the assumed solution into the energy principle that is equivalent to the governing equations of the problem. Such solution methods are called *direct methods* because the approximate solutions are obtained directly by applying the same energy principle that was used to derive the governing equations. In the energy methods, we seek solution over the total domain and, therefore, the methods yield continuous solutions throughout the domain.

The assumed solutions in the energy methods are in the form of a finite linear combination of undetermined parameters and appropriately chosen functions. Since the solution of a continuum problem, in general, cannot be represented by a finite set of functions, error is introduced into the solution. Therefore, the solution obtained is an approximation to the true solution of the equations describing the problem. As the number of linearly independent terms in the assumed solution is increased, the error in the approximation will be reduced and the assumed solution converges to the exact solution, provided certain conditions are met by the assumed solution.

The energy methods of approximation to be described here are limited to the Ritz method and the Galerkin method. Readers may consult the references [see, for example, Reddy (2002)] in the back of the book for additional details.

2.4.2 The Ritz Method

The Ritz method is based on an energy or variational principle, such as those provided by the principles of virtual work or their variants, that account for the natural boundary conditions as a part of the principle. In the Ritz method, a dependent unknown (e.g., the displacement) u is approximated by a finite linear combination U_N of the form

$$u \approx U_N = \sum_{j=1}^N c_j \varphi_j + \varphi_0 \quad (2.4.1)$$

and then determine the parameters c_j by requiring that the principle of virtual displacements or the principle of minimum total potential energy hold for the approximate problem. In Eq. (2.4.1), φ_0 represents the particular solution, while $\sum c_j \varphi_j$ is the homogeneous part of the solution. Here c_j denote undetermined parameters, and φ_j are called the *approximation functions*, which are appropriately selected functions of position, as discussed next.

Properties of Approximation Functions

In order to ensure that the algebraic equations resulting from the Ritz approximation have a solution and that the approximate solution converges to the true solution of the problem as the number of parameters N is increased, we must choose φ_j ($j = 1, 2, 3, \dots, N$) and φ_0 such that they meet certain requirements. Formal definitions of convergence and completeness require a background in functional analysis [see Reddy (1992)] and, therefore, we give some elementary and intuitive definitions of these concepts.

Convergence. A sequence $\{U_N\}$ of functions is said to *converge* to u_0 if for each $\epsilon > 0$ there is a number $M > 0$, depending on ϵ , such that

$$\|U_N(\mathbf{x}) - u_0(\mathbf{x})\| < \epsilon \quad \text{for all } N > M \quad (2.4.2)$$

where $\|\cdot\|$ denotes a *norm* or measure of the magnitude of the enclosed quantity and u_0 is called the limit of the sequence. An example of the norm of a function $u(\mathbf{x})$ with \mathbf{x} in the domain Ω is provided by

$$\|u\|^2 = \int_{\Omega} |u(\mathbf{x})|^2 d\mathbf{x} \quad (2.4.3)$$

In the above statement, U_N can be thought of as the approximate solution and u_0 as the true solution. The statement implies that the N -parameter approximate solution U_N can be made as close to u_0 as we wish, say within ϵ , by choosing N to be greater than $M = M(\epsilon)$, provided that the approximate solution is convergent. While there is no formula to determine M , a series of trials will help determine the value of N for which the approximate solution U_N is within the tolerance.

Completeness. The concept of convergence of a sequence involves a limit of the sequence. If the limit is not a part of the sequence $\{U_N\}_{N=1}^{\infty}$, then there is no hope of attaining convergence. For example, if the true solution to a certain problem is of the form $u_0(x) = ax^2 + bx^3$, where a and b are constants, then the sequence of approximations

$$U_1 = c_1 x^3, \quad U_2 = c_1 x^3 + c_2 x^4, \quad \dots, \quad U_N = c_1 x^3 + c_2 x^4 + \dots + c_N x^{N+2}$$

will not converge to the true solution because the sequence does not contain the x^2 term. The sequence is said to be incomplete. As a rule, in selecting an approximate solution one should include all admissible terms up to the desired highest order term.

Linear Independence. If a function U can be expressed as $U = \sum c_i \varphi_i$, where c_i are real numbers, we say that U is a *linear combination* of φ_i 's. An expression of the form $\sum c_i \varphi_i = 0$ is called a *linear relation* among the φ_i 's. A linear relation with all $c_i = 0$ is called a *trivial linear relation*. If at least one c_i is nonzero, the relation is called a *nontrivial relation*. A set of vectors $\{\varphi_i\}$ is said to be *linearly independent* if there exists no nontrivial relation among them. In other words, no φ_i is expressible in terms of others in the set.

We now list the requirements of a convergent Ritz approximation (2.4.1):

1. $\varphi_j (j = 1, 2, \dots, N)$ should satisfy the following three conditions:
 - (a) Each φ_j is *continuous*, as is required in the variational statement (i.e., $\delta W = 0$ or $\delta \Pi = 0$); i.e., φ_j should be such that U_N has a nonzero contribution.
 - (b) Each φ_j satisfies the *homogeneous form* of the specified essential boundary conditions.
 - (c) The set $\{\varphi_j\}$ is *linearly independent* and *complete*.
2. φ_0 has the primary role of satisfying the specified *essential* (or geometric) boundary conditions associated with the variational formulation; φ_0 plays the role of the *particular solution*. It is necessarily zero when the specified essential boundary conditions are homogeneous.

For polynomial approximations functions, the linear independence and completeness properties require φ_j to be increasingly higher-order polynomials. For example, if φ_1 is a linear polynomial, φ_2 should be a quadratic polynomial, φ_3 should be a cubic polynomial, and so on (but each φ_j need not be a complete polynomial by itself). The completeness property is essential for the convergence of the Ritz approximation [see Reddy (1992), p. 262].

Since the natural boundary conditions of the problem are included in the functional Π or the statement $\delta W = 0$, we require the Ritz approximation U_N to satisfy only the specified essential boundary conditions of the problem. This is done by selecting φ_0 to satisfy the essential boundary conditions and φ_i to satisfy the homogeneous form of the essential boundary conditions. For instance, if u is specified to be \hat{u} at a point $\mathbf{x} = \mathbf{x}_0$, then using $U_N(\mathbf{x}_0) = \hat{u}$ and $\varphi_0(\mathbf{x}_0) = \hat{u}$ in

$$u(\mathbf{x}_0) \approx U_N(\mathbf{x}_0) = \sum_{j=1}^N c_j \varphi_j(\mathbf{x}_0) + \varphi_0(\mathbf{x}_0)$$

one may conclude that

$$\sum_{j=1}^N c_j \varphi_j(\mathbf{x}_0) = 0$$

Since the above condition must hold for any independent set of parameters c_j , it follows that

$$\varphi_j(\mathbf{x}_0) = 0 \quad \text{for } j = 1, 2, \dots, N \quad (2.4.4)$$

The requirements on φ_j provide guidelines for selecting the coordinate functions; they do not give any formula for generating the functions. As a general rule, coordinate functions should be selected from a set of linearly independent functions from the lowest order to a desired order without missing any intermediate admissible functions in the representation of U_N (i.e., satisfy the completeness property). The function φ_0 has no other role to play than to satisfy specified (nonhomogeneous) essential boundary conditions; there are no continuity conditions on φ_0 . Therefore, one should select the lowest order φ_0 that satisfies the specified essential boundary conditions. When all of the specified essential boundary conditions are homogeneous, then $\varphi_0 = 0$.

Ritz Equations for the Parameters

Once the approximation functions φ_0 and φ_i are selected, the parameters c_j in Eq. (2.4.1) are determined by requiring U_N to minimize the total potential energy functional Π or satisfy the principle of virtual displacements of the problem. First consider the principle of minimum total potential energy. Upon substitution of the approximation $u \approx U_N$, $\Pi(U_N)$ becomes a function of c_1, c_2, \dots, c_N . Hence, minimization of the functional $\Pi(c_1, c_2, \dots, c_N)$ is reduced to the minimization of a function of several variables:

$$0 = \delta\Pi(U_N) = \sum_{i=1}^N \frac{\partial\Pi}{\partial c_i} \delta c_i \quad \text{or} \quad \frac{\partial\Pi}{\partial c_i} = 0 \quad (2.4.5)$$

The same procedure applies to the principle of virtual displacements. We have

$$0 = \delta W(U_N) = \sum_{i=1}^N \delta c_i W = \sum_{i=1}^N \frac{\partial W}{\partial c_i} \delta c_i \quad \text{or} \quad \frac{\partial W}{\partial c_i} = 0$$

which is the same as Eq. (2.4.5).

Equation (2.4.5) gives N algebraic equations in the N coefficients (c_1, c_2, \dots, c_N) ,

$$0 = \frac{\partial\Pi}{\partial c_i} = \sum_{j=1}^N R_{ij} c_j - F_i \quad \text{or} \quad \mathbf{R}\mathbf{c} = \mathbf{F} \quad (2.4.6)$$

where R_{ij} and F_i are known coefficients that depend on the problem parameters (e.g., geometry, material coefficients, and loads) and the approximation functions. These coefficients will be defined for each problem discussed in the sequel. Equation (2.4.6) is then solved for c_i and substituted back into Eq. (2.4.1) to obtain the N parameter Ritz solution. Some general features of the Ritz method are noted next.

1. If the coordinate functions φ_i are selected to satisfy the required conditions, the assumed approximation for the displacements converges to the true solution with an increase in the number of parameters (i.e., as $N \rightarrow \infty$). A mathematical proof of such an assertion can be found in Reddy (1992).
2. For increasing values of N , the previously computed coefficients of the algebraic equations (2.4.6) remain unchanged, provided the previously selected coordinate functions are not changed. One must add only the newly computed coefficients to the system of equations.
3. If the resulting algebraic equations are symmetric, one needs to compute only upper or lower diagonal elements in the coefficient matrix \mathbf{R} . For all problems considered here, the coefficient matrix is symmetric whenever the principles of virtual displacements or the minimum total potential energy are used.
4. If the variational (or virtual work) statement is nonlinear in u , then the resulting algebraic equations are also nonlinear in the parameters c_i . To solve such nonlinear equations, a variety of iterative methods are available; see Chapter 12.
5. Since the strains are computed from an approximate displacement field, the strains and stresses are generally less accurate than the displacements.
6. The equilibrium equations of the problem are satisfied only in the energy sense, not in the differential equation sense. Therefore, the displacements obtained from the Ritz approximation in general do not satisfy the equations of equilibrium point-wise, unless the solution converged to the exact solution.
7. Since a continuous system is approximated by a finite number of coordinates (or degrees of freedom), the approximate system is less flexible than the actual system. Consequently, the displacements obtained using the principle of minimum total potential energy and the Ritz method converge to the exact displacements from below:

$$U_1 < U_2 < \dots < U_N < U_M \dots < u(\text{exact}), \quad \text{for } M > N$$

where U_N denotes the N parameter Ritz approximation of u obtained from the principle of virtual displacements or the minimum total potential energy principle. It should be noted that the displacements obtained from the Ritz method based on the total complementary energy principle provide the upper bound.

8. The Ritz method can be applied, in principle, to any physical problem that can be cast in a *weak form* – a form that contains the natural boundary conditions of the problem. The principles of virtual displacements ($\delta W = 0$) and minimum total potential energy ($\delta\Pi = 0$) provide the weak forms directly. In particular, the Ritz method can be applied to all structural problems, linear or nonlinear, because the principle of virtual displacements applies to all problems.

Example 2.4.1

Consider axial deformation of an isotropic, elastic, nonuniform cross section bar of length L , fixed at $x = 0$ and subjected to an axial force P_0 at $x = L$ (Figure 2.4.1). In addition, suppose that the bar experiences a body force $f(x)$. We wish to determine the axial displacement $u(x)$ using the Ritz method.

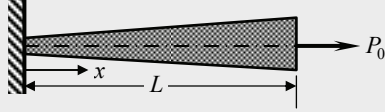


Figure 2.4.1 Axial deformation of a bar with an end load.

First, we write the boundary conditions of the problem:

$$u(0) = 0, \quad \left(EA \frac{du}{dx} \right)_{x=L} = P_0 \quad (2.4.7)$$

where E is the modulus and A is the area of cross section of the bar. The first one is a geometric (essential) boundary condition, while the second one is a force (natural) boundary condition. The principle of virtual displacements for the problem at hand can be written as

$$0 = \int_0^L \left(EA \frac{du}{dx} \frac{d\delta u}{dx} - f \delta u \right) dx - P_0 \delta u(L) \quad (2.4.8)$$

and the total potential energy of the bar is

$$\Pi(u) = \int_0^L \left[\frac{EA}{2} \left(\frac{du}{dx} \right)^2 - fu \right] dx - P_0 u(L) \quad (2.4.9)$$

The expression in Eq. (2.4.8) is equivalent to the statement $\delta\Pi = 0$.

Substituting

$$u \approx U_n = \sum_{j=1}^n c_j \varphi_j(x) + \varphi_0(x) \quad (2.4.10)$$

into the statement (2.4.8), we obtain

$$\begin{aligned} 0 &= \int_0^L \left[EA \left(\sum_{j=1}^n c_j \frac{d\varphi_j}{dx} + \frac{d\varphi_0}{dx} \right) \left(\sum_{i=1}^n \delta c_i \frac{d\varphi_i}{dx} \right) - f \left(\sum_{i=1}^n \delta c_i \varphi_i \right) \right] dx \\ &\quad - P_0 \left(\sum_{i=1}^n \delta c_i \varphi_i(L) \right) \end{aligned}$$

or

$$\begin{aligned} 0 &= \sum_{i=1}^n \delta c_i \left\{ \sum_{j=1}^n \left(\int_0^L EA \frac{d\varphi_i}{dx} \frac{d\varphi_j}{dx} dx \right) c_j + \int_0^L EA \frac{d\varphi_0}{dx} \frac{d\varphi_i}{dx} dx \right. \\ &\quad \left. - \int_0^L f \varphi_i dx - P_0 \varphi_i(L) \right\} = \sum_{i=1}^n \delta c_i \left\{ \sum_{j=1}^n R_{ij} c_j - F_i \right\} \end{aligned}$$

where

$$R_{ij} = \int_0^L EA \frac{d\varphi_i}{dx} \frac{d\varphi_j}{dx} dx, \quad F_i = \int_0^L f \varphi_i dx + P_0 \varphi_i(L) - \int_0^L EA \frac{d\varphi_0}{dx} \frac{d\varphi_i}{dx} dx$$

Since δc_i are arbitrary and linearly independent, we can write

$$0 = \sum_{j=1}^n R_{ij} c_j - F_i \quad \text{or} \quad \mathbf{R} \mathbf{c} = \mathbf{F} \quad (2.4.11)$$

The result in Eq. (2.4.11) can also be obtained from the principle of minimum total potential energy. Substituting Eq. (2.4.10) into Eq. (2.4.9), we obtain

$$\begin{aligned} \Pi = & \frac{1}{2} \int_0^L \left[EA \left(\sum_{j=1}^n c_j \frac{d\varphi_j}{dx} + \frac{d\varphi_0}{dx} \right) \left(\sum_{i=1}^n c_i \frac{d\varphi_i}{dx} + \frac{d\varphi_0}{dx} \right) \right. \\ & \left. - f \left(\sum_{i=1}^n c_i \varphi_i \right) \right] dx - P_0 \left(\sum_{i=1}^n c_i \varphi_i(L) \right) \end{aligned}$$

Thus, Π is a function of c_1, c_2, \dots, c_n , and a necessary condition for its minimum is

$$0 = \sum_{i=1}^n \frac{\partial \Pi}{\partial c_i} \delta c_i \quad \text{or} \quad \frac{\partial \Pi}{\partial c_i} = 0 \quad (i = 1, 2, \dots, n)$$

and

$$\frac{\partial \Pi}{\partial c_i} = \sum_{j=1}^n \left(\int_0^L EA \frac{d\varphi_i}{dx} \frac{d\varphi_j}{dx} dx \right) c_j + \int_0^L EA \frac{d\varphi_0}{dx} \frac{d\varphi_i}{dx} dx - \int_0^L f \varphi_i dx - P_0 \varphi_i(L)$$

which is the same as Eq. (2.4.11).

Since the specified geometric boundary condition is homogeneous, we have $\varphi_0 = 0$. The approximation functions $\varphi_i(x)$ must satisfy the condition $\varphi_i(0) = 0$. Clearly, $\varphi_i(x) = x^i$ satisfies the condition and it has a nonzero first derivative, as required in Eqs. (2.4.8) or (2.4.9). Thus, we have (the approximation functions are made nondimensional)

$$\varphi_0 = 0, \quad \varphi_i = \left(\frac{x}{L} \right)^i, \quad \frac{d\varphi_i}{dx} = \frac{i}{L} \left(\frac{x}{L} \right)^{i-1}$$

In addition, suppose that the modulus E is constant, the area of cross section A varies as $A = A_0 + (x/L)A_1$, and the body force varies as $f(x) = f_0 + (x/L)f_1$. Then

$$\begin{aligned} R_{ij} &= \int_0^L E \left(A_0 + \frac{x}{L} A_1 \right) \frac{ij}{L^2} \left(\frac{x}{L} \right)^{i+j-2} dx \\ &= \frac{E}{L} \left[\left(\frac{ij}{i+j-1} \right) A_0 + \left(\frac{ij}{i+j} \right) A_1 \right] \\ F_i &= \int_0^L \left(f_0 + \frac{x}{L} f_1 \right) \left(\frac{x}{L} \right)^i dx + P_0 = L \left(\frac{f_0}{i+1} + \frac{f_1}{i+2} \right) + P_0 \quad (2.4.12) \end{aligned}$$

In particular, we choose, for example, $A_0 = 2a_0$, $A_1 = -a_0$, and $f_1 = 0$, we obtain

$$R_{ij} = \frac{Ea_0}{L} \frac{ij(1+i+j)}{(i+j-1)(i+j)}, \quad F_i = \frac{f_0 L}{i+1} + P_0$$

For two-parameter approximation ($n = 2$), we obtain

$$\frac{Ea_0}{6L} \begin{bmatrix} 9 & 8 \\ 8 & 10 \end{bmatrix} \begin{Bmatrix} c_1 \\ c_2 \end{Bmatrix} = \frac{f_0 L}{6} \begin{Bmatrix} 3 \\ 2 \end{Bmatrix} + P_0 \begin{Bmatrix} 1 \\ 1 \end{Bmatrix} \quad (2.4.13)$$

$$c_1 = \frac{7f_0 L^2 + 6P_0 L}{13Ea_0}, \quad c_2 = \frac{3(P_0 L - f_0 L^2)}{13Ea_0}$$

$$u_2(x) = \frac{7f_0 L^2 + 6P_0 L}{13Ea_0} \left(\frac{x}{L} \right) + \frac{3(P_0 L - f_0 L^2)}{13Ea_0} \left(\frac{x^2}{L^2} \right) \quad (2.4.14)$$

The exact solution is

$$u(x) = \frac{f_0 L}{Ea_0} x + \frac{2f_0 L^2}{Ea_0} \log\left(1 - \frac{x}{2L}\right) + \frac{(f_0 L - P_0)L}{Ea_0} \log\left(1 - \frac{x}{2L}\right) \quad (2.4.15)$$

Table 2.4.1 contains comparison of the Ritz coefficients $\bar{c}_i = c_i P_0 L / Ea_0$ and the end deflection $\bar{u}(L) = (P_0 L / Ea_0) u(L) = \bar{c}_1 + \bar{c}_2 + \dots + \bar{c}_n$ for $n = 1, 2, \dots, 5$ with the exact coefficients and solution from the expansion (for $f = 0$)

$$u(x) = -\frac{P_0 L}{Ea_0} \log\left(1 - \frac{x}{2L}\right) \approx \frac{P_0 L}{Ea_0} \left(\frac{1}{2} \frac{x}{L} + \frac{1}{8} \frac{x^2}{L^2} + \frac{1}{24} \frac{x^3}{L^3} + \frac{1}{64} \frac{x^4}{L^4} + \dots \right) \quad (2.4.16)$$

Clearly, the Ritz solution converges to the exact solution as n increases. This completes the example.

Table 2.4.1 The Ritz coefficients* and the end deflection for the axial deformation of a nonuniform, isotropic bar fixed at $x = 0$ and subjected to force P_0 at $x = L$.

n	\bar{c}_1	\bar{c}_2	\bar{c}_3	\bar{c}_4	\bar{c}_5	$\bar{u}(L)$
1	0.6667					0.6667
2	0.4615	0.2308				0.6923
3	0.5079	0.0794	0.1058			0.6931
4	0.4984	0.1402	0.0000	0.0545		0.6931
5	0.5003	0.1206	0.0610	-0.0187	0.0299	0.6931
Exact	0.5000	0.1250	0.0416	0.0156	0.0062	0.6931

* $\bar{c}_i = c_i (P_0 L / Ea_0)$, $\bar{u}(L) = u(L) (P_0 L / Ea_0)$.

Example 2.4.2

This example is concerned with the study of the dynamic response (i.e., both natural vibration and transient response) of bars. Consider a uniform cross-section bar of length L with the left end fixed and the right end connected to a rigid support via a linear elastic spring with spring constant k (Figure 2.4.2). In addition, the member is subjected to a body force $f(x, t)$. The kinetic and potential energies associated with the axial motion of the member are given by

$$\begin{aligned} K &= \int_0^L \frac{\rho A}{2} \left(\frac{\partial u}{\partial t} \right)^2 dx \\ U &= \int_0^L \frac{EA}{2} \left(\frac{\partial u}{\partial x} \right)^2 dx + \frac{k}{2} [u(L, t)]^2 \\ V &= - \int_0^L f u dx \end{aligned} \quad (2.4.17)$$

Substituting for K , U , and V from Eq. (2.4.17) in Hamilton's principle, we obtain

$$\begin{aligned} 0 &= \delta \int_0^{t_0} (K - U - V) dt \\ &= \delta \int_0^{t_0} \left\{ \int_0^L \left[\frac{\rho A}{2} \left(\frac{\partial u}{\partial t} \right)^2 - \frac{EA}{2} \left(\frac{\partial u}{\partial x} \right)^2 + fu \right] dx - \frac{k}{2} [u(L, t)]^2 \right\} dt \end{aligned} \quad (2.4.18)$$

The Euler–Lagrange equations associated with Eq. (2.4.18) are

$$\frac{\partial}{\partial x} \left(EA \frac{\partial u}{\partial x} \right) - \frac{\partial}{\partial t} \left(\rho A \frac{\partial u}{\partial t} \right) + f = 0, \quad 0 < x < L; \quad t > 0 \quad (2.4.19)$$

$$\left. \left(EA \frac{\partial u}{\partial x} + ku \right) \right|_{x=L} = 0 \quad \text{for all } t \geq 0 \quad (2.4.20)$$

Natural Vibration

First, suppose that we are interested in finding the periodic motion (or natural vibration, $f = 0$) of the form

$$u(x, t) = u_0(x) e^{i\omega t}, \quad i = \sqrt{-1} \quad (2.4.21)$$

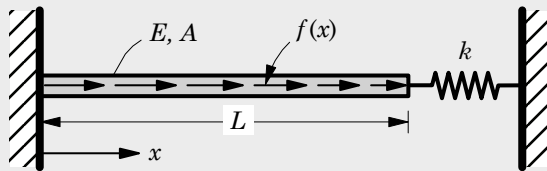


Figure 2.4.2 Axial deformation of a bar with an end spring.

where ω denotes the *frequency* of natural vibration and $u_0(x)$ is the amplitude. Substituting Eq. (2.4.21) into Eqs. (2.4.19) and (2.4.20), we obtain

$$\frac{d}{dx} \left(EA \frac{du_0}{dx} \right) + \rho A \omega^2 u_0 = 0, \quad 0 < x < L \quad (2.4.22)$$

$$\left(EA \frac{du_0}{dx} + k u_0 \right)_{x=L} = 0 \quad (2.4.23)$$

The variational statement (or weak form) associated with Eqs. (2.4.22) and (2.4.23) is given by

$$\begin{aligned} 0 &= \int_0^L \delta u_0 \left[\frac{d}{dx} \left(EA \frac{du_0}{dx} \right) + \rho A \omega^2 u_0 \right] \\ &= \int_0^L \left(-EA \frac{d\delta u_0}{dx} \frac{du_0}{dx} + \rho A \omega^2 \delta u_0 u_0 \right) dx - k \delta u_0(L) u_0(L) \end{aligned} \quad (2.4.24)$$

We use Eq. (2.4.24) and the Ritz method to determine the values of ω . The continuum system described by Eqs. (2.4.22) and (2.4.23) have an infinite number of frequencies. Any approximate method reduces a continuum problem to a discrete problem, which has a finite number of degrees of freedom and, hence, a finite number of frequencies. The number of natural frequencies obtainable by the Ritz method is equal to the number of parameters n . It is convenient to introduce nondimensional variables, $\bar{x} = x/L$ and $\bar{u} = u_0/L$. Then, we obtain

$$0 = \int_0^1 \left(\lambda \delta \bar{u} \bar{u} - \frac{d\delta \bar{u}}{dx} \frac{d\bar{u}}{dx} \right) dx - \mu \delta \bar{u}(1) \bar{u}(1) \quad (2.4.25)$$

where

$$\mu = \frac{kL}{EA}, \quad \lambda = \frac{\omega^2 \rho L^2}{E} \quad (2.4.26)$$

Following the procedure outlined in the previous example, we select (based on the condition $\varphi_i(0) = 0$)

$$\varphi_0 = 0, \quad \varphi_1 = x, \quad \varphi_2 = x^2, \quad \dots, \quad \varphi_N = x^N \quad (2.4.27)$$

Substituting $\bar{u} \approx \sum_{j=1}^N c_j x^j$ into Eq. (2.4.25), we obtain

$$\begin{aligned} 0 &= \int_0^1 \left[\lambda \left(\sum_{i=1}^N \delta c_i \varphi_i \right) \left(\sum_{j=1}^N c_j \varphi_j \right) - \left(\sum_{i=1}^N \delta c_i \frac{d\varphi_i}{dx} \right) \left(\sum_{j=1}^N c_j \frac{d\varphi_j}{dx} \right) \right] dx \\ &\quad - \mu \left(\sum_{i=1}^N \delta c_i \varphi_i(1) \right) \left(\sum_{j=1}^N c_j \varphi_j(1) \right) \\ &= \sum_{i=1}^n \delta c_i \left\{ \sum_{j=1}^N \left[\int_0^1 \left(\lambda \varphi_i \varphi_j - \frac{d\varphi_i}{dx} \frac{d\varphi_j}{dx} \right) dx - \mu \varphi_i(1) \varphi_j(1) \right] c_j \right\} \end{aligned}$$

Since δc_i are arbitrary and linearly independent, we obtain

$$0 = \sum_{j=1}^N (\lambda M_{ij} - R_{ij}) c_j \quad \text{or} \quad (\lambda[M] - [R])\{c\} = \{0\} \quad (2.4.28)$$

where

$$\begin{aligned} M_{ij} &= \int_0^1 \varphi_i \varphi_j \, dx = \frac{1}{i+j+1} \\ R_{ij} &= \int_0^1 \frac{d\varphi_i}{dx} \frac{d\varphi_j}{dx} \, dx + \mu \varphi_i(1) \varphi_j(1) = \frac{ij}{i+j-1} + \mu \end{aligned} \quad (2.4.29)$$

For $N = 2$, we have

$$\begin{aligned} M_{11} &= \frac{1}{3}, \quad M_{12} = M_{21} = \frac{1}{4}, \quad M_{22} = \frac{1}{5} \\ R_{11} &= 1 + \mu, \quad R_{12} = R_{21} = 1 + \mu = \frac{4}{3} + \mu \\ \left(\begin{bmatrix} 1+\mu & 1+\mu \\ 1+\mu & \frac{4}{3}+\mu \end{bmatrix} - \lambda \begin{bmatrix} \frac{1}{3} & \frac{1}{4} \\ \frac{1}{4} & \frac{1}{5} \end{bmatrix} \right) \begin{Bmatrix} c_1 \\ c_2 \end{Bmatrix} &= \begin{Bmatrix} 0 \\ 0 \end{Bmatrix} \end{aligned} \quad (2.4.30)$$

A nontrivial solution ($c_1 \neq 0, c_2 \neq 0$) to Eq. (2.4.30) exists only if the determinant of the coefficients matrix is zero:

$$\begin{vmatrix} 1 + \mu - \frac{\lambda}{3} & 1 + \mu - \frac{\lambda}{4} \\ 1 + \mu - \frac{\lambda}{4} & \frac{4}{3} + \mu - \frac{\lambda}{5} \end{vmatrix} = 0$$

For $\mu = 1$, we obtain

$$\frac{2}{3} - \frac{8}{45}\lambda + \frac{1}{240}\lambda^2 = 0 \quad \text{or} \quad 15\lambda^2 - 640\lambda + 2400 = 0$$

whose roots are

$$\lambda_1 = \frac{64}{3} - \frac{4}{3}\sqrt{166} \approx 4.155, \quad \lambda_2 = \frac{64}{3} + \frac{4}{3}\sqrt{166} \approx 38.512$$

and the first two natural frequencies are [$\omega = (1/L)\sqrt{E\lambda/\rho}$]

$$\omega_1 = \frac{2.038}{L} \sqrt{\frac{E}{\rho}}, \quad \omega_2 = \frac{6.206}{L} \sqrt{\frac{E}{\rho}}$$

The exact values of λ (with $\mu = 1$) are the roots of the transcendental equation

$$\lambda + \tan \lambda = 0 \quad (2.4.31)$$

whose first two roots are

$$\omega_1 = \frac{2.029}{L} \sqrt{\frac{E}{\rho}}, \quad \omega_2 = \frac{4.913}{L} \sqrt{\frac{E}{\rho}}$$

Transient Response

Here we are interested in determining the time-dependent solution $u_0(x, t)$ of Eqs. (2.4.19) and (2.4.20) under applied load $f(x, t)$. For simplicity of calculation, we introduce the following nondimensional variables:

$$\bar{x} = \frac{x}{L}, \quad u = \frac{u_0}{(f_0 L^2 / EA)}, \quad \bar{t} = \frac{t}{L\sqrt{\rho/E}}, \quad \bar{f} = \frac{f}{f_0} \quad (\text{a})$$

where f_0 is a constant. In the following discussion omit the bar over x and t . The statement in Eq. (2.4.18) takes the form

$$0 = - \int_0^T \left[\int_0^1 \left(\delta u \frac{\partial^2 u}{\partial t^2} + \frac{\partial \delta u}{\partial x} \frac{\partial u}{\partial x} \right)^2 - \bar{f} \delta u \right] dx + \bar{k} \delta u(1, t) u(1, t) dt \quad (\text{b})$$

where the first term of Eq. (2.4.18) was integrated by parts in time to relieve δu of any time derivatives, and $\bar{k} = k f_0 L^2 / EA$.

The Ritz approximation is sought in the form

$$u(x, t) \approx \sum_{j=1}^n c_j(t) \varphi_j(x) + \varphi_0(x) \quad (2.4.32)$$

where c_j are now time-dependent parameters to be determined for all times $t > 0$. Note that the Ritz approximation is used only in space to obtain ordinary differential equations among the parameters c_j , which must be solved using a suitable method. Substituting (2.4.32) into Eq. (b), we obtain

$$\begin{aligned} 0 &= - \sum_{j=1}^N \left[\left(\int_0^1 \varphi_i \varphi_j dx \right) \frac{d^2 c_j}{dt^2} + \left(\int_0^1 \frac{d \varphi_i}{dx} \frac{d \varphi_j}{dx} dx + \bar{k} \varphi_i(1) \varphi_j(1) \right) c_j \right] + \int_0^1 \phi_i \bar{f} dx \\ &= - \sum_{j=1}^N \left(M_{ij} \frac{d^2 c_j}{dt^2} + R_{ij} c_j \right) + F_i \end{aligned} \quad (2.4.33)$$

where

$$M_{ij} = \int_0^1 \varphi_i \varphi_j dx, \quad R_{ij} = \int_0^1 \frac{d \varphi_i}{dx} \frac{d \varphi_j}{dx} dx + \bar{k} \varphi_i(1) \varphi_j(1), \quad F_i = \int_0^1 \varphi_i \bar{f} dx \quad (2.4.34)$$

In the numerical calculations, we take $\bar{f} = 1$ and $\bar{k} = 1$. For one-parameter approximation $N = 1$, we have

$$M_{11} \frac{d^2 c_1}{dt^2} + R_{11} c_1 = F_1 \quad \text{or} \quad \frac{1}{3} \frac{d^2 c_1}{dt^2} + 2c_1 = \frac{1}{2} \quad (\text{c})$$

The solution to the second-order differential equation is

$$c_1(t) = A_1 \sin \sqrt{6}t + A_2 \cos \sqrt{6}t + \frac{1}{4}$$

Hence, the one-parameter Ritz solution is given by

$$u_1(x, t) = \left(A_1 \sin \sqrt{6}t + A_2 \cos \sqrt{6}t + \frac{1}{4} \right) x \quad (\text{d})$$

where A_1 and A_2 are constants to be determined using the initial conditions. For zero initial conditions $u(x, 0) = 0$ and $\dot{u}(x, 0) = 0$, we have $A_2 = -1/4$ and $A_1 = 0$, and the solution becomes

$$u_1(x, t) = \frac{1}{4} (1 - \cos \sqrt{6}t) x \quad (\text{e})$$

For $N \geq 2$, the resulting system of differential equations in time among $c_j(t)$ may be solved using a numerical method.

Example 2.4.3

Consider a simply supported straight beam of length L . We wish to find a Ritz approximation for the transverse deflection w_0 of the beam under uniformly distributed transverse load of intensity q_0 . The principle of the minimum total potential energy, $\delta\Pi = 0$, for the problem (using the Euler–Bernoulli beam theory) can be expressed as

$$\delta\Pi = 0 = \int_0^L \left(EI \frac{d^2\delta w_0}{dx^2} \frac{d^2w_0}{dx^2} - \delta w_0 q_0 \right) dx \quad (2.4.35)$$

The geometric boundary conditions are

$$w_0(0) = w_0(L) = 0 \quad (\text{a})$$

The remaining two boundary conditions are both natural and they are $M(0) = M(L) = 0$. In the Ritz method, these enter the statement of the virtual displacement (2.4.35) (work done by the zero bending moments in moving through the nonzero rotations at $x = 0$ and $x = L$ is zero).

We choose a two-parameter approximation ($N = 2$)

$$w_0(x) \approx W_2(x) = c_1\varphi_1 + c_2\varphi_2 + \varphi_0 \quad (2.4.36)$$

$$\varphi_0 = 0, \quad \varphi_1 = x(L - x), \quad \varphi_2 = x^2(L - x) \quad (2.4.37)$$

Note that $\varphi_i(0) = \varphi_i(L) = 0$. Substituting Eq. (2.4.36) into Eq. (2.4.35), we obtain

$$\begin{aligned} 0 &= \int_0^L \left[EI \left(\delta c_1 \varphi_1'' + \delta c_2 \varphi_2'' \right) \left(c_1 \varphi_1'' + c_2 \varphi_2'' \right) - (\delta c_1 \varphi_1 + \delta c_2 \varphi_2) q_0 \right] dx \\ &= \sum_{i=1}^2 \left(\sum_{j=1}^2 R_{ij} c_j - F_i \right) \delta c_i \quad \rightarrow \quad 0 = \sum_{j=1}^2 R_{ij} c_j - F_i \end{aligned} \quad (2.4.38)$$

where

$$R_{ij} = \int_0^L EI \frac{d^2\varphi_i}{dx^2} \frac{d^2\varphi_j}{dx^2} dx, \quad F_i = \int_0^L q_0 \varphi_i dx \quad (2.4.39)$$

For the particular choice of φ_i in Eq.(2.4.37), we have

$$EIL \begin{bmatrix} 4 & 2L \\ 2L & 4L^2 \end{bmatrix} \begin{Bmatrix} c_1 \\ c_2 \end{Bmatrix} = \frac{q_0 L^3}{12} \begin{Bmatrix} 2 \\ L \end{Bmatrix}$$

whose solution is

$$c_1 = \frac{q_0 L^2}{24EI}, \quad c_2 = 0 \quad (b)$$

and the two-parameter Ritz solution becomes

$$W_2(x) = \frac{q_0 L^3}{24EI} x - \frac{q_0 L^2}{24EI} x^2 \quad (2.4.40)$$

The exact solution is given by

$$w_0(x) = \frac{q_0 L^4}{24EI} \left[\left(\frac{x}{L} \right)^4 - 2 \left(\frac{x}{L} \right)^3 + \left(\frac{x}{L} \right)^2 \right] \quad (2.4.41)$$

The three-parameter approximation with $\varphi_3 = x^3(L - x)$ yields

$$EIL \begin{bmatrix} 4 & 2L & 2L^2 \\ 2L & 4L^2 & 4L^3 \\ 2L^2 & 4L^3 & 4.8L^4 \end{bmatrix} \begin{Bmatrix} c_1 \\ c_2 \\ c_3 \end{Bmatrix} = \frac{q_0 L^3}{12} \begin{Bmatrix} 2 \\ L \\ 0.6L^2 \end{Bmatrix} \quad (2.4.42)$$

$$c_1 = c_2 L = -c_3 L^2 = \frac{q_0 L^2}{24EI} \quad (2.4.43)$$

and the three-parameter Ritz approximation coincides with the exact solution.

Instead of the uniformly distributed load, suppose that the beam is subjected to a transverse point load F_0 at $x = L/2$. The virtual work statement for this case is given by

$$0 = \int_0^L EI \frac{d^2 \delta w_0}{dx^2} \frac{d^2 w_0}{dx^2} dx - F_0 \delta w_0(L/2) \quad (2.4.44)$$

Using the three-parameter approximation with $\varphi_i(x) = x^i(x - L)$, we obtain the coefficient matrix as in Eq. (2.4.42), with the right-hand side given by

$$\frac{F_0 L^2}{4} \begin{Bmatrix} \frac{1}{L} \\ \frac{2}{L^2} \\ \frac{L^2}{4} \end{Bmatrix}$$

and the solution of these equations is given by

$$c_1 = \frac{F_0 L}{12EI}, \quad c_2 = -\frac{F_0}{12EI}, \quad c_3 = -\frac{5F_0}{64EIL} \quad (c)$$

The exact solution for this case is

$$w_0(x) = \begin{cases} \frac{F_0 L}{12EI} x(L - x) + \frac{F_0}{12EI} x^2(L - x) - \frac{F_0 x L^2}{48EI} \\ \frac{F_0 L}{12EI} x(L - x) + \frac{F_0}{12EI} x^2(L - x) - \frac{F_0 x L^2}{48EI} + \frac{F_0 (2x - L)^3}{48EI} \end{cases} \quad (2.4.45)$$

The first expression is valid for $0 \leq x \leq L/2$ and the second expression for $L/2 \leq x \leq L$. The maximum deflection predicted by the three-parameter Ritz solution is

$$w_3(L/2) = \frac{7}{384} \frac{F_0 L^3}{EI} = \frac{F_0 L^3}{54.86 EI}$$

and the exact value is

$$w_0\left(\frac{L}{2}\right) = \frac{F_0 L^3}{48 EI}$$

The Ritz solution is defined by a single expression, whereas the exact solution is defined by two expressions in two parts of the beam due to the discontinuity of the applied load. Consequently, the exact shear force and bending moment are also discontinuous at $x = L/2$. Irrespective of the number of terms used in the approximation, the Ritz solution based on the total potential energy functional (2.4.44) does not yield the exact solution (2.4.47). Obviously, the variational method should also be applied separately in each part, $0 < x < L/2$ and $L/2 < x < L$, and then the continuity of the primary variables at the point $x = L/2$ should be imposed to obtain the exact solution. The *finite element method* is a technique in which the domain is divided into parts and then the Ritz method is used in each interval to develop relationships among the undetermined parameters [see Reddy (2002)]. The method will be discussed in Chapter 12.

One can also use trigonometric polynomials in place of algebraic polynomials for the coordinate functions. However, such functions can make the evaluation of R_{ij} and/or F_i a difficult task. Further, for nontrigonometric loads, the Ritz solution does not converge to the true solution for a finite number of parameters. The reason is that loads represented by algebraic polynomials (e.g., $q(x) = a_1 + a_2x + a_3x^2 + \dots$) cannot be represented by a finite trigonometric series. For instance, the simply supported beam under uniform loading can be modeled by the approximation

$$w_N(x) = c_1 \sin \frac{\pi x}{L} + c_2 \sin \frac{3\pi x}{L} + \dots + c_N \sin \frac{(2N+1)\pi x}{L} \quad (2.4.46)$$

The functions $\varphi_i = \sin(2i+1)\pi x/L$ are linearly independent and complete if all lower functions up to $\sin(2N+1)\pi x/L$ are included. However, the approximation will not coincide with the exact solution for any finite value of N because the sine series representation of a uniform load is an infinite series:

$$q_0 = \sum_{i=1,3,\dots}^{\infty} \frac{16q_0}{i\pi} \sin \frac{i\pi x}{L}$$

The approximate solution w_N in Eq. (2.4.46) converges as the number of parameters N are increased, giving almost an exact solution for only finitely large values of N . For example, a one-term approximation of a simply supported beam with uniformly distributed load of intensity q_0 is

$$w_1 = \frac{4q_0 L^4}{EI\pi^5} \sin \frac{\pi x}{L}$$

Evaluating at $x = L/2$, we obtain

$$w_1\left(\frac{L}{2}\right) = \frac{q_0 L^4}{76.5EI}$$

whereas the exact solution is

$$w_0\left(\frac{L}{2}\right) = \frac{q_0 L^4}{76.8EI}$$

The center deflection is 0.39% in error in the case of the uniform load and 1.46% in error for the point load at the center. The two-term approximation gives the deflection

$$w_2(x) = w_1(x) + \frac{4q_0 L^4}{243EI\pi^5} \sin \frac{3\pi x}{L}$$

Evaluating w_2 at $x = L/2$, we find

$$w_2\left(\frac{L}{2}\right) = \frac{q_0 L^4}{76.8EI}$$

Thus, the two-term approximation gives a center deflection that is exact for uniform load.

2.4.3 The Galerkin Method

Consider an operator equation of the form

$$A(u) = f \quad \text{in } \Omega \tag{2.4.47}$$

subjected to boundary conditions

$$B_1(u) = \hat{u} \quad \text{on } \Gamma_1, \quad B_2(u) = \hat{g} \quad \text{on } \Gamma_2 \tag{2.4.48}$$

where A is a linear or nonlinear differential operator, u is the dependent variable, f is a given force term in the domain Ω , B_1 and B_2 are boundary operators associated with essential and natural boundary conditions of the operator A , and \hat{u} and \hat{g} are specified values on the portions Γ_1 and Γ_2 of the boundary Γ of the domain. An example of Eqs. (2.4.47) and (2.4.48) is given by

$$A(u) = -\frac{d}{dx} \left(a \frac{du}{dx} \right), \quad B_1(u) = \hat{u}, \quad B_2(u) = a \frac{du}{dx}$$

Γ_1 is the point $x = 0$, Γ_2 is the point $x = L$

We seek an approximate solution of u in the form

$$U_N = \sum_{j=1}^N c_j \varphi_j + \varphi_0 \tag{2.4.49}$$

where the parameters c_j are determined by requiring that the residual of the approximation

$$\mathcal{R}_N = A \left(\sum_{j=1}^N c_j \varphi_j + \varphi_0 \right) - f \neq 0 \quad (2.4.50)$$

be orthogonal to a set of N linearly independent *weight functions* ψ_i :

$$\int_{\Omega} \psi_i \mathcal{R}_N(c_i, \varphi_i, f) d\mathbf{x} = 0, \quad i = 1, 2, \dots, N \quad (2.4.51)$$

The method based on this procedure is called a *weighted residual method*.

The coordinate function φ_0 and φ_i in a weighted residual method must satisfy the following conditions:

1. $\varphi_j (j = 1, 2, \dots, N)$ should satisfy the following three conditions:
 - (a) Each φ_j is *continuous* as required in the weighted residual statement; i.e., φ_j should be such that U_N yields a nonzero value of $A(U_N)$.
 - (b) Each φ_j satisfies the *homogeneous form* of *all* specified (i.e., essential as well as natural) boundary conditions.
 - (c) The set $\{\varphi_j\}$ is *linearly independent* and *complete*.
2. φ_0 has the main purpose of satisfying *all* specified boundary conditions associated with the equation. It is zero when the specified boundary conditions are homogeneous.
3. ψ_i should be linearly independent.

There are two main differences between the approximation functions used in the Ritz method and those used in weighted residual methods: (1) *Continuity*: The approximation functions used in the weighted residual methods are required to have the same differentiability as in the differential equation, whereas those used in the Ritz method must be differentiable as required by the weak form or the principle of virtual displacements. (2) *Boundary Conditions*: The approximation functions used in the Galerkin method must satisfy the homogeneous form of both geometric and force boundary conditions. Both of these differences require, in general, φ_i in the Galerkin method to be of a higher order than those used in the Ritz method.

Equation (2.4.51) provides N linearly independent algebraic equations for the determination of the parameters c_i . If A is a nonlinear operator, the resulting algebraic equations will be nonlinear. Whenever A is linear, we can write

$$A \left(\sum_{j=1}^N c_j \varphi_j + \varphi_0 \right) = \sum_{j=1}^N c_j A(\varphi_j) + A(\varphi_0) \quad (2.4.52)$$

and Eq. (2.4.51) becomes

$$\begin{aligned} \sum_{j=1}^N \left[\int_{\Omega} \psi_i A(\varphi_j) d\mathbf{x} \right] c_j - \int_{\Omega} \psi_i [f - A(\varphi_0)] d\mathbf{x} &= 0 \\ \sum_{j=1}^N G_{ij} c_j - q_i &= 0, \quad i = 1, 2, \dots, N \end{aligned} \quad (2.4.53)$$

where

$$G_{ij} = \int_{\Omega} \psi_i A(\varphi_j) d\mathbf{x}, \quad q_i = \int_{\Omega} \psi_i [f - A(\varphi_0)] d\mathbf{x} \quad (2.4.54)$$

Note that G_{ij} is not symmetric in general, even when $\psi_i = \varphi_i$ (Galerkin's method). It is symmetric when A is a linear operator and $\psi_i = A(\varphi_i)$ (the least-squares method).

Various special cases of the weighted residual method differ from each other due to the choice of the weight function, ψ_i . The most commonly used weight functions are:

$$\begin{aligned} \text{Galerkin's method:} \quad & \psi_i = \varphi_i \\ \text{Least-squares method:} \quad & \psi_i = A(\varphi_i) \\ \text{Collocation method:} \quad & \psi_i = \delta(\mathbf{x} - \mathbf{x}_i) \end{aligned}$$

Here $\delta(\cdot)$ denotes the Dirac delta function. The weighted residual method in the general form (2.4.51) (with $\psi_i \neq \varphi_i$) is known as the *Petrov–Galerkin method*.

The Galerkin method is a special case of the Petrov–Galerkin method in which the coordinate functions and the weighted functions are the same ($\varphi_i = \psi_i$). If the Galerkin method is used for second-order or higher-order equations, it would involve the use of higher-order coordinate functions and the solution of nonsymmetric equations.

The Ritz and Galerkin methods yield the same set of algebraic equations for the following two cases:

1. The specified boundary conditions of the problem are all essential type and, therefore, the requirements on φ_i in both methods are the same.
2. The problem has both essential and natural boundary conditions, but the coordinate functions used in the Galerkin method are also used in the Ritz method.

Example 2.4.4

Consider the bar problem of Example 2.4.2. In the weighted residual method, φ_i must also satisfy the condition $\varphi'_i(1) + \varphi_i(1) = 0$ (for the nondimensional problem). The lowest-order function that satisfies the condition is

$$\varphi_1 = 3x - 2x^2 \quad (2.4.55)$$

The one-parameter Galerkin's solution for the natural frequency can be computed using

$$0 = \int_0^1 \varphi_1 \left(\lambda c_1 \varphi_1 + c_1 \frac{d^2 \varphi_1}{dx^2} \right) dx \quad \text{or} \quad \left(\frac{4}{5} \lambda - \frac{10}{3} \right) c_1 = 0 \quad (2.4.56)$$

which gives $\lambda_1 = 50/12 = 4.167$. If the same function is used for φ_1 in the one-parameter Ritz solution, we obtain the same result as in the one-parameter Galerkin's solution.

For the transient response, we have

$$0 = \int_0^1 \varphi_1 \left(c_1 \frac{d^2 \varphi_1}{dx^2} - \frac{d^2 c_1}{dt^2} \varphi_1 + 1 \right) dx \quad \text{or} \quad \frac{4}{5} \frac{d^2 c_1}{dt^2} + \frac{10}{3} c_1 = \frac{5}{6} \quad (2.4.57)$$

whose solution is ($\sqrt{50/12} \approx 2.0412$)

$$c_1(t) = A \sin 2.04t + B \cos 2.04t + \frac{1}{4}$$

For zero initial conditions, the total solution becomes

$$u_1(x, t) = \frac{1}{4} (1 - \cos 2.04t) (3x - 2x^2)$$

Example 2.4.5

Consider the simply supported beam problem of Example 2.4.3. Since all specified boundary conditions are homogeneous, again we have $\varphi_0 = 0$. In the Galerkin method, φ_i must satisfy the homogeneous form of all specified boundary conditions ($w_0 = M_{xx} = 0$ at $x = 0, L$):

$$\varphi_i = 0, \quad \frac{d^2\varphi_i}{dx^2} = 0 \quad \text{at } x = 0, L \quad (2.4.58)$$

For the choice of algebraic polynomials, we assume a five-parameter polynomial because there are four conditions in Eq. (2.4.58):

$$\varphi_1(x) = a + bx + cx^2 + dx^3 + ex^4$$

Using the conditions in Eq. (2.4.58), we find that

$$a = c = 0, \quad bL + dL^3 + eL^4 = 0, \quad 6dL + 12eL^2 = 0$$

Thus, we have $b = eL^3$ and $d = -2eL$. The function φ_1 is given by (taking $eL^4 = 1$)

$$\varphi_1 = \frac{x}{L} \left(1 - 2\frac{x^2}{L^2} + \frac{x^4}{L^4} \right) \quad (2.4.59)$$

Substituting the one-parameter Galerkin approximation $W_1 = c_1\varphi_1$ into the residual

$$\mathcal{R} = EI \frac{d^4W_1}{dx^4} - q_0 = \frac{24EI}{L^4} c_1 - q_0 \quad (2.4.60)$$

and integrating over 0 to L yields $c_1 = q_0 L^4 / (24EI)$. Hence, the solution becomes

$$W_1(x) = \frac{q_0 L^4}{24EI} \left[\left(\frac{x}{L} \right) - 2 \left(\frac{x}{L} \right)^3 + \left(\frac{x}{L} \right)^5 \right] \quad (2.4.61)$$

which is the same as the exact solution.

It can be shown that a one-parameter Ritz solution with φ_1 given by Eq. (2.4.59) gives the exact solution. From Eq. (2.4.39) of Example 2.4.3, we have the result

$$R_{11} = \int_0^L EI \frac{d^2\phi_1}{dx^2} \frac{d^2\phi_1}{dx^2} dx = 144 \frac{EI}{L^4} \int_0^L \left(-\frac{x}{L} + \frac{x^2}{L^2} \right)^2 dx = \frac{24EIL^5}{5}$$

$$F_1 = \int_0^L q_0 \phi_1 dx = q_0 \int_0^L \left[\left(\frac{x}{L} \right) - 2 \left(\frac{x}{L} \right)^3 + \left(\frac{x}{L} \right)^4 \right] dx = \frac{q_0 L}{5}$$

Hence, we obtain $c_1 = q_0 L^4 / (24EI)$.

2.5 Summary

In this chapter, an introduction to the principle of virtual displacements and its special case, the principle of minimum total potential energy, are presented. As an offspring of the virtual work principles, Castigliano's Theorems I and II are also discussed and their use is illustrated through truss and beam problems. The energy principles provide a means for the derivation of the governing equations, provided one can write the internal and external virtual work expressions for the problem. They also yield the natural boundary conditions and give the form of the essential and natural boundary conditions.

An introduction to the Ritz and Galerkin methods is also presented in this chapter. The Ritz method makes use of the weak form provided by the principle of virtual displacements or the principles of minimum potential energy in determining the approximate solutions. The Galerkin method, on the other hand, is based on a weighted integral statement of the governing equation or equations. The Galerkin solution is required to satisfy all specified boundary conditions, whereas the Ritz solution need only satisfy the specified essential (geometric) boundary conditions. The single most difficult step in the use of these methods is the selection of the approximation functions. The requirements on the approximation functions merely provide the guidelines for their selection. The selection of coordinate functions becomes more difficult for problems with irregular domains or discontinuous data (i.e., loading or geometry). Further, the generation of coefficient matrices for the resulting algebraic equations cannot be automated for a *class* of problems that differ from each other only in the geometry of the domain, boundary conditions, or loading. These limitations of the classical variational methods can be overcome by the *finite element method*, which is discussed later in this book.

Problems

- 2.1** For the Euler–Bernoulli beam theory, the displacement field is given by Eq. (2.1.11). The stress resultants for the beam are defined in Eq. (2.1.15). Assuming linear elastic stress–strain relations, $\sigma_{xx} = E\varepsilon_{xx}$, show that the stress in the beam is related to the stress resultants by

$$\sigma_{xx} = \frac{N_{xx}}{A} + \frac{M_{xx}z}{I}$$

- 2.2** Show that the expression for the internal virtual work δW_I for an arbitrary beam of length L , axial stiffness EA , and bending stiffness EI is given by

$$\delta W_I = \int_0^L \left(EA \frac{du_0}{dx} \frac{d\delta u_0}{dx} + EI \frac{d^2 w_0}{dx^2} \frac{d^2 \delta w_0}{dx^2} \right) dx$$

Neglect the energy due to transverse shear deformation.

2.3 Show that the complementary internal virtual work δW_I^* for an arbitrary beam of length L , axial stiffness EA , and bending stiffness EI is given by

$$\delta W_I^* = \frac{1}{EA} \int_0^L N_{xx} \delta N_{xx} dx + \frac{1}{EI} \int_0^L M_{xx} \delta M_{xx} dx$$

Neglect the energy due to transverse shear forces.

2.4–2.9 Find the Euler–Lagrange equations and the natural boundary conditions associated with each of the total potential energy functionals given in Problems 2.4–2.9. The dependent variables are listed as the arguments of the functional, and only the geometric boundary conditions are stated. No other variables are functions of the dependent variables, but may be functions of position in the domain or on the boundary.

2.4 Axial deformation of a spring-supported bar: $u_0(0) = 0$

$$\Pi(u_0) = \int_0^L \left[\frac{EA}{2} \left(\frac{du_0}{dx} \right)^2 - fu_0 \right] dx + \frac{k}{2} [u_0(L)]^2 - Pu_0(L)$$

2.5 Bending of a beam on elastic foundation: $w_0(0) = w_0(L) = 0$

$$\Pi(w_0) = \int_0^L \left[\frac{EI}{2} \left(\frac{d^2w_0}{dx^2} \right)^2 + \frac{k}{2} w_0^2 - qw_0 \right] dx$$

2.6 Nonlinear bending of a beam: $u_0(0) = 0$, $w_0(0) = 0$, and $(dw_0/dx)(0) = 0$

$$\begin{aligned} \Pi(u_0, w_0) = & \int_0^L \left\{ \frac{EA}{2} \left[\frac{du_0}{dx} + \frac{1}{2} \left(\frac{dw_0}{dx} \right)^2 \right]^2 + \frac{EI}{2} \left(\frac{d^2w_0}{dx^2} \right)^2 \right\} dx \\ & - F_0 w_0(L) - Pu_0(L) \end{aligned}$$

2.7 Transverse deflection of a membrane: $u = 0$ on the portion Γ_u of the total boundary Γ ($\Gamma_\sigma = \Gamma - \Gamma_u$)

$$\Pi(u) = \int_\Omega \left[\frac{a_{11}}{2} \left(\frac{\partial u}{\partial x} \right)^2 + \frac{a_{22}}{2} \left(\frac{\partial u}{\partial y} \right)^2 - fu \right] dx dy - \int_{\Gamma_\sigma} tu ds$$

2.8 Bending of an orthotropic plate: $w_0 = 0$, $\partial w_0 / \partial n = 0$ on the boundary Γ

$$\begin{aligned} \Pi(w_0) = & \int_\Omega \left[\frac{D_{11}}{2} \left(\frac{\partial^2 w_0}{\partial x^2} \right)^2 + D_{12} \frac{\partial^2 w_0}{\partial x^2} \frac{\partial^2 w_0}{\partial y^2} + 2D_{66} \left(\frac{\partial^2 w_0}{\partial x \partial y} \right)^2 \right. \\ & \left. + \frac{D_{22}}{2} \left(\frac{\partial^2 w_0}{\partial y^2} \right)^2 - qw_0 \right] dx dy \end{aligned}$$

2.9 Plane elasticity: $u = \hat{u}$ and $v = \hat{v}$ on Γ_1 where $\Gamma_1 + \Gamma_2 = \Gamma$

$$\begin{aligned}\Pi(u, v) = & \int_{\Omega} \left\{ \frac{1}{2} \left[c_{11} \left(\frac{\partial u}{\partial x} \right)^2 + c_{22} \left(\frac{\partial v}{\partial y} \right)^2 + 2c_{12} \frac{\partial u}{\partial x} \frac{\partial v}{\partial y} \right. \right. \\ & \left. \left. + c_{33} \left(\frac{\partial u}{\partial y} + \frac{\partial v}{\partial x} \right)^2 \right] - f_1 u - f_2 v \right\} dx dy - \int_{\Gamma_2} (t_1 u + t_2 v) ds\end{aligned}$$

2.10 Show that the force and moment resultants N_{xx} , M_{xx} , and Q_x can be expressed in terms of the generalized displacements (u_0, w_0, ϕ) of the Timoshenko beam theory as

$$\begin{aligned}N_{xx} &= EA \left(\frac{\partial u_0}{\partial x} - \alpha T^0 \right), \quad M_{xx} = EI \left(\frac{\partial \phi}{\partial x} - \alpha T^1 \right) \\ Q_x &= GAK_s \left(\phi + \frac{\partial w_0}{\partial x} \right)\end{aligned}$$

where α is the thermal expansion coefficient, E the modulus, G the shear modulus, A the area of cross section, I the moment of inertia, and $\Delta T = T^0 + zT^1$ is the temperature change. Use the thermoelastic constitutive relations $\sigma_{xx} = E(\varepsilon_{xx} - \alpha\Delta T)$ and $\sigma_{xz} = G\gamma_{xz}$.

2.11 Third-Order Beam Theory: Consider the displacement field

$$\begin{aligned}u(x, z, t) &= u_0(x, t) + z\phi(x, t) - c_1 z^3 \left(\phi + \frac{\partial w_0}{\partial x} \right) \\ w(x, z, t) &= w_0(x, t)\end{aligned}\tag{1}$$

where $c_1 = 4/(3h^2)$. The displacement field accommodates quadratic variation of transverse shear strains and stresses and vanishing of transverse shear stress on the top and bottom planes of a beam.

- (a) Show that the nonzero linear strains associated with the displacement field (1) are

$$\begin{aligned}\varepsilon_{xx} &= \varepsilon_{xx}^{(0)} + z\varepsilon_{xx}^{(1)} + z^3\varepsilon_{xx}^{(3)}, \quad \gamma_{xz} = \gamma_{xz}^{(0)} + z^2\gamma_{xz}^{(2)} \\ \varepsilon_{xx}^{(0)} &= \frac{\partial u_0}{\partial x}, \quad \varepsilon_{xx}^{(1)} = \frac{\partial \phi}{\partial x}, \quad \varepsilon_{xx}^{(3)} = -c_1 \left(\frac{\partial \phi}{\partial x} + \frac{\partial^2 w_0}{\partial x^2} \right) \\ \gamma_{xz}^{(0)} &= \phi + \frac{\partial w_0}{\partial x}, \quad \gamma_{xz}^{(2)} = -c_2 \left(\phi + \frac{\partial w_0}{\partial x} \right), \quad c_2 = 4/h^2\end{aligned}\tag{2}$$

- (b) Using the dynamic version of the principle of virtual displacements, show that the equations of motion of the theory are given by

$$\frac{\partial N_{xx}}{\partial x} = I_0 \frac{\partial^2 u_0}{\partial t^2}\tag{3}$$

$$\frac{\partial \bar{Q}_x}{\partial x} + c_1 \frac{\partial^2 P_{xx}}{\partial x^2} + q = I_0 \frac{\partial^2 w_0}{\partial t^2} + c_1 \left(J_4 \frac{\partial^3 \phi}{\partial x \partial t^2} - c_1 I_6 \frac{\partial^4 w_0}{\partial x^2 \partial t^2} \right)\tag{4}$$

$$\frac{\partial \bar{M}_{xx}}{\partial x} - \bar{Q}_x = K_2 \frac{\partial^2 \phi}{\partial t^2} - c_1 J_4 \frac{\partial^3 w_0}{\partial x \partial t^2}\tag{5}$$

where

$$\begin{Bmatrix} N_{xx} \\ M_{xx} \\ P_{xx} \end{Bmatrix} = \int_{-h/2}^{h/2} \begin{Bmatrix} 1 \\ z \\ z^3 \end{Bmatrix} \sigma_{xx} dz, \quad \begin{Bmatrix} Q_x \\ R_x \end{Bmatrix} = \int_{-h/2}^{h/2} \begin{Bmatrix} 1 \\ z^2 \end{Bmatrix} \sigma_{xz} dz \quad (6)$$

$$\bar{M}_{xx} = M_{xx} - c_1 P_{xx}, \quad \bar{Q}_x = Q_x - c_2 R_x \quad (7)$$

$$J_i = I_i - c_1 I_{i+2}, \quad K_2 = I_2 - 2c_1 I_4 + c_1^2 I_6, \quad I_i = \int_{-h/2}^{h/2} \rho(z)^i dz \quad (8)$$

and (P_{xx}, R_x) denote the higher-order stress resultants. Note that the primary and secondary variables of the theory are

$$\begin{array}{ll} \text{Primary Variables :} & u_0, \quad w_0, \quad \frac{\partial w_0}{\partial x}, \quad \phi \\ \text{Secondary Variables :} & N_{xx}, \quad V_x, \quad P_{xx}, \quad \bar{M}_{xx} \end{array} \quad (9)$$

where

$$V_x \equiv \bar{Q}_x + N_{xx} \frac{\partial w_0}{\partial x} + c_1 \left[\frac{\partial P_{xx}}{\partial x} - \left(I_3 \ddot{u}_0 + J_4 \ddot{\phi}_x - c_1 I_6 \frac{\partial \ddot{w}_0}{\partial x} \right) \right] \quad (10)$$

2.12 Suppose that the displacement field of the Timoshenko beam theory (see Example 2.2.2) can be expressed in the form

$$u(x, z) = z \left(-\frac{dw^b}{dx} + \phi \right), \quad w(x, z) = w^b(x) + w^s(x) \quad (1)$$

where w^b and w^s denote the bending and shear components, respectively, of the total transverse deflection w , and ϕ denotes the shear rotation, in addition to the bending rotation, of a transverse normal about the y axis. Use the principle of virtual displacements to obtain the following Euler–Lagrange equations

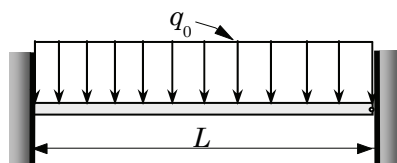
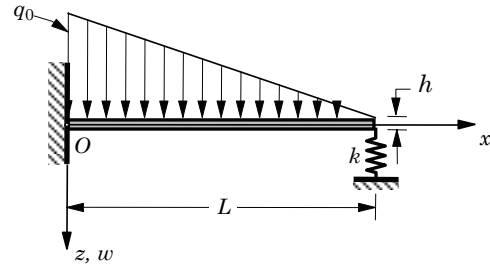
$$\delta\phi : -\frac{dM_{xx}}{dx} + Q_x = 0 \quad (2)$$

$$\delta w^b : -\frac{d^2 M_{xx}}{dx^2} - q = 0 \quad (3)$$

$$\delta w^s : -\frac{dQ_x}{dx} - q = 0 \quad (4)$$

where q is the distributed transverse load (measured per unit length), and M_{xx} and Q_x are the resultants defined in Eq. (2.2.27).

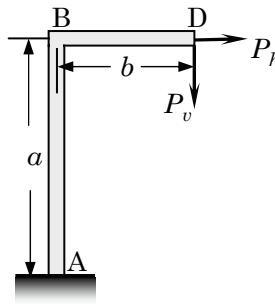
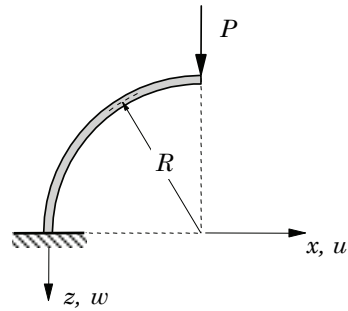
2.13 Use Castigliano's Theorem I to determine the center deflection of the beam with both ends clamped and carrying uniformly distributed load (Figure P2.13).

**Figure P2.13****Figure P2.14**

- 2.14** Use Castigliano's Theorem I to determine the compressive force and displacements in the linear elastic spring (k) supporting the free end of a cantilevered beam under triangular distributed load (Figure P2.14).

2.15 Repeat Problem 2.14 using Castigliano's Theorem II.

- 2.16** Consider the frame structure shown in Figure P2.16. Each member of the structure has the same geometric and material properties. Assume linear elastic behavior. Determine the horizontal and vertical displacements at the point of load application using Castigliano's Theorem II.

**Figure P2.16****Figure 2.17**

- 2.17** Use Castigliano's Theorem II to determine the vertical and horizontal deflections at the free end of the curved beam shown in Figure P2.17.

- 2.18** Give the approximation functions φ_1 and φ_0 required in the (i) Ritz and (ii) Galerkin methods to solve the problem of a beam clamped at both ends. Consider (a) full beam and (b) half beam (exploit symmetry). Use the Euler-Bernoulli beam theory.

- 2.19** Consider a uniform beam fixed at one end and supported by an elastic spring (k) in the vertical direction. Assume that the beam is loaded by uniformly distributed load q_0 . Determine one-parameter Ritz solution using algebraic

functions. Use the Euler–Bernoulli beam theory and the total potential energy functional

$$\Pi(w_0) = \frac{EI}{2} \int_0^L \left(\frac{d^2 w_0}{dx^2} \right)^2 dx + \frac{k}{2} [w_0(L)]^2 - \int_0^L q_0 w_0 dx$$

- 2.20** Repeat Problem 2.19 using the Timoshenko beam theory. The total potential energy functional is given by

$$\begin{aligned} \Pi(w_0, \phi) = & \frac{1}{2} \int_0^L \left[EI \left(\frac{d\phi}{dx} \right)^2 + GAK_s \left(\phi + \frac{dw_0}{dx} \right)^2 \right] dx + \frac{k}{2} [w_0(L)]^2 \\ & - \int_0^L q_0 w_0 dx \end{aligned}$$

where ϕ is the rotation and GAK_s is the shear stiffness.

- 2.21** Consider the buckling of a uniform beam according to the Timoshenko beam theory. The total potential energy functional for the problem can be written as

$$\Pi(w_0, \phi) = \frac{1}{2} \int_0^L \left[EI \left(\frac{d\phi}{dx} \right)^2 + GAK_s \left(\frac{dw_0}{dx} + \phi \right)^2 - \hat{N}_{xx} \left(\frac{dw_0}{dx} \right)^2 \right] dx$$

where \hat{N}_{xx} is the axial compressive load. We wish to determine the critical buckling load N_{cr} of a simply supported beam using the Ritz method. Assume one-parameter approximation of the form

$$w_0(x) = c_1 \sin \frac{\pi x}{L}, \quad \phi(x) = c_2 \cos \frac{\pi x}{L}$$

and determine the critical buckling load.

- 2.22** Determine the N –parameter Ritz solution for the natural frequencies of a simply supported beam. Use trigonometric functions for $\varphi_i(x)$. Use the total potential energy functional

$$\Pi(w) = \frac{EI}{2} \int_0^L \left(\frac{d^2 w}{dx^2} \right)^2 dx - \frac{\rho A \omega^2}{2} \int_0^L w^2 dx$$

- 2.23** Repeat Problem 2.22 using the Timoshenko beam theory with the total potential energy functional

$$\Pi(w, \phi) = \frac{1}{2} \int_0^L \left[EI \left(\frac{d\phi}{dx} \right)^2 + GAK_s \left(\phi + \frac{dw}{dx} \right)^2 \right] dx - \frac{\rho A \omega^2}{2} \int_0^L w^2 dx$$

- 2.24** Determine the N –parameter Ritz solution for the transient response of a simply supported beam under a step load $q(x, t) = q_0 H(t - t_0)$, where $H(t)$

denotes the Heaviside step function. Use trigonometric functions for $\varphi_i(x)$. Use the total potential energy functional

$$\Pi(w_0) = \frac{EI}{2} \int_0^L \left(\frac{\partial^2 w_0}{\partial x^2} \right)^2 dx + \frac{\rho A}{2} \int_0^L \left(\frac{\partial^2 w_0}{\partial t^2} \right)^2 dx - \int_0^L q(x, t) w_0 dx$$

- 2.25** Show that the two-parameter Ritz solution for the transient response of the bar considered in Example 2.4.2 yields the equations

$$\begin{bmatrix} \frac{1}{3} & \frac{1}{4} \\ \frac{1}{4} & \frac{1}{5} \end{bmatrix} \begin{Bmatrix} \ddot{c}_1 \\ \ddot{c}_2 \end{Bmatrix} + \begin{bmatrix} 2 & 2 \\ 2 & \frac{7}{3} \end{bmatrix} \begin{Bmatrix} c_1 \\ c_2 \end{Bmatrix} = \begin{Bmatrix} \frac{1}{2} \\ \frac{1}{3} \end{Bmatrix}$$

Use the Laplace transform method to determine the solution of these differential equations.

3

Classical Theory of Plates

3.1 Introduction

The objective of this chapter is to develop the governing equations of the classical theory of plates. A *plate* is a structural element with planform dimensions that are large compared to its thickness and is subjected to loads that cause bending deformation in addition to stretching. In most cases, the thickness is no greater than one-tenth of the smallest in-plane dimension. Because of the smallness of thickness dimension, it is often not necessary to model them using 3D elasticity equations. Simple 2D plate theories can be developed to study the deformation and stresses in plate structures.

Plate theories are developed using the semi-inverse method wherein an educated guess is made as to the form of the displacement field or stress field, leaving enough freedom in the assumed field to satisfy the equations of elasticity. In the case of beams, plates, and shells, the displacement field is in terms of unknown functions φ_i^j of the surface coordinates (x, y) and time t :

$$u_i(x, y, z, t) = \sum_{j=0}^N (z)^j \varphi_i^j(x, y, t) \quad (3.1.1)$$

and equations governing φ_i^j are determined such that the principle of virtual displacements is satisfied. The specific form of Eq. (3.1.1) depends on the kinematics of deformation to be included. For example, the Euler–Bernoulli beam theory is based on the hypothesis that the beam deforms such that a straight line normal to the beam axis before bending remains (1) straight, (2) inextensible, and (3) normal to the beam axis after deformation. This three-part hypothesis provides a clue to the form of the displacement field of the Euler–Bernoulli beam theory

$$u_1(x, y, z, t) = u_0(x, t) - z \frac{\partial w_0}{\partial x}, \quad u_2 = 0, \quad u_3(x, y, z, t) = w_0(x, t)$$

where u_0 and w_0 are functions to be determined such that the equations of elasticity or its equivalent, namely, the principle of virtual displacements is satisfied, as shown in Examples 2.1.1 and 2.2.1.

The extension of the Euler–Bernoulli beam theory to plates is known as the Kirchhoff plate theory or *classical plate theory* (CPT). The present chapter is dedicated to the development of the classical plate theory.

3.2 Assumptions of the Theory

The classical plate theory is one in which the displacement field is based on the *Kirchhoff hypothesis*, which consists of the following three parts (Figure 3.2.1):

- (1) Straight lines perpendicular to the mid-surface (i.e., transverse normals) before deformation remain straight after deformation.
- (2) The transverse normals do not experience elongation (i.e., they are inextensible).
- (3) The transverse normals rotate such that they remain perpendicular to the middle surface after deformation.

Let us examine the consequences of the Kirchhoff hypothesis. Consider a plate of uniform thickness h . We shall use the rectangular Cartesian coordinates (x, y, z) with the xy -plane coinciding with the geometric middle plane of the plate and the z -coordinate taken positive upward. Suppose that (u, v, w) denote the total displacements of a point along the (x, y, z) coordinates. A material point occupying the position (x, y, z) in the undeformed plate moves to the position $(x+u, y+v, z+w)$ in the deformed plate. The inextensibility of a transverse normal (assumptions 1 and 2) implies that the thickness normal strain is zero:

$$\varepsilon_{zz} = \frac{\partial w}{\partial z} = 0 \quad (3.2.1)$$

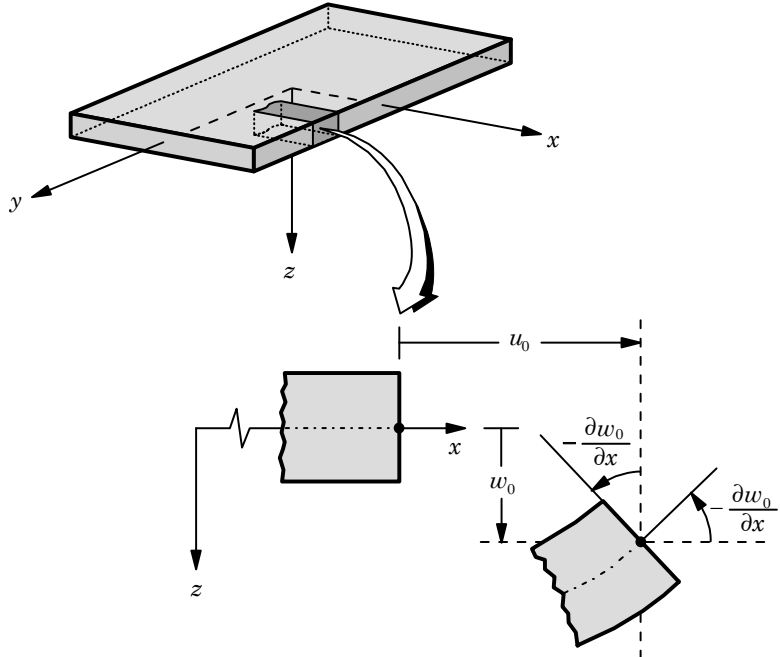


Figure 3.2.1. Undeformed and deformed geometries of an edge of a plate under the Kirchhoff assumptions.

which implies that w is independent of z . The third assumption results in zero transverse shear strains

$$\varepsilon_{xz} = \frac{\partial u}{\partial z} + \frac{\partial w}{\partial x} = 0, \quad \varepsilon_{yz} = \frac{\partial v}{\partial z} + \frac{\partial w}{\partial y} = 0 \quad (3.2.2)$$

These conditions, in turn, imply, because w is independent of z , that

$$u(x, y, z) = -z \frac{\partial w}{\partial x} + u_0(x, y), \quad v(x, y, z) = -z \frac{\partial w}{\partial y} + v_0(x, y) \quad (3.2.3)$$

where u_0 and v_0 represent the values of u and v , respectively, at the point $(x, y, 0)$. In other words, u_0 and v_0 denote the displacements along the x and y coordinates, respectively, of a point on the mid-plane.

3.3 Displacement Field and Strains

Let us denote the undeformed middle plane of the plate with the symbol Ω . The total domain of the plate is the tensor product $\Omega \times (-h/2, h/2)$. The boundary of the total domain consists of the top surface ($z = -h/2$), bottom surface ($z = h/2$), and the edge $\bar{\Gamma} \equiv \Gamma \times (-h/2, h/2)$. In general, Γ is a curved surface, with outward normal $\hat{\mathbf{n}} = n_x \hat{\mathbf{e}}_x + n_y \hat{\mathbf{e}}_y$, where n_x and n_y are the direction cosines of the unit normal (Figure 3.3.1).

The Kirchhoff hypothesis implies, as discussed above, the following form of the displacement field for time-dependent deformations

$$\begin{aligned} u(x, y, z, t) &= u_0(x, y, t) - z \frac{\partial w_0}{\partial x} \\ v(x, y, z, t) &= v_0(x, y, t) - z \frac{\partial w_0}{\partial y} \\ w(x, y, z, t) &= w_0(x, y, t) \end{aligned} \quad (3.3.1)$$

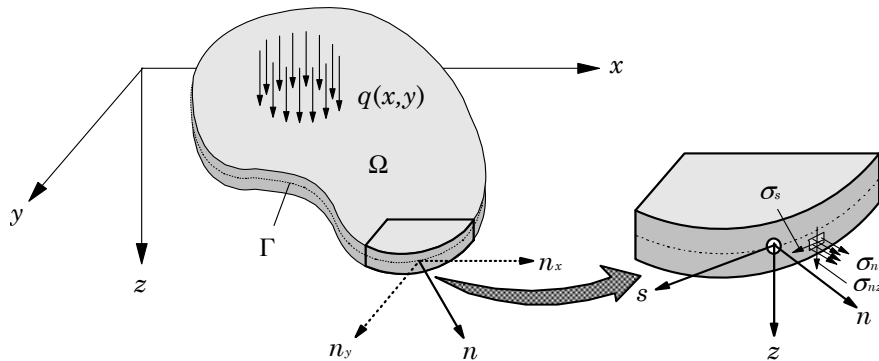


Figure 3.3.1. Geometry of a plate with curved boundary.

where (u_0, v_0, w_0) denote the displacements of a material point at $(x, y, 0)$ in (x, y, z) coordinate directions. Note that (u_0, v_0) are associated with extensional deformation of the plate while w_0 denotes the bending deflection.

The strains associated with the displacement field (3.3.1) can be computed using either the nonlinear strain-displacement relations (1.3.5) or the linear strain-displacement relations (1.3.8). The nonlinear strains are given by

$$\begin{aligned} E_{11} &= \frac{\partial u}{\partial x} + \frac{1}{2} \left[\left(\frac{\partial u}{\partial x} \right)^2 + \left(\frac{\partial v}{\partial x} \right)^2 + \left(\frac{\partial w}{\partial x} \right)^2 \right] \\ E_{22} &= \frac{\partial v}{\partial y} + \frac{1}{2} \left[\left(\frac{\partial u}{\partial y} \right)^2 + \left(\frac{\partial v}{\partial y} \right)^2 + \left(\frac{\partial w}{\partial y} \right)^2 \right] \\ E_{33} &= \frac{\partial w}{\partial z} + \frac{1}{2} \left[\left(\frac{\partial u}{\partial z} \right)^2 + \left(\frac{\partial v}{\partial z} \right)^2 + \left(\frac{\partial w}{\partial z} \right)^2 \right] \\ E_{12} &= \frac{1}{2} \left(\frac{\partial u}{\partial y} + \frac{\partial v}{\partial x} + \frac{\partial u}{\partial x} \frac{\partial u}{\partial y} + \frac{\partial v}{\partial x} \frac{\partial v}{\partial y} + \frac{\partial w}{\partial x} \frac{\partial w}{\partial y} \right) \\ E_{13} &= \frac{1}{2} \left(\frac{\partial u}{\partial z} + \frac{\partial w}{\partial x} + \frac{\partial u}{\partial x} \frac{\partial u}{\partial z} + \frac{\partial v}{\partial x} \frac{\partial v}{\partial z} + \frac{\partial w}{\partial x} \frac{\partial w}{\partial z} \right) \\ E_{23} &= \frac{1}{2} \left(\frac{\partial v}{\partial z} + \frac{\partial w}{\partial y} + \frac{\partial u}{\partial y} \frac{\partial u}{\partial z} + \frac{\partial v}{\partial y} \frac{\partial v}{\partial z} + \frac{\partial w}{\partial y} \frac{\partial w}{\partial z} \right) \end{aligned} \quad (3.3.2)$$

If the components of the displacement gradients are of the order ϵ , i.e.,

$$\frac{\partial u}{\partial x}, \frac{\partial u}{\partial y}, \frac{\partial v}{\partial x}, \frac{\partial v}{\partial y}, \frac{\partial w}{\partial z} = O(\epsilon) \quad (3.3.3)$$

then the small strain assumption implies that terms of the order ϵ^2 are omitted in the strains. Terms of order ϵ^2 are

$$\begin{aligned} &\left(\frac{\partial u}{\partial x} \right)^2, \left(\frac{\partial u}{\partial y} \right)^2, \left(\frac{\partial u}{\partial z} \right)^2, \left(\frac{\partial u}{\partial x} \right) \left(\frac{\partial u}{\partial y} \right), \left(\frac{\partial u}{\partial x} \right) \left(\frac{\partial u}{\partial z} \right), \left(\frac{\partial u}{\partial y} \right) \left(\frac{\partial u}{\partial z} \right) \\ &\left(\frac{\partial v}{\partial x} \right)^2, \left(\frac{\partial v}{\partial y} \right)^2, \left(\frac{\partial v}{\partial z} \right)^2, \left(\frac{\partial v}{\partial x} \right) \left(\frac{\partial v}{\partial y} \right), \left(\frac{\partial v}{\partial x} \right) \left(\frac{\partial v}{\partial z} \right), \left(\frac{\partial v}{\partial y} \right) \left(\frac{\partial v}{\partial z} \right) \\ &\left(\frac{\partial w}{\partial x} \right) \left(\frac{\partial w}{\partial z} \right), \left(\frac{\partial w}{\partial y} \right) \left(\frac{\partial w}{\partial z} \right), \left(\frac{\partial w}{\partial z} \right)^2 \end{aligned} \quad (3.3.4)$$

If the rotations of transverse normals are moderate (say $10^\circ - 15^\circ$), then the following terms are small, but *not* negligible compared to ϵ

$$\left(\frac{\partial w}{\partial x} \right)^2, \left(\frac{\partial w}{\partial y} \right)^2, \frac{\partial w}{\partial x} \frac{\partial w}{\partial y} \quad (3.3.5)$$

and they should be included in the strain-displacement relations. Thus, for small strains and moderate rotations, the strain-displacement relations (3.3.2) take the form

$$\begin{aligned}\varepsilon_{xx} &= \frac{\partial u}{\partial x} + \frac{1}{2} \left(\frac{\partial w}{\partial x} \right)^2, & \varepsilon_{xy} &= \frac{1}{2} \left(\frac{\partial u}{\partial y} + \frac{\partial v}{\partial x} + \frac{\partial w}{\partial x} \frac{\partial w}{\partial y} \right) \\ \varepsilon_{yy} &= \frac{\partial v}{\partial y} + \frac{1}{2} \left(\frac{\partial w}{\partial y} \right)^2, & \varepsilon_{xz} &= \frac{1}{2} \left(\frac{\partial u}{\partial z} + \frac{\partial w}{\partial x} \right) \\ \varepsilon_{zz} &= \frac{\partial w}{\partial z}, & \varepsilon_{yz} &= \frac{1}{2} \left(\frac{\partial v}{\partial z} + \frac{\partial w}{\partial y} \right)\end{aligned}\quad (3.3.6)$$

where, for this special case of geometric nonlinearity (i.e., small strains but moderate rotations), the notation ε_{ij} is used in place of E_{ij} . The corresponding Second-Piola Kirchhoff stresses will be denoted σ_{ij} .

For the displacement field in Eq. (3.3.1), $\partial w/\partial z = 0$. In view of the assumptions in Eqs. (3.3.3)–(3.3.5), the strains (3.3.6) for the displacement field (3.3.1) reduce to

$$\begin{aligned}\varepsilon_{xx} &= \frac{\partial u_0}{\partial x} + \frac{1}{2} \left(\frac{\partial w_0}{\partial x} \right)^2 - z \frac{\partial^2 w_0}{\partial x^2} \\ \varepsilon_{yy} &= \frac{\partial v_0}{\partial y} + \frac{1}{2} \left(\frac{\partial w_0}{\partial y} \right)^2 - z \frac{\partial^2 w_0}{\partial y^2}\end{aligned}\quad (3.3.7a)$$

$$\begin{aligned}\varepsilon_{xy} &= \frac{1}{2} \left(\frac{\partial u_0}{\partial y} + \frac{\partial v_0}{\partial x} + \frac{\partial w_0}{\partial x} \frac{\partial w_0}{\partial y} - 2z \frac{\partial^2 w_0}{\partial x \partial y} \right) \\ \varepsilon_{xz} &= \frac{1}{2} \left(-\frac{\partial w_0}{\partial x} + \frac{\partial w_0}{\partial x} \right) = 0 \\ \varepsilon_{yz} &= \frac{1}{2} \left(-\frac{\partial w_0}{\partial y} + \frac{\partial w_0}{\partial y} \right) = 0 \\ \varepsilon_{zz} &= 0\end{aligned}\quad (3.3.7b)$$

The strains in Eqs. (3.3.7a) are called the *von Kármán strains*, and the associated plate theory is termed the *von Kármán plate theory*. Note that the transverse strains ($\varepsilon_{xz}, \varepsilon_{yz}, \varepsilon_{zz}$) are identically zero in the classical plate theory.

The strains in Eq. (3.3.7a) have the form

$$\begin{aligned}\varepsilon_{xx} &= \varepsilon_{xx}^0 + z \varepsilon_{xx}^1 \\ \gamma_{xy} &\equiv 2\varepsilon_{xy} = \gamma_{xy}^0 + z \gamma_{xy}^1 \\ \varepsilon_{yy} &= \varepsilon_{yy}^0 + z \varepsilon_{yy}^1\end{aligned}\quad (3.3.8a)$$

where

$$\begin{aligned}\varepsilon_{xx}^0 &= \frac{\partial u_0}{\partial x} + \frac{1}{2} \left(\frac{\partial w_0}{\partial x} \right)^2, & \varepsilon_{xx}^1 &= -\frac{\partial^2 w_0}{\partial x^2} \\ \varepsilon_{yy}^0 &= \frac{\partial v_0}{\partial y} + \frac{1}{2} \left(\frac{\partial w_0}{\partial y} \right)^2, & \varepsilon_{yy}^1 &= -\frac{\partial^2 w_0}{\partial y^2} \\ \gamma_{xy}^0 &= \frac{\partial u_0}{\partial y} + \frac{\partial v_0}{\partial x} + \frac{\partial w_0}{\partial x} \frac{\partial w_0}{\partial y}, & \gamma_{xy}^1 &= -2 \frac{\partial^2 w_0}{\partial x \partial y}\end{aligned}\quad (3.3.8b)$$

where the strains of the middle surface, $(\varepsilon_{xx}^0, \varepsilon_{yy}^0, \gamma_{xy}^0)$, are called the *membrane strains*, and $(\varepsilon_{xx}^1, \varepsilon_{yy}^1, \gamma_{xy}^1)$ are the flexural (bending) strains, known as the *curvatures*. In matrix notation, Eqs. (3.3.8a,b) can be written as

$$\begin{Bmatrix} \varepsilon_{xx} \\ \varepsilon_{yy} \\ \gamma_{xy} \end{Bmatrix} = \begin{Bmatrix} \varepsilon_{xx}^0 \\ \varepsilon_{yy}^0 \\ \gamma_{xy}^0 \end{Bmatrix} + z \begin{Bmatrix} \varepsilon_{xx}^1 \\ \varepsilon_{yy}^1 \\ \gamma_{xy}^1 \end{Bmatrix} \quad (3.3.9)$$

where ε_{xx}^0 , ε_{yy}^0 , ε_{xy}^0 , ε_{xx}^1 , ε_{yy}^1 , and ε_{xy}^1 are defined in Eq. (3.3.8b).

3.4 Equations of Motion

The equations of motion of CPT are derived using the principle of virtual displacements. In the derivations, we account for thermal effects only with the understanding that the material properties are independent of the temperature and that the temperature T is a known function of position (hence, $\delta T = 0$). Thus, the temperature enters the formulation only through constitutive equations.

As noted earlier, the transverse strains (γ_{xz} , γ_{yz} , ε_{zz}) are identically zero in the classical plate theory. Consequently, the transverse stresses (σ_{xz} , σ_{yz} , σ_{zz}) do not enter the formulation because the virtual strain energy of these stresses is zero [due to the fact that kinematically consistent virtual strains must be zero; see Eq. (3.3.7b)]:

$$\delta\varepsilon_{xz} = 0, \quad \delta\varepsilon_{yz} = 0, \quad \delta\varepsilon_{zz} = 0 \quad (3.4.1)$$

Whether the transverse stresses are accounted for or not in a theory, they are present in reality to keep the plate in equilibrium. In addition, these stress components may be specified on the boundary. Thus, the transverse stresses do not enter the virtual strain energy expression, but must be accounted for in the boundary conditions and equilibrium of forces.

The dynamic version of the principle of virtual displacements [or the minimum total potential energy, $\delta\Pi = \delta(U + V - K)$] is

$$0 = \int_0^T (\delta U + \delta V - \delta K) dt \quad (3.4.2)$$

where U is the strain energy (volume integral of U_0), V is the work done by applied forces, and K is the kinetic energy. Suppose that q_b is the distributed force at the bottom ($z = -h/2$) of the plate, q_t is the distributed force at the top ($z = h/2$) of the plate, and $(\hat{\sigma}_{nn}, \hat{\sigma}_{ns}, \hat{\sigma}_{nz})$ are the specified stress components on the portion Γ_σ of the boundary Γ (Figure 3.4.1). The virtual displacements must be zero on the portion Γ_u on which the displacements are specified. We have $\Gamma = \Gamma_u + \Gamma_\sigma$.

The virtual strain energy is given by

$$\begin{aligned} \delta U &= \int_{\Omega} \int_{-\frac{h}{2}}^{\frac{h}{2}} (\sigma_{xx}\delta\varepsilon_{xx} + \sigma_{yy}\delta\varepsilon_{yy} + 2\sigma_{xy}\delta\varepsilon_{xy}) dz dx dy \\ &= \int_{\Omega} \left\{ \int_{-\frac{h}{2}}^{\frac{h}{2}} \left[\sigma_{xx} (\delta\varepsilon_{xx}^0 + z\delta\varepsilon_{xx}^1) + \sigma_{yy} (\delta\varepsilon_{yy}^0 + z\delta\varepsilon_{yy}^1) + \right. \right. \\ &\quad \left. \left. + \sigma_{xy} (\delta\gamma_{xy}^0 + z\delta\gamma_{xy}^1) \right] dz \right\} dx dy \end{aligned}$$

Next, we introduce thickness-integrated forces (N_{xx}, N_{yy}, N_{xy}) and moments (M_{xx}, M_{yy}, M_{xy}), known as the *stress resultants* (Figure 3.4.1):

$$\begin{Bmatrix} N_{xx} \\ N_{yy} \\ N_{xy} \end{Bmatrix} = \int_{-\frac{h}{2}}^{\frac{h}{2}} \begin{Bmatrix} \sigma_{xx} \\ \sigma_{yy} \\ \sigma_{xy} \end{Bmatrix} dz, \quad \begin{Bmatrix} M_{xx} \\ M_{yy} \\ M_{xy} \end{Bmatrix} = \int_{-\frac{h}{2}}^{\frac{h}{2}} \begin{Bmatrix} \sigma_{xx} \\ \sigma_{yy} \\ \sigma_{xy} \end{Bmatrix} z dz \quad (3.4.3)$$

Then the virtual strain energy can be expressed in terms of the stress resultants as

$$\delta U = \int_{\Omega} \left(N_{xx} \delta \varepsilon_{xx}^0 + M_{xx} \delta \varepsilon_{xx}^1 + N_{yy} \delta \varepsilon_{yy}^0 + M_{yy} \delta \varepsilon_{yy}^1 + N_{xy} \delta \gamma_{xy}^0 + M_{xy} \delta \gamma_{xy}^1 \right) dx dy \quad (3.4.4)$$

The virtual work done by external applied forces can be computed as follows: The external applied forces consist of the distributed transverse load $q_t(x, y)$ applied at the top surface, distributed transverse load $q_b(x, y)$ applied at the bottom surface, and the transverse reaction force of an elastic foundation (if any). In addition, forces and moments due to inplane normal stress $\hat{\sigma}_{nn}$, inplane tangential stress $\hat{\sigma}_{ns}$, and the transverse shear stress $\hat{\sigma}_{nz}$, all acting on an edge with normal $\hat{\mathbf{n}}$, also do work in moving through corresponding virtual displacements. All stresses are assumed to be positive with respect to the sign convention already established.

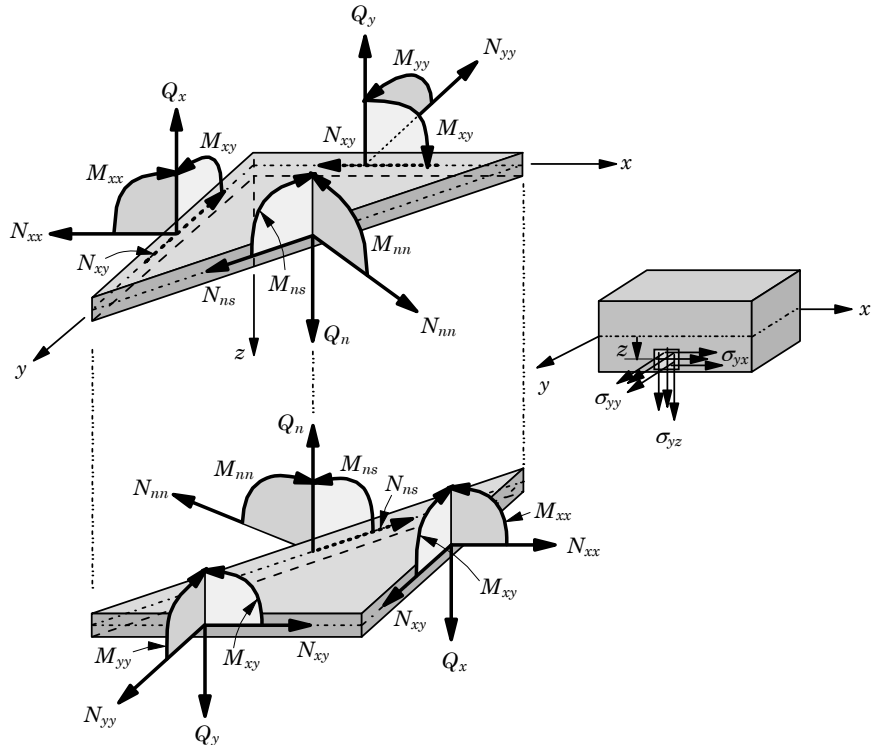


Figure 3.4.1. Thickness-integrated forces and moments on a plate element.

The virtual work done by external forces is

$$\begin{aligned}\delta V = & - \int_{\Omega} \left[q_t(x, y) \delta w(x, y, \frac{h}{2}) + q_b(x, y) \delta w(x, y, -\frac{h}{2}) \right] dx dy \\ & - \int_{\Omega} F_s(x, y) \delta w(x, y, \frac{h}{2}) dx dy \\ & - \int_{\Gamma_{\sigma}} \int_{-\frac{h}{2}}^{\frac{h}{2}} [\hat{\sigma}_{nn} \delta u_n + \hat{\sigma}_{ns} \delta u_s + \hat{\sigma}_{nz} \delta w] dz ds\end{aligned}\quad (3.4.5)$$

$$\begin{aligned} = & - \int_{\Omega} [q_b(x, y) + q_t(x, y) - kw_0] \delta w_0 dx dy \\ & - \int_{\Gamma_{\sigma}} \int_{-\frac{h}{2}}^{\frac{h}{2}} \left[\hat{\sigma}_{nn} \left(\delta u_{0n} - z \frac{\partial \delta w_0}{\partial n} \right) + \hat{\sigma}_{ns} \left(\delta u_{0s} - z \frac{\partial \delta w_0}{\partial s} \right) + \hat{\sigma}_{nz} \delta w_0 \right] dz ds \\ = & - \int_{\Omega} (q - kw_0) \delta w_0 dx dy - \int_{\Gamma_{\sigma}} \left(\hat{N}_{nn} \delta u_{0n} - \hat{M}_{nn} \frac{\partial \delta w_0}{\partial n} \right. \\ & \left. + \hat{N}_{ns} \delta u_{0s} - \hat{M}_{ns} \frac{\partial \delta w_0}{\partial s} + \hat{Q}_n \delta w_0 \right) ds\end{aligned}\quad (3.4.6)$$

where $F_s = -kw_0$; k is the foundation modulus; $q = q_b + q_t$; u_{0n} , u_{0s} , and w_0 are the displacements along the normal, tangential, and transverse directions, respectively; and

$$\left\{ \begin{array}{l} \hat{N}_{nn} \\ \hat{N}_{ns} \end{array} \right\} = \int_{-\frac{h}{2}}^{\frac{h}{2}} \left\{ \begin{array}{l} \hat{\sigma}_{nn} \\ \hat{\sigma}_{ns} \end{array} \right\} dz, \quad \left\{ \begin{array}{l} \hat{M}_{nn} \\ \hat{M}_{ns} \end{array} \right\} = \int_{-\frac{h}{2}}^{\frac{h}{2}} \left\{ \begin{array}{l} \hat{\sigma}_{nn} \\ \hat{\sigma}_{ns} \end{array} \right\} z dz, \quad \hat{Q}_n = \int_{-\frac{h}{2}}^{\frac{h}{2}} \hat{\sigma}_{nz} dz\quad (3.4.7)$$

If the plate is in dynamic equilibrium, the virtual kinetic energy must be calculated. The virtual kinetic energy due to the three velocities is

$$\begin{aligned}\delta K = & \int_{\Omega} \int_{-\frac{h}{2}}^{\frac{h}{2}} \rho (\dot{u} \delta \dot{u} + \dot{v} \delta \dot{v} + \dot{w} \delta \dot{w}) dz dx dy \\ = & \int_{\Omega} \int_{-\frac{h}{2}}^{\frac{h}{2}} \rho \left[\left(\dot{u}_0 - z \frac{\partial \dot{w}_0}{\partial x} \right) \left(\delta \dot{u}_0 - z \frac{\partial \delta \dot{w}_0}{\partial x} \right) \right. \\ & \left. + \left(\dot{v}_0 - z \frac{\partial \dot{w}_0}{\partial y} \right) \left(\delta \dot{v}_0 - z \frac{\partial \delta \dot{w}_0}{\partial y} \right) + \dot{w}_0 \delta \dot{w}_0 \right] dz dx dy \\ = & \int_{\Omega} \left[-I_0 (\dot{u}_0 \delta \dot{u}_0 + \dot{v}_0 \delta \dot{v}_0 + \dot{w}_0 \delta \dot{w}_0) + I_1 \left(\frac{\partial \delta \dot{w}_0}{\partial x} \dot{u}_0 + \frac{\partial \dot{w}_0}{\partial x} \delta \dot{u}_0 \right. \right. \\ & \left. \left. + \frac{\partial \delta \dot{w}_0}{\partial y} \dot{v}_0 + \frac{\partial \dot{w}_0}{\partial y} \delta \dot{v}_0 \right) - I_2 \left(\frac{\partial \dot{w}_0}{\partial x} \frac{\partial \delta \dot{w}_0}{\partial x} + \frac{\partial \dot{w}_0}{\partial y} \frac{\partial \delta \dot{w}_0}{\partial y} \right) \right] dx dy\end{aligned}\quad (3.4.8)$$

where the superposed dot on a variable indicates time derivative, $\dot{u}_0 = \partial u_0 / \partial t$, and (I_0, I_1, I_2) are the mass moments of inertia

$$\left\{ \begin{array}{l} I_0 \\ I_1 \\ I_2 \end{array} \right\} = \int_{-\frac{h}{2}}^{\frac{h}{2}} \left\{ \begin{array}{l} 1 \\ z \\ z^2 \end{array} \right\} \rho dz = \rho \left\{ \begin{array}{l} h \\ 0 \\ \frac{h^3}{12} \end{array} \right\}\quad (3.4.9)$$

The virtual displacements are zero on the portion of the boundary where the corresponding actual displacements are specified. For time-dependent problems, the admissible virtual displacements must also vanish at time $t = 0$ and $t = T$. Substituting for δU , δV , and δK from Eqs. (3.4.4), (3.4.6), and (3.4.8) into the virtual work statement in Eq. (3.4.2) and integrating through the thickness of the plate, we obtain

$$\begin{aligned}
0 = & \int_0^T \left\{ \int_{\Omega} \left[N_{xx} \delta \varepsilon_{xx}^0 + M_{xx} \delta \varepsilon_{xx}^1 + N_{yy} \delta \varepsilon_{yy}^0 + M_{yy} \delta \varepsilon_{yy}^1 + N_{xy} \delta \gamma_{xy}^0 \right. \right. \\
& + M_{xy} \delta \gamma_{xy}^1 + k w_0 \delta w_0 - I_0 (\dot{u}_0 \delta \dot{u}_0 + \dot{v}_0 \delta \dot{v}_0 + \dot{w}_0 \delta \dot{w}_0) \\
& + I_1 \left(\frac{\partial \delta \dot{w}_0}{\partial x} \dot{u}_0 + \frac{\partial \dot{w}_0}{\partial x} \delta \dot{u}_0 + \frac{\partial \delta \dot{w}_0}{\partial y} \dot{v}_0 + \frac{\partial \dot{w}_0}{\partial y} \delta \dot{v}_0 \right) \\
& \left. \left. - I_2 \left(\frac{\partial \dot{w}_0}{\partial x} \frac{\partial \delta \dot{w}_0}{\partial x} + \frac{\partial \dot{w}_0}{\partial y} \frac{\partial \delta \dot{w}_0}{\partial y} \right) - q \delta w_0 \right] dx dy \right\} dt \\
& - \int_0^T \left\{ \int_{\Gamma_\sigma} \left(\hat{N}_{nn} \delta u_{0n} + \hat{N}_{ns} \delta u_{0s} - \hat{M}_{nn} \frac{\partial \delta w_0}{\partial n} - \hat{M}_{ns} \frac{\partial \delta w_0}{\partial s} + \hat{Q}_n \delta w_0 \right) ds \right\} dt
\end{aligned} \tag{3.4.10}$$

The virtual strains are known in terms of the virtual displacements:

$$\begin{aligned}
\delta \varepsilon_{xx}^0 &= \frac{\partial \delta u_0}{\partial x} + \frac{\partial w_0}{\partial x} \frac{\partial \delta w_0}{\partial x}, \quad \delta \varepsilon_{xx}^1 = -\frac{\partial^2 \delta w_0}{\partial x^2} \\
\delta \varepsilon_{yy}^0 &= \frac{\partial \delta v_0}{\partial y} + \frac{\partial w_0}{\partial y} \frac{\partial \delta w_0}{\partial y}, \quad \delta \varepsilon_{yy}^1 = -\frac{\partial^2 \delta w_0}{\partial y^2} \\
\delta \gamma_{xy}^0 &= \frac{\partial \delta u_0}{\partial y} + \frac{\partial \delta v_0}{\partial x} + \frac{\partial \delta w_0}{\partial x} \frac{\partial w_0}{\partial y} + \frac{\partial w_0}{\partial x} \frac{\partial \delta w_0}{\partial y} \\
\delta \gamma_{xy}^1 &= -2 \frac{\partial^2 \delta w_0}{\partial x \partial y}
\end{aligned} \tag{3.4.11}$$

Substituting the virtual strains from Eq. (3.4.11) into Eq. (3.4.10) and integrating by parts to relieve the virtual displacements ($\delta u_0, \delta v_0, \delta w_0$) in Ω of any differentiation (so that we can use the fundamental lemma of variational calculus), we obtain

$$\begin{aligned}
0 = & \int_0^T \left\{ \int_{\Omega} \left[-N_{xx,x} \delta u_0 - \frac{\partial}{\partial x} \left(N_{xx} \frac{\partial w_0}{\partial x} \right) \delta w_0 - M_{xx,xx} \delta w_0 - N_{yy,y} \delta v_0 \right. \right. \\
& - \frac{\partial}{\partial y} \left(N_{yy} \frac{\partial w_0}{\partial y} \right) \delta w_0 - M_{yy,yy} \delta w_0 - N_{xy,y} \delta u_0 - N_{xy,x} \delta v_0 \\
& - \frac{\partial}{\partial x} \left(N_{xy} \frac{\partial w_0}{\partial y} \right) \delta w_0 - \frac{\partial}{\partial y} \left(N_{xy} \frac{\partial w_0}{\partial x} \right) \delta w_0 - 2M_{xy,xy} \delta w_0 \\
& + (k w_0 - q) \delta w_0 + I_0 (\ddot{u}_0 \delta u_0 + \ddot{v}_0 \delta v_0 + \ddot{w}_0 \delta w_0) \\
& \left. \left. - I_2 \left(\frac{\partial^2 \ddot{w}_0}{\partial x^2} + \frac{\partial^2 \ddot{w}_0}{\partial y^2} \right) \delta w_0 \right] dx dy \right\} dt \\
& + \oint_{\Gamma} \left[N_{xx} n_x \delta u_0 + \left(N_{xx} \frac{\partial w_0}{\partial x} \right) n_x \delta w_0 - M_{xx} n_x \frac{\partial \delta w_0}{\partial x} \right]
\end{aligned}$$

$$\begin{aligned}
& + M_{xx,x} n_x \delta w_0 + N_{yy} n_y \delta v_0 + \left(N_{yy} \frac{\partial w_0}{\partial y} \right) n_y \delta w_0 \\
& - M_{yy} n_y \frac{\partial \delta w_0}{\partial y} + M_{yy,y} n_y \delta w_0 - M_{xy} n_x \frac{\partial \delta w_0}{\partial y} \\
& + M_{xy,x} n_y \delta w_0 - M_{xy} n_y \frac{\partial \delta w_0}{\partial x} + M_{xy,y} n_x \delta w_0 + N_{xy} n_y \delta u_0 \\
& + N_{xy} n_x \delta v_0 + N_{xy} \frac{\partial w_0}{\partial y} n_x \delta w_0 + N_{xy} \frac{\partial w_0}{\partial x} n_y \delta w_0 \Big] ds \\
& - \int_{\Gamma_\sigma} \left(\hat{N}_{nn} \delta u_{0n} + \hat{N}_{ns} \delta u_{0s} - \hat{M}_{nn} \frac{\partial \delta w_0}{\partial n} - \hat{M}_{ns} \frac{\partial \delta w_0}{\partial s} + \hat{Q}_n \delta w_0 \right) ds \\
& + \oint_{\Gamma} I_2 \left(\frac{\partial \ddot{w}_0}{\partial x} n_x + \frac{\partial \ddot{w}_0}{\partial y} n_y \right) \delta w_0 \Big\} dt \quad (3.4.12)
\end{aligned}$$

where a comma followed by subscripts denotes differentiation with respect to the subscripts: $N_{xx,x} = \partial N_{xx}/\partial x$, $N_{xx,xx} = \partial^2 N_{xx}/\partial x^2$, and so on. Note that both spatial and time integration-by-parts were used in arriving at the last expression. The terms obtained in Ω , but evaluated at $t = 0$ and $t = T$ were set to zero because the virtual displacements are zero at $t = 0$ and $t = T$.

Collecting the coefficients of each of the virtual displacements $(\delta u_0, \delta v_0, \delta w_0)$ together and noting that the virtual displacements are zero on Γ_u , we obtain

$$\begin{aligned}
0 = \int_0^T \Bigg\{ & \int_{\Omega} \left[-(N_{xx,x} + N_{xy,y} - I_0 \ddot{u}_0) \delta u_0 - (N_{xy,x} + N_{yy,y} - I_0 \ddot{v}_0) \delta v_0 \right. \\
& - \left(M_{xx,xx} + 2M_{xy,xy} + M_{yy,yy} + \mathcal{N}(u_0, v_0, w_0) \right. \\
& \left. \left. - kw_0 + q - I_0 \ddot{w}_0 + I_2 \frac{\partial^2 \ddot{w}_0}{\partial x^2} + I_2 \frac{\partial^2 \ddot{w}_0}{\partial y^2} \right) \delta w_0 \right] dx dy \\
& + \int_{\Gamma_\sigma} \left[(N_{xx} n_x + N_{xy} n_y) \delta u_0 + (N_{xy} n_x + N_{yy} n_y) \delta v_0 \right. \\
& + \left(M_{xx,x} n_x + M_{xy,y} n_x + M_{yy,y} n_y + M_{xy,x} n_y \right. \\
& \left. + \mathcal{P}(u_0, v_0, w_0) + I_2 \frac{\partial \ddot{w}_0}{\partial x} n_x + I_2 \frac{\partial \ddot{w}_0}{\partial y} n_y \right) \delta w_0 \\
& \left. - (M_{xx} n_x + M_{xy} n_y) \frac{\partial \delta w_0}{\partial x} - (M_{xy} n_x + M_{yy} n_y) \frac{\partial \delta w_0}{\partial y} \right] ds \\
& - \int_{\Gamma_\sigma} \left(\hat{N}_{nn} \delta u_{0n} + \hat{N}_{ns} \delta u_{0s} - \hat{M}_{nn} \frac{\partial \delta w_0}{\partial n} - \hat{M}_{ns} \frac{\partial \delta w_0}{\partial s} + \hat{Q}_n \delta w_0 \right) ds \Bigg\} dt \quad (3.4.13)
\end{aligned}$$

where

$$\begin{aligned}
\mathcal{N}(u_0, v_0, w_0) &= \frac{\partial}{\partial x} \left(N_{xx} \frac{\partial w_0}{\partial x} + N_{xy} \frac{\partial w_0}{\partial y} \right) + \frac{\partial}{\partial y} \left(N_{xy} \frac{\partial w_0}{\partial x} + N_{yy} \frac{\partial w_0}{\partial y} \right) \\
\mathcal{P}(u_0, v_0, w_0) &= \left(N_{xx} \frac{\partial w_0}{\partial x} + N_{xy} \frac{\partial w_0}{\partial y} \right) n_x + \left(N_{xy} \frac{\partial w_0}{\partial x} + N_{yy} \frac{\partial w_0}{\partial y} \right) n_y
\end{aligned} \quad (3.4.14)$$

The Euler–Lagrange equations are obtained by setting the coefficients of δu_0 , δv_0 , and δw_0 in Ω to zero separately:

$$\delta u_0 : \frac{\partial N_{xx}}{\partial x} + \frac{\partial N_{xy}}{\partial y} = I_0 \frac{\partial^2 u_0}{\partial t^2} \quad (3.4.15)$$

$$\delta v_0 : \frac{\partial N_{xy}}{\partial x} + \frac{\partial N_{yy}}{\partial y} = I_0 \frac{\partial^2 v_0}{\partial t^2} \quad (3.4.16)$$

$$\begin{aligned} \delta w_0 : & \frac{\partial^2 M_{xx}}{\partial x^2} + 2 \frac{\partial^2 M_{xy}}{\partial y \partial x} + \frac{\partial^2 M_{yy}}{\partial y^2} + \mathcal{N}(u_0, v_0, w_0) - kw_0 + q \\ &= I_0 \frac{\partial^2 w_0}{\partial t^2} - I_2 \frac{\partial^2}{\partial t^2} \left(\frac{\partial^2 w_0}{\partial x^2} + \frac{\partial^2 w_0}{\partial y^2} \right) \end{aligned} \quad (3.4.17)$$

The terms involving I_2 are called *rotary* (or *rotatory*) inertia terms, and are often neglected in most books. The term can contribute to higher frequencies of vibration.

3.5 Boundary and Initial Conditions

A salient feature of energy principles is that they also yield the natural boundary conditions and identify the variables involved in the specification of the essential boundary conditions of the problem. As a rule, quantities with a variation in the boundary integrals are the *primary variables*, and their specification constitutes the geometric boundary conditions. The expressions that are coefficients of the varied quantities are termed the *secondary variables*, and their specification constitutes the natural boundary conditions.

In view of Eqs. (3.4.15)–(3.4.17), the integral over Ω in Eq. (3.4.13) is zero. Then the remaining boundary integral is also zero:

$$\begin{aligned} 0 = \int_0^T \left\{ \int_{\Gamma_\sigma} \left[& (N_{xx}n_x + N_{xy}n_y) \underline{\delta u_0} + (N_{xy}n_x + N_{yy}n_y) \underline{\delta v_0} \right. \right. \\ &+ \left(M_{xx,x}n_x + M_{xy,y}n_x + M_{yy,y}n_y + M_{xy,x}n_y \right. \\ &+ \mathcal{P}(u_0, v_0, w_0) + I_2 \frac{\partial \ddot{w}_0}{\partial x} n_x + I_2 \frac{\partial \ddot{w}_0}{\partial y} n_y \Big) \underline{\delta w_0} \\ &\left. \left. - (M_{xx}n_x + M_{xy}n_y) \frac{\partial \delta w_0}{\partial x} - (M_{xy}n_x + M_{yy}n_y) \frac{\partial \delta w_0}{\partial y} \right] ds \right\} dt \\ &- \int_{\Gamma_\sigma} \left(\hat{N}_{nn} \delta u_{0n} + \hat{N}_{ns} \delta u_{0s} - \hat{M}_{nn} \frac{\partial \delta w_0}{\partial n} - \hat{M}_{ns} \frac{\partial \delta w_0}{\partial s} + \hat{Q}_n \delta w_0 \right) ds \} dt \end{aligned} \quad (3.5.1)$$

Inspection of the above expression indicates that the quantities with variation (the underlined terms) are u_0 , v_0 , w_0 , $\partial w_0/\partial x$, and $\partial w_0/\partial y$, and, therefore, they are the primary variables for a plate with edges parallel to the x and y coordinates. Before we proceed further, we must examine whether we have the right number of primary and secondary variables associated with the equations (3.4.15)–(3.4.17) governing the bending and stretching of a plate.

We note that the equations of motion in Eqs. (3.4.15)–(3.4.17) have the total spatial differential order of eight. In other words, if the equations are expressed in terms of the displacements (u_0, v_0, w_0) , they would contain second-order spatial derivatives of u_0 and v_0 and fourth-order spatial derivatives of w_0 . Hence, the classical plate theory is said to be an *eighth-order theory*. This implies that there should be only eight (four essential and four natural) boundary conditions, whereas from Eq. (3.5.1) we note that there are five essential boundary conditions and five natural boundary conditions, giving a total of ten boundary conditions. Before we eliminate this inconsistency, we rewrite all of the boundary expressions in terms of the displacements, forces, and moments over an edge with unit normal $\hat{\mathbf{n}} = n_x \hat{\mathbf{e}}_x + n_y \hat{\mathbf{e}}_y$ (Figure 3.3.1). Suppose that the unit normal vector $\hat{\mathbf{n}}$ is oriented at an angle θ clockwise from the positive x -axis, then its direction cosines are: $n_x = \cos \theta$ and $n_y = \sin \theta$. The transverse normal coordinate r is parallel to the z -axis.

The displacement vector of a point on this edge can be written in terms of the three displacement components along three coordinate directions (n, s, r) and rotations about n and s coordinates (see Figures 3.2.2 and 3.4.1). In order to write the components of displacements, forces and moments in the (x, y, z) coordinates in terms of the (n, s, r) coordinates, we use the transformation equations (1.2.73) and (1.4.1) derived in Chapter 1. The transformation between (barred) coordinates (n, s, r) and (unbarred) coordinates (x, y, z) is given by [see Eq. (1.2.72)]

$$\begin{Bmatrix} x \\ y \\ z \end{Bmatrix} = \begin{bmatrix} \cos \theta & -\sin \theta & 0 \\ \sin \theta & \cos \theta & 0 \\ 0 & 0 & 1 \end{bmatrix} \begin{Bmatrix} n \\ s \\ r \end{Bmatrix} \equiv \begin{bmatrix} n_x & -n_y & 0 \\ n_y & n_x & 0 \\ 0 & 0 & 1 \end{bmatrix} \begin{Bmatrix} n \\ s \\ r \end{Bmatrix} \quad (3.5.2)$$

Hence, the displacements (u_{0n}, u_{0s}, w_0) are related to (u_0, v_0, w_0) by the same transformation as in Eq. (3.5.2):

$$\begin{Bmatrix} u_0 \\ v_0 \\ w_0 \end{Bmatrix} = \begin{bmatrix} n_x & -n_y & 0 \\ n_y & n_x & 0 \\ 0 & 0 & 1 \end{bmatrix} \begin{Bmatrix} u_{0n} \\ u_{0s} \\ w_0 \end{Bmatrix} \quad (3.5.3)$$

Similarly, the normal and tangential derivatives $(w_{0,n}, w_{0,s})$ are related to the derivatives $(w_{0,x}, w_{0,y})$ by the relations

$$\begin{Bmatrix} \frac{\partial w_0}{\partial x} \\ \frac{\partial w_0}{\partial y} \end{Bmatrix} = \begin{bmatrix} n_x & -n_y \\ n_y & n_x \end{bmatrix} \begin{Bmatrix} \frac{\partial w_0}{\partial n} \\ \frac{\partial w_0}{\partial s} \end{Bmatrix} \quad (3.5.4)$$

In addition, the stresses $(\sigma_{nn}, \sigma_{ns})$ are related to $(\sigma_{xx}, \sigma_{yy}, \sigma_{xy})$ by the transformation [see Eq. (1.4.1)]

$$\begin{Bmatrix} \sigma_{nn} \\ \sigma_{ns} \end{Bmatrix} = \begin{bmatrix} n_x^2 & n_y^2 & 2n_x n_y \\ -n_x n_y & n_x n_y & n_x^2 - n_y^2 \end{bmatrix} \begin{Bmatrix} \sigma_{xx} \\ \sigma_{yy} \\ \sigma_{xy} \end{Bmatrix} \quad (3.5.5)$$

Therefore, we have [see Eq. (3.4.7)]

$$\begin{Bmatrix} N_{nn} \\ N_{ns} \end{Bmatrix} = \begin{bmatrix} n_x^2 & n_y^2 & 2n_x n_y \\ -n_x n_y & n_x n_y & n_x^2 - n_y^2 \end{bmatrix} \begin{Bmatrix} N_{xx} \\ N_{yy} \\ N_{xy} \end{Bmatrix} \quad (3.5.6)$$

and

$$\begin{Bmatrix} M_{nn} \\ M_{ns} \end{Bmatrix} = \begin{bmatrix} n_x^2 & n_y^2 & 2n_x n_y \\ -n_x n_y & n_x n_y & n_x^2 - n_y^2 \end{bmatrix} \begin{Bmatrix} M_{xx} \\ M_{yy} \\ M_{xy} \end{Bmatrix} \quad (3.5.7)$$

Now we can rewrite the boundary expressions in Eq. (3.5.1) in terms of the displacements (u_{0n}, u_{0s}, w_0) and $(w_{0,n}, w_{0,s})$ and stress resultants N_{nn} , N_{ns} , M_{nn} , and M_{ns} . We have

$$\begin{aligned} (N_{xx}n_x + N_{xy}n_y)\delta u_0 + (N_{xy}n_x + N_{yy}n_y)\delta v_0 \\ = (N_{xx}n_x + N_{xy}n_y)(n_x\delta u_{0n} - n_y\delta u_{0s}) \\ + (N_{xy}n_x + N_{yy}n_y)(n_y\delta u_{0n} + n_x\delta u_{0s}) \\ = (N_{xx}n_x^2 + 2N_{xy}n_x n_y + N_{yy}n_y^2)\delta u_{0n} \\ + [-N_{xx}n_x n_y + N_{yy}n_x n_y + N_{xy}(n_x^2 - n_y^2)]\delta u_{0s} \\ = N_{nn}\delta u_{0n} + N_{ns}\delta u_{0s} \end{aligned} \quad (3.5.8)$$

Similarly,

$$\begin{aligned} (M_{xx}n_x + M_{xy}n_y)\frac{\partial \delta w_0}{\partial x} + (M_{xy}n_x + M_{yy}n_y)\frac{\partial \delta w_0}{\partial y} \\ = (M_{xx}n_x + M_{xy}n_y)(n_x\delta w_{0,n} - n_y\delta w_{0,s}) \\ + (M_{xy}n_x + M_{yy}n_y)(n_y\delta w_{0,n} + n_x\delta w_{0,s}) \\ = (M_{xx}n_x^2 + 2M_{xy}n_x n_y + M_{yy}n_y^2)\delta w_{0,n} \\ + [-M_{xx}n_x n_y + M_{yy}n_x n_y + M_{xy}(n_x^2 - n_y^2)]\delta w_{0,s} \\ = M_{nn}\delta w_{0,n} + M_{ns}\delta w_{0,s} \end{aligned} \quad (3.5.9)$$

In view of the above relations, the boundary integrals in Eq. (3.4.13) can be written as

$$\begin{aligned} 0 = \int_0^T \int_{\Gamma_\sigma} \left[(N_{nn} - \hat{N}_{nn})\delta u_{0n} + (N_{ns} - \hat{N}_{ns})\delta u_{0s} \right. \\ + \left(M_{xx,x}n_x + M_{xy,y}n_x + M_{yy,y}n_y + M_{xy,x}n_y \right. \\ + \mathcal{P}(u_0, v_0, w_0) + I_2 \frac{\partial \ddot{w}_0}{\partial x} n_x + I_2 \frac{\partial \ddot{w}_0}{\partial y} n_y - \hat{Q}_n \left. \right) \delta w_0 \\ \left. - (M_{nn} - \hat{M}_{nn})\frac{\partial \delta w_0}{\partial n} - (M_{ns} - \hat{M}_{ns})\frac{\partial \delta w_0}{\partial s} \right] ds dt \quad (3.5.10) \end{aligned}$$

Kirchhoff Free Edge Condition

To eliminate the discrepancy between the total order of the differential and the number of boundary conditions available, one may integrate the tangential derivative term by parts to obtain the boundary term

$$-\oint_{\Gamma} M_{ns} \frac{\partial \delta w_0}{\partial s} ds = \oint_{\Gamma} \frac{\partial M_{ns}}{\partial s} \delta w_0 ds - [M_{ns}\delta w_0]_{\Gamma} \quad (3.5.11)$$

The term $[M_{ns}\delta w_0]_\Gamma$ is zero when the end points of a closed curve coincide or when $M_{ns} = 0$. If $M_{ns} \neq 0$ at corners of the boundary Γ of a polygonal plate, concentrated forces of magnitude

$$F_c = -2M_{ns} \quad (3.5.12)$$

will be produced at the corners. The factor of 2 appears because M_{ns} from two sides of the corner are added there. Here we assume that $M_{ns} = 0$.

The coefficient of δw_0 in the boundary integral of Eq. (3.5.11) adds to the coefficient of δw_0 in Eq. (3.5.10) to give the *effective shear force*

$$\begin{aligned} V_n \equiv & M_{xx,x}n_x + M_{xy,y}n_x + M_{yy,y}n_y + M_{xy,x}n_y + \frac{\partial M_{ns}}{\partial s} \\ & + \mathcal{P}(u_0, v_0, w_0) + I_2 \frac{\partial \ddot{w}_0}{\partial x} n_x + I_2 \frac{\partial \ddot{w}_0}{\partial y} n_y \end{aligned} \quad (3.5.13)$$

The specification of V_n is called the *Kirchhoff free edge condition*.

The complete boundary expression in Eq. (3.5.10) becomes

$$\begin{aligned} 0 = & \int_0^T \int_{\Gamma_\sigma} \left[(N_{nn} - \hat{N}_{nn}) \delta u_{0n} + (N_{ns} - \hat{N}_{ns}) \delta u_{0s} + (V_n - \hat{V}_n) \delta w_0 \right. \\ & \left. - (M_{nn} - \hat{M}_{nn}) \frac{\partial \delta w_0}{\partial n} \right] ds dt \end{aligned} \quad (3.5.14)$$

where

$$\hat{V}_n \equiv \hat{Q}_n + \frac{\partial \hat{M}_{ns}}{\partial s} \quad (3.5.15)$$

Consequently, the primary and secondary variables of the classical plate theory are

$$\begin{aligned} \text{Primary variables: } & u_{0n}, u_{0s}, w_0, \frac{\partial w_0}{\partial n} \\ \text{Secondary variables: } & N_{nn}, N_{ns}, V_n, M_{nn} \end{aligned} \quad (3.5.16)$$

On the edge $y = b$ (i.e., $s = x$, $n = y$, $n_x = 0$, and $n_y = 1$), for example, the above variables become

$$\begin{aligned} u_{0n} &= v_0, \quad u_{0s} = u_0, \quad w_0, \quad \frac{\partial w_0}{\partial n} = \frac{\partial w_0}{\partial y}, \quad \frac{\partial w_0}{\partial s} = \frac{\partial w_0}{\partial x} \\ N_{nn} &= N_{yy}, \quad N_{ns} = N_{yx}, \quad M_{nn} = M_{yy}, \quad M_{ns} = M_{yx} \\ V_n &= V_y = \frac{\partial M_{yy}}{\partial y} + 2 \frac{\partial M_{yx}}{\partial x} + \mathcal{P}(u_0, v_0, w_0) + I_2 \frac{\partial \ddot{w}_0}{\partial y} \end{aligned} \quad (3.5.17)$$

If the primary variables are not specified on any portion of the boundary, the natural boundary conditions on that portion (Γ_σ) are then given by

$$N_{nn} - \hat{N}_{nn} = 0, \quad N_{ns} - \hat{N}_{ns} = 0, \quad M_{nn} - \hat{M}_{nn} = 0, \quad V_n - \hat{V}_n = 0 \quad (3.5.18)$$

Equations (3.4.15)–(3.4.17) with suitable boundary conditions on variables in Eq. (3.5.16) completely specify the plate problem.

Next we discuss some common types of boundary conditions for the linear bending of a rectangular plate with edges parallel to the x and y coordinates. Here we use the edge at $y = 0$ ($n_x = 0$ and $n_y = -1$) to discuss the boundary conditions (see Figure 3.4.1). It should be noted that only one element of each of the four pairs may (and should) be specified on an edge of a plate. The force boundary conditions may be expressed in terms of the generalized displacements using the plate constitutive equations discussed in the next section.

Free edge, $y = 0$: A free edge is one that is geometrically not restrained in any way. Hence, we have

$$u_0 \neq 0, \quad v_0 \neq 0, \quad w_0 \neq 0, \quad \frac{\partial w_0}{\partial y} \neq 0 \quad (3.5.19)$$

However, the edge may have applied forces and/or moments

$$N_{xy} = \hat{N}_{xy}, \quad N_{yy} = \hat{N}_{yy}, \quad V_n \equiv -Q_y - \frac{\partial M_{xy}}{\partial x} = \hat{V}_n, \quad M_{yy} = \hat{M}_{yy} \quad (3.5.20)$$

where quantities with a hat (or caret), are specified forces or moments. For free rectangular plates, $M_{xy} = 0$ and, therefore, no corner forces are developed.

Fixed (or clamped) edge, $y = 0$: A fixed edge is one that is geometrically fully restrained

$$u_0 = 0, \quad v_0 = 0, \quad w_0 = 0, \quad \frac{\partial w_0}{\partial y} = 0 \quad (3.5.21)$$

Therefore, the forces and moments on a fixed edge are not known a priori (i.e., they are reactions to be determined as a part of the analysis). For clamped rectangular plates, $M_{xy} = 0$, hence no corner forces are developed.

Simply supported edge $y = 0$: The phrase “simply supported” does not uniquely define the boundary conditions, and one must indicate what it means, especially when both inplane and bending deflections are involved. Here we *define* two types of simply supported boundary conditions:

$$\text{SS-1: } u_0 = 0, \quad w_0 = 0; \quad N_{yy} = \hat{N}_{yy}, \quad M_{yy} = \hat{M}_{yy} \quad (3.5.22)$$

$$\text{SS-2: } v_0 = 0, \quad w_0 = 0; \quad N_{xy} = \hat{N}_{xy}, \quad M_{yy} = \hat{M}_{yy} \quad (3.5.23)$$

For simply supported rectangular plates, a reacting force of $2M_{xy}$ is developed at each corner of the plate.

When transient response of a plate is of interest, we must know the initial displacement field and velocity field throughout the domain of the plate. The initial conditions of classical plate theory involve specifying the values of the displacements and their first derivatives with respect to time at $t = 0$:

$$\begin{aligned} u_n &= u_n^0, \quad u_s = u_s^0, \quad w_0 = w_0^0 \\ \dot{u}_n &= \dot{u}_n^0, \quad \dot{u}_s = \dot{u}_s^0, \quad \dot{w}_0 = \dot{w}_0^0 \end{aligned} \quad (3.5.24)$$

for all points in Ω .

3.6 Plate Stiffness Coefficients

In classical plate theory, all three transverse strain components ($\varepsilon_{zz}, \varepsilon_{xz}, \varepsilon_{yz}$) are zero by definition. Since $\varepsilon_{zz} = 0$, the transverse normal stress σ_{zz} , though not zero identically, does not appear in the virtual work statement and, hence, in the equations of motion. Consequently, it amounts to neglecting the transverse normal stress. Thus, we have, in theory, a case of both plane strain and plane stress. However, from practical considerations, a thin-to-moderately thick plate is in a state of plane stress because the thickness is small compared to the inplane dimensions. Hence, the plane stress-reduced constitutive relations may be used.

For an orthotropic material with principal materials axes (x_1, x_2, x_3) coinciding with the plate coordinates (x, y, z), the plane stress-reduced thermoelastic constitutive equations can be expressed as

$$\begin{Bmatrix} \sigma_{xx} \\ \sigma_{yy} \\ \sigma_{xy} \end{Bmatrix} = \begin{bmatrix} Q_{11} & Q_{12} & 0 \\ Q_{12} & Q_{22} & 0 \\ 0 & 0 & Q_{66} \end{bmatrix} \begin{Bmatrix} \varepsilon_{xx} - \alpha_1 \Delta T \\ \varepsilon_{yy} - \alpha_2 \Delta T \\ \gamma_{xy} \end{Bmatrix} \quad (3.6.1)$$

where Q_{ij} are the plane stress-reduced stiffness coefficients

$$\begin{aligned} Q_{11} &= \frac{E_1}{1 - \nu_{12}\nu_{21}}, & Q_{12} &= \frac{\nu_{12}E_2}{1 - \nu_{12}\nu_{21}} = \frac{\nu_{21}E_1}{1 - \nu_{12}\nu_{21}} \\ Q_{22} &= \frac{E_2}{1 - \nu_{12}\nu_{21}}, & Q_{66} &= G_{12} \end{aligned} \quad (3.6.2)$$

and $(\sigma_i, \varepsilon_i)$ are the stress and strain components, respectively, α_1 and α_2 are the coefficients of thermal expansion, and ΔT is the temperature increment from a reference state, $\Delta T = T - T_0$. The moisture strains are similar to thermal strains (i.e., for moisture strains replace ΔT and α_i with the moisture concentration increment and coefficients of hygroscopic expansion, respectively).

If the principal material axes (x_1, x_2, x_3) are such that $x_3 = z$ and the x_1x_2 -plane is rotated about the z -axis by an arbitrary angle θ , we must transform the material stiffness coefficients, as explained in Chapter 1. The stress-strain relations for this case are given by

$$\begin{Bmatrix} \sigma_{xx} \\ \sigma_{yy} \\ \sigma_{xy} \end{Bmatrix} = \begin{bmatrix} \bar{Q}_{11} & \bar{Q}_{12} & \bar{Q}_{16} \\ \bar{Q}_{12} & \bar{Q}_{22} & \bar{Q}_{26} \\ \bar{Q}_{16} & \bar{Q}_{26} & Q_{66} \end{bmatrix} \left(\begin{Bmatrix} \varepsilon_{xx} \\ \varepsilon_{yy} \\ \gamma_{xy} \end{Bmatrix} - \begin{Bmatrix} \alpha_{xx} \\ \alpha_{yy} \\ \alpha_{xy} \end{Bmatrix} \Delta T \right) \quad (3.6.3)$$

where [see Eqs. (1.4.6) and (1.4.7)]

$$\begin{aligned} \bar{Q}_{11} &= Q_{11} \cos^4 \theta + 2(Q_{12} + 2Q_{66}) \sin^2 \theta \cos^2 \theta + Q_{22} \sin^4 \theta \\ \bar{Q}_{12} &= (Q_{11} + Q_{22} - 4Q_{66}) \sin^2 \theta \cos^2 \theta + Q_{12}(\sin^4 \theta + \cos^4 \theta) \\ \bar{Q}_{22} &= Q_{11} \sin^4 \theta + 2(Q_{12} + 2Q_{66}) \sin^2 \theta \cos^2 \theta + Q_{22} \cos^4 \theta \\ \bar{Q}_{16} &= (Q_{11} - Q_{12} - 2Q_{66}) \sin \theta \cos^3 \theta + (Q_{12} - Q_{22} + 2Q_{66}) \sin^3 \theta \cos \theta \\ \bar{Q}_{26} &= (Q_{11} - Q_{12} - 2Q_{66}) \sin^3 \theta \cos \theta + (Q_{12} - Q_{22} + 2Q_{66}) \sin \theta \cos^3 \theta \\ \bar{Q}_{66} &= (Q_{11} + Q_{22} - 2Q_{12} - 2Q_{66}) \sin^2 \theta \cos^2 \theta + Q_{66}(\sin^4 \theta + \cos^4 \theta) \end{aligned} \quad (3.6.4)$$

and α_{xx} , α_{yy} , and α_{xy} are the transformed thermal coefficients of expansion

$$\begin{aligned}\alpha_{xx} &= \alpha_1 \cos^2 \theta + \alpha_2 \sin^2 \theta \\ \alpha_{yy} &= \alpha_1 \sin^2 \theta + \alpha_2 \cos^2 \theta \\ \alpha_{xy} &= 2(\alpha_1 - \alpha_2) \sin \theta \cos \theta\end{aligned}\quad (3.6.5)$$

Here θ is the angle measured counterclockwise from the x -coordinate to the x_1 -coordinate (Figure 1.4.1). In this book, we only consider orthotropic plates (i.e., $\theta = 0^\circ$ or 90°); see Reddy (2004a) for laminated composite plates and shells.

The plate constitutive equations relate the forces and moments defined in Eq. (3.4.3) to the extensional and bending strains in Eq. (3.3.8b) of the plate theory. For a plate made of a single anisotropic material (i.e., $\theta \neq 0^\circ$ or 90°), the plate constitutive relations are obtained using the definitions in Eq. (3.4.4). They are

$$\begin{aligned}\left\{ \begin{array}{c} N_{xx} \\ N_{yy} \\ N_{xy} \end{array} \right\} &= \int_{-\frac{h}{2}}^{\frac{h}{2}} \left\{ \begin{array}{c} \sigma_{xx} \\ \sigma_{yy} \\ \sigma_{xy} \end{array} \right\} dz = \int_{-\frac{h}{2}}^{\frac{h}{2}} \begin{bmatrix} \bar{Q}_{11} & \bar{Q}_{12} & \bar{Q}_{16} \\ \bar{Q}_{12} & \bar{Q}_{22} & \bar{Q}_{26} \\ \bar{Q}_{16} & \bar{Q}_{26} & \bar{Q}_{66} \end{bmatrix} \left\{ \begin{array}{c} \varepsilon_{xx}^0 + z\varepsilon_{xx}^1 - \alpha_{xx}\Delta T \\ \varepsilon_{yy}^0 + z\varepsilon_{yy}^1 - \alpha_{yy}\Delta T \\ \gamma_{xy}^0 + z\gamma_{xy}^1 - \alpha_{xy}\Delta T \end{array} \right\} dz \\ &= \begin{bmatrix} A_{11} & A_{12} & A_{16} \\ A_{12} & A_{22} & A_{26} \\ A_{16} & A_{26} & A_{66} \end{bmatrix} \left\{ \begin{array}{c} \varepsilon_{xx}^0 \\ \varepsilon_{yy}^0 \\ \gamma_{xy}^0 \end{array} \right\} - \left\{ \begin{array}{c} N_{xx}^T \\ N_{yy}^T \\ N_{xy}^T \end{array} \right\}\end{aligned}\quad (3.6.6)$$

$$\begin{aligned}\left\{ \begin{array}{c} M_{xx} \\ M_{yy} \\ M_{xy} \end{array} \right\} &= \int_{-\frac{h}{2}}^{\frac{h}{2}} \left\{ \begin{array}{c} \sigma_{xx} \\ \sigma_{yy} \\ \sigma_{xy} \end{array} \right\} z dz = \int_{-\frac{h}{2}}^{\frac{h}{2}} \begin{bmatrix} \bar{Q}_{11} & \bar{Q}_{12} & \bar{Q}_{16} \\ \bar{Q}_{12} & \bar{Q}_{22} & \bar{Q}_{26} \\ \bar{Q}_{16} & \bar{Q}_{26} & \bar{Q}_{66} \end{bmatrix} \left\{ \begin{array}{c} \varepsilon_{xx}^0 + z\varepsilon_{xx}^1 - \alpha_{xx}\Delta T \\ \varepsilon_{yy}^0 + z\varepsilon_{yy}^1 - \alpha_{yy}\Delta T \\ \gamma_{xy}^0 + z\gamma_{xy}^1 - \alpha_{xy}\Delta T \end{array} \right\} z dz \\ &= \begin{bmatrix} D_{11} & D_{12} & D_{16} \\ D_{12} & D_{22} & D_{26} \\ D_{16} & D_{26} & D_{66} \end{bmatrix} \left\{ \begin{array}{c} \varepsilon_{xx}^1 \\ \varepsilon_{yy}^1 \\ \gamma_{xy}^1 \end{array} \right\} - \left\{ \begin{array}{c} M_{xx}^T \\ M_{yy}^T \\ M_{xy}^T \end{array} \right\}\end{aligned}\quad (3.6.7)$$

where A_{ij} are *extensional stiffness coefficients* and D_{ij} are *bending stiffness coefficients*, which are defined in terms of the material elastic coefficients \bar{Q}_{ij} as

$$(A_{ij}, D_{ij}) = \int_{-\frac{h}{2}}^{\frac{h}{2}} \bar{Q}_{ij}(1, z^2) dz \quad \text{or} \quad A_{ij} = \bar{Q}_{ij}h \quad \text{and} \quad D_{ij} = \bar{Q}_{ij} \frac{h^3}{12} \quad (3.6.8)$$

and $\{N^T\}$ and $\{M^T\}$ are thermal stress resultants

$$\left\{ \begin{array}{c} N_{xx}^T \\ N_{yy}^T \\ N_{xy}^T \end{array} \right\} = \int_{-\frac{h}{2}}^{\frac{h}{2}} \left\{ \begin{array}{c} \bar{Q}_{11}\alpha_{xx} + \bar{Q}_{12}\alpha_{yy} + \bar{Q}_{16}\alpha_{xy} \\ \bar{Q}_{12}\alpha_{xx} + \bar{Q}_{22}\alpha_{yy} + \bar{Q}_{26}\alpha_{xy} \\ \bar{Q}_{16}\alpha_{xx} + \bar{Q}_{26}\alpha_{yy} + \bar{Q}_{66}\alpha_{xy} \end{array} \right\} \Delta T dz \quad (3.6.9)$$

$$\left\{ \begin{array}{c} M_{xx}^T \\ M_{yy}^T \\ M_{xy}^T \end{array} \right\} = \int_{-\frac{h}{2}}^{\frac{h}{2}} \left\{ \begin{array}{c} \bar{Q}_{11}\alpha_{xx} + \bar{Q}_{12}\alpha_{yy} + \bar{Q}_{16}\alpha_{xy} \\ \bar{Q}_{12}\alpha_{xx} + \bar{Q}_{22}\alpha_{yy} + \bar{Q}_{26}\alpha_{xy} \\ \bar{Q}_{16}\alpha_{xx} + \bar{Q}_{26}\alpha_{yy} + \bar{Q}_{66}\alpha_{xy} \end{array} \right\} \Delta T z dz \quad (3.6.10)$$

In general, \bar{Q}_{ij} and $(\alpha_{xx}, \alpha_{yy}, \alpha_{xy})$, and therefore A_{ij} and D_{ij} , can be functions of position (x, y) . Relations similar to (3.6.6) and (3.6.7) can be written for hygroscopic effects (i.e., replace ΔT by Δc , where c is the moisture concentration).

For a plate made of a single orthotropic material, we have

$$\begin{Bmatrix} N_{xx} \\ N_{yy} \\ N_{xy} \end{Bmatrix} = \begin{bmatrix} A_{11} & A_{12} & 0 \\ A_{12} & A_{22} & 0 \\ 0 & 0 & A_{66} \end{bmatrix} \begin{Bmatrix} \varepsilon_{xx}^0 \\ \varepsilon_{yy}^0 \\ \gamma_{xy}^0 \end{Bmatrix} - \begin{Bmatrix} N_{xx}^T \\ N_{yy}^T \\ 0 \end{Bmatrix} \quad (3.6.11)$$

$$\begin{Bmatrix} M_{xx} \\ M_{yy} \\ M_{xy} \end{Bmatrix} = \begin{bmatrix} D_{11} & D_{12} & 0 \\ D_{12} & D_{22} & 0 \\ 0 & 0 & D_{66} \end{bmatrix} \begin{Bmatrix} \varepsilon_{xx}^1 \\ \varepsilon_{yy}^1 \\ \gamma_{xy}^1 \end{Bmatrix} - \begin{Bmatrix} M_{xx}^T \\ M_{yy}^T \\ 0 \end{Bmatrix} \quad (3.6.12)$$

where

$$A_{11} = \frac{E_1 h}{1 - \nu_{12} \nu_{21}}, \quad A_{12} = \nu_{21} A_{11}, \quad A_{22} = \frac{E_2}{E_1} A_{11}, \quad A_{66} = G_{12} h \quad (3.6.13)$$

$$D_{11} = \frac{E_1 h^3}{12(1 - \nu_{12} \nu_{21})}, \quad D_{12} = \nu_{21} D_{11}, \quad D_{22} = \frac{E_2}{E_1} D_{11}, \quad D_{66} = \frac{G_{12} h^3}{12}$$

and

$$\begin{Bmatrix} N_{xx}^T \\ N_{yy}^T \end{Bmatrix} = \begin{Bmatrix} Q_{11}\alpha_1 + Q_{12}\alpha_2 \\ Q_{12}\alpha_1 + Q_{22}\alpha_2 \end{Bmatrix} \int_{-\frac{h}{2}}^{\frac{h}{2}} \Delta T(x, y, z) dz \quad (3.6.14)$$

$$\begin{Bmatrix} M_{xx}^T \\ M_{yy}^T \end{Bmatrix} = \begin{Bmatrix} Q_{11}\alpha_1 + Q_{12}\alpha_2 \\ Q_{12}\alpha_1 + Q_{22}\alpha_2 \end{Bmatrix} \int_{-\frac{h}{2}}^{\frac{h}{2}} \Delta T(x, y, z) z dz \quad (3.6.15)$$

where the temperature change ΔT (above a stress-free temperature) is a known function of position.

For plates made of an isotropic material, Eqs. (3.6.11)–(3.6.15) simplify to

$$\begin{Bmatrix} N_{xx} \\ N_{yy} \\ N_{xy} \end{Bmatrix} = A \begin{bmatrix} 1 & \nu & 0 \\ \nu & 1 & 0 \\ 0 & 0 & \frac{1-\nu}{2} \end{bmatrix} \begin{Bmatrix} \varepsilon_{xx}^0 \\ \varepsilon_{yy}^0 \\ \gamma_{xy}^0 \end{Bmatrix} - \frac{N^T}{1-\nu} \begin{Bmatrix} 1 \\ 1 \\ 0 \end{Bmatrix} \quad (3.6.16)$$

$$\begin{Bmatrix} M_{xx} \\ M_{yy} \\ M_{xy} \end{Bmatrix} = D \begin{bmatrix} 1 & \nu & 0 \\ \nu & 1 & 0 \\ 0 & 0 & \frac{1-\nu}{2} \end{bmatrix} \begin{Bmatrix} \varepsilon_{xx}^1 \\ \varepsilon_{yy}^1 \\ \gamma_{xy}^1 \end{Bmatrix} - \frac{M^T}{1-\nu} \begin{Bmatrix} 1 \\ 1 \\ 0 \end{Bmatrix} \quad (3.6.17)$$

where

$$A = \frac{Eh}{1 - \nu^2}, \quad D = \frac{h^2}{12} A, \quad N_T = E\alpha \int_{-\frac{h}{2}}^{\frac{h}{2}} \Delta T dz, \quad M_T = E\alpha \int_{-\frac{h}{2}}^{\frac{h}{2}} \Delta T z dz \quad (3.6.18)$$

Plates composed of multiple layers are called *laminated plates* [see Reddy (2004a) and Figure 3.6.1]. A laminated plate composed of multiple orthotropic layers that are *symmetrically disposed*, both from a material and geometric properties standpoint, about the midplane of the plate has constitutive equations that are again given by Eqs. (3.6.11) and (3.6.12), with the laminate stiffness coefficients A_{ij} and D_{ij} defined by

$$A_{ij} = \sum_{k=1}^N \bar{Q}_{ij}^{(k)} (z_{k+1} - z_k), \quad D_{ij} = \frac{1}{3} \sum_{k=1}^N \bar{Q}_{ij}^{(k)} (z_{k+1}^3 - z_k^3) \quad (3.6.19)$$

where

$$\begin{aligned} \bar{Q}_{11}^{(k)} &= \frac{E_1^k}{1 - \nu_{12}^k \nu_{21}^k}, \quad \bar{Q}_{12}^{(k)} = \frac{\nu_{21}^k E_1^k}{1 - \nu_{12}^k \nu_{21}^k}, \quad \bar{Q}_{22}^{(k)} = \frac{E_2^k}{1 - \nu_{12}^k \nu_{21}^k} \\ \bar{Q}_{16}^{(k)} &= 0, \quad \bar{Q}_{26}^{(k)} = 0, \quad \bar{Q}_{66}^{(k)} = G_{12}^k, \quad \bar{Q}_{44}^{(k)} = G_{23}^k, \quad \bar{Q}_{55}^{(k)} = G_{13}^k \end{aligned} \quad (3.6.20)$$

Here N denotes the number of layers, z_k is the z -coordinate of the bottom of the k th layer, and $(E_i^k, \nu_{ij}^k, G_{ij}^k)$ denote the engineering properties of the k th layer. The layers are numbered from the top to the bottom, in the positive z direction, as indicated in Figure 3.6.1. For a symmetrically laminated plate composed of multiple isotropic layers, the laminate stiffness coefficients A_{ij} and D_{ij} are defined by Eq. (3.6.19) with [see Reddy (2004a)]

$$\begin{aligned} \bar{Q}_{11}^{(k)} &= \bar{Q}_{22}^{(k)} = \frac{E^k}{1 - \nu_k^2}, \quad \bar{Q}_{16}^{(k)} = \bar{Q}_{26}^{(k)} = 0 \\ \bar{Q}_{12}^{(k)} &= \frac{\nu_k E^k}{1 - \nu_k^2}, \quad \bar{Q}_{44}^{(k)} = \bar{Q}_{55}^{(k)} = \bar{Q}_{66}^{(k)} = \frac{E^k}{2(1 + \nu_k)} \end{aligned} \quad (3.6.21)$$

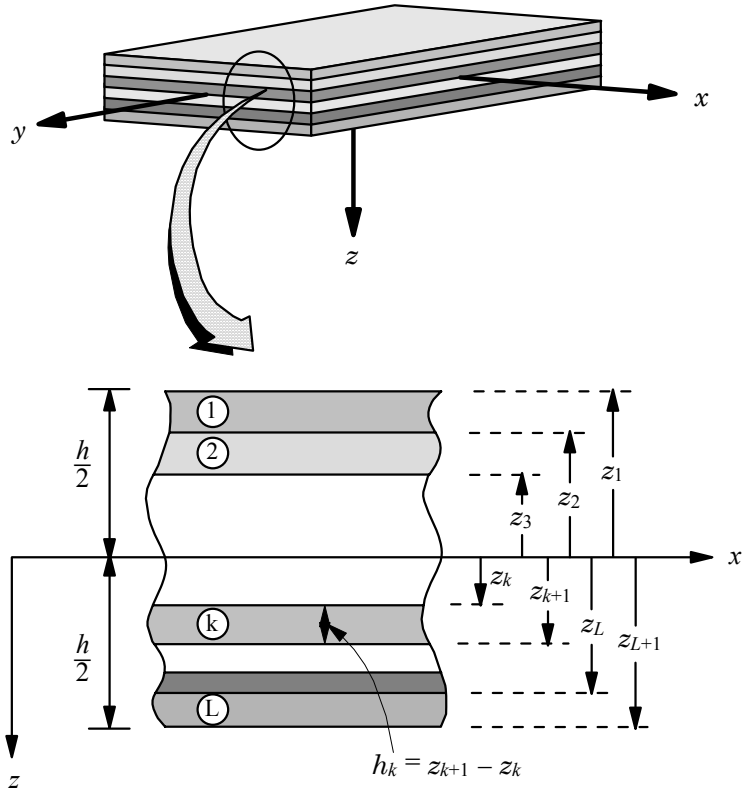


Figure 3.6.1. The layer numbering used for a typical laminated plate.

Example 3.6.1

Consider a plate made of a graphite-epoxy material with the following material properties in the principal material coordinates (see Table 1.3.1):

$$E_1 = 20 \text{ msi}, E_2 = 1.30 \text{ msi}, G_{12} = 1.03 \text{ msi}, \nu_{12} = 0.3 \quad (3.6.22)$$

The elastic coefficients Q_{ij} (in msi. $= 10^6$ psi.) in the principal material coordinates can be calculated using Eq. (3.6.2) as

$$Q_{11} = 20.118, Q_{22} = 1.3076, Q_{12} = 0.3923, Q_{66} = 1.03$$

If the plate is of thickness $h = 0.001$ in., and the plate coordinate axes coincide with the principal material coordinates, the (orthotropic) plate stiffness coefficients A_{ij} (ksi-in.) and D_{ij} (psi-in.³) can be calculated using Eq. (3.6.13) as

$$A_{11} = 201.18, A_{22} = 13.076, A_{12} = 3.9229, A_{66} = 10.300$$

$$D_{11} = 1.6765, D_{22} = 0.10897, D_{12} = 0.03269, D_{66} = 0.08583$$

If the principal material axes x_1 and x_2 are oriented at 60° to the plate (x, y) axes and $x_3 = z$, then we have

$$\bar{Q}_{11} = 2.9125, \bar{Q}_{22} = 12.318, \bar{Q}_{12} = 3.4899, \bar{Q}_{66} = 4.1276 \text{ (msi.)}$$

$$A_{11} = 29.125, A_{22} = 123.18, A_{12} = 34.899, A_{66} = 41.276 \text{ (ksi-in.)}$$

$$D_{11} = 0.24271, D_{22} = 1.0625, D_{12} = 0.29083, D_{66} = 0.34397 \text{ (psi-in.}^3\text{)}$$

If the plate is composed of three layers of the same thickness and material, but the top and bottom layers oriented at 0° and the middle layer at 90° [denoted (0/90/0) laminate], then the plate stiffness coefficients are given by

$$A_{11} = 138.48, A_{22} = 75.777, A_{12} = 3.9229, A_{66} = 10.300 \text{ (ksi-in.)}$$

$$D_{11} = 1.6184, D_{22} = 0.1670, D_{12} = 0.0327, D_{66} = 0.0858 \text{ (psi-in.}^3\text{)}$$

Example 3.6.2

Suppose that an orthotropic plate is subjected to loads such that the only nonzero strain at a point (x, y) is $\varepsilon_{xx}^0 = 10^3 \mu = 10^{-3}$ in./in. The material properties are the same as those listed in Eq. (3.6.22). We wish to determine the state of stress $(\sigma_{xx}, \sigma_{yy}, \sigma_{xy})$ in the plate. Assuming that the plate is of thickness 0.01 in., we wish to compute the plate forces and moments.

The stresses (in psi.) are given by

$$\sigma_{xx} = Q_{11}\varepsilon_{xx}^0 = 20,118, \sigma_{yy} = Q_{22}\varepsilon_{xx}^0 = 392, \sigma_{xy} = Q_{12}\varepsilon_{xx}^0 = 0$$

where Q_{ij} are given in Example 3.6.1. The tensile stress σ_{yy} is the reaction of the laminate trying to contract in the y -direction due to the Poisson effect. Since the

strain $\varepsilon_{yy} = 0$ by assumption, a tensile stress σ_{yy} is required to maintain the zero strain condition.

The forces and moments in the plate are

$$\begin{Bmatrix} N_{xx} \\ N_{yy} \\ N_{xy} \end{Bmatrix} = \begin{Bmatrix} A_{11} \\ A_{12} \\ 0 \end{Bmatrix} \varepsilon_{xx}^0 = \begin{Bmatrix} 201.18 \\ 3.92 \\ 0 \end{Bmatrix} \text{ lbs/in.}, \quad \begin{Bmatrix} M_{xx} \\ M_{yy} \\ M_{xy} \end{Bmatrix} = \begin{Bmatrix} 0 \\ 0 \\ 0 \end{Bmatrix} \text{ lbs-in.}$$

If the plate is subjected to a uniform temperature of $T^0 = 250^\circ\text{F}$, the thermal forces generated are equal to ($\alpha_1 = 10^{-6}$ in./in. $^\circ\text{F}$ and $\alpha_2 = 30 \times 10^{-6}$ in./in. $^\circ\text{F}$)

$$\begin{Bmatrix} N_{xx}^T \\ N_{yy}^T \\ N_{xy}^T \end{Bmatrix} = \begin{Bmatrix} (A_{11}\alpha_1 + A_{12}\alpha_2) \\ (A_{12}\alpha_1 + A_{22}\alpha_2) \\ 0 \end{Bmatrix} T^0 = \begin{Bmatrix} 79.72 \\ 99.05 \\ 0 \end{Bmatrix} \text{ lbs/in.}$$

Example 3.6.3

Consider the case in which the plate of Example 3.6.2 is subjected to loads such that the only nonzero strain at a point (x, y) is the curvature strain $\varepsilon_{xx}^1 = (1/12)$ /in. Hence, $\varepsilon_{xx} = z\varepsilon_{xx}^1 = \frac{z}{12}$ in./in. Then the stresses (in msi) are given by

$$\sigma_{xx} = zQ_{11}\varepsilon_{xx}^1 = 1.6765z, \quad \sigma_{yy} = zQ_{12}\varepsilon_{xx}^1 = 0.0327z, \quad \sigma_{xy} = 0$$

The stresses σ_{xx} and σ_{yy} are linear through the entire plate thickness, and σ_{xy} is zero everywhere.

The forces and moments are ($\varepsilon_{xx}^0 = 0$)

$$\begin{Bmatrix} N_{xx} \\ N_{yy} \\ N_{xy} \end{Bmatrix} = \begin{Bmatrix} 0 \\ 0 \\ 0 \end{Bmatrix} \text{ lbs/in.}, \quad \begin{Bmatrix} M_{xx} \\ M_{yy} \\ M_{xy} \end{Bmatrix} = \begin{Bmatrix} D_{11} \\ D_{12} \\ D_{16} \end{Bmatrix} \varepsilon_{xx}^1 = \begin{Bmatrix} 0.1397 \\ 0.0027 \\ 0 \end{Bmatrix} \text{ lbs-in.}$$

If the plate is subjected to a linear variation of temperature through the thickness of zT^1 with $T^1 = 250^\circ\text{F}/\text{in.}$, the thermal moments generated are equal to ($\alpha_1 = 10^{-6}$ in./in. $^\circ\text{F}$ and $\alpha_2 = 30 \times 10^{-6}$ in./in. $^\circ\text{F}$)

$$\begin{Bmatrix} M_{xx}^T \\ M_{yy}^T \\ M_{xy}^T \end{Bmatrix} = \begin{Bmatrix} (D_{11}\alpha_1 + D_{12}\alpha_2) \\ (D_{12}\alpha_1 + D_{22}\alpha_2) \\ 0 \end{Bmatrix} T^1 = \begin{Bmatrix} 0.664 \\ 0.826 \\ 0 \end{Bmatrix} 10^{-3} \text{ lbs-in.}$$

3.7 Stiffness Coefficients of Orthotropic Plates

When the engineering constants ($E_1, E_2, \nu_{12}, G_{12}$) of a plate material are available, the plate stiffness coefficients A_{ij} and D_{ij} may be computed using Eq. (3.6.13) for single-layer plates and Eqs. (3.6.19) and (3.6.20) for symmetrically laminated plates. The engineering parameters E_1, E_2, G_{12} , and ν_{12} of an orthotropic material may be determined experimentally using an appropriate test specimen made of the material. When it is not possible to determine the engineering constants experimentally,

approximate methods based on certain mathematical models are used to determine them [see Reddy (2004a)].

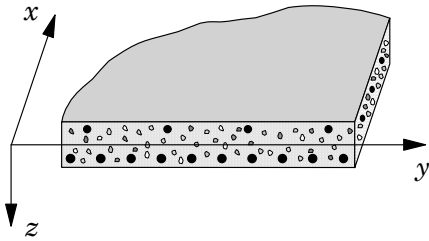
It is also common to characterize plate structures made of reinforced concrete or isotropic plates reinforced with stiffeners, and corrugated plates as orthotropic plates. Table 3.7.1 summarizes the expressions for bending stiffness coefficients (or rigidities) for some standard cases [see Timoshenko and Woinowsky-Krieger (1970), Troitsky (1976), and Huffington (1956)]. For the steel-reinforced concrete slab, the steel bars are assumed to be placed biaxially along the x - and y -axes. In the case of stiffened plates, the word “plate” refers to the portion without stiffeners. If a plate is stiffened by equidistant stiffeners in both x and y directions (Table 3.7.1 shows only along the y -direction), the rigidity D_{11} should be modified as

$$D_{11} = \frac{Eh^3}{12(1-\nu^2)} + \frac{E_s I_s}{s} \quad (3.7.1)$$

where it is assumed that the stiffeners are identical in geometry and material properties. Otherwise, the additive part, $E_s I_s/s$, should be replaced with $E_x I_x/s_x$ for stiffeners parallel to the x -direction and $E_y I_y/s_y$ for stiffeners in the y -direction, which are added to D_{11} and D_{22} , respectively.

Table 3.7.1. Extensional and bending rigidities for various orthotropic plates.

Plate Type	Plate Bending Stiffness Coefficients D_{ij}
Steel-reinforced concrete slab	

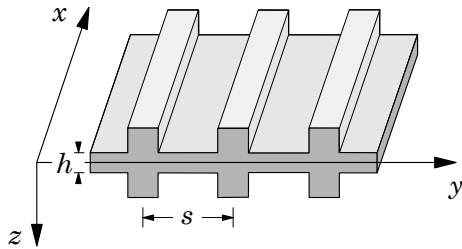


$$\begin{aligned} D_{11} &= \frac{E_c}{1-\nu_c^2} \left[I_{cx} + \left(\frac{E_s}{E_c} - 1 \right) I_{sx} \right] \\ D_{22} &= \frac{E_c}{1-\nu_c^2} \left[I_{cy} + \left(\frac{E_s}{E_c} - 1 \right) I_{sy} \right] \\ D_{12} &= \nu_c \sqrt{D_{11} D_{22}} \\ D_{66} &= \frac{1-\nu_c}{2} \sqrt{D_{11} D_{22}} \end{aligned}$$

ν_c = Poisson's ratio for concrete
 E_c, E_s = Young's modulus of concrete and steel, respectively

$I_{c\xi}, I_{s\xi}$ = Moments of inertia of the concrete and steel bars about the neutral axis in the section $\xi = \text{constant}$ ($\xi = x$ or y)

Plate Type	Plate Bending Stiffness Coefficients D_{ij}
------------	---

Plate reinforced symmetrically by equidistant stiffeners

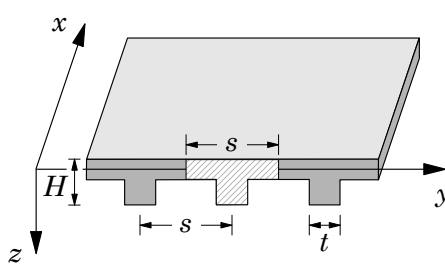
$$D_{11} = \frac{Eh^3}{12(1-\nu^2)}, \quad D_{12} = \nu D_{11}$$

$$D_{22} = \frac{Eh^3}{12(1-\nu^2)} + \frac{E_s I_s}{s}$$

E, E_s = Young's modulus of plate and stiffeners, respectively
 ν = Poisson's ratio of plate

s = Spacing between stiffeners

I_s = Moment of inertia of the stiffener with respect to the middle plane of the plate

Plate reinforced by equidistant ribs

$$D_{11} = \frac{Eh^3 s}{12[s-t+t(h/H)^3]}, \quad D_{22} = \frac{EI}{s}$$

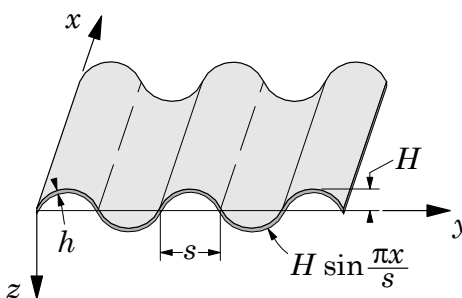
$$2D_{66} = 2G_{xy} + \frac{C}{s}, \quad D_{12} = 0 \ (\nu = 0)$$

E = Young's modulus of the plate

G_{xy} = Torsional rigidity of the plate

C = Torsional rigidity of one rib

I_s = Moment of inertia about neutral axis of a T-section (shaded)

Corrugated plate

$$D_{11} = \frac{s}{\mu} \frac{Eh^3}{12(1-\nu^2)}, \quad D_{22} = EI$$

$$2D_{66} = \frac{s}{\mu} \frac{Eh^3}{12(1+\nu)}, \quad D_{12} = 0$$

$$\mu = s \left(1 + \frac{\pi^2 H^2}{4s^2} \right)$$

$$I = 0.5H^2h \left[1 - \frac{0.81}{1+2.5(H/2s)^2} \right]$$

3.8 Equations of Motion in Terms of Displacements

The stress resultants are related to the displacement gradients and other fields, such as temperature and electric fields. The forces (N_{xx}, N_{yy}, N_{xy}) and moments (M_{xx}, M_{yy}, M_{xy}) in a single-layer orthotropic plate or a laminated plate composed of multiple orthotropic layers that are symmetrically disposed about the middle plane of the plate can be expressed in terms of the displacements (u_0, v_0, w_0) by the relations

$$\begin{Bmatrix} N_{xx} \\ N_{yy} \\ N_{xy} \end{Bmatrix} = \begin{bmatrix} A_{11} & A_{12} & 0 \\ A_{12} & A_{22} & 0 \\ 0 & 0 & A_{66} \end{bmatrix} \begin{Bmatrix} \frac{\partial u_0}{\partial x} + \frac{1}{2} \left(\frac{\partial w_0}{\partial x} \right)^2 \\ \frac{\partial v_0}{\partial y} + \frac{1}{2} \left(\frac{\partial w_0}{\partial y} \right)^2 \\ \frac{\partial u_0}{\partial y} + \frac{\partial v_0}{\partial x} + \frac{\partial w_0}{\partial x} \frac{\partial w_0}{\partial y} \end{Bmatrix} - \begin{Bmatrix} N_{xx}^T \\ N_{yy}^T \\ 0 \end{Bmatrix} \quad (3.8.1)$$

$$\begin{Bmatrix} M_{xx} \\ M_{yy} \\ M_{xy} \end{Bmatrix} = - \begin{bmatrix} D_{11} & D_{12} & 0 \\ D_{12} & D_{22} & 0 \\ 0 & 0 & D_{66} \end{bmatrix} \begin{Bmatrix} \frac{\partial^2 w_0}{\partial x^2} \\ \frac{\partial^2 w_0}{\partial y^2} \\ 2 \frac{\partial^2 w_0}{\partial x \partial y} \end{Bmatrix} - \begin{Bmatrix} M_{xx}^T \\ M_{yy}^T \\ 0 \end{Bmatrix} \quad (3.8.2)$$

where the thermal forces and moments are defined by Eqs. (3.6.14) and (3.6.15). For geometrically linear analysis, the nonlinear parts of strains in Eq. (3.8.1) are omitted.

The equations of motion (3.4.15)–(3.4.17) can be expressed in terms of displacements (u_0, v_0, w_0) by substituting for the forces and moments from Eqs. (3.8.1) and (3.8.2). For homogeneous plates (i.e., for plates with constant A_{ij} and D_{ij}), the equations of motion (3.4.15)–(3.4.17) take the form

$$\begin{aligned} A_{11} \left(\frac{\partial^2 u_0}{\partial x^2} + \frac{\partial w_0}{\partial x} \frac{\partial^2 w_0}{\partial x^2} \right) + A_{12} \left(\frac{\partial^2 v_0}{\partial x \partial y} + \frac{\partial w_0}{\partial y} \frac{\partial^2 w_0}{\partial x \partial y} \right) \\ + A_{66} \left(\frac{\partial^2 u_0}{\partial y^2} + \frac{\partial^2 v_0}{\partial x \partial y} + \frac{\partial^2 w_0}{\partial x \partial y} \frac{\partial w_0}{\partial y} + \frac{\partial w_0}{\partial x} \frac{\partial^2 w_0}{\partial y^2} \right) \\ - \left(\frac{\partial N_{xx}^T}{\partial x} + \frac{\partial N_{xy}^T}{\partial y} \right) = I_0 \frac{\partial^2 u_0}{\partial t^2} \end{aligned} \quad (3.8.3)$$

$$\begin{aligned} A_{66} \left(\frac{\partial^2 u_0}{\partial x \partial y} + \frac{\partial^2 v_0}{\partial x^2} + \frac{\partial^2 w_0}{\partial x^2} \frac{\partial w_0}{\partial y} + \frac{\partial w_0}{\partial x} \frac{\partial^2 w_0}{\partial x \partial y} \right) \\ + A_{12} \left(\frac{\partial^2 u_0}{\partial x \partial y} + \frac{\partial w_0}{\partial x} \frac{\partial^2 w_0}{\partial x \partial y} \right) + A_{22} \left(\frac{\partial^2 v_0}{\partial y^2} + \frac{\partial w_0}{\partial y} \frac{\partial^2 w_0}{\partial y^2} \right) \\ - \left(\frac{\partial N_{xy}^T}{\partial x} + \frac{\partial N_{yy}^T}{\partial y} \right) = I_0 \frac{\partial^2 v_0}{\partial t^2} \end{aligned} \quad (3.8.4)$$

$$\begin{aligned} -D_{11} \frac{\partial^4 w_0}{\partial x^4} - 2(D_{12} + 2D_{66}) \frac{\partial^4 w_0}{\partial x^2 \partial y^2} - D_{22} \frac{\partial^4 w_0}{\partial y^4} - k w_0 \\ - \left(\frac{\partial^2 M_{xx}^T}{\partial x^2} + 2 \frac{\partial^2 M_{xy}^T}{\partial y \partial x} + \frac{\partial^2 M_{yy}^T}{\partial y^2} \right) + \mathcal{N}(u_0, v_0, w_0) + q \\ = I_0 \frac{\partial^2 w_0}{\partial t^2} - I_2 \frac{\partial^2}{\partial t^2} \left(\frac{\partial^2 w_0}{\partial x^2} + \frac{\partial^2 w_0}{\partial y^2} \right) \end{aligned} \quad (3.8.5)$$

where $\mathcal{N}(u_0, v_0, w_0)$ was defined in Eq. (3.4.14), and it contains the thermal forces. For isotropic case, we have $A_{11} = A_{22} = A$, $A_{12} = \nu A$, $2A_{66} = (1 - \nu)A$, $D_{11} = D_{22} = D$, $D_{12} = \nu D$, $2D_{66} = (1 - \nu)D$ with $A = E/(1 - \nu^2)$ and $D = Ah^3/12$.

The nonlinear partial differential equations in (3.8.3)–(3.8.5) can be simplified for the linear static analysis:

$$A_{11} \frac{\partial^2 u_0}{\partial x^2} + A_{12} \frac{\partial^2 v_0}{\partial x \partial y} + A_{66} \left(\frac{\partial^2 u_0}{\partial y^2} + \frac{\partial^2 v_0}{\partial x \partial y} \right) - \left(\frac{\partial N_{xx}^T}{\partial x} + \frac{\partial N_{xy}^T}{\partial y} \right) = 0 \quad (3.8.6)$$

$$A_{66} \left(\frac{\partial^2 u_0}{\partial x \partial y} + \frac{\partial^2 v_0}{\partial x^2} \right) + A_{12} \frac{\partial^2 u_0}{\partial x \partial y} + A_{22} \frac{\partial^2 v_0}{\partial y^2} - \left(\frac{\partial N_{xy}^T}{\partial x} + \frac{\partial N_{yy}^T}{\partial y} \right) = 0 \quad (3.8.7)$$

$$\begin{aligned} D_{11} \frac{\partial^4 w_0}{\partial x^4} + 2(D_{12} + 2D_{66}) \frac{\partial^4 w_0}{\partial x^2 \partial y^2} + D_{22} \frac{\partial^4 w_0}{\partial y^4} + kw_0 \\ = q - \left(\frac{\partial^2 M_{xx}^T}{\partial x^2} + 2 \frac{\partial^2 M_{xy}^T}{\partial y \partial x} + \frac{\partial^2 M_{yy}^T}{\partial y^2} \right) \end{aligned} \quad (3.8.8)$$

Thus, the coupling between the inplane displacements (u_0, v_0) and transverse deflection w_0 disappears in the case of linear analysis, and Eq. (3.8.8) can be solved separately from Eqs. (3.8.6) and (3.8.7).

Example 3.8.1: Cylindrical Bending

If a plate is infinitely long in one direction, the plate becomes a *plate strip*. Consider a plate strip that has a finite dimension along the x -axis and is subjected to a transverse load $q(x)$ that is uniform at any section parallel to the x -axis. In such a case, the deflection w_0 and displacements (u_0, v_0) of the plate are functions of only x . Therefore, all derivatives with respect to y are zero. In such cases, the deflected surface of the plate strip is cylindrical, and it is referred to as the *cylindrical bending*. For this case, the governing equations (3.8.3)–(3.8.5) reduce to

$$A_{11} \left(\frac{\partial^2 u_0}{\partial x^2} + \frac{\partial w_0}{\partial x} \frac{\partial^2 w_0}{\partial x^2} \right) - \frac{\partial N_{xx}^T}{\partial x} = I_0 \frac{\partial^2 u_0}{\partial t^2} \quad (3.8.9)$$

$$A_{66} \frac{\partial^2 v_0}{\partial x^2} - \frac{\partial N_{xy}^T}{\partial x} = I_0 \frac{\partial^2 v_0}{\partial t^2} \quad (3.8.10)$$

$$-D_{11} \frac{\partial^4 w_0}{\partial x^4} + \frac{\partial}{\partial x} \left(N_{xx} \frac{\partial w_0}{\partial x} \right) - kw_0 + q - \frac{\partial^2 M_{xx}^T}{\partial x^2} = I_0 \frac{\partial^2 w_0}{\partial t^2} - I_2 \frac{\partial^4 w_0}{\partial x^2 \partial t^2} \quad (3.8.11)$$

Note that for the nonlinear case, the three equations are coupled through the nonlinear term (N_{xx}) in Eq. (3.8.11) and are uncoupled for the linear case. Hence, they can be solved independently of each other.

In Chapter 4, we consider static bending, buckling, and natural vibrations of plate strips governed by Eqs. (3.8.9)–(3.8.9). Analytical as well as Ritz solutions are discussed for linear problems. Since Eqs. (3.8.9) and (3.8.11) are essentially the same as those of bars and beams, respectively, known solutions of bars and beams for various boundary conditions and loads can be readily used for plate strips.

Example 3.8.2: Pure Bending of Plates

For bending of isotropic plates [$D_{11} = D_{22}$, $D_{12} = \nu D$, and $2D_{66} = (1 - \nu)D$, $\alpha_1 = \alpha_2 = \alpha$], experiencing small strains and small displacements, Eq. (3.8.8) takes the simpler form

$$D \left(\frac{\partial^4 w_0}{\partial x^4} + 2 \frac{\partial^4 w_0}{\partial x^2 \partial y^2} + \frac{\partial^4 w_0}{\partial y^4} \right) + kw_0 = q - \frac{1}{1 - \nu} \left(\frac{\partial^2 M_T}{\partial x^2} + \frac{\partial^2 M_T}{\partial y^2} \right) \quad (3.8.12)$$

where

$$M_T = E\alpha \int_{-\frac{h}{2}}^{\frac{h}{2}} \Delta T z \, dz \quad (3.8.13)$$

and $D = Eh^3/[12(1 - \nu^2)]$. Using the Laplace operator ∇^2 , we can express the above equation as

$$D\nabla^4 w_0 + kw_0 = q - \frac{1}{1 - \nu} \nabla^2 M_T \quad (3.8.14)$$

where $\nabla^4 = \nabla^2 \nabla^2$ is the biharmonic operator. Equation (3.8.14) is valid in any coordinate system.

Equation (3.8.12) or (3.8.14) must be solved in conjunction with appropriate boundary conditions of the problem for the desired response. The boundary conditions at any point on the boundary are of the form

$$\text{specify: } w_0 \quad \text{or} \quad V_n \equiv Q_n + \frac{\partial M_{ns}}{\partial s} \quad (3.8.15)$$

$$\text{specify: } \frac{\partial w_0}{\partial n} \quad \text{or} \quad M_{nn} \quad (3.8.16)$$

where

$$Q_n = \left(\frac{\partial M_{xx}}{\partial x} + \frac{\partial M_{xy}}{\partial y} \right) n_x + \left(\frac{\partial M_{xy}}{\partial x} + \frac{\partial M_{yy}}{\partial y} \right) n_y \quad (3.8.17)$$

$$\begin{aligned} M_{nn} = & - \left(D \frac{\partial^2 w_0}{\partial x^2} + \nu D \frac{\partial^2 w_0}{\partial y^2} + M_{xx}^T \right) n_x^2 \\ & - \left(\nu D \frac{\partial^2 w_0}{\partial x^2} + D \frac{\partial^2 w_0}{\partial y^2} + M_{yy}^T \right) n_y^2 - (1 - \nu) D \frac{\partial^2 w_0}{\partial x \partial y} n_x n_y \end{aligned} \quad (3.8.18)$$

$$\begin{aligned} M_{ns} = & (1 - \nu) D \left[\left(\frac{\partial^2 w_0}{\partial x^2} - \frac{\partial^2 w_0}{\partial y^2} \right) n_x n_y - \frac{\partial^2 w_0}{\partial x \partial y} (n_x^2 - n_y^2) \right] \\ & - (M_{yy}^T - M_{xx}^T) n_x n_y \end{aligned} \quad (3.8.19)$$

Note that the moments M_{nn} and M_{ns} contain thermal parts. The expressions can be simplified for isotropic plates.

The following boundary conditions will be of interest in the present study:

$$\text{Simply Supported: } w_0 = 0, \quad M_{nn} = 0 \quad (3.8.20)$$

$$\text{Clamped: } w_0 = 0, \quad \frac{\partial w_0}{\partial n} = 0 \quad (3.8.21)$$

$$\text{Free: } V_n = 0, \quad M_{nn} = 0 \quad (3.8.22)$$

3.9 Summary

This chapter is primarily concerned with the development of the classical plate theory based on the Kirchhoff hypothesis, which is valid for thin plates with side-to-thickness ratio greater than 30. The governing equations were derived using a semi-inverse method in which the form of the displacement field is assumed using the Kirchhoff hypothesis. The chosen displacement field contains, while satisfying the Kirchhoff hypothesis, three functions (u_0, v_0, w_0) that represent the displacements of a point on the midplane of the plate in the three coordinate directions. Then the equations governing (u_0, v_0, w_0) are derived using the dynamic version of the principle of virtual displacements. The plate is assumed to be made of an orthotropic material with principal material coordinates coinciding with the plate coordinates, and the von Kármán nonlinearity is accounted for in the development of the theory.

The resulting partial differential equations are nonlinear in (u_0, v_0, w_0) , and the total order of the three equations is 8 (i.e., u_0 and v_0 each is governed by a second-order equation while w_0 is governed by a fourth-order equation), requiring a total of 8 boundary conditions. Four of these are provided by the boundary conditions on the 4 primary variables $(u_{0n}, u_{0s}, w_0, \partial w_0 / \partial n)$ and the remaining 4 are provided by conditions on the secondary variables $(N_{nn}, N_{ns}, V_n, M_{nn})$, where u_{0n} and u_{0s} are the inplane normal and tangential displacements, N_{nn} and N_{ns} are the corresponding forces; V_n is the effective shear force and includes the Kirchhoff free-edge condition. The normal derivative of w_0 is dual to the normal bending moment M_{nn} .

The equations derived in this chapter can be simplified for different geometries, like beams and plate strips, as shown in Examples 3.8.1 and 3.8.2. Solutions of these equations will be discussed in the coming chapters.

Problems

- 3.1** Derive the equations of equilibrium associated with linear theory of plate bending using the free-body diagram of an infinitesimal element shown in Figure P3.1.

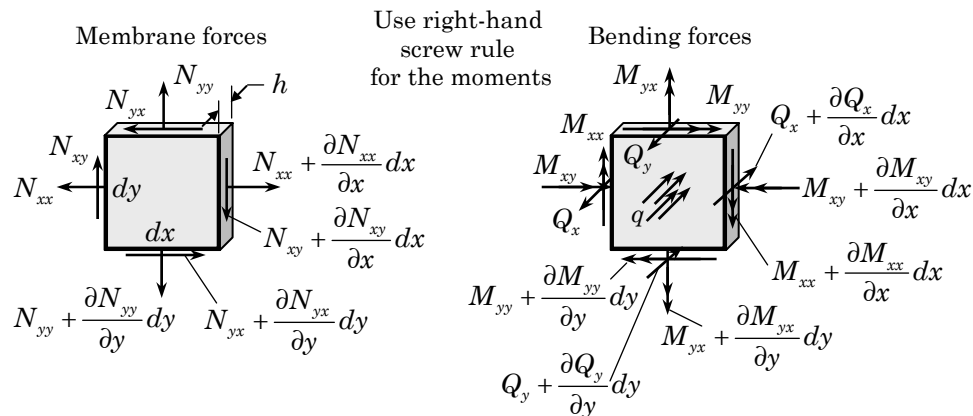


Figure P3.1

- 3.2** Starting with a linear distribution of the displacements through the plate thickness in terms of unknown functions ($u_0, v_0, w_0, F_1, F_2, F_3$)

$$\begin{aligned} u(x, y, z, t) &= u_0(x, y, t) + zF_1(x, y, t) \\ v(x, y, z, t) &= v_0(x, y, t) + zF_2(x, y, t) \\ w(x, y, z, t) &= w_0(x, y, t) + zF_3(x, y, t) \end{aligned}$$

determine the functions (F_1, F_2, F_3) such that the Kirchhoff hypothesis holds:

$$\frac{\partial w}{\partial z} = 0, \quad \frac{\partial u}{\partial z} = -\frac{\partial w}{\partial x}, \quad \frac{\partial v}{\partial z} = -\frac{\partial w}{\partial y}$$

- 3.3** Construct the total potential energy functional for an orthotropic plate in pure bending (i.e., neglect extensional displacements u_0 and v_0). Assume small strains, displacements, and rotations and that the only nonzero applied loading is the distributed load, q . Use the classical plate theory.
- 3.4** (Continuation of Problem 3.3) Derive the equation of equilibrium governing w_0 using the principle of minimum total potential energy.
- 3.5** Consider an orthotropic plate and assume that the material coordinates coincide with the plate coordinates. Compute the stresses ($\sigma_{xx}, \sigma_{yy}, \sigma_{xy}$) for the pure bending case using the constitutive equations, and then use the equilibrium equations of the three-dimensional elasticity theory to determine the transverse stresses ($\sigma_{xz}, \sigma_{yz}, \sigma_{zz}$) as a function of the thickness coordinate.
- 3.6** Consider the equations of motion of 3-D elasticity [see Eq. (1.3.26)] in the absence of body forces:

$$\begin{aligned} \frac{\partial \sigma_{xx}}{\partial x} + \frac{\partial \sigma_{xy}}{\partial y} + \frac{\partial \sigma_{xz}}{\partial z} &= \rho \frac{\partial^2 u}{\partial t^2} \\ \frac{\partial \sigma_{xy}}{\partial x} + \frac{\partial \sigma_{yy}}{\partial y} + \frac{\partial \sigma_{yz}}{\partial z} &= \rho \frac{\partial^2 v}{\partial t^2} \\ \frac{\partial \sigma_{xz}}{\partial x} + \frac{\partial \sigma_{yz}}{\partial y} + \frac{\partial \sigma_{zz}}{\partial z} &= \rho \frac{\partial^2 w}{\partial t^2} \end{aligned}$$

Integrate the above equations with respect to z over the interval $(-h/2, h/2)$ and express the results in terms of the forces (N_{xx}, N_{yy}, N_{xy}) and (Q_x, Q_y), where

$$Q_x = \int_{-h/2}^{h/2} \sigma_{xz} dz, \quad Q_y = \int_{-h/2}^{h/2} \sigma_{yz} dz$$

Next, multiply the equations of motion with z , integrate with respect to z over the interval $(-h/2, h/2)$, and express the results in terms of the moments (M_{xx}, M_{yy}, M_{xy}). Use the following boundary conditions:

$$\begin{aligned} \sigma_{xz}(x, y, -\frac{h}{2}) &= 0, \quad \sigma_{xz}(x, y, \frac{h}{2}) = 0, \quad \sigma_{yz}(x, y, -\frac{h}{2}) = 0 \\ \sigma_{yz}(x, y, \frac{h}{2}) &= 0, \quad \sigma_{zz}(x, y, -\frac{h}{2}) = -q_b, \quad \sigma_{zz}(x, y, \frac{h}{2}) = q_t \end{aligned}$$

- 3.7** (Continuation of Problem 3.6) Eliminate the shear forces Q_x and Q_y and express the equations of equilibrium only in terms of the forces (N_{xx}, N_{yy}, N_{xy}) and moments (M_{xx}, M_{yy}, M_{xy}).

4

Analysis of Plate Strips

4.1 Introduction

There are two cases of rectangular plates that can be treated as one-dimensional problems: (1) beams, and (2) cylindrical bending of plate strips. When the width b (i.e., length along the y -axis) of a plate is very small compared to the length a along the x -axis, it is treated as a beam. In cylindrical bending, the plate is assumed to be a plate strip that is very long along the y -axis and has a finite dimension a along the x -axis (Figure 4.1.1). The transverse load q is assumed to be uniform at any section parallel to the x -axis, i.e., $q = q(x)$. In such a case, the deflection w_0 and displacements (u_0, v_0) of the plate are functions of only x , and all derivatives with respect to y are zero. The cylindrical bending problem is a *plane strain* problem, whereas the beam problem is a *plane stress* problem. In this chapter, we consider cylindrical bending, buckling, and natural vibrations of plate strips.

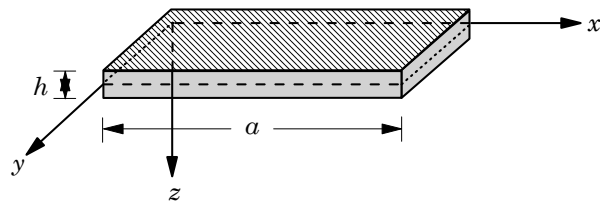
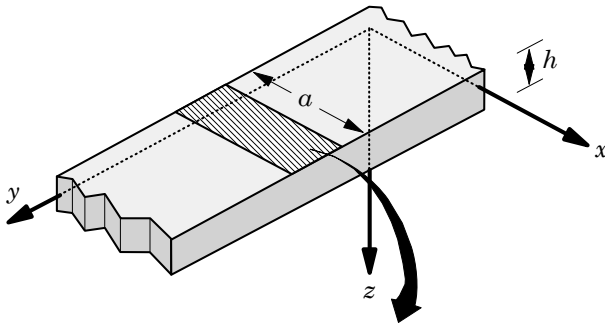


Figure 4.1.1. Geometry of a plate strip in cylindrical bending.

4.2 Governing Equations

Consider an isotropic rectangular plate strip and let the x and y coordinates be parallel to the edges of the strip. Suppose that the plate is long in the y -direction, has a finite dimension along the x -direction, and is subjected to a transverse load $q(x)$ (measured per unit area) that is uniform at any section parallel to the x -axis and the plate bends into a cylindrical surface. For this *cylindrical bending* problem (Figure 4.1.1), the governing equations of motion according to the linear classical plate theory (CPT) are given by Eqs. (3.8.9)–(3.8.11). The operator \mathcal{N} in this case must be understood as one that is due to the applied axial load \hat{N}_{xx}

$$\mathcal{N} = \frac{\partial}{\partial x} \left(\hat{N}_{xx} \frac{\partial w_0}{\partial x} \right)$$

When the nonlinear terms are neglected, Eqs. (3.8.9)–(3.8.11) reduce to

$$A_{11} \frac{\partial^2 u_0}{\partial x^2} - \frac{\partial N_{xx}^T}{\partial x} = I_0 \frac{\partial^2 u_0}{\partial t^2} \quad (4.2.1)$$

$$A_{66} \frac{\partial^2 v_0}{\partial x^2} = I_0 \frac{\partial^2 v_0}{\partial t^2} \quad (4.2.2)$$

$$-D_{11} \frac{\partial^4 w_0}{\partial x^4} - k w_0 + \frac{\partial}{\partial x} \left(\hat{N}_{xx} \frac{\partial w_0}{\partial x} \right) - \frac{\partial^2 M_{xx}^T}{\partial x^2} + q = I_0 \frac{\partial^2 w_0}{\partial t^2} - I_2 \frac{\partial^4 w_0}{\partial x^2 \partial t^2} \quad (4.2.3)$$

where \hat{N}_{xx} is an applied axial (tensile) load (measured per unit length), $I_0 = \rho h$, $I_2 = \rho h^3/12$, and the thermal force and moments are defined in Eqs. (3.6.14) and (3.6.15). For isotropic case, we set $A_{11} = A = Eh/(1-\nu^2)$, $A_{66} = A/[2(1+\nu)]$, and $D_{11} = D = Eh^3/12(1-\nu^2)$. The thermal force and moment take the form

$$N_{xx}^T = \frac{E\alpha}{1-\nu} \int_{-\frac{h}{2}}^{\frac{h}{2}} \Delta T \, dz, \quad M_{xx}^T = \frac{E\alpha}{1-\nu} \int_{-\frac{h}{2}}^{\frac{h}{2}} z \Delta T \, dz \quad (4.2.4)$$

The three equations in (4.2.1)–(4.2.3) are uncoupled from each other and, therefore, each equation can be solved independently of the other two. Here we are primarily concerned with the bending, buckling, and natural vibrations of plate strips. Equation (4.2.3) has the same form as that for a beam. Therefore, the solutions developed herein for plate strips with various boundary conditions are also valid for beams with the appropriate change of the coefficients (i.e., replace D_{11} with EI). Also, the results presented in this chapter can be specialized to isotropic plate strips by simply setting $D_{11} = D$.

4.3 Bending Analysis

4.3.1 General Solution

For linear static bending analysis in the absence of axial force \hat{N}_{xx} and elastic foundation, Eq. (4.2.3) reduces to

$$D_{11} \frac{d^4 w_0}{dx^4} = - \frac{d^2 M_{xx}^T}{dx^2} + q \quad (4.3.1)$$

Equation (4.3.1) can be integrated, given thermal and mechanical loads, to obtain $w_0(x)$. We have

$$D_{11} \frac{d^2 w_0}{dx^2} = -M_{xx}^T + \int^x \int^\xi q(\eta) d\eta d\xi + c_1 x + c_2 \quad (4.3.2)$$

$$D_{11} \frac{dw_0}{dx} = - \int^x M_{xx}^T(\xi) d\xi + \int^x \int^\xi \int^\eta q(\zeta) d\zeta d\eta d\xi + c_1 \frac{x^2}{2} + c_2 x + c_3 \quad (4.3.3)$$

$$\begin{aligned} D_{11} w_0(x) = & - \int^x \int^\xi M_{xx}^T(\eta) d\eta d\xi + \int^x \int^\xi \int^\eta \int^\zeta q(\mu) d\mu d\zeta d\eta d\xi \\ & + c_1 \frac{x^3}{6} + c_2 \frac{x^2}{2} + c_3 x + c_4 \end{aligned} \quad (4.3.4)$$

where c_1 through c_4 are constants of integration.

If the temperature distribution in an isotropic plate strip is assumed to be of the form

$$\Delta T(x, z) = T_0(x) + z T_1(x) \quad (4.3.5)$$

where T_0 and T_1 are functions of x only, then the thermal moment is

$$M_{xx}^T = \frac{E\alpha}{1-\nu} \int_{-\frac{h}{2}}^{\frac{h}{2}} T_1 z^2 dz = \alpha \frac{Eh^3}{12(1-\nu)} T_1 \equiv D_T T_1 \quad (4.3.6)$$

For uniformly distributed load $q = q_0$ and constant T_1 , Eq. (4.3.4) yields

$$Dw_0(x) = -D_T T_1 \frac{x^2}{2} + q_0 \frac{x^4}{24} + c_1 \frac{x^3}{6} + c_2 \frac{x^2}{2} + c_3 x + c_4 \quad (4.3.7)$$

The constants of integration c_i can be determined using the boundary conditions. In the following exact solutions are presented for certain conventional boundary conditions (Table 4.3.1).

4.3.2 Simply Supported Plates

For a plate strip with simply supported edges at $x = 0$ and $x = a$, the boundary conditions are

$$w_0 = 0, \quad M_{xx} \equiv -D_{11} \frac{d^2 w_0}{dx^2} - M_{xx}^T = 0 \quad (4.3.8)$$

Using boundary conditions (4.3.8) in Eqs. (4.3.2) and (4.3.4), we obtain

$$c_2 = 0, \quad c_4 = 0, \quad c_1 = -\frac{q_0 a}{2}, \quad c_3 = \frac{D_T T_1 a}{2} + \frac{q_0 a^3}{24} \quad (4.3.9)$$

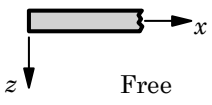
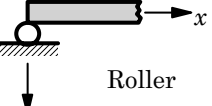
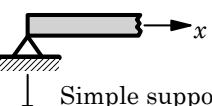
and the solution becomes

$$w_0(x) = \frac{q_0 a^4}{24 D_{11}} \left[\left(\frac{x}{a} \right)^4 - 2 \left(\frac{x}{a} \right)^3 + \left(\frac{x}{a} \right)^2 \right] - \frac{D_T T_1 a^2}{2 D_{11}} \left[\left(\frac{x}{a} \right)^2 - \left(\frac{x}{a} \right) \right] \quad (4.3.10)$$

$$M_{xx} = -\frac{q_0 a^2}{2} \left[\left(\frac{x}{a} \right)^2 - \left(\frac{x}{a} \right) \right] \quad (4.3.11)$$

where D_T here corresponds to the orthotropic case [see Eq. (3.6.15)].

Table 4.3.1. Conventional boundary conditions in the classical theory of plate strips.

Type of support	Geometric B.C.	Force B.C.
	None	$N_{xx} = 0$ $M_{xx} = 0$ $\frac{dM_{xx}}{dx} = 0$
	$w_0 = 0$	$N_{xx} = 0$ $M_{xx} = 0$
	$u_0 = 0$ $w_0 = 0$	$M_{xx} = 0$
	$u_0 = 0$ $w_0 = 0, \quad \frac{dw_0}{dx} = 0$	None

Note that the bending moment is not a function of the temperature for the case of simply supported boundary conditions. The maximum transverse deflection and bending moments occur at $x = a/2$, and are given by

$$w_{max} = w_0(a/2) = \frac{5q_0a^4}{384D_{11}} + \frac{D_T T_1 a^2}{8D_{11}}, \quad M_{max} = M_{xx}(a/2) = \frac{q_0 a^2}{8} \quad (4.3.12)$$

4.3.3 Clamped Plates

For a plate strip with clamped edges at $x = 0$ and $x = a$ (and free at $y = 0, \infty$), the boundary conditions are

$$w_0 = 0, \quad \frac{dw_0}{dx} = 0 \quad (4.3.13)$$

Using boundary conditions (4.3.13) in Eqs. (4.3.3) and (4.3.4), we obtain

$$c_3 = 0, \quad c_4 = 0, \quad c_1 = -\frac{q_0 a}{2}, \quad c_2 = D_T T_1 + \frac{q_0 a^2}{12} \quad (4.3.14)$$

The solution becomes

$$w_0(x) = \frac{q_0 a^4}{24D_{11}} \left[\left(\frac{x}{a} \right)^4 - 2 \left(\frac{x}{a} \right)^3 + \left(\frac{x}{a} \right)^2 \right] \quad (4.3.15)$$

$$M_{xx} = -\frac{q_0 a^2}{12} \left[1 - 6 \left(\frac{x}{a} \right) + 6 \left(\frac{x}{a} \right)^2 \right] - D_T T_1 \quad (4.3.16)$$

In this case, the deflection is independent of temperature, while the bending moment depends on the temperature. The maximum transverse deflection occurs at $x = a/2$ and maximum bending moments occurs at $x = 0$:

$$w_{max} = w_0(a/2) = \frac{q_0 a^4}{384 D_{11}}, \quad M_{max} = M_{xx}(0) = -\left(\frac{q_0 a^2}{12} + D_T T_1\right) \quad (4.3.17)$$

4.3.4 Plate Strips on Elastic Foundation

Here we consider the problem of the bending of a uniformly loaded plate strip supported over the entire bottom surface by an elastic foundation. In the absence of the axial force, the governing equation is given by

$$D_{11} \frac{d^2 w_0}{dx^2} + k w_0 = q_0 \quad (4.3.18)$$

where k is the foundation modulus (force per unit surface area) and q_0 is the intensity of the transverse load. The general solution of this equation is

$$\begin{aligned} w_0(x) &= \left(c_1 \sinh \frac{2\beta x}{a} + c_2 \cosh \frac{2\beta x}{a} \right) \sin \frac{2\beta x}{a} \\ &\quad + \left(c_3 \sinh \frac{2\beta x}{a} + c_4 \cosh \frac{2\beta x}{a} \right) \cos \frac{2\beta x}{a} + \frac{q_0}{k} \end{aligned} \quad (4.3.19)$$

where

$$\beta^4 = \frac{k a^4}{64 D_{11}} \quad (4.3.20)$$

and c_1 through c_4 are constants to be determined using the boundary conditions.

For a plate strip with both edges simply supported, the deflection is symmetrical with respect to the center of the strip. Hence, the slope and shear force at the center must be zero. Suppose that the origin of the coordinate system is taken at the center of the plate. Then, the boundary conditions are

$$\frac{dw_0}{dx} = \frac{d^3 w_0}{dx^3} = 0 \text{ at } x = 0; \quad w_0 = \frac{d^2 w_0}{dx^2} = 0 \text{ at } x = a/2 \quad (4.3.21)$$

The first two boundary conditions give $c_2 = c_3 = 0$. The next two boundary conditions yield

$$c_1 \sin \beta \sinh \beta + c_4 \cos \beta \cosh \beta + \frac{q_0}{k} = 0, \quad c_1 \cos \beta \cosh \beta + c_4 \sin \beta \sinh \beta = 0$$

from which we obtain

$$c_1 = -\frac{2q_0}{k} \left(\frac{\sin \beta \sinh \beta}{\cos 2\beta + \cosh 2\beta} \right), \quad c_4 = -\frac{2q_0}{k} \left(\frac{\cos \beta \cosh \beta}{\cos 2\beta + \cosh 2\beta} \right) \quad (4.3.22)$$

The deflection in Eq. (4.3.19) takes the form

$$w_0(x) = \frac{q_0 a^4}{64 D_{11} \beta^4} \left[1 - \left(\frac{2 \sin \beta \sinh \beta}{\cos 2\beta + \cosh 2\beta} \right) \sin \frac{2\beta x}{a} \sinh \frac{2\beta x}{a} - \left(\frac{2 \cos \beta \cosh \beta}{\cos 2\beta + \cosh 2\beta} \right) \cos \frac{2\beta x}{a} \cosh \frac{2\beta x}{a} \right] \quad (4.3.23)$$

The maximum deflection occurs at $x = 0$

$$w_{max} = w_0\left(\frac{a}{2}\right) = \frac{5q_0 a^4}{384 D_{11}} \varphi_1(\beta), \quad \varphi_1(\beta) = \frac{6}{5\beta^4} \left(1 - \frac{2 \cos \beta \cosh \beta}{\cos 2\beta + \cosh 2\beta} \right) \quad (4.3.24)$$

The rotation at $x = -a/2$ is given by

$$\theta_{max} = \frac{dw_0}{dx} \Big|_{x=a/2} = \frac{q_0 a^3}{24 D_{11}} \varphi_2(\beta), \quad \varphi_2(\beta) = \frac{3}{4\beta^3} \left(\frac{2 \sinh 2\beta - \sin 2\beta}{\cos 2\beta + \cosh 2\beta} \right) \quad (4.3.25)$$

The maximum bending moment occurs at $x = 0$, and it is given by

$$M_{max} = \left(-D_{11} \frac{d^2 w_0}{dx^2} \right)_{x=0} = \frac{q_0 a^2}{8} \varphi_3(\beta), \quad \varphi_3(\beta) = \frac{2}{\beta^2} \left(\frac{\sinh \beta \sin \beta}{\cos 2\beta + \cosh 2\beta} \right) \quad (4.3.26)$$

For isotropic plate strips, one may replace D_{11} with D in Eqs. (4.3.18)–(4.3.25).

4.4 Buckling under Inplane Compressive Load

4.4.1 Introduction

A plate strip subjected to compressive load $\hat{N}_{xx} = -N_{xx}^0$ along its width remains straight, but shortens as the load increases from zero to a certain magnitude. If a small additional axial or lateral disturbance applied to the plate keeps it in equilibrium, then the plate is said to be *stable*. If the small additional disturbance results in a large response and the plate does not return to its original equilibrium configuration, the plate is said to be *unstable*. The onset of instability is called *buckling* (Figure 4.4.1). The magnitude of the compressive axial load at which the plate becomes unstable is termed the *critical buckling load*. If the load is increased beyond this critical buckling load, it results in a large deflection and the plate seeks another equilibrium configuration. Thus, the load at which a plate becomes unstable is of practical importance in design. Here we determine critical buckling loads for plate strips in cylindrical bending.

The equilibrium of the plate strip under the applied inplane compressive load $\hat{N}_{xx} = -N_{xx}^0$ can be obtained from Eqs. (4.2.3) by omitting the inertia terms and thermal resultants

$$D_{11} \frac{d^4 w}{dx^4} + N_{xx}^0 \frac{d^2 w}{dx^2} = 0 \quad (4.4.1)$$

where w denotes the transverse deflection measured from the prebuckling equilibrium state.

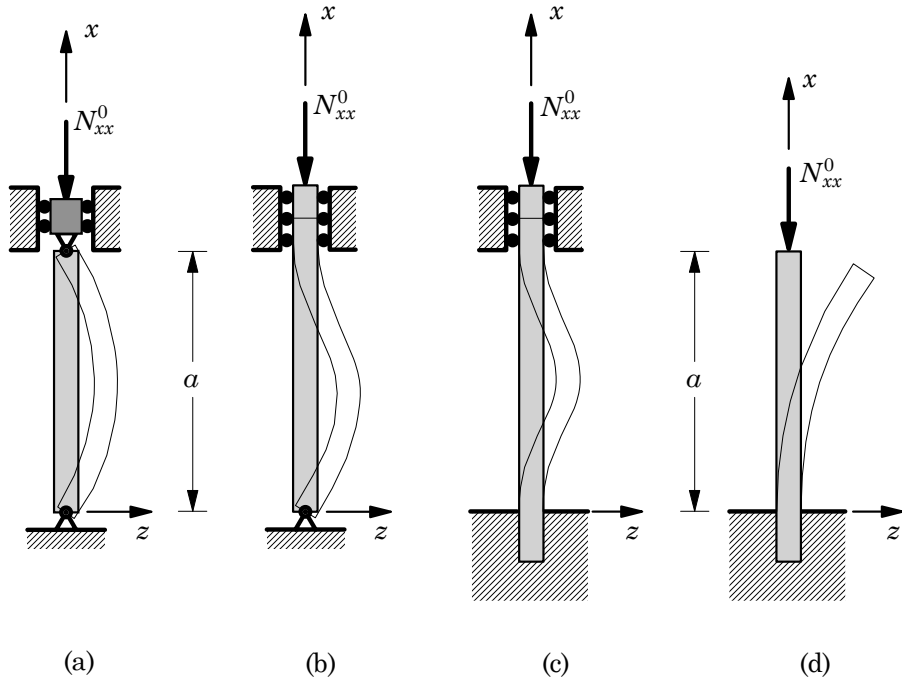


Figure 4.4.1. Buckling of plate strips under various boundary conditions (edge view): (a) hinged-hinged, (b) hinged-clamped, (c) clamped-clamped, and (d) clamped-free.

Integrating Eq. (4.4.1) twice with respect to x , we obtain

$$D_{11} \frac{d^2w}{dx^2} + N_{xx}^0 w = K_1 x + K_2 \quad (4.4.2)$$

where K_1 and K_2 are constants. Next we consider the solution of Eq. (4.4.2) in two parts: homogeneous solution and particular solution. The homogeneous solution of Eq. (4.4.2) is obtained from

$$D_{11} \frac{d^2w}{dx^2} + N_{xx}^0 w = 0 \quad \text{or} \quad \frac{d^2w}{dx^2} + \lambda^2 w = 0 \quad (4.4.3)$$

where

$$\lambda^2 = \frac{N_{xx}^0}{D_{11}} \quad \text{or} \quad N_{xx}^0 = D_{11} \lambda^2 \quad (4.4.4)$$

The homogeneous and particular solutions of the second-order equation (4.4.3) are given, respectively, by

$$\begin{aligned} w_h(x) &= c_1 \sin \lambda x + c_2 \cos \lambda x \\ w_p(x) &= \frac{1}{\lambda^2} (K_1 x + K_2) \end{aligned} \quad (4.4.5)$$

Hence, the complete solution is

$$w(x) = c_1 \sin \lambda x + c_2 \cos \lambda x + c_3 x + c_4 \quad (4.4.6)$$

where $c_3 = K_1/\lambda^2$ and $c_4 = K_2/\lambda^2$. Three of the four constants c_1, c_2, c_3, c_4 , and λ (or N_{xx}^0) are determined using (four) boundary conditions of the problem. Once λ is known, the buckling load can be determined using Eq. (4.4.4).

4.4.2 Simply Supported Plate Strips

For a simply supported plate strip (at $x = 0, a$), we have

$$w = 0, \quad \frac{d^2w}{dx^2} = 0 \quad (4.4.7)$$

Use of the boundary conditions on w gives

$$\begin{aligned} w(0) = 0 : & \quad c_2 + c_4 = 0 \quad \text{or} \quad c_4 = -c_2 \\ \frac{d^2w}{dx^2}|_{x=0} = 0 : & \quad -\lambda^2 c_2 = 0 \quad \text{or} \quad c_2 = 0 \\ w(a) = 0 : & \quad c_1 \sin \lambda a + c_3 a = 0 \\ \frac{d^2w}{dx^2}|_{x=a} = 0 : & \quad -\lambda^2 c_1 \sin \lambda a = 0 \end{aligned} \quad (4.4.8a)$$

From the above equations, it follows that

$$c_1 \sin \lambda a = 0, \quad c_2 = 0, \quad c_3 = 0, \quad c_4 = 0 \quad (4.4.8b)$$

The first equation implies that either $c_1 = 0$ or (and) $\sin \lambda a = 0$. If $c_1 = 0$, then the buckling deflection of Eq. (4.4.3) is zero, implying that the plate did not begin to buckle. For nonzero deflection w , we must have

$$\sin \lambda a = 0 \quad \text{which implies} \quad \lambda a = a \sqrt{\frac{N_{xx}^0}{D_{11}}} = n\pi \quad \text{or} \quad N_{xx}^0 = D_{11} \left(\frac{n\pi}{a} \right)^2 \quad (4.4.9)$$

The critical buckling load (i.e., the smallest value of N_{xx}^0 at which the plate buckles) occurs when $n = 1$

$$N_{cr} = \frac{D_{11}\pi^2}{a^2} \quad (4.4.10)$$

For $E_1/E_2 = 25$ and $\nu_{12} = 0.25$, we have

$$N_{cr} = \frac{E_1 h^3 \pi^2}{12(1 - \nu_{12}\nu_{21})a^2} = \frac{\pi^2}{11.97} \frac{E_1 h^3}{a^2} = 0.8245 \frac{E_1 h^3}{a^2} = 20.6125 \frac{E_2 h^3}{a^2} \quad (4.4.11)$$

For an isotropic plate ($D_{11} = D$) with $\nu = 0.25$, the buckling load becomes

$$N_{cr} = \frac{\pi^2}{11.25} \frac{E h^3}{a^2} = 0.8773 \frac{E h^3}{a^2} \quad (4.4.12)$$

4.4.3 Clamped Plate Strips

For a clamped plate strip (at $x = 0, a$), we have

$$w = 0, \quad \frac{dw}{dx} = 0 \quad (4.4.13)$$

Use of the boundary conditions on w gives

$$\begin{aligned} w(0) = 0 : & \quad c_2 + c_4 = 0 \quad \text{or} \quad c_4 = -c_2 \\ \frac{dw}{dx}|_{x=0} = 0 : & \quad \lambda c_1 + c_3 = 0 \quad \text{or} \quad c_3 = -\lambda c_1 \\ w(a) = 0 : & \quad c_1 \sin \lambda a + c_2 \cos \lambda a + c_3 a + c_4 = 0 \\ \frac{dw}{dx}|_{x=a} = 0 : & \quad \lambda(c_1 \cos \lambda a - c_2 \sin \lambda a) + c_3 = 0 \end{aligned} \quad (4.4.14)$$

Using the first two equations, c_3 and c_4 can be eliminated from the last two equations. We have

$$c_1(\sin \lambda a - \lambda a) + c_2(\cos \lambda a - 1) = 0, \quad c_1(\cos \lambda a - 1) - c_2 \sin \lambda a = 0$$

For nonzero transverse deflection (i.e., for nonzero values of c_2 and c_3), we require that the determinant of the above pair of equations be zero:

$$\begin{vmatrix} \sin \lambda a - \lambda a & \cos \lambda a - 1 \\ \cos \lambda a - 1 & -\sin \lambda a \end{vmatrix} = 0$$

or

$$\lambda a \sin \lambda a + 2 \cos \lambda a - 2 = 0 \quad (4.4.15)$$

This nonlinear (transcendental) equation can be solved by an iterative (Newton's) method for various roots of the equation. The smallest root of this equation is $\lambda = 2\pi$, and the critical buckling load becomes

$$N_{cr} = \frac{4D_{11}\pi^2}{a^2} \quad (4.4.16)$$

Thus, the buckling load of a clamped plate strip is four times that of a simply supported plate strip.

For an orthotropic plate with $E_1/E_2 = 25$ and $\nu_{12} = 0.25$, we have

$$N_{cr} = \frac{\pi^2}{11.97} \frac{E_1 h^3}{a^2} = 3.298 \frac{E_1 h^3}{a^2} = 82.45 \frac{E_2 h^3}{a^2}$$

For an isotropic plate ($D_{11} = D$) with $\nu = 0.25$, the buckling load becomes

$$N_{cr} = \frac{\pi^2}{11.25} \frac{E h^3}{a^2} = 3.5092 \frac{E h^3}{a^2}$$

4.4.4 Other Boundary Conditions

The procedure illustrated in the two previous sections to determine the buckling load can be used for any set of boundary conditions. The analytical expressions for various boundary conditions are listed in Eqs. (4.4.17)–(4.4.21) below. The boundary conditions can be used obtain relations among the constants c_1 , c_2 , c_3 , and c_4 of Eq. (4.4.6), which are listed along with the equation governing λ in Table 4.4.1 for various combinations of classical boundary conditions. These can be used to readily determine the critical buckling loads of plate strips.

Free:

$$M_{xx} = 0 \quad \text{and} \quad V_x = Q_x - N_{xx}^0 \frac{d^2 w}{dx^2} = 0$$

or

$$\frac{d^2 w}{dx^2} = 0 \quad \text{and} \quad D_{11} \frac{d^3 w}{dx^3} - N_{xx}^0 \frac{d^2 w}{dx^2} = 0 \quad (4.4.17)$$

Hinged (or) Simply Supported:

$$w = 0, \quad M_{xx} = 0 \quad \text{or} \quad \frac{d^2 w}{dx^2} = 0 \quad (4.4.18)$$

Table 4.4.1. Values of the constants and eigenvalues for buckling of plate strips with various boundary conditions [$\lambda^2 \equiv N_{xx}^0 / D_{11} = (e_n/a)^2$].

End Conditions at $x = 0$ and $x = a$	Constants [†]	Characteristic Equation and Values* of $e_n \equiv \lambda_n a$
• Hinged-Hinged	$c_1 \neq 0$ $c_2 = c_3 = c_4 = 0$ 	$\sin e_n = 0, \quad e_n = n\pi$
• Fixed-Fixed	$c_1 = 1/(\sin e_n - e_n)$ $c_3 = -1/\lambda_n, \quad c_2 = -c_4$ $c_2 = 1/(\cos e_n - 1)$ 	$e_n \sin e_n = 2(1 - \cos e_n)$ $e_n = 2\pi, 8.987, 4\pi, \dots$
• Fixed-Free	$c_1 = c_3 = 0$ $c_2 = -c_4 \neq 0$ 	$\cos e_n = 0$ $e_n = (2n - 1)\pi/2$
• Free-Free	$c_1 = c_3 = 0$ $c_2 \neq 0, \quad c_4 \neq 0$ 	$\sin e_n = 0$ $e_n = n\pi$
• Hinged-Fixed	$c_1 = 1/(e_n \cos e_n)$ $c_3 = -1, \quad c_2 = c_4 = 0$ 	$\tan e_n = e_n$ $e_n = 4.493, 7.725, \dots$

[†] See Eq. (4.4.6): $w(x) = c_1 \sin \lambda x + c_2 \cos \lambda x + c_3 x + c_4$.

*For critical buckling load, only the first (minimum) value of $e = \lambda a$ is needed.

Fixed (or) Clamped:

$$w = 0, \quad \frac{dw}{dx} = 0 \quad (4.4.19)$$

Elastically Simply Supported:

$$w = \alpha F_0, \quad M_{xx} = 0 \quad \text{or} \quad \frac{d^2w}{dx^2} = 0 \quad (4.4.20)$$

where F_0 is the vertical reacting force of the elastic support and α is the inverse of the elastic (spring) constant. When $\alpha = 0$ (i.e., the support is rigid), we recover the conventional simply supported boundary condition. When α is very large, the boundary condition approaches that of a free edge.

Elastically Clamped:

$$w = 0, \quad \frac{dw}{dx} = -\beta M_0 \quad (4.4.21)$$

where M_0 is the reacting moment (clockwise) of the elastic support and β is the torsional spring constant. When $\beta = 0$ (i.e., the restraint is rigid), we recover the conventional clamped boundary condition. On the other hand, if β is very large (i.e., the restraint is very flexible), the condition approaches that of a simply supported case.

4.5 Free Vibration

4.5.1 General Formulation

In the absence of any applied transverse mechanical and thermal loads, Eq. (4.2.3) reduces to

$$D_{11} \frac{\partial^4 w_0}{\partial x^4} = I_2 \frac{\partial^4 w_0}{\partial x^2 \partial t^2} - I_0 \frac{\partial^2 w_0}{\partial t^2} + \hat{N}_{xx} \frac{\partial^2 w_0}{\partial x^2} \quad (4.5.1)$$

For natural vibration, the solution of Eq. (4.5.1) is assumed to be periodic

$$w_0(x, t) = w(x) \cos \omega t \quad (4.5.2)$$

where ω is the natural frequency of vibration and $w(x)$ is the mode shape. Substituting for w_0 from Eq. (4.5.2) into Eq. (4.5.1) and cancelling the factor $\cos \omega t$ (because the result should hold for any time t), we obtain

$$D_{11} \frac{d^4 w}{dx^4} - \hat{N}_{xx} \frac{d^2 w}{dx^2} = I_0 \omega^2 w - I_2 \omega^2 \frac{d^2 w}{dx^2} \quad (4.5.3)$$

Equation (4.5.3) can be expressed in the general form

$$a \frac{d^4 w}{dx^4} + b \frac{d^2 w}{dx^2} - cw = 0 \quad (4.5.4a)$$

where

$$a = D_{11}, \quad b = \omega^2 I_2 - \hat{N}_{xx}, \quad c = \omega^2 I_0 \quad (4.5.4b)$$

Assume solution of the homogeneous equation in (4.5.4a) in the form

$$w(x) = Ae^{rx} \quad (4.5.5)$$

and substitute it into Eq. (4.5.4a) to obtain

$$ar^4 + br^2 - c = 0 \quad \text{or} \quad as^2 + bs - c = 0 \quad (s = r^2) \quad (4.5.6)$$

The roots of the above equation are

$$s_1 = \frac{1}{2a} (-b - \sqrt{b^2 + 4ac}) \equiv -\lambda^2, \quad s_2 = \frac{1}{2a} (-b + \sqrt{b^2 + 4ac}) \equiv \mu^2 \quad (4.5.7)$$

Hence, the solution of Eq. (4.5.4a) can be expressed as

$$w(x) = c_1 \sin \lambda x + c_2 \cos \lambda x + c_3 \sinh \mu x + c_4 \cosh \mu x \quad (4.5.8)$$

where

$$\lambda = \sqrt{\frac{1}{2a} (b + \sqrt{b^2 + 4ac})}, \quad \mu = \sqrt{\frac{1}{2a} (-b + \sqrt{b^2 + 4ac})} \quad (4.5.9)$$

and c_1, c_2, c_3 , and c_4 are integration constants, which are to be determined using the boundary conditions. In reality, the four boundary conditions (two at each edge of the plate strip) are used to determine λ and only three of the four constants.

The frequency of vibration is determined from λ (or μ) as follows. From Eq. (4.5.7) we have

$$(2a\lambda - b)^2 = b^2 + 4ac \quad \text{or} \quad a\lambda^4 - b\lambda^2 - c = 0$$

Using the definitions of a, b , and c , we obtain

$$D_{11}\lambda^4 - (\omega^2 I_2 - \hat{N}_{xx}) \lambda^2 - \omega^2 I_0 = 0$$

from which we have

$$(I_0 + \lambda^2 I_2) \omega^2 = D_{11}\lambda^4 + \hat{N}_{xx}\lambda^2$$

or

$$\omega^2 = \frac{D_{11}\lambda^4 + \hat{N}_{xx}\lambda^2}{I_0 + \lambda^2 I_2} \quad (4.5.10)$$

If the applied inplane force is zero, the natural frequency of vibration, with rotary inertia included, is given by

$$\omega^2 = \frac{D_{11}\lambda^4}{I_0 + \lambda^2 I_2} = \frac{D_{11}}{I_0} \left(1 - \frac{I_2 \lambda^2}{I_0 + \lambda^2 I_2} \right) \lambda^2 \quad (4.5.11)$$

In addition, if rotary inertia is neglected, we have

$$\omega = \lambda^2 \sqrt{\frac{D_{11}}{I_0}} \quad (4.5.12)$$

The result in Eq. (4.5.12), when the rotary inertia is neglected and there is no applied inplane force, can be obtained directly from Eq. (4.5.3), which reduces to

$$D_{11} \frac{d^4 w}{dx^4} - I_0 \omega^2 w = 0$$

The solution to this equation is also given by Eq. (4.5.8) with $\lambda = \mu$ and

$$\lambda^2 = \omega \sqrt{\frac{I_0}{D_{11}}} \quad (4.5.13)$$

In the following sections, plates with both ends simply supported or both ends clamped are considered to illustrate the procedure to evaluate the constants c_1 through c_4 and, more importantly, to determine λ and find ω . The smallest frequency is known as the *fundamental frequency*. For other boundary conditions, the reader is referred to Table 4.5.1.

Table 4.5.1. Values of the constants and eigenvalues for natural vibration of plate strips with various boundary conditions ($\lambda_n^4 \equiv \omega_n^2 I_0 / D = (e_n/a)^4$). Rotary inertia is not included.

End Conditions at $x = 0$ and $x = a$	Constants [†]	Characteristic Equation and Values of $e_n \equiv \lambda_n a$
• Hinged-Hinged 	$c_1 \neq 0$ $c_2 = c_3 = c_4 = 0$	$\sin e_n = 0, e_n = n\pi$
• Fixed-Fixed 	$c_1 = -c_3 = 1/p_n$ $-c_2 = c_4 = 1/q_n$ $p_n = (\sin e_n - \sinh e_n),$	$\cos e_n \cosh e_n - 1 = 0$ $e_n = 4.730, 7.853, \dots$ $q_n = (\cos e_n - \cosh e_n)$
• Fixed-Free 	$c_1 = -c_3 = 1/p_n$ $-c_2 = c_4 = 1/q_n$ $p_n = (\sin e_n + \sinh e_n),$	$\cos e_n \cosh e_n + 1 = 0$ $e_n = 1.875, 4.694, \dots$ $q_n = (\cos e_n + \cosh e_n)$
• Free-Free 	$c_1 = c_3 = 1/p_n$ $c_2 = c_4 = -1/q_n$ $p_n = (\sin e_n - \sinh e_n),$	$\cos e_n \cosh e_n - 1 = 0$ $e_n = 4.730, 7.853, \dots$ $q_n = (\cos e_n - \cosh e_n)$
• Hinged-Fixed 	$c_1 = 1/\sin e_n$ $c_2 = c_4 = 0$ $c_3 = 1/\sinh e_n$	$\tan e_n = \tanh e_n$ $e_n = 3.927, 7.069, \dots$
• Hinged-Free 	$c_1 = 1/\sin e_n$ $c_2 = c_4 = 0$ $c_3 = -1/\sinh e_n$	$\tan e_n = \tanh e_n$ $e_n = 3.927, 7.069, \dots$

[†] See Eq. (4.5.8): $W(x) = c_1 \sin \lambda x + c_2 \cos \lambda x + c_3 \sinh \mu x + c_4 \cosh \mu x$.

4.5.2 Simply Supported Plate Strips

For a simply supported plate strip, we use the boundary conditions

$$w = 0 \quad M_{xx} = D_{11} \frac{d^2 w}{dx^2} = 0 \quad \text{at } x = 0, a$$

and obtain

$$c_1 \sin \lambda a = 0, \quad c_2 = c_3 = c_4 = 0$$

Hence, $\lambda = \frac{n\pi}{a}$, and from Eq. (4.5.10) it follows that

$$\omega_n = \left(\frac{n\pi}{a} \right)^2 \left[\left(\frac{D_{11}}{I_0} \right) \left(1 + \frac{\hat{N}_{xx}}{(\frac{n\pi}{a})^2 D_{11}} \right) \left(\frac{1}{1 + (\frac{n\pi}{a})^2 \frac{I_2}{I_0}} \right) \right]^{\frac{1}{2}} \quad (4.5.14)$$

If the rotary inertia is neglected, we obtain

$$\omega_n = \left(\frac{n\pi}{a} \right)^2 \left[\left(\frac{D_{11}}{I_0} \right) \left(1 + \frac{\hat{N}_{xx}}{(\frac{n\pi}{a})^2 D_{11}} \right) \right]^{\frac{1}{2}} \quad (4.5.15)$$

Thus, the effect of the inplane tensile force \hat{N}_{xx} is to increase the natural frequencies. If we have a very flexible plate, say a membrane under large tension, the second term under the radical in Eq. (4.5.15) becomes very large in comparison with unity; if n is not large, we have

$$\omega_n \approx \frac{n\pi}{a} \sqrt{\frac{\hat{N}_{xx}}{I_0}} \quad (4.5.16)$$

which are natural frequencies of a stretched membrane. We also note from Eq. (4.5.15) that frequencies of natural vibration decrease when a compressive force instead of a tensile force is acting on the plate strip.

When $\hat{N}_{xx} = 0$, we obtain from Eq. (4.5.14)

$$\omega_n = \left(\frac{n\pi}{a} \right)^2 \left[\frac{D_{11}}{I_0} \left(\frac{I_0}{I_0 + (\frac{n\pi}{a})^2 I_2} \right) \right]^{\frac{1}{2}} = \left(\frac{n\pi}{a} \right)^2 \left[\frac{D_{11}}{I_0} \left(1 - \frac{I_2 (\frac{n\pi}{a})^2}{(\frac{n\pi}{a})^2 I_2 + I_0} \right) \right]^{\frac{1}{2}} \quad (4.5.17)$$

Thus, rotatory inertia decreases frequencies of natural vibration. If the rotatory inertia is neglected, we obtain

$$\omega_n = \left(\frac{n\pi}{a} \right)^2 \sqrt{\frac{D_{11}}{I_0}} \quad (4.5.18)$$

For a simply supported orthotropic plate with $E_1/E_2 = 25$, $\nu_{12} = 0.25$, $a/h = 10$ and rotatory inertia included, we obtain

$$\omega_1 = \frac{14.205}{a^2} \sqrt{\frac{E_2 h^3}{I_0}} = 14.205 \frac{h}{a^2} \sqrt{\frac{E_2}{\rho}}$$

4.5.3 Clamped Plate Strips

For a plate strip clamped at both ends, the boundary conditions

$$w = 0, \quad \frac{dw}{dx} = 0 \quad \text{at } x = 0, a$$

lead to the relations

$$c_2 + c_4 = 0, \quad \lambda c_1 + \mu c_3 = 0 \quad (4.5.19a)$$

$$\begin{bmatrix} \sin \lambda a - \left(\frac{\lambda}{\mu}\right) \sinh \mu a & \cos \lambda a - \cosh \mu a \\ \cos \lambda a - \cosh \mu a & -\sin \lambda a - \left(\frac{\mu}{\lambda}\right) \sinh \mu a \end{bmatrix} \begin{Bmatrix} c_1 \\ c_2 \end{Bmatrix} = \begin{Bmatrix} 0 \\ 0 \end{Bmatrix} \quad (4.5.19b)$$

where relations (4.5.19a) were used to eliminate c_3 and c_4 in writing the relations in (4.5.19b). For nonzero c_1 and c_2 , we require the determinant of the coefficient matrix of the above equations to vanish. This leads to the characteristic polynomial

$$-2 + 2 \cos \lambda a \cosh \mu a + \left(\frac{\lambda}{\mu} - \frac{\mu}{\lambda}\right) \sin \lambda a \sinh \mu a = 0 \quad (4.5.20)$$

The transcendental equation (4.5.20) needs to be solved iteratively for λ and μ , in conjunction with

$$\lambda^2 = \mu^2 + \frac{b}{a} = \mu^2 + \frac{I_2 \omega^2 - \hat{N}_{xx}}{D_{11}} \quad (4.5.21)$$

For natural vibration without rotatory inertia, Eq. (4.5.20) takes the simpler form

$$\cos \lambda a \cosh \lambda a - 1 = 0 \quad (4.5.22)$$

The roots of Eq. (4.5.22) are

$$\lambda_1 a = 4.730, \quad \lambda_2 a = 7.853, \quad \dots, \quad \lambda_n a \approx \left(n + \frac{1}{2}\right)\pi \quad (4.5.23)$$

In general, the roots of Eq. (4.5.22) are not the same as those of Eq. (4.5.20). If one approximates Eq. (4.5.20) as (4.5.22) (i.e., $\lambda \approx \mu$), the roots in Eq. (4.5.23) can be used to determine the natural frequencies of vibration *with rotary inertia* from Eq. (4.5.17). When rotary inertia is neglected, the frequencies are given by Eq. (4.5.18) with λ given by Eq. (4.5.23). The frequencies obtained from Eq. (4.5.17) with the values of λ from Eq. (4.5.22) are only an approximation of the frequencies with rotary inertia.

For a clamped orthotropic plate with $E_1/E_2 = 25$, $\nu_{12} = 0.25$, $a/h = 10$ and rotatory inertia included, we obtain

$$\omega_1 = \frac{32.169}{a^2} \sqrt{\frac{E_2 h^3}{I_0}} = 32.169 \frac{h}{a^2} \sqrt{\frac{E_2}{\rho}} \quad (4.5.24)$$

4.6 Transient Analysis

4.6.1 Preliminary Comments

In this section, we study the transient response of plate strips. The Ritz method or Navier's method may be used to reduce the partial differential equation (4.2.3) to an ordinary differential equation in time. In the Navier method, the deflection as well as the load are expanded using the Fourier series. The expansions are selected such that they satisfy all of the boundary conditions of the problem for any choice of the Fourier coefficients. The expansions are then substituted into the governing differential equation to obtain a differential equation in time. The Navier method may be used only for simply supported boundary conditions.

Suppose that the solution $w_0(x, t)$ of Eq. (4.2.3), either exact or approximate, is of the form

$$w_0(x, t) \approx \sum_{n=1}^N A_n(t) \varphi_n(x) \quad (4.6.1)$$

where $A_n(t)$ are parameters to be determined and $\varphi_n(x)$ are known functions of x . In the N -parameter Ritz solution, $\varphi_n(x)$ represent the approximation functions that are selected to satisfy at least the geometric boundary conditions (see section 2.3.2) of the problem for any time. In the Navier method, φ_n satisfy all of the boundary conditions of the problem. Further, N may be infinity [i.e., Eq. (4.6.1) represents an infinite series]. In both methods, an ordinary differential equation of the form

$$M_n \frac{d^2 A_n}{dt^2} + K_n A_n = F_n \quad (4.6.2)$$

is obtained, which is then solved using initial conditions of the problem. The exact form of the coefficients M_n , K_n , and F_n depend on the method used.

Suppose that we wish to solve the equation

$$D_{11} \frac{\partial^4 w_0}{\partial x^4} = q - I_0 \frac{\partial^2 w_0}{\partial t^2} + I_2 \frac{\partial^4 w_0}{\partial x^2 \partial t^2} \quad (4.6.3)$$

subjected to the simply supported boundary conditions

$$w_0 = 0, \quad M \equiv -D_{11} \frac{\partial^2 w_0}{\partial x^2} = 0 \quad (4.6.4)$$

at $x = 0, a$. Here we discuss both the Navier method and the Ritz method of reducing Eq. (4.6.3) to Eq. (4.6.2).

4.6.2 The Navier Solution

The first step in the Navier solution procedure is to expand the dependent unknown $w_0(x, t)$ in the Fourier series

$$w_0(x, t) = \sum_{n=1}^{\infty} A_n(t) \sin \alpha_n x + \sum_{n=0}^{\infty} B_n(t) \cos \alpha_n x \quad (4.6.5)$$

where (A_n, B_n) are Fourier coefficients to be determined for any time t , and $\alpha_n = n\pi/a$. The expansion in Eq. (4.6.3) must be such that w_0 satisfies the boundary conditions in Eq. (4.6.4). Clearly, the expansion in (4.6.5) satisfies the boundary conditions (4.6.4) for any A_n but $B_n = 0$.

The next step is to substitute the expansion (4.6.5) into Eq. (4.6.3)

$$\sum_{n=1}^{\infty} \left\{ [D_{11}\alpha_n^4] A_n(t) + [I_0 + I_2\alpha_n^2] \ddot{A}_n(t) \right\} \sin \alpha_n x = q \quad (4.6.6)$$

where the superposed dots on A_n denote derivatives with respect to time. Since the left side of Eq. (4.6.4) represents a Fourier sine series, the load q is also expanded in a sine series

$$q(x, t) = \sum_{n=1}^{\infty} Q_n(t) \sin \alpha_n x \quad (4.6.7)$$

Since q is a known function, it is possible to determine the coefficients Q_n from the equation

$$Q_n(t) = \frac{2}{a} \int_0^a q(x, t) \sin \alpha_n x \, dx \quad (4.6.8)$$

For example, if the beam is suddenly subjected to uniformly distributed load of intensity q_0 at time $t = 0$, we have

$$Q_n = \frac{2}{a} \int_0^a q_0 \sin \alpha_n x \, dx = \frac{4q_0}{a\alpha_n} \quad \text{when } n = 1, 3, 5, \dots \quad (4.6.9)$$

and $Q_n = 0$ when n is even.

Substituting the load expansion (4.6.7) into Eq. (4.6.6) [with q replaced by the expansion in (4.6.7)], we obtain

$$\sum_{n=1}^{\infty} [K_n A_n + M_n \ddot{A}_n - Q_n] \sin \alpha_n x = 0 \quad (4.6.10a)$$

where K_n and M_n are the parameters (independent of x)

$$K_n = D_{11}\alpha_n^4, \quad M_n = I_0 + I_2\alpha_n^2 \quad (4.6.10b)$$

Since Eq. (4.6.10a) must hold for every x and $\sin \alpha_n x$ is not zero for all x , it follows that the coefficient in the square brackets of Eq. (4.6.10a) must be zero:

$$M_n \frac{d^2 A_n}{dt^2} + K_n A_n - Q_n = 0 \quad (4.6.11)$$

This completes the application of the Navier solution approach. Note that if there is no time dependence, we set the term containing \ddot{A}_n to zero and solve for $A_n = Q_n/K_n$. Then the static solution is given by (which is exact)

$$w_0(x) = \sum_{n=1}^{\infty} \frac{Q_n}{D_{11}\alpha_n^4} \sin \alpha_n x \quad (4.6.12)$$

4.6.3 The Ritz Solution

In the Ritz method the approximation functions $\varphi_n(x)$ are chosen to satisfy the geometric boundary conditions $w_0(0, t) = w_0(a, t) = 0$ since the natural boundary conditions are included in the virtual work statement. If we were to choose trigonometric functions, we set

$$w_0(x, t) \approx W_N(x, t) = \sum_{n=1}^N A_n(t) \varphi_n(x) + \varphi_0(x) \quad (4.6.13a)$$

where

$$\varphi_n(x) = \sin \alpha_n x, \quad \alpha_n = \frac{n\pi}{a} \quad (4.6.13b)$$

The function $\varphi_0(x)$ is zero in the present case because the geometric boundary conditions are homogeneous.

Next, we substitute the approximation W_N in Eq. (4.6.13a) into the statement of the dynamic version of the principle of virtual displacements (or Hamilton's principle) and determine the equation governing $A_n(t)$:

$$0 = \int_0^T \int_0^a \left(D_{11} \frac{\partial^2 W_N}{\partial x^2} \frac{\partial^2 \delta W_N}{\partial x^2} - q W_N - I_0 \dot{W}_N \delta \dot{W}_N - I_2 \frac{\partial^2 W_N}{\partial x \partial t} \frac{\partial^2 \delta W_N}{\partial x \partial t} \right) dx dt \quad (4.6.14)$$

Substituting Eq. (4.6.13a) into Eq. (4.6.14), we obtain

$$0 = \int_0^T \left[\sum_{n=1}^N \left(M_{mn}^R \frac{d^2 A_n}{dt^2} + K_{mn}^R A_n \right) - F_n \right] dt \quad (4.6.15a)$$

for $m = 1, 2, \dots, N$, where

$$K_{mn}^R = \int_0^a D_{11} \frac{\partial^2 \varphi_m}{\partial x^2} \frac{\partial^2 \varphi_n}{\partial x^2} dx = \begin{cases} \frac{a D_{11} \alpha_n^4}{2} & \text{for } m = n \\ 0 & \text{for } m \neq n \end{cases} \quad (4.6.15b)$$

$$M_{mn}^R = \int_0^a \left(I_0 \varphi_m \varphi_n + I_2 \frac{\partial \varphi_m}{\partial x} \frac{\partial \varphi_n}{\partial x} \right) dx = \begin{cases} \frac{a}{2} (I_0 + I_2 \alpha_n^2) & \text{for } m = n \\ 0 & \text{for } m \neq n \end{cases} \quad (4.6.15c)$$

$$F_m = \int_0^a q \varphi_m dx \quad (4.6.15d)$$

Since Eq. (4.6.15a) must hold for all times $t > 0$, we have

$$\sum_{n=1}^N \left(M_{mn}^R \frac{d^2 A_n}{dt^2} + K_{mn}^R A_n \right) = F_m \quad \text{for } m = 1, 2, \dots, N \quad (4.6.16)$$

Equation (4.6.16) is similar to Eq. (4.6.11), except that Eq. (4.6.16) is a matrix equation, which, in view of the fact that the off-diagonal values are zero [see Eq. (4.6.15b)], reduces to a set of N uncoupled equations similar to Eq. (4.6.11):

$$M_n^R \frac{d^2 A_n}{dt^2} + K_n^R A_n = F_m \quad (\text{no sum on } n) \quad (4.6.17)$$

for $n = 1, 2, \dots, N$, where we set $M_{nn}^R = M_n^R$ and $K_{nn}^R = K_n^R$.

4.6.4 Transient Response

Equation (4.6.11) or (4.6.17) represents a second-order ordinary differential equation in time for each n . The general solution of (4.6.11) is given by

$$A_n(t) = A_n^0 \sin \lambda_n t + B_n^0 \cos \lambda_n t + \frac{Q_n}{K_n}, \quad \lambda_n = \sqrt{\frac{K_n}{M_n}} \quad (4.6.18)$$

where A_n^0 and B_n^0 are constants to be determined using the initial conditions of the problem. The complete solution is then given by

$$w_0(x, t) = \sum_{n=1}^{\infty} \left[A_n^0 \sin \lambda_n t + B_n^0 \cos \lambda_n t + \frac{Q_n}{K_n} \right] \sin \alpha_n x \quad (4.6.19)$$

where Q_n is as defined in (4.6.8). In the case of the Ritz solution, we write

$$W_N(x, t) = \sum_{n=1}^N \left[A_n^{0R} \sin \lambda_n t + B_n^{0R} \cos \lambda_n^R t + \frac{F_n}{K_n^R} \right] \sin \alpha_n x, \quad \lambda_n^R = \sqrt{\frac{K_n^R}{M_n}} \quad (4.6.20)$$

Let the initial conditions on the displacement and velocity be

$$w_0(x, 0) = d_0(x) = \sum_{n=1}^{\infty} D_n^0 \sin \alpha_n x, \quad \frac{\partial w_0}{\partial t}(x, 0) = v_0 = \sum_{n=1}^{\infty} V_n^0 \sin \alpha_n x \quad (4.6.21)$$

where D_n^0 and V_n^0 have the same form as Q_n in Eq. (4.6.8). These conditions give

$$B_n^0 = D_n^0 - \frac{Q_n}{K_n}, \quad A_n^0 \lambda_n = V_n^0 - \frac{1}{K_n} \frac{dQ_n}{dt} \quad (4.6.22)$$

Then the analytical solution becomes

$$\begin{aligned} w_0(x, t) &= \sum_{n=1}^{\infty} \left[D_n^0 \sin \lambda_n t + \frac{V_n^0}{\lambda_n} \cos \lambda_n t \right. \\ &\quad \left. + \frac{Q_n}{K_n} (1 - \cos \lambda_n t) - \frac{1}{K_n} \frac{dQ_n}{dt} \sin \lambda_n t \right] \sin \alpha_n x \end{aligned} \quad (4.6.23)$$

When the initial deflection and velocity are zero, we obtain

$$w_0(x, t) = \sum_{n=1}^{\infty} \left[\frac{Q_n}{K_n} (1 - \cos \lambda_n t) - \frac{1}{K_n} \frac{dQ_n}{dt} \sin \lambda_n t \right] \sin \alpha_n x \quad (4.6.24)$$

Similarly, the N -parameter Ritz solution is

$$W_N(x, t) = \sum_{n=1}^N \left[\frac{F_n}{K_n^R} (1 - \cos \lambda_n^R t) - \frac{1}{K_n^R} \frac{dF_n}{dt} \sin \lambda_n^R t \right] \sin \alpha_n x \quad (4.6.25)$$

For a beam simply supported at both ends and subjected to a suddenly applied uniform load $q = q_0 H(t)$, Q_n is defined by Eq. (4.6.9) and the analytical solution becomes

$$w_0(x, t) = \frac{4q_0}{\pi} \sum_{n=1}^{\infty} \frac{1}{nK_n} (1 - \cos \lambda_n t) \sin \alpha_n x \quad (4.6.26)$$

for n odd. In the case of the N -parameter Ritz solution, $F_n = 2q_0 a / n\pi$ for n odd, and the solution is given by

$$W_N(x, t) = \frac{2q_0 a}{\pi} \sum_{n=1}^N \frac{1}{nK_n^R} (1 - \cos \lambda_n^R t) \sin \alpha_n^R x \quad (4.6.27)$$

The static deflection can be obtained by setting the expression $(1 - \cos \lambda_n t)$ to unity.

4.6.5 Laplace Transform Method

Equation (4.6.11) or (4.6.17) can also be solved using the Laplace transform method. The Laplace transform of a function $f(t)$ is defined by

$$\bar{f}(s) \equiv \mathcal{L}[f(t)] = \int_0^\infty e^{-st} f(t) dt \quad (4.6.28)$$

The Laplace transform (or inverse transform) of some typical functions are given in Table 4.6.1.

To solve Eq. (4.6.11) by the Laplace transform method, let $\mathcal{L}[A_n(t)] = \bar{A}_n(s)$. Then Eq. (4.6.11) transforms to

$$M_n \left(s^2 \bar{A}_n(s) - s A_n(0) - \dot{A}_n(0) \right) + K_n \bar{A}_n(s) - \bar{F}_n(s) = 0 \quad (4.6.29a)$$

or

$$(s^2 + \lambda_n^2) \bar{A}_n(s) = \left(s A_n(0) + \dot{A}_n(0) + \frac{\bar{F}_n}{M_n} \right) \quad (4.6.29b)$$

Now suppose that the applied load is uniformly distributed step loading. Then

$$\bar{F}_n(s) = \left(\frac{4q_0}{a\alpha_n} \right) \frac{1}{s} \quad (4.6.30)$$

Substituting the above expression into Eq. (4.6.29b) and using the inverse Laplace transform (see Table 4.6.1), we obtain

$$A_n(t) = \left[A_n(0) \cos \lambda_n t + \frac{\dot{A}_n(0)}{\lambda_n} \sin \lambda_n t \right] + \left(\frac{4q_0}{a\alpha_n K_n} \right) (1 - \cos \lambda_n t) \quad (4.6.31)$$

where we have used the identity

$$\frac{1}{s(s^2 + \lambda_n^2)} = \frac{1}{\lambda_n^2} \left(\frac{1}{s} - \frac{s}{s^2 + \lambda_n^2} \right)$$

Table 4.6.1. The Laplace transform pairs of typical functions.[†]

$F(t)$	$\bar{F}(s)$	$f(t)$	$\bar{f}(s)$
1	$\frac{1}{s}$	$\frac{df}{dt}$	$s\bar{f}(s) - f(0)$
e^{at}	$\frac{1}{s-a}$	$\frac{d^2f}{dt^2}$	$s^2\bar{f}(s) - sf(0) - f'(0)$
$\sin at$	$\frac{a}{s^2+a^2}$	$\cos at$	$\frac{s}{s^2+a^2}$
$\frac{1}{a^2}(1 - \cos at)$	$\frac{1}{s(s^2+a^2)}$	$\frac{1}{a^3}(at - \sin at)$	$\frac{1}{s^2(s^2+a^2)}$
$\frac{1}{2a} \sin at$	$\frac{s}{(s^2+a^2)^2}$	$\frac{1}{2a^3}(\sin at - at \cos at)$	$\frac{1}{(s^2+a^2)^2}$
$t \cos at$	$\frac{s^2-a^2}{(s^2+a^2)^2}$	$\frac{1}{2a}(\sin at + at \cos at)$	$\frac{s^2}{(s^2+a^2)^2}$
$\frac{1}{b}e^{at} \sin bt$	$\frac{1}{(s-a)^2+b^2}$	$\frac{\cos at - \cos bt}{b^2-a^2}$	$\frac{s}{(s^2+a^2)(s^2+b^2)}$
$\sinh at$	$\frac{a}{s^2-a^2}$	$\cosh at$	$\frac{s}{s^2-a^2}$
$t^n f(t)$	$(-)^n \frac{d^n \bar{f}}{ds^n}$	$tf(t)$	$-\frac{d}{ds} \bar{f}(s)$
$\frac{1}{t}f(t)$	$\int_s^\infty \bar{f}(r)dr$	$\int_0^t f(\tau)d\tau$	$\frac{1}{s}\bar{f}(s)$
$e^{at}f(t)$	$\bar{f}(s-a)$	$f * g$	$\bar{f}(s)\bar{g}(s)$

[†] a and b are constants; $f * g = \int_0^t f(\tau)g(t-\tau)d\tau$.

For $A_n(0) = D_n^0$ and $\dot{A}_n(0) = V_n^0$, Eq. (4.6.31) becomes

$$A_n(t) = \left[D_n^0 \cos \lambda_n t + \frac{V_n^0}{\lambda_n} \sin \lambda_n t \right] + \left(\frac{4q_0}{a\alpha_n K_n} \right) (1 - \cos \lambda_n t) \quad (4.6.32)$$

If the initial conditions are zero, then $D_n^0 = V_n^0 = 0$ and $A_n(t)$ becomes

$$A_n(t) = \left(\frac{4q_0}{a\alpha_n K_n} \right) (1 - \cos \lambda_n t) \quad (4.6.33)$$

Equation (4.6.33) is the same as the solution obtained earlier. The complete solution is given by

$$w_0(x, t) = \sum_{n=1}^{\infty} A_n(t) \sin \alpha_n x = \sum_{n=1}^{\infty} \left(\frac{4q_0}{a\alpha_n K_n} \right) (1 - \cos \lambda_n t) \sin \alpha_n x \quad (4.6.34)$$

The procedure used to solve Eq. (4.6.11) can be used to solve Eq. (4.6.17). When the matrix equations (4.6.17) are not uncoupled (i.e., K_n^R and M_n^R are not diagonal), solution by the Laplace transform method requires us to deal with a set of (matrix) differential equations (see Problem 4.17).

4.7 Summary

In this chapter the classical plate theory is used to study the bending, buckling, natural frequency, and transient response of plate strips in cylindrical bending for the most commonly used boundary conditions. A plate strip is a long plate with relatively smaller dimension in the other planar direction, but still considerably large compared to the thickness. Each long edge is assumed to have the same boundary condition along its entire length, and any applied load is assumed to be constant along the long edges, as shown in Figure 4.1.1. Consequently, the plate problem reduces to a one-dimensional with respect to the shorter direction, and the displacements (u_0, v_0, w_0) of the plate strip are functions of the coordinate along the shorter direction. Bending, buckling, and natural vibration responses of plate strips using shear deformation theories can be obtained using algebraic relations that exist between the corresponding solutions of the classical and shear deformation theories [see Wang, Reddy, and Lee (2000) and Problems 4.18–4.21].

Problems

- 4.1** Consider a simply supported plate strip under point loads F_0 at $x = a/4$ and $x = 3a/4$ (the so-called *four-point bending*). Use the symmetry about $x = a/2$ to determine the deflection $w_0(x)$ using the classical plate theory. (*Ans:* The maximum deflection is $w_{max} = -11F_0a^3/384D_{11}$)
- 4.2** Determine the static deflection of a clamped plate strip under uniformly distributed load q_0 and a center point load F_0 using the classical plate theory.
- 4.3** Determine the static deflection of a plate strip with elastically built-in edges and under uniformly distributed load q_0 using the classical plate theory. Assume that there is no axial force. Note that the boundary conditions in Eq. (4.3.13) are now replaced with

$$w_0 = 0, \quad \frac{dw_0}{dx} = -\beta M_0$$

where β is a constant that defines the degree of the rigidity of the restraint against rotation. The larger the value of β , the more flexible is the restraint, and the boundary condition approaches that of a simply supported edge with $\beta \rightarrow \infty$ [$\beta = 0$ gives the clamped boundary condition in Eq. (4.3.13)].

- 4.4** Repeat Problem 4.3 for the case in which there is an axial force.
- 4.5** Show that the critical buckling load of a clamped-free plate strip using the classical plate theory is given by $N_{cr} = D_{11}\pi^2/(4a^2)$.
- 4.6** Show that the characteristic equation governing the buckling of a clamped-hinged plate strip using the classical plate theory is given by

$$\sin \lambda a - \lambda a \cos \lambda a = 0$$

- 4.7** Show that the characteristic equation governing the natural vibration of a clamped-free plate strip using the classical plate theory is given by

$$\cos \lambda a \cosh \lambda a + 1 = 0$$

- 4.8** Show that the characteristic equation governing the natural vibration of a clamped-hinged plate strip using the classical plate theory when rotary inertia is neglected is given by

$$\sin \lambda a \cosh \lambda a - \cos \lambda a \sinh \lambda a = 0$$

- 4.9** Derive the characteristic equation governing the natural vibration of a clamped-hinged plate strip using the classical plate theory when rotary inertia is *not* neglected.

- 4.10** Use the total potential energy functional

$$\Pi(w_0) = \frac{1}{2} \int_0^a \left[D_{11} \left(\frac{d^2 w_0}{dx^2} \right)^2 - N_{xx}^0 \left(\frac{dw_0}{dx} \right)^2 - I_0 \omega^2 w_0^2 \right] dx$$

to construct a one-parameter Ritz solution to determine the natural frequency of vibration, ω , of a *simply supported* plate strip with compressive load N_{xx}^0 . Use algebraic polynomials for the approximate functions. (*Ans:* $\omega = (1/a)\sqrt{(10/I_0)[(12D_{11}/a^2) - N_{xx}^0]}$)

- 4.11** Repeat Problem 4.10 for fixed-free boundary conditions (fixed at $x = 0$ and free at $x = a$).

- 4.12** Use the total potential energy functional

$$\Pi(w_0) = \int_0^a \left[\frac{D_{11}}{2} \left(\frac{d^2 w_0}{dx^2} \right)^2 - q w_0 \right] dx$$

to construct a one-parameter Ritz solution of w_0 for a simply supported plate strip. Use algebraic polynomials for the approximate functions. (*Ans:* $c_1 = q_0 a^2 / 24 D_{11}$)

- 4.13** Repeat Problem 4.12 for a plate strip with clamped boundary conditions at $x = 0$ and free boundary conditions at $x = a$.

- 4.14** Use the total potential energy functional

$$\Pi(w) = \frac{1}{2} \int_0^a \left[D_{11} \left(\frac{d^2 w}{dx^2} \right)^2 - N_{xx}^0 \left(\frac{dw}{dx} \right)^2 \right] dx$$

to construct a one-parameter (for each variable) Ritz solution to determine the critical buckling load N_{cr} of a plate strip with clamped boundary conditions at $x = 0$ and free boundary conditions at $x = a$. Use algebraic polynomials for the approximate functions. (*Ans:* $N_{cr} = 3D_{11}/a^2$)

- 4.15** Use the total potential energy functional

$$\Pi(w_0) = \frac{1}{2} \int_0^a \left[D_{11} \left(\frac{d^2 w}{dx^2} \right)^2 - N_{xx}^0 \left(\frac{dw}{dx} \right)^2 - I_0 \omega^2 w^2 \right] dx$$

to construct a one-parameter (for each variable) Ritz solution to determine the natural frequency of vibration, ω , of a simply supported plate strip with edge compressive load N_{xx}^0 . Use algebraic polynomials for the approximate functions. (Ans: $\omega = (1/a)\sqrt{(10/I_0)[(12D_{11}/a^2) - N_{xx}^0]}$)

4.16 Repeat Problem 4.15 for a plate strip with clamped boundary condition at $x = 0$ and free at $x = a$.

4.17 The deflection, bending moment, and shear force of the first order plate theory for cylindrical bending can be expressed in terms of the corresponding quantities of the classical plate theory. In order to establish these relationships, we use the following equations of the two theories:

$$-D_{11} \frac{d^4 w_0^c}{dx^4} = -q(x), \quad D_{11} \frac{d^3 \phi^s}{dx^3} = -q(x), \quad GhK_s \left(\frac{d\phi^s}{dx} + \frac{d^2 w_0^s}{dx^2} \right) = -q(x)$$

where K_s is the shear correction coefficient, and superscripts c and s on variables refer to the classical and shear deformation plate theories, respectively. Show that ($\beta = D_{11}/GhK_s$)

$$D_{11}w_0^s(x) = D_{11}w_0^c(x) + \beta M_{xx}^c(x) + C_1 \left(\beta x - \frac{x^3}{6} \right) - C_2 \frac{x^2}{2} - C_3 x - C_4 \quad (1)$$

$$D_{11}\phi^s(x) = -D_{11} \frac{dw_0^c}{dx} + C_1 \frac{x^2}{2} + C_2 x + C_3 \quad (2)$$

$$M_{xx}^s(x) = M_{xx}^c(x) + C_1 x + C_2, \quad Q_x^s(x) = Q_x^c(x) + C_1 \quad (3, 4)$$

where h is the plate thickness and C_1, C_2, C_3 , and C_4 are constants of integration, which are to be determined using the boundary conditions of the particular beam.

4.18 Show that for simply supported beams all C_i of Problem 4.17 are zero.

4.19 Show that for cantilevered beams all C_i except C_4 of Problem 4.17 are zero.

4.20 Consider the bending of a plate strip of length a , clamped (or fixed) at the left end and simply supported at the right, that is subjected to a uniformly distributed transverse load q_0 . The boundary conditions of the classical (CPT) and shear deformation (SDT) theories for the problem are as follows:

$$\text{CPT : } w_0^c(0) = w_0^c(a) = \frac{dw_0^c}{dx}(0) = M_{xx}^c(a) = 0 \quad (1)$$

$$\text{SDT : } w_0^s(0) = w_0^s(a) = \phi^s(0) = M_{xx}^s(a) = 0 \quad (2)$$

Determine the constants of integration in Problem 4.17.

Analysis of Circular Plates

5.1 Introduction

Circular plates are found in end plates, manhole covers, closures of pressure vessels, pump diaphragms, clutches, and turbine disks, to name a few. Therefore, it is of interest to study stretching and bending of circular plates. The state of rotational symmetry (or axisymmetric with respect to the z -axis, which is taken normal to the plane of the plate with the origin at the center of the plate) exists and the deformation is independent of the angular coordinate only when the boundary conditions, material properties, and loading are also rotationally symmetric. Consequently, the problem is reduced to a one-dimensional one. Here we consider bending of circular plates under both axisymmetric and asymmetric transverse loads.

5.2 Governing Equations

5.2.1 Transformation of Equations from Rectangular Coordinates to Polar Coordinates

The equations governing circular plates may be obtained either (1) using transformation relations between the polar coordinates (r, θ) and the rectangular Cartesian coordinates (x, y) to express the governing equations from the rectangular Cartesian coordinates in polar coordinates, or (2) by direct derivation in the polar coordinates. The former is mathematical while the latter provides more physical insight. Also, the direct derivation can be carried out either by vector approach (see Problem 5.2) or energy approach (see Section 5.2.2). To illustrate the first (transformation) method, we consider the Poisson equation

$$\nabla^2 u = f \quad (5.2.1)$$

governing a function u in a two-dimensional domain with a source f . Eq. (5.2.1) is valid in any coordinate system, and we only have to define ∇^2 in that coordinate system. In the rectangular coordinates, we have [see Eq. (1.2.22)]

$$\nabla^2 = \nabla \cdot \nabla = \left(\hat{\mathbf{e}}_x \frac{\partial}{\partial x} + \hat{\mathbf{e}}_y \frac{\partial}{\partial y} \right) \cdot \left(\hat{\mathbf{e}}_x \frac{\partial}{\partial x} + \hat{\mathbf{e}}_y \frac{\partial}{\partial y} \right) = \frac{\partial^2}{\partial x^2} + \frac{\partial^2}{\partial y^2} \quad (5.2.2)$$

In the polar coordinates, we have [see Eqs. (1.2.30)–(1.2.31)]

$$\nabla^2 = \nabla \cdot \nabla = \left(\hat{\mathbf{e}}_r \frac{\partial}{\partial r} + \frac{\hat{\mathbf{e}}_\theta}{r} \frac{\partial}{\partial \theta} \right) \cdot \left(\hat{\mathbf{e}}_r \frac{\partial}{\partial r} + \frac{\hat{\mathbf{e}}_\theta}{r} \frac{\partial}{\partial \theta} \right) = \frac{1}{r} \frac{\partial}{\partial r} \left(r \frac{\partial}{\partial r} \right) + \frac{1}{r^2} \frac{\partial^2}{\partial \theta^2} \quad (5.2.3)$$

where derivatives of the base vectors with respect to θ [see Eq. (1.3.19)] are taken into account:

$$\frac{\partial \hat{\mathbf{e}}_r}{\partial \theta} = \hat{\mathbf{e}}_\theta, \quad \frac{\partial \hat{\mathbf{e}}_\theta}{\partial \theta} = -\hat{\mathbf{e}}_r \quad (5.2.4)$$

Therefore, the Poisson equation (5.2.1) has the form

$$\frac{\partial^2 u}{\partial x^2} + \frac{\partial^2 u}{\partial y^2} = f(x, y)$$

in the rectangular coordinate system, and

$$\frac{1}{r} \frac{\partial}{\partial r} \left(r \frac{\partial u}{\partial r} \right) + \frac{1}{r^2} \frac{\partial^2 u}{\partial \theta^2} = f(r, \theta)$$

in the polar coordinate system (Figure 5.2.1).

The result in Eq. (5.2.3) can also be obtained from Eq. (5.2.2) using the transformation relations [see Eq. (1.2.23) and Figure 5.2.1]

$$\begin{aligned} x &= r \cos \theta, \quad y = r \sin \theta \\ \frac{\partial}{\partial x} &= \frac{\partial r}{\partial x} \frac{\partial}{\partial r} + \frac{\partial \theta}{\partial x} \frac{\partial}{\partial \theta}, \quad \frac{\partial}{\partial y} = \frac{\partial r}{\partial y} \frac{\partial}{\partial r} + \frac{\partial \theta}{\partial y} \frac{\partial}{\partial \theta} \end{aligned} \quad (5.2.5)$$

where [from $r^2 = x^2 + y^2$ and Eq. (5.2.5)]

$$\frac{\partial r}{\partial x} = \frac{x}{r} = \cos \theta, \quad \frac{\partial r}{\partial y} = \frac{y}{r} = \sin \theta, \quad \frac{\partial \theta}{\partial x} = -\frac{\sin \theta}{r}, \quad \frac{\partial \theta}{\partial y} = \frac{\cos \theta}{r} \quad (5.2.6)$$

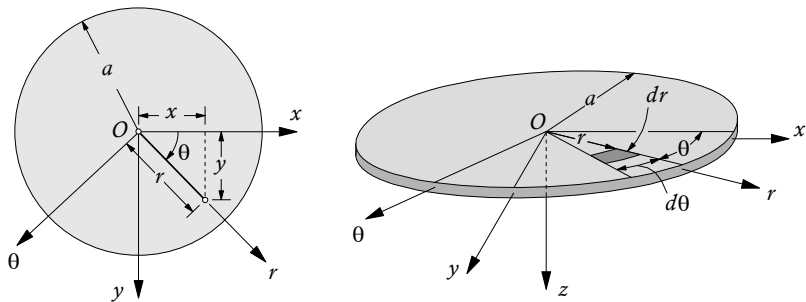


Figure 5.2.1. Transformation between rectangular and polar coordinate systems.

Hence,

$$\frac{\partial}{\partial x} = \cos \theta \frac{\partial}{\partial r} - \frac{\sin \theta}{r} \frac{\partial}{\partial \theta}, \quad \frac{\partial}{\partial y} = \sin \theta \frac{\partial}{\partial r} + \frac{\cos \theta}{r} \frac{\partial}{\partial \theta} \quad (5.2.7)$$

The second derivatives with respect to x and y can be computed using the above relations and chain rule of differentiation as follows:

$$\begin{aligned} \frac{\partial^2}{\partial x^2} &= \cos \theta \frac{\partial}{\partial r} \left(\frac{\partial}{\partial x} \right) - \frac{\sin \theta}{r} \frac{\partial}{\partial \theta} \left(\frac{\partial}{\partial x} \right) \\ &= \cos \theta \frac{\partial}{\partial r} \left(\cos \theta \frac{\partial}{\partial r} - \frac{\sin \theta}{r} \frac{\partial}{\partial \theta} \right) - \frac{\sin \theta}{r} \frac{\partial}{\partial \theta} \left(\cos \theta \frac{\partial}{\partial r} - \frac{\sin \theta}{r} \frac{\partial}{\partial \theta} \right) \\ &= \cos^2 \theta \frac{\partial^2}{\partial r^2} + \frac{\sin^2 \theta}{r} \frac{\partial}{\partial r} - \frac{\sin 2\theta}{r} \frac{\partial^2}{\partial r \partial \theta} + \frac{\sin 2\theta}{r^2} \frac{\partial}{\partial \theta} + \frac{\sin^2 \theta}{r^2} \frac{\partial^2}{\partial \theta^2} \end{aligned} \quad (5.2.8)$$

$$\frac{\partial^2}{\partial y^2} = \sin^2 \theta \frac{\partial^2}{\partial r^2} + \frac{\cos^2 \theta}{r} \frac{\partial}{\partial r} + \frac{\sin 2\theta}{r} \frac{\partial^2}{\partial r \partial \theta} - \frac{\sin 2\theta}{r^2} \frac{\partial}{\partial \theta} + \frac{\cos^2 \theta}{r^2} \frac{\partial^2}{\partial \theta^2} \quad (5.2.9)$$

$$\frac{\partial^2}{\partial x \partial y} = \frac{\sin 2\theta}{2} \frac{\partial^2}{\partial r^2} - \frac{\sin 2\theta}{2r} \frac{\partial}{\partial r} + \frac{\cos 2\theta}{r} \frac{\partial^2}{\partial r \partial \theta} - \frac{\cos 2\theta}{r^2} \frac{\partial}{\partial \theta} - \frac{\sin 2\theta}{2r^2} \frac{\partial^2}{\partial \theta^2} \quad (5.2.10)$$

Adding Eqs. (5.2.8) and (5.2.9), we arrive at the result in Eq. (5.2.3).

With the above relations in hand, one can write the equation of equilibrium governing the linear bending of an isotropic plate on elastic foundation of modulus k [see Eq. (3.8.14) with $M^T = 0$]

$$D \nabla^4 w_0 + kw_0 = q \quad (5.2.11)$$

where $w_0 = w_0(r, \theta)$ or $w_0 = w_0(x, y)$ is the transverse deflection, q the distributed transverse load, and D the flexural rigidity. Expressing the above equation in the rectangular Cartesian coordinates

$$D \left(\frac{\partial^4 w_0}{\partial x^4} + 2 \frac{\partial^4 w_0}{\partial x^2 \partial y^2} + \frac{\partial^4 w_0}{\partial y^4} \right) + kw_0 = q(x, y) \quad (5.2.12)$$

In the polar coordinates, the above equation becomes

$$D \left[\frac{1}{r} \frac{\partial}{\partial r} \left(r \frac{\partial}{\partial r} \right) + \frac{1}{r^2} \frac{\partial^2}{\partial \theta^2} \right] \left[\frac{1}{r} \frac{\partial}{\partial r} \left(r \frac{\partial w_0}{\partial r} \right) + \frac{1}{r^2} \frac{\partial^2 w_0}{\partial \theta^2} \right] + kw_0 = q(r, \theta) \quad (5.2.13)$$

Equation (5.2.12) is more suitable for the analysis of polygonal plates, while the latter equation is more suitable for circular plates.

For axisymmetric deformation, $w_0 = w_0(r)$ and Eq. (5.2.13) reduces to

$$D \left[\frac{1}{r} \frac{\partial}{\partial r} \left(r \frac{\partial}{\partial r} \right) \right] \left[\frac{1}{r} \frac{\partial}{\partial r} \left(r \frac{\partial w_0}{\partial r} \right) \right] + kw_0(r) = q(r), \quad b < r < a \quad (5.2.14)$$

where r is taken radially outward from the center of an annular circular plate with outer radius a and inner radius b . For solid circular plates, we set $b = 0$.

In order to derive the strain-displacement equations, equations of motion, and plate constitutive equations in polar coordinates from corresponding equations in the rectangular coordinates, one must first use the transformation relations between the strain components and stress components (hence, force and moment resultants) of the two coordinate systems. Then the transformation equations (5.2.7) through (5.2.10) may be used to replace the derivatives with respect to x and y in terms of the derivatives with respect to r and θ . Thus, the procedure involves quite a bit of mathematical manipulation. Alternatively, the same can be achieved by using the invariant forms of the equations and replacing the quantities and operators in terms of the polar coordinates.

For example, the moment-displacement and shear force-displacement relations [see Eq. (3.8.2)] for an isotropic homogeneous plate in the Cartesian rectangular coordinate system are given by

$$\begin{aligned} M_{xx} &= -D \left(\frac{\partial^2 w_0}{\partial x^2} + \nu \frac{\partial^2 w_0}{\partial y^2} \right) \\ M_{yy} &= -D \left(\nu \frac{\partial^2 w_0}{\partial x^2} + \frac{\partial^2 w_0}{\partial y^2} \right) \\ M_{xy} &= -2(1-\nu)D \frac{\partial^2 w_0}{\partial x \partial y} \\ Q_x &\equiv \frac{\partial M_{xx}}{\partial x} + \frac{\partial M_{xy}}{\partial y} = -D \left(\frac{\partial^3 w_0}{\partial x^3} + 2 \frac{\partial^3 w_0}{\partial x \partial y^2} \right) \\ Q_y &\equiv \frac{\partial M_{xy}}{\partial x} + \frac{\partial M_{yy}}{\partial y} = -D \left(\frac{\partial^3 w_0}{\partial y^3} + 2 \frac{\partial^3 w_0}{\partial x^2 \partial y} \right) \end{aligned} \quad (5.2.15)$$

Using the transformation relations, the above relations can be expressed in polar coordinates as (see Figure 5.2.2 for the meaning of the moments and shear forces in a cylindrical coordinate system)

$$\begin{aligned} M_{rr} &= -D \left[\frac{\partial^2 w_0}{\partial r^2} + \nu \left(\frac{1}{r} \frac{\partial w_0}{\partial r} + \frac{1}{r^2} \frac{\partial^2 w_0}{\partial \theta^2} \right) \right] \\ M_{\theta\theta} &= -D \left[\nu \frac{\partial^2 w_0}{\partial r^2} + \frac{1}{r} \frac{\partial w_0}{\partial r} + \frac{1}{r^2} \frac{\partial^2 w_0}{\partial \theta^2} \right] \\ M_{r\theta} &= -(1-\nu)D \left(\frac{1}{r} \frac{\partial^2 w_0}{\partial r \partial \theta} - \frac{1}{r^2} \frac{\partial w_0}{\partial \theta} \right) \\ Q_r &\equiv \frac{1}{r} \left[\frac{\partial}{\partial r} (r M_{rr}) + \frac{\partial M_{r\theta}}{\partial \theta} - M_{\theta\theta} \right] = -D \frac{\partial}{\partial r} \left[\frac{1}{r} \frac{\partial}{\partial r} \left(r \frac{\partial w_0}{\partial r} \right) + \frac{1}{r^2} \frac{\partial^2 w_0}{\partial \theta^2} \right] \\ Q_\theta &\equiv \frac{1}{r} \left[\frac{\partial}{\partial r} (r M_{r\theta}) + \frac{\partial M_{\theta\theta}}{\partial \theta} + M_{rr} \right] = -D \frac{1}{r} \frac{\partial}{\partial \theta} \left[\frac{1}{r} \frac{\partial}{\partial r} \left(r \frac{\partial w_0}{\partial r} \right) + \frac{1}{r^2} \frac{\partial^2 w_0}{\partial \theta^2} \right] \end{aligned} \quad (5.2.16)$$

The effective transverse shear forces V_r and V_θ are

$$V_r = Q_r + \frac{1}{r} \frac{\partial M_{r\theta}}{\partial \theta}, \quad V_\theta = Q_\theta + \frac{\partial M_{r\theta}}{\partial r} \quad (5.2.17)$$

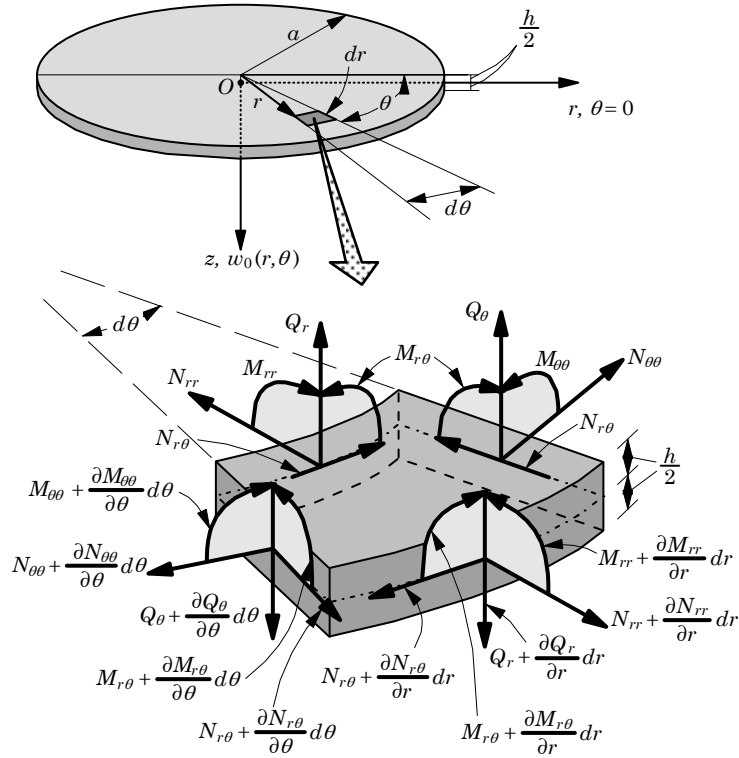


Figure 5.2.2. Moments and shear forces on an element in polar coordinates.

5.2.2 Derivation of Equations Using Hamilton's Principle

Let the r -coordinate be taken radially outward from the center of the plate, z -coordinate along the thickness (or height) of the plate, and the θ -coordinate be taken along a circumference of the plate, as shown in Figure 5.2.2. In a general case where applied loads and geometric boundary conditions are not axisymmetric, the displacements (u_r, u_θ, u_z) along the coordinates (r, θ, z) are functions of r, θ , and z coordinates.

We begin with the following displacement field for the classical plate theory (CPT):

$$\begin{aligned} u_r(r, \theta, z, t) &= u_0(r, \theta, t) - z \frac{\partial w_0}{\partial r} \\ u_\theta(r, \theta, z, t) &= v_0(r, \theta, t) - z \left(\frac{1}{r} \frac{\partial w_0}{\partial \theta} \right) \\ u_z(r, \theta, z, t) &= w_0(r, \theta, t) \end{aligned} \quad (5.2.18)$$

where (u_0, v_0, w_0) are the radial, angular, and transverse displacements, respectively, of a point on the midplane (i.e., $z = 0$) of the plate. The displacement field (5.2.18)

is based on the Kirchhoff hypothesis that straight lines normal to the middle plane before deformation remain (1) inextensible, (2) straight, and (3) normal to the middle surface after deformation.

The nonlinear strains are given by Eq. (1.3.6). Accounting only for the von Kármán nonlinearity (i.e., neglecting all nonlinear terms except for those involving only u_z), we obtain

$$\begin{aligned}\varepsilon_{rr} &= \frac{\partial u_r}{\partial r} + \frac{1}{2} \left(\frac{\partial u_z}{\partial r} \right)^2 \\ \varepsilon_{\theta\theta} &= \frac{u_r}{r} + \frac{1}{r} \frac{\partial u_\theta}{\partial \theta} + \frac{1}{2} \left(\frac{1}{r} \frac{\partial u_z}{\partial \theta} \right)^2 \\ \varepsilon_{zz} &= \frac{\partial u_z}{\partial z} + \frac{1}{2} \left(\frac{\partial u_z}{\partial z} \right)^2 \\ \varepsilon_{r\theta} &= \frac{1}{2} \left(\frac{1}{r} \frac{\partial u_r}{\partial \theta} + \frac{\partial u_\theta}{\partial r} - \frac{u_\theta}{r} + \frac{1}{r} \frac{\partial u_z}{\partial r} \frac{\partial u_z}{\partial \theta} \right) \\ \varepsilon_{z\theta} &= \frac{1}{2} \left(\frac{\partial u_\theta}{\partial z} + \frac{1}{r} \frac{\partial u_z}{\partial \theta} + \frac{1}{r} \frac{\partial u_z}{\partial \theta} \frac{\partial u_z}{\partial z} \right) \\ \varepsilon_{rz} &= \frac{1}{2} \left(\frac{\partial u_r}{\partial z} + \frac{\partial u_z}{\partial r} + \frac{\partial u_z}{\partial r} \frac{\partial u_z}{\partial z} \right)\end{aligned}\tag{5.2.19}$$

For the choice of the displacement field in Eq. (5.2.18), the only nonzero strains are

$$\varepsilon_{rr} = \varepsilon_{rr}^{(0)} + z\varepsilon_{rr}^{(1)}, \quad \varepsilon_{\theta\theta} = \varepsilon_{\theta\theta}^{(0)} + z\varepsilon_{\theta\theta}^{(1)}, \quad 2\varepsilon_{r\theta} = \gamma_{r\theta}^{(0)} + z\gamma_{r\theta}^{(1)}\tag{5.2.20}$$

where

$$\begin{aligned}\varepsilon_{rr}^{(0)} &= \frac{\partial u_0}{\partial r} + \frac{1}{2} \left(\frac{\partial w_0}{\partial r} \right)^2, & \varepsilon_{rr}^{(1)} &= -\frac{\partial^2 w_0}{\partial r^2} \\ \varepsilon_{\theta\theta}^{(0)} &= \frac{u_0}{r} + \frac{1}{r} \frac{\partial v_0}{\partial \theta} + \frac{1}{2r^2} \left(\frac{\partial w_0}{\partial \theta} \right)^2, & \varepsilon_{\theta\theta}^{(1)} &= -\frac{1}{r} \left(\frac{\partial w_0}{\partial r} + \frac{1}{r} \frac{\partial^2 w_0}{\partial \theta^2} \right) \\ \gamma_{r\theta}^{(0)} &= \frac{1}{r} \frac{\partial u_0}{\partial \theta} + \frac{\partial v_0}{\partial r} - \frac{v_0}{r} + \frac{1}{r} \frac{\partial w_0}{\partial r} \frac{\partial w_0}{\partial \theta}, & \gamma_{r\theta}^{(1)} &= -\frac{2}{r} \left(\frac{\partial^2 w_0}{\partial r \partial \theta} - \frac{1}{r} \frac{\partial w_0}{\partial \theta} \right)\end{aligned}\tag{5.2.21}$$

The dynamic version of the principle of virtual displacements or Hamilton's principle can be written as

$$\begin{aligned}0 &= \int_0^T \int_{\Omega} \int_{-\frac{h}{2}}^{\frac{h}{2}} (\sigma_{rr} \delta \varepsilon_{rr} + \sigma_{\theta\theta} \delta \varepsilon_{\theta\theta} + \sigma_{r\theta} \delta \gamma_{r\theta}) dz dr d\theta dt \\ &\quad - \int_0^T \int_{\Omega} \int_{-\frac{h}{2}}^{\frac{h}{2}} \rho (\dot{u}_r \delta \dot{u}_r + \dot{u}_\theta \delta \dot{u}_\theta + \dot{u}_z \delta \dot{u}_z) dz dr d\theta dt \\ &\quad - \int_0^T \int_{\Omega} (q + F_s) \delta w_0 dr d\theta dt\end{aligned}\tag{5.2.22}$$

where h is the plate thickness, $q = q(r, \theta, t)$ is the distributed transverse load, F_s is the reaction force of an elastic foundation, Ω denotes the mid-plane of the plate,

and the superposed dot indicates the time derivative. The virtual work done by any applied nonzero edge loads and moments should be added to the expression in Eq. (5.2.22).

Substituting for the virtual strains $\delta\varepsilon_{rr}$ and $\delta\varepsilon_{\theta\theta}$ from Eq. (5.2.21) into Eq. (5.2.22) and integrating over the plate thickness, we obtain

$$\begin{aligned} 0 = \int_0^T \int_{\Omega} & \left[N_{rr} \left(\frac{\partial \delta u_0}{\partial r} + \frac{\partial w_0}{\partial r} \frac{\partial \delta w_0}{\partial r} \right) + N_{\theta\theta} \left(\frac{\delta u_0}{r} + \frac{1}{r} \frac{\partial \delta v_0}{\partial \theta} + \frac{1}{r^2} \frac{\partial w_0}{\partial \theta} \frac{\partial \delta w_0}{\partial \theta} \right) \right. \\ & + N_{r\theta} \left(\frac{1}{r} \frac{\partial \delta u_0}{\partial \theta} + \frac{\partial \delta v_0}{\partial r} - \frac{\delta v_0}{r} + \frac{1}{r} \frac{\partial \delta w_0}{\partial r} \frac{\partial w_0}{\partial \theta} + \frac{1}{r} \frac{\partial w_0}{\partial r} \frac{\partial \delta w_0}{\partial \theta} \right) \\ & - M_{rr} \frac{\partial^2 \delta w_0}{\partial r^2} - \frac{1}{r} M_{\theta\theta} \left(\frac{\partial \delta w_0}{\partial r} + \frac{1}{r} \frac{\partial^2 \delta w_0}{\partial \theta^2} \right) - \frac{2}{r} M_{r\theta} \left(\frac{\partial^2 \delta w_0}{\partial r \partial \theta} - \frac{1}{r} \frac{\partial \delta w_0}{\partial \theta} \right) \\ & - I_0 (\dot{u}_0 \delta \dot{u}_0 + \dot{v}_0 \delta \dot{v}_0 + \dot{w}_0 \delta \dot{w}_0) - I_2 \left(\frac{\partial \dot{w}_0}{\partial r} \frac{\partial \delta \dot{w}_0}{\partial r} + \frac{1}{r^2} \frac{\partial \dot{w}_0}{\partial \theta} \frac{\partial \delta \dot{w}_0}{\partial \theta} \right) \\ & \left. - q \delta w_0 + k w_0 \delta w_0 \right] r \, dr \, d\theta \, dt \end{aligned} \quad (5.2.23)$$

where the elastic foundation reaction force is replaced with $F_s = -k w_0$, and the forces ($N_{rr}, N_{\theta\theta}, N_{r\theta}$) and moments ($M_{rr}, M_{\theta\theta}, M_{r\theta}$) are defined by

$$N_{rr} = \int_{-\frac{h}{2}}^{\frac{h}{2}} \sigma_{rr} \, dz, \quad N_{\theta\theta} = \int_{-\frac{h}{2}}^{\frac{h}{2}} \sigma_{\theta\theta} \, dz, \quad N_{r\theta} = \int_{-\frac{h}{2}}^{\frac{h}{2}} \sigma_{r\theta} \, dz \quad (5.2.24)$$

$$M_{rr} = \int_{-\frac{h}{2}}^{\frac{h}{2}} \sigma_{rr} z \, dz, \quad M_{\theta\theta} = \int_{-\frac{h}{2}}^{\frac{h}{2}} \sigma_{\theta\theta} z \, dz, \quad M_{r\theta} = \int_{-\frac{h}{2}}^{\frac{h}{2}} \sigma_{r\theta} z \, dz \quad (5.2.25)$$

The Euler–Lagrange equations can be obtained from Eq. (5.2.23) by relieving $(\delta u_0, \delta v_0, \delta w_0)$ of all differentiations using integration-by-parts and setting the coefficients of $(\delta u_0, \delta v_0, \delta w_0)$ to zero separately (i.e., using the fundamental lemma of calculus of variations). One must make note of the presence of r in the integrand when integration-by-parts is used. We obtain

$$\delta u_0 : \quad -\frac{1}{r} \left[\frac{\partial}{\partial r} (r N_{rr}) + \frac{\partial N_{r\theta}}{\partial \theta} - N_{\theta\theta} \right] + I_0 \frac{\partial^2 u_0}{\partial t^2} = 0 \quad (5.2.26)$$

$$\delta v_0 : \quad -\frac{1}{r} \left[\frac{\partial}{\partial r} (r N_{r\theta}) + \frac{\partial N_{\theta\theta}}{\partial \theta} + N_{r\theta} \right] + I_0 \frac{\partial^2 v_0}{\partial t^2} = 0 \quad (5.2.27)$$

$$\begin{aligned} \delta w_0 : \quad & -\frac{1}{r} \left[\frac{\partial^2}{\partial r^2} (r M_{rr}) - \frac{\partial M_{\theta\theta}}{\partial r} + \frac{1}{r} \frac{\partial^2 M_{\theta\theta}}{\partial \theta^2} + \frac{2}{r} \frac{\partial}{\partial r} \left(r \frac{\partial M_{r\theta}}{\partial \theta} \right) \right. \\ & + \frac{\partial}{\partial r} \left(r N_{rr} \frac{\partial w_0}{\partial r} + N_{r\theta} \frac{\partial w_0}{\partial \theta} \right) + \frac{1}{r} \frac{\partial}{\partial \theta} \left(N_{\theta\theta} \frac{\partial w_0}{\partial \theta} + r N_{r\theta} \frac{\partial w_0}{\partial r} \right) \left. \right] \\ & - q + k w_0 + I_0 \frac{\partial^2 w_0}{\partial t^2} - I_2 \frac{\partial^2}{\partial t^2} \left[\frac{1}{r} \frac{\partial}{\partial r} \left(r \frac{\partial w_0}{\partial r} \right) + \frac{1}{r^2} \frac{\partial^2 w_0}{\partial \theta^2} \right] = 0 \quad (5.2.28) \end{aligned}$$

Introducing the transverse shear forces acting on the rz -plane and θz -plane as

$$Q_r = \frac{1}{r} \left[\frac{\partial}{\partial r} (r M_{rr}) + \frac{\partial M_{r\theta}}{\partial \theta} - M_{\theta\theta} \right], \quad Q_\theta = \frac{1}{r} \left[\frac{\partial}{\partial r} (r M_{r\theta}) + \frac{\partial M_{\theta\theta}}{\partial \theta} + M_{r\theta} \right] \quad (5.2.29)$$

the third equation of motion, Eq. (5.2.28), can be expressed as

$$\begin{aligned} & -\frac{1}{r} \left[\frac{\partial}{\partial r} (r Q_r) + \frac{\partial Q_\theta}{\partial \theta} + \frac{\partial}{\partial r} \left(r N_{rr} \frac{\partial w_0}{\partial r} + N_{r\theta} \frac{\partial w_0}{\partial \theta} \right) + \frac{1}{r} \frac{\partial}{\partial \theta} \left(N_{\theta\theta} \frac{\partial w_0}{\partial \theta} + r N_{r\theta} \frac{\partial w_0}{\partial r} \right) \right] \\ & - q + k w_0 + I_0 \frac{\partial^2 w_0}{\partial t^2} - I_2 \frac{\partial^2}{\partial t^2} \left[\frac{1}{r} \frac{\partial}{\partial r} \left(r \frac{\partial w_0}{\partial r} \right) + \frac{1}{r^2} \frac{\partial^2 w_0}{\partial \theta^2} \right] = 0 \end{aligned} \quad (5.2.30)$$

The natural boundary conditions involve specifying the following expressions on an edge with unit normal $\hat{\mathbf{n}} = n_r \hat{\mathbf{e}}_r + n_\theta \hat{\mathbf{e}}_\theta$, where (n_r, n_θ) are such that $n_r = 1$ when $n_\theta = 0$ and vice versa (i.e., $\hat{\mathbf{n}} = \hat{\mathbf{e}}_r$ on a surface with fixed r and $\hat{\mathbf{n}} = \hat{\mathbf{e}}_\theta$ on a surface with fixed θ)

$$\begin{aligned} \delta u_0 : & \quad r N_{rr} n_r + N_{r\theta} n_\theta \\ \delta v_0 : & \quad r N_{r\theta} n_r + N_{\theta\theta} n_\theta \\ \delta w_0 : & \quad Q_n + \frac{\partial M_{ns}}{\partial s} + r I_2 \frac{\partial \ddot{w}_0}{\partial n} + \mathcal{P}(u_0, v_0, w_0) \\ \frac{\partial \delta w_0}{\partial n} : & \quad M_{nn} \end{aligned} \quad (5.2.31)$$

where n and s take the values of r and θ depending on the edge of the plate. For example, at a fixed r , $n = r$ and $s = \theta$; on the other hand, on a boundary with fixed θ , we have $n = \theta$ and $s = r$. The quantities introduced in Eq. (5.2.31) have the following definitions:

$$Q_n = r Q_r n_r + Q_\theta n_\theta \quad (5.2.32)$$

$$\mathcal{P} = \left(r N_{rr} \frac{\partial w_0}{\partial r} + N_{r\theta} \frac{\partial w_0}{\partial \theta} \right) n_r + \frac{1}{r} \left(N_{\theta\theta} \frac{\partial w_0}{\partial \theta} + r N_{r\theta} \frac{\partial w_0}{\partial r} \right) n_\theta \quad (5.2.33)$$

$$M_{ns} = M_{r\theta} (r n_r^2 - n_\theta^2), \quad M_{nn} = r M_{rr} n_r^2 + M_{\theta\theta} n_\theta^2 \quad (5.2.34)$$

$$\frac{\partial}{\partial n} = n_r \frac{\partial}{\partial r} + n_\theta \frac{1}{r} \frac{\partial}{\partial \theta}, \quad \frac{\partial}{\partial s} = -n_\theta \frac{\partial}{\partial r} + n_r \frac{1}{r} \frac{\partial}{\partial \theta} \quad (5.2.35)$$

and the Kirchhoff free edge condition is incorporated in Eq. (5.2.31). The boundary condition on shear force in Eq. (5.2.31) can be expressed in terms of the equivalent shear force V_n as

$$\bar{V}_n \equiv V_n + r I_2 \frac{\partial \ddot{w}_0}{\partial n} + \mathcal{P}(u_0, v_0, w_0) \quad (5.2.36)$$

$$V_n = r V_r n_r + V_\theta n_\theta, \quad V_r = Q_r + \frac{1}{r} \frac{\partial M_{r\theta}}{\partial \theta}, \quad V_\theta = Q_\theta + \frac{\partial M_{r\theta}}{\partial r} \quad (5.2.37)$$

The boundary conditions for *circular plates* involve specifying one quantity in each of the following pairs on positive r - and θ -planes:

At $r = \hat{r}$, constant:

$$\begin{aligned} u_0 &= \hat{u}_0 & \text{or} & \quad \hat{r}N_{rr} = \hat{r}\hat{N}_{rr} \\ v_0 &= \hat{v}_0 & \text{or} & \quad \hat{r}N_{r\theta} = \hat{r}\hat{N}_{r\theta} \\ w_0 &= \hat{w}_0 & \text{or} & \quad \hat{r}\bar{V}_r = \hat{r}\hat{\bar{V}}_r \\ \frac{\partial w_0}{\partial r} &= \frac{\partial \hat{w}_0}{\partial r} & \text{or} & \quad \hat{r}M_{rr} = \hat{r}\hat{M}_{rr} \end{aligned} \quad (5.2.38)$$

At $\theta = \hat{\theta}$, constant:

$$\begin{aligned} u_0 &= \hat{u}_0 & \text{or} & \quad N_{r\theta} = \hat{N}_{r\theta} \\ v_0 &= \hat{v}_0 & \text{or} & \quad N_{\theta\theta} = \hat{N}_{\theta\theta} \\ w_0 &= \hat{w}_0 & \text{or} & \quad \bar{V}_\theta = \hat{\bar{V}}_\theta \\ \frac{1}{r} \frac{\partial w_0}{\partial \theta} &= \frac{1}{r} \frac{\partial \hat{w}_0}{\partial \theta} & \text{or} & \quad M_{\theta\theta} = \hat{M}_{\theta\theta} \end{aligned} \quad (5.2.39)$$

where

$$\begin{aligned} \bar{V}_r &= Q_r + \frac{1}{r} \frac{\partial M_{r\theta}}{\partial \theta} + I_2 \frac{\partial \ddot{w}_0}{\partial r} + N_{rr} \frac{\partial w_0}{\partial r} + \frac{1}{r} N_{r\theta} \frac{\partial w_0}{\partial \theta} \\ \bar{V}_\theta &= Q_\theta + \frac{\partial M_{r\theta}}{\partial r} + I_2 \frac{\partial \ddot{w}_0}{\partial \theta} + \frac{1}{r^2} N_{\theta\theta} \frac{\partial w_0}{\partial \theta} + \frac{1}{r} N_{r\theta} \frac{\partial w_0}{\partial r} \end{aligned} \quad (5.2.40)$$

For the linear case, i.e., for the infinitesimal strains, Eq. (5.2.28) is uncoupled from Eqs. (5.2.26) and (5.2.27). For this case, Eq. (5.2.28) takes the form

$$\begin{aligned} -\frac{1}{r} \left[\frac{\partial^2}{\partial r^2} (rM_{rr}) - \frac{\partial M_{\theta\theta}}{\partial r} + \frac{1}{r} \frac{\partial^2 M_{\theta\theta}}{\partial \theta^2} + 2 \frac{\partial^2 M_{r\theta}}{\partial r \partial \theta} + \frac{2}{r} \frac{\partial M_{r\theta}}{\partial \theta} \right] + kw_0 \\ = q - I_0 \frac{\partial^2 w_0}{\partial t^2} + I_2 \frac{\partial^2}{\partial t^2} \left[\frac{1}{r} \frac{\partial}{\partial r} \left(r \frac{\partial w_0}{\partial r} \right) + \frac{1}{r^2} \frac{\partial^2 w_0}{\partial \theta^2} \right] \end{aligned} \quad (5.2.41)$$

and for the static case it reduces to

$$-\frac{1}{r} \left[\frac{\partial^2}{\partial r^2} (rM_{rr}) - \frac{\partial M_{\theta\theta}}{\partial r} + \frac{1}{r} \frac{\partial^2 M_{\theta\theta}}{\partial \theta^2} + 2 \frac{\partial^2 M_{r\theta}}{\partial r \partial \theta} + \frac{2}{r} \frac{\partial M_{r\theta}}{\partial \theta} \right] + kw_0 = q_0 \quad (5.2.42)$$

Equations (5.2.41) and (5.2.42) can be expressed in terms of the transverse displacement w_0 with the help of the moment-deflection relations (5.2.16), which are revisited next.

5.2.3 Plate Constitutive Equations

The force and moment resultants can be expressed in terms of the strains of Eq. (5.2.20) once the constitutive relations are assumed. For a *polar orthotropic* material with material axes coinciding with r and θ (e.g., a fiber-reinforced material plate with radial and circumferential fibers) and assuming that the elastic stiffnesses are independent of the temperature, we have [see Eq. (3.6.1)]

$$\begin{Bmatrix} \sigma_{rr} \\ \sigma_{\theta\theta} \\ \sigma_{r\theta} \end{Bmatrix} = \begin{bmatrix} Q_{11} & Q_{12} & 0 \\ Q_{12} & Q_{22} & 0 \\ 0 & 0 & Q_{66} \end{bmatrix} \begin{Bmatrix} \varepsilon_{rr} - \alpha_1 \Delta T \\ \varepsilon_{\theta\theta} - \alpha_2 \Delta T \\ 2\varepsilon_{r\theta} \end{Bmatrix} \quad (5.2.43)$$

where $\Delta T(r, \theta, z)$ is the temperature increment, α_1 and α_2 are the coefficients of thermal expansion, and Q_{ij} are the elastic stiffness coefficients

$$Q_{11} = \frac{E_1}{1 - \nu_{12}\nu_{21}}, \quad Q_{22} = \frac{E_2}{E_1}Q_{11}, \quad Q_{66} = G_{23} \quad (5.2.44)$$

The plate constitutive relations are those that relate the stress resultants to the membrane strains $\{\varepsilon^{(0)}\}$ and flexural strains $\{\varepsilon^{(1)}\}$ and they are given by [see Eqs. (5.2.21), (5.2.24), and (5.2.25)]

$$\begin{aligned} N_{rr} &= \int_{-\frac{h}{2}}^{\frac{h}{2}} \sigma_{rr} dz = A_{11}\varepsilon_{rr}^{(0)} + A_{12}\varepsilon_{\theta\theta}^{(0)} - N_{rr}^T \\ N_{\theta\theta} &= \int_{-\frac{h}{2}}^{\frac{h}{2}} \sigma_{\theta\theta} dz = A_{12}\varepsilon_{rr}^{(0)} + A_{22}\varepsilon_{\theta\theta}^{(0)} - N_{\theta\theta}^T \\ N_{r\theta} &= \int_{-\frac{h}{2}}^{\frac{h}{2}} \sigma_{r\theta} dz = A_{66}\gamma_{r\theta}^{(0)} \end{aligned} \quad (5.2.45a)$$

$$\begin{aligned} M_{rr} &= \int_{-\frac{h}{2}}^{\frac{h}{2}} \sigma_{rr}z dz = D_{11}\varepsilon_{rr}^{(1)} + D_{12}\varepsilon_{\theta\theta}^{(1)} - M_{rr}^T \\ M_{\theta\theta} &= \int_{-\frac{h}{2}}^{\frac{h}{2}} \sigma_{\theta\theta}z dz = D_{12}\varepsilon_{rr}^{(1)} + D_{22}\varepsilon_{\theta\theta}^{(1)} - M_{\theta\theta}^T \\ M_{r\theta} &= \int_{-\frac{h}{2}}^{\frac{h}{2}} \sigma_{r\theta}z dz = D_{66}\gamma_{r\theta}^{(1)} \end{aligned} \quad (5.2.45b)$$

where A_{ij} and D_{ij} denote the extensional and bending stiffnesses of polar orthotropic plates

$$A_{ij} = hQ_{ij}, \quad D_{ij} = \frac{h^3}{12}Q_{ij} \quad (5.2.45c)$$

and N_{rr}^T , $N_{\theta\theta}^T$, M_{rr}^T , and $M_{\theta\theta}^T$ are the thermal forces and moments

$$\begin{aligned} N_{rr}^T &= \int_{-\frac{h}{2}}^{\frac{h}{2}} (Q_{11}\alpha_1 + Q_{12}\alpha_2) \Delta T \, dz \\ N_{\theta\theta}^T &= \int_{-\frac{h}{2}}^{\frac{h}{2}} (Q_{12}\alpha_1 + Q_{22}\alpha_2) \Delta T \, dz \\ M_{rr}^T &= \int_{-\frac{h}{2}}^{\frac{h}{2}} (Q_{11}\alpha_1 + Q_{12}\alpha_2) \Delta T z \, dz \\ M_{\theta\theta}^T &= \int_{-\frac{h}{2}}^{\frac{h}{2}} (Q_{12}\alpha_1 + Q_{22}\alpha_2) \Delta T z \, dz \end{aligned} \quad (5.2.46)$$

The moments can be expressed in terms of the deflection w_0 using the strain-displacement relations. For a geometrically linear case, we have

$$\begin{aligned} M_{rr} &= - \left[D_{11} \frac{\partial^2 w_0}{\partial r^2} + D_{12} \frac{1}{r} \left(\frac{\partial w_0}{\partial r} + \frac{1}{r} \frac{\partial^2 w_0}{\partial \theta^2} \right) \right] - M_{rr}^T \\ M_{\theta\theta} &= - \left[D_{12} \frac{\partial^2 w_0}{\partial r^2} + D_{22} \frac{1}{r} \left(\frac{\partial w_0}{\partial r} + \frac{1}{r} \frac{\partial^2 w_0}{\partial \theta^2} \right) \right] - M_{\theta\theta}^T \\ M_{r\theta} &= -2D_{66} \frac{1}{r} \left(\frac{\partial^2 w_0}{\partial r \partial \theta} - \frac{1}{r} \frac{\partial w_0}{\partial \theta} \right) \end{aligned} \quad (5.2.47)$$

For isotropic plates, we set $D_{11} = D_{22} = D$, $D_{12} = \nu D$ and $2D_{66} = (1 - \nu)D$, and the bending moment-deflection relationships in Eq. (5.2.47) reduce to [cf., Eq. (5.2.16)]

$$\begin{aligned} M_{rr} &= -D \left[\frac{\partial^2 w_0}{\partial r^2} + \frac{\nu}{r} \left(\frac{\partial w_0}{\partial r} + \frac{1}{r} \frac{\partial^2 w_0}{\partial \theta^2} \right) \right] - \frac{M_T}{1 - \nu} \\ M_{\theta\theta} &= -D \left[\nu \frac{\partial^2 w_0}{\partial r^2} + \frac{1}{r} \left(\frac{\partial w_0}{\partial r} + \frac{1}{r} \frac{\partial^2 w_0}{\partial \theta^2} \right) \right] - \frac{M_T}{1 - \nu} \\ M_{r\theta} &= -(1 - \nu)D \frac{1}{r} \left(\frac{\partial^2 w_0}{\partial r \partial \theta} - \frac{1}{r} \frac{\partial w_0}{\partial \theta} \right) \end{aligned} \quad (5.2.48)$$

where

$$M_T = E\alpha \int_{-\frac{h}{2}}^{\frac{h}{2}} \Delta T(x, z) z \, dz \quad (5.2.49)$$

The equation of motion (5.2.41) or equation of equilibrium (5.2.42) can be expressed in terms of the deflection w_0 with the aid of Eq. (5.2.47) or Eq. (5.2.48). To this end, let us introduce the moment sum, called the *Marcus moment*, which is defined by

$$\mathcal{M} \equiv \frac{M_{rr} + M_{\theta\theta}}{1 + \nu} = -D \left[\frac{1}{r} \frac{\partial}{\partial r} \left(r \frac{\partial w_0}{\partial r} \right) + \frac{1}{r^2} \frac{\partial^2 w_0}{\partial \theta^2} \right] = -D\nabla^2 w_0 \quad (5.2.50)$$

Then we have

$$\begin{aligned} & \left[\frac{1}{r} \frac{\partial}{\partial r} \left(r \frac{\partial \mathcal{M}}{\partial r} \right) + \frac{1}{r^2} \frac{\partial^2 \mathcal{M}}{\partial \theta^2} \right] - \frac{1}{1-\nu} \left[\frac{1}{r} \frac{\partial}{\partial r} \left(r \frac{\partial M_T}{\partial r} \right) + \frac{1}{r^2} \frac{\partial^2 M_T}{\partial \theta^2} \right] \\ & + q - kw_0 = I_0 \frac{\partial^2 w_0}{\partial t^2} - I_2 \frac{\partial^2}{\partial t^2} \left[\frac{1}{r} \frac{\partial}{\partial r} \left(r \frac{\partial w_0}{\partial r} \right) + \frac{1}{r^2} \frac{\partial^2 w_0}{\partial \theta^2} \right] \end{aligned} \quad (5.2.51)$$

and, in terms of the deflection, we have

$$\begin{aligned} & D \left[\frac{1}{r} \frac{\partial}{\partial r} \left(r \frac{\partial}{\partial r} \right) + \frac{1}{r^2} \frac{\partial^2}{\partial \theta^2} \right] \left[\frac{1}{r} \frac{\partial}{\partial r} \left(r \frac{\partial w_0}{\partial r} \right) + \frac{1}{r^2} \frac{\partial^2 w_0}{\partial \theta^2} \right] + kw_0 - q \\ & + \frac{1}{1-\nu} \left[\frac{1}{r} \frac{\partial}{\partial r} \left(r \frac{\partial M_T}{\partial r} \right) + \frac{1}{r^2} \frac{\partial^2 M_T}{\partial \theta^2} \right] \\ & = -I_0 \frac{\partial^2 w_0}{\partial t^2} + I_2 \frac{\partial^2}{\partial t^2} \left[\frac{1}{r} \frac{\partial}{\partial r} \left(r \frac{\partial w_0}{\partial r} \right) + \frac{1}{r^2} \frac{\partial^2 w_0}{\partial \theta^2} \right] \end{aligned} \quad (5.2.52)$$

Using the Laplace operator of Eq. (5.2.3), Eq. (5.2.52) can be written simply as

$$D\nabla^2 \nabla^2 w_0 + kw_0 = q - \frac{1}{1-\nu} \nabla^2 M_T - I_0 \frac{\partial^2 w_0}{\partial t^2} + I_2 \frac{\partial^2}{\partial t^2} (\nabla^2 w_0) \quad (5.2.53)$$

For the static case, we have [cf., Eqs. (5.2.11) and (5.2.13)]

$$D\nabla^2 \nabla^2 w_0 + kw_0 = q - \frac{1}{1-\nu} \nabla^2 M_T \quad (5.2.54)$$

5.3 Axisymmetric Bending

5.3.1 Governing Equations

When isotropic or polar orthotropic circular (solid or annular) plates are subjected to rotationally symmetric (or axisymmetric) loads and the edge conditions are also axisymmetric, then all variables are only functions of the radial coordinate r (and possibly time t) and u_θ is identically zero. In this section, we consider linear, static bending of circular plates with axisymmetric loads and edge conditions. Since u_0 is uncoupled from w_0 for the linear case, we focus only on pure bending deformation and determine w_0 and bending stresses.

The nonzero linear strains, stresses, bending moments, and shear force for the axisymmetric bending are given by

$$\varepsilon_{rr} = -z \frac{d^2 w_0}{dr^2} - \alpha_1 \Delta T, \quad \varepsilon_{\theta\theta} = -z \frac{1}{r} \frac{dw_0}{dr} - \alpha_2 \Delta T \quad (5.3.1)$$

$$\sigma_{rr} = -z \left(Q_{11} \frac{d^2 w_0}{dr^2} + Q_{12} \frac{1}{r} \frac{dw_0}{dr} \right) - (Q_{11}\alpha_1 + Q_{12}\alpha_2) \Delta T \quad (5.3.2a)$$

$$\sigma_{\theta\theta} = -z \left(Q_{12} \frac{d^2 w_0}{dr^2} + Q_{22} \frac{1}{r} \frac{dw_0}{dr} \right) - (Q_{12}\alpha_1 + Q_{22}\alpha_2) \Delta T \quad (5.3.2b)$$

$$M_{rr} = - \left(D_{11} \frac{d^2 w_0}{dr^2} + D_{12} \frac{1}{r} \frac{dw_0}{dr} \right) - M_{rr}^T \quad (5.3.3a)$$

$$M_{\theta\theta} = - \left(D_{12} \frac{d^2 w_0}{dr^2} + D_{22} \frac{1}{r} \frac{dw_0}{dr} \right) - M_{\theta\theta}^T \quad (5.3.3b)$$

$$\begin{aligned} Q_r &\equiv \frac{1}{r} \left[\frac{d}{dr} (r M_{rr}) - M_{\theta\theta} \right] \\ &= -D_{11} \frac{1}{r} \frac{d}{dr} \left(r \frac{d^2 w_0}{dr^2} \right) + D_{22} \frac{1}{r^2} \frac{dw_0}{dr} - \frac{1}{r} \left[\frac{d}{dr} (r M_{rr}^T) - M_{\theta\theta}^T \right] \end{aligned} \quad (5.3.4)$$

The equation of equilibrium for the axisymmetric case can be deduced from Eq. (5.2.30) by setting the nonlinear and time-derivative terms and terms involving differentiation with respect to θ to zero, i.e.,

$$-\frac{1}{r} \frac{d}{dr} (r Q_r) + k w_0 = q \quad (5.3.5)$$

Using Eq. (5.3.4) for $r Q_r$ in Eq. (5.3.5), we find that

$$\frac{1}{r} \frac{d}{dr} \left[D_{11} \frac{d}{dr} \left(r \frac{d^2 w_0}{dr^2} \right) - D_{22} \frac{1}{r} \frac{dw_0}{dr} \right] + k w_0 = q - \frac{1}{r} \frac{d}{dr} \left[\frac{d}{dr} (r M_{rr}^T) - M_{\theta\theta}^T \right] \quad (5.3.6)$$

In view of the identity

$$\frac{d}{dr} \left(r \frac{d^2 w_0}{dr^2} \right) = r \frac{d}{dr} \left[\frac{1}{r} \frac{d}{dr} \left(r \frac{dw_0}{dr} \right) \right] + \frac{1}{r} \frac{dw_0}{dr} \quad (5.3.7)$$

we can rewrite Eq. (5.3.6) as

$$\begin{aligned} D_{11} \frac{1}{r} \frac{d}{dr} \left\{ r \frac{d}{dr} \left[\frac{1}{r} \frac{d}{dr} \left(r \frac{dw_0}{dr} \right) \right] + \left(\frac{D_{11} - D_{22}}{D_{11}} \right) \frac{1}{r} \frac{dw_0}{dr} \right\} + k w_0 \\ = q - \frac{1}{r} \frac{d}{dr} \left[\frac{d}{dr} (r M_{rr}^T) - M_{\theta\theta}^T \right] \end{aligned} \quad (5.3.8)$$

Equation (5.3.8) must be solved with appropriate boundary conditions [see Eq. (5.2.38)] on w_0 or Q_r and $\frac{dw_0}{dr}$ or M_{rr} .

For isotropic plates [$D_{11} = D_{22} = D$; $M_{rr}^T = M_{\theta\theta}^T = M_T/(1 - \nu)$], Eqs. (5.3.2)–(5.3.4) simplify to

$$\begin{aligned} \sigma_{rr} &= -\frac{Ez}{(1 - \nu^2)} \left(\frac{d^2 w_0}{dr^2} + \frac{\nu}{r} \frac{dw_0}{dr} \right) - \frac{E\alpha}{1 - \nu} \Delta T \\ \sigma_{\theta\theta} &= -\frac{Ez}{(1 - \nu^2)} \left(\nu \frac{d^2 w_0}{dr^2} + \frac{1}{r} \frac{dw_0}{dr} \right) - \frac{E\alpha}{1 - \nu} \Delta T \end{aligned} \quad (5.3.9)$$

$$\begin{aligned} M_{rr} &= -D \left(\frac{d^2 w_0}{dr^2} + \frac{\nu}{r} \frac{dw_0}{dr} \right) - \frac{M_T}{1-\nu} \\ M_{\theta\theta} &= -D \left(\nu \frac{d^2 w_0}{dr^2} + \frac{1}{r} \frac{dw_0}{dr} \right) - \frac{M_T}{1-\nu} \end{aligned} \quad (5.3.10)$$

$$\begin{aligned} Q_r &= -D \frac{d}{dr} \left[\frac{1}{r} \frac{d}{dr} \left(r \frac{dw_0}{dr} \right) \right] - \frac{1}{1-\nu} \frac{dM_T}{dr} \\ M_T &= E\alpha \int_{-\frac{h}{2}}^{\frac{h}{2}} \Delta T(r, z) z \, dz \end{aligned} \quad (5.3.11)$$

The governing equation (5.3.8) becomes

$$\frac{D}{r} \frac{d}{dr} \left\{ r \frac{d}{dr} \left[\frac{1}{r} \frac{d}{dr} \left(r \frac{dw_0}{dr} \right) \right] \right\} + kw_0 = q - \frac{1}{1-\nu} \frac{1}{r} \frac{d}{dr} \left(r \frac{dM_T}{dr} \right) \quad (5.3.12)$$

5.3.2 Analytical Solutions

In this section we develop the general analytical solution of isotropic plates and the Ritz formulation for polar orthotropic plates, i.e., for plates whose principal material coordinates (x_1, x_2) coincide with the polar coordinates (r, θ) . In the subsequent sections, these general solutions are specialized to plates with various specific boundary conditions and loads. We assume that the plate is isotropic and *not* resting on an elastic foundation (i.e., $k = 0$). Circular plates on elastic foundation and polar orthotropic plates will be considered toward the end of the chapter.

Multiplying Eq. (5.3.5) throughout with r and integrating with respect to r , we obtain

$$-rQ(r) = \int rq(r)dr + c_1 \quad (5.3.13)$$

The constant of integration c_1 can be determined using a boundary condition on shear force Q . In view of Eq. (5.3.11), Eq. (5.3.13) can be expressed in terms of w_0

$$Dr \frac{d}{dr} \left[\frac{1}{r} \frac{d}{dr} \left(r \frac{dw_0}{dr} \right) \right] + \frac{r}{1-\nu} \frac{dM_T}{dr} = \int rq(r)dr + c_1 \quad (5.3.14)$$

Successive integrations of the above equation (divide or multiply throughout by r as required) lead to the relations

$$D \frac{d}{dr} \left(r \frac{dw_0}{dr} \right) = r \int \frac{1}{r} \left(\int rq(r)dr \right) dr - \frac{rM_T}{1-\nu} + c_1 r \log r + c_2 r \quad (5.3.15)$$

$$D \frac{dw_0}{dr} = F'(r) - G'(r) + \frac{r}{4} (2 \log r - 1) c_1 + \frac{r}{2} c_2 + \frac{1}{r} c_3 \quad (5.3.16)$$

$$Dw_0(r) = F(r) - G(r) + \frac{r^2}{4} (\log r - 1) c_1 + \frac{r^2}{4} c_2 + c_3 \log r + c_4 \quad (5.3.17)$$

where

$$\begin{aligned} F(r) &= \int \frac{1}{r} \left\{ \int r \left[\int \frac{1}{r} \left(\int rq(r) dr \right) dr \right] dr \right\} dr \\ G(r) &= \frac{1}{(1-\nu)} \int \frac{1}{r} \left(\int r M_T dr \right) dr \end{aligned} \quad (5.3.18)$$

and c_i ($i = 1, 2, 3, 4$) are constants of integration that will be evaluated using boundary conditions. Typical boundary conditions for solid circular plates and annular plates are listed in Table 5.3.1 (Figure 5.3.1). Since the second derivative of w_0 is required in the moment boundary condition [see Eq. (5.3.3a)], it can be obtained by differentiating Eq. (5.3.16) with respect to r

$$D \frac{d^2 w_0}{dr^2} = F'' - G'' + \frac{1}{4}(2 \log r - 1)c_1 + \frac{1}{2}c_2 - \frac{1}{r^2}c_3 \quad (5.3.19)$$

Equations (5.3.13), (5.3.16), and (5.3.19) are useful in the determination of the constants of integration.

Once the deflection $w_0(r)$ is known, the stresses and bending moments in the plate can be determined using the following expressions [Eqs. (5.3.16) and (5.3.19) are used in Eqs. (5.3.9) and (5.3.10)]:

$$\begin{aligned} \sigma_{rr}(r, z) &= -\frac{Ez}{1-\nu^2} \left(\frac{d^2 w_0}{dr^2} + \nu \frac{1}{r} \frac{dw_0}{dr} \right) \\ &= -\frac{12z}{h^3} \left\{ \left(H'' + \frac{\nu}{r} H' \right) + \left[\frac{1+\nu}{2} \log r + \frac{1}{4}(1-\nu) \right] c_1 \right. \\ &\quad \left. + \frac{1+\nu}{2} c_2 - \frac{1-\nu}{r^2} c_3 \right\} \end{aligned} \quad (5.3.20)$$

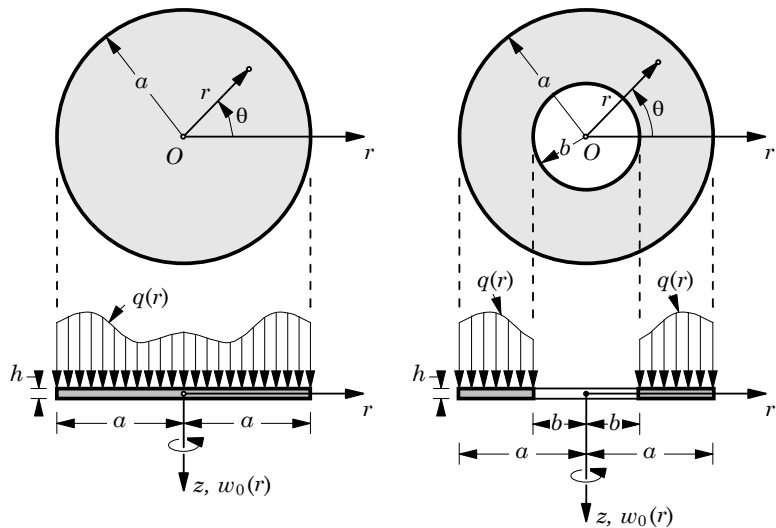


Figure 5.3.1. Axisymmetric circular and annular plates.

Table 5.3.1. Typical boundary conditions for solid circular and annular plates.[†]

Plate Type/Edge	Free	Hinged	Clamped
Solid Circular Plate			
$r = 0$ (for all cases)	$\frac{dw_0}{dr} = 0$ and $2\pi r Q_r = -Q_0$ for all cases		
$r = a$	$Q_r = Q_a$ $M_{rr} = M_a$	$w_0 = 0$ $M_{rr} = M_a$	$w_0 = 0$ $\frac{dw_0}{dr} = 0$
Annular Plate			
$r = b$	$Q_r = Q_b$ $M_{rr} = M_b$	$w_0 = 0$ $M_{rr} = M_b$	$w_0 = 0$ $\frac{dw_0}{dr} = 0$
$r = a$	$Q_r = Q_a$ $M_{rr} = M_a$	$w_0 = 0$ $M_{rr} = M_a$	$w_0 = 0$ $\frac{dw_0}{dr} = 0$

[†] Q_a, Q_b, M_a , and M_b are distributed edge forces and moments and Q_0 is a concentrated force.

$$\begin{aligned}\sigma_{\theta\theta}(r, z) &= -\frac{Ez}{1-\nu^2} \left(\nu \frac{d^2 w_0}{dr^2} + \frac{1}{r} \frac{dw_0}{dr} \right) \\ &= -\frac{12z}{h^3} \left\{ \left(\nu H'' + \frac{1}{r} H' \right) + \left[\frac{1+\nu}{2} \log r - \frac{1}{4}(1-\nu) \right] c_1 \right. \\ &\quad \left. + \frac{1+\nu}{2} c_2 + \frac{1-\nu}{r^2} c_3 \right\} \end{aligned}\quad (5.3.21)$$

$$\begin{aligned}M_{rr}(r) &= -D \left(\frac{d^2 w_0}{dr^2} + \frac{\nu}{r} \frac{dw_0}{dr} \right) \\ &= - \left(H'' + \frac{\nu}{r} H' \right) - \left[\frac{1+\nu}{2} \log r + \frac{1}{4}(1-\nu) \right] c_1 \\ &\quad - \frac{1+\nu}{2} c_2 + \frac{1-\nu}{r^2} c_3 \end{aligned}\quad (5.3.22)$$

$$\begin{aligned}M_{\theta\theta}(r) &= -D \left(\nu \frac{d^2 w_0}{dr^2} + \frac{1}{r} \frac{dw_0}{dr} \right) \\ &= - \left(\nu H'' + \frac{1}{r} H' \right) - \left[\frac{1+\nu}{2} \log r - \frac{1}{4}(1-\nu) \right] c_1 - \frac{1+\nu}{2} c_2 - \frac{1-\nu}{r^2} c_3 \end{aligned}\quad (5.3.23)$$

where $H = F - G$ and primes on F , G , and H denote derivatives with respect to r .

In general, for a solid circular plate, the boundary condition (due to the symmetry)

$$\frac{dw_0}{dr} = 0 \quad \text{at} \quad r = 0 \quad (5.3.24)$$

requires that c_3 be zero (because $r \log r = 0$ as $r \rightarrow 0$) so that the slope is finite. In addition, the shear force at $r = 0$ should equal the externally applied force Q_0

$$2\pi(rQ_r) = -Q_0 \quad \text{at} \quad r = 0 \quad (5.3.25)$$

which gives, in view of Eq. (5.3.13), the result

$$c_1 = Q_0/(2\pi) \quad (5.3.26)$$

In the absence of a point load at the center (i.e., $Q_0 = 0$), we have the condition

$$c_1 = 0 \quad (5.3.27)$$

The fact that c_1 is not equal to zero in the case of a nonzero central point load presents a problem because of the presence of the logarithmic term in the solution. In particular, the deflection, bending moments, and stresses at $r = 0$ are unbounded. This is due to the fact that in the classical theory of plates we have assumed that the transverse shear strain is zero, an assumption that does not hold in the vicinity of a point load. To alleviate the problem, the deflection, bending moments, and stresses at the center of a circular plate loaded at the center are computed by omitting the logarithmic term.

For the case of a circular plate with zero point load at the center, but under arbitrarily distributed transverse load $q(r)$ and temperature distribution $\Delta T(r, z)$, we have $c_1 = c_3 = 0$. The remaining two constants c_2 and c_4 are determined by the boundary conditions at the outer edge of the plate. The deflection, bending moments, and stresses become

$$Dw_0(r) = H(r) + c_2 \frac{r^2}{4} + c_4 \quad (5.3.28)$$

$$D \frac{dw_0}{dr} = H' + c_2 \frac{r}{2} \quad (5.3.29)$$

$$M_{rr} = -\left(H'' + \frac{\nu}{r}H'\right) - \frac{1+\nu}{2}c_2 \quad (5.3.30)$$

$$M_{\theta\theta} = -\left(\nu H'' + \frac{1}{r}H'\right) - \frac{1+\nu}{2}c_2 \quad (5.3.31)$$

$$\sigma_{rr} = -\frac{12z}{h^3} \left[\left(H'' + \frac{\nu}{r}H'\right) + \frac{1+\nu}{2}c_2 \right] \quad (5.3.32)$$

$$\sigma_{\theta\theta} = -\frac{12z}{h^3} \left[\left(\nu H'' + \frac{1}{r}H'\right) + \frac{1+\nu}{2}c_2 \right] \quad (5.3.33)$$

The maximum values of these quantities occur at $r = 0$ and are given by

$$w_{max} = w_0(0) = \frac{c_4}{D} \quad (5.3.34)$$

$$M_{max} = M_{rr}(0) = M_{\theta\theta} = -\frac{1+\nu}{2}c_2 \quad (5.3.35)$$

$$\sigma_{max} = \sigma_{rr}(0, \frac{h}{2}) = \sigma_{\theta\theta}(0, \frac{h}{2}) = -\frac{3(1+\nu)}{h^2}c_2 \quad (5.3.36)$$

In the case of annular plates, constants c_1 through c_4 are determined using the boundary conditions at the inner and outer edges of the plate. Complete analytical solutions for various boundary conditions will be presented in the subsequent sections. The Ritz formulation presented next is valid for orthotropic plates and hence to isotropic plates as a special case.

5.3.3 The Ritz Formulation

Here we consider Ritz solutions of polar orthotropic annular plates, possibly on elastic foundation. Towards this end, we first write the virtual work statement of the problem for the general case; the results can be specialized to solid circular plates by setting the inner radius to zero, $b = 0$. Specializing the virtual work statement in (5.2.23) to the static, axisymmetric and pure bending case, and adding terms due to the virtual work done by applied loads, we obtain

$$\begin{aligned} 0 &= -2\pi \int_b^a \left(M_{rr} \frac{d^2 \delta w_0}{dr^2} + M_{\theta\theta} \frac{1}{r} \frac{d\delta w_0}{dr} - kw_0 \delta w_0 + q\delta w_0 \right) r dr \\ &\quad + 2\pi \left[aQ_a \delta w_0(a) - bQ_b \delta w_0(b) - aM_a \left(\frac{d\delta w_0}{dr} \right)_a + bM_b \left(\frac{d\delta w_0}{dr} \right)_b \right] \\ &= 2\pi \int_b^a \left[\left(D_{11} \frac{d^2 w_0}{dr^2} + D_{12} \frac{1}{r} \frac{dw_0}{dr} \right) \frac{d^2 \delta w_0}{dr^2} \right. \\ &\quad \left. + \left(D_{12} \frac{d^2 w_0}{dr^2} + D_{22} \frac{1}{r} \frac{dw_0}{dr} \right) \frac{1}{r} \frac{d\delta w_0}{dr} + kw_0 \delta w_0 - q\delta w_0 \right. \\ &\quad \left. + M_{rr}^T \frac{d^2 \delta w_0}{dr^2} + M_{\theta\theta}^T \frac{1}{r} \frac{d\delta w_0}{dr} \right] r dr + 2\pi \left[aQ_a \delta w_0(a) - bQ_b \delta w_0(b) \right] \\ &\quad + 2\pi \left[-aM_a \left(\frac{d\delta w_0}{dr} \right)_a + bM_b \left(\frac{d\delta w_0}{dr} \right)_b \right] \end{aligned} \quad (5.3.37)$$

where a and b denote the outer and inner radii of the plate, respectively, k is the spring constant of the linear elastic foundation, q the distributed load, Q_a and Q_b the intensities of line loads at the outer and inner edges, respectively, and M_a and M_b the distributed edge moments at the outer and inner edges, respectively. When $b = 0$ (for solid circular plate), we have $M_b = 0$ and $2\pi b Q_b = Q_0$, Q_0 being the point load at the center of the plate.

Assume a solution of the form (assuming that all specified geometric boundary conditions are homogeneous so that we can take $\varphi_0(r) = 0$)

$$w_0(r) \approx W_N(r) = \sum_{j=1}^N c_j \varphi_j(r) \quad (5.3.38)$$

Substituting Eq. (5.3.38) into Eq. (5.3.37), we obtain

$$\begin{aligned} 0 &= 2\pi \sum_{j=1}^N c_j \int_b^a \left[\left(D_{11} \frac{d^2 \varphi_j}{dr^2} + D_{12} \frac{1}{r} \frac{d\varphi_j}{dr} \right) \frac{d^2 \phi_i}{dr^2} \right. \\ &\quad \left. + \left(D_{12} \frac{d^2 \varphi_j}{dr^2} + D_{22} \frac{1}{r} \frac{d\varphi_j}{dr} \right) \frac{1}{r} \frac{d\phi_i}{dr} + k\varphi_i \varphi_j \right] r dr \end{aligned}$$

$$\begin{aligned}
& -2\pi \int_b^a \left(q - M_{rr}^T \frac{d^2\varphi_i}{dr^2} - M_{\theta\theta}^T \frac{1}{r} \frac{d\varphi_i}{dr} \right) r dr \\
& + 2\pi \left[aQ_a \varphi_i(a) - bQ_b \varphi_i(b) - aM_a \left(\frac{d\varphi_i}{dr} \right)_a + bM_b \left(\frac{d\varphi_i}{dr} \right)_b \right]
\end{aligned}$$

or, in matrix form, we have

$$[R]\{c\} = \{F\} \quad (5.3.39)$$

where

$$\begin{aligned}
R_{ij} = & 2\pi \int_b^a \left[D_{11} \frac{d^2\varphi_i}{dr^2} \frac{d^2\varphi_j}{dr^2} + D_{12} \frac{1}{r} \left(\frac{d\varphi_i}{dr} \frac{d^2\varphi_j}{dr^2} + \frac{d^2\varphi_j}{dr^2} \frac{d\varphi_i}{dr} \right) \right. \\
& \left. + D_{22} \frac{1}{r^2} \frac{d\varphi_i}{dr} \frac{d\varphi_j}{dr} + k\varphi_i \varphi_j \right] r dr
\end{aligned} \quad (5.3.40a)$$

$$\begin{aligned}
F_i = & 2\pi \int_b^a \left[q\varphi_i - \left(M_{rr}^T \frac{d^2\varphi_i}{dr^2} + M_{\theta\theta}^T \frac{1}{r} \frac{d\varphi_i}{dr} \right) \right] r dr \\
& - 2\pi \left[aQ_a \varphi_i(a) - bQ_b \varphi_i(b) - aM_a \left(\frac{d\varphi_i}{dr} \right)_a + bM_b \left(\frac{d\varphi_i}{dr} \right)_b \right]
\end{aligned} \quad (5.3.40b)$$

The approximation functions φ_i are selected using the homogeneous form of the geometric boundary conditions of the problem. Once φ_i are known, one can compute R_{ij} and F_i , and Eq. (5.3.40) can be solved for c_i ($i = 1, 2, \dots, N$). The Ritz solution is then given by Eq. (5.3.38). In the sequel, we illustrate the selection of approximation functions and computation of the Ritz solutions of circular plates with specific boundary conditions.

5.3.4 Simply Supported Circular Plate under Distributed Load

Analytical solution

Consider a simply supported circular plate under distributed load (Figure 5.3.2). The boundary conditions associated with the simply supported outer edge are $w_0 = 0$ and $M_{rr} = 0$ at $r = a$. Using these conditions in Eqs. (5.3.28) and (5.3.30), we obtain

$$c_2 = -\frac{2}{(1+\nu)} \left(F_0'' + \frac{\nu}{a} F_0' \right), \quad c_4 = -\left(F_0 + \frac{a^2}{4} c_2 \right) \quad (5.3.41)$$

where $F_0 = F(0)$, $F_0' = F'(a)$, and $F_0'' = F''(0)$.

Uniform load. For uniformly distributed load of intensity q_0 , we have

$$F(r) = \frac{q_0 r^4}{64}, \quad F'(r) = \frac{q_0 r^3}{16}, \quad F''(r) = \frac{3q_0 r^2}{16} \quad (5.3.42a)$$

$$c_2 = -\frac{(3+\nu)}{8(1+\nu)} q_0 a^2, \quad c_4 = \frac{(5+\nu)}{64(1+\nu)} q_0 a^4 \quad (5.3.42b)$$

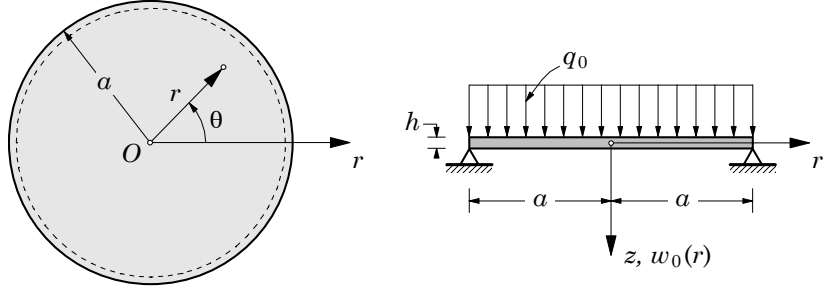


Figure 5.3.2. A simply supported circular plate under uniformly distributed load.

The deflection, bending moment, and stresses in a simply supported circular plate under uniformly distributed load are

$$w_0(r) = \frac{q_0 a^4}{64D} \left[\frac{5+\nu}{1+\nu} - 2 \left(\frac{3+\nu}{1+\nu} \right) \left(\frac{r}{a} \right)^2 + \left(\frac{r}{a} \right)^4 \right] \quad (5.3.43)$$

$$M_{rr}(r) = (3+\nu) \frac{q_0 a^2}{16} \left[1 - \left(\frac{r}{a} \right)^2 \right] \quad (5.3.44a)$$

$$M_{\theta\theta}(r) = \frac{q_0 a^2}{16} \left[(3+\nu) - (1+3\nu) \left(\frac{r}{a} \right)^2 \right] \quad (5.3.44b)$$

$$\sigma_{rr}(r, z) = 3(3+\nu) \frac{q_0 a^2}{4h^2} \frac{z}{h} \left[1 - \left(\frac{r}{a} \right)^2 \right] \quad (5.3.45a)$$

$$\sigma_{\theta\theta}(r, z) = 3 \frac{q_0 a^2}{4h^2} \frac{z}{h} \left[(3+\nu) - (1+3\nu) \left(\frac{r}{a} \right)^2 \right] \quad (5.3.45b)$$

The maximum deflection, bending moments, and stresses occur at $r = 0$:

$$w_{max} = \left(\frac{5+\nu}{1+\nu} \right) \frac{q_0 a^4}{64D}, \quad M_{max} = (3+\nu) \frac{q_0 a^2}{16}, \quad \sigma_{max} = 3(3+\nu) \frac{q_0 a^2}{8h^2} \quad (5.3.46)$$

Linearly varying load. For a linearly distributed load of the type (Figure 5.3.3)

$$q(r) = q_0 + \frac{q_1 - q_0}{a} r \quad (5.3.47)$$

we obtain

$$\begin{aligned} F(r) &= \frac{q_0 r^4}{64} + \left(\frac{q_1 - q_0}{a} \right) \frac{r^5}{225} \\ F'(r) &= \frac{q_0 r^3}{16} + \left(\frac{q_1 - q_0}{a} \right) \frac{r^4}{45} \\ F''(r) &= \frac{3q_0 r^2}{16} + \left(\frac{q_1 - q_0}{a} \right) \frac{4r^3}{45} \end{aligned} \quad (5.3.48)$$

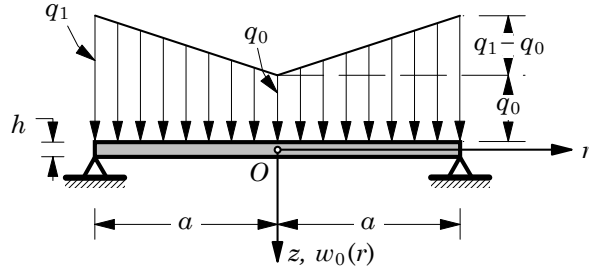


Figure 5.3.3. A simply supported circular plate under linearly varying distributed load.

$$\begin{aligned} c_2 &= -\frac{2a^2}{(1+\nu)} \left[\frac{3+\nu}{16}q_0 + \frac{4+\nu}{45}(q_1 - q_0) \right] \\ c_4 &= \frac{a^4}{(1+\nu)} \left[\frac{5+\nu}{64}q_0 + \frac{6+\nu}{150}(q_1 - q_0) \right] \end{aligned} \quad (5.3.49)$$

The deflection, bending moments, and stresses are given by Eqs. (5.3.28)–(5.3.33), and their maximum values are given by Eqs. (5.3.34)–(5.3.36).

Ritz solutions

The Ritz solution of a simply supported polar orthotropic circular plate under uniformly distributed load can be obtained using the formulation of Section 5.3.3. The primary task is to select admissible approximation functions $\varphi_i(r)$. Recall that for this problem the geometric (or essential) boundary conditions are

$$\frac{dw_0}{dr}(0) = 0, \quad w_0(a) = 0$$

and the force (or natural) boundary conditions are given by

$$M_{rr} = 0 \text{ at } r = a, \quad Q_r = \frac{1}{r} \left[\frac{d}{dr}(rM_{rr}) - M_{\theta\theta} \right] = 0 \text{ at } r = 0$$

The natural boundary conditions will have no bearing on the selection of φ_i in the Ritz method. Each φ_i must satisfy the conditions

$$\frac{d\varphi_i}{dr}(0) = 0, \quad \varphi_i(a) = 0$$

For the choice of algebraic polynomials, we assume

$$\varphi_1(r) = \alpha_1 + \alpha_2r + \alpha_3r^2$$

and determine, using the above conditions, that $\alpha_2 = 0$ and $\alpha_1 + \alpha_3a^2 = 0$. Thus, we have (for the choice of $\alpha_1 = 1$)

$$\varphi_1 = 1 - \frac{r^2}{a^2}$$

The procedure can be used to obtain a linearly independent and complete set of functions

$$\varphi_1 = 1 - \frac{r^2}{a^2}, \quad \varphi_2 = 1 - \frac{r^3}{a^3}, \quad \dots, \quad \varphi_j = 1 - \left(\frac{r}{a}\right)^{j+1} \quad (5.3.50)$$

Substituting for φ_j from the above approximation into Eqs. (5.3.40a) and (5.3.40b), and noting that $k = 0$, we obtain

$$\begin{aligned} R_{ij} &= \frac{2\pi}{a^2} [ijD_{11} + D_{12}(i+j) + D_{22}] \frac{(i+1)(j+1)}{(i+j)} (1 - \beta^{i+j}) \\ F_i &= 2\pi \left\{ q_0 a^2 \left[(i+1) - (i+3)\beta^2 + 2\beta^{i+3} \right] \frac{1}{2(i+3)} + bQ_b (1 - \beta^{i+1}) \right. \\ &\quad \left. + (1 - \beta^{i+1}) (iM_{rr}^T + M_{\theta\theta}^T) - (i+1)M_a + (i+1)\beta^{i+1}M_b \right\} \end{aligned} \quad (5.3.51)$$

where $\beta = b/a$.

Orthotropic plate. Consider the case of a circular plate ($b = 0$ or $\beta = 0$) made of a material for which we have $D_{11}/D_{22} = 10$ and $D_{12}/D_{22} = 1/3$, and subjected to only uniformly distributed load of intensity q_0 . Then

$$R_{ij} = \frac{2\pi D_{22}}{3a^2} (30ij + i + j + 3) \frac{(i+1)(j+1)}{(i+j)}, \quad F_i = 2\pi q_0 a^2 \frac{(i+1)}{2(i+2)}$$

For $N = 1$, we have

$$R_{11} = \frac{140D_{22}\pi}{3a^2}, \quad F_1 = \frac{2\pi q_0 a^2}{4}, \quad c_1 = \frac{3q_0 a^4}{280D_{22}}$$

and the one-parameter Ritz solution becomes

$$W_1(r) = \frac{3q_0 a^4}{280D_{22}} \left(1 - \frac{r^2}{a^2} \right)$$

For $N = 2$, we have

$$\frac{D_{22}}{a^2} \begin{bmatrix} \frac{70}{3} & 44 \\ 44 & \frac{381}{4} \end{bmatrix} \begin{Bmatrix} c_1 \\ c_2 \end{Bmatrix} = \frac{q_0 a^2}{20} \begin{Bmatrix} 5 \\ 6 \end{Bmatrix}$$

and the solution is given by

$$W_2(r) = \frac{q_0 a^4}{D_{22}} \left[0.03704 \left(1 - \frac{r^2}{a^2} \right) - 0.01396 \left(1 - \frac{r^3}{a^3} \right) \right]$$

For $N = 3$, we have

$$\frac{D_{22}}{a^2} \begin{bmatrix} \frac{70}{3} & 44 & \frac{194}{5} \\ 44 & \frac{381}{4} & \frac{752}{248} \\ \frac{194}{3} & \frac{752}{5} & 248 \end{bmatrix} \begin{Bmatrix} c_1 \\ c_2 \\ c_3 \end{Bmatrix} = q_0 a^2 \begin{Bmatrix} \frac{1}{4} \\ \frac{3}{10} \\ \frac{1}{3} \end{Bmatrix} \quad (5.3.52)$$

and the solution is given by

$$W_3(r) = \frac{q_0 a^4}{D_{22}} \left[0.05841 \left(1 - \frac{r^2}{a^2} \right) - 0.04493 \left(1 - \frac{r^3}{a^3} \right) + 0.01336 \left(1 - \frac{r^4}{a^4} \right) \right]$$

Isotropic plate. For an isotropic circular plate, the coefficients R_{ij} are

$$R_{ij} = \frac{2\pi D}{a^2} \left(\frac{ij+1}{i+j} + \nu \right) (i+1)(j+1)$$

For $N = 3$, we have the algebraic equations

$$\frac{D}{a^2} \begin{bmatrix} 4(1+\nu) & 6(1+\nu) & 8(1+\nu) \\ 6(1+\nu) & 9(1.25+\nu) & 12(1.4+\nu) \\ 8(1+\nu) & 12(1.4+\nu) & 16(\frac{5}{3}+\nu) \end{bmatrix} \begin{Bmatrix} c_1 \\ c_2 \\ c_3 \end{Bmatrix} = \frac{q_0 a^2}{60} \begin{Bmatrix} 15 \\ 18 \\ 20 \end{Bmatrix} \quad (5.3.53)$$

The one-, two- and three-parameter Ritz solutions are

$$\begin{aligned} W_1(r) &= \frac{q_0 a^4}{16D(1+\nu)} \left(1 - \frac{r^2}{a^2} \right) \\ W_2(r) &= \frac{q_0 a^4}{80D} \left(\frac{9+4\nu}{1+\nu} \right) \left(1 - \frac{r^2}{a^2} \right) - \frac{q_0 a^4}{30D} \left(1 - \frac{r^3}{R_0^3} \right) \\ W_3(r) &= \frac{q_0 a^4}{64D} \left(\frac{6+2\nu}{1+\nu} \right) \left(1 - \frac{r^2}{a^2} \right) - \frac{q_0 a^4}{64D} \left(1 - \frac{r^4}{a^4} \right) \\ &= \frac{q_0 a^4}{64D} \left[\frac{5+\nu}{1+\nu} - 2 \left(\frac{3+\nu}{1+\nu} \right) \left(\frac{r}{a} \right)^2 + \left(\frac{r}{a} \right)^4 \right] \end{aligned}$$

The three-parameter solution coincides with the exact solution (5.3.43).

5.3.5 Simply Supported Circular Plate under Central Point Load

Analytical solution

For this case, we have $c_1 = Q_0/2\pi$ and $c_3 = 0$ (Figure 5.3.4). Using the boundary condition $w_0(a) = 0$, we obtain from Eq. (5.3.17) the result ($F = G = 0$)

$$\frac{Q_0 a^2}{8\pi} (\log a - 1) + \frac{a^2}{4} c_2 + c_4 = 0 \quad (a)$$

If there is no applied bending moment at $r = a$, Eq. (5.3.22) yields the result

$$-\frac{Q_0}{2\pi} \left[\frac{1+\nu}{2} \log a + \frac{1-\nu}{4} \right] - \frac{1+\nu}{2} c_2 = 0 \quad (b)$$

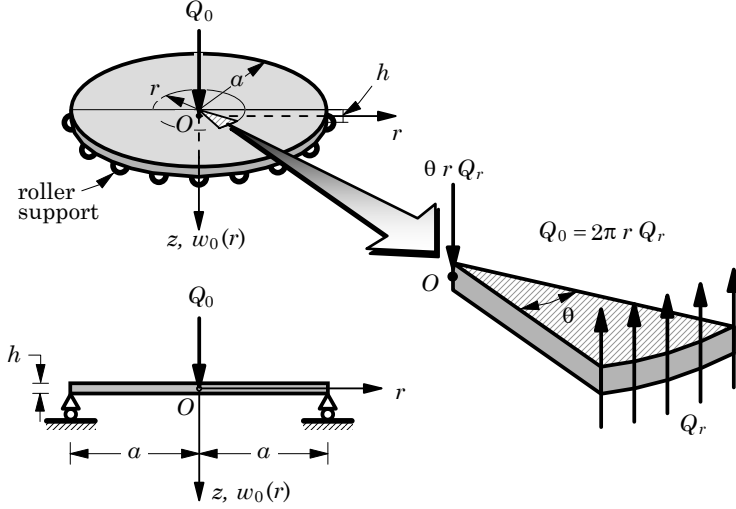


Figure 5.3.4. A simply supported circular plate under central point load.

Solving Eqs. (a) and (b) for the constants c_2 and c_4 , we obtain

$$c_2 = -\frac{Q_0}{2\pi} \left[\log a + \frac{1}{2} \left(\frac{1-\nu}{1+\nu} \right) \right], \quad c_4 = \left(\frac{3+\nu}{1+\nu} \right) \frac{Q_0 a^2}{16\pi} \quad (5.3.54)$$

The deflection for any $r \neq 0$ is given by

$$w_0(r) = \frac{Q_0 a^2}{16\pi D} \left[\left(\frac{3+\nu}{1+\nu} \right) \left(1 - \frac{r^2}{a^2} \right) + 2 \left(\frac{r}{a} \right)^2 \log \left(\frac{r}{a} \right) \right] \quad (5.3.55)$$

The stresses and bending moments are given by

$$\sigma_{rr}(r) = -\frac{3zQ_0(1+\nu)}{h^3\pi} \log \left(\frac{r}{a} \right) \quad (5.3.56a)$$

$$\sigma_{\theta\theta}(r) = -\frac{3zQ_0}{h^3\pi} \left[(1+\nu) \log \left(\frac{r}{a} \right) - (1-\nu) \right] \quad (5.3.56b)$$

$$M_{rr}(r) = -\frac{Q_0(1+\nu)}{4\pi} \log \left(\frac{r}{a} \right) \quad (5.3.57a)$$

$$M_{\theta\theta}(r) = -\frac{Q_0}{4\pi} \left[(1+\nu) \log \left(\frac{r}{a} \right) - (1-\nu) \right] \quad (5.3.57b)$$

The maximum deflection is computed at $r = 0$ by omitting the logarithmic term in Eq. (5.3.55)

$$w_{max} = w_0(0) = \frac{Q_0 a^2}{16\pi D} \left(\frac{3+\nu}{1+\nu} \right) \quad (5.3.58)$$

The maximum stresses and bending moments cannot be calculated using Eqs.(5.3.56a,b) and (5.3.57a,b) due to the logarithmic singularity (omitting the

logarithmic terms give grossly wrong values). The maximum finite stresses produced by load Q_0 on a very small circular area of radius r_c can be calculated using the so-called equivalent radius r_e in Eqs. (5.3.56a,b) and (5.3.57a,b) [see Roark and Young (1975)]

$$r_e = \sqrt{1.6r_c^2 + h^2} - 0.675h \quad \text{when } r_c < 1.7h \quad (5.3.59a)$$

$$r_e = r_c \quad \text{when } r_c \geq 1.7h \quad (5.3.59b)$$

The Ritz solution

This problem can also be solved using the Ritz method. Suppose that the circular plate is subjected to moment M_a at edge $r = a$, point load $Q_0 = 2\pi b Q_b$ at the center, and uniformly distributed load q_0 . Although the exact solution is logarithmic, we can seek an algebraic approximation of the solution. The approximation functions φ_i given in Eq. (5.3.50) are admissible for this problem.

For $N = 1$, from Eq. (5.3.51) we have $R_{11} = 8\pi D(1 + \nu)/a^2$ and $F_1 = \pi q_0 a^2/2 + Q_0 + 4\pi M_a$. Hence, the one-parameter Ritz solution is given by

$$W_1(r) = \left[\frac{q_0 a^4}{16D(1 + \nu)} + \frac{Q_0 a^2}{8\pi D(1 + \nu)} + \frac{M_a a^2}{2D(1 + \nu)} \right] \left(1 - \frac{r^2}{a^2} \right) \quad (5.3.60)$$

Note that the deflection due to the edge moment M_a is exact, the maximum deflection due to the distributed load q_0 is in 24.5% error, and the maximum deflection due to the point load Q_0 is in 40% error. It was already shown in Eq. (5.3.53) that the three-parameter Ritz solution is exact for uniformly distributed load. Hence, we consider only the point load in evaluating the two- and three-parameter solutions.

For $N = 2$, we obtain

$$c_1 = \frac{5.25 + 3\nu}{18(1 + \nu)} \left(\frac{Q_0 a^2}{\pi D} \right), \quad c_2 = -\frac{Q_0 a^2}{9\pi D} \quad (5.3.61)$$

and the solution is given by

$$W_2(r) = \frac{Q_0 a^2}{18\pi D} \left[\left(\frac{5.25 + 3\nu}{1 + \nu} \right) \left(1 - \frac{r^2}{a^2} \right) - 2 \left(1 - \frac{r^3}{a^3} \right) \right] \quad (5.3.62)$$

The maximum deflection predicted by the two-parameter approximation is 4.38% in error.

Lastly, for $N = 3$, we obtain

$$c_1 = \frac{2.96 + 2\nu}{1 + \nu} \Omega, \quad c_2 = -2.133\Omega, \quad c_3 = 0.6\Omega, \quad \Omega = \frac{Q_0 a^2}{7.68\pi D}$$

and the solution becomes

$$W_3(r) = \Omega \left[\left(\frac{2.96 + 2\nu}{1 + \nu} \right) \left(1 - \frac{r^2}{a^2} \right) - 2.133 \left(1 - \frac{r^3}{a^3} \right) + 0.6 \left(1 - \frac{r^4}{a^4} \right) \right] \quad (5.3.63)$$

The maximum deflection predicted by the three-parameter Ritz solution is only 1% in error compared to the analytical deflection in Eq. (5.3.58).

It should be noted that the method of superposition may be used to obtain the solution to a problem on a variety of loads. For example, the center deflection of a simply supported plate subjected to uniformly distributed load as well as a point load at the center may be obtained by adding the expressions in Eqs. (5.3.43) and (5.3.55).

5.3.6 Annular Plate with Simply Supported Outer Edge

Circular plates with a concentric circular hole of radius b are called annular plates [Figure 5.3.1(b)]. For this case, the solutions given in Eqs. (5.3.17) and (5.3.20)–(5.3.23) are valid for $b \leq r \leq a$. For annular plates, the edge $r = b$ can also be subjected to various geometric and/or force boundary conditions. We consider several cases here.

Suppose that the inner edge is subjected to a bending moment M_b while the outer edge is subjected to a bending moment M_a [Figure 5.3.5(a)]. The boundary conditions are then

$$\text{At } r = b : \quad M_{rr} = M_b, \quad rQ_r = 0 \quad (5.3.64a)$$

$$\text{At } r = a : \quad w_0 = 0, \quad M_{rr} = M_a \quad (5.3.64b)$$

Hence, we obtain from Eq. (5.3.13) $c_1 = 0$ and

$$\begin{aligned} -\frac{1+\nu}{2}c_2 + \frac{1-\nu}{b^2}c_3 &= M_b, \quad -\frac{1+\nu}{2}c_2 + \frac{1-\nu}{a^2}c_3 = M_a \\ \frac{a^2}{4}c_2 + c_3 \log a + c_4 &= 0 \end{aligned} \quad (5.3.65)$$

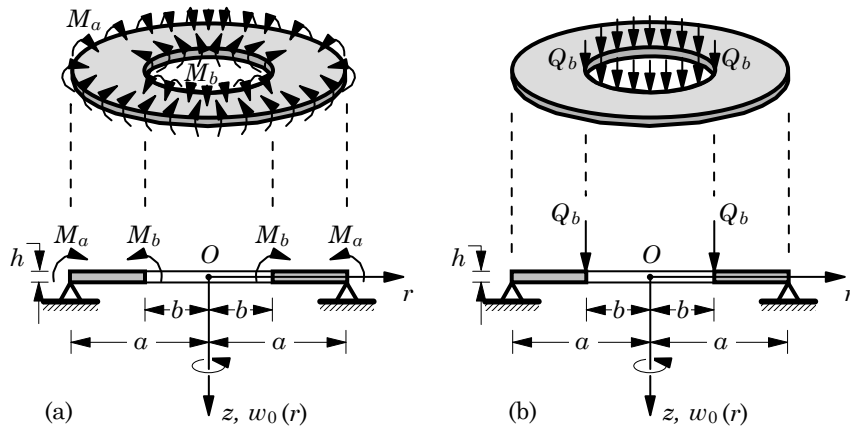


Figure 5.3.5. A simply supported annular plate with (a) edge moments or (b) inner edge-line load.

which give

$$\begin{aligned} c_3 &= \frac{M_b - M_a}{1 - \nu} \left(\frac{b^2 a^2}{a^2 - b^2} \right), \quad c_2 = \frac{2}{1 + \nu} \left(\frac{M_b b^2 - M_a a^2}{a^2 - b^2} \right) \\ c_4 &= -\frac{a^2}{2(1 + \nu)} \left(\frac{M_b b^2 - M_a a^2}{a^2 - b^2} \right) - \frac{(M_b - M_a) \log a}{1 - \nu} \left(\frac{b^2 a^2}{a^2 - b^2} \right) \end{aligned} \quad (5.3.66)$$

The deflection of Eq. (5.3.17) becomes

$$\begin{aligned} w_0 &= - \left(\frac{a^2 - r^2}{a^2 - b^2} \right) \left(\frac{M_b b^2 - M_a a^2}{2(1 + \nu)D} \right) + \left(\frac{b^2 a^2}{a^2 - b^2} \right) \left(\frac{M_a - M_b}{(1 - \nu)D} \right) \log \bar{r} \\ &= -\frac{a^2}{2D(1 - \beta^2)} \left[\beta^2 \left(\frac{1 - \bar{r}^2}{1 + \nu} - \frac{2 \log \bar{r}}{1 - \nu} \right) M_b - \left(\frac{1 - \bar{r}^2}{1 + \nu} - \frac{2\beta^2 \log \bar{r}}{1 - \nu} \right) M_a \right] \end{aligned} \quad (5.3.67)$$

$$M_{rr} = \frac{1}{1 - \beta^2} \left[\beta^2 \left(\frac{a^2}{r^2} - 1 \right) M_b + \left(1 - \beta^2 \frac{a^2}{r^2} \right) M_a \right] \quad (5.3.68)$$

$$M_{\theta\theta} = \frac{1}{1 - \beta^2} \left[-\beta^2 \left(\frac{a^2}{r^2} + 1 \right) M_b + \left(1 + \beta^2 \frac{a^2}{r^2} \right) M_a \right] \quad (5.3.69)$$

where $\bar{r} = r/a$ and $\beta = b/a$. The above results can be specialized to the case in which $M_b = 0$ or $M_a = 0$ as well as to the case of solid circular plate with applied moment at edge $r = a$ by setting $\beta = 0$.

Next consider an annular plate with the inner edge subjected to transverse line load Q_b (Figure 5.3.5b). The boundary conditions are then

$$\text{At } r = b : \quad M_{rr} = 0, \quad (r Q_r) = -b Q_b \quad (5.3.70a)$$

$$\text{At } r = a : \quad w_0 = 0, \quad M_{rr} = 0 \quad (5.3.70b)$$

Hence, we have from Eq. (5.3.13) $c_1 = b Q_b$ and

$$\begin{aligned} - \left[\frac{1 + \nu}{2} \log b + \frac{1}{4}(1 - \nu) \right] b Q_b - \frac{1 + \nu}{2} c_2 + \frac{1 - \nu}{b^2} c_3 &= 0 \\ - \left[\frac{1 + \nu}{2} \log a + \frac{1}{4}(1 - \nu) \right] b Q_b - \frac{1 + \nu}{2} c_2 + \frac{1 - \nu}{a^2} c_3 &= 0 \\ \frac{a^2}{4} (\log a - 1) b Q_b + \frac{a^2}{4} c_2 + c_3 \log a + c_4 &= 0 \end{aligned} \quad (5.3.71)$$

from which we obtain

$$\begin{aligned} c_2 &= b Q_b \left[\frac{b^2}{a^2 - b^2} \log \left(\frac{b}{a} \right) - \log a - \frac{1}{2} \left(\frac{1 - \nu}{1 + \nu} \right) \right] \\ c_3 &= b Q_b \frac{1}{2} \left(\frac{1 + \nu}{1 - \nu} \right) \frac{b^2 a^2}{a^2 - b^2} \log \left(\frac{b}{a} \right) \\ c_4 &= -b Q_b \left[\frac{a^2}{4} \left(\frac{b^2}{a^2 - b^2} \log \left(\frac{b}{a} \right) - 1 \right) - \frac{a^2}{8} \left(\frac{1 - \nu}{1 + \nu} \right) \right. \\ &\quad \left. + \frac{1}{2} \left(\frac{1 + \nu}{1 - \nu} \right) \frac{b^2 a^2}{a^2 - b^2} \log \left(\frac{b}{a} \right) \log a \right] \end{aligned} \quad (5.3.72)$$

Thus, the solution becomes

$$w_0(r) = \frac{Q_b b a^2}{8D} \left[\left(1 - \frac{r^2}{a^2}\right) \left(\frac{3+\nu}{1+\nu} - 2\kappa\right) + 2 \frac{r^2}{a^2} \log\left(\frac{r}{a}\right) + 4\kappa \left(\frac{1+\nu}{1-\nu}\right) \log\left(\frac{r}{a}\right) \right] \quad (5.3.73)$$

$$M_{rr}(r) = -\frac{b Q_b (1+\nu)}{2} \left[\log\left(\frac{r}{a}\right) + \kappa \left(1 - \frac{r^2}{a^2}\right) \right] \quad (5.3.74)$$

$$M_{\theta\theta}(r) = -\frac{b Q_b (1+\nu)}{2} \left[\log\left(\frac{r}{a}\right) - \frac{1-\nu}{1+\nu} + \kappa \left(1 + \frac{r^2}{a^2}\right) \right] \quad (5.3.75)$$

where

$$\kappa = \frac{\beta^2}{1-\beta^2} \log \beta, \quad \beta = \frac{b}{a} \quad (5.3.76)$$

Note that if the radius b of the hole becomes infinitesimally small, $b^2 \log(b/a)$ vanishes, and Eqs. (5.3.73)–(5.3.75), by letting $2\pi b Q_b = Q_0$ [or $Q_b = Q_0/(2\pi b)$], reduce to Eqs. (5.3.55), (5.3.57a), and (5.3.57b), respectively.

Uniformly distributed load. Finally, we consider a simply supported annular plate under uniformly distributed load of intensity q_0 . The boundary conditions are

$$\text{At } r = b : \quad M_{rr} = 0, \quad (r Q_r) = 0 \quad (5.3.77a)$$

$$\text{At } r = a : \quad w_0 = 0, \quad M_{rr} = 0 \quad (5.3.77b)$$

Hence, we have $c_1 = -q_0 b^2 / 2$ and

$$\begin{aligned} & -\left(\frac{3+\nu}{16}\right) q_0 b^2 + \left[\frac{1+\nu}{4} \log b + \frac{1-\nu}{8}\right] b^2 q_0 - \frac{1+\nu}{2} c_2 + \frac{1-\nu}{b^2} c_3 = 0 \\ & -\left(\frac{3+\nu}{16}\right) q_0 a^2 + \left[\frac{1+\nu}{4} \log a + \frac{1}{8}(1-\nu)\right] b^2 q_0 - \frac{1+\nu}{2} c_2 + \frac{1-\nu}{a^2} c_3 = 0 \\ & \frac{q_0 a^4}{64} - \frac{a^2}{8} (\log a - 1) q_0 b^2 + \frac{a^2}{4} c_2 + c_3 \log a + c_4 = 0 \end{aligned} \quad (5.3.78)$$

We obtain

$$\begin{aligned} c_2 &= -\left(\frac{1+3\nu}{1+\nu}\right) \frac{q_0 b^2}{8} - \left(\frac{3+\nu}{1+\nu}\right) \frac{q_0 a^2}{8} + \frac{q_0 b^2}{2} \log a - \frac{q_0 b^4}{2(a^2 - b^2)} \log \beta \\ c_3 &= -\left(\frac{3+\nu}{1-\nu}\right) \frac{q_0 b^2 a^2}{16} - \left(\frac{1+\nu}{1-\nu}\right) \frac{q_0 a^2 b^4}{4(a^2 - b^2)} \log \beta \\ c_4 &= -\frac{q_0 a^4}{64} + \left(\frac{3+\nu}{1+\nu}\right) \frac{q_0 a^2 (a^2 - b^2)}{32} + \left(\frac{3+\nu}{1-\nu}\right) \frac{q_0 b^2 a^2}{16} \log a \\ &+ \frac{q_0 b^4 a^2}{8(a^2 - b^2)} \log \beta + \left(\frac{1+\nu}{1-\nu}\right) \frac{q_0 b^4 a^2}{4(a^2 - b^2)} \log a \log \beta \end{aligned} \quad (5.3.79)$$

The deflection and bending moments become

$$\begin{aligned} w_0 &= \frac{q_0 a^4}{64D} \left\{ - \left[1 - \left(\frac{r}{a} \right)^4 \right] + \frac{2\alpha_1}{1+\nu} \left[1 - \left(\frac{r}{a} \right)^2 \right] - \frac{4\alpha_2\beta^2}{1-\nu} \log \left(\frac{r}{a} \right) \right\} \\ M_{rr} &= \frac{q_0 a^2}{16} \left\{ (3+\nu) \left[1 - \left(\frac{r}{a} \right)^2 \right] - \beta^2 (3+\nu) \left[1 + \left(\frac{r}{a} \right)^2 \right] \right. \\ &\quad \left. + 4(1+\nu)\beta^2\kappa \left[1 - \left(\frac{r}{a} \right)^2 \right] + 4(1+\nu)\beta^2 \log \left(\frac{r}{a} \right) \right\} \\ M_{\theta\theta} &= \frac{q_0 a^2}{16} \left\{ (3+\nu) \left[1 - \left(\frac{r}{a} \right)^2 \right] + \beta^2 \left[(5\nu-1) + (3+\nu) \left(\frac{r}{a} \right)^2 \right] \right. \\ &\quad \left. + 4(1+\nu)\beta^2\kappa \left[1 + \left(\frac{r}{a} \right)^2 \right] \right\} \end{aligned} \quad (5.3.80a)$$

where

$$\alpha_1 = (3+\nu)(1-\beta^2) - 4(1+\nu)\beta^2\kappa, \quad \alpha_2 = (3+\nu) + 4(1+\nu)\kappa \quad (5.3.80b)$$

and β and κ are defined in Eq. (5.3.76).

The Ritz solutions

The Ritz formulation presented in Eqs. (5.3.37)–(5.3.40) is also applicable to annular plates. The approximation functions of Eq. (5.3.50) were derived using the conditions $w_0(a) = 0$ and $dw_0/dr = 0$ at $r = 0$. While $w_0(a) = 0$ is also valid for simply supported annular plates, we no longer require that $dw_0/dr = 0$ at $r = 0$, which is not even a boundary point. The lowest order function $\varphi_1(r)$ that meets the condition $\varphi_1(a) = 0$ is $(1-r/a)$, which does not meet the continuity requirement. Hence, the next choice is $\varphi_1 = (1-r^2/a^2)$. Thus, the functions in Eq. (5.3.50) can be used for simply supported annular plates. For an isotropic annular plate with edge moments and edge forces and subjected to distributed load, Eq. (5.3.51) yields

$$\begin{aligned} R_{ij} &= \frac{2\pi D}{a^2} [ij + (1+\nu)(i+j) + 1] \frac{(i+1)(j+1)}{(i+j)} (1 - \beta^{i+j}) \\ F_i &= 2\pi \left\{ q_0 a^2 \left[(i+1) - (i+3)\beta^2 + 2\beta^{i+3} \right] \frac{1}{2(i+3)} \right. \\ &\quad \left. + bQ_b (1 - \beta^{i+1}) - (i+1)M_a + (i+1)\beta^{i+1}M_b \right\} \end{aligned} \quad (5.3.81)$$

where $\beta = b/a$. For instance, the one-parameter solution is

$$c_1 = \frac{1}{D(1+\nu)} \left[\frac{q_0 a^4 (1 - \beta^2)}{16} + \frac{Q_b a^2 b}{4} - \frac{a^2}{2(1 - \beta^2)} (\beta^2 M_b - M_a) \right]$$

Although the Ritz approximation for this choice of φ_i will not give the exact solution (because of the lack of logarithmic terms), it can give a very accurate solution as

the number of terms is increased. Alternatively, one may choose an approximation of the form

$$w_0(r) \approx c_1 \log r + c_2 r^2 \log r + \sum_{j=3}^N c_j \left(1 - \frac{r^{j+1}}{a^{j+1}}\right)$$

and obtain the exact solution. The first term is needed to capture the response due to the edge moment and distributed load, and the second term is needed to capture the response due to the point load.

5.3.7 Clamped Circular Plate under Distributed Load

Analytical solution

The boundary conditions associated with the clamped outer edges are $w_0 = 0$ and $\frac{dw_0}{dr} = 0$ at $r = a$ (Figure 5.3.6). Using these conditions in Eqs. (5.3.28) and (5.3.29), we obtain

$$c_2 = -\frac{2F'_0}{a}, \quad c_4 = -F_0 + \frac{F'_0 a}{2} \quad (5.3.82)$$

For uniformly distributed load q_0 , we have $c_2 = -q_0 a^2 / 8$ and $c_4 = q_0 a^4 / 64$. Hence, the deflection (5.3.28) becomes

$$w_0(r) = \frac{q_0 a^4}{64D} \left(1 - \frac{r^2}{a^2}\right)^2 \quad (5.3.83)$$

and the maximum deflection occurs at the center of the plate ($r = 0$):

$$w_{max} = \frac{q_0 a^4}{64D} \quad (5.3.84)$$

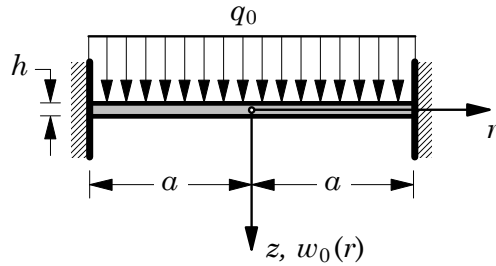


Figure 5.3.6. A clamped circular plate under a uniformly distributed load.

Expressions for the bending moments and stresses can be obtained from Eqs. (5.3.30)–(5.3.33):

$$M_{rr}(r) = \frac{q_0 a^2}{16} \left[(1 + \nu) - (3 + \nu) \frac{r^2}{a^2} \right] \quad (5.3.85)$$

$$M_{\theta\theta}(r) = \frac{q_0 a^2}{16} \left[(1 + \nu) - (1 + 3\nu) \frac{r^2}{a^2} \right] \quad (5.3.86)$$

$$\sigma_{rr}(r, z) = \frac{3q_0 a^2 z}{4h^3} \left[(1 + \nu) - (3 + \nu) \frac{r^2}{a^2} \right] \quad (5.3.87)$$

$$\sigma_{\theta\theta}(r, z) = \frac{3q_0 a^2 z}{4h^3} \left[(1 + \nu) - (1 + 3\nu) \frac{r^2}{a^2} \right] \quad (5.3.88)$$

The maximum (in magnitude) values of the bending moments are found to be at the fixed edge:

$$M_{rr}(a) = -\frac{q_0 a^2}{8}, \quad M_{\theta\theta}(a) = -\frac{\nu q_0 a^2}{8} \quad (5.3.89)$$

Hence, the maximum stress is given by

$$\sigma_{rr}(a, -\frac{h}{2}) = -\frac{6M_{rr}(a)}{h^2} = \frac{3q_0}{4} \left(\frac{a}{h}\right)^2 \quad (5.3.90)$$

The Ritz solution

Note that the one-parameter Ritz or Galerkin solution with $\varphi_1 = (1 - r^2/a^2)^2$ will yield the same solution as in Eq. (5.3.83); see Problems 5.12–5.14 at the end of the chapter.

5.3.8 Clamped Circular Plate under Central Point Load

Analytical solution

For this case, we have $c_1 = Q_0/2\pi$ and $c_3 = 0$, where Q_0 is the magnitude of the central point load (Figure 5.3.7). The boundary conditions of the clamped edge give

$$\frac{Q_0 a}{8\pi} (2 \log a - 1) + \frac{a}{2} c_2 = 0, \quad \frac{Q_0 a^2}{8\pi} (\log a - 1) + \frac{a^2}{4} c_2 + c_4 = 0$$

from which we obtain

$$c_2 = -\frac{Q_0}{4\pi} (2 \log a - 1), \quad c_4 = \frac{Q_0 a^2}{16\pi} \quad (5.3.91)$$

Hence, the solution becomes

$$w_0(r) = \frac{Q_0 a^2}{16\pi D} \left[1 - \frac{r^2}{a^2} + 2 \frac{r^2}{a^2} \log \left(\frac{r}{a} \right) \right] \quad (5.3.92)$$

$$M_{rr}(r) = -\frac{Q_0}{4\pi} \left[1 + (1 + \nu) \log \left(\frac{r}{a} \right) \right] \quad (5.3.93)$$

$$M_{\theta\theta}(r) = -\frac{Q_0}{4\pi} \left[\nu + (1 + \nu) \log \left(\frac{r}{a} \right) \right] \quad (5.3.94)$$

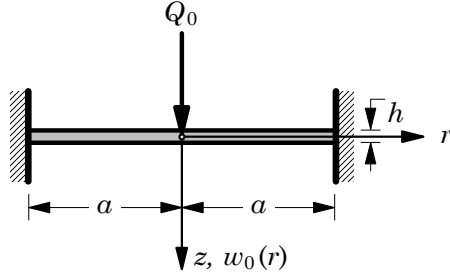


Figure 5.3.7. A clamped circular plate under a central point load.

The maximum deflection occurs at $r = 0$ and is given by

$$w_{max} = \frac{Q_0 a^2}{16\pi D} \quad (5.3.95)$$

The Ritz Solution

Let us consider a Ritz solution to the problem. The geometric boundary conditions are

$$\frac{dw}{dr} = 0 \text{ at } r = 0 \quad \text{and} \quad w = \frac{dw}{dr} = 0 \quad \text{at } r = a \quad (5.3.96)$$

The known natural boundary condition is that the shear force $2\pi(rQ_r)$ at $r = 0$ is Q_0 , which enters the variational statement [see Eq. (5.3.37)].

For $N = 2$, we choose the following approximation functions [the reader is asked to verify that the following functions satisfy the boundary conditions in Eq. (5.3.96)]:

$$\varphi_1(r) = 1 - 3\left(\frac{r}{a}\right)^2 + 2\left(\frac{r}{a}\right)^3, \quad \varphi_2(r) = \left[1 - \left(\frac{r}{a}\right)^2\right]^2 \quad (5.3.97)$$

For $q = 0$, $k = 0$, and $b = 0$, $Q_a = 0$, $2\pi b Q_b = Q_0$, and $D_{11} = D_{22} = D$, the coefficients R_{ij} and F_i are evaluated to be

$$R_{11} = \frac{18\pi D}{a^2}, \quad R_{22} = \frac{64\pi}{3a^2}, \quad R_{12} = R_{21} = \frac{96\pi}{5a^2}, \quad F_1 = F_2 = Q_0 \quad (5.3.98)$$

The Ritz parameters c_1 and c_2 are given by

$$c_1 = \frac{5Q_0 a^2}{36\pi D}, \quad c_2 = -\frac{5Q_0 a^2}{64\pi D} \quad (5.3.99)$$

and the two-parameter Ritz solution is

$$W_2(r) = \frac{5Q_0 a^2}{576\pi D} \left[7 - 30\left(\frac{r}{a}\right)^2 + 32\left(\frac{r}{a}\right)^3 - 9\left(\frac{r}{a}\right)^4 \right] \quad (5.3.100)$$

The one-parameter solution is in 11.2% error while the two-parameter solution is in 3.8% error compared to the exact solution (5.3.95).

5.3.9 Annular Plates with Clamped Outer Edges

Analytical solution

Specified bending moment on the edge. Suppose that the inner edge is subjected to a bending moment M_b while the outer edge is clamped, as shown in Figure 5.3.8(a). The boundary conditions are then

$$\text{At } r = b : \quad M_{rr} = M_b, \quad (rQ_r) = 0 \quad (5.3.101a)$$

$$\text{At } r = a : \quad w_0 = 0, \quad \frac{dw_0}{dr} = 0 \quad (5.3.101b)$$

Hence, we obtain from Eq. (5.3.13) $c_1 = 0$ and from Eqs. (5.3.16) and (5.3.17) the relations

$$-\frac{1+\nu}{2}c_2 + \frac{1-\nu}{b^2}c_3 = M_b, \quad \frac{a}{2}c_2 + \frac{1}{a}c_3 = 0, \quad \frac{a^2}{4}c_2 + c_3 \log a + c_4 = 0 \quad (5.3.102)$$

which give

$$\begin{aligned} c_2 &= -\frac{2M_bb^2}{(1+\nu)b^2 + (1-\nu)a^2}, & c_3 &= \frac{M_bb^2a^2}{(1+\nu)b^2 + (1-\nu)a^2} \\ c_4 &= \frac{1}{2} \left(\frac{M_bb^2a^2}{(1+\nu)b^2 + (1-\nu)a^2} \right) (1 - 2 \log a) \end{aligned} \quad (5.3.103)$$

Hence, the deflection and bending moments of Eqs. (5.3.17), (5.3.22) and (5.3.23) for the present problem become

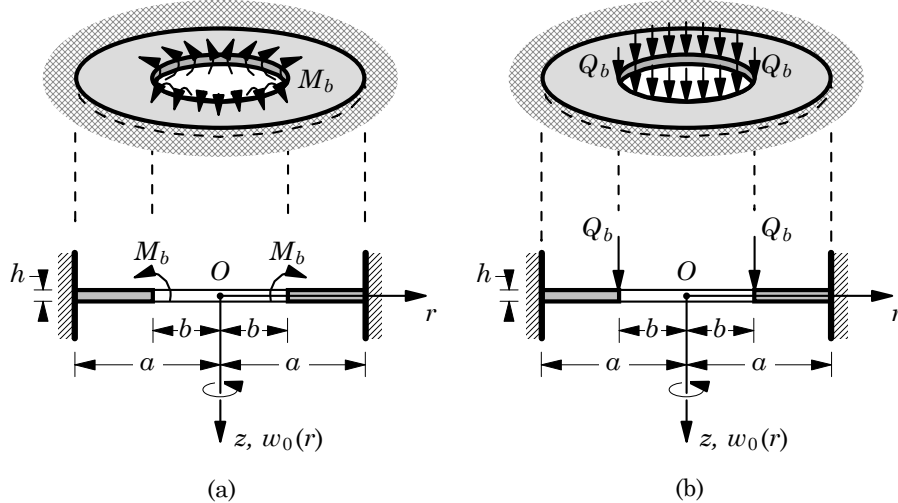


Figure 5.3.8. A clamped annular plate with the inner edge subjected to (a) a bending moment or (b) a line load.

$$w_0(r) = \frac{M_b b^2 a^2}{2[(1+\nu)b^2 + (1-\nu)a^2]} \left[1 - \frac{r^2}{a^2} + 2 \log\left(\frac{r}{a}\right) \right] \quad (5.3.104)$$

$$M_{rr}(r) = \frac{M_b b^2}{(1+\nu)b^2 + (1-\nu)a^2} \left[(1+\nu) + (1-\nu)\frac{a^2}{r^2} \right] \quad (5.3.105)$$

$$M_{\theta\theta}(r) = \frac{M_b b^2}{(1+\nu)b^2 + (1-\nu)a^2} \left[(1+\nu) - (1-\nu)\frac{a^2}{r^2} \right] \quad (5.3.106)$$

Specified edge line load. Next, we consider an annular plate with the inner edge subjected to transverse line load Q_b , as shown in Figure 5.3.8(b). The boundary conditions are then

$$\begin{aligned} \text{At } r = b : \quad M_{rr} &= 0, & rQ_r &= -bQ_b \\ \text{At } r = a : \quad w_0 &= 0, & \frac{dw_0}{dr} &= 0 \end{aligned} \quad (5.3.107)$$

Hence, we have from Eq. (5.3.13) $c_1 = bQ_b$ and

$$\begin{aligned} -\left[\frac{1+\nu}{2} \log b + \frac{1}{4}(1-\nu)\right] bQ_b - \frac{1+\nu}{2} c_2 + \frac{1-\nu}{b^2} c_3 &= 0 \\ \frac{a^2}{4} (\log a - 1) bQ_b + \frac{a^2}{4} c_2 + c_3 \log a + c_4 &= 0 \\ \frac{a}{4} (2 \log a - 1) bQ_b + \frac{a}{2} c_2 + \frac{c_3}{a} &= 0 \end{aligned} \quad (5.3.108)$$

which gives

$$\begin{aligned} c_2 &= -\frac{bQ_b}{\Delta} \left[(1-\nu) \log a + (1+\nu)\beta^2 \log b - \frac{1}{2}(1-\nu)(1-\beta^2) \right] \\ c_3 &= -\frac{a^2}{4} [(2 \log a - 1) bQ_b + 2c_2] \\ c_4 &= -\frac{a^2}{4} [(\log a - 1) bQ_b + 2c_2] - c_3 \log a \\ \Delta &= (1-\nu) + (1+\nu)\beta^2, \quad \beta = \frac{b}{a} \end{aligned} \quad (5.3.109)$$

The deflections and bending moments can be obtained from Eqs. (5.3.17), (5.3.22), and (5.3.23).

Free edge with uniform load. Now consider an annular plate under uniformly distributed load of intensity q_0 and with a free inner edge. The boundary conditions are

$$\begin{aligned} \text{At } r = b : \quad M_{rr} &= 0, & rQ_r &= 0 \\ \text{At } r = a : \quad w_0 &= 0, & \frac{dw_0}{dr} &= 0 \end{aligned} \quad (5.3.110)$$

Hence, we have $c_1 = -q_0 b^2 / 2$ and

$$\begin{aligned} -\left(\frac{3+\nu}{16}\right)q_0b^2 + \left[\frac{1+\nu}{4}\log b + \frac{1-\nu}{8}\right]b^2q_0 - \frac{1+\nu}{2}c_2 + \frac{1-\nu}{b^2}c_3 &= 0 \\ \frac{q_0a^4}{64} - \frac{q_0a^2b^2}{8}(\log a - 1) + \frac{a^2}{4}c_2 + c_3 \log a + c_4 &= 0 \\ \frac{q_0a^3}{16} - \frac{q_0ab^2}{8}(2\log a - 1) + \frac{c_2a}{2} + \frac{c_3}{a} &= 0 \end{aligned}$$

We obtain

$$\begin{aligned} c_2 &= -\frac{q_0a^2}{8\Delta} \left[(1-\nu)(1+2\beta^2) + (1+3\nu)\beta^4 - 4(1-\nu)\beta^2 \log a - 4(1+\nu)\beta^4 \log b \right] \\ c_3 &= -\frac{q_0a^4}{16} \left[1 - 2\beta^2(2\log a - 1) \right] - \frac{a^2}{2}c_2 \\ c_4 &= -\frac{q_0a^4}{64} \left[1 - 8\beta^2(\log a - 1) \right] - \frac{a^2}{4}c_2 - c_3 \log a \end{aligned} \quad (5.3.111)$$

where Δ and β are as defined in Eq. (5.3.109). Once again, the deflection and bending moments can be obtained using Eqs. (5.3.17), (5.3.22), and (5.3.23).

Inner edge welded to a rigid shaft. Next, we consider a circular plate clamped to a rigid circular inclusion of radius b at the center, and subjected to a point load Q_0 at the center (Figure 5.3.9). The boundary conditions are

$$\begin{aligned} \text{At } r = b : \quad \frac{dw_0}{dr} &= 0, \quad 2\pi(rQ_r) = -Q_0 \\ \text{At } r = a : \quad w_0 &= 0, \quad \frac{dw_0}{dr} = 0 \end{aligned} \quad (5.3.112)$$

The boundary conditions yield $c_1 = Q_0 / 2\pi$ and

$$\begin{aligned} \frac{b}{8\pi}(2\log b - 1)Q_0 + \frac{b}{2}c_2 + \frac{1}{b}c_3 &= 0 \\ \frac{a^2}{8\pi}(\log a - 1)Q_0 + \frac{a^2}{4}c_2 + \log a c_3 + c_4 &= 0 \\ \frac{a}{8\pi}(2\log a - 1)Q_0 + \frac{a}{2}c_2 + \frac{1}{a}c_3 &= 0 \end{aligned}$$

which give ($\beta = b/a$)

$$\begin{aligned} c_2 &= \frac{Q_0}{4\pi} \left(1 + \frac{2\beta^2}{1-\beta^2} \log b - \frac{2}{1-\beta^2} \log a \right) \\ c_3 &= -\frac{Q_0b^2}{4\pi} \frac{\log \beta}{1-\beta^2} \\ c_4 &= \frac{Q_0a^2}{16\pi} \left[1 - \frac{2\beta^2}{1-\beta^2} \log \beta (1 + 2\log a) \right] \end{aligned} \quad (5.3.113)$$

The deflection and bending moments are given by Eqs. (5.3.17), (5.3.22), and (5.3.23).

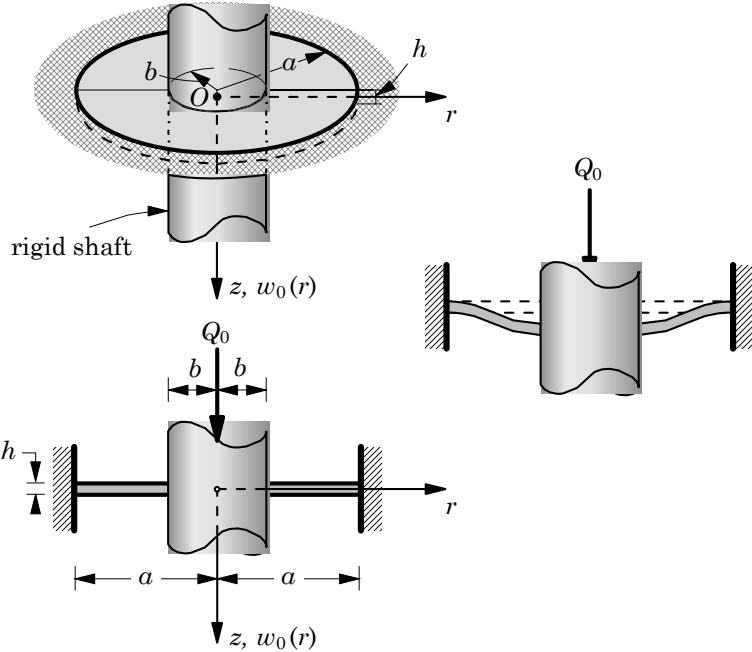


Figure 5.3.9. An annular plate with a rigid shaft at the center and subjected to a central point load.

Finally, we consider a circular plate clamped to a rigid circular inclusion of radius b at the center (Figure 5.3.10) and subjected to uniformly distributed load q_0 . In addition, suppose that it is also clamped at $r = a$. The boundary conditions are

$$\begin{aligned} \text{At } r = b : \quad & \frac{dw_0}{dr} = 0, \quad rQ_r = 0 \\ \text{At } r = a : \quad & w_0 = 0, \quad \frac{dw_0}{dr} = 0 \end{aligned} \tag{5.3.114}$$

The boundary conditions yield $c_1 = -q_0 b^2 / 2$ and

$$\begin{aligned} \frac{q_0 b^3}{16} - \frac{q_0 b^3}{8} (2 \log b - 1) + \frac{c_2 b}{2} + \frac{c_3}{b} &= 0 \\ \frac{q_0 a^4}{64} - \frac{q_0 a^4}{8} (\log a - 1) + \frac{a^2}{4} c_2 + c_3 \log a + c_4 &= 0 \\ \frac{q_0 a^3}{16} - \frac{q_0 b^2 a}{8} (2 \log a - 1) + \frac{c_2 a}{2} + \frac{c_3}{a} &= 0 \end{aligned}$$

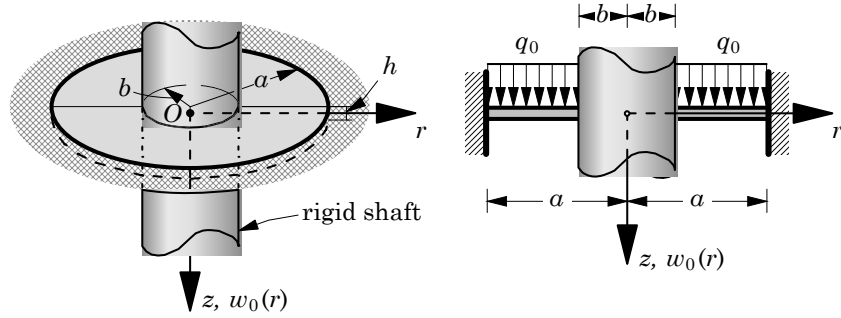


Figure 5.3.10. An annular plate with a rigid shaft at the center and subjected to uniformly distributed load.

Solving the three equations for c_1 , c_2 , and c_3 , we obtain

$$\begin{aligned} c_2 &= -\frac{q_0 a^2}{8(1-\beta^2)} \left[1 + 2\beta^2 (1 - 2 \log a) + \beta^4 (-3 + 4 \log b) \right] \\ c_3 &= \frac{q_0 a^2 b^2}{16} \left(1 - \frac{4\beta^2}{1-\beta^2} \log \beta \right) \\ c_4 &= -\frac{q_0 a^4}{64} [1 - 8(\log a - 1)] - \frac{a^2}{4} c_2 + c_3 \log a \end{aligned} \quad (5.3.115)$$

5.3.10 Circular Plates on Elastic Foundation

The Ritz solutions

The exact solutions of circular plates resting on an elastic foundation can be developed in terms of the Bessel functions [see Timoshenko and Woinowsky-Krieger (1970), Chapter 8]. Here we consider Ritz solutions of circular plates on elastic foundations. The weak form and the Ritz formulation presented in Eqs. (5.3.37)–(5.3.40) are valid here. We must select suitable approximation functions φ_i for each set of boundary conditions.

For a *free* circular plate on an elastic foundation, the approximation functions for the Ritz method are required to satisfy only the continuity and completeness conditions, as there are no boundary conditions to satisfy. We begin with the approximation ($N \geq 2$)

$$W_N(r) = c_0 + c_1 r + c_2 r^2 + \cdots + c_N r^N \quad (5.3.116)$$

and note that the c_1 -term presents difficulty (logarithmic singularity) when $b = 0$. Hence, we omit it for circular plates, but include for annular plates. For solid circular

plates, we have from Eq. (5.3.40a) the result $R_{ij} = R_{ij}^1 + R_{ij}^2$, where

$$R_{ij}^1 = 2\pi k \int_0^a \varphi_i \varphi_j r dr = \frac{2\pi k a^{i+j+2}}{i+i+2} \quad (5.3.117a)$$

when $i = 0, j = 0, 2, \dots, N$ and when $j = 0, i = 0, 2, \dots, N$, and

$$\begin{aligned} R_{ij}^2 &= 2\pi \int_b^a \left[D_{11} \frac{d^2 \varphi_i}{dr^2} \frac{d^2 \varphi_j}{dr^2} + D_{12} \frac{1}{r} \left(\frac{d\varphi_i}{dr} \frac{d^2 \varphi_j}{dr^2} + \frac{d^2 \varphi_j}{dr^2} \frac{d\varphi_i}{dr} \right) \right. \\ &\quad \left. + D_{22} \frac{1}{r^2} \frac{d\varphi_i}{dr} \frac{d\varphi_j}{dr} \right] r dr \\ &= 2\pi [ij(i-1)(j-1)D_{11} + ij(i+j-2)D_{12} + ijD_{22}] \frac{a^{i+j-2}}{i+j-2} \quad (5.3.117b) \end{aligned}$$

when $i, j = 2, 3, \dots, N$. Also, we have

$$F_i = \frac{2\pi q_0 a^{i+1}}{i+2} + \hat{Q} \delta_{i0} \quad (5.3.118)$$

Consider as an example a circular plate resting freely on an elastic foundation and subjected to a center point load Q_0 (Figure 5.3.11). For $N = 2$ (i.e., $w_0(r) \approx c_0 + c_2 r^2$) and $\hat{Q} = Q_0$, we have

$$2\pi \begin{bmatrix} \frac{ka^2}{2} & \frac{ka^4}{4} \\ \frac{ka^4}{4} & \frac{ka^6}{6} + \alpha \end{bmatrix} \begin{Bmatrix} c_0 \\ c_2 \end{Bmatrix} = Q_0 \begin{Bmatrix} 1 \\ 0 \end{Bmatrix}$$

where

$$\alpha = (2D_{11} + 4D_{12} + 2D_{22}) a^2$$

The solution is given by

$$c_0 = \frac{4Q_0}{k\pi a^2} \left(\frac{ka^6 + 6\alpha}{ka^6 + 24\alpha} \right), \quad c_2 = -\frac{6Q_0 a^2}{\pi(ka^6 + 24\alpha)} \quad (5.3.119)$$

For an isotropic plate, we have [$\alpha = 4(1+\nu)Da^2$ and $\hat{D} = D/(ka^4)$]

$$c_0 = \frac{4Q_0}{\pi ka^2} \left[\frac{1 + 24(1+\nu)\hat{D}}{1 + 96(1+\nu)\hat{D}} \right], \quad c_2 = -\frac{6Q_0}{\pi ka^4[1 + 96(1+\nu)\hat{D}]} \quad (5.3.120)$$

The maximum deflection occurs at $r = 0$ and it is given by

$$w_{max} = c_0 = \frac{4Q_0}{k\pi a^2} \left[\frac{1 + 24(1+\nu)\hat{D}}{1 + 96(1+\nu)\hat{D}} \right] \quad (5.3.121)$$

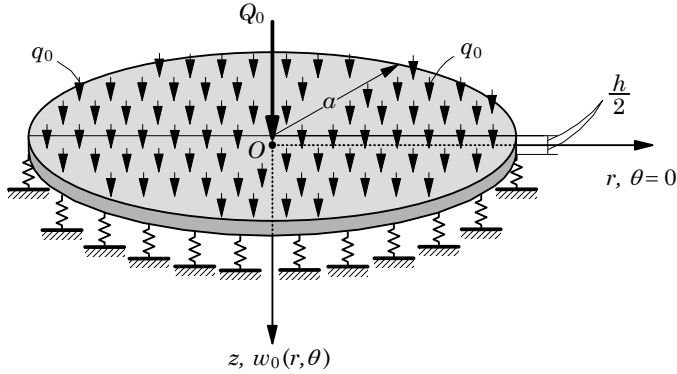


Figure 5.3.11. A circular plate on elastic foundation and subjected to a central point load.

For the following values of the parameters (data)

$$a = 5 \text{ in.}, \quad \hat{D} \equiv \frac{D}{ka^4} = 1.0, \quad \frac{Q_0}{\pi ka^2} = 408 \times 10^{-4}, \quad \nu = 0.3$$

we find that $w_{max} = c_0 = 0.04177$ in. This solution is about 3% less than that obtained using the analytical solution based on the Bessel functions.

Although the deflection obtained using the approximation $w_0 \approx c_0 + c_2 r^2$ is very accurate, the bending moments and stresses computed will not be accurate for a circular plate under a central point load. This is due to the fact that the assumed approximation does not contain a term that significantly contributes to the stress calculation. Note from Eqs. (5.3.17) and (5.3.26) that the solution of a circular plate under a central point load consists of a term of the form $r^2 \log r$. Therefore, to obtain accurate stresses around the point load, one must include this term in the approximate solution sought

$$w_0(r) \approx c_0 + c_2 r^2 + c_3 r^2 \log r \quad (5.3.122)$$

For circular plates on elastic foundation and with various boundary conditions, one may select the approximation developed earlier. For a simply supported plate on an elastic foundation and subjected to a central point load, for example, approximation functions of the form used in Eq. (5.3.50) may be employed. The coefficient matrix R_{ij}^2 of Eq. (5.3.117b) is valid for the problem, and the coefficients R_{ij}^1 can be computed with

$$\varphi_i(r) = 1 - \left(\frac{r}{a}\right)^{i+1} \quad (5.3.123)$$

We find

$$R_{ij}^1 = 2\pi ka^2 \left[\frac{1}{2} + \frac{1}{i+j+4} - \frac{i+j+6}{(i+3)(j+3)} \right] \quad (5.3.124)$$

For one-parameter Ritz solution ($N = 1$), we have

$$\left[\frac{8\pi(1+\nu)D}{a^2} + \frac{\pi ka^2}{3} \right] c_1 = Q_0 \quad \text{or} \quad c_1 = \frac{3Q_0}{\pi ka^2[1 + 24(1+\nu)\hat{D}]}$$

where $\hat{D} = D/ka^4$. The maximum deflection with the parameters $a = 5$ in., $\hat{D} = 1.0$, $Q_0/\pi ka^2 = 408 \times 10^{-4}$, and $\nu = 0.3$ is $w_{max} = c_1 = 0.0038$ in.

5.3.11 Bending of Circular Plates under Thermal Loads

Analytical solution

As discussed in Section 5.3.2, Eq. (5.3.17) gives the deflection of a circular plate (solid or annular) under arbitrary thermal loading. We have

$$Dw_0(r) = -G(r) + \frac{r^2}{4} (\log r - 1) c_1 + \frac{r^2}{4} c_2 + c_3 \log r + c_4 \quad (5.3.125)$$

where

$$G(r) = \frac{1}{(1-\nu)} \int \frac{1}{r} \int r M_T \, dr \, dr \quad (5.3.126)$$

The constants c_1 through c_4 must be determined using the boundary conditions. For solid circular plates, we necessarily have $c_1 = c_3 = 0$ and the solution becomes

$$Dw_0(r) = -G(r) + c_2 \frac{r^2}{4} + c_4 \quad (5.3.127)$$

Once the deflection is known, the stresses and bending moments may be computed using Eqs. (5.3.9) and (5.3.10).

The boundary conditions for the three standard cases are listed below:

$$\text{Hinged: } w_0 = 0, \quad D \left(\frac{d^2 w_0}{dr^2} + \frac{\nu}{r} \frac{dw_0}{dr} \right) + \frac{M_T}{1-\nu} = 0 \quad (5.3.128)$$

$$\text{Fixed: } w_0 = 0, \quad \frac{dw_0}{dr} = 0 \quad (5.3.129)$$

$$\begin{aligned} \text{Free: } & D \left(\frac{d^2 w_0}{dr^2} + \frac{\nu}{r} \frac{dw_0}{dr} \right) + \frac{M_T}{1-\nu} = 0, \quad \text{and} \\ & D \frac{d}{dr} \left[\frac{1}{r} \frac{d}{dr} \left(r \frac{dw_0}{dr} \right) \right] + \frac{1}{1-\nu} \frac{dM_T}{dr} = 0 \end{aligned} \quad (5.3.130)$$

The force boundary conditions for free thermal problems are not homogeneous because of the thermal moment M_T .

The constants for typical boundary conditions are given below. In these equations, the notation $M_T(a)$ means that $M_T(r)$ is evaluated at $r = a$.

Circular plate, simply supported at $r = a$:

$$\begin{aligned} c_2 &= \frac{2}{1+\nu} \left[G''(a) + \frac{\nu}{a} G'(a) - \frac{M_T(a)}{1-\nu} \right] \\ c_4 &= G(a) - \frac{a^2}{2(1+\nu)} \left[G''(a) + \frac{\nu}{a} G'(a) - \frac{M_T(a)}{1-\nu} \right] \end{aligned} \quad (5.3.131)$$

Circular plate, fixed at $r = a$:

$$c_2 = \frac{2}{a} G'(a), \quad c_4 = G(a) - \frac{a}{2} G'(a) \quad (5.3.132)$$

Annular plate, fixed at $r = b$ and $r = a$:

$$\begin{aligned} c_1 &= \frac{a_{22}b_1 - a_{12}b_2}{a_{11}a_{22} - a_{12}a_{21}}, \quad c_2 = \frac{a_{11}b_2 - a_{21}b_1}{a_{11}a_{22} - a_{12}a_{21}} \\ a_{11} &= \frac{1}{4} [b^2(2\log b - 1) - a^2(2\log a - 1)] \\ a_{12} &= \frac{1}{4} (b^2 - a^2), \quad a_{22} = \frac{1}{4} [b^2 - a^2(1 + \log \beta)] \\ a_{21} &= \frac{1}{4} [b^2(\log b - 1) - a^2(\log a - 1)(1 + \log \beta)] \\ b_1 &= bG'(b) - aG'(a), \quad b_2 = G'(b) - G'(a) - aG'(a)\log \beta \\ c_3 &= aG'(a) - \frac{a^2}{4} [(2\log a - 1)c_1 + c_2], \quad \beta = \frac{b}{a} \\ c_4 &= G(a) - aG'(a)\log a + \frac{a^2}{4} \{[2\log a(\log a - 1) + 1]c_1 + (\log a - 1)c_2\} \end{aligned} \quad (5.3.133)$$

For uniform temperature $\Delta T = T^0$, we find $M_T = 0$; however, N_T will not be zero. For temperature linearly varying through the thickness, $\Delta T = zT^1$, we have $M_T = E\alpha T^1 h^3/12$ and $N_T = 0$.

The Ritz formulation presented in Section 5.3.3 can also be used to determine solutions to thermal problems. In fact, solutions developed for circular and annular plates under mechanical loads can be extended/modified for thermal loads.

5.4 Asymmetrical Bending

5.4.1 General Solution

In this section, we consider the bending of circular plates under nonaxisymmetric loads. In other words, the geometry and boundary conditions are axisymmetric, but the loading is not axisymmetric. To determine solutions under such loads, we return to the governing equation (5.2.13) developed in Section 5.2. For static bending of an isotropic plate, not resting on an elastic foundation and without thermal loads, Eq. (5.2.13) becomes

$$D \left[\frac{1}{r} \frac{\partial}{\partial r} \left(r \frac{\partial}{\partial r} \right) + \frac{1}{r^2} \frac{\partial^2}{\partial \theta^2} \right] \left[\frac{1}{r} \frac{\partial}{\partial r} \left(r \frac{\partial w_0}{\partial r} \right) + \frac{1}{r^2} \frac{\partial^2 w_0}{\partial \theta^2} \right] = q(r, \theta) \quad (5.4.1)$$

The solution w_0 to this equation consists of two parts: a homogeneous solution w_h such that

$$D \left[\frac{1}{r} \frac{\partial}{\partial r} \left(r \frac{\partial}{\partial r} \right) + \frac{1}{r^2} \frac{\partial^2}{\partial \theta^2} \right] \left[\frac{1}{r} \frac{\partial}{\partial r} \left(r \frac{\partial w_h}{\partial r} \right) + \frac{1}{r^2} \frac{\partial^2 w_h}{\partial \theta^2} \right] = 0 \quad (5.4.2a)$$

and a particular solution w_p so that

$$w_0 = w_h + w_p \quad (5.4.2b)$$

The homogeneous solution may be expressed in the following form

$$w_h(r, \theta) = \sum_{n=0}^{\infty} a_n(r) \cos n\theta + \sum_{n=1}^{\infty} b_n(r) \sin n\theta \quad (5.4.3)$$

where a_n and b_n are functions of r only. Substitution of Eq. (5.4.3) into Eq. (5.4.2a) leads to the following set of equations for a_n and b_n :

$$\begin{aligned} a_0 &= A_0 + B_0 r^2 + C_0 \log r + D_0 r^2 \log r \\ a_1 &= A_1 r + B_1 r^3 + C_1 r^{-1} + D_1 r \log r \\ b_1 &= E_1 r + F_1 r^3 + G_1 r^{-1} + H_1 r \log r \\ a_n &= A_n r^n + B_n r^{-n} + C_n r^{n+2} + D_n r^{-n+2} \\ b_n &= E_n r^n + F_n r^{-n} + G_n r^{n+2} + H_n r^{-n+2} \end{aligned} \quad (5.4.4)$$

for $n = 2, 3, \dots$ where A_n, \dots, H_n are constants that are determined using boundary conditions. The solution $w_h = a_0$, which is independent of the angle θ , represents symmetrical bending of circular plates.

5.4.2 General Solution of Circular Plates under Linearly Varying Asymmetric Loading

Analytical solution

Consider a circular plate of radius a and subjected to an asymmetric loading of the type (Figure 5.4.1)

$$q(r, \theta) = q_0 + q_1 \frac{r}{a} \cos \theta \quad (5.4.5)$$

where q_0 represents the uniform part of the load for which the solution was already determined previously for various boundary conditions. The particular solution w_{p1} due to the uniform load q_0 for this case is given by [see Eq. (5.3.18)]

$$Dw_{p1} = \int \frac{1}{r} \int r \int \frac{1}{r} \int rq_0 dr dr dr dr = \frac{q_0 r^4}{64} \quad (5.4.6)$$

Similarly, the particular solution due to the second portion of the load is given by

$$Dw_{p2} = A \frac{q_1}{a} \cos \theta \left(\int \frac{1}{r} \int r \int \frac{1}{r} \int r^2 dr dr dr dr \right) = A \frac{q_1}{a} \cos \theta \left(\frac{r^5}{225} \right) \quad (5.4.7)$$

where A is a constant to be determined by substituting into

$$D \left[\frac{1}{r} \frac{\partial}{\partial r} \left(r \frac{\partial}{\partial r} \right) + \frac{1}{r^2} \frac{\partial^2}{\partial \theta^2} \right] \left[\frac{1}{r} \frac{\partial}{\partial r} \left(r \frac{\partial w_{p2}}{\partial r} \right) + \frac{1}{r^2} \frac{\partial^2 w_{p2}}{\partial \theta^2} \right] = q_1 \frac{r}{a} \cos \theta \quad (5.4.8)$$

We obtain $A = 225/192$. Thus, the particular solution is

$$w_p = w_{p1} + w_{p2} = \frac{q_0 r^4}{64D} + \frac{q_1 r^5}{192Da} \cos \theta \quad (5.4.9)$$

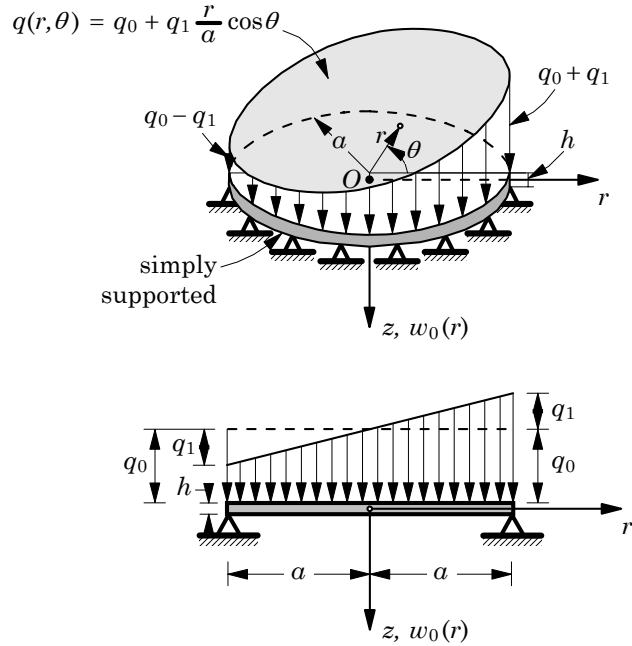


Figure 5.4.1. A circular plate subjected to an asymmetric loading.

The fourth-order derivative with respect to θ appearing in Eq. (5.4.2a) and the nature of the load distribution (5.4.5) implies that the homogeneous solution w_h is of the form [see Timoshenko and Woinowsky-Krieger (1970) and McFarland, Smith and Bernhart (1972)]

$$w_h(r) = \sum_{n=0}^{\infty} a_n(r) \cos n\theta \quad (5.4.10)$$

We take the first two terms of the series. Since the deflection must be finite at $r = 0$, it follows that $C_0 = D_0 = C_1 = D_1 = 0$ in a_0 and a_1 . Hence, the homogeneous solution is of the form

$$w_h = A_0 + B_0 r^2 + (A_1 r + B_1 r^3) \cos \theta \quad (5.4.11)$$

The complete general solution of a circular plate subjected to asymmetric loading in Eq. (5.4.5) is

$$\begin{aligned} w_0(r, \theta) &= w_p + w_h \\ &= A_0 + B_0 r^2 + \frac{q_0 r^4}{64D} + \left(\frac{q_1 r^5}{192Da} + A_1 r + B_1 r^3 \right) \cos \theta \end{aligned} \quad (5.4.12)$$

The four constants are determined using the boundary conditions. The procedure to determine the constants for clamped and simply supported plates is discussed next. The Ritz solutions are discussed in Section 5.4.6.

5.4.3 Clamped Plate under Asymmetric Loading

Analytical solution

The boundary conditions of a clamped circular plate are

$$w_0 = 0, \quad \frac{\partial w_0}{\partial r} = 0 \quad \text{at } r = a \text{ and for all } \theta \quad (5.4.13)$$

Substituting the deflection expression from Eq. (5.4.12) into the boundary conditions in Eq. (5.4.13), we arrive at

$$\begin{aligned} \frac{q_0 a^4}{64D} + A_0 + B_0 a^2 + \left(\frac{q_1 a^4}{192D} + A_1 a + B_1 a^3 \right) \cos \theta &= 0 \\ \frac{4q_0 a^3}{64D} + 2B_0 a + \left(\frac{5q_1 a^3}{192D} + A_1 + 3B_1 a^2 \right) \cos \theta &= 0 \end{aligned}$$

Since the above conditions must hold for all values of θ , it follows that

$$\begin{aligned} \frac{q_0 a^4}{64D} + A_0 + B_0 a^2 &= 0, & \frac{q_1 a^4}{192D} + A_1 a + B_1 a^3 &= 0 \\ \frac{4q_0 a^3}{64D} + 2B_0 a &= 0, & \frac{5q_1 a^3}{192D} + A_1 + 3B_1 a^2 &= 0 \end{aligned}$$

from which we obtain

$$A_0 = \frac{q_0 a^4}{64D}, \quad B_0 = -\frac{q_0 a^2}{32D}, \quad A_1 = \frac{q_1 a^3}{192D}, \quad B_1 = -\frac{q_1 a}{96D} \quad (5.4.14)$$

The deflection of a clamped plate under asymmetric loading becomes

$$w_0(r, \theta) = \left[\frac{q_0 a^4}{64D} + \frac{q_1 a^4}{192D} \left(\frac{r}{a} \right) \cos \theta \right] \left[1 - \left(\frac{r}{a} \right)^2 \right]^2 \quad (5.4.15)$$

The bending moments can be calculated using Eqs. (5.2.15a–c) and are given by

$$\begin{aligned} M_{rr} &= \frac{q_0 a^2}{16} \left[(1 + \nu) - (3 + \nu) \left(\frac{r}{a} \right)^2 \right] \\ &\quad - \frac{q_1 a^2}{48} \left[(5 + \nu) \left(\frac{r}{a} \right)^3 - (3 + \nu) \left(\frac{r}{a} \right) \right] \cos \theta \end{aligned} \quad (5.4.16)$$

$$\begin{aligned} M_{\theta\theta} &= \frac{q_0 a^2}{16} \left[(1 + \nu) - (1 + 3\nu) \left(\frac{r}{a} \right)^2 \right] \\ &\quad - \frac{q_1 a^2}{48} \left[(1 + 5\nu) \left(\frac{r}{a} \right)^3 - (1 + 3\nu) \left(\frac{r}{a} \right) \right] \cos \theta \end{aligned} \quad (5.4.17)$$

$$M_{r\theta} = -\frac{(1 - \nu) q_1 a^2}{48} \left[1 - \left(\frac{r}{a} \right)^2 \right] \sin \theta \quad (5.4.18)$$

Note that when $q_1 = 0$, all of the above results reduce to those of a clamped circular plate under a uniformly distributed load [see Eqs. (5.3.83), (5.3.85), and (5.3.86)].

5.4.4 Simply Supported Plate under Asymmetric Loading Analytical solution

The boundary conditions of a simply supported circular plate are

$$w_0 = 0, \quad M_{rr} = 0 \quad \text{at } r = a \text{ and for all } \theta \quad (5.4.19)$$

where the expression for M_{rr} in terms of the deflection is given in Eq. (5.2.16). Substituting the deflection expression from Eq. (5.4.12) into the boundary conditions in Eq. (5.4.19), we arrive at

$$\begin{aligned} \frac{q_0 a^4}{64D} + A_0 + B_0 a^2 &= 0, \quad \frac{q_1 a^3}{192D} + A_1 + B_1 a^2 = 0 \\ \frac{4(3+\nu)q_0 a^3}{64D} + 2(1+\nu)B_0 a &= 0, \quad \frac{4(5+\nu)q_1 a^2}{192D} + 2(3+\nu)B_1 a = 0 \end{aligned} \quad (5.4.20)$$

and

$$\begin{aligned} A_0 &= \left(\frac{5+\nu}{1+\nu}\right) \frac{q_0 a^4}{64D}, \quad B_0 = -\left(\frac{3+\nu}{1+\nu}\right) \frac{q_0 a^2}{32D} \\ A_1 &= \left(\frac{7+\nu}{3+\nu}\right) \frac{q_1 a^3}{192D}, \quad B_1 = -\left(\frac{5+\nu}{3+\nu}\right) \frac{q_1 a}{96D} \end{aligned} \quad (5.4.21)$$

Then the deflection of a simply supported plate under the asymmetric loading becomes

$$\begin{aligned} w_0(r, \theta) &= \frac{q_0 a^4}{64D} \left(1 - \frac{r^2}{a^2}\right) \left(\frac{5+\nu}{1+\nu} - \frac{r^2}{a^2}\right) + \frac{q_1 a^4}{(3+\nu)192D} \left(\frac{r}{a}\right) \left(1 - \frac{r^2}{a^2}\right) \\ &\times \left[7 + \nu - (3 + \nu) \frac{r^2}{a^2}\right] \cos \theta \end{aligned} \quad (5.4.22)$$

The bending moments can be calculated using Eqs. (5.2.15a–c) as before

$$M_{rr} = \frac{(3+\nu)q_0 a^2}{16} \left[1 - \left(\frac{r}{a}\right)^2\right] + \frac{(5+\nu)q_1 a^2}{48} \left[\frac{r}{a} - \left(\frac{r}{a}\right)^3\right] \cos \theta \quad (5.4.23)$$

$$\begin{aligned} M_{\theta\theta} &= \frac{(3+\nu)q_0 a^2}{16} \left[1 - \left(\frac{1+3\nu}{3+\nu}\right) \left(\frac{r}{a}\right)^2\right] \\ &+ \frac{(1+3\nu)q_1 a^2}{48} \left[\left(\frac{5+\nu}{3+\nu}\right) \frac{r}{a} - \left(\frac{1+5\nu}{1+3\nu}\right) \left(\frac{r}{a}\right)^2\right] \cos \theta \end{aligned} \quad (5.4.24)$$

$$M_{r\theta} = -\frac{(1-\nu)q_1 a^2}{48} \left[\frac{5+\nu}{3+\nu} - \left(\frac{r}{a}\right)^2\right] \sin \theta \quad (5.4.25)$$

5.4.5 Circular Plates under Noncentral Point Load

Analytical solution

Consider an isotropic circular plate with a point load Q_0 applied at point A at $r = b$. The solution can be sought by dividing the plate into two regions: the inside circle of radius b (shown with dashed line in Figure 5.4.2), and the annulus of inner radius b and outer radius a . Then Eq. (5.4.3) can be applied to each region separately. If the angle θ is measured from the radial line passing through point A , then the solution (5.4.3) containing $\cos n\theta$ should be retained because the solution is symmetric about $\theta = 0$ radial line.

For the outer (annulus) region, we have

$$w_0(r, \theta) = \sum_{n=0}^{\infty} a_n \cos n\theta \quad (5.4.26)$$

where a_0 and a_n are as defined in Eq. (5.4.4). Similarly, the solution for the inner region is

$$w_i(r, \theta) = \sum_{n=0}^{\infty} \hat{a}_n \cos n\theta \quad (5.4.27)$$

where \hat{a}_n have expressions similar to a_n .

The requirement that the deflection, slope, and moments be finite at the center of the plate forces the following constants to be zero for $n > 1$:

$$\hat{C}_0 = \hat{D}_0 = \hat{C}_1 = \hat{D}_1 = \hat{B}_n = \hat{D}_n = 0$$

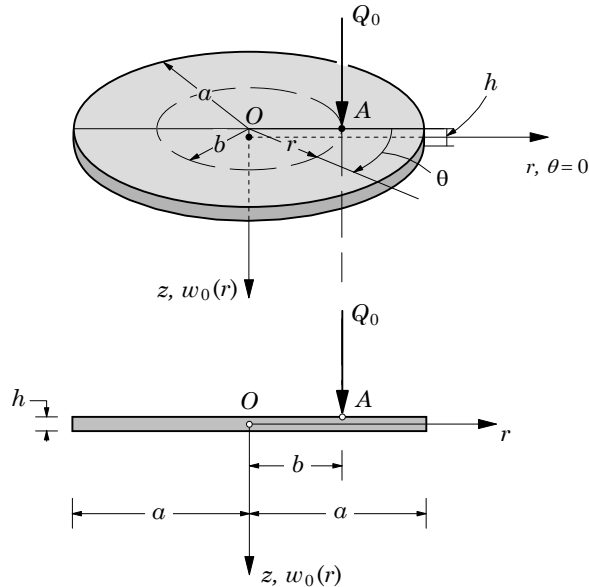


Figure 5.4.2. A circular plate subjected to an asymmetric point load.

Therefore, four constants for each term of the series (5.4.26) and two constants for each term of the series (5.4.27) must be determined. The six constants require six conditions for each n . These conditions are developed next.

The two solutions w_0 and w_i must be continuous at $r = b$

$$w_0 = w_i, \quad \frac{\partial w_0}{\partial r} = \frac{\partial w_i}{\partial r}, \quad \frac{\partial^2 w_0}{\partial r^2} = \frac{\partial^2 w_i}{\partial r^2} \quad (5.4.28)$$

In addition, the shear force is also continuous at all points of the circle except at point A . To represent this discontinuity, first the applied load Q_0 is represented in the form

$$Q_0 = \sum_{n=0}^{\infty} Q_n^0 \cos n\theta = \frac{Q_0}{2\pi} \left(\frac{1}{2} + \sum_{n=1}^{\infty} \cos n\theta \right) \quad (5.4.29)$$

Next the condition for the discontinuity of shear force is written as [see Eq. (5.2.17a)]

$$D(\nabla^2 w_0)_{r=b} - D(\nabla^2 w_i)_{r=b} = \frac{Q_0}{2\pi} \left(\frac{1}{2} + \sum_{n=1}^{\infty} \cos n\theta \right) \quad (5.4.30)$$

The outer region also has two specified boundary conditions, the nature of which depends on the type of support. For instance, if the plate is clamped, we have

$$w_0(a) = 0, \quad \left(\frac{\partial w_0}{\partial r} \right)_{r=a} = 0 \quad (5.4.31)$$

Equations (5.4.28), (5.4.30), and (5.4.31) provide the necessary six conditions to determine the six constants.

For a clamped circular plate, the functions $a_0(r), \dots, \hat{a}_n(r)$ are obtained as [see Timoshenko and Woinowsky-Krieger (1970)]

$$\begin{aligned} a_0 &= \frac{Q_0 a^2}{16\pi D} \left[2(\beta^2 + \bar{r}^2) \log \bar{r} + (1 + \beta^2)(1 - \bar{r}^2) \right] \\ \hat{a}_0 &= \frac{Q_0 a^2}{16\pi D} \left[2(\beta^2 + \bar{r}^2) \log \beta + (1 - \beta^2)(1 + \bar{r}^2) \right] \\ a_1 &= -\frac{Q_0 ab}{16\pi D} \left[\frac{\beta^2}{\bar{r}} + 2(1 - \beta^2)\bar{r} - (2 - \beta^2)\bar{r}^3 - 4\bar{r} \log \frac{1}{\bar{r}} \right] \\ \hat{a}_1 &= -\frac{Q_0 ab}{16\pi D} \left[2(1 - \beta^2)\bar{r} + \frac{(1 - \beta^2)^2}{\beta^2}\bar{r}^3 - 4\bar{r} \log \frac{1}{\beta} \right] \\ a_n &= \frac{Q_0 a^2 \alpha^n}{8\pi D} \left\{ \bar{r}^n \left[(n-1)\beta^2 - n + (n-1)\bar{r}^2 - \frac{n(n-1)}{n+1}\beta^2\bar{r}^2 \right] \right. \\ &\quad \left. + \frac{1}{\bar{r}^n} \left(\bar{r}^2 - \frac{n-1}{n+1}\beta^2 \right) \right\} \\ \hat{a}_n &= \frac{Q_0 a^2 \alpha^n}{8\pi D} \left\{ \bar{r}^n \left[(n-1)\beta^2 - n + \frac{1}{\beta^{n-2}} \right] + \frac{n-1}{n+1}\bar{r}^{n+2} \left[1 + n(1 - \beta^2) - \frac{1}{\beta^{2n}} \right] \right\} \end{aligned} \quad (5.4.32)$$

where $\alpha_n = \beta^n / [n(n-1)]$, $\bar{r} = r/a$ and $\beta = b/a$.

The deflection under the load is given by

$$w_0(b, 0) = \frac{Q_0 a^2}{16\pi D} (1 - \beta^2)^2 \quad (5.4.33)$$

5.4.6 The Ritz Solutions

Here, we present the Ritz formulation for the bending of circular plates under general loads and boundary conditions. The weak formulation or the statement of virtual work for this case was already presented in Eq. (5.2.23). For the linear case, the inplane deformation is uncoupled from the bending deformation. Hence, the virtual work statement in Eq. (5.2.23) is simplified for the present case by setting the nonlinear terms, time derivative terms, and terms involving the inplane displacements (u_0, v_0) to zero. We obtain

$$0 = \int_{\Omega} \left[-M_{rr} \frac{\partial^2 \delta w_0}{\partial r^2} - M_{\theta\theta} \left(\frac{1}{r} \frac{\partial \delta w_0}{\partial r} + \frac{1}{r^2} \frac{\partial^2 \delta w_0}{\partial \theta^2} \right) - 2M_{r\theta} \left(\frac{1}{r} \frac{\partial^2 \delta w_0}{\partial r \partial \theta} - \frac{1}{r^2} \frac{\partial \delta w_0}{\partial \theta} \right) - (q - kw_0) \delta w_0 \right] r dr d\theta \quad (5.4.34)$$

where Ω denotes the r - θ plane ($z = 0$). Rewriting Eq. (5.4.34) in terms of the displacements by employing the plate constitutive equations (5.2.47a–c), we obtain

$$\begin{aligned} 0 = \int_{\Omega} & \left\{ \left[D_{11} \frac{\partial^2 w_0}{\partial r^2} + D_{12} \left(\frac{1}{r} \frac{\partial w_0}{\partial r} + \frac{1}{r^2} \frac{\partial^2 w_0}{\partial \theta^2} \right) + M_{rr}^T \right] \frac{\partial^2 \delta w_0}{\partial r^2} \right. \\ & + \left[D_{12} \frac{\partial^2 w_0}{\partial r^2} + D_{22} \left(\frac{1}{r} \frac{\partial w_0}{\partial r} + \frac{1}{r^2} \frac{\partial^2 w_0}{\partial \theta^2} \right) + M_{\theta\theta}^T \right] \left(\frac{1}{r} \frac{\partial \delta w_0}{\partial r} + \frac{1}{r^2} \frac{\partial^2 \delta w_0}{\partial \theta^2} \right) \\ & \left. + 4D_{66} \left(\frac{1}{r} \frac{\partial^2 w_0}{\partial r \partial \theta} - \frac{1}{r^2} \frac{\partial w_0}{\partial \theta} \right) \left(\frac{1}{r} \frac{\partial^2 \delta w_0}{\partial r \partial \theta} - \frac{1}{r^2} \frac{\partial \delta w_0}{\partial \theta} \right) \right\} r dr d\theta \\ & - \int_{\Omega} (q - kw_0) \delta w_0 r dr d\theta \end{aligned} \quad (5.4.35a)$$

Rearranging the terms, we arrive at

$$\begin{aligned} 0 = \int_{\Omega} & \left[D_{11} \frac{\partial^2 w_0}{\partial r^2} \frac{\partial^2 \delta w_0}{\partial r^2} + D_{12} \frac{1}{r} \left(\frac{\partial w_0}{\partial r} \frac{\partial^2 \delta w_0}{\partial r^2} + \frac{\partial \delta w_0}{\partial r} \frac{\partial^2 w_0}{\partial r^2} \right) \right. \\ & + \frac{1}{r} \frac{\partial^2 w_0}{\partial \theta^2} \frac{\partial^2 \delta w_0}{\partial r^2} + \frac{1}{r} \frac{\partial^2 \delta w_0}{\partial \theta^2} \frac{\partial^2 w_0}{\partial r^2} \\ & + D_{22} \left(\frac{1}{r} \frac{\partial w_0}{\partial r} + \frac{1}{r^2} \frac{\partial^2 w_0}{\partial \theta^2} \right) \left(\frac{1}{r} \frac{\partial \delta w_0}{\partial r} + \frac{1}{r^2} \frac{\partial^2 \delta w_0}{\partial \theta^2} \right) \\ & + 4D_{66} \left(\frac{1}{r} \frac{\partial^2 w_0}{\partial r \partial \theta} - \frac{1}{r^2} \frac{\partial w_0}{\partial \theta} \right) \left(\frac{1}{r} \frac{\partial^2 \delta w_0}{\partial r \partial \theta} - \frac{1}{r^2} \frac{\partial \delta w_0}{\partial \theta} \right) \\ & \left. + M_{rr}^T \frac{\partial^2 \delta w_0}{\partial r^2} + M_{\theta\theta}^T \left(\frac{1}{r} \frac{\partial \delta w_0}{\partial r} + \frac{1}{r^2} \frac{\partial^2 \delta w_0}{\partial \theta^2} \right) - (q - kw_0) \delta w_0 \right] r dr d\theta \end{aligned} \quad (5.4.35b)$$

Now it is easy to identify the total potential energy functional $\Pi(w_0)$ from Eq. (5.4.35b). It is given by

$$\begin{aligned} \Pi(w_0) = & \int_{\Omega} \left[\frac{D_{11}}{2} \left(\frac{\partial^2 w_0}{\partial r^2} \right)^2 + D_{12} \left(\frac{1}{r} \frac{\partial w_0}{\partial r} \frac{\partial^2 w_0}{\partial r^2} + \frac{1}{r^2} \frac{\partial^2 w_0}{\partial \theta^2} \frac{\partial^2 w_0}{\partial r^2} \right) \right. \\ & + \frac{D_{22}}{2} \left(\frac{1}{r} \frac{\partial w_0}{\partial r} + \frac{1}{r^2} \frac{\partial^2 w_0}{\partial \theta^2} \right)^2 + 2D_{66} \left(\frac{1}{r} \frac{\partial^2 w_0}{\partial r \partial \theta} - \frac{1}{r^2} \frac{\partial w_0}{\partial \theta} \right)^2 \\ & \left. + M_{rr}^T \frac{\partial^2 w_0}{\partial r^2} + M_{\theta\theta}^T \left(\frac{1}{r} \frac{\partial w_0}{\partial r} + \frac{1}{r^2} \frac{\partial^2 w_0}{\partial \theta^2} \right) - qw_0 + \frac{k}{2} w_0^2 \right] r dr d\theta \quad (5.4.36) \end{aligned}$$

For an isotropic plate, the total potential energy functional is given by

$$\begin{aligned} \Pi(w_0) = & \int_{\Omega} \left\{ \frac{D}{2} \left[\left(\frac{\partial^2 w_0}{\partial r^2} \right)^2 + 2 \frac{\nu}{r} \left(\frac{\partial w_0}{\partial r} + \frac{1}{r} \frac{\partial^2 w_0}{\partial \theta^2} \right) \frac{\partial^2 w_0}{\partial r^2} \right. \right. \\ & + \left(\frac{1}{r} \frac{\partial w_0}{\partial r} + \frac{1}{r^2} \frac{\partial^2 w_0}{\partial \theta^2} \right)^2 + 2(1-\nu) \left(\frac{1}{r} \frac{\partial^2 w_0}{\partial r \partial \theta} - \frac{1}{r^2} \frac{\partial w_0}{\partial \theta} \right)^2 \\ & \left. \left. + \frac{M_T}{1-\nu} \left(\frac{\partial^2 w_0}{\partial r^2} + \frac{1}{r} \frac{\partial w_0}{\partial r} + \frac{1}{r^2} \frac{\partial^2 w_0}{\partial \theta^2} \right) - qw_0 + \frac{k}{2} w_0^2 \right\} r dr d\theta \quad (5.4.37) \right. \end{aligned}$$

where

$$M_T(r, \theta) = E\alpha \int_{-\frac{h}{2}}^{\frac{h}{2}} \Delta T(r, \theta, z) z dz \quad (5.4.38)$$

Assume an N -parameter Ritz approximation of the form

$$w_0(r, \theta) \approx \sum_{j=1}^N c_j \varphi_j(r, \theta) + \varphi_0(r, \theta) \quad (5.4.39)$$

Substituting Eq. (5.4.39) into Eq. (5.4.35b), we find

$$0 = \sum_{j=1}^N \left(R_{ij}^1 + R_{ij}^2 \right) c_j - \left(F_j^1 + F_i^2 \right) \quad (5.4.40a)$$

where

$$\begin{aligned} R_{ij}^1 = & \int_{\Omega} \left[D_{11} \frac{\partial^2 \varphi_i}{\partial r^2} \frac{\partial^2 \varphi_j}{\partial r^2} + D_{22} \left(\frac{1}{r} \frac{\partial \varphi_i}{\partial r} + \frac{1}{r^2} \frac{\partial^2 \varphi_i}{\partial \theta^2} \right) \left(\frac{1}{r} \frac{\partial \varphi_j}{\partial r} + \frac{1}{r^2} \frac{\partial^2 \varphi_j}{\partial \theta^2} \right) \right. \\ & + \frac{D_{12}}{r} \left(\frac{\partial \varphi_i}{\partial r} \frac{\partial^2 \varphi_j}{\partial r^2} + \frac{\partial \varphi_j}{\partial r} \frac{\partial^2 \varphi_i}{\partial r^2} + \frac{1}{r} \frac{\partial^2 \varphi_i}{\partial \theta^2} \frac{\partial^2 \varphi_j}{\partial r^2} + \frac{1}{r} \frac{\partial^2 \varphi_j}{\partial \theta^2} \frac{\partial^2 \varphi_i}{\partial r^2} \right) \\ & \left. + 4D_{66} \left(\frac{1}{r} \frac{\partial^2 \varphi_i}{\partial r \partial \theta} - \frac{1}{r^2} \frac{\partial \varphi_i}{\partial \theta} \right) \left(\frac{1}{r} \frac{\partial^2 \varphi_j}{\partial r \partial \theta} - \frac{1}{r^2} \frac{\partial \varphi_j}{\partial \theta} \right) \right] r dr d\theta \quad (5.4.40b) \end{aligned}$$

$$R_{ij}^2 = k \int_{\Omega} \varphi_i \varphi_j r dr d\theta \quad (5.4.40c)$$

$$\begin{aligned} F_i^1 &= \int_{\Omega} \left[-D_{11} \frac{\partial^2 \varphi_i}{\partial r^2} \frac{\partial^2 \varphi_0}{\partial r^2} - D_{22} \left(\frac{1}{r} \frac{\partial \varphi_i}{\partial r} + \frac{1}{r^2} \frac{\partial^2 \varphi_i}{\partial \theta^2} \right) \left(\frac{1}{r} \frac{\partial \varphi_0}{\partial r} + \frac{1}{r^2} \frac{\partial^2 \varphi_0}{\partial \theta^2} \right) \right. \\ &\quad - \frac{D_{12}}{r} \left(\frac{\partial \varphi_i}{\partial r} \frac{\partial^2 \varphi_0}{\partial r^2} + \frac{\partial \varphi_0}{\partial r} \frac{\partial^2 \varphi_i}{\partial r^2} + \frac{1}{r} \frac{\partial^2 \varphi_i}{\partial \theta^2} \frac{\partial^2 \varphi_0}{\partial r^2} + \frac{1}{r} \frac{\partial^2 \varphi_0}{\partial \theta^2} \frac{\partial^2 \varphi_i}{\partial r^2} \right) \\ &\quad \left. - 4D_{66} \left(\frac{1}{r} \frac{\partial^2 \varphi_i}{\partial r \partial \theta} - \frac{1}{r^2} \frac{\partial \varphi_i}{\partial \theta} \right) \left(\frac{1}{r} \frac{\partial^2 \varphi_0}{\partial r \partial \theta} - \frac{1}{r^2} \frac{\partial \varphi_0}{\partial \theta} \right) + q \varphi_i \right] r dr d\theta \end{aligned} \quad (5.4.40d)$$

$$F_i^2 = -\frac{1}{1-\nu} \int_{\Omega} M_T(r, \theta) \left[\frac{\partial^2 \varphi_i}{\partial r^2} + \left(\frac{1}{r} \frac{\partial \varphi_i}{\partial r} + \frac{1}{r^2} \frac{\partial^2 \varphi_i}{\partial \theta^2} \right) \right] r dr d\theta \quad (5.4.40e)$$

This completes the formulation of the Ritz equations for an arbitrarily loaded, orthotropic circular plate. Next, we consider an example of application of the formulation.

Consider a clamped circular plate on elastic foundation and subjected to asymmetric loading of the form (see Section 5.4.2)

$$q(r, \theta) = q_1 \frac{r}{a} \cos \theta \quad (5.4.41)$$

and with a temperature distribution of the form

$$\Delta T(r, \theta, z) = T(z) \cos \theta \quad (5.4.42)$$

so that $M_T = M_T^0 \cos \theta$, where

$$M_T^0 = E\alpha \int_{-\frac{h}{2}}^{\frac{h}{2}} T(z) z dz \quad (5.4.43)$$

For this case, the geometric boundary conditions are

$$w_0(r, \theta) = \frac{\partial w_0}{\partial r} = 0 \text{ at } r = a \text{ and } \frac{\partial w_0}{\partial r} = 0 \text{ at } r = 0 \quad (5.4.44)$$

for any θ . For one-parameter Ritz solution, we can assume

$$w_0(r, \theta) \approx c_1 \varphi_1(r, \theta) \equiv c_1 f_1(r) f_2(\theta) \quad (5.4.45)$$

where f_1 is only a function of r and f_2 is only a function of θ . Therefore, the conditions on the approximation functions

$$\varphi_i(r, \theta) = \frac{\partial \varphi_i}{\partial r} = 0 \text{ at } r = a \text{ and } \frac{\partial \varphi_i}{\partial r} = 0 \text{ at } r = 0 \quad (5.4.46)$$

translate into the conditions $f_1(a) = f'_1(a) = f'_1(0) = 0$. Clearly, the choice

$$f_1(r) = 1 - 3 \left(\frac{r}{a} \right)^2 + 2 \left(\frac{r}{a} \right)^3 \quad (5.4.47)$$

satisfies the conditions.

The form of the load in Eq. (5.4.41) suggests that $f_2 = \cos \theta$. Since

$$f'_1 = -\frac{6r}{a^2} + \frac{6r^2}{a^3}, \quad f''_1 = -\frac{6}{a^2} + \frac{12r}{a^3}$$

it is clear that the integrals

$$\int_0^a \frac{1}{r} f_1 f''_1 dr, \quad \int_0^a \frac{1}{r^3} f_1 f_1 dr \quad (5.4.48)$$

are to be evaluated in R_{11}^1 of Eq. (5.4.40a); however, they do not exist because of the logarithmic singularity. Thus, $f_1(r)$ defined in Eq. (5.4.47) is not admissible.

The next function that satisfies the boundary conditions $f_1(a) = f'_1(a) = f''_1(0) = 0$ is

$$f_1(r) = \left[1 - \left(\frac{r}{a} \right)^2 \right]^2 = 1 - 2 \left(\frac{r}{a} \right)^2 + \left(\frac{r}{a} \right)^4 \quad (5.4.49)$$

However, this too does not permit the evaluation of the integrals in Eq. (5.4.48).

The next admissible function is

$$f_1(r) = \frac{r}{a} \left[1 - \left(\frac{r}{a} \right)^2 \right]^2 = \frac{r}{a} - 2 \left(\frac{r}{a} \right)^3 + \left(\frac{r}{a} \right)^5 \quad (5.4.50)$$

which allow the evaluation of the necessary integrals. Substituting $\varphi_1 = f_1(r) \cos \theta$ into R_{11}^1 of Eq. (5.4.40b) with $D_{11} = D_{22} = D$, $D_{12} = \nu D$, and $2D_{66} = (1 - \nu)D$ and into F_1^1 and F_1^2 of Eqs. (5.4.40d,e), we obtain

$$\begin{aligned} R_{11}^1 &= D \int_0^{2\pi} \int_0^a \left\{ \left[f''_1 f''_1 + \left(\frac{1}{r} f'_1 - \frac{1}{r^2} f_1 \right)^2 + \frac{2\nu}{r} \left(f'_1 f''_1 - \frac{1}{r} f_1 f''_1 \right) \right. \right. \\ &\quad \left. \left. + \frac{M_T^0}{1-\nu} \right] \cos^2 \theta + 2(1-\nu) \left(\frac{1}{r} f'_1 - \frac{1}{r^2} f_1 \right)^2 \sin^2 \theta \right\} r dr d\theta \\ &= \frac{D\pi}{a^2} \left[6 + \frac{2}{3} - \nu + \frac{7\nu}{3} + \frac{4(1-\nu)}{3} \right] = \frac{8D\pi}{a^2} \end{aligned} \quad (5.4.51a)$$

$$R_{11}^2 = k \int_0^{2\pi} \int_0^a f_1 f_1 \cos^2 \theta r dr d\theta = \frac{ka^2\pi}{60} \quad (5.4.51b)$$

$$F_1^1 = \int_0^{2\pi} \int_0^a \left(q_1 \frac{r}{a} \cos \theta \right) f_1 \cos \theta r dr d\theta = \frac{q_1 a^2 \pi}{24} \quad (5.4.51c)$$

$$F_1^2 = -\frac{M_T^0}{1-\nu} \int_0^{2\pi} \int_0^a \left(f''_1 + \frac{1}{r} f'_1 - \frac{1}{r^2} f_1 \right) \cos^2 \theta r dr d\theta = \frac{8M_T^0 \pi}{15(1-\nu)} \quad (5.4.51d)$$

where we have used the identities

$$\cos^2 \theta = \frac{1}{2} (1 + \cos 2\theta), \quad \sin^2 \theta = \frac{1}{2} (1 - \cos 2\theta)$$

to evaluate the integrals. Thus, we have

$$(R_{11}^1 + R_{11}^2) c_1 = F_1^1 + F_1^2$$

Solving for c_1 , we obtain

$$c_1 = \frac{1}{\left(1 + \frac{ka^4}{480D}\right)} \left[\frac{q_1 a^4}{192D} + \frac{M_T^0 a^2}{15(1-\nu)D} \right]$$

and the Ritz solution becomes

$$w_0(r, \theta) = \frac{1}{\left(1 + \frac{ka^4}{480D}\right)} \left[\frac{q_1 a^4}{192D} + \frac{M_T^0 a^2}{15(1-\nu)D} \right] \left\{ \frac{r}{a} \left[1 - \left(\frac{r}{a} \right)^2 \right]^2 \right\} \cos \theta \quad (5.4.52)$$

This solution coincides with the exact solution in Eq. (5.4.15) for the case $q_0 = 0$, $k = 0$, and $M_T^0 = 0$.

5.5 Free Vibration

5.5.1 Introduction

In the preceding sections of this chapter, we considered bending of circular and annular plates. Here we consider natural vibration. The equation of motion of an isotropic plate is given by Eq. (5.2.53)

$$D\nabla^2\nabla^2 w_0 + kw_0 + I_0 \frac{\partial^2 w_0}{\partial t^2} - I_2 \frac{\partial^2}{\partial t^2} (\nabla^2 w_0) = 0 \quad (5.5.1)$$

where $I_0 = \rho h$ and $I_2 = \rho h^3/12$ are the principal and rotatory inertias, respectively. When free vibration is assumed, the deflection is periodic and can be expressed as

$$w_0(r, \theta, t) = W(r, \theta) \cos \omega t \quad (5.5.2)$$

where ω is the circular frequency of vibration (radians per unit time), and W is a function of only r and θ . Substituting Eq. (5.5.2) into Eq. (5.5.1), we obtain

$$D\nabla^2\nabla^2 W + kW - I_0\omega^2 W + I_2\omega^2\nabla^2 W = 0 \quad (5.5.3)$$

The presence of the rotatory inertia I_2 presents difficulties while it contributes little to the frequencies, especially to the fundamental frequency. Hence, we neglect the rotatory inertia term. Equation (5.5.3) becomes

$$(\nabla^4 - \beta^4) W = 0 \quad (5.5.4)$$

where

$$\beta^4 = \frac{I_0\omega^2 - k}{D} \quad (5.5.5)$$

Equation (5.5.4) can be factored into

$$(\nabla^2 + \beta^2)(\nabla^2 - \beta^2) W = 0 \quad (5.5.6)$$

so that the complete solution to Eq. (5.5.6) can be obtained by superimposing the solutions of the equations

$$\nabla^2 W_1 + \beta^2 W_1 = 0, \quad \nabla^2 W_2 - \beta^2 W_2 = 0 \quad (5.5.7)$$

5.5.2 General Analytical Solution

We assume solution to Eq. (5.5.4) in the form of the general Fourier series

$$W(r, \theta) = \sum_{n=0}^{\infty} W_n(r) \cos n\theta + \sum_{n=1}^{\infty} W_n^*(r) \sin n\theta \quad (5.5.8)$$

Substitution of Eq. (5.5.8) into Eq. (5.5.7) yields

$$\begin{aligned} \frac{d^2 W_{n1}}{dr^2} + \frac{1}{r} \frac{dW_{n1}}{dr} - \left(\frac{n^2}{r^2} - \beta^2 \right) W_{n1} &= 0 \\ \frac{d^2 W_{n2}}{dr^2} + \frac{1}{r} \frac{dW_{n2}}{dr} - \left(\frac{n^2}{r^2} - \beta^2 \right) W_{n2} &= 0 \end{aligned} \quad (5.5.9)$$

and two identical equations for W_n^* (W_{n1}^* and W_{n2}^*). Equations (5.5.9) are a form of Bessel's equations, which have the solutions

$$W_{n1} = A_n J_n(\beta r) + B_n Y_n(\beta r), \quad W_{n2} = C_n I_n(\beta r) + D_n K_n(\beta r) \quad (5.5.10)$$

respectively, where J_n and Y_n are the Bessel functions of first and second kind, respectively, and I_n and K_n are the modified Bessel functions of the first and second kind, respectively [see McLachlan (1948)]. The coefficients A_n , B_n , C_n , and D_n , which determine the mode shapes, are solved using the boundary conditions. Thus, the general solution of Eq. (5.5.4) is

$$\begin{aligned} W(r, \theta) &= \sum_{n=0}^{\infty} [A_n J_n(\beta r) + B_n Y_n(\beta r) + C_n I_n(\beta r) + D_n K_n(\beta r)] \cos n\theta \\ &\quad + \sum_{n=1}^{\infty} [A_n^* J_n(\beta r) + B_n^* Y_n(\beta r) + C_n^* I_n(\beta r) + D_n^* K_n(\beta r)] \sin n\theta \end{aligned} \quad (5.5.11)$$

For solid circular plates, the terms involving Y_n and K_n in the solution (5.5.11) must be discarded in order to avoid singularity of deflections and stresses (i.e., avoid infinite values) at the origin, $r = 0$. In addition, if the boundary conditions are symmetrically applied about a diameter of the plate, then the second expression containing $\sin n\theta$ is not needed to represent the solution. Then, the n th term of Eq. (5.5.11) becomes

$$W_n(r, \theta) = [A_n J_n(\beta r) + C_n I_n(\beta r)] \cos n\theta \quad (5.5.12)$$

for $n = 0, 1, \dots, \infty$. A *nodal line* is one that has zero deflection (i.e., $W_n = 0$). For circular plates, nodal lines are either concentric circles or diameters. The nodal diameters are determined by $n\theta = \pi/2, 3\pi/2, \dots$

Next we apply boundary conditions (which are homogeneous) to obtain a pair of algebraic equations among A_n and C_n for any n . For a nontrivial solution of the pair, the determinant of the matrix representing the two equations is set to zero. The resulting equation is known as the characteristic polynomial. In the following paragraphs, we consider several typical boundary conditions.

5.5.3 Clamped Circular Plates

The boundary conditions are

$$W_n = 0 \quad \text{and} \quad \frac{\partial W_n}{\partial r} = 0 \quad \text{at } r = a \text{ for any } \theta \quad (5.5.13)$$

Using Eq. (5.5.12) in Eq. (5.5.13), we obtain

$$\begin{bmatrix} J_n(\lambda) & I_n(\lambda) \\ J'_n(\lambda) & I'_n(\lambda) \end{bmatrix} \begin{Bmatrix} A_n \\ C_n \end{Bmatrix} = \begin{Bmatrix} 0 \\ 0 \end{Bmatrix} \quad (5.5.14)$$

where $\lambda = \beta a$ and the prime denotes differentiation with respect to the argument, βr . For nontrivial solution, we set the determinant of the coefficient matrix in Eq. (5.5.14) to zero

$$\begin{vmatrix} J_n(\lambda) & I_n(\lambda) \\ J'_n(\lambda) & I'_n(\lambda) \end{vmatrix} = 0 \quad (5.5.15)$$

Expanding the determinant and using the recursion relations

$$\lambda J'_n(\lambda) = nJ_n(\lambda) - \lambda J_{n+1}(\lambda), \quad \lambda I'_n(\lambda) = nI_n(\lambda) + \lambda I_{n+1}(\lambda) \quad (5.5.16)$$

we find

$$J_n(\lambda)I_{n+1}(\lambda) + I_n(\lambda)J_{n+1}(\lambda) = 0 \quad (5.5.17a)$$

or

$$\frac{J_{n+1}(\lambda)}{J_n(\lambda)} + \frac{I_{n+1}(\lambda)}{I_n(\lambda)} = 0 \quad (5.5.17b)$$

which is called the *frequency equation*. The roots λ of Eq. (5.5.17), called the eigenvalues, are used to determine the frequencies ω [see Eq. (5.5.5)]

$$\omega^2 = \frac{D\beta^4 + k}{I_0} = \frac{D\lambda^4 + ka^4}{a^4 I_0} \quad (5.5.18)$$

When $k = 0$, Eq. (5.5.18) reduces to

$$\omega^2 = \frac{D\lambda^4}{a^4 I_0} \quad \text{or} \quad \lambda^2 = \omega a^2 \sqrt{I_0/D} \quad (5.5.19)$$

Note that the frequencies of a clamped circular plate do not depend on Poisson's ratio.

There are an infinite number of roots λ of Eq. (5.5.17) for each value of n , which represents the number of nodal diameters. For instance, when $n = 0$ (i.e., when the only nodal diameter is the boundary circle) the roots in order of magnitude

correspond with $1, 2, \dots, m$ nodal circles. The mode shape associated with λ is determined using Eq. (5.5.15)

$$\frac{A_n}{C_n} = -\frac{I_n(\lambda)}{J_n(\lambda)} \quad (5.5.20)$$

where λ is the solution (i.e., root) of Eq. (5.5.17). The radii of nodal circles $\xi = r/a$ are determined from Eqs. (5.5.20) and (5.5.12)

$$\frac{J_n(\lambda\xi)}{J_n(\lambda)} = \frac{I_n(\lambda\xi)}{I_n(\lambda)} \quad (5.5.21)$$

Values of λ^2 , taken from Leissa (1969), McLachlan (1948), and Kantham (1958), are presented in Table 5.5.1, where n denotes the number of nodal diameters and m is the number of nodal circles, not including the circle $r = a$. Figure 5.5.1 shows typical nodal patterns for a clamped circular plate.

Table 5.5.1. Values of $\lambda^2 = \omega a^2 \sqrt{I_0/D}$ for a clamped circular plate.

$n \rightarrow$	0	1	2	3	4	5
$m \downarrow$						
0	10.2158	21.26	34.88	51.04	69.6659	90.7390
1	39.771	60.82	84.58	111.01	140.1079	171.8029
2	89.104	120.08	153.81	190.30	229.5185	271.4283
3	158.183	199.06	242.71	289.17	338.4113	390.3896

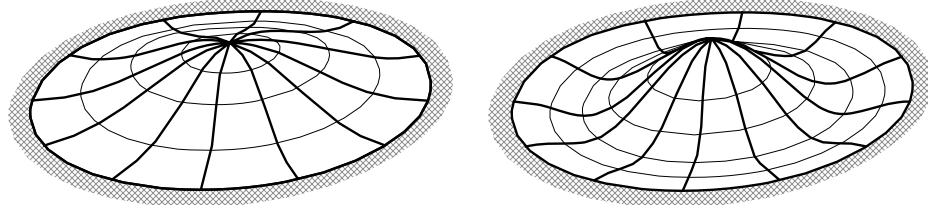


Figure 5.5.1. Typical modes of free vibration of a clamped circular plate, showing the nodal diameters and nodal circles.

5.5.4 Simply Supported Circular Plates

The boundary conditions are

$$W_n = 0 \text{ and } M_{rr} = 0 \text{ at } r = a \text{ for any } \theta \quad (5.5.22)$$

In addition, we note that $\partial^2 w_0 / \partial \theta^2 = 0$ on the boundary. Use of Eq. (5.5.12) in Eq. (5.5.21) results in the following two equations:

$$\begin{aligned} A_n J_n(\lambda) + C_n I_n(\lambda) &= 0 \\ A_n \left[J_n''(\lambda) + \frac{\nu}{\lambda} J_n'(\lambda) \right] + C_n \left[I_n''(\lambda) + \frac{\nu}{\lambda} I_n'(\lambda) \right] &= 0 \end{aligned} \quad (5.5.23)$$

These equations lead to the frequency equation

$$\frac{J_{n+1}(\lambda)}{J_n(\lambda)} + \frac{I_{n+1}(\lambda)}{I_n(\lambda)} = \frac{2\lambda}{1-\nu} \quad (5.5.24)$$

The mode shape is now determined using Eq. (5.5.23a,b)

$$\frac{A_n}{C_n} = -\frac{I_n(\lambda)}{J_n(\lambda)} \quad (5.5.25)$$

where λ is a solution of Eq. (5.5.24).

Table 5.5.2 contains values of λ^2 for various values of n and m and Poisson's ratio $\nu = 0.3$.

Table 5.5.2. Values of $\lambda^2 = \omega a^2 \sqrt{I_0/D}$ for a simply supported circular plate ($\nu = 0.3$).

$n \rightarrow$ $m \downarrow$	0	1	2
0	4.977	13.94	25.65
1	29.76	48.51	70.14
2	74.20	102.80	134.33
3	138.34	176.84	218.24

5.5.5 The Ritz Solutions

Natural frequencies of solid circular plates with other boundary conditions and annular plates with various boundary conditions can be found in the papers listed at the back of the book. In the general case, analytical solutions of free vibration lead to mathematically complex equations, often in terms of Bessel functions, and the solutions are difficult to obtain, requiring the use of approximate methods of solution. Here, the Ritz formulation for free vibration of circular plates is presented.

The equation of motion in Eq. (5.2.41), with M_{rr} , $M_{r\theta}$, and $M_{\theta\theta}$ given by Eqs. (5.2.47a–c) and no applied loads, is valid for free vibration analysis. The solution to this equation is again sought in the form of Eq. (5.5.2). The variational (or weak) form of the resulting equation is the same as that in Eq. (5.4.35b) without the thermal and mechanical loads, but with the addition of appropriate terms corresponding to the inertia terms. We find that

$$0 = \int_{\Omega} \left\{ D_{11} \frac{\partial^2 W}{\partial r^2} \frac{\partial^2 \delta W}{\partial r^2} + D_{12} \frac{1}{r} \left(\frac{\partial W}{\partial r} \frac{\partial^2 \delta W}{\partial r^2} + \frac{\partial \delta W}{\partial r} \frac{\partial^2 W}{\partial r^2} \right. \right. \\ \left. \left. + \frac{1}{r} \frac{\partial^2 W}{\partial \theta^2} \frac{\partial^2 \delta W}{\partial r^2} + \frac{1}{r} \frac{\partial^2 \delta W}{\partial \theta^2} \frac{\partial^2 W}{\partial r^2} \right) + kW \delta W \right. \\ \left. + D_{22} \left(\frac{1}{r} \frac{\partial W}{\partial r} + \frac{1}{r^2} \frac{\partial^2 W}{\partial \theta^2} \right) \left(\frac{1}{r} \frac{\partial \delta W}{\partial r} + \frac{1}{r^2} \frac{\partial^2 \delta W}{\partial \theta^2} \right) \right. \\ \left. + 4D_{66} \left(\frac{1}{r} \frac{\partial^2 W}{\partial r \partial \theta} - \frac{1}{r^2} \frac{\partial W}{\partial \theta} \right) \left(\frac{1}{r} \frac{\partial^2 \delta W}{\partial r \partial \theta} - \frac{1}{r^2} \frac{\partial \delta W}{\partial \theta} \right) \right. \\ \left. - \omega^2 \left[I_0 W \delta W + I_2 \left(\frac{\partial W}{\partial r} \frac{\partial \delta W}{\partial r} + \frac{1}{r^2} \frac{\partial W}{\partial \theta} \frac{\partial \delta W}{\partial \theta} \right) \right] \right\} r dr d\theta \quad (5.5.26)$$

where ω is the frequency of free vibration.

Assume an N -parameter Ritz approximation of the form

$$W(r, \theta) \approx \sum_{j=1}^N c_j \varphi_j(r, \theta) \quad (5.5.27)$$

Substituting Eq. (5.5.27) into Eq. (5.5.26), we obtain

$$0 = \sum_{j=1}^N \left(R_{ij}^1 + R_{ij}^2 - \omega^2 M_{ij} \right) c_j \quad (5.5.28)$$

where R_{ij}^1 and R_{ij}^2 are defined in Eqs. (5.4.40b,c), and M_{ij} is defined as

$$M_{ij} = \int_{\Omega} \left[I_0 \varphi_i \varphi_j + I_2 \left(\frac{\partial \varphi_i}{\partial r} \frac{\partial \varphi_j}{\partial r} + \frac{1}{r^2} \frac{\partial \varphi_i}{\partial \theta} \frac{\partial \varphi_j}{\partial \theta} \right) \right] r dr d\theta \quad (5.5.29)$$

In matrix notation, Eq. (5.5.28) has the form of an eigenvalue problem

$$\left([R^1 + R^2] - \omega^2 [M] \right) \{c\} = \{0\} \quad (5.5.30)$$

For a nontrivial solution, the coefficient matrix in Eq. (5.5.30) should be singular, i.e.,

$$|([R^1] + [R^2] - \omega^2 [M])| = 0 \quad (5.5.31)$$

The above formulation is valid also for annular plates.

As an example, consider free vibration of a clamped solid circular plate. For a one-parameter ($N = 1$) Ritz solution, let [see Eqs. (5.4.44) through (5.4.50)]

$$\varphi_1(r, \theta) = f_1(r) \cos n\theta \quad (5.5.32)$$

and compute R_{11}^1 , R_{11}^2 , and M_{11}

$$\begin{aligned} R_{11}^1 &= \int_0^{2\pi} \int_0^a \left\{ \left[D_{11} f_1'' f_1'' + D_{22} \left(\frac{1}{r} f_1' - \frac{n^2}{r^2} f_1 \right)^2 \right. \right. \\ &\quad \left. \left. + 2D_{12} \frac{1}{r} \left(f_1' f_1'' - \frac{n^2}{r} f_1 f_1'' \right) \right] \cos^2 n\theta \right. \\ &\quad \left. + 4D_{66} \left(\frac{n}{r} f_1' - \frac{n}{r^2} f_1 \right)^2 \sin^2 n\theta \right\} r dr d\theta \end{aligned} \quad (5.5.33a)$$

$$R_{11}^2 = k \int_0^{2\pi} \int_0^a f_1 f_1 \cos^2 n\theta r dr d\theta \quad (5.5.33b)$$

$$M_{ij} = \int_0^{2\pi} \int_0^a \left[(I_0 f_1 f_1 + f_1' f_1') \cos^2 n\theta + I_2 \frac{n^2}{r^2} f_1 f_1 \sin^2 n\theta \right] r dr d\theta \quad (5.5.33c)$$

In particular, for $n = 0$, we select the function in Eq. (5.4.49) and obtain the coefficients

$$\begin{aligned} R_{11}^1 &= 2\pi \int_0^a \left(D_{11} f_1'' f_1'' + D_{22} \frac{1}{r^2} f_1' f_1' + 2D_{12} \frac{1}{r} f_1' f_1'' \right) r dr \\ &= \frac{2\pi}{a^2} \left(8D_{11} + \frac{8}{3} D_{22} \right) \end{aligned} \quad (5.5.34a)$$

$$R_{11}^2 = 2\pi k \int_0^a f_1 f_1 r dr = 2\pi k \frac{a^2}{10} \quad (5.5.34b)$$

$$M_{11} = 2\pi \int_0^a (I_0 f_1 f_1 + I_2 f_1' f_1') r dr = 2\pi \left(\frac{a^2}{10} I_0 + \frac{3}{a^2} I_2 \right) \quad (5.5.34c)$$

We find that

$$\lambda^2 = \omega a^2 \sqrt{\frac{I_0}{D_{22}}} = \left[\frac{\frac{80}{3} \left(3 \frac{D_{11}}{D_{22}} + 1 \right) + \frac{a^4 k}{80 D_{22}}}{1 + \frac{30 I_2}{a^2 I_0}} \right]^{\frac{1}{2}} \quad (5.5.35)$$

Clearly, rotatory inertia has the effect of reducing the frequency of vibration while the elastic foundation modulus increases it.

For a clamped isotropic plate without elastic foundation, the frequency becomes ($I_2 = I_0 h^2 / 12$)

$$\lambda^2 = \omega a^2 \sqrt{\frac{I_0}{D}} = 10.328 \left[\frac{1}{1 + 2.5 \frac{h^2}{a^2}} \right]^{\frac{1}{2}} \quad (5.5.36)$$

For very thin plates, say $h/a = 0.01$, the effect of rotatory inertia is negligible. Even for $h/a = 0.1$, the effect is less than 1%. Note that the one-parameter Ritz solution differs from that listed in Table 5.5.1 (for $m = n = 0$) by less than 1%!

For $n = 1$, the function in Eq. (5.4.49) is not admissible and we select the function in Eq. (5.4.50) and obtain

$$R_{11}^1 = \frac{\pi}{a^2} \left[6D_{11} + \frac{2}{3}D_{22} - 2\left(\frac{1}{2} - \frac{7}{6}\right)D_{12} + 4\frac{2}{3}D_{66} \right] \quad (5.5.37a)$$

$$R_{11}^2 = \frac{\pi a^2}{60}k, \quad M_{11} = \frac{a^2}{60}I_0 + \frac{1}{6}I_2 \quad (5.5.37b)$$

The frequency is given by

$$\lambda^2 = \omega a^2 \sqrt{\frac{I_0}{D_{22}}} = \left[\frac{6\frac{D_{11}}{D_{22}} + \frac{2}{3} + \frac{4}{3}\frac{D_{12}+2D_{66}}{D_{22}} + \frac{a^4 k}{60 D_{22}}}{1 + \frac{10 I_2}{a^2 I_0}} \right]^{\frac{1}{2}} \quad (5.5.38)$$

For a clamped isotropic plate without elastic foundation, the frequency for the case $m = 0$, $n = 1$ becomes ($I_2 = I_0 h^2 / 12$)

$$\lambda^2 = \omega a^2 \sqrt{\frac{I_0}{D}} = 21.91 \left[\frac{1}{1 + \frac{5}{6} \frac{h^2}{a^2}} \right]^{\frac{1}{2}} \quad (5.5.39)$$

When rotatory inertia is neglected, the frequency predicted by Eq. (5.5.39) differs from the value given in Table 5.5.1 only by 3%.

For other values of n , one must select functions that are admissible (i.e., allow evaluation of the integrals). Generally, higher values of n require higher-order functions $f_i(r)$.

5.6 Axisymmetric Buckling

5.6.1 Governing Equations

Here we consider axisymmetric buckling of circular plates under inplane radial compressive load, $N_{rr} = -\hat{N}_{rr}$ (Figure 5.6.1). The equation of equilibrium for this case can be deduced from Eq. (5.2.30) as

$$-\frac{1}{r} \frac{d}{dr} (rQ_r) + \frac{1}{r} \frac{d}{dr} \left(r\hat{N}_{rr} \frac{dw}{dr} \right) = 0 \quad (5.6.1)$$

where w denotes the transverse deflection at the onset of buckling and Q_r is given in terms of the deflection by Eq. (5.3.4). Substituting for rQ_r from (5.3.4) into Eq. (5.6.1), we obtain [see Eqs. (5.3.6)–(5.3.8)]

$$D_{11} \frac{1}{r} \frac{d}{dr} \left\{ r \frac{d}{dr} \left[\frac{1}{r} \frac{d}{dr} \left(r \frac{dw}{dr} \right) \right] + \left(\frac{D_{11} - D_{22}}{D_{11}} \right) \frac{1}{r} \frac{dw}{dr} \right\} + \frac{1}{r} \frac{d}{dr} \left(r\hat{N}_{rr} \frac{dw}{dr} \right) = 0 \quad (5.6.2)$$

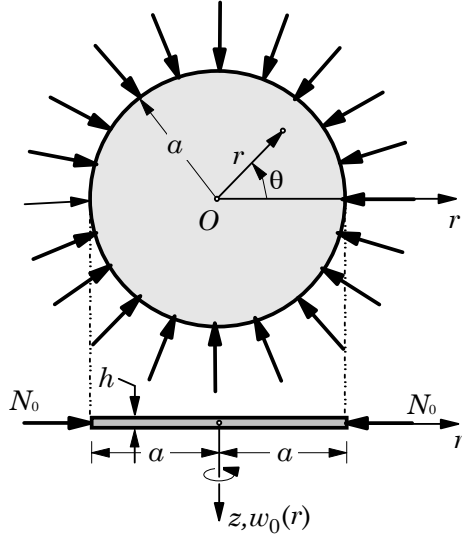


Figure 5.6.1. Buckling of a circular plate under uniform radial compressive load.

For isotropic plates Eq. (5.6.2) becomes

$$\frac{D}{r} \frac{d}{dr} \left\{ r \frac{d}{dr} \left[\frac{1}{r} \frac{d}{dr} \left(r \frac{dw}{dr} \right) \right] \right\} + \frac{1}{r} \frac{d}{dr} \left(r \hat{N}_{rr} \frac{dw}{dr} \right) = 0 \quad (5.6.3)$$

The boundary conditions involve specifying

$$w \quad \text{or} \quad r \left(Q_r - \hat{N}_{rr} \frac{dw}{dr} \right) \quad (5.6.4a)$$

and

$$\frac{dw}{dr} \quad \text{or} \quad r M_{rr} \quad (5.6.4b)$$

5.6.2 General Solution

Here we consider exact buckling solutions of circular plates. Integration of Eq. (5.6.1) gives the result

$$-Q_r(r) + \hat{N}_{rr} \frac{dw}{dr} = A$$

where A is a constant of integration. Since $Q_r - \hat{N}_{rr}(dw/dr) = 0$ at $r = 0$ [see Eq. (5.6.4a)], we obtain $A = 0$. Hence, we have

$$Q_r = \hat{N}_{rr} \frac{dw}{dr}$$

We write the above equation in terms of $\phi = (dw/dr)$, which represents the angle between the central axis of the plate and the normal to the deflected surface at any point (Figure 5.6.1), as

$$Q_r = \hat{N}_{rr} \phi \quad (5.6.5)$$

Next, consider the shear force-deflection relation (5.3.4) in the absence of thermal moments:

$$\begin{aligned} Q_r &= -D_{11} \frac{1}{r} \frac{d}{dr} \left(r \frac{d^2 w}{dr^2} \right) + D_{22} \frac{1}{r^2} \frac{dw}{dr} \\ &= -D_{11} \frac{1}{r} \frac{d}{dr} \left(r \frac{d\phi}{dr} \right) + D_{22} \frac{\phi}{r^2} \end{aligned} \quad (5.6.6)$$

so that Eq. (5.6.5) can be written as

$$r \frac{d}{dr} \left(r \frac{d\phi}{dr} \right) + \left(\frac{\hat{N}_{rr}}{D_{11}} r^2 - \frac{D_{22}}{D_{11}} \right) \phi = 0 \quad (5.6.7)$$

Using the transformation

$$\bar{r} = r \sqrt{\frac{\hat{N}_{rr}}{D_{11}}}, \quad n^2 = \frac{D_{22}}{D_{11}} \quad (5.6.8)$$

Eq. (5.6.7) can be recast in an alternative form as

$$\bar{r} \frac{d}{d\bar{r}} \left(\bar{r} \frac{d\phi}{d\bar{r}} \right) + (\bar{r}^2 - n^2) \phi = 0 \quad (5.6.9)$$

Equations (5.6.9) is known as the *Bessel's differential equation* of the n th order.

The general solution of Eq. (5.6.9) is

$$\phi(\bar{r}) = C_1 J_n(\bar{r}) + C_2 Y_n(\bar{r}) \quad (5.6.10)$$

where J_n is the Bessel function of the first kind of order n , Y_n is the Bessel function of the second kind of order n , and C_1 and C_2 are constants to be determined using the boundary conditions; we do not actually find these constants, but determine the stability criterion for various boundary conditions.

5.6.3 Clamped Plates

For a clamped plate with radius a , the boundary conditions are (dw/dr is zero at $r = 0, a$)

$$\phi(0) = 0, \quad \phi(a) = 0 \quad (5.6.11)$$

Using the general solution (5.6.10) for an isotropic plate, we obtain ($n = 1$)

$$C_1 J_1(0) + C_2 Y_1(0) = 0, \quad C_1 J_1(\alpha a) + C_2 Y_1(\alpha a) = 0, \quad \alpha^2 = \frac{\hat{N}_{rr}}{D} \quad (5.6.12)$$

Since $Y_1(0)$ is unbounded, we must have $C_2 = 0$. The fact that $J_1(0) = 0$ reduces the two equations in (5.6.10) to the single condition (since $C_1 \neq 0$ for a nontrivial solution)

$$J_1(\alpha a) = 0 \quad (5.6.13)$$

which is the stability criterion. The smallest root of the condition in (5.6.13) is $\alpha a = 3.8317$. Thus, we have

$$\hat{N}_{\text{cr}} = 14.682 \frac{D}{a^2} \quad (5.6.14)$$

5.6.4 Simply Supported Plates

For a simply supported plate, the boundary conditions are $dw/dr = 0$ at $r = 0$ and $M_{rr} = 0$ at $r = a$; expressing the boundary conditions in terms of ϕ , we have

$$\phi(0) = 0, \quad \left[D_{11} \frac{d\phi}{dr} + D_{12} \frac{1}{r} \phi \right]_{r=a} = 0 \quad (5.6.15)$$

The second boundary condition can be written in terms of \bar{r} as

$$\left[D_{11} \frac{d\phi}{d\bar{r}} + D_{12} \frac{1}{\bar{r}} \phi \right]_{\bar{r}=\alpha a} = 0 \quad (5.6.16)$$

Using the general solution (5.6.10) for an isotropic plate in the boundary conditions gives

$$C_1 J_1(0) + C_2 Y_1(0) = 0, \quad C_1 J'_1(\alpha a) + C_2 Y'_1(\alpha a) + \frac{\nu}{\alpha a} [C_1 J_1(\alpha a) + C_2 Y_1(\alpha a)] = 0 \quad (5.6.17)$$

The first equation gives $C_2 = 0$, and the second equation, in view of $C_2 = 0$ and the identity

$$\frac{dJ_n}{d\bar{r}} = J_{n-1}(\bar{r}) - \frac{1}{\bar{r}} J_n(\bar{r}) \quad (5.6.18)$$

gives

$$\alpha a J_0(\alpha a) - (1 - \nu) J_1(\alpha a) = 0 \quad (5.6.19)$$

Equation (5.6.19) defines the stability criterion for a simply supported circular plate. For $\nu = 0.3$, the smallest root of the transcendental equation (5.6.19) is $\alpha a = 2.05$. Hence, the buckling load becomes

$$\hat{N}_{\text{cr}} = 4.198 \frac{D}{a^2} \quad (5.6.20)$$

5.6.5 Simply Supported Plates with Rotational Restraint

For a simply supported plate with rotational restraint (Figure 5.6.2), the boundary conditions are

$$\phi(0) = 0, \quad \left[r D_{11} \frac{d\phi}{dr} + D_{12} \phi \right]_{r=a} + K_R a \phi(a) = 0 \quad (5.6.21)$$

where K_R denotes the rotational spring constant.

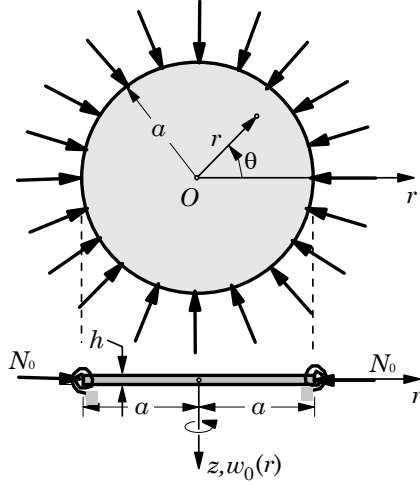


Figure 5.6.2. Buckling of a rotationally restrained circular plate under uniform radial compressive load.

For an isotropic plate, we obtain [see Reismann (1952) and Kerr (1962)]

$$\alpha a J'_0(\alpha a) - (1 - \nu - \beta) J_1(\alpha a) = 0, \quad \beta = \frac{a K_R}{D} \quad (5.6.22)$$

which is the stability criterion. When $\beta = 0$, we obtain Eq. (5.6.19), and when $\beta = \infty$, we obtain Eq. (5.6.13) as special cases. Table 5.6.1 contains exact values of the buckling load factor $\bar{N} = \hat{N}_{cr}(a^2/D)$ for various values of the parameter β (for $\nu = 0.3$).

Table 5.6.1. Critical buckling load factors $\bar{N} = \hat{N}_{cr}(a^2/D)$ for rotationally restrained circular plates.

β	0	0.1	0.5	1	5	10	100	∞
\bar{N}	4.198	4.449	5.369	6.353	10.462	12.173	14.392	14.682

5.7 Summary

A derivation of the governing equations of circular plates according to the classical plate theory is presented, followed by analytical solutions for axisymmetric bending, natural vibration, and buckling of circular plates. The Ritz solutions are also developed for bending and vibration of annular and solid circular plates. The solutions were developed for a variety of boundary conditions and loads. Additional buckling solutions, e.g., nonaxisymmetric buckling, buckling with internal ring support, buckling under intermediate and edge radial loads, and buckling of annular plates can be found in the book by Wang, et al. (2005).

Problems

- 5.1** Verify the strain-displacement relations in Eqs. (5.2.21).
- 5.2** Use the 3-D equations of equilibrium in terms of stresses [with the body forces equal to zero; see Eqs. (1.3.27)] in the cylindrical coordinate system to derive the equilibrium equations in terms of the force and moment resultants of Eqs. (5.2.24) and (5.2.25) of a circular plate (see Problem 3.6).

- 5.3** Show that

$$\frac{\partial M_{r\theta}}{\partial r} = \frac{1}{r} \frac{\partial F}{\partial \theta}, \quad \frac{\partial \mathcal{M}}{\partial r} = \frac{1}{r} \left[\frac{\partial}{\partial r} (r M_{rr}) - M_{\theta\theta} + \frac{\partial M_{r\theta}}{\partial \theta} \right] \quad (1)$$

where

$$\mathcal{M} = \frac{M_{rr} + M_{\theta\theta}}{1 + \nu}, \quad F = -(1 - \nu) D r \frac{\partial}{\partial r} \left(\frac{1}{r} \frac{\partial w_0}{\partial r} - \frac{w_0}{r^2} \right) \quad (2)$$

- 5.4** Show that the expression for the deflection of a simply supported circular plate of radius a subjected to uniformly distributed transverse load and applied bending moment $M_{rr} = M_a$ at $r = a$ is

$$w_0(r) = \bar{w}_0(r) + \frac{M_a a^2}{2D(1 + \nu)} \left(1 - \frac{r^2}{a^2} \right)$$

where \bar{w}_0 is the deflection given in Eq. (5.3.43).

- 5.5** Determine the deflection and bending moments of a circular plate under uniformly distributed transverse load q_0 when the edge $r = a$ is elastically built in. The boundary conditions are

$$w_0(a) = 0, \quad M_{rr} = \beta \frac{dw_0}{dr} \quad \text{at } r = a$$

where β denotes rotational stiffness constant. *Answer:*

$$\begin{aligned} w_0 &= \frac{q_0 a^4}{64D} \left\{ \frac{(5 + \nu)D + \beta a}{(1 + \nu)D + \beta a} - 2 \left[\frac{(3 + \nu)D + \beta a}{(1 + \nu)D + \beta a} \right] \left(\frac{r}{a} \right)^2 + \left(\frac{r}{a} \right)^4 \right\} \\ M_{rr} &= \frac{q_0 a^2}{16} \left[(1 + \nu) \frac{(3 + \nu)D + \beta a}{(1 + \nu)D + \beta a} - (3 + \nu) \left(\frac{r}{a} \right)^2 \right] \\ M_{\theta\theta} &= \frac{q_0 a^2}{16} \left[(1 + \nu) \frac{(3 + \nu)D + \beta a}{(1 + \nu)D + \beta a} - (1 + 3\nu) \left(\frac{r}{a} \right)^2 \right] \end{aligned}$$

- 5.6** Show that the deflection of a simply supported circular plate under linearly varying load $q = q_0(1 - r/a)$ is given by

$$w(r) = \frac{q_0 a^4}{14400D} \left[\frac{3(183 + 43\nu)}{1 + \nu} - \frac{10(71 + 29\nu)}{1 + \nu} \left(\frac{r}{a} \right)^2 + 255 \left(\frac{r}{a} \right)^4 - 64 \left(\frac{r}{a} \right)^5 \right]$$

and, hence, show that

$$w_{max} = \frac{q_0 a^4}{4800D} \left(\frac{183 + 43\nu}{1 + \nu} \right), \quad M_{max} = q_0 a^2 \left(\frac{71 + 29\nu}{720} \right)$$

- 5.7** Show that the maximum deflection and bending moment of a simply supported circular plate under linearly varying load, $q = q_1(r/a)$, are

$$w_{max} = \frac{q_1 a^4}{150D} \left(\frac{6 + \nu}{1 + \nu} \right), \quad M_{max} = q_1 a^2 \left(\frac{4 + \nu}{45} \right)$$

- 5.8** Show that the deflection of a clamped circular plate under the load, $q = q_0(r^2/a^2)$, is given by

$$w_0(r) = \frac{q_0 a^4}{576D} \left[2 - 3 \left(\frac{r}{a} \right)^2 + \left(\frac{r}{a} \right)^6 \right]$$

- 5.9** Show that the expressions for the deflection and bending moments of an annular plate of inner radius a and outer radius b , simply supported at the inner edge $r = a$ and subjected to bending moment $M_{rr} = M_b$ at $r = b$, are the same as those given in Eqs. (5.3.67)–(5.3.69) with $M_a = 0$.

- 5.10** Show that the expressions for the deflection and bending moments of an annular plate of inner radius a and outer radius b , simply supported at the inner edge $r = a$ and subjected to bending moment $M_{rr} = M_a$ at $r = a$, are the same as those given in Eqs. (5.3.67)–(5.3.69) with $M_b = 0$.

- 5.11** Determine the deflection and bending moments of an annular plate of inner radius b and outer radius a , clamped at the inner edge $r = b$ and subjected to uniformly distributed load q_0 .

- 5.12** Show that the expressions for the deflection and bending moments of an annular plate of inner radius a and outer radius b , simply supported at the inner edge $r = a$ and subjected to shear force $rQ_r = bQ_b$ at $r = b$, are the same as those given in Eqs. (5.3.73)–(5.3.75).

- 5.13** Show that the expression for the deflection of a clamped (at the outer edge) circular plate under linearly varying load, $q = q_0(1 - r/a)$ is

$$w_0(r) = \frac{q_0 a^4}{14400D} \left(129 - 290 \frac{r^2}{a^2} + 225 \frac{r^4}{a^4} - 64 \frac{r^5}{a^5} \right)$$

- 5.14** Show that the expressions for the deflection and bending moments of a clamped (at the outer edge) circular plate under linearly varying load $q = q_1(r/a)$ are

$$w_0(r) = \frac{q_1 a^4}{450D} \left(3 - 5 \frac{r^2}{a^2} + 2 \frac{r^5}{a^5} \right)$$

$$M_{rr}(r) = \frac{q_1 a^2}{45} \left[(1 + \nu) - (4 + \nu) \frac{r^3}{a^3} \right]$$

$$M_{\theta\theta}(r) = \frac{q_1 a^2}{45} \left[(1 + \nu) - (1 + 4\nu) \frac{r^3}{a^3} \right]$$

- 5.15** Show that the one-parameter Ritz solution for the deflection of an isotropic clamped (at the outer edge) circular plate under uniformly distributed load q_0 is given by

$$w_1(r) = c_1 \phi_1(r) = \frac{q_0 a^4}{60D} \left[1 - 3 \left(\frac{r}{a} \right)^2 + 2 \left(\frac{r}{a} \right)^3 \right]$$

- 5.16** Show that the two-parameter Ritz solution for the deflection of an isotropic, clamped (at the outer edge) circular plate under uniformly distributed load q_0 coincides with the exact solution.
- 5.17** Show that the one-parameter Galerkin's solution for the deflection of an isotropic clamped (at the outer edge) circular plate under uniformly distributed load q_0 coincides with the exact solution.
- 5.18** Use the two-parameter Ritz solution of the form

$$W_2(r, \theta) = c_1 \varphi_1(r) + c_2 \varphi_2(r) \cos \theta$$

and determine the coefficients c_1 and c_2 for a clamped circular plate subjected to asymmetric loading given in Eq. (5.4.5). You must determine φ_1 and φ_2 first (see Problem 5.16 above).

- 5.19** Determine the fundamental frequency of a simply supported circular plate using a one-parameter Ritz approximation.
- 5.20** Formulate the N -parameter Ritz approximation for axisymmetric buckling of annular plates subjected to inplane compression (Figure P5.20).

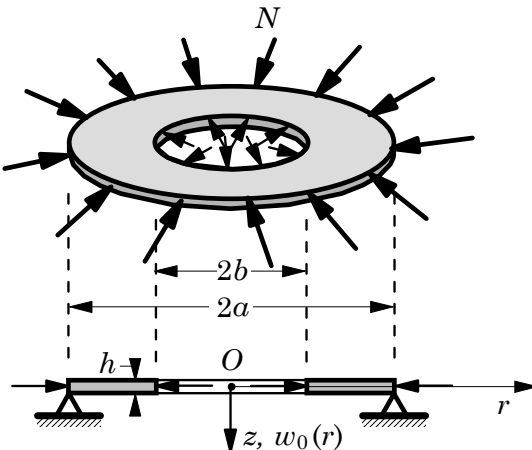


Figure P5.20

6

Bending of Simply Supported Rectangular Plates

6.1 Introduction

6.1.1 Governing Equations

In this chapter, analytical solutions for deflections and stresses of simply supported rectangular plates are developed using the Navier method, the Lévy method with the state-space approach, and the Ritz method. The Navier solutions can be developed for rectangular plates when all four edges are simply supported. The Lévy solutions can be developed for rectangular plates with two opposite edges simply supported and the remaining two edges having any possible combination of *free*, *simply supported*, and *clamped/fixed* boundary conditions. The Ritz method can be used to determine approximate solutions for more general boundary conditions, provided that suitable approximation functions that satisfy the geometric boundary conditions can be constructed.

The governing equations of rectangular plates are best described using Cartesian rectangular coordinates, as discussed in Chapter 3. For the linear analysis of plates studied here, we consider plates subjected to transverse distributed load q and thermal loads due to temperature change ΔT . When inplane forces $(\hat{N}_{xx}, \hat{N}_{yy}, \hat{N}_{xy})$ and the nonlinear terms are (\mathcal{N}) omitted, the equation governing the bending, Eq. (3.8.5), becomes uncoupled from Eqs. (3.8.3) and (3.8.4). For an orthotropic plate, we have

$$D_{11} \frac{\partial^4 w_0}{\partial x^4} + 2\hat{D}_{12} \frac{\partial^4 w_0}{\partial x^2 \partial y^2} + D_{22} \frac{\partial^4 w_0}{\partial y^4} + kw_0 = q - \left(\frac{\partial^2 M_{xx}^T}{\partial x^2} + 2 \frac{\partial^2 M_{xy}^T}{\partial x \partial y} + \frac{\partial^2 M_{yy}^T}{\partial y^2} \right) \quad (6.1.1)$$

where

$$\hat{D}_{12} = (D_{12} + 2D_{66}) \quad (6.1.2)$$

and the thermal moments M_{xx}^T , M_{xy}^T , and M_{yy}^T are defined by [see Eqs. (3.6.10) and (3.6.15)]

$$\begin{Bmatrix} M_{xx}^T \\ M_{yy}^T \\ M_{xy}^T \end{Bmatrix} = \begin{Bmatrix} Q_{11}\alpha_1 + Q_{12}\alpha_2 \\ Q_{12}\alpha_1 + Q_{22}\alpha_2 \\ 0 \end{Bmatrix} \int_{-\frac{h}{2}}^{\frac{h}{2}} \Delta T(x, y, z) z \, dz \quad (6.1.3)$$

where Q_{ij} and α_i are the elastic stiffnesses and thermal coefficients of expansion, respectively, of an orthotropic plate, and $\Delta T(x, y, z)$ is the temperature increment above a reference temperature (at which the plate is stress free). Note that M_{xy}^T is identically zero for isotropic or orthotropic plates.

For isotropic plates ($D_{11} = D_{22} = \hat{D}_{12} = D$, $\alpha_1 = \alpha_2 = \alpha$), Eq. (6.1.1) simplifies to

$$D\left(\frac{\partial^4 w_0}{\partial x^4} + 2\frac{\partial^4 w_0}{\partial x^2 \partial y^2} + \frac{\partial^4 w_0}{\partial y^4}\right) + kw_0 = q - \frac{1}{1-\nu} \left(\frac{\partial^2 M_T}{\partial x^2} + \frac{\partial^2 M_T}{\partial y^2}\right) \quad (6.1.4)$$

where

$$M_T = E\alpha \int_{-\frac{h}{2}}^{\frac{h}{2}} \Delta T(x, y, z) z \, dz \quad (6.1.5)$$

Equation (6.1.4) can be expressed in terms of the Laplace operator ∇^2 as

$$D\nabla^2 \nabla^2 w_0 + kw_0 = q - \frac{1}{(1-\nu)} \nabla^2 M_T \quad (6.1.6)$$

6.1.2 Boundary Conditions

Simply supported boundary conditions on all four edges of a rectangular plate can be expressed as

$$w_0(0, y) = 0, \quad w_0(a, y) = 0, \quad w_0(x, 0) = 0, \quad w_0(x, b) = 0 \quad (6.1.7)$$

$$M_{xx}(0, y) = 0, \quad M_{xx}(a, y) = 0, \quad M_{yy}(x, 0) = 0, \quad M_{yy}(x, b) = 0 \quad (6.1.8)$$

where the bending moments are related to the transverse deflection by

$$\begin{aligned} M_{xx} &= -\left(D_{11}\frac{\partial^2 w_0}{\partial x^2} + D_{12}\frac{\partial^2 w_0}{\partial y^2}\right) - M_{xx}^T \\ M_{yy} &= -\left(D_{12}\frac{\partial^2 w_0}{\partial x^2} + D_{22}\frac{\partial^2 w_0}{\partial y^2}\right) - M_{yy}^T \\ M_{xy} &= -2D_{66}\frac{\partial^2 w_0}{\partial x \partial y} \end{aligned} \quad (6.1.9)$$

where

$$\begin{aligned} D_{11} &= \frac{E_1 h^3}{12(1 - \nu_{12}\nu_{21})}, & D_{22} &= \frac{E_2 h^3}{12(1 - \nu_{12}\nu_{21})} \\ D_{12} &= \frac{\nu_{12}E_2 h^3}{12(1 - \nu_{12}\nu_{21})}, & D_{66} &= \frac{G_{12}h^3}{12} \end{aligned} \quad (6.1.10)$$

and a and b denote the inplane dimensions along the x and y coordinate directions of a rectangular plate. The origin of the coordinate system is taken at the upper left corner of the mid-plane (Figure 6.1.1).

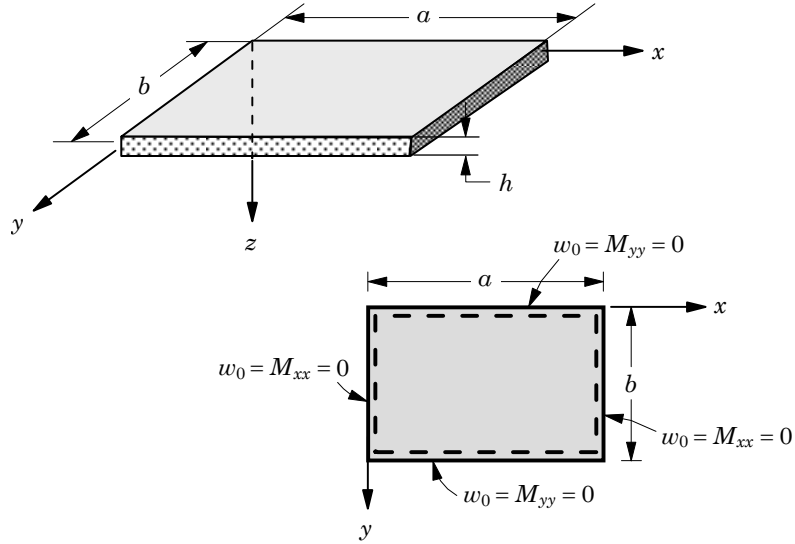


Figure 6.1.1. Geometry and coordinate system for a rectangular plate.

6.2 Navier Solutions

6.2.1 Solution Procedure

The solution of Eq. (6.1.1) for rectangular plates with simply supported boundary conditions can be obtained using Navier's method. In Navier's method, the displacement w_0 , mechanical load q , and thermal loads M_{xx}^T and M_{yy}^T are expanded in trigonometric series. The choice of the trigonometric functions used for the deflection and thermal moments is restricted to those that satisfy the boundary conditions of the problem. Substitution of the expansion for the deflection into the governing equation (6.1.1) will dictate the choice of the expansions used for the mechanical and thermal loads.

The simply supported boundary conditions in Eqs. (6.1.7) and (6.1.8) are met by the following form of the transverse deflection

$$w_0(x, y) = \sum_{n=1}^{\infty} \sum_{m=1}^{\infty} W_{mn} \sin \frac{m\pi x}{a} \sin \frac{n\pi y}{b} \quad (6.2.1)$$

where W_{mn} are coefficients to be determined such that Eq. (6.1.1) is satisfied everywhere in the domain of the plate. Substituting Eq. (6.2.1) into Eq. (6.1.1), we obtain

$$\begin{aligned} & \sum_{n=1}^{\infty} \sum_{m=1}^{\infty} \left[D_{11} \left(\frac{m\pi}{a} \right)^4 + 2\hat{D}_{12} \left(\frac{m\pi}{a} \right)^2 \left(\frac{n\pi}{b} \right)^2 + D_{22} \left(\frac{n\pi}{b} \right)^4 + k \right] \\ & \times W_{mn} \sin \frac{m\pi x}{a} \sin \frac{n\pi y}{b} = q - \left(\frac{\partial^2 M_{xx}^T}{\partial x^2} + 2 \frac{\partial^2 M_{xy}^T}{\partial x \partial y} + \frac{\partial^2 M_{yy}^T}{\partial y^2} \right) \end{aligned} \quad (6.2.2)$$

Equation (6.2.2) suggests that the right-hand side also be expanded in double sine series as

$$\begin{aligned} q(x, y) &= \sum_{n=1}^{\infty} \sum_{m=1}^{\infty} q_{mn} \sin \frac{m\pi x}{a} \sin \frac{n\pi y}{b} \\ M_{xx}^T(x, y) &= \sum_{n=1}^{\infty} \sum_{m=1}^{\infty} M_{mn}^1 \sin \frac{m\pi x}{a} \sin \frac{n\pi y}{b} \\ M_{yy}^T(x, y) &= \sum_{n=1}^{\infty} \sum_{m=1}^{\infty} M_{mn}^2 \sin \frac{m\pi x}{a} \sin \frac{n\pi y}{b} \end{aligned} \quad (6.2.3)$$

and that $M_{xy}^T = 0$, as is the case for isotropic and orthotropic plates. The coefficients q_{mn} , M_{mn}^1 , and M_{mn}^2 are calculated from (see Table 6.2.1)

$$\begin{aligned} q_{mn} &= \frac{4}{ab} \int_0^b \int_0^a q(x, y) \sin \frac{m\pi x}{a} \sin \frac{n\pi y}{b} dx dy \\ M_{mn}^1 &= \frac{4}{ab} \int_0^b \int_0^a M_{xx}^T(x, y) \sin \frac{m\pi x}{a} \sin \frac{n\pi y}{b} dx dy \\ M_{mn}^2 &= \frac{4}{ab} \int_0^b \int_0^a M_{yy}^T(x, y) \sin \frac{m\pi x}{a} \sin \frac{n\pi y}{b} dx dy \end{aligned} \quad (6.2.4)$$

For example, when $q = q_0$, q_{mn} can be computed using Eq. (6.2.4) as follows:

$$\begin{aligned} q_{mn} &= \frac{4}{ab} \int_0^b \int_0^a q_0 \sin \frac{m\pi x}{a} \sin \frac{n\pi y}{b} dx dy \\ &= \frac{4q_0}{ab} \left[-\frac{\cos \frac{m\pi x}{a}}{\frac{m\pi}{a}} \right]_0^a \left[-\frac{\cos \frac{n\pi y}{b}}{\frac{n\pi}{b}} \right]_0^b \\ &= \frac{4q_0}{mn\pi^2} (\cos m\pi - 1) (\cos n\pi - 1) \end{aligned}$$

for $m, n = 1, 2, 3, \dots$. Since $\cos n\pi = (-1)^n$, the above expression is identically zero for the even values of m and n . Hence, we have

$$q_{mn} = \frac{16q_0}{mn\pi^2}, \quad \text{for } m, n = 1, 3, 5, \dots \quad (6.2.5)$$

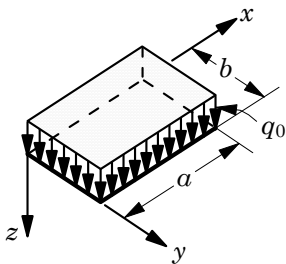
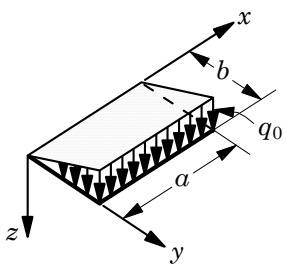
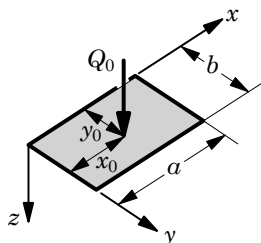
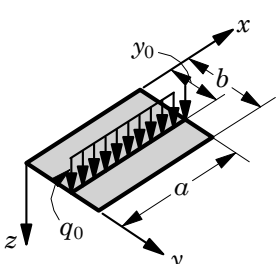
Similarly, for a point load Q_0 applied at $x = x_0$ and $y = y_0$, we set $q = Q_0\delta(x - x_0)\delta(y - y_0)$ and find

$$\begin{aligned} q_{mn} &= \frac{4}{ab} \int_0^b \int_0^a Q_0\delta(x - x_0)\delta(y - y_0) \sin \frac{m\pi x}{a} \sin \frac{n\pi y}{b} dx dy \\ &= \frac{4Q_0}{ab} \sin \frac{m\pi x_0}{a} \sin \frac{n\pi y_0}{b} \end{aligned} \quad (6.2.6)$$

for $m, n = 1, 2, 3, \dots$, where $\delta(\cdot)$ is the Dirac delta function

$$\int_{-\infty}^{\infty} F(\xi)\delta(\xi - \xi_0) d\xi = F(\xi_0) \quad (6.2.7)$$

Table 6.2.1. Coefficients in the double trigonometric series expansion of loads in the Navier method.

Loading	Coefficients q_{mn}
	Uniform load $q(x, y) = q_0$ $q_{mn} = \frac{16q_0}{\pi^2 mn}$ $(m, n = 1, 3, 5, \dots)$
	Hydrostatic load $q(x, y) = q_0 \frac{y}{b}$ $q_{mn} = \frac{8q_0}{\pi^2 mn} (-1)^{n+1}$ $(m = 1, 3, 5, \dots)$ $(n = 1, 2, 3, \dots)$
	Point load [i.e., Q_0 at (x_0, y_0)] $q_{mn} = \frac{4Q_0}{ab} \sin \frac{m\pi x_0}{a} \sin \frac{n\pi y_0}{b}$ $(m, n = 1, 2, 3, \dots)$
	Line load $q(x, y) = q_0 \delta(y - y_0)$ $q_{mn} = \frac{8q_0}{\pi b m} \sin \frac{n\pi y_0}{b}$ $(m = 1, 3, 5, \dots)$ $(n = 1, 2, 3, \dots)$

For a point load of magnitude Q_0 placed at the center of the plate (i.e., $x_0 = a/2$ and $y_0 = b/2$), we have

$$q_{mn} = \frac{4Q_0}{ab}, \quad m, n = 1, 3, 5, \dots \quad (6.2.8)$$

The coefficients q_{mn} for other types of loads are listed in Table 6.2.1.

We note that the boundary conditions (6.1.8) on bending moments are satisfied by the double sine series expansions selected for the deflection and thermal moments [see Eqs. (6.2.1) and (6.2.3)]. Therefore, the exact analytical solution of Eq. (6.1.1) is given by Eq. (6.2.1), where the coefficients W_{mn} are determined from Eq. (6.2.2) by substituting the expansions for the load and thermal moments. We find

$$\sum_{n=1}^{\infty} \sum_{m=1}^{\infty} \left\{ W_{mn} \left[D_{11} \left(\frac{m\pi}{a} \right)^4 + 2\hat{D}_{12} \left(\frac{m\pi}{a} \right)^2 \left(\frac{n\pi}{b} \right)^2 + D_{22} \left(\frac{n\pi}{b} \right)^4 + k \right] - q_{mn} - \left[\left(\frac{m\pi}{a} \right)^2 M_{mn}^1 + \left(\frac{n\pi}{b} \right)^2 M_{mn}^2 \right] \right\} \sin \frac{m\pi x}{a} \sin \frac{n\pi y}{b} = 0$$

Since the equation must hold for all points (x, y) of the domain $0 < x < a$ and $0 < y < b$, the expression in the braces must be zero for any m and n . This yields

$$W_{mn} = \frac{1}{d_{mn}} \left[q_{mn} + \left(\frac{m\pi}{a} \right)^2 M_{mn}^1 + \left(\frac{n\pi}{b} \right)^2 M_{mn}^2 \right] \quad (6.2.9)$$

$$d_{mn} = \frac{\pi^4}{b^4} \left[D_{11} m^4 s^4 + 2\hat{D}_{12} m^2 n^2 s^2 + D_{22} n^4 \right] + k \quad (6.2.10)$$

where s denotes the plate aspect ratio, $s = b/a$. The deflection in Eq. (6.1.1) becomes

$$w_0(x, y) = \sum_{n=1}^{\infty} \sum_{m=1}^{\infty} \frac{1}{d_{mn}} \left[q_{mn} + \left(\frac{m\pi}{a} \right)^2 M_{mn}^1 + \left(\frac{n\pi}{b} \right)^2 M_{mn}^2 \right] \sin \frac{m\pi x}{a} \sin \frac{n\pi y}{b} \quad (6.2.11)$$

For an isotropic plate, we have [see Eq. (6.1.4)]

$$w_0(x, y) = \sum_{n=1}^{\infty} \sum_{m=1}^{\infty} \left\{ \frac{q_{mn} + \pi^2 \left(\frac{m^2}{a^2} + \frac{n^2}{b^2} \right) M_{mn}^T}{\pi^4 D \left(\frac{m^2}{a^2} + \frac{n^2}{b^2} \right)^2 + k} \right\} \sin \frac{m\pi x}{a} \sin \frac{n\pi y}{b} \quad (6.2.12)$$

where

$$\begin{aligned} q_{mn} &= \frac{4}{ab} \int_0^b \int_0^a q(x, y) \sin \frac{m\pi x}{a} \sin \frac{n\pi y}{b} dx dy \\ M_{mn}^T &= \frac{4}{ab(1-\nu)} \int_0^b \int_0^a M_T(x, y) \sin \frac{m\pi x}{a} \sin \frac{n\pi y}{b} dx dy \end{aligned} \quad (6.2.13)$$

and M_T is defined in Eq. (6.1.5).

6.2.2 Calculation of Bending Moments, Shear Forces, and Stresses

The bending moments can be calculated using Eqs. (6.1.9) and (6.2.1) as

$$\begin{aligned} M_{xx} &= \sum_{n=1}^{\infty} \sum_{m=1}^{\infty} \left(B_{xx} W_{mn} - M_{mn}^1 \right) \sin \frac{m\pi x}{a} \sin \frac{n\pi y}{b} \\ M_{yy} &= \sum_{n=1}^{\infty} \sum_{m=1}^{\infty} \left(B_{yy} W_{mn} - M_{mn}^2 \right) \sin \frac{m\pi x}{a} \sin \frac{n\pi y}{b} \\ M_{xy} &= - \sum_{n=1}^{\infty} \sum_{m=1}^{\infty} B_{xy} W_{mn} \cos \frac{m\pi x}{a} \cos \frac{n\pi y}{b} \end{aligned} \quad (6.2.14a)$$

where

$$\begin{aligned} B_{xx} &= D_{11} \left(\frac{m\pi}{a} \right)^2 + D_{12} \left(\frac{n\pi}{b} \right)^2 \\ B_{yy} &= D_{12} \left(\frac{m\pi}{a} \right)^2 + D_{22} \left(\frac{n\pi}{b} \right)^2 \\ B_{xy} &= 2D_{66} \left(\frac{m\pi}{a} \right) \left(\frac{n\pi}{b} \right) \end{aligned} \quad (6.2.14b)$$

The transverse shear forces Q_x and Q_y are defined by

$$\begin{aligned} Q_x &= \frac{\partial M_{xx}}{\partial x} + \frac{\partial M_{xy}}{\partial y} \\ &= \sum_{n=1}^{\infty} \sum_{m=1}^{\infty} \left[S_{xx} W_{mn} - \left(\frac{m\pi}{a} \right) M_{mn}^1 \right] \cos \frac{m\pi x}{a} \sin \frac{n\pi y}{b} \end{aligned} \quad (6.2.15a)$$

$$\begin{aligned} Q_y &= \frac{\partial M_{xy}}{\partial x} + \frac{\partial M_{yy}}{\partial y} \\ &= \sum_{n=1}^{\infty} \sum_{m=1}^{\infty} \left[S_{yy} W_{mn} - \left(\frac{n\pi}{b} \right) M_{mn}^2 \right] \sin \frac{m\pi x}{a} \cos \frac{n\pi y}{b} \end{aligned} \quad (6.2.15b)$$

where

$$\begin{aligned} S_{xx} &= D_{11} \left(\frac{m\pi}{a} \right)^3 + \hat{D}_{12} \left(\frac{m\pi}{a} \right) \left(\frac{n\pi}{b} \right)^2 \\ S_{yy} &= D_{22} \left(\frac{n\pi}{b} \right)^3 + \hat{D}_{12} \left(\frac{m\pi}{a} \right)^2 \left(\frac{n\pi}{b} \right) \end{aligned} \quad (6.2.15c)$$

Reaction forces V_x and V_y along the simply supported edges $x = a$ and $y = b$, respectively, can be calculated using the definition in Eq. (3.5.15) as follows:

$$\begin{aligned} V_x(a, y) &= Q_x + \frac{\partial M_{xy}}{\partial y} = \frac{\partial M_{xx}}{\partial x} + 2 \frac{\partial M_{xy}}{\partial y} \\ &= \sum_{n=1}^{\infty} \sum_{m=1}^{\infty} (-1)^m \left[\hat{S}_{xx} W_{mn} - \left(\frac{m\pi}{a} \right) M_{mn}^1 \right] \sin \frac{n\pi y}{b} \end{aligned} \quad (6.2.16)$$

$$\begin{aligned} V_y(x, b) &= Q_y + \frac{\partial M_{xy}}{\partial x} = 2 \frac{\partial M_{xy}}{\partial x} + \frac{\partial M_{yy}}{\partial y} \\ &= \sum_{n=1}^{\infty} \sum_{m=1}^{\infty} (-1)^n \left[\hat{S}_{yy} W_{mn} - \left(\frac{n\pi}{b} \right) M_{mn}^2 \right] \sin \frac{m\pi x}{a} \end{aligned} \quad (6.2.17)$$

where

$$\begin{aligned} \hat{S}_{xx} &= D_{11} \left(\frac{m\pi}{a} \right)^3 + (D_{12} + 4D_{66}) \left(\frac{m\pi}{a} \right) \left(\frac{n\pi}{b} \right)^2 \\ \hat{S}_{yy} &= D_{22} \left(\frac{n\pi}{b} \right)^3 + (D_{12} + 4D_{66}) \left(\frac{m\pi}{a} \right)^2 \left(\frac{n\pi}{b} \right) \end{aligned} \quad (6.2.18)$$

Thus, the distribution of the reaction forces along the edges follows a sinusoidal form. Similar expressions hold for $V_x(0, y)$ and $V_y(x, 0)$.

In addition to the reactions in Eqs. (6.2.16) and (6.2.17) along the edges, the plate experiences concentrated forces [see Eq. (3.5.14)] at the corners of a rectangular plate due to the twisting moment M_{xy} per unit length (which has the dimensions of a force). The concentrated force at the corner $x = a$ and $y = b$ is given by

$$F_c = -2M_{xy} = 4D_{66} \frac{\partial^2 w_0}{\partial x \partial y} = 4D_{66} \sum_{n=1}^{\infty} \sum_{m=1}^{\infty} \left(\frac{m\pi}{a} \right) \left(\frac{n\pi}{b} \right) (-1)^{m+n} W_{mn} \quad (6.2.19)$$

Suppose that the temperature variation through thickness is of the form

$$\begin{aligned} \Delta T(x, y, z) &= T^0(x, y) + zT^1(x, y) \\ &\equiv \sum_{n=1}^{\infty} \sum_{m=1}^{\infty} \left(T_{mn}^0 + zT_{mn}^1 \right) \sin \frac{m\pi x}{a} \sin \frac{n\pi y}{b} \end{aligned} \quad (6.2.20)$$

where the coefficients T_{mn}^0 and T_{mn}^1 are computed using equations of the form (6.2.4). Using Eq. (6.2.20) in the definitions of the thermal moments, Eq. (6.1.3), we find that (note that T_{mn}^0 enters only the thermal forces and not thermal moments)

$$\begin{aligned} M_{xx}^T &= \int_{-\frac{h}{2}}^{\frac{h}{2}} (Q_{11}\alpha_1 + Q_{12}\alpha_2) \Delta T z dz \\ &= (D_{11}\alpha_1 + D_{12}\alpha_2) \sum_{n=1}^{\infty} \sum_{m=1}^{\infty} T_{mn}^1 \sin \frac{m\pi x}{a} \sin \frac{n\pi y}{b} \\ &\equiv \sum_{n=1}^{\infty} \sum_{m=1}^{\infty} M_{mn}^1 \sin \frac{m\pi x}{a} \sin \frac{n\pi y}{b} \end{aligned} \quad (6.2.21a)$$

$$\begin{aligned} M_{yy}^T &= \int_{-\frac{h}{2}}^{\frac{h}{2}} (Q_{12}\alpha_1 + Q_{22}\alpha_2) \Delta T z dz \\ &= (D_{12}\alpha_1 + D_{22}\alpha_2) \sum_{n=1}^{\infty} \sum_{m=1}^{\infty} T_{mn}^1 \sin \frac{m\pi x}{a} \sin \frac{n\pi y}{b} \\ &\equiv \sum_{n=1}^{\infty} \sum_{m=1}^{\infty} M_{mn}^2 \sin \frac{m\pi x}{a} \sin \frac{n\pi y}{b} \end{aligned} \quad (6.2.21b)$$

$$M_{mn}^1 = (D_{11}\alpha_1 + D_{12}\alpha_2) T_{mn}^1, \quad M_{mn}^2 = (D_{12}\alpha_1 + D_{22}\alpha_2) T_{mn}^1 \quad (6.2.22)$$

For the pure bending case considered here, i.e., when the membrane strains are zero, the stresses in a simply supported plate are given by

$$\begin{aligned} \begin{Bmatrix} \sigma_{xx} \\ \sigma_{yy} \\ \sigma_{xy} \end{Bmatrix} &= -z \begin{bmatrix} Q_{11} & Q_{12} & 0 \\ Q_{12} & Q_{22} & 0 \\ 0 & 0 & Q_{66} \end{bmatrix} \begin{Bmatrix} \frac{\partial^2 w_0}{\partial x^2} + \alpha_1 T^1 \\ \frac{\partial^2 w_0}{\partial y^2} + \alpha_2 T^1 \\ 2 \frac{\partial^2 w_0}{\partial x \partial y} \end{Bmatrix} \\ &= z \sum_{n=1}^{\infty} \sum_{m=1}^{\infty} \begin{Bmatrix} (R_{xx} W_{mn} - \mathcal{M}_{mn}^1) \sin \frac{m\pi x}{a} \sin \frac{n\pi y}{b} \\ (R_{yy} W_{mn} - \mathcal{M}_{mn}^2) \sin \frac{m\pi x}{a} \sin \frac{n\pi y}{b} \\ -R_{xy} W_{mn} \cos \frac{m\pi x}{a} \cos \frac{n\pi y}{b} \end{Bmatrix} \quad (6.2.23) \end{aligned}$$

where

$$\begin{aligned} R_{xx} &= \frac{\pi^2}{b^2} (Q_{11}m^2 s^2 + Q_{12}n^2), \quad R_{yy} = \frac{\pi^2}{b^2} (Q_{12}m^2 s^2 + Q_{22}n^2) \\ R_{xy} &= 2mns \frac{\pi^2}{b^2} Q_{66} \\ \mathcal{M}_{mn}^1 &= (Q_{11}\alpha_1 + Q_{12}\alpha_2) T_{mn}^1, \quad \mathcal{M}_{mn}^2 = (Q_{12}\alpha_1 + Q_{22}\alpha_2) T_{mn}^1 \end{aligned} \quad (6.2.24)$$

The maximum stresses occur at $(x, y, z) = (a/2, b/2, \pm h/2)$, depending on the nature of the thermo-mechanical loads.

In the classical plate theory, the transverse stresses ($\sigma_{xz}, \sigma_{yz}, \sigma_{zz}$) are identically zero when computed from the constitutive equations because the transverse shear strains are zero. However, they can be computed using the 3-D stress equilibrium equations for any $-h/2 \leq z \leq h/2$:

$$\begin{aligned} \sigma_{xz} &= - \int_{-\frac{h}{2}}^z \left(\frac{\partial \sigma_{xx}}{\partial x} + \frac{\partial \sigma_{xy}}{\partial y} \right) dz + C_1(x, y) \\ \sigma_{yz} &= - \int_{-\frac{h}{2}}^z \left(\frac{\partial \sigma_{xy}}{\partial x} + \frac{\partial \sigma_{yy}}{\partial y} \right) dz + C_2(x, y) \\ \sigma_{zz} &= - \int_{-\frac{h}{2}}^z \left(\frac{\partial \sigma_{xz}}{\partial x} + \frac{\partial \sigma_{yz}}{\partial y} \right) dz + C_3(x, y) \end{aligned} \quad (6.2.25)$$

where the stresses σ_{xx}, σ_{xy} , and σ_{yy} are known from Eq. (6.2.23) and C_i are functions to be determined using the conditions $\sigma_{xz}(x, y, -h/2) = \sigma_{yz}(x, y, -h/2) = \sigma_{zz}(x, y, -h/2) = 0$. We obtain $C_i = 0$ and

$$\begin{aligned} \sigma_{xz} &= \frac{h^2}{8} \left[1 - \left(\frac{2z}{h} \right)^2 \right] \sum_{n=1}^{\infty} \sum_{m=1}^{\infty} S_{mn}^{xz} \cos \frac{m\pi x}{a} \sin \frac{n\pi y}{b} \\ \sigma_{yz} &= \frac{h^2}{8} \left[1 - \left(\frac{2z}{h} \right)^2 \right] \sum_{n=1}^{\infty} \sum_{m=1}^{\infty} S_{mn}^{yz} \sin \frac{m\pi x}{a} \cos \frac{n\pi y}{b} \\ \sigma_{zz} &= - \frac{h^3}{48} \left\{ \left[1 + \left(\frac{2z}{h} \right)^3 \right] - 3 \left[1 + \left(\frac{2z}{h} \right) \right] \right\} \sum_{n=1}^{\infty} \sum_{m=1}^{\infty} S_{mn}^{zz} \sin \frac{m\pi x}{a} \sin \frac{n\pi y}{b} \end{aligned} \quad (6.2.26)$$

where

$$\begin{aligned} S_{mn}^{xz} &= \left(\frac{m\pi}{a}\right) \left(R_{xx}W_{mn} - \mathcal{M}_{mn}^1\right) + \left(\frac{n\pi}{b}\right) R_{xy}W_{mn} \\ &= S_{13}W_{mn} - T_{13}T_{mn}^1 \\ S_{mn}^{yz} &= \left(\frac{n\pi}{b}\right) \left(R_{yy}W_{mn} - \mathcal{M}_{mn}^2\right) + \left(\frac{m\pi}{a}\right) R_{xy}W_{mn} \\ &= S_{23}W_{mn} - T_{23}T_{mn}^1 \\ S_{mn}^{zz} &= \left(\frac{m\pi}{a}\right) S_{mn}^{xz} + \left(\frac{n\pi}{b}\right) S_{mn}^{yz} = S_{33}W_{mn} - T_{33}T_{mn}^1 \end{aligned} \quad (6.2.27)$$

and S_{ij} and T_{ij} are

$$\begin{aligned} S_{13} &= \left(\frac{m\pi}{a}\right)^3 Q_{11} + \left(\frac{m\pi}{a}\right) \left(\frac{n\pi}{b}\right)^2 (Q_{12} + 2Q_{66}) \\ S_{23} &= \left(\frac{n\pi}{b}\right)^3 Q_{22} + \left(\frac{m\pi}{a}\right)^2 \left(\frac{n\pi}{b}\right) (Q_{12} + 2Q_{66}) \\ S_{33} &= \left(\frac{m\pi}{a}\right)^4 Q_{11} + 2 \left(\frac{m\pi}{a}\right)^2 \left(\frac{n\pi}{b}\right)^2 (Q_{12} + 2Q_{66}) + \left(\frac{n\pi}{b}\right)^4 Q_{22} \\ T_{13} &= \left(\frac{m\pi}{a}\right) (Q_{11}\alpha_1 + Q_{12}\alpha_2), \quad T_{23} = \left(\frac{n\pi}{b}\right) (Q_{12}\alpha_1 + Q_{22}\alpha_2) \\ T_{33} &= \left(\frac{m\pi}{a}\right)^2 Q_{11}\alpha_1 + \left[\left(\frac{m\pi}{a}\right)^2 \alpha_2 + \left(\frac{n\pi}{b}\right)^2 \alpha_1\right] Q_{12} + \left(\frac{n\pi}{b}\right)^2 Q_{22}\alpha_2 \end{aligned} \quad (6.2.28)$$

Note that σ_{xz} and σ_{yz} are zero and $\sigma_{zz} = q$ at the top surface of the plate ($z = h/2$). The transverse shear stress σ_{xz} is the maximum at $(x, y, z) = (0, b/2, 0)$, σ_{yz} is the maximum at $(x, y, z) = (a/2, 0, 0)$, and the transverse normal stress σ_{zz} is the maximum at $(x, y, z) = (a/2, b/2, h/2)$.

All developments presented above can be specialized to isotropic plates by setting $\alpha_1 = \alpha_2 = \alpha$ and

$$D_{11} = D_{22} = D, \quad D_{12} = \nu D, \quad 2D_{66} = (1 - \nu)D, \quad D = \frac{Eh^3}{12(1 - \nu^2)} \quad (6.2.29)$$

The thermal resultants take the form

$$M_{mn}^1 = M_{mn}^2 = D(1 + \nu)\alpha T_{mn}^1 = \frac{Eh^3\alpha}{12(1 - \nu)} T_{mn}^1 \quad (6.2.30)$$

The transverse deflection becomes

$$w_0(x, y) = \sum_{n=1}^{\infty} \sum_{m=1}^{\infty} W_{mn} \sin \frac{m\pi x}{a} \sin \frac{n\pi y}{b} \quad (6.2.31)$$

where $s = b/a$ is the plate aspect ratio and

$$W_{mn} = \frac{b^4}{D\pi^4} \left[\frac{q_{mn} + \delta_T(m^2s^2 + n^2)}{(m^2s^2 + n^2)^2 + \hat{k}} \right], \quad \hat{k} = \frac{kb^4}{D\pi^4}, \quad \delta_T = \frac{T_{mn}^1\alpha D(1 + \nu)\pi^2}{b^2} \quad (6.2.32)$$

The bending moments become

$$\begin{aligned} M_{xx} &= D \sum_{n=1}^{\infty} \sum_{m=1}^{\infty} \left[\frac{\pi^2}{b^2} (m^2 s^2 + \nu n^2) W_{mn} - (1 + \nu) \alpha T_{mn}^1 \right] \sin \frac{m\pi x}{a} \sin \frac{n\pi y}{b} \\ M_{yy} &= D \sum_{n=1}^{\infty} \sum_{m=1}^{\infty} \left[\frac{\pi^2}{b^2} (\nu m^2 s^2 + n^2) W_{mn} - (1 + \nu) \alpha T_{mn}^1 \right] \sin \frac{m\pi x}{a} \sin \frac{n\pi y}{b} \\ M_{xy} &= -(1 - \nu) \frac{\pi^2}{b^2} D s \sum_{n=1}^{\infty} \sum_{m=1}^{\infty} mn W_{mn} \cos \frac{m\pi x}{a} \cos \frac{n\pi y}{b} \end{aligned} \quad (6.2.33)$$

The transverse shear forces Q_x and Q_y can be calculated using Eqs. (6.2.15a,b) with

$$\begin{aligned} S_{xx} &= D \left[\left(\frac{m\pi}{a} \right)^3 + \left(\frac{m\pi}{a} \right) \left(\frac{n\pi}{b} \right)^2 \right] \\ S_{yy} &= D \left[\left(\frac{n\pi}{b} \right)^3 + \left(\frac{m\pi}{a} \right)^2 \left(\frac{n\pi}{b} \right) \right] \end{aligned} \quad (6.2.34)$$

6.2.3 Sinusoidally Loaded Plates

The Navier solution for a sinusoidally distributed transverse load

$$q(x, y) = q_0 \sin \frac{\pi x}{a} \sin \frac{\pi y}{b} \quad (6.2.35)$$

is a one-term solution ($m = n = 1$ and $q_{11} = q_0$) and, therefore, it is a *closed-form solution*. For this case, the deflection in Eq. (6.2.11) becomes

$$w_0(x, y) = \frac{q_0 b^4}{\pi^4 (D_{11} s^4 + 2\hat{D}_{12} s^2 + D_{22}) + k b^4} \sin \frac{\pi x}{a} \sin \frac{\pi y}{b} \quad (6.2.36)$$

where $s = b/a$ is the plate aspect ratio. The maximum deflection occurs at $x = a/2$ and $y = b/2$:

$$w_{max} = w_0\left(\frac{a}{2}, \frac{b}{2}\right) = \frac{q_0 b^4}{\pi^4 (D_{11} s^4 + 2\hat{D}_{12} s^2 + D_{22}) + k b^4} \quad (6.2.37)$$

If $D_{11} = 25D_{22}$ and $2\hat{D}_{12} = 2.5D_{22}$ (typical of a graphite-epoxy fiber-reinforced material), $k = 0$, and $a = b$, we have

$$w_{max} = \frac{q_0 b^4}{28.5 D_{22} \pi^4} = 0.0003602 \frac{q_0 b^4}{D_{22}} = 0.0043115 \frac{q_0 b^4}{E_2 h^3} \quad (6.2.38)$$

The bending moments for the case when $k = 0$ are given by

$$\begin{aligned} M_{xx} &= \frac{q_0 b^2 (s^2 D_{11} + D_{12})}{\pi^2 (s^4 D_{11} + 2s^2 \hat{D}_{12} + D_{22})} \sin \frac{\pi x}{a} \sin \frac{\pi y}{b} \\ M_{yy} &= \frac{q_0 b^2 (s^2 D_{12} + D_{22})}{\pi^2 (s^4 D_{11} + 2s^2 \hat{D}_{12} + D_{22})} \sin \frac{\pi x}{a} \sin \frac{\pi y}{b} \\ M_{xy} &= -\frac{2s q_0 b^2 D_{66}}{\pi^2 (s^4 D_{11} + 2s^2 \hat{D}_{12} + D_{22})} \cos \frac{\pi x}{a} \cos \frac{\pi y}{b} \end{aligned} \quad (6.2.39)$$

The maximum values of the bending moments M_{xx} and M_{yy} occur at $x = a/2$ and $y = b/2$, and the maximum of M_{xy} occurs at $x = y = 0$.

The inplane stresses are

$$\begin{Bmatrix} \sigma_{xx} \\ \sigma_{yy} \\ \sigma_{xy} \end{Bmatrix} = z \frac{w_s \pi^2}{b^2} \begin{Bmatrix} (s^2 Q_{11} + Q_{12}) \sin \frac{\pi x}{a} \sin \frac{\pi y}{b} \\ (s^2 Q_{12} + Q_{22}) \sin \frac{\pi x}{a} \sin \frac{\pi y}{b} \\ -2s Q_{66} \cos \frac{\pi x}{a} \cos \frac{\pi y}{b} \end{Bmatrix} \quad (6.2.40)$$

where

$$w_s = \frac{q_0 b^4}{\pi^4 (s^4 D_{11} + 2s^2 \hat{D}_{12} + D_{22}) + kb^4} \quad (6.2.41)$$

The maximum normal stresses occur at $(x, y, z) = (a/2, b/2, h/2)$, and the shear stress is maximum at $(x, y, z) = (a, b, -h/2)$.

The transverse shear and normal stresses $(\sigma_{xz}, \sigma_{yz}, \sigma_{zz})$ computed from the equilibrium equations are

$$\begin{aligned} \sigma_{xz} &= \frac{h^2}{8} \left[1 - \left(\frac{2z}{h} \right)^2 \right] S_{13} w_s \cos \frac{\pi x}{a} \sin \frac{\pi y}{b} \\ \sigma_{yz} &= \frac{h^2}{8} \left[1 - \left(\frac{2z}{h} \right)^2 \right] S_{23} w_s \sin \frac{\pi x}{a} \cos \frac{\pi y}{b} \\ \sigma_{zz} &= -\frac{h^3}{48} \left\{ \left[1 + \left(\frac{2z}{h} \right)^3 \right] - 3 \left[1 + \left(\frac{2z}{h} \right) \right] \right\} S_{33} w_s \sin \frac{\pi x}{a} \sin \frac{\pi y}{b} \end{aligned} \quad (6.2.42)$$

where w_s is given by Eq. (6.2.41) and

$$\begin{aligned} S_{13} &= \frac{\pi^3}{b^3} \left[s^3 Q_{11} + s^2 (Q_{12} + 2Q_{66}) \right] \\ S_{23} &= \frac{\pi^3}{b^3} \left[s^3 Q_{22} + s^2 (Q_{12} + 2Q_{66}) \right] \\ S_{33} &= \frac{\pi^4}{b^4} \left[s^4 Q_{11} + 2s^2 (Q_{12} + 2Q_{66}) + Q_{22} \right] \end{aligned} \quad (6.2.43)$$

Clearly, the maximum of σ_{xz} occurs at $x = 0$, $y = b/2$, and $z = 0$; σ_{yz} is the maximum at $x = a/2$, $y = 0$, and $z = 0$; and σ_{zz} is maximum at $x = a/2$, $y = b/2$, and $z = h/2$.

For isotropic plates with $k = 0$, the deflection becomes

$$w_0(x, y) = \frac{q_0 b^4}{\pi^4 D(s^2 + 1)^2} \sin \frac{\pi x}{a} \sin \frac{\pi y}{b} \quad (6.2.44)$$

The maximum deflection occurs at $x = a/2$ and $y = b/2$

$$w_{max} = \frac{q_0 b^4}{\pi^4 D(s^2 + 1)^2} \quad (6.2.45)$$

and for a square ($s = b/a = 1$) isotropic plate, we have

$$w_{max} = \frac{q_0 a^4}{4D\pi^4} \approx 0.002566 \frac{q_0 a^4}{D} \quad (6.2.46)$$

For rectangular isotropic plates, the maximum bending moments are

$$(M_{xx})_{max} = \frac{q_0 b^2(s^2 + \nu)}{\pi^2(s^2 + 1)^2}, \quad (M_{yy})_{max} = \frac{q_0 b^2(\nu s^2 + 1)}{\pi^2(s^2 + 1)^2} \quad (6.2.47)$$

$$(M_{xy})_{max} = -\frac{q_0 s b^2(1 - \nu)}{\pi^2(s^2 + 1)^2} \quad (6.2.48)$$

and for a square isotropic plate with $\nu = 0.3$, we have

$$(M_{xx})_{max} = (M_{yy})_{max} = \frac{(1 + \nu)q_0 b^2}{4\pi^2} = 0.03293q_0 a^2 \quad (6.2.49)$$

$$(M_{xy})_{max} = -\frac{(1 - \nu)q_0 b^2}{4\pi^2} = -0.01773q_0 a^2 \quad (6.2.50)$$

The reaction force at the corner $x = a$ and $y = b$ of an isotropic rectangular plate is given by

$$R_c = \frac{2q_0 s b^2(1 - \nu)}{\pi^2(s^2 + 1)^2} \quad (6.2.51)$$

which acts in the direction of the applied load. In other words, if the load is applied downward (i.e., q_0 is positive), the corners have the tendency to lift, but this is prevented by the concentrated downward reactions at the corners. For a square isotropic plate ($\nu = 0.3$) this value is $R_c = 0.03546q_0 a^2$.

The inplane normal stresses in a rectangular isotropic plate are maximum at the center of the plate. Substituting $x = a/2$, $y = b/2$ and $z = h/2$ in Eq. (6.2.40), we find

$$\left\{ \begin{array}{l} \sigma_{xx} \\ \sigma_{yy} \end{array} \right\}_{max} = \frac{6q_0 b^2}{\pi^2 h^2(s^2 + 1)^2} \left\{ \begin{array}{l} (s^2 + \nu) \\ (\nu s^2 + 1) \end{array} \right\} \quad (6.2.52)$$

For $a > b$, $(\sigma_{xx})_{max} > (\sigma_{yy})_{max}$. The shear stress σ_{xy} is maximum at $(x, y, z) = (a, b, -h/2)$ and $(x, y, z) = (0, 0, -h/2)$. We have

$$(\sigma_{xy})_{max} = \frac{6q_0 b^2 s(1-\nu)}{\pi^2 h^2 (s^2 + 1)^2} \quad (6.2.53)$$

The maximum transverse shear stress σ_{yz} , for example, occurs at $(x, y, z) = (a/2, 0, 0)$ and its value is given by [see Eq. (6.2.42)]

$$(\sigma_{yz})_{max} = \frac{3q_0 b s^2}{2\pi h (s^2 + 1)} \quad (6.2.54)$$

If we use the formula $\tilde{\sigma}_{yz} = 3V_y/2h$, we obtain

$$(\tilde{\sigma}_{yz})_{max} = \frac{3q_0 b s^2 [1 + (2 - \nu)s^2]}{2\pi h (s^2 + 1)^2} \quad (6.2.55)$$

which is larger in value. For a square isotropic ($\nu = 0.3$) plate, the maximum stress values are

$$\begin{aligned} (\sigma_{xx})_{max} &= (\sigma_{yy})_{max} = 0.1976 \frac{q_0 a^2}{h^2}, \quad (\sigma_{xy})_{max} = 0.1064 \frac{q_0 a^2}{h^2} \\ (\sigma_{yz})_{max} &= 0.2387 \frac{q_0 a}{h} \quad \text{and} \quad (\tilde{\sigma}_{yz})_{max} = 0.3223 \frac{q_0 a}{h} \end{aligned}$$

6.2.4 Plates with Distributed and Point Loads

For loads other than sinusoidal load, the Navier solution is a series solution that can be evaluated for a desired number of terms in the series. For example, for *uniformly distributed load* $q(x, y) = q_0$, a constant, we have

$$q_{mn} = \frac{16q_0}{\pi^2 mn} \quad \text{for } m, n, \text{ odd} \quad (6.2.56)$$

and the solution becomes

$$w_0(x, y) = \frac{16q_0}{\pi^2} \sum_{n=1,3,\dots}^{\infty} \sum_{m=1,3,\dots}^{\infty} \frac{1}{mnd_{mn}} \sin \frac{m\pi x}{a} \sin \frac{n\pi y}{b} \quad (6.2.57)$$

where d_{mn} is defined in Eq. (6.2.10)

$$d_{mn} = \frac{\pi^4}{b^4} \left[D_{11} m^4 s^4 + 2\hat{D}_{12} m^2 n^2 s^2 + D_{22} n^4 \right] + k$$

For the *hydrostatic load* $q(x, y) = q_0(y/b)$, we have

$$q_{mn} = \frac{8q_0}{\pi^2 mn} (-1)^{n+1} \quad \text{for } m = 1, 3, \dots; n = 1, 2, 3, \dots \quad (6.2.58)$$

and the solution becomes

$$w_0(x, y) = \frac{8q_0}{\pi^2} \sum_{n=1,2,\dots}^{\infty} \sum_{m=1,3,\dots}^{\infty} \frac{(-1)^{n+1}}{mnd_{mn}} \sin \frac{m\pi x}{a} \sin \frac{n\pi y}{b} \quad (6.2.59)$$

For a *point load* Q_0 located at (x_0, y_0) , the load coefficients are given by Eq. (6.2.8)

$$q_{mn} = \frac{4Q_0}{ab} \sin \frac{m\pi x_0}{a} \sin \frac{n\pi y_0}{b} \quad (6.2.60)$$

and the solution becomes

$$w_0(x, y) = \frac{4Q_0}{ab} \sum_{n=1}^{\infty} \sum_{m=1}^{\infty} \frac{1}{d_{mn}} \sin \frac{m\pi x_0}{a} \sin \frac{n\pi y_0}{b} \sin \frac{m\pi x}{a} \sin \frac{n\pi y}{b} \quad (6.2.61)$$

The series in Eqs. (6.2.57) and (6.2.59) converge rapidly in the case of a uniformly distributed load, but the series in Eq. (6.2.61) for a point load has a slower convergence. The same comments apply for the calculation of bending moments and stresses for these loads, which are given below:

$$\begin{aligned} M_{xx} &= \frac{\pi^2}{b^2} \sum_{n=1}^{\infty} \sum_{m=1}^{\infty} (m^2 s^2 D_{11} + n^2 D_{12}) W_{mn} \sin \frac{m\pi x}{a} \sin \frac{n\pi y}{b} \\ M_{yy} &= \frac{\pi^2}{b^2} \sum_{n=1}^{\infty} \sum_{m=1}^{\infty} (m^2 s^2 D_{12} + n^2 D_{22}) W_{mn} \sin \frac{m\pi x}{a} \sin \frac{n\pi y}{b} \\ M_{xy} &= -\frac{2s\pi^2 D_{66}}{b^2} \sum_{n=1}^{\infty} \sum_{m=1}^{\infty} mn W_{mn} \cos \frac{m\pi x}{a} \cos \frac{n\pi y}{b} \end{aligned} \quad (6.2.62)$$

and the inplane stresses are given by

$$\left\{ \begin{array}{l} \sigma_{xx} \\ \sigma_{yy} \\ \sigma_{xy} \end{array} \right\} = z \frac{\pi^2}{b^2} \sum_{n=1}^{\infty} \sum_{m=1}^{\infty} W_{mn} \left\{ \begin{array}{l} (s^2 m^2 Q_{11} + n^2 Q_{12}) \sin \frac{m\pi x}{a} \sin \frac{n\pi y}{b} \\ (s^2 m^2 Q_{12} + n^2 Q_{22}) \sin \frac{m\pi x}{a} \sin \frac{n\pi y}{b} \\ -2smn Q_{66} \cos \frac{m\pi x}{a} \cos \frac{n\pi y}{b} \end{array} \right\} \quad (6.2.63)$$

where $W_{mn} = q_{mn}/d_{mn}$. The maximum normal stresses occur at $(x, y, z) = (a/2, b/2, h/2)$, and the shear stress is maximum at $(x, y, z) = (a, b, -h/2)$.

The transverse stresses ($\sigma_{xz}, \sigma_{yz}, \sigma_{zz}$) computed using the 3-D stress equilibrium equations for any $-h/2 \leq z \leq h/2$ are

$$\begin{aligned} \sigma_{xz} &= \frac{h^2}{8} \left[1 - \left(\frac{2z}{h} \right)^2 \right] \sum_{n=1}^{\infty} \sum_{m=1}^{\infty} S_{13} W_{mn} \cos \frac{m\pi x}{a} \sin \frac{n\pi y}{b} \\ \sigma_{yz} &= \frac{h^2}{8} \left[1 - \left(\frac{2z}{h} \right)^2 \right] \sum_{n=1}^{\infty} \sum_{m=1}^{\infty} S_{23} W_{mn} \sin \frac{m\pi x}{a} \cos \frac{n\pi y}{b} \\ \sigma_{zz} &= -\frac{h^3}{48} \left\{ \left[1 + \left(\frac{2z}{h} \right)^3 \right] - 3 \left[1 + \left(\frac{2z}{h} \right) \right] \right\} \\ &\times \sum_{n=1}^{\infty} \sum_{m=1}^{\infty} S_{33} W_{mn} \sin \frac{m\pi x}{a} \sin \frac{n\pi y}{b} \end{aligned} \quad (6.2.64a)$$

where

$$\begin{aligned} S_{13} &= \left(\frac{m\pi}{a}\right)^3 Q_{11} + \left(\frac{m\pi}{a}\right) \left(\frac{n\pi}{b}\right)^2 (Q_{12} + 2Q_{66}) \\ S_{23} &= \left(\frac{n\pi}{b}\right)^3 Q_{22} + \left(\frac{m\pi}{a}\right)^2 \left(\frac{n\pi}{b}\right) (Q_{12} + 2Q_{66}) \\ S_{33} &= \left(\frac{m\pi}{a}\right)^4 Q_{11} + 2 \left(\frac{m\pi}{a}\right)^2 \left(\frac{n\pi}{b}\right)^2 (Q_{12} + 2Q_{66}) + \left(\frac{n\pi}{b}\right)^4 Q_{22} \end{aligned} \quad (6.2.64b)$$

In integrating the stress-equilibrium equations, it is assumed that the stresses ($\sigma_{xz}, \sigma_{yz}, \sigma_{zz}$) are zero at the bottom surface of the plate ($z = -h/2$). Because of the assumptions of the plate theory, they will also be zero at $z = h/2$. The transverse shear stress σ_{xz} is the maximum at $(x, y, z) = (0, b/2, 0)$, σ_{yz} is the maximum at $(x, y, z) = (a/2, 0, 0)$, and the transverse normal stress σ_{zz} is the maximum at $(x, y, z) = (a/2, b/2, h/2)$.

Uniform load. For an isotropic rectangular plate with $k = 0$ and subjected to a uniformly distributed load, the deflection is given by

$$w_0(x, y) = \frac{16q_0b^4}{D\pi^6} \sum_{n=1,3,\dots}^{\infty} \sum_{m=1,3,\dots}^{\infty} \frac{1}{mn(m^2s^2 + n^2)^2} \sin \frac{m\pi x}{a} \sin \frac{n\pi y}{b} \quad (6.2.65)$$

The center deflection becomes

$$w_0\left(\frac{a}{2}, \frac{b}{2}\right) = \frac{16q_0b^4}{D\pi^6} \sum_{n=1,3,\dots}^{\infty} \sum_{m=1,3,\dots}^{\infty} \frac{(-1)^{\frac{m+n}{2}-1}}{mn(m^2s^2 + n^2)^2} \quad (6.2.66)$$

For a square plate ($b = a$), it reduces to

$$w_{max} = \frac{16q_0a^4}{D\pi^6} \sum_{n=1,3,\dots}^{\infty} \sum_{m=1,3,\dots}^{\infty} \frac{(-1)^{\frac{m+n}{2}-1}}{mn(m^2 + n^2)^2} \quad (6.2.67)$$

A one-term solution is given by

$$w_{max} = \frac{4q_0a^4}{D\pi^6} = 0.00416 \frac{q_0a^4}{D} \quad (6.2.68)$$

which is about 2.4% in error compared to the solution obtained with $m, n = 1, 3, \dots, 9$. Thus, the series in Eq. (6.2.66) converges rapidly. The expressions for bending moments and stresses, which involve second derivatives of w_0 , do not converge as rapidly. The first-term values are ($\nu = 0.3$)

$$(M_{xx})_{max} = 0.05338q_0a^2, \quad (\sigma_{xx})_{max} = 0.3203 \frac{q_0a^2}{h^2}$$

The first four terms of the series (i.e., $m, n = 1, 3$) yields

$$w_{max} = 0.004056 \frac{q_0a^4}{D}, \quad (M_{xx})_{max} = 0.0469q_0a^2, \quad (\sigma_{xx})_{max} = 0.2816 \frac{q_0a^2}{h^2}$$

Point load. For an isotropic rectangular plate ($k = 0$) under a point load Q_0 at (x_0, y_0) , the deflection is given by

$$w_0(x, y) = \frac{4Q_0 b^2 s}{D\pi^4} \sum_{n=1,3,\dots}^{\infty} \sum_{m=1,3,\dots}^{\infty} \frac{\sin \frac{m\pi x_0}{a} \sin \frac{n\pi y_0}{b}}{(m^2 s^2 + n^2)^2} \sin \frac{m\pi x}{a} \sin \frac{n\pi y}{b} \quad (6.2.69)$$

The center deflection when the load is applied at the center is given by

$$w_0\left(\frac{a}{2}, \frac{b}{2}\right) = \frac{4Q_0 b^2 s}{D\pi^4} \sum_{n=1,3,\dots}^{\infty} \sum_{m=1,3,\dots}^{\infty} \frac{1}{(m^2 s^2 + n^2)^2} \quad (6.2.70)$$

In the case of a square plate, the center deflection becomes

$$w_{max} = \frac{4Q_0 a^2}{D\pi^4} \sum_{n=1,3,\dots}^{\infty} \sum_{m=1,3,\dots}^{\infty} \frac{1}{(m^2 + n^2)^2} \quad (6.2.71)$$

The first term of the series yields ($\nu = 0.3$)

$$w_{max} = 0.01027 \frac{Q_0 a^2}{D}, \quad (M_{xx})_{max} = 0.1317 Q_0 a, \quad (\sigma_{xx})_{max} = 0.7903 \frac{Q_0 a}{h^2}$$

Taking the first four terms (i.e., $m, n = 1, 3$) of the series, we obtain

$$w_{max} = 0.01121 \frac{Q_0 a^2}{D}, \quad (M_{xx})_{max} = 0.199 Q_0 a, \quad (\sigma_{xx})_{max} = 1.194 \frac{Q_0 a}{h^2}$$

The deflection is about 3.4% in error compared to the solution 0.0116 ($Q_0 a^2 / D$) obtained using $m, n = 1, 3, \dots, 19$.

Table 6.2.2 contains the nondimensional maximum transverse deflections and stresses of square and rectangular plates under various types of loads:

$$\begin{aligned} \bar{w} &= w_0(0, 0) \left(E_2 h^3 / a^4 q_0 \right); & \bar{\sigma}_{xx} &= \sigma_{xx}(a/2, b/2, h/2) \left(h^2 / a^2 q_0 \right) \\ \bar{\sigma}_{yy} &= \sigma_{yy}(a/2, b/2, h/2) \left(h^2 / a^2 q_0 \right); & \bar{\sigma}_{xy} &= \sigma_{xy}(a, b, -h/2) \left(h^2 / a^2 q_0 \right) \\ \bar{\sigma}_{xz} &= \sigma_{xz}(0, b/2, 0) (h/aq_0); & \bar{\sigma}_{yz} &= \sigma_{yz}(a/2, 0, 0) (h/aq_0) \end{aligned}$$

The load consists of only sinusoidal (SL), uniform (UL), hydrostatic (HL), or central point load (PL). Since convergence for derivatives of a function is slower than the function itself, the convergence is slower for stresses, which are calculated using the derivatives of the deflection. In the case of the point load, convergence for stresses will not be reached due to the stress singularity at the center of the plate.

Deflections for other load cases can also be determined by knowing q_{mn} . For example, suppose that a uniform load of intensity q_0 is applied on a rectangular patch of size $2c \times 2d$ (Figure 6.2.1) whose center is located at (x_0, y_0) . Then, from Eq. (6.2.4), we have

Table 6.2.2. Transverse deflections and stresses in isotropic ($\nu = 0.3$) and orthotropic ($E_1/E_2 = 25$, $G_{12} = G_{13} = 0.5E_2$, $\nu_{12} = 0.25$) square and rectangular plates subjected to distributed loads ($k = 0$).

Load	\bar{w}	$\bar{\sigma}_{xx}$	$\bar{\sigma}_{yy}$	$\bar{\sigma}_{xy}$	$\bar{\sigma}_{xz}$	$\bar{\sigma}_{yz}$
Square Plates ($b/a = 1$)						
<i>Isotropic plates ($\nu = 0.3$)</i>						
SL	0.0280	0.1976	0.1976	0.1064	0.2387	0.2387
UL (19)	0.0444	0.2873	0.2873	0.1946	0.4909	0.4909
HL (19)	0.0222	0.1436	0.1436	0.0775	0.2455	0.1353
PL (29)	0.1266	2.4350	2.4350	0.3658	1.0010	1.0010
<i>Orthotropic plates</i>						
SL	0.0043	0.5387	0.0267	0.0213	0.4398	0.0376
UL (19)	0.0065	0.7866	0.0244	0.0463	0.7758	0.1811
HL (19)	0.0032	0.3933	0.0122	0.0105	0.3879	0.0092
PL (29)	0.0232	6.0075	0.8670	0.0409	1.8150	0.1338
Rectangular Plates ($b/a = 3$)						
<i>Isotropic plates ($\nu = 0.3$)</i>						
SL	0.0908	0.5088	0.2024	0.1149	0.4297	0.1432
UL (19)	0.1336	0.7130	0.2433	0.2830	0.7221	0.5110
HL (19)	0.0668	0.3565	0.1217	0.0579	0.3610	0.0636
PL (29)	0.1845	2.3523	1.8828	0.0566	0.9032	0.2257
<i>Orthotropic plates</i>						
SL	0.0048	0.6016	0.0087	0.0080	0.4746	0.0085
UL (19)	0.0062	0.7494	0.0071	0.0447	0.7310	0.1509
HL (19)	0.0031	0.3747	0.0035	0.0034	0.3655	0.0044
PL (29)	0.0227	4.8157	0.5648	0.0000	1.4820	0.0864

Note: The numbers in parentheses denote the maximum values of m and n used to evaluate the series in Eq. (6.2.69).

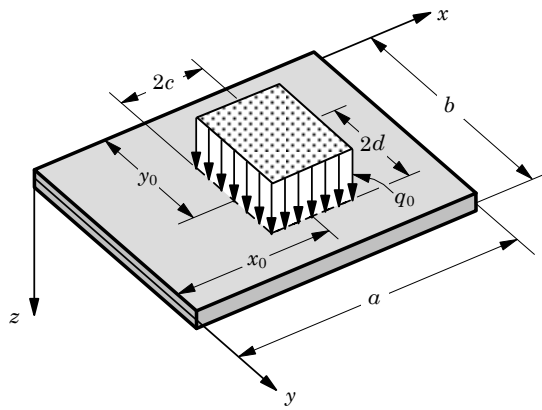


Figure 6.2.1. Rectangular plate with a patch loading.

$$\begin{aligned} q_{mn} &= \frac{4q_0}{ab} \int_{y_0-d}^{y_0+d} \int_{x_0-c}^{x_0+c} \sin \frac{m\pi x}{a} \sin \frac{n\pi y}{b} dx dy \\ &= \frac{16q_0}{\pi^2 mn} \sin \frac{m\pi x_0}{a} \sin \frac{n\pi y_0}{b} \sin \frac{m\pi c}{a} \sin \frac{n\pi d}{b} \end{aligned} \quad (6.2.72)$$

Similarly, if a point load Q_0 is applied at point (x_0, y_0) , then q_{mn} can be computed from Eq. (6.2.72) by setting $4q_0 = Q_0/(cd)$ and letting c and d approach zero. We obtain

$$q_{mn} = \frac{4Q_0}{ab} \sin \frac{m\pi x_0}{a} \sin \frac{n\pi y_0}{b} \quad (6.2.73)$$

and the deflection is given by Eq. (6.2.61).

6.2.5 Plates with Thermal Loads

If an orthotropic plate is subjected to a temperature field that varies linearly through the thickness $\Delta T = zT_1(x, y)$ and $q = k = 0$, then the solution (6.2.11) becomes

$$w_0(x, y) = \sum_{n=1}^{\infty} \sum_{m=1}^{\infty} W_{mn} \sin \frac{m\pi x}{a} \sin \frac{n\pi y}{b} \quad (6.2.74a)$$

where [see Eqs. (6.2.9) and (6.2.10) with $q_{mn} = 0$]

$$W_{mn} = \frac{T_{mn}^1 b^2}{\pi^2} \frac{[m^2 s^2 (D_{11}\alpha_1 + D_{12}\alpha_2) + n^2 (D_{12}\alpha_1 + D_{22}\alpha_2)]}{(m^4 s^4 D_{11} + 2m^2 n^2 s^2 \hat{D}_{12} + n^4 D_{22})} \quad (6.2.74b)$$

and T_{mn}^1 is defined by equation of the form (6.2.4). For a rectangular isotropic plate, the deflection is given by Eq. (6.2.74a) with

$$W_{mn} = \frac{(1+\nu)\alpha b^2}{\pi^2} \frac{T_{mn}^1}{(m^2 s^2 + n^2)} \quad (6.2.74c)$$

The bending moments can be calculated using Eqs. (6.2.14a,b) and stresses by Eqs. (6.2.23), (6.2.24), and (6.2.26)–(6.2.28), with W_{mn} defined above and M_{mn}^1 and M_{mn}^2 in Eq. (6.2.22).

Sinusoidally Distributed Temperature Field

For a sinusoidally distributed temperature field over the surface of the plate, but linear through the plate thickness, $\Delta T = zT_1(x, y)$, with

$$T_1(x, y) = T_0^1 \sin \frac{m\pi x}{a} \sin \frac{n\pi y}{b} \quad (6.2.75)$$

the coefficients T_{mn}^1 are equal to T_0^1 and the deflection becomes

$$w_0(x, y) = \hat{w} \sin \frac{\pi x}{a} \sin \frac{\pi y}{b} \quad (6.2.76a)$$

where

$$\hat{w} = \frac{b^2 [s^2 (D_{11}\alpha_1 + D_{12}\alpha_2) + (D_{12}\alpha_1 + D_{22}\alpha_2)] T_0^1}{\pi^2 (s^4 D_{11} + 2s^2 \hat{D}_{12} + D_{22})} \quad (6.2.76b)$$

For a square plate ($s = 1$), we have

$$w_0(x, y) = \frac{b^2 [(D_{11} + D_{12})\alpha_1 + (D_{12} + D_{22})\alpha_2] T_0^1}{\pi^2 (D_{11} + 2\hat{D}_{12} + D_{22})} \sin \frac{\pi x}{a} \sin \frac{\pi y}{b} \quad (6.2.77)$$

For the particular case in which $D_{11} = 25D_{22}$, $2\hat{D}_{12} = 2.5D_{22}$, $\alpha_1 = 3\alpha_2$, and $a = b$, the maximum deflection becomes

$$w_{max} = \frac{77}{28.5\pi^2} T_0^1 \alpha_2 b^2 \approx 0.2738 T_0^1 \alpha_2 a^2 \quad (6.2.78)$$

The bending moments are

$$\begin{aligned} M_{xx} &= \frac{\pi^2}{b^2} \left[(D_{11}s^2 + D_{12})\hat{w} - (Q_{11}s^2 + Q_{12})T_0^1 \right] \sin \frac{\pi x}{a} \sin \frac{\pi y}{b} \\ M_{yy} &= \frac{\pi^2}{b^2} \left[(D_{12}s^2 + D_{22})\hat{w} - (Q_{12}s^2 + Q_{22})T_0^1 \right] \sin \frac{\pi x}{a} \sin \frac{\pi y}{b} \\ M_{xy} &= -2 \frac{\pi^2}{ab} D_{66} \hat{w} \cos \frac{\pi x}{a} \cos \frac{\pi y}{b} \end{aligned} \quad (6.2.79)$$

where \hat{w} is defined by Eq. (6.2.76b).

For an isotropic square plate, the deflection becomes

$$w_0(x, y) = \frac{(1+\nu)\alpha a^2 T_0^1}{2\pi^2} \sin \frac{\pi x}{a} \sin \frac{\pi y}{b} \quad (6.2.80)$$

The maximum deflection is $w_{max} = 0.0633(\alpha a^2 T_0^1)$ when $\nu = 0.25$, and $w_{max} = 0.06586(\alpha a^2 T_0^1)$ when $\nu = 0.3$. The bending moments become

$$\begin{aligned} M_{xx} &= \frac{\pi^2 D}{a^2} \left[\frac{(1+\nu)^2 \alpha a^2 T_0^1}{2\pi^2} - \frac{E\alpha T_0^1}{1-\nu} \right] \sin \frac{\pi x}{a} \sin \frac{\pi y}{a} \\ M_{yy} &= \frac{\pi^2 D}{a^2} \left[\frac{(1+\nu)^2 \alpha b^2 T_0^1}{2\pi^2} - \frac{E\alpha T_0^1}{1-\nu} \right] \sin \frac{\pi x}{a} \sin \frac{\pi y}{a} \\ M_{xy} &= -\frac{E\alpha T_0^1 h^3}{24} \cos \frac{\pi x}{a} \cos \frac{\pi y}{a} \end{aligned} \quad (6.2.81)$$

The maximum bending moments are

$$(M_{xx})_{max} = (M_{yy})_{max} = (M_{xy})_{max} = -(h^3 E\alpha T_0^1 / 24) \quad (6.2.82a)$$

and the maximum membrane stresses (at $z = h/2$) are

$$(\sigma_{xx})_{max} = (\sigma_{yy})_{max} = (\sigma_{xy})_{max} = -(h E\alpha T_0^1 / 4) \quad (6.2.82b)$$

Uniformly Distributed Temperature Field

For a uniformly distributed temperature field, $T_1(x, y) = T_0^1$, the coefficients T_{mn}^1 are equal to $16T_0^1/\pi^2 mn$. Hence, the deflection is

$$w_0(x, y) = \sum_{n=1}^{\infty} \sum_{m=1}^{\infty} W_{mn} \sin \frac{m\pi x}{a} \sin \frac{n\pi y}{b} \quad (6.2.83)$$

where

$$W_{mn} = 16T_0^1 \frac{[m^2 s^2 (D_{11}\alpha_1 + D_{12}\alpha_2) + n^2 (D_{12}\alpha_1 + D_{22}\alpha_2)]}{mn\pi^4(m^4 s^4 D_{11} + 2m^2 n^2 s^2 \hat{D}_{12} + n^4 D_{22})} \quad (6.2.84)$$

For an isotropic rectangular plate, the deflection becomes

$$w_0(x, y) = \frac{16T_0^1 \alpha(1 + \nu)b^2}{\pi^4} \sum_{n=1}^{\infty} \sum_{m=1}^{\infty} \frac{1}{(m^2 s^2 + n^2)mn} \sin \frac{m\pi x}{a} \sin \frac{n\pi y}{b} \quad (6.2.85)$$

In general, the series for thermal problems converge more slowly than the corresponding ones for mechanical loads (see Table 6.2.3). This can be seen by comparing the denominators of the series, for example, in Eqs. (6.2.65) and (6.2.85).

Table 6.2.3. Transverse deflections and stresses in isotropic ($\nu = 0.25$) and orthotropic ($E_1/E_2 = 25$, $G_{12} = G_{13} = 0.5E_2$, $\nu_{12} = 0.25$, $\alpha_1 = 3\alpha_2$) square plates subjected to distributed temperature fields of the form $\Delta T = zT^1(x, y)$.

Load	\hat{w}	$\hat{\sigma}_{xx}$	$\hat{\sigma}_{yy}$	$\hat{\sigma}_{xy}$
<i>Isotropic plates</i>				
SL	0.0633	-0.0025	-0.0025	0.0025
UL(1)	0.1027	0.0000	0.0000	0.0000
UL(3)	0.0902	0.0030	0.0030	0.0061
UL(9)	0.0922	-0.0019	-0.0019	0.0090
UL(49)	0.0921	-0.0024	-0.0024	0.0141
UL(99)	0.0921	0.0041	0.0041	0.0163
UL(199)	0.0921	0.0041	0.0041	0.0185
<i>Orthotropic plates</i>				
SL	0.2738	-0.0352	0.0082	0.0135
UL(1)	0.4438	0.1772	0.0187	0.0219
UL(3)	0.3924	0.3615	0.0098	0.0328
UL(9)	0.3977	0.0538	0.0533	0.0464
UL(49)	0.3974	0.0334	0.0046	0.0707
UL(99)	0.3974	0.4033	0.0132	0.0812
UL(199)	0.3974	0.4045	0.0132	0.0917

Note: The numbers in parentheses denote the maximum value of m and n used to evaluate the series.

Table 6.2.3 contains the nondimensional maximum transverse deflections and stresses

$$\hat{w} = w_0(0,0)/(\alpha_2 T_0^1 a^2), \quad \hat{\sigma} = \sigma \times \beta, \quad \beta = (1/h E_2 \alpha_2 T_0^1)$$

in square plates under two types of temperature variations, of which both are assumed to vary linearly through the thickness. The first one is a sinusoidal distribution of the form

$$\Delta T = z T_0^1 \sin \frac{\pi x}{a} \sin \frac{\pi y}{b} \quad (6.2.86)$$

and the second one is the uniform temperature of the form

$$\Delta T = z T_0^1 \quad (6.2.87)$$

where T_0^1 is a constant. In the case of uniform temperature field (with respect to x and y), the double trigonometric series are evaluated using $m, n = 1, 3, \dots, 99$.

6.3 Lévy's Solutions

6.3.1 Solution Procedure

Here we consider an alternate procedure to determine the solution to simply supported rectangular plates. The solution to the problem of a rectangular plate with two opposite edges simply supported and the other two edges having arbitrary boundary conditions can be represented in terms of single Fourier series as

$$w_0(x, y) = \sum_{n=1}^{\infty} W_n(x) \sin \frac{n\pi y}{b} \quad (6.3.1)$$

which satisfies the following simply supported boundary conditions on edges $y = 0$ and $y = b$ (Figure 6.3.1):

$$w_0(x, 0) = w_0(x, b) = 0, \quad M_{yy}(x, 0) = M_{yy}(x, b) = 0 \quad (6.3.2)$$

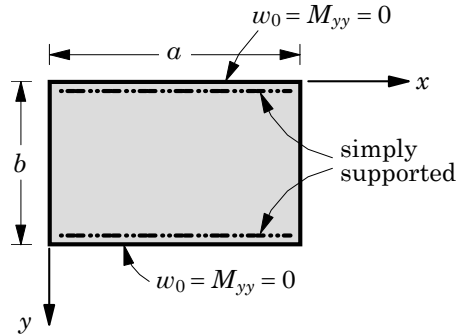


Figure 6.3.1. A rectangular plate with simply supported edges at $y = 0, b$.

Similarly, the load q and thermal moments M_{xx}^T and M_{yy}^T are represented as

$$q(x, y) = \sum_{n=1}^{\infty} q_n(x) \sin \frac{n\pi y}{b} \quad (6.3.3)$$

$$M_{xx}^T(x, y) = \sum_{n=1}^{\infty} M_n^1(x) \sin \frac{n\pi y}{b} \quad (6.3.4a)$$

$$M_{yy}^T(x, y) = \sum_{n=1}^{\infty} M_n^2(x) \sin \frac{n\pi y}{b} \quad (6.3.4b)$$

where $q_n(x)$, for example, is defined by

$$q_n(x) = \frac{2}{b} \int_0^b q(x, y) \sin \frac{n\pi y}{b} dy \quad (6.3.5)$$

The coefficients for various distributions of $q(x, y)$ are given in Table 6.3.1.

Substitution of Eqs. (6.3.1), (6.3.3), and (6.3.4a,b) into Eq. (6.1.1) results in

$$\sum_{n=1}^{\infty} \left\{ D_{11} \frac{d^4 W_n}{dx^4} - 2 \left(\frac{n\pi}{b} \right)^2 \hat{D}_{12} \frac{d^2 W_n}{dx^2} + \left[\left(\frac{n\pi}{b} \right)^4 D_{22} + k \right] W_n + \frac{d^2 M_n^1}{dx^2} - \left(\frac{n\pi}{b} \right)^2 M_n^2 - q_n \right\} \sin \frac{n\pi y}{b} = 0 \quad (6.3.6)$$

Since the result must hold for any y , it follows that the expression inside the braces must be zero:

$$\begin{aligned} D_{11} \frac{d^4 W_n}{dx^4} - 2 \left(\frac{n\pi}{b} \right)^2 \hat{D}_{12} \frac{d^2 W_n}{dx^2} + \left[\left(\frac{n\pi}{b} \right)^4 D_{22} + k \right] W_n \\ = q_n - \frac{d^2 M_n^1}{dx^2} + \left(\frac{n\pi}{b} \right)^2 M_n^2 \equiv \bar{q}_n \end{aligned} \quad (6.3.7)$$

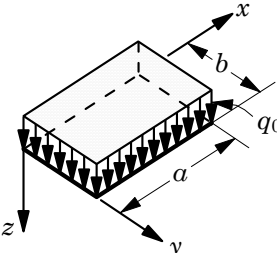
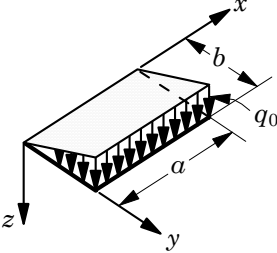
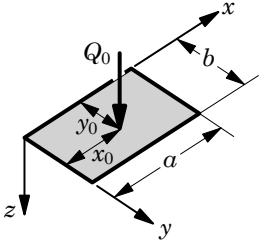
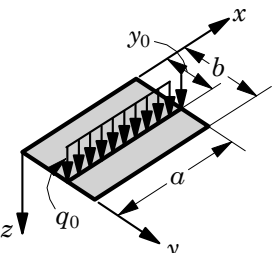
The fourth-order differential equation in Eq. (6.3.7) can be solved either analytically or by an approximate method. Analytically, Eq. (6.3.7) can be solved directly or by the *state-space approach* used in control theory. As for approximate methods, the Ritz, finite difference, and finite element methods are good candidates. Here, analytical and Ritz solutions are discussed.

6.3.2 Analytical Solution

The general form of the analytical solution to the fourth-order differential equation (6.3.7) consists of two parts: homogeneous and particular solutions. The homogeneous solution is of the form

$$W_n^h(x) = C \exp(\lambda x) \quad (6.3.8)$$

Table 6.3.1. Coefficients in the single trigonometric series expansion of loads in the Lévy method.

Loading	Coefficients $q_n(x)$
	Uniform load (UL) $q = q_0$ $q_n = \frac{4q_0}{n\pi}$ $(n = 1, 3, 5, \dots)$
	Hydrostatic load (HL) $q(x, y) = q_0 \frac{y}{b}$ $q_n = \frac{2q_0}{n\pi} (-1)^{n+1}$ $(n = 1, 2, 3, \dots)$
	Point load Q_0 at (x_0, y_0) $q_n = \frac{2Q_0}{b} \delta(x - x_0) \sin \frac{n\pi y_0}{b}$ $(n = 1, 2, 3, \dots)$
	Line load (LL) $q(x, y) = q_0 \delta(y - y_0)$ $q_n = \frac{2q_0}{b} \sin \frac{n\pi y_0}{b}$ $(n = 1, 2, 3, \dots)$

where λ denotes a root of the algebraic equation

$$D_{11}\lambda^4 - 2\left(\frac{n\pi}{b}\right)^2(D_{12} + 2D_{66})\lambda^2 + \left(\frac{n\pi}{b}\right)^4 D_{22} + k = 0 \quad (6.3.9)$$

The roots of this equation are

$$\begin{aligned} \lambda_1^2 &= \beta_n^2 \left(\frac{D_{12} + 2D_{66}}{D_{11}} \right) - \beta_n^2 \left[\left(\frac{D_{12} + 2D_{66}}{D_{11}} \right)^2 - \left(\frac{D_{22}}{D_{11}} + \frac{k}{D_{11}\beta_n^4} \right) \right]^{\frac{1}{2}} \\ \lambda_2^2 &= \beta_n^2 \left(\frac{D_{12} + 2D_{66}}{D_{11}} \right) + \beta_n^2 \left[\left(\frac{D_{12} + 2D_{66}}{D_{11}} \right)^2 - \left(\frac{D_{22}}{D_{11}} + \frac{k}{D_{11}\beta_n^4} \right) \right]^{\frac{1}{2}} \end{aligned} \quad (6.3.10)$$

where

$$\beta_n = \frac{n\pi}{b} \quad (6.3.11)$$

Since there are four roots ($\lambda_1, -\lambda_1, \lambda_2, -\lambda_2$), the solution (6.3.7) can be written as a linear combination of functions of these four roots. The true form of the solution depends on the nature of the roots, i.e., real or complex and equal or distinct. Three different cases are discussed below.

Case 1: Roots Are Real and Distinct

When $(D_{12} + 2D_{66})^2 > D_{11}(D_{22} + k/\beta_n^4)$, the roots are real and unequal: $\lambda_1, -\lambda_1, \lambda_2$, and $-\lambda_2$, where λ_1 and λ_2 are given by Eq. (6.3.10). Then the homogeneous part of the solution for this case is

$$W_n^h(x) = A_n \cosh \lambda_1 x + B_n \sinh \lambda_1 x + C_n \cosh \lambda_2 x + D_n \sinh \lambda_2 x \quad (6.3.12)$$

Case 2: Roots Are Real and Equal

When $(D_{12} + 2D_{66})^2 = D_{11}(D_{22} + k/\beta_n^4)$, the roots are real, but equal:

$$\lambda_1 = \lambda_2 = -\lambda_3 = -\lambda_4 \equiv \lambda, \quad \lambda^2 = \beta_n^2 \left(\frac{D_{12} + 2D_{66}}{D_{11}} \right) \quad (6.3.13)$$

and the homogeneous part of the solution is

$$W_n^h(x) = (A_n + B_n x) \cosh \lambda x + (C_n + D_n x) \sinh \lambda x \quad (6.3.14)$$

Case 3: Roots Are Complex

When $(D_{12} + 2D_{66})^2 < D_{11}(D_{22} + k/\beta_n^4)$, the roots are complex and they appear in complex conjugate pairs $\lambda_1 \pm i\lambda_2$ and $-\lambda_1 \pm i\lambda_2$ ($i = \sqrt{-1}$, $\lambda_1 > 0$, $\lambda_2 > 0$):

$$\begin{aligned} (\lambda_1)^2 &= \frac{\beta_n^2}{2D_{11}} \left[\sqrt{D_{11} \left(D_{22} + \frac{k}{\beta_n^4} \right)} + (D_{12} + 2D_{66}) \right] \\ (\lambda_2)^2 &= \frac{\beta_n^2}{2D_{11}} \left[\sqrt{D_{11} \left(D_{22} + \frac{k}{\beta_n^4} \right)} - (D_{12} + 2D_{66}) \right] \end{aligned} \quad (6.3.15)$$

The homogeneous part of the solution is

$$\begin{aligned} W_n^h(x) &= (A_n \cos \lambda_2 x + B_n \sin \lambda_2 x) \cosh \lambda_1 x \\ &\quad + (C_n \cos \lambda_2 x + D_n \sin \lambda_2 x) \sinh \lambda_1 x \end{aligned} \quad (6.3.16)$$

For isotropic plates, we have $D_{11} = D_{22} = D$ and $D_{12} + 2D_{66} = D$. Hence, Case 2 applies when $k = 0$ and Case 3 applies when $k \neq 0$. For isotropic plates *without* elastic foundation, the homogeneous solution is given by

$$W_n^h(x) = (A_n + B_n x) \cosh \beta_n x + (C_n + D_n x) \sinh \beta_n x \quad (6.3.17)$$

For isotropic plates on elastic foundation, Case 3 applies and we have

$$\begin{aligned} W_n^h(x) &= (A_n \cos \lambda_2 x + B_n \sin \lambda_2 x) \cosh \lambda_1 x \\ &\quad + (C_n \cos \lambda_2 x + D_n \sin \lambda_2 x) \sinh \lambda_1 x \end{aligned} \quad (6.3.18)$$

where

$$(\lambda_1)^2 = \frac{\beta_n^2}{2} \left[\sqrt{\left(1 + \frac{k}{D\beta_n^4}\right)} + 1 \right], \quad (\lambda_2)^2 = \frac{\beta_n^2}{2} \left[\sqrt{\left(1 + \frac{k}{D\beta_n^4}\right)} - 1 \right] \quad (6.3.19)$$

The particular solution W_n^p of the fourth-order differential equation (6.3.7) in the general case in which q_n , M_n^1 , and M_n^2 are functions of x can be determined by expanding the solution and the loads in Fourier series:

$$\begin{aligned} W_n^p(x) &= \sum_{m=1}^{\infty} W_{mn} \sin \frac{m\pi x}{a}, \quad q_n(x) = \sum_{m=1}^{\infty} q_{mn} \sin \frac{m\pi x}{a} \\ M_n^1(x) &= \sum_{m=1}^{\infty} M_{mn}^1 \sin \frac{m\pi x}{a}, \quad M_n^2(x) = \sum_{m=1}^{\infty} M_{mn}^2 \sin \frac{m\pi x}{a} \end{aligned} \quad (6.3.20)$$

where the coefficients q_{mn} , M_{mn}^1 , and M_{mn}^2 have the same meaning as in Eq. (6.2.4). Substituting these expressions into

$$D_{11} \frac{d^4 W_n^p}{dx^4} - 2\beta_n^2 \hat{D}_{12} \frac{d^2 W_n^p}{dx^2} + (\beta_n^4 D_{22} + k) W_n^p = q_n - \frac{d^2 M_n^1}{dx^2} + \beta_n^2 M_n^2 \quad (6.3.21)$$

we obtain [cf., Eq. (6.2.9)]

$$W_n^p(x) = \sum_{m=1}^{\infty} \frac{1}{d_{mn}} \left[q_{mn} + \left(\frac{m\pi}{a} \right)^2 M_{mn}^1 + \left(\frac{n\pi}{b} \right)^2 M_{mn}^2 \right] \sin \frac{m\pi x}{a} \quad (6.3.22)$$

where d_{mn} is defined by Eq. (6.2.10). The complete solution is given by

$$w_0(x, y) = \sum_{n=1}^{\infty} (W_n^h(x) + W_n^p(x)) \sin \beta_n y \quad (6.3.23)$$

where W_n^h for the three cases are given in Eqs. (6.3.12), (6.3.14), and (6.3.16), and W_n^p for all cases is given by Eq. (6.3.22). The four constants A_n , B_n , C_n , and D_n present in the expressions for W_n^h are determined using the four boundary conditions associated with the points $x = 0, a$ (two at each point). In particular, when the edges at $x = 0, a$ are also simply supported, the constants A_n , B_n , C_n , and D_n will be identically zero, and we obtain the solution in Eq. (6.2.11).

Alternatively, if q_n , $d^2M_n^1/dx^2$, and M_n^2 are at most linear functions of x , the particular solution is also a constant or a linear function of x , which is determined by substituting it into Eq. (6.3.21). The particular solution is given by

$$W_n^p(x) = \frac{q_n - \frac{d^2M_n^1}{dx^2} + \beta_n^2 M_n^2}{(D_{22}\beta_n^4 + k)} \equiv \frac{\bar{q}_n}{D_{22}\beta_n^4 + k} \equiv \hat{q}_n \quad (6.3.24)$$

and the complete solution becomes

$$w_0(x, y) = \sum_{n=1}^{\infty} \left(W_n^h(x) + \hat{q}_n \right) \sin \beta_n y \quad (6.3.25)$$

In this case, even for the case of simply supported boundary conditions on edges $x = 0, a$, the constants A_n , B_n , C_n , and D_n will not be zero.

The particular solution in Eq. (6.3.24) is valid for any $\bar{q}_n = q_n - (d^2M_n^1/dx^2) + \beta_n^2 M_n^2$ that is a constant or a linear function of x . Thus, $q(x, y)$ can be an arbitrary function of y , but must be a linear function of x in order for the particular solution in Eq. (6.3.24) to be valid. Note that a point load can be expressed as

$$q(x, y) = Q_0 \delta(x - x_0) \delta(y - y_0) \quad (6.3.26a)$$

and, therefore,

$$q_n = \frac{2}{b} \int_0^b q(x, y) \sin \frac{n\pi y}{b} dy = \frac{2Q_0}{b} \delta(x - x_0) \sin \frac{n\pi y_0}{b}$$

Similarly, hydrostatic load of the type

$$q(x, y) = q_0 \left(\frac{x}{a} \right) \quad (6.3.26b)$$

yields

$$q_n = \frac{2}{b} \int_0^b q(x, y) \sin \frac{n\pi y}{b} dy = \frac{2q_0}{n\pi} \left(\frac{x}{a} \right)$$

For these cases, the particular solutions are given by

$$W_n^p(x) = \frac{\frac{2Q_0}{b} \delta(x - x_0) \sin \frac{n\pi y_0}{b}}{(D_{22}\beta_n^4 + k)}, \quad W_n^p(x) = \frac{\frac{2q_0}{n\pi} \left(\frac{x}{a} \right)}{(D_{22}\beta_n^4 + k)}$$

When \bar{q}_n is a quadratic or higher-order function of x , one must use Eq. (6.3.22). In the following discussion, we assume that the loads are distributed such that \bar{q}_n is at most a linear function of x so that we can use the particular solution in Eq. (6.3.24).

6.3.3 Plates under Distributed Transverse Loads

Consider a simply supported plate subjected to a distributed transverse load $q(x, y)$ such that \bar{q}_n is independent of x . Since the simply supported boundary conditions on edges $y = 0$ and $y = b$ are identically satisfied by the assumed solution (6.3.1), the remaining simply supported boundary conditions on edges $x = 0$ and $x = a$ are

$$w_0 = 0, \quad M_{xx} \equiv -\left(D_{11}\frac{\partial^2 w_0}{\partial x^2} + D_{12}\frac{\partial^2 w_0}{\partial y^2}\right) = 0 \quad (6.3.27a)$$

Because of the form of the solution in Eq. (6.3.1), Eq. (6.3.27a) implies that

$$W_n(0) = 0, \quad -D_{11}\left(\frac{d^2 W_n}{dx^2}\right)_{x=0} + D_{12}\beta_n^2 W_n(0) = 0 \quad (6.3.27b)$$

for any n . Thus, if $w_0 = 0$ at a point, then $M_{xx} = 0$ necessarily implies that

$$\frac{\partial^2 w_0}{\partial x^2} = 0 \quad \text{at } x = 0 \quad (6.3.27c)$$

Case 1: $(D_{12} + 2D_{66})^2 > D_{11}(D_{22} + k/\beta_n^4)$. Only certain orthotropic plates fall into this category. The solution for this case is given by

$$w_0(x, y) = \sum_{n=1}^{\infty} (A_n \cosh \lambda_1 x + B_n \sinh \lambda_1 x + C_n \cosh \lambda_2 x + D_n \sinh \lambda_2 x + \hat{q}_n) \sin \beta_n y \quad (6.3.28a)$$

where λ_1 and λ_2 are defined by Eq. (6.3.10) and \hat{q}_n is defined by Eq. (6.3.24). The second derivative of w_0 with respect to x is

$$\frac{\partial^2 w_0}{\partial x^2} = \sum_{n=1}^{\infty} [\lambda_1^2 (A_n \cosh \lambda_1 x + B_n \sinh \lambda_1 x) + \lambda_2^2 (C_n \cosh \lambda_2 x + D_n \sinh \lambda_2 x)] \sin \beta_n y \quad (6.3.28b)$$

Substituting Eqs. (6.3.28a,b) into Eq. (6.3.27a), the following algebraic relations among A_n , B_n , C_n , and D_n are obtained:

$$\begin{bmatrix} 1 & 0 & 1 & 0 \\ \cosh \bar{\lambda}_1 & \sinh \bar{\lambda}_1 & \cosh \bar{\lambda}_2 & \sinh \bar{\lambda}_2 \\ \lambda_1^2 & 0 & \lambda_2^2 & 0 \\ \lambda_1^2 \cosh \bar{\lambda}_1 & \lambda_1^2 \sinh \bar{\lambda}_1 & \lambda_2^2 \cosh \bar{\lambda}_2 & \lambda_2^2 \sinh \bar{\lambda}_2 \end{bmatrix} \begin{Bmatrix} A_n \\ B_n \\ C_n \\ D_n \end{Bmatrix} = - \begin{Bmatrix} \hat{q}_n \\ \hat{q}_n \\ 0 \\ 0 \end{Bmatrix} \quad (6.3.29)$$

where $\bar{\lambda}_i = \lambda_i a$. These equations can be solved by Cramer's rule (see Section 1.2.5). The determinant of the 4×4 coefficient matrix in Eq. (6.3.29) is

$$\Delta = (\lambda_2^2 - \lambda_1^2)^2 \sinh \bar{\lambda}_1 \sinh \bar{\lambda}_2$$

and the solution of the matrix equation (6.3.29) is given by

$$\begin{aligned} A_n &= -\frac{\lambda_2^2}{(\lambda_2^2 - \lambda_1^2)} \hat{q}_n, \quad B_n = -\frac{\lambda_2^2(1 - \cosh \bar{\lambda}_1)}{(\lambda_2^2 - \lambda_1^2) \sinh \bar{\lambda}_1} \hat{q}_n \\ C_n &= \frac{\lambda_1^2}{(\lambda_2^2 - \lambda_1^2)} \hat{q}_n, \quad D_n = \frac{\lambda_1^2(1 - \cosh \bar{\lambda}_2)}{(\lambda_2^2 - \lambda_1^2) \sinh \bar{\lambda}_2} \hat{q}_n \end{aligned} \quad (6.3.30)$$

Case 2: $(D_{12} + 2D_{66})^2 = D_{11}(D_{22} + k/\beta_n^4)$. Isotropic plates without elastic foundation ($k = 0$) and certain orthotropic plates (with or without k) fall into this category. The solution for this case is given by

$$w_0(x, y) = \sum_{n=1}^{\infty} [(A_n + B_n x) \cosh \lambda x + (C_n + D_n x) \sinh \lambda x + \hat{q}_n] \sin \beta_n y \quad (6.3.31a)$$

where λ is defined by Eq. (6.3.13). The second derivative of w_0 with respect to x is

$$\begin{aligned} \frac{\partial^2 w_0}{\partial x^2} &= \sum_{n=1}^{\infty} [\lambda^2(A_n + B_n a) \cosh \lambda x + \lambda^2(C_n + D_n a) \sinh \lambda x \\ &\quad + 2\lambda(B_n \sinh \lambda x + D_n \cosh \lambda x)] \sin \beta_n y \end{aligned} \quad (6.3.31b)$$

Substituting Eqs. (6.3.31a,b) into the boundary conditions (6.3.27a,b), we obtain

$$\begin{aligned} A_n + \hat{q}_n &= 0, \quad A_n \lambda^2 + 2D_n \lambda = 0 \\ (A_n + B_n a) \cosh \lambda a + (C_n + D_n a) \sinh \lambda a + \hat{q}_n &= 0 \\ \lambda^2(A_n + B_n a) \cosh \lambda a + \lambda^2(C_n + D_n a) \sinh \lambda a \\ &\quad + 2\lambda(B_n \sinh \lambda a + D_n \cosh \lambda a) = 0 \end{aligned}$$

The solution of the above equations is

$$\begin{aligned} A_n &= -\hat{q}_n, \quad D_n = \frac{1}{2}\lambda \hat{q}_n, \quad B_n = \frac{1}{2}\left(\frac{1 - \cosh \lambda a}{\sinh \lambda a}\right)\lambda \hat{q}_n \\ C_n &= \frac{1}{2}\left(\frac{1 - \cosh \lambda a}{\sinh \lambda a}\right)\left(\frac{\lambda a - 2 \sinh \lambda a}{\sinh \lambda a}\right)\hat{q}_n \end{aligned} \quad (6.3.32)$$

Case 3: $(D_{12} + 2D_{66})^2 < D_{11}(D_{22} + k/\beta_n^4)$. Isotropic plates on elastic foundation ($k \neq 0$) and orthotropic plates (with or without k) fall into this category. The solution for this case is given by

$$\begin{aligned} w_0(x, y) &= \sum_{n=1}^{\infty} [(A_n \cos \lambda_2 x + B_n \sin \lambda_2 x) \cosh \lambda_1 x + (C_n \cos \lambda_2 x \\ &\quad + D_n \sin \lambda_2 x) \sinh \lambda_1 x + \hat{q}_n] \sin \beta_n y \end{aligned} \quad (6.3.33a)$$

where λ_1 and λ_2 are defined by Eq. (6.3.15). Note that

$$\begin{aligned} \frac{\partial^2 w_0}{\partial x^2} = & \sum_{n=1}^{\infty} \left[-\lambda_2^2 (A_n \cos \lambda_2 x + B_n \sin \lambda_2 x) \cosh \lambda_1 x \right. \\ & - \lambda_2^2 (C_n \cos \lambda_2 x + D_n \sin \lambda_2 x) \sinh \lambda_1 x \\ & + \lambda_1^2 (A_n \cos \lambda_2 x + B_n \sin \lambda_2 x) \cosh \lambda_1 x \\ & + \lambda_1^2 (C_n \cos \lambda_2 x + D_n \sin \lambda_2 x) \sinh \lambda_1 x \\ & + 2\lambda_1 \lambda_2 (-A_n \sin \lambda_2 x + B_n \cos \lambda_2 x) \sinh \lambda_1 x \\ & \left. + 2\lambda_1 \lambda_2 (-C_n \sin \lambda_2 x + D_n \cos \lambda_2 x) \cosh \lambda_1 x \right] \sin \beta_n y \quad (6.3.33b) \end{aligned}$$

Substituting Eqs. (6.3.33a,b) into the boundary conditions (6.3.27a), we obtain

$$\begin{aligned} A_n + \hat{q}_n &= 0, \quad (\lambda_1^2 - \lambda_2^2) A_n + 2\lambda_1 \lambda_2 D_n = 0 \\ (A_n \cos \lambda_2 a + B_n \sin \lambda_2 a) \cosh \lambda_1 a & \\ + (C_n \cos \lambda_2 a + D_n \sin \lambda_2 a) \sinh \lambda_1 a + \hat{q}_n &= 0 \\ (\lambda_1^2 - \lambda_2^2) [(A_n \cos \lambda_2 a + B_n \sin \lambda_2 a) \cosh \lambda_1 a & \\ + (C_n \cos \lambda_2 a + D_n \sin \lambda_2 a) \sinh \lambda_1 a] & \\ + 2\lambda_1 \lambda_2 [(-A_n \sin \lambda_2 a + B_n \cos \lambda_2 a) \sinh \lambda_1 a & \\ + (-C_n \sin \lambda_2 a + D_n \cos \lambda_2 a) \cosh \lambda_1 a] &= 0 \end{aligned}$$

The solution of these equations is

$$\begin{aligned} A_n &= -\hat{q}_n, \quad D_n = \left(\frac{\lambda_1^2 - \lambda_2^2}{2\lambda_1 \lambda_2} \right) \hat{q}_n \\ B_n &= \frac{1}{\Delta} [\sin \lambda_2 a (\cosh \lambda_1 a - \cos \lambda_2 a) \hat{q}_n \\ &\quad + \sinh \lambda_1 a (\cos \lambda_2 a + \cosh \lambda_1 a) D_n] \quad (6.3.34) \\ C_n &= \frac{1}{\Delta} [\sinh \lambda_1 a (\cos \lambda_2 a - \cosh \lambda_1 a) \hat{q}_n \\ &\quad - \sin \lambda_2 a (\cosh \lambda_1 a + \cos \lambda_2 a) D_n] \\ \Delta &= -(\sin^2 \lambda_2 a \cosh^2 \lambda_1 a + \cos^2 \lambda_2 a \sinh^2 \lambda_1 a) \end{aligned}$$

As an example, consider a simply supported plate under a distributed transverse load. For *uniformly distributed load*, we have

$$q(x, y) = q_0, \quad \hat{q}_n = \frac{4q_0 b^4}{n^5 \pi^5 D}$$

and for the case of *hydrostatic loading*, we find

$$q(x, y) = q_0 \frac{y}{b}, \quad \hat{q}_n = \frac{2q_0 b^4}{n^5 \pi^5 D} (-1)^{n+1}$$

An *isotropic plate without elastic foundation* ($k = 0$) falls into Case 2 (real, but equal roots). The solution is given by ($\lambda = \beta_n$)

$$w_0(x, y) = \sum_{n=1}^{\infty} [(A_n + B_n x) \cosh \beta_n x + (C_n + D_n x) \sinh \beta_n x + \hat{q}_n] \sin \beta_n y \quad (6.3.35)$$

where [cf., Eq.(6.3.32)]

$$\begin{aligned} A_n &= -\hat{q}_n, \quad D_n = \frac{1}{2} \beta_n \hat{q}_n, \quad B_n = \frac{1}{2} \left(\frac{1 - \cosh \beta_n a}{\sinh \beta_n a} \right) \beta_n \hat{q}_n \\ C_n &= \frac{1}{2} \left(\frac{1 - \cosh \beta_n a}{\sinh \beta_n a} \right) \left(\frac{\beta_n a - 2 \sinh \beta_n a}{\sinh \beta_n a} \right) \hat{q}_n \end{aligned} \quad (6.3.36)$$

Bending moments and stresses can be computed using the expression given for w_0 in Eq. (6.3.35).

An *isotropic plate on elastic foundation* ($k \neq 0$) falls into Case 3. The solution is given by Eq. (6.3.33a) with the constants defined in Eq. (6.3.34). The roots λ_1 and λ_2 are given by Eq. (6.3.19). We note that

$$\lambda_1^2 - \lambda_2^2 = \beta_n^2, \quad 2\lambda_1\lambda_2 = \sqrt{\frac{k}{D}} \quad (6.3.37)$$

Orthotropic plates for which $E_1 > E_2$, with or without elastic foundation, also fall into Case 3. The solution is again given by Eqs. (6.3.33a) and (6.3.34), with λ_1 and λ_2 defined by Eq. (6.3.15). In this case, we have

$$\lambda_1^2 - \lambda_2^2 = \beta_n^2 \left(\frac{D_{12} + 2D_{66}}{D_{11}} \right), \quad 2\lambda_1\lambda_2 = \sqrt{\frac{D_{22}\beta_n^4 + k}{D_{11}} - \frac{\hat{D}_{12}^2}{D_{11}^2}\beta_n^4} \quad (6.3.38)$$

Table 6.3.2 contains numerical results for the nondimensional center deflection $\bar{w} = w_0(a/2, b/2)(D/q_0 a^4) \times 10^2$ and bending moments $\bar{M} = M(a/2, b/2) \times 10/(q_0 a^2)$ obtained in the Navier and Lévy methods for various simply supported plates under uniform load (UL) or hydrostatic load (HL). The series was evaluated using a final value of 9 for m and n . Note that the number of actual terms used in evaluating the series for deflection and bending moment for a given final value of n is different in the two methods. For example, $m, n = 1, 2, 3$ in the Navier method involves four terms ($m = n = 1; m = 1, n = 3; m = 3, n = 1; m = n = 3$) of the series, while the Lévy method involves only two terms ($n = 1$ and $n = 3$). Thus, the number of terms used from each series is vastly different for increasing n .

The center deflection due to HL is one-half the center deflection due to uniform load, as it should be. The maximum deflection of a plate under HL occurs away from the center (it occurs at $y = 0.557b$). However, the value is not significantly different from the center deflection. The point of maximum deflection approaches the center of the plate as the aspect ratio a/b increases. The maximum bending moments also occur away from the center of the plate.

Table 6.3.2. Nondimensional center deflections (\bar{w}) and bending moments \bar{M}_{xx} and \bar{M}_{yy} of various simply supported plates subjected to distributed transverse loads.

Method	Variable	$\frac{b}{a} = 1$		$\frac{b}{a} = 1.5$		$\frac{b}{a} = 2$	
		HL	UL	HL	UL	HL	UL
<i>Isotropic plates ($k = 0$)</i>							
Navier	\bar{w}	0.2031	0.4062	0.3862	0.7724	0.5065	1.0130
	\bar{M}_{xx}	0.2398	0.4797	0.4063	0.8126	0.5091	1.0182
	\bar{M}_{yy}	0.2398	0.4797	0.2500	0.5000	0.2331	0.4661
Lévy	\bar{w}	0.2031	0.4062	0.3862	0.7724	0.5065	1.0130
	\bar{M}_{xx}	0.2395	0.4791	0.4060	0.8120	0.5088	1.0176
	\bar{M}_{yy}	0.2397	0.4795	0.2499	0.4998	0.2330	0.4659
<i>Isotropic plates on elastic foundation ($k = 100$)</i>							
Navier	\bar{w}	0.0503	0.1007	0.0536	0.1073	0.0524	0.1048
	\bar{M}_{xx}	0.0465	0.0930	0.0401	0.0802	0.0369	0.0738
	\bar{M}_{yy}	0.0465	0.0930	0.0176	0.0351	0.0110	0.0221
Lévy	\bar{w}	0.0503	0.1007	0.0536	0.1073	0.0524	0.1048
	\bar{M}_{xx}	0.0462	0.0923	0.0398	0.0796	0.0366	0.0732
	\bar{M}_{yy}	0.0464	0.0928	0.0175	0.0349	0.0109	0.0219
<i>Orthotropic plates ($k = 0$)</i>							
Navier	\bar{w}	0.0271	0.0543	0.0269	0.0538	0.0262	0.0524
	\bar{M}_{xx}	0.6560	1.3119	0.6458	1.2917	0.6291	1.2583
	\bar{M}_{yy}	0.0207	0.0414	0.0068	0.0136	0.0066	0.0132
Lévy	\bar{w}	0.0271	0.0543	0.0269	0.0538	0.0262	0.0524
	\bar{M}_{xx}	0.6556	1.3113	0.6455	1.2910	0.6288	1.2576
	\bar{M}_{yy}	0.0207	0.0414	0.0068	0.0136	0.0066	0.0132
<i>Orthotropic plates ($k = 100$)</i>							
Navier	\bar{w}	0.0185	0.0371	0.0178	0.0356	0.0175	0.0350
	\bar{M}_{xx}	0.4418	0.8835	0.4219	0.8438	0.4137	0.8273
	\bar{M}_{yy}	0.0115	0.0229	0.0037	0.0075	0.0049	0.0098
Lévy	\bar{w}	0.0185	0.0371	0.0178	0.0356	0.0175	0.0350
	\bar{M}_{xx}	0.4415	0.8829	0.4216	0.8432	0.4133	0.8267
	\bar{M}_{yy}	0.0115	0.0229	0.0037	0.0075	0.0049	0.0098

6.3.4 Plates with Distributed Edge Moments

Consider a simply supported (on all four edges) rectangular plate subjected to distributed bending moments along edges $x = 0, a$ (Figure 6.3.2). We wish to determine the deflections and bending moments throughout the plate using the Lévy solution procedure. The general solutions developed earlier in Eqs. (6.3.28a),

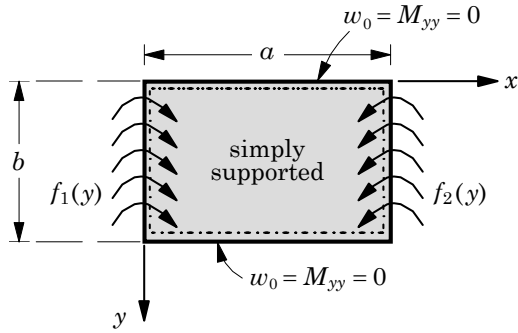


Figure 6.3.2. A rectangular plate simply supported on all four edges and subjected to distributed moments along edges $x = 0, a$.

(6.3.31a), and (6.3.33a) for rectangular plates with all four edges simply supported are valid here except that the distributed load is zero: $q = 0$ (hence, $\hat{q}_n = 0$). Instead, we have nonzero bending moments applied on edges $x = 0, a$. The constants A_n , B_n , C_n , and D_n now must be determined subjected to the boundary conditions

$$w_0(0, y) = 0, \quad M_{xx}(0, y) = f_1(y), \quad w_0(a, y) = 0, \quad M_{xx}(a, y) = f_2(y) \quad (6.3.39)$$

where f_1 and f_2 are the applied bending moment distributions along the edges $x = 0$ and $x = a$, respectively. Here we consider isotropic plates (Case 2) and orthotropic plates (Case 3) without elastic foundation ($k = 0$).

Isotropic plates. The solution for this case is given by Eq. (6.3.31a) with $\hat{q}_n = 0$ and $\lambda = \beta_n$. The boundary condition $w_0(0, y) = 0$ yields $A_n = 0$. The condition $M_{xx}(0, y) = f_1(y)$ together $w_0(0, y) = 0$ yields

$$-2D \sum_{n=1}^{\infty} \beta_n D_n \sin \beta_n y = f_1(y) \quad (6.3.40)$$

The form of Eq. (6.3.40) suggests that we must express $f_1(y)$ in the series form

$$M_{xx}(0, y) = f_1(y) = \sum_{n=1}^{\infty} F_n^1 \sin \beta_n y \quad (6.3.41)$$

where F_n^1 is calculated in the same way as before [see, for example, Eq. (6.3.5)]

$$F_n^1 = \frac{2}{b} \int_0^b f_1(y) \sin \beta_n y \, dy \quad (6.3.42)$$

Then Eq. (6.3.40) yields

$$D_n = -\frac{F_n^1}{2D\beta_n} \quad (6.3.43)$$

Using the remaining two boundary conditions, we obtain

$$\begin{aligned} aB_n \cosh \beta_n a + (C_n + D_n a) \sinh \beta_n a &= 0 \\ -2D\beta_n (B_n \sinh \beta_n a + D_n \cosh \beta_n a) &= F_n^2 \end{aligned}$$

where $f_2(y)$ is also expressed in the same form as $f_1(y)$ so that

$$F_n^2 = \frac{2}{b} \int_0^b f_2(y) \sin \beta_n y dy \quad (6.3.44)$$

Solving the above two equations, we find

$$\begin{aligned} B_n &= \frac{1}{2D\beta_n \sinh \beta_n a} (F_n^1 \cosh \beta_n a - F_n^2) \\ C_n &= \frac{a}{2D\beta_n \sinh^2 \beta_n a} (F_n^2 \cosh \beta_n a - F_n^1) \end{aligned} \quad (6.3.45)$$

Orthotropic plates. The solution for this case is given by Eq. (6.3.33a) with $\hat{q}_n = 0$. The boundary conditions give

$$\begin{aligned} A_n &= 0 \\ D_n &= -\frac{F_n^1}{2D_{11}\lambda_1\lambda_2} \\ B_n &= \frac{\sinh \lambda_1 a}{2D_{11}\lambda_1\lambda_2\Delta} (F_n^2 \cos \lambda_2 a - F_n^1 \cosh \lambda_1 a) \\ C_n &= \frac{\sin \lambda_2 a}{2D_{11}\lambda_1\lambda_2\Delta} (F_n^1 \cos \lambda_2 - F_n^2 \cosh \lambda_1 a) \\ \Delta &= -(\sin^2 \lambda_2 a \cosh^2 \lambda_1 a + \cos^2 \lambda_2 a \sinh^2 \lambda_1 a) \end{aligned} \quad (6.3.46)$$

Nondimensional deflections and bending moments of simply supported rectangular plates with uniformly distributed moments of intensity $f_1 = f_2 = M_0$ are presented in Table 6.3.3 for various aspect ratios. The results were computed using $n = 1, 3, \dots, 9$. The nondimensional variables used are as follows:

$$\begin{aligned} \text{For } \frac{a}{b} \leq 1 : \quad \bar{w} &= w_0(a/2, b/2) \frac{D_{22}}{M_0 a^2}, \quad \bar{M} = M(a/2, b/2) \frac{1}{M_0} \\ \text{For } \frac{a}{b} \geq 1 : \quad \bar{w} &= w_0(a/2, b/2) \frac{D_{22}}{M_0 b^2}, \quad \bar{M} = M(a/2, b/2) \frac{1}{M_0} \end{aligned} \quad (6.3.47)$$

Table 6.3.3. Nondimensional center deflections and bending moments of simply supported plates subjected to *uniformly distributed bending moments* along edges $x = 0, a$.

Variable	$a/b \rightarrow$	0.5	0.75	1.0	1.5	2.0	3.0
<i>Isotropic plates ($\nu = 0.3$)</i>							
\bar{w}		0.0965	0.0620	0.0368	0.0280	0.0174	0.0055
\bar{M}_{xx}		0.7701	0.4764	0.2562	0.0465	-0.0103	-0.0148
\bar{M}_{yy}		0.3873	0.4240	0.3938	0.2635	0.1530	0.0446
<i>Orthotropic plates ($E_1/E_2 = 25$, $G_{12} = 0.5E_2$, $\nu = 0.25$)</i>							
\bar{w}		0.0050	0.0052	0.0052	0.0097	0.0121	0.0099
\bar{M}_{xx}		0.9999	1.0553	1.0606	0.8560	0.5282	0.0523
\bar{M}_{yy}		0.0094	0.0139	0.0378	0.0927	0.1209	0.0990

6.3.5 An Alternate Form of the Lévy Solution

The choice of a coordinate system can simplify the development of Lévy solutions. Here we illustrate this by considering a rectangular plate with the (x, y) coordinate system such that $-b/2 \leq y \leq b/2$ and $0 \leq x \leq a$ (Figure 6.3.3). Suppose that the edges $x = 0, a$ are simply supported. The Lévy solution for the plate can be written as

$$w_0(x, y) = \sum_{m=1}^{\infty} W_m(y) \sin \frac{m\pi x}{a} \quad (6.3.48)$$

which satisfies the simply supported boundary conditions at $x = 0$ and $x = a$.

Following the procedure outlined in Section 6.3.1, we find that the complete solution of the governing equation

$$D_{11} \frac{\partial^4 w_0}{\partial x^4} + 2\hat{D}_{12} \frac{\partial^4 w_0}{\partial x^2 \partial y^2} + D_{22} \frac{\partial^4 w_0}{\partial y^4} + kw_0 = q \quad (6.3.49)$$

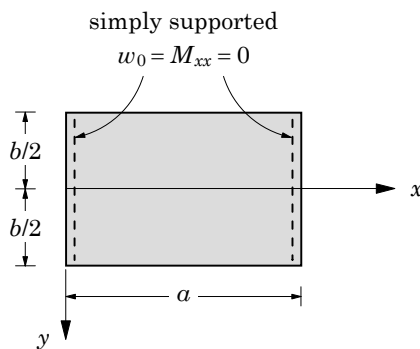


Figure 6.3.3. Geometry and coordinate system for a rectangular plate with sides $x = 0, a$ simply supported.

where $\hat{D}_{12} = (D_{12} + 2D_{66})$, is given by

$$w_0(x, y) = \sum_{m=1}^{\infty} (W_m^h(y) + W_m^p(y)) \sin \alpha_m x \quad (6.3.50)$$

Here, W_m^h denotes the homogeneous solution and W_m^p the particular solution of

$$(D_{11}\alpha_m^4 + k) W_m - 2\alpha_m^2 \hat{D}_{12} \frac{d^2 W_m}{dy^2} + D_{22} \frac{d^4 W_m}{dy^4} = q_m \quad (6.3.51)$$

and q_m is defined by

$$q_m(y) = \frac{2}{a} \int_0^a q(x, y) \sin \alpha_m x \, dx, \quad \alpha_m = \frac{m\pi}{a} \quad (6.3.52)$$

The homogeneous solution W_m^h is taken in the form [see Eq. (6.3.16)]

$$\begin{aligned} W_m^h(y) = & (A_m \cos \lambda_2 y + B_m \sin \lambda_2 y) \cosh \lambda_1 y \\ & + (C_m \cos \lambda_2 y + D_m \sin \lambda_2 y) \sinh \lambda_1 y \end{aligned} \quad (6.3.53)$$

where λ_1 and λ_2 are the roots of the equation [assuming that $(D_{12} + 2D_{66})^2 < D_{22}(D_{11} + k/\beta_n^4)$]

$$D_{22}\lambda^4 - 2\alpha_m^2 \hat{D}_{12}\lambda^2 + D_{11}\alpha_m^4 + k = 0 \quad (6.3.54)$$

and they are given by

$$\begin{aligned} (\lambda_1)^2 &= \frac{\alpha_m^2}{2D_{22}} \left[\sqrt{D_{22} \left(D_{11} + \frac{k}{\alpha_m^4} \right)} + \hat{D}_{12} \right] \\ (\lambda_2)^2 &= \frac{\alpha_m^2}{2D_{22}} \left[\sqrt{D_{22} \left(D_{11} + \frac{k}{\alpha_m^4} \right)} - \hat{D}_{12} \right] \end{aligned} \quad (6.3.55)$$

The particular solution in a general case is given by the solution of

$$(D_{11}\alpha_m^4 + k) W_m^p - 2\alpha_m^2 \hat{D}_{12} \frac{d^2 W_m^p}{dy^2} + D_{22} \frac{d^4 W_m^p}{dy^4} = q_m \quad (6.3.56)$$

Assuming solution of the form

$$W_m^p(y) = \sum_{n=1}^{\infty} W_{mn} \sin \frac{n\pi y}{b} \quad (6.3.57)$$

and expanding the load q_m also in the same form

$$q_m(y) = \sum_{n=1}^{\infty} q_{mn} \sin \frac{n\pi y}{b} \quad (6.3.58)$$

and substituting into Eq. (6.3.56), we obtain

$$W_{mn} = \frac{q_{mn}}{d_{mn}}, \quad d_{mn} = (D_{11}\alpha_m^4 + k) + 2\alpha_m^2\beta_n^2\hat{D}_{12} + D_{22}\beta_n^4 \quad (6.3.59)$$

The particular solution becomes

$$W_m^p(y) = \sum_{n=1}^{\infty} \frac{q_{mn}}{d_{mn}} \sin \frac{n\pi y}{b} \quad (6.3.60)$$

When q_m is a constant or a linear function of y , the particular solution is given by

$$W_m^p(y) = \frac{q_m}{D_{11}\alpha_m^4 + k} \equiv \hat{q}_m \quad (6.3.61)$$

The complete solution becomes

$$w_0(x, y) = \sum_{m=1}^{\infty} \left[(A_m \cos \lambda_2 y + B_m \sin \lambda_2 y) \cosh \lambda_1 y + (C_m \cos \lambda_2 y + D_m \sin \lambda_2 y) \sinh \lambda_1 y + W_m^p \right] \sin \alpha_m x \quad (6.3.62)$$

where W_m^p is given by Eq. (6.3.60), in the general case of loading, or by Eq. (6.3.61), when the loading is such that q_m is a constant or a linear function of y . The constants A_m , B_m , C_m , and D_m must be determined for the particular set of boundary conditions on edges $y = \pm b/2$.

When the applied load and boundary conditions are symmetric about the x -axis, then the deflection w_0 is also symmetric about the x -axis. Note that the choice of the coordinate system [with $-b/2 \leq y \leq b/2$] made it possible to arrive at this conclusion. Thus, only even functions of y should be kept in the expression (6.3.62), requiring the constants B_m and C_m to be zero. Of course, this can be shown by actual calculation of the constants. We have

$$w_0(x, y) = \sum_{m=1}^{\infty} (A_m \cos \lambda_2 y \cosh \lambda_1 y + D_m \sin \lambda_2 y \sinh \lambda_1 y + \hat{q}_m) \sin \alpha_m x \quad (6.3.63)$$

Once w_0 is known, the bending moments and shear forces can be computed using the relations

$$\begin{aligned} M_{xx} &= -D_{11} \frac{\partial^2 w_0}{\partial x^2} - D_{12} \frac{\partial^2 w_0}{\partial y^2} \\ M_{yy} &= -D_{12} \frac{\partial^2 w_0}{\partial x^2} - D_{22} \frac{\partial^2 w_0}{\partial y^2} \\ M_{xy} &= -2D_{66} \frac{\partial^2 w_0}{\partial x \partial y} \end{aligned} \quad (6.3.64)$$

$$\begin{aligned} Q_x &= -D_{11} \frac{\partial^3 w_0}{\partial x^3} - \hat{D}_{12} \frac{\partial^2 w_0}{\partial x \partial y^2} \\ Q_y &= -\hat{D}_{12} \frac{\partial^2 w_0}{\partial x^2 \partial y} - D_{22} \frac{\partial^3 w_0}{\partial y^3} \end{aligned} \quad (6.3.65)$$

$$\begin{aligned} V_x &= -D_{11} \frac{\partial^3 w_0}{\partial x^3} - \bar{D}_{12} \frac{\partial^2 w_0}{\partial x \partial y^2} \\ V_y &= -\bar{D}_{12} \frac{\partial^2 w_0}{\partial x^2 \partial y} - D_{22} \frac{\partial^3 w_0}{\partial y^3} \end{aligned} \quad (6.3.66)$$

where $\hat{D}_{12} = D_{12} + 2D_{66}$, $\bar{D}_{12} = D_{12} + 4D_{66}$, and

$$\frac{\partial^2 w_0}{\partial x^2} = \sum_{m=1}^{\infty} (-\alpha_m^2) [A_m f_1(y) + D_m f_2(y) + \hat{q}_m] \sin \alpha_m x \quad (6.3.67a)$$

$$\begin{aligned} \frac{\partial^2 w_0}{\partial y^2} &= \sum_{m=1}^{\infty} \left\{ (\lambda_1^2 - \lambda_2^2) [A_m f_1(y) + D_m f_2(y)] \right. \\ &\quad \left. + 2\lambda_1 \lambda_2 [-A_m f_2(y) + D_m f_1(y)] \right\} \sin \alpha_m x \end{aligned} \quad (6.3.67b)$$

$$\frac{\partial^2 w_0}{\partial x \partial y} = \sum_{m=1}^{\infty} \alpha_m [A_m f'_1(y) + D_m f'_2(y)] \cos \alpha_m x \quad (6.3.67c)$$

$$\frac{\partial^3 w_0}{\partial x^2 \partial y} = \sum_{m=1}^{\infty} (-\alpha_m^2) [A_m f'_1(y) + D_m f'_2(y)] \sin \alpha_m x \quad (6.3.67d)$$

$$\begin{aligned} \frac{\partial^3 w_0}{\partial x \partial y^2} &= \sum_{m=1}^{\infty} \alpha_m \left\{ (\lambda_1^2 - \lambda_2^2) [A_m f_1(y) + D_m f_2(y)] \right. \\ &\quad \left. + 2\lambda_1 \lambda_2 [-A_m f_2(y) + D_m f_1(y)] \right\} \cos \alpha_m x \end{aligned} \quad (6.3.67e)$$

$$\frac{\partial^3 w_0}{\partial x^3} = \sum_{m=1}^{\infty} (-\alpha_m^3) [A_m f_1(y) + D_m f_2(y) + \hat{q}_m] \cos \alpha_m x \quad (6.3.67f)$$

$$\begin{aligned} \frac{\partial^3 w_0}{\partial y^3} &= \sum_{m=1}^{\infty} \left\{ (\lambda_1^2 - \lambda_2^2) [A_m f'_1(y) + D_m f'_2(y)] \right. \\ &\quad \left. + 2\lambda_1 \lambda_2 [-A_m f'_2(y) + D_m f'_1(y)] \right\} \sin \alpha_m x \end{aligned} \quad (6.3.67g)$$

$$\begin{aligned} f_1 &= \cos \lambda_2 y \cosh \lambda_1 y, & f_2 &= \sin \lambda_2 y \sinh \lambda_1 y \\ f'_1 &= \lambda_1 g_1 - \lambda_2 g_2, & f'_2 &= \lambda_2 g_1 + \lambda_1 g_2 \\ g_1 &= \cos \lambda_2 y \sinh \lambda_1 y, & g_2 &= \sin \lambda_2 y \cosh \lambda_1 y \end{aligned} \quad (6.3.67h)$$

As a specific example, consider a rectangular plate with all its edges simply supported and subjected to distributed loads that are independent of y . For this case, the deflection of the plate is symmetric about the x -axis (or symmetric in y), and Eq. (6.3.63) is valid here. The constants A_m and D_m are determined using the boundary conditions

$$w_0(x, \pm \frac{b}{2}) = 0, \quad M_{yy}(x, \pm \frac{b}{2}) = 0 \quad (6.3.68)$$

From Eqs. (6.3.63) and (6.3.64), it follows that the conditions in Eq. (6.3.68) are equivalent to

$$w_0 = 0, \quad \frac{\partial^2 w_0}{\partial y^2} = 0 \quad (6.3.69)$$

at $y = \pm b/2$. Using Eqs. (6.3.63) and (6.3.67b) in Eq. (6.3.69), we obtain

$$\begin{aligned} A_m \cos \bar{\lambda}_2 \cosh \bar{\lambda}_1 + D_m \sin \bar{\lambda}_2 \sinh \bar{\lambda}_1 &= -\hat{q}_m \\ -A_m \sin \bar{\lambda}_2 \sinh \bar{\lambda}_1 + D_m \cos \bar{\lambda}_2 \cosh \bar{\lambda}_1 &= \gamma \hat{q}_m \end{aligned} \quad (6.3.70)$$

where

$$\bar{\lambda}_i = \frac{\lambda_i b}{2}, \quad \gamma = \frac{\lambda_1^2 - \lambda_2^2}{2\lambda_1 \lambda_2} \quad (6.3.71)$$

Equations (6.3.70a,b) give

$$\begin{aligned} A_m &= -\frac{\hat{q}_m}{\Delta} (\gamma \sinh \bar{\lambda}_1 \sin \bar{\lambda}_2 + \cosh \bar{\lambda}_1 \cos \bar{\lambda}_2) \\ D_m &= \frac{\hat{q}_m}{\Delta} (\gamma \cosh \bar{\lambda}_1 \cos \bar{\lambda}_2 - \sinh \bar{\lambda}_1 \sin \bar{\lambda}_2) \\ \Delta &= \cosh^2 \bar{\lambda}_1 \cos^2 \bar{\lambda}_2 + \sinh^2 \bar{\lambda}_1 \sin^2 \bar{\lambda}_2 \end{aligned} \quad (6.3.72)$$

The same procedure applies to simply supported plates with applied edge moments (see Problem 6.11).

Table 6.3.4 contains nondimensional deflections, moments, and shear forces

$$\bar{w} = w_0 \left(\frac{a}{2}, 0 \right) \times 10^2 \frac{D}{q_0 a^4}, \quad \bar{M}_{\xi\xi} = M_{\xi\xi} \left(\frac{a}{2}, 0 \right) \frac{10}{q_0 a^2} \quad (6.3.73a)$$

$$\bar{M}_{xy} = M_{xy} \left(0, \frac{b}{2} \right) \frac{10}{q_0 a^2}, \quad \bar{Q}_x = Q_x \left(0, 0 \right) \frac{1}{q_0 a}, \quad \bar{Q}_y = -Q_y \left(\frac{a}{2}, \frac{b}{2} \right) \frac{1}{q_0 a} \quad (6.3.73b)$$

$$\bar{V}_x = \left(Q_x + \frac{\partial M_{xy}}{\partial y} \right) \frac{1}{q_0 a}, \quad \bar{V}_y = - \left(Q_y + \frac{\partial M_{xy}}{\partial x} \right) \frac{1}{q_0 a} \quad (6.3.73c)$$

for simply supported rectangular plates under uniform loading. The effective shear forces \bar{V}_x and \bar{V}_y were also evaluated at the same points as Q_x and Q_y , respectively.

Table 6.3.4. Maximum nondimensional deflections, bending moments, and shear forces in simply supported isotropic ($\nu = 0.3$) rectangular plates subjected to *uniformly distributed load*.

$\frac{b}{a}$	\bar{w}	\bar{M}_{xx}	\bar{M}_{yy}	\bar{M}_{xy}	\bar{Q}_x	\bar{Q}_y	\bar{V}_x	\bar{V}_y
1.0(399)	0.4062	0.4789	0.4789	0.3248	0.3372	0.3377	0.4200	0.4205
1.5(249)	0.7724	0.8116	0.4984	0.4293	0.4230	0.3640	0.4848	0.4796
2.0(199)	1.0129	1.0168	0.4635	0.4627	0.4640	0.3697	0.5023	0.4958
2.5(149)	1.1496	1.1294	0.4295	0.4718	0.4827	0.3709	0.5046	0.4999
3.0(149)	1.2233	1.1886	0.4063	0.4741	0.4914	0.3712	0.5034	0.5009
3.5 (99)	1.2619	1.2191	0.3922	0.4747	0.4947	0.3712	0.5010	0.5011
4.0 (99)	1.2819	1.2346	0.3842	0.4748	0.4965	0.3712	0.4998	0.5011
4.5 (99)	1.2920	1.2424	0.3798	0.4749	0.4973	0.3712	0.4990	0.5011
5.0 (89)	1.2971	1.2462	0.3775	0.4749	0.4974	0.3712	0.4983	0.5012
10.0(39)	1.3021	1.2500	0.3750	0.4748	0.4949	0.3732	0.4949	0.5010

Note: The numbers in parentheses denote the final value of m used to evaluate the quantities.

The computation requires evaluation of hyperbolic functions [see Eq. (6.3.72)] that can cause overflow problems for large aspect ratios (b/a) and/or large values of m . Hence, the largest value of m is chosen for each aspect ratio that would not cause overflow problems in a Pentium PC. The numerical values for the shear forces may differ slightly depending on the final value of m used to evaluate them. Since the Lévy solution is not symmetric in x and y (whereas the Navier solution is), the equalities $\bar{Q}_x = \bar{Q}_y$ and $\bar{V}_x = \bar{V}_y$ for square plates and plate strips (i.e., $b/a \gg 1$) are not predicted, as evidenced by the numerical results of Table 6.3.4.

6.3.6 The Ritz Solutions

Equation (6.3.7) can also be solved using the Ritz method. Assuming that the boundary conditions on W_n are homogeneous, the Ritz method, the solution of Eq. (6.3.7) is sought in the form

$$W_n(x) \approx \sum_{j=1}^N c_j^{(n)} \varphi_j(x) \quad (6.3.74)$$

where $\varphi_j(x)$ are approximation functions that must meet the continuity and completeness conditions and satisfy the homogeneous form of the geometric boundary conditions (see Chapter 2). The parameters $c_j^{(n)}$ are then determined by requiring that the weak form of Eq. (6.3.7) be satisfied. The weak form of Eq. (6.3.7) is given by

$$0 = \int_0^a \left[D_{11} \frac{d^2 W_n}{dx^2} \frac{d^2 \delta W_n}{dx^2} + 2\hat{D}_{12} \beta_n^2 \frac{dW_n}{dx} \frac{d\delta W_n}{dx} + (D_{22} \beta_n^4 + k) W_n \delta W_n - \bar{q}_n \delta W_n \right] dx \quad (6.3.75)$$

where δW_n denotes the virtual variation in W_n and $\beta_n = n\pi/b$. In arriving at the weak form (6.3.75), it is assumed that the edges $x = 0, a$ are simply supported and that there are no applied bending moments. See Problem 6.13 for the weak form when moments are applied on edges $x = 0, a$.

Substituting Eq. (6.3.74) into (6.3.75), we obtain

$$0 = \sum_{j=1}^N c_j^{(n)} \int_0^a \left[D_{11} \frac{d^2 \varphi_j}{dx^2} \frac{d^2 \varphi_i}{dx^2} + 2\hat{D}_{12} \beta_n^2 \frac{d\varphi_j}{dx} \frac{d\varphi_i}{dx} + (D_{22} \beta_n^4 + k) \varphi_j \varphi_i \right] dx - \int_0^a \bar{q}_n \varphi_i dx \quad (6.3.76)$$

and, in matrix form, we can write

$$0 = \sum_{j=1}^N R_{ij}^{(n)} c_j^{(n)} - F_i^{(n)} \quad \text{or} \quad [R]^{(n)} \{c\}^{(n)} = \{F\}^{(n)} \quad (6.3.77a)$$

where $(R_{ij}^{(n)} = R_{ji}^{(n)})$

$$\begin{aligned} R_{ij}^{(n)} &= \int_0^a \left[D_{11} \frac{d^2 \varphi_i}{dx^2} \frac{d^2 \varphi_j}{dx^2} + 2\hat{D}_{12} \beta_n^2 \frac{d\varphi_i}{dx} \frac{d\varphi_j}{dx} + (D_{22} \beta_n^4 + k) \varphi_i \varphi_j \right] dx \\ F_i^{(n)} &= \int_0^a \bar{q}_n \varphi_i dx \end{aligned} \quad (6.3.77b)$$

Equation (6.3.77a) represents a set of N algebraic equations among the $c_i^{(n)}$ for each n . The complete solution is given by [see Eq. (6.3.1)]

$$w_0(x, y) = \sum_{n=1}^{\infty} \sum_{j=1}^N c_j^{(n)} \varphi_j(x) \sin \beta_n y \quad (6.3.78)$$

The bending moments and stresses can be computed using the deflection of Eq. (6.3.78). For example, the bending moments are given by

$$\begin{aligned} M_{xx} &= \sum_{n=1}^{\infty} \sum_{j=1}^N c_j^{(n)} \left[-D_{11} \frac{d^2 \varphi_j}{dx^2} + D_{12} \beta_n^2 \varphi_j \right] \sin \beta_n y \\ M_{yy} &= \sum_{n=1}^{\infty} \sum_{j=1}^N c_j^{(n)} \left[-D_{12} \frac{d^2 \varphi_j}{dx^2} + D_{22} \beta_n^2 \varphi_j \right] \sin \beta_n y \\ M_{xy} &= -2D_{66} \sum_{n=1}^{\infty} \sum_{j=1}^N \beta_n c_j^{(n)} \frac{d\varphi_j}{dx} \cos \beta_n y \end{aligned} \quad (6.3.79)$$

For a rectangular plate with edges $x = 0, a$ simply supported, the geometric boundary conditions are given by

$$W_n(0) = 0, \quad W_n(a) = 0 \quad (6.3.80)$$

Hence, the approximation functions φ_i must be selected such that $\varphi_i = 0$ at $x = 0, a$. If an algebraic polynomial is to be selected, one may use the polynomial

$$\varphi_i(x) = \left(\frac{x}{a}\right)^i \left(1 - \frac{x}{a}\right) = \left(\frac{x}{a}\right)^i - \left(\frac{x}{a}\right)^{i+1} \quad (6.3.81)$$

For the choice of $\varphi_i(x)$ in Eq. (6.3.81), we have

$$\begin{aligned} R_{ij} &= \frac{D_{11}}{a^3} \left[\frac{ij(i-1)(j-1)}{i+j-3} - \frac{2ij(ij-1)}{i+j-2} + \frac{ij(i+1)(j+1)}{i+j-1} \right] \\ &\quad + \frac{2\hat{D}_{12}}{a} \left[\frac{ij}{i+j-1} - \frac{2ij+i+j}{i+j} + \frac{(i+1)(j+1)}{i+j+1} \right] \beta_n^2 \\ &\quad + a \left(\beta_n^4 D_{22} + k \right) \left[\frac{1}{i+j+1} - \frac{2}{i+j+2} + \frac{1}{i+j+3} \right] \end{aligned} \quad (6.3.82)$$

The load vector $\{F^{(n)}\}$ can be evaluated for different loads \bar{q}_n .

Uniform and hydrostatic loads ($\bar{q}_n = \text{constant}$):

$$F_i^{(n)} = \frac{\bar{q}_n a}{(i+1)(i+2)} \quad (6.3.83)$$

Point load [$\bar{q}_n = \frac{2Q_0}{b} \delta(x - x_0) \sin \frac{n\pi y_0}{b}$]:

$$F_i^{(n)} = \frac{2Q_0}{b} \sin \frac{n\pi y_0}{b} \varphi_i(x_0) = \frac{2Q_0}{b} \sin \frac{n\pi y_0}{b} \left(\frac{x_0}{a}\right)^i \left(1 - \frac{x_0}{a}\right) \quad (6.3.84)$$

As a specific example, consider $N = 3$. The constants $c_i^{(n)}$ are determined by solving the equations

$$\left(\frac{D_{11}}{a^3} \begin{bmatrix} 4 & 2 & 2 \\ 2 & 4 & 4 \\ 2 & 4 & \frac{4}{5} \end{bmatrix} + \frac{2\beta_n^2 \hat{D}_{12}}{a} \begin{bmatrix} \frac{1}{3} & \frac{1}{6} & \frac{1}{5} \\ \frac{1}{6} & \frac{2}{15} & \frac{1}{5} \\ \frac{1}{5} & \frac{1}{5} & \frac{3}{35} \end{bmatrix} \right. \\ \left. + a(\beta_n^4 \hat{D}_{22} + k) \begin{bmatrix} \frac{1}{30} & \frac{1}{60} & \frac{1}{105} \\ \frac{1}{60} & \frac{1}{105} & \frac{1}{168} \\ \frac{1}{105} & \frac{1}{168} & \frac{1}{252} \end{bmatrix} \right) \begin{Bmatrix} c_1^{(n)} \\ c_2^{(n)} \\ c_3^{(n)} \end{Bmatrix} = \bar{q}_n a \begin{Bmatrix} \frac{1}{6} \\ \frac{1}{12} \\ \frac{1}{20} \end{Bmatrix}$$

For a square orthotropic plate with the material properties

$$E_1 = 25E_2, \quad G_{12} = 0.5E_2, \quad \nu_{12} = 0.25, \quad E_2 = 10^6 \text{ psi} \quad (6.3.85)$$

and $k = 0$, the above equation reduces, for instance when $n = 1$, to

$$\frac{1}{a^3} \begin{bmatrix} 9.311 & 4.656 & 4.460 \\ 4.656 & 8.706 & 8.608 \\ 4.460 & 8.608 & 10.23 \end{bmatrix} \begin{Bmatrix} c_1^{(1)} \\ c_2^{(1)} \\ c_3^{(1)} \end{Bmatrix} = q_1 a \begin{Bmatrix} 0.1667 \\ 0.0833 \\ 0.0500 \end{Bmatrix}$$

For uniformly distributed load ($\bar{q}_1 = q_1 = 4q_0/\pi$), the maximum deflection and stresses are (at $x = y = a/2$)

$$w_{max} = 0.6963 \times 10^{-2} \frac{q_0 a^4}{E_2 h^3} \quad (6.3.86)$$

$$(\sigma_{xx})_{max} = 0.8452 \frac{q_0 a^2}{h^2}, \quad (\sigma_{yy})_{max} = 0.0428 \frac{q_0 a^2}{h^2}$$

Table 6.3.5 contains a comparison of the deflections obtained through the Ritz method with those obtained through Navier's method for isotropic and orthotropic, simply supported square plates under UL, HL, and central point load (PL). The same nondimensional variables as in Table 6.2.2 are used. Clearly, the Ritz solution converges with increasing values of N . It is found that even values of N do not contribute to the solution over that obtained using the preceding odd value of N .

Table 6.3.6 contains comparison of the deflections and stresses. The subscript 'N' denotes Navier's solution and 'R' denotes the Ritz solution. The Ritz solution is not symmetric in x and y (it is algebraic in x and trigonometric in y) and, hence, may not yield $\sigma_{xx} = \sigma_{yy}$ for an isotropic plate when n is small. However, with increasing $n = N$, we do obtain $\sigma_{xx} = \sigma_{yy}$. As noted earlier, the convergence is slower for the point load case.

If we were to select trigonometric functions for φ_j of Eq. (6.3.74), we would take

$$\varphi_j(x) = \sin \frac{j\pi x}{a}, \quad j = 1, 2, \dots, N$$

because it satisfies the simply supported boundary conditions in Eq. (6.3.80).

Table 6.3.5. Transverse deflections $\bar{w} = w_0(a/2, b/2)(E_2 h^3/q_0 a^4)$ in simply supported isotropic and orthotropic square plates subjected to various types of loads.

Load	Navier solution	Ritz solution				
		$N = 1$	$N = 3$	$N = 5$	$N = 9$	$N = 9^*$
<i>Isotropic plates ($\nu = 0.3$)</i>						
UL (1)	0.0454	0.0419	0.0451	0.0449	0.0449	0.0115
UL (9)	0.0444	0.0416	0.0445	0.0444	0.0444	0.0110
PL (1)	0.1121	0.0987	0.1131	0.1161	0.1172	0.0342
PL (9)	0.1260	0.1037	0.1194	0.1233	0.1253	0.0417
<i>Orthotropic plates ($E_1/E_2 = 25$, $G_{12} = 0.5E_2$, $\nu_{12} = 0.25$)</i>						
UL (1)	0.0070	0.0057	0.0069	0.0069	0.0069	0.0048
UL (9)	0.0065	0.0053	0.0065	0.0065	0.0065	0.0044
PL (1)	0.0173	0.0134	0.0172	0.0175	0.0175	0.0123
PL (9)	0.0229	0.0177	0.0222	0.0227	0.0229	0.0174

*This column corresponds to a plate on elastic foundation, $k = 100$.

Note: The numbers in parentheses denote the maximum value of $m = n$ and N used to evaluate the series in the Navier and Ritz methods.

Table 6.3.6. Transverse deflections $\bar{w} = w_0(a/2, b/2)(E_2 h^3/q_0 a^4)$ and stresses $\bar{\sigma} = \sigma(h^2/q_0 a^2)$ in simply supported isotropic and orthotropic square plates subjected to various types of loads.

Load	\bar{w}_N	\bar{w}_R	$(\bar{\sigma}_{xx})_N$	$(\bar{\sigma}_{xx})_R$	$(\bar{\sigma}_{yy})_N$	$(\bar{\sigma}_{yy})_R$
<i>Isotropic plates ($\nu = 0.3$)</i>						
UL (9)	0.0444	0.0444	0.2878	0.2874	0.2878	0.2877
UL (29)	0.0444	0.0444	0.2873	0.2873	0.2873	0.2873
HL (9)	0.0222	0.0222	0.1439	0.1437	0.1439	0.1438
HL (29)	0.0222	0.0222	0.1437	0.1437	0.1437	0.1437
PL (9)	0.1260	0.1253	1.7546	1.5342	1.7546	1.5802
PL (29)	0.1266	0.1262	1.4350	1.8993	1.4350	1.8996
<i>Orthotropic plates ($E_1/E_2 = 25$, $G_{12} = G_{13} = 0.5E_2$, $\nu_{12} = 0.25$)</i>						
UL (9)	0.0065	0.0065	0.7872	0.7868	0.0248	0.0248
UL (29)	0.0065	0.0065	0.7867	0.7867	0.0245	0.0245
HL (9)	0.0325	0.0325	0.3936	0.3934	0.0124	0.0124
HL (29)	0.0325	0.0325	0.3933	0.3934	0.0122	0.0122
PL (9)	0.0229	0.0229	4.4530	4.0844	0.5559	0.5445
PL(29)	0.0232	0.0232	6.0075	5.2142	0.8670	0.8430

Note: The numbers in parentheses denote the maximum value of m and n used to evaluate the series in Navier's solution; it also denotes the values used for $n = N$ in the Ritz solution.

Substituting the following Ritz approximation

$$W_n(x) \approx W_n^{(N)}(x) = \sum_{j=1}^N c_j^{(n)} \sin \frac{j\pi x}{a} \quad (6.3.87)$$

into Eq. (6.3.77b) yields

$$R_{ij}^{(n)} = \begin{cases} \frac{a}{2} \left(D_{11}\alpha_i^4 + 2\hat{D}_{12}\alpha_i^2\beta_n^2 + D_{22}\beta_n^4 + k \right), & \text{for } i = j \\ 0, & \text{for } i \neq j \end{cases} \quad (6.3.88)$$

where $\alpha_i = (i\pi/b)$. For the case in which \bar{q}_n is a constant, we can evaluate $F_i^{(n)}$ using definitions in Eq. (6.3.77b).

$$F_i^{(n)} = -\frac{\bar{q}_n}{\alpha_i} \left[(-1)^i - 1 \right] = \frac{2a\bar{q}_n}{i\pi} \quad \text{for } i = 1, 3, \dots, N \quad (6.3.89)$$

Thus, Eq. (6.3.88) in the present case is a diagonal system of equations (because $[R^{(n)}]$ is a diagonal matrix) and $c_i^{(n)}$ are nontrivial only when i is an *odd* integer. We have

$$c_i^{(n)} = \frac{2a\bar{q}_n}{i\pi R_{ii}^{(n)}} \quad (\text{no sum on } i) \quad (6.3.90)$$

The complete solution becomes

$$w_0(x, y) = \sum_{n=1}^{\infty} \sum_{i=1}^N c_i^{(n)} \sin \alpha_i x \sin \beta_n y = \sum_{n=1}^{\infty} \sum_{m=1}^N c_m^{(n)} \sin \alpha_m x \sin \beta_n y \quad (6.3.91)$$

where

$$\begin{aligned} c_m^{(n)} &= \frac{q_{mn}}{d_{mn}}, \quad q_{mn} = \frac{4\bar{q}_n}{m\pi} \\ d_{mn} &= D_{11} \left(\frac{m\pi}{a} \right)^4 + 2\hat{D}_{12} \left(\frac{m\pi}{a} \right)^2 \left(\frac{n\pi}{b} \right)^2 + D_{22} \left(\frac{n\pi}{b} \right)^4 + k \end{aligned} \quad (6.3.92)$$

Comparing Eqs. (6.3.91) and (6.3.92) with Eqs. (6.2.1) and (6.2.8)–(6.2.10), we note that the Ritz solution coincides with the Navier solution for any finite values of m and n .

6.4 Summary

In this chapter, the exact solutions using Navier and Lévy methods are presented for isotropic and orthotropic rectangular plates under arbitrarily distributed transverse load. The Navier solutions are developed for plates with all four edges simply supported. The Lévy solutions are obtained for rectangular plates with two parallel edges simply supported while the other two edges, separately, may be subjected to any boundary conditions. The Ritz solutions are also presented. Numerical results of the maximum deflections and stresses are tabulated for various boundary conditions and load distributions.

The Lévy solution procedure and the Ritz formulation described in this chapter are also valid for rectangular plates with two parallel edges simply supported and other edges with *any* boundary conditions, as discussed in the next chapter. The Ritz formulation for plates with arbitrary boundary conditions will be discussed in the next chapter.

Problems

- 6.1** Verify the expressions in Eqs. (6.2.26)–(6.2.28) for σ_{xz} , σ_{yz} , and σ_{zz} .
- 6.2** Determine the maximum transverse deflection, bending moments, and stresses of an isotropic ($\nu = 0.25$), simply supported, square plate with an elastic foundation ($ka^4/D = 1125$) and subjected to a sinusoidally distributed transverse load of intensity q_0 . *Ans.:* $w_{max} = 0.66 \times 10^{-3}(q_0 a^4/D)$, $(M_{xx})_{max} = 0.008145 q_0 a^2$, $(\sigma_{xx})_{max} = 0.04887(q_0 a^2/h^2)$.
- 6.3** Determine the maximum transverse deflection of an isotropic ($\nu = 0.25$), simply supported square plate with an elastic foundation ($ka^4/D = 1125$) and subjected to uniformly distributed transverse load of intensity q_0 . Use the first term of the series to evaluate the deflection. *Ans.:* $w_{max}^{(1)} = 0.01204(q_0 a^4/Eh^3)$, $w_{max}^{(3)} = 0.01098(q_0 a^4/Eh^3)$.
- 6.4** Repeat Problem 6.3 when the plate is subjected to a central point load of intensity Q_0 . Use the first term of the series to evaluate the deflection. *Ans.:* $w_{max}^{(1)} = 0.02971(Q_0 a^3/Eh^3)$, $w_{max}^{(3)} = 0.03937(Q_0 a^3/Eh^3)$.
- 6.5** Determine the deflection of a simply supported plate ($k = 0$) when the plate is subjected to a load of the type

$$q(x, y) = q_0 \sin \frac{\pi x}{a}$$

where q_0 is a constant.

- 6.6** Determine the deflection of a simply supported plate ($k = 0$) when the plate is subjected to a line load of the type

$$q(x, y) = q^1 \sin \frac{\pi x}{a} \delta(y - y_0)$$

where q^1 is a constant and $\delta(y)$ is the Dirac delta function.

- 6.7** Determine the deflection of a simply supported isotropic plate when the plate is subjected to a concentrated force Q_0 at $(x, y) = (x_0, y_0)$

$$q(x, y) = Q_0 \delta(x - x_0) \delta(y - y_0)$$

and uniform compressive inplane force N_{xx}^0 . *Ans.:* The deflection is given by Eq. (6.2.1) with

$$W_{mn} = \frac{4Q_0 \sin \frac{m\pi x_0}{a} \sin \frac{n\pi y_0}{b}}{abD\pi^4 \left[\left(\frac{m^2}{a^2} + \frac{n^2}{b^2} \right)^2 + k - \frac{m^2 N_{xx}^0}{a^2 \pi^2 D} \right]}$$

6.8 Verify Eqs. (6.3.29) and (6.3.30).

6.9 Verify the expressions for A_n, B_n, C_n , and D_n given in Eq. (6.3.32).

6.10 Verify the expressions for A_n, B_n, C_n , and D_n given in Eq. (6.3.34).

6.11 Consider a simply supported plate subjected to uniformly distributed bending moments on edges $y = \pm b/2$ (Figure 6.3.3). Determine the constants A_m and D_m of Eq. (6.3.63) (with $\hat{q}_m = 0$) so that the boundary conditions

$$w_0(x, \pm \frac{b}{2}) = 0, \quad M_{yy}(x, \pm \frac{b}{2}) = M_0 \quad (1)$$

are satisfied, where M_0 is the value of the applied bending moment. In particular, show that

$$A_m = \frac{M_m \sinh \bar{\lambda}_1 \sin \bar{\lambda}_2}{2D_{22}\lambda_1\lambda_2\Delta}, \quad D_m = -\frac{M_m \cosh \bar{\lambda}_1 \cos \bar{\lambda}_2}{2D_{22}\lambda_1\lambda_2\Delta}$$

$$\Delta = \cosh^2 \bar{\lambda}_1 \cos^2 \bar{\lambda}_2 + \sinh^2 \bar{\lambda}_1 \sin^2 \bar{\lambda}_2 \quad (2)$$

where $M_m = (4M_0/m\pi)$ and $\bar{\lambda}_i = \lambda_i b/2$.

6.12 Evaluate the Ritz equations for a square isotropic ($\nu = 0.25$ and $k = 0$) plate under uniform loading when $n = 1$ and for $N = 1, 2$, and 3, and determine the maximum deflection [see Eqs. (6.3.77a,b), (6.3.82), and (6.3.83)].

Ans.: For $N = 3$, we have

$$\frac{1}{a^3} \begin{bmatrix} 1.2290 & 0.6145 & 0.4357 \\ 0.6145 & 0.6720 & 0.5826 \\ 0.4357 & 0.5826 & 0.6114 \end{bmatrix} \begin{Bmatrix} c_1^{(1)} \\ c_2^{(1)} \\ c_3^{(1)} \end{Bmatrix} = q_0 a \begin{Bmatrix} 0.2122 \\ 0.1061 \\ 0.0637 \end{Bmatrix}$$

$$w_{max} = 0.04644 \frac{q_0 a^4}{E h^3}$$

6.13 Show that the weak form for a simply supported rectangular plate with edge moments is given by [note that $W_n(0) = W_n(a) = 0$]

$$0 = \int_0^a \left[D_{11} \frac{d^2 W_n}{dx^2} \frac{d^2 \delta W_n}{dx^2} + 2\hat{D}_{12} \beta_n^2 \frac{dW_n}{dx} \frac{d\delta W_n}{dx} + D_{22} \beta_n^4 W_n \delta W_n \right] dx$$

$$- F_n^1 \left(\frac{d\delta W_n}{dx} \right)_{x=0} + F_n^2 \left(\frac{d\delta W_n}{dx} \right)_{x=a} \quad (1)$$

where F_n^1 and F_n^2 are defined in Eqs. (6.3.42) and (6.3.44), respectively.

6.14 Formulate the Ritz equations for a simply supported, isotropic ($\nu = 0.3$), square plate with distributed edge moments of magnitude M_0 at $x = 0, a$, and determine the solution for $N = 3$ and $n = 1$. *Ans.*:

$$\frac{1}{a^3} \begin{bmatrix} 1.266 & 0.6331 & 0.4489 \\ 0.6331 & 0.6923 & 0.6002 \\ 0.4489 & 0.6002 & 0.6299 \end{bmatrix} \begin{Bmatrix} c_1^{(1)} \\ c_2^{(1)} \\ c_3^{(1)} \end{Bmatrix} = \frac{4M_0}{a\pi} \begin{Bmatrix} 2 \\ 1 \\ 1 \end{Bmatrix}$$

$$w_0(a/2, b/2) = 0.0367 \frac{M_0 a^2}{D}, \quad M_{xx}(a/2, b/2) = 0.242 M_0$$

$$M_{yy}(a/2, b/2) = 0.397 M_0$$

Compare these results with those in Table 6.3.3.

- 6.15** Determine the Ritz solution of a simply supported, isotropic ($\nu = 0.3$), square plate under hydrostatic load $q = q_0(y/b)$ for $N = 3$ and $n = 1$. *Ans:*

$$w_0(a/2, b/2) = 0.002064 \frac{q_0 a^4}{D}, \quad M_{xx}(a/2, b/2) = 0.0254 q_0 a^2$$

$$M_{yy}(a/2, b/2) = 0.0262 q_0 a^2$$

Bending of Rectangular Plates with Various Boundary Conditions

7.1 Introduction

In the previous chapter, analytical solutions using Navier's, Lévy's, and the Ritz methods were presented for bending of rectangular plates with all four edges simply supported. In this chapter, solutions will be developed for rectangular plates with various boundary conditions. First, we use the Lévy method to determine solutions of rectangular plates with two opposite edges simply supported while each of the remaining two edges are free, simply supported, or clamped. The Lévy method was discussed in Section 6.3, and only pertinent equations are repeated here for the sake of completeness. Next, the Ritz solutions are developed for rectangular plates with general boundary conditions.

7.2 Lévy Solutions

7.2.1 Basic Equations

Consider a rectangular plate with simply supported edges along $y = 0, b$ (Figure 7.2.1) and subjected to a distributed transverse load q . The other two edges at $x = 0$ and $x = a$ can each be free, simply supported, or clamped. The solution to the problem is represented as

$$w_0(x, y) = \sum_{n=1}^{\infty} W_n(x) \sin \frac{n\pi y}{b} \quad (7.2.1)$$

which satisfies the simply supported boundary conditions at $y = 0$ and $y = b$. Similarly, the load q and thermal moments M_{xx}^T and M_{yy}^T are represented as

$$q(x, y) = \sum_{n=1}^{\infty} q_n(x) \sin \frac{n\pi y}{b} \quad (7.2.2)$$

$$M_{xx}^T(x, y) = \sum_{n=1}^{\infty} M_n^1(x) \sin \frac{n\pi y}{b}, \quad M_{yy}^T(x, y) = \sum_{n=1}^{\infty} M_n^2(x) \sin \frac{n\pi y}{b} \quad (7.2.3)$$

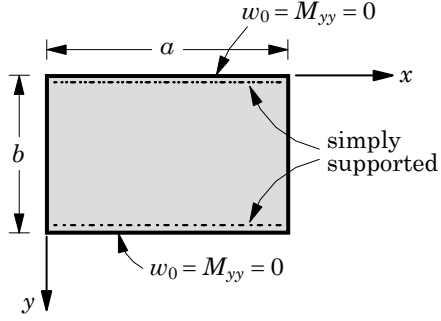


Figure 7.2.1. Geometry and coordinate system for a rectangular plate with sides $y = 0, b$ simply supported.

The coefficients q_n , for example, are given in Table 6.3.1 for various distributions of $q(x, y)$.

Substitution of Eqs. (7.2.1)–(7.2.3) into Eq. (6.1.1) results in the following ordinary differential equation in $W_n(x)$:

$$\begin{aligned} D_{11} \frac{d^4 W_n}{dx^4} - 2 \left(\frac{n\pi}{b} \right)^2 \hat{D}_{12} \frac{d^2 W_n}{dx^2} + \left[\left(\frac{n\pi}{b} \right)^4 D_{22} + k \right] W_n \\ = q_n - \frac{d^2 M_n^1}{dx^2} + \left(\frac{n\pi}{b} \right)^2 M_n^2 \equiv \bar{q}_n \end{aligned} \quad (7.2.4)$$

The solution of Eq. (7.2.4) is of the form $W_n(x) = W_n^h(x) + W_n^p(x)$ so that the complete solution is given by

$$w_0(x, y) = \sum_{n=1}^{\infty} (W_n^h(x) + W_n^p(x)) \sin \beta_n y \quad (7.2.5)$$

where W_n^h is the homogeneous solution and W_n^p is the particular solution of Eq. (7.2.4). The form of the homogeneous solution depends on the nature of the roots λ of the equation

$$D_{11} \lambda^4 - 2 \left(\frac{n\pi}{b} \right)^2 (D_{12} + 2D_{66}) \lambda^2 + \left(\frac{n\pi}{b} \right)^4 D_{22} + k = 0 \quad (7.2.6)$$

The following three cases were discussed in Section 6.3 and are summarized here.

Case 1: $(D_{12} + 2D_{66})^2 > D_{11}(D_{22} + k/\beta_n^4)$

$$W_n^h = A_n \cosh \lambda_1 x + B_n \sinh \lambda_1 x + C_n \cosh \lambda_3 x + D_n \sinh \lambda_3 x \quad (7.2.7a)$$

$$\lambda_1^2 = \beta_n^2 \left(\frac{D_{12} + 2D_{66}}{D_{11}} \right) - \beta_n^2 \left[\left(\frac{D_{12} + 2D_{66}}{D_{11}} \right)^2 - \left(\frac{D_{22}}{D_{11}} + \frac{k}{D_{11}\beta_n^4} \right) \right]^{\frac{1}{2}}$$

$$\lambda_2^2 = \beta_n^2 \left(\frac{D_{12} + 2D_{66}}{D_{11}} \right) + \beta_n^2 \left[\left(\frac{D_{12} + 2D_{66}}{D_{11}} \right)^2 - \left(\frac{D_{22}}{D_{11}} + \frac{k}{D_{11}\beta_n^4} \right) \right]^{\frac{1}{2}} \quad (7.2.7b)$$

Case 2: $(D_{12} + 2D_{66})^2 = D_{11}(D_{22} + k/\beta_n^4)$

$$W_n^h(x) = (A_n + B_n x) \cosh \lambda x + (C_n + D_n x) \sinh \lambda x \quad (7.2.8a)$$

$$\lambda^2 = \beta_n^2 \left(\frac{D_{12} + 2D_{66}}{D_{11}} \right) \quad (7.2.8b)$$

Case 3: $(D_{12} + 2D_{66})^2 < D_{11}(D_{22} + k/\beta_n^4)$

$$W_n^h(x) = (A_n \cos \lambda_2 x + B_n \sin \lambda_2 x) \cosh \lambda_1 x + (C_n \cos \lambda_2 x + D_n \sin \lambda_2 x) \sinh \lambda_1 x \quad (7.2.9a)$$

$$(\lambda_1)^2 = \frac{\beta_n^2}{2D_{11}} \left[\sqrt{D_{11} \left(D_{22} + \frac{k}{\beta_n^4} \right)} + (D_{12} + 2D_{66}) \right]$$

$$(\lambda_2)^2 = \frac{\beta_n^2}{2D_{11}} \left[\sqrt{D_{11} \left(D_{22} + \frac{k}{\beta_n^4} \right)} - (D_{12} + 2D_{66}) \right] \quad (7.2.9b)$$

The four constants, A_n , B_n , C_n , and D_n , are determined in each case by using the boundary conditions on edges $x = 0, a$.

The particular solution W_n^p may be determined in two alternative ways. In the general case, in which \bar{q}_n is an arbitrary function of x , the particular solution is determined by expanding the solution and the loads in Fourier series

$$\begin{aligned} W_n^p(x) &= \sum_{m=1}^{\infty} W_{mn} \sin \frac{m\pi x}{a} \\ q_n(x) &= \sum_{m=1}^{\infty} q_{mn} \sin \frac{m\pi x}{a} \\ M_n^1(x) &= \sum_{m=1}^{\infty} M_{mn}^1 \sin \frac{m\pi x}{a} \\ M_n^2(x) &= \sum_{m=1}^{\infty} M_{mn}^2 \sin \frac{m\pi x}{a} \end{aligned} \quad (7.2.10)$$

where the coefficients q_{mn} , M_{mn}^1 , and M_{mn}^2 have the same meaning as in Eqs. (6.2.3) and (6.2.4). The particular solution is given by

$$W_n^p(x) = \sum_{m=1}^{\infty} W_{mn} \sin \frac{m\pi x}{a} \quad (7.2.11)$$

$$W_{mn} = \frac{1}{d_{mn}} \left[q_{mn} + \left(\frac{m\pi}{a} \right)^2 M_{mn}^1 + \left(\frac{n\pi}{b} \right)^2 M_{mn}^2 \right] \quad (7.2.12a)$$

$$d_{mn} = D_{11} \left(\frac{m\pi}{a} \right)^4 + 2\hat{D}_{12} \left(\frac{m\pi}{a} \right)^2 \left(\frac{n\pi}{b} \right)^2 + D_{22} \left(\frac{n\pi}{b} \right)^4 + k \quad (7.2.12b)$$

When the applied loads are such that \bar{q}_n is a constant or a linear function of x , the particular solution may be determined directly, as discussed in Eqs. (6.3.24)–(6.3.26). The particular solution is given by

$$W_n^p = \frac{\bar{q}_n}{(D_{22}\beta_n^4 + k)} \equiv \hat{q}_n, \quad \bar{q}_n = q_n - \frac{d^2 M_n^1}{dx^2} + \beta_n^2 M_n^2 \quad (7.2.13)$$

where $\beta_n = (n\pi/b)$. The complete solution for the deflection becomes

$$w_0(x, y) = \sum_{n=1}^{\infty} \left(W_n^h(x) + \hat{q}_n \right) \sin \beta_n y \quad (7.2.14)$$

7.2.2 Plates with Edges $x = 0, a$ Clamped (CCSS)

Here we consider rectangular plates with the first ($x = 0$) and second ($x = a$) edges clamped (C), and the third ($y = 0$) and fourth ($y = b$) edges simply supported (S) (Figure 7.2.2). We shall label it as the CCSS plate. The notation SCFS, for example, means that edge $x = 0$ is simply supported (S), edge $x = a$ clamped (C), edge $y = 0$ free (F), and edge $y = b$ simply supported (S). Thus, the first two letters indicate boundary conditions on edges $x = 0, a$ and the next two letters indicate the boundary conditions on edges $y = 0, b$.

The clamped boundary conditions are

$$w_0 = 0, \quad \frac{\partial w_0}{\partial x} = 0 \quad \text{on edges } x = 0, a \quad (7.2.15)$$

We consider (1) isotropic plates without elastic foundation, and (2) isotropic plates with elastic foundation or orthotropic plates with $(D_{12} + 2D_{66})^2 < D_{11}(D_{22} + k/\beta_n^4)$ and determine the constants A_n , B_n , C_n , and D_n . The solution to the first problem falls into Case 2 and the second one into Case 3, as discussed in Chapter 6. The first problem also includes orthotropic plates on elastic foundation for which we have $(D_{12} + 2D_{66})^2 = D_{11}(D_{22} + k/\beta_n^4)$.

Isotropic Plates ($k = 0$)

First, we consider the particular solution in the form of Eq. (7.2.11). The complete solution for this case is given by

$$w_0 = \sum_{n=1}^{\infty} \left[(A_n + B_n x) \cosh \beta_n x + (C_n + D_n x) \sinh \beta_n x + \sum_{m=1}^{\infty} W_{mn} \sin \alpha_m x \right] \sin \beta_n y \quad (7.2.16)$$

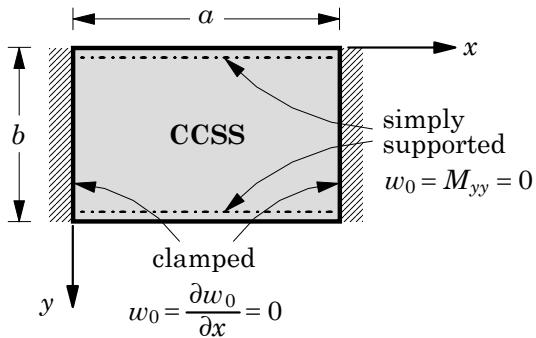


Figure 7.2.2. Geometry and coordinate system for a rectangular plate with sides $x = 0, a$ clamped and $y = 0, b$ simply supported (CCSS).

where W_{mn} is given by

$$W_{mn} = \frac{q_{mn} + \alpha_m^2 M_{mn}^1 + \beta_n^2 M_{mn}^2}{D (\alpha_m^2 + \beta_n^2)^2} \quad (7.2.17a)$$

and

$$\alpha_m = \frac{m\pi}{a}, \quad \beta_n = \frac{n\pi}{b} \quad (7.2.17b)$$

Differentiating Eq. (7.2.16), we obtain

$$\begin{aligned} \frac{\partial w_0}{\partial x} = \sum_{n=1}^{\infty} & \left[\beta_n (A_n + B_n x) \sinh \beta_n x + B_n \cosh \beta_n x \right. \\ & + \beta_n (C_n + D_n x) \cosh \beta_n x + D_n \sinh \beta_n x \\ & \left. + \sum_{m=1}^{\infty} \alpha_m W_{mn} \cos \alpha_m x \right] \sin \beta_n y \end{aligned} \quad (7.2.18)$$

Substitution of Eqs. (7.2.16) and (7.2.18) into Eq. (7.2.15) yields

$$\begin{aligned} A_n = 0, \quad B_n + \beta_n C_n + \sum_{m=1}^{\infty} \alpha_m W_{mn} &= 0 \\ (A_n + B_n a) \cosh \bar{\beta}_n + (C_n + D_n a) \sinh \bar{\beta}_n &= 0 \\ \beta_n (A_n + B_n a) \sinh \bar{\beta}_n + \beta_n (C_n + D_n a) \cosh \bar{\beta}_n & \\ + B_n \cosh \bar{\beta}_n + D_n \sinh \bar{\beta}_n + \sum_{m=1}^{\infty} (-1)^m \alpha_m W_{mn} &= 0 \end{aligned} \quad (7.2.19)$$

where $\bar{\beta}_n = a\beta_n = n\pi a/b$. The solution of these equations is ($A_n = 0$)

$$\begin{aligned} B_n &= \frac{1}{\Delta_n} \left(\sinh \bar{\beta}_n \hat{q}_n^0 + \bar{\beta}_n \hat{q}_n^1 \right) \sinh \bar{\beta}_n, \quad \Delta_n = \bar{\beta}_n^2 - \sinh^2 \bar{\beta}_n \\ C_n &= -\frac{1}{\Delta_n} \left(\bar{\beta}_n \hat{q}_n^0 + \sinh \bar{\beta}_n \hat{q}_n^1 \right) \\ D_n &= -\frac{1}{\Delta_n} \left[(-\bar{\beta}_n + \cosh \bar{\beta}_n \sinh \bar{\beta}_n) \hat{q}_n^0 + (\bar{\beta}_n \cosh \bar{\beta}_n - \sinh \bar{\beta}_n) \hat{q}_n^1 \right] \\ \hat{q}_n^0 &= \sum_{m=1}^{\infty} \alpha_m W_{mn}, \quad \hat{q}_n^1 = \sum_{m=1}^{\infty} (-1)^m \alpha_m W_{mn} \end{aligned} \quad (7.2.20)$$

Next, we consider the case in which the applied loads are such that \bar{q}_n is a constant. The complete solution is given by

$$w_0(x, y) = \sum_{n=1}^{\infty} \left[(A_n + B_n x) \cosh \beta_n x + (C_n + D_n x) \sinh \beta_n x + \frac{\bar{q}_n}{D \beta_n^4} \right] \sin \beta_n y \quad (7.2.21)$$

where \bar{q}_n is defined in Eq. (7.2.4) and q_n , M_n^1 , and M_n^2 can be calculated using equations of the form

$$q_n(x) = \frac{2}{b} \int_0^b q(x, y) \sin \beta_n y \, dy \quad (7.2.22)$$

Using the boundary conditions in Eq. (7.2.15), we obtain

$$\begin{aligned} A_n + \frac{\bar{q}_n b^4}{D n^4 \pi^4} &= 0, & B_n + \beta_n C_n &= 0 \\ (A_n + B_n a) \cosh \bar{\beta}_n + (C_n + D_n a) \sinh \bar{\beta}_n + \frac{\bar{q}_n b^4}{D n^4 \pi^4} &= 0 \end{aligned} \quad (7.2.23)$$

$$\begin{aligned} \beta_n (A_n + B_n a) \sinh \bar{\beta}_n + \beta_n (C_n + D_n a) \cosh \bar{\beta}_n \\ + B_n \cosh \bar{\beta}_n + D_n \sinh \bar{\beta}_n &= 0 \end{aligned}$$

Solving these equations, we find that

$$\begin{aligned} A_n &= -\frac{\bar{q}_n b^4}{n^4 \pi^4 D}, & B_n &= -\beta_n A_n \left(\frac{1 - \cosh \bar{\beta}_n}{\bar{\beta}_n + \sinh \bar{\beta}_n} \right) \\ C_n &= A_n \left(\frac{1 - \cosh \bar{\beta}_n}{\bar{\beta}_n + \sinh \bar{\beta}_n} \right), & D_n &= -\beta_n A_n \left(\frac{\sinh \bar{\beta}_n}{\bar{\beta}_n + \sinh \bar{\beta}_n} \right) \end{aligned} \quad (7.2.24)$$

The bending moments and stresses can be computed using the deflection in Eq. (7.2.21). First note that

$$\begin{aligned} \frac{\partial^2 w_0}{\partial x^2} &= \sum_{n=1}^{\infty} \beta_n \{ [\beta_n (A_n + B_n x) + 2D_n] \cosh \beta_n x \\ &\quad + [\beta_n (C_n + D_n x) + 2B_n] \sinh \beta_n x \} \sin \beta_n y \\ \frac{\partial^2 w_0}{\partial y^2} &= - \sum_{n=1}^{\infty} \beta_n^2 \left[(A_n + B_n x) \cosh \beta_n x + (C_n + D_n x) \sinh \beta_n x - A_n \right] \sin \beta_n y \end{aligned} \quad (7.2.25)$$

Next, we consider several specific load cases.

Uniformly distributed load, q_0 . For this case, we have $\bar{q}_n = q_n$ and

$$q_n = \frac{4q_0}{n\pi}, \quad A_n = -\frac{4q_0 b^4}{n^5 \pi^5 D} \quad (7.2.26)$$

The deflection is given by Eq. (7.2.21), with A_n given by Eq. (7.2.26) and B_n , C_n , and D_n defined by Eq. (7.2.24). For $n = 1$ and $b/a = 1$, the center deflection and bending moments are given by

$$w_0\left(\frac{a}{2}, \frac{b}{2}\right) = 0.001962 \left(\frac{q_0 a^4}{D} \right), \quad M_{xx}\left(\frac{a}{2}, \frac{b}{2}\right) = 0.03461 q_0 a^2, \quad M_{yy}\left(\frac{a}{2}, \frac{b}{2}\right) = 0.028 q_0 a^2$$

The bending moments at the center of the clamped edge are

$$M_{xx}(0, \frac{b}{2}) = -0.07383q_0a^2, \quad M_{yy}(0, \frac{b}{2}) = -0.02215q_0a^2$$

Table 7.2.1 contains nondimensional deflections and bending moments

$$\hat{w} = w_0\left(\frac{a}{2}, \frac{b}{2}\right)\left(\frac{D}{q_0b^4}\right) \times 10^2, \quad \hat{M} = M\left(\frac{1}{q_0b^2}\right) \times 10 \quad (7.2.27)$$

$$\bar{w} = w_0\left(\frac{a}{2}, \frac{b}{2}\right)\left(\frac{D}{q_0a^4}\right) \times 10^2, \quad \bar{M} = M\left(\frac{1}{q_0a^2}\right) \times 10 \quad (7.2.28)$$

for various aspect ratios of isotropic plates. The first set of nondimensional parameters is used for $b/a \leq 1$ (the first three columns of values) and the second set is used for $b/a > 1$ (the last three columns of values). The values are obtained using the first five terms of the series ($n = 1, 3, \dots, 9$).

Hydrostatic load. The hydrostatic load is assumed to be of the form

$$q(x, y) = q_0 \frac{y}{b} \quad (7.2.29)$$

Then $\bar{q}_n = q_n$ is given by (see Table 6.3.1)

$$q_n = \frac{2q_0}{n\pi}(-1)^{n+1}, \quad A_n = -\frac{2q_0b^4}{n^5\pi^5 D}(-1)^{n+1} \quad (7.2.30)$$

for $n = 1, 2, 3, \dots, \infty$. For $n = 1$ and $b/a = 1$, the center deflection and bending moments are given by

$$w_0\left(\frac{a}{2}, \frac{b}{2}\right) = 0.000981\left(\frac{q_0a^4}{D}\right), \quad M_{xx}\left(\frac{a}{2}, \frac{b}{2}\right) = 0.01731q_0a^2, \quad M_{yy}\left(\frac{a}{2}, \frac{b}{2}\right) = 0.014q_0a^2$$

The bending moments at the center of the clamped edge are

$$M_{xx}(0, b/2) = -0.03691q_0a^2, \quad M_{yy}(0, b/2) = -0.01107q_0a^2$$

Table 7.2.1. Maximum nondimensional deflections and bending moments in isotropic ($\nu = 0.3$) rectangular plates with edges $y = 0, b$ simply supported and edges $x = 0, a$ clamped (CCSS), and subjected to uniformly distributed load.

Variable	$\frac{b}{a} = \frac{1}{3}$	$\frac{b}{a} = \frac{1}{2}$	$\frac{b}{a} = 1$	$\frac{b}{a} = \frac{3}{2}$	$\frac{b}{a} = 2$	$\frac{b}{a} = 3$
$\hat{w}(a/2, b/2)$	1.1681	0.8445	0.1917	0.2476	0.2612	0.2619
$\hat{M}_{xx}(a/2, b/2)$	0.4214	0.4738	0.3326	0.4067	0.4214	0.4201
$\hat{M}_{yy}(a/2, b/2)$	1.1442	0.8693	0.2445	0.1794	0.1441	0.1302
$-\hat{M}_{xx}(0, b/2)$	1.2467	1.1915	0.6990	0.8233	0.8451	0.8417
$-\hat{M}_{yy}(0, b/2)$	0.3740	0.3574	0.2097	0.2470	0.2535	0.2525

and the bending moments at $y = 3b/4$ of the clamped edge are

$$M_{xx}(0, 3b/4) = -0.0261q_0a^2, \quad M_{yy}(0, 3b/4) = -0.00783q_0a^2$$

Table 7.2.2 contains nondimensional deflections and bending moments [see Eqs. (7.2.27) and (7.2.28)] for various aspect ratios of isotropic plates. The values are obtained using the first nine terms of the series ($n = 1, 2, 3, \dots, 9$).

Table 7.2.2. Maximum nondimensional deflections and bending moments in isotropic ($\nu = 0.3$) rectangular plates with edges $y = 0, b$ simply supported and edges $x = 0, a$ clamped (CCSS), and subjected to hydrostatic load.

Variable	$\frac{b}{a} = \frac{1}{3}$	$\frac{b}{a} = \frac{1}{2}$	$\frac{b}{a} = 1$	$\frac{b}{a} = \frac{3}{2}$	$\frac{b}{a} = 2$	$\frac{b}{a} = 3$
$\hat{w}(a/2, b/2)$	0.5841	0.4222	0.0959	0.1238	0.1306	0.1309
$\hat{M}_{xx}(a/2, b/2)$	0.2107	0.2369	0.1663	0.2033	0.2107	0.2100
$\hat{M}_{yy}(a/2, b/2)$	0.5721	0.4346	0.1222	0.0897	0.0721	0.0651
$-\hat{M}_{xx}(0, b/2)$	0.6233	0.5957	0.3495	0.4117	0.4225	0.4209
$-\hat{M}_{yy}(0, b/2)$	0.1870	0.1787	0.1048	0.1235	0.1267	0.1263
$\hat{w}(a/2, 3b/4)$	0.4368	0.3218	0.0841	0.1313	0.1614	0.1884
$\hat{M}_{xx}(a/2, 3b/4)$	0.1803	0.1997	0.1562	0.2276	0.2705	0.3055
$\hat{M}_{yy}(a/2, 3b/4)$	0.5085	0.4097	0.1640	0.1665	0.1509	0.1153
$-\hat{M}_{xx}(0, 3b/4)$	0.5449	0.5254	0.3475	0.4810	0.5566	0.6140
$-\hat{M}_{yy}(0, 3b/4)$	0.1635	0.1576	0.1042	0.1443	0.1670	0.1842

Orthotropic Plates

For isotropic plates on elastic foundation or orthotropic plates with $(D_{12} + 2D_{66})^2 < D_{11}(D_{22} + k/\beta_n^4)$, the homogeneous solution is given by Eq. (7.2.9a). When the applied loads are such that \bar{q}_n is a constant or linear function of x , the complete solution is given by

$$w_0(x, y) = \sum_{n=1}^{\infty} \left[\frac{q_n}{D_{22}\beta_n^4 + k} + (A_n \cos \lambda_2 x + B_n \sin \lambda_2 x) \cosh \lambda_1 x + (C_n \cos \lambda_2 x + D_n \sin \lambda_2 x) \sinh \lambda_1 x \right] \sin \beta_n y \quad (7.2.31a)$$

where λ_1 and λ_2 are given by Eq. (7.2.9b). Differentiating Eq. (7.2.31a), we obtain

$$\begin{aligned} \frac{\partial w_0}{\partial x} = \sum_{n=1}^{\infty} & \left[\lambda_2 (-A_n \sin \lambda_2 x + B_n \cos \lambda_2 x) \cosh \lambda_1 x \right. \\ & + \lambda_1 (A_n \cos \lambda_2 x + B_n \sin \lambda_2 x) \sinh \lambda_1 x \\ & + \lambda_2 (-C_n \sin \lambda_2 x + D_n \cos \lambda_2 x) \sinh \lambda_1 x \\ & \left. + \lambda_1 (C_n \cos \lambda_2 x + D_n \sin \lambda_2 x) \cosh \lambda_1 x \right] \sin \beta_n y \end{aligned} \quad (7.2.31b)$$

Using Eqs. (7.2.30a,b) in Eq. (7.2.15), we find that

$$\begin{aligned} A_n + \frac{\bar{q}_n}{D_{22}\beta_n^4 + k} &= 0, \quad \lambda_2 B_n + \lambda_1 C_n = 0 \\ \frac{\bar{q}_n}{D_{22}\beta_n^4 + k} + (A_n \cos \lambda_2 a + B_n \sin \lambda_2 a) \cosh \lambda_1 a &+ (C_n \cos \lambda_2 a + D_n \sin \lambda_2 a) \sinh \lambda_1 a = 0 \\ \lambda_2 (-A_n \sin \lambda_2 a + B_n \cos \lambda_2 a) \cosh \lambda_1 a &+ \lambda_1 (A_n \cos \lambda_2 a + B_n \sin \lambda_2 a) \sinh \lambda_1 a \\ + \lambda_2 (-C_n \sin \lambda_2 a + D_n \cos \lambda_2 a) \sinh \lambda_1 a &+ \lambda_1 (C_n \cos \lambda_2 a + D_n \sin \lambda_2 a) \cosh \lambda_1 a = 0 \end{aligned} \quad (7.2.32)$$

which can be solved for A_n , B_n , C_n , and D_n . We have

$$\begin{aligned} A_n &= -\frac{\bar{q}_n}{D_{22}\beta_n^4 + k}, \quad C_n = \frac{b_1 a_{22} - b_2 a_{12}}{a_{11} a_{22} - a_{12} a_{21}}, \quad D_n = \frac{b_2 a_{11} - b_1 a_{21}}{a_{11} a_{22} - a_{12} a_{21}} \\ B_n &= -\frac{\lambda_2}{\lambda_1} C_n, \quad b_1 = (1 - \cos \lambda_2 a \cosh \lambda_1 a) A_n \\ b_2 &= (\lambda_2 \sin \lambda_2 a \cosh \lambda_1 a - \lambda_1 \cos \lambda_2 a \sinh \lambda_1 a) A_n \\ a_{11} &= \cos \lambda_2 a \sinh \lambda_1 a - \frac{\lambda_1}{\lambda_2} \sin \lambda_2 a \cosh \lambda_1 a \\ a_{12} &= \sin \lambda_2 a \sinh \lambda_1 a, \quad a_{21} = -\left(\frac{\lambda_2^2 + \lambda_1^2}{\lambda_2}\right) \sin \lambda_2 a \sinh \lambda_1 a \\ a_{22} &= \lambda_1 \sin \lambda_2 a \cosh \lambda_1 a + \lambda_2 \cos \lambda_2 a \sinh \lambda_1 a \end{aligned} \quad (7.2.33)$$

The bending moments can be calculated using Eqs. (6.1.9a–c). Note that the second derivatives of w_0 in Eq. (7.2.31a) with respect to x and y are given by

$$\begin{aligned} \frac{\partial^2 w_0}{\partial x^2} &= \sum_{n=1}^{\infty} \left[\left(\lambda_1^2 - \lambda_2^2 \right) (A_n \cos \lambda_2 x + B_n \sin \lambda_2 x) \cosh \lambda_1 x \right. \\ &\quad + 2\lambda_1 \lambda_2 (-A_n \sin \lambda_2 x + B_n \cos \lambda_2 x) \sinh \lambda_1 x \\ &\quad \left. + \left(\lambda_1^2 - \lambda_2^2 \right) (C_n \cos \lambda_2 x + D_n \sin \lambda_2 x) \sinh \lambda_1 x \right. \\ &\quad \left. + 2\lambda_1 \lambda_2 (-C_n \sin \lambda_2 x + D_n \cos \lambda_2 x) \cosh \lambda_1 x \right] \sin \beta_n y \end{aligned} \quad (7.2.34)$$

$$\begin{aligned} \frac{\partial^2 w_0}{\partial y^2} &= -\sum_{n=1}^{\infty} \beta_n^2 \left[\hat{q}_n + (A_n \cos \lambda_2 x + B_n \sin \lambda_2 x) \cosh \lambda_1 x \right. \\ &\quad \left. + (C_n \cos \lambda_2 x + D_n \sin \lambda_2 x) \sinh \lambda_1 x \right] \sin \beta_n y \end{aligned} \quad (7.2.35)$$

where $\hat{q}_n = \bar{q}_n / (D_{22}\beta_n^4 + k)$.

Table 7.2.3 contains nondimensional deflections and bending moments [see Eqs. (7.2.27) and (7.2.28) for the nondimensional parameters] for various aspect ratios of orthotropic and isotropic plates on elastic foundation under uniform load (UL) or hydrostatic load (HL). The values are obtained using the first nine terms of the series ($n = 1, 2, 3, \dots, 9$). The values in column “ $k = 0$ ” were obtained with the procedure of this section, but by setting $k = 10^{-6}$.

Table 7.2.3. Maximum nondimensional deflections and bending moments in isotropic ($\nu = 0.3$) and orthotropic ($E_1/E_2 = 25$, $G_{12} = G_{13} = 0.5E_2$, $\nu_{12} = 0.25$) square plates with edges $y = 0, b$ simply supported and edges $x = 0, a$ clamped (CCSS), and subjected to distributed loads.

Variable	$k = 0$	$k = 1$	$k = 10$	$k = 10^2$	$k = 10^3$	$k = 10^4$
<i>Isotropic plates on elastic foundation, UL</i>						
$\hat{w}(a/2, b/2)$	0.1917	0.1892	0.1688	0.0795	0.0103	0.0009
$\hat{M}_{xx}(a/2, b/2)$	0.3326	0.3277	0.2888	0.1199	0.0025	0.0000
$-\hat{M}_{xx}(0, b/2)$	0.6990	0.6908	0.6258	0.3392	0.0978	0.0308
<i>Orthotropic plates on elastic foundation, UL</i>						
$\hat{w}(a/2, b/2)$	0.0108	0.0108	0.0107	0.0098	0.0053	0.0009
$\hat{M}_{xx}(a/2, b/2)$	0.4331	0.4327	0.4285	0.3909	0.1998	0.0180
$-\hat{M}_{xx}(0, b/2)$	0.8630	0.8622	0.8554	0.7930	0.4748	0.1479
<i>Isotropic plates on elastic foundation, HL</i>						
$\hat{w}(a/2, b/2)$	0.0958	0.0946	0.0844	0.0397	0.0051	0.0004
$\hat{M}_{xx}(a/2, b/2)$	0.1663	0.1639	0.1444	0.0599	0.0012	0.0000
$\hat{w}(a/2, 3b/4)$	0.0841	0.0831	0.0754	0.0404	0.0075	0.0007
$\hat{M}_{xx}(a/2, 3b/4)$	0.4607	0.4553	0.4119	0.2091	0.0157	0.0005
$-\hat{M}_{xx}(0, 3b/4)$	1.3370	1.3265	1.2416	0.8271	0.2989	0.0608
$-\hat{M}_{yy}(0, 3b/4)$	0.4011	0.3979	0.3725	0.2481	0.0897	0.0183
<i>Orthotropic plates on elastic foundation, HL</i>						
$\hat{w}(a/2, 3b/4)$	0.0054	0.0054	0.0053	0.0049	0.0027	0.0004
$\hat{M}_{xx}(a/2, 3b/4)$	0.2166	0.2163	0.2143	0.1954	0.0999	0.0090
$\hat{w}(a/2, 3b/4)$	0.0078	0.0078	0.0078	0.0072	0.0042	0.0007
$\hat{M}_{xx}(a/2, 3b/4)$	1.4317	1.4304	1.4188	1.3117	0.7186	0.0602
$-\hat{M}_{xx}(0, 3b/4)$	2.6650	2.6628	2.6432	2.4616	1.4520	0.2867
$-\hat{M}_{yy}(0, 3b/4)$	0.0266	0.0266	0.0264	0.0246	0.0145	0.0028

7.2.3 Plates with Edge $x = 0$ Clamped and Edge $x = a$ Simply Supported (CSSS)

The boundary conditions for this case are (Figure 7.2.3)

$$w_0 = \frac{\partial w_0}{\partial x} = 0 \text{ at } x = 0 \quad \text{and} \quad w_0 = M_{xx} = 0 \text{ at } x = a \quad (7.2.36)$$

Here we consider Case 3 for orthotropic plates; isotropic plate solutions can be obtained as a special case. The solution is given by Eq. (7.2.31a). Using Eqs. (7.2.31b), (7.2.34), and (7.2.35) in Eq. (7.2.36), we obtain

$$A_n + \hat{q}_n = 0, \quad \lambda_2 B_n + \lambda_1 C_n = 0 \quad (7.2.37a)$$

$$\begin{aligned} \hat{q}_n + (A_n \cos \lambda_2 a + B_n \sin \lambda_2 a) \cosh \lambda_1 a \\ + (C_n \cos \lambda_2 a + D_n \sin \lambda_2 a) \sinh \lambda_1 a = 0 \end{aligned} \quad (7.2.37b)$$

$$\begin{aligned} [(-A_n \sin \lambda_2 a + B_n \cos \lambda_2 a) \sinh \lambda_1 a + (-C_n \sin \lambda_2 a \\ + D_n \cos \lambda_2 a) \cosh \lambda_1 a] - \hat{q}_n \left(\frac{\lambda_1^2 - \lambda_2^2}{2\lambda_1\lambda_2} \right) = 0 \end{aligned} \quad (7.2.37c)$$

which can be solved for the constants A_n , B_n , C_n , and D_n , and the deflection is given by Eq. (7.2.31a). It should be noted that the solution of Eqs. (7.2.37a–c) includes plates on elastic foundation.

Nondimensional deflections and bending moments [see Eqs. (7.2.27) and (7.2.28)] for various aspect ratios of isotropic and orthotropic plates under uniformly distributed transverse load q_0 are presented in Table 7.2.4. The values are obtained using the first five terms of the series ($n = 1, 3, \dots, 9$). Table 7.2.5 contains the same quantities for hydrostatic loading. For square isotropic plates under uniform loading, the magnitude of the bending moment at the middle of the clamped edge is $M_{xx}(0, b/2) = -0.0839q_0b^2$, which is numerically larger than the corresponding moment $M_{xx}(0, b/2) = -0.0699q_0b^2$ for square isotropic plates with two edges clamped (see Table 7.2.3). The deflections and moments of hydrostatically loaded plates are equal to one-half of the corresponding deflections and moments of uniformly loaded plates, as they should be.

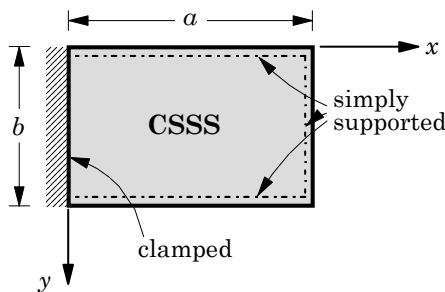


Figure 7.2.3. Geometry and coordinate system for a rectangular plate with side $x = 0$ clamped, side $x = a$ simply supported, and sides $y = 0, b$ simply supported (CSSS).

Table 7.2.4. Non-dimensional deflections and bending moments in isotropic and orthotropic rectangular plates with side $x = 0$ clamped, side $x = a$ simply supported, and sides $y = 0, b$ simply supported (CSSS), and subjected to *uniformly distributed load*.

Variable	$\frac{b}{a} = \frac{1}{3}$	$\frac{b}{a} = \frac{1}{2}$	$\frac{b}{a} = 1$	$\frac{b}{a} = \frac{3}{2}$	$\frac{b}{a} = 2$	$\frac{b}{a} = 3$
<i>Isotropic plates ($\nu = 0.3$)</i>						
$\hat{w}(a/2, b/2)$	1.0526	0.9270	0.2786	0.4250	0.4880	0.5193
$\hat{M}_{xx}(a/2, b/2)$	8.4196	0.4689	0.3920	0.5442	0.6021	0.6267
$\hat{M}_{yy}(a/2, b/2)$	-6.8394	0.9419	0.3395	0.2862	0.2373	0.2002
$-\hat{M}_{xx}(0, b/2)$	1.2484	1.2157	0.8394	1.1135	1.2143	1.2562
$-\hat{M}_{yy}(0, b/2)$	0.3745	0.3647	0.2518	0.3341	0.3643	0.3769
<i>Orthotropic plates ($E_1/E_2 = 25$, $G_{12} = 0.5E_2$, $\nu_{12} = 0.25$)</i>						
$\hat{w}(a/2, b/2)$	0.7735	0.2873	0.0221	0.0210	0.0209	0.0212
$\hat{M}_{xx}(a/2, b/2)$	2.6029	2.1967	0.6651	0.6304	0.6262	0.6354
$\hat{M}_{yy}(a/2, b/2)$	0.7524	0.2691	0.0109	0.0059	0.0085	0.0104
$-\hat{M}_{xx}(0, b/2)$	6.2887	4.5522	1.3224	1.2648	1.2605	1.2785
$-\hat{M}_{yy}(0, b/2)$	0.0629	0.0455	0.0132	0.0126	0.0126	0.0128

Table 7.2.5. Maximum nondimensional deflections and bending moments in isotropic and orthotropic rectangular plates with edges $y = 0, b$ and $x = a$ simply supported and edge $x = 0$ clamped (CSSS), and subjected to *hydrostatic load*.

Variable	$\frac{b}{a} = \frac{1}{3}$	$\frac{b}{a} = 0.5$	$\frac{b}{a} = 1$	$\frac{b}{a} = 1.5$	$\frac{b}{a} = 2$	$\frac{b}{a} = 3$
<i>Isotropic plates ($\nu = 0.3$)</i>						
$\hat{w}(a/2, b/2)$	0.5263	0.4635	0.1393	0.2125	0.2440	0.2596
$\hat{M}_{xx}(a/2, b/2)$	4.2098	0.2344	0.1960	0.2721	0.3011	0.3134
$\hat{M}_{yy}(a/2, b/2)$	-3.4197	0.4710	0.1697	0.1431	0.1187	0.1001
$-\hat{M}_{xx}(0, b/2)$	0.6242	0.6079	0.4197	0.5568	0.6072	0.6281
$-\hat{M}_{yy}(0, b/2)$	0.1873	0.1824	0.1259	0.1670	0.1821	0.1884
<i>Orthotropic plates ($E_1/E_2 = 25$, $G_{12} = 0.5E_2$, $\nu_{12} = 0.25$)</i>						
$\hat{w}(a/2, b/2)$	0.3867	0.1436	0.0110	0.0105	0.0104	0.0106
$\hat{M}_{xx}(a/2, b/2)$	1.3014	1.0984	0.3326	0.3152	0.3131	0.3177
$\hat{M}_{yy}(a/2, b/2)$	0.3762	0.1345	0.0054	0.0030	0.0042	0.0052
$-\hat{M}_{xx}(0, b/2)$	3.1444	2.2761	0.6612	0.6324	0.6302	0.6393
$-\hat{M}_{yy}(0, b/2)$	0.0314	0.0228	0.0066	0.0063	0.0063	0.0064

7.2.4 Plates with Edge $x = 0$ Clamped and Edge $x = a$ Free (CFSS)

Here we consider rectangular plates with edge $x = 0$ clamped, edge $x = a$ free, and edges $y = 0, b$ simply supported (Figure 7.2.4). The boundary conditions at the free edge $x = a$ are

$$M_{xx} = 0, \quad V_x \equiv \frac{\partial M_{xx}}{\partial x} + 2 \frac{\partial M_{xy}}{\partial y} = 0 \quad (7.2.38a)$$

or, in terms of the deflection,

$$-\left(D_{11} \frac{\partial^2 w_0}{\partial x^2} + D_{12} \frac{\partial^2 w_0}{\partial y^2} \right) = 0, \quad -\left(D_{11} \frac{\partial^3 w_0}{\partial x^3} + \bar{D}_{12} \frac{\partial^3 w_0}{\partial x \partial y^2} \right) = 0 \quad (7.2.38b)$$

where $\bar{D}_{12} = (D_{12} + 4D_{66})$. The third-order derivatives of w_0 are obtained from Eqs. (7.2.31b), (7.2.34), and (7.2.35) as

$$\begin{aligned} \frac{\partial^3 w_0}{\partial x^3} &= \sum_{n=1}^{\infty} \left\{ \left(\lambda_1^2 - \lambda_2^2 \right) [\lambda_1 (A_n \cos \lambda_2 x + B_n \sin \lambda_2 x) \sinh \lambda_1 x \right. \\ &\quad + \lambda_2 (-A_n \sin \lambda_2 x + B_n \cos \lambda_2 x) \cosh \lambda_1 x] \\ &\quad + 2\lambda_1^2 \lambda_2 (-A_n \sin \lambda_2 x + B_n \cos \lambda_2 x) \cosh \lambda_1 x \\ &\quad - 2\lambda_1 \lambda_2^2 (A_n \cos \lambda_2 x + B_n \sin \lambda_2 x) \sinh \lambda_1 x \\ &\quad + \left(\lambda_1^2 - \lambda_2^2 \right) [\lambda_1 (C_n \cos \lambda_2 x + D_n \sin \lambda_2 x) \cosh \lambda_1 x \\ &\quad + \lambda_2 (-C_n \sin \lambda_2 x + D_n \cos \lambda_2 x) \sinh \lambda_1 x] \\ &\quad + 2\lambda_1^2 \lambda_2 (-C_n \sin \lambda_2 x + D_n \cos \lambda_2 x) \sinh \lambda_1 x \\ &\quad \left. - 2\lambda_1 \lambda_2^2 (C_n \cos \lambda_2 x + D_n \sin \lambda_2 x) \cosh \lambda_1 x \right\} \sin \beta_n y \end{aligned} \quad (7.2.39)$$

$$\begin{aligned} \frac{\partial^3 w_0}{\partial x \partial y^2} &= - \sum_{n=1}^{\infty} \beta_n^2 \left[\lambda_2 (-A_n \sin \lambda_2 x + B_n \cos \lambda_2 x) \cosh \lambda_1 x \right. \\ &\quad + \lambda_1 (A_n \cos \lambda_2 x + B_n \sin \lambda_2 x) \sinh \lambda_1 x \\ &\quad + \lambda_2 (-C_n \sin \lambda_2 x + D_n \cos \lambda_2 x) \sinh \lambda_1 x \\ &\quad \left. + \lambda_1 (C_n \cos \lambda_2 x + D_n \sin \lambda_2 x) \cosh \lambda_1 x \right] \sin \beta_n y \end{aligned} \quad (7.2.40)$$

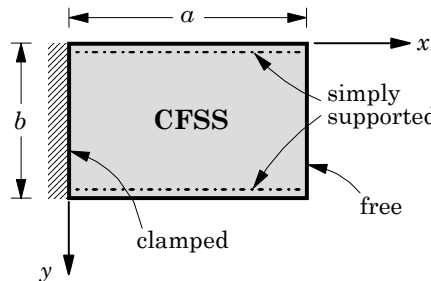


Figure 7.2.4. Rectangular plate with sides $y = 0, b$ simply supported, edge $x = 0$ clamped, and edge $x = a$ free (CFSS).

The boundary conditions in Eq. (7.2.38b), coupled with Eq. (7.2.37a) associated with the clamped edge at $x = 0$, yield the following relations among the four constants, A_n , B_n , C_n , and D_n [$\hat{q}_n = \bar{q}_n/(D_{22}\beta_n^4 + k)$]:

$$A_n + \hat{q}_n = 0, \quad \lambda_2 B_n + \lambda_1 C_n = 0 \quad (7.2.41a)$$

$$\begin{aligned} D_{11} & \left[\left(\lambda_1^2 - \lambda_2^2 \right) (A_n \cos \lambda_2 a + B_n \sin \lambda_2 a) \cosh \lambda_1 a \right. \\ & \quad + 2\lambda_1 \lambda_2 (-A_n \sin \lambda_2 a + B_n \cos \lambda_2 a) \sinh \lambda_1 a \\ & \quad + \left(\lambda_1^2 - \lambda_2^2 \right) (C_n \cos \lambda_2 a + D_n \sin \lambda_2 a) \sinh \lambda_1 a \\ & \quad \left. + 2\lambda_1 \lambda_2 (-C_n \sin \lambda_2 a + D_n \cos \lambda_2 a) \cosh \lambda_1 a \right] \\ & - D_{12} \beta_n^2 \left[\hat{q}_n + (A_n \cos \lambda_2 a + B_n \sin \lambda_2 a) \cosh \lambda_1 a \right. \\ & \quad \left. + (C_n \cos \lambda_2 a + D_n \sin \lambda_2 a) \sinh \lambda_1 a \right] = 0 \end{aligned} \quad (7.2.41b)$$

$$\begin{aligned} D_{11} & \left\{ \left(\lambda_1^2 - \lambda_2^2 \right) [\lambda_1 (A_n \cos \lambda_2 a + B_n \sin \lambda_2 a) \sinh \lambda_1 a \right. \\ & \quad + \lambda_2 (-A_n \sin \lambda_2 a + B_n \cos \lambda_2 a) \cosh \lambda_1 a] \\ & \quad + 2\lambda_1^2 \lambda_2 (-A_n \sin \lambda_2 a + B_n \cos \lambda_2 a) \cosh \lambda_1 a \\ & \quad - 2\lambda_1 \lambda_2^2 (A_n \cos \lambda_2 a + B_n \sin \lambda_2 a) \sinh \lambda_1 a \\ & \quad + \left(\lambda_1^2 - \lambda_2^2 \right) [\lambda_1 (C_n \cos \lambda_2 a + D_n \sin \lambda_2 a) \cosh \lambda_1 a \\ & \quad + \lambda_2 (-C_n \sin \lambda_2 a + D_n \cos \lambda_2 a) \sinh \lambda_1 a] \\ & \quad + 2\lambda_1^2 \lambda_2 (-C_n \sin \lambda_2 a + D_n \cos \lambda_2 a) \sinh \lambda_1 a \\ & \quad \left. - 2\lambda_1 \lambda_2^2 (C_n \cos \lambda_2 a + D_n \sin \lambda_2 a) \cosh \lambda_1 a \right\} \\ & - \bar{D}_{12} \beta_n^2 \left[\lambda_2 (-A_n \sin \lambda_2 a + B_n \cos \lambda_2 a) \cosh \lambda_1 a \right. \\ & \quad + \lambda_1 (A_n \cos \lambda_2 a + B_n \sin \lambda_2 a) \sinh \lambda_1 a \\ & \quad + \lambda_2 (-C_n \sin \lambda_2 a + D_n \cos \lambda_2 a) \sinh \lambda_1 a \\ & \quad \left. + \lambda_1 (C_n \cos \lambda_2 a + D_n \sin \lambda_2 a) \cosh \lambda_1 a \right] = 0 \end{aligned} \quad (7.2.41c)$$

The maximum nondimensional deflections $\bar{w}_{\max} = w_{\max} D / (q_0 a^4)$ and bending moments of isotropic and orthotropic plates under uniformly distributed load are presented in Table 7.2.6 for various aspect ratios. The values of the bending moments listed in the first row of each aspect ratio are to be multiplied with $q_0 a^2$ whereas those in the second row (for aspect ratios $b/a = 1.5, 2.0, 2.5$, and 3.0) are to be multiplied with $q_0 b^2$. The deflection is the maximum at the center of the free edge. The values were obtained using the first five terms of the series ($n = 1, 3, \dots, 9$). The bending moments at the center of the clamped edge as well as at the center of the free edge are tabulated. The maximum bending moment also occurs at the center of the free edge.

Table 7.2.6. Maximum nondimensional deflections and bending moments in rectangular plates (CFSS) subjected to *uniformly distributed load*.

$\frac{b}{a}$	\bar{w}_{max}	$-M_{xx}(0, b/2)$	$-M_{yy}(0, b/2)$	$M_{yy}(a, b/2)$	Factor
<i>Isotropic plates ($\nu = 0.3$)</i>					
1.0	0.0112	0.1185	0.0355	0.0972	$q_0 a^2$
1.5	0.0335	0.2271	0.0681	0.1258	$q_0 a^2$
		0.1009	0.0303	0.0559	$q_0 b^2$
2.0	0.0582	0.3192	0.0958	0.1173	$q_0 a^2$
		0.0798	0.0239	0.0293	$q_0 b^2$
2.5	0.0788	0.3850	0.1155	0.0946	$q_0 a^2$
		0.0616	0.0185	0.0151	$q_0 b^2$
3.0	0.0940	0.4285	0.1285	0.0710	$q_0 a^2$
		0.0476	0.0143	0.0079	$q_0 b^2$
<i>Orthotropic plates ($E_1/E_2 = 25$, $G_{12} = G_{13} = 0.5E_2$, $\nu_{12} = 0.25$)</i>					
1.0	0.0039	0.4289	0.0043	0.0344	$q_0 a^2$
1.5	0.0051	0.5189	0.0052	0.0146	$q_0 a^2$
2.0	0.0053	0.5262	0.0053	0.0039	$q_0 a^2$
2.5	0.0052	0.5160	0.0052	0.0002	$q_0 a^2$
3.0	0.0051	0.5078	0.0051	-0.0002	$q_0 a^2$

7.2.5 Plates with Edge $x = 0$ Simply Supported and Edge $x = a$ Free (SFSS)

Consider rectangular plates with edges $y = 0, b$ and $x = 0$ simply supported and the edge ($x = a$) free (F) (Figure 7.2.5). When \hat{q}_n is a constant, the boundary conditions on the edge $x = 0$ yield the following relations for A_n and D_n :

$$A_n = -\hat{q}_n, \quad D_n = -\left(\frac{\lambda_1^2 - \lambda_2^2}{2\lambda_1\lambda_2}\right) A_n \quad (7.2.42)$$

The relations among B_n and C_n are provided by Eqs. (7.2.41a–c).

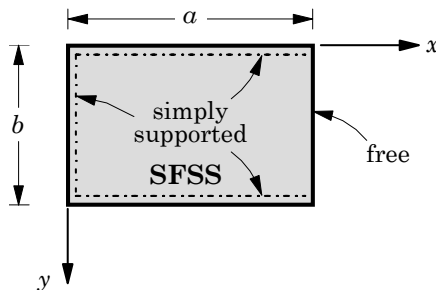


Figure 7.2.5. Rectangular plate with sides $y = 0, b$ and $x = 0$ simply supported and edge $x = a$ free (SFSS).

Table 7.2.7. Maximum nondimensional deflections and bending moments in rectangular plates (SFSS) subjected to *uniformly distributed load*.

$\frac{b}{a}$	\bar{w}_{max}	$\bar{M}_{yy}(a, b/2)$	$\bar{M}_{yy}(a/2, b/2)$	$\bar{M}_{xx}(a/2, b/2)$
3.0	0.00399	0.0330	0.0207	0.0125
2.5	0.00526	0.0442	0.0279	0.0166
2.0	0.00709	0.0602	0.0386	0.0223
1.5	0.00968	0.0833	0.0552	0.0303
1.0	0.01285	0.1185	0.0390	0.0799
2/3	0.01461	0.1274	0.1011	0.0421
0.5	0.01507	0.1320	0.1127	0.0415
1/3	0.01521	0.1321	0.1209	0.0388

The nondimensional deflections $\bar{w}_{max} = w_{max}D/(q_0b^4)$ and bending moments $\bar{M} = Mb^2/q_0$ at the middle of the free edge of uniformly loaded plates (SFSS) are presented in Table 7.2.7. The last two columns contain bending moments at the center of the plate. The first five terms of the series are used to evaluate the quantities.

When the plate is loaded by hydrostatic load of the form

$$q(x, y) = q_0 \left(1 - \frac{x}{a}\right) \quad (7.2.43)$$

the particular solution is given by

$$W_n^p(x) = \frac{q_n}{D_{22}\beta_n^4} \left(1 - \frac{x}{a}\right) \quad (7.2.44)$$

The values of A_n and D_n given in Eq. (7.2.42) remain unchanged with $\bar{q}_n = q_n$. However, equations relating B_n and C_n must be modified as

$$\begin{aligned} D_{11} & \left[\left(\lambda_1^2 - \lambda_2^2\right) (A_n \cos \lambda_2 a + B_n \sin \lambda_2 a) \cosh \lambda_1 a \right. \\ & + 2\lambda_1 \lambda_2 (-A_n \sin \lambda_2 a + B_n \cos \lambda_2 a) \sinh \lambda_1 a \\ & + \left(\lambda_1^2 - \lambda_2^2\right) (C_n \cos \lambda_2 a + D_n \sin \lambda_2 a) \sinh \lambda_1 a \\ & \left. + 2\lambda_1 \lambda_2 (-C_n \sin \lambda_2 a + D_n \cos \lambda_2 a) \cosh \lambda_1 a \right] \\ & - D_{12}\beta_n^2 \left[(A_n \cos \lambda_2 a + B_n \sin \lambda_2 a) \cosh \lambda_1 a \right. \\ & \left. + (C_n \cos \lambda_2 a + D_n \sin \lambda_2 a) \sinh \lambda_1 a \right] = 0 \end{aligned} \quad (7.2.45)$$

$$\begin{aligned}
D_{11} \left\{ & \left(\lambda_1^2 - \lambda_2^2 \right) [\lambda_1 (A_n \cos \lambda_2 a + B_n \sin \lambda_2 a) \sinh \lambda_1 a \right. \\
& + \lambda_2 (-A_n \sin \lambda_2 a + B_n \cos \lambda_2 a) \cosh \lambda_1 a] \\
& + 2\lambda_1^2 \lambda_2 (-A_n \sin \lambda_2 a + B_n \cos \lambda_2 a) \cosh \lambda_1 a \\
& - 2\lambda_1 \lambda_2^2 (A_n \cos \lambda_2 a + B_n \sin \lambda_2 a) \sinh \lambda_1 a \\
& + \left(\lambda_1^2 - \lambda_2^2 \right) [\lambda_1 (C_n \cos \lambda_2 a + D_n \sin \lambda_2 a) \cosh \lambda_1 a \\
& + \lambda_2 (-C_n \sin \lambda_2 a + D_n \cos \lambda_2 a) \sinh \lambda_1 a] \\
& + 2\lambda_1^2 \lambda_2 (-C_n \sin \lambda_2 a + D_n \cos \lambda_2 a) \sinh \lambda_1 a \\
& \left. - 2\lambda_1 \lambda_2^2 (C_n \cos \lambda_2 a + D_n \sin \lambda_2 a) \cosh \lambda_1 a \right\} \\
& - \bar{D}_{12} \beta_n^2 \left[- \frac{q_n}{a D_{22} \beta_n^4} + \lambda_2 (-A_n \sin \lambda_2 a + B_n \cos \lambda_2 a) \cosh \lambda_1 a \right. \\
& + \lambda_1 (A_n \cos \lambda_2 a + B_n \sin \lambda_2 a) \sinh \lambda_1 a \\
& + \lambda_2 (-C_n \sin \lambda_2 a + D_n \cos \lambda_2 a) \sinh \lambda_1 a \\
& \left. + \lambda_1 (C_n \cos \lambda_2 a + D_n \sin \lambda_2 a) \cosh \lambda_1 a \right] = 0 \quad (7.2.46)
\end{aligned}$$

and the solution is given by

$$\begin{aligned}
w_0(x, y) = \sum_{n=1}^{\infty} \left[\left(1 - \frac{x}{a} \right) \frac{q_n}{D_{22} \beta_n^4} + (A_n \cos \lambda_2 x + B_n \sin \lambda_2 x) \cosh \lambda_1 x \right. \\
\left. + (C_n \cos \lambda_2 x + D_n \sin \lambda_2 x) \sinh \lambda_1 x \right] \sin \beta_n y \quad (7.2.47)
\end{aligned}$$

The nondimensional deflections and bending moments, as defined by

$$\begin{aligned}
\bar{w} &= w_0(a, b/2) \frac{D}{q_0 b^4}, \quad \hat{w} = w_0(a/2, b/2) \frac{D}{q_0 b^4} \\
\bar{M} &= M(a, b/2) \frac{1}{q_0 b^2}, \quad \hat{M} = M(a/2, b/2) \frac{1}{q_0 b^4}
\end{aligned}$$

at the middle of the free edge and at the center of hydrostatically loaded plates (SFSS), are presented in Table 7.2.8.

The solutions for the hydrostatic loading

$$q(x, y) = q_0 \left(\frac{y}{b} \right)$$

can be obtained as discussed before. The magnitudes of maximum deflections and bending moments would be one-half of those presented in Table 7.2.8.

Table 7.2.8. Maximum nondimensional deflections and bending moments in rectangular plates with edges $y = 0, b$ and $x = 0$ simply supported and edge $x = a$ free (SFSS) and subjected to *hydrostatic load*, $q = q_0(1 - x/a)$.

$\frac{b}{a}$	\bar{w}	\bar{M}_{yy}	\hat{w}	\hat{M}_{yy}	\hat{M}_{xx}
2.5	0.00172	0.0145	0.00095	0.0103	0.0085
2.0	0.00229	0.0197	0.00134	0.0146	0.0117
1.5	0.00304	0.0265	0.00199	0.0215	0.0162
1.0	0.00368	0.0325	0.00314	0.0331	0.0214
2/3	0.00347	0.0308	0.00445	0.0455	0.0231
0.5	0.00291	0.0258	0.00533	0.0531	0.0223

The solutions for other boundary conditions and loads, within the limitations of the Lévy solutions discussed, may be obtained in the manner illustrated in this section. Solutions of plates with more general boundary conditions (e.g., plates with two adjacent edges clamped while the other edges simply supported) may be obtained using the method of superposition, where the solution of a given problem is represented as the sum of the solutions of plates for which solutions can be either developed or readily available [see Timoshenko and Woinowsky-Krieger (1970)], as shown next. In Section 7.3, we use the Ritz method to determine solutions of plates with various boundary conditions.

7.2.6 Solution by the Method of Superposition

The linear solutions of rectangular plates with any edge conditions and loads can be determined using the method of superposition. There are two types of problems that can be solved by the method of superposition: (1) plates with multiple loads, and (2) plates with different boundary conditions. Deflections, bending moments, and stresses in a plate with specific boundary conditions and subjected to several different loads (the first type) can be obtained by simply adding the solutions of plates with the same boundary conditions, but subjected to one load at a time. For instance, the deflection of a rectangular plate with all edges simply supported and subjected to hydrostatic load $q = q_0(x/a)$ and distributed bending moment M_0 along the edges $x = 0, a$ can be obtained by simply adding the deflection due to the hydrostatic load and that due to distributed edge moment. An example of the second type of problems is provided by the plate shown in Figure 7.2.6. The deflection of the problem can be obtained for any applied loading by the superposition of the deflections of two different plate problems: (1) a simply supported plate under the applied loading, and (2) a simply supported plate with applied edge moments M_{yy} necessary to make the rotations $\partial w_0/\partial y$ vanish at the clamped edges. Note that solutions of the two problems whose solutions are superposed are known from the Navier and/or Lévy solution procedures. Of course, the solution to the problem shown in Figure 7.2.6 can be derived directly using the Lévy method (see Section 7.2.2). The procedure for the SSCC plate is illustrated below.

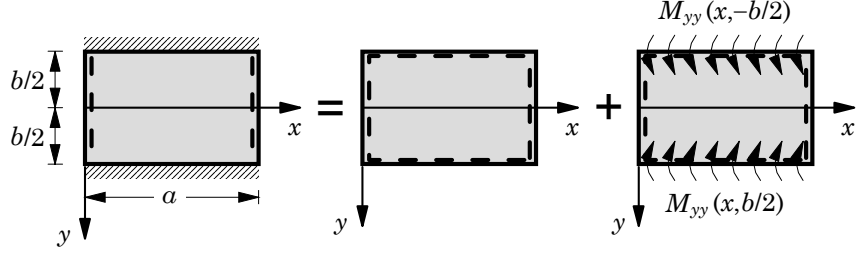


Figure 7.2.6. Application of the method of superposition to a rectangular plate with edges $x = 0, a$ simply supported and edges $y = \pm b/2$ clamped (SSCC).

Consider the SSCC plate shown in Figure 7.2.6 under uniformly distributed transverse load q_0 . The deflection of the problem is represented as the sum of the deflection w_1 of a simply supported plate under distributed transverse load and deflection w_2 of a simply supported plate with distributed edge moments M_{yy} at $y = \pm b/2$. The edge moments M_{yy} are determined such that the rotations are zero along the edges $y = \pm b/2$. The general solution of plates with simply supported edges at $x = 0, a$ is given by [see Section 6.3.5 and Eq. (6.3.63)]

$$w_0(x, y) = \sum_{m=1}^{\infty} (A_m \cos \lambda_2 y \cosh \lambda_1 y + D_m \sin \lambda_2 y \sinh \lambda_1 y + \hat{q}_m) \sin \alpha_m x \quad (7.2.48)$$

where

$$\hat{q}_m = \frac{4q_0 a^4}{m^5 \pi^5 D_{11}} \quad (7.2.49)$$

The deflection of a simply supported plate under distributed transverse load is given by

$$w_1(x, y) = \sum_{m=1}^{\infty} \hat{q}_m \left(A_m^{(1)} \cos \lambda_2 y \cosh \lambda_1 y + D_m^{(1)} \sin \lambda_2 y \sinh \lambda_1 y + 1 \right) \sin \alpha_m x \quad (7.2.50)$$

where $A_m^{(1)}$ and $D_m^{(1)}$ are defined by [see Eq. (6.3.72)]

$$\begin{aligned} A_m^{(1)} &= -\frac{1}{\Delta} (\gamma \sinh \bar{\lambda}_1 \sin \bar{\lambda}_2 + \cosh \bar{\lambda}_1 \cos \bar{\lambda}_2) \\ D_m^{(1)} &= \frac{1}{\Delta} (\gamma \cosh \bar{\lambda}_1 \cos \bar{\lambda}_2 - \sinh \bar{\lambda}_1 \sin \bar{\lambda}_2) \\ \Delta^{(1)} &= \cosh^2 \bar{\lambda}_1 \cos^2 \bar{\lambda}_2 + \sinh^2 \bar{\lambda}_1 \sin^2 \bar{\lambda}_2 \\ \bar{\lambda}_i &= \frac{\lambda_i b}{2}, \quad \gamma = \frac{\lambda_1^2 - \lambda_2^2}{2\lambda_1 \lambda_2} \end{aligned} \quad (7.2.51)$$

and the deflection of a simply supported plate with edge moment

$$M_{yy}(x, \pm \frac{b}{2}) = f(x) = \sum_{m=1}^{\infty} F_m \sin \alpha_m x \quad (7.2.52)$$

is given by

$$w_2(x, y) = \sum_{m=1}^{\infty} \frac{F_m}{2D_{22}\lambda_1\lambda_2} \left(A_m^{(2)} \cos \lambda_2 y \cosh \lambda_1 y + D_m^{(2)} \sin \lambda_2 y \sinh \lambda_1 y \right) \sin \alpha_m x \quad (7.2.53)$$

where $A_m^{(2)}$ and $D_m^{(2)}$ are defined by

$$\begin{aligned} A_m^{(2)} &= \frac{\sinh \bar{\lambda}_1 \sin \bar{\lambda}_2}{\Delta}, \quad D_m^{(2)} = -\frac{\cosh \bar{\lambda}_1 \cos \bar{\lambda}_2}{\Delta} \\ \Delta^{(2)} &= \cosh^2 \bar{\lambda}_1 \cos^2 \bar{\lambda}_2 + \sinh^2 \bar{\lambda}_1 \sin^2 \bar{\lambda}_2 \end{aligned} \quad (7.2.54)$$

The slope of the deflection surface w_1 along the edge $y = b/2$ is

$$\begin{aligned} \left(\frac{\partial w_1}{\partial x} \right)_{y=\frac{b}{2}} &= \sum_{m=1}^{\infty} \hat{q}_m \left[A_m^{(1)} (\lambda_1 \cos \bar{\lambda}_2 \sinh \bar{\lambda}_1 - \lambda_2 \cosh \bar{\lambda}_1 \sin \bar{\lambda}_2) \right. \\ &\quad \left. + D_m^{(1)} (\lambda_1 \sin \bar{\lambda}_2 \cosh \bar{\lambda}_1 + \lambda_2 \sinh \bar{\lambda}_1 \cos \bar{\lambda}_2) \right] \sin \alpha_m x \end{aligned} \quad (7.2.55)$$

The slope of the deflection surface w_2 along the edge $y = b/2$ is

$$\begin{aligned} \left(\frac{\partial w_2}{\partial x} \right)_{y=\frac{b}{2}} &= \sum_{m=1}^{\infty} \frac{F_m}{2D_{22}\lambda_1\lambda_2} \left[A_m^{(2)} (\lambda_1 \cos \bar{\lambda}_2 \sinh \bar{\lambda}_1 - \lambda_2 \cosh \bar{\lambda}_1 \sin \bar{\lambda}_2) \right. \\ &\quad \left. + D_m^{(2)} (\lambda_1 \sin \bar{\lambda}_2 \cosh \bar{\lambda}_1 + \lambda_2 \sinh \bar{\lambda}_1 \cos \bar{\lambda}_2) \right] \sin \alpha_m x \end{aligned} \quad (7.2.56)$$

To satisfy the actual boundary conditions along the clamped edges, we equate the negative of the slope produced by the moment distribution F_m to that given in Eq. (7.2.55) and solve for F_m . We obtain

$$F_m = 2\lambda_1\lambda_2 D_{22} \hat{q}_m \left(\frac{W_m^1}{W_m^2} \right) \quad (7.2.57)$$

$$\begin{aligned} W_m^1 &= A_m^{(1)} (\lambda_1 \cos \bar{\lambda}_2 \sinh \bar{\lambda}_1 - \lambda_2 \cosh \bar{\lambda}_1 \sin \bar{\lambda}_2) \\ &\quad + D_m^{(1)} (\lambda_1 \sin \bar{\lambda}_2 \cosh \bar{\lambda}_1 + \lambda_2 \sinh \bar{\lambda}_1 \cos \bar{\lambda}_2) \\ W_m^2 &= A_m^{(2)} (\lambda_1 \cos \bar{\lambda}_2 \sinh \bar{\lambda}_1 - \lambda_2 \cosh \bar{\lambda}_1 \sin \bar{\lambda}_2) \\ &\quad + D_m^{(2)} (\lambda_1 \sin \bar{\lambda}_2 \cosh \bar{\lambda}_1 + \lambda_2 \sinh \bar{\lambda}_1 \cos \bar{\lambda}_2) \end{aligned} \quad (7.2.58)$$

Hence, the bending moment along the clamped edge is

$$M_{yy}(x, \pm \frac{b}{2}) = 2D_{22} \sum_{m=1}^{\infty} \lambda_1\lambda_2 \hat{q}_m \left(\frac{W_m^1}{W_m^2} \right) \sin \alpha_m x \quad (7.2.59)$$

The deflection of the SSCC plate is now given by

$$w_0(x, y) = w_1(x, y) - w_2(x, y) \quad (7.2.60)$$

where F_m of Eq. (7.2.53) is defined by Eq. (7.2.57).

7.3 Approximate Solutions by the Ritz Method

7.3.1 Analysis of the Lévy Plates

We recall from Section 6.3.6 that the ordinary differential equation resulting from the application of the Lévy solution procedures, namely Eq. (7.2.4), can be solved by the Ritz method. The Ritz solutions of the Lévy equation (7.2.4) were presented for simply supported plates in Section 6.3.6. Here we use the method for other boundary conditions. Towards this end, first we construct the weak form of Eq. (7.2.4) for general boundary conditions at $x = 0, a$. We have

$$\begin{aligned} 0 = \int_0^a & \left[D_{11} \frac{d^2 W_n}{dx^2} \frac{d^2 \delta W_n}{dx^2} + 2\hat{D}_{12}\beta_n^2 \frac{dW_n}{dx} \frac{d\delta W_n}{dx} \right. \\ & \left. + (D_{22}\beta_n^4 + k) W_n \delta W_n - q_n \delta W_n \right] dx \\ & + \left[\left(D_{11} \frac{d^3 W_n}{dx^3} - 2\hat{D}_{12}\beta_n^2 \frac{dW_n}{dx} \right) \delta W_n - D_{11} \frac{d^2 W_n}{dx^2} \frac{d\delta W_n}{dx} \right]_0^a \end{aligned} \quad (7.3.1)$$

$\hat{D}_{12} = D_{12} + 2D_{66}$. For a simply supported edge without an applied edge moment [$W_n = 0$ and $(d^2 W_n / dx^2) = 0$] or a clamped edge [$W_n = 0$ and $(dW_n / dx) = 0$], the boundary terms in Eq. (7.3.1) vanish identically. However, for a free edge, the vanishing of bending moment and effective shear force require

$$D_{11} \frac{d^2 W_n}{dx^2} - D_{12}\beta_n^2 W_n = 0, \quad D_{11} \frac{d^3 W_n}{dx^3} - \bar{D}_{12}\beta_n^2 \frac{dW_n}{dx} = 0 \quad (7.3.2)$$

where $\bar{D}_{12} = D_{12} + 4D_{66}$. Hence, on a free edge, the boundary expression of Eq. (7.3.1) can be simplified to

$$\begin{aligned} & \left[\left(D_{11} \frac{d^3 W_n}{dx^3} - 2\hat{D}_{12}\beta_n^2 \frac{dW_n}{dx} \right) \delta W_n - D_{11} \frac{d^2 W_n}{dx^2} \frac{d\delta W_n}{dx} \right]_0^a \\ & = -\beta_n^2 D_{12} \left[W_n \frac{d\delta W_n}{dx} + \frac{dW_n}{dx} \delta W_n \right]_0^a \end{aligned} \quad (7.3.3)$$

The weak forms for various plates are summarized next.

SSSS, CCSS, and CSSS Plates:

$$\begin{aligned} 0 = \int_0^a & \left[D_{11} \frac{d^2 W_n}{dx^2} \frac{d^2 \delta W_n}{dx^2} + 2\hat{D}_{12}\beta_n^2 \frac{dW_n}{dx} \frac{d\delta W_n}{dx} \right. \\ & \left. + (D_{22}\beta_n^4 + k) W_n \delta W_n - q_n \delta W_n \right] dx \end{aligned} \quad (7.3.4)$$

CFSS and SFSS Plates:

$$0 = \int_0^a \left[D_{11} \frac{d^2 W_n}{dx^2} \frac{d^2 \delta W_n}{dx^2} + 2\hat{D}_{12}\beta_n^2 \frac{dW_n}{dx} \frac{d\delta W_n}{dx} \right. \\ \left. + (D_{22}\beta_n^4 + k) W_n \delta W_n - q_n \delta W_n \right] dx \\ - \beta_n^2 D_{12} \left[W_n \frac{d\delta W_n}{dx} + \frac{dW_n}{dx} \delta W_n \right]_0^a \quad (7.3.5)$$

FFSS Plates:

$$0 = \int_0^a \left[D_{11} \frac{d^2 W_n}{dx^2} \frac{d^2 \delta W_n}{dx^2} + 2\hat{D}_{12}\beta_n^2 \frac{dW_n}{dx} \frac{d\delta W_n}{dx} \right. \\ \left. + (D_{22}\beta_n^4 + k) W_n \delta W_n - q_n \delta W_n \right] dx \\ - \beta_n^2 D_{12} \left[W_n \frac{d\delta W_n}{dx} + \frac{dW_n}{dx} \delta W_n \right]_0^a \quad (7.3.6)$$

The Ritz equations are obtained by substituting the approximation

$$W_n(x) \approx \sum_{j=1}^N c_j \varphi_j(x) \quad (7.3.7)$$

into the weak forms (7.3.4)–(7.3.6). We obtain

$$[R + B]^{(n)} \{c\}^{(n)} = \{F\}^{(n)} \quad (7.3.8)$$

where

$$R_{ij}^{(n)} = \int_0^a \left[D_{11} \frac{d^2 \varphi_i}{dx^2} \frac{d^2 \varphi_j}{dx^2} + 2\beta_n^2 \hat{D}_{12} \frac{d\varphi_i}{dx} \frac{d\varphi_j}{dx} + (D_{22}\beta_n^4 + k) \varphi_i \varphi_j \right] dx \quad (7.3.9a)$$

$$B_{ij}^{(n)} = -\beta_n^2 D_{12} \left[\varphi_j \frac{d\varphi_i}{dx} + \frac{d\varphi_j}{dx} \varphi_i \right]_0^a, \quad F_i^{(n)} = \int_0^a q_n \varphi_i dx \quad (7.3.9b)$$

The coefficients $B_{ij}^{(n)}$ are nonzero only for the CFSS, SFSS, and FFSS plates.

Limiting our choice of the approximation functions to algebraic polynomials and using the *geometric* boundary conditions, we can derive φ_i for various plates. The geometric boundary conditions and the approximation functions are presented below.

SSSS Plates:

$$W_n(0) = 0, \quad W_n(a) = 0 \quad (7.3.10)$$

$$\varphi_i = \left(\frac{x}{a} \right)^i - \left(\frac{x}{a} \right)^{i+1}$$

$$\frac{d\varphi_i}{dx} = \frac{1}{a} \left[i \left(\frac{x}{a} \right)^{i-1} - (i+1) \left(\frac{x}{a} \right)^i \right]$$

$$\frac{d^2 \varphi_i}{dx^2} = \frac{1}{a^2} \left[i(i-1) \left(\frac{x}{a} \right)^{i-2} - i(i+1) \left(\frac{x}{a} \right)^{i-1} \right] \quad (7.3.11)$$

CCSS Plates:

$$W_n = 0, \quad \frac{dW_n}{dx} = 0 \quad \text{for } x = 0, a \quad (7.3.12)$$

$$\begin{aligned} \varphi_i &= \left(\frac{x}{a}\right)^{i+1} - 2\left(\frac{x}{a}\right)^{i+2} + \left(\frac{x}{a}\right)^{i+3} \\ \frac{d\varphi_i}{dx} &= \frac{1}{a} \left[(i+1) \left(\frac{x}{a}\right)^i - 2(i+2) \left(\frac{x}{a}\right)^{i+1} + (i+3) \left(\frac{x}{a}\right)^{i+2} \right] \\ \frac{d^2\varphi_i}{dx^2} &= \frac{1}{a^2} \left[i(i+1) \left(\frac{x}{a}\right)^{i-1} - 2(i+1)(i+2) \left(\frac{x}{a}\right)^i \right. \\ &\quad \left. + (i+2)(i+3) \left(\frac{x}{a}\right)^{i+1} \right] \end{aligned} \quad (7.3.13)$$

CSSS Plates:

$$W_n(0) = 0, \quad \frac{dW_n}{dx}(0) = 0, \quad W_n(a) = 0 \quad (7.3.14)$$

$$\begin{aligned} \varphi_i &= \left(\frac{x}{a}\right)^{i+1} - \left(\frac{x}{a}\right)^{i+2} \\ \frac{d\varphi_i}{dx} &= \frac{1}{a} \left[(i+1) \left(\frac{x}{a}\right)^i - (i+2) \left(\frac{x}{a}\right)^{i+1} \right] \\ \frac{d^2\varphi_i}{dx^2} &= \frac{1}{a^2} \left[i(i+1) \left(\frac{x}{a}\right)^{i-1} - (i+1)(i+2) \left(\frac{x}{a}\right)^i \right] \end{aligned} \quad (7.3.15)$$

CFSS Plates:

$$W_n(0) = 0, \quad \frac{dW_n}{dx}(0) = 0 \quad (7.3.16)$$

$$\begin{aligned} \varphi_i &= \left(\frac{x}{a}\right)^{i+1} \\ \frac{d\varphi_i}{dx} &= \frac{(i+1)}{a} \left(\frac{x}{a}\right)^i \\ \frac{d^2\varphi_i}{dx^2} &= \frac{1}{a^2} \left[i(i+1) \left(\frac{x}{a}\right)^{i-1} \right] \end{aligned} \quad (7.3.17)$$

SFSS Plates:

$$W_n(0) = 0 \quad (7.3.18)$$

$$\begin{aligned} \varphi_i &= \left(\frac{x}{a}\right)^i \\ \frac{d\varphi_i}{dx} &= \frac{i}{a} \left(\frac{x}{a}\right)^{i-1} \\ \frac{d^2\varphi_i}{dx^2} &= \frac{1}{a^2} \left[i(i-1) \left(\frac{x}{a}\right)^{i-2} \right] \end{aligned} \quad (7.3.19)$$

FFSS Plates: ($N > 1$)

$$\begin{aligned}\varphi_i &= \left(\frac{x}{a}\right)^{i-1} \\ \frac{d\varphi_i}{dx} &= \frac{(i-1)}{a} \left(\frac{x}{a}\right)^{i-2} \\ \frac{d^2\varphi_i}{dx^2} &= \frac{1}{a^2} \left[(i-1)(i-2) \left(\frac{x}{a}\right)^{i-3} \right]\end{aligned}\quad (7.3.20)$$

Table 7.3.1 contains numerical results obtained using the approximation functions in Eqs. (7.3.11), (7.3.13), (7.3.15), (7.3.17), (7.3.19), and (7.3.20) for various plates under center point load Q_0 and uniformly distributed transverse load q_0 . The results were obtained using $n = 1, 3, \dots, 9$ and $N = 9$. The nondimensional deflections and moments are defined as follows:

$$\bar{w} = w_0(a/2, b/2) \left(D/q_0 a^4 \right), \quad \bar{M} = M(a/2, b/2) \left(1/q_0 a^2 \right) \quad (7.3.21a)$$

$$\hat{w} = w_0(a, b/2) \left(D/q_0 a^4 \right), \quad \hat{M} = M(a, b/2) \left(1/q_0 a^2 \right) \quad (7.3.21b)$$

$$\tilde{M} = M(0, b/2) \left(1/q_0 a^2 \right) \quad (7.3.21c)$$

In the case of point load Q_0 , the above nondimensional parameters hold with $q_0 a^2 = Q_0$.

Table 7.3.1. Transverse deflections and bending moments in isotropic square plates with various boundary conditions and subjected to central point load or uniformly distributed load .

Plate	\bar{w}	\hat{w}	\bar{M}_{xx}	\bar{M}_{yy}	\hat{M}_{yy}	\tilde{M}_{xx}	\tilde{M}_{yy}
<i>Uniformly Distributed Load</i> ($q_n = \frac{4q_0}{n\pi}$)							
SSSS	0.00406	0.00000	0.0479	0.0479	0.0000	0.0000	0.0000
CCSS	0.00192	0.00000	0.0333	0.0244	-0.0210	-0.0699	-0.0210
CSSS	0.00279	0.00000	0.0392	0.0339	0.0210	-0.0839	-0.0252
CFSS	0.00567	0.01124	0.0280	0.0564	0.0973	-0.1185	-0.0355
SFSS	0.00793	0.01285	0.0390	0.0799	0.1118	0.0000	0.0000
FFSS	0.01309	0.01501	0.0271	0.1226	0.1312	0.0000	0.1312
<i>Central Point Load</i> [$q_n = \frac{2Q_0}{b} \delta(x - \frac{a}{2}) \sin \frac{n\pi}{2}$]							
SSSS	0.01145	0.00000	0.2557	0.2729	0.0000	0.0000	0.0000
CCSS	0.00695	0.00000	0.2398	0.2309	-0.0601	-0.2002	-0.0601
CSSS	0.00876	0.00000	0.2373	0.2429	0.0000	-0.1566	-0.0470
CFSS	0.01223	0.01363	0.2237	0.2700	0.1385	-0.1980	-0.0594
SFSS	0.01640	0.01664	0.2250	0.3026	0.1381	0.0000	0.0000
FFSS	0.02304	0.01942	0.2095	0.3576	0.1630	0.1630	-0.0494

7.3.2 Formulation for General Plates

In this section, we discuss applications of the Ritz method to the bending of rectangular plates with various boundary conditions. The virtual work statement (or weak form) and the total potential energy expressions for an orthotropic rectangular plate are [see Eq. (3.4.10)]

$$\begin{aligned} 0 = \int_0^b \int_0^a & \left[D_{11} \frac{\partial^2 w_0}{\partial x^2} \frac{\partial^2 \delta w_0}{\partial x^2} + D_{12} \left(\frac{\partial^2 w_0}{\partial y^2} \frac{\partial^2 \delta w_0}{\partial x^2} + \frac{\partial^2 w_0}{\partial x^2} \frac{\partial^2 \delta w_0}{\partial y^2} \right) \right. \\ & + 4D_{66} \frac{\partial^2 w_0}{\partial x \partial y} \frac{\partial^2 \delta w_0}{\partial x \partial y} + D_{22} \frac{\partial^2 w_0}{\partial y^2} \frac{\partial^2 \delta w_0}{\partial y^2} - q \delta w_0 \Big] dx dy \\ & - \int_{\Gamma} \left(-\hat{M}_{nn} \frac{\partial \delta w_0}{\partial n} + \hat{V}_n \delta w_0 \right) ds \end{aligned} \quad (7.3.22)$$

where \hat{M}_{nn} and \hat{V}_n are applied edge moment and effective shear force, respectively, on the boundary Γ . The total potential energy functional is given by

$$\begin{aligned} \Pi(w_0) = \frac{1}{2} \int_0^b \int_0^a & \left[D_{11} \left(\frac{\partial^2 w_0}{\partial x^2} \right)^2 + 2D_{12} \frac{\partial^2 w_0}{\partial x^2} \frac{\partial^2 w_0}{\partial y^2} + 4D_{66} \left(\frac{\partial^2 w_0}{\partial x \partial y} \right)^2 \right. \\ & \left. + D_{22} \left(\frac{\partial^2 w_0}{\partial y^2} \right)^2 - 2q w_0 \right] dx dy - \int_{\Gamma} \left(-\hat{M}_{nn} \frac{\partial w_0}{\partial n} + \hat{V}_n w_0 \right) ds \end{aligned} \quad (7.3.23)$$

We seek an N -parameter Ritz solution in the form

$$w_0(x, y) \approx \sum_{j=1}^N c_j \varphi_j(x, y) \quad (7.3.24)$$

and substitute it into Eq. (7.3.22) to obtain

$$[R]\{c\} = \{F\} \quad (7.3.25)$$

where

$$\begin{aligned} R_{ij} = \int_0^b \int_0^a & \left[D_{11} \frac{\partial^2 \varphi_i}{\partial x^2} \frac{\partial^2 \varphi_j}{\partial x^2} + D_{12} \left(\frac{\partial^2 \varphi_i}{\partial y^2} \frac{\partial^2 \varphi_j}{\partial x^2} + \frac{\partial^2 \varphi_i}{\partial x^2} \frac{\partial^2 \varphi_j}{\partial y^2} \right) \right. \\ & \left. + 4D_{66} \frac{\partial^2 \varphi_i}{\partial x \partial y} \frac{\partial^2 \varphi_j}{\partial x \partial y} + D_{22} \frac{\partial^2 \varphi_i}{\partial y^2} \frac{\partial^2 \varphi_j}{\partial y^2} \right] dx dy \end{aligned} \quad (7.3.26a)$$

$$F_i = \int_0^b \int_0^a q \varphi_i dx dy + \int_{\Gamma} \left(-\hat{M}_{nn} \frac{\partial \varphi_i}{\partial n} + \hat{V}_n \varphi_i \right) ds \quad (7.3.26b)$$

In view of the rectangular geometry, it is convenient to express the Ritz approximation in the form

$$w_0(x, y) \approx W_{mn}(x, y) = \sum_{i=1}^N \sum_{j=1}^N c_{ij} \varphi_{ij}(x, y) \quad (7.3.27)$$

and write $\varphi_{ij}(x, y)$ as a tensor product of the one-dimensional functions X_i and Y_j

$$\varphi_{ij}(x, y) = X_i(x)Y_j(y) \quad (7.3.28)$$

$i, j = 1, 2, \dots, N$. The functions given in Eqs. (7.3.11), (7.3.13), (7.3.15), (7.3.17), (7.3.19), and (7.3.20) are candidates for X_i and Y_j . An alternative choice is provided by the characteristic equations of beams (see Table 4.5.1; set $\mu = \lambda$). These sets of functions are summarized below for typical boundary conditions (Figure 7.3.1). In the case of characteristic polynomials, the roots λ_i are to be determined by solving a nonlinear equation. The first few values of $\lambda_i a$ are given in Table 4.5.1.

CCSS Plates:

Algebraic polynomials

$$X_i(x) = \left(\frac{x}{a}\right)^{i+1} - 2\left(\frac{x}{a}\right)^{i+2} + \left(\frac{x}{a}\right)^{i+3}, \quad Y_j(y) = \left(\frac{y}{b}\right)^j - \left(\frac{y}{b}\right)^{j+1} \quad (7.3.29)$$

Characteristic polynomials

$$X_i(x) = \sin \lambda_i x - \sinh \lambda_i x + \alpha_i (\cosh \lambda_i x - \cos \lambda_i x), \quad Y_j(y) = \sin \frac{n\pi y}{b} \quad (7.3.30a)$$

where λ_i are the roots of the characteristic equation

$$\cos \lambda_i a \cosh \lambda_i a - 1 = 0 \quad (7.3.30b)$$

and α_i are defined by

$$\alpha_i = \frac{\sinh \lambda_i a - \sin \lambda_i a}{\cosh \lambda_i a - \cos \lambda_i a} \quad (7.3.30c)$$

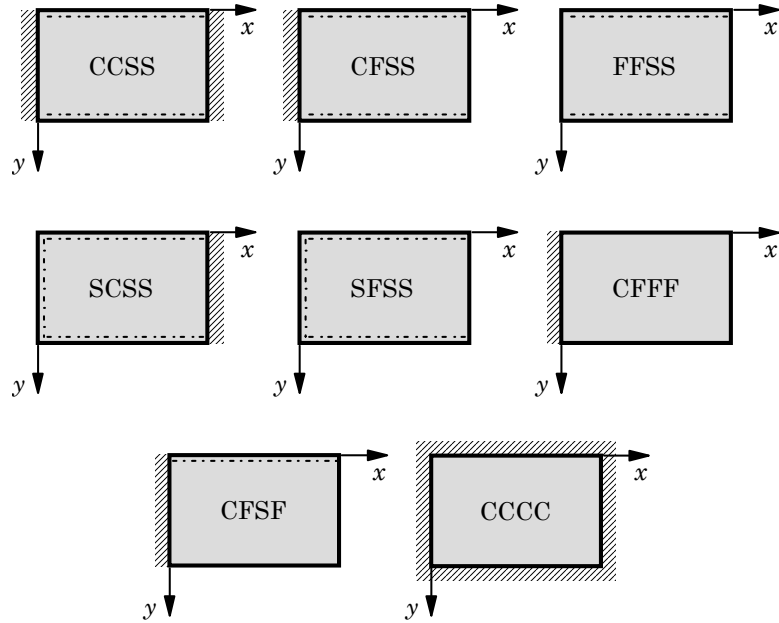


Figure 7.3.1. Rectangular plates with various boundary conditions along the four sides.

CFSS Plates:*Algebraic polynomials*

$$X_i(x) = \left(\frac{x}{a}\right)^{i+1}, \quad Y_j(x) = \left(\frac{y}{b}\right)^j - \left(\frac{y}{b}\right)^{j+1} \quad (7.3.31)$$

Characteristic polynomials

$$\begin{aligned} X_i(x) &= \sin \lambda_i x - \sinh \lambda_i x + \alpha_i (\cosh \lambda_i x - \cos \lambda_i x), \quad Y_j(y) = \sin \frac{n\pi y}{b} \\ \cos \lambda_i a \cosh \lambda_i a + 1 &= 0, \quad \alpha_i = \frac{\sinh \lambda_i a + \sin \lambda_i a}{\cosh \lambda_i a + \cos \lambda_i a} \end{aligned} \quad (7.3.32)$$

FFSS Plates:*Algebraic polynomials ($M > 1$)*

$$X_i(x) = \left(\frac{x}{a}\right)^{i-1}, \quad Y_j(x) = \left(\frac{y}{b}\right)^j - \left(\frac{y}{b}\right)^{j+1} \quad (7.3.33)$$

Characteristic polynomials

$$\begin{aligned} X_i(x) &= \sin \lambda_i x + \sinh \lambda_i x - \alpha_i (\cosh \lambda_i x + \cos \lambda_i x), \quad Y_j(y) = \sin \frac{n\pi y}{b} \\ \cos \lambda_i a \cosh \lambda_i a - 1 &= 0, \quad \alpha_i = \frac{\sinh \lambda_i a - \sin \lambda_i a}{\cosh \lambda_i a - \cos \lambda_i a} \end{aligned} \quad (7.3.34)$$

SCSS Plates:*Algebraic polynomials*

$$X_i(x) = \left(\frac{x}{a}\right) \left[1 - \left(\frac{x}{a}\right)\right]^{i+1}, \quad Y_j(x) = \left(\frac{y}{b}\right)^j - \left(\frac{y}{b}\right)^{j+1} \quad (7.3.35)$$

Characteristic polynomials

$$\begin{aligned} X_i(x) &= \sinh \lambda_i a \sin \lambda_i x + \sin \lambda_i a \sinh \lambda_i x, \quad Y_j(y) = \sin \frac{n\pi y}{b} \\ \tan \lambda_i a - \tanh \lambda_i a &= 0 \end{aligned} \quad (7.3.36)$$

SFSS Plates:*Algebraic polynomials*

$$X_i(x) = \left(\frac{x}{a}\right)^i, \quad Y_j(x) = \left(\frac{y}{b}\right)^j - \left(\frac{y}{b}\right)^{j+1} \quad (7.3.37)$$

Characteristic polynomials

$$\begin{aligned} X_i(x) &= \sinh \lambda_i a \sin \lambda_i x - \sin \lambda_i a \sinh \lambda_i x, \quad Y_j(y) = \sin \frac{n\pi y}{b} \\ \tan \lambda_i a - \tanh \lambda_i a &= 0 \end{aligned} \quad (7.3.38)$$

CFFF Plates: ($N > 1$)*Algebraic polynomials*

$$X_i(x) = \left(\frac{x}{a}\right)^{i+1}, \quad Y_j(y) = \left(\frac{y}{b}\right)^{j-1} \quad (7.3.39)$$

Characteristic polynomials

$$\begin{aligned} X_i(x) &= \sin \lambda_i x - \sinh \lambda_i x + \alpha_i (\cosh \lambda_i x - \cos \lambda_i x) \\ Y_j(y) &= \sin \mu_j y + \sinh \mu_j y - \beta_j (\cosh \mu_j y + \cos \mu_j y) \end{aligned} \quad (7.3.40a)$$

$$\cos \lambda_i a \cosh \lambda_i a + 1 = 0, \quad \cos \mu_j b \cosh \mu_j b - 1 = 0 \quad (7.3.40b)$$

$$\alpha_i = \frac{\sinh \lambda_i a + \sin \lambda_i a}{\cosh \lambda_i a + \cos \lambda_i a}, \quad \beta_j = \frac{\sinh \mu_j b - \sin \mu_j b}{\cosh \mu_j b - \cos \mu_j b} \quad (7.3.40c)$$

CFSF Plates:*Algebraic polynomials*

$$X_i(x) = \left(\frac{x}{a}\right)^{i+1}, \quad Y_j(y) = \left(\frac{y}{b}\right)^j \quad (7.3.41)$$

Characteristic polynomials

$$\begin{aligned} X_i(x) &= \sin \lambda_i x - \sinh \lambda_i x + \alpha_i (\cosh \lambda_i x - \cos \lambda_i x) \\ Y_j(y) &= \sinh \mu_j b \sin \mu_j y - \sin \mu_j b \sinh \mu_j y \end{aligned} \quad (7.3.42a)$$

$$\cos \lambda_i a \cosh \lambda_i a + 1 = 0, \quad \tan \mu_j b - \tanh \mu_j b = 0 \quad (7.3.42b)$$

$$\alpha_i = \frac{\sinh \lambda_i a + \sin \lambda_i a}{\cosh \lambda_i a + \cos \lambda_i a} \quad (7.3.42c)$$

CCCC Plates:*Algebraic polynomials*

$$X_i(x) = \left(\frac{x}{a}\right)^{i+1} - 2 \left(\frac{x}{a}\right)^{i+2} + \left(\frac{x}{a}\right)^{i+3} \quad (7.3.43a)$$

$$Y_j(y) = \left(\frac{y}{b}\right)^{j+1} - 2 \left(\frac{y}{b}\right)^{j+2} + \left(\frac{y}{b}\right)^{j+3} \quad (7.3.43b)$$

Characteristic polynomials

$$\begin{aligned} X_i(x) &= \sin \lambda_i x - \sinh \lambda_i x + \alpha_i (\cosh \lambda_i x - \cos \lambda_i x) \\ Y_j(y) &= \sin \lambda_j y - \sinh \lambda_j y + \alpha_j (\cosh \lambda_j y - \cos \lambda_j y) \end{aligned} \quad (7.3.44a)$$

$$\cos \lambda_i a \cosh \lambda_i a - 1 = 0 \quad (7.3.44b)$$

$$\alpha_i = \frac{\sinh \lambda_i a - \sin \lambda_i a}{\cosh \lambda_i a - \cos \lambda_i a} = \frac{\cosh \lambda_i a - \cos \lambda_i a}{\sinh \lambda_i a + \sin \lambda_i a} \quad (7.3.44c)$$

The examples given above indicate how one can construct the approximation functions for any combination of fixed, hinged, and free boundary conditions on the four edges of a rectangular plate. The difficult task is to evaluate the integrals of these functions as required in Eqs. (7.3.26a,b). One may use a symbolic manipulator, such as *Mathematica* or *Maple*, to evaluate the integrals. In general, the Ritz method for general rectangular plates with arbitrary boundary conditions is algebraically more complicated than a numerical method, such as the finite element method.

7.3.3 Clamped Plates (CCCC)

For clamped plates, the Navier or Lévy methods cannot be used. As an example of the application of the Ritz method to plates with arbitrary boundary conditions, we consider a CCCC plate subjected to distributed transverse load $q(x, y)$. The approximation functions φ_{ij} of Eqs. (7.3.43a,b) or Eqs. (7.3.44a–c) may be used. Substituting Eq. (7.3.27) into Eq. (7.3.22) (with $\delta w_{0,n} = \delta w_0 = 0$ on Γ), we obtain

$$0 = \sum_{i=1}^m \sum_{j=1}^n \left\{ \int_0^b \int_0^a \left[D_{11} \frac{d^2 X_i}{dx^2} Y_j \frac{d^2 X_p}{dx^2} Y_q + 4D_{66} \frac{dX_i}{dx} \frac{dY_j}{dy} \frac{dX_p}{dx} \frac{dY_q}{dy} \right. \right. \\ \left. \left. + D_{12} \left(X_i \frac{d^2 Y_j}{dy^2} \frac{d^2 X_p}{dx^2} Y_q + \frac{d^2 X_i}{dx^2} Y_j X_p \frac{d^2 Y_q}{dy^2} \right) \right. \right. \\ \left. \left. + D_{22} X_i \frac{d^2 Y_j}{dy^2} X_p \frac{d^2 Y_q}{dy^2} \right] dx dy \right\} c_{ij} - \int_0^b \int_0^a q X_p Y_q dx dy \quad (7.3.45)$$

Equation (7.3.45) represents $m \times n$ algebraic equations among the coefficients c_{ij} . Note that all integrals in (7.3.45) are line integrals, and they involve evaluating the following five different integrals:

$$\int_0^a X_i dx, \quad \int_0^a X_i X_p dx, \quad \int_0^a \frac{dX_i}{dx} \frac{dX_p}{dx} dx, \quad \int_0^a X_i \frac{d^2 X_p}{dx^2} dx, \quad \int_0^a \frac{d^2 X_i}{dx^2} \frac{d^2 X_p}{dx^2} dx \quad (7.3.46)$$

First, we consider the algebraic functions in Eqs. (7.3.43a,b) with $m = n = 1$ and $q = q_0$ (uniformly distributed load of intensity q_0). The integrals in Eq. (7.3.46) for this case are given by

$$\begin{aligned} \int_0^a X_1 dx &= \frac{a}{30}, & \int_0^a X_1 X_1 dx &= \frac{a}{630}, & \int_0^a \frac{dX_1}{dx} \frac{dX_1}{dx} dx &= \frac{2}{105a} \\ \int_0^a X_1 \frac{d^2 X_1}{dx^2} dx &= -\frac{2}{105a}, & \int_0^a \frac{d^2 X_1}{dx^2} \frac{d^2 X_1}{dx^2} dx &= \frac{4}{5a^3} \end{aligned} \quad (7.3.47)$$

and Eq. (7.3.45) takes the form

$$\begin{aligned} 0 = & \left[\left(\frac{4}{5a^3} \right) \left(\frac{b}{630} \right) D_{11} + 4D_{66} \left(\frac{2}{105a} \right) \left(\frac{2}{105b} \right) \right. \\ & \left. + 2D_{12} \left(-\frac{2}{105a} \right) \left(-\frac{2}{105b} \right) + \left(\frac{a}{630} \right) \left(\frac{4}{5b^3} \right) D_{22} \right] c_{11} - \left(\frac{ab}{900} \right) q_0 \end{aligned}$$

or

$$\left[\frac{7}{a^4} D_{11} + \frac{4}{a^2 b^2} (D_{12} + 2D_{66}) + \frac{7}{b^4} D_{22} \right] c_{11} = \frac{49}{8} q_0 \quad (7.3.48)$$

and the one-parameter Ritz solution becomes

$$W_{11}(x, y) = \left(\frac{49}{8} \right) \frac{q_0 a^4 \left[\frac{x}{a} - \left(\frac{x}{a} \right)^2 \right]^2 \left[\frac{y}{b} - \left(\frac{y}{b} \right)^2 \right]^2}{7D_{11} + 4(D_{12} + 2D_{66})s^2 + 7D_{22}s^4} \quad (7.3.49)$$

where $s = a/b$ denotes the plate aspect ratio. The maximum deflection occurs at $x = a/2$ and $y = b/2$:

$$W_{11}\left(\frac{a}{2}, \frac{b}{2}\right) = 0.00342 \frac{q_0 a^4}{D_{11} + 0.5714(D_{12} + 2D_{66})s^2 + D_{22}s^4} \quad (7.3.50)$$

Next, we use the characteristic functions in Eqs. (7.3.44a,b) for $m = n = 1$

$$\begin{aligned} X_1(x) &= \sin \frac{4.73x}{a} - \sinh \frac{4.73x}{a} + 1.0178 \left(\cosh \frac{4.73x}{a} - \cos \frac{4.73x}{a} \right) \\ Y_1(y) &= \sin \frac{4.73y}{b} - \sinh \frac{4.73y}{b} + 1.0178 \left(\cosh \frac{4.73y}{b} - \cos \frac{4.73y}{b} \right) \end{aligned} \quad (7.3.51)$$

Evaluating the integrals in Eq. (7.3.46), we obtain

$$\begin{aligned} \int_0^a X_1 \, dx &= 0.84555a, \quad \int_0^a X_1 X_1 \, dx = 1.035966a, \quad \int_0^a \frac{dX_1}{dx} \frac{dX_1}{dx} \, dx = \frac{12.7442}{a} \\ \int_0^a X_1 \frac{d^2 X_1}{dx^2} \, dx &= -\frac{12.7442}{a}, \quad \int_0^a \frac{d^2 X_1}{dx^2} \frac{d^2 X_1}{dx^2} \, dx = \frac{518.531}{a^3} \end{aligned}$$

and Eq. (7.3.45) becomes

$$\left[\frac{537.181b}{a^3} D_{11} + \frac{324.829}{ab} (D_{12} + 2D_{66}) + \frac{537.181a}{b^3} D_{22} \right] c_{11} = 0.715q_0 ab$$

The maximum deflection is given by ($X_1(a/2) = Y_1(b/2) = 1.6164$)

$$W_{11}\left(\frac{a}{2}, \frac{b}{2}\right) = 0.00348 \frac{q_0 a^4}{D_{11}b^4 + 0.6047(D_{12} + 2D_{66})s^2 + D_{22}s^4} \quad (7.3.52)$$

For an isotropic square plate, the maximum deflection in Eq. (7.3.52) becomes $W_{11}(a/2, b/2) = 0.00134(q_0 a^4/D)$, whereas Eq. (7.3.50) gives $W_{11}(a/2, b/2) = 0.00133(q_0 a^4/D)$. The “exact” solution [see Timoshenko and Woinowsky-Krieger (1970), p. 202] is $W_{11}(a/2, b/2) = 0.00126(q_0 a^4/D)$.

7.4 Summary

The Lévy solution procedure is used to develop exact solutions of rectangular plates with two parallel sides simply supported while the other two sides are independently subjected to other boundary conditions (i.e., free, clamped, simply supported) under a variety of loads. The Ritz solution procedure is also presented for solving the two-dimensional plate problem as well as the one-dimensional differential equation resulting from the Lévy solution procedure. Numerical results for maximum deflections and stresses are tabulated for various boundary conditions and loads.

Problems

- 7.1** Write the necessary algebraic equations to determine the constants A_n , B_n , C_n , and D_n in the solution (7.2.31a) of a rectangular plate with edges $x = 0, a$ free and edges $y = 0, b$ simply supported (FFSS), and subjected to loads in which q_n is a constant. Note that conditions in Eq. (7.2.38b) must be satisfied at $x = 0, a$. *Ans:* From Eqs. (7.2.34), (7.2.35), (7.2.39), and (7.3.40), we have

$$\begin{aligned} D_{11} \left[(\lambda_1^2 - \lambda_2^2) A_n + 2\lambda_1\lambda_2 D_n \right] - D_{12}\beta_n^2 \left[\frac{q_n}{D_{22}\beta_n^4 + k} + A_n \right] &= 0 \\ D_{11} \left[(\lambda_1^2 - \lambda_2^2) (\lambda_2 B_n + \lambda_1 C_n) + 2\lambda_1\lambda_2 (\lambda_1 B_n - \lambda_2 C_n) \right] \\ - \bar{D}_{12}\beta_n^2 (\lambda_2 B_n + \lambda_1 C_n) &= 0 \end{aligned}$$

The remaining two relations are provided by Eqs. (7.2.41b,c).

- 7.2** Repeat Problem 7.1 for the case of plates with hydrostatic loading of the type $q = q_0(x/a)$.
- 7.3** Determine a one-parameter Ritz solution of an isotropic rectangular plate with all edges clamped and subjected to uniformly distributed transverse load q_0 . Use the approximation

$$W(x, y) = c_{11} \left(1 - \cos \frac{2\pi x}{a} \right) \left(1 - \cos \frac{2\pi y}{b} \right) \quad (1)$$

Determine the maximum deflection of a square plate. *Ans:*

$$c_{11} = \frac{q_0 a^4}{4\pi^4 D} \left(\frac{1}{3 + 2s^2 + 3s^4} \right), \quad s = \frac{a}{b}$$

The maximum deflection for $a = b$ is $w_{max} = 0.00128(q_0 a^4 / D)$.

- 7.4** Determine a one-parameter Ritz solution of an isotropic rectangular plate with all edges clamped and subjected to a central point load Q_0 using approximation in Eq. (1) of Problem 7.3 and find the maximum deflection of a square plate. *Ans:*

$$c_{11} = \frac{Q_0 a^4}{ab\pi^4 D} \left(\frac{1}{3 + 2s^2 + 3s^4} \right), \quad s = \frac{a}{b}$$

The maximum deflection for $a = b$ is $w_{max} = 0.00513(Q_0 a^2/D)$.

- 7.5** Determine a one-parameter Ritz solution of an isotropic rectangular plate with edges $x = 0, a$ clamped and edges $y = 0, b$ simply supported, and subjected to uniformly distributed transverse load q_0 . Use the approximation

$$W(x, y) = c_{11} \left(1 - \cos \frac{2\pi x}{a} \right) \sin \frac{\pi y}{b} \quad (1)$$

to determine the maximum deflection of a square plate. *Ans:*

$$c_{11} = \frac{8q_0 a^4}{\pi^5 D} \left(\frac{1}{16 + 8s^2 + 3s^4} \right), \quad s = \frac{a}{b}$$

The maximum deflection for $a = b$ is $w_{max} = 0.00194(q_0 a^4/D)$.

- 7.6** Determine a one-parameter Ritz solution of an isotropic rectangular plate with edges $x = 0, a$ clamped and edges $y = 0, b$ simply supported, and subjected to a center point load Q_0 transverse load. Use the approximation in Eq. (1) of Problem 7.5. Determine the maximum deflection of a square plate. *Ans:*

$$c_{11} = \frac{8Q_0 a^3}{b\pi^4 D} \left(\frac{1}{16 + 8s^2 + 3s^4} \right), \quad s = \frac{a}{b}$$

The maximum deflection for $a = b$ is $w_{max} = 0.00610(Q_0 a^2/D)$.

- 7.7** Give the functions X_i and Y_j of Eq. (7.3.28) for a rectangular plate with edges $x = 0, a$ and $y = 0$ clamped and edge $y = b$ simply supported.
- 7.8** Give the functions X_i and Y_j of Eq. (7.3.28) for a rectangular plate with edge $x = 0$ clamped and the remaining edges free.
- 7.9** Give the functions X_i and Y_j of Eq. (7.3.28) for a rectangular plate with edges $x = 0, a$ and $y = 0$ clamped and edge $y = b$ free.
- 7.10** Give the functions X_i and Y_j of Eq. (7.3.28) for a rectangular plate with edges $x = 0$ and $y = 0$ clamped and edges $x = a$ and $y = b$ free.

Problems on Nonrectangular Plates

- 7.11** Consider an equilateral triangular plate (Figure P7.11). Suppose that all edges are simply supported. The equations of the edges, with respect to the coordinate system shown, are

$$\begin{aligned} \frac{x}{a} + \frac{1}{3} &= 0 \quad \text{on BC} \\ \frac{1}{\sqrt{3}} \frac{x}{a} + \frac{y}{a} - \frac{2}{3\sqrt{3}} &= 0 \quad \text{on AC} \\ \frac{1}{\sqrt{3}} \frac{x}{a} - \frac{y}{a} - \frac{2}{3\sqrt{3}} &= 0 \quad \text{on AB} \end{aligned}$$

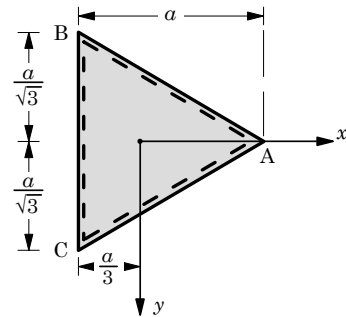


Figure P7.11

Use a one-parameter Ritz approximation of the form

$$\begin{aligned} w_0(x, y) &= c_1 \left(\frac{x}{a} + \frac{1}{3} \right) \left(\frac{1}{\sqrt{3}} \frac{x}{a} + \frac{y}{a} - \frac{2}{3\sqrt{3}} \right) \left(\frac{1}{\sqrt{3}} \frac{x}{a} - \frac{y}{a} - \frac{2}{3\sqrt{3}} \right) \\ &= d_1 \left[\frac{4}{27} - \left(\frac{x}{a} \right)^2 - \left(\frac{y}{a} \right)^2 - 3 \left(\frac{x}{a} \right) \left(\frac{y}{a} \right)^2 + \left(\frac{x}{a} \right)^3 \right] \\ &\equiv d_1 \varphi_1(x, y) \end{aligned}$$

and determine $d_1 = c_1/3$ when the plate is subjected to uniformly distributed transverse load q_0 . The exact deflection of an isotropic plate is given by (can be verified by substitution into the governing equation)

$$\begin{aligned} w_0(x, y) &= \frac{q_0 a^4}{64D} \left[\frac{4}{27} - \left(\frac{x}{a} \right)^2 - \left(\frac{y}{a} \right)^2 - 3 \left(\frac{x}{a} \right) \left(\frac{y}{a} \right)^2 + \left(\frac{x}{a} \right)^3 \right] \\ &\quad \times \left[\frac{4}{9} - \left(\frac{x}{a} \right)^2 - \left(\frac{y}{a} \right)^2 \right] \end{aligned}$$

The exact maximum deflection for an isotropic plate is $w_{max} = w_0(0, 0) = (q_0 a^4 / 972D)$.

- 7.12** Consider the equilateral triangular plate of Figure P7.11. Suppose that all edges are simply supported and loaded by a uniform moment $\hat{M}_{nn} = M_0$ along its edges. Use a one-parameter Ritz solution of Problem 7.11 and determine F_1 (R_{11} is known from Problem 7.11). Show that

$$w_0(x, y) = \frac{M_0 a^2}{4D} \left[\frac{4}{27} - \left(\frac{x}{a} \right)^2 - \left(\frac{y}{a} \right)^2 - 3 \left(\frac{x}{a} \right) \left(\frac{y}{a} \right)^2 + \left(\frac{x}{a} \right)^3 \right]$$

which is the exact deflection.

Hint: Evaluate the line integral

$$F_1 = \oint_{\Gamma} M_0 \left(n_x \frac{\partial \varphi_1}{\partial x} + n_y \frac{\partial \varphi_1}{\partial y} \right) ds$$

where Γ denotes the boundary of the triangle and (n_x, n_y) are the direction cosines of the line segment.

- 7.13** Determine the deflection surface $w_0(x, y)$ of the simply supported triangular plate of Figure P7.11 using a one-parameter Ritz approximation in Eq. (a) of Problem 7.11 when the plate is loaded by a point load Q_0 at the centroid $(x, y) = (0, 0)$. Assume that the plate is made of an isotropic material. *Ans:* $d_1 = (Q_0 a^2 / 36\sqrt{3}D)$.

- 7.14** Consider an isotropic elliptic plate with major and minor axes $2a$ and $2b$, respectively. Obtain a one-parameter Galerkin solution for the case in which the plate is clamped and subjected to uniformly distributed load q_0 .

Hint: Take

$$\varphi_1(x, y) = \left(1 - \frac{x^2}{a^2} - \frac{y^2}{b^2}\right)^2$$

which satisfies the geometric boundary conditions

$$w_0 = \frac{\partial w_0}{\partial x} = \frac{\partial w_0}{\partial y} = 0$$

Ans: The Galerkin solution, which coincides with the exact solution, is given by

$$w_0(x, y) = \frac{q_0 a^4}{8D(3s^4 + 2s^2 + 3)} \left(1 - \frac{x^2}{a^2} - \frac{y^2}{b^2}\right)^2$$

where $s = a/b$. When $a = b$, the solution reduces to that of a circular plate.

- 7.15** Repeat Problem 7.14 for the case in which the plate is subjected to distributed load $q = q_0(x/a)$. *Ans:* The solution is

$$w_0(x, y) = \frac{q_0 a^4 x}{24D(s^4 + 2s^2 + 5)} \left(1 - \frac{x^2}{a^2} - \frac{y^2}{b^2}\right)^2$$

- 7.16** Determine a one-parameter Ritz solution of a simply supported, isotropic elliptic plate under uniformly distributed load.

Hint: Use

$$\varphi_1(x, y) = \left(1 - \frac{x^2}{a^2} - \frac{y^2}{b^2}\right)$$

which satisfies the geometric boundary condition $w_0 = 0$. *Ans:* The Ritz solution, which *does not* coincide with the exact solution, is given by ($s = a/b$)

$$w_0(x, y) = \frac{q_0 a^4}{8D(1 + 2\nu s^2 + s^4)} \left(1 - \frac{x^2}{a^2} - \frac{y^2}{b^2}\right)$$

- 7.17** *Solution by State-Space Approach.* An alternative method of solving Eq. (7.2.4) is provided by the state-space approach [see Brogan (1985), Franklin (1968), and Gopal (1984)]. The approach involves writing a p th-order ordinary differential equation as a set of p first-order equations in matrix form, and then its solution is obtained in terms of the eigenvalues of the matrix operator. In the present case, Eq. (7.2.4) is a fourth-order equation with constant coefficients that can be expressed in terms of four first-order equations. Let

$$Z_1 = W_n, \quad Z_2 = Z'_1 = W'_n, \quad Z_3 = Z'_2 = W''_n, \quad Z_4 = Z'_3 = W'''_n$$

Then, we have

$$Z'_1 = Z_2, \quad Z'_2 = Z_3, \quad Z'_3 = Z_4, \quad Z'_4 = C_1 Z_1 + C_2 Z_3 + \hat{q}_n$$

or in matrix form

$$\{Z'\} = [T]\{Z\} + \{F\}$$

where

$$\{Z\} = \begin{Bmatrix} W_n \\ W'_n \\ W''_n \\ W'''_n \\ W_n \end{Bmatrix}, \quad [T] = \begin{bmatrix} 0 & 1 & 0 & 0 \\ 0 & 0 & 1 & 0 \\ 0 & 0 & 0 & 1 \\ C_1 & 0 & C_2 & 0 \end{bmatrix}, \quad \{F\} = \begin{Bmatrix} 0 \\ 0 \\ 0 \\ \hat{q}_n \end{Bmatrix}$$

$$C_1 = -\frac{1}{D_{11}} (D_{22}\beta_n^4 + k), \quad C_2 = 2\frac{\hat{D}_{12}}{D_{11}}\beta_n^2, \quad \hat{q}_n = \frac{\bar{q}_n}{D_{11}}$$

The general solution of $\{Z'\} = [T]\{Z\} + \{F\}$ is given by

$$\mathbf{Z}(x) = e^{\mathbf{T}x} \left(\mathbf{K} + \int^x e^{-\mathbf{T}\xi} \mathbf{F}(\xi) d\xi \right) \equiv \mathbf{G}(x)\mathbf{K} + \mathbf{H}(x)$$

Here, $e^{\mathbf{T}x}$ denotes the matrix product

$$e^{\mathbf{T}x} = [E] \begin{bmatrix} e^{\lambda_1 x} & & 0 \\ & \ddots & \\ 0 & & e^{\lambda_4 x} \end{bmatrix} [E]^{-1}$$

Here, $[E]$ is the matrix of distinct eigenvectors of matrix $[T]$, $[E]^{-1}$ denotes its inverse, λ_j ($j = 1, 2, 3, 4$) are the eigenvalues associated with matrix $[T]$, and $\{K\}$ is a vector of constants to be determined using the boundary conditions of the problem.

Consider an orthotropic, simply supported, rectangular plate ($k = 0$) subjected to uniformly distributed load of intensity q_0 . The simply supported boundary conditions at $x = 0, a$ imply

$$W_n = 0, \quad -D_{11}W_n'' + D_{12}\beta_n^2 W_n = 0$$

Show that these four conditions yield the following four algebraic equations among K_i ($i = 1, 2, 3, 4$):

$$\begin{aligned} \sum_{j=1}^4 G_{1j}(0)K_j + H_1(0) &= 0, \quad \sum_{j=1}^4 G_{1j}(a)K_j + H_1(a) = 0 \\ \sum_{j=1}^4 \left(D_{11}G_{3j}(0) - \beta^2 D_{12}G_{1j}(0) \right) K_j + D_{11}H_3(0) - D_{12}\beta^2 H_1(0) &= 0 \\ \sum_{j=1}^4 \left(D_{11}G_{3j}(a) - \beta^2 D_{12}G_{1j}(a) \right) K_j + D_{11}H_3(a) - D_{12}\beta^2 H_1(a) &= 0 \end{aligned}$$

General Buckling of Rectangular Plates

8.1 Buckling of Simply Supported Plates under Compressive Loads

8.1.1 Governing Equations

When a plate is subjected to uniform compressive forces applied in the middle plane of the plate, and if the forces are sufficiently small, the force-displacement response is linear. The linear relationship holds until a certain load is reached. At that load, called the *buckling load*, the stable state of the plate is disturbed and the plate seeks an alternative equilibrium configuration accompanied by a change in the load-deflection behavior. The phenomenon of changing the equilibrium configuration at the same load and without drastic changes in deformation is termed *bifurcation*. The load-deflection curve for buckled plates is often bilinear. The magnitude of the buckling load depends, as will be shown shortly, on geometry, material properties, and the buckling mode shape, i.e., geometric configuration of the plate at buckling.

In the present study, we assume that the only applied loads are the uniform inplane forces and that all other mechanical and thermal loads are zero. Since the prebuckling deformation w_0 is that of an equilibrium configuration, it satisfies the equilibrium equations, and the equation governing buckling deflection w is given by

$$D_{11} \frac{\partial^4 w}{\partial x^4} + 2\hat{D}_{12} \frac{\partial^4 w}{\partial x^2 \partial y^2} + D_{22} \frac{\partial^4 w}{\partial y^4} + kw = \hat{N}_{xx} \frac{\partial^2 w}{\partial x^2} + \hat{N}_{yy} \frac{\partial^2 w}{\partial y^2} \quad (8.1.1)$$

where $\hat{D}_{12} = D_{12} + 2D_{66}$, and $\hat{N}_{xx} < 0$ and $\hat{N}_{yy} < 0$ for compressive forces. Here we wish to determine a nonzero deflection w that satisfies Eq. (8.1.1) when the inplane forces are (Figure 8.1.1)

$$\hat{N}_{xx} = -N_0, \quad \hat{N}_{yy} = -\gamma N_0, \quad \gamma = \frac{\hat{N}_{yy}}{\hat{N}_{xx}} \quad (8.1.2)$$

and the edges are simply supported.

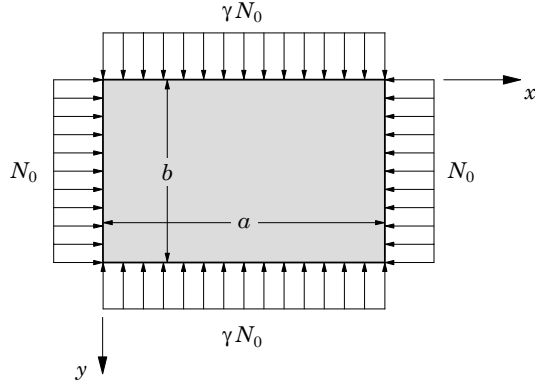


Figure 8.1.1. Rectangular plate subjected to biaxial inplane compression ($\hat{N}_{xx} = -N_0$ and $\hat{N}_{yy} = \gamma N_0$).

8.1.2 The Navier Solution

As in the case of bending, we select an expansion for w that satisfies the boundary conditions on edges $x = 0, a$ and $y = 0, b$

$$w(0, y) = 0, \quad w(a, y) = 0, \quad w(x, 0) = 0, \quad w(x, b) = 0 \quad (8.1.3)$$

$$M_{xx}(0, y) = 0, \quad M_{xx}(a, y) = 0, \quad M_{yy}(x, 0) = 0, \quad M_{yy}(x, b) = 0 \quad (8.1.4)$$

We take

$$w(x, y) = W_{mn} \sin \alpha_m x \sin \beta_n y, \quad \alpha_m = \frac{m\pi}{a}, \quad \beta_n = \frac{n\pi}{b} \quad (8.1.5)$$

Substituting Eq. (8.1.5) into Eq. (8.1.1), we obtain, for any m and n , the relation

$$0 = \left\{ \left[D_{11}\alpha_m^4 + 2\hat{D}_{12}\alpha_m^2\beta_n^2 + D_{22}\beta_n^4 + k \right] - (\alpha_m^2 + \gamma\beta_n^2)N_0 \right\} \times W_{mn} \sin \alpha_m x \sin \beta_n y \quad (8.1.6)$$

for any pair of (m, n) . Since Eq. (8.1.6) must hold for every point (x, y) of the domain for nontrivial buckling mode $w(x, y)$ (i.e., $W_{mn} \neq 0$), the expression inside the braces is zero for every m and n . This yields

$$N_0(m, n) = \frac{\pi^2}{b^2} \left(\frac{D_{11}s^4m^4 + 2\hat{D}_{12}s^2m^2n^2 + D_{22}n^4 + \bar{k}}{s^2m^2 + \gamma n^2} \right) \quad (8.1.7)$$

where $s = b/a$ is the plate aspect ratio and k is the elastic foundation modulus

$$s = \frac{b}{a}, \quad \bar{k} = \frac{kb^4}{\pi^4} \quad (8.1.8)$$

Thus, for each choice of m and n there corresponds a unique value of N_0 . The *critical buckling load* is the smallest of $N_0(m, n)$. For a given plate, this value is dictated by a particular combination of the values of m and n , value of γ , plate geometry, and material properties. It is difficult to determine the critical buckling load for an arbitrary plate. Next, we investigate critical buckling loads of rectangular plates with various combination of inplane loads.

8.1.3 Biaxial Compression of a Plate

For a square orthotropic plate subjected to the same magnitude of uniform compressive forces N_{xx} and N_{yy} on both edges (i.e., biaxial compression with $\gamma = 1$; see Figure 8.1.1), Eq. (8.1.7) yields

$$N_0(m, n) = \frac{\pi^2}{a^2} \left(\frac{m^4 D_{11} + 2m^2 n^2 \hat{D}_{12} + n^4 D_{22} + \bar{k}}{m^2 + n^2} \right) \quad (8.1.9)$$

where $\bar{k} = ka^4/\pi^4$. Now suppose that $D_{11} > D_{22}$. Then, $D_{11}m^2$ increases more rapidly than the decrease in D_{22}/m^2 with an increase in m . Thus, the minimum of N_0 occurs when $m = 1$:

$$N_0(1, n) = \left(\frac{\pi^2}{a^2} \right) \left(\frac{D_{11} + 2\hat{D}_{12}n^2 + D_{22}n^4 + \bar{k}}{1 + n^2} \right) \quad (8.1.10)$$

The buckling load is a minimum when n is the nearest positive integer to the real number R

$$R^2 = \left(1 + \frac{D_{11} - 2\hat{D}_{12} + k}{D_{22}} \right)^{\frac{1}{2}} - 1 \quad (8.1.11)$$

For example, for modulus ratios of $D_{11}/D_{22} = 10$ and $\hat{D}_{12}/D_{22} = 1$ and $k = 0$, the minimum buckling load occurs at $n = 1$ (because $R = \sqrt{2}$) and it is given by

$$N_{cr} \equiv N_0(1, 1) = 6.5 \left(\frac{\pi^2 D_{22}}{a^2} \right) \quad (8.1.12)$$

For modulus ratios $12 \leq D_{11}/D_{22} \leq 26$ and $\hat{D}_{12}/D_{22} = 1$ and $k = 0$, the value of R is $1.52 \leq R \leq 2$. Hence, the minimum buckling load occurs for $n = 2$. In particular, for $D_{11}/D_{22} = 12$, we have

$$N_{cr} = 7.2 \left(\frac{\pi^2 D_{22}}{a^2} \right) \quad (8.1.13a)$$

and the mode shape is given by

$$W_{12} = \sin \frac{\pi x}{a} \sin \frac{2\pi y}{a} \quad (8.1.13b)$$

For a rectangular isotropic [$D_{11} = D_{22} = D$, $D_{12} = \nu D$, $2D_{66} = (1 - \nu)D$ or $\hat{D}_{12} = D$] plate under biaxial compression, the buckling load can be calculated using Eq. (8.1.7):

$$N_0(m, n) = \frac{\pi^2 D}{b^2} \left(m^2 s^2 + n^2 + \frac{\hat{k}}{m^2 s^2 + n^2} \right), \quad \hat{k} = \frac{k b^4}{D \pi^4} \quad (8.1.14)$$

where s is the plate aspect ratio $s = b/a$. Clearly, the critical buckling load for the case in which $k = 0$ occurs at $m = n = 1$ and it is equal to

$$N_{cr} = (1 + s^2) \frac{\pi^2 D}{b^2}, \quad s = \frac{b}{a} \quad (8.1.15a)$$

and for a square plate ($s = 1$) it reduces to

$$N_{cr} = \frac{2\pi^2 D}{b^2} \quad (8.1.15b)$$

When $k \neq 0$, N_0 is not a minimum for any finite values of m and n .

8.1.4 Biaxial Loading of a Plate

When the edges $x = 0$ and $x = a$ of a square plate are subjected to compressive load $\hat{N}_{xx} = -N_0$ and the edges $y = 0$ and $y = b$ are subjected to tensile load $\hat{N}_{yy} = \gamma N_0$ (Figure 8.1.2), Eq. (8.1.7) becomes

$$N_0(m, n) = \frac{\pi^2}{a^2} \left(\frac{m^4 D_{11} + 2m^2 n^2 \hat{D}_{12} + n^4 D_{22} + \frac{ka^4}{\pi^4}}{m^2 - \gamma n^2} \right) \quad (8.1.16)$$

when $\gamma n^2 < m^2$. For example, when $\gamma = 0.5$ and $k = 0$, the minimum buckling load occurs at $m = 1$ and $n = 1$:

$$N_0(1, 1) = \frac{2\pi^2}{a^2} (D_{11} + 2\hat{D}_{12} + D_{22}) \quad (8.1.17)$$

If $D_{11}/D_{22} = 10$ and $\hat{D}_{12}/D_{22} = 1$, then the critical buckling load becomes

$$N_{cr} = \frac{26\pi^2 D_{22}}{a^2} \quad (8.1.18)$$

For a rectangular isotropic plate (when $k = 0$), the buckling load under biaxial loading ($N_{xx} = -N_0$ and $N_{yy} = \gamma N_0$) becomes

$$N_0(m, n) = \left(\frac{\pi^2 D}{b^2} \right) \frac{(m^2 s^2 + n^2)^2}{m^2 s^2 - \gamma n^2} \quad (8.1.19)$$

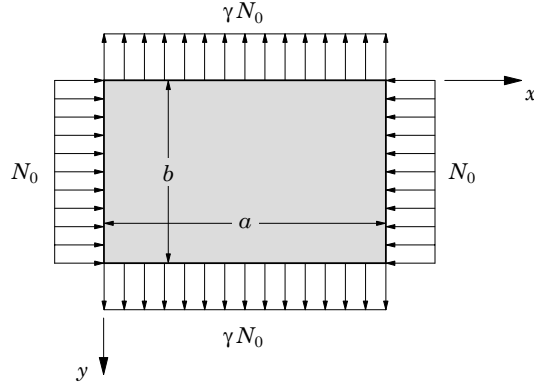


Figure 8.1.2. Plate subjected to uniform compression along x ($\hat{N}_{xx} = -N_0$) and uniform tension along y ($\hat{N}_{yy} = \gamma N_0$).

and the minimum buckling load occurs for $n = 1$

$$N_0(m, 1) = \left(\frac{\pi^2 D}{b^2} \right) \frac{(m^2 s^2 + 1)^2}{m^2 s^2 - \gamma} \quad (8.1.20)$$

In theory, the minimum of $N_0(m, 1)$ occurs when $m^2 s^2 = 1 + 2\gamma$. For a square plate with $\gamma = 0.5$, we find

$$N_0(1, 1) = \frac{8\pi^2 D}{a^2}, \quad N_0(2, 1) = 7.1429 \frac{\pi^2 D}{a^2} = N_{cr}$$

8.1.5 Uniaxial Compression of a Rectangular Plate

When a rectangular plate with $k = 0$ is subjected to uniform compressive load N_0 on edges $x = 0$ and $x = a$, i.e., when $\gamma = 0$, the buckling load can be calculated using Eq. (8.1.7)

$$N_0(m, n) = \frac{\pi^2}{m^2 s^2 b^2} \left(m^4 s^4 D_{11} + 2s^2 m^2 n^2 \hat{D}_{12} + n^4 D_{22} \right) \quad (8.1.21)$$

An examination of the expression in Eq. (8.1.21) shows that the smallest value of N_0 for any m occurs for $n = 1$:

$$N_0(m, 1) = \frac{\pi^2 D_{22}}{b^2} \left(m^2 s^2 \frac{D_{11}}{D_{22}} + 2 \frac{\hat{D}_{12}}{D_{22}} + \frac{1}{m^2 s^2} \right) \quad (8.1.22)$$

Thus, the plate buckles in such a way that there can be several ($m \geq 1$) half-waves in the direction of compression, but only one ($n = 1$) half-wave in the perpendicular direction. The critical buckling load is then determined by finding the minimum of $N_0 = N_0(m)$ in Eq. (8.1.22) with respect to m . We have

$$\frac{dN_0}{dm} = 0 \quad \text{gives} \quad m_c^4 = \frac{1}{s^4} \frac{D_{22}}{D_{11}}, \quad s = \frac{b}{a} \quad (8.1.23)$$

The second derivative of N_0 with respect to m can be shown to be positive. Since the value of m from Eq. (8.1.23) is not always an integer, the minimum buckling load cannot be predicted by substituting the value of m_c from Eq. (8.1.23) for m into Eq. (8.1.22). The minimum value of N_0 is given by Eq. (8.1.22) when m_c is the nearest integer value given by Eq. (8.1.23). Since the value of m_c depends on the ratio of the principal bending stiffnesses D_{11} and D_{22} as well as plate aspect ratio $s = b/a$, we must investigate the variation of N_0 with aspect ratio s for different values of m_c for a given rectangular plate.

For instance, consider a plate with $D_{11}/D_{22} = 10$ and $a/b = 1.778$. Then, we have

$$N_0(m, 1) = \frac{\pi^2 D_{22}}{b^2} \left(10m^2 s^2 + 2 + \frac{1}{s^2 m^2} \right) \quad (8.1.24a)$$

$$m_c^4 = \frac{D_{22}}{D_{11}} \left(\frac{a}{b} \right)^4 = 0.1 \times (1.778)^4 = 0.9994 \approx 1 \quad (8.1.24b)$$

In fact, for $(a/b) < 2.66$, we have

$$m_c^4 = \frac{D_{22}}{D_{11}} \left(\frac{a}{b} \right)^4 = 0.1 \times (2.66)^4 \quad \text{or} \quad m_c = 1.496 \quad (8.1.25)$$

Thus, the closest integer is $m = 1$. The critical buckling load of a laminate with

$$\frac{D_{11}}{D_{22}} = 10, \quad (D_{12} + 2D_{66}) = D_{22}, \quad \frac{a}{b} < 2.66 \quad (8.1.26)$$

is given by

$$N_{cr} \equiv N_0(1, 1) = \frac{\pi^2 D_{22}}{s^2 b^2} \left(10s^4 + 2s^2 + 1 \right) \quad (8.1.27)$$

For various aspect ratios, we have

$$\frac{a}{b} = 1 : \quad N_{cr} = 13 \frac{\pi^2 D_{22}}{b^2}; \quad \frac{a}{b} = 1.5 : \quad N_{cr} = 8.69 \frac{\pi^2 D_{22}}{b^2}$$

$$\frac{a}{b} = 2 : \quad N_{cr} = 8.5 \frac{\pi^2 D_{22}}{b^2}; \quad \frac{a}{b} = 2.5 : \quad N_{cr} = 9.85 \frac{\pi^2 D_{22}}{b^2}$$

and the buckling mode is

$$W_{11} = \sin \frac{\pi x}{a} \sin \frac{\pi y}{a}$$

It can be shown that if the plate aspect ratio a/b is greater than 2.66, but less than 4.44, the buckling load is the minimum for $n = 1$ and $m = 2$. For example, for $a/b = 3$, Eq. (8.1.24a) yields

$$\begin{aligned}N_0(1,1) &= \frac{109}{9} \frac{\pi^2 D_{22}}{b^2} \approx 12.11 \frac{\pi^2 D_{22}}{b^2} \\N_0(2,1) &= \frac{313}{36} \frac{\pi^2 D_{22}}{b^2} \approx 8.69 \frac{\pi^2 D_{22}}{b^2} = N_{cr} \\N_0(3,1) &= 13 \frac{\pi^2 D_{22}}{b^2}\end{aligned}$$

Thus, for aspect ratios between 2.66 and 4.44, the plate buckles into two half-waves in the x -direction and one half-wave in the y -direction. The larger aspect ratios lead to higher modes of buckling. Figure 8.1.3 contains a plot of the nondimensional buckling load $\bar{N} = N_0 b^2 / (\pi^2 D_{22})$ versus plate aspect ratio a/b for laminates whose material properties are $D_{11}/D_{22} = 10$ and $\hat{D}_{12}/D_{22} = 1$. For aspect ratios less than 2.5, the plate buckles into a single half-wave in the x -direction. As the aspect ratio increases, the plate buckles into more and more half-waves in the x -direction. Note that intersections of two consecutive modes correspond to certain aspect ratios (Figure 8.1.4). Thus, for each of these aspect ratios, there are two possible buckled mode shapes. The \bar{N} versus a/b curve gets flatter with the increasing aspect ratio, and it approaches the value

$$N_{cr} = \frac{2\pi^2 D_{22}}{b^2} \left(\sqrt{\frac{D_{11}}{D_{22}}} + \frac{\hat{D}_{12}}{D_{22}} \right) \quad (8.1.28)$$

which is obtained from Eq. (8.1.22) after substituting for $m^2 = m_c^2$ from Eq. (8.1.23). For the data in Eq. (8.1.26), this limiting value of the critical buckling load is

$$N_{cr} = 8.325 \left(\frac{\pi^2 D_{22}}{b^2} \right) \quad (8.1.29)$$

For an isotropic plate, Eqs. (8.1.21) and (8.1.22) reduce to

$$N_0(m, n) = \frac{\pi^2 a^2 D}{m^2} \left(\frac{m^2}{a^2} + \frac{n^2}{b^2} \right)^2 \quad (8.1.30)$$

$$N_0(m, 1) = \frac{\pi^2 D}{a^2} \left(m + \frac{1}{m} \frac{a^2}{b^2} \right)^2 \quad (8.1.31)$$

For a given aspect ratio, two different modes, m_1 and m_2 , will have the same buckling load when $\sqrt{m_1 m_2} = a/b$. In particular, the point of intersection of curves m and $m+1$ occurs for aspect ratios

$$\frac{a}{b} = \sqrt{2}, \sqrt{6}, \sqrt{12}, \sqrt{20}, \dots, \sqrt{m^2 + m}$$

Thus, there is a mode change at these aspect ratios from m half-waves to $m+1$ half-waves. Putting $m=1$ in Eq. (8.1.31), we find

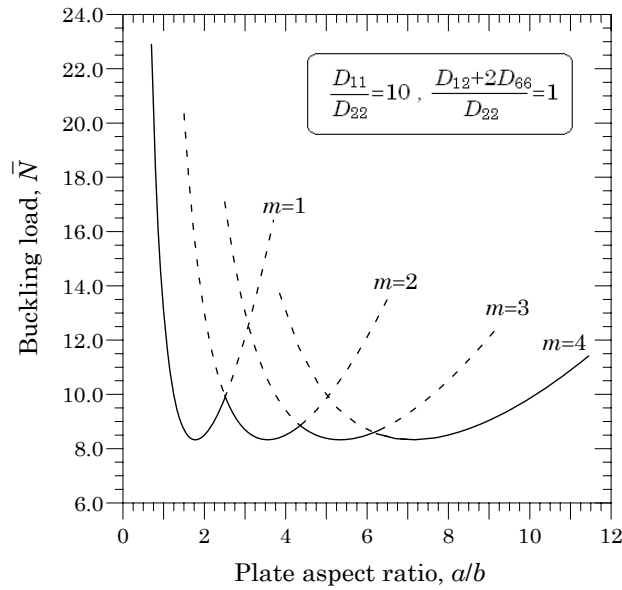


Figure 8.1.3. Nondimensional buckling load $\bar{N} = N_0 b^2 / (\pi^2 D_{22})$ versus plate aspect ratio a/b .

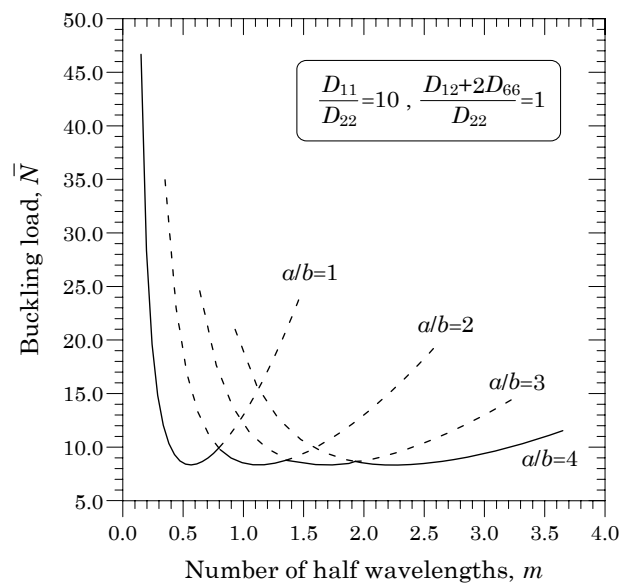


Figure 8.1.4. Nondimensional buckling load \bar{N} versus number of half wavelengths m in the x -direction.

$$N_{cr} = \frac{\pi^2 D}{b^2} \left(\frac{a}{b} + \frac{b}{a} \right)^2 \quad (8.1.32)$$

For a square plate Eq. (8.1.32) yields

$$N_{cr} = \frac{4\pi^2 D}{b^2} \quad (8.1.33)$$

The critical value of the compressive stress is given by $\sigma_{cr} = N_{cr}/h$, where h is the thickness of the plate.

The results presented in Table 8.1.1 show the effect of plate aspect ratio and modulus ratio (orthotropy) on the critical buckling loads $\bar{N} = N_{cr}b^2/(\pi^2 D_{22})$ of rectangular isotropic ($\nu = 0.3$) and orthotropic ($G_{12} = 0.5E_2$, $\nu_{12} = 0.25$) plates under uniform axial compression ($\gamma = 0$) and biaxial compression ($\gamma = 1$). In all cases, the critical buckling mode is $(m, n) = (1, 1)$, except as indicated. The nondimensional buckling load increases as the modulus ratio increases. The effect of aspect ratio and mode on critical buckling loads \bar{N} of simply supported (SSSS) isotropic and orthotropic plates are shown in Figure 8.1.5 and Figure 8.1.6, respectively.

All of the discussion presented in this section was for simply supported rectangular plates under various types of inplane loads. In the next section, we consider rectangular plates with two parallel edges simply supported while the remaining two edges having various combinations (e.g., free, clamped, simply supported) boundary conditions.

Table 8.1.1. Effect of plate aspect ratio and modulus ratio on the nondimensional buckling loads \bar{N} of simply supported (SSSS) rectangular plates under uniform axial compression ($\gamma = 0$) and biaxial compression ($\gamma = 1$).

γ	$\frac{a}{b}$	$\frac{E_1}{E_2} = 1$	$\frac{E_1}{E_2} = 3$	$\frac{E_1}{E_2} = 10$	$\frac{E_1}{E_2} = 25$
0	0.5	6.250	14.708	42.737	102.750
	1.0	4.000	6.458	13.488	28.495
	1.5	4.340 ^{(2,1)†}	6.042	9.182	15.856
	2.0	4.000 ^(2,1)	6.458 ^(2,1)	8.987	12.745
	2.5	4.134 ^(3,1)	5.941 ^(2,1)	10.338	12.745
	3.0	4.000 ^(3,1)	6.042 ^(2,1)	9.182 ^(2,1)	14.273
1	0.5	5.000	11.767	25.427 ^(1,3)	40.784 ^(1,4)
	1.0	2.000	3.229	6.744	10.196 ^(1,2)
	1.5	1.444	1.859	2.825	4.879
	2.0	1.250	1.442	1.798	2.549
	2.5	1.160	1.267	1.426	1.758
	3.0	1.111	1.179	1.260	1.427

† Denotes mode numbers (m, n) at which the critical buckling load occurred; $(m, n) = (1, 1)$ for all other cases.

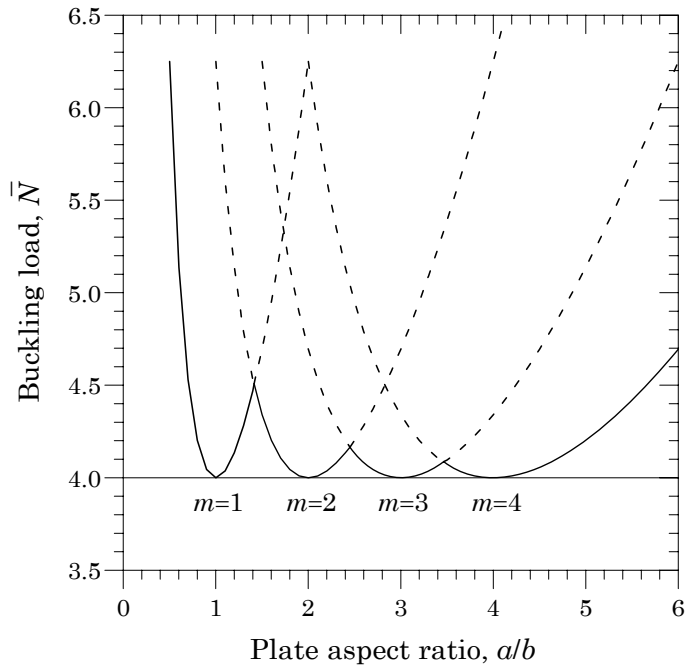


Figure 8.1.5. Nondimensional buckling load, $\bar{N} = N_0 b^2 / (\pi^2 D_{22})$, versus plate aspect ratio a/b for isotropic SSSS plates.

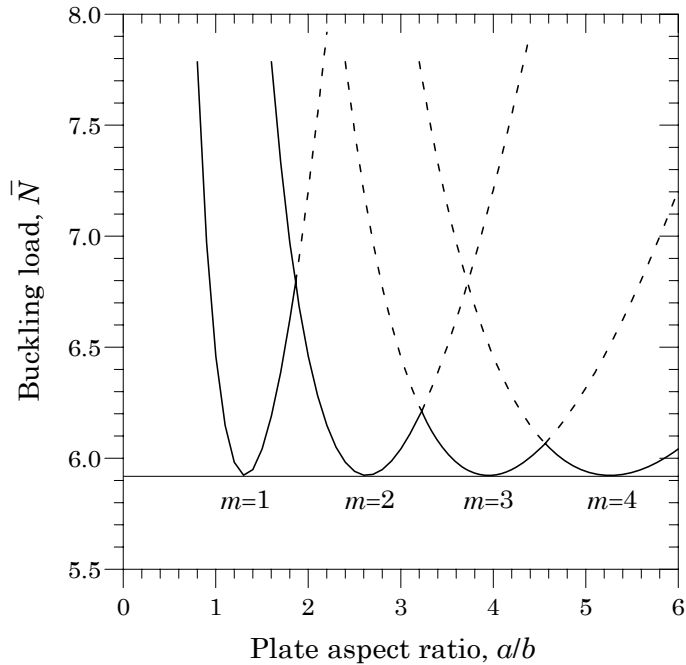


Figure 8.1.6 Nondimensionalized buckling load, $\bar{N} = N_0 b^2 / (\pi^2 D_{22})$, versus plate aspect ratio a/b for orthotropic SSSS plates.

8.2 Buckling of Plates Simply Supported along Two Opposite Sides and Compressed in the Direction Perpendicular to Those Sides

8.2.1 The Lévy Solution

Here we consider buckling of uniformly compressed rectangular plates simply supported along two opposite edges perpendicular to the direction of compression (Figure 8.2.1) and having various edge conditions along the other two sides. We use the Lévy method of solution to reduce the governing partial differential equation (8.1.1) to an ordinary differential equation in y .

For the case of uniform compression along the x -axis, we have $\hat{N}_{xx} = -N_0$ and $\hat{N}_{yy} = 0$, and Eq. (8.1.1) reduces to ($k = 0$)

$$D_{11} \frac{\partial^4 w}{\partial x^4} + 2\hat{D}_{12} \frac{\partial^4 w}{\partial x^2 \partial y^2} + D_{22} \frac{\partial^4 w}{\partial y^4} = -N_0 \frac{\partial^2 w}{\partial x^2} \quad (8.2.1)$$

where $\hat{D}_{12} = D_{12} + 2D_{66}$. This equation must be solved for the buckling load N_0 and mode shape w for any given boundary conditions.

We assume solution of Eq. (8.2.1) in the form

$$w(x, y) = W(y) \sin \frac{m\pi x}{a} \quad (8.2.2)$$

i.e., under the action of compressive forces the plate buckles into m sinusoidal half-waves. The function $W(y)$, which is to be determined later, represents the buckling shape along the y -axis. The assumed solution in Eq. (8.2.2) satisfies the following boundary conditions along the simply supported edges $x = 0, a$ of the plate:

$$w = 0, \quad M_{xx} \equiv - \left(D_{11} \frac{\partial^2 w}{\partial x^2} + D_{12} \frac{\partial^2 w}{\partial y^2} \right) = 0 \quad \text{at } x = 0, a \quad (8.2.3)$$

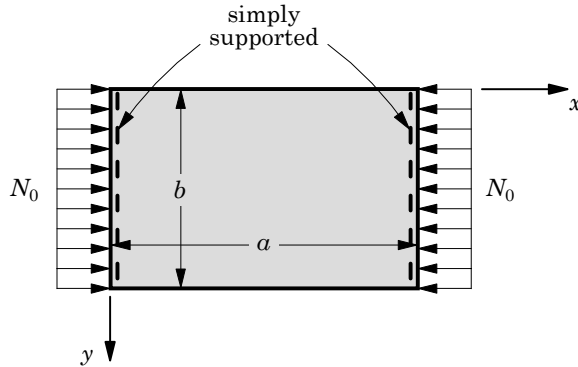


Figure 8.2.1. Uniformly compressed rectangular plates simply supported along two opposite sides ($x = 0, a$) perpendicular to the direction of compression and having various boundary conditions along the other two sides ($y = 0, b$).

Substituting Eq. (8.2.2) into Eq. (8.2.1), we obtain

$$\left(D_{11}\alpha_m^4 - N_0\alpha_m^2 \right) W - 2\alpha_m^2 \hat{D}_{12} \frac{d^2W}{dy^2} + D_{22} \frac{d^4W}{dy^4} = 0 \quad (8.2.4)$$

The form of the solution to Eq. (8.2.4) depends on the nature of the roots λ of the equation

$$D_{22}\lambda^4 - 2\alpha_m^2 \hat{D}_{12}\lambda^2 + \left(\alpha_m^4 D_{11} - \alpha_m^2 N_0 \right) = 0 \quad (8.2.5)$$

Due to the geometric constraints on the edges $y = 0, b$, the buckling load N_0 [see Eq. (8.1.22)] is such that

$$N_0 > \alpha_m^2 D_{11} \quad (8.2.6)$$

Hence, the solution to Eq. (8.2.4) is of the form

$$W(y) = A \cosh \lambda_1 y + B \sinh \lambda_1 y + C \cos \lambda_2 y + D \sin \lambda_2 y \quad (8.2.7)$$

where

$$(\lambda_1)^2 = \sqrt{\alpha_m^2 \frac{N_0}{D_{22}} - \alpha_m^4 \frac{D_{11}}{D_{22}} + \alpha_m^4 \left(\frac{\hat{D}_{12}}{D_{22}} \right)^2 + \frac{\hat{D}_{12}}{D_{22}} \alpha_m^2} \quad (8.2.8a)$$

$$(\lambda_2)^2 = \sqrt{\alpha_m^2 \frac{N_0}{D_{22}} - \alpha_m^4 \frac{D_{11}}{D_{22}} + \alpha_m^4 \left(\frac{\hat{D}_{12}}{D_{22}} \right)^2 - \frac{\hat{D}_{12}}{D_{22}} \alpha_m^2} \quad (8.2.8b)$$

For isotropic plates, Eqs. (8.2.8a,b) reduce to

$$(\lambda_1)^2 = \sqrt{\alpha_m^2 \frac{N_0}{D}} + \alpha_m^2, \quad (\lambda_2)^2 = \sqrt{\alpha_m^2 \frac{N_0}{D}} - \alpha_m^2 \quad (8.2.8c)$$

8.2.2 Buckling of SSSF Plates

Consider buckling of uniformly compressed rectangular plates with side $y = 0$ simply supported and side $y = b$ free (Figure 8.2.2). The boundary conditions on the simply supported and free edges are

$$w = 0, \quad M_{yy} = - \left(D_{12} \frac{\partial^2 w}{\partial x^2} + D_{22} \frac{\partial^2 w}{\partial y^2} \right) = 0 \quad \text{at } y = 0 \quad (8.2.9)$$

$$M_{yy} = 0, \quad V_y = - \left(D_{22} \frac{\partial^3 w}{\partial y^3} + \bar{D}_{12} \frac{\partial^3 w}{\partial x^2 \partial y} \right) = 0 \quad \text{at } y = b \quad (8.2.10)$$

where $\bar{D}_{12} = D_{12} + 4D_{66}$.

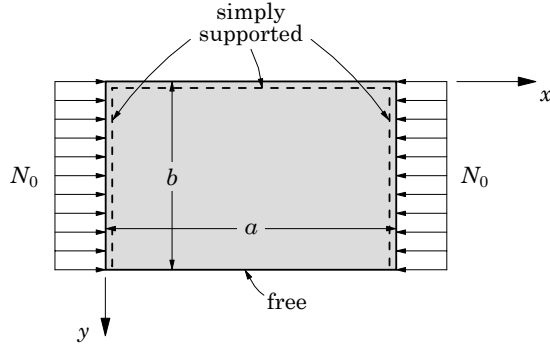


Figure 8.2.2. Uniformly compressed rectangular plate simply supported along two opposite sides ($x = 0, a$) perpendicular to the direction of compression, and simply supported on side $y = 0$ and free on side $y = b$ (SSSF).

Using the solution (8.2.7) in Eq. (8.2.9) yields $A = C = 0$, and using it in Eq. (8.2.10) yields the following two linear relations among B and D :

$$\begin{aligned} & \left(D_{12}\alpha_m^2 - D_{22}\lambda_1^2 \right) B \sinh \lambda_1 b + \left(D_{12}\alpha_m^2 + D_{22}\lambda_2^2 \right) D \sin \lambda_2 b = 0 \\ & \lambda_1 \left(\bar{D}_{12}\alpha_m^2 - D_{22}\lambda_1^2 \right) B \cosh \lambda_1 b + \lambda_2 \left(\bar{D}_{12}\alpha_m^2 + D_{22}\lambda_2^2 \right) D \cos \lambda_2 b = 0 \end{aligned} \quad (8.2.11)$$

One possible solution of these homogeneous equations is that $B = D = 0$. Then, the deflection at each point of the plate is zero, which is the flat form of equilibrium of the plate. The buckled form of equilibrium of the plate is possible only if equations in (8.2.11) yield nonzero values of B and D . This requires that the determinant of the two linear equations in (8.2.11) be zero. We obtain

$$\lambda_2 \Omega_1^2 \sinh \lambda_1 b \cos \lambda_2 b - \lambda_1 \Omega_2^2 \cosh \lambda_1 b \sin \lambda_2 b = 0 \quad (8.2.12)$$

where Ω_1 and Ω_2 are defined by

$$\Omega_1 = \left(\lambda_1^2 - \frac{D_{12}}{D_{22}} \alpha_m^2 \right), \quad \Omega_2 = \left(\lambda_2^2 + \frac{D_{12}}{D_{22}} \alpha_m^2 \right) \quad (8.2.13)$$

Since λ_1 and λ_2 contain N_0 [see Eqs. (8.2.8a–c)], Eq. (8.2.12) can be solved for the smallest N_0 once the geometric and material parameters of the plate are known. The critical buckling load may be written as

$$N_{cr} = \kappa \frac{\pi^2 D_{22}}{b^2} \quad (8.2.14)$$

where κ is a numerical factor depending on the plate aspect ratio b/a and material properties. The magnitude of the corresponding critical compressive stress is given by $(\sigma_{xx})_{cr} = N_{cr}/h$. The general mode shape is given by

$$w(x, y) = (\Omega_1 \sinh \lambda_1 b \sin \lambda_2 y + \Omega_2 \sinh \lambda_1 y \sin \lambda_2 b) \sin \alpha_m x \quad (8.2.15)$$

Table 8.2.1 contains buckling loads of isotropic ($\nu = 0.25$) and orthotropic ($G_{12} = 0.5E_2$, $\nu_{12} = 0.25$) plates (SSSF) for various values of a/b and modes $m = 1, 2$. The critical buckling load occurs in mode $m = 1$ for isotropic as well orthotropic plates with aspect ratio $0 < a/b \leq 6$. The mode shape associated with the critical buckling load is

$$w(x, y) = (\Omega_1 \sinh \lambda_1 b \sin \lambda_2 y + \Omega_2 \sinh \lambda_1 y \sin \lambda_2 b) \sin \frac{\pi x}{a}$$

Table 8.2.1. Effect of plate aspect ratio and modulus ratio on the nondimensional buckling loads $\bar{N} = N_0 b^2 / (\pi^2 D_{22})$ of rectangular plates (SSSF) under uniform compression $\hat{N}_{xx} = -N_0$.

$\frac{a}{b}$	$\frac{E_1}{E_2} = 1$		$\frac{E_1}{E_2} = 3$		$\frac{E_1}{E_2} = 10$	
	$m = 1$	$m = 2$	$m = 1$	$m = 2$	$m = 1$	$m = 2$
0.4	6.6367	25.2899	19.2688	75.4387	63.0270	250.448
0.6	3.1921	11.4675	8.8763	33.8266	28.3288	111.613
0.8	1.9894	6.3667	5.2425	19.2688	16.1880	63.027
1.0	1.4342	4.4036	3.5626	12.5334	10.5707	40.542
1.5	0.8880	2.2022	1.9075	5.8859	5.0268	18.338
2.0	0.6979	1.4342	1.3307	3.5626	3.0891	10.571
2.5	0.6104	1.0798	1.0648	2.4893	2.1932	6.977
3.0	0.5630	0.8879	0.9208	1.9075	1.7071	5.027
3.5	0.5345	0.7726	0.8341	1.5574	1.4142	3.851
4.0	0.5161	0.6979	0.7780	1.3307	1.2242	3.089
4.5	0.5034	0.6469	0.7396	1.1755	1.0939	2.567
5.0	0.4944	0.6104	0.7121	1.0648	1.0008	2.193
5.5	0.4877	0.5835	0.6918	0.9829	0.9319	1.917
6.0	0.4826	0.5630	0.6764	0.9208	0.8795	1.707

8.2.3 Buckling of SSCF Plates

Here we consider buckling of uniformly compressed rectangular plates with side $y = 0$ clamped and side $y = b$ free (Figure 8.2.3). The boundary conditions are

$$w = 0, \quad \frac{\partial w}{\partial y} = 0 \quad \text{at } y = 0 \quad (8.2.16)$$

$$M_{yy} = 0, \quad V_y = -D_{22} \frac{\partial^3 w}{\partial y^3} - \bar{D}_{12} \frac{\partial^3 w}{\partial x^2 \partial y} = 0 \quad \text{at } y = b \quad (8.2.17)$$

Substituting for w from Eq. (8.2.7) into the boundary conditions, we obtain $C = -A$, $D = -(\lambda_1/\lambda_2)B$, and

$$\begin{aligned} -\Omega_1 (A \cosh \lambda_1 b + B \sinh \lambda_1 b) + \Omega_2 (C \cos \lambda_2 b + D \sin \lambda_2 b) &= 0 \\ -\lambda_1 \Omega_1 (A \sinh \lambda_1 b + B \cosh \lambda_1 b) + \lambda_2 \Omega_2 (-C \sin \lambda_2 b + D \cos \lambda_2 b) &= 0 \end{aligned} \quad (8.2.18)$$

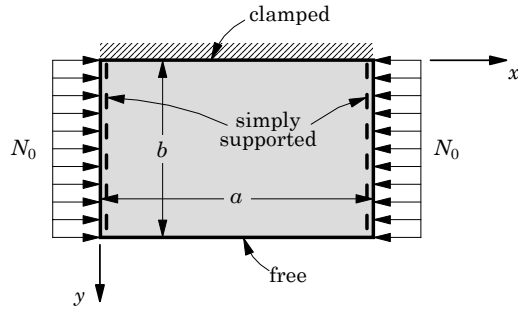


Figure 8.2.3. Uniformly compressed rectangular plate simply supported along two opposite sides ($x = 0, a$), clamped on side $y = 0$, and free on side $y = b$ (SSCF).

Setting the determinant of these equations, after substituting for $C = -A$ and $D = -(\lambda_1/\lambda_2)B$, to zero, we obtain

$$2\Omega_1\Omega_2 + (\Omega_1^2 + \Omega_2^2) \cosh \lambda_1 b \cos \lambda_2 b - \frac{1}{\lambda_1 \lambda_2} (\lambda_1^2 \Omega_2^2 - \lambda_2^2 \Omega_1^2) \sinh \lambda_1 b \sin \lambda_2 b = 0 \quad (8.2.19)$$

Figures 8.2.4 and 8.2.5 contain plots of nondimensional buckling load $\bar{N} = N_0 b^2 / (\pi^2 D_{22})$ versus plate aspect ratio for modes $m = 1, 2, 3$ of isotropic ($\nu = 0.25$) and orthotropic ($G_{12} = 0.5E_2$, $\nu_{12} = 0.25$) SSCF plates, respectively (Table 8.2.2). It is seen that at the beginning, the buckling load of an isotropic plate decreases with an increase in the aspect ratio a/b . The minimum value of the buckling load $\bar{N}_{cr} = 1.329$ occurs at $a/b = 1.635$. There is a mode change at $a/b = 2.3149$ from $m = 1$ and $m = 2$, and the buckling load for this aspect ratio is $\bar{N}_{cr} = 1.503$. The minimum buckling load ($\bar{N}_{cr} = 1.329$) for mode $m = 2$ occurs at $a/b = 3.27$. For comparatively long isotropic plates, the critical buckling load can be taken with sufficient accuracy as $\bar{N}_{cr} = 1.329$. For orthotropic plates with $E_1/E_2 = 3$, the minimum buckling load ($\bar{N}_{cr} = 2.0606$) occurs at $a/b = 2.168$.

Table 8.2.2. Nondimensional buckling loads \bar{N} of SSCF rectangular plates under uniform axial compression $\hat{N}_{xx} = -N_0$.

$\frac{a}{b}$	$\frac{E_1}{E_2} = 1$	$\frac{E_1}{E_2} = 3$	$\frac{E_1}{E_2} = 10$	$\frac{a}{b}$	$\frac{E_1}{E_2} = 1$	$\frac{E_1}{E_2} = 3$	$\frac{E_1}{E_2} = 10$
0.5	4.518	12.665	40.674	3.5	1.336	2.174	3.239
1.0	1.698	3.861	10.871	4.0	1.386	2.076	3.529
1.5	1.339	2.407	5.529	4.5	1.339 [†]	2.064	3.459 [†]
2.0	1.386	2.076	3.838	5.0	1.329	2.110	3.242
2.5	1.432 [†]	2.110	3.242	5.5	1.347	2.129 [†]	3.138
3.0	1.339	2.407 [†]	3.114	6.0	1.339 [†]	2.076	3.114

[†]Denotes change to next higher mode.

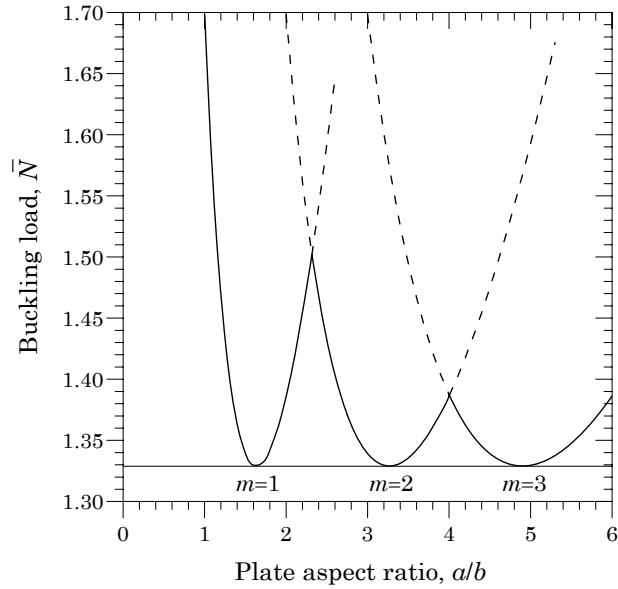


Figure 8.2.4. Nondimensional buckling load, $\bar{N} = N_0 b^2 / (\pi^2 D_{22})$, versus plate aspect ratio a/b for isotropic SSCF plates.

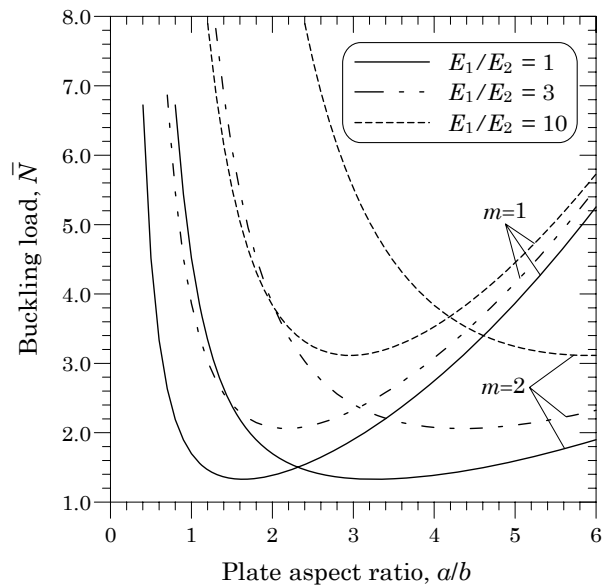


Figure 8.2.5 Nondimensional buckling load, $\bar{N} = N_0 b^2 / (\pi^2 D_{22})$, versus plate aspect ratio a/b for orthotropic SSCF plates.

8.2.4 Buckling of SSCC Plates

Here, we consider buckling of uniformly compressed rectangular plates with sides $y = 0, b$ clamped (Figure 8.2.6). The boundary conditions are

$$w = 0, \quad \frac{\partial w}{\partial y} = 0 \quad \text{at } y = 0, b \quad (8.2.20)$$

Substitution of Eq. (8.2.7) into the boundary conditions yields

$$\begin{aligned} A (\cosh \lambda_1 b - \cos \lambda_2 b) + B \left(\sinh \lambda_1 b - \frac{\lambda_1}{\lambda_2} \sin \lambda_2 b \right) &= 0 \\ A (\lambda_1 \sinh \lambda_1 b + \lambda_2 \sin \lambda_2 b) + B \lambda_1 (\cosh \lambda_1 b - \cos \lambda_2 b) &= 0 \end{aligned} \quad (8.2.21)$$

The determinant of these equations is

$$2(1 - \cosh \lambda_1 b \cos \lambda_2 b) + \left(\frac{\lambda_1}{\lambda_2} - \frac{\lambda_2}{\lambda_1} \right) \sinh \lambda_1 b \sin \lambda_2 b = 0 \quad (8.2.22)$$

where λ_1 and λ_2 are defined by Eqs. (8.2.8a,b), respectively.

Figures 8.2.7 and 8.2.8 contain plots of nondimensional buckling load $\bar{N}_{cr} = N_0 b^2 / (\pi^2 D_{22})$ versus plate aspect ratio for modes $m = 1, 2, 3$ of isotropic ($\nu = 0.25$) and orthotropic ($G_{12} = 0.2E_2$, $\nu_{12} = 0.25$) plates (Table 8.2.3). The minimum value of the buckling load $\bar{N}_{cr} = 0.697$ occurs at $a/b = 0.661$. There is a mode change at $a/b = 0.9349$ from $m = 1$ to $m = 2$, and the buckling load for this aspect ratio is $\bar{N}_{cr} = 8.097$. The minimum buckling load ($\bar{N}_{cr} = 0.697$) for mode $m = 2$ occurs at $a/b = 1.322$. For orthotropic plates with $E_1/E_2 = 3$, the minimum buckling load ($\bar{N}_{cr} = 10.866$) occurs at $a/b = 0.871$. The minimum buckling load ($\bar{N}_{cr} = 17.407$) for $E_1/E_2 = 10$ occurs at $a/b = 1.181$.

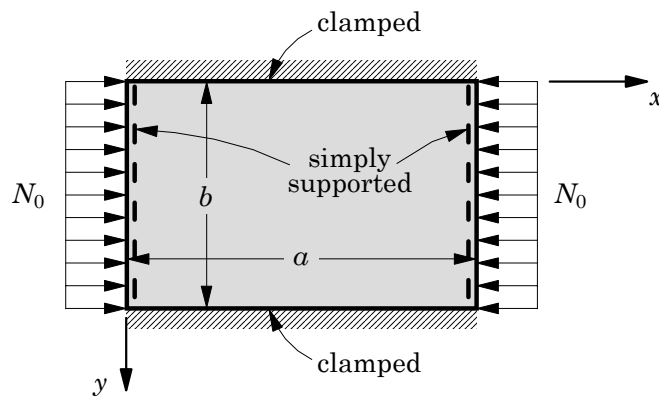


Figure 8.2.6. Uniformly compressed SSCC rectangular plate.

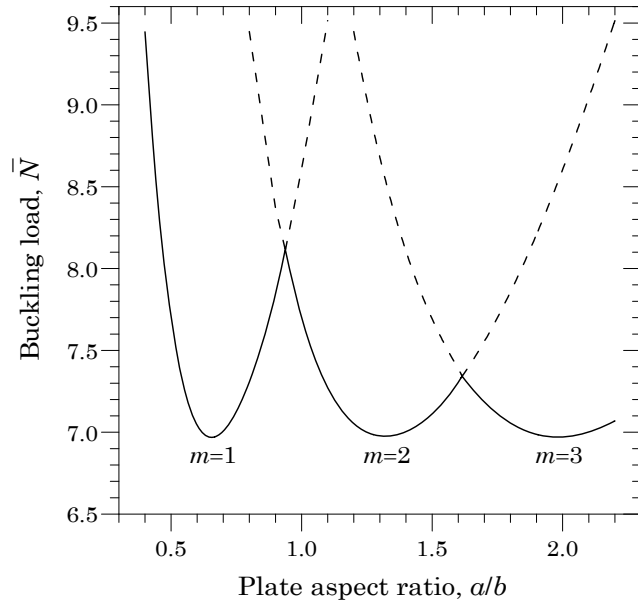


Figure 8.2.7. Nondimensional buckling load, $\bar{N} = N_0 b^2 / (\pi^2 D_{22})$, versus plate aspect ratio a/b for isotropic SSCC plates.

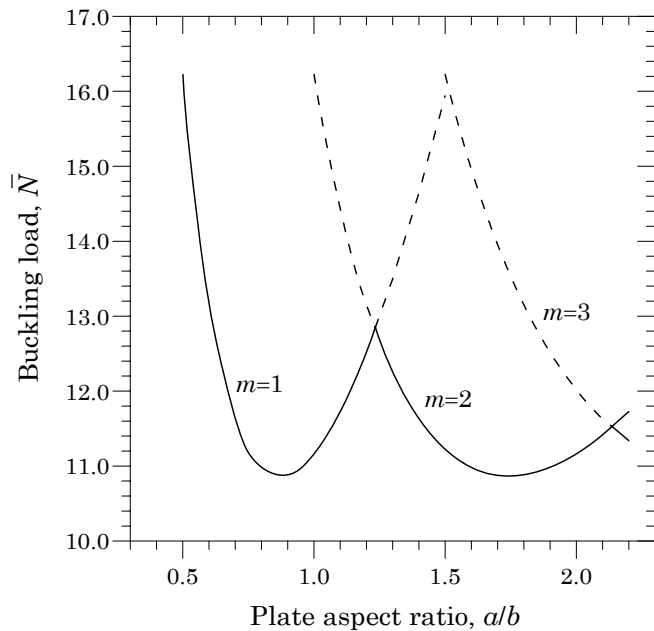


Figure 8.2.8 Nondimensional buckling load, $\bar{N} = N_0 b^2 / (\pi^2 D_{22})$, versus plate aspect ratio a/b for orthotropic SSCC plates.

Table 8.2.3. Nondimensional buckling loads \bar{N}_{cr} of SSCC rectangular plates under uniform axial compression $\hat{N}_{xx} = -N_0$.

$\frac{a}{b}$	$\frac{E_1}{E_2} = 1$	$\frac{E_1}{E_2} = 3$	$\frac{E_1}{E_2} = 10$	$\frac{a}{b}$	$\frac{E_1}{E_2} = 1$	$\frac{E_1}{E_2} = 3$	$\frac{E_1}{E_2} = 10$
0.4	9.448	22.473	66.256	1.4	7.001	11.631†	18.252
0.6	7.055	13.153	32.632	1.6	7.304	10.981	20.145
0.8	7.304	10.981	21.954	1.8	7.055†	10.882	19.559†
1.0	7.691†	11.163	18.198	2.0	6.972	11.163	18.198
1.2	7.055	12.518	17.415	2.2	7.069	11.337†	17.548

† Denotes change to next higher mode.

8.3 Buckling of Rectangular Plates Using the Ritz Method

8.3.1 Analysis of the Lévy Plates

As was shown in Section 7.3.1 for the bending case, the buckling equation obtained after the application of the Lévy method, namely Eq. (8.2.4), can also be solved using the Ritz method. The weak form of Eq. (8.2.4) is

$$\begin{aligned} & \int_0^b \left[D_{22} \frac{d^2 W}{dy^2} \frac{d^2 \delta W}{dy^2} + 2\alpha_m^2 \hat{D}_{12} \frac{dW}{dy} \frac{d\delta W}{dy} + (D_{11}\alpha_m^4 - N_0\alpha_m^2) W \delta W \right] dy \\ & + \left[\left(D_{22} \frac{d^3 W}{dy^3} - 2\hat{D}_{12}\alpha_m^2 \frac{dW}{dy} \right) \delta W - D_{22} \frac{d^2 W}{dy^2} \frac{d\delta W}{dy} \right]_0^b = 0 \end{aligned} \quad (8.3.1)$$

where $\hat{D}_{12} = D_{12} + 2D_{66}$.

For a simply supported edge [$W = 0$ and $(d^2 W/dy^2) = 0$] or a clamped edge [$W = 0$ and $(dW/dy) = 0$] the boundary terms in Eq. (8.3.1) vanish identically. However, for a free edge, the vanishing of bending moment and effective shear force require

$$D_{22} \frac{d^2 W}{dy^2} - \alpha_m^2 D_{12} W = 0, \quad D_{22} \frac{d^3 W}{dy^3} - \alpha_m^2 \bar{D}_{12} \frac{dW}{dy} = 0 \quad (8.3.2)$$

where $\bar{D}_{12} = D_{12} + 4D_{66}$. Hence, on a free edge, the boundary expression of Eq. (8.3.1) can be simplified by using the relations in Eq. (8.3.2)

$$\begin{aligned} & \left[\left(D_{22} \frac{d^3 W}{dy^3} - 2\hat{D}_{12}\alpha_m^2 \frac{dW}{dy} \right) \delta W - D_{22} \frac{d^2 W}{dy^2} \frac{d\delta W}{dy} \right]_0^b \\ & = -\alpha_m^2 D_{12} \left[W \frac{d\delta W}{dy} + \frac{dW}{dy} \delta W \right]_0^b \end{aligned} \quad (8.3.3)$$

In summary, the weak form for SSSS, SSCC, and SSCS plates becomes

$$0 = \int_0^b \left[D_{22} \frac{d^2 W}{dy^2} \frac{d^2 \delta W}{dy^2} + 2\hat{D}_{12}\alpha_m^2 \frac{dW}{dy} \frac{d\delta W}{dy} + (D_{11}\alpha_m^4 - N_0\alpha_m^2) W\delta W \right] dy \quad (8.3.4)$$

and, for SSSF and SSCF plates, it is given by

$$\begin{aligned} 0 = & \int_0^b \left[D_{22} \frac{d^2 W}{dy^2} \frac{d^2 \delta W}{dy^2} + 2\hat{D}_{12}\alpha_m^2 \frac{dW}{dy} \frac{d\delta W}{dy} + (D_{11}\alpha_m^4 - N_0\alpha_m^2) W\delta W \right] dy \\ & - \alpha_m^2 D_{12} \left[W \frac{d\delta W}{dy} + \frac{dW}{dy} \delta W \right]_0^b \end{aligned} \quad (8.3.5)$$

Assume an approximation of the form

$$W(y) \approx \sum_{j=1}^N c_j \varphi_j(y) \quad (8.3.6)$$

where φ_j are the approximation functions [see Eqs. (7.3.10)–(7.3.20); replace x with y and a with b]. Substituting the approximation (8.3.6) into the weak form (8.3.5), we obtain

$$([R] - N_0[B]) \{c\} = \{0\} \quad (8.3.7)$$

where

$$\begin{aligned} R_{ij} = & \int_0^b \left(D_{22} \frac{d^2 \varphi_i}{dy^2} \frac{d^2 \varphi_j}{dy^2} + 2\alpha_m^2 \hat{D}_{12} \frac{d\varphi_i}{dy} \frac{d\varphi_j}{dy} + D_{11}\alpha_m^4 \varphi_i \varphi_j \right) dy \\ & - \alpha_m^2 D_{12} \left[\varphi_j \frac{d\varphi_i}{dy} + \frac{d\varphi_j}{dy} \varphi_i \right]_0^b \end{aligned} \quad (8.3.8a)$$

$$B_{ij} = \alpha_m^2 \int_0^b \varphi_i \varphi_j dy, \quad \alpha_m = \frac{m\pi}{a} \quad (8.3.8b)$$

The boundary term in R_{ij} is *nonzero* only for SSSF and SSCF plates. Equation (8.3.7) has a nontrivial solution, $c_i \neq 0$, only if the determinant of the coefficient matrix is zero

$$|[R] - N_0[B]| = 0 \quad (8.3.9)$$

Equation (8.3.9) yields an N th order polynomial in N_0 that depends on m . Hence, for any given aspect ratio a/b , the critical buckling load is the smallest value of N_0 for all m .

Table 8.3.1 contains numerical values of nondimensional critical buckling loads $\bar{N}_{cr} = N_{cr}b^2/(\pi^2 D_{22})$ obtained using the algebraic approximation functions given in Eqs. (7.3.10)–(7.3.20) (replace x with y and a with b) for various boundary conditions. The accuracy of the buckling loads predicted by the three-parameter Ritz approximation are in very good agreement with the analytical solutions derived in Section 8.2.

Table 8.3.1. Nondimensional buckling loads \bar{N} of rectangular isotropic ($\nu = 0.25$) plates under uniform compression $\hat{N}_{xx} = -N_0$ (Ritz solutions).

$\frac{a}{b}$	N	SSSS	SSCC	SSCS	SSCF	SSSF	SSFF
0.5	1	6.334	7.725	7.915	4.896	4.456	4.000
	3	6.250	7.693	6.860	4.526	4.436	3.958
	E	6.250	7.691	6.853	4.518	4.404	—
1.0	1	4.258	8.606	8.149	2.050	1.456	1.000
	3	4.001	8.605	5.741	1.699	1.445	0.972
	E	4.000	8.604	5.740	1.698	1.434	—
1.5	1	4.497 [†]	7.120 [†]	7.040 [†]	1.751	0.900	0.988
	3	4.341	7.116	5.432	1.339	0.894	0.426
	E	4.340	7.116	5.431	1.339	0.888	—
2.0	1	4.258	8.606	8.149	1.915	0.706	0.250
	3	4.001	8.605	5.741	1.386	0.702	0.238
	E	4.000	8.604	5.740	1.386	0.698	—

[†] Denotes change to the next higher mode; E denotes the “exact” solution obtained in Section 8.2.

8.3.2 General Formulation

In this section, we consider buckling of orthotropic rectangular plates using the Ritz method. Buckling problems of plates with combined bending and compression or under pure inplane shear stress do not permit analytical solutions; therefore, we use the Ritz method to solve such problems. Of course, the method can be used for any combination of boundary conditions and edges loads. The statement of the principle of virtual displacements or the minimum total potential energy for plates subjected to inplane edge forces \hat{N}_{xx} , \hat{N}_{yy} , and \hat{N}_{xy} can be expressed as

$$0 = \int_0^b \int_0^a \left[D_{11} \frac{\partial^2 w}{\partial x^2} \frac{\partial^2 \delta w}{\partial x^2} + D_{12} \left(\frac{\partial^2 w}{\partial y^2} \frac{\partial^2 \delta w}{\partial x^2} + \frac{\partial^2 w}{\partial x^2} \frac{\partial^2 \delta w}{\partial y^2} \right) \right. \\ + 4D_{66} \frac{\partial^2 w}{\partial x \partial y} \frac{\partial^2 \delta w}{\partial x \partial y} + D_{22} \frac{\partial^2 w}{\partial y^2} \frac{\partial^2 \delta w}{\partial y^2} \\ + \hat{N}_{xx} \frac{\partial w}{\partial x} \frac{\partial \delta w}{\partial x} + \hat{N}_{yy} \frac{\partial w}{\partial y} \frac{\partial \delta w}{\partial y} \\ \left. + \hat{N}_{xy} \left(\frac{\partial w}{\partial y} \frac{\partial \delta w}{\partial x} + \frac{\partial w}{\partial x} \frac{\partial \delta w}{\partial y} \right) \right] dx dy \quad (8.3.10)$$

In general, the applied edge forces are functions of position and they are independent of each other. Let

$$\hat{N}_{xx} = -N_0, \quad \hat{N}_{yy} = -\gamma_1 N_0, \quad \hat{N}_{xy} = -\gamma_2 N_0 \quad (8.3.11)$$

where N_0 is a constant and γ_1 and γ_2 are possibly functions of position.

Using an N -parameter Ritz solution of the form

$$w(x, y) \approx \sum_{j=1}^N c_j \varphi_j(x, y) \quad (8.3.12)$$

in Eq. (8.3.10), we obtain

$$([R] - N_0[B]) \{c\} = \{0\} \quad (8.3.13)$$

where

$$\begin{aligned} R_{ij} &= \int_0^b \int_0^a \left[D_{11} \frac{\partial^2 \varphi_i}{\partial x^2} \frac{\partial^2 \varphi_j}{\partial x^2} + D_{12} \left(\frac{\partial^2 \varphi_i}{\partial y^2} \frac{\partial^2 \varphi_j}{\partial x^2} + \frac{\partial^2 \varphi_i}{\partial x^2} \frac{\partial^2 \varphi_j}{\partial y^2} \right) \right. \\ &\quad \left. + 4D_{66} \frac{\partial^2 \varphi_i}{\partial x \partial y} \frac{\partial^2 \varphi_j}{\partial x \partial y} + D_{22} \frac{\partial^2 \varphi_i}{\partial y^2} \frac{\partial^2 \varphi_j}{\partial y^2} \right] dx dy \end{aligned} \quad (8.3.14a)$$

$$B_{ij} = \int_0^b \int_0^a \left[\frac{\partial \varphi_i}{\partial x} \frac{\partial \varphi_j}{\partial x} + \gamma_1 \frac{\partial \varphi_i}{\partial y} \frac{\partial \varphi_j}{\partial y} + \gamma_2 \left(\frac{\partial \varphi_i}{\partial x} \frac{\partial \varphi_j}{\partial y} + \frac{\partial \varphi_i}{\partial y} \frac{\partial \varphi_j}{\partial x} \right) \right] dx dy \quad (8.3.14b)$$

As discussed in Section 7.3.2, it is convenient to express the Ritz approximation of rectangular plates in the form

$$w(x, y) \approx W_{mn}(x, y) = \sum_{i=1}^M \sum_{j=1}^N c_{ij} X_i(x) Y_j(y) \quad (8.3.15)$$

The functions X_i and Y_j for various boundary conditions are given in Eqs. (7.3.29)–(7.3.44). Substituting Eq. (8.3.15) into Eq. (8.3.10), we obtain Eq. (8.3.13) with the following definitions of the coefficients

$$\begin{aligned} R_{(ij)(k\ell)} &= \int_0^b \int_0^a \left[D_{11} \frac{d^2 X_i}{dx^2} \frac{d^2 X_k}{dx^2} Y_j Y_\ell + D_{22} X_i X_k \frac{d^2 Y_j}{dy^2} \frac{d^2 Y_\ell}{dy^2} \right. \\ &\quad \left. + D_{12} \left(X_i \frac{d^2 X_k}{dx^2} \frac{d^2 Y_j}{dy^2} Y_\ell + \frac{d^2 X_i}{dx^2} X_k Y_j \frac{d^2 Y_\ell}{dy^2} \right) \right. \\ &\quad \left. + 4D_{66} \frac{dX_i}{dx} \frac{dX_k}{dx} \frac{dY_j}{dy} \frac{dY_\ell}{dy} \right] dx dy \end{aligned} \quad (8.3.16a)$$

$$\begin{aligned} B_{(ij)(k\ell)} &= \int_0^b \int_0^a \left[\frac{dX_i}{dx} \frac{dX_k}{dx} Y_j Y_\ell + \gamma_1 X_i X_k \frac{dY_j}{dy} \frac{dY_\ell}{dy} \right. \\ &\quad \left. + \gamma_2 \left(\frac{dX_i}{dx} X_k Y_j \frac{dY_\ell}{dy} + X_i \frac{dX_k}{dx} \frac{dY_j}{dy} Y_\ell \right) \right] dx dy \end{aligned} \quad (8.3.16b)$$

As an example, consider a simply supported plate. For the choice of algebraic functions

$$X_i(x) = \left(\frac{x}{a} \right)^i - \left(\frac{x}{a} \right)^{i+1}, \quad Y_j(y) = \left(\frac{y}{b} \right)^j - \left(\frac{y}{b} \right)^{j+1} \quad (8.3.17)$$

and for $M = N = 1$, we obtain

$$\begin{aligned} R_{(11)(11)} &= \frac{2b}{15a^3}D_{11} + \frac{2}{9ab}\hat{D}_{12} + \frac{2a}{15b^3}D_{22} \\ B_{(11)(11)} &= \frac{1}{90} + \frac{\gamma_1}{90} + \gamma_2 \times 0 \end{aligned} \quad (8.3.18)$$

Note that the buckling load under inplane shear cannot be determined with one-parameter approximation. The buckling load under uniaxial compression along the x -axis is given by setting $\gamma_1 = 0$

$$N_{cr}^u = \frac{12b}{a^3}D_{11} + \frac{20}{ab}\hat{D}_{12} + \frac{12a}{b^3}D_{22} \quad (8.3.19a)$$

and the critical buckling load under biaxial compression is given by ($\gamma_1 = 1$)

$$N_{cr}^b = \frac{6b}{a^3}D_{11} + \frac{10}{ab}\hat{D}_{12} + \frac{6a}{b^3}D_{22} \quad (8.3.19b)$$

For square isotropic plates, the above expressions become

$$N_{cr}^u = 44\frac{D}{a^2} = 4.458\frac{D\pi^2}{a^2}, \quad N_{cr}^b = 22\frac{D}{a^2} = 2.229\frac{D\pi^2}{a^2}$$

The exact values for the two cases are $4D\pi^2/a^2$ and $2D\pi^2/a^2$, respectively (see Table 8.1.1). The results are in about -11.5% error, and the values do not change for $N = M = 2$.

For a square isotropic plate clamped on all sides and subjected to uniaxial compression or biaxial compression, the buckling loads obtained using the Ritz method with algebraic polynomials given in Eqs. (7.3.43a,b) are (for $N = M = 1$ or 2)

$$N_{cr}^u = 10.943\frac{D\pi^2}{a^2}, \quad N_{cr}^b = 5.471\frac{D\pi^2}{a^2}$$

8.3.3 Buckling of a Simply Supported Plate under Combined Bending and Compression

Let us consider a simply supported rectangular plate (Figure 8.3.1) with distributed inplane forces applied in the middle plane of the plate on sides $x = 0, a$. The distribution of the applied forces is assumed to be

$$\hat{N}_{xx} = -N_0\gamma_1 = -N_0\left(1 - c_0\frac{y}{b}\right) \quad (8.3.20)$$

where N_0 is the magnitude of the compressive force at $y = 0$ and c_0 is a parameter that defines the relative bending and compression. For example, $c_0 = 0$ corresponds to the case of uniformly distributed compressive force, as discussed in Section 8.2, and for $c_0 = 2$ we obtain the case of pure bending. All other values give a combination of bending and compression or tension.

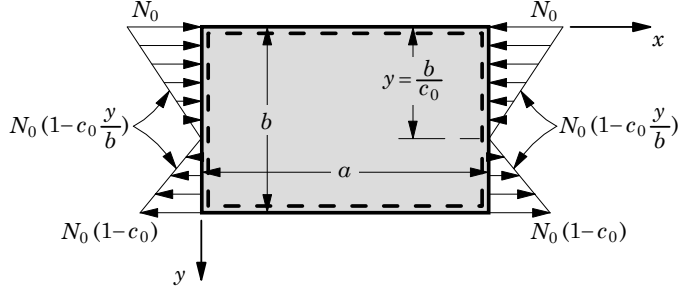


Figure 8.3.1. Buckling of simply supported plates under combined bending and compression.

We seek the deflection of the buckled plate, which is simply supported on all sides, in the form of a double sine series

$$w(x, y) \approx W_{MN} = \sum_{n=1}^N \sum_{m=1}^M c_{mn} \sin \frac{m\pi x}{a} \sin \frac{n\pi y}{b} \quad (8.3.21)$$

that satisfies the geometric as well as the force boundary conditions of the problem.

Substituting Eq. (8.3.21) for w and

$$\delta w = \sin \frac{p\pi x}{a} \sin \frac{q\pi y}{b}$$

into Eq. (8.3.10) with $\hat{N}_{yy} = \hat{N}_{xy} = 0$, we obtain

$$\begin{aligned} 0 &= \sum_{n=1}^N \sum_{m=1}^M c_{mn} \left\{ D_{11} \left(\frac{m\pi}{a} \right)^2 \left(\frac{p\pi}{a} \right)^2 + D_{22} \left(\frac{n\pi}{b} \right)^2 \left(\frac{q\pi}{b} \right)^2 \right. \\ &\quad \left. + D_{12} \left[\left(\frac{n\pi}{b} \right)^2 \left(\frac{p\pi}{a} \right)^2 + \left(\frac{m\pi}{a} \right)^2 \left(\frac{q\pi}{b} \right)^2 \right] \right\} I_1 \\ &\quad + \sum_{n=1}^N \sum_{m=1}^M c_{mn} 4D_{66} \left(\frac{m\pi}{a} \right) \left(\frac{n\pi}{b} \right) \left(\frac{p\pi}{a} \right) \left(\frac{q\pi}{b} \right) I_2 \\ &\quad - \sum_{n=1}^N \sum_{m=1}^M \sum_{q=1}^M c_{mq} N_0 \left(\frac{m\pi}{a} \right) \left(\frac{p\pi}{a} \right) I_{nq} \end{aligned} \quad (8.3.22)$$

where I_1 and I_2 are nonzero only when $p = m$ and $q = n$

$$\begin{aligned} I_1 &= \int_0^b \int_0^a \sin \frac{m\pi x}{a} \sin \frac{n\pi y}{b} \sin \frac{p\pi x}{a} \sin \frac{q\pi y}{b} dx dy = \frac{ab}{4} \\ I_2 &= \int_0^b \int_0^a \cos \frac{m\pi x}{a} \cos \frac{n\pi y}{b} \cos \frac{p\pi x}{a} \cos \frac{q\pi y}{b} dx dy = \frac{ab}{4} \end{aligned} \quad (8.3.23a)$$

and I_{nq} is defined as

$$I_{nq} = \int_0^b \int_0^a \left(1 - c_0 \frac{y}{b}\right) \cos \frac{m\pi x}{a} \cos \frac{p\pi x}{a} \sin \frac{n\pi y}{b} \sin \frac{q\pi y}{b} dx dy \quad (8.3.23b)$$

which can be computed with the help of the following identities:

$$\begin{aligned} I_0 &\equiv \int_0^b y \sin \frac{n\pi y}{b} \sin \frac{q\pi y}{b} dy \\ &= \frac{b^2}{4} \text{ when } n = q \\ &= 0 \text{ when } n \neq q \text{ and } n \pm q \text{ an even number} \\ &= -\frac{b^2}{\pi^2} \frac{2nq}{(n^2 - q^2)^2} \text{ when } n \neq q \text{ and} \\ &\quad n \pm q \text{ an odd number} \end{aligned} \quad (8.3.24)$$

Thus, $I_{nq} = 0$, if $p \neq m$ and

$$I_{nq} = \frac{a}{2} \left(\frac{b}{2} - \frac{c_0}{b} I_0 \right) \quad (8.3.25)$$

when $p = m$. For any m and n , Eq. (8.3.22) becomes

$$\begin{aligned} 0 &= \left[D_{11} \left(\frac{m\pi}{a} \right)^4 + D_{22} \left(\frac{n\pi}{b} \right)^4 + 2\hat{D}_{12} \left(\frac{n\pi}{b} \right)^2 \left(\frac{m\pi}{a} \right)^2 \right] c_{mn} \\ &\quad - N_0 \left(\frac{m\pi}{a} \right)^2 \left[c_{mn} - \frac{c_0}{2} \left(c_{mn} - \frac{8}{\pi^2} \sum_{q=1}^M \frac{2nqc_{mq}}{(n^2 - q^2)^2} \right) \right] \end{aligned} \quad (8.3.26)$$

where the summation is taken over all numbers q such that $n \pm q$ is an odd number. Taking $m = 1$ in Eq. (8.3.26), we obtain

$$\begin{aligned} &\left(D_{11}s^4 + D_{22}n^4 + 2\hat{D}_{12}n^2s^2 \right) c_{1n} \\ &= N_0 \frac{s^2b^2}{\pi^2} \left[c_{1n} \left(1 - \frac{c_0}{2} \right) + \frac{8c_0}{\pi^2} \sum_{q=1}^M \frac{nqc_{1q}}{(n^2 - q^2)^2} \right] \end{aligned} \quad (8.3.27)$$

where s denotes the aspect ratio $s = b/a$. A nontrivial solution, i.e., for nonzero c_{1i} , the determinant of the linear equations in (8.3.27) must be zero if the plate buckles.

For one-parameter approximation ($N = M = 1$), we obtain

$$N_0 = \frac{\pi^2}{s^2b^2} \left(s^4 D_{11} + D_{22}n^4 + 2\hat{D}_{12}n^2s^2 \right) \frac{1}{1 - 0.5c_0} \quad (8.3.28)$$

which gives a satisfactory result only for small values of c_0 , i.e., in cases where the bending stresses are small compared with the uniform compressive stress. In particular, when $c_0 = 0$, Eq. (8.3.28) gives the result in Eq. (8.1.22) for $m = 1$. Higher-order approximations yield sufficiently accurate results for the case of pure

bending. Table 8.3.2 contains critical buckling loads $\bar{N} = N_0(b^2/\pi^2 D)$ obtained using two-parameter approximation, except for $c_0 = 2$, where the three-parameter approximation was used [see Timoshenko and Gere (1961)].

Table 8.3.2. Nondimensional critical buckling loads \bar{N} of simply supported rectangular isotropic plates under combined bending and inplane compression [$\hat{N}_{xy} = N_0(1 - c_0y/b)$].

c_0	$\frac{a}{b} \rightarrow$	0.4	0.5	0.6	$\frac{2}{3}$	0.75	0.8	0.9	1.0	1.5
2		29.1	25.6	24.1	23.9	24.1	24.4	25.6	25.6	24.1
4/3		18.7	—	12.9	—	11.5	11.2	—	11.0	11.5
1		15.1	—	9.7	—	8.4	8.1	—	7.8	8.4
4/5		13.3	—	8.3	—	7.1	6.9	—	6.6	7.1
2/3		10.8	—	7.1	—	6.1	6.0	—	5.8	6.1

8.3.4 Buckling of a Simply Supported Plate under Inplane Shear

When the plate is simply supported on all its edges and subjected to uniformly distributed inplane shear force $\hat{N}_{xy} = -N_{xy}^0$ (Figure 8.3.2), the Navier or Lévy solution procedure cannot be used to determine the critical buckling load. Hence, we will seek an approximate solution by the Ritz or Galerkin method.

Let us seek the solution in the form

$$w(x, y) \approx W_{MN} = \sum_{n=1}^N \sum_{m=1}^M c_{mn} \sin \frac{m\pi x}{a} \sin \frac{n\pi y}{b} \quad (8.3.29)$$

The approximate solution satisfies the geometric ($w = 0$) as well as the natural ($M_{xx} = 0$ on sides $x = 0, a$ and $M_{yy} = 0$ on sides $y = 0, b$) boundary conditions of the problem. Therefore, both the Ritz and Galerkin methods yield the same solutions.

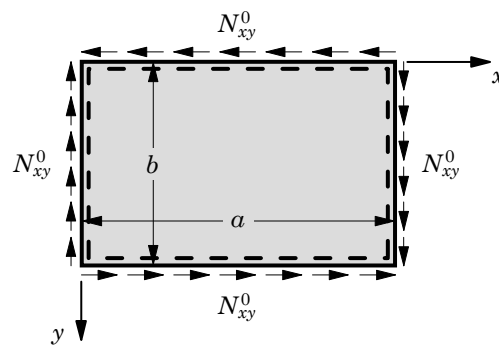


Figure 8.3.2. Buckling of rectangular plates under the action of shearing stresses.

The Galerkin solution is obtained by substituting Eq. (8.3.29) in the “weighted-residual” statement

$$0 = \int_0^b \int_0^a \left[D_{11} \frac{\partial^4 w}{\partial x^4} + 2\hat{D}_{12} \frac{\partial^4 w}{\partial x^2 \partial y^2} + D_{22} \frac{\partial^4 w}{\partial y^4} - 2N_{xy}^0 \frac{\partial^2 w}{\partial x \partial y} \right] \varphi_{pq} \, dx dy \quad (8.3.30)$$

We obtain

$$\begin{aligned} 0 = \frac{ab}{4} & \left[D_{11} \left(\frac{p\pi}{a} \right)^4 + (D_{12} + 2D_{66}) \left(\frac{p\pi}{a} \right)^2 \left(\frac{q\pi}{b} \right)^2 + D_{22} \left(\frac{q\pi}{b} \right)^4 \right] c_{pq} \\ & - 2N_{xy}^0 \sum_{m=1}^N \sum_{n=1}^M \left(\frac{m\pi}{a} \right) \left(\frac{n\pi}{b} \right) I_{mp} I_{nq} c_{mn} \end{aligned} \quad (8.3.31)$$

where

$$I_{mp} = \int_0^a \cos \frac{m\pi x}{a} \sin \frac{p\pi x}{a} \, dx = \left(\frac{2a}{\pi^2} \right) \frac{p}{(p^2 - m^2)} \quad \text{for } p^2 \neq m^2 \quad (8.3.32a)$$

$$I_{nq} = \int_0^b \cos \frac{n\pi y}{b} \sin \frac{q\pi y}{b} \, dy = \left(\frac{2b}{\pi^2} \right) \frac{q}{(q^2 - n^2)} \quad \text{for } q^2 \neq n^2 \quad (8.3.32b)$$

and the integral I_{mp} is zero when $p = m$ or $p \pm m$ is an even number, and I_{nq} is zero when $q = n$ or $q \pm n$ is an even number. The set of mn homogeneous equations (8.3.31) define an eigenvalue problem

$$\sum_{m=1}^N \sum_{n=1}^M \left(A_{(mn),(pq)} - N_{xy}^0 G_{(mn)(pq)} \right) c_{mn} = 0 \quad \text{or} \quad ([A] - N_{xy}^0 [G]) \{c\} = \{0\} \quad (8.3.33a)$$

where

$$\begin{aligned} A_{(mn)(pq)} &= \delta_{mp} \delta_{nq} \frac{ab}{4} \left[D_{11} \alpha_m^2 \alpha_p^2 + 2\hat{D}_{12} \alpha_m \alpha_p \beta_n \beta_q + D_{22} \beta_n^2 \beta_q^2 \right] \\ G_{(mn)(pq)} &= 2\alpha_m \beta_n I_{mp} I_{nq} \\ \hat{D}_{12} &= D_{12} + 2D_{66}, \quad \alpha_m = \frac{m\pi}{a}, \quad \beta_n = \frac{n\pi}{b} \end{aligned} \quad (8.3.33b)$$

which has a nontrivial solution (i.e., $c_{mn} \neq 0$) when the determinant of the coefficient matrix is zero. Note that $[A]$ is a diagonal matrix while $[G]$ is a nonpositive-definite matrix; hence, the solution of (8.3.33a) requires an eigenvalue routine that is suitable for nonpositive-definite matrices. It is found that the solution of (8.3.33a) converges very slowly with increasing values of M and N . We note that $[G]$ does not exist for $M = N = 1$.

For $M = N = 2$, we find from Eq. (8.3.33a) the result ($g_{(11)(12)} = g_{(11)(21)} = 0$)

$$\left(\begin{bmatrix} a_{11} & 0 \\ 0 & a_{22} \end{bmatrix} - N_{xy}^0 \begin{bmatrix} 0 & g_{(11)(22)} \\ g_{(22)(11)} & 0 \end{bmatrix} \right) \begin{Bmatrix} c_{11} \\ c_{22} \end{Bmatrix} = \begin{Bmatrix} 0 \\ 0 \end{Bmatrix} \quad (8.3.34)$$

where the coefficients are given by

$$\begin{aligned} a_{(11)(11)} &= \frac{\pi^4}{4sb^2} (D_{11}s^4 + 2\hat{D}_{12}s^2 + D_{22}), \quad a_{(22)(22)} = 16a_{(11)(11)} \\ g_{(11)(11)} = g_{(22)(22)} &= 0, \quad g_{(11)(22)} = g_{(22)(11)} = \frac{32}{9} \end{aligned} \quad (8.3.35)$$

where $s = b/a$ is the plate aspect ratio. Setting the determinant of the coefficient matrix in Eq. (8.3.34) to zero, we obtain

$$N_{xy}^0 = \pm \frac{9\pi^4}{32sb^2} (D_{11}s^4 + 2\hat{D}_{12}s^2 + D_{22}) \quad (8.3.36)$$

The two signs indicate that the value of the critical buckling load does not depend on sign.

Timoshenko and Gere (1961) obtained the following equation for short isotropic plates ($a/b < 2$) using a five-term approximation:

$$\lambda^2 = \frac{s^4}{81(1+s^2)^4} \left[1 + \frac{81}{625} + \frac{81}{25} \left(\frac{1+s^2}{9+s^2} \right)^2 + \frac{81}{25} \left(\frac{1+s^2}{1+9s^2} \right)^2 \right] \quad (8.3.37)$$

where

$$s = \frac{b}{a}, \quad \lambda = -\frac{\pi^4 D}{32ab N_{xy}^0} \quad (8.3.38)$$

For a square plate, Eq. (8.3.38) yields the critical buckling load

$$(N_{xy}^0)_{cr} = 9.4 \frac{\pi^2 D}{b^2} \quad (8.3.39)$$

whereas the value obtained with a larger (than 5) number of equations give 9.34 in place of 9.4. Table 8.3.3 contains the critical buckling loads $\bar{N} = (N_{xy}^0)_{cr}(b^2/\pi^2 D)$ obtained using a large number of parameters [see Timoshenko and Gere (1961)].

Table 8.3.3. Nondimensional critical buckling loads \bar{N} of rectangular isotropic ($\nu = 0.25$) plates under uniform shear $\hat{N}_{xy} = N_{xy}^0$ (Ritz solution).

$\frac{a}{b}$	1.0	1.2	1.4	1.5	1.6	1.8	2.0	2.5	3	4
\bar{N}	9.34	8.0	7.3	7.1	7.0	6.8	6.6	6.1	5.9	5.7

8.3.5 Buckling of Clamped Plates under Inplane Shear

The total potential energy expression for the clamped rectangular plate under inplane shear load N_{xy}^0 is

$$\begin{aligned} \Pi(w) &= \frac{1}{2} \int_0^b \int_0^a \left[D_{11} \left(\frac{\partial^2 w}{\partial x^2} \right)^2 + 2D_{12} \frac{\partial^2 w}{\partial x^2} \frac{\partial^2 w}{\partial y^2} + 4D_{66} \left(\frac{\partial^2 w}{\partial x \partial y} \right)^2 \right. \\ &\quad \left. + D_{22} \left(\frac{\partial^2 w}{\partial y^2} \right)^2 - 2N_{xy}^0 \left(\frac{\partial w}{\partial x} \frac{\partial w}{\partial y} \right) \right] dx dy \end{aligned} \quad (8.3.40)$$

The minimum total potential energy principle requires that $\delta\Pi = 0$. We have

$$\begin{aligned} 0 = \int_0^b \int_0^a & \left[D_{11} \frac{\partial^2 w}{\partial x^2} \frac{\partial^2 \delta w}{\partial x^2} + D_{12} \left(\frac{\partial^2 w}{\partial y^2} \frac{\partial^2 \delta w}{\partial x^2} + \frac{\partial^2 w}{\partial x^2} \frac{\partial^2 \delta w}{\partial y^2} \right) \right. \\ & + 4D_{66} \frac{\partial^2 w}{\partial x \partial y} \frac{\partial^2 \delta w}{\partial x \partial y} + D_{22} \frac{\partial^2 w}{\partial y^2} \frac{\partial^2 \delta w}{\partial y^2} \\ & \left. - N_{xy}^0 \left(\frac{\partial \delta w}{\partial x} \frac{\partial w}{\partial y} + \frac{\partial w}{\partial x} \frac{\partial \delta w}{\partial y} \right) \right] dx dy \end{aligned} \quad (8.3.41)$$

We assume a Ritz approximation of the form

$$w(x, y) \approx W_{MN}(x, y) = \sum_{j=1}^N \sum_{i=1}^M c_{ij} X_i(x) Y_j(y) \quad (8.3.42)$$

Substituting Eq. (8.3.42) into Eq. (8.3.41), we obtain

$$\begin{aligned} 0 = \sum_{j=1}^N \sum_{i=1}^M c_{ij} & \left\{ \int_0^b \int_0^a \left[D_{11} \frac{d^2 X_i}{dx^2} Y_j \frac{d^2 X_p}{dx^2} Y_q + D_{22} X_i \frac{d^2 Y_j}{dy^2} X_p \frac{d^2 Y_q}{dy^2} \right. \right. \\ & + 2\hat{D}_{12} \frac{dX_i}{dx} \frac{dY_j}{dy} \frac{dX_p}{dx} \frac{dY_q}{dy} \\ & \left. \left. - N_{xy}^0 \left(\frac{dX_i}{dx} Y_j X_p \frac{dY_q}{dy} + X_i \frac{dY_j}{dy} \frac{dX_p}{dx} Y_q \right) \right] dx dy \right\} c_{ij} \end{aligned} \quad (8.3.43a)$$

$$= \sum_{j=1}^N \sum_{i=1}^M c_{ij} \left(a_{(ij)(pq)} - N_{xy}^0 g_{(ij)(pq)} \right) c_{ij} \quad (8.3.43b)$$

Using the two-parameter approximation of the form

$$w(x, y) \approx c_{11} X_1(x) Y_1(y) + c_{22} X_2(x) Y_2(y) \quad (8.3.44)$$

with

$$\begin{aligned} X_1(x) &= \sin \frac{4.73x}{a} - \sinh \frac{4.73x}{a} + 1.0178 \left(\cosh \frac{4.73x}{a} - \cos \frac{4.73x}{a} \right) \\ X_2(x) &= \sin \frac{7.853x}{a} - \sinh \frac{7.853x}{a} + 0.9992 \left(\cosh \frac{7.853x}{a} - \cos \frac{7.853x}{a} \right) \\ Y_1(y) &= \sin \frac{4.73y}{b} - \sinh \frac{4.73y}{b} + 1.0178 \left(\cosh \frac{4.73y}{b} - \cos \frac{4.73y}{b} \right) \\ Y_2(y) &= \sin \frac{7.853y}{b} - \sinh \frac{7.853y}{b} + 0.9992 \left(\cosh \frac{7.853y}{b} - \cos \frac{7.853y}{b} \right) \end{aligned} \quad (8.3.45)$$

we obtain

$$\begin{bmatrix} b_{11} & -N_{xy}^0 b_{12} \\ -N_{xy}^0 b_{12} & b_{22} \end{bmatrix} \begin{Bmatrix} c_{11} \\ c_{22} \end{Bmatrix} = - \begin{Bmatrix} 0 \\ 0 \end{Bmatrix} \quad (8.3.46)$$

where

$$\begin{aligned} b_{11} &= \frac{537.181}{a^4} D_{11} + \frac{324.829}{a^2 b^2} \hat{D}_{12} + \frac{537.181}{b^4} D_{22}, \quad b_{12} = \frac{23.107}{ab} \\ b_{22} &= \frac{3791.532}{a^4} D_{11} + \frac{4227.255}{a^2 b^2} \hat{D}_{12} + \frac{3791.532}{b^4} D_{22} \end{aligned} \quad (8.3.47)$$

and $\hat{D}_{12} = D_{12} + 2D_{66}$. For a nontrivial solution, the determinant of the coefficient matrix in Eq. (8.3.46) should be zero, $b_{11}b_{22} - b_{12}b_{12}(N_{xy}^0)^2 = 0$. Solving for the buckling load N_{xy}^0 , we obtain

$$N_{xy}^0 = \pm \frac{1}{a_{12}} \sqrt{a_{11}a_{22}} \quad (8.3.48)$$

The \pm sign indicates that the shear buckling load may be either positive or negative.

For an isotropic square plate, we have $a = b$ and $D_{11} = D_{22} = (D_{12} + 2D_{66}) = D$, and the shear buckling load predicted by Eq. (8.3.48) is

$$N_{xy}^0 = \pm 176 \frac{D}{a^2} \quad (8.3.49)$$

whereas the “exact” critical buckling load is

$$N_{xy}^0 = \pm 145 \frac{D}{a^2} \quad (8.3.50)$$

The two-term Ritz solution (8.3.49) is over 21% in error.

8.4 Summary

In this chapter, buckling of rectangular plates under inplane loads is studied. Exact buckling loads using the Navier and Lévy solution methods and approximate buckling loads using the Ritz and Galerkin methods are obtained. The Ritz and Galerkin methods prove to be very powerful in obtaining approximate critical buckling loads of rectangular plates for boundary conditions for which the Navier and Lévy solution procedures do not apply. In particular, buckling loads of rectangular plates clamped on all four edges can be determined using the Ritz method.

Exact buckling loads of rectangular and polygonal plates with thickness changes or internal line hinges can be found in the book by Wang et al. (2005).

Problems

- 8.1** Consider buckling of uniformly compressed rectangular plates with edges $x = 0, a$ and $y = 0, b$ simply supported. The boundary conditions are

$$w = 0, \quad M_{yy} = -D_{12} \frac{\partial^2 w}{\partial x^2} - D_{22} \frac{\partial^2 w}{\partial y^2} = 0 \quad \text{at } y = 0, b$$

Use the boundary conditions (a) to show that the constants A through C in Eq. (8.2.7) are $A = C = 0$ and

$$B \sinh \lambda_1 b + D \sin \lambda_2 b = 0, \quad \lambda_1^2 B \sinh \lambda_1 b - \lambda_2^2 D \sin \lambda_2 b = 0$$

Show that the buckled form of equilibrium of the plate is possible only if

$$\lambda_2 = \frac{n\pi}{b} = \beta_n$$

Then, using Eq. (8.2.8b), show that

$$N_0(m, n) = \frac{1}{\alpha_m^2} \left(D_{11}\alpha_m^4 + 2\alpha_m^2\beta_n^2\hat{D}_{12} + D_{22}\beta_n^4 \right)$$

which is the same as Eq. (8.1.21).

- 8.2** Use the *state-space approach* of Problem 7.17 to find the general solution of Eq. (8.2.4) for the case of biaxial buckling. In particular, show that the characteristic equation is given by

$$\lambda^4 - C_2\lambda^2 - C_1 = 0$$

Hint: The constants C_1 and C_2 of Problem 7.17 for the present case are given by

$$C_1 = -\frac{1}{D_{11}} \left(D_{22}\beta_n^4 + \hat{N}_{yy}\beta_n^2 \right), \quad C_2 = \frac{2\beta_n^2\hat{D}_{12} + \hat{N}_{xx}}{D_{11}}$$

Then, find the eigenvalues of the matrix $[T]$.

- 8.3** Consider the buckling of uniformly compressed rectangular SSCS plates with sides $x = 0, a$ simply supported, side $y = 0$ clamped, and side $y = b$ simply supported. The boundary conditions are

$$w = 0, \quad \frac{\partial w}{\partial y} = 0 \quad \text{at } y = 0$$

$$w = 0, \quad M_{yy} = -D_{22}\frac{\partial^2 w}{\partial y^2} - D_{12}\frac{\partial^2 w}{\partial x^2} = 0 \quad \text{at } y = 0$$

Show that the characteristic equation is given by

$$\lambda_2 \tanh \lambda_1 b - \lambda_1 \tan \lambda_2 b = 0$$

- 8.4** Establish the following identities with the help of Eqs. (8.2.8a,b):

$$\Omega_1\bar{\Omega}_2 = \Omega_1^2, \quad \Omega_2\bar{\Omega}_1 = \Omega_2^2$$

where ($\bar{D}_{12} = D_{12} + 4D_{66}$)

$$\begin{aligned} \Omega_1 &= \lambda_1^2 - \frac{D_{12}}{D_{22}}\alpha_m^2, & \Omega_2 &= \lambda_2^2 + \frac{D_{12}}{D_{22}}\alpha_m^2 \\ \bar{\Omega}_1 &= \lambda_1^2 - \frac{\bar{D}_{12}}{D_{22}}\alpha_m^2, & \bar{\Omega}_2 &= \lambda_2^2 + \frac{\bar{D}_{12}}{D_{22}}\alpha_m^2 \end{aligned}$$

- 8.5** Establish the characteristic equation of SSSF plates, i.e., Eq. (8.2.12).
- 8.6** Derive the boundary condition on the *free edge* $y = b$ of a plate when it is biaxially compressed. *Hint:* Use Eqs. (3.5.11) and (3.5.15) to show that
- $$V_y(b) = \left(M_{yy,y} + 2M_{xy,x} + \hat{N}_{yy} \frac{\partial w}{\partial y} \right)_{y=b}$$
- 8.7** Derive the characteristic equation associated with a rectangular plate simply supported on edges $x = 0, a$, elastically restrained on edge $y = 0$ (i.e., $V + kw = 0$), and free on edge $y = b$.
- 8.8** Show that the one-parameter Ritz approximation (8.3.15) with X_i and Y_j defined by Eq. (8.3.17) yields the following critical buckling load for a simply supported plate under combined bending and compression

$$N_{cr} = \left(\frac{12b}{a^3} D_{11} + \frac{20}{ab} \hat{D}_{12} + \frac{12a}{b^3} D_{22} \right) \frac{1}{(1 - 0.5c_0)}$$

- 8.9** Show that the two-parameter Ritz approximation of the form in Eq. (8.3.21) yields the equations [see Eq. (8.3.27)]

$$\begin{aligned} & \left[\left(1 + \frac{a^2}{b^2} \right)^2 - N_0 \frac{a^2}{\pi^2 D} (1 - 0.5c_0) \right] c_{11} - N_0 c_0 \frac{16a^2}{9\pi^4 D} c_{12} = 0 \\ & -N_0 c_0 \frac{16a^2}{9\pi^4 D} c_{11} + \left[\left(1 + 4 \frac{a^2}{b^2} \right)^2 - N_0 \frac{a^2}{\pi^2 D} (1 - 0.5c_0) \right] c_{12} = 0 \end{aligned}$$

and show that the associated characteristic equation is

$$A\lambda^2 - B\lambda + C = 0$$

where $\lambda = N_0(a^2/\pi^2 D)$ and

$$\begin{aligned} A &= (1 - 0.5c_0)^2 - \left(\frac{16a^2}{9\pi^4 D} \right)^2 \\ B &= (1 - 0.5c_0) \left[\left(1 + \frac{a^2}{b^2} \right)^2 + \left(1 + 4 \frac{a^2}{b^2} \right)^2 \right] \\ C &= \left(1 + \frac{a^2}{b^2} \right)^2 \left(1 + 4 \frac{a^2}{b^2} \right)^2 \end{aligned}$$

- 8.10** Show that the first three equations of the system in Eq. (8.3.27) for $c_0 = 2$ are

$$\begin{aligned} & \left(1 + \frac{a^2}{b^2} \right)^2 c_{11} - \frac{32}{9} \frac{N_0 a^2}{\pi^4 D} c_{12} = 0 \\ & -\frac{32}{9} \frac{N_0 a^2}{\pi^4 D} c_{11} + \left(1 + 4 \frac{a^2}{b^2} \right)^2 c_{12} - \frac{96}{25} \frac{N_0 a^2}{\pi^4 D} c_{13} = 0 \\ & -\frac{96}{25} \frac{N_0 a^2}{\pi^4 D} c_{12} + \left(1 + 9 \frac{a^2}{b^2} \right)^2 c_{13} = 0 \end{aligned}$$

Dynamic Analysis of Rectangular Plates

9.1 Introduction

9.1.1 Governing Equations

The equation of motion governing the linear bending of elastic plates is given by Eq. (3.8.5). In the absence of thermal loads and without elastic foundation (i.e., $k = 0$), the equation reduces to

$$D_{11} \frac{\partial^4 w_0}{\partial x^4} + 2\hat{D}_{12} \frac{\partial^4 w_0}{\partial x^2 \partial y^2} + D_{22} \frac{\partial^4 w_0}{\partial y^4} + I_0 \frac{\partial^2 w_0}{\partial t^2} - I_2 \left(\frac{\partial^4 w_0}{\partial t^2 \partial x^2} + \frac{\partial^4 w_0}{\partial t^2 \partial y^2} \right) = q \quad (9.1.1)$$

where $\hat{D}_{12} = 2(D_{12} + 2D_{66})$ and

$$I_0 = \rho_0 h, \quad I_2 = \frac{\rho_0 h^3}{12} \quad (9.1.2)$$

We use Eq. (9.1.1) to determine the natural frequencies of vibration and the transient response of rectangular plates.

9.1.2 Natural Vibration

For natural vibration, the solution is assumed to be periodic

$$w_0(x, y, t) = w(x, y)e^{i\omega t} \quad (9.1.3)$$

where $i = \sqrt{-1}$ and ω is the frequency of natural vibration associated with mode shape w . Substituting Eq. (9.1.3) in Eq. (9.1.1) and setting $q = 0$, we obtain

$$\left\{ D_{11} \frac{\partial^4 w}{\partial x^4} + 2\hat{D}_{12} \frac{\partial^4 w}{\partial x^2 \partial y^2} + D_{22} \frac{\partial^4 w}{\partial y^4} - \omega^2 \left[I_0 w - I_2 \left(\frac{\partial^2 w}{\partial x^2} + \frac{\partial^2 w}{\partial y^2} \right) \right] \right\} e^{i\omega t} = 0 \quad (9.1.4)$$

which must hold for any time t . Hence, we have

$$D_{11} \frac{\partial^4 w}{\partial x^4} + 2\hat{D}_{12} \frac{\partial^4 w}{\partial x^2 \partial y^2} + D_{22} \frac{\partial^4 w}{\partial y^4} - \omega^2 \left[I_0 w - I_2 \left(\frac{\partial^2 w}{\partial x^2} + \frac{\partial^2 w}{\partial y^2} \right) \right] = 0 \quad (9.1.5)$$

We wish to find values of ω such that Eq. (9.1.5) has a nontrivial solution w .

9.1.3 Transient Analysis

The determination of the solution $w_0(x, y, t)$ of Eq. (9.1.1) for all times $t > 0$ under any applied load $q(x, y, t)$ is termed *transient response*. The transient response of rectangular plates can be determined by assuming that the solution is of the form

$$w_0(x, y, t) = w(x, y)T(t) \quad (9.1.6)$$

where $w(x, y)$ is only a function of the spatial coordinates x and y and T is a function of time t only (i.e., use the *separation of variables* technique). The Navier or Lévy methods can be used to determine the spatial part of the solution, and then the resulting ordinary differential equation in time is solved analytically or by a numerical method.

9.2 Natural Vibration of Simply Supported Plates

Consider a rectangular plate with all four sides simply supported. The boundary conditions of a simply supported plate can be expressed in terms of w as

$$w = 0, \quad \frac{\partial^2 w}{\partial x^2} = \frac{\partial^2 w}{\partial y^2} = 0 \quad (9.2.1)$$

on all four edges. In the Navier solution procedure, we assume a solution of the form

$$w(x, y) = W_{mn} \sin \frac{m\pi x}{a} \sin \frac{n\pi y}{b} \quad (9.2.2)$$

that satisfies the boundary conditions in Eq. (9.2.1). Equation (9.2.2) represents the mode shape of the plate for mode (m, n) and W_{mn} are the amplitudes of vibration. Substituting Eq. (9.2.2) into Eq. (9.1.5), we obtain the following relation for any m and n :

$$D_{11}\alpha_m^4 + 2\hat{D}_{12}\alpha_m^2\beta_n^2 + D_{22}\beta_n^4 - \omega^2 \left[I_0 + (\alpha_m^2 + \beta_n^2)I_2 \right] = 0 \quad (9.2.3)$$

where $\alpha_m = m\pi/a$ and $\beta_n = n\pi/b$. Solving Eq. (9.2.3) for ω , we obtain

$$\omega^2 = \frac{\pi^4}{\tilde{I}_0 b^4} \left[D_{11}m^4 \left(\frac{b}{a} \right)^4 + 2(D_{12} + 2D_{66})m^2n^2 \left(\frac{b}{a} \right)^2 + D_{22}n^4 \right] \quad (9.2.4)$$

where

$$\tilde{I}_0 = I_0 + I_2 \left[\left(\frac{m\pi}{a} \right)^2 + \left(\frac{n\pi}{b} \right)^2 \right] \quad (9.2.5)$$

For different values of m and n , there correspond a unique frequency ω_{mn} and mode shape given by Eq. (9.2.2). The smallest value of ω_{mn} is called the *fundamental frequency*. When the rotatory inertia I_2 is not zero, it is not easy to find the lowest natural frequency. Equation (9.2.4) shows that the rotatory (or rotary) inertia has the effect of reducing the magnitude of the frequency of vibration and its relative effect depends on m and n , degree of orthotropy, and the plate thickness-to-side ratio h/b . For most plates with $h/b < 0.1$, the rotary inertia may be neglected.

When the rotatory inertia I_2 is neglected, the frequency of a rectangular orthotropic plate is ($I_0 = \rho h$)

$$\omega_{mn}^2 = \frac{\pi^4}{\rho h b^4} \left[D_{11} m^4 \left(\frac{b}{a} \right)^4 + 2(D_{12} + 2D_{66}) m^2 n^2 \left(\frac{b}{a} \right)^2 + D_{22} n^4 \right] \quad (9.2.6)$$

For isotropic rectangular plates, when the rotatory inertia I_2 is neglected, we have

$$\omega_{mn} = \frac{\pi^2}{b^2} \sqrt{\frac{D}{\rho h}} \left(m^2 \frac{b^2}{a^2} + n^2 \right) \quad (9.2.7)$$

For a square isotropic plate, the expression reduces to

$$\omega_{mn} = \frac{\pi^2}{a^2} \sqrt{\frac{D}{\rho h}} (m^2 + n^2) \quad (9.2.8)$$

and the fundamental frequency is given by

$$\omega_{11} = \frac{2\pi^2}{a^2} \sqrt{\frac{D}{\rho h}} \quad (9.2.9)$$

Nondimensional frequencies, $\bar{\omega}_{mn} = \omega_{mn}(b^2/\pi^2)\sqrt{\rho h/D_{22}}$, of isotropic ($\nu = 0.25$) plates and orthotropic ($G_{12}/E_2 = 0.5$, $\nu_{12} = 0.25$) plates with modulus ratios $E_1/E_2 = 3$ and $E_1/E_2 = 10$ are presented in Table 9.2.1. The fundamental frequency increases with modular ratio E_1/E_2 . The effect of including rotary inertia is to decrease the frequency of vibration, and the effect is negligible for plates with $h/b < 0.1$. Figure 9.2.1 shows a plot of nondimensional fundamental frequency $\bar{\omega}_{11}$ as a function of plate aspect ratio a/b for isotropic and orthotropic plates. The natural frequency increases with the degree of orthotropy E_1/E_2 . For long plates, the frequency approaches that of a plate strip ($\bar{\omega}_{11} = 1.0$).

Table 9.2.1. Fundamental frequencies $\bar{\omega}_{11} = \omega_{11}(b^2/\pi^2)\sqrt{\rho h/D_{22}}$ of simply supported (SSSS) isotropic and orthotropic plates.[†]

a/b	Isotropic			$E_1/E_2 = 3$			$E_1/E_2 = 10$		
	w/o	0.01	0.1	w/o	0.01	0.1	w/o	0.01	0.1
0.5	5.000	4.999	4.900	7.670	7.669	7.517	13.075	13.072	12.814
1.0	2.000	2.000	1.984	2.541	2.541	2.521	3.672	3.672	3.643
1.5	1.444	1.444	1.436	1.639	1.639	1.629	2.020	2.020	2.008
2.0	1.250	1.250	1.244	1.342	1.342	1.336	1.499	1.499	1.491
2.5	1.160	1.160	1.154	1.213	1.212	1.207	1.286	1.286	1.280
3.0	1.111	1.111	1.106	1.145	1.145	1.139	1.183	1.183	1.178

[†] w/o = without rotary inertia; the second and third columns contain frequencies when the rotary inertia is included for $h/b = 0.01$ and 0.1, respectively.

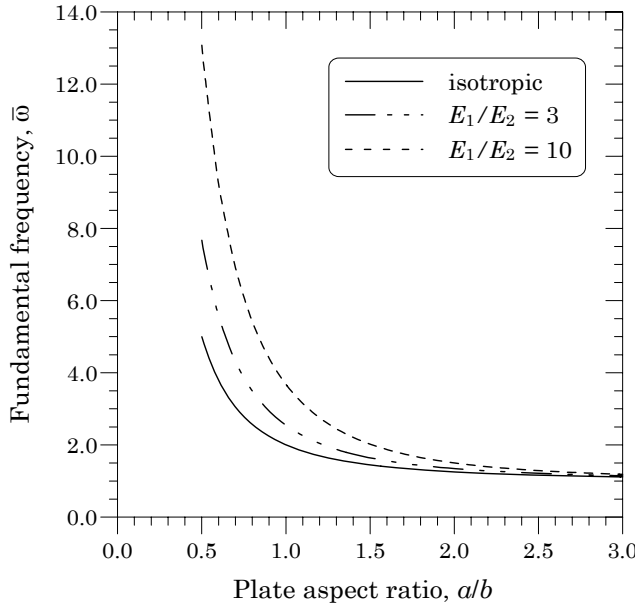


Figure 9.2.1 Nondimensional fundamental frequency versus aspect ratio for simply supported plates.

9.3 Natural Vibration of Plates with Two Parallel Sides Simply Supported

9.3.1 The Lévy Solution

The Lévy method introduced in the previous chapters can also be used to determine natural frequencies of rectangular plates for which two opposite edges are simply supported and the other two edges have any combination of fixed, hinged, and free boundary conditions.

Recall from Section 8.2 that in the Lévy method, the partial differential equation (9.1.5) is reduced to an ordinary differential equation in y by assuming solution in the form of a single Fourier series

$$w(x, y) = W_m(y) \sin \alpha_m x, \quad \alpha_m = \frac{m\pi}{a} \quad (9.3.1)$$

that satisfies the simply supported boundary conditions

$$w = 0, \quad M_{xx} = - \left(D_{11} \frac{\partial^2 w}{\partial x^2} + D_{12} \frac{\partial^2 w}{\partial y^2} \right) = 0 \quad \text{on } x = 0, a \quad (9.3.2)$$

Substituting Eq. (9.3.1) into Eq. (9.1.5), we obtain

$$\left[D_{11} \alpha_m^4 - \left(I_0 + \alpha_m^2 I_2 \right) \omega^2 \right] W - \left(2\alpha_m^2 \hat{D}_{12} - I_2 \omega^2 \right) \frac{d^2 W}{dy^2} + D_{22} \frac{d^4 W}{dy^4} = 0 \quad (9.3.3)$$

The ordinary differential equation (9.3.3) obtained in the Lévy method can be solved for the natural frequencies and mode shapes either analytically or by means of the Ritz method. We will discuss both procedures in the following sections. Since the effect of rotary inertia I_2 is negligible on the fundamental frequency in majority of cases, we will neglect it in the subsequent study.

9.3.2 Analytical Solution

The form of the solution to Eq. (9.3.3) depends on the nature of the roots λ of the equation

$$D_{22}\lambda^4 - 2\alpha_m^2 \hat{D}_{12}\lambda^2 + (\alpha_m^4 D_{11} - I_0\omega^2) = 0 \quad (9.3.4)$$

There are two cases: (1) the case in which $\omega^2 \geq \alpha_m^4 D_{11}/I_0$, and (2) the case in which $\omega^2 < \alpha_m^4 D_{11}/I_0$. The general solution of Eq. (9.3.3) when $\omega^2 \geq \alpha_m^4 D_{11}/I_0$ is given by [see Eq. (8.2.7)]

$$W_n(x) = A \cosh \lambda_1 y + B \sinh \lambda_1 y + C \cos \lambda_2 y + D \sin \lambda_2 y \quad (9.3.5)$$

and the solution for the case $\omega^2 < \alpha_m^4 D_{11}/I_0$ is given by

$$W_n(x) = A \cosh \lambda_1 y + B \sinh \lambda_1 y + C \cosh \lambda_2 y + D \sinh \lambda_2 y \quad (9.3.6)$$

where [see Eqs. (8.2.8a,b); replace $\alpha_m^2 N_0$ with $I_0\omega^2$]

$$\begin{aligned} (\lambda_1)^2 &= \sqrt{\omega^2 \frac{I_0}{D_{22}} - \alpha_m^4 \frac{D_{11}}{D_{22}} + \alpha_m^4 \left(\frac{\hat{D}_{12}}{D_{22}} \right)^2 + \frac{\hat{D}_{12}}{D_{22}} \alpha_m^2} \\ (\lambda_2)^2 &= \sqrt{\omega^2 \frac{I_0}{D_{22}} - \alpha_m^4 \frac{D_{11}}{D_{22}} + \alpha_m^4 \left(\frac{\hat{D}_{12}}{D_{22}} \right)^2 - \frac{\hat{D}_{12}}{D_{22}} \alpha_m^2} \end{aligned} \quad (9.3.7)$$

and A, B, C , and D are integration constants, which are determined using the boundary conditions. However, we do not actually determine these constants. Instead, the values of ω are determined by setting the determinant of the coefficient matrix of the four equations among the constants A, B, C and D to zero. The procedure is exactly parallel to that used in determining the buckling loads. Indeed, the characteristic equations derived in connection with the Lévy solutions of plates for various boundary conditions hold for natural vibrations as well for the correspondence

$$N_0 = \frac{I_0}{\alpha_m^2} \omega^2 \quad (9.3.8)$$

In the sections that follow, we present natural frequencies for rectangular plates with various boundary conditions.

9.3.3 Vibration of SSSF Plates

Consider natural vibrations of rectangular plates with sides $x = 0, a$ and $y = 0$ simply supported and side $y = b$ free, as shown in Figure 8.2.2. The boundary conditions on edges $y = 0, b$ are

$$w = 0, \quad M_{yy} = -\left(D_{12}\frac{\partial^2 w}{\partial x^2} + D_{22}\frac{\partial^2 w}{\partial y^2}\right) = 0 \quad \text{at } y = 0 \quad (9.3.9)$$

$$M_{yy} = 0, \quad V_y = -\left(D_{22}\frac{\partial^3 w}{\partial y^3} + \bar{D}_{12}\frac{\partial^3 w}{\partial x^2 \partial y}\right) = 0 \quad \text{at } y = b \quad (9.3.10)$$

where $\bar{D}_{12} = D_{12} + 4D_{66}$. It should be noted that when rotary inertia is included, the shear force V_y will include an additional term $-I_2\omega^2(dw/dy)$.

For the solution in Eq. (9.3.5), the boundary conditions in Eqs. (9.3.9) and (9.3.10) yield $A = C = 0$ and

$$\begin{aligned} -(\Omega_1 \sinh \lambda_1 b) B + (\Omega_2 \sin \lambda_2 b) D &= 0 \\ (\lambda_1 \bar{\Omega}_1 \cosh \lambda_1 b) B + (\lambda_2 \bar{\Omega}_2 \cos \lambda_2 b) D &= 0 \end{aligned} \quad (9.3.11)$$

where

$$\begin{aligned} \Omega_1 &= \left(\lambda_1^2 - \frac{D_{12}}{D_{22}}\alpha_m^2\right), \quad \Omega_2 = \left(\lambda_2^2 + \frac{D_{12}}{D_{22}}\alpha_m^2\right) \\ \bar{\Omega}_1 &= \left(\lambda_1^2 - \frac{\bar{D}_{12}}{D_{22}}\alpha_m^2\right), \quad \bar{\Omega}_2 = \left(\lambda_2^2 + \frac{\bar{D}_{12}}{D_{22}}\alpha_m^2\right) \end{aligned} \quad (9.3.12)$$

Setting the determinant of the coefficient matrix of the two equations in (9.3.11) to zero, we obtain the following characteristic equation for the natural vibration of SSSF plates:

$$\lambda_2 \Omega_1 \bar{\Omega}_2 \sinh \lambda_1 b \cos \lambda_2 b - \lambda_1 \Omega_2 \bar{\Omega}_1 \cosh \lambda_1 b \sin \lambda_2 b = 0 \quad (9.3.13)$$

For the solution in Eq. (9.3.6), the boundary conditions in Eqs. (9.3.9) and (9.3.10) yield $A = C = 0$ and

$$\begin{aligned} (\Omega_1 \sinh \lambda_1 b) B + (\Omega_3 \sin \lambda_3 b) D &= 0 \\ (\lambda_1 \bar{\Omega}_1 \cosh \lambda_1 b) B + (\lambda_3 \bar{\Omega}_3 \cos \lambda_3 b) D &= 0 \end{aligned} \quad (9.3.14)$$

which results in the characteristic equation

$$\lambda_2 \Omega_1 \bar{\Omega}_3 \sinh \lambda_1 b \cosh \lambda_3 b - \lambda_1 \Omega_3 \bar{\Omega}_1 \cosh \lambda_1 b \sinh \lambda_3 b = 0 \quad (9.3.15)$$

$$\Omega_3 = \left(\lambda_3^2 - \frac{D_{12}}{D_{22}}\alpha_m^2\right), \quad \bar{\Omega}_3 = \left(\lambda_3^2 - \frac{\bar{D}_{12}}{D_{22}}\alpha_m^2\right) \quad (9.3.16)$$

Equations (9.3.13) and (9.3.15) can be solved iteratively using, for example, the bisection method for the roots ω_{mn} for a given m once the geometric and material parameters of the plate are known. Here, m gives the number of half-sine waves in the x -direction, and n is the n th lowest frequency for a given value of m . Care must be taken in the iterative procedure not to miss any roots, from the least to a desired number. The mode shape for the case $\omega^2 > \alpha_m^4 D_{11}/I_0$ is given by

$$w(x, y) = (\Omega_1 \sinh \lambda_1 b \sin \lambda_2 y + \Omega_2 \sinh \lambda_1 y \sin \lambda_2 b) \sin \alpha_m x \quad (9.3.17)$$

and for the case $\omega^2 < \alpha_m^4 D_{11}/I_0$, it is given by

$$w(x, y) = (\Omega_1 \sinh \lambda_1 b \sinh \lambda_2 y + \Omega_2 \sinh \lambda_1 y \sinh \lambda_2 b) \sin \alpha_m x \quad (9.3.18)$$

For the SSSF plates there exist no real roots of Eq. (9.3.15).

Table 9.3.1 contains the first seven natural frequencies $\bar{\omega}$ of isotropic ($\nu = 0.25$) and orthotropic plates for various aspect ratios. The following material properties were used for orthotropic plates:

$$E_1 = 3E_2 \text{ and } 10E_2, \quad G_{12} = 0.5E_2, \quad \nu_{12} = 0.25 \quad (9.3.19)$$

Table 9.3.1. Effect of plate aspect ratio and modulus ratio on the nondimensional frequencies of rectangular plates (SSSF) [$\bar{\omega}_{mn} = \omega_{mn}a^2(\sqrt{\rho h/D_{22}})$].

$\frac{E_1}{E_2}$	(m, n)	Mode					
		Plate aspect ratio, $\frac{a}{b}$					
0.5	1.0	1.5	2.0	2.5	3.0		
1	(1,1)	10.356	11.820	13.950	16.491	19.278	22.217
	(1,2)	14.860	27.995	48.195	75.678	110.653	153.226
	(1,3)	23.742	62.076	124.811	212.363	324.839	462.273
	(2,1)	39.884	41.422	43.939	47.278	51.280	55.801
	(2,2)	44.650	59.437	82.156	111.981	148.811	192.779
	(2,3)	54.074	94.969	159.641	248.304	361.421	499.245
	(3,1)	89.131	90.628	93.200	96.752	101.181	106.376
3	(1,1)	17.471	18.629	20.447	22.770	25.461	28.412
	(1,2)	21.038	33.066	52.768	80.024	114.882	157.387
	(1,3)	28.884	66.067	128.423	215.816	328.213	465.602
	(2,1)	68.714	69.882	71.834	74.515	77.859	81.786
	(2,2)	72.220	84.150	104.267	132.266	167.896	211.074
	(2,3)	79.569	115.536	177.233	264.268	376.446	513.691
	(3,1)	154.139	155.280	157.234	159.973	163.462	167.660
10	(1,1)	31.421	32.089	33.192	34.693	36.541	38.686
	(1,2)	33.558	42.220	59.019	84.358	118.016	159.757
	(1,3)	38.999	71.181	131.225	217.577	365.412	466.531
	(2,1)	125.029	125.684	126.795	128.355	130.352	132.769
	(2,2)	127.012	134.232	147.800	168.878	198.202	236.077
	(2,3)	131.375	155.997	206.153	284.726	391.315	524.901
	(3,1)	281.055	281.692	282.789	284.342	286.347	288.798

9.3.4 Vibration of SSCF Plates

Next, consider vibration of rectangular plates with sides $x = 0, a$ simply supported, side $y = 0$ clamped, and side $y = b$ free (Figure 8.2.3). The boundary conditions on edges $y = 0, b$ are

$$w = 0, \quad \frac{\partial w}{\partial y} = 0 \quad \text{at } y = 0 \quad (9.3.20)$$

$$M_{yy} = 0, \quad V_y = -D_{22} \frac{\partial^3 w}{\partial y^3} - \bar{D}_{12} \frac{\partial^3 w}{\partial x^2 \partial y} = 0 \quad \text{at } y = b \quad (9.3.21)$$

Substitution of Eq. (9.3.5) into the boundary conditions (9.3.20) and (9.3.21) results in the following characteristic equation:

$$2\Omega_1\Omega_2 + (\Omega_1^2 + \Omega_2^2) \cosh \lambda_1 b \cos \lambda_2 b - \frac{1}{\lambda_1 \lambda_2} (\lambda_1^2 \Omega_2^2 - \lambda_2^2 \Omega_1^2) \sinh \lambda_1 b \sin \lambda_2 b = 0 \quad (9.3.22)$$

Tables 9.3.2 and 9.3.3 contain natural frequencies of isotropic and orthotropic plates, respectively. Table 9.3.2 contains the first five roots (i.e., $n = 1, 2, \dots, 5$) of Eq. (9.3.22) for $m = 1, 2, \dots, 6$ and for aspect ratios $a/b = 0.5, 1.0, 1.5$, and 2.0 of isotropic plates. The first six roots for $m = 1, 2, 3$ are presented in Table 9.3.3 for orthotropic plates. The orthotropic material properties used are

$$E_1 = 3E_2 \text{ and } 10E_2, \quad G_{12} = 0.4E_2, \quad \nu_{12} = 0.25 \quad (9.3.23)$$

Table 9.3.2. Effect of plate aspect ratio on the nondimensional frequencies $\bar{\omega}_{mn} = \omega_{mn}b^2(\sqrt{\rho h/D})$ of isotropic ($\nu = 0.25$) rectangular plates (SSCF).

$\frac{a}{b}$	m	$\bar{\omega}_{mn} = \omega_{mn}b^2\sqrt{\rho h/D}$ for values of n					
		1	2	3	4	5	6
0.5	1	41.958	63.434	103.670	162.867	241.577	340.009
	2	159.782	180.971	222.271	282.892	362.616	461.579
	3	356.671	377.544	418.698	479.750	560.319	660.219
	4	632.519	653.260	694.146	755.122	835.918	936.313
	5	987.303	1008.030	1048.700	1109.490	1190.240	1290.780
1.0	1	12.862	33.317	72.605	131.592	210.391	308.977
	2	41.958	63.434	103.670	162.867	241.577	340.009
	3	90.971	112.381	153.435	213.415	292.520	391.068
	4	159.782	180.971	222.271	282.892	362.616	461.579
	5	248.354	269.358	310.630	371.576	451.818	551.286
2.0	1	5.810	25.036	64.462	123.589	202.499	301.164
	2	12.862	33.317	72.605	131.592	210.391	308.977
	3	24.907	46.116	85.774	144.752	223.456	321.948
	4	41.958	63.434	103.670	162.867	241.577	340.009
	5	63.985	85.478	126.208	185.779	264.631	363.077

Note that frequencies of certain mode and aspect ratios are identical to those of another mode and aspect ratio. For example, the frequencies ω_{1n} for aspect ratio $a/b = 0.5$ are identical to ω_{2n} for aspect ratio $a/b = 1.0$, ω_{3n} for aspect ratio $a/b = 1.5$, and ω_{4n} for aspect ratio $a/b = 2.0$. Similar correspondence can be found among other frequencies of Tables 9.3.2 and 9.3.3. The effect of orthotropy on the frequencies is to increase their magnitude. The increase is more in the fundamental and lower modes, and it is almost negligible in higher modes.

Table 9.3.3. Effect of the plate aspect ratio and the modulus ratio on the nondimensional frequencies $\bar{\omega}_{mn} = \omega_{mn} b^2 (\sqrt{\rho h / D_{22}})$ of orthotropic rectangular plates (SSCF).

$\frac{a}{b}$	m	$\bar{\omega}_{mn} = \omega_{mn} b^2 \sqrt{\rho h / D_{22}}$ for values of n					
		1	2	3	4	5	6
Modulus ratio, $E_1/E_2 = 3$							
0.5	1	69.901	84.921	118.563	173.237	249.143	345.828
	2	274.662	287.897	316.217	362.353	428.564	516.092
	3	616.269	628.968	655.256	696.923	755.968	834.208
1.0	1	19.042	36.395	74.275	132.684	211.209	309.646
	2	69.901	84.921	118.563	173.237	249.143	345.828
	3	155.162	168.997	199.340	249.263	320.417	413.114
1.5	1	9.880	28.126	67.051	125.991	204.806	303.416
	2	32.143	48.577	85.092	142.573	220.542	318.636
	3	69.901	84.921	118.563	173.237	249.143	345.828
2.0	1	6.828	25.381	64.654	123.733	202.622	301.276
	2	19.042	36.395	74.275	132.684	211.209	309.646
	3	40.145	56.166	91.948	148.825	226.397	324.236
Modulus ratio, $E_1/E_2 = 10$							
0.5	1	125.694	134.707	158.222	202.607	270.537	361.680
	2	500.009	507.477	524.214	553.485	599.190	664.909
	3	1124.060	1131.150	1146.130	1170.670	1207.040	1257.870
1.0	1	32.331	44.871	78.843	135.351	212.940	310.868
	2	125.694	134.707	158.222	202.607	270.537	361.680
	3	281.625	289.557	308.403	342.994	397.943	475.999
1.5	1	15.254	30.479	68.106	126.582	205.192	303.694
	2	56.477	67.279	97.091	150.134	225.581	322.211
	3	125.694	134.707	158.222	202.607	270.537	361.680
2.0	1	94.590	26.242	65.017	123.939	202.759	301.378
	2	32.331	44.871	78.843	135.351	212.940	310.868
	3	71.171	81.370	109.294	160.232	234.148	329.778

9.3.5 Vibration of SSCC Plates

The boundary conditions on edges $y = 0, b$ of SSCC rectangular plates (with sides $x = 0, a$ simply supported and sides $y = 0, b$ clamped; see Figure 8.2.6) are

$$w = 0, \quad \frac{\partial w}{\partial y} = 0 \quad (9.3.24)$$

Substitution of Eq. (9.3.5) into Eq. (9.3.24) yields the following characteristic equation:

$$2(1 - \cosh \lambda_1 b \cos \lambda_2 b) + \left(\frac{\lambda_1}{\lambda_2} - \frac{\lambda_2}{\lambda_1}\right) \sinh \lambda_1 b \sin \lambda_2 b = 0 \quad (9.3.25)$$

The frequency equation obtained with Eq. (9.3.6) is

$$2(1 - \cosh \lambda_1 b \cosh \lambda_2 b) + \left(\frac{\lambda_1}{\lambda_2} + \frac{\lambda_2}{\lambda_1}\right) \sinh \lambda_1 b \sinh \lambda_2 b = 0 \quad (9.3.26)$$

and it does not have any roots when $\rho h \omega^2 < \alpha_m^4 (D_{11}/D_{22})$.

The first six roots of Eq. (9.3.25) for $m = 1, 2, \dots, 6$ and for $a/b = 0.5, 1.0, 1.5$, and 2.0 of isotropic ($\nu = 0.25$) rectangular plates are presented in Table 9.3.4. The first five frequencies for modulus ratios $E_1/E_2 = 1, 3$, and 10 ($\nu_{12} = 0.25$ and $G_{12} = 0.4$) are listed in Table 9.3.5.

Table 9.3.4. Effect of plate aspect ratio on the frequencies ($\bar{\omega}_{mn}$) of isotropic ($\nu = 0.25$) rectangular plates (SSCC).

		$\bar{\omega}_{mn} = \omega_{mn} b^2 \sqrt{\rho h / D}$ for values of n					
$\frac{a}{b}$	m	1	2	3	4	5	6
0.5	1	54.743	94.585	154.775	234.585	333.952	452.911
	2	170.346	206.696	265.195	344.536	444.034	563.379
	3	366.816	401.078	457.437	535.161	633.640	752.449
	4	642.726	730.684	806.895	904.072	1021.870	1160.010
	5	1084.000	1255.060	1371.790	1509.030	1666.580	1844.290
	6	1431.870	1463.800	1516.910	1591.070	1686.130	1801.920
1.0	1	28.951	69.327	129.095	208.391	307.316	425.914
	2	54.743	94.585	154.775	234.585	333.952	452.911
	3	102.216	140.204	199.809	279.650	379.267	498.532
	4	170.346	206.696	265.195	344.536	444.034	563.379
	5	258.613	293.755	351.112	429.676	528.750	647.924
	6	366.816	401.078	457.437	535.161	633.640	752.449
2.0	1	23.815	63.534	122.930	201.982	300.739	419.218
	2	28.951	69.327	129.095	208.391	307.316	425.914
	3	39.089	79.525	139.622	219.207	318.354	437.124
	4	54.743	94.585	154.775	234.585	333.952	452.911
	5	75.841	114.779	174.785	254.686	354.221	473.354
	6	102.216	140.204	199.809	279.650	379.267	498.532

Table 9.3.5. Effect of modulus ratio on the first five nondimensional frequencies ($\bar{\omega}_{mn}$) of square plates (SSCC).

$\frac{E_1}{E_2}$	$\bar{\omega}_{mn} = \omega_{mn}a^2(\sqrt{\rho h/D_{22}})$ for (m, n)				
1	28.951 ^(1,1)	54.743 ^(2,1)	69.327 ^(1,2)	94.585 ^(2,2)	102.216 ^(3,1)
3	32.263 ^(1,1)	70.930 ^(1,2)	78.386 ^(2,1)	110.370 ^(2,2)	130.098 ^(1,3)
10	41.539 ^(1,1)	75.654 ^(1,2)	130.632 ^(2,1)	132.778 ^(1,3)	152.094 ^(2,2)

9.3.6 Vibration of SSCS Plates

The boundary conditions on edges $y = 0, b$ of SSCS rectangular plates (with sides $x = 0, a$ and $y = b$ simply supported and side $y = 0$ clamped) are

$$w = 0, \quad \frac{\partial w}{\partial y} = 0 \quad \text{at } y = 0 \quad (9.3.27a)$$

$$w = 0, \quad M_{yy} = -\left(D_{12}\frac{\partial^2 w}{\partial x^2} + D_{22}\frac{\partial^2 w}{\partial y^2}\right) = 0 \quad \text{at } y = b \quad (9.3.27b)$$

These boundary conditions in conjunction with the solution in Eq. (9.3.5) yield the characteristic equation

$$\lambda_1 \cosh \lambda_1 b \sin \lambda_2 b - \lambda_2 \sinh \lambda_1 b \cos \lambda_2 b = 0 \quad (9.3.28)$$

The frequency equation obtained with Eq. (9.3.6) is

$$\lambda_1 \cosh \lambda_1 b \sinh \lambda_2 b - \lambda_2 \sinh \lambda_1 b \cosh \lambda_2 b = 0 \quad (9.3.29)$$

and it does not have any roots when $\rho h \omega^2 < \alpha_m^4 (D_{11}/D_{22})$. The mode shapes associated with the frequencies obtained from Eq. (9.3.28) are

$$w(x, y) = (\sin \lambda_2 b \sinh \lambda_1 y - \sinh \lambda_1 b \sin \lambda_2 y) \sin \alpha_m x \quad (9.3.30)$$

The first six frequencies for modulus ratios $E_1/E_2 = 1, 3$, and 10 ($\nu_{12} = 0.25$ and $G_{12} = 0.5$) are listed in Table 9.3.6, and the first six roots of Eq. (9.3.28) for $m = 1, 2, \dots, 6$ and for $a/b = 0.5, 1.0, 1.5$, and 2.0 of isotropic ($\nu = 0.25$) rectangular plates are presented in Table 9.3.7.

Table 9.3.6. Effect of the modulus ratio on the first six nondimensional frequencies ($\bar{\omega}_{mn}$) of square plates (SSCS).

$\frac{E_1}{E_2}$	$\bar{\omega}_{mn} = \omega_{mn}a^2(\sqrt{\rho h/D_{22}})$ for (m, n)					
1	23.646 ^(1,1)	51.674 ^(2,1)	58.646 ^(1,2)	86.134 ^(2,2)	100.270 ^(3,1)	113.228 ^(1,3)
3	28.365 ^(1,1)	61.867 ^(1,2)	77.345 ^(2,1)	106.306 ^(2,2)	115.933 ^(1,3)	156.998 ^(2,3)
10	38.596 ^(1,1)	67.244 ^(1,2)	118.951 ^(1,3)	130.017 ^(2,1)	149.195 ^(2,2)	188.854 ^(2,3)

Table 9.3.7. Effect of the plate aspect ratio on the nondimensional frequencies of isotropic ($\nu = 0.25$) rectangular plates (SSCS).

$\frac{a}{b}$	m	$\bar{\omega}_{mn} = \omega_{mn} b^2 \sqrt{\rho h / D}$ for values of n					
		1	2	3	4	5	6
0.5	1	86.134	140.846	215.294	309.403	423.178	556.634
	2	168.959	201.725	255.469	329.574	423.682	537.614
	3	365.950	450.482	523.760	617.315	730.935	864.474
	4	642.100	673.388	725.392	797.937	890.842	1003.940
	5	997.288	1028.250	1079.770	1151.750	1244.090	1356.660
	6	1431.470	1462.210	1513.390	1584.950	1676.830	1788.940
1.0	1	23.646	58.646	113.228	187.437	281.322	394.910
	2	51.674	86.134	140.846	215.294	309.403	423.178
	3	100.270	133.791	188.113	262.517	356.723	470.639
	4	168.959	201.725	255.469	329.574	423.682	537.614
	5	257.544	289.762	342.950	416.648	510.515	624.335
	6	365.950	397.768	450.482	523.760	617.315	730.935
1.5	1	18.901	53.776	108.221	182.335	276.156	389.697
	2	30.668	65.616	120.305	194.612	288.574	402.221
	3	51.674	86.134	140.846	215.294	309.403	423.178
	4	81.822	115.645	170.135	244.589	338.784	452.665
	5	120.947	154.191	208.327	282.652	376.845	490.782
	6	168.959	201.725	255.469	329.574	423.682	537.614
2.0	1	17.332	52.098	106.479	180.555	274.350	387.874
	2	23.646	58.646	113.228	187.437	281.322	394.910
	3	35.051	69.912	124.633	198.986	292.988	406.666
	4	51.674	86.134	140.846	215.294	309.403	423.178
	5	73.439	107.420	161.982	236.448	330.630	444.488
	6	100.270	133.791	188.113	262.517	356.723	470.639
3.0	1	16.252	50.909	105.238	179.285	273.061	386.572
	2	18.901	53.776	108.221	182.335	276.156	389.687
	3	23.646	58.646	113.228	187.437	281.322	394.910
	4	30.668	65.616	120.305	194.612	288.574	402.221
	5	40.015	74.762	129.497	203.889	297.929	411.639
	6	51.674	86.134	140.846	215.294	309.403	423.178

9.3.7 Vibration of SSFF Plates

The boundary conditions on edges $y = 0, b$ of SSFF rectangular plates (with sides $x = 0, a$ simply supported and sides $y = 0, b$ free) are

$$M_{yy} = - \left(D_{12} \frac{\partial^2 w}{\partial x^2} + D_{22} \frac{\partial^2 w}{\partial y^2} \right) = 0 \quad \text{at } y = 0, b \quad (9.3.31a)$$

$$V_y = - \left(D_{22} \frac{\partial^3 w}{\partial y^3} + \bar{D}_{12} \frac{\partial^3 w}{\partial x^2 \partial y} \right) = 0 \quad \text{at } y = 0, b \quad (9.3.31b)$$

These boundary conditions in conjunction with the solution in Eq. (9.3.5) yield the characteristic equation

$$2(1 - \cosh \lambda_1 b \cos \lambda_2 b) + \left(\mu_0 - \frac{1}{\mu_0} \right) \sinh \lambda_1 b \sin \lambda_2 b = 0 \quad (9.3.32)$$

where

$$\mu_0 = \frac{\lambda_1 \Omega_2 \bar{\Omega}_1}{\lambda_2 \bar{\Omega}_1 \bar{\Omega}_2} \quad (9.3.33)$$

and Ω_i and $\bar{\Omega}_i$ are defined by Eqs. (9.3.12). The frequency equation obtained with Eq. (9.3.6) is

$$2(1 - \cosh \lambda_1 b \cosh \lambda_2 b) + \left(\mu_0 + \frac{1}{\mu_0} \right) \sinh \lambda_1 b \sinh \lambda_2 b = 0 \quad (9.3.34)$$

which does have some roots when $\rho h \omega^2 < \alpha_m^4(D_{11}/D_{22})$.

The first eight frequencies for modulus ratios $E_1/E_2 = 1, 3$, and 10 ($\nu_{12} = 0.25$ and $G_{12} = 0.5$) are listed in Table 9.3.8. For $E_1/E_2 = 1$ and 3 , the frequencies ω_{11} , ω_{21} , and ω_{31} are the only frequencies among the first nine frequencies of SSFF plates with $\rho h \omega^2 < \alpha_m^4(D_{11}/D_{22})$ [i.e., roots of Eq. (9.3.34)]. The remaining frequencies are the roots of Eq. (9.3.32). For $E_1/E_2 = 10$, there are no roots of Eq. (9.3.34). Table 9.3.9 contains the first five roots of Eq. (9.3.32) or Eq. (9.3.34), whichever is the minimum, for $m = 1, 2, \dots, 4$ and for $a/b = 0.5, 0.6, 0.8, 1.0$, and 2.0 of isotropic ($\nu = 0.3$) rectangular plates.

Finally, Figure 9.3.1 contains plots of frequency parameters $\bar{\omega} = \omega_{mn} a^2(\sqrt{\rho h/D})$ for various plate aspect ratios a/b of a rectangular isotropic ($\nu = 0.3$) plate. Each set of three curves corresponds to $n = 1, 2$, and 3 , and the three sets corresponds to $m = 1, 2$, and 3 . The intersections indicate that two modes can exist simultaneously. For example, the third root for $m = 1$ and the second root for $m = 2$ can exist simultaneously for a plate having an a/b ratio of approximately 1.25.

Table 9.3.8. Effect of the modulus ratio on the first eight natural frequencies ($\bar{\omega}_{mn}$) of square plates (SSFF).

$\frac{E_1}{E_2}$	$\bar{\omega}_{mn} = \omega_{mn} a^2(\sqrt{\rho h/D_{22}})$ for (m, n)							
	ω_{11}	ω_{12}	ω_{13}	ω_{21}	ω_{22}	ω_{23}	ω_{31}	ω_{32}
1	9.710 [†]	16.491	37.176	39.128 [†]	47.278	71.559	88.282 [†]	96.752
3	17.013 [†]	22.770	42.319	68.204 [†]	74.515	95.091	153.583 [†]	159.973
10	34.693	49.863	84.358	128.355	141.431	168.878	284.342	296.666

[†] Frequencies computed using Eq. (9.3.34); all other frequencies are computed using Eq. (9.3.32).

Table 9.3.9. Effect of the plate aspect ratio on the nondimensional frequencies of isotropic ($\nu = 0.3$) rectangular plates (SSFF).

		$\bar{\omega}_{mn} = \omega_{mn}a^2\sqrt{\rho h/D}$ for values of n				
$\frac{a}{b}$	m	1	2	3	4	5
0.5	1	9.736	11.684	17.685	27.756	42.384
	2	39.188	41.196	47.966	59.065	74.525
	3	88.363	90.294	97.342	108.918	125.016
	4	157.260	159.080	166.291	178.095	194.542
0.6	1	9.713	12.434	20.715	34.935	55.909
	2	39.138	42.042	51.556	67.149	88.991
	3	88.287	91.133	101.118	117.513	140.301
	4	157.159	159.888	170.125	186.928	210.311
0.8	1	9.670	14.170	27.943	52.748	90.033
	2	39.040	44.147	60.249	86.824	124.707
	3	88.135	93.289	110.481	138.656	177.963
	4	156.955	162.014	179.766	208.911	249.424
1.0	1	9.631	16.135	36.725	75.283	133.704
	2	38.945	46.738	70.739	111.024	169.537
	3	87.987	96.040	122.039	164.694	224.756
	4	156.752	164.786	191.866	236.260	298.100
2.0	1	9.512	27.522	105.489	260.870	496.633
	2	38.525	64.538	146.901	301.132	534.817
	3	87.285	116.831	206.579	363.202	596.068
	4	155.780	186.951	282.958	444.097	678.146

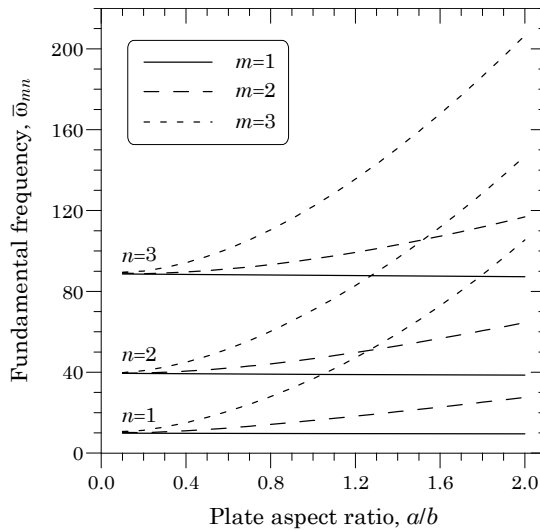


Figure 9.3.1 Plots of the frequency parameters $\omega_{mn}a^2(\sqrt{\rho h/D})$ for various a/b ratios of isotropic ($\nu = 0.3$) rectangular plates (SSFF).

9.3.8 The Ritz Solutions

As discussed in Section 8.3.1, Eq. (9.3.3) can also be solved using the Ritz method. The weak form of Eq. (9.3.3) is given by

$$\begin{aligned} & \int_0^b \left[D_{22} \frac{d^2 W}{dy^2} \frac{d^2 \delta W}{dy^2} + k_1 \frac{dW}{dy} \frac{d\delta W}{dy} + k_2 W \delta W \right] dy \\ & + \left[\left(D_{22} \frac{d^3 W}{dy^3} - k_1 \frac{dW}{dy} \right) \delta W - D_{22} \frac{d^2 W}{dy^2} \frac{d\delta W}{dy} \right]_0^b = 0 \end{aligned} \quad (9.3.35)$$

where

$$k_1 = \left(2\alpha_m^2 \hat{D}_{12} - I_2 \omega^2 \right), \quad k_2 = \left[D_{11} \alpha_m^4 - \left(I_0 + \alpha_m^2 I_2 \right) \omega^2 \right] \quad (9.3.36)$$

For a simply supported edge [$W = 0$ and $(d^2 W/dy^2) = 0$] or a clamped edge [$W = 0$ and $(dW/dy) = 0$], the boundary terms in Eq. (9.3.35) vanish identically. However, for a free edge the vanishing of bending moment and effective shear force require

$$D_{22} \frac{d^2 W}{dy^2} - \alpha_m^2 \bar{D}_{12} W = 0, \quad D_{22} \frac{d^3 W}{dy^3} - \alpha_m^2 \bar{D}_{12} \frac{dW}{dy} = 0 \quad (9.3.37)$$

where $\bar{D}_{12} = D_{12} + 4D_{66}$. These conditions can be used, as shown in Eqs. (8.3.3)–(8.3.5), to simplify the weak form (9.3.35) for various boundary conditions on sides $y = 0, b$.

Assume an N -parameter Ritz approximation of the form

$$W(y) \approx \sum_{j=1}^N c_j \varphi_j(y) \quad (9.3.38)$$

where φ_j are the functions given in Eqs. (7.3.10)–(7.3.20). Substituting the approximation (9.3.38) into the simplified weak form (9.3.35), we obtain

$$([R] - \omega^2 [B]) \{c\} = \{0\} \quad (9.3.39)$$

where [cf. Eq. (8.3.8a,b)]

$$\begin{aligned} R_{ij} &= \int_0^b \left(D_{22} \frac{d^2 \varphi_i}{dy^2} \frac{d^2 \varphi_j}{dy^2} + 2\alpha_m^2 \hat{D}_{12} \frac{d\varphi_i}{dy} \frac{d\varphi_j}{dy} + D_{11} \alpha_m^4 \varphi_i \varphi_j \right) dy \\ &- \alpha_m^2 D_{12} \left[\varphi_j \frac{d\varphi_i}{dy} + \frac{d\varphi_j}{dy} \varphi_i \right]_0^b \end{aligned} \quad (9.3.40a)$$

$$B_{ij} = \int_0^b \left[I_2 \alpha_m^2 \frac{d\varphi_i}{dy} \frac{d\varphi_j}{dy} + (I_0 + \alpha_m^2 I_2) \varphi_i \varphi_j \right] dy \quad (9.3.40b)$$

where the boundary term in the expression for R_{ij} is zero for SSSS, SSCC, and SSCS plates.

Equation (9.3.39) is an eigenvalue problem much the same way as Eq. (8.3.9), and it can be solved for the first n frequencies ω_{mn}^2 for any choice of m . Due to the similarity of the buckling problem and natural vibration problem, we will not discuss any examples of application of Eq. (9.3.39).

9.4 Natural Vibration of Plates with General Boundary Conditions

9.4.1 The Ritz Solution

In the preceding sections, we discussed analytical solutions based on the Navier solution method for plates with all sides simply supported and solutions based on the Lévy method for plates with two opposite edges simply supported while the other two had any combination of simple support, clamped, and free edge conditions. For rectangular plates with boundary conditions that do not fall into the above categories (e.g., a plate with all four edges clamped), the natural frequencies may be computed using approximate methods. Here, we consider the Ritz method of solution.

The weak form of Eq. (9.1.5) governing plates undergoing natural vibration can be expressed as [cf. Eq. (8.3.10)]

$$0 = \int_0^b \int_0^a \left\{ D_{11} \frac{\partial^2 w}{\partial x^2} \frac{\partial^2 \delta w}{\partial x^2} + D_{12} \left(\frac{\partial^2 w}{\partial y^2} \frac{\partial^2 \delta w}{\partial x^2} + \frac{\partial^2 w}{\partial x^2} \frac{\partial^2 \delta w}{\partial y^2} \right) \right. \\ \left. + 4D_{66} \frac{\partial^2 w}{\partial x \partial y} \frac{\partial^2 \delta w}{\partial x \partial y} + D_{22} \frac{\partial^2 w}{\partial y^2} \frac{\partial^2 \delta w}{\partial y^2} \right. \\ \left. - \omega^2 \left[I_0 w \delta w + I_2 \left(\frac{\partial w}{\partial x} \frac{\partial \delta w}{\partial x} + \frac{\partial w}{\partial y} \frac{\partial \delta w}{\partial y} \right) \right] \right\} dx dy \quad (9.4.1)$$

Using an N -parameter Ritz solution of the form

$$w(x, y) \approx \sum_{j=1}^N c_j \varphi_j(x, y) \quad (9.4.2)$$

in Eq. (9.4.1), we obtain

$$([R] - \omega^2[B]) \{c\} = \{0\} \quad (9.4.3)$$

where

$$R_{ij} = \int_0^b \int_0^a \left[D_{11} \frac{\partial^2 \varphi_i}{\partial x^2} \frac{\partial^2 \varphi_j}{\partial x^2} + D_{12} \left(\frac{\partial^2 \varphi_i}{\partial y^2} \frac{\partial^2 \varphi_j}{\partial x^2} + \frac{\partial^2 \varphi_i}{\partial x^2} \frac{\partial^2 \varphi_j}{\partial y^2} \right) \right. \\ \left. + 4D_{66} \frac{\partial^2 \varphi_i}{\partial x \partial y} \frac{\partial^2 \varphi_j}{\partial x \partial y} + D_{22} \frac{\partial^2 \varphi_i}{\partial y^2} \frac{\partial^2 \varphi_j}{\partial y^2} \right] dx dy \quad (9.4.4a)$$

$$B_{ij} = \int_0^b \int_0^a \left[I_0 \varphi_i \varphi_j + I_2 \left(\frac{\partial \varphi_i}{\partial x} \frac{\partial \varphi_j}{\partial x} + \frac{\partial \varphi_i}{\partial y} \frac{\partial \varphi_j}{\partial y} \right) \right] dx dy \quad (9.4.4b)$$

As discussed in Sections 7.3.2 and 8.3.2, it is convenient to express the Ritz approximation of rectangular plates in the form

$$w(x, y) \approx W_{mn}(x, y) = \sum_{i=1}^M \sum_{j=1}^N c_{ij} X_i(x) Y_j(y) \quad (9.4.5)$$

The functions X_i and Y_j for various boundary conditions are given in Eqs. (7.3.29)–(7.3.44). These functions satisfy only the geometric boundary conditions of the problem. Substituting Eq. (9.4.5) into Eq. (9.4.1), we obtain Eq. (9.4.3) in which $R_{(ij)(k\ell)}$ of $[R]$ are defined by Eq. (8.3.16a) and coefficients $B_{(ij)(k\ell)}$ of $[B]$ are defined by

$$B_{ij,k\ell} = \int_0^b \int_0^a \left[I_0 X_i X_k Y_j Y_\ell + I_2 \left(\frac{dX_i}{dx} \frac{dX_k}{dx} Y_j Y_\ell + X_i X_k \frac{dY_j}{dy} \frac{dY_\ell}{dy} \right) \right] dx dy \quad (9.4.6)$$

The size of the matrix $[R]$ is $MN \times MN$, and Eq. (9.4.3) can be used to calculate first MN frequencies of the infinite set.

9.4.2 Simply Supported Plates (SSSS)

For a rectangular plate simply supported on all sides (Figure 9.4.1), we may select the following approximation functions

$$\varphi_{ij} = X_i(x) Y_j(y) \quad (9.4.7a)$$

$$X_i(x) = \left(\frac{x}{a} \right)^i - \left(\frac{x}{a} \right)^{i+1}, \quad Y_j(y) = \left(\frac{y}{b} \right)^j - \left(\frac{y}{b} \right)^{j+1} \quad (9.4.7b)$$

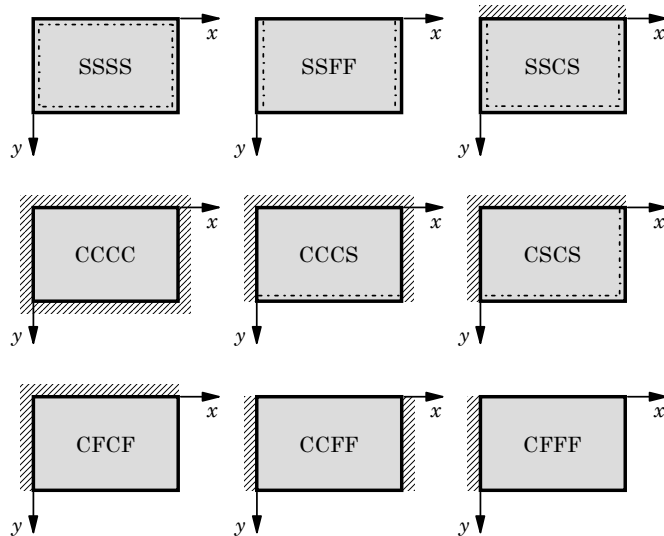


Figure 9.4.1 Rectangular plates with various boundary conditions.

For isotropic ($\nu = 0.25$) square plates with $M = N = 2$ [see Eq. (9.4.5)], the matrices $[R]$ and $[B]$ are given by

$$\begin{aligned}[R] &= \begin{bmatrix} 0.4346 & 0.2173 & 0.2173 & 0.1086 \\ 0.2173 & 0.2314 & 0.1086 & 0.1157 \\ 0.2173 & 0.1086 & 0.2314 & 0.1157 \\ 0.1086 & 0.1157 & 0.1157 & 0.0993 \end{bmatrix} \times 10^{-1} \\ [B] &= \begin{bmatrix} 1.1111 & 0.5556 & 0.5556 & 0.2778 \\ 0.5556 & 0.3175 & 0.2778 & 0.1587 \\ 0.5556 & 0.2778 & 0.3175 & 0.1587 \\ 0.2778 & 0.1587 & 0.1587 & 0.0907 \end{bmatrix} \times 10^{-5}\end{aligned}\quad (9.4.8)$$

where the following notation is used to store the coefficients

$$\begin{aligned}R_{11} &= R_{11,11}, \quad R_{12} = R_{11,12}, \quad R_{13} = R_{11,21}, \quad R_{14} = R_{11,22} \\ R_{21} &= R_{12,11}, \quad R_{22} = R_{12,12}, \quad R_{23} = R_{12,21}, \quad R_{24} = R_{12,22} \\ R_{31} &= R_{21,11}, \quad R_{32} = R_{21,12}, \quad R_{33} = R_{21,21}, \quad R_{34} = R_{21,22} \\ R_{41} &= R_{22,11}, \quad R_{42} = R_{22,12}, \quad R_{43} = R_{22,21}, \quad R_{44} = R_{22,22}\end{aligned}$$

The first four frequencies ($\bar{\omega}_{mn} = \omega_{mn}a^2\sqrt{\rho h/D}$) are

$$\bar{\omega}_{11} = 20.973, \quad \bar{\omega}_{12} = 58.992, \quad \bar{\omega}_{21} = 59.007, \quad \bar{\omega}_{22} = 92.529 \quad (9.4.9)$$

The exact frequencies [see Eq. (9.2.8)] are

$$\bar{\omega}_{11} = 19.739, \quad \bar{\omega}_{12} = \bar{\omega}_{21} = 49.348, \quad \bar{\omega}_{22} = 88.826 \quad (9.4.10)$$

For larger values of N and M , the Ritz method will yield increasingly accurate and more frequencies.

9.4.3 Clamped Plates (CCCC)

Both the Ritz and Lévy methods cannot be used to determine the frequencies of clamped plates. Therefore, here we use the Ritz method to determine the natural frequencies. For a rectangular plate clamped on all sides, we may select the following approximation functions

$$\varphi_{ij} = X_i(x)Y_j(y) \quad (9.4.11)$$

$$X_i(x) = \left(\frac{x}{a}\right)^{i+1} - 2\left(\frac{x}{a}\right)^{i+2} + \left(\frac{x}{a}\right)^{i+3} \quad (9.4.12a)$$

$$Y_j(y) = \left(\frac{y}{b}\right)^{j+1} - 2\left(\frac{y}{b}\right)^{j+2} + \left(\frac{y}{b}\right)^{j+3} \quad (9.4.12b)$$

For isotropic ($\nu = 0.25$) square plates with $M = N = 2$, the matrices $[R]$ and $[B]$ are given by

$$\begin{aligned}
 [R] &= \begin{bmatrix} 0.2902 & 0.1451 & 0.1451 & 0.0725 \\ 0.1451 & 0.1007 & 0.0725 & 0.0503 \\ 0.1451 & 0.0725 & 0.1007 & 0.0503 \\ 0.0725 & 0.0503 & 0.0503 & 0.0335 \end{bmatrix} \times 10^{-3} \\
 [B] &= \begin{bmatrix} 0.2520 & 0.1260 & 0.1260 & 0.0630 \\ 0.1260 & 0.0687 & 0.0630 & 0.0344 \\ 0.1260 & 0.0630 & 0.0687 & 0.0344 \\ 0.0630 & 0.0344 & 0.0344 & 0.0187 \end{bmatrix} \times 10^{-7}
 \end{aligned} \tag{9.4.13}$$

The first four nondimensional frequencies ($\bar{\omega}_{mn} = \omega_{mn}a^2\sqrt{\rho h/D}$) are

$$\bar{\omega}_{11} = 36.000, \quad \bar{\omega}_{12} = 74.296, \quad \bar{\omega}_{21} = 74.297, \quad \bar{\omega}_{22} = 108.592 \tag{9.4.14a}$$

The approximate frequencies obtained by Ödman (1955) [see Leissa (1969)] are

$$\bar{\omega}_{11} = 35.999, \quad \bar{\omega}_{12} = 73.405, \quad \bar{\omega}_{21} = 73.405, \quad \bar{\omega}_{22} = 108.237 \tag{9.4.14b}$$

Table 9.4.1 contains the first four natural frequencies of clamped rectangular plates. The results are obtained with $M = N = 2$ in Eq. (9.4.5) (see Leissa (1969), Tables 4.28 and 4.29; no mention is made of Poisson's ratio used). The frequencies listed for the orthotropic plate are the first four frequencies. The mode shape is of the form

$$w(x, y) = X_1(c_1Y_1 + c_2Y_2) + X_2(c_3Y_1 + c_4Y_2) \tag{9.4.15}$$

Table 9.4.1. Effect of the plate aspect ratio on the nondimensional frequencies of isotropic ($\nu = 0.25$) and orthotropic clamped rectangular plates (CCCC).

m	n	$\omega_{mn}a^2\sqrt{\rho h/D_{22}}$ for values of a/b					
		0.25	0.5	0.667	1.0	1.5	2.0
<i>Isotropic Plates ($\nu = 0.25$)</i>							
1	1	22.890	24.647	27.047	36.000	60.856	98.590
	2	24.196	31.867	41.899	74.296	94.273	127.466
2	1	63.466	65.234	69.297	74.297	151.419	260.938
	2	64.943	71.941	80.394	108.592	180.887	287.766
<i>Orthotropic Plates ($E_1 = 10E_2, G_{12} = 0.5E_2, \nu = 0.25$)</i>							
1	1	71.164	71.840	72.792	76.826	91.637	120.569
	2	71.677	74.939	80.036	101.555	167.460	230.036
2	1	199.206	199.898	200.708	203.511	212.381	271.393
	2	199.793	202.613	206.212	219.947	265.488	349.607

The vectors $\{c\}^i$ for the four modes in the case of $a/b = 0.25$, for example, are given by

$$\{c\}^1 = \begin{Bmatrix} 1.0 \\ 0.0 \\ 0.0 \\ 0.0 \end{Bmatrix}, \quad \{c\}^2 = \begin{Bmatrix} -0.5 \\ 1.0 \\ 0.0 \\ 0.0 \end{Bmatrix}, \quad \{c\}^3 = \begin{Bmatrix} -0.50 \\ 0.08 \\ 1.00 \\ 0.16 \end{Bmatrix}, \quad \{c\}^4 = \begin{Bmatrix} 0.25 \\ -0.50 \\ -0.50 \\ 1.00 \end{Bmatrix}$$

The vectors $\{c\}^i$ for the four modes in the case of $a/b = 1$ are given by

$$\{c\}^1 = \begin{Bmatrix} 1.0 \\ 0.0 \\ 0.0 \\ 0.0 \end{Bmatrix}, \quad \{c\}^2 = \begin{Bmatrix} -0.5 \\ 1.0 \\ 0.0 \\ 0.0 \end{Bmatrix}, \quad \{c\}^3 = \begin{Bmatrix} -0.5 \\ 0.0 \\ 1.0 \\ 0.0 \end{Bmatrix}, \quad \{c\}^4 = \begin{Bmatrix} 0.25 \\ -0.50 \\ -0.50 \\ 1.00 \end{Bmatrix}$$

9.4.4 CCCS Plates

Consider natural vibrations of rectangular plates with sides $x = 0, a$ and $y = 0$ clamped and side $y = b$ simply supported (Figure 9.4.1). For this case, the approximation functions are given by

$$X_i = \left(\frac{x}{a}\right)^{i+1} - 2\left(\frac{x}{a}\right)^{i+2} + \left(\frac{x}{a}\right)^{i+3}, \quad Y_j = \left(\frac{y}{b}\right)^{j+1} - \left(1 - \frac{y}{b}\right)^{j+2} \quad (9.4.16)$$

The first four natural frequencies of rectangular plates are presented in Table 9.4.2 for various aspect ratios.

Table 9.4.2. Effect of the plate aspect ratio on the nondimensional frequencies of isotropic and orthotropic rectangular plates (CCCS).

Mode (m, n)	$\omega_{mn}a^2\sqrt{\rho h/D_{22}}$ for values of a/b					
	0.25	0.5	0.667	1.0	1.5	2.0
<i>Isotropic Plates ($\nu = 0.25$)</i>						
(1,1)	22.840	24.215	25.913	31.849	48.217	73.573
(1,2)	24.654	34.421	46.951	72.025	86.045	108.452
(2,1)	63.411	64.957	66.663	86.497	179.342	310.663
(2,2)	65.444	74.254	84.914	120.087	208.448	337.474
<i>Orthotropic Plates ($E_1 = 10E_2, G_{12} = 0.5E_2, \nu = 0.25$)</i>						
(1,1)	71.146	71.685	72.365	74.942	83.725	101.066
(1,2)	71.859	76.161	82.957	111.066	193.427	219.912
(2,1)	199.162	199.773	200.452	202.629	208.753	319.871
(2,2)	200.015	203.605	208.276	226.356	285.872	392.681

9.4.5 CSCS Plates

Here we consider natural vibrations of rectangular plates with sides $x = 0$ and $y = 0$ clamped and sides $x = a$ and $y = b$ simply supported (Figure 9.4.1). For this case, the approximation functions are

$$X_i = \left(\frac{x}{a}\right)^{i+1} - \left(1 - \frac{x}{a}\right)^{i+2}, \quad Y_j = \left(\frac{y}{b}\right)^{j+1} - \left(1 - \frac{y}{b}\right)^{j+2} \quad (9.4.17)$$

The first four natural frequencies of rectangular plates are presented in Table 9.4.3 for various aspect ratios.

Table 9.4.3. Effect of the plate aspect ratio on the nondimensional frequencies of isotropic and orthotropic rectangular plates (CSCS).

Mode (m, n)	$\omega_{mn}a^2\sqrt{\rho h/D_{22}}$ for values of a/b					
	0.25	0.5	0.667	1.0	1.5	2.0
<i>Isotropic Plates ($\nu = 0.25$)</i>						
(1,1)	15.985	17.818	19.991	27.087	44.979	71.272
(1,2)	18.386	30.012	43.638	84.399	98.194	120.056
(2,1)	75.839	77.413	79.132	84.517	178.042	309.642
(2,2)	77.892	86.649	97.076	131.386	218.411	346.580
<i>Orthotropic Plates ($E_1 = 10E_2, G_{12} = 0.5E_2, \nu = 0.25$)</i>						
(1,1)	49.070	49.815	50.754	54.272	65.694	86.527
(1,2)	50.052	55.904	64.724	97.935	185.878	258.208
(2,1)	238.427	239.047	239.728	241.879	247.752	315.079
(2,2)	239.240	242.788	247.265	264.141	319.351	420.586

9.4.6 CFCF, CCFF, and CFFF Plates

First we consider natural vibrations of rectangular plates with sides $x = 0$ and $y = 0$ clamped and sides $x = a$ and $y = b$ free (Figure 9.4.1). The first choice of the approximation functions is

$$X_i = \left(\frac{x}{a}\right)^{i+1}, \quad Y_j = \left(\frac{y}{b}\right)^{j+1} \quad (9.4.18)$$

The first four natural frequencies of rectangular plates are presented in Table 9.4.4 for various aspect ratios (first row of numbers for each mode). These results differ considerably from those presented by Young (1950) [see Leissa (1969), p. 73]. The reason for this is that the functions in Eq. (9.4.18) do not satisfy the force boundary conditions on the free edges when $M = N = 2$. The functions

$$X_i(x) = \left(\frac{x}{a}\right)^{i+1} - \frac{2i}{i+2} \left(\frac{x}{a}\right)^{i+2} + \frac{i(i+1)}{(i+2)(i+3)} \left(\frac{x}{a}\right)^{i+3} \quad (9.4.19a)$$

Table 9.4.4. Effect of the plate aspect ratio on the nondimensional frequencies of isotropic ($\nu = 0.3$) rectangular plates (CFCF).

Mode (m, n)	$\omega_{mn}a^2\sqrt{\rho h/D}$ for values of a/b					
	0.25	0.5	0.667	1.0	1.5	2.0
(1,1) [†]	3.719	4.408	5.162	7.229	11.614	17.634
	3.685	4.317	5.020	6.996	11.296	17.269
(1,2)	6.347	12.739	18.982	33.888	42.710	50.955
	5.095	9.257	13.478	24.696	30.327	37.030
(2,1)	35.041	35.832	36.828	43.044	82.863	143.328
	22.888	23.447	24.079	27.056	54.177	93.789
(2,2)	39.111	50.516	60.882	86.665	136.984	202.065
	24.552	29.848	35.066	49.113	78.898	119.391

[†] The first row of numbers for each mode corresponds to the frequencies obtained using the functions in Eq. (9.4.18), while the second row corresponds to those obtained using the functions in Eqs. (9.4.19a,b).

$$Y_j(y) = \left(\frac{y}{b}\right)^{j+1} - \frac{2j}{j+2} \left(\frac{y}{b}\right)^{j+2} + \frac{j(j+1)}{(j+2)(j+3)} \left(\frac{y}{b}\right)^{j+3} \quad (9.4.19b)$$

satisfy the conditions

$$X_i''(a) = X_i'''(a) = 0 \quad \text{and} \quad Y_j''(b) = Y_j'''(b) = 0 \quad (9.4.20)$$

and, hence, provide a better choice. The first four natural frequencies obtained with the functions in Eqs. (9.4.19a,b) are listed in the second row of each mode. The values for the square plate are 6.996, 24.696, 27.056, and 49.113, which are close to those of Young: 6.958, 24.80, 26.80, and 48.05.

Next, consider the natural vibrations of CCFF and CFFF plates. For CCFF plates (sides $x = 0, a$ clamped and sides $y = 0, b$ free) the approximation functions are

$$X_i = \left(\frac{x}{a}\right)^{i+1} - 2 \left(\frac{x}{a}\right)^{i+2} + \left(\frac{x}{a}\right)^{i+3}, \quad Y_j = \left(\frac{y}{b}\right)^{j-1} \quad (9.4.21)$$

For CFFF plates, we have the choice of

$$X_i = \left(\frac{x}{a}\right)^{i+1}, \quad Y_j = \left(\frac{y}{b}\right)^{j-1} \quad (9.4.22)$$

or

$$X_i(x) = \left(\frac{x}{a}\right)^{i+1} - \frac{2i}{i+2} \left(\frac{x}{a}\right)^{i+2} + \frac{i(i+1)}{(i+2)(i+3)} \left(\frac{x}{a}\right)^{i+3}, \quad Y_j = \left(\frac{y}{b}\right)^{j-1} \quad (9.4.23)$$

The first four natural frequencies of CCFF and CFFF plates are presented in Table 9.4.5 for various aspect ratios. The mode shapes associated with these plates are of the form given in Eq. (9.4.15). The amplitudes $\{c\}^i$ associated with the four modes of CCFF plates are

$$\{c\}^1 = \begin{Bmatrix} 1.0 \\ 0.0 \\ 0.0 \\ 0.0 \end{Bmatrix}, \quad \{c\}^2 = \begin{Bmatrix} 0.5 \\ -1.0 \\ 0.0 \\ 0.0 \end{Bmatrix}, \quad \{c\}^3 = \begin{Bmatrix} 0.5 \\ 0.0 \\ -1.0 \\ -0.0 \end{Bmatrix}, \quad \{c\}^4 = \begin{Bmatrix} 0.25 \\ -0.5 \\ -0.5 \\ 1.0 \end{Bmatrix}$$

The amplitudes of CFFF plates based on Eq. (9.4.22) are

$$\{c\}^1 = \begin{Bmatrix} 1.0 \\ 0.0 \\ -0.4 \\ 0.0 \end{Bmatrix}, \quad \{c\}^2 = \begin{Bmatrix} 0.5 \\ -1.0 \\ -0.3 \\ 0.6 \end{Bmatrix}, \quad \{c\}^3 = \begin{Bmatrix} 0.8 \\ 0.0 \\ -1.0 \\ 0.0 \end{Bmatrix}, \quad \{c\}^4 = \begin{Bmatrix} 0.4 \\ -0.8 \\ -0.5 \\ 1.0 \end{Bmatrix}$$

and those based on Eq. (9.4.23) are

$$\{c\}^1 = \begin{Bmatrix} 1.0 \\ 0.0 \\ 0.2 \\ 0.0 \end{Bmatrix}, \quad \{c\}^2 = \begin{Bmatrix} 0.5 \\ -1.0 \\ -0.4 \\ 0.9 \end{Bmatrix}, \quad \{c\}^3 = \begin{Bmatrix} 0.5 \\ 0.0 \\ -1.0 \\ 0.0 \end{Bmatrix}, \quad \{c\}^4 = \begin{Bmatrix} 0.3 \\ -0.5 \\ -0.5 \\ 1.0 \end{Bmatrix}$$

Table 9.4.5. Effect of plate aspect ratio on the nondimensional frequencies of isotropic ($\nu = 0.3$) CCFF and CFFF plates.

Mode (m, n)	$\omega_{mn}a^2\sqrt{\rho h/D}$ for values of a/b					
	0.25	0.5	0.667	1.0	1.5	2.0
<i>CCFF Plates</i>						
(1,1)	22.450	22.450	22.450	22.450	22.450	22.450
(1,2)	22.729	23.546	24.364	26.563	30.945	36.199
(2,1)	62.928	62.928	62.928	62.928	62.928	62.928
(2,2)	63.294	64.380	65.487	68.550	74.987	83.167
<i>CFFF Plates</i> [†]						
(1,1)	3.533	3.533	3.533	3.533	3.533	3.533
	3.516	3.516	3.516	3.516	3.516	3.516
(1,2)	4.176	5.612	6.715	8.984	12.383	15.792
	4.139	5.514	6.555	8.664	11.794	14.937
(2,1)	34.807	34.807	34.807	34.807	34.807	34.807
	22.712	22.712	22.712	22.712	22.712	22.712
(2,2)	35.684	38.205	40.666	47.029	58.946	72.446
	23.378	25.289	27.151	31.938	40.800	50.721

[†] The first row corresponds to the frequencies obtained using the functions in Eq. (9.4.22), while the second row corresponds to those obtained using the functions in Eq. (9.4.23).

It is interesting to note that the predicted frequencies ω_{11} and ω_{21} are independent of the plate aspect ratio, a/b . This can be attributed to the low order of approximation used in the y coordinate direction.

9.5 Transient Analysis

9.5.1 Spatial Variation of the Solution

The equation of motion governing bending deflection w_0 of an orthotropic plate, assuming no applied inplane and thermal forces, is

$$\begin{aligned} D_{11} \frac{\partial^4 w_0}{\partial x^4} + 2(D_{12} + 2D_{66}) \frac{\partial^4 w_0}{\partial x^2 \partial y^2} + D_{22} \frac{\partial^4 w_0}{\partial y^4} - q(x, y, t) \\ + I_0 \ddot{w}_0 - I_2 \left(\frac{\partial^2 \ddot{w}_0}{\partial x^2} + \frac{\partial^2 \ddot{w}_0}{\partial y^2} \right) = 0 \end{aligned} \quad (9.5.1)$$

Suppose that the plate is simply supported with the boundary conditions

$$\begin{aligned} w_0(x, 0, t) = 0, \quad w_0(x, b, t) = 0, \quad w_0(0, y, t) = 0, \quad w_0(a, y, t) = 0 \\ M_{xx}(0, y, t) = 0, \quad M_{xx}(a, y, t) = 0, \quad M_{yy}(x, 0, t) = 0, \quad M_{yy}(x, b, t) = 0 \end{aligned} \quad (9.5.2)$$

for $t > 0$, and assume that the initial conditions are

$$w_0(x, y, 0) = d_0(x, y), \quad \frac{\partial w_0}{\partial t}(x, y, 0) = v_0(x, y) \quad \text{for all } x \text{ and } y \quad (9.5.3)$$

where d_0 and v_0 are the initial displacement and velocity, respectively.

We assume the following expansion of the transverse deflection to satisfy the boundary conditions (9.5.2) for any time $t \geq 0$

$$w_0(x, y, t) = \sum_{n=1}^{\infty} \sum_{m=1}^{\infty} W_{mn}(t) \sin \alpha_m x \sin \beta_n y \quad (9.5.4)$$

Similarly, we assume that the transverse load, initial displacement, and initial velocity can be expanded as

$$q(x, y, t) = \sum_{n=1}^{\infty} \sum_{m=1}^{\infty} Q_{mn}(t) \sin \alpha_m x \sin \beta_n y \quad (9.5.5)$$

$$d_0(x, y) = \sum_{n=1}^{\infty} \sum_{m=1}^{\infty} D_{mn} \sin \alpha_m x \sin \beta_n y \quad (9.5.6)$$

$$v_0(x, y) = \sum_{n=1}^{\infty} \sum_{m=1}^{\infty} V_{mn} \sin \alpha_m x \sin \beta_n y \quad (9.5.7)$$

where $\alpha_m = m\pi/a$, $\beta_n = n\pi/b$, and Q_{mn} , for example, is given by

$$Q_{mn}(t) = \frac{4}{ab} \int_0^b \int_0^a q(x, y, t) \sin \alpha_m x \sin \beta_n y dx dy \quad (9.5.8)$$

Substituting the expansions (9.5.4) and (9.5.5) into Eq. (9.5.1), we obtain

$$\sum_{n=1}^{\infty} \sum_{m=1}^{\infty} \left\{ W_{mn} \left[D_{11}\alpha_m^4 + 2(D_{12} + 2D_{66})\alpha_m^2\beta_n^2 + D_{22}\beta_n^4 \right] + \left[I_0 + I_2 (\alpha_m^2 + \beta_n^2) \right] \ddot{W}_{mn} - Q_{mn} \right\} \sin \alpha_m x \sin \beta_n y = 0 \quad (9.5.9)$$

Since the above expression must hold for all x and y , it follows that

$$\begin{aligned} W_{mn} \left[D_{11}\alpha_m^4 + 2(D_{12} + 2D_{66})\alpha_m^2\beta_n^2 + D_{22}\beta_n^4 \right] \\ + \left[I_0 + I_2 (\alpha_m^2 + \beta_n^2) \right] \ddot{W}_{mn} - Q_{mn} = 0 \end{aligned} \quad (9.5.10a)$$

or

$$K_{mn} W_{mn}(t) + M_{mn} \ddot{W}_{mn} = Q_{mn}(t) \quad (9.5.10b)$$

where

$$\begin{aligned} K_{mn} &= D_{11}\alpha_m^4 + 2(D_{12} + 2D_{66})\alpha_m^2\beta_n^2 + D_{22}\beta_n^4 \\ M_{mn} &= I_0 + I_2 (\alpha_m^2 + \beta_n^2) \end{aligned} \quad (9.5.10c)$$

9.5.2 Time Integration

The second-order differential equation (9.5.10a) can be solved either exactly or numerically. The numerical time integration methods will be discussed in Chapter 12. To solve it exactly, we first write Eq. (9.5.10a) in the form

$$\frac{d^2 W_{mn}}{dt^2} + \left(\frac{K_{mn}}{M_{mn}} \right) W_{mn} = \frac{1}{M_{mn}} Q_{mn}(t) \equiv \hat{Q}_{mn}(t) \quad (9.5.11)$$

The solution of Eq. (9.5.11) is given by

$$W_{mn}(t) = C_1 e^{\lambda_1 t} + C_2 e^{\lambda_2 t} + W_{mn}^p(t) \quad (9.5.12)$$

where C_1 and C_2 are constants to be determined using the initial conditions, $W_{mn}^p(t)$ is the particular solution

$$W_{mn}^p(t) = \int^t \frac{r_1(\tau)r_2(t) - r_1(t)r_2(\tau)}{r_1(\tau)\dot{r}_2(\tau) - \dot{r}_1(\tau)r_2(\tau)} \hat{Q}_{mn}(\tau) d\tau \quad (9.5.13a)$$

with $r_1(t) = e^{\lambda_1 t}$ and $r_2(t) = e^{\lambda_2 t}$, and λ_1 and λ_2 are the roots of the equation

$$\lambda^2 + \frac{K_{mn}}{M_{mn}} = 0; \quad \lambda_1 = -i\mu, \quad \lambda_2 = i\mu, \quad i = \sqrt{-1}, \quad \mu = \sqrt{\frac{K_{mn}}{M_{mn}}} \quad (9.5.13b)$$

The solution becomes

$$W_{mn}(t) = A \cos \mu t + B \sin \mu t + W_{mn}^p(t) \quad (9.5.14a)$$

$$W_{mn}^p(t) = \frac{1}{2i\mu} \left(e^{i\mu t} \int^t e^{-i\mu\tau} \hat{Q}_{mn}(\tau) d\tau - e^{-i\mu t} \int^t e^{i\mu\tau} \hat{Q}_{mn}(\tau) d\tau \right) \quad (9.5.14b)$$

Once the load distribution – both spatially and with time – is known, the solution can be determined from Eq. (9.5.14a).

For a step loading, $Q_{mn}(t) = Q_{mn}^0 H(t)$, where $H(t)$ denotes the Heaviside step function, Eq. (9.5.14a) takes the form

$$W_{mn}(t) = A_{mn} \cos \mu t + B_{mn} \sin \mu t + \frac{1}{K_{mn}} Q_{mn}^0 \quad (9.5.15a)$$

Using the initial conditions (9.5.3), we obtain

$$A_{mn} = D_{mn} - \frac{1}{K_{mn}} Q_{mn}^0, \quad B_{mn} = \frac{V_{mn}}{\mu} \quad (9.5.15b)$$

Thus, the final solution (9.5.4) is given by

$$w_0(x, y, t) = \sum_{n=1}^{\infty} \sum_{m=1}^{\infty} \left[D_{mn} \cos \mu t + \frac{V_{mn}}{\mu} \sin \mu t + \frac{Q_{mn}^0}{K_{mn}} (1 - \cos \mu t) \right] \times \sin \alpha_m x \sin \beta_n y \quad (9.5.16)$$

The coefficients Q_{mn}^0 were given in Table 6.3.1 for various types of distributions. The same holds for D_{mn} and V_{mn} .

It should be noted that the procedure outlined above is valid irrespective of how one arrives at Eq. (9.5.10b), e.g., Eq. (9.5.10b) could have been obtained using the Ritz method or other methods. The exact solution of the differential equation (9.5.10b) can also be obtained using the Laplace transform method (see Table 4.6.1 for the Laplace transform pairs). Once the solution w_0 is known, stresses can be computed using the constitutive equations.

9.6 Summary

This chapter was dedicated to natural vibration and transient analysis of rectangular plates. Exact, as well as the Ritz, solutions were developed. The exact solutions were based on the Navier and Lévy solution procedures. Numerical values of natural frequencies of plates are tabulated for various modulus ratios and boundary conditions.

Problems

9.1 Consider the natural vibration of a rectangular plate with all edges simply supported. Use the Lévy solution method and establish the result in Eq. (9.2.6).

9.2 Assuming that $(I_0 \omega^2 / D_{22}) < \alpha_m^4 (D_{11} / D_{22})$, show that the frequency equation of SSSF plates is

$$\Omega_1 \Lambda_2 \cosh \lambda_2 b \sinh \lambda_1 b - \Lambda_1 \Omega_2 \cosh \lambda_1 b \sinh \lambda_2 b = 0$$

where

$$\Omega_1 = \lambda_1^2 - \frac{D_{12}}{D_{22}}\alpha_m^2, \quad \Omega_2 = \lambda_2^2 - \frac{D_{12}}{D_{22}}\alpha_m^2$$

$$\Lambda_1 = \lambda_1^2 - \frac{\bar{D}_{12}}{D_{22}}\alpha_m^2, \quad \Lambda_2 = \lambda_2^2 - \frac{\bar{D}_{12}}{D_{22}}\alpha_m^2$$

and $\bar{D}_{12} = D_{12} + 4D_{66}$.

- 9.3** Assuming that $(I_0\omega^2/D_{22}) < \alpha_m^4(D_{11}/D_{22})$, show that the frequency equation of SSCC plates is

$$2\lambda_1\lambda_2(1 - \cosh \lambda_1 b \cosh \lambda_2 b) + (\lambda_1^2 + \lambda_2^2) \sinh \lambda_1 b \sinh \lambda_2 b = 0$$

- 9.4** Assuming that $(I_0\omega^2/D_{22}) < \alpha_m^4(D_{11}/D_{22})$, show that the frequency equation of SSCS plates is

$$\lambda_2 \cosh \lambda_2 b \sinh \lambda_1 b - \lambda_1 \cosh \lambda_1 b \sinh \lambda_2 b = 0$$

- 9.5** Assuming that $(I_0\omega^2/D_{22}) < \alpha_m^4(D_{11}/D_{22})$, show that the frequency equation of SSCF plates is

$$\begin{aligned} &\lambda_1\lambda_2 [\Omega_1\Lambda_1 + \Omega_2\Lambda_2 - (\Omega_1\Lambda_2 + \Omega_2\Lambda_1) \cosh \lambda_1 b \cosh \lambda_2 b] \\ &+ (\lambda_1^2\Omega_2\Lambda_1 + \lambda_2^2\Omega_1\Lambda_2) \sinh \lambda_1 b \sinh \lambda_2 b = 0 \end{aligned}$$

- 9.6** Assuming that $(I_0\omega^2/D_{22}) > \alpha_m^4(D_{11}/D_{22})$, show that the frequency equation of SSCC plates is given by Eq. (9.3.26).

- 9.7** Assuming that $(I_0\omega^2/D_{22}) > \alpha_m^4(D_{11}/D_{22})$, show that the frequency equation of SSCS plates is given by Eq. (9.3.28).

- 9.8** Derive the approximation functions X_i and Y_j in Eqs. (9.4.19a,b) for CFCF plates so that they satisfy the geometric and force boundary conditions of Eq. (9.4.20).

- 9.9** Derive the explicit form of the coefficients $R_{(ij)(k\ell)}$ and $B_{(ij)(k\ell)}$ for CSCS plates using the functions in Eq. (9.4.17).

Shear Deformation Plate Theories

10.1 First-Order Shear Deformation Plate Theory

10.1.1 Preliminary Comments

The preceding chapters of the book were devoted to the study of bending, buckling, and natural vibrations of rectangular plates using the classical plate theory (CPT), in which transverse normal and shear stresses are neglected. The first-order shear deformation plate theory (FSDT) extends the kinematics of the CPT by relaxing the normality restriction (see Section 3.2) and allowing for arbitrary but constant rotation of transverse normals. The third-order shear deformation plate theory (TSĐT) further relaxes the kinematic hypothesis by removing the straightness assumption; i.e., straight normal to the middle plane before deformation may become cubic curves after deformation. In this chapter, the first-order and third-order shear deformation plate theories are developed and they are employed in the bending, buckling, and natural vibration analysis of rectangular plates.

The most significant difference between the classical and shear deformation theories is the effect of including transverse shear deformation on the predicted deflections, frequencies, and buckling loads. As will be seen in the sequel, the classical plate theory underpredicts deflections and overpredicts frequencies as well as buckling loads of plates with side-to-thickness ratios of the order of 20 or less (i.e., thick plates). For this reason alone it is necessary to use the first-order or third-order shear deformation plate theory in the analysis of relatively thick plates.

10.1.2 Kinematics

Under the same assumptions and restrictions as in the classical laminate theory, but relaxing the normality condition, the displacement field of the first-order theory can be expressed in the form (Figure 10.1.1)

$$\begin{aligned} u(x, y, z, t) &= u_0(x, y, t) + z\phi_x(x, y, t) \\ v(x, y, z, t) &= v_0(x, y, t) + z\phi_y(x, y, t) \\ w(x, y, z, t) &= w_0(x, y, t) \end{aligned} \tag{10.1.1}$$

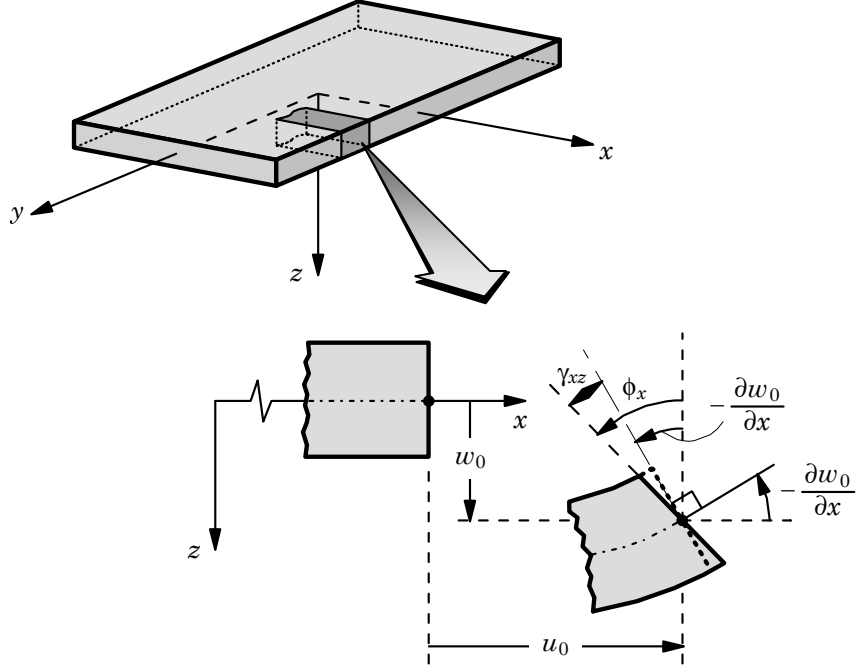


Figure 10.1.1. Undeformed and deformed geometries of an edge of a plate under the assumptions of the first-order shear deformation plate theory (FSDT).

As in CPT, \$(u_0, v_0, w_0)\$ denote the displacements of a point on the plane \$z = 0\$ and \$\phi_x\$ and \$\phi_y\$ are the rotations of a transverse normal about the \$y\$- and \$x\$-axes, respectively (Figure 10.1.1)

$$\frac{\partial u}{\partial z} = \phi_x, \quad \frac{\partial v}{\partial z} = \phi_y$$

The quantities \$(u_0, v_0, w_0, \phi_x, \phi_y)\$ are called the *generalized displacements*.

The notation that \$\phi_x\$ denotes the rotation of a transverse normal about the \$y\$-axis and \$\phi_y\$ denotes the rotation about the \$x\$-axis may be confusing to some because they do not follow the right-hand rule. However, the notation has been used extensively in the literature, and we will not depart from it. If \$(\beta_x, \beta_y)\$ denote the rotations about the \$x\$- and \$y\$-axes, respectively, that follow the right-hand rule, then

$$\beta_x = \phi_y, \quad \beta_y = -\phi_x \quad (10.1.2)$$

For thin plates, i.e., when the plate inplane characteristic dimension to thickness ratio is on the order of 50 or greater, the rotation functions \$\phi_x\$ and \$\phi_y\$ should approach the respective slopes of the transverse deflection:

$$\phi_x \rightarrow -\frac{\partial w_0}{\partial x}, \quad \phi_y \rightarrow -\frac{\partial w_0}{\partial y} \quad (10.1.3)$$

Indeed, the first-order shear deformation theory can be derived from the classical plate theory using the conditions (10.1.3) as constraints [see Reddy (2004a), pp. 520–523].

The von Kármán nonlinear strains associated with the displacement field (10.1.1) are

$$\begin{aligned}\varepsilon_{xx} &= \frac{\partial u_0}{\partial x} + \frac{1}{2} \left(\frac{\partial w_0}{\partial x} \right)^2 + z \frac{\partial \phi_x}{\partial x} \\ \varepsilon_{yy} &= \frac{\partial v_0}{\partial y} + \frac{1}{2} \left(\frac{\partial w_0}{\partial y} \right)^2 + z \frac{\partial \phi_y}{\partial y} \\ \gamma_{xy} &= \left(\frac{\partial u_0}{\partial y} + \frac{\partial v_0}{\partial x} + \frac{\partial w_0}{\partial x} \frac{\partial w_0}{\partial y} \right) + z \left(\frac{\partial \phi_x}{\partial y} + \frac{\partial \phi_y}{\partial x} \right) \\ \gamma_{xz} &= \frac{\partial w_0}{\partial x} + \phi_x, \quad \gamma_{yz} = \frac{\partial w_0}{\partial y} + \phi_y, \quad \varepsilon_{zz} = 0\end{aligned}\tag{10.1.4}$$

Note that the strains $(\varepsilon_{xx}, \varepsilon_{yy}, \gamma_{xy})$ are linear through the plate thickness, while the transverse shear strains $(\gamma_{xz}, \gamma_{yz})$ are constant. The strains in Eq. (10.1.4) can be expressed in the vector form as

$$\begin{Bmatrix} \varepsilon_{xx} \\ \varepsilon_{yy} \\ \gamma_{yz} \\ \gamma_{xz} \\ \gamma_{xy} \end{Bmatrix} = \begin{Bmatrix} \varepsilon_{xx}^0 \\ \varepsilon_{yy}^0 \\ \gamma_{yz} \\ \gamma_{xz} \\ \gamma_{xy}^0 \end{Bmatrix} + z \begin{Bmatrix} \varepsilon_{xx}^1 \\ \varepsilon_{yy}^1 \\ 0 \\ 0 \\ \gamma_{xy}^1 \end{Bmatrix} \quad \text{or} \quad \{\varepsilon\} = \{\varepsilon^0\} + z\{\varepsilon^1\}\tag{10.1.5a}$$

$$\{\varepsilon^0\} = \begin{Bmatrix} \frac{\partial u_0}{\partial x} + \frac{1}{2} \left(\frac{\partial w_0}{\partial x} \right)^2 \\ \frac{\partial v_0}{\partial y} + \frac{1}{2} \left(\frac{\partial w_0}{\partial y} \right)^2 \\ \frac{\partial w_0}{\partial y} + \phi_y \\ \frac{\partial w_0}{\partial x} + \phi_x \\ \frac{\partial u_0}{\partial y} + \frac{\partial v_0}{\partial x} + \frac{\partial w_0}{\partial x} \frac{\partial w_0}{\partial y} \end{Bmatrix}, \quad \{\varepsilon^1\} = \begin{Bmatrix} \frac{\partial \phi_x}{\partial x} \\ \frac{\partial \phi_y}{\partial y} \\ 0 \\ 0 \\ \frac{\partial \phi_x}{\partial y} + \frac{\partial \phi_y}{\partial x} \end{Bmatrix}\tag{10.1.5b}$$

10.1.3 Equations of Motion

The governing equations of the first-order plate theory can be derived using the dynamic version of the principle of virtual displacements (or Hamilton's principle of Section 2.2.3)

$$0 = \int_0^T (\delta U + \delta V - \delta K) dt\tag{10.1.6}$$

where the virtual strain energy δU , virtual work done by applied forces δV , and the virtual kinetic energy δK are given by

$$\begin{aligned}\delta U = \int_{\Omega} \left\{ \int_{-\frac{h}{2}}^{\frac{h}{2}} \left[\sigma_{xx} \left(\delta \varepsilon_{xx}^0 + z \delta \varepsilon_{xx}^1 \right) + \sigma_{yy} \left(\delta \varepsilon_{yy}^0 + z \delta \varepsilon_{yy}^1 \right) \right. \right. \\ \left. \left. + \sigma_{xy} \left(\delta \gamma_{xy}^0 + z \delta \gamma_{xy}^1 \right) + \sigma_{xz} \delta \gamma_{xz}^0 + \sigma_{yz} \delta \gamma_{yz}^0 \right] dz \right\} dx dy\end{aligned}\tag{10.1.7a}$$

$$\delta V = - \int_{\Gamma_\sigma} \int_{-\frac{h}{2}}^{\frac{h}{2}} \left[\hat{\sigma}_{nn} (\delta u_n + z \delta \phi_n) + \hat{\sigma}_{ns} (\delta u_s + z \delta \phi_s) + \hat{\sigma}_{nz} \delta w_0 \right] dz ds \\ - \int_{\Omega} (q_b + q_t - kw_0) \delta w_0 dx dy \quad (10.1.7b)$$

$$\delta K = \int_{\Omega_0} \int_{-\frac{h}{2}}^{\frac{h}{2}} \rho \left[(\dot{u}_0 + z \dot{\phi}_x) (\delta \dot{u}_0 + z \delta \dot{\phi}_x) + (\dot{v}_0 + z \dot{\phi}_y) (\delta \dot{v}_0 + z \delta \dot{\phi}_y) \right. \\ \left. + \dot{w}_0 \delta \dot{w}_0 \right] dz dx dy \quad (10.1.8)$$

where Ω denotes the middle plane of the plate, h the total thickness, ρ the density of the plate, and k the modulus of the elastic foundation.

Substituting for δU , δV , and δK from Eqs. (10.1.7a,b) and (10.1.8) into the virtual work statement in Eq. (10.1.6) and integrating through the thickness of the laminate, we obtain

$$0 = \int_0^T \left\{ \int_{\Omega} \left[N_{xx} \delta \varepsilon_{xx}^0 + M_{xx} \delta \varepsilon_{xx}^1 + N_{yy} \delta \varepsilon_{yy}^0 + M_{yy} \delta \varepsilon_{yy}^1 + N_{xy} \delta \gamma_{xy}^0 \right. \right. \\ + M_{xy} \delta \gamma_{xy}^1 + Q_x \delta \gamma_{xz}^0 + Q_y \delta \gamma_{yz}^0 + kw_0 \delta w_0 - q \delta w_0 \\ - I_1 (\dot{\phi}_x \delta \dot{u}_0 + \dot{\phi}_y \delta \dot{v}_0 + \delta \dot{\phi}_x \dot{u}_0 + \delta \dot{\phi}_y \dot{v}_0) \\ \left. - I_0 (\dot{u}_0 \delta \dot{u}_0 + \dot{v}_0 \delta \dot{v}_0 + \dot{w}_0 \delta \dot{w}_0) - I_2 (\dot{\phi}_x \delta \dot{\phi}_x + \dot{\phi}_y \delta \dot{\phi}_y) \right] dx dy \\ \left. - \int_{\Gamma_\sigma} (\hat{N}_{nn} \delta u_n + \hat{N}_{ns} \delta u_s + \hat{M}_{nn} \delta \phi_n + \hat{M}_{ns} \delta \phi_s + \hat{Q}_n \delta w_0) ds \right\} dt \quad (10.1.9)$$

where $q = q_b + q_t$, the stress resultants ($N_{xx}, N_{yy}, N_{xy}, M_{xx}, M_{yy}, M_{xy}$) and the inertias (I_0, I_1, I_2) were defined in Eqs. (3.4.3) and (3.4.9), respectively, ($N_{nn}, N_{ns}, M_{nn}, M_{ns}$) in Eq. (3.4.7) [also, see Eqs. (3.5.6) and (3.5.7)], and the transverse force resultants (Q_x, Q_y) are defined by

$$\begin{Bmatrix} Q_x \\ Q_y \end{Bmatrix} = \int_{-\frac{h}{2}}^{\frac{h}{2}} \begin{Bmatrix} \sigma_{xz} \\ \sigma_{yz} \end{Bmatrix} dz \quad (10.1.10)$$

Shear Correction Factors

Since the transverse shear strains are represented as constant through the laminate thickness, it follows that the transverse shear stresses will also be constant. It is well known from elementary theory of homogeneous beams that the transverse shear stress variation is parabolic through the beam thickness. This discrepancy between the actual stress state and the constant stress state predicted by the first-order theory is often corrected, only in the energy sense, in computing the transverse shear force resultants (Q_x, Q_y) by multiplying the integrals in Eq. (10.1.10) with a parameter K_s , called *shear correction coefficient*:

$$\begin{Bmatrix} Q_x \\ Q_y \end{Bmatrix} = K_s \int_{-\frac{h}{2}}^{\frac{h}{2}} \begin{Bmatrix} \sigma_{xz} \\ \sigma_{yz} \end{Bmatrix} dz \quad (10.1.11)$$

This amounts to modifying the plate transverse shear stiffnesses. The factor K_s is computed such that the strain energy due to transverse shear stresses in Eq. (10.1.11) equals the strain energy due to the true transverse stresses predicted by the three-dimensional elasticity theory.

For example, consider a homogeneous beam with rectangular cross section, with width b and height h . The actual shear stress distribution through the thickness of the beam is given by

$$\sigma_{xz}^c = \frac{3Q_0}{2bh} \left[1 - \left(\frac{2z}{h} \right)^2 \right], \quad -\frac{h}{2} \leq z \leq \frac{h}{2} \quad (10.1.12)$$

where Q_0 is the transverse load. The transverse shear stress in the first-order theory is a constant, $\sigma_{xz}^f = Q_0/bh$. The strain energies due to transverse shear stresses in the two theories are

$$\begin{aligned} U_s^c &= \frac{1}{2G_{13}} \int_A (\sigma_{xz}^c)^2 dA = \frac{3Q_0^2}{5G_{13}bh} \\ U_s^f &= \frac{1}{2G_{13}} \int_A (\sigma_{xz}^f)^2 dA = \frac{Q_0^2}{2G_{13}bh} \end{aligned} \quad (10.1.13)$$

The shear correction factor is the ratio of U_s^f to U_s^c , which gives $K_s = 5/6$. The shear correction factor, in general, depends on the geometry and material properties of the plate.

Returning to the virtual work statement in Eq. (10.1.9), we substitute for the virtual strains into Eq. (10.1.9) and integrate-by-parts to relieve the virtual generalized displacements $(\delta u_0, \delta v_0, \delta w_0, \delta \phi_x, \delta \phi_y)$ in Ω of any differentiation, so that we can use the fundamental lemma of variational calculus. We obtain

$$\begin{aligned} 0 &= \int_0^T \int_{\Omega} \left[- \left(N_{xx,x} + N_{xy,y} - I_0 \ddot{u}_0 - I_1 \ddot{\phi}_x \right) \delta u_0 \right. \\ &\quad - \left(N_{xy,x} + N_{yy,y} - I_0 \ddot{v}_0 - I_1 \ddot{\phi}_y \right) \delta v_0 \\ &\quad - \left(M_{xx,x} + M_{xy,y} - Q_x - I_2 \ddot{\phi}_x - I_1 \ddot{u}_0 \right) \delta \phi_x \\ &\quad - \left(M_{xy,x} + M_{yy,y} - Q_y - I_2 \ddot{\phi}_y - I_1 \ddot{v}_0 \right) \delta \phi_y \\ &\quad \left. - (Q_{x,x} + Q_{y,y} - k w_0 + \mathcal{N} + q - I_0 \ddot{w}_0) \delta w_0 \right] dx dy \\ &\quad + \int_0^T \int_{\Gamma} \left[(N_{nn} - \hat{N}_{nn}) \delta u_n + (N_{ns} - \hat{N}_{ns}) \delta u_s + (Q_n - \hat{Q}_n) \delta w_0 \right. \\ &\quad \left. + (M_{nn} - \hat{M}_{nn}) \delta \phi_n + (M_{ns} - \hat{M}_{ns}) \delta \phi_s \right] ds dt \quad (10.1.14) \end{aligned}$$

where \mathcal{N} and \mathcal{P} were defined in Eq. (3.4.14)

$$\begin{aligned}\mathcal{N} &= \frac{\partial}{\partial x} \left(N_{xx} \frac{\partial w_0}{\partial x} + N_{xy} \frac{\partial w_0}{\partial y} \right) + \frac{\partial}{\partial y} \left(N_{xy} \frac{\partial w_0}{\partial x} + N_{yy} \frac{\partial w_0}{\partial y} \right) \\ \mathcal{P} &= \left(N_{xx} \frac{\partial w_0}{\partial x} + N_{xy} \frac{\partial w_0}{\partial y} \right) n_x + \left(N_{xy} \frac{\partial w_0}{\partial x} + N_{yy} \frac{\partial w_0}{\partial y} \right) n_y\end{aligned}\quad (10.1.15)$$

and the boundary expressions were arrived by expressing ϕ_x and ϕ_y in terms of the normal and tangential rotations, (ϕ_n, ϕ_s) :

$$\phi_x = n_x \phi_n - n_y \phi_s, \quad \phi_y = n_y \delta \phi_n + n_x \delta \phi_s \quad (10.1.16)$$

The Euler–Lagrange equations are

$$\delta u_0 : \quad \frac{\partial N_{xx}}{\partial x} + \frac{\partial N_{xy}}{\partial y} = I_0 \frac{\partial^2 u_0}{\partial t^2} + I_1 \frac{\partial^2 \phi_x}{\partial t^2} \quad (10.1.17)$$

$$\delta v_0 : \quad \frac{\partial N_{xy}}{\partial x} + \frac{\partial N_{yy}}{\partial y} = I_0 \frac{\partial^2 v_0}{\partial t^2} + I_1 \frac{\partial^2 \phi_y}{\partial t^2} \quad (10.1.18)$$

$$\delta w_0 : \quad \frac{\partial Q_x}{\partial x} + \frac{\partial Q_y}{\partial y} - k w_0 + \mathcal{N} + q = I_0 \frac{\partial^2 w_0}{\partial t^2} \quad (10.1.19)$$

$$\delta \phi_x : \quad \frac{\partial M_{xx}}{\partial x} + \frac{\partial M_{xy}}{\partial y} - Q_x = I_2 \frac{\partial^2 \phi_x}{\partial t^2} + I_1 \frac{\partial^2 u_0}{\partial t^2} \quad (10.1.20)$$

$$\delta \phi_y : \quad \frac{\partial M_{xy}}{\partial x} + \frac{\partial M_{yy}}{\partial y} - Q_y = I_2 \frac{\partial^2 \phi_y}{\partial t^2} + I_1 \frac{\partial^2 v_0}{\partial t^2} \quad (10.1.21)$$

The natural boundary conditions are

$$\begin{aligned}N_{nn} - \hat{N}_{nn} &= 0, \quad N_{ns} - \hat{N}_{ns} = 0, \quad Q_n - \hat{Q}_n = 0 \\ M_{nn} - \hat{M}_{nn} &= 0, \quad M_{ns} - \hat{M}_{ns} = 0\end{aligned}\quad (10.1.22)$$

where

$$Q_n \equiv Q_x n_x + Q_y n_y + \mathcal{P} \quad (10.1.23)$$

Thus, the primary and secondary variables of the theory are

$$\begin{aligned}&\text{primary variables: } u_n, u_s, w_0, \phi_n, \phi_s \\ &\text{secondary variables: } N_{nn}, N_{ns}, Q_n, M_{nn}, M_{ns}\end{aligned}\quad (10.1.24)$$

The initial conditions of the theory involve specifying the values of the displacements and their first derivatives with respect to time at $t = 0$:

$$\begin{aligned}u_n &= u_n^0, \quad u_s = u_s^0, \quad w_0 = w_0^0, \quad \phi_n = \phi_n^0, \quad \phi_s = \phi_s^0 \\ \dot{u}_n &= \dot{u}_n^0, \quad \dot{u}_s = \dot{u}_s^0, \quad \dot{w}_0 = \dot{w}_0^0, \quad \dot{\phi}_n = \dot{\phi}_n^0, \quad \dot{\phi}_s = \dot{\phi}_s^0\end{aligned}\quad (10.1.25)$$

for all points in Ω .

10.1.4 Plate Constitutive Equations

The plate constitutive equations in Eqs. (3.6.6) and (3.6.7) are valid also for the first-order plate theory. In addition, we have

$$Q_x = A_{55}\gamma_{xz}, \quad Q_y = A_{44}\gamma_{yz} \quad (10.1.26)$$

The plate stiffnesses A_{ij} and D_{ij} are given by [see Eqs. (3.6.13)]

$$\begin{aligned} A_{11} &= \frac{E_1 h}{1 - \nu_{12}\nu_{21}}, \quad A_{12} = \frac{\nu_{12}E_2 h}{1 - \nu_{12}\nu_{21}}, \quad A_{22} = \frac{E_2 h}{1 - \nu_{12}\nu_{21}} \\ D_{11} &= \frac{E_1 h^3}{12(1 - \nu_{12}\nu_{21})}, \quad D_{12} = \frac{\nu_{12}E_2 h^3}{12(1 - \nu_{12}\nu_{21})}, \quad D_{22} = \frac{E_2 h^3}{12(1 - \nu_{12}\nu_{21})} \\ D_{66} &= \frac{G_{12}h^3}{12}, \quad A_{44} = G_{23}h, \quad A_{55} = G_{13}h, \quad A_{66} = G_{12}h \end{aligned} \quad (10.1.27)$$

where h is the plate thickness. The stress resultants in an *orthotropic* plate are related to the generalized displacements $(u_0, v_0, w_0, \phi_x, \phi_y)$ by

$$\begin{Bmatrix} N_{xx} \\ N_{yy} \\ N_{xy} \end{Bmatrix} = \begin{bmatrix} A_{11} & A_{12} & 0 \\ A_{12} & A_{22} & 0 \\ 0 & 0 & A_{66} \end{bmatrix} \begin{Bmatrix} \frac{\partial u_0}{\partial x} + \frac{1}{2}(\frac{\partial w_0}{\partial x})^2 \\ \frac{\partial v_0}{\partial y} + \frac{1}{2}(\frac{\partial w_0}{\partial y})^2 \\ \frac{\partial u_0}{\partial y} + \frac{\partial v_0}{\partial x} + \frac{\partial w_0}{\partial x} \frac{\partial w_0}{\partial y} \end{Bmatrix} \quad (10.1.28)$$

$$\begin{Bmatrix} M_{xx} \\ M_{yy} \\ M_{xy} \end{Bmatrix} = \begin{bmatrix} D_{11} & D_{12} & 0 \\ D_{12} & D_{22} & 0 \\ 0 & 0 & D_{66} \end{bmatrix} \begin{Bmatrix} \frac{\partial \phi_x}{\partial x} \\ \frac{\partial \phi_y}{\partial y} \\ \frac{\partial \phi_x}{\partial y} + \frac{\partial \phi_y}{\partial x} \end{Bmatrix} \quad (10.1.29)$$

$$\begin{Bmatrix} Q_y \\ Q_x \end{Bmatrix} = K_s \begin{bmatrix} A_{44} & 0 \\ 0 & A_{55} \end{bmatrix} \begin{Bmatrix} \frac{\partial w_0}{\partial y} + \phi_y \\ \frac{\partial w_0}{\partial x} + \phi_x \end{Bmatrix} \quad (10.1.30)$$

Note that the transverse shear strains $(\gamma_{xz}, \gamma_{yz}) = (\gamma_{xz}^0, \gamma_{yz}^0)$ in FSDT are constant through the plate thickness. Hence, the transverse shear stresses are also constant through the thickness. This is inconsistent with the actual distributions of transverse shear strains and stresses. As we shall see in Section 10.3, the third-order shear deformation plate theory accounts for quadratic variations of these quantities through the plate thickness.

10.1.5 Equations of Motion in Terms of Displacements

The equations of motion (10.1.17)–(10.1.21) can be expressed in terms of displacements $(u_0, v_0, w_0, \phi_x, \phi_y)$ by substituting for the force and moment resultants from Eqs. (10.1.28)–(10.1.30). For homogeneous plates, the equations of motion take the form

$$\begin{aligned} A_{11} \left(\frac{\partial^2 u_0}{\partial x^2} + \frac{\partial w_0}{\partial x} \frac{\partial^2 w_0}{\partial x^2} \right) + A_{12} \left(\frac{\partial^2 v_0}{\partial y \partial x} + \frac{\partial w_0}{\partial y} \frac{\partial^2 w_0}{\partial y \partial x} \right) \\ + A_{66} \left(\frac{\partial^2 u_0}{\partial y^2} + \frac{\partial^2 v_0}{\partial x \partial y} + \frac{\partial^2 w_0}{\partial x \partial y} \frac{\partial w_0}{\partial y} + \frac{\partial w_0}{\partial x} \frac{\partial^2 w_0}{\partial y^2} \right) \\ - \left(\frac{\partial N_{xx}^T}{\partial x} + \frac{\partial N_{xy}^T}{\partial y} \right) = I_0 \frac{\partial^2 u_0}{\partial t^2} \end{aligned} \quad (10.1.31)$$

$$\begin{aligned}
& A_{66} \left(\frac{\partial^2 u_0}{\partial y \partial x} + \frac{\partial^2 v_0}{\partial x^2} + \frac{\partial^2 w_0}{\partial x^2} \frac{\partial w_0}{\partial y} + \frac{\partial w_0}{\partial x} \frac{\partial^2 w_0}{\partial y \partial x} \right) \\
& + A_{12} \left(\frac{\partial^2 u_0}{\partial x \partial y} + \frac{\partial w_0}{\partial x} \frac{\partial^2 w_0}{\partial x \partial y} \right) + A_{22} \left(\frac{\partial^2 v_0}{\partial y^2} + \frac{\partial w_0}{\partial y} \frac{\partial^2 w_0}{\partial y^2} \right) \\
& - \left(\frac{\partial N_{xy}^T}{\partial x} + \frac{\partial N_{yy}^T}{\partial y} \right) = I_0 \frac{\partial^2 v_0}{\partial t^2} \quad (10.1.32)
\end{aligned}$$

$$\begin{aligned}
& K_s A_{55} \left(\frac{\partial^2 w_0}{\partial x^2} + \frac{\partial \phi_x}{\partial x} \right) + K_s A_{44} \left(\frac{\partial^2 w_0}{\partial y^2} + \frac{\partial \phi_y}{\partial y} \right) - k w_0 \\
& + \mathcal{N}(u_0, v_0, w_0) + q(x, y) = I_0 \frac{\partial^2 w_0}{\partial t^2} \quad (10.1.33)
\end{aligned}$$

$$\begin{aligned}
& D_{11} \frac{\partial^2 \phi_x}{\partial x^2} + D_{12} \frac{\partial^2 \phi_y}{\partial y \partial x} + D_{66} \left(\frac{\partial^2 \phi_x}{\partial y^2} + \frac{\partial^2 \phi_y}{\partial y \partial x} \right) \\
& - K_s A_{55} \left(\frac{\partial w_0}{\partial x} + \phi_x \right) - \left(\frac{\partial M_{xx}^T}{\partial x} + \frac{\partial M_{xy}^T}{\partial y} \right) = I_2 \frac{\partial^2 \phi_x}{\partial t^2} \quad (10.1.34)
\end{aligned}$$

$$\begin{aligned}
& D_{66} \left(\frac{\partial^2 \phi_x}{\partial x \partial y} + \frac{\partial^2 \phi_y}{\partial x^2} \right) + D_{12} \frac{\partial^2 \phi_x}{\partial x \partial y} + D_{22} \frac{\partial^2 \phi_y}{\partial y^2} \\
& - K_s A_{44} \left(\frac{\partial w_0}{\partial y} + \phi_y \right) - \left(\frac{\partial M_{xy}^T}{\partial x} + \frac{\partial M_{yy}^T}{\partial y} \right) = I_2 \frac{\partial^2 \phi_y}{\partial t^2} \quad (10.1.35)
\end{aligned}$$

Equations (10.1.31)–(10.1.35) describe five second-order nonlinear partial differential equations in terms of the five generalized displacements u_0 , v_0 , w_0 , ϕ_x , and ϕ_y . When the strains and rotations are small, Eqs. (10.1.31) and (10.1.32) that govern inplane stretching (u_0, v_0) are uncoupled from Eqs. (10.1.33)–(10.1.35) which govern bending (w_0, ϕ_x, ϕ_y). In the following sections, we consider bending, buckling, and natural vibrations using these linear equations of bending.

10.2 The Navier Solutions of FSST

10.2.1 General Solution

As in the case of the classical plate theory, exact analytical solutions of the first-order shear deformation plate theory can be obtained for simply supported plates using Navier's method. The simply supported boundary conditions for the first-order shear deformation plate theory (FSST) can be expressed as (Figure 10.2.1)

$$\begin{aligned}
& w_0(x, 0, t) = 0, \quad w_0(x, b, t) = 0, \quad w_0(0, y, t) = 0, \quad w_0(a, y, t) = 0 \\
& \phi_x(x, 0, t) = 0, \quad \phi_x(x, b, t) = 0, \quad \phi_y(0, y, t) = 0, \quad \phi_y(a, y, t) = 0 \quad (10.2.1) \\
& M_{yy}(x, 0, t) = 0, \quad M_{yy}(x, b, t) = 0, \quad M_{xx}(0, y, t) = 0, \quad M_{xx}(a, y, t) = 0
\end{aligned}$$

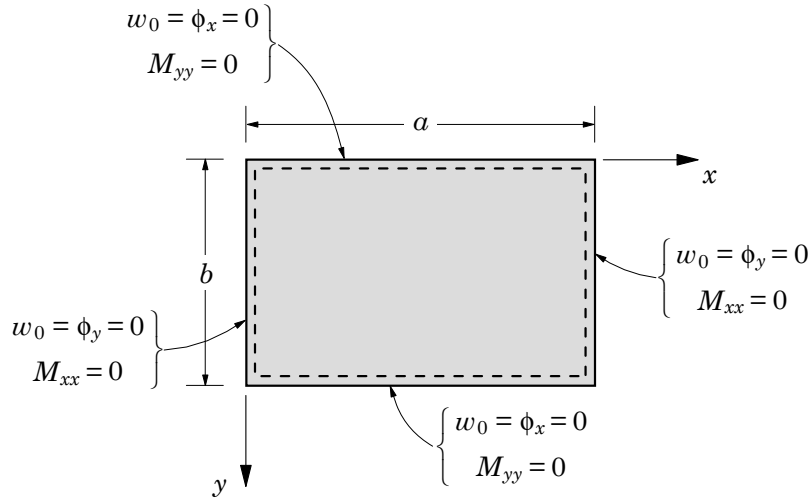


Figure 10.2.1. The simply supported boundary conditions of the first-order shear deformation theory (FSDT).

The boundary conditions in Eq. (10.2.1) are satisfied by the following expansions of the displacements:

$$w_0(x, y, t) = \sum_{n=1}^{\infty} \sum_{m=1}^{\infty} W_{mn}(t) \sin \frac{m\pi x}{a} \sin \frac{n\pi y}{b} \quad (10.2.2)$$

$$\phi_x(x, y, t) = \sum_{n=1}^{\infty} \sum_{m=1}^{\infty} X_{mn}(t) \cos \frac{m\pi x}{a} \sin \frac{n\pi y}{b} \quad (10.2.3)$$

$$\phi_y(x, y, t) = \sum_{n=1}^{\infty} \sum_{m=1}^{\infty} Y_{mn}(t) \sin \frac{m\pi x}{a} \cos \frac{n\pi y}{b} \quad (10.2.4)$$

where a and b denote the dimensions of the rectangular plate. The mechanical and thermal loads are also expanded in double Fourier sine series

$$q(x, y, t) = \sum_{n=1}^{\infty} \sum_{m=1}^{\infty} Q_{mn}(t) \sin \frac{m\pi x}{a} \sin \frac{n\pi y}{b} \quad (10.2.5)$$

$$\Delta T(x, y, z, t) = \sum_{n=1}^{\infty} \sum_{m=1}^{\infty} T_{mn}(z, t) \sin \frac{m\pi x}{a} \sin \frac{n\pi y}{b} \quad (10.2.6)$$

where

$$Q_{mn}(t) = \frac{4}{ab} \int_0^a \int_0^b q(x, y, t) \sin \frac{m\pi x}{a} \sin \frac{n\pi y}{b} dx dy \quad (10.2.7)$$

$$T_{mn}(z, t) = \frac{4}{ab} \int_0^a \int_0^b \Delta T(x, y, z, t) \sin \frac{m\pi x}{a} \sin \frac{n\pi y}{b} dx dy \quad (10.2.8)$$

Substitution of Eqs. (10.2.2)–(10.2.6) into Eqs. (10.1.33)–(10.1.35) yields the following equations for the coefficients (W_{mn}, X_{mn}, Y_{mn}):

$$\begin{aligned} \begin{bmatrix} \hat{s}_{11} + \tilde{s}_{11} & \hat{s}_{12} & \hat{s}_{13} \\ \hat{s}_{12} & \hat{s}_{22} & \hat{s}_{23} \\ \hat{s}_{13} & \hat{s}_{23} & \hat{s}_{33} \end{bmatrix} \begin{Bmatrix} W_{mn} \\ X_{mn} \\ Y_{mn} \end{Bmatrix} + \begin{bmatrix} \hat{m}_{11} & 0 & 0 \\ 0 & \hat{m}_{22} & 0 \\ 0 & 0 & \hat{m}_{33} \end{bmatrix} \begin{Bmatrix} \ddot{W}_{mn} \\ \ddot{X}_{mn} \\ \ddot{Y}_{mn} \end{Bmatrix} \\ = \begin{Bmatrix} Q_{mn} \\ 0 \\ 0 \end{Bmatrix} - \begin{Bmatrix} 0 \\ \alpha_m M_{mn}^1 \\ \beta_n M_{mn}^2 \end{Bmatrix} \end{aligned} \quad (10.2.9)$$

where \hat{s}_{ij} and \hat{m}_{ij} are defined by

$$\begin{aligned} \hat{s}_{11} &= K_s(A_{55}\alpha_m^2 + A_{44}\beta_n^2) + k, \quad \tilde{s}_{11} = \hat{N}_{xx}\alpha_m^2 + \hat{N}_{yy}\beta_n^2 \\ \hat{s}_{12} &= K_s A_{55}\alpha_m, \quad \hat{s}_{13} = K_s A_{44}\beta_n, \quad \hat{s}_{22} = (D_{11}\alpha_m^2 + D_{66}\beta_n^2 + K_s A_{55}) \\ \hat{s}_{23} &= (D_{12} + D_{66})\alpha_m\beta_n, \quad \hat{s}_{33} = (D_{66}\alpha_m^2 + D_{22}\beta_n^2 + K_s A_{44}) \\ \hat{m}_{11} &= I_0, \quad \hat{m}_{22} = I_2, \quad \hat{m}_{33} = I_2 \end{aligned} \quad (10.2.10)$$

where the thermal coefficients M_{mn}^1 and M_{mn}^2 are defined by Eqs. (6.2.4), and $\alpha_m = m\pi/a$ and $\beta_n = n\pi/b$.

10.2.2 Bending Analysis

The static solution can be obtained from Eq. (10.2.9) by setting the time derivative terms and edge forces ($\hat{N}_{xx}, \hat{N}_{yy}$) to zero:

$$\begin{bmatrix} \hat{s}_{11} & \hat{s}_{12} & \hat{s}_{13} \\ \hat{s}_{12} & \hat{s}_{22} & \hat{s}_{23} \\ \hat{s}_{13} & \hat{s}_{23} & \hat{s}_{33} \end{bmatrix} \begin{Bmatrix} W_{mn} \\ X_{mn} \\ Y_{mn} \end{Bmatrix} = \begin{Bmatrix} Q_{mn} \\ 0 \\ 0 \end{Bmatrix} - \begin{Bmatrix} 0 \\ \alpha_m M_{mn}^1 \\ \beta_n M_{mn}^2 \end{Bmatrix} \quad (10.2.11)$$

Solution of Eq. (10.2.11) for each $m, n = 1, 2, \dots$ gives (W_{mn}, X_{mn}, Y_{mn}) , which can then be used to compute the solution (w_0, ϕ_x, ϕ_y) from Eqs. (10.2.2)–(10.2.4). We obtain

$$\begin{aligned} W_{mn} &= \frac{1}{b_{mn}} \left[b_0 Q_{mn} + \hat{s}_{12} \left(\alpha_m M_{mn}^1 \hat{s}_{33} - \beta_n M_{mn}^2 \hat{s}_{23} \right) \right. \\ &\quad \left. - \hat{s}_{13} \left(\alpha_m M_{mn}^1 \hat{s}_{23} - \beta_n M_{mn}^2 \hat{s}_{22} \right) \right] \\ X_{mn} &= \frac{1}{b_0} \left[b_1 W_{mn} - \left(\alpha_m M_{mn}^1 \hat{s}_{33} - \beta_n M_{mn}^2 \hat{s}_{23} \right) \right] \\ Y_{mn} &= \frac{1}{b_0} \left[b_2 W_{mn} + \left(\alpha_m M_{mn}^1 \hat{s}_{23} - \beta_n M_{mn}^2 \hat{s}_{22} \right) \right] \end{aligned} \quad (10.2.12)$$

where

$$\begin{aligned} b_{mn} &= \hat{s}_{11} b_0 + \hat{s}_{12} b_1 + \hat{s}_{13} b_2, \quad b_0 = \hat{s}_{22} \hat{s}_{33} - \hat{s}_{23} \hat{s}_{23} \\ b_1 &= \hat{s}_{23} \hat{s}_{13} - \hat{s}_{12} \hat{s}_{33}, \quad b_2 = \hat{s}_{12} \hat{s}_{23} - \hat{s}_{22} \hat{s}_{13} \end{aligned} \quad (10.2.13)$$

When thermal effects are absent, we have

$$W_{mn} = \frac{b_0}{b_{mn}} Q_{mn}, \quad X_{mn} = \frac{b_1}{b_{mn}} Q_{mn}, \quad Y_{mn} = \frac{b_2}{b_{mn}} Q_{mn} \quad (10.2.14)$$

The bending moments are given by

$$\begin{aligned} M_{xx} &= - \sum_{n=1}^{\infty} \sum_{m=1}^{\infty} (D_{11}\alpha_m X_{mn} + D_{12}\beta_n Y_{mn}) \sin \alpha_m x \sin \beta_n y \\ M_{yy} &= - \sum_{n=1}^{\infty} \sum_{m=1}^{\infty} (D_{12}\alpha_m X_{mn} + D_{22}\beta_n Y_{mn}) \sin \alpha_m x \sin \beta_n y \\ M_{xy} &= D_{66} \sum_{n=1}^{\infty} \sum_{m=1}^{\infty} (\beta_n X_{mn} + \alpha_m Y_{mn}) \cos \alpha_m x \cos \beta_n y \end{aligned} \quad (10.2.15)$$

The inplane stresses and transverse shear stresses can be computed using the constitutive equations:

$$\begin{Bmatrix} \sigma_{xx} \\ \sigma_{yy} \\ \sigma_{xy} \end{Bmatrix} = -z \sum_{n=1}^{\infty} \sum_{m=1}^{\infty} \begin{Bmatrix} (Q_{11}\alpha_m X_{mn} + Q_{12}\beta_n Y_{mn}) \sin \alpha_m x \sin \beta_n y \\ (Q_{12}\alpha_m X_{mn} + Q_{22}\beta_n Y_{mn}) \sin \alpha_m x \sin \beta_n y \\ -Q_{66}(\beta_n X_{mn} + \alpha_m Y_{mn}) \cos \alpha_m x \cos \beta_n y \end{Bmatrix} \quad (10.2.16)$$

$$\begin{Bmatrix} \sigma_{yz} \\ \sigma_{xz} \end{Bmatrix} = \sum_{n=1}^{\infty} \sum_{m=1}^{\infty} \begin{Bmatrix} Q_{44}(Y_{mn} + \beta_n W_{mn}) \sin \alpha_m x \cos \beta_n y \\ Q_{55}(X_{mn} + \alpha_m W_{mn}) \cos \alpha_m x \sin \beta_n y \end{Bmatrix} \quad (10.2.17)$$

The transverse shear stresses can also be computed using 3-D equilibrium equations in terms of stresses [see Chapter 6, Eqs. (6.2.25)–(6.2.28)]. They are given by

$$\begin{aligned} \sigma_{xz} &= -\frac{h^2}{8} \left[1 - \left(\frac{2z}{h} \right)^2 \right] (T_{11}X_{mn} + T_{12}Y_{mn}) \cos \alpha_m x \sin \beta_n y \\ \sigma_{yz} &= -\frac{h^2}{8} \left[1 - \left(\frac{2z}{h} \right)^2 \right] (T_{12}X_{mn} + T_{22}Y_{mn}) \sin \alpha_m x \cos \beta_n y \\ \sigma_{zz} &= \frac{h^3}{48} \left\{ \left[1 + \left(\frac{2z}{h} \right)^3 \right] - 3 \left[1 + \left(\frac{2z}{h} \right) \right] \right\} (T_{31}X_{mn} + T_{32}Y_{mn}) \\ &\quad \times \sin \alpha_m x \sin \beta_n y \end{aligned} \quad (10.2.18a)$$

where

$$\begin{aligned} T_{11} &= \alpha_m^2 Q_{11} + \beta_n^2 Q_{66}, \quad T_{12} = \alpha_m \beta_n (Q_{12} + Q_{66}) \\ T_{22} &= \alpha_m^2 Q_{66} + \beta_n^2 Q_{22}, \quad T_{31} = \alpha_m^3 Q_{11} + \alpha_m \beta_n^2 (2Q_{66} + Q_{12}) \\ T_{32} &= \alpha_m^2 \beta_n (Q_{12} + 2Q_{66}) + \beta_n^3 Q_{22} \end{aligned} \quad (10.2.18b)$$

The following nondimensional variables are used to present the numerical results in tabular (Table 10.2.1) and graphical (Fig. 10.2.2) forms:

$$\begin{aligned} \bar{w} &= w_0 \left(E_2 h^3 / b^4 q_0 \right), \quad \hat{w} = w_0 \left(D_{22} / b^4 q_0 \right) \times 10^2 \\ \bar{\sigma}_{xx} &= \sigma_{xx} \left(h^2 / b^2 q_0 \right), \quad \bar{\sigma}_{yy} = \sigma_{yy} \left(h^2 / b^2 q_0 \right) \\ \bar{\sigma}_{xy} &= \sigma_{xy} \left(h^2 / b^2 q_0 \right), \quad \bar{\sigma}_{xz} = \sigma_{xz} (h / bq_0), \quad \bar{\sigma}_{yz} = \sigma_{yz} (h / bq_0) \end{aligned} \quad (10.2.19)$$

Table 10.2.1. Effect of the transverse shear deformation on deflections and stresses in isotropic and orthotropic square plates under distributed loads.*

Load	$\frac{b}{h}$	\hat{w}	$\bar{\sigma}_{xx}$	$\bar{\sigma}_{yy}$	$\bar{\sigma}_{xy}$	$\bar{\sigma}_{xz}$	$\bar{\sigma}_{yz}$
<i>Isotropic plates ($\nu = 0.25$)</i>							
SL	10	0.2702	0.1900	0.1900	0.1140	0.1910	0.1910
						0.2387	0.2387†
	20	0.2600	0.1900	0.1900	0.1140	0.1910	0.1910
	50	0.2572	0.1900	0.1900	0.1140	0.1910	0.1910
	100	0.2568	0.1900	0.1900	0.1140	0.1910	0.1910
	CPT	0.2566	0.1900	0.1900	0.1140	—	—
UL (19)	10	0.4259	0.2762	0.2762	0.2085	0.3927	0.3927
						0.4909	0.4909†
	20	0.4111	0.2762	0.2762	0.2085	0.3927	0.3927
	50	0.4070	0.2762	0.2762	0.2085	0.3927	0.3927
	100	0.4060	0.2762	0.2762	0.2085	0.3927	0.3927
	CPT	0.4062	0.2762	0.2762	0.2085	—	—
<i>Orthotropic plates</i>							
SL	10	0.0533	0.5248	0.0338	0.0246	0.3452	0.0367
						0.4315	0.0459
	20	0.0404	0.5350	0.0286	0.0222	0.3501	0.0319
						0.4376	0.0399
	50	0.0367	0.5380	0.0270	0.0214	0.3515	0.0304
						0.4394	0.0380
	100	0.0362	0.5385	0.0267	0.0213	0.3517	0.0302
						0.4397	0.0377
	CPT	0.0360	0.5387	0.0267	0.0213	—	—
						0.4398	0.0376
UL (19)	10	0.0795	0.7706	0.0352	0.0539	0.6147	0.1529
						0.7684	0.1911
	20	0.0607	0.7828	0.0272	0.0487	0.6194	0.1466
						0.7742	0.1833
	50	0.0553	0.7860	0.0249	0.0468	0.6207	0.1452
						0.7756	0.1814
	100	0.0545	0.7865	0.0245	0.0464	0.6206	0.1449
						0.7757	0.1812
	CPT	0.0543	0.7866	0.0244	0.0463	—	—
						0.7758	0.1811

* See Figure 10.2.1 for the plate geometry and coordinate system.

† Stresses computed using the stress equilibrium equations (10.2.18a,b); results are independent of b/h for isotropic plates.

Note: The numbers in parentheses denote the maximum values of m and n used to evaluate the series.

Table 10.2.1 contains the maximum nondimensional deflections (\bar{w}) and stresses of simply supported square plates under sinusoidally distributed load (SSL) and uniformly distributed load (UDL), and for different side-to-thickness ratios ($E_1 = 25E_2$, $G_{12} = G_{13} = 0.5E_2$, $G_{23} = 0.2E_2$, $\nu_{12} = 0.25$, $K_s = 5/6$, $k = 0$). The maximum stresses were evaluated at the locations indicated below:

$$\bar{\sigma}_{xx}(a/2, b/2, \frac{h}{2}), \quad \bar{\sigma}_{yy}(a/2, b/2, \frac{h}{2}), \quad \bar{\sigma}_{xy}(a, b, -\frac{h}{2})$$

$$\bar{\sigma}_{xz}(0, b/2, \frac{h}{2}), \quad \bar{\sigma}_{yz}(a/2, 0, \frac{h}{2})$$

The transverse shear stresses are calculated using the constitutive equations as well as equilibrium equations. Of course, the constitutively-derived transverse stresses in the first-order shear deformation plate theory are independent of the z coordinate (i.e., constant through the thickness). The nondimensional quantities in the classical plate theory are independent of the side-to-thickness ratio. It is clear from the results that the influence of transverse shear deformation is to increase the transverse deflection. The difference between the deflections predicted by the first-order shear deformation theory and classical plate theory decreases with the increase in the side-to-thickness ratio a/h , as can be seen from Figure 10.2.2.

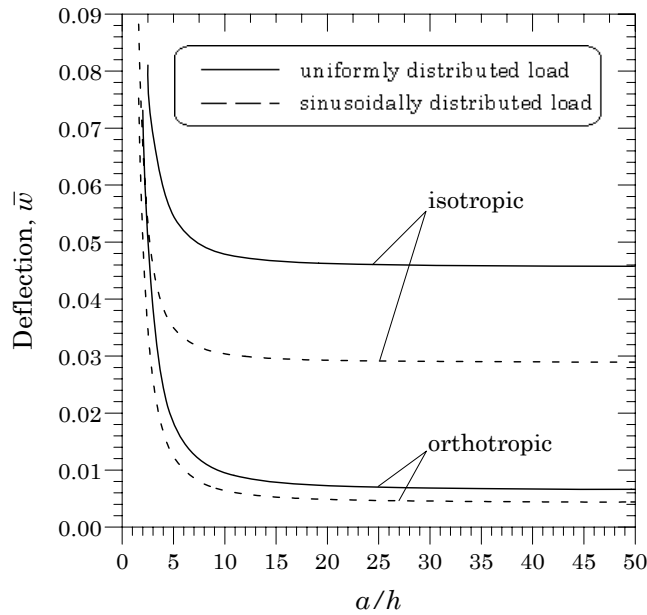


Figure 10.2.2. Nondimensional center transverse deflection (\bar{w}) versus side-to-thickness ratio (a/h) for simply supported square plates.

10.2.3 Buckling Analysis

For buckling analysis, we assume that the only applied loads are the inplane compressive forces

$$\hat{N}_{xx} = -N_0, \quad \hat{N}_{yy} = -\gamma N_0, \quad \gamma = \frac{\hat{N}_{yy}}{\hat{N}_{xx}} \quad (10.2.20)$$

and all other mechanical and thermal loads are zero (and $k = 0$). From Eq. (10.2.9), we have

$$\begin{bmatrix} \hat{s}_{11} - N_0 (\alpha_m^2 + \gamma \beta_n^2) & \hat{s}_{12} & \hat{s}_{13} \\ \hat{s}_{12} & \hat{s}_{22} & \hat{s}_{23} \\ \hat{s}_{13} & \hat{s}_{23} & \hat{s}_{33} \end{bmatrix} \begin{Bmatrix} W_{mn} \\ X_{mn} \\ Y_{mn} \end{Bmatrix} = \begin{Bmatrix} 0 \\ 0 \\ 0 \end{Bmatrix} \quad (10.2.21)$$

For a nontrivial solution the determinant of the coefficient matrix in Eq. (10.2.21) must be zero. This gives the following expression for the buckling load:

$$N_0 = \left(\frac{1}{\alpha_m^2 + \gamma \beta_n^2} \right) \left[\frac{K_s^2 A_{44} A_{55} \hat{c}_{33} + (K_s A_{55} \alpha_m^2 + K_s A_{44} \beta_n^2) c_1}{c_1 + K_s A_{44} c_2 + K_s A_{55} c_3 + K_s^2 A_{44} A_{55}} \right] \quad (10.2.22)$$

$$= \left(\frac{1}{\alpha_m^2 + \gamma \beta_n^2} \right) \left[\frac{c_0 + \left(\frac{\alpha_m^2}{K_s A_{44}} + \frac{\beta_n^2}{K_s A_{55}} \right) c_1}{1 + \frac{c_1}{K_s^2 A_{44} A_{55}} + \frac{c_2}{K_s A_{55}} + \frac{c_3}{K_s A_{44}}} \right] \quad (10.2.22)$$

$$\begin{aligned} c_0 &= D_{11} \alpha_m^4 + 2(D_{12} + 2D_{66}) \alpha_m^2 \beta_n^2 + D_{22} \beta_n^4, \quad c_1 = c_2 c_3 - (c_4)^2 > 0 \\ c_2 &= D_{11} \alpha_m^2 + D_{66} \beta_n^2, \quad c_3 = D_{66} \alpha_m^2 + D_{22} \beta_n^2, \quad c_4 = (D_{12} + D_{66}) \alpha_m \beta_n \end{aligned} \quad (10.2.23)$$

When the effect of transverse shear deformation is neglected (i.e., set K_s to a large value), Eq. (10.2.22) yields the result (8.1.7) obtained using the classical plate theory. The expression in (10.2.22) is of the form

$$\frac{c_0 + k_1}{1 + k_2} \quad \text{with} \quad k_1 < k_2, \quad \text{which implies} \quad c_0 \geq \frac{c_0 + k_1}{1 + k_2}$$

indicating that transverse shear deformation has the effect of reducing the buckling load (as long as $c_0 > 1$).

In general, no conclusions can be drawn from the complicated expression of the buckling load concerning its minimum. For an isotropic plate ($D_{11} = D_{22} = D_{12} + 2D_{66} = D$), the critical buckling load occurs for $m = n = 1$ and it is given by

$$N_{cr} = 4D \left(\frac{\pi}{a} \right)^2 \frac{\left[1 + \frac{3(1-\nu^2)\pi^2(h/a)^2}{K_s} \right]}{\left[1 + \frac{72(1+\nu)(1-\nu^2)\pi^4(h/a)^4}{K_s^2} + \frac{6(1+\nu)(3-\nu)\pi^2(h/a)^2}{K_s} \right]} \quad (10.2.24)$$

Table 10.2.2 contains the critical buckling loads $\bar{N} = N_{cr} b^2 / (\pi^2 D_{22})$ as a function of the plate aspect ratio a/b , side-to-thickness ratio b/h , and modulus ratio E_1/E_2 for uniaxial ($\gamma = 0$) and biaxial ($\gamma = 1$) compression. The classical plate theory (CPT) results are also included for comparison (see Table 8.1.1). The effect of

transverse shear deformation is significant for lower aspect ratios, thick plates, and larger modular ratios. For thin plates, irrespective of the aspect ratio and modular ratio, the buckling loads predicted by the shear deformation plate theory (Figure 10.2.3) are very close to those of the classical plate theory.

Table 10.2.2. Nondimensional buckling loads \bar{N} of simply supported plates under inplane uniform compression ($\gamma = 0$) and biaxial compression ($\gamma = 1$).

γ	$\frac{a}{b}$	$\frac{h}{b}$	$\frac{E_1}{E_2} = 1$	$\frac{E_1}{E_2} = 3$	$\frac{E_1}{E_2} = 10$	$\frac{E_1}{E_2} = 25$
0	0.5	10	5.523	11.583	23.781	34.701
		20	6.051	13.779	35.615	68.798
		100	6.242	14.669	42.398	100.750
		CPT	6.250	14.708	42.737	102.750
	1.0	10	3.800	5.901	11.205	19.252
		20	3.948	6.309	12.832	25.412
		100	3.998	6.452	13.460	28.357
		CPT	4.000	6.458	13.488	28.495
1.5	0.5	10	4.045 ^(2,1)	5.664	8.354	13.166
		20	4.262 ^(2,1)	5.942	8.959	15.077
		100	4.337 ^(2,1)	6.037	9.173	15.823
		CPT	4.340 ^(2,1)	6.042	9.182	15.856
	1.0	10	3.800 ^(3,1)	5.664 ^(2,1)	8.354 ^(2,1)	13.166 ^(2,1)
		20	3.948 ^(3,1)	5.942 ^(2,1)	8.959 ^(2,1)	14.052
		100	3.998 ^(3,1)	6.037 ^(2,1)	9.173 ^(2,1)	14.264
		CPT	4.000 ^(3,1)	6.042 ^(2,1)	9.182 ^(2,1)	14.273
3.0	0.5	10	4.418	9.405	15.191 ^(1,3)	17.773 ^(1,3)
		20	4.841	11.070	21.565 ^(1,3)	30.073 ^(1,4)
		100	4.993	11.737	25.241 ^(1,3)	40.157 ^(1,4)
		CPT	5.000	11.767	25.427 ^(1,3)	40.784 ^(1,4)
	1.0	10	1.900	3.015	5.662	7.518 ^(1,2)
		20	1.974	3.173	6.433	9.308 ^(1,2)
		100	1.999	3.227	6.731	10.156 ^(1,2)
		CPT	2.000	3.229	6.744	10.196 ^(1,2)
1.5	0.5	10	1.391	1.788	2.614	4.093
		20	1.431	1.841	2.769	4.651
		100	1.444	1.858	2.823	4.869
		CPT	1.444	1.859	2.825	4.879
	1.0	10	1.079	1.151	1.227	1.375
		20	1.103	1.172	1.251	1.414
		100	1.111	1.179	1.259	1.426
		CPT	1.111	1.179	1.260	1.427

Note: The pair of numbers in parentheses denote mode numbers (m, n) at which the critical buckling load occurred; $(m, n) = (1, 1)$ for all other cases.

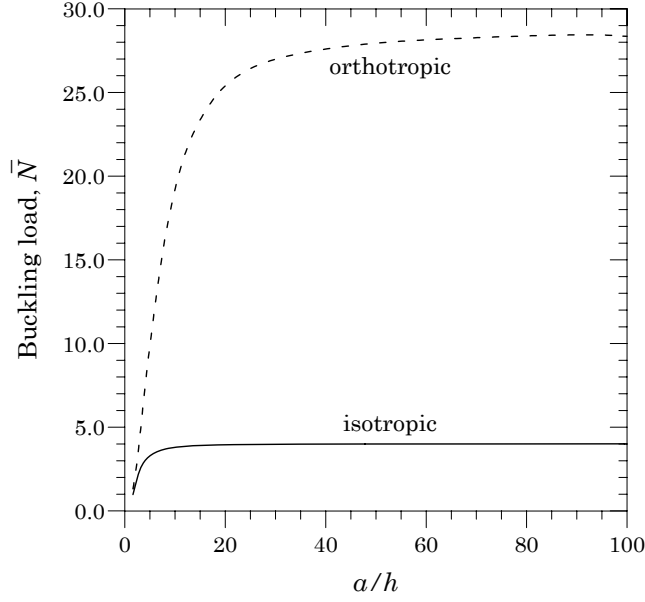


Figure 10.2.3. Nondimensional critical buckling load (\bar{N}) versus side-to-thickness ratio (a/h) for simply supported square plates.

10.2.4 Natural Vibration

For free vibration, we set the thermal and mechanical loads to zero and seek periodic solution to Eq. (10.2.9) in the form

$$W_{mn}(t) = W_{mn}^0 e^{i\omega t}, \quad X_{mn}(t) = X_{mn}^0 e^{i\omega t}, \quad Y_{mn}(t) = Y_{mn}^0 e^{i\omega t} \quad (10.2.25)$$

and obtain the following 3×3 system of eigenvalue problem:

$$\left(\begin{bmatrix} \hat{s}_{11} & \hat{s}_{12} & \hat{s}_{13} \\ \hat{s}_{12} & \hat{s}_{22} & \hat{s}_{23} \\ \hat{s}_{13} & \hat{s}_{23} & \hat{s}_{33} \end{bmatrix} - \omega^2 \begin{bmatrix} \hat{m}_{11} & 0 & 0 \\ 0 & \hat{m}_{22} & 0 \\ 0 & 0 & \hat{m}_{33} \end{bmatrix} \right) \begin{Bmatrix} W_{mn}^0 \\ X_{mn}^0 \\ Y_{mn}^0 \end{Bmatrix} = \begin{Bmatrix} 0 \\ 0 \\ 0 \end{Bmatrix} \quad (10.2.26)$$

where \hat{s}_{ij} and \hat{m}_{ij} are defined in Eq. (10.2.10). Setting the determinant of the coefficient matrix in Eq. (10.2.26) yields the frequency equation.

If the rotatory inertia I_2 is omitted (i.e., $\hat{m}_{22} = \hat{m}_{33} = 0$), the frequency equation can be solved for ω^2

$$\omega^2 = \frac{1}{\hat{m}_{11}} \left(\hat{s}_{11} - \frac{\hat{s}_{13}\hat{s}_{23} - \hat{s}_{12}\hat{s}_{33}}{\hat{s}_{22}\hat{s}_{33} - \hat{s}_{23}\hat{s}_{23}} \hat{s}_{12} - \frac{\hat{s}_{12}\hat{s}_{23} - \hat{s}_{13}\hat{s}_{22}}{\hat{s}_{22}\hat{s}_{33} - \hat{s}_{23}\hat{s}_{23}} \hat{s}_{13} \right) \quad (10.2.27)$$

Table 10.2.3 contains the first four frequencies of isotropic plates. The effect of the shear correction factor is to decrease the frequencies, i.e., the smaller the K_s , the smaller are the frequencies. The rotary inertia (RI) also has the effect of decreasing the frequencies. Table 10.2.4 contains fundamental natural frequencies of square plates for various values of side-to-thickness ratio a/b and modulus ratios $E_1/E_2 = 1$ and 10. Figure 10.2.4 shows the effect of transverse shear deformation

and rotary inertia on fundamental natural frequencies of orthotropic square plates. The effect of rotary inertia is negligible in FSDT and, therefore, not shown in the figure.

Table 10.2.3. Effect of the shear deformation, rotatory inertia, and shear correction coefficient on nondimensional natural frequencies of simply supported isotropic square plates ($\bar{\omega} = \omega(a^2/h)\sqrt{\rho/E}$; $\nu = 0.3$, $a/h = 10$).

m	n	CPT w/o RI	CPT with RI	K_s	FSDT w/o RI	FSDT with RI
1	1	5.973	5.925	5/6	5.812	5.769
				2/3	5.773	5.732
				1.0	5.838	5.794
2	1	14.933	14.635	5/6	13.980	13.764
				2/3	13.769	13.568
				1.0	14.127	13.899
2	2	23.893	23.144	5/6	21.582	21.121
				2/3	21.103	20.688
				1.0	21.922	21.424
3	1	29.867	28.709	5/6	26.378	25.734
				2/3	25.682	25.115
				1.0	26.875	26.171

Note: “w/o RI” means without rotary inertia.

Table 10.2.4. Effect of shear deformation, material orthotropy, rotatory inertia on dimensionless fundamental frequencies of simply supported square plates [$\bar{\omega} = \omega(a^2/h)\sqrt{\rho/E_2}$, $K_s = 5/6$].

Theory	$a/h \rightarrow$	5	10	20	25	50	100
$E_1/E_2 = 1$, $\nu = 0.25$							
FSDT	w-RI	5.232	5.694	5.835	5.853	5.877	5.883
	w/o-RI	5.349	5.736	5.847	5.860	5.879	5.883
CPT	(5.885)	5.700	5.837	5.873	5.877	5.883	5.885
$E_1 = 10E_2$, $G_{12} = G_{13} = 0.5E_2$, $G_{23} = 0.2E_2$, $\nu_{12} = 0.25$							
FSDT	w-RI	7.709	9.509	10.218	10.316	10.450	10.484
	w/o-RI	7.810	9.567	10.238	10.329	10.454	10.486
CPT	(10.496)	10.167	10.411	10.475	10.483	10.493	10.495

Note: “w-RI” means with rotatory inertia; “w/o-RI” means without rotatory inertia. Values in the parentheses are the frequencies without rotatory inertia.

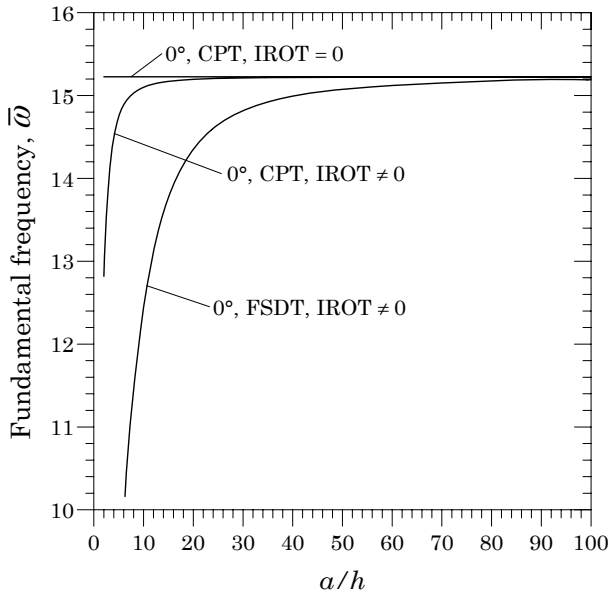


Figure 10.2.4. Fundamental frequency ($\bar{\omega}$) versus side-to-thickness ratio (a/b) for simply supported orthotropic plates.

10.3 The Third-Order Plate Theory

10.3.1. General Comments

In principle, one may expand the displacement field of a plate in terms of the thickness coordinate up to any desired degree. However, due to the algebraic complexity and computational effort involved with higher-order theories in return for a marginal gain in accuracy, theories higher than third order have not been attempted. The reason for expanding the displacements up to the cubic term in the thickness coordinate is to have quadratic variation of the transverse shear strains and transverse shear stresses through the plate thickness. This avoids the need for shear correction coefficients used in the first-order shear deformation plate theory (FSDT).

There are many papers on third-order plate theories and review is presented in Reddy (2004a). Although many of them seem to differ from each other on the surface, the displacement fields of these theories are related. Here we present the original third-order shear deformation plate theory (TSDT) of Reddy (1984a) that contains other lower-order plate theories, including CPT and FSDT, as special cases. For additional details, see Chapter 11 of Reddy (2004a).

10.3.2. Displacement Field

The third-order plate theory to be presented here is also based on the same assumptions as the classical and first-order plate theories, except that the assumption on the straightness and normality of a transverse normal after deformation is relaxed by expanding the displacements (u, v, w) as cubic functions

of the thickness coordinate. Figure 10.3.1 shows the kinematics of deformation of a transverse normal on edge $y = 0$ in the classical, first-order, and third-order plate theories.

Consider the displacement field

$$\begin{aligned} u(x, y, z, t) &= u_0(x, y, t) + z\phi_x(x, y, t) - \frac{4z^3}{3h^2} \left(\phi_x + \frac{\partial w_0}{\partial x} \right) \\ v(x, y, z, t) &= v_0(x, y, t) + z\phi_y(x, y, t) - \frac{4z^3}{3h^2} \left(\phi_y + \frac{\partial w_0}{\partial y} \right) \\ w(x, y, z, t) &= w_0(x, y, t) \end{aligned} \quad (10.3.1)$$

where (u_0, v_0, w_0) have the same meaning as in FSDT except that (ϕ_x, ϕ_y) now denote slopes of a transverse normal at $z = 0$

$$\left. \frac{\partial u}{\partial z} \right|_{z=0} = \phi_x, \quad \left. \frac{\partial v}{\partial z} \right|_{z=0} = \phi_y$$

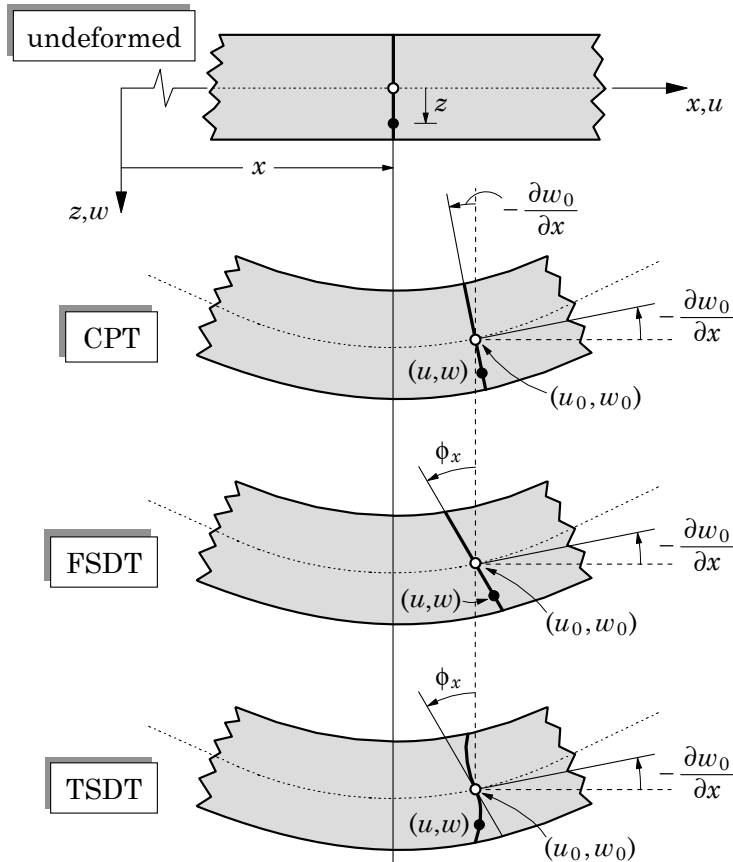


Figure 10.3.1. Deformation of a transverse normal according to the classical, first-order, and third-order plate theories.

Note that the displacement field in Eq. (10.3.1) suggests that a straight line perpendicular to the undeformed middle plane becomes a cubic curve after the plate deforms (Figure 10.3.1). As will be seen shortly, this choice of the displacement field is arrived to satisfy the following stress-free boundary conditions on the bottom and top faces of the plate:

$$\sigma_{xz}(x, y, \pm\frac{h}{2}) = \sigma_{yz}(x, y, \pm\frac{h}{2}) = 0 \quad (10.3.2)$$

10.3.3. Strains and Stresses

Substitution of the displacement field (10.3.1) into the linear strain-displacement relations of Eq. (1.4.8) yields the strains

$$\begin{Bmatrix} \varepsilon_{xx} \\ \varepsilon_{yy} \\ \gamma_{xy} \end{Bmatrix} = \begin{Bmatrix} \varepsilon_{xx}^{(0)} \\ \varepsilon_{yy}^{(0)} \\ \gamma_{xy}^{(0)} \end{Bmatrix} + z \begin{Bmatrix} \varepsilon_{xx}^{(1)} \\ \varepsilon_{yy}^{(1)} \\ \gamma_{xy}^{(1)} \end{Bmatrix} + z^3 \begin{Bmatrix} \varepsilon_{xx}^{(3)} \\ \varepsilon_{yy}^{(3)} \\ \gamma_{xy}^{(3)} \end{Bmatrix} \quad (10.3.3a)$$

$$\begin{Bmatrix} \gamma_{yz} \\ \gamma_{xz} \end{Bmatrix} = \begin{Bmatrix} \gamma_{yz}^{(0)} \\ \gamma_{xz}^{(0)} \end{Bmatrix} + z^2 \begin{Bmatrix} \gamma_{yz}^{(2)} \\ \gamma_{xz}^{(2)} \end{Bmatrix} \quad (10.3.3b)$$

where

$$\begin{Bmatrix} \varepsilon_{xx}^{(0)} \\ \varepsilon_{yy}^{(0)} \\ \gamma_{xy}^{(0)} \end{Bmatrix} = \begin{Bmatrix} \frac{\partial u_0}{\partial x} \\ \frac{\partial v_0}{\partial y} \\ \frac{\partial u_0}{\partial y} + \frac{\partial v_0}{\partial x} \end{Bmatrix}, \quad \begin{Bmatrix} \varepsilon_{xx}^{(1)} \\ \varepsilon_{yy}^{(1)} \\ \gamma_{xy}^{(1)} \end{Bmatrix} = \begin{Bmatrix} \frac{\partial \phi_x}{\partial x} \\ \frac{\partial \phi_y}{\partial y} \\ \frac{\partial \phi_x}{\partial y} + \frac{\partial \phi_y}{\partial x} \end{Bmatrix} \quad (10.3.4a)$$

$$\begin{Bmatrix} \varepsilon_{xx}^{(3)} \\ \varepsilon_{yy}^{(3)} \\ \gamma_{xy}^{(3)} \end{Bmatrix} = -c_1 \begin{Bmatrix} \left(\frac{\partial \phi_x}{\partial x} + \frac{\partial^2 w_0}{\partial x^2} \right) \\ \left(\frac{\partial \phi_y}{\partial y} + \frac{\partial^2 w_0}{\partial y^2} \right) \\ \left(\frac{\partial \phi_x}{\partial y} + \frac{\partial \phi_y}{\partial x} + 2 \frac{\partial^2 w_0}{\partial x \partial y} \right) \end{Bmatrix} \quad (10.3.4b)$$

$$\begin{Bmatrix} \gamma_{yz}^{(0)} \\ \gamma_{xz}^{(0)} \end{Bmatrix} = \begin{Bmatrix} \phi_y + \frac{\partial w_0}{\partial y} \\ \phi_x + \frac{\partial w_0}{\partial x} \end{Bmatrix}, \quad \begin{Bmatrix} \gamma_{yz}^{(2)} \\ \gamma_{xz}^{(2)} \end{Bmatrix} = -c_2 \begin{Bmatrix} \left(\phi_y + \frac{\partial w_0}{\partial y} \right) \\ \left(\phi_x + \frac{\partial w_0}{\partial x} \right) \end{Bmatrix} \quad (10.3.4c)$$

and

$$c_1 = \frac{4}{3h^2}, \quad c_2 = 3c_1 = \frac{4}{h^2} \quad (10.3.5)$$

Assuming linear elastic behavior, the inplane stresses ($\sigma_{xx}, \sigma_{yy}, \sigma_{xy}$) and transverse shear stresses (σ_{xz}, σ_{yz}) can be expressed as

$$\begin{Bmatrix} \sigma_{xx} \\ \sigma_{yy} \\ \sigma_{xy} \end{Bmatrix} = \begin{bmatrix} Q_{11} & Q_{12} & 0 \\ Q_{12} & Q_{22} & 0 \\ 0 & 0 & Q_{66} \end{bmatrix} \begin{Bmatrix} \varepsilon_{xx} \\ \varepsilon_{yy} \\ \gamma_{xy} \end{Bmatrix} \quad (10.3.6a)$$

$$\begin{Bmatrix} \sigma_{yz} \\ \sigma_{xz} \end{Bmatrix} = \begin{bmatrix} Q_{44} & 0 \\ 0 & Q_{55} \end{bmatrix} \begin{Bmatrix} \gamma_{yz} \\ \gamma_{xz} \end{Bmatrix} \quad (10.3.6b)$$

Thus, the inplane stresses vary as cubic functions of the thickness coordinate (z) while the transverse shear stresses are quadratic through the thickness. Note that the transverse normal stress σ_{zz} is assumed to be zero, like in CPT and FSDT, and this assumption was used in deriving the plane-stress-reduced stiffness coefficients Q_{ij} in Section 1.4 [see Eqs. (1.3.36) and (1.3.37)], which are related to the engineering constants E_1 , E_2 , ν_{12} , G_{12} , G_{13} , and G_{23} by

$$\begin{aligned} Q_{11} &= \frac{E_1}{1 - \nu_{12}\nu_{21}}, \quad Q_{12} = \frac{\nu_{12}E_2}{1 - \nu_{12}\nu_{21}}, \quad Q_{22} = \frac{E_2}{1 - \nu_{12}\nu_{21}} \\ Q_{66} &= G_{12}, \quad Q_{44} = G_{23}, \quad Q_{55} = G_{13} \end{aligned} \quad (10.3.7)$$

It can be readily seen that the transverse shear stresses obtained using the constitutive equations are zero at $z = \pm(h/2)$

$$\sigma_{yz} = Q_{44} \left(\gamma_{yz}^{(0)} + z^2 \gamma_{yz}^{(2)} \right) = Q_{44} \left[1 - 4 \left(\frac{z}{h} \right)^2 \right] \left(\phi_y + \frac{\partial w_0}{\partial y} \right) \quad (10.3.8a)$$

$$\sigma_{xz} = Q_{44} \left(\gamma_{xz}^{(0)} + z^2 \gamma_{xz}^{(2)} \right) = Q_{55} \left[1 - 4 \left(\frac{z}{h} \right)^2 \right] \left(\phi_x + \frac{\partial w_0}{\partial x} \right) \quad (10.3.8b)$$

10.3.4 Equations of Motion

The equations of motion of the third-order plate theory can be derived using the dynamic version of the principle of virtual displacements. The virtual strain energy δU , virtual work done by applied forces δV , and the virtual kinetic energy δK are given by

$$\begin{aligned} \delta U &= \int_{\Omega} \left\{ \int_{-\frac{h}{2}}^{\frac{h}{2}} \left[\sigma_{xx} \left(\delta \varepsilon_{xx}^{(0)} + z \delta \varepsilon_{xx}^{(1)} - c_1 z^3 \delta \varepsilon_{xx}^{(3)} \right) \right. \right. \\ &\quad + \sigma_{yy} \left(\delta \varepsilon_{yy}^{(0)} + z \delta \varepsilon_{yy}^{(1)} - c_1 z^3 \delta \varepsilon_{yy}^{(3)} \right) \\ &\quad + \sigma_{xy} \left(\delta \gamma_{xy}^{(0)} + z \delta \gamma_{xy}^{(1)} - c_1 z^3 \delta \gamma_{xy}^{(3)} \right) \\ &\quad \left. \left. + \sigma_{xz} \left(\delta \gamma_{xz}^{(0)} + z^2 \delta \gamma_{xz}^{(2)} \right) + \sigma_{yz} \left(\delta \gamma_{yz}^{(0)} + z^2 \delta \gamma_{yz}^{(2)} \right) \right] dz \right\} dxdy \\ &= \int_{\Omega} \left(N_{xx} \delta \varepsilon_{xx}^{(0)} + M_{xx} \delta \varepsilon_{xx}^{(1)} - c_1 P_{xx} \delta \varepsilon_{xx}^{(3)} + N_{yy} \delta \varepsilon_{yy}^{(0)} + M_{yy} \delta \varepsilon_{yy}^{(1)} \right. \\ &\quad - c_1 P_{yy} \delta \varepsilon_{yy}^{(3)} + N_{xy} \delta \gamma_{xy}^{(0)} + M_{xy} \delta \gamma_{xy}^{(1)} - c_1 P_{xy} \delta \gamma_{xy}^{(3)} \\ &\quad \left. + Q_x \delta \gamma_{xz}^{(0)} - c_2 R_x \delta \gamma_{xz}^{(2)} + Q_y \delta \gamma_{yz}^{(0)} - c_2 R_y \delta \gamma_{yz}^{(2)} \right) dxdy \quad (10.3.9) \end{aligned}$$

$$\begin{aligned} \delta V &= - \int_{\Omega} [(q_b - kw_0) \delta w_0 + q_t \delta w_0] dxdy \\ &\quad - \int_{\Gamma} \int_{-\frac{h}{2}}^{\frac{h}{2}} [\hat{\sigma}_{nn} \left(\delta u_n + z \delta \phi_n - c_1 z^3 \delta \varphi_n \right) \\ &\quad + \hat{\sigma}_{ns} \left(\delta u_s + z \delta \phi_s - c_1 z^3 \delta \varphi_{ns} \right) + \hat{\sigma}_{nr} \delta w_0] dz d\Gamma \end{aligned}$$

$$= - \int_{\Omega} (q - kw_0) \delta w_0 dx dy - \int_{\Gamma} (\hat{N}_{nn} \delta u_n + \hat{M}_{nn} \delta \phi_n - c_1 \hat{P}_{nn} \delta \varphi_n \\ + \hat{N}_{ns} \delta u_s + \hat{M}_{ns} \delta \phi_s - c_1 \hat{P}_{ns} \delta \varphi_{ns} + \hat{Q}_n \delta w_0) d\Gamma \quad (10.3.10)$$

$$\begin{aligned} \delta K = & \int_{\Omega_0} \int_{-\frac{h}{2}}^{\frac{h}{2}} \rho \left[\left(\dot{u}_0 + z\dot{\phi}_x - c_1 z^3 \dot{\varphi}_x \right) \left(\delta \dot{u}_0 + z\delta \dot{\phi}_x - c_1 z^3 \delta \dot{\varphi}_x \right) \right. \\ & + \left(\dot{v}_0 + z\dot{\phi}_y - c_1 z^3 \dot{\varphi}_y \right) \left(\delta \dot{v}_0 + z\delta \dot{\phi}_y + z^3 \delta \dot{\varphi}_y \right) \\ & \left. + \dot{w}_0 \delta \dot{w}_0 \right] dv \\ = & \int_{\Omega_0} \left\{ I_0 \dot{u}_0 \delta \dot{u}_0 + I_0 \dot{v}_0 \delta \dot{v}_0 + \left[I_2 \dot{\phi}_x - c_1 I_4 \left(\dot{\phi}_x + \frac{\partial \dot{w}_0}{\partial x} \right) \right] \delta \dot{\phi}_x \right. \\ & - c_1 \left[I_4 \dot{\phi}_x - c_1 I_6 \left(\dot{\phi}_x + \frac{\partial \dot{w}_0}{\partial x} \right) \right] \left(\delta \dot{\phi}_x + \frac{\partial \delta \dot{w}_0}{\partial x} \right) \\ & + \left[I_2 \dot{\phi}_y - c_1 I_4 \left(\dot{\phi}_y + \frac{\partial \dot{w}_0}{\partial y} \right) \right] \delta \dot{\phi}_y \\ & \left. - c_1 \left[I_4 \dot{\phi}_y - c_1 I_6 \left(\dot{\phi}_y + \frac{\partial \dot{w}_0}{\partial y} \right) \right] \left(\delta \dot{\phi}_y + \frac{\partial \delta \dot{w}_0}{\partial y} \right) \right\} dx dy \quad (10.3.11) \end{aligned}$$

where Ω denotes the middle plane of the laminate, the superposed dot denotes derivative with respect to time, and the stress resultants and mass inertias are defined by

$$\begin{Bmatrix} N_{\alpha\beta} \\ M_{\alpha\beta} \\ P_{\alpha\beta} \end{Bmatrix} = \int_{-\frac{h}{2}}^{\frac{h}{2}} \sigma_{\alpha\beta} \begin{Bmatrix} 1 \\ z \\ z^3 \end{Bmatrix} dz, \quad \begin{Bmatrix} Q_{\alpha} \\ R_{\alpha} \end{Bmatrix} = \int_{-\frac{h}{2}}^{\frac{h}{2}} \sigma_{\alpha z} \begin{Bmatrix} 1 \\ z^2 \end{Bmatrix} dz \quad (10.3.12)$$

$$I_i = \int_{-\frac{h}{2}}^{\frac{h}{2}} \rho(z)^i dz \quad (i = 0, 1, 2, \dots, 6) \quad (10.3.13)$$

In Eq. (10.3.12), α and β take the symbols x and y . The same definitions hold for the stress resultants with a hat (caret), which are specified. The inertias I_1 , I_3 , and I_5 are zero for homogeneous plates.

The Euler–Lagrange equations of the third-order shear deformation theory (TSDT) can be derived by substituting for δU , δV , and δK from Eqs. (10.3.9)–(10.3.11) into the virtual work statement, noting that the virtual strains can be written in terms of the generalized displacements using Eqs. (10.3.3a,b) and (10.3.4a–c), integrating by parts to relieve the virtual generalized displacements δu_0 , δv_0 , δw_0 , $\delta \phi_x$, and $\delta \phi_y$ in Ω of any differentiation, and using the fundamental lemma of calculus of variations. The equations involve higher-order stress resultants (P_{xx} , P_{yy} , P_{xy}) and (R_x , R_y), which are mathematically similar to the conventional moments (M_{xx} , M_{yy} , M_{xy}) and shear forces (Q_x , Q_y), respectively. However, they do present a difficulty when one is required to specify them on the boundary.

We obtain the following Euler–Lagrange equations:

$$\frac{\partial N_{xx}}{\partial x} + \frac{\partial N_{xy}}{\partial y} = I_0 \ddot{u}_0 \quad (10.3.14)$$

$$\frac{\partial N_{xy}}{\partial x} + \frac{\partial N_{yy}}{\partial y} = I_0 \ddot{v}_0 \quad (10.3.15)$$

$$\begin{aligned} \frac{\partial \bar{Q}_x}{\partial x} + \frac{\partial \bar{Q}_y}{\partial y} + c_1 \left(\frac{\partial^2 P_{xx}}{\partial x^2} + 2 \frac{\partial^2 P_{xy}}{\partial x \partial y} + \frac{\partial^2 P_{yy}}{\partial y^2} \right) + q - kw_0 \\ = I_0 \ddot{w}_0 - c_1^2 I_6 \left(\frac{\partial^2 \ddot{w}_0}{\partial x^2} + \frac{\partial^2 \ddot{w}_0}{\partial y^2} \right) + c_1 J_4 \left(\frac{\partial \ddot{\phi}_x}{\partial x} + \frac{\partial \ddot{\phi}_y}{\partial y} \right) \end{aligned} \quad (10.3.16)$$

$$\frac{\partial \bar{M}_{xx}}{\partial x} + \frac{\partial \bar{M}_{xy}}{\partial y} - \bar{Q}_x = K_2 \ddot{\phi}_x - c_1 J_4 \frac{\partial \ddot{w}_0}{\partial x} \quad (10.3.17)$$

$$\frac{\partial \bar{M}_{xy}}{\partial x} + \frac{\partial \bar{M}_{yy}}{\partial y} - \bar{Q}_y = K_2 \ddot{\phi}_y - c_1 J_4 \frac{\partial \ddot{w}_0}{\partial y} \quad (10.3.18)$$

where c_1 and c_2 are given in Eq. (10.3.5), and

$$\bar{M}_{\alpha\beta} = M_{\alpha\beta} - c_1 P_{\alpha\beta}, \quad \bar{Q}_\alpha = Q_\alpha - c_2 R_\alpha \quad (10.3.19)$$

$$J_i = I_i - c_1 I_{i+2}, \quad K_2 = I_2 - 2c_1 I_4 + c_1^2 I_6 \quad (10.3.20)$$

and (P_{xx}, P_{yy}, P_{xy}) and (R_x, R_y) denote the higher-order stress resultants

$$\begin{Bmatrix} P_{xx} \\ P_{yy} \\ P_{xy} \end{Bmatrix} = \int_{-\frac{h}{2}}^{\frac{h}{2}} \begin{Bmatrix} \sigma_{xx} \\ \sigma_{yy} \\ \sigma_{xy} \end{Bmatrix} z^3 dz, \quad \begin{Bmatrix} R_x \\ R_y \end{Bmatrix} = \int_{-\frac{h}{2}}^{\frac{h}{2}} \begin{Bmatrix} \sigma_{yz} \\ \sigma_{xz} \end{Bmatrix} z^2 dz \quad (10.3.21)$$

The primary and secondary variables of the theory are

$$\text{Primary variables : } u_n, u_s, w_0, \frac{\partial w_0}{\partial n}, \phi_n, \phi_s \quad (10.3.22)$$

$$\text{Secondary variables : } N_{nn}, N_{ns}, \bar{V}_n, P_{nn}, \bar{M}_{nn}, \bar{M}_{ns} \quad (10.3.23)$$

where u_n, u_s, N_{nn}, N_{ns} , and so on have the same meaning as in the classical and first-order plate theory [see Eqs. (3.5.3)–(3.5.8)],

$$\begin{aligned} \bar{V}_n \equiv c_1 & \left[\left(\frac{\partial P_{xx}}{\partial x} + \frac{\partial P_{xy}}{\partial y} \right) n_x + \left(\frac{\partial P_{xy}}{\partial x} + \frac{\partial P_{yy}}{\partial y} \right) n_y \right] \\ & - c_1 \left[\left(J_4 \ddot{\phi}_x - c_1 I_6 \frac{\partial \ddot{w}_0}{\partial x} \right) n_x + \left(J_4 \ddot{\phi}_y - c_1 I_6 \frac{\partial \ddot{w}_0}{\partial y} \right) n_y \right] \\ & + (\bar{Q}_x n_x + \bar{Q}_y n_y) + c_1 \frac{\partial P_{ns}}{\partial s} \end{aligned} \quad (10.3.24)$$

P_{nn} and P_{ns} are defined by [see Eq. (3.5.8)]

$$\begin{Bmatrix} P_{nn} \\ P_{ns} \end{Bmatrix} = \begin{bmatrix} n_x^2 & n_y^2 & 2n_x n_y \\ -n_x n_y & n_x n_y & n_x^2 - n_y^2 \end{bmatrix} \begin{Bmatrix} P_{xx} \\ P_{yy} \\ P_{xy} \end{Bmatrix} \quad (10.3.25)$$

and (n_x, n_y) are the direction cosines of the unit normal on the boundary.

The stress resultants are related to the strains by

$$\begin{Bmatrix} \{N\} \\ \{M\} \\ \{P\} \end{Bmatrix} = \begin{bmatrix} [A] & [0] & [0] \\ [0] & [D] & [F] \\ [0] & [F] & [H] \end{bmatrix} \begin{Bmatrix} \{\varepsilon^{(0)}\} \\ \{\varepsilon^{(1)}\} \\ \{\varepsilon^{(3)}\} \end{Bmatrix} \quad (10.3.26)$$

$$\begin{Bmatrix} \{Q\} \\ \{R\} \end{Bmatrix} = \begin{bmatrix} [A] & [D] \\ [D] & [F] \end{bmatrix} \begin{Bmatrix} \{\gamma^{(0)}\} \\ \{\gamma^{(2)}\} \end{Bmatrix} \quad (10.3.27)$$

$$(A_{ij}, D_{ij}, F_{ij}, H_{ij}) = \int_{-\frac{h}{2}}^{\frac{h}{2}} Q_{ij} (1, z^2, z^4, z^6) dz \quad (10.3.28a)$$

$$(A_{ij}, D_{ij}, F_{ij}) = \int_{-\frac{h}{2}}^{\frac{h}{2}} Q_{ij} (1, z^2, z^6) dz \quad (10.3.28b)$$

The stiffnesses in Eq. (10.3.28a) are defined for $i, j = 1, 2, 6$ and those in Eq. (10.3.28b) are defined for $i, j = 4, 5$. The coefficients A_{ij} and D_{ij} were given in terms of the material constants and plate thickness h in Eq. (3.6.13) for single-layer orthotropic plates, and in Eq. (3.6.19) for symmetrically laminated plates with principal material axes coinciding with those of the plate. The higher-order stiffness coefficients introduced in the third-order theory are given by

$$\begin{aligned} F_{ij} &= \frac{1}{5} \sum_{k=1}^N Q_{ij}^{(k)} \left[(z_{k+1})^5 - (z_k)^5 \right] \\ H_{ij} &= \frac{1}{7} \sum_{k=1}^N Q_{ij}^{(k)} \left[(z_{k+1})^7 - (z_k)^7 \right] \end{aligned} \quad (10.3.29)$$

This completes the development of TSDT. Note that the equations of motion of the first-order theory are obtained from the present third-order theory by setting $c_1 = 0$. The displacement field in Eq. (10.3.1) contains, as special cases, the displacement fields used by other researchers to derive a third-order plate theory, as given in Table 10.3.1. Therefore, the third-order plate theories reported in the literature, despite the different looks of the assumed displacement fields, are indeed equivalent.

Table 10.3.1. Relationship of the displacements of other third-order theories to the one in Eq. (10.3.1).

References	Displacement Field [†]	Correspondence with Eq. (10.3.1) [‡]
Vlasov (1964), Jemielita (1975)	$u_\alpha = u_\alpha^0 + f(z)\psi_\alpha - c_1 z^3 u_{3,\alpha}^0$	$\varphi_\alpha = \psi_\alpha + u_{3,\alpha}^0$
Schmidt (1977)	$u_\alpha = u_\alpha^0 - z u_{3,\alpha}^0 + \frac{3}{2} f(z) \varepsilon_\alpha$	$\varphi_\alpha = \frac{3}{2} \varepsilon_\alpha$
Krishna Murty (1977), Levinson (1980), Reddy (1984a)	$u_\alpha = u_\alpha^0 - z u_{3,\alpha}^0 - c_3 f(z) \theta_\alpha$	$\varphi_\alpha = -c_3 \theta_\alpha$
Reddy (1987)	$u_\alpha = u_\alpha^0 + f(z) \hat{\phi}_\alpha - z u_{3,\alpha}^b - c_1 h z^3 u_{3,\alpha}^0$	$\varphi_\alpha = \hat{\phi}_\alpha + u_{3,\alpha}^s$ $w_0 = u_3^s + u_3^b$
Reddy (1990)	$u_\alpha = u_\alpha^0 - z u_{3,\alpha}^0 + f(z) \phi_\alpha$	$\varphi_\alpha = \phi_\alpha$

[†] $c_1 = \frac{4}{3h^2}$, $c_3 = \frac{3}{4h}$, $c_4 = \frac{5}{3h^2}$, $f(z) = z(1 - c_1 z^2)$. [‡] $\varphi_\alpha \equiv \phi_\alpha + u_{3,\alpha}^0$, $u_3^0 = w_0$.

10.4 The Navier Solutions of TSDT

10.4.1 Preliminary Comments

Except for additional higher-order terms, the third-order plate theory equations are very similar to those of the first-order plate theory. They too admit exact solutions for the case of simply supported rectangular plates. Following the same steps as in the case of the first-order plate theory, here we present the Navier solutions of the third-order plate theory for bending, buckling, and vibrations of simply supported rectangular plates. Since the stretching deformation is uncoupled from the bending, we can analyze three equations, Eqs. (10.3.16)–(10.3.18), independent of Eqs. (10.3.14) and (10.3.15).

The simply supported boundary conditions on the edges of a rectangular plate for the third-order shear deformation plate theory are (Figure 10.4.1)

$$w_0(x, 0, t) = 0, \quad w_0(x, b, t) = 0, \quad w_0(0, y, t) = 0, \quad w_0(a, y, t) = 0 \quad (10.4.1a)$$

$$\phi_x(x, 0, t) = 0, \quad \phi_x(x, b, t) = 0, \quad \phi_y(0, y, t) = 0, \quad \phi_y(a, y, t) = 0 \quad (10.4.1b)$$

$$\bar{M}_{xx}(0, y, t) = 0, \quad \bar{M}_{xx}(a, y, t) = 0, \quad \bar{M}_{yy}(x, 0, t) = 0, \quad \bar{M}_{yy}(x, b, t) = 0 \quad (10.4.1c)$$

10.4.2 General Solution

The boundary conditions in (10.4.1a–c) are satisfied by the following expansions of the generalized displacements:

$$w_0(x, y, t) = \sum_{n=1}^{\infty} \sum_{m=1}^{\infty} W_{mn}(t) \sin \alpha_m x \sin \beta_n y \quad (10.4.2a)$$

$$\phi_x(x, y, t) = \sum_{n=1}^{\infty} \sum_{m=1}^{\infty} X_{mn}(t) \cos \alpha_m x \sin \beta_n y \quad (10.4.2b)$$

$$\phi_y(x, y, t) = \sum_{n=1}^{\infty} \sum_{m=1}^{\infty} Y_{mn}(t) \sin \alpha_m x \cos \beta_n y \quad (10.4.2c)$$

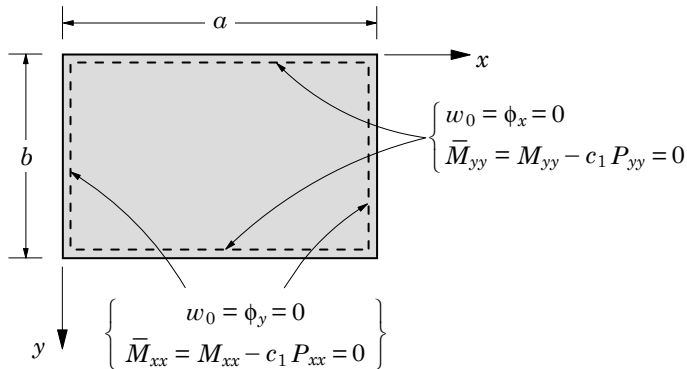


Figure 10.4.1. Simply supported boundary conditions for the third-order shear deformation plate theory (TSDT).

where $\alpha_m = m\pi/a$ and $\beta_n = n\pi/b$. The assumed form of the generalized displacements in Eqs. (10.4.2a-c) also satisfies the boundary conditions of FSDT for simply supported plates. The transverse load q is also expanded in double Fourier sine series

$$q(x, y, t) = \sum_{n=1}^{\infty} \sum_{m=1}^{\infty} Q_{mn}(t) \sin \alpha_m x \sin \beta_n y \quad (10.4.3a)$$

$$Q_{mn}(z, t) = \frac{4}{ab} \int_0^a \int_0^b q(x, y, t) \sin \alpha_m x \sin \beta_n y dx dy \quad (10.4.3b)$$

Substitution of Eqs. (10.4.2) and (10.4.3) into Eqs. (10.3.16)–(10.3.18) results in the following equations for the undetermined coefficients (W_{mn}, X_{mn}, Y_{mn})

$$\begin{aligned} & \begin{bmatrix} \hat{s}_{11} + \tilde{s}_{11} & \hat{s}_{12} & \hat{s}_{13} \\ \hat{s}_{12} & \hat{s}_{22} & \hat{s}_{23} \\ \hat{s}_{13} & \hat{s}_{23} & \hat{s}_{33} \end{bmatrix} \begin{Bmatrix} W_{mn} \\ X_{mn} \\ Y_{mn} \end{Bmatrix} + \begin{bmatrix} \hat{m}_{11} & \hat{m}_{12} & \hat{m}_{13} \\ \hat{m}_{12} & \hat{m}_{22} & 0 \\ \hat{m}_{23} & 0 & \hat{m}_{33} \end{bmatrix} \begin{Bmatrix} \ddot{W}_{mn} \\ \ddot{X}_{mn} \\ \ddot{Y}_{mn} \end{Bmatrix} \\ &= \begin{Bmatrix} Q_{mn} \\ 0 \\ 0 \end{Bmatrix} - \begin{Bmatrix} 0 \\ \alpha_m \hat{M}_{mn}^1 \\ \beta_n \hat{M}_{mn}^2 \end{Bmatrix} \end{aligned} \quad (10.4.4)$$

where \hat{s}_{ij} and \hat{m}_{ij} are defined by

$$\begin{aligned} \hat{s}_{11} &= \bar{A}_{55}\alpha_m^2 + \bar{A}_{44}\beta_n^2 + k + c_1^2 [H_{11}\alpha_m^4 + 2(H_{12} + 2H_{66})\alpha_m^2\beta_n^2 + H_{22}\beta_n^4] \\ \hat{s}_{12} &= \bar{A}_{55}\alpha_m - c_1 [\hat{F}_{11}\alpha_m^3 + (\hat{F}_{12} + 2\hat{F}_{66})\alpha_m\beta_n^2] \\ \hat{s}_{13} &= \bar{A}_{44}\beta_n - c_1 [\hat{F}_{22}\beta_n^3 + (\hat{F}_{12} + 2\hat{F}_{66})\alpha_m^2\beta_n] \\ \hat{s}_{22} &= \bar{A}_{55} + \bar{D}_{11}\alpha_m^2 + \bar{D}_{66}\beta_n^2, \quad \hat{s}_{23} = (\bar{D}_{12} + \bar{D}_{66})\alpha_m\beta_n \\ \hat{s}_{33} &= \bar{A}_{44} + \bar{D}_{66}\alpha_m^2 + \bar{D}_{22}\beta_n^2, \quad \hat{s}_{11} = \hat{N}_{xx}\alpha_m^2 + \hat{N}_{yy}\beta_n^2 \end{aligned} \quad (10.4.5a)$$

$$\hat{m}_{11} = I_0 + c_1^2 I_6 (\alpha_m^2 + \beta_n^2), \quad \hat{m}_{12} = -c_1 J_4 \alpha_m \quad (10.4.5b)$$

$$\hat{m}_{13} = -c_1 J_4 \beta_n, \quad \hat{m}_{22} = K_2, \quad \hat{m}_{33} = K_2 \quad (10.4.5b)$$

$$\hat{D}_{ij} = D_{ij} - c_1 F_{ij}, \quad \hat{F}_{ij} = F_{ij} - c_1 H_{ij}, \quad \bar{D}_{ij} = \hat{D}_{ij} - c_1 \hat{F}_{ij} \quad (10.4.6a)$$

for $i, j = 1, 2, 6$, and

$$\hat{A}_{ij} = A_{ij} - c_2 D_{ij}, \quad \hat{D}_{ij} = D_{ij} - c_2 \hat{F}_{ij}, \quad \bar{A}_{ij} = \hat{A}_{ij} - c_2 \bar{D}_{ij} \quad (10.4.6b)$$

for $i, j = 4, 5$. The thermal resultants are defined by

$$\begin{Bmatrix} N_{xx}^T \\ N_{yy}^T \\ N_{xy}^T \end{Bmatrix} = \sum_{n=1}^{\infty} \sum_{m=1}^{\infty} \begin{Bmatrix} N_{mn}^1(t) \\ N_{mn}^2(t) \\ N_{mn}^6(t) \end{Bmatrix} \sin \alpha_m x \sin \beta_n y \quad (10.4.7a)$$

$$\begin{Bmatrix} M_{xx}^T \\ M_{yy}^T \\ M_{xy}^T \end{Bmatrix} = \sum_{n=1}^{\infty} \sum_{m=1}^{\infty} \begin{Bmatrix} M_{mn}^1(t) \\ M_{mn}^2(t) \\ M_{mn}^6(t) \end{Bmatrix} \sin \alpha_m x \sin \beta_n y \quad (10.4.7b)$$

$$\begin{Bmatrix} P_{xx}^T \\ P_{yy}^T \\ P_{xy}^T \end{Bmatrix} = \sum_{n=1}^{\infty} \sum_{m=1}^{\infty} \begin{Bmatrix} P_{mn}^1(t) \\ P_{mn}^2(t) \\ P_{mn}^6(t) \end{Bmatrix} \sin \alpha_m x \sin \beta_n y \quad (10.4.7c)$$

where

$$\{N_{mn}(t)\} = \int_{-\frac{h}{2}}^{\frac{h}{2}} [Q]\{\alpha\} T_{mn}(z, t) dz \quad (10.4.8a)$$

$$\{M_{mn}(t)\} = \int_{-\frac{h}{2}}^{\frac{h}{2}} [Q]\{\alpha\} T_{mn}(z, t) z dz \quad (10.4.8b)$$

$$\{P_{mn}(t)\} = \int_{-\frac{h}{2}}^{\frac{h}{2}} [Q]\{\alpha\} T_{mn}(z, t) z^3 dz \quad (10.4.8c)$$

and

$$\Delta T(x, y, z, t) = \sum_{m=1}^{\infty} \sum_{n=1}^{\infty} (T_{mn}^0 + z T_{mn}^1) \sin \alpha_m x \sin \beta_n y \quad (10.4.9a)$$

$$(T_{mn}^0, T_{mn}^1) = \frac{4}{ab} \int_0^a \int_0^b (T_0, T_1) \sin \alpha_m x \sin \beta_n y dx dy \quad (10.4.9b)$$

$$\{\hat{M}_{mn}\} = \{M_{mn}\} - c_1 \{P_{mn}\} \quad (10.4.10)$$

Equation (10.4.4) can be specialized to static bending analysis, buckling, and natural vibration, as discussed next.

10.4.3 Bending Analysis

The static solution can be obtained from Eqs. (10.4.4) by setting the time derivative terms to zero. The resulting equations are identical to those in Eq. (10.2.11) but with \hat{s}_{ij} defined by Eq. (10.4.5a).

The inplane stresses can be computed from the equations

$$\begin{Bmatrix} \sigma_{xx} \\ \sigma_{yy} \\ \sigma_{xy} \end{Bmatrix} = \begin{bmatrix} Q_{11} & Q_{12} & 0 \\ Q_{12} & Q_{22} & 0 \\ 0 & 0 & Q_{66} \end{bmatrix} \left(\begin{Bmatrix} \varepsilon_{xx} \\ \varepsilon_{yy} \\ \gamma_{xy} \end{Bmatrix} - \begin{Bmatrix} \alpha_{xx} \\ \alpha_{yy} \\ 2\alpha_{xy} \end{Bmatrix} \Delta T \right) \quad (10.4.11)$$

$$\begin{Bmatrix} \varepsilon_{xx} \\ \varepsilon_{yy} \\ \gamma_{xy} \end{Bmatrix} = \begin{Bmatrix} \varepsilon_{xx}^{(0)} \\ \varepsilon_{yy}^{(0)} \\ \gamma_{xy}^{(0)} \end{Bmatrix} + z \begin{Bmatrix} \varepsilon_{xx}^{(1)} \\ \varepsilon_{yy}^{(1)} \\ \gamma_{xy}^{(1)} \end{Bmatrix} + z^3 \begin{Bmatrix} \varepsilon_{xx}^{(3)} \\ \varepsilon_{yy}^{(3)} \\ \gamma_{xy}^{(3)} \end{Bmatrix}$$

$$= \sum_{m=1}^{\infty} \sum_{n=1}^{\infty} \begin{Bmatrix} (z S_{mn}^{xx} + c_1 z^3 T_{mn}^{xx}) \sin \alpha_m x \sin \beta_n y \\ (z S_{mn}^{yy} + c_1 z^3 T_{mn}^{yy}) \sin \alpha_m x \sin \beta_n y \\ (z S_{mn}^{xy} + c_1 z^3 T_{mn}^{xy}) \cos \alpha_m x \cos \beta_n y \end{Bmatrix} \quad (10.4.12)$$

$$\begin{Bmatrix} S_{mn}^{xx} \\ S_{mn}^{yy} \\ S_{mn}^{xy} \end{Bmatrix} = \begin{Bmatrix} -\alpha_m X_{mn} \\ -\beta_n Y_{mn} \\ \beta_n X_{mn} + \alpha_m Y_{mn} \end{Bmatrix} \quad (10.4.13a)$$

$$\begin{Bmatrix} T_{mn}^{xx} \\ T_{mn}^{yy} \\ T_{mn}^{xy} \end{Bmatrix} = \begin{Bmatrix} \alpha_m X_{mn} + \alpha_m^2 W_{mn} \\ \beta_n Y_{mn} + \beta_n^2 W_{mn} \\ -(\beta_n X_{mn} + \alpha_m Y_{mn} + 2\alpha_m \beta_n W_{mn}) \end{Bmatrix} \quad (10.4.13b)$$

The transverse shear stresses from the constitutive equations are given by

$$\begin{aligned}\sigma_{yz} &= (1 - c_2 z^2) \sum_{m=1}^{\infty} \sum_{n=1}^{\infty} Q_{44} (Y_{mn} + \beta_n W_{mn}) \sin \alpha_m x \cos \beta_n y \\ \sigma_{xz} &= (1 - c_2 z^2) \sum_{m=1}^{\infty} \sum_{n=1}^{\infty} Q_{55} (X_{mn} + \alpha_m W_{mn}) \cos \alpha_m x \sin \beta_n y\end{aligned}\quad (10.4.14)$$

where $c_2 = 4/h^2$. Note that the transverse shear stresses are quadratic through the thickness.

The transverse shear stresses can also be determined using the equilibrium equations of 3-D elasticity. In the absence of thermal effects, they are given by

$$\begin{aligned}\sigma_{xz} &= \sum_{m=1}^{\infty} \sum_{n=1}^{\infty} \left[\frac{1}{2} (z^2 - z_b^2) \mathcal{B}_{mn} + \frac{c_1}{4} (z^4 - z_b^4) \mathcal{E}_{mn} \right] \cos \alpha_m x \sin \beta_n y \\ \sigma_{yz} &= \sum_{m=1}^{\infty} \sum_{n=1}^{\infty} \left[\frac{1}{2} (z^2 - z_b^2) \mathcal{D}_{mn} + \frac{c_1}{4} (z^4 - z_b^4) \mathcal{F}_{mn} \right] \sin \alpha_m x \cos \beta_n y\end{aligned}\quad (10.4.15)$$

where $z_b = -h/2$ and

$$\begin{aligned}\mathcal{B}_{mn} &= \left[(\alpha_m^2 Q_{11} + \beta_n^2 Q_{66}) X_{mn} + \alpha_m \beta_n (Q_{12} + Q_{66}) Y_{mn} \right] \\ \mathcal{D}_{mn} &= \left[\alpha_m \beta_n (Q_{12} + Q_{66}) X_{mn} + (\alpha_m^2 Q_{66} + \beta_n^2 Q_{22}) Y_{mn} \right] \\ \mathcal{E}_{mn} &= - \left[\alpha^3 Q_{22} + \alpha_m \beta_n^2 (Q_{12} + 2Q_{66}) \right] W_{mn} - \mathcal{B}_{mn} \\ \mathcal{F}_{mn} &= - \left[\beta^3 Q_{22} + \alpha_m^2 \beta_n (Q_{12} + 2Q_{66}) \right] W_{mn} - \mathcal{D}_{mn}\end{aligned}\quad (10.4.16)$$

Table 10.4.1 contains the maximum nondimensional deflections (\bar{w}) and stresses ($\bar{\sigma}$) of simply supported, isotropic ($\nu = 0.3$), square plates under sinusoidally distributed load (SSL) and uniformly distributed load (UDL), and for different side-to-thickness ratios. The nondimensional variables used are the same as in Eq. (10.2.19), and the locations of the maximum stresses are the same as given before:

$$\begin{aligned}\bar{\sigma}_{xx}(\frac{a}{2}, \frac{b}{2}, \frac{h}{2}), \quad \bar{\sigma}_{yy}(\frac{a}{2}, \frac{b}{2}, \frac{h}{2}), \quad \bar{\sigma}_{xy}(a, b, -\frac{h}{2}) \\ \bar{\sigma}_{xz}(0, \frac{b}{2}, \frac{h}{2}), \quad \bar{\sigma}_{yz}(\frac{a}{2}, 0, \frac{h}{2})\end{aligned}\quad (10.4.17)$$

Table 10.4.2 contains the results for orthotropic plates. The following material properties are used:

$$\begin{aligned}E_1 &= 20.83 \text{ msi}, \quad E_2 = 10.94 \text{ msi}, \quad \nu_{12} = 0.44, \quad k = 0 \\ G_{12} &= 6.10 \text{ msi}, \quad G_{13} = 3.71 \text{ msi}, \quad G_{23} = 6.19 \text{ msi}\end{aligned}\quad (10.4.18)$$

The difference between the deflections predicted by the first-order theory ($K_s = 5/6$) and the third-order theory is not significant. This is clear from an examination of

Table 10.4.1. Effect of transverse shear deformation on deflections and stresses in isotropic ($\nu = 0.3$) square plates subjected to distributed loads.

Theory	$\frac{b}{h}$	$10\bar{w}$	$\bar{\sigma}_{xx}$	$\bar{\sigma}_{xy}$	$(\bar{\sigma}_{xz})^\dagger$	$\bar{\sigma}_{xz}$
<i>Sinusoidal Load</i>						
CPT*		0.2803	0.1976	0.1064	—	0.2387
FSDT	5	0.3435	0.1976	0.1064	0.1910	0.2387
TSDT	5	0.3433	0.2050	0.1104	0.2381	0.2365
FSDT	10	0.2961	0.1976	0.1064	0.1910	0.2387
TSDT	10	0.2961	0.1994	0.1074	0.2386	0.2382
FSDT	100	0.2804	0.1976	0.1064	0.1910	0.2387
TSDT	100	0.2804	0.1976	0.1064	0.2387	0.2387
<i>Uniform Load</i> ($m, n = 1, 3, \dots, 19$)						
CPT*		0.4436	0.2873	0.1946	—	0.4909
FSDT	5	0.5355	0.2873	0.1946	0.3927	0.4909
TSDT	5	0.5354	0.2944	0.2112	0.4840	0.4668
FSDT	10	0.4666	0.2873	0.1946	0.3927	0.4909
TSDT	10	0.4666	0.2890	0.1990	0.4890	0.4843
FSDT	100	0.4438	0.2873	0.1946	0.3927	0.4909
TSDT	100	0.4438	0.2873	0.1946	0.4909	0.4909

† Transverse shear stress computed using the constitutive equation (10.4.14); the next column shows the transverse shear stress computed using the stress equilibrium equation (10.4.15).

* The nondimensional quantities in CPT are independent of the ratio a/h .

the higher-order stiffnesses, F_{ij} and H_{ij} , which contain the fifth and seventh powers, respectively, of the plate thickness h , and, therefore, are expected to contribute little to the displacements. The main advantage of the third-order theory is that the transverse shear strains and stresses are represented quadratically, a state of stress that is close to the 3-D elasticity solution and, consequently, *no shear correction coefficients are needed*. Note that the constitutively derived transverse shear stresses of TSDT are close to the equilibrium-derived values, and they are zero at $z = \pm(h/2)$.

10.4.4 Buckling Analysis

The buckling problem associated with the third-order shear deformation theory is again given by Eq. (10.2.21), with \hat{S}_{ij} given by Eq. (10.4.5a) (see Problem 10.3). Table 10.4.3 contains the critical buckling loads $\bar{N} = N_{cr}b^2/(\pi^2 D_{22})$ as a function of the plate aspect ratio a/b , side-to-thickness ratio b/h , and modulus ratio E_1/E_2 for uniaxial ($\gamma = 0$) and biaxial ($\gamma = 1$) compression. It is clear that the difference between the buckling loads predicted by the third-order plate theory and the first-order plate theory is negligible. For the biaxial case, there is a small difference between the two solutions, with the buckling loads predicted by the third-order theory being slightly lower. Thus, there is no real advantage to using the third-order plate theory for the prediction of buckling loads.

Table 10.4.2. Effect of transverse shear deformation on deflections and stresses in orthotropic plates subjected to uniformly distributed load ($m, n = 1, 3, \dots, 29$).

Theory	$\frac{b}{h}$	$10\bar{w}$	$\bar{\sigma}_{xx}$	$\bar{\sigma}_{yy}$	$\bar{\sigma}_{xy}$	$\bar{\sigma}_{xz}$	$\bar{\sigma}_{yz}$
<i>Aspect Ratio, $\frac{a}{b} = 1.0$</i>							
CPT		0.3022	0.3609	0.2162	0.1939	—	0.4393 [†]
FSDT	100	0.3024	0.3609	0.2163	0.1939	0.4399 0.5499	0.3514 0.4393
TSDT	100	0.3024	0.3609	0.2163	0.1939	0.5498 0.5496	0.4393 0.4392
FSDT	20	0.3079	0.3597	0.2171	0.1941	0.4394 0.5493	0.3520 0.4401
TSDT	20	0.3079	0.3608	0.2175	0.1957	0.5477 0.5437	0.4395 0.4381
FSDT	10	0.3252	0.3562	0.2196	0.1947	0.4381 0.5476	0.3537 0.4422
TSDT	10	0.3252	0.3604	0.2213	0.2010	0.5420 0.5279	0.4400 0.4348
<i>Aspect Ratio, $\frac{a}{b} = 2.0$</i>							
CPT		0.5862	0.1021	0.1346	0.0804	—	—
FSDT	100	0.5864	0.1021	0.1346	0.0804	0.2527 0.3159	0.2611 0.3264
TSDT	100	0.5864	0.1021	0.1346	0.0804	0.3159 0.3159	0.3264 0.3264
FSDT	20	0.5908	0.1019	0.1348	0.0803	0.2524 0.3155	0.2613 0.3266
TSDT	20	0.5908	0.1020	0.1349	0.0807	0.3151 0.3141	0.3263 0.3256
FSDT	10	0.6046	0.1013	0.1352	0.0800	0.2515 0.3143	0.2615 0.3269
TSDT	10	0.6046	0.1017	0.1357	0.0816	0.3128 0.3089	0.3259 0.3233

[†] Stresses computed using the stress equilibrium equations.

Table 10.4.3. Nondimensional buckling loads \bar{N} of simply supported plates under inplane uniform compression ($\gamma = 0$) and biaxial compression ($\gamma = 1$).

γ	$\frac{a}{b}$	$\frac{h}{b}$	$\frac{E_1}{E_2} = 1$		$\frac{E_1}{E_2} = 10$	
					FSDT	TSDT
0	1.0	10	3.800	3.800	11.205	11.209
		20	3.948	3.948	12.832	12.832
		100	3.998	3.998	13.460	13.460
		CPT	4.000	4.000	13.488	13.488
3.0	10	3.800 ^(3,1)	3.800 ^(3,1)	8.354 ^(2,1)	8.355 ^(2,1)	
		3.948 ^(3,1)	3.948 ^(3,1)	8.959 ^(2,1)	8.959 ^(2,1)	
		3.998 ^(3,1)	3.998 ^(3,1)	9.173 ^(2,1)	9.173 ^(2,1)	
		CPT	4.000 ^(3,1)	4.000 ^(3,1)	9.182 ^(2,1)	9.182 ^(2,1)
1	1.0	10	1.900	1.900	5.662	5.605
		20	1.974	1.974	6.433	6.416
		100	1.999	1.999	6.731	6.730
		CPT	2.000	2.000	6.744	6.744
3.0	10	1.079	1.079	1.227	1.195	
		1.103	1.103	1.251	1.243	
		1.111	1.111	1.259	1.259	
		CPT	1.111	1.111	1.260	1.260

Note: The pair of numbers in parentheses denote mode numbers (m, n) at which the critical buckling load occurred; $(m, n) = (1, 1)$ for all other cases.

10.4.5 Natural Vibration

For natural vibration, Eq. (10.4.4) becomes

$$\left(\begin{bmatrix} \hat{s}_{11} & \hat{s}_{12} & \hat{s}_{13} \\ \hat{s}_{12} & \hat{s}_{22} & \hat{s}_{23} \\ \hat{s}_{13} & \hat{s}_{23} & \hat{s}_{33} \end{bmatrix} - \omega^2 \begin{bmatrix} \hat{m}_{11} & \hat{m}_{12} & \hat{m}_{13} \\ \hat{m}_{12} & \hat{m}_{22} & 0 \\ \hat{m}_{13} & 0 & \hat{m}_{33} \end{bmatrix} \right) \begin{Bmatrix} W_{mn}^0 \\ X_{mn}^0 \\ Y_{mn}^0 \end{Bmatrix} = \begin{Bmatrix} 0 \\ 0 \\ 0 \end{Bmatrix} \quad (10.4.19)$$

where \hat{s}_{ij} and \hat{m}_{ij} are defined in Eqs. (10.4.5a,b).

Table 10.4.4 contains natural frequencies $\hat{\omega} = \omega h(\sqrt{\rho/G})$ of isotropic ($\nu = 0.3$) rectangular plates as predicted by the first-order (FSDT), third-order (TSDT), and classical (CPT) plate theories. Once again, we find that the difference between the frequencies predicted by the first- and third-order theories is negligible, and that both are in close agreement with the 3-D elasticity results.

Table 10.4.4. Nondimensional frequencies $\hat{\omega}$ of simply supported isotropic ($\nu = 0.3$) rectangular plates ($a/h = 10$, $k = 0$).

$\frac{b}{a}$	m	n	Exact	TSDT	FSDT	CPT ^a	CPT
1.0	1	1	0.0932 ^b	0.0930	0.0930	0.0955	0.0963
	2	1	0.2260	0.2219	0.2219	0.2360	0.2408
	2	2	0.3421	0.3406	0.3406	0.3732	0.3853
	1	3	0.4171	0.4106	0.4149	0.4629	0.4816
	2	3	0.5239	0.5208	0.5206	0.5951	0.6261
$\sqrt{2}$	1	1	0.0704 ^c	0.0704	0.0704	0.0718	0.0722
	1	2	0.1376	0.1374	0.1373	0.1427	0.1445
	2	1	0.2018	0.2013	0.2012	0.2128	0.2167
	1	3	0.2431	0.2423	0.2423	0.2591	0.2649
	2	2	0.2634	0.2625	0.2625	0.2821	0.2889
	2	3	0.3612	0.3596	0.3595	0.3957	0.4093
	1	4	0.3800	0.3783	0.3782	0.4182	0.4334
	3	1	0.3987	0.3968	0.3967	0.4406	0.4575
	3	2	0.4535	0.4511	0.4509	0.5073	0.5297
	2	4	0.4890	0.4863	0.4861	0.5513	0.5779
	3	3	0.5411	0.5378	0.5375	0.6168	0.6501

^a CPT solution without rotatory inertia and all other solutions include rotatory inertia;

^b 3-D elasticity solution of Srinivas and Rao (1970);

^c 3-D elasticity solution of Reismann and Lee (1969); also see Reddy (2002), pp. 410–412.

10.5 Relationships between Solutions of Classical and Shear Deformation Theories

10.5.1 Introduction

As seen from the previous sections of this chapter, the shear deformation plate theories involve more dependent unknowns and algebraically complicated governing equations than the classical plate theory. The classical plate theory is the most commonly used, and analytical solutions for bending, vibration, and buckling of the classical plate theories are available for a vast number of plate problems as discussed in Chapters 6 through 9. Therefore, it is desirable to have algebraic relationships between solutions of shear deformation theories and those of the classical plate theory. Such relationships have been developed by Wang (1995), Wang et al. (1997, 2000), Reddy et al. (1997a-c, 1998, 2000a,b), and Lim and Reddy (2003). The book by Wang, Reddy, and Lee (2000) presents relationships between various shear deformation theories and classical theories for deflections, buckling loads, and natural frequencies of beams and plates. Such relationships enable one to obtain the solutions of the shear deformation plate theories for specific problems and, thereby, reduce the effort of solving the complicated equations of shear deformation theories. Here, we present a brief discussion of the bending relationships for circular and polygonal plates made of an isotropic material.

10.5.2 Circular Plates

The governing equations of the classical plate theory and first-order shear deformation plate theory share certain common mathematical structure. To see this, we first summarize the governing equations of the two theories.

CPT:

$$\frac{1}{r} \frac{d}{dr} (r Q_r^C) = -q \quad (10.5.1)$$

where

$$r Q_r^C \equiv \frac{d}{dr} (r M_{rr}^C) - M_{\theta\theta}^C \quad (10.5.2)$$

$$M_{rr}^C = -D \left(\frac{d^2 w_0^C}{dr^2} + \frac{\nu}{r} \frac{dw_0^C}{dr} \right)$$

$$M_{\theta\theta}^C = -D \left(\nu \frac{d^2 w_0^C}{dr^2} + \frac{1}{r} \frac{dw_0^C}{dr} \right) \quad (10.5.3)$$

FSDT:

$$\frac{1}{r} \frac{d}{dr} (r Q_r^F) = -q, \quad r Q_r^F = \frac{d}{dr} (r M_{rr}^F) - M_{\theta\theta}^F \quad (10.5.4)$$

where

$$M_{rr}^F = D \left(\frac{d\phi_r^F}{dr} + \frac{\nu}{r} \phi_r^F \right) \quad (10.5.5)$$

$$M_{\theta\theta}^F = D \left(\nu \frac{d\phi_r^F}{dr} + \frac{1}{r} \phi_r^F \right) \quad (10.5.6)$$

$$Q_r^F = K_s G h \left(\phi_r^F + \frac{dw_0^F}{dr} \right) \quad (10.5.7)$$

where the superscripts C and F on variables refer to the theory: C for CPT and F for FSDT.

Next, we introduce the moment sum, known also as the Marcus moment,

$$\mathcal{M} = \frac{M_{rr} + M_{\theta\theta}}{1 + \nu} \quad (10.5.8)$$

Using Eqs. (10.5.1)–(10.5.7), we can show that

$$\mathcal{M}^C = -D \left(\frac{d^2 w_0^C}{dr^2} + \frac{1}{r} \frac{dw_0^C}{dr} \right) = -D \frac{1}{r} \frac{d}{dr} \left(r \frac{dw_0^C}{dr} \right) \quad (10.5.9)$$

$$\mathcal{M}^F = D \left(\frac{d\phi_r^F}{dr} + \frac{1}{r} \phi_r^F \right) = D \frac{1}{r} \frac{d}{dr} (r \phi_r) \quad (10.5.10)$$

$$r \frac{d\mathcal{M}^C}{dr} = \frac{d}{dr} (r M_{rr}^C) - M_{\theta\theta}^C = r Q_r^C \quad (10.5.11)$$

$$r \frac{d\mathcal{M}^F}{dr} = \frac{d}{dr} (r M_{rr}^F) - M_{\theta\theta}^F = r Q_r^F \quad (10.5.12)$$

Therefore, the equations of equilibrium, Eqs. (10.5.1) and (10.5.4), can be expressed in terms of the moment sum as

$$\frac{1}{r} \frac{d}{dr} \left(r \frac{d\mathcal{M}^C}{dr} \right) = -q, \quad \frac{1}{r} \frac{d}{dr} \left(r \frac{d\mathcal{M}^F}{dr} \right) = -q \quad (10.5.13)$$

From Eqs. (10.5.1) and (10.5.4), because the load q being the same, it follows that

$$rQ_r^F = rQ_r^C + C_1 \quad (10.5.14)$$

and from Eqs. (10.5.11)–(10.5.14), we have

$$r \frac{d\mathcal{M}^F}{dr} = r \frac{d\mathcal{M}^C}{dr} + C_1 \rightarrow \mathcal{M}^F = \mathcal{M}^C + C_1 \log r + C_2 \quad (10.5.15)$$

where C_1 and C_2 are constants of integration. Next, from Eqs. (10.5.9), (10.5.10), and (10.5.15), we have

$$\phi_r = -\frac{dw_0^C}{dr} + \frac{C_1 r}{4D} (2 \log r - 1) + \frac{C_2 r}{2D} + \frac{C_3}{rD} \quad (10.5.16)$$

Finally, from Eqs. (10.5.7), (10.5.11), (10.5.12), (10.5.15), and (10.5.16), we obtain

$$\frac{dw_0^F}{dr} = -\phi_r^F + \frac{1}{K_s G h} \left(Q_r^C + \frac{C_1}{r} \right) \quad (10.5.17)$$

and noting that $Q_r^C = d\mathcal{M}^C/dr$, we have

$$w_0^F = w_0^C + \frac{\mathcal{M}^C}{K_s G h} + \frac{C_1 r^2}{4D} (1 - \log r) + \frac{C_1}{K_s G h} \log r - \frac{C_2 r^2}{4D} - \frac{C_3 \log r}{D} + \frac{C_4}{D} \quad (10.5.18)$$

The four constants of integration are determined using the boundary conditions. The boundary conditions for various cases are given below.

Free edge:

$$rQ_r^F = rQ_r^C = 0, \quad rM_{rr}^F = rM_{rr}^C = 0 \quad (10.5.19)$$

Simply supported edge:

$$w_0^F = w_0^C = 0, \quad rM_{rr}^F = rM_{rr}^C = 0 \quad (10.5.20)$$

Clamped edge:

$$w_0^F = w_0^C = 0, \quad \phi_r^F = \frac{dw_0^C}{dr} = 0 \quad (10.5.21)$$

Solid circular plate at $r = 0$ (i.e., at the plate center):

$$\phi_r^F = \frac{dw_0^C}{dr} = 0, \quad C_1 = 0 \quad (10.5.22)$$

Example 10.5.1: _____

Consider a circular plate of radius a and subjected to a linearly varying axisymmetric load $q = q_0(1 - r/a)$ (set $q_1 = 0$ in Figure 10.5.1). For simply supported as well as clamped (at $r = a$) circular plates, the boundary conditions (10.5.20) and (10.5.21) give

$$C_1 = C_2 = C_3 = 0 \quad \text{and} \quad C_4 = -\frac{D\mathcal{M}_a^C}{K_s Gh} \quad (10.5.23)$$

where \mathcal{M}_a^C is the moment sum at the simply supported or clamped edge ($r = a$) of the classical plate theory, and it is given as follows:

Simply supported edge:

$$\mathcal{M}_a^C = \frac{M_{\theta\theta}^C(a)}{1 + \nu} = -\frac{D(1 - \nu)}{a} \frac{dw_0^C}{dr} \Big|_{r=a} = \frac{D(1 - \nu)}{\nu} \frac{d^2 w_0^C}{dr^2} \Big|_{r=a} \quad (10.5.24)$$

Clamped edge:

$$\mathcal{M}_a^C = -D \frac{d^2 w_0^C}{dr^2} \Big|_{r=a} \quad (10.5.25)$$

Hence, the relationships (10.5.16) and (10.5.18) become

$$\phi_r(r) = -\frac{dw_0^C}{dr} \quad (10.5.26)$$

$$w_0^F(r) = w_0^C + \frac{\mathcal{M}_a^C(r) - \mathcal{M}_a^C}{K_s Gh} \quad (10.5.27)$$

The classical plate theory solution for such plates is given by (see Problem 5.6)

$$w_0^C = \frac{q_0 a^4}{14400 D} \left[\frac{3(183 + 43\nu)}{1 + \nu} - \frac{10(71 + 29\nu)}{1 + \nu} \left(\frac{r}{a}\right)^2 + 255 \left(\frac{r}{a}\right)^4 - 64 \left(\frac{r}{a}\right)^5 \right] \quad (10.5.28)$$

for simply supported plates, and

$$w_0^C = \frac{q_0 a^4}{14400 D} \left[129 - 290 \left(\frac{r}{a}\right)^2 + 225 \left(\frac{r}{a}\right)^4 - 64 \left(\frac{r}{a}\right)^5 \right] \quad (10.5.29)$$

for clamped plates (see Problem 5.13). Substitution of Eqs. (10.5.28) and (10.5.29) into Eqs. (10.5.24) and the result into Eq. (10.5.25), yields the deflection of the simply supported plate according to the first-order shear deformation plate theory

$$w_0^F = w_0^C + \frac{q_0 a^4}{36 K_s Gh} \left[5 - 9 \left(\frac{r}{a}\right)^2 + 4 \left(\frac{r}{a}\right)^3 \right] \quad (10.5.30)$$

The maximum deflection occurs at $r = 0$

$$w_{max}^F = w_{max}^C + \frac{5q_0 a^4}{36 K_s Gh}$$

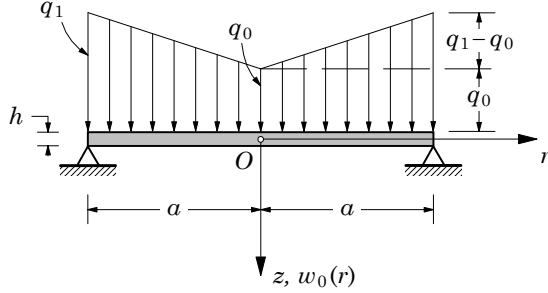


Figure 10.5.1. Simply supported solid circular plate under linearly varying axisymmetric load.

10.5.3 Polygonal Plates

Next, we consider the relationships between the bending solutions of the classical plate theory and the first-order shear deformation plate theory for polygonal plates (i.e., plates with multiple straight edges). The equations of equilibrium of plates according to the classical plate theory [see Eqs. (3.4.17) and (3.8.2)] and the first-order shear deformation theory [see Eqs. (10.1.19)–(10.1.21), (10.1.29) and (10.1.30)] are summarized below for isotropic plates under mechanical loads only.

CPT:

$$\frac{\partial^2 M_{xx}}{\partial x^2} + 2 \frac{\partial^2 M_{xy}}{\partial y \partial x} + \frac{\partial^2 M_{yy}}{\partial y^2} + q = 0 \quad (10.5.31)$$

where

$$\begin{Bmatrix} M_{xx} \\ M_{yy} \\ M_{xy} \end{Bmatrix} = -D \begin{bmatrix} 1 & \nu & 0 \\ \nu & 1 & 0 \\ 0 & 0 & \frac{1-\nu}{2} \end{bmatrix} \begin{Bmatrix} \frac{\partial^2 w_0}{\partial x^2} \\ \frac{\partial^2 w_0}{\partial y^2} \\ 2 \frac{\partial^2 w_0}{\partial x \partial y} \end{Bmatrix} \quad (10.5.32)$$

FSDT:

$$\frac{\partial Q_x}{\partial x} + \frac{\partial Q_y}{\partial y} + q = 0 \quad (10.5.33)$$

$$\frac{\partial M_{xx}}{\partial x} + \frac{\partial M_{xy}}{\partial y} - Q_x = 0 \quad (10.5.34)$$

$$\frac{\partial M_{xy}}{\partial x} + \frac{\partial M_{yy}}{\partial y} - Q_y = 0 \quad (10.5.35)$$

where

$$\begin{Bmatrix} M_{xx} \\ M_{yy} \\ M_{xy} \end{Bmatrix} = D \begin{bmatrix} 1 & \nu & 0 \\ \nu & 1 & 0 \\ 0 & 0 & \frac{1-\nu}{2} \end{bmatrix} \begin{Bmatrix} \frac{\partial \phi_x}{\partial x} \\ \frac{\partial \phi_y}{\partial y} \\ \frac{\partial \phi_x}{\partial y} + \frac{\partial \phi_y}{\partial x} \end{Bmatrix} \quad (10.5.36)$$

$$\begin{Bmatrix} Q_y \\ Q_x \end{Bmatrix} = \frac{K_s Eh}{2(1+\nu)} \begin{bmatrix} 1 & 0 \\ 0 & 1 \end{bmatrix} \begin{Bmatrix} \frac{\partial w_0}{\partial y} + \phi_y \\ \frac{\partial w_0}{\partial x} + \phi_x \end{Bmatrix} \quad (10.5.37)$$

The above equations can be expressed in terms of the deflection w_0 and the moment sum \mathcal{M} of each theory,

$$\mathcal{M}^C = \frac{M_{xx}^C + M_{yy}^C}{1 + \nu}, \quad \mathcal{M}^F = \frac{M_{xx}^F + M_{yy}^F}{1 + \nu} \quad (10.5.38)$$

as

$$\nabla^2 \mathcal{M}^C = -q, \quad \nabla^2 w_0^C = -\frac{\mathcal{M}^C}{D} \quad (10.5.39a, b)$$

$$\nabla^2 \mathcal{M}^F = -q, \quad \nabla^2 \left(w_0^F - \frac{\mathcal{M}^F}{K_s G h} \right) = -\frac{\mathcal{M}^F}{D} \quad (10.5.40a, b)$$

where the superscripts C and F refer to quantities of the classical and first-order plate theories, respectively; D is the flexural rigidity; and ν Poisson's ratio. The moment sum in each theory is related to the generalized displacements of the theory by the relations

$$\mathcal{M}^C = -D \left(\frac{\partial^2 w_0^C}{\partial x^2} + \frac{\partial^2 w_0^C}{\partial y^2} \right) \quad (10.5.41)$$

$$\mathcal{M}^F = D \left(\frac{\partial \phi_x}{\partial x} + \frac{\partial \phi_y}{\partial y} \right) \quad (10.5.42)$$

From Eqs. (10.5.39a) and (10.5.40a), since q is the same in both equations, it follows that

$$\mathcal{M}^F = \mathcal{M}^C + D \nabla^2 \Phi \quad (10.5.43)$$

where Φ is a function such that it satisfies the biharmonic equation

$$\nabla^4 \Phi = 0 \quad (10.5.44)$$

Using this result in Eqs. (10.5.39b) and (10.5.40b), we arrive at the relationship

$$w_0^F = w_0^C + \frac{\mathcal{M}^C}{K_s G h} + \Psi - \Phi \quad (10.5.45)$$

$$= w_0^C + \frac{h^2}{6 K_s (1 - \nu)} \nabla^2 w_0^C + \Psi - \Phi \quad (10.5.46)$$

where Ψ is a harmonic function that satisfies the Laplace equation

$$\nabla^2 \Psi = 0 \quad (10.5.47)$$

Note that the relationship (10.5.46) is valid for all plates with arbitrary boundary conditions and transverse load. One must determine Φ and Ψ from Eqs. (10.5.44) and (10.5.47), respectively, subject to the boundary conditions of the plate. However, it is difficult to determine these functions for arbitrary geometries and boundary conditions.

In cases where $w_0^F = w_0^C$ on the boundary of the polygonal plates and \mathcal{M}^C is either zero or equal to a constant \mathcal{M}^{*C} (which can be zero) over the boundary, $(\Psi - \Phi)$ simply takes on the value of $-\mathcal{M}^{*C}/(K_s Gh)$. However, if \mathcal{M}^C varies over the boundary, the functions Ψ and Φ must be determined separately. Restricting our analysis to the former case, Eq. (10.5.45) can be written as

$$w_0^F(x, y) = w_0^C(x, y) + \frac{\mathcal{M}^C - \mathcal{M}^{*C}}{K_s Gh} \quad (10.5.48)$$

Equation (10.5.48) can be used to establish relationships between deflection gradients, bending moments, twisting moment, and shear forces of the classical and first-order shear deformation plate theories, as given below:

$$\frac{\partial w_0^F}{\partial x} = \frac{\partial w_0^C}{\partial x} + \frac{Q_x^C}{K_s Gh} \quad (10.5.49)$$

$$\frac{\partial w_0^F}{\partial y} = \frac{\partial w_0^C}{\partial y} + \frac{Q_y^C}{K_s Gh} \quad (10.5.50)$$

$$\begin{aligned} M_{xx}^F &= M_{xx}^C + \frac{D(1-\nu)}{2K_s Gh} \left[\frac{\partial}{\partial x} (Q_x^F - Q_x^C) - \frac{\partial}{\partial y} (Q_y^F - Q_y^C) \right] \\ &= M_{xx}^C + \frac{D}{K_s Gh} \left[\frac{\partial}{\partial x} (Q_x^F - Q_x^C) + \nu \frac{\partial}{\partial y} (Q_y^F - Q_y^C) \right] \\ &= M_{xx}^C + \frac{D(1-\nu)}{K_s Gh} \frac{\partial}{\partial x} (Q_x^F - Q_x^C) \end{aligned} \quad (10.5.51)$$

$$\begin{aligned} M_{yy}^F &= M_{yy}^C + \frac{D(1-\nu)}{2K_s Gh} \left[\frac{\partial}{\partial y} (Q_y^F - Q_y^C) - \frac{\partial}{\partial x} (Q_x^F - Q_x^C) \right] \\ &= M_{yy}^C + \frac{D}{K_s Gh} \left[\frac{\partial}{\partial y} (Q_y^F - Q_y^C) + \nu \frac{\partial}{\partial x} (Q_x^F - Q_x^C) \right] \\ &= M_{yy}^C + \frac{D(1-\nu)}{K_s Gh} \frac{\partial}{\partial y} (Q_y^F - Q_y^C) \end{aligned} \quad (10.5.52)$$

$$M_{xy}^F = M_{xy}^C + \frac{D(1-\nu)}{2K_s Gh} \left[\frac{\partial}{\partial y} (Q_x^F - Q_x^C) - \frac{\partial}{\partial x} (Q_y^F - Q_y^C) \right] \quad (10.5.53)$$

The above relationships are exact if $w_0^F = w_0^C$ at the boundaries and the Marcus moments in both theories at the boundary are equal to the same constant.

In the case of simply supported polygonal plates, it can be shown that the Marcus moment in the classical plate theory is zero along with the deflection:

$$w_0^C = \mathcal{M}^C = 0 \text{ along the straight simply supported edges} \quad (10.5.54)$$

In the first-order plate theory, the simply supported boundary condition involves specifying, in addition to the deflection and normal bending moment, the tangential rotation on the edge. This, boundary condition is known as the simple support of the “hard” type:

$$w_0^F = 0, \quad M_{nn}^F = 0, \quad \phi_s = 0 \quad (10.5.55)$$

where n is the direction normal to the simply supported edge and s is the direction tangential to the edge. Owing to these conditions, $\partial\phi_s/\partial s = 0$ and the Marcus moment \mathcal{M}^F is, thus, equal to zero. The boundary conditions of the FSDT for the simply supported plate are, therefore

$$w_0^F = \mathcal{M}^F = 0 \text{ along the straight simply supported edges.} \quad (10.5.56)$$

Since the Marcus moments at the boundaries of plates with any polygonal shape and simply supported edges are equal to zero, Eq. (10.5.48) applies to such plates with $\mathcal{M}^{*C} = 0$. We have

$$w_0^F = w_0^C + \frac{\mathcal{M}^C}{K_s G h} \quad (10.5.57)$$

Equation (10.5.57) is an important relationship between the deflections w_0^F and w_0^C of a simply supported polygonal plate. That is, if deflection of a simply supported plate using the classical plate theory is available, we can immediately determine the deflection according to the first-order theory for the same problem from Eq. (10.5.57), thus bypassing the task of solving the equations of the first-order shear deformation plate theory. Using the same reasoning, one may readily deduce that Eq. (10.5.48) holds for simply supported polygonal plates under a constant distributed moment \mathcal{M}^{*K} along their edges. For additional results on this topic, the reader may consult the book by Wang, Lee, and Reddy (2000) and references therein.

Example 10.5.2: _____

Consider the simply supported equilateral triangular plate shown in Figure 10.5.2 (see Problem 7.11). Equation (c) of that problem contains the analytical solution of CPT for the deflection of the plate under uniform load q_0 :

$$w_0^C = \frac{q_0 a^4}{64D} \left[\bar{x}^3 - 3\bar{y}^2\bar{x} - (\bar{x}^2 + \bar{y}^2) + \frac{4}{27} \right] \left(\frac{4}{9} - \bar{x}^2 - \bar{y}^2 \right) \quad (10.5.58)$$

where $\bar{x} = x/a$ and $\bar{y} = y/a$ (Figure 10.5.2). The Marcus moment is given by

$$\mathcal{M}^C = -D\nabla^2 w_0^C = \frac{q_0 L^2}{4} \left[\bar{x}^3 - 3\bar{x}\bar{y}^2 - (\bar{x}^2 - \bar{y}^2) + \frac{4}{27} \right]. \quad (10.5.59)$$

Therefore, the deflection w_0^F according to the first-order plate theory of the same problem is given by Eq. (10.5.57) as

$$w_0^F = \frac{q_0 a^4}{4D} \left[\bar{x}^3 - 3\bar{y}^2 - (\bar{x}^2 + \bar{y}^2) + \frac{4}{27} \right] \left[\frac{\frac{4}{9} - \bar{x}^2 - \bar{y}^2}{16} + \frac{D}{K_s G a^2} \right] \quad (10.5.60)$$

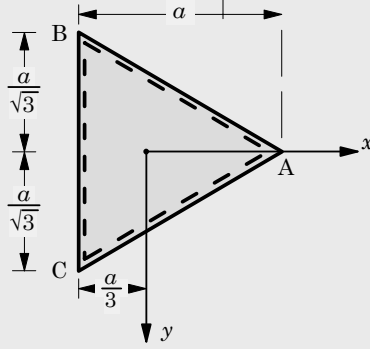


Figure 10.5.2. Simply supported equilateral triangular plate.

Example 10.5.3:

Consider a simply supported rectangular plate of side lengths $a \times b$, as shown in Figure 10.5.3. The plate is subjected to a distributed load $q(x, y)$. The deflection of this problem according to the classical plate theory is given by Eq. (6.2.11) with $M_{mn}^T = 0$ and $k = 0$:

$$w_0^C = \sum_{n=1}^{\infty} \sum_{m=1}^{\infty} \left[\frac{q_{mn}}{\pi^4 D \left(\frac{m^2}{a^2} + \frac{n^2}{b^2} \right)^2} \right] \sin \frac{m\pi x}{a} \sin \frac{n\pi y}{b} \quad (10.5.61)$$

where

$$q_{mn} = \frac{4}{ab} \int_0^b \int_0^a q(x, y) \sin \frac{m\pi x}{a} \sin \frac{n\pi y}{b} dx dy \quad (10.5.62)$$

The Marcus moment is given by

$$\mathcal{M}^C = -D \nabla^2 w_0^C = - \sum_{n=1}^{\infty} \sum_{m=1}^{\infty} \left[\frac{q_{mn}}{\pi^2 \left(\frac{m^2}{a^2} + \frac{n^2}{b^2} \right)} \right] \sin \frac{m\pi x}{a} \sin \frac{n\pi y}{b} \quad (10.5.63)$$

Using Eq. (10.5.57), the deflection w_0^F according to the first-order plate theory applied to the simply supported rectangular plate under distributed load is given by

$$w_0^F = \sum_{n=1}^{\infty} \sum_{m=1}^{\infty} \left[\frac{Q_{mn}}{\pi^4 \left(\frac{m^2}{a^2} + \frac{n^2}{b^2} \right)^2} \right] \sin \frac{m\pi x}{a} \sin \frac{n\pi y}{b} \quad (10.5.64)$$

where

$$Q_{mn} = q_{mn} \left[1 + \frac{\pi^2 \left(\frac{m^2}{a^2} + \frac{n^2}{b^2} \right)}{6K_s G} \right] \quad (10.5.65)$$

This solution can be verified to be the same as that in Eq. (10.4.2a) with W_{mn} defined by the solution of Eq. (10.4.4). In particular, for sinusoidally distributed load

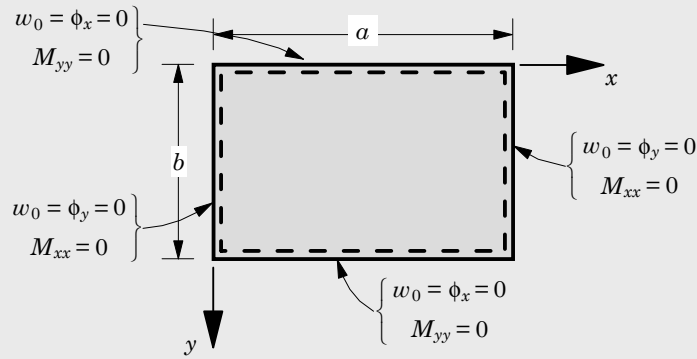


Figure 10.5.3. Simply supported rectangular plate.

$$q(x, y) = q_0 \sin \frac{\pi x}{a} \sin \frac{\pi y}{b} \quad (10.5.66)$$

The deflection becomes ($q_{mn} = q_0$)

$$w_0^F = \frac{q_0 b^4}{\pi^4 (1 + s^2)^2} \left[1 + \frac{\pi^2 (1 + s^2)}{6 K_s G b^2} \right] \sin \frac{\pi x}{a} \sin \frac{\pi y}{b} \quad (10.5.67)$$

where s is the plate aspect ratio, $s = b/a$.

10.6 Summary

This chapter is dedicated to the development of the first-order and third-order shear deformation plate theories. Beginning with assumed displacement fields and using the principle of virtual displacements, governing equations and associated natural boundary conditions are derived. The Navier solutions of the theories are presented for bending, natural vibration, and buckling of rectangular plates. Also, a section on the relationships between the classical plate theory and shear deformation plate theories is also presented. The relationships allow one to determine the solution of a problem according the first-order theory or the third-order theory if classical plate theory solution to the problem is available. Additional details on these relationships can be found in the book by Wang, Reddy, and Lee (2000).

Problems

10.1 Show that the solution of Eq. (10.2.11) is given by

$$\begin{aligned} W_{mn} &= \frac{1}{b_{mn}} \left(a_1 Q_{mn} - a_2 \alpha_m M_{mn}^1 - a_3 \beta_n M_{mn}^2 \right) \\ X_{mn} &= \frac{1}{b_{mn}} \left(a_2 Q_{mn} - a_4 \alpha_m M_{mn}^1 - a_5 \beta_n M_{mn}^2 \right) \\ Y_{mn} &= \frac{1}{b_{mn}} \left(a_3 Q_{mn} - a_5 \alpha_m M_{mn}^1 - a_6 \beta_n M_{mn}^2 \right) \end{aligned}$$

where

$$b_{mn} = \begin{vmatrix} \hat{s}_{11} & \hat{s}_{12} & \hat{s}_{13} \\ \hat{s}_{12} & \hat{s}_{22} & \hat{s}_{23} \\ \hat{s}_{13} & \hat{s}_{23} & \hat{s}_{33} \end{vmatrix} = \hat{s}_{11}a_1 + \hat{s}_{12}a_2 + \hat{s}_{13}a_3$$

$$a_1 = \hat{s}_{22}\hat{s}_{33} - \hat{s}_{23}\hat{s}_{23}, \quad a_2 = \hat{s}_{23}\hat{s}_{13} - \hat{s}_{12}\hat{s}_{33}, \quad a_3 = \hat{s}_{12}\hat{s}_{23} - \hat{s}_{22}\hat{s}_{13}$$

$$a_4 = \hat{s}_{11}\hat{s}_{33} - \hat{s}_{13}\hat{s}_{13}, \quad a_5 = \hat{s}_{12}\hat{s}_{13} - \hat{s}_{11}\hat{s}_{23}, \quad a_6 = \hat{s}_{11}\hat{s}_{22} - \hat{s}_{12}\hat{s}_{12}$$

10.2 Derive the expressions for transverse stresses in FSDT presented in Eqs. (10.2.18a,b).

10.3 Show that the expression for the critical buckling load, using Eq. (10.2.21), is

$$N_0 = \frac{1}{\alpha_m^2 + \gamma\beta_n^2} \left(\hat{s}_{11} + \frac{\hat{s}_{12}\hat{s}_{33} - \hat{s}_{13}\hat{s}_{23}}{\hat{s}_{22}\hat{s}_{33} - \hat{s}_{23}\hat{s}_{23}} \hat{s}_{12} + \frac{\hat{s}_{22}\hat{s}_{13} - \hat{s}_{23}\hat{s}_{12}}{\hat{s}_{22}\hat{s}_{33} - \hat{s}_{23}\hat{s}_{23}} \hat{s}_{13} \right)$$

10.4 Show that the equations of equilibrium [see Eqs. (10.1.33)–(10.1.35)] for bending of the first-order shear deformation plate theory can be expressed in matrix form as

$$\begin{bmatrix} L_{11} & L_{12} & L_{13} \\ L_{12} & L_{22} & L_{23} \\ L_{13} & L_{23} & L_{33} \end{bmatrix} \begin{Bmatrix} w_0 \\ \phi_x \\ \phi_y \end{Bmatrix} = \begin{Bmatrix} q \\ 0 \\ 0 \end{Bmatrix}$$

where the coefficients $L_{ij} = L_{ji}$ are

$$L_{11} = -K_s A_{55} \frac{\partial^2}{\partial x^2} - K_s A_{44} \frac{\partial^2}{\partial y^2}, \quad L_{12} = -K_s A_{55} \frac{\partial}{\partial x}$$

$$L_{13} = -K_s A_{44} \frac{\partial}{\partial y}, \quad L_{22} = -K_s A_{55} + D_{11} \frac{\partial^2}{\partial x^2} + D_{66} \frac{\partial^2}{\partial y^2}$$

$$L_{23} = (D_{12} + D_{66}) \frac{\partial^2}{\partial x \partial y}, \quad L_{33} = -K_s A_{44} + D_{66} \frac{\partial^2}{\partial x^2} + D_{22} \frac{\partial^2}{\partial y^2}$$

10.5 In the Lévy method, the generalized displacements are expressed as products of undetermined functions and known trigonometric functions so as to satisfy the simply supported boundary conditions. Suppose that the edges at $y = 0, b$ of a rectangular plate are simply supported

$$w_0 = \phi_x = N_{yy} = M_{yy} = 0$$

Then, the displacement field (w_0, ϕ_x, ϕ_y) can be represented as

$$\begin{Bmatrix} w_0(x, y) \\ \phi_x(x, y) \\ \phi_y(x, y) \end{Bmatrix} = \sum_{n=1}^{\infty} \begin{Bmatrix} W_n(x) \\ X_n(x) \\ Y_n(x) \end{Bmatrix} \cos \beta_n y$$

where $\beta_n = n\pi/b$. The transverse load is also expanded as

$$q(x, y) = \sum_{n=1}^{\infty} q_n \sin \beta_n y, \quad q_n(x) = \frac{2}{b} \int_0^b q(x, y) \sin \beta_n y \, dy$$

Show that the substitution of the displacement field into governing equations (10.1.33)–(10.1.35) (see Problem 10.4) results in the following three ordinary differential equations

$$\begin{aligned} W_n'' &= C_{11}W_n + C_{12}X'_n + C_{13}Y_n + C_0q_n \\ X_n'' &= C_{21}W'_n + C_{22}X_n + C_{23}Y'_n \\ Y_n'' &= C_{31}W_n + C_{32}X'_n + C_{33}Y_n \end{aligned}$$

where a prime denotes the derivative with respect to x . The coefficients C_i are given by

$$\begin{aligned} C_0 &= -\frac{1}{K_s A_{55}}, & C_{11} &= \frac{A_{44}}{A_{55}}\beta_n^2, & C_{12} &= -1, & C_{13} &= \frac{A_{44}}{A_{55}}\beta_n \\ C_{21} &= \frac{K_s A_{55}}{D_{11}}, & C_{22} &= \frac{(K_s A_{55} + D_{66}\beta_n^2)}{D_{11}}, & C_{23} &= \frac{(D_{12} + D_{66})}{D_{11}}\beta_n \\ C_{31} &= -\frac{K_s A_{44}}{D_{66}}\beta_n, & C_{32} &= \frac{(D_{12} + D_{66})}{D_{66}}\beta_n, & C_{33} &= \frac{(K_s A_{44} + D_{22}\beta_n^2)}{D_{66}} \end{aligned}$$

10.6 The first-order shear deformation plate theory (FSDT) for axisymmetric bending of circular plates is based on the displacement field

$$u_r(r, z, t) = u(r, t) + z\phi(r, t), \quad u_z(r, z, t) = w(r, t) \quad (1)$$

where ϕ denotes rotation of a transverse normal in the plane $\theta = \text{constant}$. Use Hamilton's principle (or the dynamics version of the principle of virtual work) to show that the equations of motion are given by

$$\begin{aligned} -\frac{1}{r} \left[\frac{\partial}{\partial r} (rN_{rr}) - N_{\theta\theta} \right] + I_0 \frac{\partial^2 u}{\partial t^2} &= 0 \\ -\frac{1}{r} \frac{\partial}{\partial r} (rQ_r) - \frac{1}{r} \frac{\partial}{\partial r} \left(rN_{rr} \frac{\partial w}{\partial r} \right) - q + I_0 \frac{\partial^2 w}{\partial t^2} &= 0 \\ -\frac{1}{r} \left[\frac{\partial}{\partial r} (rM_{rr}) - M_{\theta\theta} \right] + Q_r + I_2 \frac{\partial^2 \phi}{\partial t^2} &= 0 \end{aligned} \quad (2)$$

Include the von Kármán nonlinear strains.

10.7 (Continuation of Problem 10.6) Express the stress resultants (N_{rr} , $N_{\theta\theta}$, M_{rr} , $M_{\theta\theta}$, Q_r) in terms of the strains in the axisymmetric bending of polar orthotropic circular plates by assuming linear constitutive equations in the form

$$\begin{aligned} \sigma_{rr} &= Q_{11}\varepsilon_{rr} + Q_{12}\varepsilon_{\theta\theta} \\ \sigma_{\theta\theta} &= Q_{12}\varepsilon_{rr} + Q_{22}\varepsilon_{\theta\theta} \\ \sigma_{rz} &= 2Q_{44}\varepsilon_{rz} \end{aligned} \quad (1)$$

where Q_{ij} are the plane stress-reduced elastic stiffnesses, which are known in terms of four independent material (engineering) constants E_1 , E_2 , ν_{12} and G_{13} :

$$\begin{aligned} Q_{11} &= \frac{E_1}{1 - \nu_{12}\nu_{21}}, & Q_{12} &= \frac{\nu_{12}E_2}{1 - \nu_{12}\nu_{21}} \\ Q_{22} &= \frac{E_2}{1 - \nu_{12}\nu_{21}}, & Q_{44} &= G_{13} \end{aligned} \quad (2)$$

Poisson's ratio ν_{21} is known through the reciprocal relation $\nu_{21} = E_1\nu_{12}/E_2$.

- 10.8** Use the results of Problems 10.6 and 10.7 to determine the general solution (w, ϕ) of the linear, static, bending of circular plates under axisymmetric loads.
- 10.9** For a clamped solid circular plate under uniform load of intensity q_0 , determine the constants c_1 through c_4 of Problem 10.8 and obtain the following expressions for the transverse deflection and rotation:

$$\begin{aligned} w(r) &= \frac{q_0 a^4}{64D} \left(1 - \frac{r^2}{a^2}\right)^2 + \frac{q_0 a^2}{4K_s Gh} \left(1 - \frac{r^2}{a^2}\right) \\ \phi(r) &= \frac{q_0 a^3 r}{16D a} \left(1 - \frac{r^2}{a^2}\right) \end{aligned}$$

- 10.10** For a simply supported solid circular plate under uniform load of intensity q_0 , determine the constants c_1 through c_4 of Problem 10.8 and obtain the following expressions for the transverse deflection and rotation:

$$\begin{aligned} w(r) &= \frac{q_0 a^4}{64D} \left(\frac{r^4}{a^4} - 2\frac{3+\nu}{1+\nu}\frac{r^2}{a^2} + \frac{5+\nu}{1+\nu}\right) + \frac{q_0 a^2}{4K_s Gh} \left(1 - \frac{r^2}{a^2}\right) \\ \phi(r) &= \frac{q_0 a^3 r}{16D a} \left[\frac{(3+\nu)}{(1+\nu)} - \frac{r^2}{a^2}\right] \end{aligned}$$

- 10.11** The third-order plate theory of Reddy (1984a) is based on the displacement field (for axisymmetric bending)

$$u_r(r, z, t) = u(r, t) + z\phi(r, t) - c_1 z^3 \left(\phi + \frac{\partial w}{\partial r}\right), \quad u_z(r, z, t) = w(r, t) \quad (1)$$

where $c_1 = 4/(3h^2)$ and h denotes the total thickness of the plate. Derive the governing equations of motion using Hamilton's principle. Include the von Kármán nonlinear strains.

Theory and Analysis of Shells

11.1 Introduction

11.1.1 Preliminary Comments

In the preceding chapters, we studied the theory and the analysis of flat plates. In this chapter, we consider theories of shells. Shells are common structural elements in many engineering structures, including pressure vessels, submarine hulls, ship hulls, wings and fuselages of airplanes, containment structures of nuclear power plants, pipes, exteriors of rockets, missiles, automobile tires, concrete roofs, chimneys, cooling towers, liquid storage tanks, and many other structures. They are also found in nature in the form of eggs, leaves, inner ear, skulls, and geological formations (Figure 11.1.1). Shell structures have been built by man for centuries, mostly in the form of masonry and stone domes, roofs and arches, and some of which still exist around the world.

A number of historical papers and text books on shells are available. For example, see Ambartsumyan (1964), Bert (1974), Sanders (1959), Budiansky and Sanders (1963), Dikeman (1982), Donnell (1933, 1976), Flügge (1973), Green (1962), Heyman (1977), Koiter (1967), Kraus (1967), Librescu (1975), Love (1888), Naghdi (1963, 1972), Novozhilov (1964), Sanders (1959, 1963), and Vlasov (1964). Many of the shell theories were developed originally for thin shells and are based on the Kirchhoff-Love kinematic hypothesis that straight lines normal to the undeformed middle surface remain straight and normal to the middle surface after deformation. Other shell theories can be found in the works of Naghdi (1956, 1963) and a detailed study of thin isotropic shells can be found in the books by Ambartsumyan (1964), Kraus (1967), Timoshenko and Woinowsky-Krieger (1970), Flügge (1973), Leissa (1973), Ugural (1999), and Farshad (1992). The first-order shear deformation theory of shells, also known as the Sanders shell theory, can be found in the books by Kraus (1967) and Leissa (1973).

The theories based on Kirchhoff-Love's hypotheses, in which the transverse shear deformation is neglected, are also known as the Love's first-approximation theories [see Love (1988)]. They are expected to yield sufficiently accurate results when (1) the radius-to-thickness ratio is large, (2) the dynamic excitations are within the low-frequency range, and (3) the material anisotropy is not severe. However, the application of such theories to thick shells or anisotropic composite shells could lead to 10% or more errors in deflections, stresses, buckling loads and frequencies.

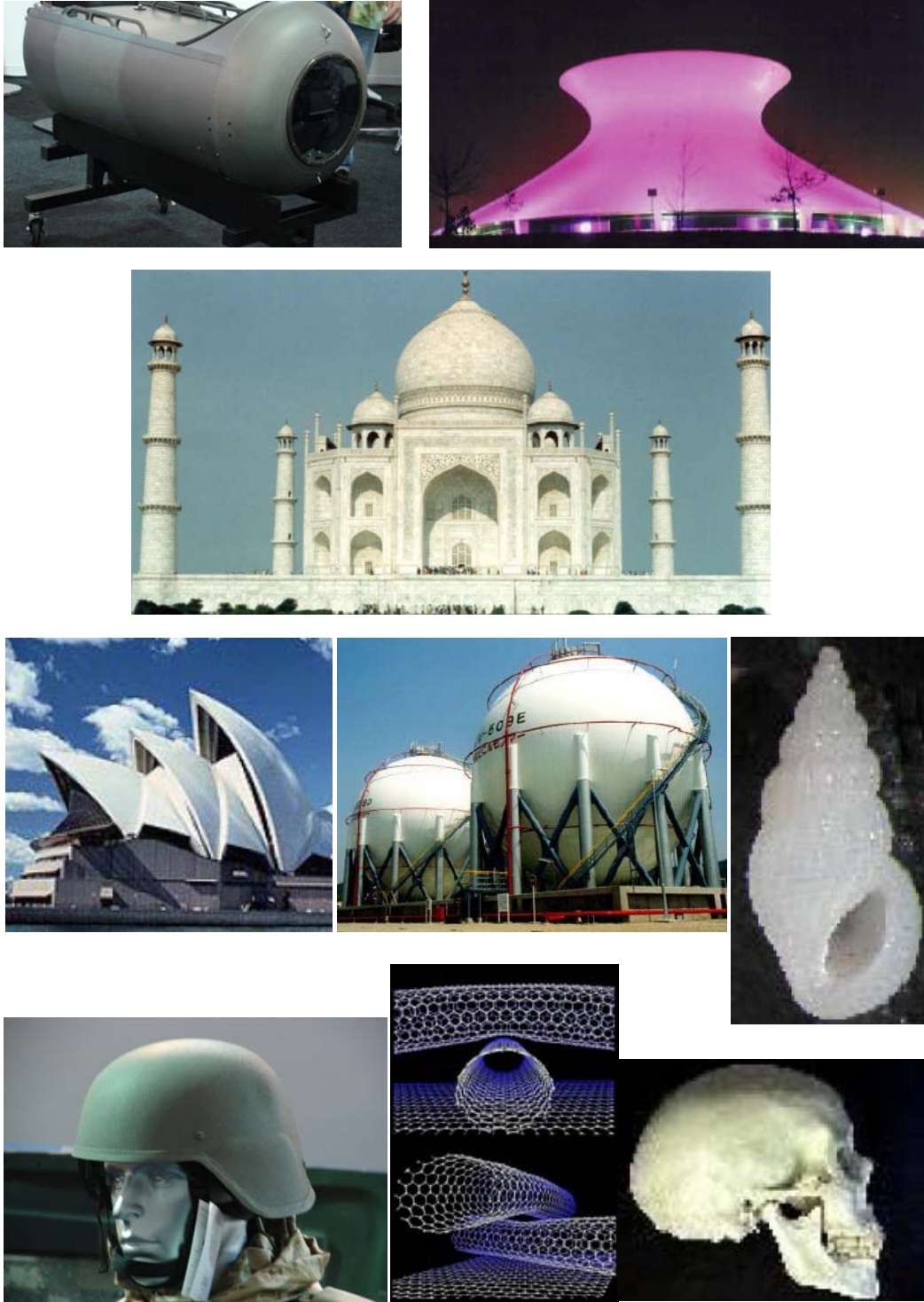


Figure 11.1.1. Various forms of manmade shells and shells found in nature.

11.1.2 Classification of Shell Surfaces

It is useful to classify shell surfaces using the so-called Gaussian curvature. The curves formed by the intersection of shell surface and a plane normal to the surface is called *normal section* of the surface at that point, as shown in Figure 11.1.2(a). In general, each of these curves has a unique curvature of its own. Of all these curves, there is one curve that has a maximum value of curvature K_1 and another one with a minimum value of curvature K_2 . These two curves are called *principal curves* and their curvatures, K_1 and K_2 , are called *principal curvatures* of the surface. Using differential geometry, it can be shown that these two principal curves are orthogonal to each other. The product of the principal curvatures K_1 and K_2 is called the *Gaussian curvature*, K . If $K_2 = 0$ and $K_1 \neq 0$, then the surface is said to have zero Gaussian curvature (e.g., cylindrical shell). If $K = K_1 K_2 > 0$, the surface is said to have positive Gaussian curvature or *synclastic surface*, and if $K < 0$, it is said to have negative Gaussian curvature or *anticlastic surface* [Figure 11.1.2(b)].

A curved surface is said to be *developable* if it can be reduced to a planar surface without stretching (i.e., deforming) the surface. For example, a cylindrical panel [Figure 11.1.3(a)] is developable because it can be unfolded to a rectangular plate. A *nondevelopable* surface, on the other hand, requires cutting or deforming to collapse it into a planar surface. An example of nondevelopable surface is provided by a spherical dome [Figure 11.1.3(b)]. Thus, nondevelopable surfaces are stronger than developable surfaces because they take additional forces to collapse compared to planar surfaces.

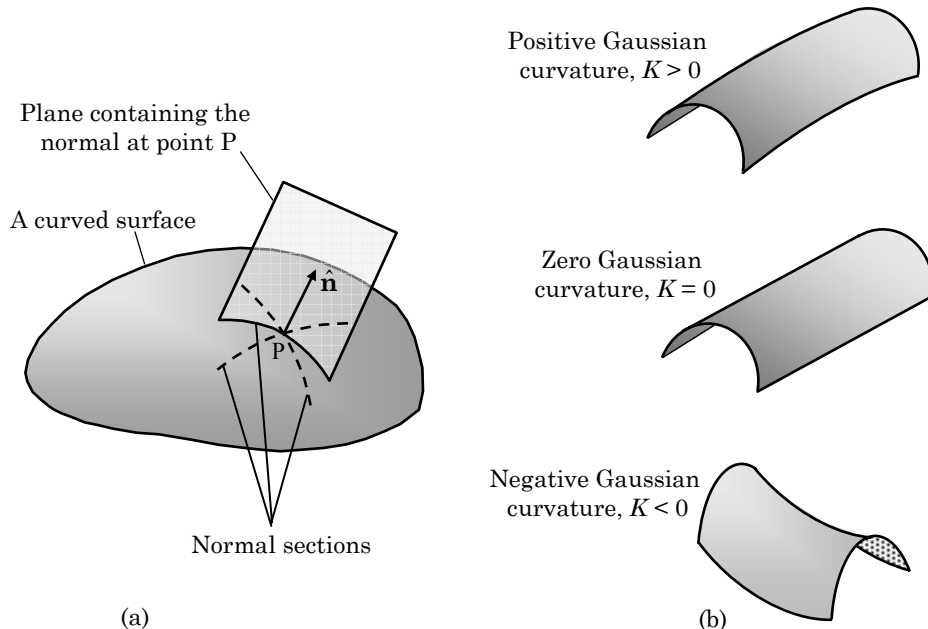


Figure 11.1.2. (a) Principal curves. (b) Surfaces with positive, zero, and negative Gaussian curvatures.

Surfaces of revolution are those generated by rotating a plane curve about an axis, called the *axis of revolution*. Examples of surfaces of revolution are shown in Figure 11.1.4.

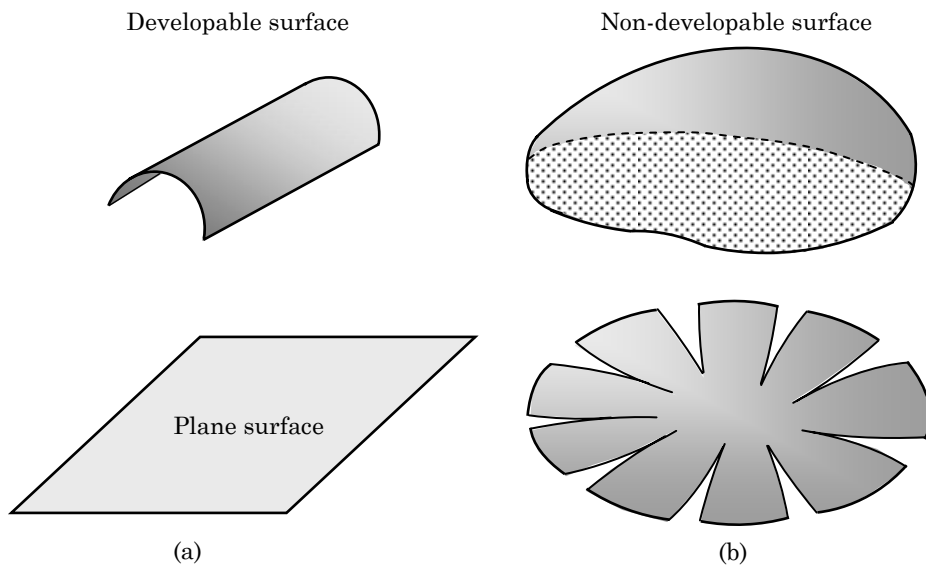


Figure 11.1.3. (a) Developable surface. (b) Nondevelopable surface.

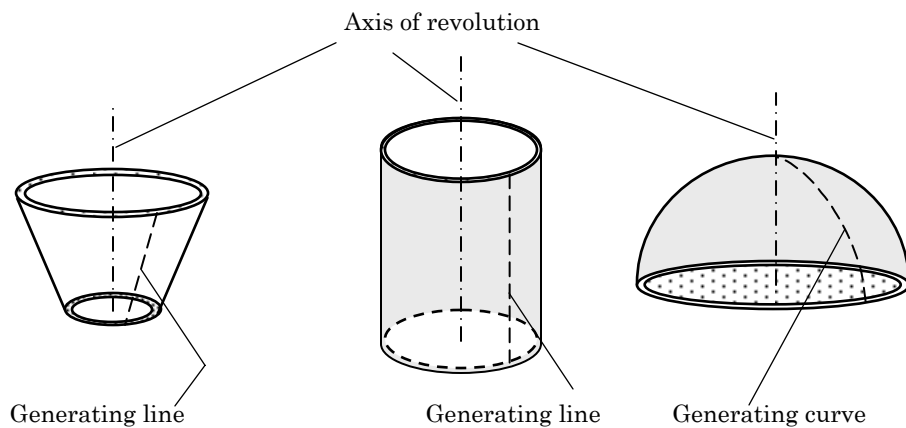


Figure 11.1.4. Surfaces of revolution.

11.2 Governing Equations

11.2.1 Geometric Properties of the Shell

Based on the geometry, shells can be classified broadly into the following groups:

- *Singly-curved shells.* Examples are provided by circular or noncircular cylinders, cones, and developable shells of revolution. A developable shell is one that can be stretched into a plane without cutting or stretching its middle surface.
- *Doubly-curved shells.* Examples are provided by spherical domes and shells of revolution (ellipsoids of revolution and paraboloids of revolution).
- *Combined shells.* Part of the shell is a singly-curved shell and other part is a doubly-curved shell.

A uniform thickness curved shell element is shown in Figure 11.2.1(a), where (ξ_1, ξ_2, ζ) denote the curvilinear coordinates such that ξ_1 and ξ_2 curves are the lines of curvature on the middle surface ($\zeta = 0$), as shown in Figure 11.2.1(b). The position vector of a typical point $(\xi_1, \xi_2, 0)$ on the middle surface is denoted by \mathbf{r} , and the position of an arbitrary point (ξ_1, ξ_2, ζ) is denoted by \mathbf{R} [Figure 11.2.1(c)]. A differential line element on the middle surface can be written as

$$d\mathbf{r} = \frac{\partial \mathbf{r}}{\partial \xi_\alpha} d\xi_\alpha = \mathbf{g}_\alpha d\xi_\alpha, \quad \mathbf{g}_\alpha = \frac{\partial \mathbf{r}}{\partial \xi_\alpha} \quad (\alpha = 1, 2) \quad (11.2.1)$$

where the vectors \mathbf{g}_1 and \mathbf{g}_2 are tangent to the ξ_1 and ξ_2 coordinate lines, as shown in Figure 11.2.1(b). The components of the *surface metric tensor* $g_{\alpha\beta}$ ($\alpha, \beta = 1, 2$) are

$$\mathbf{g}_\alpha \cdot \mathbf{g}_\beta \equiv g_{\alpha\beta}, \quad a_1 = \sqrt{g_{11}}, \quad a_2 = \sqrt{g_{22}}, \quad \mathbf{g}_1 \cdot \mathbf{g}_2 = a_1 a_2 \cos \chi \quad (11.2.2)$$

where χ denotes the angle between the coordinate curves. The unit vector normal to the middle surface (hence, normal to both \mathbf{g}_1 and \mathbf{g}_2) can be determined from

$$\hat{\mathbf{n}} = \frac{\mathbf{g}_1 \times \mathbf{g}_2}{a_1 a_2 \sin \chi} \quad (11.2.3)$$

In general, $\hat{\mathbf{n}}$, a_1 and a_2 are functions of ξ_1 and ξ_2 . The square of the distance ds between points $(\xi_1, \xi_2, 0)$ and $(\xi_1 + d\xi_1, \xi_2 + d\xi_2, 0)$ on the middle surface is determined by

$$(ds)^2 = d\mathbf{r} \cdot d\mathbf{r} = g_{\alpha\beta} d\xi_\alpha d\xi_\beta = a_1^2 (d\xi_1)^2 + a_2^2 (d\xi_2)^2 + 2a_1 a_2 \cos \chi d\xi_1 d\xi_2 \quad (11.2.4)$$

The right-hand side of the above equation is known as the *first quadratic form of the surface*, which allows us to determine the infinitesimal lengths, the angle between the curves, and area of the surface. The terms a_1^2 , a_2^2 , and $a_1 a_2 \cos \chi$ are called the “first fundamental quantities.”

Let $\mathbf{r} = \mathbf{r}(s)$ be the equation of a curve on the surface. The unit vector tangent to the curve is

$$\hat{\mathbf{t}} = \frac{d\mathbf{r}}{ds} = \frac{\partial \mathbf{r}}{\partial \xi_\alpha} \frac{d\xi_\alpha}{ds} = \mathbf{g}_\alpha \frac{d\xi_\alpha}{ds} \quad (11.2.5)$$

According to Frenet’s formula [see Kreyszig (2006)], the derivative of this unit vector is

$$\frac{d\hat{\mathbf{t}}}{ds} = \frac{\hat{\mathbf{N}}}{\rho} \quad (11.2.6)$$

where $1/\rho$ is the curvature of the curve, and $\hat{\mathbf{N}}$ is the unit vector of the principal normal to the curve. From Eqs. (11.2.5) and (11.2.6), we obtain

$$\frac{\hat{\mathbf{N}}}{\rho} = \frac{d}{ds} \left(\frac{d\mathbf{r}}{ds} \right) = \frac{\partial \mathbf{g}_\alpha}{\partial \xi_\beta} \frac{d\xi_\alpha}{ds} \frac{d\xi_\beta}{ds} + \mathbf{g}_\alpha \frac{d^2 \xi_\alpha}{ds^2} \quad (11.2.7)$$

Let φ be the angle between the normal to the surface, $\hat{\mathbf{n}}$, and the principal normal to the curve, $\hat{\mathbf{N}}$; i.e., $\cos \varphi = \hat{\mathbf{n}} \cdot \hat{\mathbf{N}}$. Then, taking the dot product of both sides of Eq. (11.2.7), we obtain

$$\frac{\cos \varphi}{\rho} = \frac{L(d\xi_1)^2 + 2M d\xi_1 d\xi_2 + N(d\xi_2)^2}{ds^2} \quad (11.2.8)$$

where

$$L = \hat{\mathbf{n}} \cdot \frac{\partial^2 \mathbf{r}}{\partial \xi_1^2}, \quad M = \hat{\mathbf{n}} \cdot \frac{\partial^2 \mathbf{r}}{\partial \xi_1 \partial \xi_2}, \quad N = \hat{\mathbf{n}} \cdot \frac{\partial^2 \mathbf{r}}{\partial \xi_2^2} \quad (11.2.9)$$

The numerator on the right-hand side of Eq. (11.2.8) is called the “second quadratic form” of the surface, and the quantities L , M , and N are the coefficients of the quadratic form.

Equation (11.2.9) can be used to compute the curvatures of the curves obtained by intersecting the surface with normal planes. For the curve generated by a normal plane, $\hat{\mathbf{n}}$ and $\hat{\mathbf{N}}$ have opposite directions ($\varphi = \pi$) because the outward normal (to the right of the curve) is taken positive as we traverse along $d\mathbf{r}$. Thus, Eq. (11.2.9) yields

$$\frac{1}{R} = -\frac{L(d\xi_1)^2 + 2M d\xi_1 d\xi_2 + N(d\xi_2)^2}{a_1^2(d\xi_1)^2 + 2a_1 a_2 \cos \chi d\xi_1 d\xi_2 + a_2^2(d\xi_2)^2} \quad (11.2.10)$$

In particular, the curvatures of the ξ_1 curve ($\xi_2 = \text{constant}$) and ξ_2 curve ($\xi_1 = \text{constant}$) are

$$\frac{1}{R_1} = -\frac{L}{a_1^2}, \quad \frac{1}{R_2} = -\frac{N}{a_2^2} \quad (11.2.11)$$

From this point forward, we assume that ξ_1 and ξ_2 are orthogonal, i.e., curves $\xi_1 = \text{constant}$ and $\xi_2 = \text{constant}$ are lines of principal curvature of the undeformed middle surface; then $\cos \chi = 0$ and $M = 0$. The derivatives of the vectors $\hat{\mathbf{n}}$ and $\hat{\mathbf{e}}_\alpha \equiv \mathbf{g}_\alpha/a_\alpha$ (no sum on α) are given by [see Kraus (1967)]

$$\begin{aligned} \frac{\partial \hat{\mathbf{n}}}{\partial \xi_\alpha} &= \frac{a_\alpha}{R_\alpha} \hat{\mathbf{e}}_\alpha = \frac{\mathbf{g}_\alpha}{R_\alpha} \quad (\alpha = 1, 2) \\ \frac{\partial \hat{\mathbf{e}}_\alpha}{\partial \xi_\beta} &= \frac{1}{a_\alpha} \frac{\partial a_\beta}{\partial \xi_\alpha} \hat{\mathbf{e}}_\beta \quad (\alpha \neq \beta) \\ \frac{\partial \hat{\mathbf{e}}_\alpha}{\partial \xi_\alpha} &= -\frac{1}{a_\beta} \frac{\partial a_\alpha}{\partial \xi_\beta} \hat{\mathbf{e}}_\beta - \frac{a_\alpha}{R_\alpha} \hat{\mathbf{n}} \quad (\alpha \neq \beta) \end{aligned} \quad (11.2.12)$$

In Eq. (11.2.12), no sum on repeated indices is implied. The first equation in (11.2.12) is known as the *Theorem of Rodrigues* and the second and third relations are known as the *Weingarten formulas*.

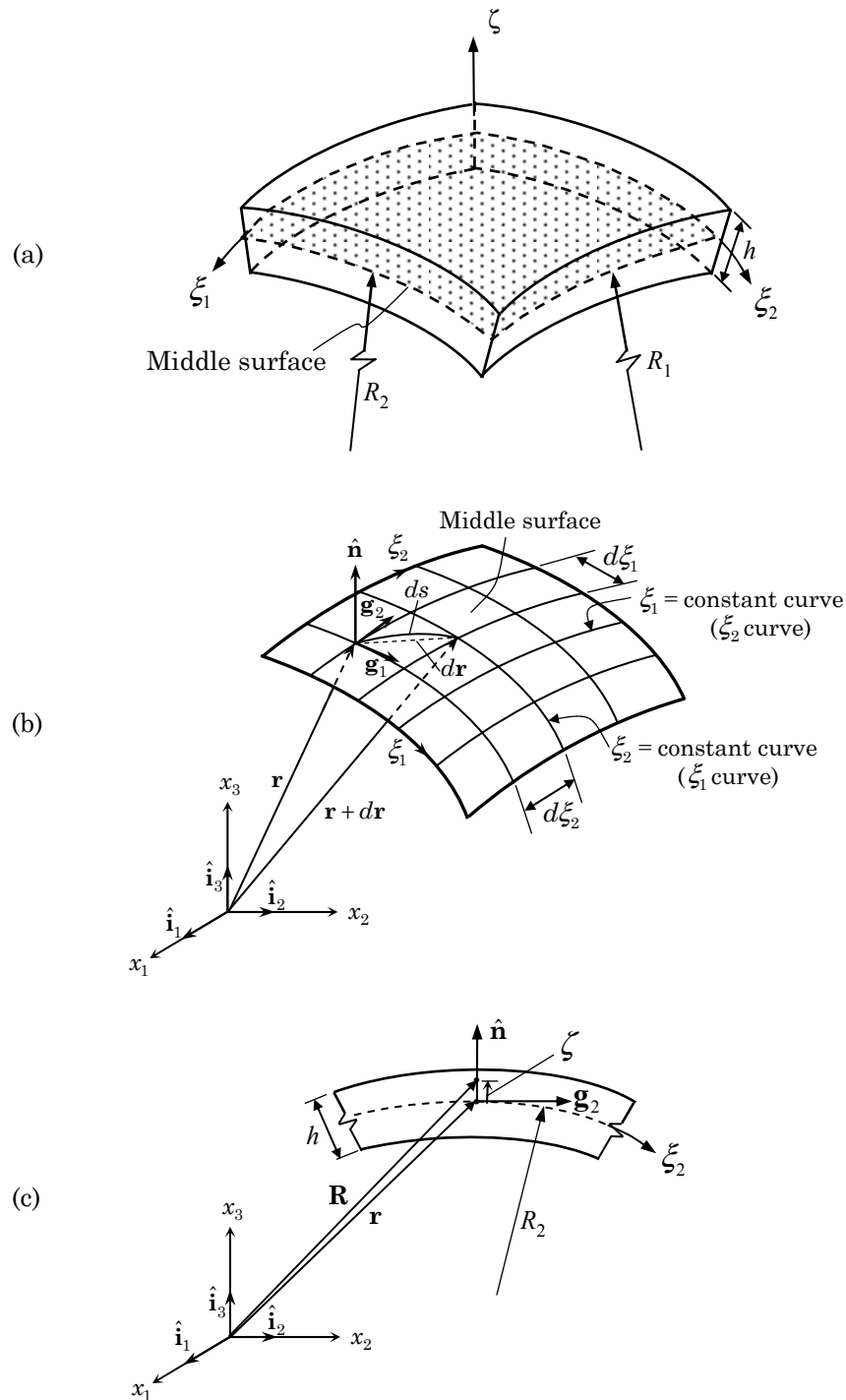


Figure 11.2.1. (a) Shell geometry. (b) Position vector of a point and coordinates on the middle surface. (c) Position vectors of points on the middle surface and above the middle surface.

In addition, we have the identities (see Problem 11.1)

$$\frac{\partial}{\partial \xi_1} \left(\frac{1}{a_1} \frac{\partial a_2}{\partial \xi_1} \right) + \frac{\partial}{\partial \xi_2} \left(\frac{1}{a_2} \frac{\partial a_1}{\partial \xi_2} \right) = -\frac{a_1 a_2}{R_1 R_2} = -\frac{a_1 a_2}{K} \quad (11.2.13)$$

$$\frac{\partial}{\partial \xi_2} \left(\frac{a_1}{R_1} \right) = \frac{1}{R_2} \frac{\partial a_1}{\partial \xi_2}, \quad \frac{\partial}{\partial \xi_1} \left(\frac{a_2}{R_2} \right) = \frac{1}{R_1} \frac{\partial a_2}{\partial \xi_1} \quad (11.2.14)$$

where $1/K = 1/R_1 R_2$ is called, as stated earlier, the Gaussian curvature. Equation (11.2.13) is known as the *Gauss characteristic equation* and the formulas given in Eq. (11.2.14) are called *Mainardi–Codazzi relations*.

The position vector \mathbf{R} of an arbitrary point (ξ_1, ξ_2, ζ) in the shell can be expressed as [Figure 11.2.1(c)]

$$\mathbf{R} = \mathbf{r} + \zeta \hat{\mathbf{n}} \quad (11.2.15)$$

where ζ is the distance of the point measured from the middle surface along $\hat{\mathbf{n}}$. The differential line element on a surface away from the middle surface is

$$d\mathbf{R} = \frac{\partial \mathbf{R}}{\partial \xi_i} d\xi_i = \frac{\partial \mathbf{R}}{\partial \xi_\alpha} d\xi_\alpha + \frac{\partial \mathbf{R}}{\partial \zeta} d\zeta = \mathbf{G}_\alpha d\xi_\alpha + \hat{\mathbf{n}} d\zeta \quad (11.2.16)$$

where

$$\mathbf{G}_\alpha = \frac{\partial \mathbf{R}}{\partial \xi_\alpha} = \frac{\partial \mathbf{r}}{\partial \xi_\alpha} + \zeta \frac{\partial \hat{\mathbf{n}}}{\partial \xi_\alpha} = \left(1 + \frac{\zeta}{R_\alpha} \right) \mathbf{g}_\alpha \quad (\text{no sum on } \alpha) \quad (11.2.17)$$

where the Theorem of Rodrigues [i.e., first equation in (11.2.12)] is used in arriving at the last step. The components of the metric tensor $G_{\alpha\beta}$ are defined by

$$G_{\alpha\beta} = \mathbf{G}_\alpha \cdot \mathbf{G}_\beta, \quad A_1 = \sqrt{G_{11}}, \quad A_2 = \sqrt{G_{22}}, \quad A_3 = 1 \quad (11.2.18)$$

where A_1 , A_2 , and A_3 are known as the *Lamé coefficients*, and they can be expressed in terms of a_α as

$$A_\alpha = a_\alpha \left(1 + \frac{\zeta}{R_\alpha} \right) \quad (\text{no sum on } \alpha) \quad (11.2.19)$$

The square of the distance dS between points (ξ_1, ξ_2, ζ) and $(\xi_1 + d\xi_1, \xi_2 + d\xi_2, \zeta + d\zeta)$ is given by

$$\begin{aligned} (dS)^2 &= d\mathbf{R} \cdot d\mathbf{R} = G_{\alpha\beta} d\xi_\alpha d\xi_\beta + (d\zeta)^2 \\ &= A_1^2 (d\xi_1)^2 + A_2^2 (d\xi_2)^2 + A_3^2 (d\zeta)^2 \end{aligned} \quad (11.2.20)$$

The Gauss characteristic equation (11.2.13) and the Mainardi–Codazzi equations (11.2.14) can be generalized for a surface at a distance ζ from the middle surface. We have

$$\frac{\partial}{\partial \xi_1} \left(\frac{1}{A_1} \frac{\partial A_2}{\partial \xi_1} \right) + \frac{\partial}{\partial \xi_2} \left(\frac{1}{A_2} \frac{\partial A_1}{\partial \xi_2} \right) = -\frac{a_1 a_2}{R_1 R_2} \quad (11.2.21)$$

$$\frac{\partial^2 A_1}{\partial \xi_2 \partial \zeta} = \frac{1}{A_2} \frac{\partial A_1}{\partial \xi_2} \frac{\partial A_2}{\partial \zeta}, \quad \frac{\partial^2 A_2}{\partial \xi_1 \partial \zeta} = \frac{1}{A_1} \frac{\partial A_2}{\partial \xi_1} \frac{\partial A_1}{\partial \zeta} \quad (11.2.22)$$

In view of the Mainardi–Codazzi conditions in Eq. (11.2.14), relations (11.2.22) reduce to

$$\frac{1}{A_2} \frac{\partial A_1}{\partial \xi_2} = \frac{1}{a_2} \frac{\partial a_1}{\partial \xi_2}, \quad \frac{1}{A_1} \frac{\partial A_2}{\partial \xi_1} = \frac{1}{a_1} \frac{\partial a_2}{\partial \xi_1} \quad (11.2.23)$$

Under the assumption that (ξ_1, ξ_2, ζ) is a curvilinear orthogonal system with two principal curvatures, the cross-sectional areas of the edge faces of the shell element shown in Figure 11.2.2 are

$$\begin{aligned} dS_1 d\zeta &= A_1 d\xi_1 d\zeta = a_1 \left(1 + \frac{\zeta}{R_1} \right) d\xi_1 d\zeta \\ dS_2 d\zeta &= A_2 d\xi_2 d\zeta = a_2 \left(1 + \frac{\zeta}{R_2} \right) d\xi_2 d\zeta \end{aligned} \quad (11.2.24)$$

An elemental area of the middle surface ($\zeta = 0$) is determined by [Figure 11.2.3(a)]

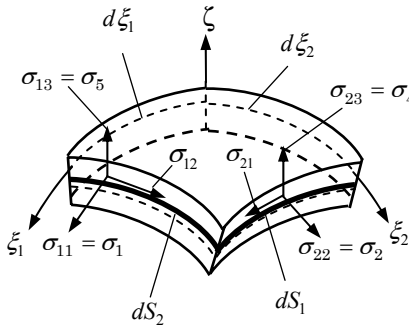
$$dA_0 = d\mathbf{r}_1 \times d\mathbf{r}_2 \cdot \hat{\mathbf{n}} = \left(\frac{\partial \mathbf{r}}{\partial \xi_1} \times \frac{\partial \mathbf{r}}{\partial \xi_2} \cdot \hat{\mathbf{n}} \right) d\xi_1 d\xi_2 = a_1 a_2 d\xi_1 d\xi_2 \quad (11.2.25)$$

and an elemental area of the surface at ζ is given by [Figure 11.2.3(b)]

$$dA_\zeta = d\mathbf{R}_1 \times d\mathbf{R}_2 \cdot \hat{\mathbf{n}} = \left(\frac{\partial \mathbf{R}}{\partial \xi_1} \times \frac{\partial \mathbf{R}}{\partial \xi_2} \cdot \hat{\mathbf{n}} \right) d\xi_1 d\xi_2 = A_1 A_2 d\xi_1 d\xi_2 \quad (11.2.26)$$

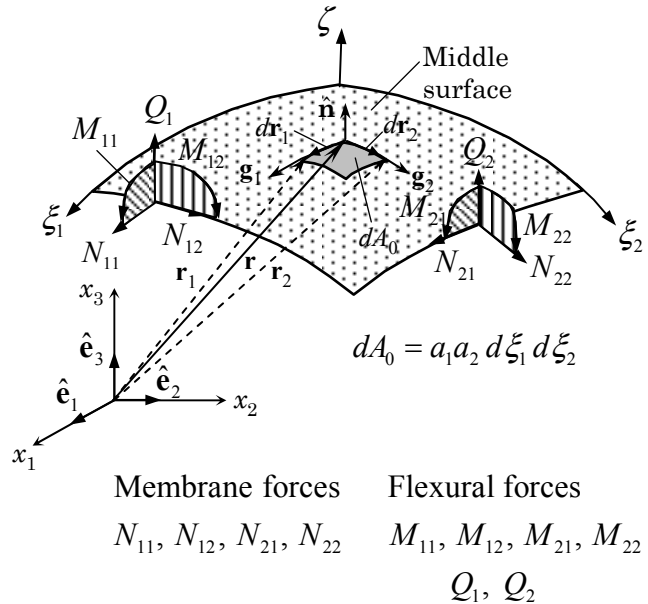
The volume of a differential shell element is given by

$$\begin{aligned} dV &= d\mathbf{R}_1 \times d\mathbf{R}_2 \cdot \hat{\mathbf{n}} d\zeta = dA_\zeta d\zeta = A_1 A_2 d\xi_1 d\xi_2 d\zeta \\ &= \left[a_1 \left(1 + \frac{\zeta}{R_1} \right) \right] \left[a_2 \left(1 + \frac{\zeta}{R_2} \right) \right] d\xi_1 d\xi_2 d\zeta \end{aligned} \quad (11.2.27)$$

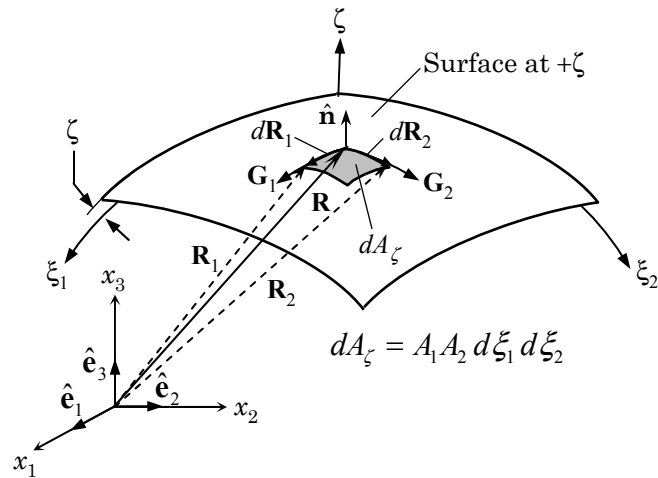


$$dS_1 = a_1 \left(1 + \frac{\zeta}{R_1} \right) d\xi_1 = A_1 d\xi_1, \quad dS_2 = a_2 \left(1 + \frac{\zeta}{R_2} \right) d\xi_2 = A_2 d\xi_2$$

Figure 11.2.2. A differential element of the shell (dS_1 and dS_2 denote the arc lengths).



(a)



(b)

Figure 11.2.3. (a) Area element on the middle surface ($\zeta = 0$). (b) Area element on a surface at $+\zeta$.

11.2.2 General Strain–Displacement Relations

Let \mathbf{u} be the displacement vector, with components $u_i(\xi_1, \xi_2, \zeta)$ ($i = 1, 2, 3$) in an orthogonal curvilinear coordinate system (ξ_1, ξ_2, ζ) . Then the normal (ε_{ij} for $i = j$) and shear ($2\varepsilon_{ij} = \gamma_{ij}$ for $i \neq j$) components of the Green–Lagrange strain tensor are given by [no sum on repeated indices; see Sokolnikoff (1956) and Palazotto and Dennis (1992)]

$$\begin{aligned}\varepsilon_i &= \frac{\partial}{\partial \xi_i} \left(\frac{u_i}{A_i} \right) + \frac{1}{A_i} \sum_{k=1}^3 \frac{u_k}{A_k} \frac{\partial A_i}{\partial \xi_k} + \frac{1}{2} \left[\frac{\partial}{\partial \xi_i} \left(\frac{u_i}{A_i} \right) + \frac{1}{A_i} \sum_{k=1}^3 \frac{u_k}{A_k} \frac{\partial A_i}{\partial \xi_k} \right]^2 \\ &\quad + \frac{1}{2A_i^2} \sum_{k=1, k \neq i}^3 \left(\frac{\partial u_k}{\partial \xi_i} - \frac{u_i}{A_k} \frac{\partial A_i}{\partial \xi_k} \right)^2 \quad (i = 1, 2, 3)\end{aligned}\quad (11.2.28)$$

$$\begin{aligned}\gamma_{ij} &= \frac{A_i}{A_j} \frac{\partial}{\partial \xi_j} \left(\frac{u_i}{A_i} \right) + \frac{A_j}{A_i} \frac{\partial}{\partial \xi_i} \left(\frac{u_j}{A_j} \right) \\ &\quad + \sum_{k \neq i, k \neq j}^3 \frac{1}{A_i A_j} \left(\frac{\partial u_k}{\partial \xi_i} - \frac{u_i}{A_k} \frac{\partial A_i}{\partial \xi_k} \right) \left(\frac{\partial u_k}{\partial \xi_j} - \frac{u_j}{A_k} \frac{\partial A_j}{\partial \xi_k} \right) \\ &\quad + \frac{1}{A_j} \left(\frac{\partial u_i}{\partial \xi_j} - \frac{u_j}{A_i} \frac{\partial A_i}{\partial \xi_j} \right) \left[\frac{\partial}{\partial \xi_i} \left(\frac{u_i}{A_i} \right) + \frac{1}{A_i} \sum_{k=1}^3 \frac{u_k}{A_k} \frac{\partial A_i}{\partial \xi_k} \right] \\ &\quad + \frac{1}{A_i} \left(\frac{\partial u_j}{\partial \xi_i} - \frac{u_i}{A_j} \frac{\partial A_i}{\partial \xi_i} \right) \left[\frac{\partial}{\partial \xi_j} \left(\frac{u_j}{A_j} \right) + \frac{1}{A_j} \sum_{k=1}^3 \frac{u_k}{A_k} \frac{\partial A_j}{\partial \xi_k} \right]\end{aligned}\quad (11.2.29)$$

where $i \neq j$ ($i, j = 1, 2, 3$) in Eq. (11.2.29), and

$$\xi_3 = \zeta, \quad A_1 = a_1 \left(1 + \frac{\zeta}{R_1} \right), \quad A_2 = a_2 \left(1 + \frac{\zeta}{R_2} \right), \quad A_3 = a_3 = 1 \quad (11.2.30)$$

Substituting Eq. (11.2.30) into Eqs. (11.2.28) and (11.2.29) and making use of conditions (11.2.12)–(11.2.14) and (11.2.23), one obtains

$$\begin{aligned}\varepsilon_1 &= \varepsilon_{11} = \frac{1}{A_1} \left(\frac{\partial u_1}{\partial \xi_1} + \frac{u_2}{a_2} \frac{\partial a_1}{\partial \xi_2} + \frac{a_1}{R_1} u_3 \right) + \frac{1}{2A_1^2} \left[\left(\frac{\partial u_1}{\partial \xi_1} + \frac{u_2}{a_2} \frac{\partial a_1}{\partial \xi_2} + \frac{a_1}{R_1} u_3 \right)^2 \right. \\ &\quad \left. + \left(\frac{\partial u_2}{\partial \xi_1} - \frac{u_1}{a_2} \frac{\partial a_1}{\partial \xi_2} \right)^2 + \left(\frac{\partial u_3}{\partial \xi_1} - \frac{a_1}{R_1} u_1 \right)^2 \right] \\ \varepsilon_2 &= \varepsilon_{22} = \frac{1}{A_2} \left(\frac{\partial u_2}{\partial \xi_2} + \frac{u_1}{a_1} \frac{\partial a_2}{\partial \xi_1} + \frac{a_2}{R_2} u_3 \right) + \frac{1}{2A_2^2} \left[\left(\frac{\partial u_2}{\partial \xi_2} + \frac{u_1}{a_1} \frac{\partial a_2}{\partial \xi_1} + \frac{a_2}{R_2} u_3 \right)^2 \right. \\ &\quad \left. + \left(\frac{\partial u_1}{\partial \xi_2} - \frac{u_2}{a_1} \frac{\partial a_2}{\partial \xi_1} \right)^2 + \left(\frac{\partial u_3}{\partial \xi_2} - \frac{a_2}{R_2} u_2 \right)^2 \right] \\ \varepsilon_3 &= \varepsilon_{33} = \frac{\partial u_3}{\partial \zeta} + \frac{1}{2} \left[\left(\frac{\partial u_1}{\partial \zeta} \right)^2 + \left(\frac{\partial u_2}{\partial \zeta} \right)^2 + \left(\frac{\partial u_3}{\partial \zeta} \right)^2 \right] \\ \varepsilon_4 &= 2\varepsilon_{23} = \frac{1}{A_2} \frac{\partial u_3}{\partial \xi_2} + A_2 \frac{\partial}{\partial \zeta} \left(\frac{u_2}{A_2} \right) + \frac{1}{A_2} \left[\frac{\partial u_2}{\partial \zeta} \left(\frac{\partial u_2}{\partial \xi_2} + \frac{u_1}{a_1} \frac{\partial a_2}{\partial \xi_1} + \frac{a_2}{R_2} u_3 \right) \right.\end{aligned}$$

$$\begin{aligned}
& + \frac{\partial u_1}{\partial \zeta} \left(\frac{\partial u_1}{\partial \xi_2} - \frac{u_2}{a_1} \frac{\partial a_2}{\partial \xi_1} \right) + \frac{\partial u_3}{\partial \zeta} \left(\frac{\partial u_3}{\partial \xi_2} - \frac{a_2}{R_2} u_2 \right) \Big] \\
\varepsilon_5 = 2\varepsilon_{13} &= \frac{1}{A_1} \frac{\partial u_3}{\partial \xi_1} + A_1 \frac{\partial}{\partial \zeta} \left(\frac{u_1}{A_1} \right) + \frac{1}{A_1} \left[\frac{\partial u_1}{\partial \zeta} \left(\frac{\partial u_1}{\partial \xi_1} + \frac{u_2}{a_2} \frac{\partial a_1}{\partial \xi_2} + \frac{a_1}{R_1} u_3 \right) \right. \\
&\quad \left. + \frac{\partial u_2}{\partial \zeta} \left(\frac{\partial u_2}{\partial \xi_1} - \frac{u_1}{a_2} \frac{\partial a_1}{\partial \xi_2} \right) + \frac{\partial u_3}{\partial \zeta} \left(\frac{\partial u_3}{\partial \xi_1} - \frac{a_1}{R_1} u_1 \right) \right] \\
\varepsilon_6 = 2\varepsilon_{12} &= \frac{A_2}{A_1} \frac{\partial}{\partial \xi_1} \left(\frac{u_2}{A_2} \right) + \frac{A_1}{A_2} \frac{\partial}{\partial \xi_2} \left(\frac{u_1}{A_1} \right) \\
&\quad + \frac{1}{A_1 A_2} \left[\left(\frac{\partial u_1}{\partial \xi_2} - \frac{u_2}{a_1} \frac{\partial a_2}{\partial \xi_1} \right) \left(\frac{\partial u_1}{\partial \xi_1} + \frac{1}{a_2} \frac{\partial a_1}{\partial \xi_2} u_2 + \frac{a_1}{R_1} u_3 \right) \right. \\
&\quad + \left(\frac{\partial u_2}{\partial \xi_1} - \frac{u_1}{a_2} \frac{\partial a_1}{\partial \xi_2} \right) \left(\frac{\partial u_2}{\partial \xi_2} + \frac{1}{a_1} \frac{\partial a_2}{\partial \xi_1} u_1 + \frac{a_2}{R_2} u_3 \right) \\
&\quad \left. + \left(\frac{\partial u_3}{\partial \xi_1} - \frac{a_1}{R_1} u_1 \right) \left(\frac{\partial u_3}{\partial \xi_2} - \frac{a_2}{R_2} u_2 \right) \right] \tag{11.2.31}
\end{aligned}$$

The linear strain-displacement relations are obtained by setting the terms in the square brackets of Eq. (11.2.31) to zero.

11.2.3 Stress Resultants

Next, we introduce the stress resultants acting on a shell element. The tensile force measured per unit length along a ξ_2 -coordinate line on a cross section perpendicular to a ξ_1 coordinate line [Figure 11.2.1(c)] is $\sigma_{11} dS_2$. The total tensile force on the differential element in the ξ_1 -direction can be computed by integrating over the entire thickness of the shell:

$$\int_{-h/2}^{h/2} \sigma_{11} dS_2 d\zeta = a_2 \left[\int_{-h/2}^{h/2} \sigma_{11} \left(1 + \frac{\zeta}{R_2} \right) d\zeta \right] d\xi_2 \equiv N_{11} a_2 d\xi_2 \tag{11.2.32}$$

where h is the total thickness of the shell, $\zeta = -h/2$ and $\zeta = h/2$ denote the bottom and top surfaces of the shell, and N_{11} is the membrane force per unit length in ξ_1 direction, acting on a surface perpendicular to the ξ_1 -coordinate (Figure 11.2.3):

$$N_{11} = \int_{-h/2}^{h/2} \sigma_{11} \left(1 + \frac{\zeta}{R_2} \right) d\zeta$$

Similarly, the moment of the force $\sigma_{11} dS_2$ about the ξ_2 -axis is

$$\int_{-h/2}^{h/2} \sigma_{11} dS_2 \zeta d\zeta = a_2 \left[\int_{-h/2}^{h/2} \sigma_{11} \left(1 + \frac{\zeta}{R_2} \right) \zeta d\zeta \right] d\xi_2 \equiv M_{11} a_2 d\xi_2 \tag{11.2.33}$$

Thus, the stress resultants per unit length (Figure 11.2.4) can be defined as

$$\begin{aligned}
\begin{Bmatrix} N_{11} \\ N_{12} \\ Q_1 \end{Bmatrix} &= \int_{-h/2}^{h/2} \begin{Bmatrix} \sigma_{11} \\ \sigma_{12} \\ K_s \sigma_{13} \end{Bmatrix} \left(1 + \frac{\zeta}{R_2} \right) d\zeta \\
\begin{Bmatrix} N_{22} \\ N_{21} \\ Q_2 \end{Bmatrix} &= \int_{-h/2}^{h/2} \begin{Bmatrix} \sigma_{22} \\ \sigma_{21} \\ K_s \sigma_{23} \end{Bmatrix} \left(1 + \frac{\zeta}{R_1} \right) d\zeta \tag{11.2.34}
\end{aligned}$$

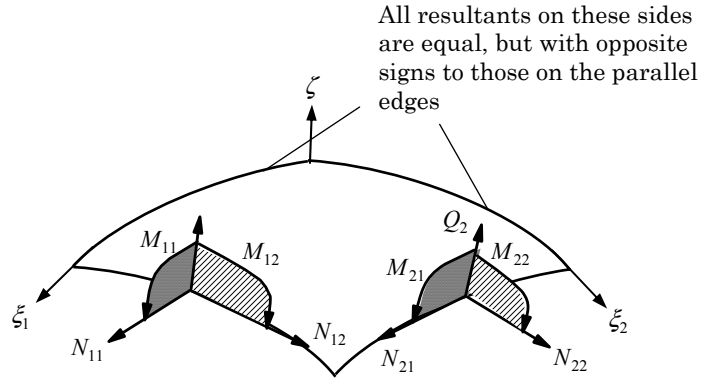


Figure 11.2.4. Stress resultants on a shell element.

$$\begin{aligned}\left\{ \begin{array}{l} M_{11} \\ M_{12} \end{array} \right\} &= \int_{-h/2}^{h/2} \left\{ \begin{array}{l} \sigma_{11} \\ \sigma_{12} \end{array} \right\} \left(1 + \frac{\zeta}{R_2} \right) \zeta d\zeta \\ \left\{ \begin{array}{l} M_{22} \\ M_{21} \end{array} \right\} &= \int_{-h/2}^{h/2} \left\{ \begin{array}{l} \sigma_{22} \\ \sigma_{21} \end{array} \right\} \left(1 + \frac{\zeta}{R_1} \right) \zeta d\zeta\end{aligned}\quad (11.2.35)$$

where K_s is the shear correction factor. Note that, in general, $N_{\alpha\beta} \neq N_{\beta\alpha}$ and $M_{\alpha\beta} \neq M_{\beta\alpha}$ for $\alpha \neq \beta$ ($\alpha, \beta = 1, 2$). However, if we assume that the thickness of the shell is small compared to the smallest radius of curvature of the middle surface, one can neglect ζ/R_1 and ζ/R_2 . Such shells are called *thin shells*, and for thin shells we have $N_{\alpha\beta} = N_{\beta\alpha}$ and $M_{\alpha\beta} = M_{\beta\alpha}$, as in a plate theory.

11.2.4 Displacement Field and Strains

In developing a moderately thick shell theory with the von Kármán type nonlinearity, the following assumptions (as in the case of plates):

1. The transverse normal is inextensible (i.e., $\varepsilon_3 \approx 0$) and the transverse normal stress is small compared with the other normal stress components and may be neglected.
2. Normals to the undeformed middle surface of the shell before deformation remain straight, but not necessarily normal after deformation.
3. The deflections and strains are sufficiently small so that the quantities of second- and higher-order magnitude, except for second-order rotations about the transverse normals, may be neglected in comparison with the first-order terms.
4. The rotations about the ξ_1 and ξ_2 axes are moderate so that we retain second-order terms (i.e., terms that are products and squares of the terms $(\partial u_3 / \partial \xi_\alpha) - (a_\alpha u_\alpha / R_\alpha)$) in the strain-displacement relations (the von Kármán nonlinearity).

The Love's *first approximation theory* further assumes that (1) the thickness of the shell is small compared with the other dimensions, (2) the transverse normals to the undeformed middle surface not only remain straight, but also normal to the deformed middle surface after deformation, and (3) the strains are infinitesimal so that all nonlinear terms are neglected. The first assumption allows us to neglect the higher powers of ζ/R and h/R in the derivation of shell theories. The second assumption (also known as the Kirchhoff hypothesis) results in the neglect of transverse shear strains.

Consistent with the assumptions (1)–(4) of a moderately thick shell theory, we assume the following form of the displacement components u_i :

$$\begin{aligned} u_1(\xi_1, \xi_2, \zeta, t) &= u_1^0(\xi_1, \xi_2, t) + \zeta \varphi_1(\xi_1, \xi_2, t) \\ u_2(\xi_1, \xi_2, \zeta, t) &= u_2^0(\xi_1, \xi_2, t) + \zeta \varphi_2(\xi_1, \xi_2, t) \\ u_3(\xi_1, \xi_2, \zeta, t) &= u_3^0(\xi_1, \xi_2, t) \end{aligned} \quad (11.2.36)$$

where u_i^0 are the displacements of a point $(\xi_1, \xi_2, 0)$ on the middle surface of the shell in the ξ_i -direction, and (φ_1, φ_2) are the rotations of a normal to the reference surface about the ξ_2 and ξ_1 axes, respectively

$$\varphi_1 = \frac{\partial u_1}{\partial \zeta}, \quad \varphi_2 = \frac{\partial u_2}{\partial \zeta} \quad (11.2.37)$$

The five variables $(u_1^0, u_2^0, u_3^0, \varphi_1, \varphi_2)$ completely determine the displacements of an arbitrary point (ξ_1, ξ_2, ζ) in the shell.

In writing the von Kármán strains, we make approximations of the type $\zeta^2 \varphi_\alpha^2 \approx 0$, $\zeta u_\alpha^0 \varphi_\alpha \approx 0$, and $\zeta u_{3,\alpha} \varphi_\alpha \approx 0$ (no sum on α) and

$$\left[\frac{\partial u_3}{\partial \xi_\alpha} - \frac{a_\alpha}{R_\alpha} (u_\alpha^0 + \zeta \varphi_\alpha) \right]^2 \approx \left(\frac{\partial u_3^0}{\partial \xi_\alpha} - \frac{a_\alpha u_\alpha^0}{R_\alpha} \right)^2 \quad (11.2.38)$$

and use the identity

$$A_\alpha \frac{\partial}{\partial \zeta} \left(\frac{u_\alpha}{A_\alpha} \right) = \frac{\partial u_\alpha}{\partial \zeta} + A_\alpha u_\alpha \frac{\partial}{\partial \zeta} \left(\frac{1}{A_\alpha} \right) = \frac{\partial u_\alpha}{\partial \zeta} - \frac{u_\alpha}{A_\alpha} \frac{a_\alpha}{R_\alpha} = \frac{a_\alpha}{A_\alpha} \left(\varphi_\alpha - \frac{u_\alpha^0}{R_\alpha} \right) \quad (11.2.39)$$

For example, $\varepsilon_1 = \varepsilon_{11}$ and $\varepsilon_4 = 2\varepsilon_{23}$ are given by

$$\begin{aligned} \varepsilon_1 &= \frac{1}{A_1} \left(\frac{\partial u_1^0}{\partial \xi_1} + \zeta \frac{\partial \varphi_1}{\partial \xi_1} + \frac{u_2^0 + \zeta \varphi_2}{a_2} \frac{\partial a_1}{\partial \xi_2} + \frac{a_1}{R_1} u_3^0 \right) \\ &\quad + \frac{1}{2A_1^2} \left\{ \left(\frac{\partial u_1^0}{\partial \xi_1} + \zeta \frac{\partial \varphi_1}{\partial \xi_1} + \frac{u_2^0 + \zeta \varphi_2}{a_2} \frac{\partial a_1}{\partial \xi_2} + \frac{a_1}{R_1} u_3^0 \right)^2 \right. \\ &\quad \left. + \left(\frac{\partial u_2^0}{\partial \xi_1} + \zeta \frac{\partial \varphi_2}{\partial \xi_1} - \frac{u_1^0 + \zeta \varphi_1}{a_2} \frac{\partial a_1}{\partial \xi_2} \right)^2 + \left[\frac{\partial u_3^0}{\partial \xi_1} - \frac{a_1}{R_1} (u_1^0 + \zeta \varphi_1) \right]^2 \right\} \\ &\approx \frac{1}{A_1} \left[\frac{\partial u_1^0}{\partial \xi_1} + \frac{u_2^0 \partial a_1}{a_2 \partial \xi_2} + \frac{a_1 u_3^0}{R_1} + \frac{1}{2A_1} \left(\frac{\partial u_3^0}{\partial \xi_1} - \frac{a_1 u_1^0}{R_1} \right)^2 + \zeta \left(\frac{\partial \varphi_1}{\partial \xi_1} + \frac{\varphi_2 \partial a_1}{a_2 \partial \xi_2} \right) \right] \end{aligned}$$

$$\begin{aligned}
\varepsilon_4 &= \frac{1}{A_2} \frac{\partial u_3^0}{\partial \xi_2} + \frac{a_2}{A_2} \left(\varphi_2 - \frac{u_2^0}{R_2} \right) + \frac{1}{A_2} \left[\varphi_1 \left(\frac{\partial u_1^0}{\partial \xi_2} + \zeta \frac{\partial \varphi_1}{\partial \xi_2} - \frac{u_2^0 + \zeta \varphi_2}{a_1} \frac{\partial a_2}{\partial \xi_1} \right) \right. \\
&\quad \left. + \varphi_2 \left(\frac{\partial u_2^0}{\partial \xi_2} + \zeta \frac{\partial \varphi_2}{\partial \xi_2} + \frac{u_1^0 + \zeta \varphi_1}{a_1} \frac{\partial a_2}{\partial \xi_1} + \frac{a_2}{R_2} u_3^0 \right) + \frac{\partial u_3^0}{\partial \zeta} \left(\frac{\partial u_3^0}{\partial \xi_2} - \frac{a_2}{R_2} u_2^0 + \zeta \varphi_2 \right) \right] \\
&\approx \frac{a_2}{A_2} \left(\frac{1}{a_2} \frac{\partial u_3^0}{\partial \xi_2} + \varphi_2 - \frac{u_2^0}{R_2} \right)
\end{aligned}$$

where the second and third terms are neglected on account of the assumption that the strains are small and the last term is replaced using the approximation in Eq. (11.2.26). Thus, the von Kármán nonlinear strain-displacement relations are given by

$$\begin{aligned}
\varepsilon_1 &= \frac{1}{A_1} \left[\frac{\partial u_1^0}{\partial \xi_1} + \frac{u_2^0}{a_2} \frac{\partial a_1}{\partial \xi_2} + \frac{a_1 u_3^0}{R_1} + \frac{1}{2A_1} \left(\frac{\partial u_3^0}{\partial \xi_1} - \frac{a_1 u_1^0}{R_1} \right)^2 + \zeta \left(\frac{\partial \varphi_1}{\partial \xi_1} + \frac{\varphi_2}{a_2} \frac{\partial a_1}{\partial \xi_2} \right) \right] \\
\varepsilon_2 &= \frac{1}{A_2} \left[\frac{\partial u_2^0}{\partial \xi_2} + \frac{u_1^0}{a_1} \frac{\partial a_2}{\partial \xi_1} + \frac{a_2 u_3^0}{R_2} + \frac{1}{2A_2} \left(\frac{\partial u_3^0}{\partial \xi_2} - \frac{a_2 u_2^0}{R_2} \right)^2 + \zeta \left(\frac{\partial \varphi_2}{\partial \xi_2} + \frac{\varphi_1}{a_1} \frac{\partial a_2}{\partial \xi_1} \right) \right] \\
\varepsilon_3 &= 0, \quad \varepsilon_4 = \frac{a_2}{A_2} \left(\frac{1}{a_2} \frac{\partial u_3^0}{\partial \xi_2} + \varphi_2 - \frac{u_2^0}{R_2} \right), \quad \varepsilon_5 = \frac{a_1}{A_1} \left(\frac{1}{a_1} \frac{\partial u_3^0}{\partial \xi_1} + \varphi_1 - \frac{u_1^0}{R_1} \right) \\
\varepsilon_6 &= \frac{A_2}{A_1} \frac{\partial}{\partial \xi_1} \left(\frac{u_2^0}{A_2} \right) + \frac{A_1}{A_2} \frac{\partial}{\partial \xi_2} \left(\frac{u_1^0}{A_1} \right) + \frac{1}{A_1 A_2} \left(\frac{\partial u_3^0}{\partial \xi_1} - \frac{a_1}{R_1} u_1^0 \right) \left(\frac{\partial u_3^0}{\partial \xi_2} - \frac{a_2}{R_2} u_2^0 \right) \\
&\quad + \zeta \left[\frac{A_2}{A_1} \frac{\partial}{\partial \xi_1} \left(\frac{\varphi_2}{A_2} \right) + \frac{A_1}{A_2} \frac{\partial}{\partial \xi_2} \left(\frac{\varphi_1}{A_1} \right) \right]
\end{aligned} \tag{11.2.40}$$

The total strains can be decomposed into membrane strains ε_i^0 and flexural strains ε_i^1 ($i = 1, 2, 4, 5, 6$)

$$\{\varepsilon\} = \{\varepsilon^0\} + \zeta \{\varepsilon^1\} \tag{11.2.41}$$

where

$$\begin{Bmatrix} \varepsilon_1^0 \\ \varepsilon_2^0 \\ \varepsilon_4^0 \\ \varepsilon_5^0 \\ \varepsilon_6^0 \end{Bmatrix} = \begin{Bmatrix} \frac{1}{A_1} \left[\frac{\partial u_1^0}{\partial \xi_1} + \frac{u_2^0}{a_2} \frac{\partial a_1}{\partial \xi_2} + \frac{a_1 u_3^0}{R_1} + \frac{1}{2A_1} \left(\frac{\partial u_3^0}{\partial \xi_1} - \frac{a_1 u_1^0}{R_1} \right)^2 \right] \\ \frac{1}{A_2} \left[\frac{\partial u_2^0}{\partial \xi_2} + \frac{u_1^0}{a_1} \frac{\partial a_2}{\partial \xi_1} + \frac{a_2 u_3^0}{R_2} + \frac{1}{2A_2} \left(\frac{\partial u_3^0}{\partial \xi_2} - \frac{a_2 u_2^0}{R_2} \right)^2 \right] \\ \frac{a_2}{A_2} \left(\frac{1}{a_2} \frac{\partial u_3^0}{\partial \xi_2} - \frac{u_2^0}{R_2} + \varphi_2 \right) \\ \frac{a_1}{A_1} \left(\frac{1}{a_1} \frac{\partial u_3^0}{\partial \xi_1} - \frac{u_1^0}{R_1} + \varphi_1 \right) \\ \frac{1}{A_1} \left[\frac{\partial u_2^0}{\partial \xi_1} - \frac{u_1^0}{a_2} \frac{\partial a_1}{\partial \xi_2} + \frac{1}{2A_2} \left(\frac{\partial u_3^0}{\partial \xi_1} - \frac{a_1 u_1^0}{R_1} \right) \left(\frac{\partial u_3^0}{\partial \xi_2} - \frac{a_2 u_2^0}{R_2} \right) \right] \\ + \frac{1}{A_2} \left[\frac{\partial u_1^0}{\partial \xi_2} - \frac{u_2^0}{a_1} \frac{\partial a_2}{\partial \xi_1} + \frac{1}{2A_1} \left(\frac{\partial u_3^0}{\partial \xi_2} - \frac{a_1 u_2^0}{R_1} \right) \left(\frac{\partial u_3^0}{\partial \xi_1} - \frac{a_2 u_1^0}{R_2} \right) \right] \end{Bmatrix} \tag{11.2.42}$$

$$\begin{Bmatrix} \varepsilon_1^1 \\ \varepsilon_2^1 \\ \varepsilon_4^1 \\ \varepsilon_5^1 \\ \varepsilon_6^1 \end{Bmatrix} = \begin{Bmatrix} \frac{1}{A_1} \left(\frac{\partial \varphi_1}{\partial \xi_1} + \frac{\varphi_2}{a_2} \frac{\partial a_1}{\partial \xi_2} \right) \\ \frac{1}{A_2} \left(\frac{\partial \varphi_2}{\partial \xi_2} + \frac{\varphi_1}{a_1} \frac{\partial a_2}{\partial \xi_1} \right) \\ 0 \\ 0 \\ \frac{1}{A_1} \left(\frac{\partial \varphi_2}{\partial \xi_1} - \frac{\varphi_1}{a_2} \frac{\partial a_1}{\partial \xi_2} \right) + \frac{1}{A_2} \left(\frac{\partial \varphi_1}{\partial \xi_2} - \frac{\varphi_2}{a_1} \frac{\partial a_2}{\partial \xi_1} \right) \end{Bmatrix} \tag{11.2.43}$$

The Love–Kirchhoff assumption of vanishing of transverse shear strains requires

$$\varphi_1 = \frac{u_1^0}{R_1} - \frac{1}{a_1} \frac{\partial u_3^0}{\partial \xi_1}, \quad \varphi_2 = -\frac{u_2^0}{R_2} - \frac{1}{a_2} \frac{\partial u_3^0}{\partial \xi_2} \quad (11.2.44)$$

The strain–displacement relations in Eq. (11.2.420) take different forms in different theories. The *linear* strain–displacement relations of some of the most well-known cases are listed below ([with φ_1 and φ_2 defined by Eq. (11.2.44)]. For additional equations, see Leissa (1973).

Equations of Byrne, Flügge, Goldenveizer, Lur'ye, and Novozhilov: The strains are of the form

$$\varepsilon_{\alpha\beta} = \varepsilon_{\alpha\beta}^0 + \zeta \varepsilon_{\alpha\beta}^1, \quad (\alpha, \beta = 1, 2) \quad (11.2.45)$$

with

$$\begin{aligned} \varepsilon_{11}^0 &= \frac{1}{A_1} \left(\frac{\partial u_1^0}{\partial \xi_1} + \frac{u_2^0}{a_2} \frac{\partial a_1}{\partial \xi_2} + \frac{a_1 u_3^0}{R_1} \right), & \varepsilon_{11}^1 &= \frac{1}{A_1} \left(\frac{\partial \varphi_1}{\partial \xi_1} + \frac{\varphi_2}{a_2} \frac{\partial a_1}{\partial \xi_2} \right) \\ \varepsilon_{22}^0 &= \frac{1}{A_2} \left(\frac{\partial u_2^0}{\partial \xi_2} + \frac{u_1^0}{a_1} \frac{\partial a_2}{\partial \xi_1} + \frac{a_2 u_3^0}{R_2} \right), & \varepsilon_{22}^1 &= \frac{1}{A_2} \left(\frac{\partial \varphi_2}{\partial \xi_2} + \frac{\varphi_1}{a_1} \frac{\partial a_2}{\partial \xi_1} \right) \\ \varepsilon_{12}^0 &= \frac{A_2}{A_1} \frac{\partial}{\partial \xi_1} \left(\frac{u_2^0}{A_2} \right) + \frac{A_1}{A_2} \frac{\partial}{\partial \xi_2} \left(\frac{u_1^0}{A_1} \right), & \varepsilon_{12}^1 &= \frac{A_2}{A_1} \frac{\partial}{\partial \xi_1} \left(\frac{\varphi_2}{A_2} \right) + \frac{A_1}{A_2} \frac{\partial}{\partial \xi_2} \left(\frac{\varphi_1}{A_1} \right) \end{aligned} \quad (11.2.46)$$

Equations of Love and Timoshenko: Neglect ζ/R_α after indicated differentiations in (11.2.46) are carried out and obtain the strains in Eq. (11.2.45) with

$$\begin{aligned} \varepsilon_{11}^0 &= \frac{1}{a_1} \left(\frac{\partial u_1^0}{\partial \xi_1} + \frac{u_2^0}{a_2} \frac{\partial a_1}{\partial \xi_2} + \frac{a_1 u_3^0}{R_1} \right), & \varepsilon_{11}^1 &= \frac{1}{a_1} \left(\frac{\partial \varphi_1}{\partial \xi_1} + \frac{\varphi_2}{a_2} \frac{\partial a_1}{\partial \xi_2} \right) \\ \varepsilon_{22}^0 &= \frac{1}{a_2} \left(\frac{\partial u_2^0}{\partial \xi_2} + \frac{u_1^0}{a_1} \frac{\partial a_2}{\partial \xi_1} + \frac{a_2 u_3^0}{R_2} \right), & \varepsilon_{22}^1 &= \frac{1}{a_2} \left(\frac{\partial \varphi_2}{\partial \xi_2} + \frac{\varphi_1}{a_1} \frac{\partial a_2}{\partial \xi_1} \right) \\ \varepsilon_{12}^0 &= \frac{a_2}{a_1} \frac{\partial}{\partial \xi_1} \left(\frac{u_2^0}{a_2} \right) + \frac{a_1}{a_2} \frac{\partial}{\partial \xi_2} \left(\frac{u_1^0}{a_1} \right) & & \\ \varepsilon_{12}^1 &= \frac{a_2}{a_1} \frac{\partial}{\partial \xi_1} \left(\frac{\varphi_2}{a_2} \right) + \frac{a_1}{a_2} \frac{\partial}{\partial \xi_2} \left(\frac{\varphi_1}{a_1} \right) + \frac{1}{a_2 R_1} \left(\frac{\partial u_1^0}{\partial \xi_2} - \frac{u_2^0}{a_1} \frac{\partial a_2}{\partial \xi_1} \right) \\ &+ \frac{1}{a_1 R_2} \left(\frac{\partial u_2^0}{\partial \xi_1} - \frac{u_1^0}{a_2} \frac{\partial a_1}{\partial \xi_2} \right) & & \end{aligned} \quad (11.2.47)$$

Equations of Reissner and Naghdi: In this case, ζ/R_α is neglected early on in the derivation. We obtain the strains in Eq. (11.2.45) with

$$\begin{aligned} \varepsilon_{11}^0 &= \frac{1}{a_1} \left(\frac{\partial u_1^0}{\partial \xi_1} + \frac{u_2^0}{a_2} \frac{\partial a_1}{\partial \xi_2} + \frac{a_1 u_3^0}{R_1} \right), & \varepsilon_{11}^1 &= \frac{1}{a_1} \left(\frac{\partial \varphi_1}{\partial \xi_1} + \frac{\varphi_2}{a_2} \frac{\partial a_1}{\partial \xi_2} \right) \\ \varepsilon_{22}^0 &= \frac{1}{a_2} \left(\frac{\partial u_2^0}{\partial \xi_2} + \frac{u_1^0}{a_1} \frac{\partial a_2}{\partial \xi_1} + \frac{a_2 u_3^0}{R_2} \right), & \varepsilon_{22}^1 &= \frac{1}{a_2} \left(\frac{\partial \varphi_2}{\partial \xi_2} + \frac{\varphi_1}{a_1} \frac{\partial a_2}{\partial \xi_1} \right) \\ \varepsilon_{12}^0 &= \frac{a_2}{a_1} \frac{\partial}{\partial \xi_1} \left(\frac{u_2^0}{a_2} \right) + \frac{a_1}{a_2} \frac{\partial}{\partial \xi_2} \left(\frac{u_1^0}{a_1} \right), & \varepsilon_{12}^1 &= \frac{a_2}{a_1} \frac{\partial}{\partial \xi_1} \left(\frac{\varphi_2}{a_2} \right) + \frac{a_1}{a_2} \frac{\partial}{\partial \xi_2} \left(\frac{\varphi_1}{a_1} \right) \end{aligned} \quad (11.2.48)$$

11.2.5 Equations of Motion of a General Shell

Here we derive the equations governing generalized Sanders shell theory. The generalization is to include the von Kármán strains. The displacement field in Eq. (11.2.36) and strains in Eq. (11.2.40) are used to derive the governing equations by means of Hamilton's principle

$$\int_0^T \delta L dt \equiv \int_0^T [\delta K - (\delta U + \delta V)] dt = 0 \quad (11.2.49)$$

where δK denotes the virtual kinetic energy, δU the virtual strain energy, and δV the virtual potential energy due to the applied loads. To write the expressions for these virtual energies, let Ω denote the middle surface and Γ its boundary, and circle on the integral implies that it is on the total boundary of the shell. Here we develop the first-order shell theory with the von Kármán nonlinear strains in Eq. (11.2.40).

The virtual energies associated with the displacement field (11.2.36) and strains in (11.2.40) are

$$\begin{aligned} \delta K &= \int_V \rho(\dot{u}_1 \delta \dot{u}_1 + \dot{u}_2 \delta \dot{u}_2 + \dot{u}_3 \delta \dot{u}_3) dV \\ &= \int_{\Omega} \left\{ \int_{-h/2}^{h/2} \rho[(\dot{u}_1^0 + \zeta \dot{\varphi}_1)(\delta \dot{u}_1^0 + \zeta \delta \dot{\varphi}_1) + (\dot{u}_2^0 + \zeta \dot{\varphi}_2)(\delta \dot{u}_2^0 + \zeta \delta \dot{\varphi}_2) \right. \\ &\quad \left. + \dot{u}_3^0 \delta \dot{u}_3^0] A_1 A_2 d\zeta \right\} d\xi_1 d\xi_2 \\ &= \int_{\Omega} [I_0(\dot{u}_1^0 \delta \dot{u}_1^0 + \dot{u}_2^0 \delta \dot{u}_2^0 + \dot{u}_3^0 \delta \dot{u}_3^0) + I_2(\dot{\varphi}_1 \delta \dot{\varphi}_1 + \dot{\varphi}_2 \delta \dot{\varphi}_2) \\ &\quad + I_1(\dot{u}_1^0 \delta \dot{\varphi}_1 + \delta \dot{u}_1^0 \dot{\varphi}_1 + \dot{u}_2^0 \delta \dot{\varphi}_2 + \delta \dot{u}_2^0 \dot{\varphi}_2)] a_1 a_2 d\xi_1 d\xi_2 \end{aligned} \quad (11.2.50)$$

$$\begin{aligned} \delta U &= \int_V \sigma_{ij} \delta \varepsilon_{ij} dV = \int_{\Omega} \left\{ \int_{-h/2}^{h/2} \sigma_{ij} \delta \varepsilon_{ij} A_1 A_2 d\zeta \right\} d\xi_1 d\xi_2 \\ &= \int_{\Omega} \left\{ \int_{-h/2}^{h/2} \left[\sigma_1 (1 + \zeta/R_2) a_2 A_1 (\delta \varepsilon_1^0 + \zeta \delta \varepsilon_1^1) \right. \right. \\ &\quad + \sigma_2 (1 + \zeta/R_1) a_1 A_2 (\delta \varepsilon_2^0 + \zeta \delta \varepsilon_2^1) \\ &\quad + \sigma_6 (1 + \zeta/R_2) a_2 A_1 (\delta \omega_1^0 + \zeta \delta \omega_1^1) \\ &\quad + \sigma_6 (1 + \zeta/R_1) a_1 A_2 (\delta \omega_2^0 + \zeta \delta \omega_2^1) \\ &\quad \left. \left. + \sigma_4 (1 + \zeta/R_1) a_1 A_2 \delta \varepsilon_4^0 + \sigma_5 (1 + \zeta/R_2) a_2 A_1 \delta \varepsilon_5^0 \right] d\zeta \right\} d\xi_1 d\xi_2 \\ &= \int_{\Omega} \left\{ a_2 N_{11} \left(\frac{\partial \delta u_1^0}{\partial \xi_1} + \frac{1}{a_2} \frac{\partial a_1}{\partial \xi_2} \delta u_2^0 + \frac{a_1 \delta u_3^0}{R_1} \right) \right. \\ &\quad + \frac{a_2}{a_1} \hat{N}_{11} \left(\frac{\partial u_3^0}{\partial \xi_1} - \frac{a_1 u_1^0}{R_1} \right) \left(\frac{\partial \delta u_3^0}{\partial \xi_1} - \frac{a_1 \delta u_1^0}{R_1} \right) \\ &\quad \left. + a_1 N_{22} \left(\frac{\partial \delta u_2^0}{\partial \xi_2} + \frac{1}{a_1} \frac{\partial a_2}{\partial \xi_1} \delta u_1^0 + \frac{a_2 \delta u_3^0}{R_2} \right) \right\} \end{aligned}$$

$$\begin{aligned}
& + \frac{a_1}{a_2} \hat{N}_{22} \left(\frac{\partial u_3^0}{\partial \xi_2} - \frac{a_2 u_2^0}{R_2} \right) \left(\frac{\partial \delta u_3^0}{\partial \xi_2} - \frac{a_2 \delta u_2^0}{R_2} \right) \\
& + a_2 M_{11} \left(\frac{\partial \delta \varphi_1}{\partial \xi_1} + \frac{1}{a_2} \frac{\partial a_1}{\partial \xi_2} \delta \varphi_2 \right) + a_1 M_{22} \left(\frac{\partial \delta \varphi_2}{\partial \xi_2} + \frac{1}{a_1} \frac{\partial a_2}{\partial \xi_1} \delta \varphi_1 \right) \\
& + a_2 N_{12} \left(\frac{\partial \delta u_2^0}{\partial \xi_1} - \frac{1}{a_2} \frac{\partial a_1}{\partial \xi_2} \delta u_1^0 \right) + a_1 N_{21} \left(\frac{\partial \delta u_1^0}{\partial \xi_2} - \frac{1}{a_1} \frac{\partial a_2}{\partial \xi_1} \delta u_2^0 \right) \\
& + a_2 M_{12} \left(\frac{\partial \delta \varphi_2}{\partial \xi_1} - \frac{1}{a_2} \frac{\partial a_1}{\partial \xi_2} \delta \varphi_1 \right) + a_1 M_{21} \left(\frac{\partial \delta \varphi_1}{\partial \xi_2} - \frac{1}{a_1} \frac{\partial a_2}{\partial \xi_1} \delta \varphi_2 \right) \\
& + \tilde{N}_{12} \left[\left(\frac{\partial \delta u_3^0}{\partial \xi_1} - \frac{a_1 \delta u_1^0}{R_1} \right) \left(\frac{\partial u_3^0}{\partial \xi_2} - \frac{a_2 u_2^0}{R_2} \right) + \left(\frac{\partial u_3^0}{\partial \xi_1} - \frac{a_1 u_1^0}{R_1} \right) \left(\frac{\partial \delta u_3^0}{\partial \xi_2} - \frac{a_2 \delta u_2^0}{R_2} \right) \right] \\
& + a_1 a_2 \left[Q_2 \left(\frac{1}{a_2} \frac{\partial \delta u_3^0}{\partial \xi_2} - \frac{\delta u_2^0}{R_2} + \delta \varphi_2 \right) + Q_1 \left(\frac{1}{a_1} \frac{\partial \delta u_3^0}{\partial \xi_1} - \frac{\delta u_1^0}{R_1} + \delta \varphi_1 \right) \right] \} d\xi_1 d\xi_2
\end{aligned} \tag{11.2.51}$$

$$\delta V = - \int_{\Omega} \left(f_1 \delta u_1^0 + f_2 \delta u_2^0 + f_3 \delta u_3^0 \right) a_1 a_2 d\xi_1 d\xi_2 \tag{11.2.52}$$

where

$$\begin{aligned}
\omega_1^0 &= \frac{1}{A_1} \left[\frac{\partial u_2^0}{\partial \xi_1} - \frac{u_1^0}{a_2} \frac{\partial a_1}{\partial \xi_2} + \frac{1}{2A_2} \left(\frac{\partial u_3^0}{\partial \xi_1} - \frac{a_1 u_1^0}{R_1} \right) \left(\frac{\partial u_3^0}{\partial \xi_2} - \frac{a_2 u_2^0}{R_2} \right) \right] \\
\omega_2^0 &= \frac{1}{A_2} \left[\frac{\partial u_1^0}{\partial \xi_2} - \frac{u_2^0}{a_1} \frac{\partial a_2}{\partial \xi_1} + \frac{1}{2A_1} \left(\frac{\partial u_3^0}{\partial \xi_1} - \frac{a_1 u_1^0}{R_1} \right) \left(\frac{\partial u_3^0}{\partial \xi_2} - \frac{a_2 u_2^0}{R_2} \right) \right] \\
\omega_1^1 &= \frac{1}{A_1} \left(\frac{\partial \varphi_2}{\partial \xi_1} - \frac{\varphi_1}{a_2} \frac{\partial a_1}{\partial \xi_2} \right), \quad \omega_2^1 = \frac{1}{A_2} \left(\frac{\partial \varphi_1}{\partial \xi_2} - \frac{\varphi_2}{a_1} \frac{\partial a_2}{\partial \xi_1} \right)
\end{aligned} \tag{11.2.53}$$

$$\begin{aligned}
\hat{N}_{11} &= \int_{-h/2}^{h/2} \sigma_1 \left(1 + \frac{\zeta}{R_2} \right) \left(1 + \frac{\zeta}{R_1} \right)^{-1} d\zeta \\
\hat{N}_{22} &= \int_{-h/2}^{h/2} \sigma_2 \left(1 + \frac{\zeta}{R_1} \right) \left(1 + \frac{\zeta}{R_2} \right)^{-1} d\zeta \\
\tilde{N}_{12} &= \tilde{N}_{21} = \int_{-h/2}^{h/2} \sigma_6 d\zeta \\
I_i &= \int_{-h/2}^{h/2} \rho \left(1 + \frac{\zeta}{R_1} \right) \left(1 + \frac{\zeta}{R_2} \right) (\zeta)^i d\zeta
\end{aligned} \tag{11.2.54}$$

and f_i is the i th component of the equivalent middle surface load, $(N_{\alpha\beta}, M_{\alpha\beta}, Q_\alpha)$ are the stress resultants defined in Eqs. (11.2.34) and (11.2.35), ρ is the mass density, and I_i are the mass inertias. It is assumed that there are no applied forces or moments on the shell.

To derive the Euler–Lagrange equations (or equations of motions of the shell) from Eq. (11.2.49), we substitute the expressions for δK , δU and δV , and then integrate the expressions by parts (or use the Green–Gauss theorem) to relieve the varied generalized displacements $(\delta u_1^0, \delta u_2^0, \delta u_3^0, \delta \varphi_1, \delta \varphi_2)$ of any derivatives with respect to ξ_1 , ξ_2 and t :

$$\begin{aligned}
0 = & - \int_0^T \int_{\Omega} [(I_0 \ddot{u}_1^0 + I_1 \ddot{\varphi}_1) \delta u_1^0 + (I_0 \ddot{u}_2^0 + I_1 \ddot{\varphi}_2) \delta u_2^0 + I_0 \ddot{u}_3^0 \delta u_3^0 \\
& + (I_1 \ddot{u}_1^0 + I_2 \ddot{\varphi}_1) \delta \varphi_1 + (I_1 \ddot{u}_2^0 + I_2 \ddot{\varphi}_2) \delta \varphi_2] a_1 a_2 d\xi_1 d\xi_2 dt \\
& + \int_0^T \int_{\Omega} \left\{ \left[\frac{\partial}{\partial \xi_1} (a_2 N_{11}) + \frac{\partial}{\partial \xi_2} (a_1 N_{21}) + N_{12} \frac{\partial a_1}{\partial \xi_2} - N_{22} \frac{\partial a_2}{\partial \xi_1} + \frac{a_1 a_2}{R_1} Q_1 \right. \right. \\
& + \frac{a_2}{R_1} \hat{N}_{11} \left(\frac{\partial u_3^0}{\partial \xi_1} - \frac{a_1 u_1^0}{R_1} \right) + \frac{a_1}{R_1} \hat{N}_{12} \left(\frac{\partial u_3^0}{\partial \xi_2} - \frac{a_2 u_2^0}{R_2} \right) + a_1 a_2 f_1 \Big] \delta u_1^0 \\
& + \left[\frac{\partial}{\partial \xi_2} (a_1 N_{22}) + \frac{\partial}{\partial \xi_1} (a_2 N_{12}) + N_{21} \frac{\partial a_2}{\partial \xi_1} - N_{11} \frac{\partial a_1}{\partial \xi_2} + \frac{a_1 a_2}{R_2} Q_2 \right. \\
& + \frac{a_1}{R_2} \hat{N}_{22} \left(\frac{\partial u_3^0}{\partial \xi_2} - \frac{a_2 u_2^0}{R_2} \right) + \frac{a_2}{R_2} \hat{N}_{12} \left(\frac{\partial u_3^0}{\partial \xi_1} - \frac{a_1 u_1^0}{R_1} \right) + a_1 a_2 f_2 \Big] \delta u_2^0 \\
& + \left\{ - a_1 a_2 \left(\frac{N_{11}}{R_1} + \frac{N_{22}}{R_2} \right) + \frac{\partial}{\partial \xi_1} (a_2 Q_1) + \frac{\partial}{\partial \xi_2} (a_1 Q_2) \right. \\
& + \frac{\partial}{\partial \xi_1} \left[\frac{a_2}{a_1} \hat{N}_{11} \left(u_{3,1}^0 - \frac{a_1 u_1^0}{R_1} \right) \right] + \frac{\partial}{\partial \xi_2} \left[\frac{a_1}{a_2} \hat{N}_{22} \left(u_{3,2}^0 - \frac{a_2 u_2^0}{R_2} \right) \right] \\
& + \left. \frac{\partial}{\partial \xi_2} \left[\tilde{N}_{12} \left(u_{3,1}^0 - \frac{a_1 u_1^0}{R_1} \right) \right] + \frac{\partial}{\partial \xi_1} \left[\tilde{N}_{12} \left(u_{3,2}^0 - \frac{a_2 u_2^0}{R_2} \right) \right] + a_1 a_2 f_3 \right\} \delta u_3^0 \\
& + \left[\frac{\partial}{\partial \xi_1} (a_2 M_{11}) + M_{12} \frac{\partial a_1}{\partial \xi_2} + \frac{\partial}{\partial \xi_2} (a_1 M_{21}) - M_{22} \frac{\partial a_2}{\partial \xi_1} - a_1 a_2 Q_1 \right] \delta \varphi_1 \\
& + \left. \left[\frac{\partial}{\partial \xi_1} (a_2 M_{12}) + \frac{\partial}{\partial \xi_2} (a_1 M_{22}) + M_{21} \frac{\partial a_2}{\partial \xi_1} - M_{11} \frac{\partial a_1}{\partial \xi_2} - a_1 a_2 Q_2 \right] \delta \varphi_2 \right\} d\xi_1 d\xi_2 dt
\end{aligned} \tag{11.2.55}$$

where the virtual generalized displacements are set to zero at $t = 0$ and $t = T$; they are also set to zero on the boundary for any $t > 0$. The equations of motion are obtained by setting the coefficients of the virtual generalized displacements to zero:

$$\begin{aligned} & \frac{1}{a_2 a_1} \left[\frac{\partial}{\partial \xi_1} (a_2 N_{11}) + \frac{\partial}{\partial \xi_2} (a_1 N_{21}) + N_{12} \frac{\partial a_1}{\partial \xi_2} - N_{22} \frac{\partial a_2}{\partial \xi_1} \right] + \frac{Q_1}{R_1} + f_1 \\ & + \frac{\hat{N}_{11}}{a_1 R_1} \left(\frac{\partial u_3^0}{\partial \xi_1} - \frac{a_1 u_1^0}{R_1} \right) + \frac{\tilde{N}_{12}}{a_2 R_1} \left(\frac{\partial u_3^0}{\partial \xi_2} - \frac{a_2 u_2^0}{R_2} \right) = I_0 \frac{\partial^2 u_1^0}{\partial t^2} + I_1 \frac{\partial^2 \varphi_1}{\partial t^2} \quad (11.2.56) \end{aligned}$$

$$\begin{aligned} & \frac{1}{a_1 a_2} \left[\frac{\partial}{\partial \xi_2} (a_1 N_{22}) + \frac{\partial}{\partial \xi_1} (a_2 N_{12}) + N_{21} \frac{\partial a_2}{\partial \xi_1} - N_{11} \frac{\partial a_1}{\partial \xi_2} \right] + \frac{Q_2}{R_2} + f_2 \\ & + \frac{\hat{N}_{22}}{a_2 R_2} \left(\frac{\partial u_3^0}{\partial \xi_2} - \frac{a_2 u_2^0}{R_2} \right) + \frac{\tilde{N}_{12}}{a_1 R_2} \left(\frac{\partial u_3^0}{\partial \xi_1} - \frac{a_1 u_1^0}{R_1} \right) = I_0 \frac{\partial^2 u_2^0}{\partial t^2} + I_1 \frac{\partial^2 \varphi_2}{\partial t^2} \quad (11.2.57) \end{aligned}$$

$$\begin{aligned} & \frac{1}{a_1 a_2} \left\{ \frac{\partial}{\partial \xi_1} \left[\frac{a_2}{a_1} \hat{N}_{11} \left(\frac{\partial u_3^0}{\partial \xi_1} - \frac{a_1 u_1^0}{R_1} \right) + \tilde{N}_{12} \left(\frac{\partial u_3^0}{\partial \xi_2} - \frac{a_2 u_2^0}{R_2} \right) \right] \right. \\ & + \frac{\partial}{\partial \xi_2} \left[\frac{a_1}{a_2} \hat{N}_{22} \left(\frac{\partial u_3^0}{\partial \xi_2} - \frac{a_2 u_2^0}{R_2} \right) + \tilde{N}_{12} \left(\frac{\partial u_3^0}{\partial \xi_1} - \frac{a_1 u_1^0}{R_1} \right) \right] \\ & \left. + \frac{\partial}{\partial \xi_1} (a_2 Q_1) + \frac{\partial}{\partial \xi_2} (a_1 Q_2) \right\} - \left(\frac{N_{11}}{R_1} + \frac{N_{22}}{R_2} \right) + f_3 = I_0 \frac{\partial^2 u_3^0}{\partial t^2} \end{aligned} \quad (11.2.58)$$

$$\begin{aligned} \frac{1}{a_1 a_2} & \left[\frac{\partial}{\partial \xi_1} (a_2 M_{11}) + \frac{\partial}{\partial \xi_2} (a_1 M_{21}) + M_{12} \frac{\partial a_1}{\partial \xi_2} - M_{22} \frac{\partial a_2}{\partial \xi_1} \right] - Q_1 \\ & = I_1 \frac{\partial^2 u_1^0}{\partial t^2} + I_2 \frac{\partial^2 \varphi_1}{\partial t^2} \end{aligned} \quad (11.2.59)$$

$$\begin{aligned} \frac{1}{a_2 a_1} & \left[\frac{\partial}{\partial \xi_1} (a_2 M_{12}) + \frac{\partial}{\partial \xi_2} (a_1 M_{22}) + M_{21} \frac{\partial a_2}{\partial \xi_1} - M_{11} \frac{\partial a_1}{\partial \xi_2} \right] - Q_2 \\ & = I_1 \frac{\partial^2 u_2^0}{\partial t^2} + I_2 \frac{\partial^2 \varphi_2}{\partial t^2} \end{aligned} \quad (11.2.60)$$

The form of the natural boundary conditions is obvious from Eq. (11.2.55). In deriving the equations of motion, we have not assumed that $N_{\alpha\beta} = N_{\beta\alpha}$ and $M_{\alpha\beta} = M_{\beta\alpha}$ for $\alpha \neq \beta$.

The vanishing of the moments about the normal to the differential element (Figure 11.2.2) yields an additional relation among the twisting moments and surface shear forces:

$$\frac{M_{21}}{R_2} - \frac{M_{12}}{R_1} + N_{21} - N_{12} = 0 \quad (11.2.61)$$

which must be accounted for in the formulation; otherwise, it will lead to inconsistency associated with rigid body rotations (i.e., a rigid body rotation gives a nonvanishing torsion except for flat plates and spherical shells). To account for this discrepancy, we must add the term

$$\int_0^T \int_{\Omega} \left(\frac{M_{21}}{R_2} - \frac{M_{12}}{R_1} + N_{21} - N_{12} \right) \delta \varphi_n a_1 a_2 d\xi_1 d\xi_2 dt \quad (11.2.62)$$

to the virtual strain energy functional δU . Here φ_n denotes the rotation about the transverse normal to the shell surface and is equal to the normal component of the curl of the displacement vector \mathbf{u}

$$\begin{aligned} \varphi_n & \equiv (\nabla \times \mathbf{u}) \cdot \hat{\mathbf{n}} = \frac{1}{2A_1 A_2} \left[\frac{\partial}{\partial \xi_1} (u_2^0 a_2) - \frac{\partial}{\partial \xi_2} (u_1^0 a_1) \right] \\ & = \frac{1}{2A_1 A_2} \left(a_2 \frac{\partial u_2^0}{\partial \xi_1} + u_2^0 \frac{\partial a_2}{\partial \xi_1} - a_1 \frac{\partial u_1^0}{\partial \xi_2} - u_1^0 \frac{\partial a_1}{\partial \xi_2} \right) \end{aligned} \quad (11.2.63)$$

The condition in Eq. (11.2.62) amounts to modifying the ω_{α}^0 and ω_{α}^1 in Eq. (11.2.53) as follows:

$$\begin{aligned} \tilde{\omega}_1^0 & = \omega_1^0 - \varphi_n, & \tilde{\omega}_2^0 & = \omega_2^0 + \varphi_n \\ \tilde{\omega}_1^1 & = \omega_1^1 - \frac{\varphi_n}{R_1}, & \tilde{\omega}_2^1 & = \omega_2^1 + \frac{\varphi_n}{R_2} \end{aligned} \quad (11.2.64)$$

Since $\tilde{\omega}_1^0 + \tilde{\omega}_2^0 = \omega_1^0 + \omega_2^0$, there is no change as far as N_{12} and N_{21} terms are concerned in Eqs. (11.2.56) and (11.2.57). Substituting for φ_n from Eq. (11.2.63) into Eq. (11.2.64), we obtain the following expressions for $\tilde{\omega}_1^1$ and $\tilde{\omega}_2^1$:

$$\begin{aligned}\tilde{\omega}_1^1 &= \frac{1}{A_1} \left(\frac{\partial \varphi_2}{\partial \xi_1} - \frac{\varphi_1}{a_2} \frac{\partial a_1}{\partial \xi_2} \right) + \frac{1}{2R_1 A_1 A_2} \left[a_1 \left(\frac{\partial u_1^0}{\partial \xi_2} - \frac{u_2^0}{a_1} \frac{\partial a_2}{\partial \xi_1} \right) - a_2 \left(\frac{\partial u_2^0}{\partial \xi_1} - \frac{u_1^0}{a_2} \frac{\partial a_1}{\partial \xi_2} \right) \right] \\ \tilde{\omega}_2^1 &= \frac{1}{A_2} \left(\frac{\partial \varphi_1}{\partial \xi_2} - \frac{\varphi_2}{a_1} \frac{\partial a_2}{\partial \xi_1} \right) - \frac{1}{2R_2 A_1 A_2} \left[a_1 \left(\frac{\partial u_1^0}{\partial \xi_2} - \frac{u_2^0}{a_1} \frac{\partial a_2}{\partial \xi_1} \right) - a_2 \left(\frac{\partial u_2^0}{\partial \xi_1} - \frac{u_1^0}{a_2} \frac{\partial a_1}{\partial \xi_2} \right) \right]\end{aligned}\quad (11.2.65)$$

Use of the modified $\tilde{\omega}_1^1$ and $\tilde{\omega}_2^1$ from (11.2.65) in place of ω_1^1 and ω_2^1 in (11.2.51) yields the following equations of motion (note that only the first two equations are affected):

$$\begin{aligned}&\frac{1}{a_2 a_1} \left\{ \frac{\partial}{\partial \xi_1} (a_2 N_{11}) + \frac{\partial}{\partial \xi_2} (a_1 N_{21}) + N_{12} \frac{\partial a_1}{\partial \xi_2} - N_{22} \frac{\partial a_2}{\partial \xi_1} + C_0 a_1 \frac{\partial \tilde{M}_{12}}{\partial \xi_2} \right\} \\ &+ \frac{\hat{N}_{11}}{a_1 R_1} \left(\frac{\partial u_3^0}{\partial \xi_1} - \frac{a_1 u_1^0}{R_1} \right) + \frac{\tilde{N}_{12}}{a_2 R_1} \left(\frac{\partial u_3^0}{\partial \xi_2} - \frac{a_2 u_2^0}{R_2} \right) \\ &+ \frac{Q_1}{R_1} + f_1 = I_0 \frac{\partial^2 u_1^0}{\partial t^2} + I_1 \frac{\partial^2 \varphi_1}{\partial t^2}\end{aligned}\quad (11.2.66)$$

$$\begin{aligned}&\frac{1}{a_1 a_2} \left\{ \frac{\partial}{\partial \xi_2} (a_1 N_{22}) + \frac{\partial}{\partial \xi_1} (a_2 N_{12}) + N_{21} \frac{\partial a_2}{\partial \xi_1} - N_{11} \frac{\partial a_1}{\partial \xi_2} - C_0 a_2 \frac{\partial \tilde{M}_{12}}{\partial \xi_1} \right\} \\ &+ \frac{\tilde{N}_{22}}{a_2 R_2} \left(\frac{\partial u_3^0}{\partial \xi_2} - \frac{a_2 u_2^0}{R_2} \right) + \frac{\tilde{N}_{12}}{a_1 R_2} \left(\frac{\partial u_3^0}{\partial \xi_1} - \frac{a_1 u_1^0}{R_1} \right) \\ &+ \frac{Q_2}{R_2} + f_2 = I_0 \frac{\partial^2 u_2^0}{\partial t^2} + I_1 \frac{\partial^2 \varphi_2}{\partial t^2}\end{aligned}\quad (11.2.67)$$

$$\begin{aligned}&\frac{1}{a_1 a_2} \left\{ \frac{\partial}{\partial \xi_1} \left[\frac{a_2}{a_1} \hat{N}_{11} \left(\frac{\partial u_3^0}{\partial \xi_1} - \frac{a_1 u_1^0}{R_1} \right) + \tilde{N}_{12} \left(\frac{\partial u_3^0}{\partial \xi_2} - \frac{a_2 u_2^0}{R_2} \right) \right] \right. \\ &+ \frac{\partial}{\partial \xi_2} \left[\frac{a_1}{a_2} \hat{N}_{22} \left(\frac{\partial u_3^0}{\partial \xi_2} - \frac{a_2 u_2^0}{R_2} \right) + \tilde{N}_{12} \left(\frac{\partial u_3^0}{\partial \xi_1} - \frac{a_1 u_1^0}{R_1} \right) \right] \\ &\left. + \frac{\partial}{\partial \xi_1} (a_2 Q_1) + \frac{\partial}{\partial \xi_2} (a_1 Q_2) \right\} - \left(\frac{N_{11}}{R_1} + \frac{N_{22}}{R_2} \right) + f_3 = I_0 \frac{\partial^2 u_3^0}{\partial t^2}\end{aligned}\quad (11.2.68)$$

$$\begin{aligned}&\frac{1}{a_1 a_2} \left[\frac{\partial}{\partial \xi_1} (a_2 M_{11}) + \frac{\partial}{\partial \xi_2} (a_1 M_{21}) - M_{22} \frac{\partial a_2}{\partial \xi_1} + M_{12} \frac{\partial a_1}{\partial \xi_2} \right] - Q_1 \\ &= I_1 \frac{\partial^2 u_1^0}{\partial t^2} + I_2 \frac{\partial^2 \varphi_1}{\partial t^2}\end{aligned}\quad (11.2.69)$$

$$\begin{aligned}&\frac{1}{a_2 a_1} \left[\frac{\partial}{\partial \xi_1} (a_2 M_{12}) + \frac{\partial}{\partial \xi_2} (a_1 M_{22}) + M_{21} \frac{\partial a_2}{\partial \xi_1} - M_{11} \frac{\partial a_1}{\partial \xi_2} \right] - Q_2 \\ &= I_1 \frac{\partial^2 u_2^0}{\partial t^2} + I_2 \frac{\partial^2 \varphi_2}{\partial t^2}\end{aligned}\quad (11.2.70)$$

where

$$\tilde{M}_{12} = \tilde{M}_{21} = \int_{-h/2}^{h/2} \zeta \sigma_6 d\zeta, \quad C_0 = \frac{1}{2} \left(\frac{1}{R_1} - \frac{1}{R_2} \right)\quad (11.2.71)$$

and other quantities are defined in Eq. (11.2.54).

We note, even for isotropic shells, the surface (or membrane) equations of motion, Eqs. (11.2.66) and (11.2.67), are coupled to the bending (flexural) equations of motion, Eqs. (11.2.68)–(11.2.70), due to the presence of the bending stress resultants Q_1 , Q_2 , and $C_0 \tilde{M}_{21}$ in Eqs. (11.2.66) and (11.2.67), and membrane stress resultants N_{11} , N_{22} , \tilde{N}_{11} , \tilde{N}_{22} and \tilde{N}_{12} in Eq. (11.2.68). This coupling, which is not zero for shells, is responsible for the extraordinary capacity of an egg, despite its thinness, to withstand normal forces. Thus, a shell is a more efficient structure than a straight beam or a flat plate. It is the reason why most structures in nature are shell structures (e.g., egg, skull, and sea shells).

11.2.6 Equations of Motion of Thin Shells

In this book, we are primarily concerned with shells for which $h/R_\alpha \ll 1$. This approximation may be invoked at various stages during the derivation of a shell theory. In Love's first-approximation shell theory (1888) and in the theories developed by Timoshenko and Woinowsky-Krieger (1970), Naghdi and Berry (1964), and Sanders (1959), the approximation is made in the definition of stress resultants and strains. If we omit the term z/R_α in the definition of the stress resultants

$$\left(1 + \frac{\zeta}{R_\alpha}\right) \approx 1, \quad A_\alpha = a_\alpha \quad (11.2.72)$$

then we have

$$\begin{aligned} N_{12} &= N_{21} = \tilde{N}_{12} = \int_{-h/2}^{h/2} \sigma_6 \, d\zeta, \quad N_{11} = \tilde{N}_{11} = \int_{-h/2}^{h/2} \sigma_1 \, d\zeta \\ N_{22} &= \tilde{N}_{22} = \int_{-h/2}^{h/2} \sigma_2 \, d\zeta, \quad M_{12} = M_{21} = \tilde{M}_{12} = \int_{-h/2}^{h/2} \zeta \sigma_6 \, d\zeta \\ M_{11} &= \int_{-h/2}^{h/2} \zeta \sigma_1 \, d\zeta, \quad M_{22} = \int_{-h/2}^{h/2} \zeta \sigma_2 \, d\zeta \end{aligned} \quad (11.2.73)$$

Then Eqs. (11.2.66)–(11.2.70) simplify to

$$\begin{aligned} \frac{\partial N_{11}}{\partial x_1} + \frac{\partial N_{12}}{\partial x_2} + C_0 \frac{\partial M_{12}}{\partial x_2} + \frac{Q_1}{R_1} + f_1 + \frac{2}{a_1} N_{12} \frac{\partial a_1}{\partial x_2} + \frac{1}{a_2} \frac{\partial a_2}{\partial x_1} (N_{11} - N_{22}) \\ + \frac{N_{11}}{R_1} \left(\frac{\partial u_3^0}{\partial x_1} - \frac{u_1^0}{R_1} \right) + \frac{N_{12}}{R_1} \left(\frac{\partial u_3^0}{\partial x_2} - \frac{u_2^0}{R_2} \right) = I_0 \frac{\partial^2 u_1^0}{\partial t^2} + I_1 \frac{\partial^2 \varphi_1}{\partial t^2} \end{aligned} \quad (11.2.74)$$

$$\begin{aligned} \frac{\partial N_{12}}{\partial x_1} + \frac{\partial N_{22}}{\partial x_2} - C_0 \frac{\partial M_{12}}{\partial x_1} + \frac{Q_2}{R_2} + f_2 + \frac{2}{a_2} N_{12} \frac{\partial a_2}{\partial x_1} - \frac{1}{a_1} \frac{\partial a_1}{\partial x_1} (N_{11} - N_{22}) \\ + \frac{N_{12}}{R_2} \left(\frac{\partial u_3^0}{\partial x_1} - \frac{u_1^0}{R_1} \right) + \frac{N_{22}}{R_2} \left(\frac{\partial u_3^0}{\partial x_2} - \frac{u_2^0}{R_2} \right) = I_0 \frac{\partial^2 u_2^0}{\partial t^2} + I_1 \frac{\partial^2 \varphi_2}{\partial t^2} \end{aligned} \quad (11.2.75)$$

$$\begin{aligned} \frac{\partial Q_1}{\partial x_1} + \frac{\partial Q_2}{\partial x_2} - \left(\frac{N_{11}}{R_1} + \frac{N_{22}}{R_2} \right) + f_3 + \frac{Q_1}{a_2} \frac{\partial a_2}{\partial x_1} + \frac{Q_2}{a_1} \frac{\partial a_1}{\partial x_2} \\ + \frac{1}{a_2} \frac{\partial}{\partial x_1} \left[a_2 N_{11} \left(\frac{\partial u_3^0}{\partial x_1} - \frac{u_1^0}{R_1} \right) + a_2 N_{12} \left(\frac{\partial u_3^0}{\partial x_2} - \frac{u_2^0}{R_2} \right) \right] \end{aligned}$$

$$+ \frac{1}{a_1} \frac{\partial}{\partial x_2} \left[a_1 N_{22} \left(\frac{\partial u_3^0}{\partial x_2} - \frac{u_2^0}{R_2} \right) + a_1 N_{12} \left(\frac{\partial u_3^0}{\partial x_1} - \frac{u_1^0}{R_1} \right) \right] = I_0 \frac{\partial^2 u_3^0}{\partial t^2} \quad (11.2.76)$$

$$\begin{aligned} \frac{\partial M_{11}}{\partial x_1} + \frac{\partial M_{12}}{\partial x_2} + \frac{1}{a_2} \frac{\partial a_2}{\partial x_1} (M_{11} - M_{22}) + \frac{1}{a_1} \frac{\partial a_1}{\partial x_2} M_{12} - Q_1 \\ = I_1 \frac{\partial^2 u_1^0}{\partial t^2} + I_2 \frac{\partial^2 \varphi_1}{\partial t^2} \end{aligned} \quad (11.2.77)$$

$$\begin{aligned} \frac{\partial M_{12}}{\partial x_1} + \frac{\partial M_{22}}{\partial x_2} - \frac{1}{a_1} \frac{\partial a_1}{\partial x_2} (M_{11} - M_{22}) + \frac{1}{a_2} \frac{\partial a_2}{\partial x_1} M_{12} - Q_2 \\ = I_1 \frac{\partial^2 u_2^0}{\partial t^2} + I_2 \frac{\partial^2 \varphi_2}{\partial t^2} \end{aligned} \quad (11.2.78)$$

where we have used the notation $dx_1 = a_1 d\xi_1$ and $dx_2 = a_2 d\xi_2$.

11.2.7 Constitutive Equations of a General Shell

Suppose that the shell is made of orthotropic material. The stress-strain relations are [see Eqs. (3.6.1)–(3.6.5)]

$$\begin{Bmatrix} \sigma_1 \\ \sigma_2 \\ \sigma_4 \\ \sigma_5 \\ \sigma_6 \end{Bmatrix} = \begin{bmatrix} Q_{11} & Q_{12} & 0 & 0 & 0 \\ Q_{12} & Q_{22} & 0 & 0 & 0 \\ 0 & 0 & Q_{44} & 0 & 0 \\ 0 & 0 & 0 & Q_{55} & 0 \\ 0 & 0 & 0 & 0 & Q_{66} \end{bmatrix} \begin{Bmatrix} \varepsilon_1^0 + \zeta \varepsilon_1^1 \\ \varepsilon_2^0 + \zeta \varepsilon_2^1 \\ \varepsilon_4^0 \\ \varepsilon_5^0 \\ \varepsilon_6^0 + \zeta \varepsilon_6^1 \end{Bmatrix} \quad (11.2.79)$$

where Q_{ij} are the material stiffness coefficients

$$\begin{aligned} Q_{11} = \frac{E_1}{1 - \nu_{12}\nu_{21}}, \quad Q_{12} = \frac{\nu_{12}E_2}{1 - \nu_{12}\nu_{21}}, \quad Q_{22} = \frac{E_2}{1 - \nu_{12}\nu_{21}} \\ Q_{66} = G_{12}, \quad Q_{44} = G_{23}, \quad Q_{55} = G_{13} \end{aligned} \quad (11.2.80)$$

The strains ε_i^0 and ε_i^1 , which are still functions of (ξ_1, ξ_2, ζ) , can be expressed as

$$\begin{Bmatrix} \varepsilon_1^0 + \zeta \varepsilon_1^1 \\ \varepsilon_2^0 + \zeta \varepsilon_2^1 \\ \varepsilon_4^0 \\ \varepsilon_5^0 \\ \varepsilon_6^0 + \zeta \varepsilon_6^1 \end{Bmatrix} = \begin{Bmatrix} (1 + \zeta/R_1)^{-1} [\varepsilon_1^{0L} + (1 + \zeta/R_1)^{-1} \varepsilon_1^{0N} + \zeta \hat{\varepsilon}_1^1] \\ (1 + \zeta/R_2)^{-1} [\varepsilon_2^{0L} + (1 + \zeta/R_2)^{-1} \varepsilon_2^{0N} + \zeta \hat{\varepsilon}_2^1] \\ (1 + \zeta/R_2)^{-1} \hat{\varepsilon}_4^0 \\ (1 + \zeta/R_1)^{-1} \hat{\varepsilon}_5^0 \\ (1 + \zeta/R_1)^{-1} [\omega_1^{0L} + (1 + \zeta/R_2)^{-1} \omega_1^{0N} + \zeta \hat{\omega}_2^1] \\ + (1 + \zeta/R_2)^{-1} [\omega_2^{0L} + (1 + \zeta/R_1)^{-1} \omega_2^{0N} + \zeta \hat{\omega}_2^1] \end{Bmatrix} \quad (11.2.81)$$

where

$$\begin{aligned} \begin{Bmatrix} \varepsilon_1^{0L} \\ \varepsilon_2^{0L} \\ \varepsilon_4^{0L} \\ \varepsilon_5^{0L} \\ \omega_1^0 \\ \omega_2^0 \end{Bmatrix} &= \left\{ \begin{array}{l} \frac{1}{a_1} \left(\frac{\partial u_1^0}{\partial \xi_1} + \frac{u_2^0}{a_2} \frac{\partial a_1}{\partial \xi_2} + \frac{a_1 u_3^0}{R_1} \right) \\ \frac{1}{a_2} \left(\frac{\partial u_2^0}{\partial \xi_2} + \frac{u_1^0}{a_1} \frac{\partial a_2}{\partial \xi_1} + \frac{a_2 u_3^0}{R_2} \right) \\ \frac{1}{a_2} \frac{\partial u_3^0}{\partial \xi_2} - \frac{u_2^0}{R_2} + \varphi_2 \\ \frac{1}{a_1} \frac{\partial u_3^0}{\partial \xi_1} - \frac{u_1^0}{R_1} + \varphi_1 \\ \frac{1}{a_1} \left(\frac{\partial u_2^0}{\partial \xi_1} - \frac{u_1^0}{a_2} \frac{\partial a_1}{\partial \xi_2} \right) \\ \frac{1}{a_2} \left(\frac{\partial u_1^0}{\partial \xi_2} - \frac{u_2^0}{a_1} \frac{\partial a_2}{\partial \xi_1} \right) \end{array} \right\} \\ \begin{Bmatrix} \hat{\varepsilon}_1^1 \\ \hat{\varepsilon}_2^1 \\ \hat{\omega}_1^1 \\ \hat{\omega}_2^1 \end{Bmatrix} &= \left\{ \begin{array}{l} \frac{1}{a_1} \left(\frac{\partial \varphi_1}{\partial \xi_1} + \frac{\varphi_2}{a_2} \frac{\partial a_1}{\partial \xi_2} \right) \\ \frac{1}{a_2} \left(\frac{\partial \varphi_2}{\partial \xi_2} + \frac{\varphi_1}{a_1} \frac{\partial a_2}{\partial \xi_1} \right) \\ \frac{1}{a_1} \left(\frac{\partial \varphi_2}{\partial \xi_1} - \frac{\varphi_1}{a_2} \frac{\partial a_1}{\partial \xi_2} \right) \\ \frac{1}{a_2} \left(\frac{\partial \varphi_1}{\partial \xi_2} - \frac{\varphi_2}{a_1} \frac{\partial a_2}{\partial \xi_1} \right) \end{array} \right\} \\ \begin{Bmatrix} \varepsilon_1^{0N} \\ \varepsilon_2^{0N} \\ \omega_1^{0N} \\ \omega_2^{0N} \end{Bmatrix} &= \left\{ \begin{array}{l} \frac{1}{2a_1^2} \left(\frac{\partial u_3^0}{\partial \xi_1} - \frac{a_1 u_1^0}{R_1} \right)^2 \\ \frac{1}{2a_2^2} \left(\frac{\partial u_3^0}{\partial \xi_2} - \frac{a_2 u_2^0}{R_2} \right)^2 \\ \frac{1}{2a_1 a_2} \left(\frac{\partial u_3^0}{\partial \xi_1} - \frac{a_1 u_1^0}{R_1} \right) \left(\frac{\partial u_3^0}{\partial \xi_2} - \frac{a_2 u_2^0}{R_2} \right) \\ \frac{1}{2a_1 a_2} \left(\frac{\partial u_3^0}{\partial \xi_1} - \frac{a_1 u_1^0}{R_1} \right) \left(\frac{\partial u_3^0}{\partial \xi_2} - \frac{a_2 u_2^0}{R_2} \right) \end{array} \right\} \end{aligned} \quad (11.2.82)$$

When the shell is made of orthotropic layers with material principal axes (\bar{x}_1, \bar{x}_2) oriented at an arbitrary angle to the shell axes (x_1, x_2) , the material stiffnesses Q_{ij} need to be transformed from \bar{x}_1, \bar{x}_2 to (x_1, x_2) with $\bar{x}_3 = \zeta$ [see Section 1.4 and Reddy (2004b)]. Thus, for laminated shells Q_{ij} must be replaced by \bar{Q}_{ij} of Eq. (1.4.6).

The stress resultants defined in Eqs. (11.2.34), (11.2.35), (11.2.54), and (11.2.71) can be expressed in terms of the membrane and bending strains. For example, we have

$$\begin{aligned} N_{11} &= \int_{-\frac{h}{2}}^{\frac{h}{2}} \left(1 + \frac{\zeta}{R_2} \right) \sigma_{11} d\zeta \\ &= \int_{-\frac{h}{2}}^{\frac{h}{2}} \left(1 + \frac{\zeta}{R_2} \right) \left\{ Q_{11} \left(1 + \frac{\zeta}{R_1} \right)^{-1} \left[\varepsilon_1^{0L} + \left(1 + \frac{\zeta}{R_1} \right)^{-1} \varepsilon_1^{0N} + \zeta \hat{\varepsilon}_1^1 \right] + \right. \\ &\quad \left. Q_{12} \left(1 + \frac{\zeta}{R_2} \right)^{-1} \left[\varepsilon_2^{0L} + \left(1 + \frac{\zeta}{R_2} \right)^{-1} \varepsilon_2^{0N} + \zeta \hat{\varepsilon}_2^1 \right] \right\} d\zeta \\ &= A_{11}^{21} \varepsilon_1^{0L} + A_{11}^{211} \varepsilon_1^{0N} + B_{11}^{21} \hat{\varepsilon}_1^1 + A_{12}^{22} \varepsilon_2^{0L} + A_{12}^{222} \varepsilon_2^{0N} + B_{12}^{22} \hat{\varepsilon}_2^1 \end{aligned} \quad (11.2.83)$$

and

$$\begin{aligned}
M_{11} &= \int_{-\frac{h}{2}}^{\frac{h}{2}} \left(1 + \frac{\zeta}{R_2}\right) \sigma_{11} \zeta \, d\zeta \\
&= \int_{-\frac{h}{2}}^{\frac{h}{2}} \left(1 + \frac{\zeta}{R_2}\right) \zeta \left\{ Q_{11} \left(1 + \frac{\zeta}{R_1}\right)^{-1} \left[\varepsilon_1^{0L} + \left(1 + \frac{\zeta}{R_1}\right)^{-1} \varepsilon_1^{0N} + \zeta \hat{\varepsilon}_1^1 \right] + \right. \\
&\quad \left. Q_{12} \left(1 + \frac{\zeta}{R_2}\right)^{-1} \left[\varepsilon_2^{0L} + \left(1 + \frac{\zeta}{R_2}\right)^{-1} \varepsilon_2^{0N} + \zeta \hat{\varepsilon}_2^1 \right] \right\} d\zeta \\
&= B_{11}^{21} \varepsilon_1^{0L} + B_{11}^{211} \varepsilon_1^{0N} + D_{11}^{21} \hat{\varepsilon}_1^1 + B_{12}^{22} \varepsilon_2^{0L} + B_{12}^{222} \varepsilon_2^{0N} + D_{12}^{22} \hat{\varepsilon}_2^1 \quad (11.2.84)
\end{aligned}$$

where the shell stiffnesses are defined by

$$\begin{aligned}
A_{ij}^{\alpha\beta} &= \int_{-\frac{h}{2}}^{\frac{h}{2}} Q_{ij} \left(1 + \frac{\zeta}{R_\alpha}\right) \left(1 + \frac{\zeta}{R_\beta}\right)^{-1} d\zeta \\
B_{ij}^{\alpha\beta} &= \int_{-\frac{h}{2}}^{\frac{h}{2}} Q_{ij} \left(1 + \frac{\zeta}{R_\alpha}\right) \left(1 + \frac{\zeta}{R_\beta}\right)^{-1} \zeta d\zeta \\
D_{ij}^{\alpha\beta} &= \int_{-\frac{h}{2}}^{\frac{h}{2}} Q_{ij} \left(1 + \frac{\zeta}{R_\alpha}\right) \left(1 + \frac{\zeta}{R_\beta}\right)^{-1} \zeta^2 d\zeta \\
A_{ij}^{\alpha\beta\gamma} &= \int_{-\frac{h}{2}}^{\frac{h}{2}} Q_{ij} \left(1 + \frac{\zeta}{R_\alpha}\right) \left(1 + \frac{\zeta}{R_\beta}\right)^{-1} \left(1 + \frac{\zeta}{R_\gamma}\right)^{-1} d\zeta \\
B_{ij}^{\alpha\beta\gamma} &= \int_{-\frac{h}{2}}^{\frac{h}{2}} Q_{ij} \left(1 + \frac{\zeta}{R_\alpha}\right) \left(1 + \frac{\zeta}{R_\beta}\right)^{-1} \left(1 + \frac{\zeta}{R_\gamma}\right)^{-1} \zeta d\zeta \\
D_{ij}^{\alpha\beta\gamma} &= \int_{-\frac{h}{2}}^{\frac{h}{2}} Q_{ij} \left(1 + \frac{\zeta}{R_\alpha}\right) \left(1 + \frac{\zeta}{R_\beta}\right)^{-1} \left(1 + \frac{\zeta}{R_\gamma}\right)^{-1} \zeta^2 d\zeta \quad (11.2.85)
\end{aligned}$$

Note that (no sum on α)

$$\begin{aligned}
A_{ij}^{\alpha\beta} &\neq A_{ij}^{\beta\alpha} \quad \text{for } \alpha \neq \beta, \quad A_{ij}^{\alpha\alpha} = \int_{-\frac{h}{2}}^{\frac{h}{2}} Q_{ij} \, d\zeta \equiv A_{ij} = A_{ji} \\
B_{ij}^{\alpha\beta} &\neq B_{ij}^{\beta\alpha} \quad \text{for } \alpha \neq \beta, \quad B_{ij}^{\alpha\alpha} = \int_{-\frac{h}{2}}^{\frac{h}{2}} Q_{ij} \zeta \, d\zeta \equiv B_{ij} = B_{ji} = 0 \quad (11.2.86) \\
D_{ij}^{\alpha\beta} &\neq D_{ij}^{\beta\alpha} \quad \text{for } \alpha \neq \beta, \quad D_{ij}^{\alpha\alpha} = \int_{-\frac{h}{2}}^{\frac{h}{2}} Q_{ij} \zeta^2 \, d\zeta \equiv D_{ij} = D_{ji}
\end{aligned}$$

Thus, the shell constitutive equations are

$$\begin{Bmatrix} N_{11} \\ N_{22} \\ N_{12} \\ N_{21} \end{Bmatrix} = \begin{bmatrix} A_{11}^{21} & A_{12}^{22} & 0 & 0 \\ A_{12}^{21} & A_{22}^{22} & 0 & 0 \\ 0 & 0 & A_{66}^{21} & 0 \\ 0 & 0 & 0 & A_{66}^{12} \end{bmatrix} \begin{Bmatrix} \varepsilon_1^{0L} \\ \varepsilon_2^{0L} \\ \omega_1^{0L} \\ \omega_2^{0L} \end{Bmatrix} + \begin{bmatrix} B_{11}^{21} & B_{12}^{22} & 0 & 0 \\ B_{12}^{21} & B_{22}^{22} & 0 & 0 \\ 0 & 0 & B_{66}^{21} & 0 \\ 0 & 0 & 0 & B_{66}^{12} \end{bmatrix} \begin{Bmatrix} \hat{\varepsilon}_1^1 \\ \hat{\varepsilon}_2^1 \\ \hat{\omega}_1^1 \\ \hat{\omega}_2^1 \end{Bmatrix}$$

$$+ \begin{bmatrix} A_{11}^{211} & A_{12}^{222} & 0 & 0 \\ A_{12}^{111} & A_{22}^{122} & 0 & 0 \\ 0 & 0 & A_{66}^{212} & 0 \\ 0 & 0 & 0 & A_{66}^{112} \end{bmatrix} \begin{Bmatrix} \varepsilon_1^{0N} \\ \varepsilon_2^{0N} \\ \omega_1^{0N} \\ \omega_2^{0N} \end{Bmatrix} \quad (11.2.87)$$

$$\begin{Bmatrix} M_{11} \\ M_{22} \\ M_{12} \\ M_{21} \end{Bmatrix} = \begin{bmatrix} B_{11}^{21} & B_{12}^{22} & 0 & 0 \\ B_{12}^{21} & B_{22}^{22} & 0 & 0 \\ 0 & 0 & B_{66}^{21} & 0 \\ 0 & 0 & 0 & B_{66}^{12} \end{bmatrix} \begin{Bmatrix} \varepsilon_1^{0L} \\ \varepsilon_2^{0L} \\ \omega_1^{0L} \\ \omega_2^{0L} \end{Bmatrix} + \begin{bmatrix} D_{11}^{21} & D_{12}^{22} & 0 & 0 \\ D_{12}^{21} & D_{22}^{22} & 0 & 0 \\ 0 & 0 & D_{66}^{21} & 0 \\ 0 & 0 & 0 & D_{66}^{12} \end{bmatrix} \begin{Bmatrix} \hat{\varepsilon}_1^1 \\ \hat{\varepsilon}_2^1 \\ \hat{\omega}_1^1 \\ \hat{\omega}_2^1 \end{Bmatrix}$$

$$+ \begin{bmatrix} B_{11}^{211} & B_{12}^{222} & 0 & 0 \\ B_{12}^{111} & B_{22}^{122} & 0 & 0 \\ 0 & 0 & B_{66}^{212} & 0 \\ 0 & 0 & 0 & B_{66}^{112} \end{bmatrix} \begin{Bmatrix} \varepsilon_1^{0N} \\ \varepsilon_2^{0N} \\ \omega_1^{0N} \\ \omega_2^{0N} \end{Bmatrix} \quad (11.2.88)$$

$$\begin{Bmatrix} Q_2 \\ Q_1 \end{Bmatrix} = K_s \begin{bmatrix} A_{44} & 0 \\ 0 & A_{55} \end{bmatrix} \begin{Bmatrix} \varepsilon_4^0 \\ \varepsilon_5^0 \end{Bmatrix} \quad (11.2.89)$$

11.2.8 Constitutive Equations of Thin Shells

For thin shells, $(1 + \zeta/R_\alpha) \approx 1$ and the stiffnesses $A_{ij}^{\alpha\beta}$, $A_{ij}^{\alpha\beta\gamma}$, etc. are independent of α , β , and γ . In particular, for thin orthotropic shells, the constitutive equations are given by

$$\begin{Bmatrix} N_{11} \\ N_{22} \\ N_{12} \end{Bmatrix} = \begin{bmatrix} A_{11} & A_{12} & 0 \\ A_{12} & A_{22} & 0 \\ 0 & 0 & A_{66} \end{bmatrix} \begin{Bmatrix} \varepsilon_1^0 \\ \varepsilon_2^0 \\ \varepsilon_6^0 \end{Bmatrix} \quad (11.2.90)$$

$$\begin{Bmatrix} M_{11} \\ M_{22} \\ M_{12} \end{Bmatrix} = \begin{bmatrix} D_{11} & D_{12} & 0 \\ D_{12} & D_{22} & 0 \\ 0 & 0 & D_{66} \end{bmatrix} \begin{Bmatrix} \varepsilon_1^1 \\ \varepsilon_2^1 \\ \varepsilon_6^1 \end{Bmatrix} \quad (11.2.91)$$

$$\begin{Bmatrix} Q_2 \\ Q_1 \end{Bmatrix} = K_s \begin{bmatrix} A_{44} & 0 \\ 0 & A_{55} \end{bmatrix} \begin{Bmatrix} \varepsilon_4^0 \\ \varepsilon_5^0 \end{Bmatrix} \quad (11.2.92)$$

where

$$A_{ij} = \int_{-\frac{h}{2}}^{\frac{h}{2}} Q_{ij} d\zeta = Q_{ij} h \quad (i, j = 1, 2, 4, 5, 6) \quad (11.2.93)$$

$$D_{ij} = \int_{-\frac{h}{2}}^{\frac{h}{2}} Q_{ij} \zeta^2 d\zeta = Q_{ij} \frac{h^3}{12} \quad (i, j = 1, 2, 6)$$

and

$$\begin{Bmatrix} \varepsilon_1^0 \\ \varepsilon_2^0 \\ \varepsilon_4^0 \\ \varepsilon_5^0 \\ \varepsilon_6^0 \end{Bmatrix} = \left\{ \begin{array}{l} \frac{1}{a_1} \left(\frac{\partial u_1^0}{\partial \xi_1} + \frac{u_2^0}{a_2} \frac{\partial a_1}{\partial \xi_2} + \frac{a_1 u_3^0}{R_1} \right) \\ \frac{1}{a_2} \left(\frac{\partial u_2^0}{\partial \xi_2} + \frac{u_1^0}{a_1} \frac{\partial a_2}{\partial \xi_1} + \frac{a_2 u_3^0}{R_2} \right) \\ \frac{1}{a_2} \frac{\partial u_3^0}{\partial \xi_2} - \frac{u_2^0}{R_2} + \varphi_2 \\ \frac{1}{a_1} \frac{\partial u_3^0}{\partial \xi_1} - \frac{u_1^0}{R_1} + \varphi_1 \\ \frac{1}{a_1} \left(\frac{\partial u_2^0}{\partial \xi_1} - \frac{u_1^0}{a_2} \frac{\partial a_1}{\partial \xi_2} \right) + \frac{1}{a_2} \left(\frac{\partial u_1^0}{\partial \xi_2} - \frac{u_2^0}{a_1} \frac{\partial a_2}{\partial \xi_1} \right) \end{array} \right\} \quad (11.2.94)$$

$$\begin{Bmatrix} \varepsilon_1^1 \\ \varepsilon_2^1 \\ \varepsilon_6^1 \end{Bmatrix} = \begin{Bmatrix} \frac{1}{a_1} \left(\frac{\partial \varphi_1}{\partial \xi_1} + \frac{\varphi_2}{a_2} \frac{\partial a_1}{\partial \xi_2} \right) \\ \frac{1}{a_2} \left(\frac{\partial \varphi_2}{\partial \xi_2} + \frac{\varphi_1}{a_1} \frac{\partial a_2}{\partial \xi_1} \right) \\ \frac{1}{a_1} \left(\frac{\partial \varphi_2}{\partial \xi_1} - \frac{\varphi_1}{a_2} \frac{\partial a_1}{\partial \xi_2} \right) + \frac{1}{a_2} \left(\frac{\partial \varphi_1}{\partial \xi_2} - \frac{\varphi_2}{a_1} \frac{\partial a_2}{\partial \xi_1} \right) \end{Bmatrix} \quad (11.2.95)$$

For isotropic shells, Eqs. (11.2.90)-(11.2.92) simplify to

$$\begin{Bmatrix} N_{11} \\ N_{22} \\ N_{12} \end{Bmatrix} = A \begin{bmatrix} 1 & \nu & 0 \\ \nu & 1 & 0 \\ 0 & 0 & \frac{1-\nu}{2} \end{bmatrix} \begin{Bmatrix} \varepsilon_1^0 \\ \varepsilon_2^0 \\ \varepsilon_6^0 \end{Bmatrix} \quad (11.2.96)$$

$$\begin{Bmatrix} M_{11} \\ M_{22} \\ M_{12} \end{Bmatrix} = D \begin{bmatrix} 1 & \nu & 0 \\ \nu & 1 & 0 \\ 0 & 0 & \frac{1-\nu}{2} \end{bmatrix} \begin{Bmatrix} \varepsilon_1^1 \\ \varepsilon_2^1 \\ \varepsilon_6^1 \end{Bmatrix} \quad (11.2.97)$$

$$\begin{Bmatrix} Q_2 \\ Q_1 \end{Bmatrix} = S \begin{bmatrix} 1 & 0 \\ 0 & 1 \end{bmatrix} \begin{Bmatrix} \varepsilon_4^0 \\ \varepsilon_5^0 \end{Bmatrix} \quad (11.2.98)$$

where

$$A = \frac{Eh}{1-\nu^2}, \quad D = \frac{Eh^3}{12(1-\nu^2)}, \quad S = K_s Gh \quad (11.2.99)$$

Then from Eqs. (11.2.79) and (11.2.96)–(11.2.98), it follows that the stresses $(\sigma_{11}, \sigma_{22}, \sigma_{12})$ in isotropic shells can be computed using $(\zeta = z)$

$$\begin{aligned} \sigma_{11} &= \frac{N_{11}}{h} + \frac{12M_{11}z}{h^3} \\ \sigma_{22} &= \frac{N_{22}}{h} + \frac{12M_{22}z}{h^3} \\ \sigma_{12} &= \frac{N_{12}}{h} + \frac{12M_{12}z}{h^3} \end{aligned} \quad (11.2.100)$$

The transverse shear stresses $(\sigma_{13}, \sigma_{23})$ can be computed using either the constitutive equations

$$\sigma_{13} = \frac{Q_1}{K_s h}, \quad \sigma_{23} = \frac{Q_2}{K_s h} \quad (11.2.101)$$

or the stress equilibrium equations of 3D elasticity as

$$\sigma_{13} = \frac{3Q_1}{2h} \left[1 - \left(\frac{2z}{h} \right)^2 \right], \quad \sigma_{23} = \frac{3Q_2}{2h} \left[1 - \left(\frac{2z}{h} \right)^2 \right] \quad (11.2.102)$$

Note that for the thin shell theory, Q_1 and Q_2 are defined by Eqs. (11.2.77) and (11.2.78):

$$Q_1 = \frac{\partial M_{11}}{\partial x_1} + \frac{\partial M_{12}}{\partial x_2} + \frac{1}{a_2} \frac{\partial a_2}{\partial x_1} (M_{11} - M_{22}) + \frac{1}{a_1} \frac{\partial a_1}{\partial x_2} M_{12} \quad (11.2.103)$$

$$Q_2 = \frac{\partial M_{12}}{\partial x_1} + \frac{\partial M_{22}}{\partial x_2} - \frac{1}{a_1} \frac{\partial a_1}{\partial x_2} (M_{11} - M_{22}) + \frac{1}{a_2} \frac{\partial a_2}{\partial x_1} M_{12} \quad (11.2.104)$$

11.3 Analytical Solutions of Thin Cylindrical Shells

11.3.1 Introduction

Analytical solutions of Eqs. (11.2.48)–(11.2.52) can be obtained only for certain geometries and boundary conditions in the case of small strains, displacements and rotations. In this section, we discuss analytical solutions to certain problems of thin cylindrical and spherical shells governed by the equations derived in Section 11.2. For additional problems, the reader is advised to consult the excellent book by Timoshenko and Woinowsky-Krieger (1970), which contains analytical solutions to a number of shell problems.

For cylindrical shells, we set $(1/R_1) = 0$, $R_2 = R$, the radius of the cylinder, $a_1\xi_1 = x_1$, $a_2\xi_2 = x_2$, $a_1 = 1$ and $a_2 = R$ (Figure 11.3.1). When the nonlinear terms are omitted, Eqs. (11.2.74)–(11.2.78) reduce to the following linear partial differential equations:

$$\frac{\partial N_{11}}{\partial x_1} + \frac{\partial}{\partial x_2}(N_{21} + C_0\tilde{M}_{12}) + f_1 = I_0 \frac{\partial^2 u_1^0}{\partial t^2} + I_1 \frac{\partial^2 \varphi_1}{\partial t^2} \quad (11.3.1)$$

$$\frac{\partial}{\partial x_1}(N_{12} - C_0\tilde{M}_{12}) + \frac{\partial N_{22}}{\partial x_2} + \frac{Q_2}{R} + f_2 = I_0 \frac{\partial^2 u_2^0}{\partial t^2} + I_1 \frac{\partial^2 \varphi_2}{\partial t^2} \quad (11.3.2)$$

$$\frac{\partial Q_1}{\partial x_1} + \frac{\partial Q_2}{\partial x_2} - \frac{N_{22}}{R} + f_3 = I_0 \frac{\partial^2 u_3^0}{\partial t^2} \quad (11.3.3)$$

$$\frac{\partial M_{11}}{\partial x_1} + \frac{\partial M_{21}}{\partial x_2} - Q_1 = I_1 \frac{\partial^2 u_1^0}{\partial t^2} + I_2 \frac{\partial^2 \varphi_1}{\partial t^2} \quad (11.3.4)$$

$$\frac{\partial M_{12}}{\partial x_1} + \frac{\partial M_{22}}{\partial x_2} - Q_2 = I_1 \frac{\partial^2 u_2^0}{\partial t^2} + I_2 \frac{\partial^2 \varphi_2}{\partial t^2} \quad (11.3.5)$$

For thin cylindrical shells, we obtain the following equations of equilibrium from Eqs. (11.3.1)–(11.3.5) ($a_1\xi_1 = x_1 = x$, $a_2\xi_2 = x_2 = R\theta$, $C_0 = -1/2R$, $N_{11} = N_{xx}$, $N_{12} = N_{x\theta}$, $N_{22} = N_{\theta\theta}$, $M_{11} = M_{xx}$, $M_{12} = M_{x\theta}$, $M_{22} = M_{\theta\theta}$, $Q_1 = Q_x$, $Q_2 = Q_\theta$, $u_1^0 = u_0$, $u_2^0 = v_0$, $u_3^0 = w_0$, $\varphi_1 = \varphi_x$, and $\varphi_2 = \varphi_\theta$)

$$\begin{aligned} \frac{\partial N_{xx}}{\partial x} + \frac{1}{R} \frac{\partial}{\partial \theta} \left(N_{x\theta} - \frac{1}{2R} M_{x\theta} \right) + f_x &= 0 \\ \frac{\partial}{\partial x} \left(N_{x\theta} + \frac{1}{2R} M_{x\theta} \right) + \frac{1}{R} \frac{\partial N_{\theta\theta}}{\partial \theta} + \frac{Q_\theta}{R} + f_\theta &= 0 \\ \frac{\partial Q_x}{\partial x} + \frac{1}{R} \frac{\partial Q_\theta}{\partial \theta} - \frac{N_{\theta\theta}}{R} + f_z &= 0 \end{aligned} \quad (11.3.6)$$

$$\begin{aligned} \frac{\partial M_{xx}}{\partial x} + \frac{1}{R} \frac{\partial M_{x\theta}}{\partial \theta} - Q_x &= 0 \\ \frac{\partial M_{x\theta}}{\partial x} + \frac{1}{R} \frac{\partial M_{\theta\theta}}{\partial \theta} - Q_\theta &= 0 \end{aligned} \quad (11.3.7)$$

The shell constitutive equations in Eqs. (11.2.95)–(11.2.97) become

$$\begin{Bmatrix} N_{xx} \\ N_{\theta\theta} \\ N_{x\theta} \end{Bmatrix} = \frac{Eh}{(1-\nu^2)} \begin{bmatrix} 1 & \nu & 0 \\ \nu & 1 & 0 \\ 0 & 0 & \frac{1-\nu}{2} \end{bmatrix} \begin{Bmatrix} \frac{\partial u_0}{\partial x} \\ \frac{1}{R} \frac{\partial v_0}{\partial \theta} + \frac{w_0}{R} \\ \frac{\partial v_0}{\partial x} + \frac{1}{R} \frac{\partial u_0}{\partial \theta} \end{Bmatrix} \quad (11.3.8)$$

$$\begin{Bmatrix} M_{xx} \\ M_{\theta\theta} \\ M_{x\theta} \end{Bmatrix} = \frac{Eh^3}{12(1-\nu^2)} \begin{bmatrix} 1 & \nu & 0 \\ \nu & 1 & 0 \\ 0 & 0 & \frac{1-\nu}{2} \end{bmatrix} \begin{Bmatrix} \frac{\partial \varphi_x}{\partial x} \\ \frac{1}{R} \frac{\partial \varphi_\theta}{\partial \theta} \\ \frac{\partial \varphi_\theta}{\partial x} + \frac{1}{R} \frac{\partial \varphi_x}{\partial \theta} \end{Bmatrix} \quad (11.3.9)$$

$$\begin{Bmatrix} Q_\theta \\ Q_x \end{Bmatrix} = K_s G h \begin{Bmatrix} 2\varepsilon_{\theta z} \\ 2\varepsilon_{xz} \end{Bmatrix} = K_s G h \begin{Bmatrix} \frac{1}{R} \frac{\partial w_0}{\partial \theta} - \frac{w_0}{R} + \varphi_\theta \\ \frac{\partial w_0}{\partial x} + \varphi_x \end{Bmatrix} \quad (11.3.10)$$

where $\varepsilon_4^0 = 2\varepsilon_{\theta z}$ and $\varepsilon_5^0 = 2\varepsilon_{xz}$.

11.3.2 Membrane Theory

In some shell problems the bending stresses can be neglected. If a shell experiences negligible bending deformation and stresses, the shell is said to be in a state of *membrane behavior* and the membrane normal and shear forces are assumed to be uniformly distributed through the shell thickness. The equilibrium equations governing the membrane state of deformation and stress, called the *membrane theory*, are obtained by setting bending moments and transverse shear forces to zero in Eq. (11.3.6):

$$\frac{\partial N_{xx}}{\partial x} + \frac{1}{R} \frac{\partial N_{x\theta}}{\partial \theta} + f_x = 0 \quad (11.3.11)$$

$$\frac{\partial N_{x\theta}}{\partial x} + \frac{1}{R} \frac{\partial N_{\theta\theta}}{\partial \theta} + f_\theta = 0 \quad (11.3.12)$$

$$-\frac{N_{\theta\theta}}{R} + f_z = 0 \quad (11.3.13)$$

where the x -axis is taken parallel to the axis of the cylinder (Figure 11.3.1).

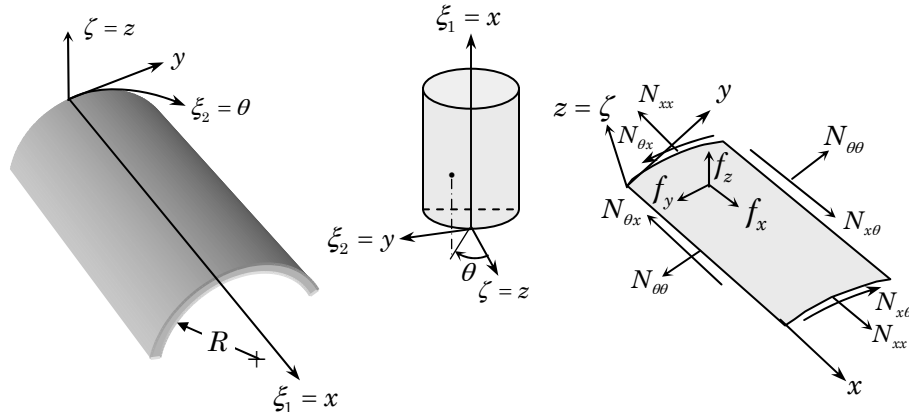


Figure 11.3.1. Cylindrical shell geometry and coordinate system.

Pure membrane state of stress exists only in few cases; a *thin* spherical container and a long and *thin* cylindrical shell subjected to uniform internal pressure normal to the surface of the shell provide examples of pure membrane state of stress. If the cylinder has built-in ends, some bending will occur near the edges because the ends are not free to expand radially. In many cases, bending is of local character and the membrane theory gives sufficiently accurate state of stress in those portions of a shell that are far away from these local regions, which are typically near the edges or points of concentrated loads. The accuracy of the membrane theory in predicting the state of stress depends on the geometry of the shell, loads, and boundary conditions, as illustrated in Figure 11.3.2.

In the following we consider a number of examples to determine the membrane forces in shells with dominant membrane behavior. The corresponding membrane stresses are obtained by dividing the force with the thickness h [see Eq. (11.2.100)]

Example 11.3.1

Consider a circular cylindrical shell of radius R and thickness h , filled with liquid, and simply supported at its ends (Figure 11.3.3). We wish to determine $N_{\theta\theta}$, $N_{x\theta}$, and N_{xx} assuming that there are no axial forces at the ends of the shell and the bending deformation is negligible.

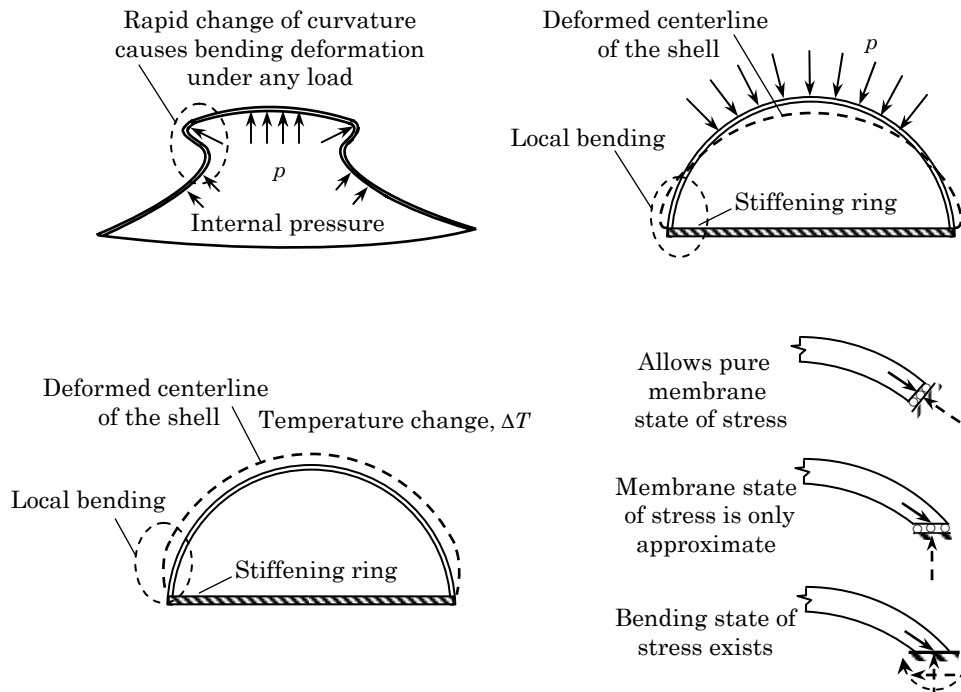


Figure 11.3.2. Examples of pure and approximate membrane states of stress and general bending state of stress.

The components of load for this case are $f_x = f_\theta = 0$ and $f_z = p_0 - \gamma R \cos \theta$, where p_0 is the pressure at the axis of the tube and γ is the specific weight of the liquid. From Eq. (11.3.13), we obtain

$$N_{\theta\theta} = p_0 R - \gamma R^2 \cos \theta$$

From Eqs. (11.3.12) and (11.3.11) we obtain

$$\begin{aligned}\frac{\partial N_{x\theta}}{\partial x} &= -\frac{1}{R} \frac{\partial N_{\theta\theta}}{\partial \theta} = -\gamma R \sin \theta \rightarrow N_{x\theta} = -x \gamma R \sin \theta + A(\theta) \\ \frac{\partial N_{xx}}{\partial x} &= -\frac{1}{R} \frac{\partial N_{x\theta}}{\partial \theta} = x \gamma \cos \theta - \frac{A'(\theta)}{R} \rightarrow N_{xx} = \frac{x^2}{2} \gamma \cos \theta - \frac{x}{R} A'(\theta) + B(\theta)\end{aligned}$$

Using the end conditions $N_{xx}(0, \theta) = 0$ and $N_{xx}(L, \theta) = 0$, we obtain

$$\begin{aligned}N_{xx}(0, \theta) = 0 : \quad B(\theta) &= 0 \\ N_{xx}(L, \theta) = 0 : \quad A'(\theta) &= \frac{1}{2} \gamma R L \cos \theta \rightarrow A(\theta) = \frac{1}{2} \gamma R L \sin \theta + C\end{aligned}$$

Thus, we have

$$N_{\theta\theta} = p_0 R - \gamma R^2 \cos \theta, \quad N_{x\theta} = \gamma R(0.5L - x) \sin \theta + C, \quad N_{xx} = -\frac{\gamma}{2}(xL - x^2) \cos \theta$$

The constant clearly represents the uniform state of shear force $N_{x\theta}$ along the edge of the cylinder, which can possibly be due to a torsional moment on the cylinder. In the absence of any torsional moment, we have $C = 0$. The membrane stresses are obtained from

$$\sigma_{xx} = \frac{N_{xx}}{h}, \quad \sigma_{x\theta} = \frac{N_{x\theta}}{h}, \quad \sigma_{\theta\theta} = \frac{N_{\theta\theta}}{h}$$

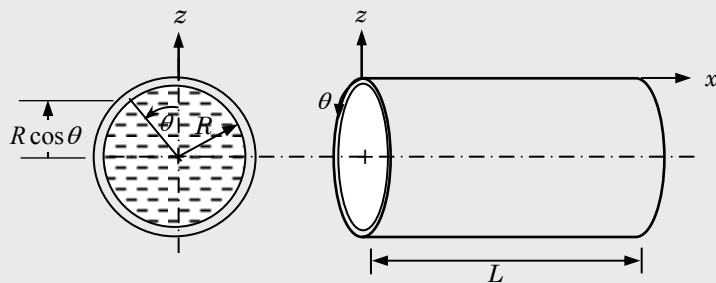


Figure 11.3.3. Circular cylinder filled with liquid and simply supported at the ends.

Example 11.3.2

Consider a cylindrical shell of semicircular cross section supporting its own weight, which is assumed to be distributed uniformly over the surface of the shell. The shell is assumed to be supported at the four corners A, B, C, and D, but the edges AB and CD are free, as shown in Figure 11.3.4(a). Using the membrane theory of shells and assuming that there are no axial forces at the ends of the shell, $N_{xx}(-L/2) = 0$ and $N_{xx}(L/2) = 0$, we wish to determine the forces N_θ , $N_{x\theta}$, and N_{xx} , and displacements u_0 , v_0 , and w_0 .

The body force components are

$$f_x = 0, \quad f_\theta = p \sin \theta, \quad f_z = -p \cos \theta$$

where p is the weight per unit area. From Eq. (11.3.13), we obtain

$$N_\theta = -pR \cos \theta$$

Equations (11.3.12) and (11.3.11), respectively, yield

$$N_{x\theta} = -2xp \sin \theta + C_1(\theta), \quad N_{xx} = \frac{p}{R}x^2 \cos \theta - \frac{x}{R}C'_1(\theta) + C_2(\theta)$$

Since $N_{x\theta}(-L/2, \theta) = -N_{x\theta}(L/2, \theta)$ (by symmetry), we must have $C_1(\theta) = 0$. Also, the boundary conditions $N_{xx}(\pm L/2) = 0$ give

$$C_2(\theta) = -\frac{pL^2}{4R} \cos \theta$$

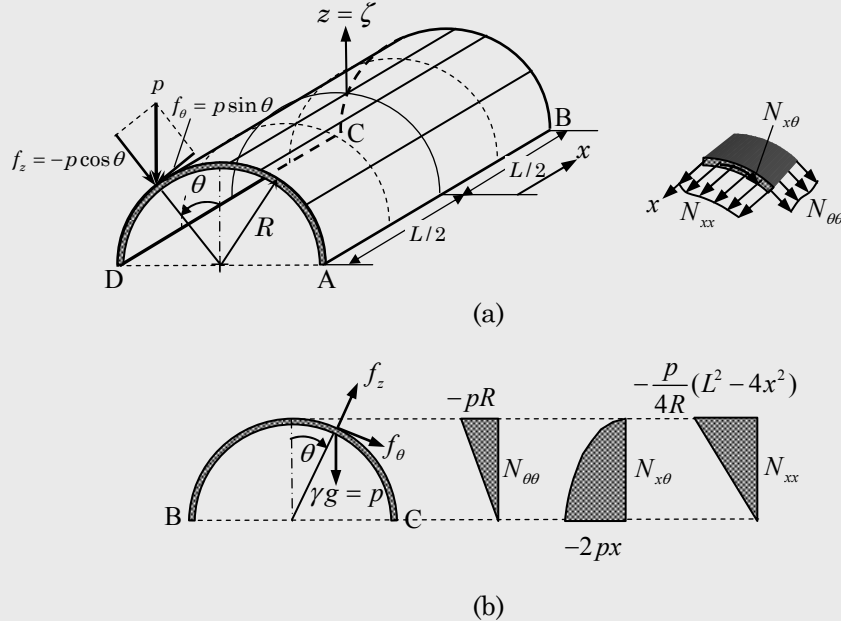


Figure 11.3.4. (a) Semicircular cylindrical shell loaded by its own weight.
(b) Variation of forces in the shell with θ .

Thus, the complete solution is

$$N_\theta = -pR \cos \theta, \quad N_{x\theta} = -2xp \sin \theta, \quad N_{xx} = -\frac{p}{4R}(L^2 - 4x^2) \cos \theta$$

Plots of the variations of these forces with θ , for a fixed x , are shown in Figure 11.3.4(b). The displacements can be determined using the constitutive relations in Eq. (11.3.8). Inverting the relation in Eq. (11.3.8), we obtain

$$\begin{Bmatrix} \varepsilon_{xx} \\ \varepsilon_{\theta\theta} \\ 2\varepsilon_{x\theta} \end{Bmatrix} = \begin{Bmatrix} \frac{\partial u_0}{\partial x} \\ \frac{1}{R} \frac{\partial v_0}{\partial \theta} + \frac{w_0}{R} \\ \frac{1}{R} \frac{\partial u_0}{\partial \theta} + \frac{\partial v_0}{\partial x} \end{Bmatrix} = \frac{1}{Eh} \begin{bmatrix} 1 & -\nu & 0 \\ -\nu & 1 & 0 \\ 0 & 0 & 2(1+\nu) \end{bmatrix} \begin{Bmatrix} N_{xx} \\ N_{\theta\theta} \\ N_{x\theta} \end{Bmatrix} \quad (11.3.14)$$

From the first equation, we have

$$\frac{\partial u_0}{\partial x} = \frac{1}{Eh} (N_{xx} - \nu N_{\theta\theta}) = \frac{p}{ERh} \left(x^2 - \frac{L^2}{4} + \nu R^2 \right) \cos \theta$$

Upon integration, we obtain

$$u_0(x, \theta) = \frac{px}{ERh} \left(\frac{x^2}{3} - \frac{L^2}{4} + \nu R^2 \right) \cos \theta + C_3(\theta)$$

Using the boundary condition (by symmetry) $u_0(0, \theta) = 0$, we find $C_3(\theta) = 0$. The third equation in (11.3.14) can now be expressed as

$$\frac{\partial v_0}{\partial x} = -\frac{1}{R} \frac{\partial u_0}{\partial \theta} + \frac{2(1+\nu)}{Eh} N_{x\theta} = \frac{px}{ER^2h} \left[\frac{x^2}{3} - \frac{L^2}{4} - (4+3\nu)R^2 \right] \sin \theta$$

Upon integration, we obtain

$$v_0(x, \theta) = \frac{px^2}{2ER^2h} \left[\frac{x^2}{6} - \frac{L^2}{4} - (4+3\nu)R^2 \right] \sin \theta + C_4(\theta)$$

The boundary condition $v_0(L/2, \theta) = 0$ allows us to calculate $C_4(\theta)$ as

$$C_4(\theta) = \frac{pL^2}{8ER^2h} \left[\frac{5L^2}{24} + (4+3\nu)R^2 \right] \sin \theta$$

and we have

$$v_0(x, \theta) = \frac{p}{192ER^2h^2} (L^2 - 4x^2) \left[(5L^2 - 4x^2) + 24(4+3\nu)R^2 \right] \sin \theta$$

Finally, using the second equation (11.3.14), we can write

$$\begin{aligned} w_0 &= -\frac{\partial v_0}{\partial \theta} + \frac{R}{Eh} (N_{\theta\theta} - \nu N_{xx}) \\ &= -\frac{p}{192ER^2h^2} \left\{ (L^2 - 4x^2) \left[(5L^2 - 4x^2) + 24(4+\nu)R^2 \right] + 192R^4 \right\} \cos \theta \end{aligned}$$

Thus, the displacement field is given by

$$\begin{aligned} u_0(x, \theta) &= \frac{px}{12EhR} (4x^2 - 3L^2 + 12\nu R^2) \cos \theta \\ v_0(x, \theta) &= \frac{p}{192EhR^2} (L^2 - 4x^2) [(5L^2 - 4x^2) + 24(4 + 3\nu)R^2] \sin \theta \\ w_0(x, \theta) &= -\frac{p}{192EhR^2} \left\{ (L^2 - 4x^2) [(5L^2 - 4x^2) + 24(4 + \nu)R^2] + 192R^4 \right\} \cos \theta \end{aligned} \quad (11.3.15)$$

We note that $w_0(L/2, \theta) \neq 0$, implying that there is some bending state of stress at $x = L/2$.

11.3.3 Flexural Theory for Axisymmetric Loads

If the cylindrical shell is axisymmetrically loaded, i.e., the shell is subjected to only forces normal to the surface, the deformation is independent of θ , $N_{x\theta}$, $M_{x\theta}$, and Q_θ are zero, and $N_{\theta\theta}$ and $M_{\theta\theta}$ are constant. Then the second equation in (11.3.6) and the second equation in (11.3.7) are trivially satisfied, and the remaining three equations of (11.3.6) and (11.3.7) take the form

$$N_{xx} = 0 \quad (11.3.16)$$

$$\begin{aligned} \frac{dQ_x}{dx} - \frac{N_{\theta\theta}}{R} &= -f_z \\ \frac{dM_{xx}}{dx} - Q_x &= 0 \end{aligned} \quad (11.3.17)$$

Equation (11.3.17) consists of two equations in three unknowns ($N_{\theta\theta}$, Q_x , M_{xx}). Hence, we must use the constitutive and kinematic (i.e., strain-displacement) relations to solve the equations. Here we consider a *thin* cylinder made of *isotropic* material [$A_{11} = A_{22} = A = Eh/(1 - \nu^2)$, $D_{11} = D_{22} = D = Eh^3/12(1 - \nu^2)$, $A_{12} = \nu A$ and $D_{12} = \nu D$].

From symmetry considerations of the problem, the displacement in the circumferential direction is zero, $v_0 = 0$. In the thin shell theory, we assume that the transverse shear strains are zero: $\varepsilon_5^0 = \varepsilon_{xz} = 0$ and $\varepsilon_4^0 = \varepsilon_{\theta z} = 0$. From Eq. (11.3.10) it follows that $\varphi_x = -dw_0/dx$ and $\varphi_\theta = 0$. Then the linear relations between $(N_{xx}, N_{\theta\theta}, M_{xx})$ and (u_0, w_0) are given by Eqs. (11.3.8) and (11.3.9):

$$\begin{aligned} N_{xx} &= \frac{Eh}{1 - \nu^2} \left(\frac{du_0}{dx} + \nu \frac{w_0}{R} \right) = 0 \rightarrow \frac{du_0}{dx} = -\nu \frac{w_0}{R} \\ N_{\theta\theta} &= \frac{Eh}{1 - \nu^2} \left(\nu \frac{du_0}{dx} + \frac{w_0}{R} \right) = \frac{Ehw_0}{R} \\ M_{xx} &= \frac{Eh^3}{12(1 - \nu^2)} \frac{d\varphi_1}{dx} = -D \frac{d^2w_0}{dx^2} \\ M_{\theta\theta} &= \nu M_{xx} = -\nu D \frac{d^2w_0}{dx^2} \\ Q_x &= \frac{dM_{xx}}{dx} = -D \frac{d^3w_0}{dx^3} \end{aligned} \quad (11.3.18)$$

From Eq. (11.3.17) we have

$$\frac{d^2 M_{xx}}{dx^2} - \frac{N_{\theta\theta}}{R} = -f_z \quad \text{or} \quad \frac{d^2}{dx^2} \left(D \frac{d^2 w_0}{dx^2} \right) + \frac{Eh w_0}{R^2} = f_z \quad (11.3.19)$$

which resembles the equation governing bending of a beam with flexural stiffness D , resting on a continuous elastic foundation with foundation modulus Eh/R^2 , and subjected to distributed load f_z . Next we consider couple of examples of application of Eq. (11.3.19).

Example 11.3.3

Consider a *long* circular cylindrical shell of radius R , subjected to uniform bending moment M_0 and shearing forces Q_0 at the end $x = 0$ (Figure 11.3.5). We wish to determine the deflection w_0 .

The general solution to Eq. (11.3.19) when D is a constant and $f_z = 0$ is given by

$$w_0(x) = e^{\alpha x} (K_1 \cos \alpha x + K_2 \sin \alpha x) + e^{-\alpha x} (K_3 \cos \alpha x + K_4 \sin \alpha x) \quad (11.3.20)$$

where

$$\alpha^4 = \frac{Eh}{4R^2 D} \quad (11.3.21)$$

Since the applied loads M_0 and Q_0 are expected to produce local bending and shear and their influence on the solution $w_0(x)$ is expected to die out rapidly with x increasing (St. Venant's principle), the constants K_1 and K_2 must be zero, giving the solution

$$w_0(x) = e^{-\alpha x} (K_3 \cos \alpha x + K_4 \sin \alpha x) \quad (11.3.22)$$

The remaining constants, K_3 and K_4 , are determined using the boundary conditions at $x = 0$:

$$M_{xx}(0) = \left(-D \frac{d^2 w_0}{dx^2} \right)_{x=0} = -M_0, \quad Q_x(0) = \left(-D \frac{d^3 w_0}{dx^3} \right)_{x=0} = -Q_0 \quad (11.3.23)$$

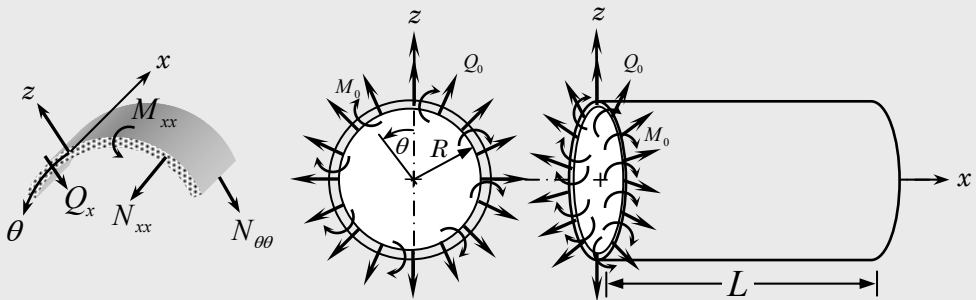


Figure 11.3.5. Circular cylindrical shell with end moments and shear forces.

We obtain

$$K_3 = \frac{Q_0 + \alpha M_0}{2\alpha^3 D}, \quad K_4 = -\frac{M_0}{2\alpha^2 D}$$

and

$$w_0(x) = \frac{1}{2\alpha^3 D} e^{-\alpha x} [\alpha M_0(\cos \alpha x - \sin \alpha x) + Q_0 \cos \alpha x] \quad (11.3.24)$$

We introduce the following notation to represent the expressions for deflection and stress resultants:

$$\begin{aligned} f_1(\alpha x) &= e^{-\alpha x} (\cos \alpha x + \sin \alpha x) \\ f_2(\alpha x) &= e^{-\alpha x} (\cos \alpha x - \sin \alpha x) \\ f_3(\alpha x) &= e^{-\alpha x} \cos \alpha x \\ f_4(\alpha x) &= e^{-\alpha x} \sin \alpha x \end{aligned} \quad (11.3.25)$$

Then we can express $w_0(x)$ and the stress resultants as

$$\begin{aligned} w_0 &= \frac{1}{2\alpha^3 D} [\alpha M_0 f_2(\alpha x) + Q_0 f_3(\alpha x)] \\ \frac{dw_0}{dx} &= \frac{1}{2\alpha^2 D} [2\alpha M_0 f_3(\alpha x) + Q_0 f_1(\alpha x)] \\ M_{xx} &= \frac{1}{\alpha} [\alpha M_0 f_1(\alpha x) + Q_0 f_4(\alpha x)] \\ M_{\theta\theta} &= \frac{\nu}{\alpha} [\alpha M_0 f_1(\alpha x) + Q_0 f_4(\alpha x)] \\ N_{\theta\theta} &= \frac{Eh}{2R\alpha^3 D} [\alpha M_0 f_2(\alpha x) + Q_0 f_3(\alpha x)] \end{aligned} \quad (11.3.26)$$

The maximum deflection occurs at $x = 0$ and it is given by

$$w_0(0) = w_{\max} = \frac{1}{2\alpha^3 D} (\alpha M_0 + Q_0) \quad (11.3.27)$$

Example 11.3.4

Consider a *long* circular cylindrical shell of radius R and thickness h , subjected to uniform circumferential line load of intensity P at $x = 0$ (Figure 11.3.6). We wish to determine the deflection w_0 and bending moment M_x .

Since the cylinder is long, we can use symmetry about $x = 0$ and analyze half of the shell using the solution obtained in Example 11.3.3, with $Q_0 = -P/2$ and M_0 to be determined. From Eq. (11.3.24) the deflection for the right half of the shell is

$$w_0(x) = \frac{1}{2\alpha^3 D} e^{-\alpha x} \left[\alpha M_0 (\cos \alpha x - \sin \alpha x) - \frac{P}{2} \cos \alpha x \right] \quad (11.3.28)$$

The bending moment M_0 at $x = 0$ is determined using the condition that the slope, dw_0/dx , is zero at $x = 0$:

$$\begin{aligned} \left(\frac{dw_0}{dx} \right)_{x=0} &= \frac{1}{2\alpha^2 D} e^{-\alpha x} \left[-2\alpha M_0 \cos \alpha x + \frac{P}{2} (\sin \alpha x + \cos \alpha x) \right]_{x=0} \\ &= \frac{1}{2\alpha^2 D} \left(-2\alpha M_0 + \frac{P}{2} \right) = 0 \end{aligned} \quad (11.3.29)$$

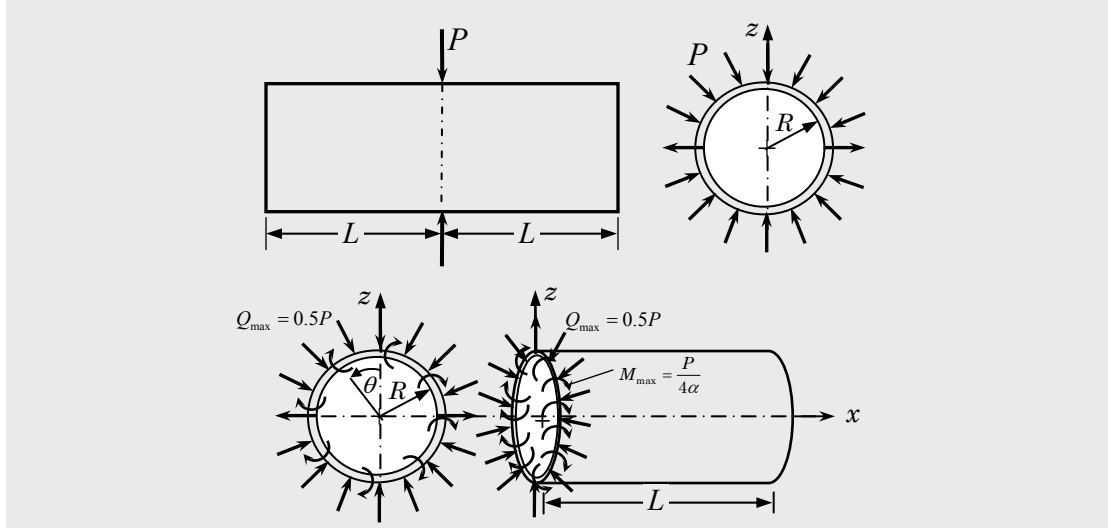


Figure 11.3.6. Circular cylindrical shell with circumferential line load at $x = 0$.

from which we obtain $M_0 = (P/4\alpha)$ and the deflection of the shell is

$$w_0(x) = -\frac{P}{8\alpha^3 D} e^{-\alpha x} (\cos \alpha x + \sin \alpha x) = -\frac{\sqrt{2}P}{8\alpha^3 D} e^{-\alpha x} \sin(\alpha x + \frac{\pi}{4}) \quad (11.3.30)$$

The negative sign in Eq. (11.3.30) indicates that the deflection $w_0(x)$ is taken positive outward.

The deflection w_0 in (11.3.30) and its derivatives can be expressed in terms of $f_i(\alpha x)$ as

$$\begin{aligned} w_0 &= -\frac{P}{8D\alpha^3} f_1(\alpha x), \quad \frac{dw_0}{dx} = \frac{P}{4D\alpha^2} f_4(\alpha x) \\ \frac{d^2w_0}{dx^2} &= \frac{P}{4D\alpha} f_2(\alpha x), \quad \frac{d^3w_0}{dx^3} = \frac{P}{2D} f_3(\alpha x) \end{aligned} \quad (11.3.31)$$

Then the stress resultants $(N_{\theta\theta}, M_{xx}, M_{\theta\theta}, Q_x)$ can be computed using Eq. (11.3.18)

$$\begin{aligned} N_{\theta\theta} &= \frac{EhP}{8RD\alpha^3} f_1(\alpha x), \quad M_{xx} = -\frac{P}{4\alpha} f_2(\alpha x) \\ M_{\theta\theta} &= -\frac{\nu P}{4\alpha} f_2(\alpha x), \quad Q_x = \frac{P}{2} f_3(\alpha x) \end{aligned} \quad (11.3.32)$$

The maximum values of the deflection, bending moment, and shear force occur at $x = 0$ and they are given by

$$w_{\max} = -\frac{P}{8\alpha^3 D} = -\frac{PR^2\alpha}{2Eh}, \quad M_{\max} = -\frac{P}{4\alpha}, \quad Q_{\max} = \frac{P}{2} \quad (11.3.33)$$

The maximum axial and circumferential stresses occur at $x = 0$ and $z = \zeta = h/2$

$$(\sigma_{xx})_{\max} = \frac{3P}{2\alpha h^2}, \quad (\sigma_{\theta\theta})_{\max} = -\frac{PR\alpha}{2h} \left(1 - \frac{3\nu}{\alpha^2 Rh}\right)$$

Example 11.3.5

Consider a long isotropic circular cylindrical shell of radius R and thickness h , subjected to uniform internal pressure of intensity p (Figure 11.3.7). We wish to determine the deflection w_0 and bending moment M_{xx} when the edges are built-in.

If the shell is free of any geometric constraints, the shell experiences membrane forces and hoop and circumferential stresses of

$$N_{xx} = \frac{pR}{2}, \quad N_{\theta\theta} = pR, \quad \sigma_{xx} = \frac{pR}{2h}, \quad \sigma_{\theta\theta} = \frac{pR}{h} \quad (11.3.34)$$

where h is the thickness of the cylinder. The cylinder experiences an increase in the radius of the cylinder by the amount

$$\delta_0 = R\varepsilon_{\theta\theta} = \frac{R}{E}(\sigma_{\theta\theta} - \nu\sigma_{xx}) = \frac{pR^2}{2Eh}(2 - \nu) \quad (11.3.35)$$

Since the ends of the cylinder are restrained from moving out, the shell develops local bending stresses at the edges. If the shell is sufficiently long, we can use the solution (11.3.24) to determine the bending moment M_0 and shear force Q_0 developed at the ends that produce zero deflection and slope there. Thus, the deflection for the present problem is the sum of the deflection in Eq. (11.3.24) and δ_0

$$w_0(x) = \frac{1}{2\alpha^3 D} e^{-\alpha x} [\alpha M_0(\cos \alpha x - \sin \alpha x) + Q_0 \cos \alpha x] + \delta_0 \quad (11.3.36)$$

The boundary conditions $w_0 = 0$ and $dw_0/dx = 0$ at $x = 0$ yield

$$\frac{1}{2\alpha^3 D}(\alpha M_0 + Q_0) + \delta_0 = 0, \quad -\frac{1}{2\alpha^2 D}(2\alpha M_0 + Q_0) = 0$$

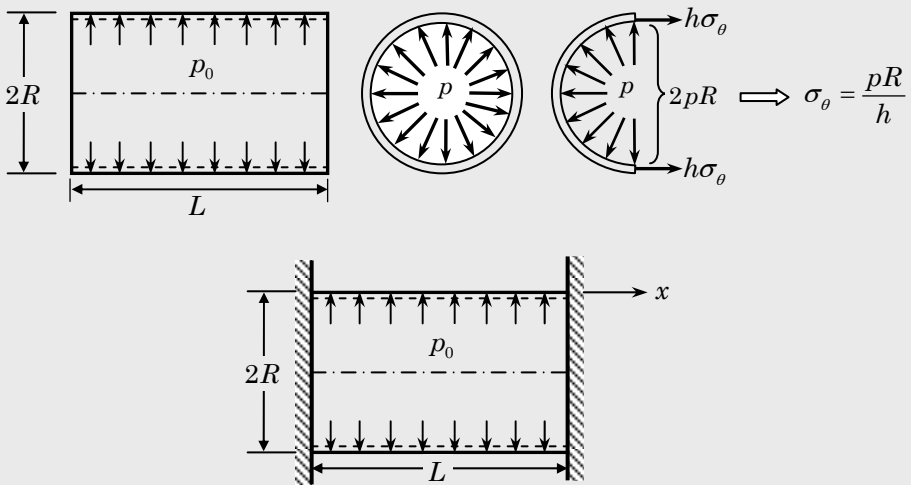


Figure 11.3.7. Circular cylindrical shell with uniform internal pressure and built-in ends.

from which we obtain

$$M_0 = 2\alpha^2 D \delta_0 = \frac{p}{2\alpha^2}, \quad Q_0 = -4\alpha^3 D \delta_0 = -\frac{p}{\alpha} \quad (11.3.37)$$

Hence, the deflection in Eq. (11.3.36) becomes

$$\begin{aligned} w_0(x) &= \delta_0 [1 - e^{-\alpha x} (\cos \alpha x + \sin \alpha x)] \\ &= \frac{pR^2}{Eh} [1 - e^{-\alpha x} (\cos \alpha x + \sin \alpha x)] \end{aligned} \quad (11.3.38)$$

The bending moment and shear force are

$$M_{xx}(x) = \frac{p}{2\alpha^2} e^{-\alpha x} (\sin \alpha x - \cos \alpha x), \quad Q_x(x) = \frac{p}{\alpha} e^{-\alpha x} \cos \alpha x \quad (11.3.39)$$

The maximum deflection occurs for large values of x and it is equal to δ_0 ; the maximum bending and shear forces occur at $x = 0$ and they are

$$M_{\max} = -\frac{p}{2\alpha^2}, \quad Q_{\max} = \frac{p}{\alpha} \quad (11.3.40)$$

The analytical solutions developed herein can also be applied to shells of other geometric shapes (e.g., spherical shells, conical shells, and so on). In the next section, we consider shells with double curvature. As special cases, we obtain solutions of conical, ellipsoidal and toroidal shells.

11.4 Analytical Solutions of Shells with Double Curvature

11.4.1 Introduction and Geometry

Here we study shells of revolution with double curvature. Shells of revolution are those in which the shell surface is formed by revolving a line, straight or curved, called *meridian line*, around a certain axis lying in the plane of the curve, known as the *axis of symmetry*. For example, a cylindrical shell is a shell of revolution generated by a straight line by revolving it around a parallel line (axis of symmetry) that is at a distance R , where R denotes the radius of the cylinder (Figure 11.1.4). However, the cylinder has only one curvature. A shell of revolution with double curvature is generated by two meridian lines that are perpendicular to each other.

The geometry of a shell of revolution with double curvature is shown in Figure 11.4.1. A typical volume element of the shell is located between two adjacent meridian lines and two sections perpendicular to the meridians, as shown in Figure 11.4.1. In general, the radii curvature of the meridian and section perpendicular to it are not constant, but for shells with double curvature, they are assumed to be constant. The *principal radii of curvature* r_1 and r_2 at any point on the surface of the shell are associated with the meridian curve (CD) and the section (AC) perpendicular to the meridian. The center of radius r_1 is located at point P, while the center of radius r_2 is located at point O on the axis of symmetry.

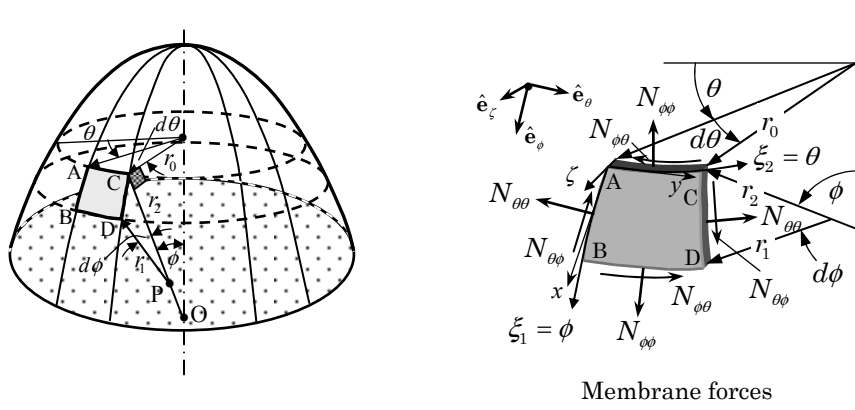


Figure 11.4.1. A shell of revolution with double curvature.

The coordinates of point A are conveniently taken to be (ϕ, θ, ζ) . The lengths of the sides of the curvilinear element ABCD are

$$dS_{CD} = r_1 d\phi, \quad dS_{AC} = r_0 d\theta = r_2 \sin \phi d\theta \quad (11.4.1)$$

Note that, for cylindrical shells, we have

$$a_1 d\phi = dx, \quad \phi = \pi/2, \quad \frac{1}{R_1} = 0, \quad a_2 = r_0 = R \quad (11.4.2)$$

and $R_1 = R_2 = R$ for spherical shells of radius R .

11.4.2 Equations of Equilibrium

The equations of equilibrium of shells of revolution with double curvature are obtained from Eqs. (11.2.66)–(11.2.70) by setting $\xi_1 = \phi$ and $\xi_2 = \theta$ and omitting the inertia terms

$$\begin{aligned} \frac{1}{a_1} \frac{\partial}{\partial \phi} (a_2 N_{\phi\phi}) + \frac{\partial N_{\theta\phi}}{\partial \theta} - N_{\theta\theta} \frac{1}{a_1} \frac{\partial a_2}{\partial \phi} + C_0 \frac{\partial \tilde{M}_{\phi\theta}}{\partial \theta} \\ + a_2 \frac{Q_\phi}{R_1} + a_2 f_\phi = 0 \end{aligned} \quad (11.4.3)$$

$$\begin{aligned} \frac{1}{a_1} \frac{\partial}{\partial \phi} (a_2 N_{\phi\theta}) + \frac{\partial N_{\theta\theta}}{\partial \theta} + N_{\theta\phi} \frac{1}{a_1} \frac{\partial a_2}{\partial \phi} - C_0 \frac{a_2}{a_1} \frac{\partial \tilde{M}_{\phi\theta}}{\partial \phi} \\ + a_2 \frac{Q_\theta}{R_2} + a_2 f_\theta = 0 \end{aligned} \quad (11.4.4)$$

$$\frac{1}{a_1} \frac{\partial}{\partial \phi} (a_2 Q_\phi) + \frac{\partial Q_\theta}{\partial \theta} - a_2 \left(\frac{N_{\phi\phi}}{R_1} + \frac{N_{\theta\theta}}{R_2} \right) + a_2 f_\zeta = 0 \quad (11.4.5)$$

$$\frac{1}{a_1} \frac{\partial}{\partial \phi} (a_2 M_{\phi\phi}) + \frac{\partial M_{\theta\phi}}{\partial \theta} - \frac{1}{a_1} \frac{\partial a_2}{\partial \phi} M_{\theta\theta} - a_2 Q_\phi = 0 \quad (11.4.6)$$

$$\frac{1}{a_1} \frac{\partial}{\partial \phi} (a_2 M_{\phi\theta}) + \frac{\partial M_{\theta\theta}}{\partial \theta} + \frac{1}{a_1} \frac{\partial a_2}{\partial \phi} M_{\theta\phi} - a_2 Q_\theta = 0 \quad (11.4.7)$$

For shells of revolution, loaded symmetrically about its axis of symmetry ($f_\theta = 0$), the stress resultants are independent of θ and $N_{\theta\phi} = N_{\phi\theta} = M_{\theta\phi} = M_{\phi\theta} = Q_\theta = 0$. For this case, the second and fifth equations in Eqs. (11.4.3)–(11.4.7) are trivially satisfied. The remaining three equations of equilibrium are given by ($a_1 = r_1$ and $a_2 = r_0 = r_2 \sin \phi$, and $\partial a_2 / \partial \phi = dr_0 / d\phi = r_1 \cos \phi$; see Problem 11.20)

$$\frac{\partial}{\partial \phi} (r_0 N_{\phi\phi}) + r_1 \frac{\partial N_{\theta\phi}}{\partial \theta} - N_{\theta\theta} r_1 \cos \phi + r_1 r_0 \frac{Q_\phi}{R_1} + r_1 r_0 f_\phi = 0 \quad (11.4.8)$$

$$\frac{\partial}{\partial \phi} (r_0 Q_\phi) - r_1 r_0 \left(\frac{N_{\phi\phi}}{R_1} + \frac{N_{\theta\theta}}{R_2} \right) + r_1 r_0 f_\zeta = 0 \quad (11.4.9)$$

$$\frac{\partial}{\partial \phi} (r_0 M_{\phi\phi}) - r_1 \cos \phi M_{\theta\theta} - r_1 r_0 Q_\phi = 0 \quad (11.4.10)$$

The above equations contain five unknowns: $N_{\phi\phi}$, $N_{\theta\theta}$, Q_ϕ , $M_{\phi\phi}$, and $M_{\theta\theta}$. Hence, we must use the constitutive equations to solve them. The constitutive relations for an isotropic shell are

$$\begin{aligned} N_{\phi\phi} &= \frac{Eh}{1-\nu^2} (\varepsilon_{\phi\phi}^0 - \nu \varepsilon_{\theta\theta}^0), & N_{\theta\theta} &= \frac{Eh}{1-\nu^2} (\varepsilon_{\theta\theta}^0 - \nu \varepsilon_{\phi\phi}^0) \\ M_{\phi\phi} &= \frac{Eh}{1-\nu^2} (\varepsilon_{\phi\phi}^1 - \nu \varepsilon_{\theta\theta}^1), & M_{\theta\theta} &= \frac{Eh^3}{12(1-\nu^2)} (\varepsilon_{\theta\theta}^1 - \nu \varepsilon_{\phi\phi}^1) \end{aligned} \quad (11.4.11)$$

$$Q_\phi = K_s A_{55} \left(\varphi_\phi - \frac{u_0}{R_1} + \frac{1}{R_1} \frac{\partial w_0}{\partial \phi} \right) \quad (11.4.12)$$

where [see Eqs. (11.2.76) and (11.2.77) with $u_1^0 = u_0$, $u_2^0 = v_0 = 0$, $u_3^0 = w_0$, $\varphi_\theta = 0$, $r_1 = R_1$, and $r_2 = R_2$]

$$\begin{aligned} \varepsilon_{\phi\phi}^0 &= \frac{1}{R_1} \frac{\partial u_0}{\partial \phi} + \frac{w_0}{R_1}, & \varepsilon_{\theta\theta}^0 &= \frac{u_0}{R_2} \cot \phi + \frac{w_0}{R_2} \\ \varepsilon_{\phi\phi}^1 &= \frac{1}{R_1} \frac{\partial \varphi_\phi}{\partial \phi}, & \varepsilon_{\theta\theta}^1 &= \frac{1}{R_2} \varphi_\phi \cot \phi \end{aligned} \quad (11.4.13)$$

For thin shells, we replace φ_ϕ in $\varepsilon_{\phi\phi}^1$ and $\varepsilon_{\theta\theta}^1$ with

$$\varphi_\phi = \frac{u_0}{R_1} - \frac{1}{R_1} \frac{\partial w_0}{\partial \phi} \quad (11.4.14)$$

and Q_ϕ in Eq. (11.4.9) is replaced by solving Eq. (11.4.10) for Q_ϕ .

11.4.3 Membrane Stresses in Symmetrically Loaded Shells

Here, a number of problems of symmetrically loaded shells of revolution are discussed to determine their *membrane load carrying ability*. In this case, only Eq. (11.4.9) along with the equation obtained by considering the equilibrium of the shell above a parallel circle defined by the angle ϕ , as shown in Figure 11.4.2. If the shell is loaded symmetrically by a uniformly distributed load of intensity p , the resultant vertical force is

$$F_R = \int_0^{2\pi} \int_0^\phi p R_1 d\phi r_0 d\theta \quad (11.4.15)$$

From the equilibrium of forces in vertical direction, we obtain

$$F_R + 2\pi r_0 N_{\phi\phi} \sin \phi = 0 \quad \text{or} \quad N_{\phi\phi} = -\frac{F_R}{2\pi R_2 \sin^2 \phi} \quad (11.4.16)$$

The circumferential force $N_{\theta\theta}$ is obtained from Eq. (11.4.9)

$$\frac{N_{\phi\phi}}{R_1} + \frac{N_{\theta\theta}}{R_2} = f_\zeta \quad (11.4.17)$$

Next, we consider examples of application of Eqs. (11.4.15)–(11.4.17).

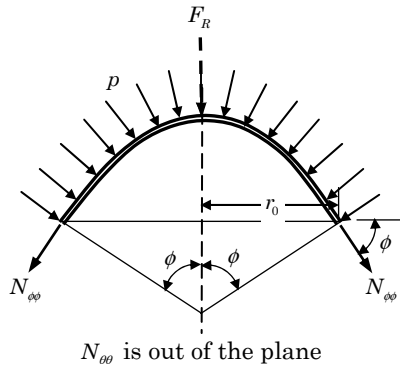


Figure 11.4.2. A shell of revolution subjected to an axisymmetric load.

Example 11.4.1

Consider a spherical dome of radius R with subtended angle α . The supports are assumed to be such that the support reaction is perpendicular to the meridian (Figure 11.4.3). The dome is subjected to its own weight, which is assumed to be distributed uniformly with intensity p per unit area. The vertical component of the body force is $f_\zeta = -p \cos \phi$. The resultant force F_R becomes ($r = R \sin \phi$ and $R_1 = R$)

$$F_R = 2\pi R^2 p \int_0^\phi \sin \phi d\phi = 2\pi R^2 p (1 - \cos \phi)$$

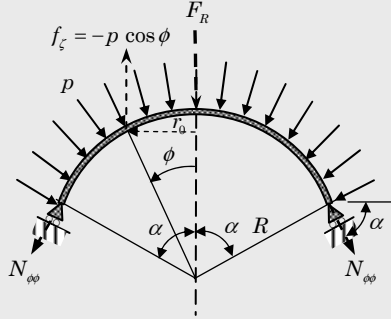


Figure 11.4.3. A spherical dome subjected to its own weight.

The forces $N_{\phi\phi}$ and $N_{\theta\theta}$ are

$$\left. \begin{aligned} N_{\phi\phi} &= -\frac{pR(1-\cos\phi)}{\sin^2\phi} = -\frac{pR}{(1+\cos\phi)} \\ N_{\theta\theta} &= -N_{\phi\phi} + Rf_\zeta = pR\left(\frac{1}{1+\cos\phi} - \cos\phi\right) \end{aligned} \right\} \quad 0 \leq \phi \leq \alpha \leq \frac{\pi}{2} \quad (11.4.18)$$

It is clear that $N_{\phi\phi}$ is compressive for all values of ϕ , while $N_{\theta\theta}$ is negative for small angles ϕ and it becomes positive when ϕ is greater than ϕ_0 , where ϕ_0 is given by

$$\frac{1}{1+\cos\phi_0} - \cos\phi_0 = 0$$

The smallest value of ϕ_0 that satisfies the above equation is $\phi_0 \approx 51.8^\circ$. We have

$$N_{\phi\phi}(0) = -\frac{pR}{2}, \quad N_{\phi\phi}(\pi/2) = -pR, \quad N_{\theta\theta}(\phi_0) = 0 \quad (11.4.19)$$

To determine the displacements (u_0, w_0) , we use the inverse of the first of Eq. (11.4.11)

$$\varepsilon_{\phi\phi}^0 = \frac{1}{Eh}(N_{\phi\phi} - \nu N_{\theta\theta}), \quad \varepsilon_{\theta\theta}^0 = \frac{1}{Eh}(N_{\theta\theta} - \nu N_{\phi\phi})$$

where h denotes the shell thickness and [see Eq. (11.4.13)]

$$\varepsilon_{\phi\phi}^0 = \frac{1}{R} \frac{du_0}{d\phi} + \frac{w_0}{R}, \quad \varepsilon_{\theta\theta}^0 = \frac{u_0}{R} \cot\phi + \frac{w_0}{R}$$

Then,

$$R(\varepsilon_{\phi\phi}^0 - \varepsilon_{\theta\theta}^0) = \frac{du_0}{d\phi} - u_0 \cot\phi = \frac{R(1+\nu)}{Eh} (N_{\phi\phi} - N_{\theta\theta}) \quad (11.4.20)$$

Using Eq. (11.4.18), we can write

$$\frac{du_0}{d\phi} - u_0 \cot\phi = \frac{(1+\nu)pR^2}{Eh} \left[\cos\phi - \frac{2}{(1+\cos\phi)} \right] \quad (11.4.21)$$

Towards solving the differential equation (11.4.21), we first note that

$$\frac{du_0}{d\phi} - u_0 \cot \phi = \sin \phi \frac{d}{d\phi} \left(\frac{u_0}{\sin \phi} \right) \quad (11.4.22)$$

$$\begin{aligned} \cos \phi - \frac{2}{(1 + \cos \phi)} &= \frac{\cos \phi + \cos^2 \phi - 2}{1 + \cos \phi} = \frac{-(1 - \cos \phi) - (1 - \cos^2 \phi)}{1 + \cos \phi} \\ &= -\frac{\sin^2 \phi}{(1 + \cos \phi)^2} - \frac{\sin^2 \phi}{1 + \cos \phi} \end{aligned} \quad (11.4.23)$$

Hence, we have

$$\begin{aligned} u_0 &= \left\{ \frac{(1 + \nu)pR^2}{Eh} \left[\int \frac{-\sin \phi}{(1 + \cos \phi)^2} + \frac{-\sin \phi}{(1 + \cos \phi)} \right] d\phi + C \right\} \sin \phi \\ &= \left\{ \frac{(1 + \nu)pR^2}{Eh} \left[-\frac{1}{(1 + \cos \phi)} + \log(1 + \cos \phi) \right] + C \right\} \sin \phi \end{aligned} \quad (11.4.24)$$

where the constant of integration, C , is determined using the boundary condition $u_0(\alpha) = 0$. We obtain

$$C = \frac{(1 + \nu)pR^2}{Eh} \left[\frac{1}{(1 + \cos \alpha)} - \log(1 + \cos \alpha) \right]$$

Thus, u_0 is given by

$$u_0(\phi) = \frac{(1 + \nu)pR^2}{Eh} \left[\log \frac{1 + \cos \phi}{1 + \cos \alpha} - \frac{1}{(1 + \cos \phi)} + \frac{1}{(1 + \cos \alpha)} \right] \sin \phi \quad (11.4.25)$$

Then, w_0 can be determined from $[\varepsilon_{\theta\theta} = (N_{\theta\theta} - \nu N_{\phi\phi})/Eh]$

$$\begin{aligned} w_0(\phi) &= -u_0 \cot \phi + \frac{R}{Eh} (N_{\theta\theta} - \nu N_{\phi\phi}) \\ &= -\frac{(1 + \nu)pR^2}{Eh} \left(\log \frac{1 + \cos \phi}{1 + \cos \alpha} - \frac{1}{1 + \cos \phi} + \frac{1}{1 + \cos \alpha} \right) \cos \phi \\ &\quad + \frac{pR^2}{Eh} \left(\frac{1 + \nu}{1 + \cos \phi} - \cos \phi \right) \end{aligned} \quad (11.4.26)$$

When the dome is resting on horizontal supports, a reinforcing ring is used at the bottom to take the horizontal components of $N_{\phi\phi}$; the ring undergoes a uniform circumferential extension and, thus, a small bending will occur near the supporting ring. Often the upper portion of the dome is removed and reinforced with a ring to take the weight of the upper structure, as shown in Figure 11.4.4. The weight of the upper structure is represented as line load P per unit length of the upper reinforcing ring. The resultant force F_R in this case becomes

$$F_R = 2\pi R^2 p \int_{\phi_0}^{\phi} \sin \phi d\phi + 2\pi RP \sin \phi_0 = 2\pi R^2 p (\cos \phi_0 - \cos \phi) + 2\pi RP \sin \phi_0$$

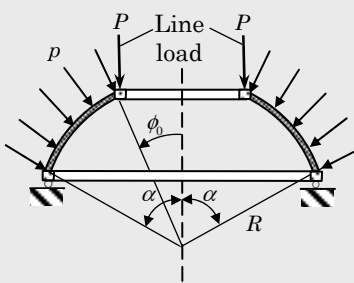


Figure 11.4.4. Spherical dome with upper and lower reinforcing rings.

The forces $N_{\phi\phi}$ and $N_{\theta\theta}$ are

$$\left. \begin{aligned} N_{\phi\phi} &= -pR \frac{\cos \phi_0 - \cos \phi}{\sin^2 \phi} - P \frac{\sin \phi_0}{\sin^2 \phi} \\ N_{\theta\theta} &= pR \left(\frac{\cos \phi_0 - \cos \phi}{\sin^2 \phi} - \cos \phi \right) + P \frac{\sin \phi_0}{\sin^2 \phi} \end{aligned} \right\} \quad \phi_0 \leq \phi \leq \alpha \leq \frac{\pi}{2} \quad (11.4.27)$$

Example 11.4.2

Consider a spherical tank of radius R supported at a parallel circle OO' (Figure 11.4.5) and filled with liquid of specific weight γ . The internal pressure for any angle ϕ is

$$p = -f_\zeta \cos \phi = -\gamma R(1 - \cos \phi) \cos \phi$$

The resultant vertical force is given by

$$\begin{aligned} F_R &= -2\pi R^3 \gamma \int_0^\phi (1 - \cos \phi) \cos \phi \sin \phi d\phi \\ &= -2\pi R^3 \gamma \left[\frac{1}{2}(1 - \cos^2 \phi) - \frac{1}{3}(1 - \cos^3 \phi) \right] \\ &= -\frac{\gamma \pi R^3}{3} (1 - 3 \cos^2 \phi + 2 \cos^3 \phi) \\ &= -\frac{\gamma \pi R^3}{3} [\sin^2 \phi - 2 \cos^2 \phi (1 - \cos \phi)] \end{aligned}$$

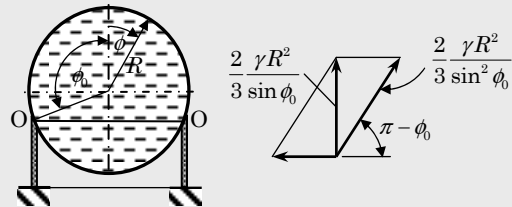


Figure 11.4.5. Spherical tank filled with liquid and supported at the bottom.

The forces $N_{\phi\phi}$ and $N_{\theta\theta}$ are

$$\left. \begin{aligned} N_{\phi\phi} &= \frac{\gamma R^2}{6} \left(1 - \frac{2 \cos^2 \phi}{1 + \cos \phi} \right) \\ N_{\theta\theta} &= \frac{\gamma R^2}{6} \left(5 - 6 \cos \phi + \frac{2 \cos^2 \phi}{1 + \cos \phi} \right) \end{aligned} \right\} \quad 0 \leq \phi \leq \phi_0 \quad (11.4.28)$$

For $\phi > \phi_0$, the resultant force F_R must include the vertical reaction exerted by the support at OO. The support reaction is equal to the total weight of the liquid, $4\gamma\pi R^3/3$, acting upward. Thus,

$$F_R = -\frac{4\gamma\pi R^3}{3} - \frac{\gamma\pi R^3}{3} [\sin^2 \phi - 2 \cos^2 \phi (1 - \cos \phi)]$$

The forces $N_{\phi\phi}$ and $N_{\theta\theta}$ are

$$\left. \begin{aligned} N_{\phi\phi} &= \frac{\gamma R^2}{6} \left(5 + \frac{2 \cos^2 \phi}{1 - \cos \phi} \right) \\ N_{\theta\theta} &= \frac{\gamma R^2}{6} \left(1 - 6 \cos \phi - \frac{2 \cos^2 \phi}{1 - \cos \phi} \right) \end{aligned} \right\} \quad \phi_0 \leq \phi \leq \pi \quad (11.4.29)$$

Note that $N_{\phi\phi}$ has a jump in the amount of $2\gamma R^2/(3 \sin^2 \phi_0)$ at the supporting ring OO, indicating that local bending takes place near the supporting ring.

Example 11.4.3

Here we consider a conical shell of height H subjected to a vertical force P at the apex of the cone [Figure 11.4.6(a)]. The cone will experience certain membrane forces. Equilibrium of forces yields ($\sin \phi = \cos \alpha$)

$$N_{\phi\phi} = -\frac{P}{2\pi r_0 \cos \alpha} \quad (11.4.30)$$

where α is the half angle and r_0 is the radius at the bottom of the cone. Since $1/R_1 = 0$ for a cone, Eq. (11.4.9) gives $N_{\theta\theta} = 0$ in the absence of distributed transverse load.

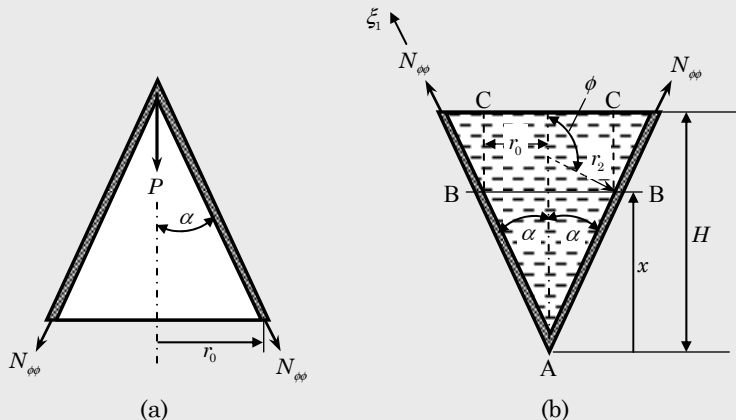


Figure 11.4.6. Conical shell (a) with a vertical force and (b) filled with liquid.

If the cone is subjected to symmetrically distributed vertical forces, the membrane forces $N_{\phi\phi} = N_{xx}$ and $N_{\theta\theta}$ can be independently calculated from [see the inverted cone in Figure 11.4.6(b)]

$$N_{\phi\phi} = -\frac{F_R}{2\pi r_0 \sin \phi}, \quad N_{\theta\theta} = r_2 f_\zeta = \frac{r_0 f_\zeta}{\sin \phi} \quad (11.4.31)$$

where F_R is the vertical resultant force (acting upward) due to the known distributed forces. For example, if the cone is filled with a liquid of specific weight γ , the pressure at any parallel circle BB, located at a vertical distance x from the bottom of the cone, is

$$p = f_\zeta = \gamma(H - x)$$

Note that the angle ϕ and r_0 are related to the cone angle α by $\phi = \alpha + \pi/2$ and $r_0 = x \tan \alpha$. The vertical resultant force F_R in this case is given by ($d\xi_1 \cos \alpha = dx$)

$$\begin{aligned} F_R &= - \int_0^{2\pi} \int_0^x p \sin \alpha d\xi_1 r_0 d\theta = -2\pi\gamma \int_0^x (H - x)x \tan^2 \alpha dx \\ &= -\pi\gamma x^2 \left(H - \frac{2}{3}x \right) \tan^2 \alpha \end{aligned} \quad (11.4.32)$$

Note that $-F_R$ is numerically equal to sum of the weight of the liquid in the conical part ABB and that in the cylindrical part AAC. Then, we have ($\sin \phi = \cos \alpha$)

$$N_{\phi\phi} = -\frac{F_R}{2\pi r_0 \sin \phi} = \frac{\gamma x(H - \frac{2}{3}x) \tan \alpha}{2 \cos \alpha}, \quad N_{\theta\theta} = \frac{\gamma(H - x)x \tan \alpha}{\cos \alpha} \quad (11.4.33)$$

The maximum values of $N_{\phi\phi}$ and $N_{\theta\theta}$ occur, respectively, at $x = 3H/4$ and $x = H/2$, and their values are

$$N_{\phi\phi} = \frac{3}{16} \frac{\gamma H^2 \tan \alpha}{\cos \alpha}, \quad N_{\theta\theta} = \frac{\gamma H^2 \tan \alpha}{4 \cos \alpha} \quad (11.4.34)$$

Example 11.4.4

Ends of a pressure vessel or boiler are in the form of an half ellipsoid of revolution, as shown in Figure 11.4.7. We wish to determine the membrane forces in the shell when the pressure inside the vessel is p .

The principal radii of curvature in this case are

$$R_1(\phi) = \frac{a^2 b^2}{(a^2 \sin^2 \phi + b^2 \cos^2 \phi)^{\frac{3}{2}}}, \quad R_2(\phi) = \frac{a^2}{(a^2 \sin^2 \phi + b^2 \cos^2 \phi)^{\frac{1}{2}}} \quad (11.4.35)$$

The membrane forces $N_{\phi\phi}$ and $N_{\theta\theta}$ are then given by Eqs. (11.4.16) and (11.4.17) with $F_R = -\pi r_0^2 p$

$$\begin{aligned} N_{\phi\phi} &= \frac{pr_0}{2 \sin \phi} = \frac{pr_2}{2} \\ N_{\theta\theta} &= -r_2 p - \frac{r_2}{r_1} N_{\phi\phi} = p \left(r_2 - \frac{r_2^2}{2r_1} \right) \end{aligned} \quad (11.4.36)$$

The forces at point O and section AA are

$$\begin{aligned} \text{Point O } (r_1 = r_2 = a^2/b) : \quad N_{\phi\phi} = N_{\theta\theta} &= \frac{pa^2}{2b} \\ \text{Section AA } (r_1 = b^2/2, r_2 = a) : \quad N_{\phi\phi} &= \frac{pa}{2}, \quad N_{\theta\theta} = pa \left(1 - \frac{a^2}{2b^2}\right) \end{aligned} \quad (11.4.37)$$

Note that $N_{\phi\phi}$ is always positive while $N_{\theta\theta}$ becomes negative when $a^2 > 2b^2$. Also, when $a = b = R$ (i.e., spherical end cap), the forces everywhere are

$$N_{\phi\phi} = N_{\theta\theta} = \frac{pR}{2} \quad (11.4.38)$$

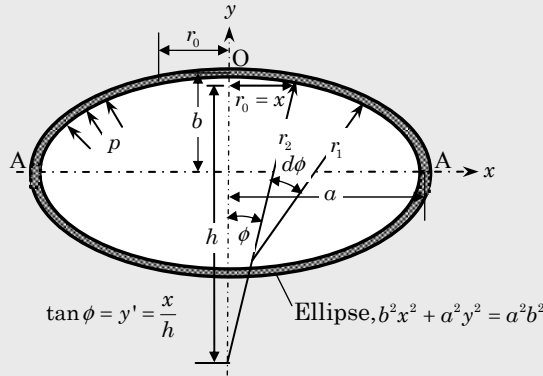


Figure 11.4.7. Half of an ellipsoidal shell of revolution.

Example 11.4.5

Here we consider a shell in the form of a *torus* of circular cross section (a torus is obtained by rotation of a circle of radius a about a vertical axis) and subjected to internal pressure p , as shown in Figure 11.4.8(a). We wish to determine the membrane forces in the shell.

Considering the equilibrium of vertical forces on the sectorial-ring shown in Figure 11.4.8(b), we obtain the result

$$2\pi r_0 N_{\phi\phi} \sin \phi = \pi p(r_0^2 - R_0^2)$$

or

$$N_{\phi\phi} = \frac{p(r_0^2 - R_0^2)}{2r_0 \sin \phi} = \frac{pa(r_0 + R_0)}{2r} \quad (11.4.39)$$

Since $f_\zeta = -p$, $N_{\theta\theta}$ is given by

$$N_{\theta\theta} = \frac{pr_2(r_0 - R_0)}{2r_0} = \frac{pa}{2} \quad (11.4.40)$$

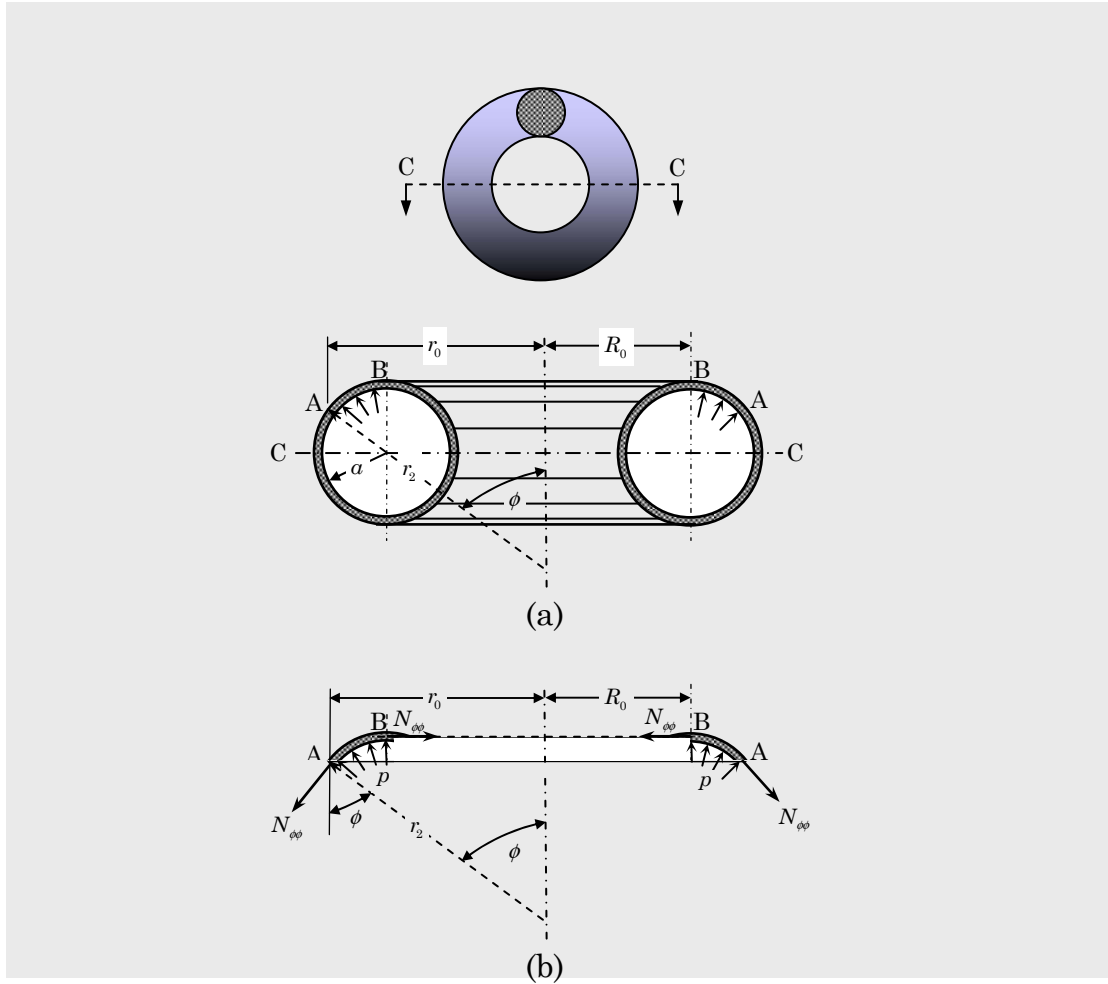


Figure 11.4.8. (a) Toroidal shell of revolution with circular cross section.
(b) Equilibrium of forces.

11.4.4 Membrane Stresses in Unsymmetrically Loaded Shells

A shell of revolution under unsymmetric loading experiences not only normal forces $N_{\phi\phi}$ and $N_{\theta\theta}$, but also shearing forces $N_{\phi\theta} = N_{\theta\phi}$, all of which are functions of both ϕ and θ . For this case, Eqs. (11.4.6) and (11.4.7) are omitted and Eqs. (11.4.3)–(11.4.5) reduce to (see Problem 11.20)

$$\frac{\partial}{\partial \phi}(r_0 N_{\phi\phi}) + r_1 \frac{\partial N_{\theta\phi}}{\partial \theta} - N_{\theta\theta} r_1 \cos \phi + r_1 r_0 f_\phi = 0 \quad (11.4.41)$$

$$\frac{\partial}{\partial \phi}(r_0 N_{\phi\theta}) + r_1 \frac{\partial N_{\theta\theta}}{\partial \theta} + N_{\theta\phi} r_1 \cos \phi + r_1 r_0 f_\theta = 0 \quad (11.4.42)$$

$$R_2 N_{\phi\phi} + R_1 N_{\theta\theta} = R_1 R_2 f_\zeta \quad (11.4.43)$$

The constitutive equations relating $(N_{\phi\phi}, N_{\theta\theta}, N_{\phi\theta} = N_{\theta\phi})$ to the displacements

(u_0, v_0, w_0) in an isotropic shell are given by

$$\begin{Bmatrix} N_{\phi\phi} \\ N_{\theta\theta} \\ N_{\phi\theta} \end{Bmatrix} = \frac{Eh}{1-\nu^2} \begin{bmatrix} 1 & \nu & 0 \\ \nu & 1 & 0 \\ 0 & 0 & \frac{1-\nu}{2} \end{bmatrix} \begin{Bmatrix} \frac{1}{R_1} \frac{\partial u_0}{\partial \phi} + \frac{w_0}{R_1} \\ \frac{u_0}{R_2} \cot \phi + \frac{w_0}{R_2} \\ \frac{1}{R_1} \frac{\partial v_0}{\partial \phi} + \frac{1}{R_2 \sin \phi} \frac{\partial u_0}{\partial \theta} - \frac{v_0}{R_2} \cot \phi \end{Bmatrix} \quad (11.4.44)$$

In particular, we consider the action of wind pressure on a shell. Suppose that the direction of the wind is in the meridian plane $\theta = 0$ and that the pressure p is normal to the surface. Then

$$f_\phi = f_\theta = 0, \quad f_\zeta = -p \sin \phi \cos \theta \quad (11.4.45)$$

Substituting for f_ϕ , f_θ , and f_ζ from Eq. (11.4.45) and eliminating $N_{\theta\theta}$ using Eq. (11.4.43) from Eqs. (11.4.41) and (11.4.42), we obtain

$$\frac{\partial N_{\phi\phi}}{\partial \phi} + \left(\frac{1}{r_0} \frac{dr_0}{d\phi} + \cot \phi \right) N_{\phi\phi} + \frac{r_1}{r_0} \frac{\partial N_{\theta\phi}}{\partial \theta} = -pr_1 \cos \phi \cos \theta \quad (11.4.46)$$

$$\frac{\partial N_{\theta\phi}}{\partial \phi} + \left(\frac{1}{r_0} \frac{dr_0}{d\phi} + \frac{r_1}{r_2} \cot \phi \right) N_{\phi\theta} - \frac{1}{\sin \phi} \frac{\partial N_{\phi\phi}}{\partial \theta} = -pr_1 \sin \theta \quad (11.4.47)$$

Next, we consider couple of specific examples of stresses induced in shells of revolution by wind pressure.

Example 11.4.6

Consider a spherical shell ($r_1 = r_2 = R_1 = R_2 = R$) subjected to wind pressure. Assuming solution of Eqs. (11.4.46) and (11.4.47) in the form

$$N_{\phi\phi} = N_{\phi\phi}^0(\phi) \cos \theta, \quad N_{\phi\theta} = N_{\phi\theta}^0(\phi) \sin \theta \quad (11.4.48)$$

and substituting into Eqs. (11.4.46) and (11.4.47), we obtain the following ordinary differential equations:

$$\begin{aligned} \frac{dN_{\phi\phi}^0}{d\phi} + 2 \cot \phi N_{\phi\phi}^0 + \frac{1}{\sin \phi} N_{\phi\theta}^0 &= -pR \cos \phi \\ \frac{dN_{\phi\theta}^0}{d\phi} + 2 \cot \phi N_{\phi\theta}^0 + \frac{1}{\sin \phi} N_{\phi\phi}^0 &= -pR \end{aligned} \quad (11.4.49)$$

In view of the form of the above equations, we introduce the variables

$$S_1 = N_{\phi\phi}^0 + N_{\phi\theta}^0, \quad S_2 = N_{\phi\phi}^0 - N_{\phi\theta}^0 \quad (11.4.50)$$

and reduce Eqs. (11.4.49) to

$$\begin{aligned} \frac{dS_1}{d\phi} + \left(2 \cot \phi + \frac{1}{\sin \phi} \right) S_1 &= -pR (1 + \cos \phi) \\ \frac{dS_2}{d\phi} + \left(2 \cot \phi + \frac{1}{\sin \phi} \right) S_2 &= pR (1 - \cos \phi) \end{aligned} \quad (11.4.51)$$

The solution of these first-order ordinary differential equations is given by

$$\begin{aligned} S_1 &= \frac{1 + \cos \phi}{\sin^3 \phi} \left[C_1 + \frac{pR \cos \phi}{3} (3 - \cos^2 \phi) \right] \\ S_2 &= \frac{1 - \cos \phi}{\sin^3 \phi} \left[C_2 - \frac{pR \cos \phi}{3} (3 - \cos^2 \phi) \right] \end{aligned} \quad (11.4.52)$$

where C_1 and C_2 are constants of integration that can be determined using the boundary conditions. The membrane forces $N_{\phi\phi}$ and $N_{\phi\theta}$ are given by

$$\begin{aligned} N_{\phi\phi}(\phi, \theta) &= \frac{\cos \theta}{\sin^3 \phi} \left[\frac{C_1 + C_2}{2} + \frac{C_1 - C_2}{2} \cos \phi + \frac{pR \cos^2 \phi}{3} (3 - \cos^2 \phi) \right] \\ N_{\phi\theta}(\phi, \theta) &= \frac{\sin \theta}{\sin^3 \phi} \left[\frac{C_1 - C_2}{2} + \frac{C_1 + C_2}{2} \cos \phi + \frac{pR \cos \phi}{3} (3 - \cos^2 \phi) \right] \end{aligned} \quad (11.4.53)$$

To determine the constants C_1 and C_2 , suppose that the shell under consideration is a hemisphere, as shown in Figure 11.4.9. Since the pressure at each point of the shell is normal to the shell, the moment of the wind forces with respect to the diameter of the sphere perpendicular to the plane $\theta = 0$ is zero. This requires

$$0 = \int_0^{2\pi} R N_{\phi\phi}(\pi/2, \theta) \cos \theta R d\theta = R^2 \frac{C_1 + C_2}{2} \int_0^{2\pi} \cos^2 \theta d\theta \rightarrow C_1 = -C_2 \quad (11.4.54)$$

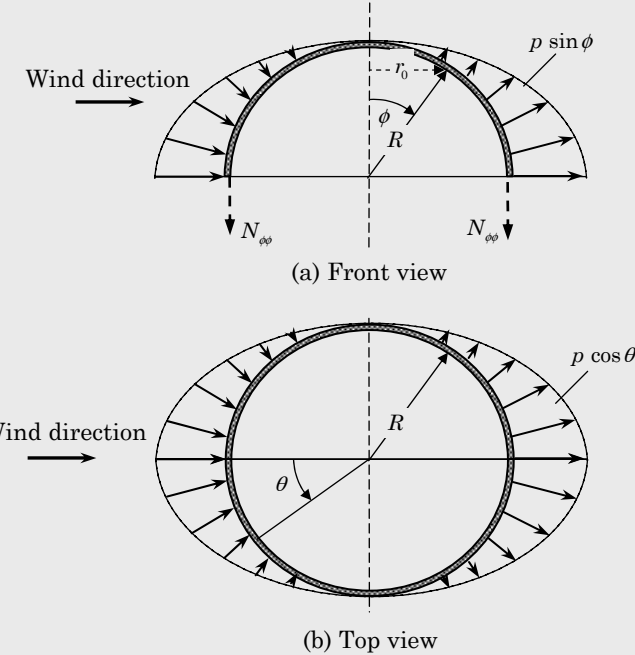


Figure 11.4.9. Hemispherical shell of revolution under wind pressure in the meridian plane $\theta = 0$; the pressure p is normal to the surface.

The second condition is provided by the equilibrium requirement that the sum of all forces acting on the half sphere in the direction of the horizontal diameter in the plane $\theta = 0$ be equal to zero:

$$\int_0^{2\pi} N_{\phi\theta}(\pi/2, \theta) \sin \theta R d\theta + \int_0^{\frac{\pi}{2}} \int 2\pi_0 pR \sin \phi \cos \theta \sin \phi \sin \phi \cos \theta d\phi R d\theta = 0$$

or

$$\pi R \frac{C_1 - C_2}{2} = -\frac{2}{3}\pi R^2 p \quad (11.4.55)$$

From Eqs. (11.4.54) and (11.4.55), we obtain

$$C_1 = -\frac{2}{3}pR, \quad C_2 = \frac{2}{3}pR \quad (11.4.56)$$

Substituting the values of the constants into Eqs. (11.4.53) and using Eq. (11.4.43), we obtain the membrane forces in a hemispherical shell under wind pressure p in the meridian plane $\theta = 0$ (the pressure p is acting normal to the surface)

$$\begin{aligned} N_{\phi\phi}(\phi, \theta) &= -\frac{pR \cos \phi \cos \theta}{3 \sin^3 \phi} (2 - 3 \cos \phi + \cos^3 \phi) \\ N_{\phi\theta}(\phi, \theta) &= -\frac{pR \sin \theta}{3 \sin^3 \phi} (2 - 3 \cos \phi + \cos^3 \phi) \\ N_{\theta\theta}(\phi, \theta) &= \frac{pR \cos \theta}{3 \sin^3 \phi} (2 \cos \phi - 3 \sin^2 \phi - 2 \cos^4 \phi) \end{aligned} \quad (11.4.57)$$

Note that the normal forces acting at the edge $\phi = \pi/2$ of the shell are zero, $N_{\phi\phi}(\pi/2, \theta) = 0$. The shearing forces on the same edge are equal to the horizontal resultant of the wind pressure.

Example 11.4.7

Consider a conical shell ($r_1 = R_1$ and $1/R_1 = 0$) supported by column at the vertex and subjected to wind pressure, as shown in Figure 11.4.10. An elemental length ds of the meridian can be written as $ds = a_1 d\phi = r_1 d\phi$, and

$$r_0 = s \sin \alpha, \quad \frac{dr_0}{ds} = \sin \alpha, \quad r_2 = s \tan \alpha, \quad f_\zeta = -p \sin \phi \cos \theta$$

The equations of equilibrium, Eqs. (11.4.41)–(11.4.43), after eliminating $N_{\theta\theta}$, reduce to ($a_2 = r_2 \sin \phi = r_2 \cos \alpha$)

$$\begin{aligned} \frac{\partial N_{\phi\phi}}{\partial s} + \frac{N_{\phi\phi}}{s} + \frac{1}{s \sin \alpha} \frac{\partial N_{\theta\phi}}{\partial \theta} &= -p \sin \alpha \cos \theta \\ \frac{\partial N_{\theta\phi}}{\partial s} + 2 \frac{N_{\theta\phi}}{s} &= -p \sin \theta \end{aligned} \quad (11.4.58)$$

Noting that

$$\frac{\partial N_{\theta\phi}}{\partial s} + 2 \frac{N_{\theta\phi}}{s} = \frac{1}{s^2} \frac{\partial}{\partial s} (s^2 N_{\theta\phi})$$

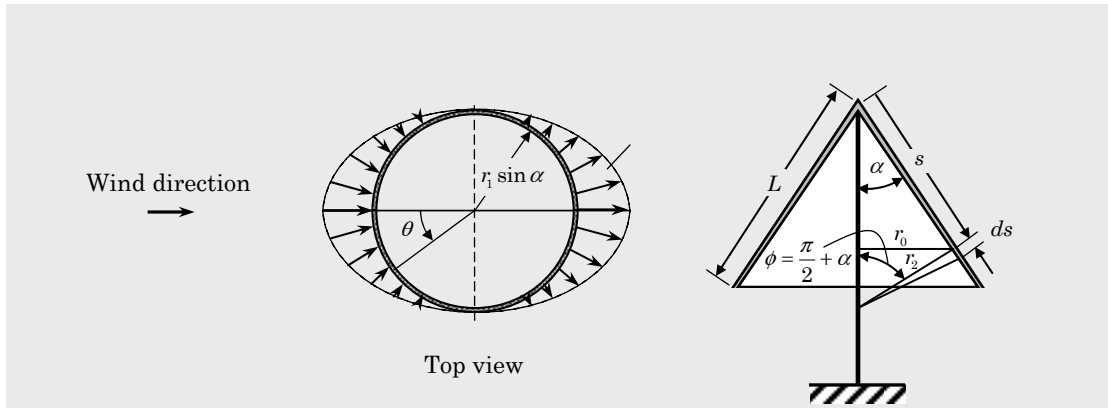


Figure 11.4.10. Conical shell of revolution under wind pressure in the meridian plane $\theta = 0$; the pressure p is normal to the surface.

the second equation in (11.4.58) can be readily integrated to give

$$N_{\theta\phi} = -\frac{1}{s^2} \left(\frac{ps^3}{3} + C_1 \right) \sin \theta \quad (11.4.59)$$

where C_1 is a constant of integration. Using the condition that the edge of the shell, $s = L$, is free from forces, we obtain $C_1 = -pL^3/3$ and $N_{\theta\phi}$ becomes

$$N_{\theta\phi}(s, \theta) = \frac{p}{3} \left(\frac{L^3 - s^3}{s^2} \right) \sin \theta \quad (11.4.60)$$

Substituting $N_{\theta\phi}$ from Eq. (11.4.60) into the first equation in Eq. (11.4.58), we obtain

$$\frac{1}{s} \frac{\partial(sN_{\phi\phi})}{\partial s} = - \left[\frac{1}{s \sin \alpha} \frac{p}{3} \left(\frac{L^3 - s^3}{s^2} \right) + p \sin \alpha \right] \cos \theta \quad (11.4.61)$$

Integrating with respect s , we obtain

$$N_{\phi\phi}(s, \theta) = \left[\frac{p}{3 \sin \alpha} \left(\frac{L^3}{s^2} + \frac{s}{2} \right) + p - \frac{ps}{2} \sin \alpha + \frac{C_2}{s} \right] \cos \theta \quad (11.4.62)$$

where the constant of integration, C_2 is determined using the boundary condition $N_{\phi,\phi}(L, \theta) = 0$. We obtain

$$C_2 = -\frac{pL^2}{2} \frac{\cos^2 \alpha}{\sin \alpha} \quad (11.4.63)$$

The force $N_{\theta\theta}$ can be calculated from Eq. (11.4.43). Thus, the forces are

$$N_{\phi\phi}(s, \theta) = \frac{p \cos \theta}{\sin \alpha} \left(\frac{L^3 - s^3}{3s^2} - \frac{L^2 - s^2}{2s} \cos^2 \alpha \right) \quad (11.4.64)$$

$$N_{\theta\theta} = -ps \sin \alpha \cos \theta$$

Example 11.4.8

Consider a cylindrical pressure vessel with hemispherical ends, as shown in Figure 11.4.11(a). As noted earlier, the stresses induced in the cylindrical portion at sufficient distances from the joints AA and BB can be determined accurately using membrane theory, as discussed in Section 11.3.2. However, at the joints AA and BB, the membrane stresses are accompanied by local bending stresses. The local bending stresses in the cylindrical portion can be determined with sufficient accuracy, as discussed in Example 11.3.3. Finding the bending stresses in the hemispherical ends is a more challenging problem, and it will be discussed in Section 11.4.5. Here we obtain an approximate solution by assuming that the bending is of importance in the portion of the spherical shell close to the joint and this zone can be considered as a portion of the long cylindrical shell.

For the cylindrical portion sufficiently far from the joints AA and BB, the membrane forces are given by [see Eq. (11.3.34)]

$$N_{xx}^c = \frac{pR}{2}, \quad N_{\theta\theta}^c = pR \quad (11.4.65)$$

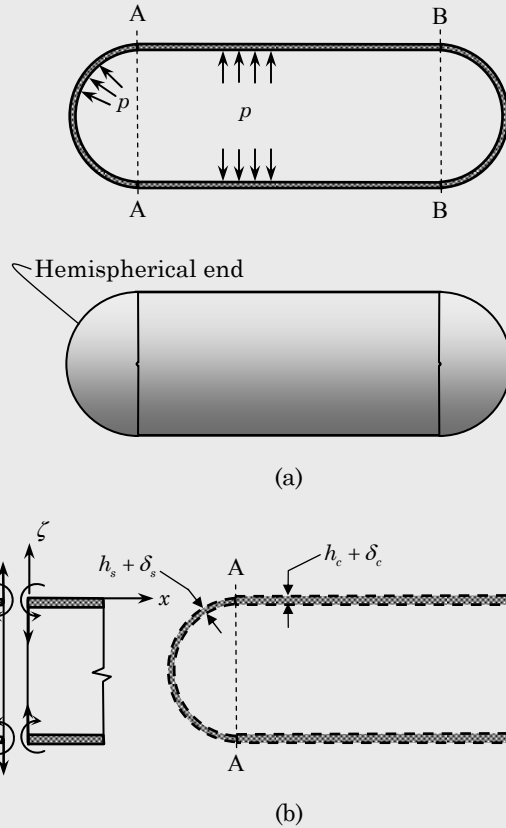


Figure 11.4.11. (a) Cylindrical pressure vessel with hemispherical ends.
(b) Radial elongations and bending forces at the joint.

where p is the pressure and R is the radius of the shell. Then the uniform tensile force in the spherical ends is given by

$$N_{xx}^s = \frac{pR}{2}$$

The radial elongation of the cylindrical shell due to the forces in Eq. (11.4.65) is

$$\delta_c = R\varepsilon_{\theta\theta} = \frac{R}{E}(\sigma_{\theta\theta} - \nu\sigma_{xx}) = \frac{pR^2}{2Eh_c}(2 - \nu)$$

and the radial elongation in spherical shell is ($\sigma_{\phi\phi} = \sigma_{\theta\theta}$)

$$\delta_s = R\varepsilon_{\theta\theta} = \frac{R(1 - \nu)}{E}\sigma_{\theta\theta} = \frac{pR^2}{2Eh_s}(1 - \nu)$$

The difference in δ_c and δ_s indicates that there exists a shear force Q_0 and a bending moment M_0 at the joint. If both portions are of equal thickness, $h_c = h_s = h$, then the bending moment $M_0 = 0$. The magnitude of Q_0 can be determined from the condition that the sum of the numerical values of the deflections of the two parts must be equal to the difference $\delta_c - \delta_s$. Using Eq. (11.3.25) for the deflection at the joint, we obtain

$$\left(\frac{Q_0}{2\alpha^3 D}\right)_c + \left(\frac{Q_0}{2\alpha^3 D}\right)_s = \delta_c - \delta_s = \frac{pR^2}{2Eh} \quad \text{or} \quad Q_0 = \frac{p}{8\alpha} \quad (11.4.66)$$

Then the deflection w_0 in the cylindrical portion can be computed using Eq. (11.3.24), and the bending moment M_{xx} is obtained using $M_{xx} = -D(d^2w_0/dx^2)$:

$$\begin{aligned} w_0(x) &= -\frac{Q_0}{2\alpha^3 D} e^{-\alpha x} \cos \alpha x = -\frac{pR^2}{4Eh} e^{-\alpha x} \cos \alpha x \\ M_{xx}(x) &= \frac{Q_0}{\alpha} e^{-\alpha x} \sin \alpha x = \frac{pRh}{8\sqrt{3(1-\nu^2)}} e^{-\alpha x} \sin \alpha x \end{aligned} \quad (11.4.67)$$

The largest axial stress occurs at the outer surface, $\zeta = h/2$, at $\alpha x = \pi/4$ of the shell ($\nu = 0.3$)

$$\begin{aligned} (\sigma_{xx})_{\max} &= \left[\frac{N_{xx}}{h} + \frac{12M_{xx}\zeta}{h^3} \right]_{x=\pi/4\alpha, \zeta=h/2} \\ &= \frac{pR}{2h} + \frac{3}{4} \frac{pR}{h\sqrt{6(1-\nu^2)}} e^{-\pi/4} = 0.647 \frac{pR}{h} \end{aligned} \quad (11.4.68)$$

The maximum hoop stress also occurs at the outer surface of the shell ($\nu = 0.3$) at $\alpha x = 1.85$

$$\begin{aligned} (\sigma_{\theta\theta})_{\max} &= \left[\frac{N_{\theta\theta}}{h} + \frac{12M_{\theta\theta}\zeta}{h^3} \right]_{x=1.85/\alpha, \zeta=h/2} = \left[\frac{pR}{h} - \frac{Ew_0}{R} - \frac{6\nu}{h^2} M_{xx} \right]_{x=1.85/\alpha, \zeta=h/2} \\ &= \frac{pR}{h} \left[1 - \frac{1}{4} f_3(\alpha x) + \frac{3\nu}{4\sqrt{3(1-\nu^2)}} f_4(\alpha x) \right]_{\alpha x=1.85, \zeta=h/2} \\ &= 1.6032 \frac{pR}{h} \end{aligned} \quad (11.4.69)$$

11.4.5 Bending Stresses in Spherical Shells

Returning to the equilibrium equations in Eqs. (11.4.8)–(11.4.10), we rewrite the stress resultants in terms of the displacements using Eqs. (11.4.11)–(11.4.14). For isotropic case, we have

$$\begin{aligned} N_{\phi\phi} &= A \left[\frac{1}{R_1} \frac{du_0}{d\phi} + \frac{w_0}{R_1} + \nu \left(\frac{u_0}{R_2} \cot \phi + \frac{w_0}{R_2} \right) \right] \\ N_{\theta\theta} &= A \left[\frac{u_0}{R_2} \cot \phi + \frac{w_0}{R_2} + \nu \left(\frac{1}{R_1} \frac{du_0}{d\phi} + \frac{w_0}{R_1} \right) \right] \\ M_{\phi\phi} &= D \left[\frac{1}{R_1} \frac{d}{d\phi} \left(\frac{u_0}{R_1} - \frac{1}{R_1} \frac{dw_0}{d\phi} \right) + \frac{\nu}{R_2} \left(\frac{u_0}{R_1} - \frac{1}{R_1} \frac{dw_0}{d\phi} \right) \cot \phi \right] \\ M_{\theta\theta} &= D \left[\frac{1}{R_2} \left(\frac{u_0}{R_1} - \frac{1}{R_1} \frac{dw_0}{d\phi} \right) \cot \phi + \frac{\nu}{R_1} \frac{d}{d\phi} \left(\frac{u_0}{R_1} - \frac{1}{R_1} \frac{dw_0}{d\phi} \right) \right] \end{aligned} \quad (11.4.70)$$

where

$$A = \frac{Eh}{1 - \nu^2}, \quad D = \frac{Eh^3}{12(1 - \nu^2)} \quad (11.4.71)$$

Now consider spherical shells ($R_1 = R_2 = R$) and introduce the variable U as

$$U = \frac{u_0}{R} - \frac{1}{R} \frac{dw_0}{d\phi} \quad (11.4.72)$$

which denotes the total rotation of the edge AC. Then $M_{\phi\phi}$ and $M_{\theta\theta}$ can be expressed as

$$M_{\phi\phi} = \frac{D}{R} \left(\frac{dU}{d\phi} + \nu U \cot \phi \right), \quad M_{\theta\theta} = \frac{D}{R} \left(U \cot \phi + \nu \frac{dU}{d\phi} \right) \quad (11.4.73)$$

Thus, we have

$$M_{\phi\phi} - M_{\theta\theta} = \frac{D(1 - \nu)}{R} \left(\frac{dU}{d\phi} - U \cot \phi \right) \quad (11.4.74)$$

Substituting the above expressions into Eq. (11.4.10), we arrive at

$$\frac{d^2U}{d\phi^2} + \frac{dU}{d\phi} \cot \phi - U(\nu + \cot^2 \phi) - \frac{R^2}{D} Q_\phi = 0 \quad (11.4.75)$$

Equations (11.4.3) and (11.4.4) for spherical shells subjected to uniform normal pressure p (symmetrically loaded; Figure 11.4.12) reduce to

$$\begin{aligned} \frac{d}{d\phi} (\sin \phi N_{\phi\phi}) - \cos \phi N_{\theta\theta} + \sin \phi Q_\phi &= 0 \\ \sin \phi N_{\phi\phi} + \sin \phi N_{\theta\theta} - \frac{d}{d\phi} (\sin \phi Q_\phi) &= pR \sin \phi \end{aligned} \quad (11.4.76)$$

Eliminating $N_{\theta\theta}$ between the above two equations, we arrive at

$$-\frac{d}{d\phi} (N_{\phi\phi} \sin^2 \phi) + \frac{d}{d\phi} (Q_\phi \sin \phi \cos \phi) + \frac{d}{d\phi} \left(\frac{pR}{2} \sin^2 \phi \right) = 0 \quad (11.4.77)$$

Integrating with respect to ϕ gives

$$N_{\phi\phi} = Q_\phi \cot \phi + \frac{pR}{2} \quad (11.4.78)$$

where the constant of integration is set to zero. Then $N_{\theta\theta}$ is obtained from the first equation in (11.4.76)

$$N_{\theta\theta} = \frac{dQ_\phi}{d\phi} + \frac{pR}{2} \quad (11.4.79)$$

Thus, both the meridional and hoop forces ($N_{\phi\phi}$, $N_{\theta\theta}$) are expressed in terms of the shear force Q_ϕ .

From the first two equations of (11.4.70) we obtain, for spherical shells, the relations

$$\frac{du_0}{d\phi} + w_0 = \frac{R}{Eh}(N_{\phi\phi} - \nu N_{\theta\theta}), \quad u_0 \cot \phi + w_0 = \frac{R}{Eh}(N_{\theta\theta} - \nu N_{\phi\phi}) \quad (11.4.80)$$

Subtracting the second equation from the first to eliminate w_0 , we obtain

$$\frac{du_0}{d\phi} - u_0 \cot \phi = \frac{R(1+\nu)}{Eh}(N_{\phi\phi} - N_{\theta\theta}) \quad (11.4.81)$$

Differentiating the second equation in (11.4.80),

$$\frac{du_0}{d\phi} \cot \phi - \frac{u_0}{\sin^2 \phi} + \frac{dw_0}{d\phi} = \frac{R}{Eh} \left(\frac{dN_{\theta\theta}}{d\phi} - \nu \frac{dN_{\phi\phi}}{d\phi} \right) \quad (11.4.82)$$

Substituting for $du_0/d\phi$ from Eq. (11.4.81) into Eq. (11.4.82), we arrive at

$$RU \equiv u_0 - \frac{dw_0}{d\phi} = \frac{R}{Eh} \left[(1+\nu) \cot \phi (N_{\phi\phi} - N_{\theta\theta}) - \left(\frac{dN_{\theta\theta}}{d\phi} - \nu \frac{dN_{\phi\phi}}{d\phi} \right) \right] \quad (11.4.83)$$

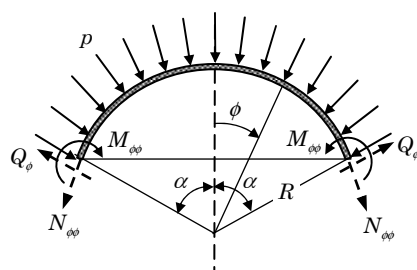


Figure 11.4.12. Spherical pressure vessel subjected to uniform normal pressure.

Finally, substituting for $N_{\phi\phi}$ and $N_{\theta\theta}$ from Eqs. (11.4.78) and (11.4.79) into Eq. (11.4.83), we obtain

$$\frac{d^2Q_\phi}{d\phi^2} + \cot\phi \frac{dQ_\phi}{d\phi} - Q_\phi(\cot^2\phi - \nu) + EhU = 0 \quad (11.4.84)$$

Thus, the problem of solving the bending of a spherical shell under uniform pressure is reduced to the solution of Eqs. (11.4.75) and (11.4.84) for U and Q_ϕ . The solution of these equations is complicated and their approximate solutions are often sought by omitting U , Q_ϕ , and their first derivatives, which are found to be negligibly smaller than their second derivatives in Eqs. (11.4.75) and (11.4.84). See Timoshenko and Woinowsky-Krieger (1970) for additional details.

Under the assumption that U , Q_ϕ , and their first derivatives are negligible, Eqs. (11.4.75) and (11.4.84) reduce to

$$\frac{d^2U}{d\phi^2} - \frac{R^2}{D}Q_\phi = 0, \quad \frac{d^2Q_\phi}{d\phi^2} + EhU = 0 \quad (11.4.85)$$

Eliminating U from the above two equations, we obtain

$$\frac{d^4Q_\phi}{d\phi^4} + 4\lambda^4Q_\phi = 0 \quad (11.4.86)$$

where

$$\lambda^4 = \frac{EhR^2}{4D} = 3(1 - \nu^2)\left(\frac{R}{h}\right)^2 \quad (11.4.87)$$

The general solution of Eq. (11.4.86) is

$$Q_\phi = e^{\lambda\phi}(C_1 \cos \lambda\phi + C_2 \sin \lambda\phi) + e^{-\lambda\phi}(C_3 \cos \lambda\phi + C_4 \sin \lambda\phi) \quad (11.4.88)$$

where C_1 through C_4 are constants to be determined using the boundary conditions at the edges.

Since the bending of shells is of local character, we expect the distributed edge forces to die out towards the interior of the shell. Thus, only the first two terms of the solution (11.4.88) are retained, which decrease with a decrease in ϕ . The solution becomes

$$Q_\phi = e^{\lambda\phi}(C_1 \cos \lambda\phi + C_2 \sin \lambda\phi) \quad (11.4.89)$$

From Eqs. (11.4.78) and (11.4.79), the meridional and hoop forces ($N_{\phi\phi}$, $N_{\theta\theta}$) are computed as

$$\begin{aligned} N_{\phi\phi} &= e^{\lambda\phi}[C_1 \cos \lambda\phi + C_2 \sin \lambda\phi] \cot\phi + \frac{pR}{2} \\ N_{\theta\theta} &= \lambda e^{\lambda\phi} [(C_1 + C_2) \cos \lambda\phi + (C_2 - C_1) \sin \lambda\phi] + \frac{pR}{2} \end{aligned} \quad (11.4.90)$$

Next, we consider couple of examples of spherical shells with specific edge conditions and determine the constants C_1 and C_2 .

Example 11.4.9

Consider a spherical shell with half angle α and subjected to (a) bending moments M_α at the edges [Figure 11.4.13(a)] and (b) horizontal forces F_H [Figure 11.4.13(b)]. We wish to determine the forces and moments in the shell.

For convenience, the solution in Eq. (11.4.89) is expressed in the following alternative form

$$Q_\phi(\psi) = Ce^{-\lambda\psi} \sin(\lambda\psi + \beta) \quad (11.4.91)$$

where $\psi = \alpha - \phi$ and C and β are constants to be determined using the boundary conditions. The forces $N_{\phi\phi}$ and $N_{\theta\theta}$ become ($p = 0$)

$$\begin{aligned} N_{\phi\phi}(\psi) &= Q_\phi \cot \phi = Ce^{-\lambda\psi} \sin(\lambda\psi + \beta) \cot(\alpha - \psi) \\ N_{\theta\theta}(\psi) &= \frac{dQ_\phi}{d\phi} = \sqrt{2} \lambda Ce^{-\lambda\psi} \sin\left(\lambda\psi + \beta - \frac{\pi}{4}\right) \end{aligned} \quad (11.4.92)$$

The function U is computed using Eq. (11.4.85)

$$U(\psi) = -\frac{1}{Eh} \frac{d^2 Q_\phi}{d\phi^2} = \frac{2\lambda^2}{Eh} Ce^{-\lambda\psi} \cos(\lambda\psi + \beta) \quad (11.4.93)$$

The approximate bending moments are obtained by neglecting U (but not its derivative) from Eq. (11.4.73)

$$\begin{aligned} M_{\phi\phi}(\psi) &= \frac{D}{R} \frac{dU}{d\phi} = -\frac{R}{\sqrt{2}\lambda} Ce^{-\lambda\psi} \sin(\lambda\psi + \beta + \frac{\pi}{4}) \\ M_{\theta\theta}(\psi) &= \frac{\nu D}{R} \frac{dU}{d\phi} = \frac{D}{R} \frac{dU}{d\phi} = -\frac{\nu R}{\sqrt{2}\lambda} Ce^{-\lambda\psi} \sin(\lambda\psi + \beta + \frac{\pi}{4}) \end{aligned} \quad (11.4.94)$$

The horizontal displacement δ_H in a plane of the parallel circles can be obtained projecting the displacement components u_0 and w_0 on that plane. We have

$$\delta_H = u_0 \cos \phi + w_0 \sin \phi$$

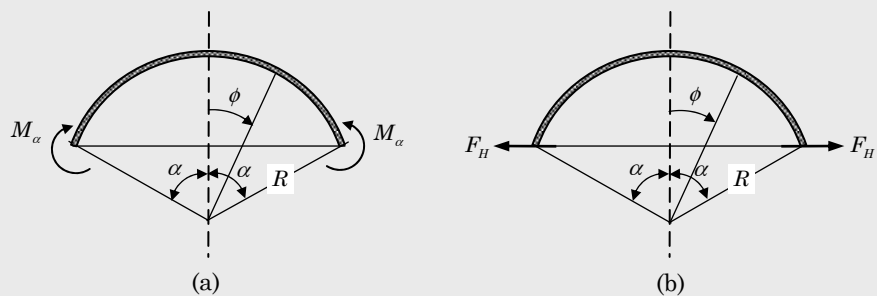


Figure 11.4.13. Spherical pressure vessel subjected to different edge conditions. (a) Subjected to end moments M_α . (b) Subjected to horizontal forces F_H .

Since δ_H represents the increase in the radius of r_0 of the parallel circle, we can also compute it from

$$\begin{aligned}\delta_H(\psi) &= R \sin \phi \varepsilon_{\theta\theta} = \frac{R \sin \phi}{Eh} (N_{\theta\theta} - \nu N_{\phi\phi}) \\ &= \frac{R}{Eh} \sqrt{2} \lambda C e^{-\lambda\psi} \sin(\lambda\psi + \beta - \frac{\pi}{4})\end{aligned}\quad (11.4.95)$$

For the shell in Figure 11.4.13(a), the boundary conditions at $\phi = \alpha$ or $\psi = 0$ are

$$M_{\phi\phi}(0) = M_\alpha, \quad N_{\phi\phi}(0) = 0 \quad (11.4.96)$$

The second boundary condition is satisfied by taking $\beta = 0$ [see Eq. (11.4.92)]. The first boundary condition yields [see Eq. 11.4.94)]

$$C = -\frac{2\lambda}{R} M_\alpha \quad (11.4.97)$$

The edge forces, moments, and displacement are obtained by substituting the value of C from Eq. (11.4.97) and setting $\psi = \beta = 0$ in Eqs. (11.4.90)–(11.4.95). In particular, the rotation U and horizontal displacement δ_H of the edge are

$$U(0) = \frac{4\lambda^3 M_\alpha}{EhR}, \quad \delta_H(0) = -\frac{2\lambda^2 M_\alpha \sin \alpha}{Eh} \quad (11.4.98)$$

For the shell in Figure 11.4.13(b), the boundary conditions at $\phi = \alpha$ or $\psi = 0$ are

$$M_{\phi\phi}(0) = 0, \quad N_{\phi\phi}(0) = -F_H \cos \alpha \quad (11.4.99)$$

The first boundary condition is satisfied by taking $\beta = -\frac{\pi}{4}$ [see Eq. (11.4.94)]. The second boundary condition yields [see Eq. (11.4.92)]

$$C = \frac{2F_H \sin \alpha}{\sqrt{2}} \quad (11.4.100)$$

The edge forces, moments, and displacement are obtained by substituting the value of C from Eq. (11.4.100) and setting $\psi = 0$ and $\beta = -(\pi/4)$ in Eqs. (11.4.90)–(11.4.95). The rotation U and horizontal displacement δ_H of the edge are

$$U(0) = -\frac{2\lambda^2 F_H \sin \alpha}{Eh}, \quad \delta_H(0) = \frac{2R\lambda F_H \sin^2 \alpha}{Eh} \quad (11.4.101)$$

Example 11.4.10

Consider a spherical shell with half angle α , clamped at its edges and subjected to uniformly distributed force p , as shown in Figure 11.4.14(a). We wish to determine the forces and moments in the shell.

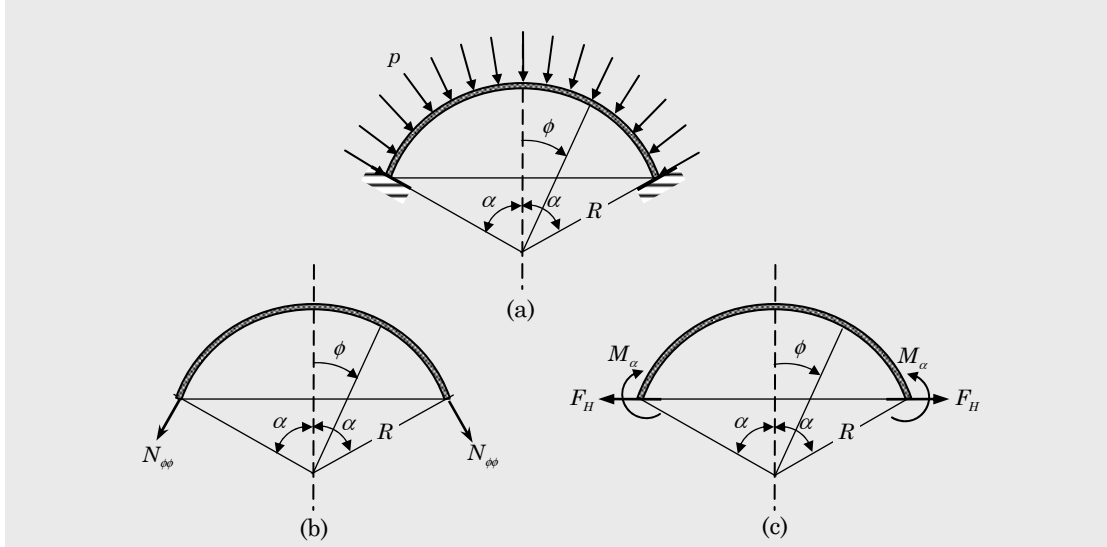


Figure 11.4.14. (a) Clamped spherical shell subjected to uniform normal pressure. (b) Membrane forces. (c) Bending forces.

In this case, the shell experiences the membrane force field shown in Figure 11.4.14(b) and the forces and bending moments shown in Figure 11.4.14(c). The membrane forces are given by

$$N_{\phi\phi} = N_{\theta\theta} = \frac{pR}{2} \quad (11.4.102)$$

The edge experiences no rotation and undergoes horizontal displacement of δ_H if it were free to move horizontally

$$\delta_H = \frac{R \sin \alpha}{Eh} (N_{\theta\theta} - \nu N_{\phi\phi}) = \frac{pR^2(1-\nu)}{2Eh} \sin \alpha \quad (11.4.103)$$

The bending moment M_α and shear force F_H are such that they produce a horizontal displacement of $-\delta_H$ and zero rotation.

Superposing the rotations and displacements from Eqs. (11.4.98) and (11.4.101) of Example 11.4.9, we require

$$\begin{aligned} \frac{4\lambda^3 M_\alpha}{EhR} - \frac{2\lambda^2 F_H \sin \alpha}{Eh} &= 0 \\ -\frac{2\lambda^2 M_\alpha \sin \alpha}{Eh} + \frac{2R\lambda F_H \sin^2 \alpha}{Eh} &= -\frac{pR^2(1-\nu)}{2Eh} \end{aligned} \quad (11.4.104)$$

whose solution gives

$$\begin{aligned} M_\alpha &= -\frac{pR^2(1-\nu)}{4\lambda^2} = -\frac{pRh}{4} \sqrt{\frac{1-\nu}{3(1+\nu)}} \\ F_H &= \frac{2\lambda M_\alpha}{R \sin \alpha} = -\frac{pR(1-\nu)}{2\lambda \sin \alpha} \end{aligned} \quad (11.4.105)$$

11.5 Vibration and Buckling of Circular Cylinders

11.5.1 Equations of Motion

In this section, we consider analytical solutions for free vibration and buckling of cylindrical shells. Although the procedure presented here can be used to study bending response, the discussion is limited to vibration and buckling. We consider consider the case of thin shells, so that we can assume $N_{12} = N_{21}$ and $M_{12} = M_{21}$.

The equations of motion of a circular cylindrical shell ($1/R_1 = 0$ and $R_2 = R$) with $C_0 = 0$ and in the absence of body forces can be obtained from Eqs. (11.3.1)–(11.3.5) for the first-order shear deformations shell theory (FST):

$$\begin{aligned}\frac{\partial N_{11}}{\partial x_1} + \frac{\partial N_{21}}{\partial x_2} &= I_0 \frac{\partial^2 u_1^0}{\partial t^2} \\ \frac{\partial N_{12}}{\partial x_1} + \frac{\partial N_{22}}{\partial x_2} + \frac{Q_2}{R} &= I_0 \frac{\partial^2 u_2^0}{\partial t^2} \\ \frac{\partial M_{11}}{\partial x_1} + \frac{\partial M_{21}}{\partial x_2} - Q_1 &= I_2 \frac{\partial^2 \phi_1}{\partial t^2} \\ \frac{\partial M_{12}}{\partial x_1} + \frac{\partial M_{22}}{\partial x_2} - Q_2 &= I_2 \frac{\partial^2 \phi_2}{\partial t^2} \\ \frac{\partial Q_1}{\partial x_1} + \frac{\partial Q_2}{\partial x_2} - \frac{N_{22}}{R} - \hat{N} \frac{\partial^2 u_3^0}{\partial x_1^2} &= I_0 \frac{\partial^2 u_3^0}{\partial t^2}\end{aligned}\quad (11.5.1)$$

where R is the radius of the cylinder, \hat{N} is the axial compressive load (positive in compression), (u_1^0, u_2^0, u_3^0) are the displacement components along the $(x_1, x_2, x_3 = \zeta)$ axes (Figure 11.5.1), ϕ_1 and ϕ_2 are the rotation functions, and I_i ($i = 0, 2$) are the mass inertia terms defined in Eq. (11.2.54):

$$I_i = \int_{-\frac{h}{2}}^{\frac{h}{2}} \rho(\zeta)^i d\zeta, \quad i = 0, 1, 2 \quad (11.5.2)$$

Here, ρ is the material mass density.

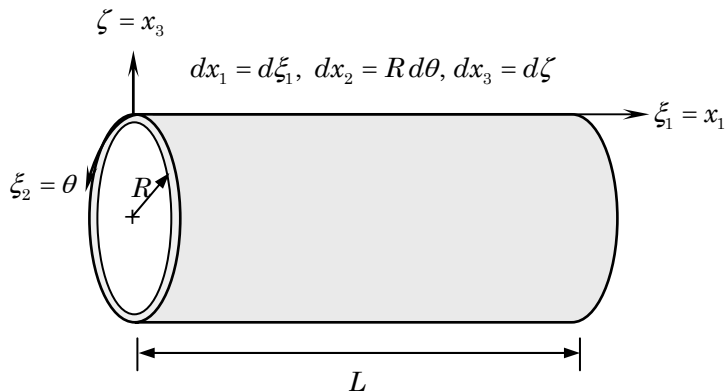


Figure 11.5.1. Geometry and coordinate system used for a cylinder.

The stress resultants can be expressed in terms of strains as

$$\begin{aligned} N_{11} &= A_{11}\varepsilon_{11}^0 + A_{12}\varepsilon_{22}^0, \quad N_{22} = A_{12}\varepsilon_{11}^0 + A_{22}\varepsilon_{22}^0 \\ M_{11} &= D_{11}\varepsilon_{11}^1 + D_{12}\varepsilon_{22}^1, \quad M_{22} = D_{12}\varepsilon_{11}^1 + D_{22}\varepsilon_{22}^1 \\ N_{12} &= N_{21} = A_{66}\varepsilon_{12}^0, \quad M_{12} = M_{21} = D_{66}\varepsilon_{12}^1 \\ Q_1 &= K_s A_{55}\varepsilon_{13}^0, \quad Q_2 = K_s A_{44}\varepsilon_{23}^0 \end{aligned} \quad (11.5.3)$$

where K_s is the shear correction factor, and the strains are given by

$$\begin{aligned} \varepsilon_{11}^0 &= \frac{\partial u_1^0}{\partial x_1}, & \varepsilon_{11}^1 &= \frac{\partial \phi_1}{\partial x_1}, & \varepsilon_{22}^0 &= \frac{\partial u_2^0}{\partial x_2} + \frac{u_3^0}{R} \\ \varepsilon_{22}^1 &= \frac{\partial \phi_2}{\partial x_2}, & \varepsilon_{12}^0 &= \frac{\partial u_2^0}{\partial x_1} + \frac{\partial u_1^0}{\partial x_2}, & \varepsilon_{12}^1 &= \frac{\partial \phi_2}{\partial x_1} + \frac{\partial \phi_1}{\partial x_2} \\ \varepsilon_{23}^0 &= \phi_2 + \frac{\partial u_3^0}{\partial x_2}, & \varepsilon_{13}^0 &= \phi_1 + \frac{\partial u_3^0}{\partial x_1} \end{aligned} \quad (11.5.4)$$

The equations of motion of the classical shell theory (CST), wherein the transverse shear strains ε_4^0 and ε_5^0 are neglected, are obtained from Eq. (11.5.1) by setting

$$\phi_1 = -\frac{\partial u_3^0}{\partial x_1}, \quad \phi_2 = -\frac{\partial u_3^0}{\partial x_2}$$

and replacing Q_1 and Q_2 in the second and fifth equations using the third and fourth equations of Eq. (11.5.1):

$$\begin{aligned} \frac{\partial N_{11}}{\partial x_1} + \frac{\partial N_{12}}{\partial x_2} &= I_0 \frac{\partial^2 u_1^0}{\partial t^2} \\ \frac{\partial N_{12}}{\partial x_1} + \frac{\partial N_{22}}{\partial x_2} + \frac{1}{R} \left(\frac{\partial M_{12}}{\partial x_1} + \frac{\partial M_{22}}{\partial x_2} \right) &= I_0 \frac{\partial^2 u_2^0}{\partial t^2} - \frac{I_2}{R} \frac{\partial^3 u_3^0}{\partial x_1 \partial t^2} \\ \frac{\partial^2 M_{11}}{\partial x_1^2} + \frac{\partial^2 M_{22}}{\partial x_2^2} + 2 \frac{\partial^2 M_{12}}{\partial x_1 \partial x_2} - \frac{N_2}{R} - \hat{N} \frac{\partial^2 u_3^0}{\partial x_1^2} &= I_0 \frac{\partial^2 u_3^0}{\partial t^2} - I_2 \frac{\partial^2}{\partial t^2} \left(\frac{\partial^2 u_3^0}{\partial x_1^2} + \frac{\partial^2 u_3^0}{\partial x_2^2} \right) \end{aligned} \quad (11.5.5)$$

11.5.2 Governing Equations in Terms of Displacements

The equations of motion can be expressed in terms of generalized displacements, $(u_1^0, u_2^0, u_3^0, \phi_1, \phi_2)$ in FST and (u_1^0, u_2^0, u_3^0) in CST, by substituting Eqs. (11.5.4) into equations (11.5.3) and the results into Eq. (11.5.1) for FST and Eq. (11.5.5) for CST. The resulting partial differential equations can be expressed in matrix operator form as

$$[L]\{\Delta\} = \{0\} \quad (11.5.6)$$

where the coefficients of the linear operator L ($L_{ij} = L_{ji}$) and displacement vector $\{\Delta\}$ for the two theories are given below. Note that the second inertia term of the second equation in (11.5.5) is neglected to facilitate the solution.

Classical shell theory (CST): $\{\Delta\} = \{u_1^0, u_2^0, u_3^0\}^T$

$$\begin{aligned} L_{11} &= A_{11} \frac{\partial^2}{\partial x_1^2} + A_{66} \frac{\partial^2}{\partial x_2^2} - I_0 \frac{\partial^2}{\partial t^2} \\ L_{12} &= (A_{12} + A_{66}) \frac{\partial^2}{\partial x_1 \partial x_2}, \quad L_{13} = \frac{A_{12}}{R} \frac{\partial}{\partial x_1} \\ L_{22} &= A_{66} \frac{\partial^2}{\partial x_1^2} + A_{22} \frac{\partial^2}{\partial x_2^2} - I_0 \frac{\partial^2}{\partial t^2}, \quad L_{23} = \frac{A_{22}}{R} \frac{\partial}{\partial x_2} \\ L_{33} &= D_{11} \frac{\partial^4}{\partial x_1^4} + 2(D_{12} + 2D_{66}) \frac{\partial^4}{\partial x_1^2 \partial x_2^2} + D_{22} \frac{\partial^4}{\partial x_2^4} + \hat{N} \\ &\quad + \frac{A_{22}}{R^2} + I_0 \frac{\partial^2}{\partial t^2} - I_2 \frac{\partial^2}{\partial t^2} \left(\frac{\partial^2}{\partial x_1^2} + \frac{\partial^2}{\partial x_2^2} \right) \end{aligned} \quad (11.5.7)$$

First-order shell theory (FST): $\{\Delta\} = \{u_1^0, u_2^0, \phi_1, \phi_2, u_3^0\}^T$

$$\begin{aligned} L_{11} &= A_{11} \frac{\partial^2}{\partial x_1^2} + A_{66} \frac{\partial^2}{\partial x_2^2} - I_0 \frac{\partial^2}{\partial t^2}, & L_{12} &= (A_{12} + A_{66}) \frac{\partial^2}{\partial x_1 \partial x_2} \\ L_{22} &= A_{66} \frac{\partial^2}{\partial x_1^2} + A_{22} \frac{\partial^2}{\partial x_2^2} - I_0 \frac{\partial^2}{\partial t^2}, & L_{15} &= \frac{A_{12}}{R} \frac{\partial}{\partial x_1} \\ L_{33} &= -K_s A_{55} + D_{11} \frac{\partial^2}{\partial x_1^2} + D_{66} \frac{\partial^2}{\partial x_2^2} - I_2 \frac{\partial^2}{\partial t^2}, & L_{25} &= \frac{A_{22}}{R} \frac{\partial}{\partial x_2} \\ L_{35} &= -K_s A_{55} \frac{\partial}{\partial x_1}, & L_{34} &= (D_{12} + D_{66}) \frac{\partial^2}{\partial x_1 \partial x_2} \\ L_{44} &= -K_s A_{44} + D_{66} \frac{\partial^2}{\partial x_1^2} + D_{22} \frac{\partial^2}{\partial x_2^2} - I_2 \frac{\partial^2}{\partial t^2}, & L_{45} &= -K_s A_{44} \frac{\partial}{\partial x_2} \\ L_{55} &= \frac{A_{22}}{R} + (\hat{N} - K_s A_{55}) \frac{\partial^2}{\partial x_1^2} - K_s A_{44} \frac{\partial^2}{\partial x_2^2} + I_0 \frac{\partial^2}{\partial t^2} \end{aligned} \quad (11.5.8)$$

and $L_{13} = L_{14} = L_{23} = L_{24} = 0$. Note that the longitudinal, circumferential and rotary inertia terms are included. The bending-extensional coupling is reflected in the coefficients L_{13} and L_{23} of CST and coefficients L_{15} and L_{25} of FST, which are never zero for shells; of course, for plates ($R \rightarrow \infty$), the bending and extensional deformations become uncoupled.

11.5.3 The Lévy Solutions

Here we discuss the Lévy-type solution procedure for shells [see Nosier and Reddy (1992a,b)]. The coordinate system in Figure 11.5.1 is shifted to the center of the shell such that $-L/2 \leq x_1 \leq L/2$ for convenience. For circular cylindrical shells with arbitrary boundary conditions at $x_1 = \pm L/2$, we assume the following representation for the generalized displacement components:

$$\begin{Bmatrix} u_1^0 \\ u_2^0 \\ \phi_1 \\ \phi_2 \\ u_3^0 \end{Bmatrix} = \begin{Bmatrix} U_m(x_1) \cos \beta x_2 \\ V_m(x_1) \sin \beta x_2 \\ X_m(x_1) \cos \beta x_2 \\ Y_m(x_1) \sin \beta x_2 \\ W_m(x_1) \cos \beta x_2 \end{Bmatrix} T_m(t), \quad \beta = m/R \quad (m = 0, 1, 2, \dots) \quad (11.5.9)$$

where $T_m = e^{i\omega_m t}$ and $i = \sqrt{-1}$, ω_m being the natural frequency corresponding to the m th mode when performing an eigenfrequency analysis (we keep in mind that there are denumerable infinite frequencies for each value of m). Since the solution technique presented for these equations is general, we present only the equations of FST and include the numerical results of CST for the sake of comparison. Substitution of Eq. (11.5.9) into Eq. (11.5.6) results in five for FST and three for CST coupled ordinary differential equations. For FST, they can be expressed in the form

$$\begin{aligned} U''_m &= C_1 U_m + C_2 V'_m + C_3 X_m + C_4 Y'_m + C_5 W'_m \\ V''_m &= C_6 U'_m + C_7 V_m + C_8 X'_m + C_9 Y_m + C_{10} W_m \\ X''_m &= C_{11} U_m + C_{12} V'_m + C_{13} X_m + C_{14} Y'_m + C_{15} W'_m \\ Y''_m &= C_{14} U'_m + C_{17} V_m + C_{18} X'_m + C_{19} Y_m + C_{20} W_m \\ W''_m &= C_{21} U'_m + C_{22} V_m + C_{23} X'_m + C_{24} Y_m + C_{25} W_m \end{aligned} \quad (11.5.10)$$

where a prime indicates a derivative with respect to x_1 . The coefficients C_j ($j = 1, 2, \dots, 25$) are given for free vibration analysis by

$$\begin{aligned} C_1 &= (e_2 - e_1 e_{14})/e_{26}, & C_2 &= (e_3 - e_1 e_{17})/e_{26}, & C_3 &= (e_4 - e_1 e_{16})/e_{26} \\ C_4 &= (e_5 - e_1 e_{17})/e_{26}, & C_5 &= (e_6 - e_1 e_{18})/e_{26}, & C_6 &= (e_8 - e_7 e_{20})/e_{27} \\ C_7 &= (e_3 - e_7 e_{21})/e_{27}, & C_8 &= (e_{10} - e_7 e_{22})/e_{27}, & C_9 &= (e_{11} - e_7 e_{23})/e_{27} \\ C_{10} &= (e_{12} - e_7 e_{24})/e_{27}, & C_{11} &= (e_{14} - e_{13} e_2)/e_{26}, & C_{12} &= (e_{15} - e_{13} e_3)/e_{26} \\ C_{13} &= (e_{16} - e_{13} e_4)/e_{26}, & C_{14} &= (e_{17} - e_{13} e_5)/e_{26}, & C_{15} &= (e_{18} - e_{13} e_6)/e_{26} \\ C_{16} &= (e_{20} - e_{19} e_8)/e_{27}, & C_{17} &= (e_{21} - e_{19} e_9)/e_{27}, & C_{18} &= (e_{22} - e_{19} e_{10})/e_{27} \\ C_{19} &= (e_{23} - e_{19} e_{11})/e_{27}, & C_{20} &= (e_{24} - e_{19} e_{12})/e_{27}, & C_{21} &= e_{28}/e_{25} \\ C_{22} &= e_{29}/e_{25}, & C_{23} &= e_{30}/e_{25}, & C_{24} &= e_{31}/e_{25}, & C_{25} &= e_{32}/e_{25} \end{aligned} \quad (11.5.11)$$

where

$$\begin{aligned} e_1 &= B_{11}/A_{11}, & e_2 &= (A_{66}\beta^2 - \omega_m^2 I_0)/A_{11}, & e_3 &= -\beta(A_{12} + A_{66})/A_{11} \\ e_4 &= B_{66}\beta^2, & e_5 &= -\beta(B_{12} + B_{66})/A_{11}, & e_6 &= -A_{12}/(A_{11}R) \\ e_7 &= B_{66}/A_{66}, & e_8 &= \beta(A_{12} + A_{66})/A_{66}, & e_9 &= (A_{22}\beta^2 - \omega_m^2 I_0)/A_{66} \\ e_{10} &= \beta(B_{12} + B_{66})/A_{66}, & e_{11} &= B_{22}\beta^2, & e_{12} &= \beta A_{22}/(A_{66}R) \\ e_{13} &= B_{11}/D_{11}, & e_{14} &= B_{66}\beta^2, & e_{15} &= -\beta(B_{12} + B_{66})/D_{11} \\ e_{16} &= (K_s A_{55} + D_{66}\beta^2 - \omega_m^2 I_2)/D_{11}, & e_{17} &= -\beta(D_{12} + D_{66})/D_{11} \\ e_{18} &= -(B_{12}/R - K_s A_{55})/D_{11}, & e_{19} &= B_{66}/D_{66}, & e_{20} &= \beta(B_{12} + B_{66})/D_{66} \\ e_{21} &= B_{22}\beta^2, & e_{22} &= \beta(D_{12} + D_{66})/D_{66} \\ e_{23} &= (K_s A_{44} + D_{22}\beta^2 - \omega_m^2 I_2)/D_{66}, & e_{24} &= \beta(B_{22}/R - K_s A_{44})/D_{66} \\ e_{25} &= K_s A_{55} - \hat{N}, & e_{26} &= 1 - e_1 e_{13}, & e_{27} &= 1 - e_7 e_{19}, & e_{28} &= A_{12}/R \\ e_{29} &= \beta A_{22}/R, & e_{30} &= -K_s A_{55} + B_{12}/R, & e_{31} &= \beta(-K_s A_{44} + B_{22}/R) \\ e_{32} &= K_s A_{44}\beta^2 - \omega_m^2 I_0 + A_{22}/R^2 \end{aligned} \quad (11.5.12)$$

In the stability analysis, we let $\omega_m \rightarrow 0$ in e_j ($j = 1, 2, \dots, 32$).

With some simple algebraic operations, it is made sure that only one unknown variable with its highest derivative appears in equations (11.5.10). This will save the computational time required in the method that we introduce next for solving equations (11.5.10).

There exists a number of ways to solve a system of ordinary differential equations. However, when there are more than three governing equations, as in Eq. (11.5.10), it is more practical to introduce new unknown variables and replace the original system of equations by an equivalent system of first-order equations (to be able to use the state-space approach). We introduce the following variables:

$$\begin{aligned} Z_{1m} &= U_m(x_1), & Z_{2m}(x_1) &= U'_m(x_1) = Z'_{1m}(x_1) \\ Z_{3m} &= V_m(x_1), & Z_{4m}(x_1) &= V'_m(x_1) = Z'_{3m}(x_1) \\ Z_{5m} &= X_m(x_1), & Z_{6m}(x_1) &= X'_m(x_1) = Z'_{5m}(x_1) \\ Z_{7m} &= Y_m(x_1), & Z_{8m}(x_1) &= Y'_m(x_1) = Z'_{9m}(x_1) \\ Z_{9m} &= W_m(x_1), & Z_{10m}(x_1) &= W'_m(x_1) = Z'_{9m}(x_1) \end{aligned} \quad (11.5.13)$$

for $m = 1, 2, \dots$. In view of the definitions in (11.5.13), Eqs. (11.5.10) along with relations in (11.5.13) can be expressed in the form

$$\{Z'\} = [A]\{Z\} \quad (11.5.14)$$

where

$$\{Z'\} = \{Z'_{1m}, Z'_{2m}, \dots, Z'_{10m}\}^T, \quad \{Z\} = \{Z_{1m}, Z_{2m}, \dots, Z_{10m}\}^T \quad (11.5.15)$$

and the coefficient matrix $[A]$ is

$$[A] = \begin{bmatrix} 0 & 1 & 0 & 0 & 0 & 0 & 0 & 0 & 0 & 0 \\ C_1 & 0 & 0 & C_2 & C_3 & 0 & 0 & C_4 & 0 & C_5 \\ 0 & 0 & 0 & 1 & 0 & 0 & 0 & 0 & 0 & 0 \\ 0 & C_4 & C_7 & 0 & 0 & C_8 & C_9 & 0 & C_{10} & 0 \\ 0 & 0 & 0 & 0 & 1 & 0 & 0 & 0 & 0 & 0 \\ C_{11} & 0 & C_{12} & C_{13} & 0 & 0 & C_{14} & 0 & C_{15} & 0 \\ 0 & 0 & 0 & 0 & 0 & 0 & 1 & 0 & 0 & 0 \\ 0 & C_{16} & C_{17} & 0 & 0 & C_{18} & C_{19} & 0 & C_{20} & 0 \\ 0 & 0 & 0 & 0 & 0 & 0 & 0 & 0 & 0 & 1 \\ 0 & C_{21} & C_{22} & 0 & 0 & C_{23} & C_{24} & 0 & C_{25} & 0 \end{bmatrix} \quad (11.5.16)$$

A formal solution of Eq. (11.5.14) is obtained using the state-space approach [see Gopal (1984) and Ogata (1967)] as

$$\{Z(x_1)\} = \Psi(x_1)\{D\} \quad (11.5.17)$$

where $\Psi(x_1)$ is a fundamental matrix, the columns of which consist of 10 linearly independent solutions of equations (11.5.10) and $\{D\}$ is an unknown constant vector. Some or all components of this vector, as will be seen later, are in general complex. The nonsingular fundamental matrix $\Psi(x_1)$ is not unique. However, all fundamental matrices differ from each other by a multiplicative constant matrix. Since equations

(11.5.17) are the solutions of equations (11.5.10) and $\Psi(0)$ is a nonsingular constant matrix, a special fundamental matrix $\Phi(x_1)$ (known as the state transition matrix) for Eq. (11.5.10) can be defined from Eq. (11.5.17) such that

$$\{Z(x_1)\} = \Phi(x_1)\{Z(0)\} \quad (11.5.18)$$

are also the solutions of equations (11.5.10), with

$$\Phi(x_1) = \Psi(x_1)\Psi^{-1}(0) \quad \text{and} \quad \{D\} = \Psi^{-1}(0)\{Z(0)\} \quad (11.5.19)$$

Since $[A]$ is a constant matrix, the state transition matrix is given by a matrix exponential function as

$$\Phi(x_1) = e^{[A]x_1} \quad (11.5.20)$$

By imposing the 10 boundary conditions at $x_1 = \pm L/2$ on the solution given by Eq. (11.5.17), a homogeneous system of algebraic equations can be found:

$$[M]\{Z(0)\} = \{0\} \quad (11.5.21)$$

For a nontrivial solution of natural frequency or critical buckling load, the determinant of the coefficient matrix $[M]$ must be set to zero

$$|M| = 0 \quad (11.5.22)$$

Since the constant vector $\{Z(0)\}$ is real, the determinant of $[M]$ is also real. Hence, in a trial and error procedure, one can easily find the correct value of natural frequency (in a free vibration problem) or of critical buckling load (in a stability problem), which would make $|M| = 0$. A nonzero compressive (or tensile) edge load can also be included in the free vibration analysis.

Numerous methods are available [e.g., see Gopal (1984) and Ogata (1967)] for determining the matrix exponential, $e^{[A]x_1}$, appearing in equation (11.5.20). However, regardless of any method used, it is found that $|M|$ becomes ill conditioned when the ratio of the characteristic length of the structure to its thickness is near or larger than 20. This is also the case in the Lévy-type eigenfrequency and stability problems of laminated plates and shell panels when shear deformation theories are used.

When the eigenvalues of the coefficient matrix $[A]$ are distinct, the fundamental matrix $\Psi(x_1)$ is given by

$$\Psi(x_1) = [U][Q(x_1)], \quad (11.5.23)$$

where $[Q(x_1)]$ is another fundamental matrix, defined as

$$[Q(x_1)] = \begin{bmatrix} e^{\lambda_1 x_1} & & & 0 \\ & e^{\lambda_2 x_1} & & \\ & & \ddots & \\ 0 & & & e^{\lambda_{10} x_1} \end{bmatrix} \quad (11.5.24)$$

and $[U]$ is a modal matrix that transforms $[A]$ into a diagonal form (i.e., the j th column of $[U]$ constitutes the eigenvectors of $[A]$ corresponding to the j th eigenvalue

of $[A]$). In Eq. (11.5.20), λ_j ($j = 1, 2, \dots, 10$) are the distinct eigenvalues of $[A]$, which in general can be real and complex. We note that the eigenvalues of $[A]$ are the same as the roots of the auxiliary equation of (11.5.19). These eigenvalues in most eigenfrequency and stability problems of plates and shells are distinct. The axisymmetric buckling problem and axisymmetric eigenfrequency problem (when all inertia forces, except the radial inertia force, are neglected) of a cylindrical shell are two examples where two of the eigenvalues, as will be seen, are identical. When the eigenvalues are repeated, Eq. (11.5.24) is no longer valid and a Jordan canonical form of $[A]$ must be used.

Substituting Eq. (11.5.23) into Eqs. (11.5.19) yields

$$\Phi(x_1) = [U][Q(x_1)][U]^{-1} \quad (11.5.25)$$

and

$$\{D\} = [U]^{-1}\{Z(0)\} \quad (11.5.26)$$

Equations (11.5.18) and (11.5.25) were used in Nosier and Reddy (1992a). However, due to the occurrence of an ill-conditioned determinant $|M|$ in Eq. (11.5.22), Nosier and Reddy (1992b) proposed the following approach. Instead of imposing the boundary conditions on Eq. (11.5.18), impose the boundary conditions on Eq. (11.5.17), which have a simpler form. This way we come up with a set of homogeneous algebraic equations of the form

$$[K]\{D\} = \{0\} \quad (11.5.27)$$

For a nontrivial solution of Eq. (11.5.27) to exist, the determinant of the generally complex coefficient matrix $[K]$ must vanish. Since, in general, $[K]$ can be complex, it may be computationally more convenient to substitute Eq. (11.5.26) into Eq. (11.5.27) to obtain

$$[K][U]^{-1}\{Z(0)\} = \{0\} \quad (11.5.28a)$$

and set the coefficient matrix in Eq. (11.5.28a) to zero:

$$|([K][U]^{-1})| = 0 \quad (11.5.28b)$$

In this way the determinant in Eq. (11.5.28b) will always be a real number. However, it will have the same computational problem as $|M|$ in Eq. (11.5.22). The key point in overcoming this difficulty is to rewrite Eq. (11.5.28b) as

$$|K|/|U| = 0 \quad (11.5.29)$$

that is, to evaluate the determinants of $[K]$ and $[U]$ separately, rather than evaluating the determinant of $([K][U]^{-1})$. It should also be noted that, in this way, the inverse of $[U]$ is never needed. For very thin shells (or long shells), computer overflow and underflow may occur when we evaluate the elements of the coefficient matrix $[K]$. However, it should be kept in mind that the determinant of $[K]$ never becomes ill conditioned. In summary, after assuming a trial value for natural frequency (in free vibration analysis) or for buckling load (in stability analysis) for a particular m , we will impose the 10 boundary conditions at $x_1 = \pm L/2$ on Eq. (11.5.17), derive Eq.

(11.5.27) and check whether Eq. (11.5.29) is satisfied. It should be remembered that $|U|$ appearing in Eq. (11.5.29) is never zero, since the eigenvectors in $[U]$ are independent of each other.

A remark must be made concerning the computation of eigenvalues and eigenvectors of the coefficient matrix $[A]$. Since the diagonal elements of $[A]$ are all zero, during the computation of eigenvalues and eigenvectors computer overflow or underflow may occur. To resolve this problem, we can subtract a nonzero constant number from the diagonal elements of $[A]$ and compute the eigenvalues and eigenvectors of the new matrix. The eigenvalues of $[A]$ can then be obtained by adding the same number to each eigenvalue of the new matrix. The eigenvectors of $[A]$ will be identical to those of the new matrix.

11.5.4 Boundary Conditions

A combination of boundary conditions may be assumed to exist at the edges of the shell. Here we classify these boundary conditions for the FST according to Nosier and Reddy (1992b):

Simply supported

$$\begin{aligned} S1: \quad & u_3^0 = M_1 = \phi_2 = N_1 = N_6 = 0, \quad S2: \quad u_3^0 = M_1 = \phi_2 = u_1^0 = N_6 = 0 \\ S3: \quad & u_3^0 = M_1 = \phi_2 = N_1 = u_2^0 = 0, \quad S4: \quad u_3^0 = M_1 = \phi_2 = u_1^0 = u_2^0 = 0 \end{aligned} \quad (11.5.30)$$

Clamped

$$\begin{aligned} C1: \quad & u_3^0 = \phi_1 = \phi_2 = N_1 = N_6 = 0, \quad C2: \quad u_3^0 = \phi_1 = \phi_2 = u_1^0 = N_6 = 0 \\ C3: \quad & u_3^0 = \phi_1 = \phi_2 = N_1 = u_2^0 = 0, \quad C4: \quad u_3^0 = \phi_1 = \phi_2 = u_1^0 = u_2^0 = 0 \end{aligned} \quad (11.5.31)$$

Free edge

$$F: \quad N_1 = N_4 = M_1 = M_4 = Q_1 - \hat{N} \frac{\partial u_3^0}{\partial x_1} = 0 \quad (11.5.32)$$

The boundary type S3 is referred to as a shear diaphragm by Leissa (1973). Similar boundary conditions may also be classified for the CST [see Nosier and Reddy (1992b)].

In the above discussion, it was assumed that $m \neq 0$ (nonaxisymmetric case). For axisymmetric mode (i.e., when $m = 0$), we have $u_2^0 = \phi_2 = 0$, and Eqs. (11.5.9) and (11.5.10) become

$$(u_1^0, \phi_1, u_3^0) = (U_0, X_0, W_0)T_0(t) \quad (11.5.33)$$

and

$$\begin{aligned} U_0'' &= \bar{C}_1 U_0 + \bar{C}_3 X_0 + \bar{C}_3 W_0' \\ X_0'' &= \bar{C}_4 U_0 + \bar{C}_5 X_0 + \bar{C}_4 W_0' \\ W_0'' &= \bar{C}_7 U_0' + \bar{C}_8 X_0' + \bar{C}_9 W_0 \end{aligned} \quad (11.5.34)$$

where $T_0(t) = e^{i\omega_0 t}$ for free vibration and $T_0(t) = 1$ for stability problems. The coefficients \bar{C}_j ($j = 1, 2, \dots, 9$) appearing in Eq. (11.5.34) are

$$\begin{aligned}\bar{C}_1 &= (e_2 - e_1 e_6)/e_{13}, & \bar{C}_2 &= (e_3 - e_1 e_7)/e_{13}, & \bar{C}_3 &= (e_4 - e_1 e_8)/e_{13} \\ \bar{C}_4 &= (e_6 - e_5 e_2)/e_{13}, & \bar{C}_5 &= (e_7 - e_5 e_3)/e_{13}, & \bar{C}_6 &= (e_8 - e_5 e_4)/e_{13} \\ \bar{C}_7 &= e_9/e_{12}, & \bar{C}_8 &= e_{10}, & \bar{C}_9 &= e_{11}/e_{12} \\ e_1 &= B_{11}/A_{11}, & e_2 &= I_0 \omega_0^2/A_{11}, & e_3 &= 0, & e_4 &= -A_{12}/(R A_{11}) \\ e_5 &= B_{11}/D_{11}, & e_6 &= 0, & e_7 &= (K_s A_{55} - I_2 \omega_0^2)/D_{11} \\ e_8 &= (K_s A_{55} - B_{12}/R)/D_{11}, & e_9 &= A_{12}/R, & e_{10} &= B_{12}/R - K_s A_{55} \\ e_{11} &= A_{22}/R^2 - I_0 \omega_0^2, & e_{12} &= K_s A_{55} - \hat{N}, & e_{13} &= 1 - e_1 e_5\end{aligned}\quad (11.5.35)$$

In the stability problem, we let $\omega_0 \rightarrow 0$ in e_j ($j = 1, 2, \dots, 13$). In the vibration problem, when only the radial inertia is included, we will have

$$e_2 = 0, \quad e_7 = K_s A_{55}/D_{11}$$

11.5.5 Numerical Results

Numerical results are presented here for an isotropic material with Poisson ratio $\nu = 0.25$. It is assumed that the total thickness h of the shell is equal to 1 in. in all numerical examples presented here.

The results for dimensionless fundamental frequency with dimensionless minimum axisymmetric frequency of a shell according to FST are tabulated in Table 11.5.1 for cases C1–C1 through C4–C4. Two minimum axisymmetric frequencies are presented. The second number, which is slightly larger than the first one, corresponds to the case when only the radial force is included. The numerical results indicate that, unless the shell is extremely short, the minimum axisymmetric frequency is always much larger than the fundamental frequency.

The influence of various simply supported boundary conditions on the critical buckling load of isotropic shells can be seen from the results presented in Table 11.5.2.

Table 11.5.1: Comparison of the dimensionless fundamental frequency with dimensionless minimum axisymmetric frequency of a shell according to FST ($R/h = 60$, $L/R = 1$, $\hat{N}=0$ and $\bar{\omega}_m = \omega_m(L^2/10h)\sqrt{\rho/E_2}$).

C1–C1	C2–C2	C3–C3	C4–C4
1.9928 (6)	2.1882 (5)	2.0196 (6)	1.2090 (6)
6.0155 (0)	6.1657 (0)	6.0155 (0)	6.1657 (0)
6.0155 (0)	6.1657 (0)	6.0155 (0)	6.1657 (0)
6.0368 (0)	6.1685 (0)	6.0368 (0)	6.1685 (0)

Table 11.5.2: The effects of various simply supported conditions on the dimensionless critical buckling load \bar{N} of an isotropic shell ($\bar{N} = \hat{N}L^2/(10h^3E)$; $R/h = 40$ and $L/R = 2$).

	Theory	S1–S1	S2–S2	S3–S3	S4–S4
FST	4.7535 (1)	4.7560 (1)	9.4428 (3)	9.4440 (3)	
	9.5074 (0)	9.5128 (0)	9.5074 (0)	9.5128 (0)	
CST	4.8062 (1)	4.8090 (1)	9.5548 (4)	9.5492 (3)	
	9.5923 (0)	9.5977 (0)	9.5923 (0)	9.5977 (0)	

11.6 Summary

In this chapter, the governing equations of Sanders shell theory that accounts for the transverse shear deformation and the von Kármán nonlinear strains are derived using the dynamic version of the principle of virtual displacements. The equations of the Love–Kirchhoff shell theory (or Love's first-approximation shell theory) are obtained as a special case. Analytical solutions are presented for membrane forces and bending forces of a variety of thin shells, including cylindrical and spherical shells, using the thin shell theory. A brief study of buckling and vibration of cylindrical shells is also presented. The Lévy solution procedure is used to study free vibration and buckling analysis of cylindrical shells and numerical results are presented.

Problems

11.1 Establish the Gauss characteristic equation in (11.2.13) and Mainardi–Codazzi relations in Eq. (11.2.14).

11.2 Verify the strain–displacement relations in (11.2.31).

11.3 Prove the following identity [see Eq. (11.2.39)]:

$$A_\alpha \frac{\partial}{\partial \zeta} \left(\frac{u_\alpha}{A_\alpha} \right) = \frac{a_\alpha}{A_\alpha} \left(\phi_\alpha - \frac{u_\alpha^0}{R_\alpha} \right)$$

11.4 Derive the equations of motion in Eqs. (11.2.56)–(11.2.60) using Hamilton's principle (11.2.37).

11.5 Verify the equations of motion in Eqs. (11.2.66)–(11.2.70).

11.6 Derive the equilibrium equations in (11.3.11)–(11.3.13) by considering the free-body diagram of an infinitesimal element of cylindrical shell shown in Figure P11.6.

11.7 Derive the linear membrane strain–displacement relations for a cylindrical shell by considering the deformed shell element shown in Figure P11.7.

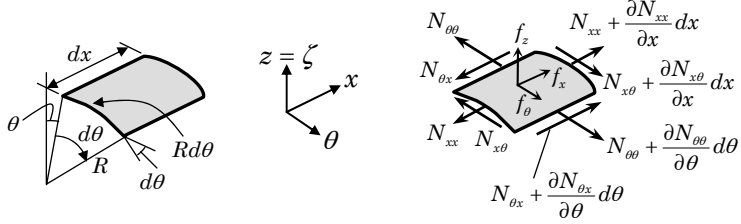


Figure P11.6

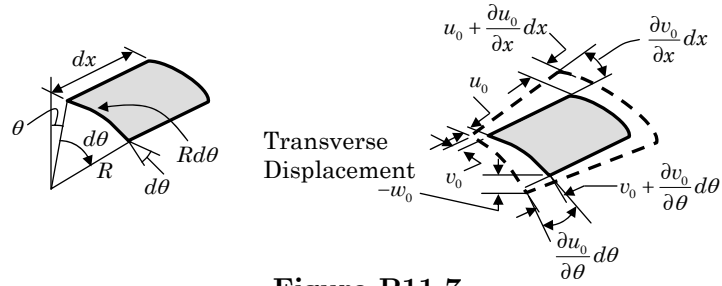


Figure P11.7

11.8 Express the equilibrium equations in (11.3.11)–(11.3.13) of the membrane theory of cylindrical shells in terms of the displacements u_0 and w_0 .

11.9 Consider a horizontal circular cylindrical shell of radius R , filled with liquid and with built-in ends. Determine N_θ , $N_{x\theta}$, and N_x . Hint: See Example 11.3.1. Use the condition that the length of the cylinder remains unchanged

$$\int_0^L (N_{xx} - \nu N_{\theta\theta}) dx = 0$$

11.10 Consider a cylindrical shell of semicircular cross section supporting its own weight, which is assumed to be distributed uniformly over the surface of the shell (Figure P11.10). Using the membrane theory of shells, determine $N_{\theta\theta}$, $N_{x\theta}$, and N_{xx} assuming that there are no axial forces at the ends of the tube $N_{xx}(-L/2, \theta) = 0$ and $N_{xx}(L/2, \theta) = 0$.

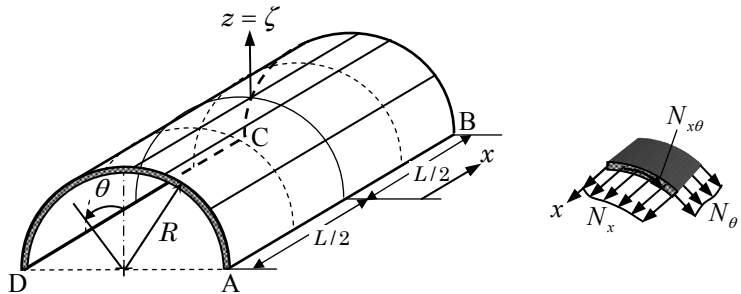
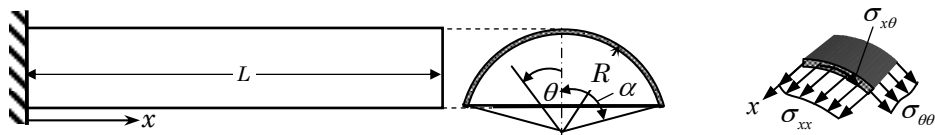
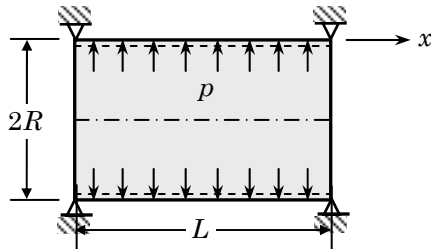


Figure P11.10

- 11.11** A cylindrical shell of length L , radius R , and half angle α is cantilevered (fixed) at its left end (Figure P11.11). Determine the stress distributions in the shell due to its own weight. *Hint:* See Examples 11.3.1 and 11.3.2.

**Figure P11.11**

- 11.12** Consider a long circular cylindrical shell of radius R with uniform internal pressure p (Figure P11.12). If the edges are simply supported, determine the deflection and the bending moment and shear forces generated at the simply supported edges. *Hint:* Make use of the solution procedure of Examples 11.3.3 through 11.3.5 and suitable boundary conditions.

**Figure P11.12**

- 11.13** In Example 11.3.4, it was assumed that the length of the cylindrical shell is large. For finite length cylinders, the solution in Eq. (11.3.20) is valid. For a short cylinder with uniform internal pressure and simply supported edges, determine the complete solution for the deflection. Assume the homogeneous solution to Eq. (11.3.19) in the alternative form

$$w_0^h(x) = \sin \alpha x (K_1 \sinh \alpha x + K_2 \cosh \alpha x) + \cos \alpha x (K_3 \sinh \alpha x + K_4 \cosh \alpha x)$$

The particular solution is given by $w_0^p(x) = \delta_0 = pR^2/Eh$. Take the origin of the coordinate system at the center of the cylinder and determine the constants K_1, K_2, K_3 and K_4 using the boundary conditions at $x = \pm L/2$. *Hint:* Constants K_2 and K_3 must be zero due to the symmetry of the solution about $x = 0$.

- 11.14** Consider a tall cylindrical tank of uniform wall thickness h filled with liquid of specific weight γ . If the bottom of the cylindrical tank is freely resting on its bottom, what are the membrane forces in the shell? Assuming that the bottom of the tank is built-in and the top is open (Figure P11.14), determine the deflection w_0 , force $N_{\theta\theta}$, and moments M_{xx} and $M_{\theta\theta}$. Hint: Take $f_z = \gamma(L - x)$, where L is the height of the tank. Use the homogeneous solution in Eq. (11.3.22), and the particular solution is given by $\gamma(L - x)R^2/Eh$.

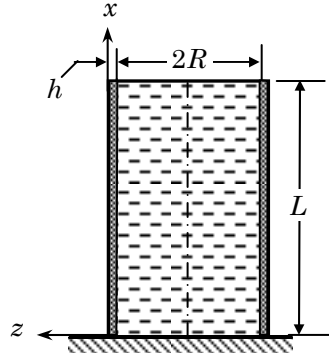


Figure P11.14

- 11.15** Show that when shear deformation is not neglected, Eqs. (11.3.17) reduce to the solution of

$$D \frac{d^4 w_0}{dx^4} - \frac{D}{2(1+\nu)K_s R^2} \frac{d^2 w_0}{dx^2} + \frac{Eh}{R^2} w_0 = f_z - \frac{D}{K_s G h} \frac{d^2 f_z}{dx^2}$$

and

$$\frac{d\varphi_x}{dx} = \frac{E}{K_s G R^2} w_0 - \frac{d^2 w_0}{dx^2} - \frac{f_z}{K_s G h}$$

- 11.16** Use Eq. (11.3.19) to derive the governing equation of a cylindrical shell with linearly varying thickness, $h(x) = kx$, where k is a constant (Figure P11.16).

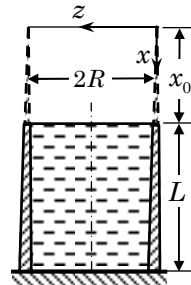


Figure P11.16

11.17 Obtain the membrane forces, Eq. (11.3.34), in a cylindrical shell subjected to internal pressure p from those of a cone (see Example 11.4.3).

11.18 Consider a truncated cone, as shown in Figure P11.18. Determine the membrane forces due to its own weight, the magnitude of which per unit area is constant and equal to p .

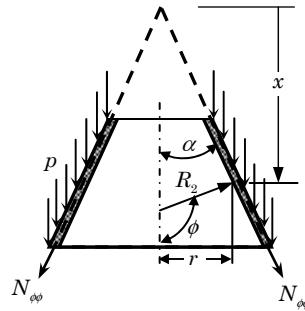


Figure P11.18

11.19 Establish the following principal radii curvature relations in Eq. (11.4.35):

$$R_1(\phi) = \frac{a^2 b^2}{(a^2 \sin^2 \phi + b^2 \cos^2 \phi)^{\frac{3}{2}}}, \quad R_2(\phi) = \frac{a^2}{(a^2 \sin^2 \phi + b^2 \cos^2 \phi)^{\frac{1}{2}}}$$

Hint: The equation of the ellipse is $b^2 x^2 + a^2 y^2 = a^2 b^2$ or $y = \pm b \sqrt{a^2 - x^2}/a$ and $\tan \phi = y' = \frac{y}{x}$. Compute $(dy/dx) \equiv y'$ and y'' and use the familiar expression for the radius of curvature, $R_1 = [1 + (y')^2]^{3/2}/y''$.

11.20 Establish the identities (Figure P11.20)

$$\frac{dr_0}{d\phi} = r_1 \cos \phi, \quad \frac{dz}{d\phi} = r_1$$

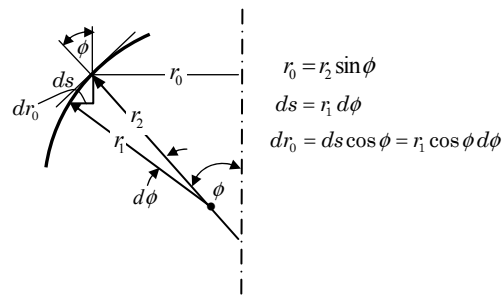


Figure P11.20

- 11.21** Derive the equilibrium equations governing membrane theory of shells of revolution using the free-body diagram of a typical shell element shown in Figure P11.21.

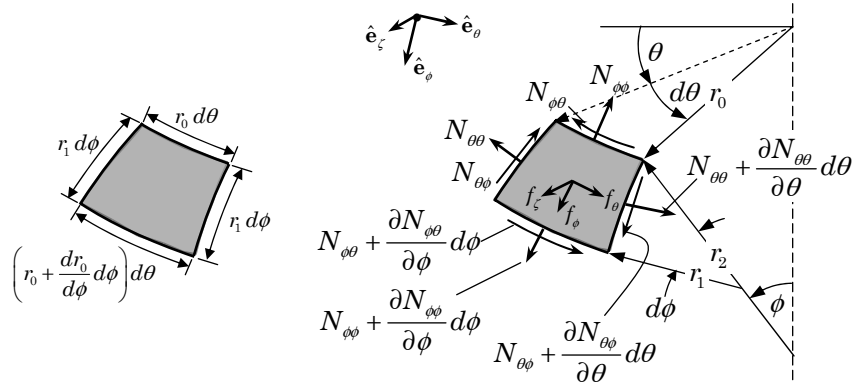


Figure P11.21

- 11.22** Determine the forces in a cylindrical pressure shell with ellipsoidal ends (Figure P11.22).

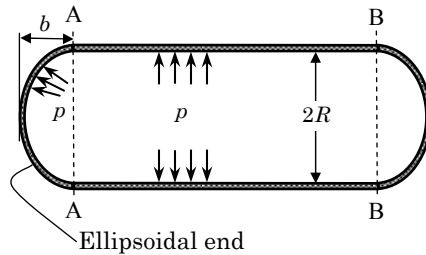


Figure P11.22

12

Finite Element Analysis of Plates

12.1 Introduction

In Chapters 4 through 11, analytical or numerical solutions of the differential equations governing beams, plates, and shells using exact integration, the Navier and Lévy methods, or the Ritz method were presented for regular geometries. Analytical or the Ritz solutions cannot be readily developed when the geometry of the plate is not circular or rectangular, different portions of the plate boundary are subjected to different boundary conditions or nonlinearities are involved. In such cases, one must resort to approximate methods of analysis that are capable of predicting accurate solutions.

The *finite element method* is a powerful numerical method for the solution of differential equations that arise in various fields of engineering and applied science. The basic idea of the finite element method is to view a given domain as an assemblage of simple geometric shapes, called *finite elements*, for which it is possible to systematically generate the approximation functions needed in the solution of differential equations over a typical element. Thus, the finite element method is a piecewise application of the Ritz method, Galerkin's method, least-squares method, and so on. For a given differential equation, it is possible to develop different finite element models, depending on the choice of the method used to generate algebraic equations among the undetermined coefficients of the approximate solution. The ability to represent geometrically complicated domains and ease of application of physical boundary conditions made the finite element method a practical tool of engineering analysis and design. For a detailed introduction to the finite element method, the reader is advised to consult the books by Zienkiewicz (1977), Zienkiewicz and Taylor (1991), Bathe (1996), Cook et al. (1989), and Reddy (2004b, 2006).

In this chapter, we develop finite element models of classical and first-order shear deformation theories of plates; shell finite element models are not included as they are considerably more complicated than plates. Interested readers may consult finite element books in the list of references. The objective here is to present an introduction to the finite element method in the context of the material covered in this book. While the coverage is not exhaustive in terms of solving complicated

problems, it is hoped that the reader gains a basic understanding of the finite element method in the analysis of plate problems. It is important to bear in mind that any approximate method is a means to analyze a practical engineering problem and that analysis is not an end in itself, but rather an aid to design and manufacturing. The value of the theory and analytical solutions presented in the preceding chapters to gain insight into the behavior of simple plate problems is immense in the numerical modelling of complicated problems by any numerical method.

12.2 Finite Element Models of CPT

12.2.1 Introduction

In this section, the displacement finite element model of Eq. (3.8.8) governing the motion of plates according to the classical plate theory is developed. The finite element models of plates are considerably complicated by the fact that two-dimensional problems are described by partial differential equations over geometrically complex regions. The boundary Γ of a two-dimensional domain Ω is, in general, a curve. Therefore, the two-dimensional finite elements must be simple geometric shapes that can be used to approximate a given two-dimensional domain as well as the solution over it. Consequently, the finite element solution will have errors due to the approximation of the solution as well as the domain. In two dimensions, there is more than one geometric shape that can be used as a finite element (Figure 12.2.1).

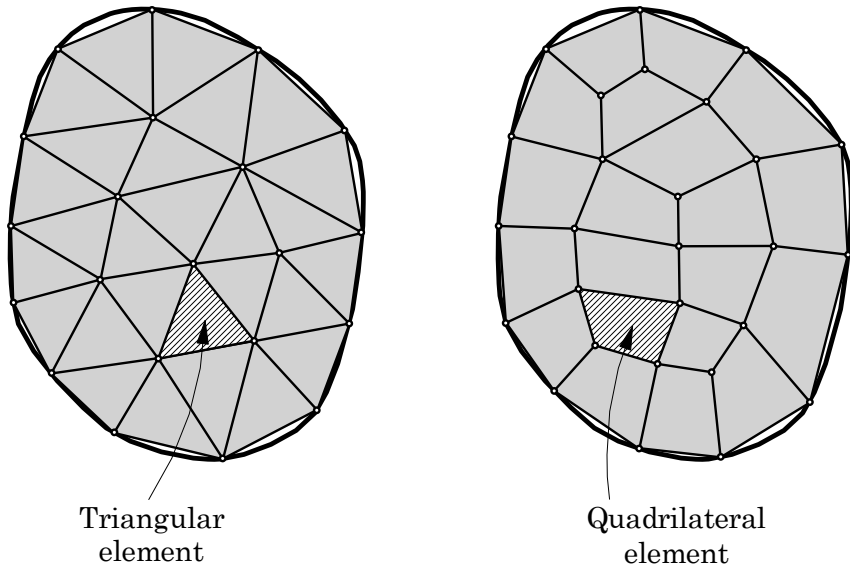


Figure 12.2.1. Finite element discretization of a two-dimensional domain using triangular and quadrilateral elements.

12.2.2 General Formulation

The finite element model of a plate theory is developed using its virtual work statement and an interpolation of the displacement field over an element. In the following sections, several standard plate bending elements are discussed.

The virtual work statement of the classical plate theory over typical finite element Ω^e is given by [from Eq. (3.4.10)]

$$\begin{aligned}
 0 = & \int_0^T \int_{\Omega^e} \left[-\frac{\partial^2 \delta w_0}{\partial x^2} M_{xx} - 2 \frac{\partial^2 \delta w_0}{\partial x \partial y} M_{xy} - \frac{\partial^2 \delta w_0}{\partial y^2} M_{yy} + k \delta w_0 w_0 \right. \\
 & + \frac{\partial \delta w_0}{\partial x} \left(\hat{N}_{xx} \frac{\partial w_0}{\partial x} + \hat{N}_{xy} \frac{\partial w_0}{\partial y} \right) + \frac{\partial \delta w_0}{\partial y} \left(\hat{N}_{xy} \frac{\partial w_0}{\partial x} + \hat{N}_{yy} \frac{\partial w_0}{\partial y} \right) \\
 & + I_0 \delta w_0 \ddot{w}_0 + I_2 \left(\frac{\partial \delta w_0}{\partial x} \frac{\partial \ddot{w}_0}{\partial x} + \frac{\partial \delta w_0}{\partial y} \frac{\partial \ddot{w}_0}{\partial y} \right) - \delta w_0 q \Big] dx dy dt \\
 & + \int_0^T \oint_{\Gamma^e} \left[-\delta w_0 \left(\frac{\partial M_{xx}}{\partial x} + \frac{\partial M_{xy}}{\partial y} + \hat{N}_{xx} \frac{\partial w_0}{\partial x} + \hat{N}_{xy} \frac{\partial w_0}{\partial y} \right) n_x \right. \\
 & - \delta w_0 \left(\frac{\partial M_{xy}}{\partial x} + \frac{\partial M_{yy}}{\partial y} + \hat{N}_{xy} \frac{\partial w_0}{\partial x} + \hat{N}_{yy} \frac{\partial w_0}{\partial y} \right) n_y \\
 & + I_2 \delta w_0 \left(\frac{\partial \ddot{w}_0}{\partial x} n_x + \frac{\partial \ddot{w}_0}{\partial y} n_y \right) + \frac{\partial \delta w_0}{\partial x} (M_{xx} n_x + M_{xy} n_y) \\
 & \left. + \frac{\partial \delta w_0}{\partial y} (M_{xy} n_x + M_{yy} n_y) \right] ds dt \tag{12.2.1}
 \end{aligned}$$

where (n_x, n_y) denote the direction cosines of the unit normal on the element boundary Γ^e , (M_{xx}, M_{xy}, M_{yy}) are the bending moments defined in Eq. (6.1.9a–c), and $(\hat{N}_{xx}, \hat{N}_{xy}, \hat{N}_{yy})$ are the inplane compressive and shear forces (to study buckling of plates). Integration by parts of the inertia terms in the last equation is necessitated by the symmetry considerations of the mass matrix in the finite element model.

We note from the boundary terms in Eq. (12.2.1) that w_0 , $\partial w_0 / \partial x$, and $\partial w_0 / \partial y$ are the primary variables (or generalized displacements), and

$$T_x \equiv M_{xx} n_x + M_{xy} n_y, \quad T_y \equiv M_{xy} n_x + M_{yy} n_y \tag{12.2.2}$$

$$\begin{aligned}
 Q_n \equiv & \left(\frac{\partial M_{xx}}{\partial x} + \frac{\partial M_{xy}}{\partial y} + \hat{N}_{xx} \frac{\partial w_0}{\partial x} + \hat{N}_{xy} \frac{\partial w_0}{\partial y} - I_2 \frac{\partial^3 w_0}{\partial x \partial t^2} \right) n_x \\
 & + \left(\frac{\partial M_{xy}}{\partial x} + \frac{\partial M_{yy}}{\partial y} + \hat{N}_{xy} \frac{\partial w_0}{\partial x} + \hat{N}_{yy} \frac{\partial w_0}{\partial y} - I_2 \frac{\partial^3 w_0}{\partial y \partial t^2} \right) n_y \tag{12.2.3}
 \end{aligned}$$

are the secondary degrees of freedom (or generalized forces). Thus, finite elements based on the classical plate theory require continuity of the transverse deflection and its normal derivative across element boundaries. Also, to satisfy the constant displacement (rigid body mode) and constant strain requirements, the polynomial expansion for w_0 should be a complete cubic.

Assume finite element approximation of the form

$$w_0(x, y, t) = \sum_{j=1}^n \Delta_j^e(t) \varphi_j^e(x, y) \quad (12.2.4)$$

where Δ_j^e are the values of w_0 and its derivatives at the nodes, and φ_j^e are the interpolation functions, the specific form of which will depend on the geometry of the element and the nodal degrees of freedom interpolated. Substituting approximations (12.2.4) for w_0 and φ_i^e for the virtual displacement δw_0 into Eq. (12.2.1), we obtain the i th equation

$$\sum_{j=1}^n \left[(K_{ij}^e + G_{ij}^e) \Delta_j^e + M_{ij}^e \ddot{\Delta}_j^e \right] = F_i^e + F_i^{eT} \quad (12.2.5)$$

where $i, j = 1, 2, \dots, n$. The coefficients of the stiffness matrix $K_{ij}^e = K_{ji}^e$, mass matrix $M_{ij}^e = M_{ji}^e$, geometric stiffness (or stability) matrix $G_{ij}^e = G_{ji}^e$, and force vectors F_i^e and F_i^{eT} are defined as follows:

$$\begin{aligned} K_{ij}^e &= \int_{\Omega^e} \left[D_{11} T_{ij}^{xxxx} + D_{12} (T_{ij}^{xxyy} + T_{ij}^{yyxx}) + 4D_{66} T_{ij}^{xyxy} \right. \\ &\quad \left. + D_{22} T_{ij}^{yyyy} + k S_{ij}^{00} \right] dx dy \\ G_{ij}^e &= \int_{\Omega^e} \left[\hat{N}_{xx} S_{ij}^{xx} + \hat{N}_{xy} (S_{ij}^{xy} + S_{ij}^{yx}) + \hat{N}_{yy} S_{ij}^{yy} \right] dx dy \\ M_{ij}^e &= \int_{\Omega^e} \left[I_0 S_{ij}^{00} + I_2 (S_{ij}^{xx} + S_{ij}^{yy}) \right] dx dy \\ F_i^e &= \int_{\Omega^e} q \varphi_i^e dx dy + \oint_{\Gamma^e} \left(Q_n \varphi_i^e - T_x \frac{\partial \varphi_i^e}{\partial x} - T_y \frac{\partial \varphi_i^e}{\partial y} \right) ds \\ F_i^{eT} &= \int_{\Omega^e} \left(\frac{\partial^2 \varphi_i^e}{\partial x^2} M_{xx}^T + 2 \frac{\partial^2 \varphi_i^e}{\partial x \partial y} M_{xy}^T + \frac{\partial^2 \varphi_i^e}{\partial y^2} M_{yy}^T \right) dx dy \end{aligned} \quad (12.2.6a)$$

where D_{ij} are the bending stiffnesses given in Eq. (10.1.27), N_{xx}^T , M_{xx}^T , etc. are the thermal forces and moments, and

$$T_{ij}^{\xi\eta\zeta\mu} = \frac{\partial^2 \varphi_i^e}{\partial \xi \partial \eta} \frac{\partial^2 \varphi_j^e}{\partial \zeta \partial \mu} dx dy, \quad S_{ij}^{\xi\eta} = \frac{\partial \varphi_i^e}{\partial \xi} \frac{\partial \varphi_j^e}{\partial \eta} dx dy \quad (12.2.6b)$$

and ξ, η, ζ , and μ take on the symbols x and y . In matrix notation, Eq. (12.2.5) can be expressed as

$$([K^e] + [G^e]) \{\Delta^e\} + [M^e] \{\ddot{\Delta}^e\} = \{F^e\} + \{F^{eT}\} \quad (12.2.7)$$

This completes the finite element model development of the classical plate theory. The finite element model in Eq. (12.2.5) or (12.2.7) is called a *displacement finite element model* because it is based on equations of motion expressed in terms of the displacements, and the generalized displacements are the primary nodal degrees of freedom.

12.2.3 Plate-Bending Elements

There exists a large body of literature on triangular and rectangular plate-bending finite elements of isotropic or orthotropic plates based on the classical plate theory. There are two kinds of plate-bending elements of the classical plate theory. A *conforming element* is one in which the inter-element continuity of w_0 , $\theta_x \equiv \partial w_0 / \partial x$, and $\theta_y \equiv \partial w_0 / \partial y$ (or $\partial w_0 / \partial n$) are satisfied, and a *nonconforming element* is one in which the continuity of the normal slope, $\partial w_0 / \partial n$, is not satisfied.

An effective nonconforming triangular element (the BCIZ triangle) was developed by Bazeley, Cheung, Irons, and Zienkiewicz (1965), and it consists of three degrees of freedom (w_0, θ_x, θ_y) at the three vertex nodes (Figure 12.2.2). Thus, a nine-term polynomial approximation of w_0 is required

$$w_0(x, y, t) = \sum_{k=1}^9 \Delta_k^e(t) \varphi_k^e(x, y) \quad (12.2.8)$$

where Δ_k^e the values of w_0 , $\partial w_0 / \partial x$, and $\partial w_0 / \partial y$ at the three nodes

$$\{\Delta^e\}^T = \{w_1, \theta_{x1}, \theta_{y1}, w_2, \theta_{x2}, \theta_{y2}, w_3, \theta_{x3}, \theta_{y3}\}^e \quad (12.2.9)$$

The interpolation functions φ_k^e for this element can be expressed in terms of the area coordinates [(see Reddy (2006)) as

$$\left\{ \begin{array}{l} \varphi_1^e \\ \varphi_2^e \\ \varphi_3^e \\ \varphi_4^e \\ \varphi_5^e \\ \varphi_6^e \\ \varphi_7^e \\ \varphi_8^e \\ \varphi_9^e \end{array} \right\} = \left\{ \begin{array}{l} L_1 + L_1^2 L_2 + L_1^2 L_3 - L_1 L_2^2 - L_1 L_3^2 \\ x_{31}(L_3 L_1^2 - f) - x_{12}(L_1^2 L_2 + f) \\ y_{31}(L_3 L_1^2 + f) - y_{12}(L_1^2 L_2 + f) \\ L_2 + L_2^2 L_3 + L_2^2 L_1 - L_2 L_3^2 - L_2 L_1^2 \\ x_{12}(L_1 L_2^2 - f) - x_{23}(L_2^2 L_3 + f) \\ y_{12}(L_1 L_2^2 + f) - y_{23}(L_2^2 L_3 + f) \\ L_3 + L_3^2 L_1 + L_3^2 L_2 - L_3 L_1^2 - L_3 L_2^2 \\ x_{23}(L_2 L_3^2 - f) - x_{31}(L_3^2 L_1 + f) \\ y_{23}(L_2 L_3^2 + f) - y_{31}(L_3^2 L_1 + f) \end{array} \right\} \quad (12.2.10a)$$

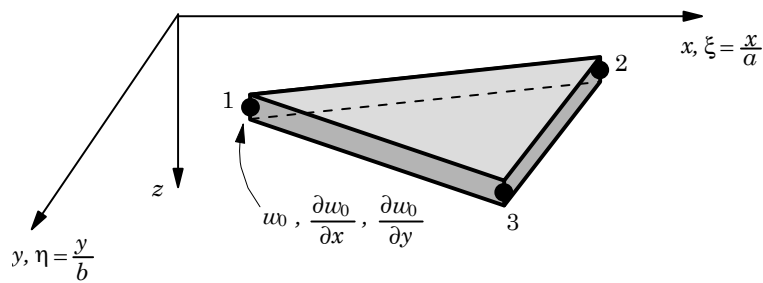


Figure 12.2.2. A nonconforming triangular element with three degrees of freedom ($w_0, \partial w_0 / \partial x, \partial w_0 / \partial y$) per node.

where $f = 0.5L_1L_2L_3$, $x_{ij} = x_i - x_j$, $y_{ij} = y_i - y_j$, (x_i, y_i) being the global coordinates of the i th node, and L_i being the area coordinates defined within an element

$$L_i = \frac{A_i}{A}, \quad A = \sum_{i=1}^3 A_i \quad (12.2.10b)$$

A conforming triangular element due to Clough and Tocher (1965) is an assemblage of three triangles as shown in Figure 12.2.3. The normal slope continuity is enforced at the mid-side nodes between the sub-triangles. In each sub-triangle, the transverse deflection is represented by the polynomial ($i = 1, 2, 3$)

$$w_0^i(x, y) = a_i + b_i\xi + c_i\eta + d_i\xi\eta + e_i\xi^2 + f_i\eta^2 + g_i\xi^3 + h_i\xi^2\eta + k_i\xi\eta^2 + \ell_i\eta^3 \quad (12.2.11)$$

where (ξ, η) are the local coordinates, as shown in the Figure 12.2.3. The 30 coefficients are reduced to 9, 3 ($w_0, \partial w_0 / \partial x, \partial w_0 / \partial y$) at each vertex of the triangle, by equating the variables from the vertices of each sub-triangle at the common points and normal slope between the mid-side points of sub-triangles.

A nonconforming rectangular element has w_0, θ_x , and θ_y as the nodal variables (Figure 12.2.4). The element was developed by Melosh (1963) and Zienkiewicz and Cheung (1964). The normal slope variation is cubic along an edge, whereas there are only two values of $\partial w_0 / \partial n$ available on the edge. Therefore, the cubic polynomial for the normal derivative of w_0 is not the same on the edge common to two elements. The interpolation functions for this element can be expressed compactly as

$$\begin{aligned} \varphi_i^e &= g_{i1} \quad (i = 1, 4, 7, 10) \\ \varphi_i^e &= g_{i2} \quad (i = 2, 5, 8, 11) \\ \varphi_i^e &= g_{i3} \quad (i = 3, 6, 9, 12) \end{aligned} \quad (12.2.12a)$$

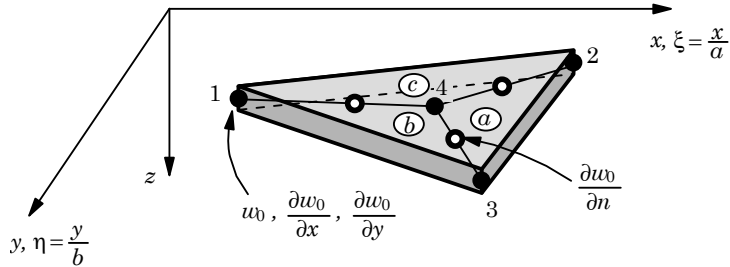


Figure 12.2.3. A conforming triangular element.

$$\begin{aligned}
 g_{i1} &= \frac{1}{8}(1 + \xi_0)(1 + \eta_0)(2 + \xi_0 + \eta_0 - \xi^2 - \eta^2) \\
 g_{i2} &= \frac{1}{8}\xi_i(\xi_0 - 1)(1 + \eta_0)(1 + \xi_0)^2 \\
 g_{i3} &= \frac{1}{8}\eta_i(\eta_0 - 1)(1 + \xi_0)(1 + \eta_0)^2 \\
 \xi &= (x - x_c)/2, \quad \eta = (y - y_c)/b, \quad \xi_0 = \xi\xi_i, \quad \eta_0 = \eta\eta_i
 \end{aligned} \tag{12.2.12b}$$

where $2a$ and $2b$ are the sides of the rectangle, and (x_c, y_c) are the global coordinates of the center of the rectangle.

A conforming rectangular element with w_0 , $\partial w_0/\partial x$, $\partial w_0/\partial y$, and $\partial^2 w_0/\partial x \partial y$ as the nodal variables was developed by Bogner, Fox, and Schmidt (1965). The interpolation functions for this element (Figure 12.2.5) are

$$\begin{aligned}
 \varphi_i^e &= g_{i1} \quad (i = 1, 5, 9, 13); \quad \varphi_i^e = g_{i2} \quad (i = 2, 6, 10, 14) \\
 \varphi_i^e &= g_{i3} \quad (i = 3, 7, 11, 15); \quad \varphi_i^e = g_{i4} \quad (i = 4, 8, 12, 16)
 \end{aligned} \tag{12.2.13a}$$

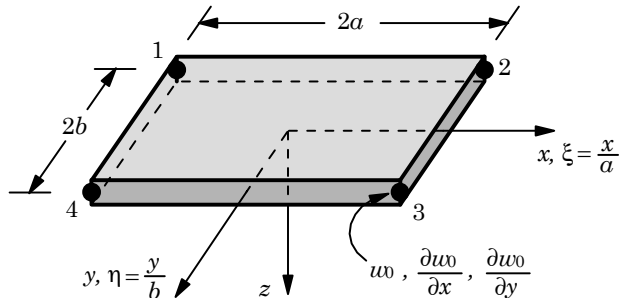


Figure 12.2.4. A nonconforming rectangular element.

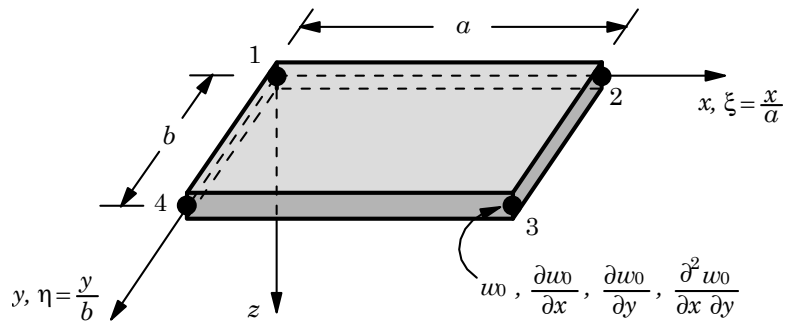


Figure 12.2.5. A conforming rectangular element.

$$\begin{aligned}
g_{i1} &= \frac{1}{16}(\xi + \xi_i)^2(\xi_0 - 2)(\eta + \eta_i)^2(\eta_0 - 2) \\
g_{i2} &= \frac{1}{16}\xi_i(\xi + \xi_i)^2(1 - \xi_0)(\eta + \eta_i)^2(\eta_0 - 2) \\
g_{i3} &= \frac{1}{16}\eta_i(\xi + \xi_i)^2(\xi_0 - 2)(\eta + \eta_i)^2(1 - \eta_0) \\
g_{i4} &= \frac{1}{16}\xi_i\eta_i(\xi + \xi_i)^2(1 - \xi_0)(\eta + \eta_i)^2(1 - \eta_0)
\end{aligned} \tag{12.2.13b}$$

The combined conforming element has four degrees of freedom per node, whereas the nonconforming element has three degrees of freedom per node. For the conforming rectangular element the total number of bending nodal degrees of freedom per element is 16, and 12 for the nonconforming element.

12.2.4 Fully Discretized Finite Element Models

Static Bending

In the case of static bending under applied mechanical and thermal loads, Eq. (12.2.7) reduces to

$$([K^e] + [G^e]) \{\Delta^e\} = \{F^e\} + \{F^{eT}\} \tag{12.2.14}$$

where it is understood that all time-derivative terms are zero.

Once the nodal values of generalized displacements ($w_0, \partial w_0 / \partial x, \partial w_0 / \partial y$) have been obtained by solving the assembled equations of a problem, the strains are evaluated in each element by differentiating the displacements. The strains and stresses are the most accurate if they are computed at the center of the element.

Buckling

In the case of buckling under applied inplane compressive and shear edge loads, Eq. (12.2.7) reduces to

$$\left([K^e] - \lambda [\hat{G}^e] \right) \{\Delta^e\} = \{\bar{F}\} \tag{12.2.15}$$

where

$$\lambda = -\hat{N}_{xx}/\hat{N}_{xx}^0 = -\hat{N}_{yy}/\hat{N}_{yy}^0 = -\hat{N}_{xy}/\hat{N}_{xy}^0 \tag{12.2.16a}$$

$$\begin{aligned}
\hat{G}_{ij}^e &= \int_{\Omega^e} \left[\hat{N}_{xx}^0 S_{ij}^{xx} + \hat{N}_{xy}^0 \left(S_{ij}^{xy} + S_{ij}^{yx} \right) + \hat{N}_{yy}^0 S_{ij}^{yy} \right] dx dy \\
\bar{F}_k &= \oint_{\Gamma^e} \left(Q_n \varphi_k^e - T_x \frac{\partial \varphi_k^e}{\partial x} - T_y \frac{\partial \varphi_k^e}{\partial y} \right) ds
\end{aligned} \tag{12.2.16b}$$

Natural Vibration

In the case of natural vibration, the response of the plate is assumed to be periodic. Equation (12.2.7) becomes

$$\left([K^e] - \omega^2 [M^e] \right) \{\Delta^e\} = \{\bar{F}^e\} \tag{12.2.17}$$

where ω denotes the frequency of natural vibration.

Transient Response

In the case of time dependent response, Eq. (12.2.7) governs the motion, and the ordinary differential equations in time must be integrated to determine the nodal values $\Delta_j^e(t)$ as functions of time. Although the matrix equation (12.2.7) can be solved, in principle, using the Laplace transforms for certain load cases, it is a tedious exercise and involves more computational effort than using a numerical time-approximation scheme. Here we consider the Newmark family of time-integration schemes that are used widely in structural dynamics.

In the Newmark method, the first and second time derivatives are approximated as

$$\begin{aligned}\{\dot{\Delta}^e\}_{s+1} &= \{\dot{\Delta}^e\}_s + a_1\{\ddot{\Delta}^e\}_s + a_2\{\ddot{\Delta}^e\}_{s+1} \\ \{\ddot{\Delta}^e\}_{s+1} &= a_3(\{\Delta^e\}_{s+1} - \{\Delta^e\}_s) - a_4\{\dot{\Delta}^e\}_s - a_5\{\dot{\Delta}^e\}_s\end{aligned}\quad (12.2.18a)$$

where the superposed dot denotes differentiation with respect to time

$$a_1 = (1 - \alpha)\delta t_s, \quad a_2 = \alpha\delta t_s, \quad a_3 = \frac{2}{\gamma(\delta t_s)^2}, \quad a_4 = \delta t_s a_3, \quad a_5 = \frac{(1 - \gamma)}{\gamma} \quad (12.2.18b)$$

δt is the time increment, $\delta t_s = t_{s+1} - t_s$, and $\{\cdot\}_s$, for example, denotes the value of the enclosed vector at time t_s .

The parameters α and γ in the Newmark scheme are selected such that the scheme is either stable or conditionally stable; i.e., the error introduced through the time approximation (12.2.18a) does not grow unboundedly as we march in time. All schemes for which $\gamma \geq \alpha \geq 1/2$ are unconditionally stable. Schemes for which $\gamma < \alpha$ and $\alpha \geq 0.5$ are conditionally stable, and the stability condition is

$$\delta t \leq \delta t_{cr} \equiv \left[\frac{1}{2} \omega_{max} (\alpha - \gamma) \right]^{-\frac{1}{2}} \quad (12.2.19)$$

where ω_{max} denotes the maximum frequency associated with the finite element equations (12.2.7).

The Newmark family contains the following widely used schemes:

$$\begin{aligned}\alpha &= \frac{1}{2}, \quad \gamma = \frac{1}{2}, \quad \text{the constant average acceleration method (stable)} \\ \alpha &= \frac{1}{2}, \quad \gamma = \frac{1}{3}, \quad \text{the linear acceleration method (conditionally stable)} \\ \alpha &= \frac{1}{2}, \quad \gamma = \frac{1}{6}, \quad \text{the Fox-Goodwin scheme (conditionally stable)} \\ \alpha &= \frac{1}{2}, \quad \gamma = 0, \quad \text{the centered difference method (conditionally stable)} \\ \alpha &= \frac{3}{2}, \quad \gamma = \frac{8}{5}, \quad \text{the Galerkin method (stable)} \\ \alpha &= \frac{3}{2}, \quad \gamma = 2, \quad \text{the backward difference method (stable)}\end{aligned}\quad (12.2.20)$$

Premultiplying the second equation in (12.2.18a) with $[M^e]_{s+1}$ and using Eq. (12.2.7) at $t = t_{s+1}$ to replace $[M^e]_{s+1}\{\Delta^e\}_{s+1}$, we obtain

$$[\hat{K}^e]\{\Delta^e\}_{s+1} = \{\hat{F}^e\} \quad (12.2.21)$$

where

$$\begin{aligned} [\hat{K}^e] &= ([K^e]_{s+1} + [G^e]_{s+1}) + a_3[M^e]_{s+1} \\ \{\hat{F}^e\} &= \{F^e\}_{s+1} + [M^e]_{s+1} (a_3\{\Delta^e\}_s + a_4\{\dot{\Delta}^e\}_s + a_5\{\ddot{\Delta}^e\}_s) \end{aligned} \quad (12.2.22)$$

Note that for the centered difference scheme ($\gamma = 0$), it is necessary to use an alternative form of Eq. (12.2.21).

Equation (12.2.21) represents a system of algebraic equations among the (discrete) values of $\{\Delta^e(t)\}$ at time $t = t_{s+1}$ in terms of known values at time $t = t_s$. At the first time step (i.e., $s = 0$), the values $\{\Delta^e\}_0 = \{\Delta^e(0)\}$ and $\{\dot{\Delta}^e\}_0 = \{\dot{\Delta}^e(0)\}$ are known from the initial conditions of the problem, and Eq. (12.2.7) is used to determine $\{\ddot{\Delta}^e\}_0$ at $t = 0$

$$\{\ddot{\Delta}^e\}_0 = [M^e]^{-1} \{ \{F^e\} - ([K^e] + [G^e]) \{w^e\}_0 \} \quad (12.2.23)$$

12.2.5 Numerical Results

Here we use the conforming (C) and nonconforming (NC) rectangular finite elements to analyze plates for bending and natural vibration. A note should be made of the fact that the finite element model developed herein is not restricted to any particular geometry, boundary conditions, or loading. Take advantage of available problem symmetries to identify the computational domain because they reduce computational effort. For example, a 2×2 mesh in a quadrant of the plate is the same as 4×4 mesh in the total plate, and the results obtained with the two meshes would be identical, within the round-off errors of the computation, if the solution exhibits biaxial symmetry. The notation “ $m \times n$ mesh” denotes m subdivisions along the x -axis and n subdivisions along the y -axis with the same type of elements. A solution is symmetric about a line only if (1) the geometry, including boundary conditions, (2) the material properties, and (3) the loading are symmetric about the line. The boundary conditions along a line of symmetry should be correctly identified and imposed in the finite element model. When one is not sure of the solution symmetry, it is advised that the whole plate be modelled.

Bending

For a rectangular orthotropic plate with simply supported edges, a quadrant of the plate may be used as the computational domain. The boundary conditions along the symmetry lines are shown in Figure 12.2.6. In the case of the conforming element, it is necessary that the cross-derivative $\partial^2 w_0 / \partial x \partial y$ also be set to zero at the center of the plate when a quarter-plate model is used. Otherwise, the results will be less accurate. The stresses in the finite element analysis were computed at the center of the elements. The foundation modulus k is set to zero.

A comparison of finite element solutions with the analytical solutions of simply supported isotropic and orthotropic square plates under uniformly distributed transverse load is presented in Table 12.2.1. The analytical solutions were evaluated using $m, n = 1, 3, \dots, 19$. The exact maximum deflection occurs at $x = y = 0$, maximum stresses σ_{xx} and σ_{yy} occur at $(0, 0, h/2)$, and the maximum shear stress σ_{xy}

occurs at $(a/2, b/2, -h/2)$. The geometric boundary conditions of the computational domain (see the shaded quadrant in Figure 12.2.6) are

$$\frac{\partial w_0}{\partial x} = 0 \text{ at } x = 0; \quad \frac{\partial w_0}{\partial y} = 0 \text{ at } y = 0 \quad (12.2.24)$$

$$w_0 = \frac{\partial w_0}{\partial x} = 0 \text{ at } x = \frac{a}{2}; \quad w_0 = \frac{\partial w_0}{\partial y} = 0 \text{ at } y = \frac{b}{2} \quad (12.2.25)$$

Table 12.2.1. A comparison of the maximum transverse deflections and stresses[†] of simply supported (SSSS) square ($a = b$) plates under a uniformly distributed transverse load.

Variable	Nonconforming			Conforming			Analytical Solution
	2×2	4×4	8×8	2×2	4×4	8×8	
<i>Isotropic Plate ($\nu = 0.25$)</i>							
\bar{w}	4.8571	4.6425	4.5883	4.7619	4.5989	4.5739	4.5701
$\bar{\sigma}_{xx}$	0.2405	0.2673	0.2740	0.2239	0.2631	0.2731	0.2762
$\bar{\sigma}_{yy}$	0.2405	0.2673	0.2740	0.2239	0.2631	0.2731	0.2762
$\bar{\sigma}_{xy}$	0.1713	0.1964	0.2050	0.1688	0.1936	0.2040	0.2085
<i>Orthotropic Plate ($E_1/E_2 = 25$, $G_{12} = G_{13} = 0.5E_2$, $\nu_{12} = 0.25$)</i>							
\bar{w}	0.7082	0.6635	0.6531	0.7532	0.6651	0.6517	0.6497
$\bar{\sigma}_{xx}$	0.7148	0.7709	0.7828	0.5772	0.7388	0.7759	0.7866
$\bar{\sigma}_{yy}$	0.0296	0.0253	0.0246	0.0283	0.0249	0.0246	0.0244
$\bar{\sigma}_{xy}$	0.0337	0.0421	0.0444	0.0369	0.0416	0.0448	0.0463

[†] $\bar{w} = 10^2[w_0 E_2 h^3 / (q_0 a^4)]$, $\bar{\sigma} = \sigma h^2 / (q_0 a^2)$.

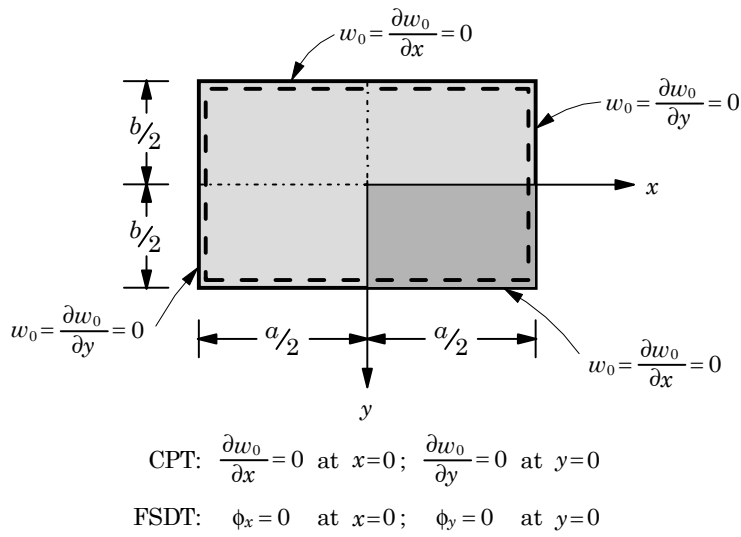


Figure 12.2.6. Symmetry boundary conditions for rectangular plates (SSSS).

In addition, $\partial^2 w_0 / \partial x \partial y = 0$ was used at $x = y = 0$ for the conforming element. Therefore, the locations of the maximum normal stresses are $(a/8, b/8)$, $(a/16, b/16)$, and $(a/32, b/32)$ for uniform meshes 2×2 , 4×4 , and 8×8 , respectively, while those of σ_{xy} are $(3a/8, 3b/8)$, $(7a/16, 7b/16)$, and $(15a/32, 15b/32)$ for the three meshes.

Similar results are presented in Table 12.2.2 for a clamped square plate. The locations of the normal stresses reported for the three meshes are

$$2 \times 2 : (a/8, b/8); \quad 4 \times 4 : (a/16, b/16); \quad 8 \times 8 : (a/32, b/32)$$

and the locations of the shear stress for the three meshes are

$$2 \times 2 : (3a/8, 3b/8); \quad 4 \times 4 : (7a/16, 7b/16); \quad 8 \times 8 : (15a/32, 15b/32)$$

These stresses are not necessarily the maximum ones in the plate. For example, for an 8×8 mesh, the maximum normal stress in the isotropic plate is found to be 0.2316 at $(0.46875a, 0.03125b, -h/2)$ and the maximum shear stress is 0.0225 at $(0.28125a, 0.09375b, -h/2)$ for the nonconforming element.

Table 12.2.2. Maximum transverse deflections and stresses[†] of clamped (CCCC), isotropic and orthotropic, square plates ($a = b$) under a uniformly distributed transverse load.

Variable	Nonconforming			Conforming		
	2×2	4×4	8×8	2×2	4×4	8×8
<i>Isotropic Plate</i> ($\nu = 0.25$)						
\bar{w}	1.5731	1.4653	1.4342	1.7245	1.5327	1.4539
$\bar{\sigma}_{xx}$	0.0987	0.1238	0.1301	0.1115	0.1247	0.1305
$\bar{\sigma}_{yy}$	0.0987	0.1238	0.1301	0.1115	0.1247	0.1305
$\bar{\sigma}_{xy}$	0.0497	0.0222	0.0067	0.0700	0.0297	0.0086
<i>Orthotropic Plate</i> ($E_1/E_2 = 25$, $G_{12} = G_{13} = 0.5E_2$, $\nu_{12} = 0.25$)						
\bar{w}	0.1434	0.1332	0.1314	0.3120	0.1889	0.1467
$\bar{\sigma}_{xx}$	0.1962	0.2491	0.2598	0.2287	0.2700	0.2650
$\bar{\sigma}_{yy}$	0.0085	0.0046	0.0042	0.0171	0.0126	0.0074
$\bar{\sigma}_{xy}$	0.0076	0.0046	0.0019	0.0104	0.0049	0.0019

[†] $\bar{w} = 10^2 [w_0 E_2 h^3 / (q_0 a^4)]$, $\bar{\sigma} = \sigma h^2 / (q_0 a^2)$.

The conforming element yields slightly better solutions than the nonconforming element, and both elements show good convergence. However, convergence of the displacements is always faster than stresses for the displacement-based finite elements, and the rate of convergence of stresses is two orders less than that of displacements for the CPT-based element. Since the stresses in the finite element analysis are computed at locations different from the analytical solutions, they are expected to be different. Mesh refinement not only improves the accuracy of the solution, but the Gauss point locations also get closer to the true locations of the maximum values.

Vibration

For natural vibration, the use of solution symmetry yields symmetric modes and associated frequencies. Since, fundamental (i.e., minimum) frequency does not always correspond to a symmetric mode, one should exercise caution in finite element modelling of vibration response.

Table 12.2.3 contains fundamental frequencies for isotropic and orthotropic simply supported and clamped plates. The results were obtained using the conforming plate bending element. Only a quadrant was modelled and rotary inertia was included ($b/h = 0.1$).

12.3 Finite Element Models of FSDT

12.3.1 Virtual Work Statements

Following the procedure described in Section 12.2, we can develop the finite element models of the equations governing the FSDT. We consider the linear equations of motion of FSDT from Eqs. (10.1.19)–(10.1.21), which are in terms of the stress resultants, but equivalent to Eqs. (10.1.33) through (10.1.35). The generalized displacements of FSDT are (w_0, ϕ_x, ϕ_y) . The virtual work statements required for the finite element model development can be identified from Eq. (10.1.9); they are

$$0 = \int_{\Omega^e} \left[\frac{\partial \delta w_0}{\partial x} Q_x + \frac{\partial \delta w_0}{\partial y} Q_y - \delta w_0 q + k w_0 \delta w_0 + I_0 \delta w_0 \frac{\partial^2 w_0}{\partial t^2} + \frac{\partial \delta w_0}{\partial x} \left(\hat{N}_{xx} \frac{\partial w_0}{\partial x} + \hat{N}_{xy} \frac{\partial w_0}{\partial y} \right) + \frac{\partial \delta w_0}{\partial y} \left(\hat{N}_{xy} \frac{\partial w_0}{\partial x} + \hat{N}_{yy} \frac{\partial w_0}{\partial y} \right) \right] dx dy$$

Table 12.2.3. A comparison of the fundamental frequencies[†] of simply supported (SSSS) and clamped (CCCC) rectangular plates.

$\frac{a}{b}$	SSSS Plates			CCCC Plates		
	2×2	4×4	Exact	2×2	4×4	Ritz [‡]
<i>Isotropic Plate ($\nu = 0.25$)</i>						
0.5	4.8301	4.9752	4.9003	7.8213	9.1185	9.9891
1.0	1.9736	1.9959	1.9838	3.3103	3.5203	3.6476
1.5	1.4144	1.4395	1.4359	2.3435	2.5861	2.7404
2.0	1.2074	1.2439	1.2436	1.9551	2.2781	2.4973
<i>Orthotropic Plate ($E_1/E_2 = 25$, $G_{12} = G_{13} = 0.5E_2$, $\nu_{12} = 0.25$)</i>						
0.5	17.6756	19.8085	19.8682	24.4927	33.1670	40.5568
1.0	4.9917	5.2801	5.2947	8.1276	10.1619	11.6406
1.5	2.5558	2.6388	2.6390	4.6561	5.2791	5.6483
2.0	1.7387	1.7785	1.7759	3.3358	3.6045	3.7424

[†] $\bar{\omega} = \omega \frac{b^2}{\pi^2} \sqrt{\frac{\rho h}{D_{22}}}$; foundation modulus $k = 0$. [‡] Ritz solution discussed in Section 9.4.3.

$$-\oint_{\Gamma^e} \left[\left(Q_x + \hat{N}_{xx} \frac{\partial w_0}{\partial x} + \hat{N}_{xy} \frac{\partial w_0}{\partial y} \right) n_x + \left(Q_y + \hat{N}_{xy} \frac{\partial w_0}{\partial x} + \hat{N}_{yy} \frac{\partial w_0}{\partial y} \right) n_y \right] \delta w_0 \, ds \quad (12.3.1a)$$

$$0 = \int_{\Omega^e} \left(\frac{\partial \delta \phi_x}{\partial x} M_{xx} + \frac{\partial \delta \phi_x}{\partial y} M_{xy} + \delta \phi_x Q_x + I_2 \delta \phi_x \frac{\partial^2 \phi_x}{\partial t^2} \right) dx dy - \oint_{\Gamma^e} T_x \delta \phi_x \, ds \quad (12.3.1b)$$

$$0 = \int_{\Omega^e} \left(\frac{\partial \delta \phi_y}{\partial x} M_{xy} + \frac{\partial \delta \phi_y}{\partial y} M_{yy} + \delta \phi_y Q_y + I_2 \delta \phi_y \frac{\partial^2 \phi_y}{\partial t^2} \right) dx dy - \oint_{\Gamma^e} T_y \delta \phi_y \, ds \quad (12.3.1c)$$

We note from the boundary terms in Eqs. (12.3.1a–c) that $(u_0, v_0, w_0, \phi_x, \phi_y)$ are the primary variables (or generalized displacements). Unlike in the classical plate theory, the rotations (ϕ_x, ϕ_y) are independent of w_0 . Note also that no derivatives of w_0 are in the list of the primary variables and, therefore, the element is called C^0 element. The secondary variables are

$$\begin{aligned} T_x &\equiv M_{xx} n_x + M_{xy} n_y, \quad T_y \equiv M_{xy} n_x + M_{yy} n_y \\ Q_n &\equiv \left(Q_x + \hat{N}_{xx} \frac{\partial w_0}{\partial x} + \hat{N}_{xy} \frac{\partial w_0}{\partial y} \right) n_x + \left(Q_y + \hat{N}_{xy} \frac{\partial w_0}{\partial x} + \hat{N}_{yy} \frac{\partial w_0}{\partial y} \right) n_y \end{aligned} \quad (12.3.2)$$

12.3.2 Lagrange Interpolation Functions

The virtual work statements in Eqs. (12.3.1a–c) of the FSDT contain at the most only the first derivatives of the dependent variables (w_0, ϕ_x, ϕ_y) . Therefore, they can all be approximated using the Lagrange interpolation functions. In principle, w_0 and (ϕ_x, ϕ_y) can be approximated with differing degrees of functions. For simplicity, we use the same order of interpolation for all variables. Let

$$w_0(x, y, t) = \sum_{j=1}^n w_j(t) \psi_j^e(x, y) \quad (12.3.3)$$

$$\phi_x(x, y, t) = \sum_{j=1}^n S_j^1(t) \psi_j^e(x, y) \quad (12.3.4a)$$

$$\phi_y(x, y, t) = \sum_{j=1}^n S_j^2(t) \psi_j^e(x, y) \quad (12.3.4b)$$

where ψ_j^e are Lagrange interpolation functions. One may use linear, quadratic, or higher-order interpolations of these variables. Lower-order interpolations are plagued with shear locking, as will be discussed in the sequel. A discussion of the Lagrange interpolation functions follows.

The simplest Lagrange element in two dimensions is the triangular element with nodes at its vertices (Figure 12.3.1), and its interpolation functions have the form

$$\psi_i^e(x, y) = a_i + b_i x + c_i y \quad (12.3.5)$$

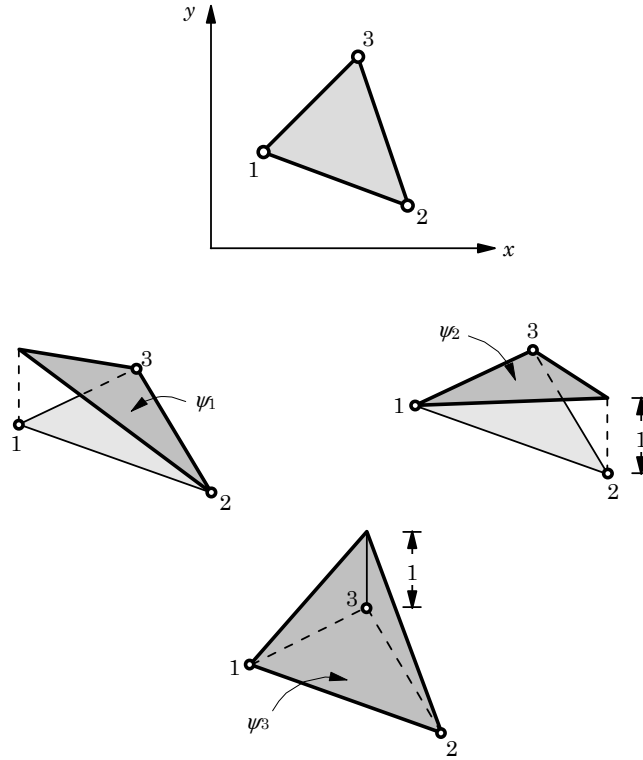


Figure 12.3.1. Linear Lagrange triangular element and its interpolation functions.

The functions are continuous in x and y and *complete* (i.e., contain all lower order terms of the polynomial). An element with quadratic variation of the dependent variables requires six nodes, because a complete quadratic polynomial in two dimensions has six coefficients

$$\psi_i^e(x, y) = a_i + b_i x + c_i y + d_i x y + e_i x^2 + f_i y^2 \quad (12.3.6)$$

The three vertex nodes uniquely describe the geometry of the element (as in the linear element), and the other three nodes are placed at the midpoints of the sides (Figure 12.3.2). The interpolation functions for linear and quadratic triangular elements are presented below in terms of the area coordinates, L_i (Figure 12.3.2)

$$L_i = \frac{A_i}{A}, \quad A = \sum_{i=1}^3 A_i \quad (12.3.7a)$$

$$\begin{Bmatrix} \psi_1^e \\ \psi_2^e \\ \psi_3^e \end{Bmatrix} = \begin{Bmatrix} L_1 \\ L_2 \\ L_3 \end{Bmatrix}, \quad \begin{Bmatrix} \psi_1^e \\ \psi_2^e \\ \psi_3^e \\ \psi_4^e \\ \psi_5^e \\ \psi_6^e \end{Bmatrix} = \begin{Bmatrix} L_1(2L_1 - 1) \\ L_2(2L_2 - 1) \\ L_3(2L_3 - 1) \\ 4L_1L_2 \\ 4L_2L_3 \\ 4L_3L_1 \end{Bmatrix} \quad (12.3.7b)$$

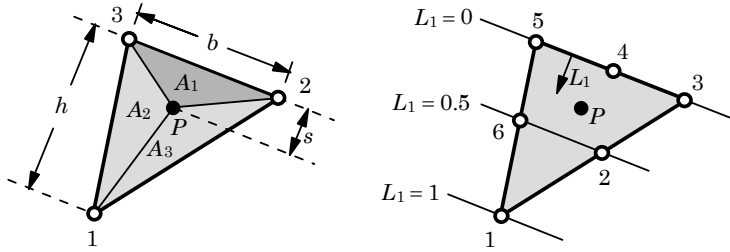


Figure 12.3.2. Quadratic Lagrange triangular element.

The simplest rectangular element has four nodes at its vertices (Figure 12.3.3) that define the geometry. The interpolation functions for this element have the form

$$\psi_i^e(x, y) = a_i + b_i x + c_i y + d_i xy \quad (12.3.8)$$

A complete quadratic polynomial representation

$$\begin{aligned} \psi_i^e(x, y) = & a_i + b_i x + c_i y + d_i xy + e_i x^2 + f_i y^2 + g_i x^2 y \\ & + h_i xy^2 + k_i x^2 y^2 \end{aligned} \quad (12.3.9)$$

for a rectangular element contains 9 parameters and, hence, 9 nodes (Figure 12.3.4a).

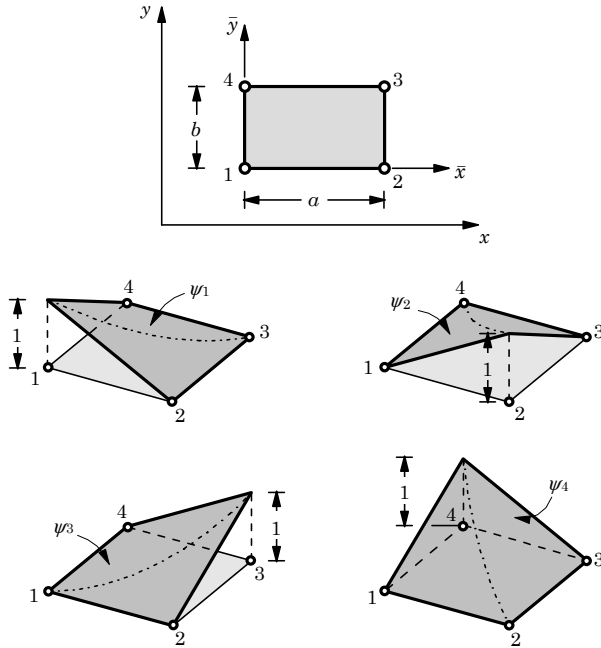


Figure 12.3.3. Linear rectangular element and its interpolation functions.

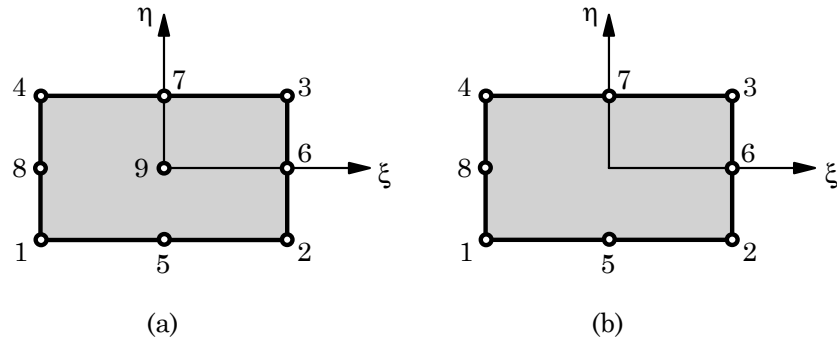


Figure 12.3.4. Nine- and eight-node quadratic rectangular elements.

The linear and quadratic Lagrange interpolation functions of rectangular elements are given in terms of the element or natural coordinates (ξ, η) as

$$\begin{Bmatrix} \psi_1^e \\ \psi_2^e \\ \psi_3^e \\ \psi_4^e \end{Bmatrix} = \frac{1}{4} \begin{Bmatrix} (1-\xi)(1-\eta) \\ (1+\xi)(1-\eta) \\ (1+\xi)(1+\eta) \\ (1-\xi)(1+\eta) \end{Bmatrix} \quad (12.3.10)$$

and

$$\begin{Bmatrix} \psi_1^e \\ \psi_2^e \\ \psi_3^e \\ \psi_4^e \\ \psi_5^e \\ \psi_6^e \\ \psi_7^e \\ \psi_8^e \\ \psi_9^e \end{Bmatrix} = \frac{1}{4} \begin{Bmatrix} (1-\xi)(1-\eta)(-\xi-\eta-1) + (1-\xi^2)(1-\eta^2) \\ (1+\xi)(1-\eta)(\xi-\eta-1) + (1-\xi^2)(1-\eta^2) \\ (1+\xi)(1+\eta)(\xi+\eta-1) + (1-\xi^2)(1-\eta^2) \\ (1-\xi)(1+\eta)(-\xi+\eta-1) + (1-\xi^2)(1-\eta^2) \\ 2(1-\xi^2)(1-\eta) - (1-\xi^2)(1-\eta^2) \\ 2(1+\xi)(1-\eta^2) - (1-\xi^2)(1-\eta^2) \\ 2(1-\xi^2)(1+\eta) - (1-\xi^2)(1-\eta^2) \\ 2(1-\xi)(1-\eta^2) - (1-\xi^2)(1-\eta^2) \\ 4(1-\xi^2)(1-\eta^2) \end{Bmatrix} \quad (12.3.11)$$

The *serendipity* family of Lagrange elements are those elements that have no interior nodes. Serendipity elements have fewer nodes compared to the higher-order Lagrange elements. The interpolation functions of the serendipity elements are not complete, and they cannot be obtained using tensor products of one-dimensional Lagrange interpolation functions. Instead, an alternative procedure must be employed, as discussed in Reddy (2006). The interpolation functions for the quadratic serendipity element are given by (Figure 12.3.4b).

$$\begin{Bmatrix} \psi_1^e \\ \psi_2^e \\ \psi_3^e \\ \psi_4^e \\ \psi_5^e \\ \psi_6^e \\ \psi_7^e \\ \psi_8^e \end{Bmatrix} = \frac{1}{4} \begin{Bmatrix} (1-\xi)(1-\eta)(-\xi-\eta-1) \\ (1+\xi)(1-\eta)(\xi-\eta-1) \\ (1+\xi)(1+\eta)(\xi+\eta-1) \\ (1-\xi)(1+\eta)(-\xi+\eta-1) \\ 2(1-\xi^2)(1-\eta) \\ 2(1+\xi)(1-\eta^2) \\ 2(1-\xi^2)(1+\eta) \\ 2(1-\xi)(1-\eta^2) \end{Bmatrix} \quad (12.3.12)$$

Although the interpolation functions are not complete because the last term in Eq. (12.3.9) is omitted, the serendipity elements have proven to be very effective in most practical applications (*serendipity*!).

12.3.3 Finite Element Model

Substituting Eqs. (12.3.3) and (12.3.4a,b) for (w_0, ϕ_x, ϕ_y) into Eqs. (12.3.1a–c), we obtain the following semidiscrete finite element model of the FSDT:

$$\begin{aligned} & \left(\begin{bmatrix} [K^{11}] & [K^{12}] & [K^{13}] \\ [K^{12}]^T & [K^{22}] & [K^{23}] \\ [K^{13}]^T & [K^{23}]^T & [K^{33}] \end{bmatrix} + \begin{bmatrix} [G] & [0] & [0] \\ [0] & [0] & [0] \\ [0] & [0] & [0] \end{bmatrix} \right) \begin{Bmatrix} \{w^e\} \\ \{S^1\} \\ \{S^2\} \end{Bmatrix} \\ & + \begin{bmatrix} [M^{11}] & [0] & [0] \\ [0] & [M^{22}] & [0] \\ [0] & [0] & [M^{33}] \end{bmatrix} \begin{Bmatrix} \{\ddot{w}^e\} \\ \{\ddot{S}^1\} \\ \{\ddot{S}^2\} \end{Bmatrix} = \begin{Bmatrix} \{F^1\} \\ \{F^2\} - \{F^{T2}\} \\ \{F^3\} - \{F^{T3}\} \end{Bmatrix} \end{aligned} \quad (12.3.13a)$$

or

$$[K^e]\{\Delta^e\} + [M^e]\{\ddot{\Delta}^e\} = \{F^e\} \quad (12.3.13b)$$

where the coefficients of the submatrices $[K^{\alpha\beta}]$ and $[M^{\alpha\beta}]$ and vectors $\{F^\alpha\}$ are defined for $(\alpha, \beta = 1, 2, 3)$ by the expressions

$$\begin{aligned} K_{ij}^{11} &= \int_{\Omega^e} \left(K_s A_{55} \frac{\partial \psi_i^e}{\partial x} \frac{\partial \psi_j^e}{\partial x} + K_s A_{44} \frac{\partial \psi_i^e}{\partial y} \frac{\partial \psi_j^e}{\partial y} + k \psi_i^e \psi_j^e \right) dx dy \\ K_{ij}^{12} &= \int_{\Omega^e} K_s A_{55} \frac{\partial \psi_i^e}{\partial x} \psi_j^e dx dy, \quad K_{ij}^{13} = \int_{\Omega^e} K_s A_{44} \frac{\partial \psi_i^e}{\partial y} \psi_j^e dx dy \\ K_{ij}^{22} &= \int_{\Omega^e} \left(D_{11} \frac{\partial \psi_i^e}{\partial x} \frac{\partial \psi_j^e}{\partial x} + D_{66} \frac{\partial \psi_i^e}{\partial y} \frac{\partial \psi_j^e}{\partial y} + K_s A_{55} \psi_i^e \psi_j^e \right) dx dy \\ K_{ij}^{23} &= \int_{\Omega^e} \left(D_{12} \frac{\partial \psi_i^e}{\partial x} \frac{\partial \psi_j^e}{\partial y} + D_{66} \frac{\partial \psi_i^e}{\partial y} \frac{\partial \psi_j^e}{\partial x} \right) dx dy \\ K_{ij}^{33} &= \int_{\Omega^e} \left(D_{66} \frac{\partial \psi_i^e}{\partial x} \frac{\partial \psi_j^e}{\partial x} + D_{22} \frac{\partial \psi_i^e}{\partial y} \frac{\partial \psi_j^e}{\partial y} + K_s A_{44} \psi_i^e \psi_j^e \right) dx dy \\ M_{ij}^{11} &= \int_{\Omega^e} I_0 \psi_i^e \psi_j^e dx dy, \quad M_{ij}^{22} = \int_{\Omega^e} I_2 \psi_i^e \psi_j^e dx dy = M_{ij}^{33} \\ F_i^1 &= \int_{\Omega^e} q \psi_i^e dx dy + \oint_{\Gamma_e} Q_n \psi_i^e ds \\ F_i^2 &= \oint_{\Gamma_e} T_x \psi_i^e dx dy, \quad F_i^3 = \int_{\Gamma_e} T_y \psi_i^e dx dy \\ F_i^{T2} &= \oint_{\Gamma_e} \left(\frac{\partial \psi_i^e}{\partial x} M_{xx}^T + \frac{\partial \psi_i^e}{\partial y} M_{xy}^T \right) dx dy \\ F_i^{T3} &= \int_{\Gamma_e} \left(\frac{\partial \psi_i^e}{\partial x} M_{xy}^T + \frac{\partial \psi_i^e}{\partial y} M_{yy}^T \right) dx dy \end{aligned} \quad (12.3.14)$$

where A_{ij} and D_{ij} are the plate stiffnesses given in Eq. (10.1.27) and M_{xx}^T, M_{yy}^T , and M_{xy}^T are the thermal moments.

The displacement-based C^0 plate-bending element of Eq. (12.3.13b) is often referred to in the finite element literature as the *Mindlin plate element* due to the fact that it is based on the so-called Mindlin plate theory, which is labelled in this book as the first-order shear deformation plate theory (FSDT). When the bilinear rectangular element is used for all generalized displacements (w_0, ϕ_x, ϕ_y) , the element stiffness matrices are of the order 12×12 ; and for the nine-node quadratic element, they are 27×27 (Figure 12.3.5).

Equation (12.3.13b) can be simplified for static bending, buckling, natural vibration, and transient analysis, as described for the classical plate element in Section 12.2. The simplifications are obvious and, therefore, are not repeated for the FSDT element. Numerical results for bending, buckling, and natural vibration will be discussed next.

The C^0 plate-bending elements based on the first-order shear deformation plate theory are among the simplest available in the literature. Unfortunately, when lower order (quadratic or less) equal interpolation of the transverse deflection and rotations is used, the elements become excessively stiff in the thin plate limit, yielding displacements that are too small compared to the true solution. This type of behavior is known as *shear locking*. A commonly used technique is to under-integrate the transverse shear stiffnesses (i.e., coefficients in $K_{ij}^{\alpha\beta}$ that contain A_{44} and A_{55}). Higher-order elements or refined meshes of lower-order elements experience relatively less locking, but sometimes at the expense of rate of convergence. With the suggested Gauss rule, highly distorted elements tend to have slower rates of convergence, but they give sufficiently accurate results [see Reddy (2004b)].

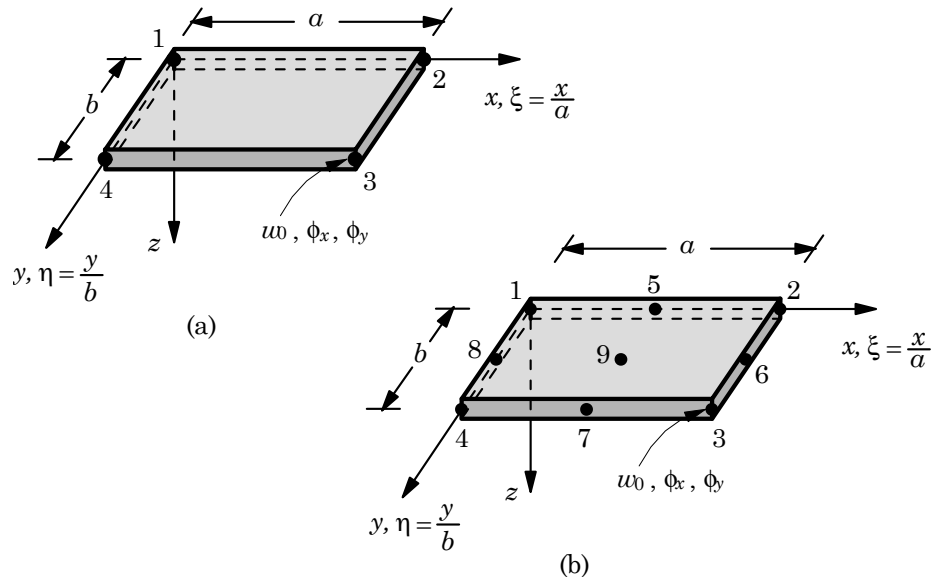


Figure 12.3.5. Linear and nine-node quadratic rectangular elements for the first-order shear deformation theory.

12.3.4 Numerical Results

The effect of the integration rule and the convergence characteristics of the C^0 finite element model based on equal interpolation is illustrated using a simply supported square plates. An isotropic ($\nu = 0.3$) plate subjected to a sinusoidally distributed transverse load

$$q(x, y) = q_0 \cos \frac{\pi x}{a} \sin \frac{\pi y}{b} \quad (12.3.15)$$

and an orthotropic plate under uniformly distributed load of intensity q_0 are analyzed using various meshes of four-node and nine-node elements. The orthotropic material properties used are [see Eq. (10.4.18)]

$$\begin{aligned} E_1 &= 20.83 \text{ msi}, & E_2 &= 10.94 \text{ msi}, & \nu_{12} &= 0.44 \\ G_{12} &= 6.10 \text{ msi}, & G_{13} &= 3.71 \text{ msi}, & G_{23} &= 6.19 \text{ msi} \end{aligned} \quad (12.3.16)$$

As noted earlier, the stresses in the finite element analysis are computed at the reduced Gauss points [see Barlow (1976, 1989)], irrespective of the Gauss rule used for the evaluation of the element stiffness coefficients. The Gauss point locations differ for each mesh used. The Gauss point coordinates A and B are shown in Table 12.3.1 for various meshes of linear (four-node) and quadratic (nine-node) rectangular elements. The finite element solutions are compared with the analytical solutions (ANS) of Chapter 10 (see Tables 10.4.1 and 10.4.2) in Table 12.3.2 for thin ($a/h = 100$) and thick ($a/h = 10$) plates. Results obtained with full integration (F) and selective integration (S) rules are presented. The following nondimensional variables are used [$\sigma(\cdot, z_0) = -\sigma(\cdot, -z_0)$] in Table 12.3.2:

$$\begin{aligned} \bar{w} &= 10w_0(0, 0) \frac{E_2 h^3}{b^4 q_0}, & \bar{\sigma}_{xx} &= \sigma_{xx}(A, A, \frac{h}{2}) \frac{h^2}{b^2 q_0} \\ \bar{\sigma}_{yy} &= \sigma_{yy}(A, A, \frac{h}{2}) \frac{h^2}{b^2 q_0}, & \bar{\sigma}_{xy} &= \sigma_{xy}(B, B, -\frac{h}{2}) \frac{h^2}{b^2 q_0} \\ \bar{\sigma}_{xz} &= \sigma_{xz}(B, A) \frac{h}{b q_0}, & \bar{\sigma}_{yz} &= \sigma_{yz}(A, B) \frac{h}{b q_0} \end{aligned} \quad (12.3.17)$$

where the values of (A, B) are given in Table 12.3.1, and the origin of the coordinate system is taken at the center of the plate, $-a/2 \leq x \leq a/2, -a/2 \leq y \leq a/2$, and $-h/2 \leq z \leq h/2$. The notation $nL4$ stands for $n \times n$ uniform mesh of linear rectangular elements and $nQ9$ for $n \times n$ uniform mesh of nine-node quadratic elements in a quarter plate.

Table 12.3.1. The Gauss point locations at which the stresses are computed in the finite element analysis.

Coordinate	2L	4L	8L	2Q9	4Q9	Exact
A	$0.125a$	$0.0625a$	$0.03125a$	$0.05283a$	$0.02642a$	0.00
B	$0.375a$	$0.4375a$	$0.46875a$	$0.44717a$	$0.47358a$	$0.5a$

Table 12.3.2. Effect of the Gauss integration rules used for the evaluation of bending and transverse shear coefficients of the element stiffness matrix on the nondimensional maximum deflections \bar{w} and stresses $\bar{\sigma}$ of simply supported square plates (isotropic plates under sinusoidal load and orthotropic plates under uniform load).

a/h	Source	\bar{w}	$\bar{\sigma}_{xx}$	$\bar{\sigma}_{yy}$	$\bar{\sigma}_{xy}$	$-10^2 \bar{\sigma}_{xz}$	$-10^2 \bar{\sigma}_{yz}$
<i>Isotropic plates under sinusoidal load</i>							
100	4L4-F [†]	0.0118	0.0078	0.0078	0.0042	0.1840	0.1840
	4L4-S	0.2780	0.1860	0.1860	0.1001	0.1837	0.1837
	2Q9-F	0.2723	0.1800	0.1800	0.1011	0.1846	0.1846
	2Q9-S	0.2806	0.1917	0.1917	0.1033	0.1850	0.1850
	8L4-F	0.0419	0.0290	0.0290	0.0156	0.1885	0.1885
	8L4-S	0.2798	0.1946	0.1946	0.1048	0.1892	0.1892
	4Q9-F	0.2787	0.1934	0.1934	0.1051	0.1896	0.1896
	4Q9-S	0.2804	0.1962	0.1962	0.1056	0.1896	0.1896
	ANS	0.2804	0.1976	0.1976	0.1064	0.1910	0.1910
10	4L4-F	0.2421	0.1513	0.1513	0.0815	0.1813	0.1813
	4L4-S	0.2940	0.1860	0.1860	0.1001	0.1837	0.1837
	2Q9-F	0.2940	0.1886	0.1886	0.1027	0.1855	0.1855
	2Q9-S	0.2962	0.1917	0.1917	0.1032	0.1855	0.1855
	8L4-F	0.2804	0.1841	0.1841	0.0991	0.1813	0.1813
	8L4-S	0.2956	0.1946	0.1946	0.1048	0.1819	0.1819
	4Q9-F	0.2959	0.1959	0.1959	0.1056	0.1897	0.1897
	4Q9-S	0.2961	0.1962	0.1962	0.1056	0.1897	0.1897
	ANS	0.2961	0.1976	0.1976	0.1064	0.1910	0.1910
<i>Orthotropic plates under uniform load</i>							
100	8L4-F	0.0548	0.0655	0.0407	0.0324	0.3319	0.4362
	8L4-S	0.3024	0.3575	0.2144	0.1864	0.4115	0.3237
	4Q9-F	0.3012	0.3578	0.2150	0.1876	0.4176	0.3292
	4Q9-S	0.3024	0.3591	0.2153	0.1898	0.4159	0.3279
	ANS	0.3024	0.3609	0.2163	0.1939	0.4399	0.3514
10	8L4-F	0.3117	0.3380	0.2096	0.1787	0.4056	0.3319
	8L4-S	0.3250	0.3528	0.2177	0.1872	0.4098	0.3259
	4Q9-F	0.3252	0.3544	0.2187	0.1906	0.4144	0.3304
	4Q9-S	0.3253	0.3545	0.2186	0.1905	0.4143	0.3302
	ANS	0.3252	0.3562	0.2196	0.1947	0.4381	0.3537

[†]F = Full integration of all coefficients; S = Full integration of all except the transverse shear coefficients, which are evaluated using reduced integration rule.

* The CPT solution is independent of side-to-thickness ratio, a/h .

An examination of the numerical results presented in Table 12.3.2 shows that the FSDT finite element with equal interpolation of all generalized displacements does not experience shear locking for thick plates even when the full integration rule is used. Shear locking is evident when the element is used to model thin plates ($a/h \geq 100$) with full integration rule (F). Also, higher-order elements show less locking, but with slower convergence. The element behaves uniformly well for thin and thick plates when selectively reduced integration (S) rule is used. The transverse shear stresses are not affected by the integration rule.

The finite element results are in excellent agreement with the analytical solutions of the FSDT. The displacements converge faster than stresses. This is expected with all displacement finite element models because the rate of convergence of gradients of the solution is one order less than the rate of convergence of the solution.

Next, we consider a sandwich plate subjected to sinusoidally distributed transverse load [see Reddy (2004a)]. The sandwich plate is treated as a three-layer plate with different thickness of the face sheets (layers 1 and 3) and the core (layer 2). The face sheets are assumed to be orthotropic with the following material properties

$$\begin{aligned} E_1 &= 25E_2, \quad E_2 = 10^6 \text{ psi}, \quad G_{12} = G_{13} = 0.5E_2 \\ G_{23} &= 0.2E_2, \quad \nu_{12} = 0.25 \end{aligned} \quad (12.3.19)$$

and the core material is transversely isotropic and is characterized by the following material properties:

$$\begin{aligned} E_1 &= E_2 = 10^6 \text{ psi}, \quad G_{13} = G_{23} = 0.06 \times 10^6 \text{ psi}, \quad \nu_{12} = 0.25 \\ G_{12} &= \frac{E_1}{2(1 + \nu_{12})} = 0.016 \times 10^6 \text{ psi} \end{aligned} \quad (12.3.20)$$

Each face sheet is assumed to be one-tenth of the total thickness of the sandwich plate ($a = b$). The finite element results obtained with 4×4 mesh of eight-node quadratic elements with reduced integration (4Q8-R) are compared with the closed-form solution and elasticity solution of Pagano (1970) in Table 12.3.3. The nondimensional stresses as defined before are used and their locations with respect to a coordinate system whose origin is at the center of the plate are as follows:

$$\begin{aligned} \sigma_{xx}(0, 0, \frac{h}{2}), \quad \sigma_{yy}(0, 0, \frac{h}{2}), \quad \sigma_{xy}(a/2, b/2, -\frac{h}{2}) \\ \sigma_{xz}(0, b/2, 0), \quad \sigma_{yz}(a/2, 0, 0) \end{aligned}$$

The results indicate that the effect of shear deformation on deflections is significant in sandwich plates even at large values of a/h . The equilibrium-derived transverse shear stresses are surprisingly close to those predicted by the elasticity theory for $a/h \geq 10$, while those computed from constitutive equations are considerably underestimated for small side-to-thickness ratios. The transverse shear stress component σ_{yz} is significantly overestimated by CPT. Figures 12.3.6 and 12.3.7 show the variation of the transverse shear stresses through the thickness of the sandwich plates for side-to-thickness ratios $a/h = 2, 10$, and 100 .

Table 12.3.3. Comparison of nondimensional maximum deflections and stresses in a simply supported sandwich plate subjected to sinusoidally varying transverse load ($h_1 = h_3 = 0.1h$, $h_2 = 0.8h$, $K = 5/6$).

a/h	Source	$\bar{w} \times 10^2$	$\bar{\sigma}_{xx}$	$\bar{\sigma}_{yy}$	$\bar{\sigma}_{xy}$	$\bar{\sigma}_{xz}$	$\bar{\sigma}_{yz}$
2	ELS	—	3.278	0.4517	0.2338	0.185	0.1399
	CFS	14.928	0.7378	0.2328	0.1263	0.1084	0.0781
	FEM	14.927	0.7326	0.2311	0.1254	0.1077	0.0776
4	ELS	—	1.556	0.2595	0.1481	0.239	0.1072
	CFS	4.7666	0.8918	0.1562	0.0907	0.1229	0.0537
	FEM	4.7663	0.8856	0.1551	0.0901	0.1221	0.0534
10	ELS	—	1.153	0.1104	0.0717	0.300	0.0527
	CFS	1.5604	1.0457	0.0798	0.0552	0.1374	0.0293
	FEM	1.5603	1.0384	0.0792	0.0548	0.1365	0.0278
20	ELS	—	1.110	0.0700	0.0511	0.317	0.0361
	CFS	1.0524	1.0831	0.0612	0.0466	0.1409	0.0234
	FEM	1.0523	1.0755	0.0608	0.0462	0.1399	0.0233
50	ELS	—	1.099	0.0569	0.0446	0.323	0.0306
	CFS	0.9063	1.0947	0.0554	0.0439	0.1420	0.0216
	FEM	0.9061	1.087	0.0551	0.0436	0.1410	0.0214
100	ELS	—	1.098	0.0550	0.0437	0.324	0.0297
	CFS	0.8852	1.0964	0.0546	0.0435	0.1422	0.0213
	FEM	0.8851	1.0887	0.0542	0.0432	0.1412	0.0161
	CPT	0.8782	1.0970	0.0543	0.0433	0.3243	0.0295

† Values computed from equilibrium equations.

The same sandwich plate discussed above is analyzed for simply supported and clamped boundary conditions when uniformly distributed load is used. Once again a quarter plate model is used with 4×4 mesh of quadratic FSDT elements and 8×8 mesh of CPT conforming cubic elements. The results are presented in Table 12.3.4. The effect of shear deformation on the deflections is even more significant in clamped plates than in simply supported plates.

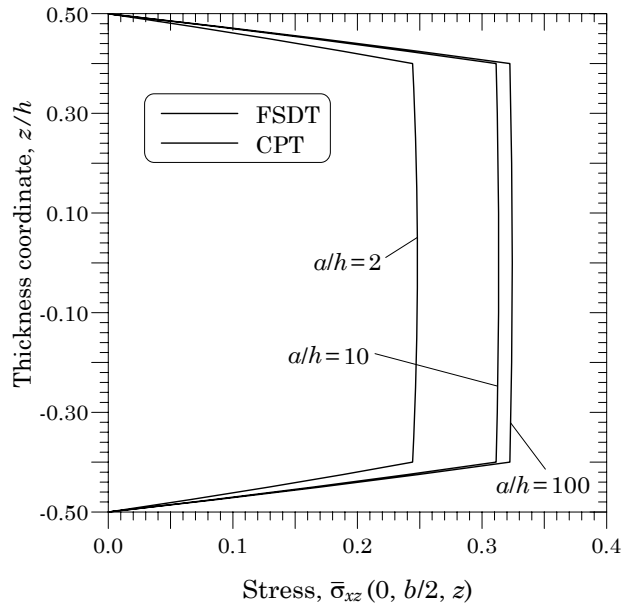


Figure 12.3.6. Distribution of transverse shear stress σ_{xz} through the thickness of a simply supported sandwich plate under sinusoidally distributed transverse load.

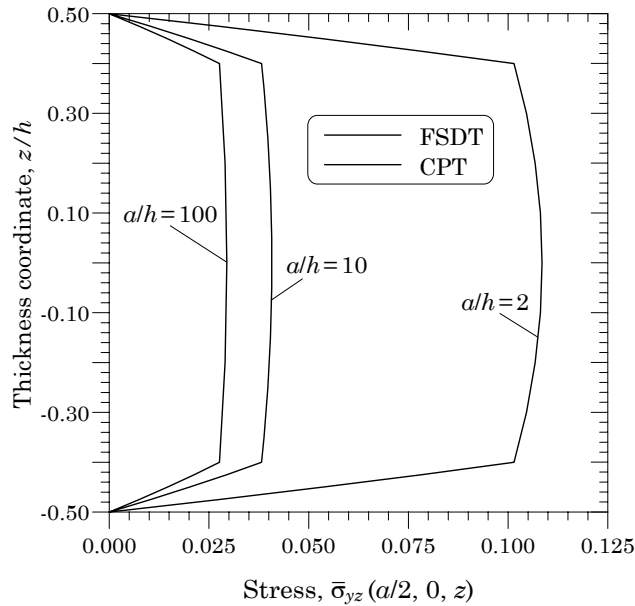


Figure 12.3.7. Distribution of transverse shear stress σ_{yz} through the thickness of a simply supported sandwich plate under sinusoidally distributed transverse load.

Effects of side-to-thickness ratio, integration, and type of element on the nondimensional fundamental frequency $\bar{\omega}$ of simply supported square laminates (0/90/90/0) on the accuracy of the natural frequencies can be seen from the results presented in Table 12.3.5. The lamina material properties are taken to be $E_1 = 40E_2$, $G_{12} = G_{13} = 0.6E_2$, $G_{23} = 0.5E_2$, and $\nu_{12} = 0.25$. A 2×2 mesh in a quarter plate is used to obtain the results (rotary inertia included). From the results obtained, it is clear that both full (F) and selective (S) integrations give good results for thick plates ($a/h \leq 10$), whereas reduced integration (R) gives the best results for thin plates ($a/h \geq 100$). However, the reduced integration and selective integration rules both give good results for a wide range of side-to-thickness ratios.

Table 12.3.4. Nondimensional maximum deflections and stresses in a square sandwich plate with simply supported and clamped boundary conditions ($h_1 = h_3 = 0.1h$, $h_2 = 0.8h$, $K = 5/6$).

a/h	Source	$\bar{w} \times 10^2$	$\bar{\sigma}_{xx}$	$\bar{\sigma}_{yy}$	$\bar{\sigma}_{xy}$	$\bar{\sigma}_{xz}$	$\bar{\sigma}_{yz}$
<i>Simply supported plate under uniformly distributed load</i>							
10	4Q8-R	2.3370	1.5430	0.0883	0.1136	0.2396	0.0991
50	4Q8-R	1.3671	1.5964	0.0526	0.0916	0.2433	0.0881
100	4Q8-R	1.3359	1.5978	0.0514	0.0906	0.2394	0.0880
CLPT	8CC-F [†]	1.3296	1.5830	0.0509	0.0906	—	—
<i>Clamped plate under uniformly distributed load</i>							
10	4Q9-R [†]	1.2654	0.5018	0.0550	0.0120	0.2318	0.1445
50	4Q9-R	0.3111	0.5356	0.0108	0.0039	0.2406	0.1160
100	4Q9-R	0.2785	0.5347	0.0094	0.0030	0.2400	0.1148
CPT	8CC-F [‡]	0.2951	0.5401	0.0145	0.0605	—	—

[†] The 4Q9-S element gives the same results as 4Q9-R.

[‡] 8×8 mesh of conforming cubic elements with full integration for stiffness coefficient evaluation and one-point Gauss rule for stresses.

Table 12.3.5. Effects of side-to-thickness ratio, integration, and type of element on the nondimensional fundamental frequency $\bar{\omega} = \omega(a^2/h)\sqrt{\rho/E_2}$ of simply supported square laminates (0/90/90/0).

a/h	Serendipity Element			Lagrange Element			Exact
	F	R	S	F	R	S	
2	5.502	5.503	5.501	5.502	5.503	5.501	5.500
10	15.174	15.179	15.159	15.182	15.193	15.172	15.143
100	19.171	18.841	18.808	19.225	18.883	18.933	18.836

12.4 Nonlinear Finite Element Models

12.4.1 Introduction

In the nonlinear formulation of plate theories based on small strains and moderate rotations, the geometry of the structure is assumed to remain unchanged during the loading, and the geometric nonlinearity in the form of the von Kármán strains is included. Here we only consider static case without temperature effects. For additional details and complications, see Reddy (2004a, 2004b).

The displacement finite element models of the classical plate theory require C^1 approximation of w_0 , but C^0 approximation of u_0 and v_0 , whereas the first-order shear deformation theory requires C^0 approximation of all generalized displacements ($u_0, v_0, w_0, \phi_x, \phi_y$). These finite element models are discussed in detail next. Since the resulting finite element models consist of a set of nonlinear algebraic equations, iterative methods to solve them are also discussed.

12.4.2 Classical Plate Theory

Governing Equations

The equations of equilibrium of the classical theory of plates are [see Eqs. (3.4.15)–(3.4.17)]

$$\begin{aligned} -\left(\frac{\partial N_{xx}}{\partial x} + \frac{\partial N_{xy}}{\partial y}\right) &= 0 \\ -\left(\frac{\partial N_{xy}}{\partial x} + \frac{\partial N_{yy}}{\partial y}\right) &= 0 \\ -\left(\frac{\partial^2 M_{xx}}{\partial x^2} + 2\frac{\partial^2 M_{xy}}{\partial y \partial x} + \frac{\partial^2 M_{yy}}{\partial y^2}\right) - \mathcal{N}(u_0, v_0, w_0) - q &= 0 \end{aligned} \quad (12.4.1)$$

where the nonlinear expression \mathcal{N} is defined by

$$\mathcal{N}(u_0, v_0, w_0) = \frac{\partial}{\partial x} \left(N_{xx} \frac{\partial w_0}{\partial x} + N_{xy} \frac{\partial w_0}{\partial y} \right) + \frac{\partial}{\partial y} \left(N_{xy} \frac{\partial w_0}{\partial x} + N_{yy} \frac{\partial w_0}{\partial y} \right) \quad (12.4.2)$$

The stress resultants (N_{xx}, N_{yy}, N_{xy}) and (M_{xx}, M_{yy}, M_{xy}) are known in terms of the displacements by [see Eqs. (3.6.6) and (3.6.7)]

$$\begin{aligned} \begin{Bmatrix} N_{xx} \\ N_{yy} \\ N_{xy} \end{Bmatrix} &= \begin{bmatrix} A_{11} & A_{12} & 0 \\ A_{12} & A_{22} & 0 \\ 0 & 0 & A_{66} \end{bmatrix} \begin{Bmatrix} \frac{\partial u_0}{\partial x} + \frac{1}{2} \left(\frac{\partial w_0}{\partial x} \right)^2 \\ \frac{\partial v_0}{\partial y} + \frac{1}{2} \left(\frac{\partial w_0}{\partial y} \right)^2 \\ \frac{\partial u_0}{\partial y} + \frac{\partial v_0}{\partial x} + \frac{\partial w_0}{\partial x} \frac{\partial w_0}{\partial y} \end{Bmatrix} \\ \begin{Bmatrix} M_{xx} \\ M_{yy} \\ M_{xy} \end{Bmatrix} &= \begin{bmatrix} D_{11} & D_{12} & 0 \\ D_{12} & D_{22} & 0 \\ 0 & 0 & D_{66} \end{bmatrix} \begin{Bmatrix} -\frac{\partial^2 w_0}{\partial x^2} \\ -\frac{\partial^2 w_0}{\partial y^2} \\ -2 \frac{\partial^2 w_0}{\partial x \partial y} \end{Bmatrix} \end{aligned} \quad (12.4.3)$$

Here A_{ij} and D_{ij} denote the extensional and bending stiffnesses of the plate

$$(A_{ij}, D_{ij}) = \int_{-h/2}^{h/2} Q_{ij}(1, z) dz \quad (12.4.4)$$

and the plane stress-reduced elastic coefficients Q_{ij} of an orthotropic material [see Eq. (3.6.2)]. We have

$$\begin{aligned} A_{11} &= Q_{11}h = \frac{E_1 h}{1 - \nu_{12}\nu_{21}}, & A_{22} &= Q_{22}h = \frac{E_2 h}{1 - \nu_{12}\nu_{21}} \\ D_{11} &= Q_{11} \frac{h^3}{12} = \frac{E_1 h^3}{12(1 - \nu_{12}\nu_{21})}, & D_{12} &= Q_{12} \frac{h^3}{12} = \frac{\nu_{12}E_2 h^3}{12(1 - \nu_{12}\nu_{21})} \\ D_{22} &= Q_{22} \frac{h^3}{12} = \frac{E_2 h^3}{12(1 - \nu_{12}\nu_{21})}, & D_{66} &= Q_{66} \frac{h^3}{12} = \frac{G_{12}h^3}{12} \\ A_{66} &= Q_{66}h = G_{12}h, & A_{44} &= G_{23}h, & A_{55} &= G_{13}h \end{aligned} \quad (12.4.5)$$

Weak Forms

The weak forms of Eqs. (12.4.1)–(12.4.3) over a typical finite element are obtained from the principle of virtual work statement (3.4.10) [but after including the Kirchhoff free-edge term (3.5.13)]

$$\begin{aligned} 0 &= \int_{\Omega^e} \left[\left(\frac{\partial \delta u_0}{\partial x} + \frac{\partial \delta w_0}{\partial x} \frac{\partial w_0}{\partial x} \right) N_{xx} + \left(\frac{\partial \delta v_0}{\partial y} + \frac{\partial \delta w_0}{\partial y} \frac{\partial w_0}{\partial y} \right) N_{yy} \right. \\ &\quad + \left(\frac{\partial \delta u_0}{\partial y} + \frac{\partial \delta v_0}{\partial x} + \frac{\partial \delta w_0}{\partial x} \frac{\partial w_0}{\partial y} + \frac{\partial \delta w_0}{\partial y} \frac{\partial w_0}{\partial x} \right) N_{xy} \\ &\quad \left. - \frac{\partial^2 \delta w_0}{\partial x^2} M_{xx} - \frac{\partial^2 \delta w_0}{\partial y^2} M_{yy} - 2 \frac{\partial^2 \delta w_0}{\partial x \partial y} M_{xy} - \delta w_0 q \right] dx dy \\ &\quad - \oint_{\Gamma^e} \left(\delta u_{0n} N_{nn} + \delta u_{0s} N_{ns} \delta w_0 V_n - \frac{\partial w_0}{\partial n} M_{nn} \right) ds \end{aligned} \quad (12.4.6)$$

where [see Eqs. (3.5.4)–(3.5.8) and (3.5.15)]

$$\begin{aligned} u_{0n} &= u_0 n_x + v_0 n_y, & u_{0s} &= -u_0 n_y + v_0 n_x \\ N_{nn} &= (N_{xx} n_x + N_{xy} n_y) n_x + (N_{xy} n_x + N_{yy} n_y) n_y \\ N_{ns} &= -(M_{xx} n_x + M_{xy} n_y) n_y + (M_{xy} n_x + M_{yy} n_y) n_x \\ M_{nn} &= (M_{xx} n_x + M_{xy} n_y) n_x + (M_{xy} n_x + M_{yy} n_y) n_y \\ M_{ns} &= -(M_{xx} n_x + M_{xy} n_y) n_y + (M_{xy} n_x + M_{yy} n_y) n_x \end{aligned} \quad (12.4.7)$$

$$\begin{aligned} V_n &= \frac{\partial M_{ns}}{\partial s} + \left(\frac{\partial M_{xx}}{\partial x} + \frac{\partial M_{xy}}{\partial y} + N_{xx} \frac{\partial w_0}{\partial x} + N_{xy} \frac{\partial w_0}{\partial y} \right) n_x \\ &\quad + \left(\frac{\partial M_{xy}}{\partial x} + \frac{\partial M_{yy}}{\partial y} + N_{xy} \frac{\partial w_0}{\partial x} + N_{yy} \frac{\partial w_0}{\partial y} \right) n_y \end{aligned}$$

and (n_x, n_y) are the direction cosines of the unit normal on the element boundary Γ^e .

The virtual work statement (12.4.6) can be expressed in terms of displacements (u_0, v_0, w_0) by substituting for the stress resultants from Eq. (12.4.3). Then the virtual work statement over a typical plate finite element can be separated into three statements that correspond to the virtual displacements $(\delta u_0, \delta v_0, \delta w_0)$

$$0 = \int_{\Omega^e} \left[\frac{\partial \delta u_0}{\partial x} \left\{ A_{11} \left[\frac{\partial u_0}{\partial x} + \frac{1}{2} \left(\frac{\partial w_0}{\partial x} \right)^2 \right] + A_{12} \left[\frac{\partial v_0}{\partial y} + \frac{1}{2} \left(\frac{\partial w_0}{\partial y} \right)^2 \right] \right\} \right. \\ \left. + A_{66} \frac{\partial \delta u_0}{\partial y} \left(\frac{\partial u_0}{\partial y} + \frac{\partial v_0}{\partial x} + \frac{\partial w_0}{\partial x} \frac{\partial w_0}{\partial y} \right) \right] dx dy \\ - \oint_{\Gamma^e} \delta u_0 (N_{nn} n_x - N_{ns} n_y) ds \quad (12.4.8a)$$

$$0 = \int_{\Omega^e} \left[\frac{\partial \delta v_0}{\partial y} \left\{ A_{12} \left[\frac{\partial u_0}{\partial x} + \frac{1}{2} \left(\frac{\partial w_0}{\partial x} \right)^2 \right] + A_{22} \left[\frac{\partial v_0}{\partial y} + \frac{1}{2} \left(\frac{\partial w_0}{\partial y} \right)^2 \right] \right\} \right. \\ \left. + A_{66} \frac{\partial \delta v_0}{\partial x} \left(\frac{\partial u_0}{\partial y} + \frac{\partial v_0}{\partial x} + \frac{\partial w_0}{\partial x} \frac{\partial w_0}{\partial y} \right) \right] dx dy \\ - \oint_{\Gamma^e} \delta v_0 (N_{nn} n_y + N_{ns} n_x) ds \quad (12.4.8b)$$

$$0 = \int_{\Omega^e} \left[\frac{\partial \delta w_0}{\partial x} \frac{\partial w_0}{\partial x} \left\{ A_{11} \left[\frac{\partial u_0}{\partial x} + \frac{1}{2} \left(\frac{\partial w_0}{\partial x} \right)^2 \right] + A_{12} \left[\frac{\partial v_0}{\partial y} + \frac{1}{2} \left(\frac{\partial w_0}{\partial y} \right)^2 \right] \right\} \right. \\ \left. + \frac{\partial \delta w_0}{\partial y} \frac{\partial w_0}{\partial y} \left\{ A_{12} \left[\frac{\partial u_0}{\partial x} + \frac{1}{2} \left(\frac{\partial w_0}{\partial x} \right)^2 \right] + A_{22} \left[\frac{\partial v_0}{\partial y} + \frac{1}{2} \left(\frac{\partial w_0}{\partial y} \right)^2 \right] \right\} \right. \\ \left. + A_{66} \left(\frac{\partial \delta w_0}{\partial x} \frac{\partial w_0}{\partial y} + \frac{\partial \delta w_0}{\partial y} \frac{\partial w_0}{\partial x} \right) \left(\frac{\partial u_0}{\partial y} + \frac{\partial v_0}{\partial x} + \frac{\partial w_0}{\partial x} \frac{\partial w_0}{\partial y} \right) \right. \\ \left. + \frac{\partial^2 \delta w_0}{\partial x^2} \left(D_{11} \frac{\partial^2 w_0}{\partial x^2} + D_{12} \frac{\partial^2 w_0}{\partial y^2} \right) + \frac{\partial^2 \delta w_0}{\partial y^2} \left(D_{12} \frac{\partial^2 w_0}{\partial x^2} + D_{22} \frac{\partial^2 w_0}{\partial y^2} \right) \right. \\ \left. + 4D_{66} \frac{\partial^2 \delta w_0}{\partial x \partial y} \frac{\partial^2 w_0}{\partial x \partial y} - \delta w_0 q \right] dx dy - \oint_{\Gamma^e} \left(V_n \delta w_0 - M_n \frac{\partial \delta w_0}{\partial n} \right) ds \quad (12.4.8c)$$

Finite Element Model

Assume finite element approximation of the form

$$u_0(x, y) = \sum_{j=1}^m u_j^e \psi_j^e(x, y), \quad v_0(x, y) = \sum_{j=1}^m v_j^e \psi_j^e(x, y) \\ w_0(x, y) = \sum_{j=1}^n \Delta_j^e \varphi_j^e(x, y) \quad (12.4.9)$$

where ψ_j^e are the Lagrange interpolation functions, Δ_j^e are the values of w_0 and its derivatives at the nodes, and φ_j^e are the interpolation functions, the specific form of which will depend on the geometry of the element and the nodal degrees of freedom interpolated. Substituting approximations (12.4.9) into Eqs. (12.4.8), we obtain

$$\begin{bmatrix} [K^{11}] & [K^{12}] & [K^{13}] \\ [K^{21}] & [K^{22}] & [K^{23}] \\ [K^{31}] & [K^{32}] & [K^{33}] \end{bmatrix} \begin{Bmatrix} \{u\} \\ \{v\} \\ \{\Delta\} \end{Bmatrix} = \begin{Bmatrix} \{F^1\} \\ \{F^2\} \\ \{F^3\} \end{Bmatrix}$$

or, in compact form

$$[K^e]\{\bar{\Delta}^e\} = \{F^e\} \quad (12.4.10)$$

The stiffness coefficients $K_{ij}^{\alpha\beta}$ (not symmetric) and force vectors F_i^α ($\alpha, \beta = 1, 2, 3$) are defined as follows:

$$\begin{aligned} K_{ij}^{11} &= \int_{\Omega^e} \left(A_{11} \frac{\partial \psi_i^e}{\partial x} \frac{\partial \psi_j^e}{\partial x} + A_{66} \frac{\partial \psi_i^e}{\partial y} \frac{\partial \psi_j^e}{\partial y} \right) dx dy \\ K_{ij}^{12} &= \int_{\Omega^e} \left(A_{12} \frac{\partial \psi_i^e}{\partial x} \frac{\partial \psi_j^e}{\partial y} + A_{66} \frac{\partial \psi_i^e}{\partial y} \frac{\partial \psi_j^e}{\partial x} \right) dx dy = K_{ji}^{21} \\ K_{ij}^{13} &= \frac{1}{2} \int_{\Omega^e} \left[\frac{\partial \psi_i^e}{\partial x} \left(A_{11} \frac{\partial w_0}{\partial x} \frac{\partial \varphi_j^e}{\partial x} + A_{12} \frac{\partial w_0}{\partial y} \frac{\partial \varphi_j^e}{\partial y} \right) \right. \\ &\quad \left. + A_{66} \frac{\partial \psi_i^e}{\partial y} \left(\frac{\partial w_0}{\partial x} \frac{\partial \varphi_j^e}{\partial y} + \frac{\partial w_0}{\partial y} \frac{\partial \varphi_j^e}{\partial x} \right) \right] dx dy \\ K_{ij}^{22} &= \int_{\Omega^e} \left(A_{66} \frac{\partial \psi_i^e}{\partial x} \frac{\partial \psi_j^e}{\partial x} + A_{22} \frac{\partial \psi_i^e}{\partial y} \frac{\partial \psi_j^e}{\partial y} \right) dx dy \\ K_{ij}^{23} &= \frac{1}{2} \int_{\Omega^e} \left[\frac{\partial \psi_i^e}{\partial y} \left(A_{12} \frac{\partial w_0}{\partial x} \frac{\partial \varphi_j^e}{\partial x} + A_{22} \frac{\partial w_0}{\partial y} \frac{\partial \varphi_j^e}{\partial y} \right) \right. \\ &\quad \left. + A_{66} \frac{\partial \psi_i^e}{\partial x} \left(\frac{\partial w_0}{\partial x} \frac{\partial \varphi_j^e}{\partial y} + \frac{\partial w_0}{\partial y} \frac{\partial \varphi_j^e}{\partial x} \right) \right] dx dy \\ K_{ij}^{31} &= \int_{\Omega^e} \left[\frac{\partial \varphi_i^e}{\partial x} \left(A_{11} \frac{\partial w_0}{\partial x} \frac{\partial \psi_j^e}{\partial x} + A_{66} \frac{\partial w_0}{\partial y} \frac{\partial \psi_j^e}{\partial y} \right) \right. \\ &\quad \left. + \frac{\partial \varphi_i^e}{\partial y} \left(A_{66} \frac{\partial w_0}{\partial x} \frac{\partial \psi_j^e}{\partial y} + A_{12} \frac{\partial w_0}{\partial y} \frac{\partial \psi_j^e}{\partial x} \right) \right] dx dy \\ K_{ij}^{32} &= \int_{\Omega^e} \left[\frac{\partial \varphi_i^e}{\partial x} \left(A_{12} \frac{\partial w_0}{\partial x} \frac{\partial \psi_j^e}{\partial y} + A_{66} \frac{\partial w_0}{\partial y} \frac{\partial \psi_j^e}{\partial x} \right) \right. \\ &\quad \left. + \frac{\partial \varphi_i^e}{\partial y} \left(A_{66} \frac{\partial w_0}{\partial x} \frac{\partial \psi_j^e}{\partial x} + A_{22} \frac{\partial w_0}{\partial y} \frac{\partial \psi_j^e}{\partial y} \right) \right] dx dy \\ K_{ij}^{33} &= \int_{\Omega^e} \left[D_{11} \frac{\partial^2 \varphi_i^e}{\partial x^2} \frac{\partial^2 \varphi_j^e}{\partial x^2} + D_{22} \frac{\partial^2 \varphi_i^e}{\partial y^2} \frac{\partial^2 \varphi_j^e}{\partial y^2} \right. \\ &\quad \left. + D_{12} \left(\frac{\partial^2 \varphi_i^e}{\partial x^2} \frac{\partial^2 \varphi_j^e}{\partial y^2} + \frac{\partial^2 \varphi_i^e}{\partial y^2} \frac{\partial^2 \varphi_j^e}{\partial x^2} \right) \right. \\ &\quad \left. + 4D_{66} \frac{\partial^2 \varphi_i^e}{\partial x \partial y} \frac{\partial^2 \varphi_j^e}{\partial x \partial y} + k \varphi_i^e \varphi_j^e \right] dx dy \end{aligned}$$

$$\begin{aligned}
& + \frac{1}{2} \int_{\Omega^e} \left\{ \left[A_{11} \left(\frac{\partial w_0}{\partial x} \right)^2 + A_{66} \left(\frac{\partial w_0}{\partial y} \right)^2 \right] \frac{\partial \varphi_i^e}{\partial x} \frac{\partial \varphi_j^e}{\partial x} \right. \\
& \quad + \left[A_{66} \left(\frac{\partial w_0}{\partial x} \right)^2 + A_{22} \left(\frac{\partial w_0}{\partial y} \right)^2 \right] \frac{\partial \varphi_i^e}{\partial y} \frac{\partial \varphi_j^e}{\partial y} \\
& \quad \left. + (A_{12} + A_{66}) \frac{\partial w_0}{\partial x} \frac{\partial w_0}{\partial y} \left(\frac{\partial \varphi_i^e}{\partial x} \frac{\partial \varphi_j^e}{\partial y} + \frac{\partial \varphi_i^e}{\partial y} \frac{\partial \varphi_j^e}{\partial x} \right) \right\} dx dy \\
F_i^1 &= \oint_{\Gamma^e} N_n \psi_i^e ds, \quad F_i^2 = \oint_{\Gamma^e} N_s \psi_i^e ds \\
F_i^3 &= \int_{\Omega^e} q \varphi_i^e dx dy + \oint_{\Gamma^e} \left(V_n \varphi_i^e - M_n \frac{\partial \varphi_i^e}{\partial n} \right) ds
\end{aligned} \tag{12.4.11}$$

The plate-bending elements discussed in Section 12.2.3, in connection with linear finite element models of the classical plate theory, can be used here with a choice of Lagrange interpolation of the inplane displacements (u_0, v_0) and Hermite interpolation of w_0 . For example, linear interpolation of (u_0, v_0) and Hermite cubic interpolation of w_0 will have 20 element degrees of freedom for nonconforming rectangular element and 25 degrees of freedom for conforming rectangular element. A discussion of iterative methods for the solution of the nonlinear algebraic equations resulting from (12.4.10) is presented in Section 12.4.4; also, see Reddy (2004b).

12.4.3 First-Order Shear Deformation Plate Theory Governing Equations

The equations of equilibrium of the first-order shear deformation plate theory (FSDT) are given by

$$\begin{aligned}
& - \left(\frac{\partial N_{xx}}{\partial x} + \frac{\partial N_{xy}}{\partial y} \right) = 0 \\
& - \left(\frac{\partial N_{xy}}{\partial x} + \frac{\partial N_{yy}}{\partial y} \right) = 0 \\
& - \left(\frac{\partial Q_x}{\partial x} + \frac{\partial Q_y}{\partial y} \right) - \mathcal{N}(u_0, v_0, w_0) - q = 0 \\
& - \left(\frac{\partial M_{xx}}{\partial x} + \frac{\partial M_{xy}}{\partial y} \right) + Q_x = 0 \\
& - \left(\frac{\partial M_{xy}}{\partial x} + \frac{\partial M_{yy}}{\partial y} \right) + Q_y = 0
\end{aligned} \tag{12.4.12}$$

where \mathcal{N} is defined by Eq. (12.4.2), and the stress resultants are given by

$$\begin{Bmatrix} N_{xx} \\ N_{yy} \\ N_{xy} \end{Bmatrix} = \begin{bmatrix} A_{11} & A_{12} & 0 \\ A_{12} & A_{22} & 0 \\ 0 & 0 & A_{66} \end{bmatrix} \begin{Bmatrix} \frac{\partial u_0}{\partial x} + \frac{1}{2} \left(\frac{\partial w_0}{\partial x} \right)^2 \\ \frac{\partial v_0}{\partial y} + \frac{1}{2} \left(\frac{\partial w_0}{\partial y} \right)^2 \\ \frac{\partial u_0}{\partial y} + \frac{\partial v_0}{\partial x} + \frac{\partial w_0}{\partial x} \frac{\partial w_0}{\partial y} \end{Bmatrix} \tag{12.4.13a}$$

$$\begin{Bmatrix} M_{xx} \\ M_{yy} \\ M_{xy} \end{Bmatrix} = \begin{bmatrix} D_{11} & D_{12} & 0 \\ D_{12} & D_{22} & 0 \\ 0 & 0 & D_{66} \end{bmatrix} \begin{Bmatrix} \frac{\partial \phi_x}{\partial x} \\ \frac{\partial \phi_y}{\partial y} \\ + \frac{\partial \phi_y}{\partial x} \end{Bmatrix} \tag{12.4.13b}$$

$$\begin{Bmatrix} Q_y \\ Q_x \end{Bmatrix} = K_s \begin{bmatrix} A_{44} & 0 \\ 0 & A_{55} \end{bmatrix} \begin{Bmatrix} \frac{\partial w_0}{\partial y} + \phi_y \\ \frac{\partial w_0}{\partial x} + \phi_x \end{Bmatrix} \quad (12.4.13c)$$

and the shear stiffnesses (A_{44}, A_{55}) are defined by

$$(A_{44}, A_{55}) = \sum_{k=1}^N (\bar{Q}_{44}^{(k)}, \bar{Q}_{55}^{(k)})(z_{k+1} - z_k) \quad (12.4.14)$$

Virtual Work Statements

The weak forms of the equations of equilibrium associated with the FSDT are

$$0 = \int_{\Omega^e} \left(\frac{\partial \delta u_0}{\partial x} N_{xx} + \frac{\partial \delta u_0}{\partial y} N_{xy} \right) dx dy - \oint_{\Gamma^e} (N_{xx} n_x + N_{xy} n_y) \delta u_0 ds \quad (12.4.15a)$$

$$0 = \int_{\Omega^e} \left(\frac{\partial \delta v_0}{\partial x} N_{xy} + \frac{\partial \delta v_0}{\partial y} N_{yy} \right) dx dy - \oint_{\Gamma^e} (N_{xy} n_x + N_{yy} n_y) \delta v_0 ds \quad (12.4.15b)$$

$$\begin{aligned} 0 = & \int_{\Omega^e} \left[\frac{\partial \delta w_0}{\partial x} Q_x + \frac{\partial \delta w_0}{\partial y} Q_y + \frac{\partial \delta w_0}{\partial x} \left(N_{xx} \frac{\partial w_0}{\partial x} + N_{xy} \frac{\partial w_0}{\partial y} \right) \right. \\ & \left. + \frac{\partial \delta w_0}{\partial y} \left(N_{xy} \frac{\partial w_0}{\partial x} + N_{yy} \frac{\partial w_0}{\partial y} \right) - \delta w_0 q + k w_0 \delta w_0 \right] dx dy \\ & - \oint_{\Gamma^e} \left[\left(Q_x + N_{xx} \frac{\partial w_0}{\partial x} + N_{xy} \frac{\partial w_0}{\partial y} \right) n_x \right. \\ & \left. + \left(Q_y + N_{xy} \frac{\partial w_0}{\partial x} + N_{yy} \frac{\partial w_0}{\partial y} \right) n_y \right] \delta w_0 ds \end{aligned} \quad (12.4.15c)$$

$$\begin{aligned} 0 = & \int_{\Omega^e} \left(\frac{\partial \delta \phi_x}{\partial x} M_{xx} + \frac{\partial \delta \phi_x}{\partial y} M_{xy} + \delta \phi_x Q_x \right) dx dy \\ & - \oint_{\Gamma^e} (M_{xx} n_x + M_{xy} n_y) \delta \phi_x ds \end{aligned} \quad (12.4.15d)$$

$$\begin{aligned} 0 = & \int_{\Omega^e} \left(\frac{\partial \delta \phi_y}{\partial x} M_{xy} + \frac{\partial \delta \phi_y}{\partial y} M_{yy} + \delta \phi_y Q_y \right) dx dy \\ & - \oint_{\Gamma^e} (M_{xy} n_x + M_{yy} n_y) \delta \phi_y ds \end{aligned} \quad (12.4.15e)$$

We note from the boundary terms in Eqs. (12.4.15) that $u_0, v_0, w_0, \phi_x, \phi_y$ are used as the primary variables (or generalized displacements) as opposed to $u_{0n}, u_{0s}, w_0, \phi_n, \phi_s$. Unlike in the CPT, the rotations (ϕ_x, ϕ_y) are independent of w_0 . Since no derivatives of $(u_0, v_0, w_0, \phi_x, \phi_y)$ appear in the list of the primary variables, all generalized displacements may be interpolated using the Lagrange interpolation functions. Thus, the FSDT requires only C^0 approximation of all dependent unknowns.

We identify the secondary variables of the formulation as

$$\begin{aligned} \hat{N}_n &\equiv N_{xx} n_x + N_{xy} n_y, \quad \hat{N}_s \equiv N_{xy} n_x + N_{yy} n_y \\ \hat{M}_n &\equiv M_{xx} n_x + M_{xy} n_y, \quad \hat{M}_s \equiv M_{xy} n_x + M_{yy} n_y \\ \hat{Q}_n &\equiv \left(Q_x + N_{xx} \frac{\partial w_0}{\partial x} + N_{xy} \frac{\partial w_0}{\partial y} \right) n_x \\ &+ \left(Q_y + N_{xy} \frac{\partial w_0}{\partial x} + N_{yy} \frac{\partial w_0}{\partial y} \right) n_y \end{aligned} \quad (12.4.16)$$

Finite Element Model

The virtual work statements in Eqs. (12.4.15a–e) contain at the most only the first derivatives of the dependent variables $(u_0, v_0, w_0, \phi_x, \phi_y)$. Therefore, they can all be approximated using the Lagrange interpolation functions. In principle, (u_0, v_0) , w_0 , and (ϕ_x, ϕ_y) can be approximated with differing degrees of functions. Let

$$\begin{aligned} u_0(x, y) &= \sum_{j=1}^m u_j \psi_j^{(1)}(x, y), & v_0(x, y) &= \sum_{j=1}^m v_j \psi_j^{(1)}(x, y) \\ w_0(x, y) &= \sum_{j=1}^n w_j \psi_j^{(2)}(x, y) \\ \phi_x(x, y) &= \sum_{j=1}^p S_j^1 \psi_j^{(3)}(x, y), & \phi_y(x, y) &= \sum_{j=1}^p S_j^2 \psi_j^{(3)}(x, y) \end{aligned} \quad (12.4.17)$$

where $\psi_j^{(\alpha)}$ ($\alpha = 1, 2, 3$) are Lagrange interpolation functions. One can use linear, quadratic, or higher-order interpolations of these variables.

Substituting Eqs. (12.4.17) for $(u_0, v_0, w_0, \phi_x, \phi_y)$ into Eqs. (12.4.15), we obtain the following finite element model:

$$\begin{bmatrix} [K^{11}] & [K^{12}] & [K^{13}] & [K^{14}] & [K^{15}] \\ [K^{21}] & [K^{22}] & [K^{23}] & [K^{24}] & [K^{25}] \\ [K^{31}] & [K^{32}] & [K^{33}] & [K^{34}] & [K^{35}] \\ [K^{41}] & [K^{42}] & [K^{43}] & [K^{44}] & [K^{45}] \\ [K^{51}] & [K^{52}] & [K^{53}] & [K^{54}] & [K^{55}] \end{bmatrix} \begin{Bmatrix} \{u^e\} \\ \{v^e\} \\ \{w^e\} \\ \{S^1\} \\ \{S^2\} \end{Bmatrix} = \begin{Bmatrix} \{F^1\} \\ \{F^2\} \\ \{F^3\} \\ \{F^4\} \\ \{F^5\} \end{Bmatrix}$$

or, in compact matrix form

$$[K^e]\{\Delta^e\} = \{F^e\} \quad (12.4.18)$$

where the coefficients of the sub-matrices $[K^{\alpha\beta}]$ and vectors $\{F^\alpha\}$ are defined for $(\alpha, \beta = 1, 2, 3, 4, 5)$ by the expressions

$$\begin{aligned} K_{ij}^{11} &= \int_{\Omega^e} \left(A_{11} \frac{\partial \psi_i^{(1)}}{\partial x} \frac{\partial \psi_j^{(1)}}{\partial x} + A_{66} \frac{\partial \psi_i^{(1)}}{\partial y} \frac{\partial \psi_j^{(1)}}{\partial y} \right) dx dy \\ K_{ij}^{12} &= \int_{\Omega^e} \left(A_{12} \frac{\partial \psi_i^{(1)}}{\partial x} \frac{\partial \psi_j^{(1)}}{\partial y} + A_{66} \frac{\partial \psi_i^{(1)}}{\partial y} \frac{\partial \psi_j^{(1)}}{\partial x} \right) dx dy \\ K_{ij}^{13} &= \frac{1}{2} \int_{\Omega^e} \left[\frac{\partial \psi_i^{(1)}}{\partial x} \left(A_{11} \frac{\partial w_0}{\partial x} \frac{\partial \psi_j^{(2)}}{\partial x} + A_{12} \frac{\partial w_0}{\partial y} \frac{\partial \psi_j^{(2)}}{\partial y} \right) \right. \\ &\quad \left. + A_{66} \frac{\partial \psi_i^{(1)}}{\partial y} \left(\frac{\partial w_0}{\partial x} \frac{\partial \psi_j^{(2)}}{\partial y} + \frac{\partial w_0}{\partial y} \frac{\partial \psi_j^{(2)}}{\partial x} \right) \right] dx dy \\ K_{ij}^{22} &= \int_{\Omega^e} \left(A_{66} \frac{\partial \psi_i^{(1)}}{\partial x} \frac{\partial \psi_j^{(1)}}{\partial x} + A_{22} \frac{\partial \psi_i^{(1)}}{\partial y} \frac{\partial \psi_j^{(1)}}{\partial y} \right) dx dy \end{aligned}$$

$$\begin{aligned}
K_{ij}^{23} &= \frac{1}{2} \int_{\Omega^e} \left[\frac{\partial \psi_i^{(1)}}{\partial y} \left(A_{12} \frac{\partial w_0}{\partial x} \frac{\partial \psi_j^{(2)}}{\partial x} + A_{22} \frac{\partial w_0}{\partial y} \frac{\partial \psi_j^{(2)}}{\partial y} \right) \right. \\
&\quad \left. + A_{66} \frac{\partial \psi_i^{(1)}}{\partial x} \left(\frac{\partial w_0}{\partial x} \frac{\partial \psi_j^{(2)}}{\partial y} + \frac{\partial w_0}{\partial y} \frac{\partial \psi_j^{(2)}}{\partial x} \right) \right] dx dy \\
K_{ij}^{31} &= \int_{\Omega^e} \left[\frac{\partial \psi_i^{(2)}}{\partial x} \left(A_{11} \frac{\partial w_0}{\partial x} \frac{\partial \psi_j^{(1)}}{\partial x} + A_{66} \frac{\partial w_0}{\partial y} \frac{\partial \psi_j^{(1)}}{\partial y} \right) \right. \\
&\quad \left. + \frac{\partial \psi_i^{(2)}}{\partial y} \left(A_{66} \frac{\partial w_0}{\partial x} \frac{\partial \psi_j^{(1)}}{\partial y} + A_{12} \frac{\partial w_0}{\partial y} \frac{\partial \psi_j^{(1)}}{\partial x} \right) \right] dx dy \\
K_{ij}^{32} &= \int_{\Omega^e} \left[\frac{\partial \psi_i^{(2)}}{\partial x} \left(A_{12} \frac{\partial w_0}{\partial x} \frac{\partial \psi_j^{(1)}}{\partial y} + A_{66} \frac{\partial w_0}{\partial y} \frac{\partial \psi_j^{(1)}}{\partial x} \right) \right. \\
&\quad \left. + \frac{\partial \psi_i^{(2)}}{\partial y} \left(A_{66} \frac{\partial w_0}{\partial x} \frac{\partial \psi_j^{(1)}}{\partial x} + A_{22} \frac{\partial w_0}{\partial y} \frac{\partial \psi_j^{(1)}}{\partial y} \right) \right] dx dy \\
K_{ij}^{33} &= \int_{\Omega^e} \left(K_s A_{55} \frac{\partial \psi_i^{(e)}}{\partial x} \frac{\partial \psi_j^{(2)}}{\partial x} + K_s A_{44} \frac{\partial \psi_i^{(2)}}{\partial y} \frac{\partial \psi_j^{(2)}}{\partial y} + k \psi_i^{(e)} \psi_j^{(2)} \right) dx dy \\
&\quad + \frac{1}{2} \int_{\Omega^e} \left\{ \left[A_{11} \left(\frac{\partial w_0}{\partial x} \right)^2 + A_{66} \left(\frac{\partial w_0}{\partial y} \right)^2 \right] \frac{\partial \psi_i^{(e)}}{\partial x} \frac{\partial \psi_j^{(2)}}{\partial x} \right. \\
&\quad \left. + \left[A_{66} \left(\frac{\partial w_0}{\partial x} \right)^2 + A_{22} \left(\frac{\partial w_0}{\partial y} \right)^2 \right] \frac{\partial \psi_i^{(2)}}{\partial y} \frac{\partial \psi_j^{(2)}}{\partial y} \right. \\
&\quad \left. + (A_{12} + A_{66}) \frac{\partial w_0}{\partial x} \frac{\partial w_0}{\partial y} \left(\frac{\partial \psi_i^{(2)}}{\partial x} \frac{\partial \psi_j^{(2)}}{\partial y} + \frac{\partial \psi_i^{(2)}}{\partial y} \frac{\partial \psi_j^{(2)}}{\partial x} \right) \right\} dx dy \\
K_{ij}^{34} &= \int_{\Omega^e} K_s A_{55} \frac{\partial \psi_i^{(2)}}{\partial x} \psi_j^{(3)} dx dy, \quad K_{ij}^{35} = \int_{\Omega^e} K_s A_{44} \frac{\partial \psi_i^{(2)}}{\partial y} \psi_j^{(3)} dx dy \\
K_{ij}^{44} &= \int_{\Omega^e} \left(D_{11} \frac{\partial \psi_i^{(3)}}{\partial x} \frac{\partial \psi_j^{(3)}}{\partial x} + D_{66} \frac{\partial \psi_i^{(3)}}{\partial y} \frac{\partial \psi_j^{(3)}}{\partial y} + K_s A_{55} \psi_i^{(3)} \psi_j^{(3)} \right) dx dy \\
K_{ij}^{45} &= \int_{\Omega^e} \left(D_{12} \frac{\partial \psi_i^{(3)}}{\partial x} \frac{\partial \psi_j^{(3)}}{\partial y} + D_{66} \frac{\partial \psi_i^{(3)}}{\partial y} \frac{\partial \psi_j^{(3)}}{\partial x} \right) dx dy \\
K_{ij}^{55} &= \int_{\Omega^e} \left(D_{66} \frac{\partial \psi_i^{(3)}}{\partial x} \frac{\partial \psi_j^{(3)}}{\partial x} + D_{22} \frac{\partial \psi_i^{(3)}}{\partial y} \frac{\partial \psi_j^{(3)}}{\partial y} + K_s A_{44} \psi_i^{(3)} \psi_j^{(3)} \right) dx dy \\
F_i^1 &= \oint_{\Gamma^e} \hat{N}_n \psi_i^{(1)} ds, \quad F_i^2 = \oint_{\Gamma^e} \hat{N}_s \psi_i^{(1)} ds, \quad F_i^3 = \int_{\Omega^e} q \psi_i^{(2)} dx dy + \oint_{\Gamma^e} \hat{Q}_n \psi_i^{(2)} ds \\
F_i^4 &= \oint_{\Gamma^e} \hat{M}_n \psi_i^{(3)} ds, \quad F_i^5 = \oint_{\Gamma^e} \hat{M}_s \psi_i^{(3)} ds \\
K_{ij}^{21} &= K_{ji}^{12}; \quad K_{ij}^{43} = K_{ji}^{34}; \quad K_{ij}^{53} = K_{ji}^{35}; \quad K_{ij}^{54} = K_{ji}^{45} \tag{12.4.19}
\end{aligned}$$

and all other stiffness coefficients are zero. It is noted that the element stiffness matrix is *not* symmetric. When the bilinear rectangular element is used for all generalized displacements ($u_0, v_0, w_0, \phi_x, \phi_y$), the element stiffness matrices are of the order 20×20 and, for the nine-node quadratic element, they are 45×45 (Figure 12.3.5).

12.4.4 The Newton–Raphson Iterative Method

Here we discuss the solution of equations of the form in (12.4.10) and (12.4.18), which represent systems of nonlinear algebraic equations. These equations must be solved using an iterative method. The Newton–Raphson iteration method is discussed below.

The Newton–Raphson iterative method is based on Taylor’s series expansion of the set of nonlinear algebraic equations, for example, Eqs. (12.4.18) about the known solution. Suppose that Eq. (12.4.18) is to be solved for the generalized displacement vector $\{\Delta\}$. Because the coefficient matrix $[\hat{K}(\{\Delta\})]$ depends on the unknown solution, the equations are solved iteratively. To formulate the equations to be solved at the $(r+1)$ st iteration by the Newton–Raphson method, we assume that the solution at the r th iteration, $\{\Delta\}^r$, is known. Then define

$$\{R\}(\{\Delta\}) \equiv [\hat{K}(\{\Delta\})]\{\Delta\} - \{\hat{F}\} = 0 \quad (12.4.20)$$

where $\{R\}$ is called the *residual*, which is a nonlinear function of the unknown solution $\{\Delta\}$. Expanding $\{R\}$ in Taylor’s series about $\{\Delta\}^r$, we obtain

$$\begin{aligned} \{0\} &= \{R\}(\{\Delta\}) = \{R\}^r + \left[\frac{\partial \{R\}}{\partial \{\Delta\}} \right]^r (\{\Delta\}^{r+1} - \{\Delta\}^r) \\ &\quad + \frac{1}{2!} \left[\frac{\partial^2 \{R\}}{\partial \{\Delta\} \partial \{\Delta\}} \right]^r (\{\Delta\}^{r+1} - \{\Delta\}^r)^2 + \dots \\ &= \{R\}^r + ([\hat{K}^T(\{\Delta\}^r)]) \{\delta\Delta\} + O(\{\delta\Delta\}^2) \end{aligned} \quad (12.4.21)$$

where $O(\cdot)$ denotes the higher-order terms in $\{\delta\Delta\}$, and $[\hat{K}^T]$ is known as the *tangent stiffness matrix* (or geometric stiffness matrix)

$$[\hat{K}^T(\{\Delta\}^r)] \equiv \left[\frac{\partial \{R\}}{\partial \{\Delta\}} \right]^r, \quad \{R\}^r = [\hat{K}(\{\Delta\}^r)]\{\Delta\}^r - \{\hat{F}\} \quad (12.4.22)$$

Equations (12.4.20)–(12.4.22) are also applicable to a typical finite element. In other words, the coefficient matrix in Eq. (12.4.22) can be assembled after the element tangent stiffness matrices and force residual vectors are computed. The assembled equations are then solved for the incremental displacement vector after imposing the boundary conditions of the problem

$$\{\delta\Delta\} = -[\hat{K}^T(\{\Delta\}^r)]^{-1}\{R\}^r \quad (12.4.23)$$

The total displacement vector is obtained from

$$\{\Delta\}^{r+1} = \{\Delta\}^r + \{\delta\Delta\} \quad (12.4.24)$$

Note that the element tangent stiffness matrix as well as the residual vector are evaluated using the latest known solution $\{\Delta\}^r$. After assembly and imposition of the boundary conditions, the linearized system of equations are solved for $\{\delta\Delta\}$.

At the beginning of the iteration (i.e., $r = 0$), we assume that $\{\Delta\}^0 = \{0\}$ so that the solution at the first iteration is the linear solution because the nonlinear stiffness matrix reduces to the linear one. The iteration process is continued [i.e., Eq. (12.4.23) is solved in each iteration] until the difference between $\{\Delta\}^r$ and $\{\Delta\}^{r+1}$ reduces to a preselected error tolerance. The *error criterion* is of the form

$$\left(\sqrt{\sum_{I=1}^N |\Delta_I^{r+1} - \Delta_I^r|^2} \Big/ \sqrt{\sum_{I=1}^N |\Delta_I^{r+1}|^2} \right) < \epsilon \quad (\text{say } 10^{-3}) \quad (12.4.25)$$

where N is the total number of nodal generalized displacements in the finite element mesh, and ϵ is the error tolerance.

In the Newton–Raphson method the global tangent stiffness matrix and residual vector must be updated using the latest available solution $\{\Delta\}^r$ before Eq. (12.4.23) is solved. If the tangent stiffness matrix is kept constant for a preselected number of iterations, but the residual vector is updated during each iteration, the method is known as the *modified Newton–Raphson method*. The approach often takes more iterations to obtain convergence. The Newton–Raphson method fails to trace the nonlinear equilibrium path through the limit points where the tangent matrix $[K_T]$ becomes singular and the iteration procedure diverges. Riks (1972) and Wempner (1971) suggested a procedure to predict the nonlinear equilibrium path through limit points. The method, known as the *Riks–Wempner method* provides the Newton–Raphson method and its modifications with a technique to control progress along the equilibrium path.

12.4.5 Tangent Stiffness Coefficients

Classical Plate Theory (CPT)

The Newton–Raphson iterative method involves solving equations of the form

$$\begin{bmatrix} [T^{11}] & [T^{12}] & [T^{13}] \\ [T^{21}] & [T^{22}] & [T^{23}] \\ [T^{31}] & [T^{32}] & [T^{33}] \end{bmatrix} \begin{Bmatrix} \{\delta\Delta^1\} \\ \{\delta\Delta^2\} \\ \{\delta\Delta^3\} \end{Bmatrix} = - \begin{Bmatrix} \{R^1\} \\ \{R^2\} \\ \{R^3\} \end{Bmatrix} \quad (12.4.26)$$

where

$$\Delta_i^1 = u_i, \quad \Delta_i^2 = v_i, \quad \Delta_i^3 = \bar{\Delta}_i \quad (12.4.27)$$

the coefficients of the sub-matrices $[T^{\alpha\beta}]$ are defined by

$$T_{ij}^{\alpha\beta} = \frac{\partial R_i^\alpha}{\partial \Delta_j^\beta} \quad (12.4.28)$$

the components of the residual vector $\{R^\alpha\}$ are

$$R_i^\alpha = \sum_{\gamma=1}^3 \sum_{k=1}^{n*} K_{ik}^{\alpha\gamma} \Delta_k^\gamma - F_i^\alpha \quad (12.4.29)$$

and $n*$ denotes n or m , depending on the nodal degree of freedom. Thus, we have

$$T_{ij}^{\alpha\beta} = \frac{\partial}{\partial \Delta_j^\beta} \left(\sum_{\gamma=1}^3 \sum_{k=1}^{n*} K_{ik}^{\alpha\gamma} \Delta_k^\gamma - F_i^\alpha \right) = \sum_{\gamma=1}^3 \sum_{k=1}^{n*} \frac{\partial K_{ik}^{\alpha\gamma}}{\partial \Delta_j^\beta} \Delta_k^\gamma + K_{ij}^{\alpha\beta} \quad (12.4.30)$$

The only coefficients that depend on the solution are K_{ij}^{13} , K_{ij}^{23} , K_{ij}^{31} , K_{ij}^{32} , and K_{ij}^{33} , and they are functions of only $\Delta_i^3 = \bar{\Delta}_i$. Hence, derivatives of all stiffness coefficients with respect to $\Delta^1 = u_j$ and $\Delta^2 = v_j$ are zero.

Thus, we have

$$T_{ij}^{11} = \sum_{\gamma=1}^3 \sum_{k=1}^{n*} \frac{\partial K_{ik}^{1\gamma}}{\partial u_j} \Delta_k^\gamma + K_{ij}^{11} = K_{ij}^{11}, \quad T_{ij}^{12} = \sum_{\gamma=1}^3 \sum_{k=1}^{n*} \frac{\partial K_{ik}^{1\gamma}}{\partial v_j} \Delta_k^\gamma + K_{ij}^{12} = K_{ij}^{12}$$

$$T_{ij}^{21} = \sum_{\gamma=1}^3 \sum_{k=1}^{n*} \frac{\partial K_{ik}^{2\gamma}}{\partial u_j} \Delta_k^\gamma + K_{ij}^{21} = K_{ij}^{21}, \quad T_{ij}^{22} = \sum_{\gamma=1}^3 \sum_{k=1}^{n*} \frac{\partial K_{ik}^{2\gamma}}{\partial v_j} \Delta_k^\gamma + K_{ij}^{22} = K_{ij}^{22}$$

$$T_{ij}^{31} = \sum_{\gamma=1}^3 \sum_{k=1}^{n*} \frac{\partial K_{ik}^{3\gamma}}{\partial u_j} \Delta_k^\gamma + K_{ij}^{31} = K_{ij}^{31}, \quad T_{ij}^{32} = \sum_{\gamma=1}^3 \sum_{k=1}^{n*} \frac{\partial K_{ik}^{3\gamma}}{\partial v_j} \Delta_k^\gamma + K_{ij}^{32} = K_{ij}^{32}$$

$$\begin{aligned} T_{ij}^{13} &= \sum_{\gamma=1}^3 \sum_{k=1}^{n*} \frac{\partial K_{ik}^{1\gamma}}{\partial \bar{\Delta}_j^3} \Delta_k^\gamma + K_{ij}^{13} = \sum_{k=1}^n \frac{\partial K_{ik}^{13}}{\partial \bar{\Delta}_j^3} \bar{\Delta}_k^3 + K_{ij}^{13} \\ &= \frac{1}{2} \sum_{k=1}^n \bar{\Delta}_k^3 \frac{\partial}{\partial \bar{\Delta}_j^3} \left\{ \int_{\Omega^e} \left[\frac{\partial \psi_i^e}{\partial x} \left(A_{11} \frac{\partial w_0}{\partial x} \frac{\partial \varphi_k^e}{\partial x} + A_{12} \frac{\partial w_0}{\partial y} \frac{\partial \varphi_k^e}{\partial y} \right) \right. \right. \\ &\quad \left. \left. + A_{66} \frac{\partial \psi_i^e}{\partial y} \left(\frac{\partial w_0}{\partial x} \frac{\partial \varphi_k^e}{\partial y} + \frac{\partial w_0}{\partial y} \frac{\partial \varphi_k^e}{\partial x} \right) \right] dx dy \right\} + K_{ij}^{13} \end{aligned}$$

$$\begin{aligned} &= \frac{1}{2} \sum_{k=1}^n \bar{\Delta}_k^3 \left\{ \int_{\Omega^e} \left[\frac{\partial \psi_i^e}{\partial x} \left(A_{11} \frac{\partial \varphi_j^e}{\partial x} \frac{\partial \varphi_k^e}{\partial x} + A_{12} \frac{\partial \varphi_j^e}{\partial y} \frac{\partial \varphi_k^e}{\partial y} \right) \right. \right. \\ &\quad \left. \left. + A_{66} \frac{\partial \psi_i^e}{\partial y} \left(\frac{\partial \varphi_j^e}{\partial x} \frac{\partial \varphi_k^e}{\partial y} + \frac{\partial \varphi_j^e}{\partial y} \frac{\partial \varphi_k^e}{\partial x} \right) \right] dx dy \right\} + K_{ij}^{13} \end{aligned}$$

$$\begin{aligned} &= \frac{1}{2} \int_{\Omega^e} \left[\frac{\partial \psi_i^e}{\partial x} \left(A_{11} \frac{\partial w_0}{\partial x} \frac{\partial \varphi_j^e}{\partial x} + A_{12} \frac{\partial w_0}{\partial y} \frac{\partial \varphi_j^e}{\partial y} \right) \right. \\ &\quad \left. + A_{66} \frac{\partial \psi_i^e}{\partial y} \left(\frac{\partial w_0}{\partial x} \frac{\partial \varphi_j^e}{\partial y} + \frac{\partial w_0}{\partial y} \frac{\partial \varphi_j^e}{\partial x} \right) \right] dx dy + K_{ij}^{13} \\ &= K_{ij}^{13} + K_{ij}^{13} = 2K_{ij}^{13} (= T_{ji}^{31}) \end{aligned}$$

$$\begin{aligned} T_{ij}^{23} &= \sum_{\gamma=1}^3 \sum_{k=1}^{n*} \frac{\partial K_{ik}^{2\gamma}}{\partial \bar{\Delta}_j^3} \Delta_k^\gamma + K_{ij}^{23} = \sum_{k=1}^n \frac{\partial K_{ik}^{23}}{\partial \bar{\Delta}_j^3} \bar{\Delta}_k^3 + K_{ij}^{23} \\ &= \frac{1}{2} \sum_{k=1}^n \bar{\Delta}_k^3 \frac{\partial}{\partial \bar{\Delta}_j^3} \left\{ \int_{\Omega^e} \left[\frac{\partial \psi_i^e}{\partial y} \left(A_{12} \frac{\partial w_0}{\partial x} \frac{\partial \varphi_k^e}{\partial x} + A_{22} \frac{\partial w_0}{\partial y} \frac{\partial \varphi_k^e}{\partial y} \right) \right. \right. \\ &\quad \left. \left. + A_{66} \frac{\partial \psi_i^e}{\partial x} \left(\frac{\partial w_0}{\partial x} \frac{\partial \varphi_k^e}{\partial y} + \frac{\partial w_0}{\partial y} \frac{\partial \varphi_k^e}{\partial x} \right) \right] dx dy \right\} + K_{ij}^{23} \end{aligned}$$

$$\begin{aligned}
&= \frac{1}{2} \sum_{k=1}^n \bar{\Delta}_k^3 \left\{ \int_{\Omega^e} \left[\frac{\partial \psi_i^e}{\partial y} \left(A_{12} \frac{\partial \varphi_j^e}{\partial x} \frac{\partial \varphi_k^e}{\partial x} + A_{22} \frac{\partial \varphi_j^e}{\partial y} \frac{\partial \varphi_k^e}{\partial y} \right) \right. \right. \\
&\quad \left. \left. + A_{66} \frac{\partial \psi_i^e}{\partial x} \left(\frac{\partial \varphi_j^e}{\partial x} \frac{\partial \varphi_k^e}{\partial y} + \frac{\partial \varphi_j^e}{\partial y} \frac{\partial \varphi_k^e}{\partial x} \right) \right] dx dy \right\} + K_{ij}^{23} \\
&= \frac{1}{2} \int_{\Omega^e} \left[\frac{\partial \psi_i^e}{\partial y} \left(A_{12} \frac{\partial w_0}{\partial x} \frac{\partial \varphi_j^e}{\partial x} + A_{22} \frac{\partial w_0}{\partial y} \frac{\partial \varphi_j^e}{\partial y} \right) \right. \\
&\quad \left. + A_{66} \frac{\partial \psi_i^e}{\partial x} \left(\frac{\partial w_0}{\partial y} \frac{\partial \varphi_j^e}{\partial x} + \frac{\partial w_0}{\partial x} \frac{\partial \varphi_j^e}{\partial y} \right) \right] dx dy + K_{ij}^{23} \\
&= K_{ij}^{23} + K_{ij}^{23} = 2K_{ij}^{23} (= T_{ji}^{32}) \tag{12.4.31}
\end{aligned}$$

The computation of T_{ij}^{33} requires the calculation of three parts

$$\begin{aligned}
T_{ij}^{33} &= \sum_{\gamma=1}^3 \sum_{k=1}^{n*} \frac{\partial K_{ik}^{3\gamma}}{\partial \bar{\Delta}_j^3} \Delta_k^\gamma + K_{ij}^{33} \\
&= \sum_{k=1}^{n*} \left(\frac{\partial K_{ik}^{31}}{\partial \bar{\Delta}_j^3} u_k + \frac{\partial K_{ik}^{32}}{\partial \bar{\Delta}_j^3} v_k + \frac{\partial K_{ik}^{33}}{\partial \bar{\Delta}_j^3} \bar{\Delta}_k^3 \right) + K_{ij}^{33} \tag{12.4.32}
\end{aligned}$$

We shall compute these terms first. We have

$$\begin{aligned}
\sum_{k=1}^{n*} u_k \frac{\partial K_{ik}^{31}}{\partial \bar{\Delta}_j^3} &= \sum_{k=1}^m u_k \frac{\partial}{\partial \bar{\Delta}_j^3} \left\{ \int_{\Omega^e} \left[\frac{\partial \varphi_i^e}{\partial x} \left(A_{11} \frac{\partial w_0}{\partial x} \frac{\partial \psi_k^e}{\partial x} + A_{66} \frac{\partial w_0}{\partial y} \frac{\partial \psi_k^e}{\partial y} \right) \right. \right. \\
&\quad \left. \left. + \frac{\partial \varphi_i^e}{\partial y} \left(A_{66} \frac{\partial w_0}{\partial x} \frac{\partial \psi_k^e}{\partial y} + A_{12} \frac{\partial w_0}{\partial y} \frac{\partial \psi_k^e}{\partial x} \right) \right] dx dy \right\} \\
&= \sum_{k=1}^m u_k \left\{ \int_{\Omega^e} \left[\frac{\partial \varphi_i^e}{\partial x} \left(A_{11} \frac{\partial \varphi_j^e}{\partial x} \frac{\partial \psi_k^e}{\partial x} + A_{66} \frac{\partial \varphi_j^e}{\partial y} \frac{\partial \psi_k^e}{\partial y} \right) \right. \right. \\
&\quad \left. \left. + \frac{\partial \varphi_i^e}{\partial y} \left(A_{66} \frac{\partial \varphi_j^e}{\partial x} \frac{\partial \psi_k^e}{\partial y} + A_{12} \frac{\partial \varphi_j^e}{\partial y} \frac{\partial \psi_k^e}{\partial x} \right) \right] dx dy \right\} \\
&= \int_{\Omega^e} \left[\frac{\partial \varphi_i^e}{\partial x} \left(A_{11} \frac{\partial u_0}{\partial x} \frac{\partial \varphi_j^e}{\partial x} + A_{66} \frac{\partial u_0}{\partial y} \frac{\partial \varphi_j^e}{\partial y} \right) \right. \\
&\quad \left. + \frac{\partial \varphi_i^e}{\partial y} \left(A_{66} \frac{\partial u_0}{\partial x} \frac{\partial \varphi_j^e}{\partial y} + A_{12} \frac{\partial u_0}{\partial x} \frac{\partial \varphi_j^e}{\partial y} \right) \right] dx dy \tag{12.4.33}
\end{aligned}$$

$$\begin{aligned}
\sum_{k=1}^{n*} v_k \frac{\partial K_{ik}^{32}}{\partial \bar{\Delta}_j^3} &= \sum_{k=1}^m v_k \frac{\partial}{\partial \bar{\Delta}_j^3} \left\{ \int_{\Omega^e} \left[\frac{\partial \varphi_i^e}{\partial x} \left(A_{12} \frac{\partial w_0}{\partial x} \frac{\partial \psi_k^e}{\partial y} + A_{66} \frac{\partial w_0}{\partial y} \frac{\partial \psi_k^e}{\partial x} \right) \right. \right. \\
&\quad \left. \left. + \frac{\partial \varphi_i^e}{\partial y} \left(A_{66} \frac{\partial w_0}{\partial x} \frac{\partial \psi_k^e}{\partial x} + A_{22} \frac{\partial w_0}{\partial y} \frac{\partial \psi_k^e}{\partial y} \right) \right] dx dy \right\} \\
&= \sum_{k=1}^m v_k \left\{ \int_{\Omega^e} \left[\frac{\partial \varphi_i^e}{\partial x} \left(A_{12} \frac{\partial \varphi_j^e}{\partial x} \frac{\partial \psi_k^e}{\partial y} + A_{66} \frac{\partial \varphi_j^e}{\partial y} \frac{\partial \psi_k^e}{\partial x} \right) \right. \right. \\
&\quad \left. \left. + \frac{\partial \varphi_i^e}{\partial y} \left(A_{66} \frac{\partial \varphi_j^e}{\partial x} \frac{\partial \psi_k^e}{\partial x} + A_{22} \frac{\partial \varphi_j^e}{\partial y} \frac{\partial \psi_k^e}{\partial y} \right) \right] dx dy \right\}
\end{aligned}$$

$$\begin{aligned}
& + \frac{\partial \varphi_i^e}{\partial y} \left(A_{66} \frac{\partial \varphi_j^e}{\partial x} \frac{\partial \psi_k^e}{\partial x} + A_{22} \frac{\partial \varphi_j^e}{\partial y} \frac{\partial \psi_k^e}{\partial y} \right) \Big] dx dy \Big\} \\
& = \int_{\Omega^e} \left[\frac{\partial \varphi_i^e}{\partial x} \left(A_{12} \frac{\partial v_0}{\partial y} \frac{\partial \varphi_j^e}{\partial x} + A_{66} \frac{\partial v_0}{\partial x} \frac{\partial \varphi_j^e}{\partial y} \right) \right. \\
& \quad \left. + \frac{\partial \varphi_i^e}{\partial y} \left(A_{66} \frac{\partial v_0}{\partial x} \frac{\partial \varphi_j^e}{\partial x} + A_{22} \frac{\partial v_0}{\partial y} \frac{\partial \varphi_j^e}{\partial y} \right) \right] dx dy \quad (12.4.34)
\end{aligned}$$

$$\begin{aligned}
\sum_{k=1}^{n*} \bar{\Delta}_k^3 \frac{\partial K_{ik}^{33}}{\partial \bar{\Delta}_j^3} & = \frac{1}{2} \sum_{k=1}^n \bar{\Delta}_k^3 \frac{\partial}{\partial \bar{\Delta}_j^3} \left\{ \int_{\Omega^e} \left\{ \left[A_{11} \left(\frac{\partial w_0}{\partial x} \right)^2 + A_{66} \left(\frac{\partial w_0}{\partial y} \right)^2 \right] \frac{\partial \varphi_i^e}{\partial x} \frac{\partial \varphi_k^e}{\partial x} \right. \right. \\
& \quad \left. + \left[A_{66} \left(\frac{\partial w_0}{\partial x} \right)^2 + A_{22} \left(\frac{\partial w_0}{\partial y} \right)^2 \right] \frac{\partial \varphi_i^e}{\partial y} \frac{\partial \varphi_k^e}{\partial y} \right. \\
& \quad \left. + (A_{12} + A_{66}) \frac{\partial w_0}{\partial x} \frac{\partial w_0}{\partial y} \left(\frac{\partial \varphi_i^e}{\partial x} \frac{\partial \varphi_k^e}{\partial y} + \frac{\partial \varphi_i^e}{\partial y} \frac{\partial \varphi_k^e}{\partial x} \right) \right\} dx dy \Big\} \\
& = \frac{1}{2} \sum_{k=1}^n \bar{\Delta}_k^3 \left\{ \int_{\Omega^e} \left[\left(2A_{11} \frac{\partial w_0}{\partial x} \frac{\partial \varphi_j^e}{\partial x} + 2A_{66} \frac{\partial w_0}{\partial y} \frac{\partial \varphi_j^e}{\partial y} \right) \frac{\partial \varphi_i^e}{\partial x} \frac{\partial \varphi_k^e}{\partial x} \right. \right. \\
& \quad \left. + \left(2A_{66} \frac{\partial w_0}{\partial x} \frac{\partial \varphi_j^e}{\partial x} + 2A_{22} \frac{\partial w_0}{\partial y} \frac{\partial \varphi_j^e}{\partial y} \right) \frac{\partial \varphi_i^e}{\partial y} \frac{\partial \varphi_k^e}{\partial y} + (A_{12} + A_{66}) \right. \\
& \quad \times \left. \left(\frac{\partial w_0}{\partial x} \frac{\partial \varphi_j^e}{\partial y} + \frac{\partial w_0}{\partial y} \frac{\partial \varphi_j^e}{\partial x} \right) \left(\frac{\partial \varphi_i^e}{\partial x} \frac{\partial \varphi_k^e}{\partial y} + \frac{\partial \varphi_i^e}{\partial y} \frac{\partial \varphi_k^e}{\partial x} \right) \right] dx dy \Big\} \\
& = \int_{\Omega^e} \left[A_{11} \left(\frac{\partial w_0}{\partial x} \right)^2 \frac{\partial \varphi_i^e}{\partial x} \frac{\partial \varphi_j^e}{\partial x} + A_{66} \frac{\partial w_0}{\partial x} \frac{\partial w_0}{\partial y} \frac{\partial \varphi_i^e}{\partial x} \frac{\partial \varphi_j^e}{\partial y} \right. \\
& \quad \left. + A_{66} \frac{\partial w_0}{\partial x} \frac{\partial w_0}{\partial y} \frac{\partial \varphi_i^e}{\partial y} \frac{\partial \varphi_j^e}{\partial x} + A_{22} \left(\frac{\partial w_0}{\partial y} \right)^2 \frac{\partial \varphi_i^e}{\partial y} \frac{\partial \varphi_j^e}{\partial y} + \left(\frac{A_{12} + A_{66}}{2} \right) \right. \\
& \quad \times \left. \left(\frac{\partial w_0}{\partial x} \frac{\partial \varphi_j^e}{\partial y} + \frac{\partial w_0}{\partial y} \frac{\partial \varphi_j^e}{\partial x} \right) \left(\frac{\partial \varphi_i^e}{\partial x} \frac{\partial w_0}{\partial y} + \frac{\partial \varphi_i^e}{\partial y} \frac{\partial w_0}{\partial x} \right) \right] dx dy \\
& = \int_{\Omega^e} \left[A_{11} \left(\frac{\partial w_0}{\partial x} \right)^2 \frac{\partial \varphi_i^e}{\partial x} \frac{\partial \varphi_j^e}{\partial x} + A_{22} \left(\frac{\partial w_0}{\partial y} \right)^2 \frac{\partial \varphi_i^e}{\partial y} \frac{\partial \varphi_j^e}{\partial y} \right. \\
& \quad \left. + A_{66} \frac{\partial w_0}{\partial x} \frac{\partial w_0}{\partial y} \left(\frac{\partial \varphi_i^e}{\partial x} \frac{\partial \varphi_j^e}{\partial y} + \frac{\partial \varphi_i^e}{\partial y} \frac{\partial \varphi_j^e}{\partial x} \right) + \left(\frac{A_{12} + A_{66}}{2} \right) \right. \\
& \quad \times \left. \left(\frac{\partial \varphi_i^e}{\partial x} \frac{\partial w_0}{\partial y} + \frac{\partial \varphi_i^e}{\partial y} \frac{\partial w_0}{\partial x} \right) \left(\frac{\partial w_0}{\partial x} \frac{\partial \varphi_j^e}{\partial y} + \frac{\partial w_0}{\partial y} \frac{\partial \varphi_j^e}{\partial x} \right) \right] dx dy \quad (12.4.35)
\end{aligned}$$

Therefore, T_{ij}^{33} is given by

$$\begin{aligned}
T_{ij}^{33} & = \int_{\Omega^e} \left[D_{11} \frac{\partial^2 \varphi_i^e}{\partial x^2} \frac{\partial^2 \varphi_j^e}{\partial x^2} + D_{22} \frac{\partial^2 \varphi_i^e}{\partial y^2} \frac{\partial^2 \varphi_j^e}{\partial y^2} \right. \\
& \quad \left. + D_{12} \left(\frac{\partial^2 \varphi_i^e}{\partial x^2} \frac{\partial^2 \varphi_j^e}{\partial y^2} + \frac{\partial^2 \varphi_i^e}{\partial y^2} \frac{\partial^2 \varphi_j^e}{\partial x^2} \right) + 4D_{66} \frac{\partial^2 \varphi_i^e}{\partial x \partial y} \frac{\partial^2 \varphi_j^e}{\partial x \partial y} + k \varphi_i^e \varphi_j^e \right] dx dy
\end{aligned}$$

$$\begin{aligned}
& + \int_{\Omega^e} \left\{ (N_{xx} + N_{xx}^T) \frac{\partial \varphi_i^e}{\partial x} \frac{\partial \varphi_j^e}{\partial x} + (N_{yy} + N_{yy}^T) \frac{\partial \varphi_i^e}{\partial y} \frac{\partial \varphi_j^e}{\partial y} \right. \\
& \quad + N_{xy} \left(\frac{\partial \varphi_i^e}{\partial x} \frac{\partial \varphi_j^e}{\partial y} + \frac{\partial \varphi_i^e}{\partial y} \frac{\partial \varphi_j^e}{\partial x} \right) \\
& \quad + (A_{12} + A_{66}) \frac{\partial w_0}{\partial x} \frac{\partial w_0}{\partial y} \left(\frac{\partial \varphi_i^e}{\partial x} \frac{\partial \varphi_j^e}{\partial y} + \frac{\partial \varphi_i^e}{\partial y} \frac{\partial \varphi_j^e}{\partial x} \right) \\
& \quad + \left[A_{11} \left(\frac{\partial w_0}{\partial x} \right)^2 + A_{66} \left(\frac{\partial w_0}{\partial y} \right)^2 \right] \frac{\partial \varphi_i^e}{\partial x} \frac{\partial \varphi_j^e}{\partial x} \\
& \quad \left. + \left[A_{66} \left(\frac{\partial w_0}{\partial x} \right)^2 + A_{22} \left(\frac{\partial w_0}{\partial y} \right)^2 \right] \frac{\partial \varphi_i^e}{\partial y} \frac{\partial \varphi_j^e}{\partial y} \right\} dx dy \tag{12.4.36}
\end{aligned}$$

Clearly, the tangent stiffness matrix of an element is symmetric (while the original element stiffness is *not* symmetric). This completes the finite element model development of the classical plate theory.

First-Order Plate Theory (FSDT)

Since the source of nonlinearity in the classical and first-order shear deformation plate theories is the same, the nonlinear parts of the tangent stiffness coefficients derived for the classical plate theory are also applicable to the first-order theory. For the sake of completeness, they are presented here again.

The coefficients of the submatrices $[T^{\alpha\beta}]$ ($\alpha, \beta = 1, 2, \dots, 5$) are defined by

$$T_{ij}^{\alpha\beta} = \frac{\partial R_i^\alpha}{\partial \Delta_j^\beta}, \quad R_i^\alpha = \sum_{\gamma=1}^5 \sum_{k=1}^{n*} K_{ik}^{\alpha\gamma} \Delta_k^\gamma - F_i^\alpha \tag{12.4.37}$$

where

$$\Delta_i^1 = u_i, \quad \Delta_i^2 = v_i, \quad \Delta_i^3 = w_i, \quad \Delta_i^4 = S_i^1, \quad \Delta_i^5 = S_i^2 \tag{12.4.38}$$

and $n*$ denotes n , m , or p , depending on the nodal degree of freedom. Thus, we have

$$T_{ij}^{\alpha\beta} = \frac{\partial}{\partial \Delta_j^\beta} \left(\sum_{\gamma=1}^5 \sum_{k=1}^{n*} K_{ik}^{\alpha\gamma} \Delta_k^\gamma - F_i^\alpha \right) = \sum_{\gamma=1}^5 \sum_{k=1}^{n*} \frac{\partial K_{ik}^{\alpha\gamma}}{\partial \Delta_j^\beta} \Delta_k^\gamma + K_{ij}^{\alpha\beta} \tag{12.4.39}$$

It should be noted that only coefficients that depend on the solution are K_{ij}^{13} , K_{ij}^{23} , K_{ij}^{31} , K_{ij}^{32} , and K_{ij}^{33} . Since they are functions of only w_0 (or functions of w_j), derivatives of all stiffness coefficients with respect to u_j , v_j , S_j^1 , and S_j^2 are zero. Thus, we have

$$\begin{aligned}
T_{ij}^{11} &= \sum_{\gamma=1}^5 \sum_{k=1}^{n*} \frac{\partial K_{ik}^{1\gamma}}{\partial u_j} \Delta_k^\gamma + K_{ij}^{11} = K_{ij}^{11}, \quad T_{ij}^{12} = \sum_{\gamma=1}^5 \sum_{k=1}^{n*} \frac{\partial K_{ik}^{1\gamma}}{\partial v_j} \Delta_k^\gamma + K_{ij}^{12} = K_{ij}^{12} \\
T_{ij}^{14} &= \sum_{\gamma=1}^5 \sum_{k=1}^{n*} \frac{\partial K_{ik}^{1\gamma}}{\partial S_j^1} \Delta_k^\gamma + K_{ij}^{14} = K_{ij}^{14}, \quad T_{ij}^{15} = \sum_{\gamma=1}^5 \sum_{k=1}^{n*} \frac{\partial K_{ik}^{1\gamma}}{\partial S_j^2} \Delta_k^\gamma + K_{ij}^{15} = K_{ij}^{15}
\end{aligned}$$

$$\begin{aligned}
T_{ij}^{21} &= \sum_{\gamma=1}^5 \sum_{k=1}^{n*} \frac{\partial K_{ik}^{2\gamma}}{\partial u_j} \Delta_k^\gamma + K_{ij}^{21} = K_{ij}^{21}, \quad T_{ij}^{22} = \sum_{\gamma=1}^5 \sum_{k=1}^{n*} \frac{\partial K_{ik}^{2\gamma}}{\partial v_j} \Delta_k^\gamma + K_{ij}^{22} = K_{ij}^{22} \\
T_{ij}^{24} &= \sum_{\gamma=1}^5 \sum_{k=1}^{n*} \frac{\partial K_{ik}^{2\gamma}}{\partial S_j^1} \Delta_k^\gamma + K_{ij}^{24} = K_{ij}^{24}, \quad T_{ij}^{25} = \sum_{\gamma=1}^5 \sum_{k=1}^{n*} \frac{\partial K_{ik}^{2\gamma}}{\partial S_j^2} \Delta_k^\gamma + K_{ij}^{25} = K_{ij}^{25} \\
T_{ij}^{31} &= \sum_{\gamma=1}^5 \sum_{k=1}^{n*} \frac{\partial K_{ik}^{3\gamma}}{\partial u_j} \Delta_k^\gamma + K_{ij}^{31} = K_{ij}^{31}, \quad T_{ij}^{32} = \sum_{\gamma=1}^5 \sum_{k=1}^{n*} \frac{\partial K_{ik}^{3\gamma}}{\partial v_j} \Delta_k^\gamma + K_{ij}^{32} = K_{ij}^{32} \\
T_{ij}^{13} &= \sum_{\gamma=1}^5 \sum_{k=1}^{n*} \frac{\partial K_{ik}^{1\gamma}}{\partial w_j} \Delta_k^\gamma + K_{ij}^{13} = \sum_{k=1}^n \frac{\partial K_{ik}^{13}}{\partial w_j} w_k + K_{ij}^{13} \\
&= \frac{1}{2} \int_{\Omega^e} \left[\frac{\partial \psi_i^{(1)}}{\partial x} \left(A_{11} \frac{\partial w_0}{\partial x} \frac{\partial \psi_j^{(2)}}{\partial x} + A_{12} \frac{\partial w_0}{\partial y} \frac{\partial \psi_j^{(2)}}{\partial y} \right) \right. \\
&\quad \left. + A_{66} \frac{\partial \psi_i^{(1)}}{\partial y} \left(\frac{\partial w_0}{\partial x} \frac{\partial \psi_j^{(2)}}{\partial y} + \frac{\partial w_0}{\partial y} \frac{\partial \psi_j^{(2)}}{\partial x} \right) \right] dx dy + K_{ij}^{13} \\
&= K_{ij}^{13} + K_{ij}^{13} = 2K_{ij}^{13} (= T_{ji}^{31} = K_{ji}^{31}) \\
T_{ij}^{23} &= \sum_{\gamma=1}^5 \sum_{k=1}^{n*} \frac{\partial K_{ik}^{2\gamma}}{\partial w_j} \Delta_k^\gamma + K_{ij}^{23} = \sum_{k=1}^n \frac{\partial K_{ik}^{23}}{\partial w_j} w_k + K_{ij}^{23} \\
&= \frac{1}{2} \int_{\Omega^e} \left[\frac{\partial \psi_i^{(1)}}{\partial y} \left(A_{12} \frac{\partial w_0}{\partial x} \frac{\partial \psi_j^{(2)}}{\partial x} + A_{22} \frac{\partial w_0}{\partial y} \frac{\partial \psi_j^{(2)}}{\partial y} \right) \right. \\
&\quad \left. + A_{66} \frac{\partial \psi_i^{(1)}}{\partial x} \left(\frac{\partial w_0}{\partial y} \frac{\partial \psi_j^{(2)}}{\partial x} + \frac{\partial w_0}{\partial x} \frac{\partial \psi_j^{(2)}}{\partial y} \right) \right] dx dy + K_{ij}^{23} \\
&= K_{ij}^{23} + K_{ij}^{23} = 2K_{ij}^{23} (= T_{ji}^{32} = K_{ji}^{32}) \\
T_{ij}^{33} &= \sum_{\gamma=1}^5 \sum_{k=1}^{n*} \frac{\partial K_{ik}^{3\gamma}}{\partial w_j} \Delta_k^\gamma + K_{ij}^{33} = \sum_{k=1}^{n*} \left(\frac{\partial K_{ik}^{31}}{\partial w_j} u_k + \frac{\partial K_{ik}^{32}}{\partial w_j} v_k + \frac{\partial K_{ik}^{33}}{\partial w_j} w_k \right) + K_{ij}^{33} \\
&= \int_{\Omega^e} \left(K_s A_{55} \frac{\partial \psi_i^{(2)}}{\partial x} \frac{\partial \psi_j^{(2)}}{\partial x} + K_s A_{44} \frac{\partial \psi_i^{(2)}}{\partial y} \frac{\partial \psi_j^{(2)}}{\partial y} + k \psi_i^{(2)} \psi_j^{(2)} \right) dx dy \\
&\quad + \int_{\Omega^e} \left\{ (N_{xx} + N_{xx}^T) \frac{\partial \psi_i^{(2)}}{\partial x} \frac{\partial \psi_j^{(2)}}{\partial x} + (N_{yy} + N_{yy}^T) \frac{\partial \psi_i^{(2)}}{\partial y} \frac{\partial \psi_j^{(2)}}{\partial y} \right. \\
&\quad \left. + N_{xy} \left(\frac{\partial \psi_i^{(2)}}{\partial x} \frac{\partial \psi_j^{(2)}}{\partial y} + \frac{\partial \psi_i^{(2)}}{\partial y} \frac{\partial \psi_j^{(2)}}{\partial x} \right) \right. \\
&\quad \left. + \left(A_{12} + A_{66} \right) \frac{\partial w_0}{\partial x} \frac{\partial w_0}{\partial y} \left(\frac{\partial \psi_i^{(2)}}{\partial x} \frac{\partial \psi_j^{(2)}}{\partial y} + \frac{\partial \psi_i^{(2)}}{\partial y} \frac{\partial \psi_j^{(2)}}{\partial x} \right) \right. \\
&\quad \left. + \left[A_{11} \left(\frac{\partial w_0}{\partial x} \right)^2 + A_{66} \left(\frac{\partial w_0}{\partial y} \right)^2 \right] \frac{\partial \psi_i^{(2)}}{\partial x} \frac{\partial \psi_j^{(2)}}{\partial x} \right. \\
&\quad \left. + \left[A_{66} \left(\frac{\partial w_0}{\partial x} \right)^2 + A_{22} \left(\frac{\partial w_0}{\partial y} \right)^2 \right] \frac{\partial \psi_i^{(2)}}{\partial y} \frac{\partial \psi_j^{(2)}}{\partial y} \right\} dx dy
\end{aligned}$$

$$\begin{aligned}
T_{ij}^{34} &= \sum_{\gamma=1}^5 \sum_{k=1}^{n*} \frac{\partial K_{ik}^{3\gamma}}{\partial S_j^1} \Delta_k^\gamma + K_{ij}^{34} = K_{ij}^{34}, & T_{ij}^{35} &= \sum_{\gamma=1}^5 \sum_{k=1}^{n*} \frac{\partial K_{ik}^{3\gamma}}{\partial S_j^2} \Delta_k^\gamma + K_{ij}^{35} = K_{ij}^{35} \\
T_{ij}^{44} &= \sum_{\gamma=1}^5 \sum_{k=1}^{n*} \frac{\partial K_{ik}^{4\gamma}}{\partial S_j^1} \Delta_k^\gamma + K_{ij}^{44} = K_{ij}^{44}, & T_{ij}^{45} &= \sum_{\gamma=1}^5 \sum_{k=1}^{n*} \frac{\partial K_{ik}^{4\gamma}}{\partial S_j^2} \Delta_k^\gamma + K_{ij}^{45} = K_{ij}^{45} \\
T_{ij}^{55} &= \sum_{\gamma=1}^5 \sum_{k=1}^{n*} \frac{\partial K_{ik}^{5\gamma}}{\partial S_j^2} \Delta_k^\gamma + K_{ij}^{55} = K_{ij}^{55}
\end{aligned} \tag{12.4.40}$$

Note that all nonlinear coefficients are the same as those derived for the CPT. Once again, we note that the tangent stiffness matrix of the FSDT element is symmetric.

12.4.6 Membrane Locking

Recall from Section 12.3.3 that when lower order (quadratic or less) equal interpolation of the generalized displacements is used, the FSDT elements become excessively stiff in the thin plate limit, yielding displacements that are too small compared to the true solution. This behavior is known as *shear locking* [see Reddy (2004b) and references therein]. As discussed earlier, shear locking is avoided by using selective integration: full integration to evaluate all linear stiffness coefficients and reduced integration to evaluate the transverse shear stiffnesses (i.e., all coefficients in $K_{ij}^{\alpha\beta}$ that contain A_{44} and A_{55}).

Another type of locking, known as the *membrane locking*, occurs in plates and shells due to the inconsistency of approximation of the inplane displacements (u_0, v_0) and the transverse displacement w_0 . The membrane locking can be explained by considering, for simplicity, the Timoshenko beam finite element (see Problem 13.12). The discussion also applies to the plate elements.

When the element is used to analyze pure bending deformation, it should experience no axial (or membrane) strain

$$\varepsilon_{xx}^0 \equiv \frac{du_0}{dx} + \frac{1}{2} \left(\frac{dw_0}{dx} \right)^2 = 0 \quad (\text{for pure bending}) \tag{12.4.41}$$

In order that the above constraint be satisfied for independent approximations of u_0 and w_0 , the term should cancel the second term in Eq. (12.4.41). This in turn requires that

$$\text{degree of polynomial of } \frac{du_0}{dx} \sim \text{degree of polynomial of } \left(\frac{dw_0}{dx} \right)^2 \tag{12.4.42}$$

If both variables are approximated with sufficiently higher-order polynomials, the coefficients in the polynomials get adjusted to satisfy the constraint (12.4.41). Also, when both u_0 and w_0 are approximated using linear polynomials, the correspondence (12.4.42) is met and, hence, the constraint in (12.4.41) is automatically satisfied; however, when quadratic interpolation of both u_0 and w_0 is used, then $\frac{du_0}{dx}$ is linear and $(\frac{dw_0}{dx})^2$ is quadratic and there is no possibility of cancelling the coefficient in quadratic term. If u_0 is interpolated with cubic polynomials and w_0 is interpolated with quadratic polynomials, we have

$$\frac{du_0}{dx} \quad (\text{quadratic}) \sim \left(\frac{dw_0}{dx} \right)^2 \quad (\text{quadratic}) \tag{12.4.43}$$

Thus, the constraint (12.4.41) is again satisfied. In summary, the element does not experience membrane locking for the following two cases:

- (1) u_0 is linear and w is linear
- (2) u_0 is cubic and w_0 is quadratic

and it experiences locking when both u_0 and w_0 are interpolated using quadratic polynomials.

Since quadratic approximation of u_0 and w_0 is common in practice, it is necessary to find a way to avoid membrane locking of the element. It is found that, for this case, the membrane locking can be avoided by using selective integrations of the terms of the form in ε_{xx} . For example, consider the coefficient $(K_{ij}^{22})^{tan}$ of the Timoshenko beam element (see Problem 12.13)

$$(K_{ij}^{22})^{tan} = \int_{x_a}^{x_b} E_{xx}^b A \left[\frac{du_0}{dx} + \frac{3}{2} \left(\frac{dw_0}{dx} \right)^2 \right] \frac{d\psi_i}{dx} \frac{d\psi_j}{dx} dx \quad (12.4.44)$$

For quadratic interpolation of u_0 and w_0 , the first term is a cubic ($p = 3$) polynomial and the second term is a fourth-order ($p = 4$) polynomial. Thus, the exact evaluation of the first term requires $NGP = (p+1)/2 = 2$ and the second term requires $NGP = [(p+1)/2] = 3$, where NGP denotes the number of Gauss points. For constant $E_{xx}^b A$, the three-point Gauss quadrature yields exact values of both integrals. However, the two-point Gauss rule would yield an exact value for the first term

$$\int_{x_a}^{x_b} \frac{du_0}{dx} \frac{d\psi_i}{dx} \frac{d\psi_j}{dx} dx$$

and, at the same time, the second term

$$\int_{x_a}^{x_b} \left(\frac{dw_0}{dx} \right)^2 \frac{d\psi_i}{dx} \frac{d\psi_j}{dx} dx$$

is approximated as the same degree polynomial as the first term. This amounts to using an interpolation for w_0 that satisfies the constraint $\varepsilon_{xx}^0 = 0$.

12.4.7 Numerical Examples

In this section several examples of isotropic and orthotropic plates with various edge conditions are presented to illustrate the use of the CPT and FSDT elements in the geometrically nonlinear (in the von Kármán sense) analysis. The effect of the integration rule to evaluate the nonlinear and transverse shear stiffness coefficients on the response is investigated in the first example. *Unless stated otherwise, a uniform mesh of 4×4 nine-node quadratic elements is used in a quarter plate for the FSDT.* For this choice of mesh, full integration (F) is to use 3×3 Gauss rule, and reduced integration (R) is to use 2×2 Gauss rule. Stresses are calculated at the center of the element. The shear correction coefficient is taken to be $K_s = 5/6$. A tolerance of $\epsilon = 10^{-2}$ is used for convergence in the Newton–Raphson iteration scheme to check for convergence of the nodal displacements.

Example 12.4.1:

Consider an isotropic, square plate with

$$a = b = 10 \text{ in.}, \quad h = 1 \text{ in.}, \quad E = 7.8 \times 10^6 \text{ psi}, \quad \nu = 0.3 \quad (12.4.45)$$

Two types of simply supported boundary conditions are studied. The displacement boundary conditions used for SS-1 and SS-3 are

$$\begin{aligned} \text{SS-1:} \quad & \text{At } x = a/2 : \quad v_0 = w_0 = \phi_y = 0 \\ & \text{At } y = b/2 : \quad u_0 = w_0 = \phi_x = 0 \end{aligned} \quad (12.4.46)$$

$$\text{SS-3:} \quad u_0 = v_0 = w_0 = 0 \quad \text{on simply supported edges} \quad (12.4.47)$$

Uniformly distributed load of intensity q_0 is used. The boundary conditions along the symmetry lines for both cases are given by

$$\text{At } x = 0 : \quad u_0 = \phi_x = 0; \quad \text{At } y = 0 : \quad v_0 = \phi_y = 0 \quad (\text{symm. lines}) \quad (12.4.48)$$

It is clear that SS-3 provides more edge restraint than SS-1 and, therefore, should produce lower transverse deflections.

Using the load parameter, $\bar{P} \equiv q_0 a^4 / Eh^4$, the incremental load vector is chosen to be $\{\Delta P\} = \{6.25, 6.25, 12.5, 25.0, 25.0, \dots, 25.0\}$. Table 12.4.1 contains the deflections $w_0(0, 0)$ and normal stresses $\bar{\sigma}_{xx} = \sigma_{xx}(a^2/Eh^2)$ at the center of the first element for various integration rules (Figure 12.4.1). The linear FSDT plate solution for load $q_0 = 4875$ psi (or $\bar{P} = 6.25$) is $w_0 = 0.2917$ in. for SS-1 and $w_0 = 0.3151$ in. for SS-3.

Table 12.4.1. Center deflection \bar{w} and stresses $\bar{\sigma}_{xx}$ of simply supported (SS-1 and SS-3) plates under uniformly distributed load.

\bar{P}	SS-3			SS-1		
	R-R*	F-R	F-F	R-R	F-R	F-F
<i>Deflections, $w_0(0, 0)$</i>						
6.25	0.2790 (3) [†]	0.2790 (4)	0.2780 (3)	0.2813 (3)	0.2813 (3)	0.2812 (3)
12.5	0.4630 (3)	0.4630 (3)	0.4619 (3)	0.5186 (3)	0.5186 (3)	0.5185 (3)
25.0	0.6911 (3)	0.6911 (3)	0.6902 (3)	0.8673 (4)	0.8673 (4)	0.8672 (4)
50.0	0.9575 (3)	0.9575 (3)	0.9570 (3)	1.3149 (4)	1.3149 (4)	1.3147 (4)
75.0	1.1333 (3)	1.1333 (3)	1.1330 (3)	1.6241 (3)	1.6239 (3)	1.6237 (3)
100.0	1.2688 (3)	1.2688 (3)	1.2686 (3)	1.8687 (3)	1.8683 (3)	1.8679 (3)
125.0	1.3809 (2)	1.3809 (2)	1.3808 (2)	2.0758 (2)	2.0751 (2)	2.0746 (2)
150.0	1.4774 (2)	1.4774 (2)	1.4774 (2)	2.2567 (2)	2.2556 (2)	2.2549 (2)
175.0	1.5628 (2)	1.5629 (2)	1.5629 (2)	2.4194 (2)	2.4177 (2)	2.4168 (2)
200.0	1.6398 (2)	1.6399 (2)	1.6399 (2)	2.5681 (2)	2.5657 (2)	2.5645 (2)

Table 12.4.1 (continued)

\bar{P}	SS-3			SS-1		
	R-R*	F-R	F-F	R-R	F-R	F-F
<i>Normal stresses, $\bar{\sigma}_{xx}(0.3125, 0.3125, h/2)$</i>						
6.25	1.861	1.861	1.856	1.779	1.779	1.780
12.5	3.305	3.305	3.300	3.396	3.396	3.398
25.0	5.319	5.320	5.317	5.882	5.882	5.885
50.0	8.001	8.002	8.001	9.159	9.162	9.165
75.0	9.983	9.984	9.983	11.458	11.462	11.465
100.0	11.633	11.634	11.634	13.299	13.307	13.308
125.0	13.084	13.085	13.085	14.878	14.890	14.889
150.0	14.396	14.398	14.398	16.278	16.293	16.290
175.0	15.608	15.610	15.610	17.553	17.572	17.567
200.0	16.741	16.743	16.743	18.733	18.755	18.748

* The first letter refers to the integration rule used for the nonlinear terms while the second letter refers to the integration rule used for the shear terms.

† Number of iterations taken for convergence.

Example 12.4.2:

Orthotropic plates with

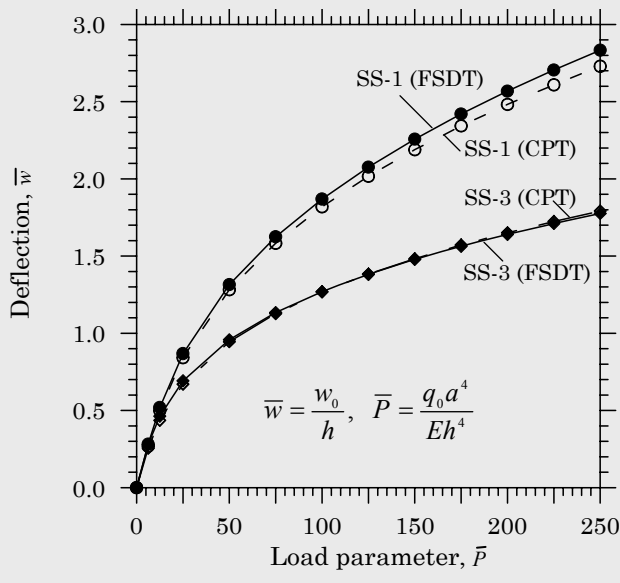
$$\begin{aligned} a = b = 12 \text{ in.}, \quad h = 0.138 \text{ in.}, \quad E_1 = 3 \times 10^6 \text{ psi}, \quad E_2 = 1.28 \times 10^6 \text{ psi} \\ G_{12} = G_{13} = G_{23} = 0.37 \times 10^6 \text{ psi}, \quad \nu_{12} = 0.32 \end{aligned} \quad (12.4.49)$$

and subjected to uniformly distributed transverse load (i.e., $q = q_0 = \text{constant}$) are analyzed. A uniform mesh of 4×4 Q9 elements with reduced integration is used in a quadrant. The incremental load vector is chosen to be

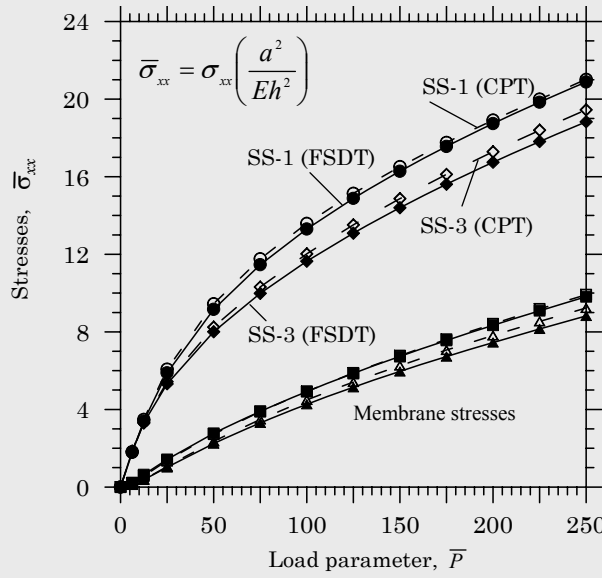
$$\{\Delta P\} = \{0.05, 0.05, 0.1, 0.2, 0.2, \dots, 0.2\}$$

Twelve load steps are used, and a tolerance of $\epsilon = 0.01$ is used for convergence.

Table 12.4.2 contains the center deflection and total as well as membrane normal stress $\bar{\sigma}_{xx}$ as a function of the load for SS-1 and SS-3 boundary conditions. The linear FSDT solution for load $q_0 = 0.05$ is $w_0 = 0.01132$ for SS-1 and $w_0 = 0.01140$ for SS-3. Plots of load q_0 (psi) vs. center deflection w_0 (in.) and q_0 versus normal stress $\bar{\sigma}_{xx} = \sigma_{xx}(a^2/E_2h^2)$ are shown in Figure 12.4.2 for SS-1 and SS-3 plates. The figure also shows the results obtained using 8×8 mesh of conforming CPT elements. In Figure 12.4.2, broken lines with open symbols are used for the CPT solutions and solid lines with dark symbols are used for the FSDT solutions.



(a)



(b)

Figure 12.4.1. Plots of center deflection w_0 versus load \bar{P} and center normal stress $\bar{\sigma}_{xx}$ versus load \bar{P} for isotropic ($\nu = 0.3$), simply supported square plates under uniform load (4×4Q9 for FSDT and 8×8C for CPT).

Table 12.4.2. Center deflection w_0 and normal stress $\bar{\sigma}_{xx}$ for simply supported orthotropic square plates under uniform load (4×4 Q9).

q_0	SS-1			SS-3		
	CPT w_0	FSDT w_0	FSDT $\bar{\sigma}_{xx}$	CPT w_0	FSDT w_0	FSDT $\bar{\sigma}_{xx}$
0.05	0.0113 (2)	0.0113	1.034	0.0112	0.0113	1.056
0.10	0.0224 (2)	0.0224	2.070	0.0217	0.0218	2.116
0.20	0.0438 (3)	0.0439	4.092	0.0395	0.0397	4.058
0.40	0.0812 (3)	0.0815	7.716	0.0648	0.0650	7.103
0.60	0.1116 (3)	0.1122	10.702	0.0823	0.0824	9.406
0.80	0.1367 (3)	0.1377	13.169	0.0957	0.0959	11.284
1.00	0.1581 (2)	0.1594	15.255	0.1068	0.1069	12.894
1.20	0.1767 (2)	0.1783	17.050	0.1162	0.1162	14.316
1.40	0.1932 (2)	0.1951	18.631	0.1245	0.1244	15.602
1.60	0.2081 (2)	0.2103	20.044	0.1318	0.1318	16.783
1.80	0.2217 (2)	0.2241	21.324	0.1385	0.1384	17.880
2.00	0.2343 (2)	0.2370	22.495	0.1447	0.1445	18.909

Example 12.4.3:

Here, we analyze an orthotropic plate with clamped edges; i.e., all generalized displacements are set to zero on the boundary. The boundary conditions of a clamped edge are taken to be

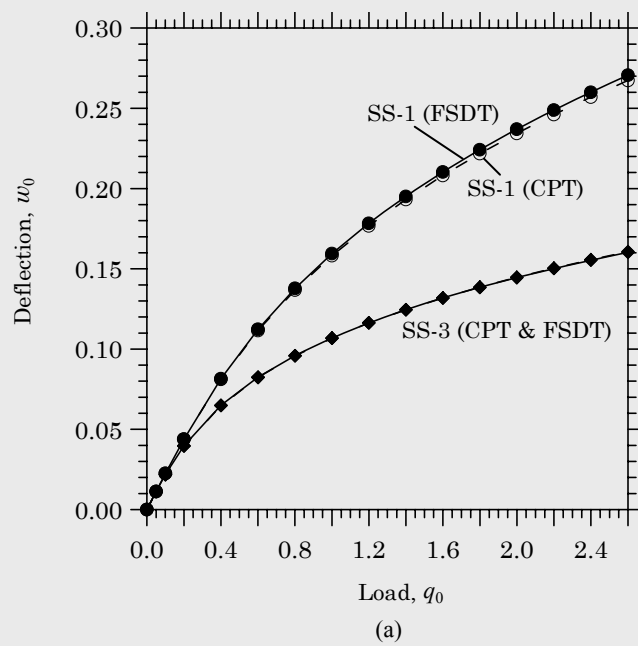
$$u_0 = v_0 = w_0 = \phi_x = \phi_y = 0 \quad (12.4.50)$$

The geometric and material parameters used are the same as those listed in Eq. (12.4.5). A uniform load of intensity q_0 is used.

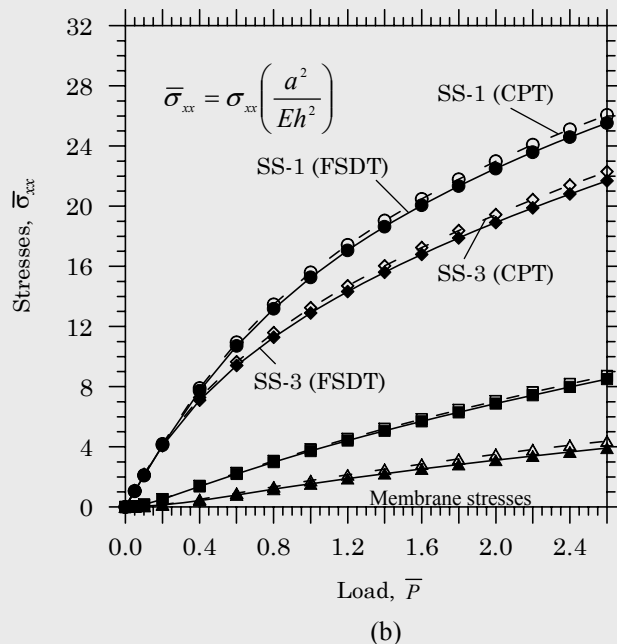
The linear solution for load $q_0 = 0.5$ is $w_0 = 0.0301$. Table 12.4.3 contains center deflections and stresses for the problem (see Reddy 2004b). Figure 12.4.3 contains plots of load versus center deflection of an isotropic plate ($h = 0.138$ in., $E = 1.28 \times 10^6$ psi, and $\nu = 0.3$); the CPT deflections were obtained using 8×8 mesh of the nonconforming elements and the FSDT deflections were obtained with 4×4 Q9 mesh (mesh of nine-node Lagrange elements).

12.5 Summary

In this chapter, finite element models of the CPT and FSDT for geometrically linear and nonlinear (i.e., with the von Kármán nonlinear strains) problems were developed. Numerical examples of bending of rectangular plates are presented and the influence of geometric nonlinearity on bending response are presented. The Newton–Raphson iterative method of solution is discussed, and the tangent stiffness matrix coefficients of the FSDT element are derived. Numerical results of the nonlinear analysis using the FSDT plate elements are presented to illustrate the influence of symmetry boundary conditions and the geometric nonlinearity on the deflections and stresses.



(a)



(b)

Figure 12.4.2. Center deflection $w_0(0, 0)$ and stresses $\bar{\sigma}_{xx}$ as functions of the load q_0 for simply supported, orthotropic, square plates under uniformly distributed load.

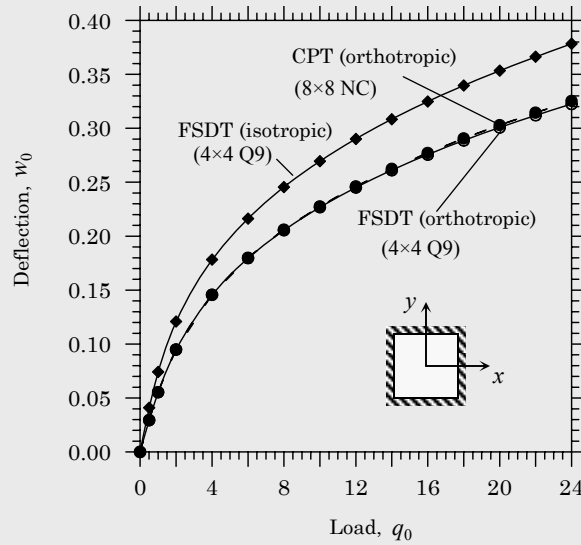


Figure 12.4.3. Nonlinear center deflection w_0 versus load parameter q_0 for clamped, orthotropic, square plates under uniform load.

Table 12.4.3: Center deflection w_0 and normal stress $\bar{\sigma}_{xx}$ for clamped orthotropic square plates under uniformly distributed load ($4 \times 4Q9$).

q_0	w_0	$\bar{\sigma}_{xx}$	q_0	w_0	$\bar{\sigma}_{xx}$
0.5	0.0294 (3)	4.317	12.0	0.2450 (2)	46.001
1.0	0.0552 (3)	8.467	14.0	0.2610 (2)	49.851
2.0	0.0948 (3)	15.309	16.0	0.2754 (2)	53.431
4.0	0.1456 (3)	24.811	18.0	0.2886 (2)	56.800
6.0	0.1795 (3)	31.599	20.0	0.3006 (2)	59.998
8.0	0.2054 (3)	37.078	22.0	0.3119 (2)	63.053
10.0	0.2268 (2)	41.793	24.0	0.3224 (2)	65.986

Problems

12.1 The principle of total potential energy for axisymmetric bending of annular plates is given by

$$0 = - \int_b^a \left(M_{rr} \frac{d^2 \delta w_0}{dr^2} + M_{\theta\theta} \frac{1}{r} \frac{d \delta w_0}{dr} \right) r dr - \int_b^a q \delta w_0 r dr \quad (1)$$

where

$$M_{rr} = - \left(D_{11} \frac{d^2 w_0}{dr^2} + D_{12} \frac{1}{r} \frac{dw_0}{dr} \right), \quad M_{\theta\theta} = - \left(D_{12} \frac{d^2 w_0}{dr^2} + D_{22} \frac{1}{r} \frac{dw_0}{dr} \right) \quad (2)$$

Formulate the displacement finite element model of axisymmetric circular plates in algebraic form, $\mathbf{K}^e \Delta^e = \mathbf{F}^e$, and define all of the expressions. The circular finite element is located between $r = r_a$ and $r = r_b$, as shown in Figure P12.1. Use Hermite cubic interpolation of $w_0(r)$ to derive the finite element model

$$w_0(r) = \sum_{j=1}^4 \Delta_j \phi_j(r) \quad (3)$$

where Δ_1 and Δ_3 are the transverse displacements at $r = r_a$, $r = r_b$, Δ_2 and Δ_4 are the rotations $-dw_0/dr$ at $r = r_a$ and $r = r_b$, and ϕ_i are the Hermite interpolation functions.

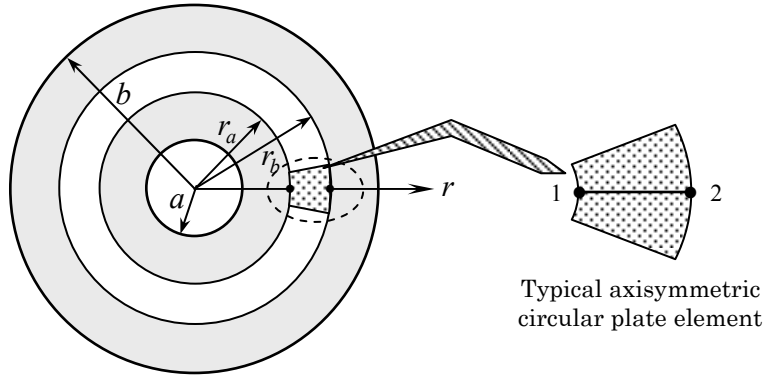


Figure P12.1

- 12.2** When cylindrical tanks of variable thickness are to be analyzed, the bending stiffness D appearing in Eq. (11.3.19) is no longer constant, but a function of the axial coordinate x because $h = h(x)$. Considering the case in which the thickness is a linear function of x (Figure P11.16 on page 476), the flexural rigidity becomes a cubic function of x

$$h(x) = kx, \quad D = \frac{Ek^3}{12(1-\nu^2)} x^3 \equiv D_0 x^3$$

and Eq. (11.3.19) takes the form

$$\frac{d^2}{dx^2} \left(D_0 x^3 \frac{d^2 w_0}{dx^2} \right) + \frac{Ek}{R^2} x w_0 = \gamma(x - x_0)$$

Develop the finite element model of the equation.

- 12.3** Investigate the displacement and slope compatibility of the nonconforming rectangular element CPT(N). *Hint:* Use the edge connecting nodes 1 and 2 and check if the displacement w and slopes $\partial w/\partial x$ and $\partial w/\partial y$ are continuous.

- 12.4** Consider the equations governing thin shells with double curvature, Eqs. (11.2.74)–(11.2.78). Displacement finite element models of these equations can be derived in a manner similar to that of plates. In fact, the finite element model of shells with double curvature is identical to that of FSDT (for FSDT, set $C_0 = 0$, $1/R_1 = 0$, and $1/R_2 = 0$) with additional terms in the stiffness coefficients. As a first step towards developing the finite element model, construct the weak forms of the linear equations associated with Eqs. (11.2.74)–(11.2.78).
- 12.5** (Continuation of Problem 12.4) Develop finite element model of a thin shell with double curvature.
- 12.6** Consider the following displacement field for pure bending of a beam according to the Euler–Bernoulli beam theory:

$$u_1(x, z) = u_0(x) - z \frac{dw_0}{dx}, \quad u_2 = 0, \quad u_3(x, z) = w_0(x) \quad (1)$$

where $u_0 = u_0(x)$ and $w_0 = w_0(x)$ are the axial and transverse displacements of a point on the centroidal axis of the beam. Write the expression for the principle of virtual work done, accounting for the von Kármán nonlinear strains. Express the final result in terms of the displacements u_0 and w_0 .

- 12.7** (Continuation of Problem 12.6) Develop the nonlinear finite element model of the Euler–Bernoulli beam using the weak forms developed in Problem 12.6. Assume finite element interpolation of u_0 and w_0 in the form

$$\begin{aligned} u_0(x) &= \sum_{j=1}^2 u_j \psi_j(x), \quad w_0(x) = \sum_{j=1}^4 \bar{\Delta}_j \varphi_j(x) \\ \bar{\Delta}_1 &= w_1, \quad \bar{\Delta}_2 = \theta_1, \quad \bar{\Delta}_3 = w_2, \quad \bar{\Delta}_4 = \theta_2 \end{aligned} \quad (1)$$

and ψ_j are the linear Lagrange interpolation functions, φ_j are the Hermite cubic interpolation functions, and $\theta = -\frac{dw_0}{dx}$.

- 12.8** (Continuation of Problems 12.6 and 12.7) Compute the tangent stiffness matrix associated with the Euler–Bernoulli beam element developed in Problem 12.7.

- 12.9** Beginning with the displacement field of the Timoshenko beam theory

$$u_1(x, z) = u_0(x) + z\phi_x(x), \quad u_2(x, z) = 0, \quad u_3(x, z) = w_0(x) \quad (1)$$

compute the von Kármán nonlinear strains and develop the expression for the statement of the principle of virtual displacements for the problem.

- 12.10** (Continuation of Problem 12.9) Assume the following finite element approximation of the generalized displacements (u_0, w_0, ϕ_x):

$$u_0 = \sum_{j=1}^m u_j \psi_j^{(1)}, \quad w_0 = \sum_{j=1}^n w_j \psi_j^{(2)}, \quad \phi_x = \sum_{j=1}^p S_j \psi_j^{(3)} \quad (1)$$

and develop the finite element model of the Timoshenko beam theory.

12.11 (Continuation of Problem 12.10) Compute the tangent stiffness matrix coefficients associated with the nonlinear Timoshenko beam finite element.

12.12 Consider the following equations of motion of the FSDT:

$$I_0 \frac{\partial^2 u_0}{\partial t^2} - \frac{\partial N_{xx}}{\partial x} - \frac{\partial N_{xy}}{\partial y} = 0 \quad (1)$$

$$I_0 \frac{\partial^2 v_0}{\partial t^2} - \frac{\partial N_{xy}}{\partial x} - \frac{\partial N_{yy}}{\partial y} = 0 \quad (2)$$

$$\begin{aligned} I_0 \frac{\partial^2 w_0}{\partial t^2} - \frac{\partial}{\partial x} \left(N_{xx} \frac{\partial w_0}{\partial x} + N_{xy} \frac{\partial w_0}{\partial y} \right) - \frac{\partial}{\partial y} \left(N_{xy} \frac{\partial w_0}{\partial x} + N_{yy} \frac{\partial w_0}{\partial y} \right) \\ - \frac{\partial Q_x}{\partial x} - \frac{\partial Q_y}{\partial y} - q = 0 \end{aligned} \quad (3)$$

$$I_2 \frac{\partial^2 \phi_x}{\partial t^2} - \frac{\partial M_{xx}}{\partial x} - \frac{\partial M_{xy}}{\partial y} + Q_x = 0 \quad (4)$$

$$I_2 \frac{\partial^2 \phi_y}{\partial t^2} - \frac{\partial M_{xy}}{\partial x} - \frac{\partial M_{yy}}{\partial y} + Q_y = 0 \quad (5)$$

where I_0 and I_2 are the principal and rotatory inertias

$$I_0 = \rho h, \quad I_2 = \frac{\rho h^3}{12} \quad (6)$$

and the inplane forces (N_{xx}, N_{xy}, N_{yy}), transverse shear forces (Q_x, Q_y), and moments (M_{xx}, M_{xy}, M_{yy}) were defined in Eqs. (12.4.13a–c). Develop the finite element model of the equations of motion.

References

- Ambartsumyan, S. A., *Theory of Anisotropic Shells*, Moscow (1961); English translation, NASA-TT-F-118 (1964).
- Averill, R. C. and Reddy, J. N., “Behavior of Plate Elements Based on the First-Order Shear Deformation Theory,” *Engineering Computations*, **7**, 57–74 (1990).
- Barbero, E. J. and Reddy, J. N., “General Two-Dimensional Theory of Laminated Cylindrical Shells,” *AIAA Journal*, **28**, 544–553 (1990).
- Barlow, J., “Optimal Stress Location in Finite Element Models,” *International Journal for Numerical Methods in Engineering*, **10**, 243–251 (1976).
- Barlow, J., “More on Optimal Stress Points — Reduced Integration Element Distortions and Error Estimation,” *International Journal for Numerical Methods in Engineering*, **28**, 1486–1504 (1989).
- Bartlett, C.C., “The Vibration and Buckling of a Circular Plate Clamped on Part of its Boundary and Simply Supported on the Remainder,” *Quarterly Journal of Mechanics and Applied Mathematics*, **16**, 431–440 (1963).
- Basset, A. B., “On the Extension and Flexure of Cylindrical and Spherical Thin Elastic Shells,” *Philosophical Transactions of the Royal Society*, (London) Ser. A, **181** (6), 433–480 (1890).
- Bathe, K. J.: *Finite Element Procedures*, Prentice-Hall, Englewood Cliffs, NJ (1996).
- Bathe, K. J. and Dvorkin, E. N., “A Four-Node Plate Bending Element Based on Mindlin/Reissner Plate Theory and Mixed Interpolation,” *International Journal for Numerical Methods in Engineering*, **21**, 367–383 (1985).
- Batoz, J. L., “An Explicit Formulation for an Efficient Triangular Plate Bending Element,” *International Journal for Numerical Methods in Engineering*, **18**(7), 1077–1089 (1985).
- Batoz, J. L., Bathe, K. J., and Ho, L. W., “A Study of Three-Node Triangular Plate Bending Elements,” *International Journal for Numerical Methods in Engineering*, **15**(12), 1771–1812 (1980).

- Batoz, J. L. and Tahar, M. B., "Evaluation of a New Quadrilateral Thin Plate Bending Element," *International Journal for Numerical Methods in Engineering*, **18**, 1655–1677 (1982).
- Bazeley, G. P., Cheung, Y. K., Irons, B. M., and Zienkiewicz, O. C., "Triangular Elements in Bending – Conforming and Non-Conforming Solutions," *Proceedings of the Conference on Matrix Methods in Structural Mechanics*, Air Force Institute of Technology, Wright-Patterson Air Force Base, Ohio, 547–576 (1965).
- Bell, K., "A Refined Triangular Plate Bending Finite Element," *International Journal for Numerical Methods in Engineering*, **1**, 101–122 (1969).
- Belytschko, T., Tsay, C. S., and Liu, W. K., "Stabilization Matrix for the Bilinear Mindlin Plate Element," *Computer Methods in Applied Mechanics and Engineering*, **29**, 313–327 (1981).
- Bert, C. W., "Analysis of Shells," *Structural Design and Analysis, Part I*, C. C. Chamis (Ed.), Vol. 7 of *Composite Materials*, L. J. Broutman and R. H. Krock (Eds.) Academic Press, New York, 207–258 (1974).
- Bogner, F. K., Fox, R. L., and Schmidt, L. A., Jr., "The Generation of Interelement-Compatible Stiffness and Mass Matrices by the Use of Interpolation Formulas," *Proceedings of the Conference on Matrix Methods in Structural Mechanics*, Air Force Institute of Technology, Wright-Patterson Air Force Base, Ohio, 397–443 (1965).
- Boley, B. A. and Weiner, J. H., *Theory of Thermal Stresses*, John Wiley, New York (1960).
- Bowen, R. M. and Wang, C. C., *Introduction to Vectors and Tensors*, Vols. I and II, Plenum, New York (1976).
- Brebbia, C. and Connor, J., "Geometrically Nonlinear Finite Element Analysis," *Journal of Engineering Mechanics*, 463–483 (1969).
- Brogan, W. L., *Modern Control Theory*, Prentice-Hall, Englewood Cliffs, NJ (1985).
- Budiansky, B. and Sanders, J. L., "On the 'Best' First-Order Linear Shell Theory," *Progress in Applied Mechanics, The Prager Anniversary Volume*, Macmillan, New York, 129–140 (1963).
- Byrne, R., "Theory of Small Deformations of a Thin Elastic Shell," Seminar Reports in Mathematics, University of California, **2** (1), 103–152 (1944).
- Cantin, G. and Clough, R. W., "A Curved Cylindrical Shell Finite Element," *AIAA Journal*, **6**, 1057 (1968).
- Castigliano, A., *Theorie de l'équilibre des systèmes élastiques et ses applications*, A. F. Negro, Turin, Italy (1879).
- Cheng, S. and Ho, B. P. C., "Stability of Heterogeneous Aeolotropic Cylindrical Shells under Combined Loading," *AIAA Journal*, **1**(4), 892–898 (1963).

- Cho, M. and Roh, H. Y., "Development of Geometrically Exact New Elements Based on General Curvilinear Coordinates," *International Journal for Numerical Methods in Engineering* **56**, 81–115 (2003).
- Clough, R. W. and Penzien, J., *Dynamics of Structures*, McGraw-Hill, New York (1975).
- Clough, R. W. and Tocher, J. L., "Finite Element Stiffness Matrices for Analysis of Plates in Bending," *Proceedings of the Conference on Matrix Methods in Structural Mechanics*, AFFDL-TR-66-80, Air Force Institute of Technology, Wright-Patterson Air Force Base, Ohio, 515–545 (1965).
- Clough, R. W. and Felippa, C. A., "A Refined Quadrilateral Element for Analysis of Plate Bending," *Proceedings of the Second Conference on Matrix Methods in Structural Mechanics*, AFFDL-TR-66-80, Air Force Institute of Technology, Wright-Patterson Air Force Base, Ohio, 399–440 (1968).
- Cook, R. D., Malkus, D. S., and Plesha, M. E., *Concepts and Applications of Finite Element Analysis*, 3d ed., John Wiley & Sons, New York (1989).
- Dikeman, M., *Theory of Thin Elastic Shells*, Pitman, Boston, MA (1982).
- Donnell, L. H., "Stability of Thin Walled Tubes in Torsion," NACA Report 479 (1933).
- Donnell, L. H., *Beams, Plates, and Shells*, McGraw-Hill, New York (1976).
- Eringen, A. C., *Mechanics of Continua*, John Wiley & Sons, New York (1967).
- Farshad, M., *Design and Analysis of Shell Structures*, Kluwer Academic Publishers, Dordrecht, Netherlands (1992).
- Flügge, W., *Stresses in Shells*, 2nd ed., Springer-Verlag, Berlin (1973).
- Fraeijs de Veubeke, B., "A Conforming Finite Element for Plate Bending," *International Journal of Solids and Structures*, **4**(1), 95–108 (1968).
- Franklin, J. N., *Matrix Theory*, Prentice-Hall, Englewood Cliffs, NJ (1968).
- Fung, Y. C., *Foundations of Solid Mechanics*, Prentice-Hall, Englewood Cliff, NJ (1965).
- Gibson, R. F., *Principles of Composite Material Mechanics*, McGraw-Hill, New York (1994).
- Goldenveizer, A. L., *Theory of Thin Shells*, Pergamon Press, New York (1962).
- Gopal, M., *Modern Control System Theory*, Wiley Eastern, New York (1984).
- Gould, P. L., *Analysis of Shells and Plates*, Prentice-Hall, Upper Saddle River, NJ (1999).
- Green, A. E., "On the Linear Theory of Thin Elastic Shells," *Proceedings of the Royal Society, Series A*, **266** (1962).
- Hashin, Z., "Analysis of Properties of Fiber Composites with Anisotropic Constituents," *Journal of Applied Mechanics*, **46**, 543–550 (1979).

- Hearman, R. F. S., "The Frequency of Flexural Vibration of Rectangular Orthotropic Plates with Clamped or Supported Edges," *Journal of Applied Mechanics*, **26**(4), 537–540 (1959).
- Heyman, J., *Equilibrium of Shell Structures*, Oxford University Press, UK (1977).
- Hildebrand, F. B., Reissner, E., and Thomas, G. B., "Notes on the Foundations of the Theory of Small Displacements of Orthotropic Shells," NACA TN-1833, Washington, D.C. (1949).
- Hrabok, M. M. and Hrudey, T. M., "A Review and Catalog of Plate Bending Finite Elements," *Computers and Structures* **19**(3), 479–495 (1984).
- Huang, H. C. and Hinton, E., "A Nine-Node Lagrangian Plate Element with Enhanced Shear Interpolation," *Engineering Computations*, **1**, 369–379 (1984).
- Huffington, H. J., "Theoretical Determination of Rigidity Properties of Orthotropic Stiffened Plates," *Journal of Applied Mechanics*, **23**, 15–18 (1956).
- Hughes, T. J. R., Taylor, R. L., and Kanoknukulchai, W., "A Simple and Efficient Element for Plate Bending," *International Journal for Numerical Methods in Engineering*, **11**(10), 1529–1543 (1977).
- Hughes, T. J. R. and Cohen, M., "The 'Heterosis' Finite Element for Plate Bending," *Computers and Structures*, **9**(5), 445–450 (1978).
- Hughes, T. J. R., Cohen, M., and Haroun, M., "Reduced and Selective Integration Techniques in the Finite Element Analysis of Plates," *Nuclear Engineering and Design*, **46**, 203–222 (1981).
- Irons, B. M., "A Conforming Quartic Triangular Element for Plate Bending", *International Journal for Numerical Methods in Engineering* **1**, 29–45 (1969).
- Jeffreys, H., *Cartesian Tensors*, Cambridge University Press, London (1965).
- Jemielita, G., "Techniczna Teoria Płyty Średniej Grubbosci," (Technical Theory of Plates with Moderate Thickness), *Rozprawy Inżynierskie, Polska Akademia Nauk*, **23**(3), 483–499 (1975).
- Joga Rao, C. V. and Pickett, G., "Vibrations of Plates of Irregular Shapes and Plates with Holes," *Journal of Aeronautical Society of India*, **13**(3), 83–88 (1961).
- Kantham, C. L., "Bending and Vibration of Elastically Restrained Circular Plates," *Journal Franklin Institute*, **265**(6), 483–491 (1958).
- Kerr, A. D., "On the stability of circular plates," *Journal of Aerospace Science*, **29**(4), 486–487 (1962).
- Khdeir, A. A. and Reddy, J. N., "Buckling and Vibration of Laminated Composite Plates Using Various Plate Theories," *AIAA Journal*, **27**(12), 1808–1817 (1989).
- Kirchhoff, G., "Über die Gleichungen des Gleichgewichts eines elastischen Körpers bei nicht unendlich kleinen Verschiebungen seiner Theile," *Sitzungsber. Akad. Wiss., Wien (Vienna)*, **9**, 762–773 (1852).

- Koiter, W. T., "Foundations and Basic Equations of Shell Theory. A Survey of Recent Progress," *Theory of Shells*, F. I. Niordson (Ed.), IUTAM Symposium, Copenhagen, 93–105 (1967).
- Kraus, H., *Thin Elastic Shells*, John Wiley & Sons, New York (1967).
- Kreyszig, E., *Advanced Engineering Mathematics*, 9th ed., John Wiley & Sons, New York (2006).
- Krishna Murty, A. V., "Higher Order Theory for Vibration of Thick Plates," *AIAA Journal*, **15**(2), 1823–1824 (1977).
- Lanczos, C., *The Variational Principles of Mechanics*, The University of Toronto Press, Toronto (1964).
- Langhaar, H. L., *Energy Methods in Applied Mechanics*, John Wiley & Sons, New York (1962).
- Leissa, A. W., *Vibration of Plates*, NASA SP-160, Washington, D.C. (1969).
- Leissa, A. W., *Vibration of Shells*, NASA SP-288, Washington, D.C. (1973).
- Levinson, M., "An Accurate, Simple Theory of the Static and Dynamics of Elastic Plates," *Mechanics Research Communications*, **7**(6), 343–350 (1980).
- Librescu, L., *Elastostatics and Kinetics of Anisotropic and Heterogeneous Shell-Type Structures*, Noordhoff, Leyden, The Netherlands (1975).
- Lim, G. T. and Reddy, J. N., "On Canonical Bending Relationships for Plates," *International Journal of Solids Structures*, **40**, 3039–3067 (2003).
- Love, A. E. H., "The Small Free Vibrations and Deformations of a Thin Elastic Shell," *Philosophical Transactions of the Royal Society (London)*, Ser. A, **179**, 491–549 (1888).
- Lukasiewicz, S., *Local Loads in Plates and Shells*, Sijthoff & Noordhoff, Alphen aan den Rijn, The Netherlands (1979).
- Lur'ye, A. I., "General Theory of Elastic Shells," *Prikl. Mat. Mekh.*, **4** (1), 7–34 (1940).
- Malvern, L. E., *Introduction to the Mechanics of a Continuous Medium*, Prentice-Hall, Englewood Cliffs, NJ (1969).
- McFarland, D., Smith, B. L., and Bernhart, W. D., *Analysis of Plates*, Spartan Books, Philadelphia, PA (1972).
- McLachlan, N., *Bessel Functions for Engineers*, Oxford University Press, London (1948).
- Melosh, R. J., "Basis of Derivation of Matrices for the Direct Stiffness Method," *AIAA Journal*, **1**, 1631–1637 (1963).
- Mikhlin, S. G., *Variational Methods in Mathematical Physics*, (translated from the 1957 Russian edition by T. Boddington) MacMillan, New York (1964).

- Mikhlin, S. G., *The Problem of the Minimum of a Quadratic Functional* (translated from the 1952 Russian edition by A. Feinstein), Holden-Day, San Francisco (1965).
- Mikhlin, S. G., *An Advanced Course of Mathematical Physics*, American Elsevier, New York (1970).
- Morley, L. S. D., "An Improvement of Donnell's Approximation of Thin-Walled Circular Cylinders," *Quarterly Journal of Mechanics and Applied Mathematics*, **8**, 169–176 (1959).
- Morley, L. S. D., "A Triangular Equilibrium Element with Linearly Varying Bending Moments for Plate Bending Problems," Technical Note, *Journal of the Aeronautical Society*, **71** (1967).
- Morley, L. S. D., "The Triangular Equilibrium Element in the Solution of Plate Bending Problems," *Journal of the Aeronautical Society*, **72** (1968).
- Morley, L. S. D., "The Constant-Moment Plate Bending Element," *Journal of Strain Analysis*, **6**(1), 20–24 (1971).
- Naghdi, P. M., "Foundations of Elastic Shell Theory," in *Progress in Solid Mechanics*, volume IV, I. N. Sneddon and R. Hill (Eds.), North-Holland, Amsterdam, Netherlands (1963).
- Naghdi, P. M., "The Theory of Shells and Plates," in *Principles of Classical Mechanics and Field Theory*, volume VI, S. Flügge (Ed.) *Encyclopedia of Physics*, part A2, pp. 425–640, Springer-Verlag, Berlin (1972).
- Naghdi, P. M. and Berry, J. G., "On the Equations of Motion of Cylindrical Shells," in *Journal of Applied Mechanics*, **21**(2), pp. 160–166 (1964).
- Newmark, N. M., "A Method for Computation of Structural Dynamics," *Journal of Engineering Mechanics*, **85**, 67–94 (1959).
- Nickell, R. E. and Secor, G.A., "Convergence of Consistently Derived Timoshenko Beam Finite Elements," *International Journal for Numerical Methods in Engineering*, **5**, 243–253 (1972).
- Niordson, F. I., *Shell Theory*, North-Holland, Amesterdam, The Netherlands (1985).
- Nosier, A. and Reddy, J. N., "Vibration and Stability Analyses of Cross-Ply Laminated Circular Cylindrical Shells," *Journal of Sound and Vibration*, **157**(1), 139–159 (1992a).
- Nosier, A. and Reddy, J. N., "On Vibration and Buckling of Symmetric Laminated Plates According to Shear Deformation Theories. Parts I and II," *Acta Mechanica*, **94**(3-4), 123–170 (1992b).
- Novozhilov, V. V., *The Theory of Thin Elastic Shells*, P. Noordhoff, Gröningen, The Netherlands (1964). Translated from the 2nd Russian edition by P. G. Lowe (edited by J. R. M. Radok).

- Nowinski, J. L., *Theory of Thermoelasticity with Applications*, Sijthoff & Noordhoff, Alphen aan den Rijn, The Netherlands (1978).
- Oden, J. T. and Reddy, J. N., *Variational Methods in Theoretical Mechanics*, 2nd ed., Springer-Verlag, Berlin (1982).
- Oden, J. T. and Ripperger, E. A., *Mechanics of Elastic Structures*, 2nd ed., Hemisphere, New York (1981).
- Ödman, S. T. A., "Studies of Boundary Value Problems. Part II. Characteristic Functions of Rectangular Plates," *Proc. NR 24*, Swedish Cement and Concrete Research Institute, Royal Institute of Technology, Stockholm, 7–62 (1955).
- Ogata, K., *State Space Analysis of Control Systems*, Prentice-Hall, Englewood Cliffs, NJ (1967).
- Pagano, N. J., "Exact Solutions for Rectangular Bidirectional Composites and Sandwich Plates," *Journal of Composite Materials*, **4**(1), 20–34 (1970).
- Pagano, N. J., and Hatfield, S. J., "Elastic Behavior of Multilayered Bidirectional Composites," *AIAA Journal*, **10**(7), 931–933 (1972).
- Palazotto, A. N. and Dennis, S. T., *Nonlinear Analysis of Shell Structures*, AIAA Education Series, Washington, D.C. (1992).
- Panc, V., *Theories of Elastic Plates*, Noordhoff, Leyden, The Netherlands (1975).
- Phan, N. D., and Reddy, J. N., "Analysis of Laminated Composite Plates Using a Higher-Order Shear Deformation Theory," *International Journal for Numerical Methods in Engineering*, **21**, 2201–2219 (1985).
- Pietraszkiewicz, W., "Geometrically Nonlinear Theories of Thin Elastic Shells," in *Advances in Mechanics*, **12** (1), 52–130 (1989).
- Pipes, L. A. and Harvill, L. R., *Applied Mathematics for Engineers and Physicists*, 3rd ed., McGraw-Hill, New York (1970).
- Raju, P. N., "Vibrations of Annular Plates," *Journal of Aeronautical Society of India*, **14**(2), 37–52 (1962).
- Rao, K. P., "A Rectangular Laminated Anisotropic Shallow Thin Shell Finite Element," *Computer Methods in Applied Mechanics and Engineering*, **15**, 13–33 (1978).
- Reddy, J. N., "Simple Finite Elements with Relaxed Continuity for Non-Linear Analysis of Plates," *Proceedings of the Third International Conference in Australia on Finite Element Methods*, University of New South Wales, Sydney, July 2–6 (1979).
- Reddy, J. N., "A Penalty Plate-Bending Element for the Analysis of Laminated Anisotropic Composite Plates," *International Journal for Numerical Methods in Engineering*, **15**(8), 1187–1206 (1980).
- Reddy, J. N., "On the Solutions to Forced Motions of Rectangular Composite Plates," *Journal of Applied Mechanics*, **49**, 403–408 (1982).

- Reddy, J. N., "A Simple Higher-Order Theory for Laminated Composite Plates," *Journal of Applied Mechanics*, **51**, 745–752 (1984a).
- Reddy, J. N., "Exact Solutions of Moderately Thick Laminated Shells," *Journal of Engineering Mechanics*, **110**(5), 794–809 (1984b).
- Reddy, J. N., *Energy and Variational Methods in Applied Mechanics* (1st ed.), John Wiley & Sons, New York (1984c).
- Reddy, J. N., "A Small Strain and Moderate Rotation Theory of Laminated Anisotropic Plates," *Journal of Applied Mechanics*, **54**, 623–626 (1987).
- Reddy, J. N., "A General Non-Linear Third-Order Theory of Plates with Moderate Thickness," *International Journal of Non-linear Mechanics*, **25**(6), 677–686 (1990).
- Reddy, J. N., *Applied Functional Analysis and Variational Methods in Engineering*, McGraw-Hill, New York, 1986; reprinted by Krieger, Melbourne, FL (1992).
- Reddy, J. N., "On Locking-Free Shear Deformable Beam Finite Elements," *Computer Methods in Applied Mechanics and Engineering*, **149**, 113–132 (1997).
- Reddy, J. N., "On the Dynamic Behavior of the Timoshenko Beam Finite Elements," *Sadhana* (Indian Academy of Sciences), **24**, Pt. 3, 175–198 (1999).
- Reddy, J. N. and Chao, W. C., "A Comparison of Closed-Form and Finite Element Solutions of Thick Laminated Anisotropic Rectangular Plates," *Nuclear Engineering and Design*, **64**, 153–167 (1981).
- Reddy, J. N. and Phan, N. D., "Stability and Vibration of Isotropic Orthotropic and Laminated Plates According to a Higher-Order Shear Deformation Theory," *Journal of Sound and Vibration*, **98**, 157–170 (1985).
- Reddy, J. N. and Wang, C. M., "Relationships Between Classical and Shear Deformation Theories of Axisymmetric Bending of Circular Plates," *AIAA Journal*, **35**(12), 1862–1868 (1997).
- Reddy, J. N., Wang, C. M., and Lee, K. H., "Relationships Between Bending Solutions of Classical and Shear Deformation Beam Theories," *International Journal of Solids and Structures*, **34**(26), 3373–3384 (1997).
- Reddy, J. N., Wang, C. M., and Lam, K. Y., "Unified Beam Finite Elements Based on the Classical and Shear Deformation Theories of Beams and Axisymmetric Circular Plates," *Communications in Numerical Methods in Engineering*, **13**, 495–510 (1997).
- Reddy, J. N. and Wang, C. M., "Deflection Relationships Between Classical and Third-Order Plate Theories," *Acta Mechanica*, **130**(3-4), 199–208 (1998).
- Reddy, J. N. and Wang, C. M., "An Overview of the Relationships Between Solutions of the Classical and Shear Deformation Plate Theories," *Composites Science and Technology*, **60**, 2327–2335 (2000).
- Reddy, J. N., Wang, C. M., and Kitipornchai, S., "Relationship Between

- Vibration Frequencies of Reddy and Kirchhoff Polygonal Plates with Simply Supported Edges," *ASME Journal of Vibration and Acoustics*, **122**(1), 77–81 (2000).
- Reddy, J. N., *Energy Principles and Variational Methods in Applied Mechanics*, 2nd ed., John Wiley & Sons, New York (2002).
- Reddy, J. N., *Mechanics of Laminated Composite Plates and Shells: Theory and Analysis*, 2nd ed., CRC Press, Boca Raton, FL (2004a).
- Reddy, J. N., *An Introduction to Nonlinear Finite Element Analysis*, Oxford University Press, Oxford, UK (2004b).
- Reddy, J. N., *An Introduction to the Finite Element Method*, 3rd ed., McGraw-Hill, New York (2006).
- Reddy, J. N., *An Introduction to Continuum Mechanics with Applications*, Cambridge University Press, New York (in press).
- Reismann, H. "Bending and buckling of an elastically restrained circular plate," *Journal of Applied Mechanics*, **19**, 167–172 (1952).
- Reismann, H. and Lee, Y.-C., "Forced Motions of Rectangular Plates," *Developments in Theoretical and Applied Mechanics*, Pergamon, New York, p. 3 (1969).
- Riks, E., "The Application of Newton's Method to the Problem of Elastic Stability," *Journal of Applied Mechanics*, **39**, 1060–1066 (1972).
- Roark, J. R. and Young, W. C., *Formulas for Stress and Strain*, McGraw-Hill, New York (1975).
- Roberson, R. E., "Vibrations of a Clamped Circular Plate Carrying Concentrated Mass," *Journal of Applied Mechanics*, **18**(4), 349–352 (1951).
- Sanders, J. L. Jr., "An Improved First-Approximation Theory for Thin Shells," NASA TR-R24, Washington, D.C. (1959).
- Sanders, J. L. Jr., "Nonlinear Theories for Thin Shells," *Quarterly of Applied Mathematics*, **21**, 21–36 (1963).
- Schapery, R. A., "Thermal Expansion Coefficients of Composite Materials Based on Energy Principles," *Journal of Composite Materials*, **2**(3), pp. 380-404 (1968).
- Schmidt, R., "A Refined Nonlinear Theory for Plates with Transverse Shear Deformation," *Journal of Industrial Mathematics Society*, **27**(1), 23–38 (1977).
- Scordelis, A. C. and Lo, K. S., "Computer Analysis of Cylindrical Shells," *Journal of American Concrete Institute*, 538–560 (1964).
- Simo, J. C., Fox, D. D., and Rifai, M. S., "On a Stress Resultant Geometrically Exact Shell Model. Part II: The Linear Theory," *Computer Methods in Applied Mechanics and Engineering*, **73**, 53–92 (1989).
- Sokolnikoff, I. S., *Mathematical Theory of Elasticity*, McGraw-Hill, New York (1956).

- Southwell, R. V., "On the Free Transverse Vibrations of a Uniform Circular Disc Clamped at its Center and on the Effect of Rotation," *Proceedings of the Royal Society (London)*, Series A, **101**, 133–153 (1922).
- Srinivas, S. and Rao, A. K., "Bending, Vibration, and Buckling of Simply Supported Thick Orthotropic Rectangular Plates and Laminates," *International Journal of Solids and Structures*, **6**, 1463–1481 (1970).
- Stavsky, Y., "Thermoelasticity of Heterogeneous Aeolotropic Plates," *Journal of Engineering Mechanics Division*, **EM2**, 89–105 (1963).
- Szilard, R., *Theories and Applications of Plate Analysis. Classical, Numerical and Engineering Methods*, John Wiley & Sons, New York (2004).
- Timoshenko, S. P., "On the Transverse Vibrations of Bars of Uniform Cross Section," *Philosophical Magazine*, **43**, 125–131 (1922).
- Timoshenko, S. P. and Gere, J. M., *Theory of Elastic Stability*, 2nd ed., McGraw-Hill, New York (1961).
- Timoshenko, S. P. and Woinowsky-Krieger, S., *Theory of Plates and Shells*, McGraw-Hill, Singapore (1970).
- Timoshenko, S. P. and Young, D. H., *Vibration Problems in Engineering*, 3rd ed., D. Van Nostrand, New York (1955).
- Troitsky, M. S., *Stiffened Plates-Bending, Stability, and Vibrations*, Elsevier, New York (1976).
- Ugural, A. C., *Stresses in Plates and Shells*, 2nd ed., McGraw-Hill, New York (1999).
- Vlasov, B. F., "Ob uravnieniakh izgiba plastinok (On Equations of Bending of Plates)," *Doklady Akademii Nauk Azerbeijanskoi SSR*, **3**, 955–959 (1957).
- Vlasov, V. Z., *General Theory of Shells and Its Applications in Engineering*, (Translation of *Obshchaya teoriya obolochek i yeye prilozheniya v tekhnike*), NASA TT F-99, NASA, Washington, D.C. (1964).
- Wang, C. M., "Timoshenko Beam-Bending Solutions in Terms of Euler–Bernoulli Solutions," *Journal of Engineering Mechanics*, ASCE, **121**(6), 763–765 (1995).
- Wang, C. M. and Reddy, J. N., "Buckling Load Relationship Between Reddy and Kirchhoff Plates of Polygonal Shape with Simply Supported Edges," *Mechanics Research Communications*, **24**(1), 103–108 (1997).
- Wang, C. M., Reddy, J. N., and Lee, K. H., *Shear Deformable Beams and Plates. Relationships with Classical Solutions*, Elsevier, Oxford, UK (2000).
- Wang, C. M., Wang, C. Y., and Reddy, J. N., *Exact Solutions for Buckling of Structural Members*, CRC Press, Boca Raton, FL (2005).
- Warburton, G. B., "The Vibration of Rectangular Plates," *Proceedings of the Institution of Mechanical Engineering*, Series A, **168**(12), 371–384 (1954).

- Washizu, K., *Variational Methods in Elasticity and Plasticity*, 3rd ed., Pergamon Press, New York (1982).
- Weaver, W., Jr., Timoshenko, S. P., and Young, D. H., *Vibration Problems in Engineering*, 5th ed., John Wiley & Sons, New York (1990).
- Wempner, G. A., "Discrete Approximations Related to Nonlinear Theories of Solids," *International Journal of Solids and Structures*, **7**, 1581–1599 (1971).
- Yamaki, N., "Influence of Large Amplitudes on Flexural Vibrations of Elastic Plates," *ZAMM*, **41**, 501–510 (1967).
- Young, D., "Vibrations of Rectangular Plates by the Ritz Method," *Journal of Applied Mechanics*, **17**, 448–453 (1950).
- Young, D. and Felgar, F. P., *Tables of Characteristic Functions Representing the Normal Modes of Vibration of a Beam*, University of Texas, Austin, Publication No. 4913 (1949).
- Zaghoul, S. A. and Kennedy, J. B., "Nonlinear Behavior of Symmetrically Laminated Plates," *Journal of Applied Mechanics*, **42**, 234–236 (1975).
- Zienkiewicz, O. C. and Cheung, Y. K., "The Finite Element Method for Analysis of Elastic Isotropic and Orthotropic Slabs," *Proceeding of the Institute of Civil Engineers*, London, **28**, 471–488 (1964).
- Zienkiewicz, O. C., Too, J. J. M., and Taylor, R. L., "Reduced Integration Technique in General Analysis of Plates and Shells," *International Journal for Numerical Methods in Engineering*, **3**, 275–290 (1971).
- Zienkiewicz, O. C., *The Finite Element Method*, McGraw-Hill, New York (1977).
- Zienkiewicz, O. C. and Taylor, R. L., *The Finite Element Method*, vol. 1, *Basic Formulation and Linear Problems*, McGraw-Hill, London (1991).
- Zienkiewicz, O. C. and Taylor, R. L., *The Finite Element Method*, vol. 2, *Solid and Fluid Mechanics, Dynamics and Non-Linearity*, McGraw-Hill, London (1991).

SUBJECT INDEX

- Adjoint, 12
Adjunct, *see* Adjoint
Admissible configurations, 40,52
Admissible variations, 40,49,52
Alternating symbol, 4
Analytical (exact) solutions
 of bars, 75,78
 of beams, 81,86
 of circular plates, 162,167,171,174,
 178–185,187,190–195
 of plate strips, 127–145
 see Navier’s and Lévy solutions
Anisotropic body, 28
Anisotropic plates, 111
Annular plates, 163,174,180,188
 boundary conditions, 164,169,
 174–176,180,182–184,191,198,202,209
 clamped, 128,133,139
 elastically supported, 135
 simply supported, 127,129,132,138
Anticlastic surface, 405
Approximation functions, 69,70
 for bars, 74,77
 for beams, 80,86,92
 for circular plates, 170,180,185,
 197–199,205
 for rectangular plates, 254,284–291,
 320,327,347–352
Area coordinates, 493
Asymmetrical bending, 189–200
Axisymmetric bending, 160–189
Basis vectors, 2
 Cartesian, 2
 cylindrical, 8,9
 derivatives of, 9,10,150
 orthonormal, 3,10
 spherical, 10,11
Bending stiffnesses, 87,111,116
Bessel functions, 185,201
Biharmonic equation, 395
Biharmonic operator, 120
Boundary conditions
 annular plates, 164
 circular plates, 164
 clamped, 128,133,139,178
 elastically supported, 135
 essential, 49
 force, 49
 geometric, 49
 homogeneous form of, 49
 natural, 49
 simply supported, 127,132,134,138,216
Buckling load
 biaxial compression, 301
 critical, 130
 inplane shear, 324
 plate strips, 130
 rectangular plates, 300
 uniaxial compression, 303
Cartesian basis, 3
Castigliano’s theorems, 61–68
Cauchy stress formula, 25
Cauchy stress tensor, 25
Characteristic equation, 134
Characteristic polynomials, 139
Circular inclusion, 183
Circular plates
 asymmetric bending of, 189
 axisymmetric bending of, 160
 classical theory of, 153–160
 equations of motion of, 160
 first-order theory of, 391
 on elastic foundation, 185
 under thermal loads, 160,187,233
 with clamped edges, 178
Classical plate theory (CPT)
 circular plates, 153–160
 displacement field, 97,153
 equations of motion, 105,155
 finite element models, 480

- Collocation method, 85
- Compatibility conditions, 21
- Completeness, 70
- Compliance coefficients, 29
- Conforming element, 483
- Constitutive equations
 - for anisotropic materials, 28
 - for orthotropic materials, 29
 - for plates, 100–113, 365, 381
 - for shells, 425–428
 - thermoelastic, 31
- Contracted notation, 28
- Convergence, 69
- Coordinate functions
 - see* Approximation functions
- Coordinates
 - Cartesian, 3
 - curvilinear, 411
 - cylindrical, 8
 - material, 18
 - rectangular, 2
 - spherical, 10
 - transformation of, 14
- Cramer's rule, 13
- Critical buckling load, 130
- Curl operator, 6
- Curvature of a shell, 408
- Cylindrical bending, 119
- Cylindrical coordinates, 8
- Deformation, 18
- Del operator, 5–11
- Developable surface, 405
- Dirac delta function, 85, 218
- Directional derivative, 6
- Displacement field of
 - circular plates, 153
 - CLPT, 97
 - Euler–Bernoulli beam, 45
 - FSDT, 359
 - shells, 415, 416
 - third-order beam, 89
 - Timoshenko beam, 56
 - TSTD, 377
- Divergence, 6
- Divergence theorem, 50
- Dummy index, 3
- Dyads
 - see* tensor, second-order
- Dynamic analysis, 65, 167, 239, 391
 - see also* Transient response
- Effective shear force, 108, 121, 251, 253, 283
- Elastic coefficients, 28
- Engineering constants
 - see* Material constants
- Epsilon–delta identity, 5
- Equations of equilibrium
 - 3-D elasticity, 25–27
 - circular plates, 157
 - cylindrical coordinates, 38
 - Euler–Bernoulli assumptions, 56
 - Euler–Bernoulli beam theory, 54, 530
 - Timoshenko beam theory, 56, 534
- Equations of motion
 - 3-D elasticity, 25, 122
 - circular plates, 155–160
 - CLPT, 105, 120
 - cylindrical bending, 119
 - third-order beam theory, 90
 - third-order plate theory, 380, 381
 - Timoshenko beam theory, 58, 90
- Equivalent shear force, 156
 - for plane stress, 30
- Euler–Bernoulli hypothesis, 25
- Euler–Lagrange equations, 49, 58, 420
- Finite element method, 479
- Finite element model
 - of beams, 530–535
 - of plates (CPT), 480, 505–508
 - of plates (FSDT), 491, 509–511
- First-order shear deformation theory (FSDT)
 - bending solutions of, 366–369
 - buckling analysis of, 372
 - displacement field of, 359
 - equations of motion of, 364
 - finite element models, 491, 509–511
 - Navier's solution, 366
 - plate constitutive equations, 110, 365, 381
 - shear correction factors, 362
 - transverse force resultants, 362
 - vibration analysis of, 389
- Free vibration of
 - see* Natural vibration of
- Frenet's formula, 407
- Frequency equation
 - of plate strips, 132–133
 - of rectangular plates, 311
 - see also* Characteristic equation
- Fully discretized model, 486
- Functional, 47, 88
- Fundamental frequency, 135, 137, 331–356
- Fundamental lemma, 48
- Galerkin method, 83
- Gauss characteristic equation, 410

- Gauss quadrature, 498
 Gaussian curvature, 405
 Gradient vector, 6
see also Del operator
 Green–Gauss theorem, 420
 Green–Lagrange strain tensor, 18–20, 413
 Hamilton’s principle, 55, 419
 Hooke’s law, generalized, 28
 Hyperelastic materials, 29
 Infinitesimal strain tensor, 20
 Internal virtual work, 43
 Internal work, 43
 Invariant, 2
 Isotropic materials, 28
 Isotropic plates, 112
 Kinematics, 18
 Kinetic energy, 55
 Kirchhoff assumptions, 96, 416
 Kirchhoff free edge condition, 107, 108, 189
 Kirchhoff hypothesis, 96, 416
 Kronecker delta, 4
 Lagrange element
 interpolation functions of, 492–495,
 rectangular, 494
 triangular, 492
 Lagrangian, 55, 59
 Lame’s coefficients, 410
 Laminate stiffness, 112–117, 365, 382
 Laminated plates, 112
 Laminated shells, 426
 Laplace equation, 395
 Laplacian operator, 7, 9, 11, 36, 120, 149
 Laplace transform, 144, 145
 Least-squares method, 85
 Lévy solution, 236, 249, 263, 466
 Linear functional, 48
 Linear independence, 70
 Local coordinates, 484,
 Love’s first-approximation shell theory, 424
 Love–Kirchhoff assumption, 418
 Marcus moment, 159, 396
 Mainardi–Codazzi relations, 410
 Mass inertias, 102, 380, 420, 404
 Material constants, 30
 Material stiffnesses, 34
 Matrices, 11
 determinant of, 12
 orthogonal, 3, 15
 Membrane locking, 520
 Meridian line, 441
 Method of superposition, 280
 Moment sum, 159, 396
 Natural coordinates, 495
 Natural vibration of
 bars, 76
 beams, 135
 circular plates, 200–204
 cylindrical shells, 464
 rectangular plates 332, 374, 389
 Navier’s solution, 217
 bending, 217, 366, 383
 buckling, 300, 372, 385
 vibration, 332, 374, 389
 Newmark family of
 approximations, 487
 Nodal circles, 203
 Nodal diameter, 201
 Nodal line, 203
 Nonconforming element, 483
 Normal derivative, 51
 Normal section, 405
 Orthogonal system, 411
 Orthonormal basis, 3, 10
 Orthotropic material, 29, 110, 270, 425
 Particular solution, 69, 131
 Permutation symbol, 4
 Petrov–Galerkin method, 85
 Physical vector, 2
 Plane strain, 110
 Plane stress, 30, 110
 Plane stress-reduced stiffness, 30, 110
 Plate stiffnesses, 110,
 Plate strip, 119, 125
 buckling, 130
 on elastic foundation, 129, 166
 Plates
 annular, 163, 166, 174, 180
 circular, 149–211
 classical theory of, 95
 first-order theory of, 359
 third-order theory of, 376
 Potential, 59
 Potential function, 29
 Potential energy functional, 60, 326, 531
 Primary variables, 49
 Principal
 curvature, 405
 curves, 405
 radius of curvature, 441

- Principle of the minimum
total potential energy, 58,60,80,92,327
- Quadratic forms of the surface, 407,408
Quadratic functional, 48
- Ritz approximation
see Ritz solution
Ritz method, 69–72
Ritz solution, 75,80,142,166,169,195,
204,254,283,345
- Rectangular plates, 215
under hydrostatic load, 219,231
under line load, 219,231
under point load, 218,219,231
under sinusoidal load, 231
under uniform load, 218,231
with clamped edges, 291
with distributed edge moments, 246
with patch loading, 232
with simply supported edges, 215
with thermal loads, 220,235
- Reduced integration, 497–500
- Rotary inertia, 105
Rotatory inertia, 105
see also Rotary inertia
- Sanders shell theory, 419
Secondary variable, 49
Serendipity family, 495
Shear correction coefficient 57,362,415
Shear deformation, 146,359
Shear force resultants, 362
Shear locking, 497,519
Shells
analytical solutions, 430–463
assumptions, 415
bending stresses in, 458
conical, 448
constitutive equations of, 425–429
cylindrical, 430–441,464
differential element of, 411
doubly-curved, 407
ellipsoidal, 450
equations of Byrne, 418
equations of Love, 418
equations of motion, 419–425
equations of Naghdi, 418
flexural forces in, 412
flexural theory of, 436–441
geometric properties of, 407
geometry of, 409
governing equations of, 407
Love's first-approximation, 424
membrane forces in, 412
- membrane stresses in, 444,451
membrane theory of, 431
of double curvature, 441–463
of revolution, 406,442
Sanders theory of, 419–423
spherical, 444–448
singly-curved, 407
strain–displacement relations of,
413–418
stress resultants of, 414,426–429
toroidal, 441,451
unsymmetrically loaded, 451–457
vibration, 464
virtual energies of, 419
- Spherical dome, 444
- Spherical tank, 447
- Stability *see* Buckling load
- State–space approach, 229,237,330,468
- Strain components
in Cartesian coordinates, 20
in cylindrical coordinates, 20,38
infinitesimal, 20
nonlinear, 19,99
of circular plates, 154
of CLPT, 99
of Euler–Bernoulli beams, 45
of Timoshenko beams, 56
- Strain energy, 43,57,58,64
- Strain energy density, 29,43,59
- Stress components
Cartesian, 24
cylindrical, 26
- Stress measures, 23–25
- Stress resultants
in plates, 101,362,381
in shells, 414
- Stress tensor, 24
- Stress vector, 24
- Summation convention, 43
- Surface metric tensor, 407
- Symmetric laminates, 113
- Synclastic surface, 405
- Tensor
alternating, 4
Cauchy stress, 25
nth order, 17
second order, 3,7,11,15,17,24
strain, 18
stress, 24
transformation of, 14–17
- Theorem of Rodrigues, 408
- Thermal
forces, 111,126,159
moments, 126,159

- Thermal coefficients of expansion
 31,34,111
- Thermoelastic constitutive relations,
 31,35,158
- Third-order beam theory, 89
- Third-order plate theory, 376–390
 bending, 385
 buckling, 387
 displacement field of, 377
 equations of motion of, 380
 natural vibration, 389
 stress resultants of, 381
- Time approximations, 487
- Timoshenko beam theory, 56,89,90,92,532
- Total potential energy
 see Potential energy functional
- Transformation of
 material stiffness, 34
 strain components, 33
 stress components, 32
 tensors, 15
 thermal coefficients, 34
 vectors, 14–16
- Transient response, 79,93,140–145,332,354
- True stress, 25
- Variational operator, 46
- Vector differential, 6
- Vector gradient, 6
- Vector transformations, 14
- Vectors
 cross product of, 4
 curl of, 6
 divergence of, 6
 dot product of, 4
 stress, 23
- Vibration
 of bars, 76
 of circular plates, 200
 of plate strips, 135
 of rectangular plates, 332
- Virtual complementary
 strain energy, 45,66,67,419
- Virtual displacements, 40
 principle of, 52,100,154,361,379
- Virtual forces, 40
- Virtual strain energy, 43,419
- Virtual strains, 43,100,155,361,379
- Virtual work, 42
 external, 42
 internal, 43
- Voigt–Kelvin notation, 28
- von Kármán strains, 99,154,361,416,
 504,520,524,529,532
- Weak form, 72,205
- Weight functions, 84
- Weighted-residual method, 84,85
- Weingarten formulas, 408

Mechanical Engineering

Praise for the First Edition

"This new book by J.N. Reddy digests more than two decades of research by him in plate theories, variational methods, and finite elements into an excellent textbook, which can be used very well by beginning or advanced graduate students, or by many engineers who deal with aerospace, automotive, and civil engineering structure....the material is presented carefully and thoroughly in language that is easy to follow...it is the best book available..."

—Arthur W. Leissa (Ohio State University), *Applied Mechanics Reviews*

Theory and Analysis of Elastic Plates and Shells, Second Edition presents a complete, up-to-date, and unified treatment of classical and shear deformation plates and shells, from the basic derivation of theories to analytical and numerical solutions.

Revised and updated, this second edition incorporates new information in most chapters, along with some rearrangement of topics to improve the clarity of the overall presentation. The book presents new material on the theory and analysis of shells, featuring an additional chapter devoted to the topic. The author also includes new sections that address Castigliano's theorems, axisymmetric buckling of circular plates, the relationships between the solutions of classical and shear deformation theories, and the nonlinear finite element analysis of plates. The book provides many illustrations of theories, formulations, and solution methods, resulting in an easy-to-understand presentation of the topics.

Like the previous edition, this book remains a suitable textbook for a course on plates and shells in aerospace, civil, and mechanical engineering curricula and continues to serve as a reference for industrial and academic structural engineers and scientists.

Features

- Presents self-contained coverage of the necessary background on vectors and tensors, basic equations of elasticity, and variational methods
- Contains new material on the theory and analysis of shells
- Covers classical as well as current shear deformation theories of plates and shells
- Explores linear and nonlinear finite element analysis of plates
- Includes numerous worked examples and problem sets in each chapter

8415

ISBN 0-8493-8415-X

9 0000



9 780849 384158



CRC Press

Taylor & Francis Group

an Informa business

www.taylorandfrancisgroup.com

6000 Broken Sound Parkway, NW
Suite 300, Boca Raton, FL 33487
270 Madison Avenue
New York, NY 10016
2 Park Square, Milton Park
Abingdon, Oxon OX14 4RN, UK